British Journal of Pharmacology

October 1994

Volume 113 Number 2 pages 331–658

Dr S J Coker
Department of Pharmacology
University of Liverpool
P.O. Box 147
LIVERPOOL L69 3BX

Br. J. Pharmacol. (1994), **113**, 331–333

SPECIAL REPORT

© Macmillan Press Ltd, 1994

Mutations in transmembrane segment VII of the AT_1 receptor differentiate between closely related insurmountable and competitive angiotensin antagonists

[1]Hans T. Schambye, Bjørn v. Wijk, Siv A. Hjorth, *Wolfgang Wienen, *Michael Entzeroth, †Derk J. Bergsma & Thue W. Schwartz

Laboratory for Molecular Endocrinology, University Dept. of Clinical Biochemistry, Rigshospitalet 6321, DK-2100 Copenhagen, Denmark; *Department of Biochemical Research, Cardiovascular Pharmacology, Dr. Karl Thomae GmbH, D-88397 Biberach an der Riss, Germany and †Dept. of Molecular Genetics, SmithKline Beecham Pharmaceuticals, King of Prussia, Pennsylvania 19406, U.S.A.

Chimeric constructs between the human and the *Xenopus laevis* AT_1 receptor have demonstrated, that the binding of non-peptide angiotensin antagonists is dependent on non-conserved residues located deep in transmembrane segment VII of the AT_1 receptor. Here we have studied four pairs of closely related antagonists each consisting of a competitive and an insurmountable compound differentiated by one out of three different types of minor chemical modifications. None of the antagonists bound to the *Xenopus* receptor and the binding of all of the compounds to the human receptor was severely impaired by the introduction of non-conserved residues from transmembrane segment VII of the *Xenopus* receptor. In all four pairs of antagonists the competitive compound was affected more by these substitutions than the corresponding insurmountable one (209 vs. 22, 281 vs. 29, 290 vs. 29 and 992 vs. 325-fold increase in K_i values). A similar pattern was observed in response to substitution of a single non-conserved residue in transmembrane segment VII, Asn^{295} to Ser. These results indicate that a common molecular mechanism distinguishes the interaction of insurmountable and competitive antagonists with the AT_1 receptor.

Keywords: Angiotensin AT_1 receptor; non-peptide antagonists; insurmountable antagonism; competitive antagonism; chimeric receptors; mutagenesis

Introduction The newly developed non-peptide antagonists for the angiotensin AT_1 receptor behave as competitive compounds in binding assays with radiolabelled angiotensin II (AII) (Wexler *et al.*, 1992; Wienen *et al.*, 1992; 1993). However, in bioassays a subset of these compounds exhibit insurmountable antagonism; i.e. the dose-response curve for the agonist is not only shifted to the right, but the maximal response is also reduced (Kenakin, 1987; Wexler *et al.*, 1992; Wienen *et al.*, 1992; 1993).

By construction of chimeric receptors between the human and the *Xenopus* AT_1 receptor, which does not bind the non-peptide compounds (Bergsma *et al.*, 1993), we recently identified residues in transmembrane segment (TM) VII, especially Asn^{295}, to be important for the binding of non-peptide ligands but not for angiotensin II (Schambye *et al.*, 1994). Surprisingly, insurmountable and competitive antagonists were differently affected by these exchanges in TM-VII as a larger decrease in binding affinity was observed for competitive than for insurmountable compounds (Schambye *et al.*, 1994).

In the present study we have selected four pairs of closely related angiotensin antagonists in which only a minor chemical modification distinguishes the insurmountable compound from its competitive counterpart. The chemical differences were located in three different parts of the compounds' common molecular scaffold (Figure 1).

Methods Rabbit aorta contraction after angiotensin II stimulation was measured as previously described (Wienen *et al.*, 1992). The apparent dissociation constants, pK_B, for competitive and insurmountable antagonism were calculated as described (Kenakin, 1987).

Chimeric receptors were constructed using an overlap extension technique based on PCR, as described by Schambye *et al.* (1994). Constructs were verified by dideoxynucleotide sequencing (Sequenase kit, U.S. Biochemicals Co.).

The binding to wildtype human and *Xenopus* AT_1 and the mutant receptors were studied in transfected COS 7 and CHO cells (Gether *et al.*, 1993). Binding experiments were performed on whole cells for 24 h at 4°C, as described by Schambye *et al.* (1994).

Peptide and non-peptide ligands Angiotensin II (AII) and [Sar^1,Leu^8]-AII were purchased from Peninsula (St. Helens, Merseyside, UK). BIBR247, BIBR179, BIBR277, BIBR255, BIBS39 and BIBR237 were synthesized by Drs N. Hauel and B. Narr at Dr Karl Thomae GmbH, Germany. Losartan and EXP3174 were kindly provided by P.B.M.W.M. Timmermans [The DuPont Merck Pharmaceutical Company (Wexler *et al.*, 1992)].

Results All of the tested compounds were potent inhibitors of AII-induced aortic contraction with a pK_B of between 7.0 and 9.78 (Table 1). Four compounds (losartan, BIBR255, BIBS39 and BIBR237) acted as classical competitive antagonists and induced a parallel shift of the concentration-contractile curve without depression of the maximal response (Table 1), whereas four other compounds (EXP3174, BIBR247, BIBR179 and BIBR277) acted as insurmountable antagonists, thus reducing the maximal response to agonist stimulation by 24% to 60% (Table 1).

All of the non-peptide antagonists were bound with high affinities by the wildtype human AT_1 receptor with K_I values ranging from 0.87 nM to 25.4 nM (Table 1). In contrast, none of the non-peptide antagonists were able to displace the ^{125}I-[Sar^1,Leu^8]-AII from the *Xenopus* AT_1 receptor (results not shown).

The chimeric AT_1 receptor constructs HX7-hAT_1, where TM-VII and the C-terminal tail of the human receptor were exchanged with the corresponding segments from the

[1] Author for correspondence.

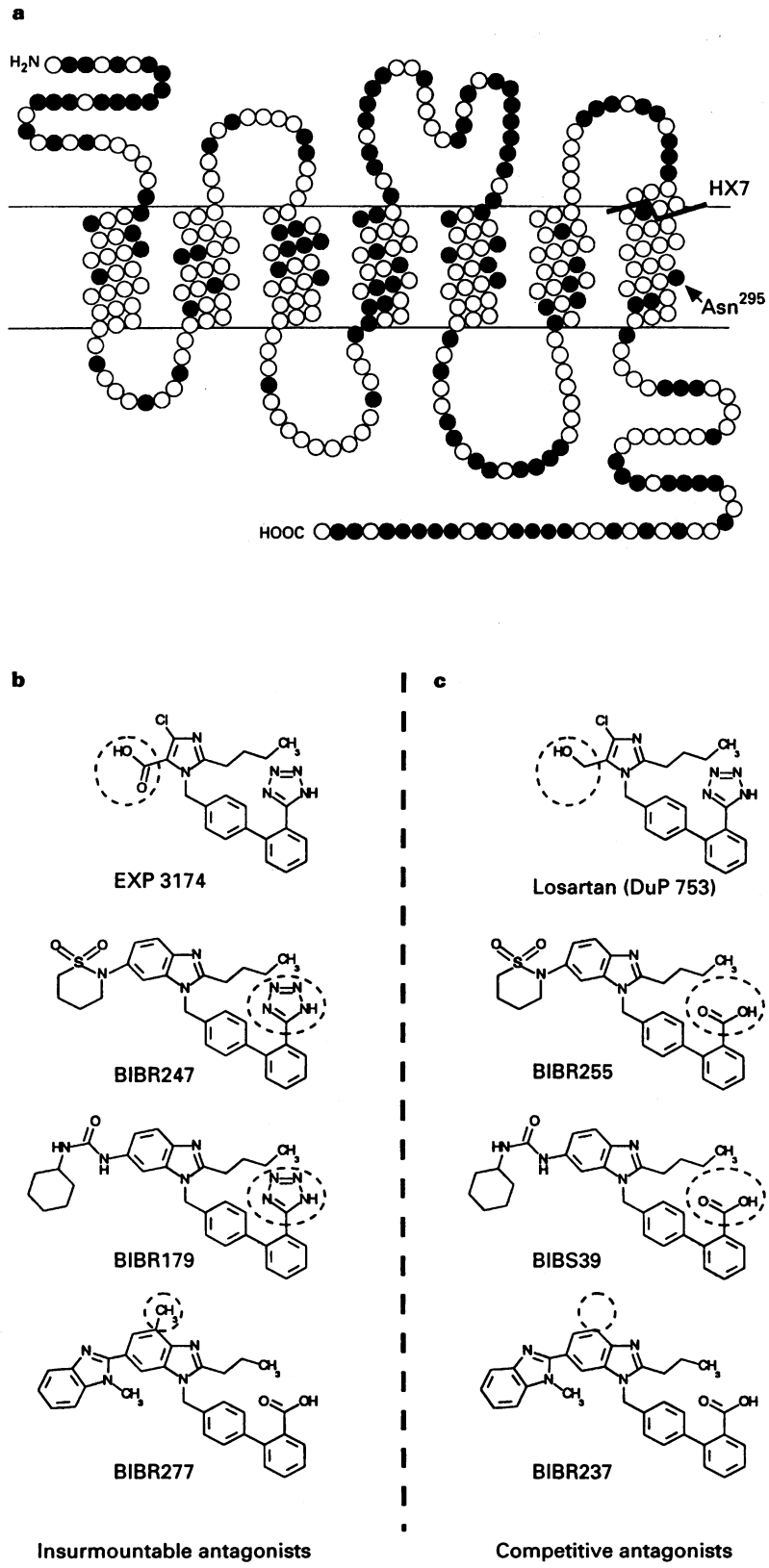


Figure 1 Structure of the human angiotensin II AT_1 receptor and of the employed non-peptide angiotensin antagonists. (a) Diagram of the human angiotensin AT_1 receptor (Bergsma *et al.*, 1992) with the splice-junction for the chimeric receptor HX7-hAT_1 indicated by a crossing line and the Asn^{295} residue located in TM-VII indicated by an arrow: (○) amino acid conserved between the human and the *Xenopus* AT_1 receptors (Bergsma *et al.*, 1993); (●) amino acid residues specific for the human AT_1 receptor. (b) and (c) The non-peptide antagonists are grouped according to their antagonist properties. The chemical differences between the two compounds in each pair are indicated by circles.

Table 1 Inhibition of angiotensin II (AII)-induced aortic contractions and binding affinity of peptide and non-peptide ligands for the human wildtype receptor and chimeric human/*Xenopus* receptor constructs

	Aorta contraction			*Receptor binding*							
Ligand	pK_B	(*n*)	*Reduction of Max. response*	*Human AT_1* K_I (nM)	(*n*)	*HX7-hAT_1* K_I (nM)	(*n*)	F_{mut}	*(Asn^{295}→Ser) hAT_1* K_I (nM)	(*n*)	F_{mut}
Angiotensin II	–		–	0.19 ± 0.03	(7)	0.34 ± 0.05	(3)	1.8	0.51 ± 0.05	(7)	2.7
BIBS39	8.14 ± 0.08	(4)	NR	8.90 ± 2.02	(6)	1865 ± 91	(4)	209	244 ± 26	(5)	27
BIBR179	7.00	(4)	32%	25.4 ± 3.9	(9)	550 ± 9	(5)	22	150 ± 10	(5)	6
BIBR237	7.85 ± 0.05	(3)	NR	5.68 ± 0.62	(9)	1594 ± 140	(4)	281	168 ± 15	(5)	30
BIBR277	9.48	(6)	60%	4.86 ± 0.98	(8)	143 ± 18	(5)	29	17.6 ± 2.7	(5)	4
BIBR255	7.85 ± 0.05	(4)	NR	6.02 ± 0.77	(9)	1748 ± 168	(4)	290	318 ± 34	(5)	53
BIBR247	7.90	(3)	39%	1.77 ± 0.49	(9)	52 ± 7	(5)	29	9.9 ± 1.3	(5)	6
Losartan (DuP753)	8.01 ± 0.02	(6)	NR	1.42 ± 0.35	(7)	1406 ± 207	(5)	992	107 ± 11	(5)	75
EXP3174	9.78	(4)	24%	0.87 ± 0.16	(7)	282 ± 33	(5)	325	14.8 ± 1.3	(5)	17

The pK_B value for the compounds are given (mean ± s.e.mean, $n = 3-6$, mean only for insurmountable compounds). The reduction of the maximum contractile response is measured in the presence of 1 μM of antagonist. NR - no reduction. The antagonists are listed as the chemically related pairs (see Figure 1). K_I values are presented in nM (mean ± s.e.). The effect of the mutations on the binding affinity is expressed as the mutation factor, $F_{mut} = K_I$ (mutant receptor)/K_I (human AT_1 receptor). B_{max} values (mean ± s.e.mean, $n = 5-8$): wildtype human AT_1, 3.0 ± 0.8 fmol/10^5 cells; HX7-hAT_1, 13.7 ± 3.8 fmol/10^5 cells; (Asn^{295}→Ser)hAT_1 4.9 ± 1.3 fmol/10^5 cells.

Xenopus receptor (Figure 1) and the (Asn^{295}-Ser)hAT_1 mutant both bound AII and [Sar^1,Leu^8]-AII with affinities comparable to those of the wildtype receptors suggesting that the mutant receptors have a normal overall structure (Table 1) (Schambye *et al.*, 1994). In contrast, the affinity of all of the non-peptide compounds was severely reduced by the HX7-hAT_1 exchange, the K_I value increased 22 to 992 fold (the mutational factor, F_{mut}, in Table 1). Substitution of Asn^{295} with Ser in TM-VII led to a decrease in binding affinity of 4 to 75 fold (Table 1). For each of the pairs of antagonists the binding affinity of the competitive compound was more reduced by the chimeric exchanges in TM-VII, than the insurmountable counterpart was (Table 1). Thus, in HX7-hAT_1 the mutational factor for the four competitive antagonists BIBS39, BIBR237, BIBR255 and losartan was 209, 281, 290 and 992, respectively, as compared to 22, 29, 29 and 325 for their insurmountable counterparts, BIBR179, BIBR277, BIBR247 and EXP3174 (Table 1). In the (Asn^{295}→Ser)hAT_1 mutant the same pattern was observed, albeit the effect of this minor modification of the receptor was smaller, with a mutational factor between 27 and 75 for the competitive antagonists and between 4 and 17 for the corresponding insurmountable compounds (Table 1).

Discussion The binding of all of the non-peptide antagonists is critically dependent on non-conserved residues in TM-VII, especially Asn^{295}, – residues which do not seem to participate in peptide binding (Schambye *et al.*, 1994). DuP753 and EXP3174 were more affected by the exchange of TM-VII than the other six compounds. Possibly these relatively smaller compounds (Figure 1) have fewer points of interaction with the receptor, making binding more dependent upon interaction with the non-conserved residues in TM-VII.

Despite the fact, that the chemical modifications, which differentiate the four competitive compounds from their insurmountable counterparts, are located in three different parts of the compounds common molecular scaffold (Figure 1), the competitive analogue was in all four cases affected approximately 10 fold more than the insurmountable one by the substitutions in TM-VII (Table 1).

It is difficult to conceive of a direct common interaction between, for example, Asn^{295} and the decisive chemical moiety in all four pairs of antagonists, as the chemical differences are located so differently (Figure 1 and Table 1). More likely Asn^{295} either interacts directly with a common chemical moiety of the antagonists, or the Asn^{295} to Ser substitution changes the overall structure of the receptor and thereby indirectly affects the binding of the antagonists in a way which is more detrimental to competitive than the insurmountable compounds. In any case, as there is a strong correlation between the compounds pharmacological properties and the degree to which they were affected by the mutations these results indicate, that a common molecular mechanism distinguishes insurmountable and competitive antagonists in their interaction with AT_1 receptors.

We thank Dorte Frederiksen, Lisa Zeh and Tina Jakobsen for expert technical assistance. Supported by grants from the Danish Heart Association, the Danish Medical Research Foundation, the Novo Nordisk Foundation.

References

BERGSMA, D.J., ELLIS, C., KUMAR, C., NUTHULAGANTI, P., KERSTEN, H., ELSHOURBAGY, N., GRIFFIN, E., STADEL, J.M. & AIYAR, N. (1992). Cloning and characterization of a human angiotensin-II type-1 receptor. *Biochem. Biophys. Res. Commun.*, **183**, 989–995.

BERGSMA, D.J., ELLIS, C., NUTHULAGANTI, P.R., NAMBI, P., SCAIFE, K., KUMAR, C. & AIYER, N. (1993). Isolation and expression of a novel angiotensin-II receptor from Xenopus-laevis heart. *Mol. Pharmacol.*, **44**, 277–284.

GETHER, U., JOHANSEN, T.E. & SCHWARTZ, T.W. (1993). Chimeric NK1 (substance P)/NK3 (neurokinin B) receptors. *J. Biol. Chem.*, **268**, 7893–7898.

KENAKIN, T.P. (1987). Drug antagonism. In *Pharmacological Analysis of Drug Receptor Interaction*. ed. Kenakin, T.P. pp. 205–244. New York: Raven Press.

SCHAMBYE, H.T., HJORTH, S.A., BERGSMA, D.J., SATHE, G. & SCHWARTZ, T.W. (1994). Differentiation between binding sites for angiotensin II and non-peptide antagonists on the angiotensin II type I receptors. *Proc. Natl. Acad. Sci. U.S.A.*, (in press).

WEXLER, R.R., CARINI, D.J, DUNCIA, J.V., JOHNSON, A.L., WELLS, G.J., CHIU, A.T., WONG, P.C. & TIMMERMANS, P.B.M.W.M. (1992). Rationale for the chemical development of angiotensin II receptor antagonists. *Am. J. Hypertens.*, **5**, 209–220.

WIENEN, W., HAUEL, N., VAN MEEL, J.C.A., NARR, B., RIES, U. & ENTZEROTH, M. (1993). Pharmacological characterization of the novel nonpeptide angiotensin-II receptor antagonist, BIBR-277. *Br. J. Pharmacol.*, **110**, 245–252.

WIENEN, W., MAUZ, A.B.M., VAN MEEL, J.C.A. & ENTZEROTH, M. (1992). Different types of receptor interaction of peptide and nonpeptide angiotensin-II antagonists revealed by receptor binding and functional studies. *Mol. Pharmacol.*, **41**, 1081–1088.

(Received May 10, 1994
Accepted June 27, 1994)

Br. J. Pharmacol. (1994), **113**, 334–335

SPECIAL REPORT

© Macmillan Press Ltd., 1994

Parallel tolerance between platelet cyclic GMP and preload effects of nitroglycerin in anaesthetized mini-pigs

Christopher P. Baines, Richard S. Szwarc & [1]Howard A. Ball

Cardiovascular Biology Research Development, Ciba-Geigy Ltd, CH-4002 Basel Switzerland

The effects of acute intravenous nitroglycerin (NTG) administration on platelet cyclic GMP in relation to changes in indices of preload (end-diastolic volume) and afterload (effective arterial elastance) were evaluated in the anaesthetized mini-pig, using pressure-volume analysis. NTG (1–30 $\mu g\ kg^{-1}\ min^{-1}$, i.v.) elicited a dose-dependent fall in preload and afterload, and an increase in arterial blood platelet cyclic GMP. Repeated doses of NTG (30 $\mu g\ kg^{-1}\ min^{-1}$) resulted in tolerance to the preload but not afterload effects. The increases in platelet cyclic GMP were also attenuated, being highly correlated with the preload changes. Therefore, platelet cyclic GMP appears to reflect NTG-induced venous tolerance, rather than arterial responsiveness. The measurement of platelet cyclic GMP may represent a simple approach for monitoring the degree of venous tolerance to NTG in animals or patients, facilitating further mechanistic investigations.

Keywords: Nitroglycerin; platelet cyclic GMP; tolerance; preload; afterload; nitric oxide

Introduction Nitroglycerin (NTG) causes both venous and arterial peripheral vasodilatation resulting in reductions in preload and afterload (Imhof *et al.*, 1980). Continuous exposure to NTG leads to an attenuation of its haemodynamic effects, i.e. tolerance, which is primarily exhibited by the venous circulation (Ghio *et al.*, 1992). The vasodilator actions of NTG are due to its metabolic conversion, by vascular smooth muscle cells, to nitric oxide (NO) which activates vascular soluble guanylate cyclase leading to an accumulation of intracellular guanosine 3′:5′-cyclic monophosphate (cyclic GMP) (Ignarro *et al.*, 1981). Platelets also contain soluble guanylate cyclase, and although they do not appear to possess the enzyme required for the direct conversion of NTG, it is believed that sufficient NO can be released from NTG by the vascular tissue enzyme to enable activation of the platelet guanylate cyclase (Gerzer *et al.*, 1989). Thus platelet cyclic GMP might be an index of the tone, or state of relaxation of the vessels (Watanabe *et al.*, 1993; Fung *et al.*, 1993) following intravenous NTG.

The aim of the present study, in the anaesthetized mini-pig, was to quantify the effects of acute intravenous NTG administration on platelet cyclic GMP in relation to changes in indices of preload (end-diastolic volume) and afterload (effective arterial elastance). Pressure-volume analysis (Kass *et al.*, 1988) was chosen as a sensitive approach to quantify changes in left-ventricular preload, afterload and contractility.

Methods Male Göttinger mini-pigs (10.5–15.5 kg) were anaesthetized with sodium pentobarbitone (75 $mg\ kg^{-1}$, i.p.; followed by 0.2–0.25 $mg\ kg^{-1}\ min^{-1}$, i.v.) and ventilated with oxygen-enriched air. Left ventricular pressure was measured with a 5F micromanometer-tipped pressure catheter (Millar), and ventricular volume with an 8-electrode 6F conductance catheter, calibrated as previously described (Kass *et al.*, 1988). A 5F Swan-Ganz thermodilution catheter was used to measure cardiac output for calibration purposes. The left femoral artery was catheterized with a fluid-filled catheter (tip in thoracic aorta) for measurement of arterial blood pressure and sampling of blood.

Protocol Intravenous doses of 1, 3, 10 and 30 $\mu g\ kg^{-1}\ min^{-1}$ NTG ($n = 10$), or an equivalent volume of saline ($n = 6$), were each infused for 3 min; 15 min separated each infusion. Pilot studies had shown 30 $\mu g\ kg^{-1}\ min^{-1}$ NTG to

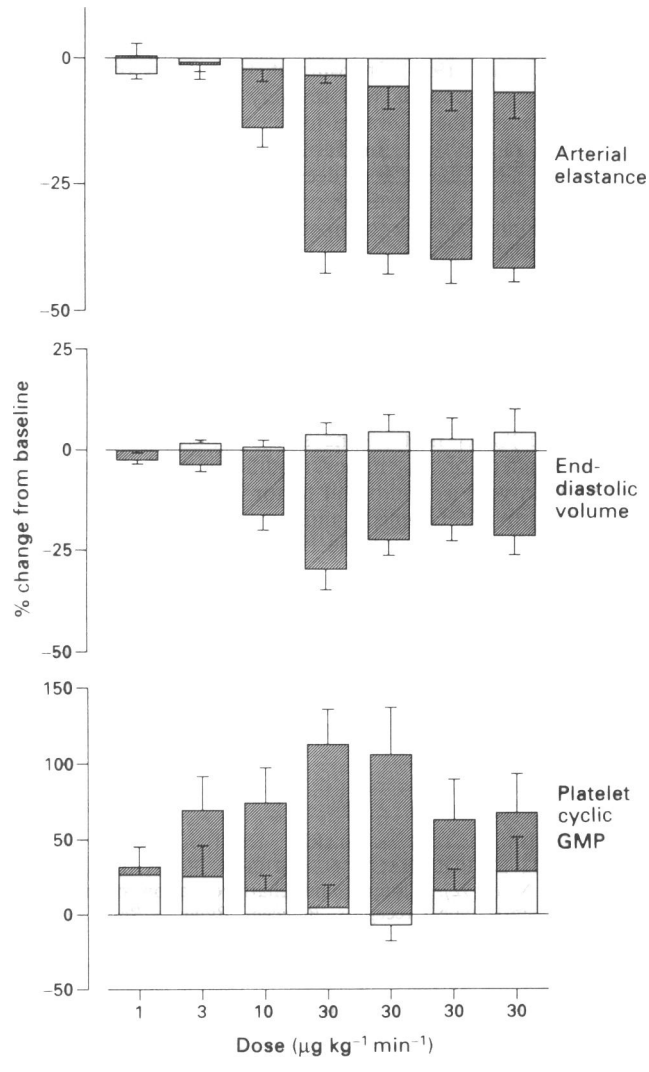


Figure 1 Effects of intravenous infusion of nitroglycerin (hatched columns) or saline vehicle (open columns) on arterial elastance (afterload index), left ventricular end-diastolic volume (preload index), and arterial blood platelet cyclic GMP. There were dose-related changes in all parameters between 1 and 30 $\mu g\ kg^{-1}\ min^{-1}$. Repeated doses caused a reproducible fall in arterial elastance. However, there was a parallel tolerance to the effects of NTG on end-diastolic volume and platelet cyclic GMP.

[1] Author for correspondence.

be equivalent to an ED_{60} for lowering of arterial blood pressure. Fifteen min following completion of the dose-response curve, $3 \times 30\,\mu g\,kg^{-1}\,min^{-1}$, i.v. NTG or saline were each infused for 5 min, allowing 15 min between infusions for parameters to return to baseline.

Arterial blood samples were withdrawn prior to and 1 min following each infusion. Cyclic GMP was extracted according to Watanabe *et al.* (1993) and the aqueous phase analysed using a [^{3}H]-cyclic GMP radioimmunoassay kit (Amersham). All data were calculated as the mean ± s.e.mean.

Materials Sodium pentobarbitone was purchased from Sigma Chemical Company (St. Louis, MO, U.S.A.). NTG (in 96% ethanol) was diluted 1 in 100 with saline immediately prior to use. All solvents and buffer constituents for extraction were obtained from Merck (Darmstadt, Germany).

Results NTG elicited dose-related decreases in arterial elastance and end-diastolic volume (max. fall 38.4 ± 4.2%; $P<0.001$, and 29.6 ± 5.1%; $P<0.01$, respectively) and increases in arterial platelet cyclic GMP (112.8 ± 23.1%; $P<0.01$) (Figure 1). However, whereas the maximum fall in arterial elastance was reproducible with repeated $30\,\mu g\,kg^{-1}\,min^{-1}$ doses, a significant attenuation of the maximum effect of NTG on EDV was observed. This was mirrored by a similar attenuation of the increase in platelet cyclic GMP. In fact, the changes in cyclic GMP were highly correlated with end-diastolic volume ($r = 0.743$, $P<0.05$) but not arterial elastance ($r = 0.597$, $P>0.1$). Contractility, as measured by end-systolic elastance was not affected by NTG.

The intravenous infusion of NTG caused a dose-related reduction in mean arterial blood pressure. The maximum fall (from 106 ± 3 to 64 ± 4 mmHg; $P<0.001$), like arterial elastance, was found to be reproducible with repeated $30\,\mu g\,kg^{-1}\,min^{-1}$ doses. The decrease in pressure was accompanied by a transient rise in heart rate (HR) with a peak increase from 88 ± 5 to 96 ± 3 beats min^{-1} ($P<0.05$), following the $10\,\mu g\,kg^{-1}\,min^{-1}$ dose. Saline had no effect on any measured parameter.

Discussion NTG dose-dependently reduced both preload and afterload: the peak effect of NTG on preload was significantly attenuated following repeated dosing whilst afterload was still reduced to the same extent. This suggests that tolerance develops to NTG in the venous circulation in agreement with similar findings (Ghio *et al.*, 1992) in patients.

Kukovetz & Holzmann (1986) showed that the *in vitro* exposure of vascular tissue to NTG caused a dose-related increase in intracellular cyclic GMP which correlated with the simultaneous relaxation of the preparation, with both effects being impaired after prolonged incubation with NTG. Similar findings were reported *in vivo* (Watanabe *et al.*, 1993) where the increase in platelet cyclic GMP correlated with epicardial coronary artery diameter. Both platelet cyclic GMP and the coronary artery changes were less pronounced in those patients receiving nitrate therapy. The present study further extends these findings by showing that repeated doses of NTG resulted in tolerance to the preload but not afterload effects. Additionally, the increases in platelet cyclic GMP were also attenuated, being highly correlated with the preload changes. This would also suggest that clinical tolerance to NTG, i.e. reduced venodilatation is, at least partly, due to biochemical tolerance at the cellular level.

In conclusion, platelet cyclic GMP appears to reflect NTG-induced venous tolerance, rather than arterial responsiveness. The measurement of platelet cyclic GMP may represent a simple approach for monitoring the degree of venous tolerance to NTG in animals or patients, facilitating further mechanistic investigations.

The excellent technical assistance of Miss Elizabeth Braun is gratefully acknowledged.

References

FUNG, H.L. (1993). Solving the mystery of nitrate tolerance: a new scent on the trail (Editorial). *Circulation*, **88**, 322–324.

GERZER, R., DRUMMER, C., KARRENBROCK, B. & HEIM, J.-M. (1989). Inhibition of platelet activating factor-induced aggregation by molsidomine, SIN-1, and nitrates in vitro and ex vivo. *J. Cardiovasc. Pharmacol.*, **14**, Suppl. 11, 115–119.

GHIO, S., DE SERVI, S., PEROTTI, R., ELEUTERI, E., MONTEMARTINI, C. & SPECCHIA, G. (1992). Different susceptibility to the development of nitroglycerin tolerance in the arterial and venous circulation in humans. Effects of N-acetylcysteine administration. *Circulation*, **86**, 798–802.

IGNARRO, L.J., LIPPTON, H., EDWARDS, J.C., BARICOS, W.H., HYMAN, A.L., KADOWITZ, P.J. & GRUETTER, C.A. (1981). Mechanism of vascular smooth muscle relaxation by organic nitrates, nitrites, nitroprusside and nitric oxide: evidence for the involvement of S-nitrosothiols as active intermediates. *J. Pharmacol. Exp. Ther.*, **218**, 739–749.

IMHOF, P.R., OTT, B., FRANKHAUSER, P., CHU, L.C. & HODLER, J. (1980). Difference in nitroglycerin dose-response in the venous and arterial beds. *Eur. J. Clin. Pharmacol.*, **18**, 455–460.

KASS, D.A., MIDEI, M., GRAVES, W., BRINKLER, J.A. & MAUGHAN, W.L. (1988). Use of a conductance (volume) catheter and transient inferior vena caval occlusion for rapid determination of pressure-volume relationships in man. *Cathet. Cardiovasc. Diagn.*, **15**, 192–202.

KUKOVETZ, W.R. & HOLZMANN, S. (1986). Mode of action of nitrates with regard to vasodilatation and tolerance. *Z. Kardiol.*, **75**, Suppl. 3, 8–11.

WATANABE, H., KAKIHANA, M., OHSTSUKA, S., ENOMOTO, T., YASUI, K. & SUGISHITA, Y. (1993). Platelet cyclic GMP: a potentially useful indicator to evaluate the effects of nitroglycerin and nitrate tolerance. *Circulation*, **88**, 29–36.

(Received June 13, 1994
Accepted June 29, 1994)

Br. J. Pharmacol. (1994), **113**, 336–338

SPECIAL REPORT

© Macmillan Press Ltd., 1994

Synergistic inhibition by BQ-123 and BQ-788 of endothelin-1-induced contractions of the rabbit pulmonary artery

[1]Takahiro Fukuroda, Satoshi Ozaki, Masaki Ihara, Kiyofumi Ishikawa, Mitsuo Yano & Masaru Nishikibe

Tsukuba Research Institute, Banyu Pharmaceutical, Tsukuba, Ibaraki 300-33, Japan

In the rabbit isolated pulmonary artery, neither the ET_A receptor antagonist, BQ-123 (10 μM), nor the ET_B receptor antagonist, BQ-788 (10 μM), inhibited the contractions induced by 1 nM endothelin-1 (ET-1). However, the combination of BQ-123 and BQ-788 completely inhibited the ET-1-induced contraction. In contrast, the ET_B-selective agonist, sarafotoxin S6c (1 nM)-induced contraction was completely inhibited by BQ-788 but not by BQ-123. In receptor binding assays, [^{125}I]-ET-1 specific binding to pulmonary arterial membranes was inhibited by BQ-123 (1 μM) by approximately 20% and additive treatment with BQ-788 (1 μM) completely inhibited the BQ-123-resistant component of [^{125}I]-ET-1 specific binding. The present study demonstrates synergistic inhibition by BQ-123 and BQ-788 of ET-1-induced contraction of the rabbit pulmonary artery and the coexistence of ET_A and ET_B receptors, suggesting that the activation of either only ET_A or only ET_B receptors may be sufficient to cause complete vasoconstriction. Therefore, blockade of both receptor subtypes would be necessary for the inhibition of some ET_A/ET_B composite types of responses.

Keywords: Endothelin-1; rabbit pulmonary artery; BQ-123; ET_A receptor antagonist; BQ-788; ET_B receptor antagonist; endothelin receptor subtypes; ET_A receptor; ET_B receptor

Introduction Endothelin-1 (ET-1) is a potent vasoconstrictor peptide isolated from the culture medium of porcine aortic endothelial cells, and ET-2 and ET-3 are isopeptides that were subsequently identified (Yanagisawa & Masaki, 1989). At least two distinct ET receptor subtypes, ET_A and ET_B receptors, exist in mammalian tissues (Arai *et al.*, 1990; Sakurai *et al.*, 1990). ET-1 is an ET_A/ET_B non-selective agonist, while sarafotoxin S6c (S6c), a peptide structurally related to ET-2, is an ET_B-selective agonist (Williams *et al.*, 1991).

It is well known that ET_A receptors mediate ET-1-induced vasocontraction. However, recent studies with ET_A-selective antagonists showed that non-ET_A receptors also mediated ET-1-induced contraction in some blood vessels (Fukuroda *et al.*, 1992; Sumner *et al.*, 1992). Furthermore, the ET-1-induced contraction of rabbit pulmonary artery was shown to be mediated through ET_A and ET_B receptors using an ET_B receptor-desensitized preparation (LaDouceur *et al.*, 1993). Very recently, BQ-788 (N-*cis*-2,6-dimethylpiperidinocarbonyl-L-γMeLeu-D-Trp(COOMe)-D-Nle-ONa) has been identified as a potent and selective ET_B receptor antagonist (Ishikawa *et al.*, 1994). In the present study, BQ-123 (cycro(-D-Trp-D-Asp(ONa)-Pro-D-Val-Leu)), an ET_A-selective antagonist (Ihara *et al.*, 1992), and BQ-788 were used to characterize endothelin receptors mediating contraction of rabbit pulmonary artery.

Methods The pulmonary arteries were removed from a male albino rabbit (approx. 3 kg body weight). The endothelium was removed mechanically from arterial spiral preparations. The preparations were placed under 1 g tension in 5 ml organ baths containing modified Krebs-Henseleit solution (composition in mM: NaCl 115.0, KCl 4.7, $CaCl_2$ 2.5, $MgCl_2$-$6H_2O$ 1.2, KH_2PO_4 1.2, $NaHCO_3$ 25.0 and glucose 5.6) maintained at 37°C and gassed with 95% O_2 and 5% CO_2. Functional responses were recorded isometrically and displayed on a multi-channel polygraph. The arteries were exposed to 50 mM KCl 1 h after equilibration. Contractile responses to ET-1 and S6c are expressed as percentages of the reference contractions. Tissues were treated with BQ-788, BQ-123 or 0.1% dimethylsulphoxide DMSO (as a vehicle) and 20 min later, ET-1 or S6c were added to the baths.

For receptor binding experiments, the pulmonary arterial segments were homogenized and the microsome fractions (the fraction between 10,000 *g* and 90,000 *g*) were collected. The membrane preparations were incubated at 25°C with 10 pM [^{125}I]-ET-1 in the presence or absence of BQ-123 and BQ-788 in 50 mM Tris HCl buffer. Four hours later, the incubation solutions were rapidly filtered through Whatman GF/C glass fibre filters. The filters were washed with 5 mM HEPES/Tris buffer and counted in a gamma counter. Non-specific binding was defined by adding 200 nM ET-1 to the assay mixture.

All data are given as mean ± s.e.mean. Statistical comparisons were made by one-way analysis of variance followed by the Neuman-Keuls test. ET-1 and S6c were purchased from Peptide Institute (Osaka, Japan). [^{125}I]-ET-1 (2000 Ci mmol^{-1}) was obtained from Amersham Japan (Tokyo). BQ-788 and BQ-123 were synthesized in our laboratory.

Results Our preliminary experiments demonstrated that 1 nM ET-1 and 1 nM S6c caused submaximal contractions in the rabbit isolated pulmonary artery (not shown). Neither the ET_A receptor antagonist, BQ-123 (10 μM), nor the ET_B receptor antagonist, BQ-788 (10 μM), inhibited the contractile response to 1 nM ET-1, while the combination of BQ-123 and BQ-788 completely inhibited the ET-1-induced contraction (Figure 1a). On the other hand, the S6c (1 nM)-induced contraction was completely inhibited by BQ-788, but not by BQ-123 (Figure 1b).

In receptor binding experiments, BQ-123 (1 μM) inhibited [^{125}I]-ET-1 binding to rabbit pulmonary arterial membranes

[1] Author for correspondence at: Department of Pharmacology, Tsukuba Research Institute, Banyu Pharmaceutical Co., Ltd., Tsukuba Techno-Park Oho, Okubo 3, Tsukuba, Ibaraki 300-33, Japan.

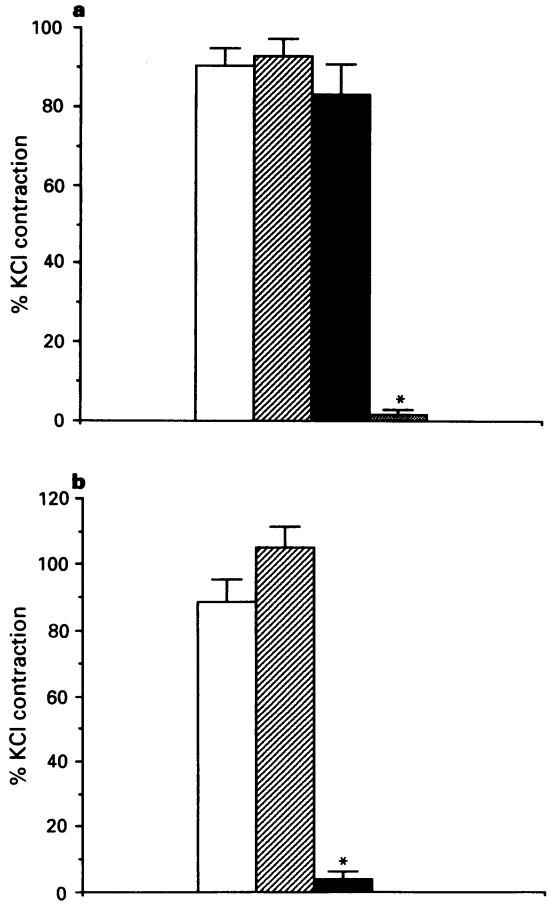


Figure 1 (a) Effect of 1 μM BQ-123 alone (hatched column, $n = 6$), 1 μM BQ-788 alone (solid column, $n = 7$) and combined treatment (stippled column, $n = 5$) on 1 nM ET-1-induced contraction in rabbit pulmonary artery. Vehicle control: open column, $n = 11$. (b) Effect of 1 μM BQ-123 alone (hatched column, $n = 7$) and 1 μM BQ-788 alone (solid column, $n = 8$) on 1 nM S6c-induced contraction in rabbit pulmonary artery. Vehicle control: open column, $n = 8$. Data are expressed as mean ± s.e.mean. $*P < 0.05$ when compared to vehicle control.

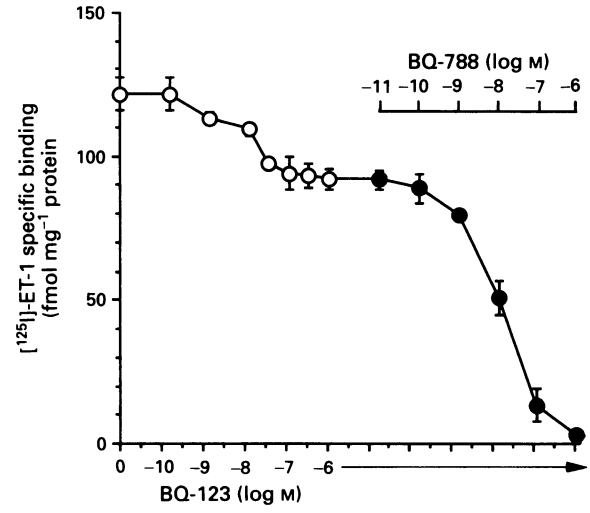


Figure 2 The effects of BQ-123 (0.1 nM to 1 μM, ○) and 1 μM BQ-123 plus BQ-788 (10 pM to 1 μM, ●) on [^{125}I]-ET-1 specific binding to rabbit pulmonary arterial membranes. Data are expressed as mean ± s.e.mean of three observations.

by approximately 20%, and additive treatment with BQ-788 (1 μM) completely inhibited the BQ-123-resistant component of [^{125}I]-ET-1 binding to the membranes (Figure 2).

Discussion In many vascular tissues, ET-1-induced contractions are mediated through ET_A receptors (Yanagisawa & Masaki, 1989). Recent studies using ET_A-selective antagonists including BQ-123 (Ihara *et al.*, 1992) have shown that ET_B receptors mediate ET-1-induced vasocontractions in some blood vessels (Fukuroda *et al.*, 1992; Sumner *et al.*, 1992). We previously reported that the ET-1-induced contraction of rabbit pulmonary artery was entirely resistant to BQ-123, suggesting that the response in this artery was mediated through ET_B receptors (Fukuroda *et al.*, 1994). However, the involvement of both ET_A and ET_B receptors in the ET-1-induced contraction of rabbit pulmonary artery was suggested by the antagonistic effects of BQ-123 in ET_B-desensitized preparations (LaDouceur *et al.*, 1993). In the present study, we examined the characteristics of the endothelin receptors mediating contraction of rabbit pulmonary artery by using BQ-123 or BQ-788, a novel ET_B-selective antagonist (Ishikawa *et al.*, 1994), or a combination of both antagonists. Neither BQ-123 alone nor BQ-788 alone inhibited the ET-1-induced contraction of rabbit pulmonary artery, whereas the combination of BQ-123 and BQ-788 completely inhibited the ET-1-induced contraction. Antagonism of ET_B receptors by 10 μM BQ-788 was confirmed by complete inhibition of the contractile response to S6c, an ET_B-selective agonist (Williams *et al.*, 1991). BQ-123 (10 μM) is known to inhibit completely the ET_A-mediated vasocontractions induced by 1 nM ET-1 (Ihara *et al.*, 1992). Thus, ET_A-selective and ET_B-selective antagonists, acting in a synergistic manner, inhibited ET-1-induced contraction of rabbit pulmonary artery. These results confirm the simultaneous involvement of ET_A and ET_B receptors in ET-1-induced contraction and suggest that the activation of either ET_A or ET_B receptors can signal the message that causes a vasocontraction with full activity in this tissue.

In the present study, the receptor binding experiments showed that there were no other endothelin receptor subtypes with the exception of BQ-123-sensitive ET_A and BQ-788-sensitive ET_B receptors. It appeared that the BQ-123-resistant component of [^{125}I]-ET-1 binding which had been observed previously (LaDouceur *et al.*, 1993; Fukuroda *et al.*, 1994) is due to ET_B receptors. This observation also indicated the simultaneous involvement of ET_A and ET_B receptors in the ET-1-induced contraction in this tissue. However, neither BQ-123 nor BQ-788 alone inhibited the ET-1-induced contraction of rabbit pulmonary artery and only the combination of both antagonists could inhibit it completely. Although the lack of effect of BQ-123 alone or BQ-788 alone on ET-1-induced contraction cannot be clearly explained at present, these results suggest that the full contractile response to ET-1 is induced by activation of either endothelin receptor subtype in this artery. Simultaneous blockade of both ET receptor subtypes is needed for the inhibition of some ET_A/ET_B-composite types of responses. Single or combined treatment with the two selective antagonists (BQ-123 and BQ-788) should be useful for characterizing ET receptor subtypes mediating responses to endothelins.

In summary, the present study clearly showed synergistic inhibition of ET-1-induced contraction of the rabbit pulmonary artery by BQ-123, an ET_A-selective antagonist, and BQ-788, an ET_B-selective antagonist. These observations demonstrated the coexistence of ET_A and ET_B receptors, and suggest that the activation of either ET_A or ET_B receptors exclusively can signal a message sufficient to cause full vasocontraction.

References

ARAI, H., HORI, S., ARAMORI, I., OHKUBO, H. & NANISHI, S. (1990). Cloning and expression of a cDNA encoding an endothelin receptor. *Nature*, **348**, 730–732.

FUKURODA, T., KOBAYASHI, M., OZAKI, S., YANO, M., MIYAUCHI, T., ONIZUKA, M, SUGISHITA, Y., GOTO, K. & NISHIKIBE, M. (1994). Endothelin receptor subtypes in human versus rabbit pulmonary arteries. *J. Appl. Physiol.*, **76**, 1976–1982.

FUKURODA, T., NISHIKIBE, M., OHTA, Y., IHARA, M., YANO, M., ISHIKAWA, K., FUKAMI, T. & IKEMOTO, F. (1992). Analysis of responses to endothelins in isolated porcine blood vessels by using a novel endothelin antagonist BQ-153. *Life Sci.*, **50**, PL107–PL112.

IHARA, M., NOGUCHI, K., SAEKI, T., FUKURODA, T., TSUCHIDA, S., KIMURA, S., FUKAMI, T., ISHIKAWA, K., NISHIKIBE, M. & YANO, M. (1992). Biological profiles of highly potent novel endothelin antagonists selective for the ETA receptor. *Life Sci.*, **50**, 247–255.

ISHIKAWA, K., IHARA, M., NOGUCHI, K., MASE, T., MINO, N., SAEKI, T., FUKURODA, T., FUKAMI, T., OZAKI, S., NAGASE, T., NISHIKIBE, M. & YANO, M. (1994). Biochemical and pharmacological profile of a potent and selective endothelin B-receptor antagonist, BQ-788. *Proc. Natl. Acad. Sci. U.S.A.*, **91**, 4892–4896.

LADOUCEUR, D.M., FLYNN, M.A., KEISER, J.A., REYNOLDS, E. & HALEEN, S.J. (1993). ET_A and ET_B receptors coexist on rabbit pulmonary artery vascular smooth muscle mediating contraction. *Biochem. Biophys. Res. Commun.*, **196**, 209–215.

SAKURAI, T., YANAGISAWA, M., TAKUWA, Y., MIYAZAKI, H., KIMURA, S., GOTO, K. & MASAKI, T. (1990). Cloning of a cDNA encoding a non-isopeptide-selective subtype of the endothelin receptor. *Nature*, **348**, 732–735.

SUMNER, M.J., CANNON, T.R., MUNDIN, J.W., WHITE, D.G. & WATTS, I.S. (1992). Endothelin ET_A and ET_B receptors mediate vascular smooth muscle contraction. *Br. J. Pharmacol.*, **107**, 858–860.

WILLIAMS, D.L., JONES, K.L., PETTIBONE, D.J., LIS, E.V. & CLINE-SCHMIDT, B.V. (1991). Sarafotoxin S6c: an agonist which distinguishes between endothelin receptor subtypes. *Biochem. Biophys. Res. Commun.*, **175**, 556–561.

YANAGISAWA, M. & MASAKI, T. (1989). Endothelin, a novel endothelium-derived peptide. Pharmacological activities regulation and possible roles in cardiovascular control. *Biochem. Pharmacol.*, **38**, 1877–1883.

(Received June 13, 1994
Accepted July 7, 1994)

Br. J. Pharmacol. (1994), **113**, 339–341

SPECIAL REPORT

© Macmillan Press Ltd., 1994

Cyclothiazide unmasks AMPA-evoked stimulation of [^{3}H]-L-glutamate release from rat hippocampal synaptosomes

Janine M. Barnes, Kumlesh K. Dev & [1]Jeremy M. Henley

Department of Pharmacology, Medical School, University of Birmingham, Edgbaston, Birmingham BH15 2TT

The effect of α-amino-3-hydroxy-5-methylisoxazolepropionate (AMPA) on Ca^{2+}-sensitive, tetrodotoxin (TTX)-insensitive K^+-stimulated [^{3}H]-L-glutamate release from rat hippocampal synaptosomes was determined. AMPA in the presence, but not in the absence of cyclothiazide, a drug which blocks AMPA receptor desensitization, elicited a dose-dependent increase in K^+-stimulated [^{3}H]-L-glutamate release but had no effect on basal release. The AMPA/cyclothiazide stimulation was blocked by CNQX and by GYKI 52466, an antagonist at the cyclothiazide site. These results indicate that AMPA receptors are present on presynaptic terminals and suggest that they may play a role in the regulation of neurotransmitter release.

Keywords: AMPA; GYKI; cyclothiazide; CNQX; synaptic plasticity; glutamate release; autoreceptors

Introduction Ionotropic glutamate receptors can be subdivided into N-methyl-D-aspartate (NMDA) and non-NMDA (kainate and α-amino-3-hydroxy-5-methylisoxazolepropionate (AMPA)) subtypes and, to date, at least seven separate cDNAs encoding non-NMDA receptor subunits have been cloned and characterized. Among these GluR1-GluR4 are proposed as the constituent subunits of functional AMPA receptors (Wenthold *et al.*, 1992).

AMPA receptors are important in a range of physiological (Barnes & Henley, 1992) and pathophysiological (Choi, 1992) processes including a long-term potentiation (LTP) in the rat hippocampus. LTP is of widespread interest since it has been proposed as an underlying molecular mechanism for learning and memory (Bliss & Collingridge, 1993). Nonetheless, while the involvement of postsynaptic AMPA receptors in LTP has been demonstrated (Bliss & Collingridge, 1993) the existence of presynaptic AMPA receptors has not been established. Here we present evidence for funtionally relevant AMPA receptors on the presynaptic terminals in the rat hippocampus which regulate the release of neurotransmitter.

Methods The hippocampil were dissected from two female Wistar rats (100–170 g) per experiment and synaptosomes were prepared as described previously (McMahon *et al.*, 1989). The synaptosomes were incubated in pre-gassed (O_2/CO_2; 95/5%) Krebs buffer (mM; NaCl 118.0, KCl 4.75, KH_2PO_4 1.2, $MgSO_4$ 1.2, $CaCl_2$ 2.5, $NaHCO_3$ 25.0, glucose 11.0) plus [^{3}H]-L-glutamate (25 nM; 50 Ci mmol^{-1}) at 37°C for 7 min. The uptake reaction was terminated by two washes in 10 volumes of ice-cold Krebs buffer and the washed [^{3}H]-L-glutamate-loaded synaptosomes were resuspended to 5 ml in fresh ice-cold Krebs.

Aliquots (0.1 ml) were added to 0.9 ml of either pre-warmed Krebs buffer, high K^+-Krebs buffer (containing an additional 20 mM KCl which gives approximately half-maximal stimulation of release) or Krebs buffer containing 50 μM 4-aminopyridine (4-AP) in the absence (control) or presence of drugs and incubated at 37°C for 2 min. Released [^{3}H]-L-glutamate was separated from synaptosomal [^{3}H]-L-glutamate by rapid filtration through GF/B filters followed by a 1 ml wash with ice-cold Krebs buffer. The data are expressed as percentage of control stimulated release as defined by the difference between the basal and K^+-stimulated [^{3}H]-L-glutamate release in the absence of drugs (100%).

[1] Author for correspondence.

Greater than 75% of the K^+-stimulated [^{3}H]-L-glutamate release was Ca^{2+}-dependent and K^+-stimulated release was not blocked by the voltage-sensitive Na^+ channel blocker tetrodotoxin (100 nM) indicating that release was from synaptosomes comprising presynaptic terminals. Analysis by high performance liquid chromatography (h.p.l.c.) confirmed that the tritium released was in the form of [^{3}H]-L-glutamate rather than any ^{3}H-labelled metabolic product (data not shown).

Results The pharmacological integrity of the synaptomes was confirmed using the previously characterized ability of carbachol to inhibit endogenous and exogenously applied neurotransmitter release (Marchi *et al.*, 1989) Consistent with those previous observations, in our assay system carbachol (100 μM) reduced K^+-stimulated release by 40% and that inhibition was completely inhibited by 0.1 μM atropine (Figure 1).

AMPA alone had no effect on stimulated release but in the presence of cyclothiazide AMPA potentiated K^+-stimulated but not basal [^{3}H]-L-glutamate release (Figure 2a) in a concentration-dependent manner (Figure 2b). The maximum

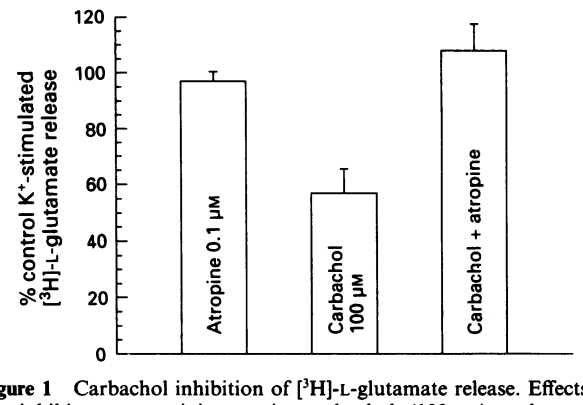


Figure 1 Carbachol inhibition of [^{3}H]-L-glutamate release. Effects of the inhibitory mucarinic agonist carbachol (100 μM) and specific antagonist atropine (0.1 μM) on 25 mM K^+-stimulated [^{3}H]-L-glutamate release. The data are the mean ± s.e.mean of 6–8 separate experiments each performed in triplicate. In normal Krebs buffer 100 μl aliquots of synaptosomes prepared as described in the Methods released ~10,000 d.p.m. into the supernatant during the 2 min time course of the experiment. In the presence, but not in the absence of $CaCl_2$, high K^+-Krebs resulted in 13,000–15,000 d.p.m. and 50 μM 4-AP resulted in ~15,000 d.p.m. of [^{3}H]-L-glutamate being released.

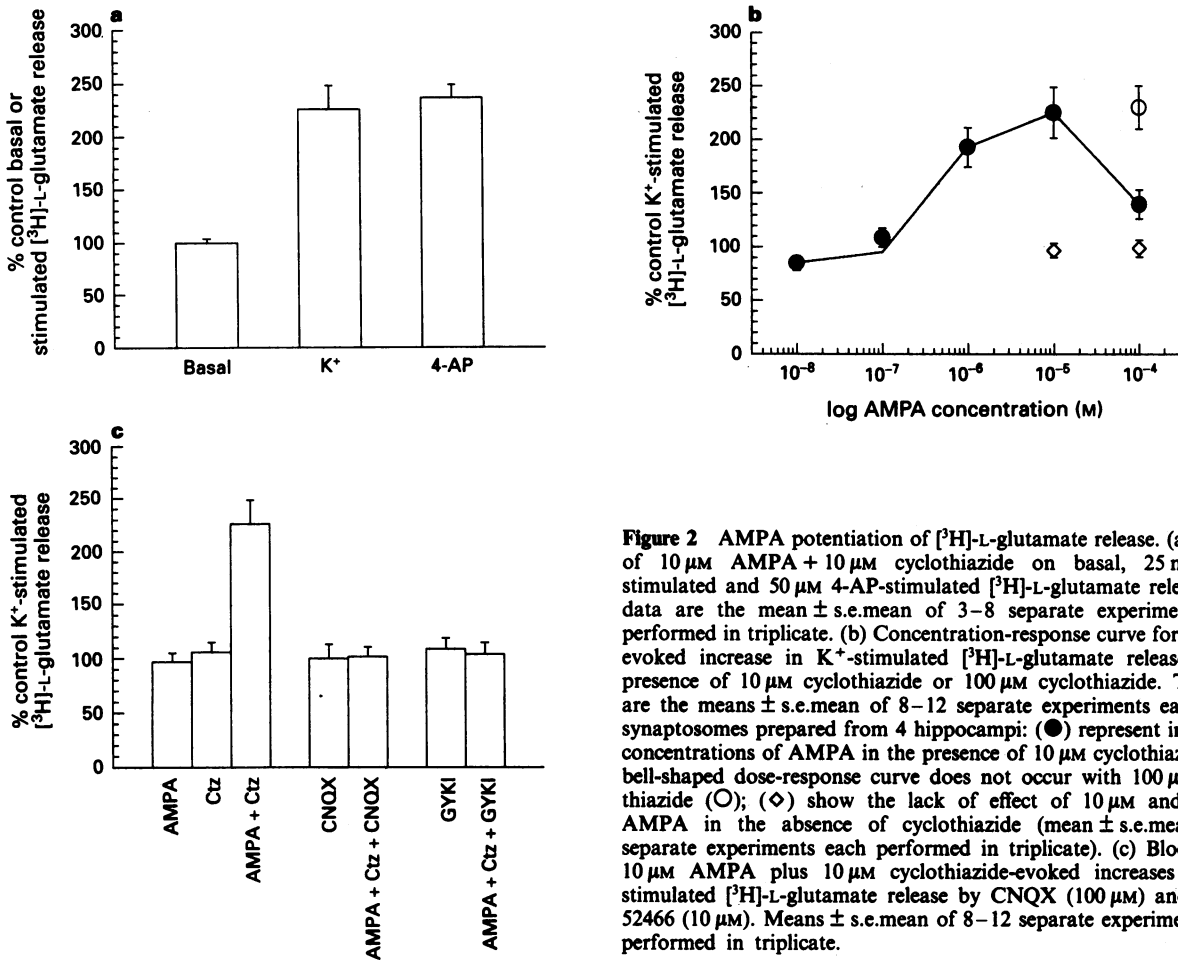


Figure 2 AMPA potentiation of [^{3}H]-L-glutamate release. (a) Effects of 10 μM AMPA + 10 μM cyclothiazide on basal, 25 mM K^+-stimulated and 50 μM 4-AP-stimulated [^{3}H]-L-glutamate release. The data are the mean ± s.e.mean of 3–8 separate experiments each performed in triplicate. (b) Concentration-response curve for AMPA-evoked increase in K^+-stimulated [^{3}H]-L-glutamate release in the presence of 10 μM cyclothiazide or 100 μM cyclothiazide. The data are the means ± s.e.mean of 8–12 separate experiments each using synaptosomes prepared from 4 hippocampi: (●) represent increasing concentrations of AMPA in the presence of 10 μM cyclothiazide. The bell-shaped dose-response curve does not occur with 100 μM cyclothiazide (○); (◇) show the lack of effect of 10 μM and 100 μM AMPA in the absence of cyclothiazide (mean ± s.e.mean of 4 separate experiments each performed in triplicate). (c) Blockade of 10 μM AMPA plus 10 μM cyclothiazide-evoked increases in K^+-stimulated [^{3}H]-L-glutamate release by CNQX (100 μM) and GYKI 52466 (10 μM). Means ± s.e.mean of 8–12 separate experiments each performed in triplicate.

increase in K^+-stimulated [^{3}H]-L-glutamate release was ~220% with an EC_{50} value of 0.3 μM. The AMPA/cyclothiazide response was blocked by CNQX (6-cyano-7-nitroquinoxaline-2,3-dione) and the 2,4-benzodiazepine GYKI 52466 (1-(4'amino-phenyl)-3-acethyl-4-methyl-3,4-dihydro-7,8-methylenedioxy-5H-2,3-benzodiazepine) (Figure 2c).

Discussion The bell-shaped dose-response for AMPA (Figure 2b) can be attributed to 10 μM cyclothiazide failing to block 100 μM AMPA-evoked receptor desensitization since the decrease does not occur with 100 μM cyclothiazide. Consistent with the results presented here, cyclothiazide potentiation of AMPA-induced [^{3}H]-noradrenaline release from rat hippocampal slices has also been observed recently but antagonism by GYKI 52466 was not reported (Desai *et al.*, 1994).

The AMPA/cyclothiazide reponse was inhibited by CNQX and GYKI 52466. CNQX is a well characterized competitive antagonist at the AMPA binding site (Barnes & Henley, 1992) whereas GYKI 52466 is a highly selective non-competitive antagonist of AMPA-evoked responses (Donevan & Rogawski, 1993) and excitotoxicity (Zorumski *et al.*, 1993) in rat CNS. The mechanism of inhibition by GYKI 52466 has been proposed as promoting the rate of desensitization of AMPA receptors by interaction at the cyclothiazide site. Thus GYKI 52466 is believed to be a competitive antagonist at the same allosteric site at which cyclothiazide is an agonist (Zorumski *et al.*, 1993).

The results presented here are relevant to the debate over possible presynaptic mechanisms for the induction and maintenance of LTP. While the molecular mechanisms regulating neurotransmitter release *in vivo* remain to be determined, our data indicate that activation of presynaptic AMPA receptors, under conditions where desensitization is prevented, can increase release. Furthermore, we demonstrate that the recently available compounds cyclothiazide and GYKI 52466 and their subsequent derivatives will provide invaluable tools to study the properties of pre- and post-synaptic AMPA receptors.

We are grateful to Dr D. Schoepp (Eli Lilley, Indianapolis) for cyclothiazide, Dr Istvan Tarnawa (IDR, Budapest) for GYKI 52466 and Dr Ewart Davies (Birmingham) for help with the h.p.l.c. Supported by MRC and Wellcome Trust grants to JMH. K.D. is an MRC-Novo Nordisk collaborative PhD scholar.

References

BARNES, J.M. & HENLEY, J.M. (1992). Molecular characteristics of excitatory amino acid receptors. *Prog. Neurobiol.*, **39**, 113–133.

BLISS, T.V.P. & COLLINGRIDGE, G.L. (1993). A synaptic model of memory: long-term potentiation in the hippocampus. *Nature*, **361**, 31–39.

CHOI, D.W. (1992). Excitotoxic cell death. *J. Neurobiol.*, **23**, 1261–1276.

DESAI, M.A., BURNETT, J.P. & SCHOEPP, D.D. (1994). Cyclothiazide selectively potentiates AMPA- and kainate- induced [^{3}H]-norepinephrine release from rat hippocampal slices. *J. Neurochem.*, **63**, 231–237.

DONEVAN, S.D. & ROGAWSKI, M.A. (1993). GYKI 52466, a 2,3-benzodiazepine, is a highly selective, noncompetitive antagonist of AMPA/Kainate receptor responses. *Neuron*, **10**, 51–59.

MARCHI, M., BOCCHIERI, P., GARBARINO, L. & RAITERI, M. (1989). Muscarinic inhibition of endogenous glutamate release from rat hippocampal synaptosomes. *Neurosci. Lett.*, **96**, 229–234.

MCMAHON, H.T., BARRIE, A.P., LOWE, M. & NICHOLLS, D.G. (1989). Glutamate release from guinea-pig synaptosomes: stimulation by reuptake-induced depolarisation. *J. Neurochem.*, **53**, 71–79.

WENTHOLD, R.J., YOKOTANI, N., DOI, K. & WADA, K. (1992). Immunochemical characterisation of the non-NMDA glutamate receptor using subunit specific antibodies. *J. Biol. Chem.*, **267**, 501–507.

ZORUMSKI, C.F., YAMADA, K.A., PRICE, M.T. & OLNEY, J.W. (1993). A benzodiazepine recognition site associated with the non-NMDA glutamate receptor. *Neuron.*, **10**, 61–67.

(Received June 30, 1994
Accepted July 18, 1994)

Br. J. Pharmacol. (1994), **113**, 342–344 © Macmillan Press Ltd, 1994

Sustained prejunctional facilitation of noradrenergic neurotransmission by adrenaline as a co-transmitter in the portal vein of freely moving rats

[1]R.P. Coppes, F. Brouwer, I. Freie, J. Smit & J. Zaagsma

Department of Medicinal Chemistry and Molecular Pharmacology, University of Groningen, Ant. Deusinglaan 2, 9713 AW Groningen, The Netherlands

1 The duration of the facilitatory effect of adrenaline on the electrically evoked overflow of noradrenaline was studied in the portal vein of permanently adreno-demedullated freely moving rats.

2 Rats were infused with adrenaline (20 or 100 ng min^{-1}) for 2 h. After an interval of 1 h, when plasma adrenaline had returned to undetectable levels, electrical stimulation resulted in an enhanced catecholamine overflow amounting to 219% (noradrenaline) and 241% (noradrenaline plus adrenaline) of control (saline infusion), respectively.

3 When stimulation was applied again, in the same animal, at 24, 48 and 72 h after the first stimulation episode, the evoked noradrenaline overflow was 150, 111 and 102% (after 20 ng ml^{-1} adrenaline) and 158, 134 and 105% (after 100 ng min^{-1} adrenaline) of control.

4 The β_2-adrenoceptor antagonist, ICI 118,551 (0.3 mg kg^{-1}), blocked the facilitatory effect obtained after the 100 ng min^{-1} adrenaline infusion on all days.

5 The results show that adrenaline, after being taken up by and released from sympathetic nerve terminals, is able to facilitate the evoked noradrenaline overflow through activation of prejunctional β_2-adrenoceptors for at least 48 h after administration.

Keywords: Catecholamine overflow; adrenaline; prejunctional β_2-adrenoceptors; sustained facilitation; portal vein; freely moving rats

Introduction

Prejunctional β_2-adrenoceptors, facilitating noradrenaline release from sympathetic varicosities, are thought to be activated *in vivo* by circulating adrenaline and/or by adrenaline taken up by and released from the nerve terminals as a co-transmitter (Rand *et al.*, 1979; Majewski *et al.*, 1981). Using permanently instrumented freely moving adreno-demedullated rats, we have recently found that the latter process has a major significance. Infusion of adrenaline, 100 ng min^{-1} for 2 h, followed by an interval of 1 h, during which plasma adrenaline had returned to pre-infusion undetectable levels, strongly potentiated electrically evoked noradrenaline overflow from the portal vein sympathetic nerves; at the same time adrenaline was released as well (Coppes *et al.*, 1993). It is known that the half-life of adrenaline, which in plasma is less than 30 s (Ferreira & Vane, 1967), is greatly enhanced once it is taken up by sympathetic nerves and Majewski *et al.* (1981) have found [^{3}H]-adrenaline release from rat atria *in vitro* up to 24 h after administration of the radiolabelled catecholamine *in vivo*.

These data induced us to investigate in a new series of experiments the duration of the facilitatory effect of adrenaline on evoked catecholamine overflow from the portal vein nervous plexus *in vivo* after preloading the animals with two different concentrations of adrenaline (20 and 100 ng min^{-1} for 2 h). As before, adreno-demedullated rats were used to prevent interference by adrenaline released from the adrenal medulla.

Methods

Male Wistar rats, weighing 270–350 g, underwent surgical bilateral adreno-demedullation under ether anaesthesia. Two weeks recovery was allowed for adrenocortical regeneration, during which the animal had free access to 0.9% NaCl in addition to normal drinking water, but they hardly used saline. Subsequently, the rats were provided with a sample and an infusion cannula in the portal vein together with a bipolar stimulation electrode as described (Remie *et al.*, 1988; Coppes *et al.*, 1993). Cannulae and electrode wires were run subcutaneously to emerge at the crown of the head where they were fixed. Experiments started approximately 10 days after instrumentation when animals had completely regained their preoperative weight.

(−)-Adrenaline (20 ng min^{-1} or 100 ng min^{-1} in saline containing 0.05% ascorbic acid) or saline (containing 0.05% ascorbic acid) was infused for 2 h (1.2 ml h^{-1}). Sixty minutes after the end of the infusion, electrical stimulation (2 Hz, 3 ms, 5 mA, biphasic pulses) was started ($t = 0$ min). The stimulation lasted for 2 min. Blood samples were drawn at $t = -10$ min, $t = 0$ min, every 15 s during and 1 min after stimulation. Electrical stimulation and blood sampling were repeated 24, 48 and 72 h after the first stimulation episode. ICI 118,551 (0.3 mg kg^{-1}) or saline (1 ml kg^{-1}) was injected at $t = -10$ min, just after the first blood sample was taken. A transfusion of 200 µl of heparinized donor blood, obtained from adreno-demedullated donor rats, was given after each blood sample but not during the stimulation period since sampling time did not allow this. After stimulation, the total amount of blood sampled during stimulation was replaced. Each animal was subjected to all four subsequent stimulation episodes after which at least 1 week of rest was allowed; then another set of experiments was performed. The animals were used up to 6 weeks after operation.

Plasma catecholamines were determined by high performance liquid chromatography with electrochemical detection (Remie *et al.*, 1988, slightly modified by Coppes *et al.*, 1993).

Data analysis

The increase in plasma catecholamines during stimulation was expressed as area under the curve (AUC), calculated by

[1] Author for correspondence.

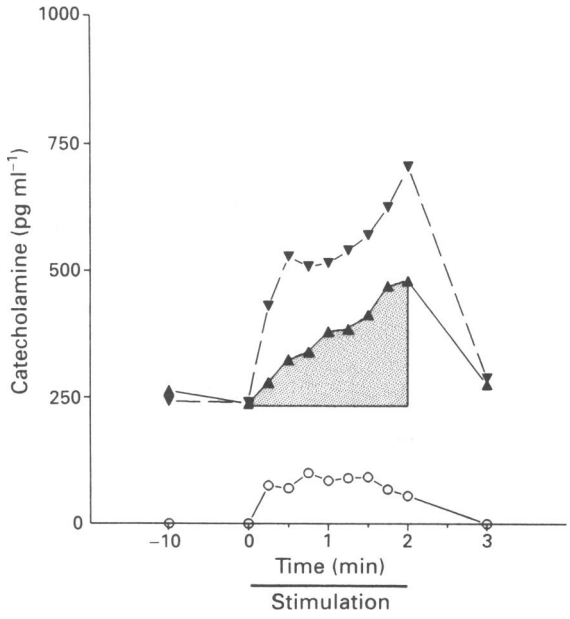


Figure 1 Typical experiment showing the effect of adrenaline infusion (100 ng min^{-1} for 2 h) followed by an interval of 1 h, on the electrically (2 Hz, 3 ms, 5 mA) evoked noradrenaline (▼) and adrenaline (○) overflow as compared to control noradrenaline overflow after saline infusion (▲). The area under the curve (stippled area) represents the control overflow of noradrenaline from the portal vein nervous plexus during the 2 min stimulation period.

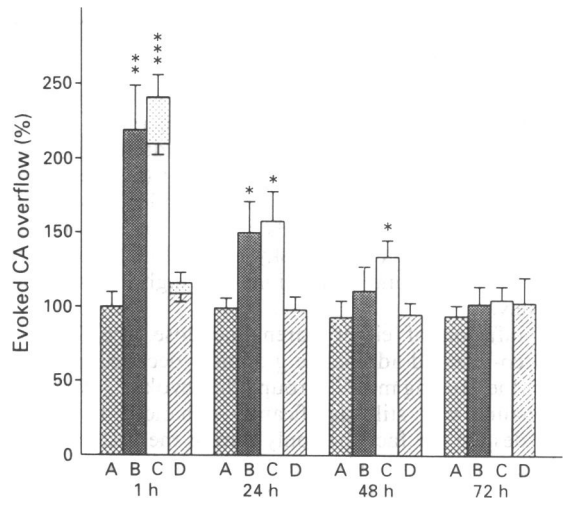


Figure 2 Development with time of the evoked catecholamine (CA, noradrenaline + adrenaline) overflow after a single saline or adrenaline infusion (20 ng min^{-1} and 100 ng min^{-1} for 2 h on the first day) during four subsequent days. Results are presented as % of the control area under the curve (saline infusion) on the first day (60 min after termination of infusion, indicated as 1 h) which was set at 100%. Crossed hatched columns (A), control ($n = 6$); grey columns (B), 20 ng min^{-1} adrenaline infusion ($n = 5$); open columns (C), 100 ng min^{-1} adrenaline infusion ($n = 7$); hatched columns (D), 100 ng min^{-1} adrenaline infusion followed by ICI 118,551 (0.3 mg kg^{-1}, $n = 5$); stippled areas, evoked adrenaline overflow. ***$P <$ 0.001, **$P < 0.01$, *$P < 0.05$ compared to controls on the same day.

trapezoid integration as described by Remie *et al.* (1988), and was compared to control stimulation (saline infusion in the absence of drugs) which was set at 100% (see Figure 1). Results are expressed as means ± s.e.mean. Statistical significance was analysed by Student's *t* test for unpaired data. *P* values of less than 0.05 were regarded as being significant.

Drugs

(−)-Adrenaline bitartrate (Sigma, St Louis, U.S.A.); ICI 118,551 ((±)-1-[(2,3-dihydro-7-methyl-1H-inden-4-yl)oxy]-3-[(1-methylethyl)amino]-2-butanol hydrochloride) was a kind gift from ICI (Macclesfield, UK). All drugs were dissolved in sterile saline. The dose of adrenaline refers to the base, the dose of ICI 118,551 to the salt.

Results

The basal adrenaline concentration ($t = 0$ min) in the portal plasma of the demedullated rats was below the limit of detection (< 10 pg ml^{-1}). Adrenaline reached levels of 750–1000 pg ml^{-1} during the 20 ng min^{-1} adrenaline infusion, and 3500–4000 pg ml^{-1} during the 100 ng min^{-1} infusion. After termination of the infusion, plasma adrenaline levels had returned to zero (undetectable) at 10 min prior to the first electrical stimulation. Basal noradrenaline levels (at $t = 0$ min, 239 ± 22 pg ml^{-1}; $n = 6$; 1 h after saline infusion) did not change during the subsequent days and were not changed by pre-infusion of adrenaline. ICI 118,551 (0.3 mg kg^{-1}) did not change the basal plasma noradrenaline concentration either (data not shown).

One hour after saline infusion, plasma noradrenaline levels increased to reach a maximum at $t = 2$ min during electrical stimulation for 2 min (Figure 1). The control AUC amounted to 5262 ± 421 pg 2 min^{-1} (100 ± 8%, $n = 6$). One hour following the 20 ng min^{-1} adrenaline infusion, plasma adrenaline could not be detected during stimulation, but the noradrenaline overflow (AUC) was significantly increased to 219% as compared to saline infusion ($n = 5$; $P < 0.01$; Figure 2). One hour after the 100 ng min^{-1} adrenaline infusion, an adrenaline concentration of up to 150 pg ml^{-1} was detected during stimulation (Figure 1). The combined areas under the curve of noradrenaline and adrenaline overflow were significantly increased to 241% ($n = 7$; $P < 0.001$) of which 32% was adrenaline (Figure 2).

After saline infusion on day 1 the electrically evoked noradrenaline overflow measured after 24, 48 and 72 h was not significantly different from the first stimulation period (Figure 2).

In the 20 ng min^{-1} and 100 ng min^{-1} adrenaline animals, electrically evoked overflow after 24 h was still significantly enhanced to 150% ($n = 5$; $P < 0.05$) and 158% ($n = 5$; $P < 0.05$), respectively. However, adrenaline was no longer detected during stimulation. After 48 h, evoked noradrenaline overflow was slightly but not significantly elevated in 20 ng min^{-1} adrenaline infused animals, whereas in the 100 ng min^{-1} adrenaline preloaded animals the AUC was still significantly elevated to 134% ($n = 7$; $P < 0.05$) (Figure 2), again without measurable adrenaline release. After 72 h, evoked noradrenaline overflow was similar in all animal groups.

ICI 118,551 (0.3 mg kg^{-1}), when given 10 min prior to electrical stimulation of animals preloaded with adrenaline, prevented the potentiation of noradrenaline overflow both immediately and after 24 and 48 h (Figure 2). The evoked adrenaline overflow 1 h after termination of the 100 ng min^{-1} adrenaline infusion was also inhibited by ICI 118,551 (Figure 2).

Discussion

Using permanently instrumented freely moving adrenodemedullated rats we have recently found that exogenously applied adrenaline, given by infusion of 100 ng min^{-1} for 2 h in the portal vein, is taken up by sympathetic nerve terminals through cocaine-sensitive carriers. During electrical stimulation adrenaline is co-released with noradrenaline and facili-

tates neurotransmitter overflow to about 200% of control through activation of pre-junctional β_2-adrenoceptors (Coppes *et al.*, 1993).

In the present study the duration of this effect was investigated, using both 20 ng min^{-1} and 100 ng min^{-1} infusions. During these infusions, portal plasma adrenaline reached levels of 750–1000 and 3500–4000 pg ml^{-1} (i.e. about 5 and 20 nM), respectively. Since physical immobilization stress increases plasma adrenaline levels in rats to 11.4 pmol ml^{-1} (about 2000 pg ml^{-1}) (Kvetnansky *et al.*, 1992), these conditions would correspond to medium and high levels of stress, respectively.

After infusion of either adrenaline dose, the facilitatory effect of co-released adrenaline gradually declined in time. At 48 h in the 100 ng min^{-1} group the evoked overflow of noradrenaline was still significantly enhanced to 134% of control, despite the fact that only during the first stimulation episode, performed 1 h after the infusion, but not at 24 h and later, some evoked adrenaline release could be measured. This indicates that uptake and breakdown strongly limit spillover into plasma, in agreement with findings in anaesthetized dogs that only 12% of adrenaline released from the cardiac sympathetic nerves escapes neuronal and extraneuronal uptake (Eisenhofer *et al.*, 1992). This is also illustrated by the 20 ng min^{-1} infusion experiments where no released adrenaline, although clearly capable of facilitating noradrenaline overflow, was detected in the plasma.

ICI 118,551 blocked the facilitation of noradrenaline overflow by co-released adrenaline at all time-points; moreover the electrically evoked adrenaline overflow, measured 1 h after preloading with 100 ng min^{-1}, was strongly inhibited by ICI 118,551 as well (Figure 2), indicating that also the adrenaline overflow is under facilitatory control of prejunctional β_2-adrenoceptors.

Adrenaline is assumed to play a role in the development of hypertension (for review see Floras, 1992). In man infusion of adrenaline (15 ng kg^{-1} min^{-1} for 6 h) amplified the blood pressure response to stress and exercise for at least 18 h after cessation of the infusion (Blankenstijn *et al.*, 1991). When spontaneously hypertensive rats (SHR) were adrenodemedullated at a prehypertensive age (4 weeks), the development of hypertension was attenuated but could be restored by implantation of adrenaline depots, and this pro-hypertensive effect of adrenaline was abolished by concomitant treatment with a β_2-adrenoceptor antagonist (Borkowski & Quinn, 1985; Borkowski, 1991). Furthermore, plasma levels of both adrenaline and noradrenaline are elevated in adult SHR (Remie *et al.*, 1992). It is very likely that the prolonged time during which adrenaline is released from sympathetic nerve endings and facilitates noradrenaline overflow through prejunctional β_2-adrenoceptors is a key factor in these processes.

We wish to thank Dr A.F. Roffel for valuable discussions on the manuscript.

References

BLANKENSTIJN, P.J., TULEN, J., MAN IN 'T VELD, A.J., BOOMSMA, F.& SCHALEKAMP, M.A.D.H. (1991). 'Stress' levels of adrenaline mediate a protracted amplification of the blood pressure response to sympathetic stimulation in man. *J. Hypertens.*, **9**, (Suppl 6), S76–S77.

BORKOWSKI, K.R. (1991). Effects of adrenal demedullation and adrenaline on hypertension development and vascular reactivity in young spontaneously hypertensive rats. *J. Auton. Pharmacol.*, **11**, 1–14.

BORKOWSKI, K.R. & QUINN, P. (1985). Adrenaline and the development of spontaneous hypertension in rats. *J. Auton. Pharmacol.*, **5**, 89–100.

COPPES, R.P., SMIT, J., NASHID KHALI, N., BROUWER, F. & ZAAGSMA, J. (1993). Strong activation of vascular prejunctional β_2-adrenoceptors in freely moving rats by adrenaline released as a co-transmitter. *Eur. J. Pharmacol.*, **243**, 273–279.

EISENHOFER, G., SMOLICH, J.J. & ESLER, M.D. (1992). Disposition of endogenous adrenaline compared to noradrenaline released by cardiac sympathetic nerves in the anaesthetized dog. *Naunyn-Schmied. Arch. Pharmacol.*, **345**, 160–171.

FERREIRA, S.H. & VANE, J.R. (1967). Half-lifes of peptide and amines in the circulation. *Nature*, **215**, 1237–1240.

FLORAS, J.S. (1992). Epinephrine and the genesis of hypertension. *Hypertension*, **19**, 1–18.

KVETNANSKY, R., GOLDSTEIN, D.S., WEISE, V.K., HOLMES, C., SZEMEREDI, K., BADGY, G. & KOPIN, I.J. (1992). Effects of handling or immobilization on plasma levels of 3,4-dihydroxyphenylalanine, catecholamines, and metabolites in rats. *J. Neurochem.*, **58**, 2296–2302.

MAJEWSKI, H., RAND, M.J. & TUNG, L.-H. (1981). Activation of prejunctional β-adrenoceptors in rat atria by adrenaline applied exogenously or released as a co-transmitter. *Br. J. Pharmacol.*, **73**, 669–679.

RAND, M., MAJEWSKI, H., MCCULLOCH, M.W. & STORY, D.F. (1979). An adrenaline-mediated positive feedback loop in the sympathetic transmission and its possible role in hypertension. In *Presynaptic Receptor*. ed. Langer, S.Z. & Dubocovich, M.L. pp. 263–269. Paris, Iuphar Satellite Meeting, Oxford, New York: Pergamon Press.

REMIE, R., KNOT, H.J., KOLKER, H.J. & ZAAGSMA, J. (1988). Pronounced facilitation of endogenous noradrenaline release by presynaptic β_2-adrenoceptors in the vasculature of freely moving rats. *Naunyn-Schmied. Arch. Pharmacol.*, **338**, 215–220.

REMIE, R., VAN ROSSUM, J.X.M., COPPES, R.P. & ZAAGSMA, J. (1992). Dysfunctional presynaptic α_2-adrenoceptors expose facilitatory β_2-adrenoceptors in the vasculature of spontaneously hypertensive rats. *Eur. J. Pharmacol.*, **211**, 257–261.

(Received December 14, 1993
Revised June 10, 1994
Accepted June 20, 1994)

Br. J. Pharmacol. (1994), **113**, 345–348 © Macmillan Press Ltd, 1994

NO-dependent and -independent elevation of plasma levels of insulin and glucose in rats by L-arginine

T. Jun & [1]Å. Wennmalm

Division of Clinical Physiology, Göteborg University, Sahlgrenska Hospital, S-413 45 Göteborg, Sweden

1 L-Arginine elevates plasma insulin in man. Recent *in vitro* data indicate that this is based on stimulation of endogenous nitric oxide (NO) with subsequent pancreatic release of insulin by L-arginine. L-Arginine also raises plasma glucose.

2 We studied plasma levels of insulin, glucose and NO metabolites, as well as systemic blood pressure, in anaesthetized rats during i.v. infusion of L-arginine (25–200 mg kg^{-1} min^{-1}) or glucose (55 mg kg^{-1} min^{-1}), before and after administration of the NO synthesis inhibitor, N^{ω}-nitro-L-arginine methyl ester (L-NAME, 50 mg kg^{-1}).

3 Before L-NAME, L-arginine elevated plasma insulin from about 15 to 65 u l^{-1} and glucose from 5.2 to 6.7 mmol l^{-1}. These effects of L-arginine were not dose-related.

4 L-NAME alone had no effect on plasma insulin and glucose levels, but diminished the effects of a low dose (25 mg kg^{-1} min^{-1}) of L-arginine on plasma insulin by about 40%, and that on plasma glucose by more than 90%. In contrast, the effects of a high dose (200 mg kg^{-1} min^{-1}) of L-arginine on plasma insulin and glucose levels were not affected by L-NAME.

5 L-NAME elevated systemic blood pressure by about 35 mmHg. L-Arginine (25–100 mg kg^{-1} min^{-1}) had no effect on systemic blood pressure, either before or after L-NAME. L-Arginine (200 mg kg^{-1} min^{-1}) lowered systemic blood pressure, both before and after L-NAME.

6 Glucose infusion elevated plasma glucose from about 5.5 to 6.8 mmol l^{-1}, and plasma insulin from about 18 to 26 u l^{-1}.

7 The basal plasma levels of the NO metabolite nitrate (18 ± 4 μmol l^{-1}) were not affected by L-arginine (200 mg kg^{-1} min^{-1}). Plasma nitrosohaemoglobin was likewise unaffected by L-arginine (200 mg kg^{-1} min^{-1}).

8 We conclude that L-arginine separately elevates plasma insulin and glucose levels, both by NO-dependent and -independent mechanisms.

Keywords: Anaesthetized rat; L-arginine; blood pressure; glucose; insulin; nitrate; nitric oxide

Introduction

Nitric oxide (NO), formerly known as endothelium-derived relaxing factor (EDRF; Furchgott & Zawadzki, 1980), is formed when the amino acid, L-arginine, enzymatically incorporates molecular oxygen and converts it to L-citrulline (Palmer *et al.*, 1988). NO is a biomediator with widespread biological actions in tissues (Moncada *et al.*, 1991).

L-Arginine, when given intravenously, stimulated insulin release in man (Floyd *et al.*, 1966); it also had a glucogenic action. The latter effect was, however, moderate and considered not responsible for the increase in plasma insulin (Floyd *et al.*, 1966).

Recently it was demonstrated that insulin release stimulated by L-arginine in the presence of D-glucose required an intact formation of nitric oxides (NOs) (Schmidt *et al.*, 1992). The assumption was based on evidence obtained in anaesthetized rats, isolated islets of Langerhans from rats, and a glucose-responsive clonal pancreatic β cell line (Schmidt *et al.*, 1992).

To explore further the possible role of endogenously formed NO in the release of insulin, we infused different doses of L-arginine in rats, before and following pretreatment with the NO synthase inhibitor, N^{ω}-nitro-L-arginine methyl ester (L-NAME). Plasma levels of insulin, glucose and nitrate (metabolite of NO) were followed at intervals and blood pressure was recorded continuously. The plasma insulin response to direct infusions of glucose was also assessed.

[1] Author for correspondence.

Methods

Experimental procedures

Male Wistar rats, weighing 200–250 g, were anaesthetized with sodium pentobarbitone (60 mg kg^{-1}, i.p.) and tracheotomized. A polyethylene catheter flushed with heparin was inserted into the right carotid artery, and connected via a pressure transducer (Harvard Apparatus, Millis, MA, U.S.A.) to a polygraph (Model 7D, Grass Instruments, Quincy, MA, U.S.A.) for continuous recording of systemic blood pressure. Heart rate was recorded from the blood pressure tracing. Another catheter was inserted into the right femoral vein, for administration of infusion solution or drug. A third catheter was inserted into the right femoral artery and used for blood sampling. After insertion of catheters the rats were allowed to stabilize for at least 10 min before the experiment was started.

Forty non-fasted rats, divided into four groups, were studied. One group was given L-arginine (free base, Sigma Chemial Co., St. Louis, MO, U.S.A.; 25, 100, or 200 mg kg^{-1} min^{-1}) at infusion rates of 0.1, 0.1 and 0.2 ml min^{-1}, respectively. The second group was pretreated with L-NAME (Sigma, 50 mg kg^{-1}, given i.v. during 5 min) 8–10 min prior to administration of L-arginine as above. Each rat was given one infusion only, and each infusion of L-arginine was maintained for 5 min. Blood samples for analysis of insulin and glucose were drawn before and at the end of the 5 min infusion of L-arginine. The third group was given glucose i.v. (55 mg kg^{-1} min^{-1}) for 5 min, and blood samples were taken as above. The fourth group was given L-arginine (200 mg kg^{-1} min^{-1}) as above, and blood samples were taken before

and at the end of the 5 min infusion of L-arginine for measurement of plasma nitrate. Blood pressure was recorded continuously in all groups throughout the experiments.

Analyses

Plasma insulin was measured by a clinical routine assay (Insulin radioimmunoassay kit, Pharmacia Diagnostics, Uppsala, Sweden). Plasma glucose was measured by an enzyme membrane analyser (Eppendorff).

Plasma nitrate was determined with a stable isotope ($Na^{15}NO_3$) dilution assay developed in our laboratory, utilizing positive ion/chemical ionization gas chromatography/mass spectrometry, after conversion of endogenous and labelled nitrate in the samples to nitrotoluene. The method has been described in detail elsewhere (Wennmalm *et al.*, 1993).

Analysis of nitroso-haemoglobin (HbNO) was performed as described previously (Wennmalm *et al.*, 1990). Samples of whole blood were rapidly centrifuged, followed by freezing of the cell fraction in quartz tubes in liquid nitrogen. Electron paramagnetic resonance (EPR) spectra of the samples were recorded at 77K in a Varian EPR spectrometer (Varian, Palo Alto, CA, U.S.A.) at a microwave frequency of 9.24 Hz and a microwave power of 10 mW. Spectra were scanned from 3.000 to 3.500 gauss with a modulation amplitude of 10 gauss and a scan rate of 25 gauss cm^{-1}.

Calculations

Differences between groups were analysed by Student's *t* test (two-tailed) for paired or unpaired observations, as appropriate. A *P* value <0.05 was considered significant. Data are presented as mean ± standard error (s.e.).

Results

Effect of L-arginine on plasma insulin and glucose, before and after L-NAME

The basal plasma levels of insulin and glucose in the anaesthetized rats, prior to infusion of L-arginine, were 14.6 ± 0.7 ($n = 15$) u l^{-1} and 5.24 ± 0.23 ($n = 15$) mmol l^{-1}, respectively.

Infusion of L-arginine (25 mg kg^{-1} min^{-1}) for 5 min increased plasma insulin to 31.4 ± 27 u l^{-1} ($P<0.001$; $n = 5$), and plasma glucose to 7.04 ± 0.10 mmol l^{-1} ($P<0.001$; $n = 5$). Infusion of L-arginine (100 mg kg^{-1} min^{-1}) for 5 min elevated plasma insulin to 65.3 ± 7.2 u l^{-1} ($P<0.01$; $n = 5$), and plasma glucose to 6.65 ± 0.11 ($P<0.001$; $n = 5$) mmol l^{-1}. L-Arginine (200 mg kg^{-1} min^{-1}) increased plasma insulin to 52.2 ± 3.1 u l^{-1} ($P<0.001$; $n = 5$), and plasma glucose to 6.58 ± 0.15 mmol l^{-1} ($P<0.001$; $n = 5$). The increases in plasma insulin and glucose levels are shown in Figure 1.

Pretreatment with L-NAME (50 mg kg^{-1}) did not affect the basal plasma concentrations of insulin or glucose, the levels reached after drug treatment being 13.9 ± 0.8 ($n = 15$) u l^{-1}, and 5.43 ± 0.12 ($n = 15$) mmol l^{-1}. The plasma insulin and glucose responses to infusion of L-arginine were, however, diminished. Following pretreatment with L-NAME, L-arginine (25 mg kg^{-1} min^{-1}) elevated plasma insulin to 23.0 ± 2.7 ($P<0.001$; $n = 5$) u l^{-1}. The difference in plasma insulin levels following infusion of L-arginine (25 mg kg^{-1} min^{-1}), before and after pretreatment with L-NAME, is of borderline significance ($P = 0.056$). Plasma glucose was not significantly affected by L-arginine (25 mg kg^{-1} min^{-1}) after pretreatment with L-NAME. The difference in plasma glucose levels following infusion of L-arginine (25 mg kg^{-1} min^{-1}), before and after pretreatment with L-NAME, is therefore highly significant ($P<0.001$).

The plasma insulin and glucose responses to L-arginine (100 mg kg^{-1} min^{-1}) were also diminished by L-NAME. Plasma insulin rose to 45.4 ± 3.6 ($P<0.01$; $n = 5$) u l^{-1}, and plasma glucose increased to 5.99 ± 0.18 ($P<0.01$; $n = 5$) mmol l^{-1}. Both the insulin and glucose levels following infusion of L-arginine (100 mg kg^{-1} min^{-1}) were lower ($P<0.05$ for both) after compared to before L-NAME. Infusion of L-arginine (200 mg kg^{-1} min^{-1}) increased plasma insulin to 51.3 ± 3.0 ($P<0.001$; $n = 5$) u l^{-1}, and plasma glucose to 6.51 ± 0.40 ($P<0.05$; $n = 5$) mmol l^{-1}. These levels do not differ from the plasma insulin and glucose levels obtained following infusion of L-arginine (200 mg kg^{-1} min^{-1}) in the absence of L-NAME.

The increases in plasma insulin and glucose levels in response to infusion of L-arginine (25–200 mg kg^{-1} min^{-1}) following pretreatment with L-NAME are shown in Figure 1.

Effect of L-arginine on systemic blood pressure before and after L-NAME

Basal heart rate and mean systemic blood pressure in the anaesthetized rats, prior to infusion of L-arginine, were 403 ± 10 ($n = 15$) beats min^{-1} and 111 ± 3 ($n = 15$) mmHg, respectively. Infusion of L-arginine (25 or 100 mg kg^{-1} min^{-1}) did not affect heart rate or systemic blood pressure, while L-arginine (200 mg kg^{-1} min^{-1}) lowered heart rate to 364 ± 11 ($P<0.05$; $n = 5$) beats min^{-1}, and systemic blood pressure to 70 ± 6 ($P<0.001$; $n = 5$) mmHg.

Infusion of L-NAME (50 mg kg^{-1} min^{-1}) decreased the heart rate to 348 ± 7 ($P<0.001$; $n = 15$) beats min^{-1}, and elevated systemic blood pressure to 140 ± 2 ($P<0.001$; $n = 15$) mmHg. Infusion of L-arginine (25 or 100 mg kg^{-1} min^{-1}) after pretreatment with L-NAME failed to affect heart rate or systemic blood pressure, while L-arginine (200 mg kg^{-1} min^{-1}) lowered heart rate to 324 ± 7 ($P<0.05$; $n = 5$) beats min^{-1}, and systemic blood pressure to 86 ± 9 ($P<0.01$, $n = 5$) mmHg.

Effect of infusion of glucose on plasma levels of insulin and glucose

Infusion of glucose (55 mg kg^{-1} min^{-1}) for 5 min elevated plasma insulin from 18.1 ± 0.8 ($n = 5$) IR u ml^{-1} to 26.2 ± 2.6 IR u ml^{-1} ($P<0.05$). In parallel, the plasma concentration of glucose rose, from 5.49 ± 0.17 ($n = 5$) to 6.82 ± 0.25 mmol l^{-1} ($P<0.01$). The plasma glucose and insulin levels

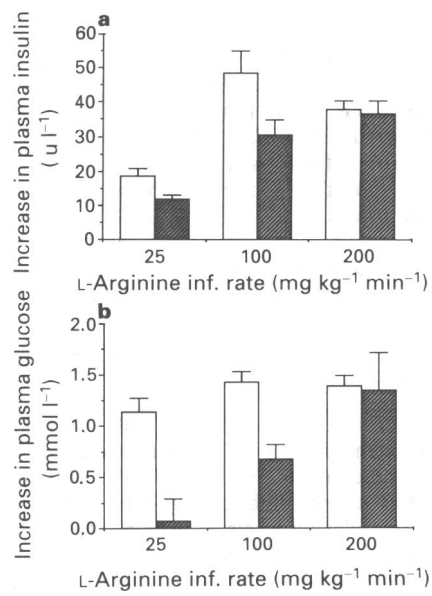


Figure 1 Increases in plasma insulin (a) and glucose (b) in rats after 5 min of infusion of L-arginine at the doses indicated. Open columns: no pretreatment. Hatched columns: animals pretreated with N^{ω}-nitro-L-arginine methyl ester (L-NAME, 50 mg kg^{-1}). Columns show mean with s.e. ($n = 5$).

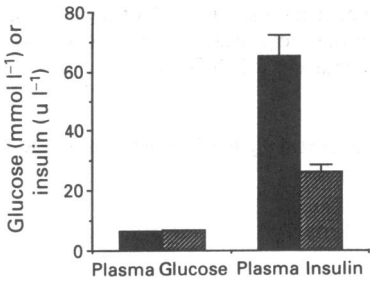


Figure 2 Increases in plasma glucose and insulin in rats after 5 min of infusion of L-arginine (100 mg kg^{-1} min^{-1}) or glucose (55 mg kg^{-1} min^{-1}). Solid columns: infusion of L-arginine. Hatched columns: infusion of glucose. Columns show mean with s.e. ($n = 5$).

after infusion of L-arginine (100 mg kg^{-1} min^{-1}) or of glucose (55 mg kg^{-1} min^{-1}) are shown in Figure 2. Glucose infusion did not affect the systemic blood pressure (120 ± 6 and 121 ± 7 mmHg before and after, respectively, the infusion).

Effect of L-arginine on plasma nitrate and red blood cell HbNO

The basal plasma level of nitrate was 18.3 ± 3.6 ($n = 5$) μmol l^{-1}. EPR spectrometry revealed no significant amounts of HbNO in the red blood cells. Following infusion of L-arginine (200 mg kg^{-1} min^{-1}) plasma nitrate was 16.9 ± 2.6 μmol min^{-1}. The difference compared to before infusion is not significant. EPR spectrometry did not display any significant effect of infusion of L-arginine on red blood cell levels of HbNO.

Discussion

Infusion of L-arginine (25–200 mg kg^{-1} min^{-1}) caused a marked increase in plasma insulin, and a moderate elevation of plasma glucose in the present study. Neither of these effects of L-arginine was dose-dependent. After administration of the NO synthase inhibitor, L-NAME, the effects of L-arginine (25–100 mg kg^{-1} min^{-1}) on plasma insulin and glucose were diminished, while the effect of L-arginine (200 mg kg^{-1} min^{-1}) was unaffected. Also, after L-NAME the effects of L-arginine on plasma insulin and glucose levels became dose-dependent. L-Arginine had no effects on plasma levels of NO metabolites, and failed to affect NO-dependent regulation of systemic blood pressure.

The presently observed effect of L-arginine (100 mg kg^{-1} min^{-1}) on plasma insulin concentration was more marked than that of L-arginine (25 mg kg^{-1} min^{-1}), suggesting a dose-dependence of the effect in the interval 25–100 mg kg^{-1} min^{-1}. However, at a dose of 200 mg kg^{-1} min^{-1}, the effect of L-arginine on plasma insulin dropped somewhat, in comparison to that obtained at 100 mg kg^{-1} min^{-1}. Schmidt *et al.* (1992) reported that in pancreatic β-cells with normal islet insulin secretory response, L-arginine elicited insulin release with an EC_{50} of 150 μM; above this concentration L-arginine was less effective. The present data are consistent with a similar type of dose-dependence *in vivo*. Hence, it appears that L-arginine also stimulates pancreatic secretion of insulin in intact animals.

In parallel to its stimulatory effect on insulin secretion, L-arginine elevated plasma glucose. This effect also failed to present any clear dose-dependence. L-Arginine is, like several other amino acids, glucogenic. The proposed mechanism is that L-arginine is converted to glutamate, which is transaminated to form alpha-glutarate and, after entering the citric acid cycle, is metabolised or increases the glucose level (Orten & Neuhaus, 1975). The parallel increases in insulin and glucose induced by L-arginine might be taken to indicate that the insulin response was secondary to the glucogenic effect of L-arginine. The experiments in which glucose was infused made it clear, however, that the increases in plasma glucose could not account solely for the elevation of plasma insulin. Infusion of glucose increased plasma glucose at least as much as L-arginine (100 mg kg^{-1} min^{-1}), but the resulting increase in plasma insulin was much smaller during the infusion of glucose than during infusion of L-arginine (100 mg kg^{-1} min^{-1}).

L-NAME is an efficient inhibitor of the constitutive NO synthase (Rees *et al.*, 1990). In accordance with previous observations (Gardiner *et al.*, 1990), administration of L-NAME (50 mg kg^{-1}) caused a marked increase in mean arterial blood pressure in the rats presently studied, indicating that endothelial NOS was inhibited. L-Arginine (25–100 mg kg^{-1} min^{-1}) was unable to lower the blood pressure after L-NAME, suggesting that the inhibition of NOS could not be reversed by a large increase in substrate availability. The highest dose of L-arginine (200 mg kg^{-1} min^{-1}) did lower the blood pressure quite substantially. However, we do not interpret this effect of the amino acid as based on an increased endothelial formation of NO. The reason for this is that a similar effect of L-arginine was observed also in the absence of L-NAME. The assumption of an unspecific, i.e. not related to NO formation, effect of L-arginine is further supported by observations that both L-arginine and D-arginine (the latter not being substrate for NO synthase) act as vasodilators in human superficial veins and resistance vessels *in vivo* (Calver *et al.*, 1991).

L-NAME did not affect the basal plasma levels of insulin or glucose, suggesting that the secretion of insulin and the regulation of glucose homeostasis in the basal state are not under influence of NO. However, after L-NAME the stimulatory effect of L-arginine on plasma insulin and glucose levels changed both qualitatively and quantitatively. The effect of L-arginine, both on plasma insulin and glucose levels, became clearly dose-related. The lowest dose of L-arginine, i.e. 25 mg kg^{-1} min^{-1}, was less potent in stimulating plasma insulin, and furthermore, was no longer able to elevate plasma glucose. In contrast, the highest dose of L-arginine, 200 mg kg^{-1} min^{-1}, was equally efficient in raising both plasma insulin and glucose levels before and after L-NAME.

The data available are not sufficient to interpret conclusively the mechanism behind the change in response pattern caused by L-NAME. One possibility would be that L-NAME did inhibit NOS at the sites of secretion of insulin and glucose, and that the remaining responses after NOS inhibition displayed effects of L-arginine on insulin and glucose secretion that are not NO-dependent. Another possibility would be that the NOS at the sites of insulin and glucose secretion had other kinetic properties than endothelial NOS (which was probably inhibited), and that the increasing doses of L-arginine given were able to break through progressively the inhibition caused by L-NAME. A third possibility would be that after L-NAME, the direct stimulatory effect of L-arginine on glucose secretion was sufficient to cause the observed elevation of plasma insulin. However, this alternative is not entirely likely inasmuch as plasma insulin, after L-NAME, was significantly increased by the lowest dose of L-arginine (25 mg kg^{-1} min^{-1}) while plasma glucose was not.

In addition to these alternative explanations, others must be considered as well. Despite the uncertainty in the interpretation of the results, the data obtained seem to merit the following conclusions. L-Arginine elevated plasma insulin and glucose by mechanisms that were independent of each other, i.e. the insulin response to L-arginine could not be entirely due to the glucogenic effect of the amino acid. Furthermore, both the insulin and glucose effects of L-arginine were partly blocked by L-NAME, indicating that NO formation participated to a certain extent both in the insulin and glucose secretory responses to L-arginine.

The extent to which the observed NO-dependent mechanisms for insulin and glucose secretion *in vivo* bear any relation to the impairment of glucose homeostasis in diabetes requires further studies. Infusion of L-arginine is a frequently used tool for stimulation of insulin secretion *in vivo*. The potentiating effect of arginine on the secretion of insulin in response to glucose is decreased in patients with non-insulin dependent diabetes mellitus (Ward *et al.*, 1984). The present data call for studies to reveal if such a decrease is related to an impaired formation of NO.

This study was supported by the Swedish Medical Research Council (project 4341).

References

CALVER, A., COLLIER, J. & VALLANCE, P. (1991). Dilator actions of arginine in human peripheral vasculature. *Clin. Sci.*, **81**, 695–700.

FLOYD, Jr., C.F., FAJANS, S.S., CONN, J.W., KNOPF, R.F. & RULL, J. (1966). Stimulation of insulin secretion by amino acids. *J. Clin. Invest.*, **45**, 1487–1502.

FURCHGOTT, R.F. & ZAWADZKI, J.V. (1980). The obligatory role of endothelial cells in the relaxation of arterial smooth muscle by acetylcholine. *Nature*, **288**, 373–376.

GARDINER, S.M., COMPTON, A.M., BENNET, T., PALMER, R.M.J. & MONCADA, S. (1990). Regional haemodynamic changes during oral ingestion of N^G-monomethyl-L-arginine or N^G-nitro-L-arginine methyl ester in conscious Brattleboro rats. *Br. J. Pharmacol.*, **101**, 10–12.

MONCADA, S., PALMER, R.M.J. & HIGGS, E.A. (1991). Nitric oxide: physiology, pathophysiology, and pharmacology. *Pharmacol. Rev.*, **43**, 109–142.

ORTEN, J.M. & NEUHAUS, O.W. (1975). Amino acid metabolism. In *Human Biochemistry*, pp. 293–355. St. Louis: C.V. Mosby Co.

PALMER, R.M.J., ASHTON, D.S. & MONCADA, S. (1988). Vascular endothelial cells synthesize nitric oxide from L-arginine. *Nature*, **333**, 664–666.

REES, D.D., PALMER, R.M.J., SCHULZ, R., HODSON, H.F. & MONCADA, S. (1990). Characterization of three inhibitors of endothelial nitric oxide synthase *in vitro* and *in vivo*. *Br. J. Pharmacol.*, **101**, 746–752.

SCHMIDT, H.H.H.W., WARNER, T.D., ISCHII, K., SHENG, H. & MURAD, F. (1992). Insulin secretion from pancreatic B cells caused by L-arginine-derived nitrogen oxides. *Science*, **255**, 721–723.

WARD, W.K., BOLGIANO, D.C., McKNIGHT, B., HALTER, J.B. & PORTE, Jr, D. (1984). Diminished B cell secretory capacity in patients with non-insulin-dependent diabetes mellitus. *J. Clin. Invest.*, **74**, 1318–1328.

WENNMALM, Å., BENTHIN, G., EDLUND, A., JUNGERSTEN, L., KIELER-JENSEN, S., LUNDIN, S., NATHORST WESTFELT, U., PETERSSON, A.-S. & WAAGSTEIN, F. (1993). Metabolism and excretion of nitric oxide in man. An experimental and clinical study. *Circ. Res.*, **73**, 1121–1127.

WENNMALM, Å., LANNE, B. & PETERSSON, A.-S. (1990). Detection of endothelial-derived relaxing factor in human plasma in the basal state and following ischemia using electron paramagnetic resonance spectrometry. *Anal. Biochem.*, **187**, 359–363.

(Received January 4, 1994
Revised March 21, 1994
Accepted April 26, 1994)

Br. J. Pharmacol. (1994), **113**, 349–354 © Macmillan Press Ltd, 1994

Blockade of P_{2X}-purinoceptors by trypan blue in rat vas deferens

[1]Ralph Bültmann, Marie Trendelenburg & Klaus Starke

Pharmakologisches Institut, Universität Freiburg, Hermann-Herder-Strasse 5, D-79104 Freiburg i.Br., Germany

1 The possibility of an antagonist effect of trypan blue at P_{2X}-purinoceptors was studied in rat vas deferens.

2 Trypan blue (3.2–320 μM) shifted the concentration-contraction response curve of α,β-methylene ATP (α,β-MeATP) to the right and simultaneously increased the maximum of the curve by up to 40%. The Schild plot had a slope not significantly different from unity and yielded a pA_2 value of 5.3 (K_B 4.9 μM).

3 Suramin (32 μM) also shifted the concentration-response curve of α,β-MeATP to the right, K_B 2.6 μM, and increased the maximum by 31%. In the presence of suramin (32 μM), trypan blue (32 μM) did not change the concentration-response curve of α,β-MeATP.

4 1-Amino-8-naphthol-3, 6-disulphonate (H-acid) 10 mM, the sulphonic acid-carrying moiety of trypan blue, shifted the concentration-response curve of α,β-MeATP to the right, K_B 1.4 mM, and increased the maximum by 33%.

5 Trypan blue did not change contractions elicited by high K^+ and noradrenaline.

6 Trypan blue attenuated the purinergic component of neurogenic contractions, IC_{50} 44.9 μM, but did not change the adrenergic component.

7 It is concluded that trypan blue blocks P_{2X}-purinoceptors in rat vas deferens. The increase of the maximum of the α,β-MeATP concentration-response curve is similar in mechanism to the increase produced by suramin.

Keywords: Rat vas deferens; trypan blue; suramin; α,β-methylene ATP; P_{2X}-purinoceptor; P_2-purinoceptor antagonists; co-transmission; purinergic transmission

Introduction

Reactive blue 2 (Kerr & Krantis, 1979) and suramin (Dunn & Blakeley, 1988) are perhaps the best characterized P_2-purinoceptor antagonists at present (see Cusack, 1993, for a review on purinoceptor classification). Reactive blue 2 is fairly selective for P_{2Y}-purinoceptors (see Kennedy, 1990), whereas suramin possesses similar affinity for several P_2 subtypes (see Cusack, 1993). Other substances have been tested only on a few preparations. Cibacron blue 3GA, an isomer of reactive blue 2, and brilliant blue G act as antagonists at the P_{2Z}-purinoceptors of rat parotid acinar cells (Soltoff *et al.*, 1989) and the P_{2Y}-like receptors on sympathetic nerve terminals (Fuder & Muth, 1993; von Kügelgen *et al.*, 1994). 4,4′-Diisothiocyanatostilbene-2,2′-disulphonate (DIDS) also blocks the rat parotid P_{2Z}-purinoceptor (McMillian *et al.*, 1988; Soltoff *et al.*, 1993) and in addition the P_{2X}-purinoceptor in rat vas deferens (Bültmann & Starke, 1994a). Pyridoxalphosphate-6-azophenyl-2′,4′-disulphonic acid (PPADS; Lambrecht *et al.*, 1992) and the 2′,5′-disulphonic acid isomer iso-PPADS block P_{2X}-purinoceptors in a variety of smooth muscle tissues (McLaren *et al.*, 1993; Ziganshin *et al.*, 1993; Bültmann & Starke, 1994b). Finally, we have recently shown that Evans blue is a P_{2X} antagonist in rat vas deferens (Bültmann & Starke, 1993).

Trypan blue, which like suramin was introduced as a trypanocide early in this century, differs from Evans blue in the position of the two sulphonic acid residues at the naphthalene rings. We examined whether trypan blue blocks P_{2X}-purinoceptors in rat vas deferens.

Methods

Male Wistar rats (240–300 g) were decapitated and the vasa deferentia removed and cleaned of adherent tissue. The medium used for incubation and superfusion contained (mM): NaCl 118, KCl 4.8, $CaCl_2$ 2.5, $MgSO_4$ 1.2, KH_2PO_4 0.9, $NaHCO_3$ 25, glucose 11, ascorbic acid 0.3 and disodium EDTA 0.03. It was saturated with 95% O_2/5% CO_2 and kept at 37°C.

Whole vasa deferentia or (in experiments with α,β-methylene ATP, α,β-MeATP) prostatic thirds were suspended vertically in a 5.7 ml organ bath. The lower end was fixed and the upper end attached to an isometric force transducer (K30, Hugo Sachs Elektronik, Hugstetten, Germany) under an initial tension of 9.8 mN (Graphtec thermal pen recorder, Ettlingen, Germany). The medium was replaced every 15 min. Tissues relaxed to about 3 mN during a 60 min equilibration period. This final resting tension remained constant for the remainder of the experiments.

Contractions were elicited by α,β-MeATP, high K^+, noradrenaline or electrical field stimulation. High K^+ was added as 35 mM KCl (final K^+ concentration therefore 40.7 mM) without osmotic compensation. Agonists and high K^+ were washed out immediately after contractions had peaked. Field stimulation (single pulses, 0.3 ms pulse width, 100 mA) was applied via platinum electrodes located at the top and the bottom of the organ bath (Stimulator II, Hugo Sachs Elektronik). Concentration-response data were analysed by logistic curve fitting to the weighted mean contraction values using equation No. 25 of Waud (1976) and non-linear regression. The calculation yielded the maximal effect and the EC_{50} or IC_{50} for each curve, EC_{50} or IC_{50} being the concentration producing 50% of the maximum of that curve.

Antagonist effects on concentration-response curves of α,β-MeATP and noradrenaline were examined as follows. Two concentration-response curves of the agonist were determined in each vas deferens, the first before, the second 60 min after addition of the antagonist or its solvent. The EC_{50} for each curve was obtained as mentioned. The shift caused by the antagonist was then quantified as the ratio 'EC_{50} in second

[1] Author for correspondence.

curve (with antagonist)' over 'EC_{50} in first curve (before antagonist)', corrected for the shift in solvent controls. Antagonist K_B values were calculated from the shifts either by means of the method of Arunlakshana & Schild (1959) or by means of equation No. 4 of Furchgott (1972). The procedure was analogous when the effect of trypan blue on the concentration-response curve of α,β-MeATP was studied in tissues exposed to suramin throughout the experiment.

α,β-Methylene ATP lithium salt (α,β-MeATP), trypan blue, (−)-noradrenaline bi-(+)-tartrate (Sigma, Deisenhofen, Ger-

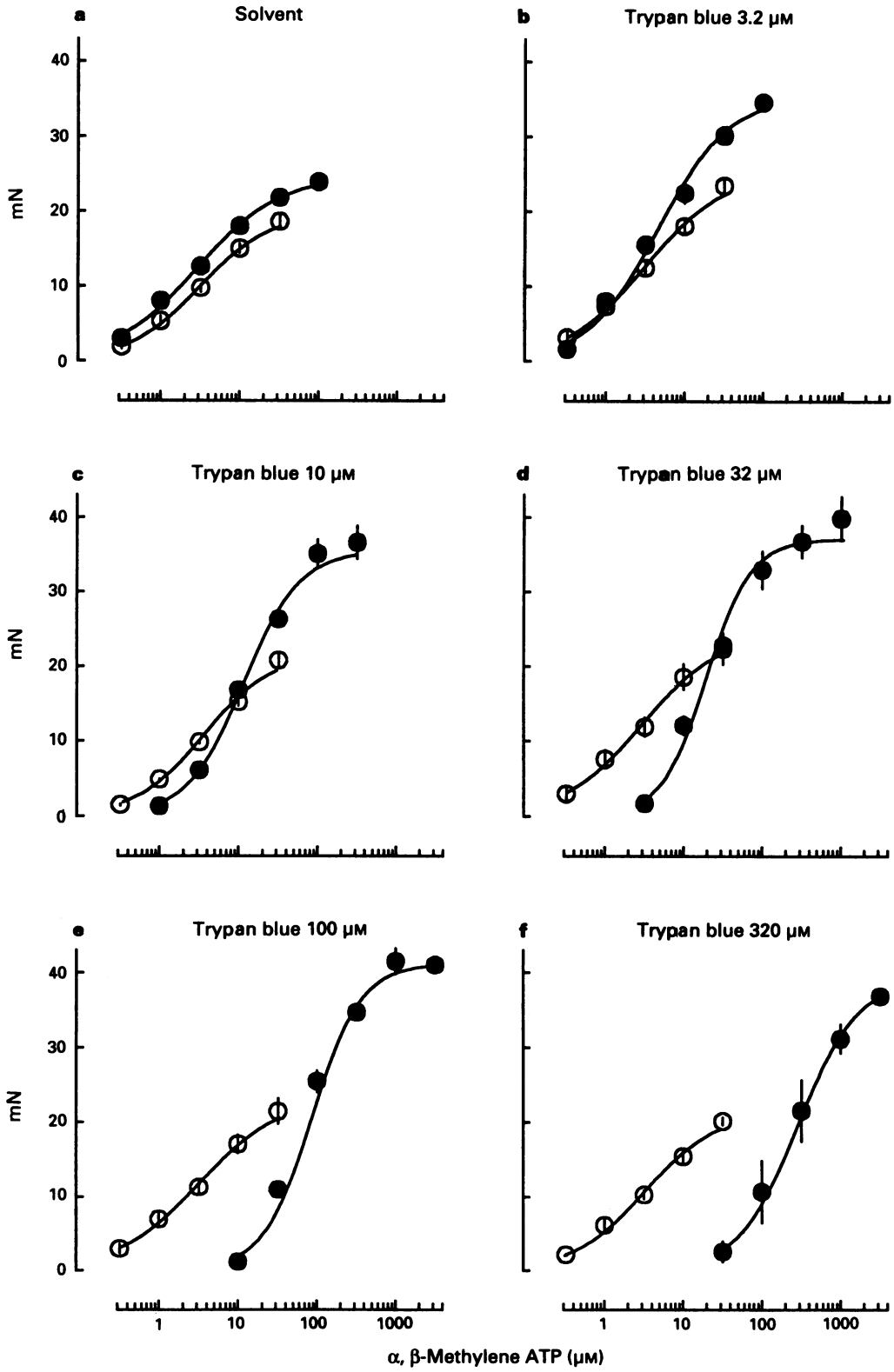


Figure 1 Effect of trypan blue on the concentration-response curve of α,β-methylene ATP. Increasing concentrations of α,β-methylene ATP were added every 30 min and washed out immediately after the contraction had peaked. Two concentration-response curves were determined in each tissue. Solvent (a) or trypan blue (b–f) was added to the medium after completion of the first curve (○) and the second curve was determined 60 min later (●). Abscissae, agonist concentration. Ordinates show contraction (mN). Means ± s.e.mean from 4 to 9 experiments.

many) and suramin (Bayer, Wuppertal, Germany) were dissolved in distilled water. KCl for high K^+ was dissolved in medium. 1-Amino-8-naphthol-3, 6-disulphonic acid monosodium salt (H-acid; Aldrich, Steinheim, Germany) was dissolved in medium with addition of the same molar amount of NaOH. Solutions of drugs were added to the organ bath in aliquots not exceeding 32 μl.

Data are expressed as either the arithmetic mean ± s.e. mean; or the EC_{50} or IC_{50} and maximal effect with the standard error as defined by Waud (1976) in the case of fitted curves; or the pA_2 with 95% confidence interval. Differences between means were tested for significance by the Mann-Whitney test. Differences between fitted curves were tested according to p. 371 of Motulsky & Ransnas (1987). $P<0.05$ was taken as the limit of statistical significance.

Results

In initial experiments, contractions were elicited by K^+ (35 mM), noradrenaline (30 μM) and α,β-MeATP (3 μM) in each single tissue, given at 5 min intervals and repeated after 70 and 140 min. Contractions were 14.1 ± 1.3, 10.9 ± 0.9 and 10.8 ± 0.6 mN, respectively, upon the first exposure ($n = 13$) and increased by 13 to 52% upon the second and third exposure 70 and 140 min later in solvent controls ($n = 6$). Compared with these controls, responses to high K^+ and noradrenaline were not changed 70 min after addition of trypan blue 100 μM, whereas responses to α,β-MeATP were greatly reduced (by 96 ± 2%; second exposure; $n = 7$; $P<0.005$). The response to α,β-MeATP recovered to control levels after 70 min of washout of trypan blue (third exposure; $n = 7$).

The effect of trypan blue on the concentration-response curve of α,β-MeATP was then determined. Increasing concentrations of α,β-MeATP elicited contractions with a maximum of 24.3 ± 1.7 mN and an EC_{50} of 4.2 ± 0.9 μM ($n = 37$; all first concentration-response curves pooled; open circles in Figures 1 and 3). A second curve after addition of solvent was very similar to the first one (solid circles in Figure 1a). Trypan blue (3.2–320 μM) caused two changes: it increased the maximal effect of α,β-MeATP, and it shifted the concentration-response curve progressively to the right (Figure 1b–f). The greatest increase of the maximum (by 40%) was obtained with trypan blue 100 μM. A plot according to Arunlakshana & Schild (1959) yielded a slope of 1.09, not significantly different from unity, and a pA_2 value of 5.31 (5.19 to 5.44, 95% confidence interval; K_B 4.9 μM). It should be noted, however, that the simultaneous increase of the maximum, here as well as in the cases of antagonism described below, leaves some doubt in the validity of the K_B calculations; the results obtained should be considered as 'apparent' K_B values.

Concentration-response curves of noradrenaline (0.1–1,000 μM) were also determined using the protocol of Figure 1. The EC_{50} was 6.7 ± 2.0 μM and the maximal contraction 22.3 ± 1.5 mN. Trypan blue (320 μM) changed neither the maximum nor the EC_{50} ($n = 4$ and 6 controls).

An increase of the maximum response to α,β-MeATP,

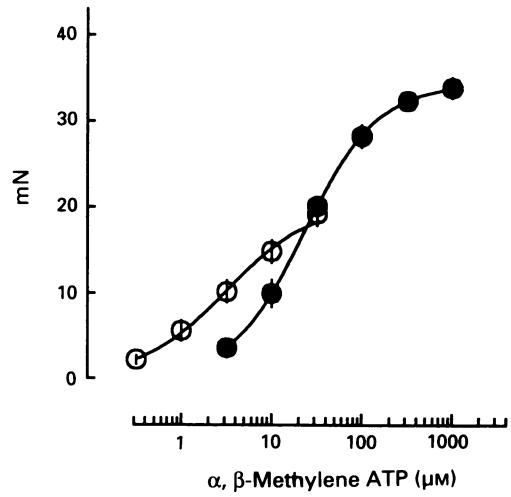


Figure 3 Effect of 1-amino-8-naphthol-3,6-disulphonic acid (H-acid) on the concentration-response curve of α,β-methylene ATP. Increasing concentrations of α,β-methylene ATP were added every 30 min and washed out immediately after the contraction had peaked. Two concentration-response curves were determined in each tissue. H-acid was added to the medium after completion of the first curve (○) and the second curve was determined 60 min later (●). Abscissae, agonist concentration. Ordinates show contraction (mN). Means ± s.e.mean from 4 experiments.

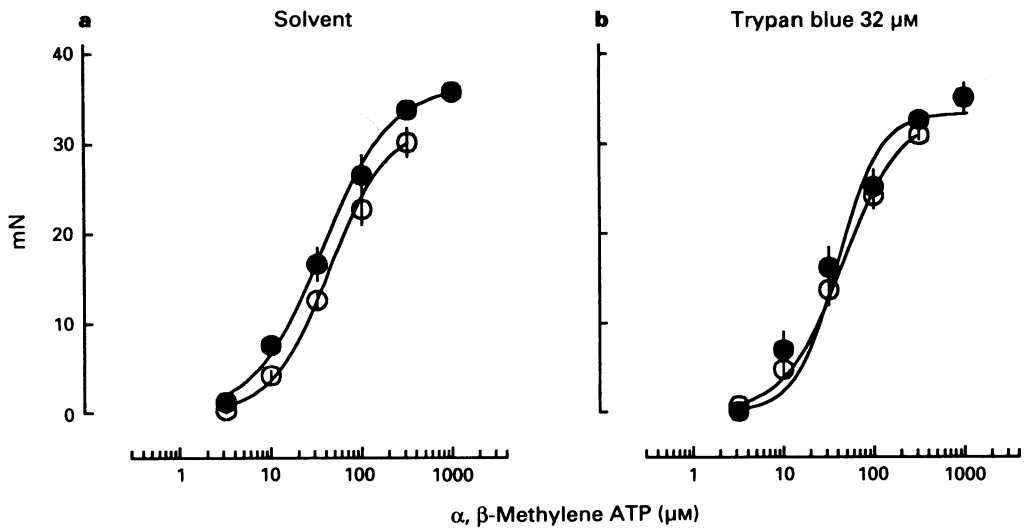


Figure 2 Effect of trypan blue on the concentration-response curve of α,β-methylene ATP in the presence of suramin. The medium contained suramin 32 μM from the beginning. Increasing concentrations of α,β-methylene ATP were added every 30 min and washed out immediately after the contraction had peaked. Two concentration-response curves were determined in each tissue. Solvent (a) or trypan blue 32 μM (b) was added to the medium after completion of the first curve (○) and the second curve was determined 60 min later (●). Abscissae, agonist concentration. Ordinates show contraction (mN). Means ± s.e.mean from 4 experiments each.

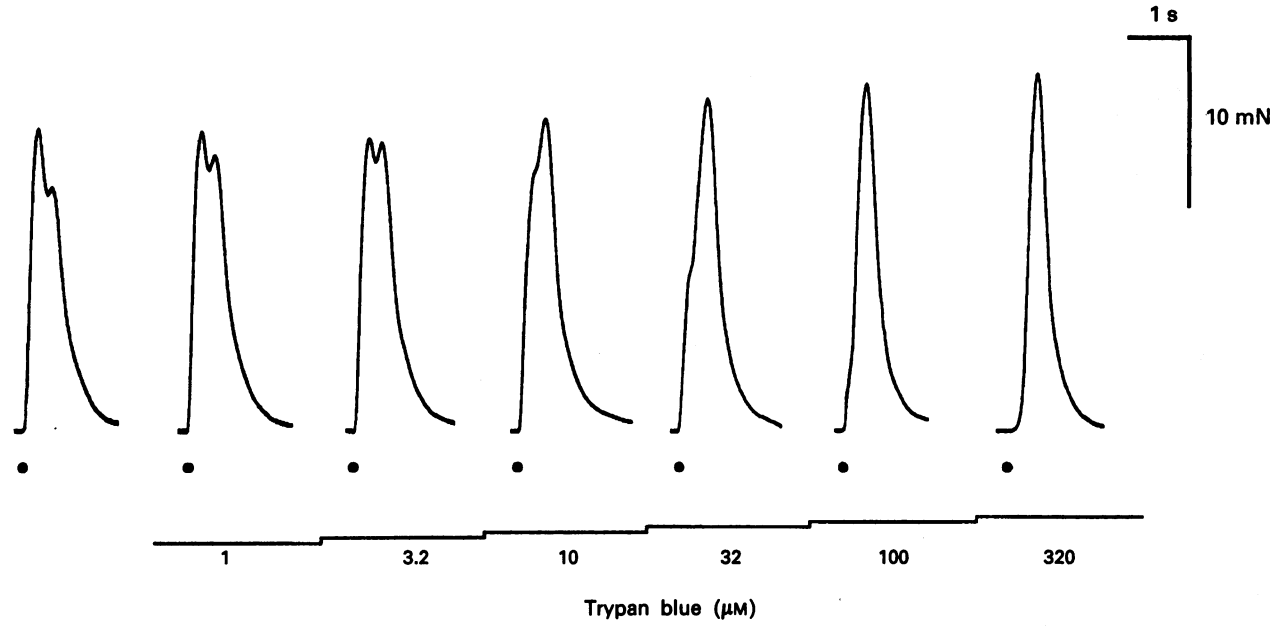


Figure 4 Effect of trypan blue on neurogenic contractions. Tissues were electrically stimulated by single pulses every 60 min (dots). Trypan blue was added at increasing concentrations immediately after the first and all following stimulations. Representative tracings from 5 experiments.

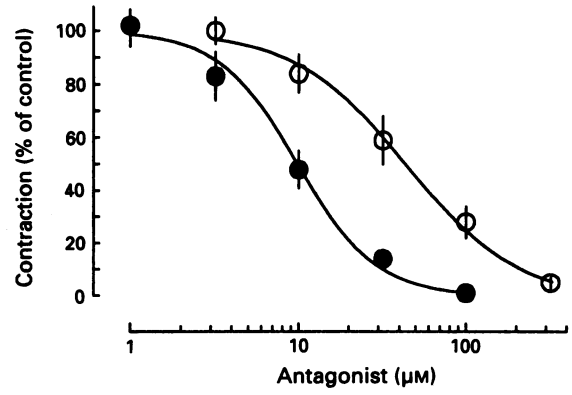


Figure 5 Effect of trypan blue and suramin on the purinergic component of neurogenic contractions. The medium contained prazosin 0.3 μM from the beginning. Tissues were electrically stimulated by single pulses every 60 min. Trypan blue (○) or suramin (●) was added at increasing concentrations immediately after the first and all following stimulations. Abscissae, antagonist concentration. Ordinates show contraction as a percentage of the first, pre-antagonist, contraction, corrected for any change observed in controls (solvent). Means ± s.e.mean from 4 to 5 experiments.

similar to that caused by trypan blue, has also been reported for suramin (e.g. von Kügelgen *et al.*, 1990). We studied the interaction of trypan blue with suramin in order to find out whether the mechanism might be the same. Suramin (32 μM) alone, when added like trypan blue in the experiments of Figure 1, shifted the concentration-response curve of α,β-MeATP to the right by a factor of 13 and increased the maximum by 31% ($n = 4$). A K_B value of 2.6 μM was calculated from the shift. In subsequent experiments, suramin 32 μM, 12.3 times K_B, was present from the beginning, i.e. 60 min before the first α,β-MeATP concentration-response curve, and either solvent or trypan blue 32 μM, 6.5 times K_B, was administered after the first curve. The maximal effect of α,β-MeATP was 31.9 ± 2.1 mN in the presence of suramin and the EC_{50} was 41.9 ± 8.1 μM (first concentration-response curves; $n = 8$; both values are higher than in the absence of suramin, $P < 0.005$). A second concentration-response curve in the presence of suramin alone, after addition of solvent, was very similar to the first one (solid circles in Figure 2a). When tested in the presence of suramin (32 μM), trypan blue (32 μM) failed to change the concentration-response curve of α,β-MeATP: the maximum was no longer increased, and the measured shift to the right, corrected for the solvent controls, was only 1.1 fold (compare Figure 2a and b).

1-Amino-8-naphthol-3, 6-disulphonate (H-acid) is the naphthalene derivative which in the trypan blue molecule carries the sulphonic acid residues. At a concentration of 10 mM, H-acid shifted the concentration-response curve of α,β-MeATP to the right and increased the maximum by 33% (Figure 3). From the shift to the right a K_B value of 1.4 mM was calculated.

Electrical stimulation of vasa deferentia with single pulses every 60 min elicited biphasic contractions (Figure 4) which remained approximately constant in solvent controls ($n = 5$). Trypan blue reduced the rapid purinergic phase in a concentration-dependent manner but did not alter the slow adrenergic phase (Figure 4). When the adrenergic phase was suppressed by prazosin 0.3 μM (Bültmann *et al.*, 1993), contractions became monophasic and amounted to 8.0 ± 0.6 mN (first contraction; $n = 15$). These purinergic responses again remained approximately constant upon repeated stimulation in solvent controls ($n = 6$). Trypan blue progressively reduced and eventually abolished the purinergic contractions (IC_{50} 44.9 ± 4.2 μM), as did suramin (IC_{50} 9.9 ± 1.3 μM; Figure 5).

Discussion

α,β-Methylene ATP (α,β-MeATP) elicits contraction of the rat vas deferens by activation of P_{2X}-purinoceptors (Bültmann & Starke, 1994b). Trypan blue reversibly inhibited these contractions. The lack of effect against noradrenaline and high K^+ indicates some degree of selectivity, although blockade of other P_2-purinoceptors (which also exist in rat vas deferens: Bültmann & Starke, 1994b) was not ruled out. The apparent affinity of trypan blue (K_B 4.9 μM) was slightly lower than that of suramin (K_B 2.6 μM; compare Hoyle *et al.*, 1990; Leff *et al.*, 1990; von Kügelgen *et al.*, 1990). The interaction of trypan blue with suramin (Figure 2) is in accord with an identical site of their antagonist action:

trypan blue, when given at 6.5 times its K_B, caused only a 1.1 fold, non-significant, shift of the concentration-response curve of α,β-MeATP beyond the shift caused by suramin alone, given at 12.3 times its K_B; from the law of mass action, the shift should be 1.5 fold, experimentally indistinguishable from the 1.1 found, if α,β-MeATP, suramin and trypan blue acted at the same site.

Trypan blue produced an additional change: it increased the maximum of the concentration-response curve of α,β-MeATP. The same was observed, and has previously been observed (Hoyle *et al.*, 1990; von Kügelgen *et al.*, 1990; Blakeley *et al.*, 1991; Mallard *et al.*, 1992; Trezise *et al.*, 1993; Venkova & Krier, 1993), for suramin. The potentiation by trypan blue of the maximal response to α,β-MeATP disappeared when suramin was present throughout, indicating that the potentiation mechanism was the same for both antagonists. Since suramin (Figures 5 and 6 of von Kügelgen *et al.*, 1990) and trypan blue enhanced the maximal effect of α,β-MeATP over the same range of concentrations that shifted the α,β-MeATP curve to the right, it seems possible that they produced enhancement of the maximum and antagonism against α,β-MeATP at the same site. For example, the antagonists might interfere with a process of fast desensitization limiting the contraction response to high agonist concentrations (von Kügelgen *et al.*, 1990). Another possibility is that suramin and trypan blue abolished an inherent relaxant effect of high concentrations of α,β-MeATP (von Kügelgen *et al.*, 1990), possibly mediated by P_{2Y}-purinoceptors (Blakeley *et al.*, 1991; see also Boland *et al.*, 1992).

Evans blue, previously shown to be a P_{2X} antagonist in rat vas deferens (Bültmann & Starke, 1993), differs chemically from trypan blue in the position of the two sulphonic acid residues at the terminal naphthalene rings. Pharmacologically, there were two differences. First, Schild analysis of the antagonism of Evans blue against α,β-MeATP yielded a slope different from unity. Second, Evans blue enhanced responses to noradrenaline and high K^+ in addition to enhancing the maximum of the α,β-MeATP concentration-response curve. The position of the sulphonic acid residues, hence, determines the mode of interaction with the P_{2X}-purinoceptor as well as the occurrence of non-specific effects.

The basic pharmacological properties of trypan blue (M_R 873) were retained in H-acid (M_R 319), the naphthalene moiety which carries the sulphonic acid residues and of which two occur per molecule of trypan blue. However, H-acid was about 300 fold less potent than trypan blue, indicating that the proper positioning of two naphthalene disulphonate groups in one molecule, connected by a central tolidine residue, greatly enhances the affinity for P_{2X}-purinoceptors.

Like suramin (Mallard *et al.*, 1992) and DIDS (Bültmann & Starke, 1994a), trypan blue also acted selectively against the components of neurogenic contractions in rat vas deferens: the purinergic, P_{2X}-receptor-mediated component of single pulse-evoked twitches was decreased, whereas the adrenergic component was unchanged, thus confirming noradrenaline-ATP co-transmission. The IC_{50} values of suramin (9.9 μM) and trypan blue (44.9 μM) were higher than their P_{2X}-purinoceptor K_B values (2.6 and 4.9 μM, respectively), possibly because very high concentrations of purinergic transmitter are generated upon single pulse stimulation in the vicinity of postjunctional P_{2X}-purinoceptors.

This study was supported by the Deutsche Forschungsgemeinschaft (SFB 325). We thank Bayer for suramin.

References

ARUNLAKSHANA, O. & SCHILD, H.O. (1959). Some quantitative uses of drug antagonists. *Br. J. Pharmacol. Chemother.*, **14**, 48–58.

BLAKELEY, A.G.H., BROCKBANK, J.E., KELLY, S.S. & PETERSEN, S.A. (1991). Effects of suramin on the concentration-response relationship of α,β-methylene ATP on the mouse vas deferens. *J. Auton. Pharmacol.*, **11**, 45–49.

BOLAND, P., HIMPENS, B., VINCENT, M.F., GILLIS, J.M. & CASTEELS, R. (1992). ATP activates P_{2x}-contracting and P_{2y}-relaxing purinoceptors in the smooth muscle of mouse vas deferens. *Br. J. Pharmacol.*, **107**, 1152–1158.

BÜLTMANN, R. & STARKE, K. (1993). Evans blue blocks P_{2X}-purinoceptors in rat vas deferens. *Naunyn-Schmied. Arch. Pharmacol.*, **348**, 684–687.

BÜLTMANN, R. & STARKE, K. (1994a). Blockade by 4,4'-diisothiocyanatostilbene-2,2'-disulphonate (DIDS) of P_{2X}-purinoceptors in rat vas deferens. *Br. J. Pharmacol.*, **112**, 650–654.

BÜLTMANN, R. & STARKE, K. (1994b). P_2-purinoceptor antagonists discriminate three contraction-mediating receptors for ATP in rat vas deferens. *Naunyn-Schmied. Arch. Pharmacol.*, **349**, 74–80.

BÜLTMANN, R., SZABO, B. & STARKE, K. (1993). Inhibition by ethanol of contractions of rat vas deferens: no evidence for selective blockade of P_{2X}-purinoceptors. *Naunyn-Schmied. Arch. Pharmacol.*, **347**, 527–533.

CUSACK, N.J. (1993). P_2 Receptor: subclassification and structure-activity relationships. *Drug Dev. Res.*, **28**, 244–252.

DUNN, P.M. & BLAKELY, A.G.H. (1988). Suramin: a reversible P_2-purinoceptor antagonist in the mouse vas deferens. *Br. J. Pharmacol.*, **93**, 243–245.

FUDER, H. & MUTH, U. (1993). ATP and endogenous agonists inhibit evoked [^{3}H]-noradrenaline release in rat iris via A_1 and P_{2y}-like purinoceptors. *Naunyn-Schmied. Arch. Pharmacol.*, **348**, 352–357.

FURCHGOTT, R.F. (1972). The classification of adrenoceptors (adrenergic receptors). An evaluation from the standpoint of receptor theory. In *Catecholamines. Handbook of Experimental Pharmacology*, vol 33. ed. Blaschko, H. & Muscholl, E. pp. 283–335. Berlin Heidelberg New York: Springer.

HOYLE, C.H.V., KNIGHT, G.E. & BURNSTOCK, G. (1990). Suramin antagonizes responses to P_2-purinoceptor agonists and purinergic nerve stimulation in the guinea-pig urinary bladder and taenia coli. *Br. J. Pharmacol.*, **99**, 617–621.

KENNEDY, C. (1990). P_1- and P_2-purinoceptor subtypes – an update. *Arch. Int. Pharmacodyn.*, **303**, 30–50.

KERR, D.I.B. & KRANTIS, A. (1979). A new class of ATP antagonist. *Proc. Austr. Physiol. Pharmacol. Soc.*, **10**, 156P.

LAMBRECHT, G., FRIEBE, T., GRIMM, U., WINDSCHEIF, U., BUNGARDT, E., HILDEBRANDT, C., BÄUMERT, H.G., SPATZ-KÜMBEL, G. & MUTSCHLER, E. (1992). PPADS, a novel functionally selective antagonist of P_2 purinoceptor-mediated responses. *Eur. J. Pharmacol.*, **217**, 217–219.

LEFF, P., WOOD, B.E. & O'CONNOR, S.E. (1990). Suramin is a slowly-equilibrating but competitive antagonist at P_{2X}-receptors in the rabbit isolated ear artery. *Br. J. Pharmacol.*, **101**, 645–649.

MALLARD, N., MARSHALL, R., SITHERS, A. & SPRIGGS, B. (1992). Suramin: a selective inhibitor of purinergic neurotransmission in rat isolated vas deferens. *Eur. J. Pharmacol.*, **220**, 1–10.

MCLAREN, G.J., SNEDDON, P., KENNEDY, C., LAMBRECHT, G., BURNSTOCK, G., MUTSCHLER, E., BAUMERT, H.G. & HOYLE, C.H.V. (1993). Investigation of a putative P_{2X}-purinoceptor antagonist in guinea-pig isolated vas deferens. *Br. J. Pharmacol.*, **109**, 109P.

MCMILLIAN, M.K., SOLTOFF, S.P., LECHLEITER, J.D., CANTLEY, L.C. & TALAMO, B.R. (1988). Extracellular ATP increases free cytosolic calcium in rat parotid acinar cells. *Biochem. J.*, **255**, 291–300.

MOTULSKY, H.J. & RANSNAS, L.A. (1987). Fitting curves to data using nonlinear regression: a practical and nonmathematical review. *FASEB J.*, **1**, 365–374.

SOLTOFF, S.P., MCMILLIAN, M.K. & TALAMO, B.R. (1989). Coomassie brilliant blue G is a more potent antagonist of P_2 purinergic responses than reactive blue 2 (cibacron blue 3GA) in rat parotid acinar cells. *Biochem. Biophys. Res. Commun.*, **165**, 1279–1285.

SOLTOFF, S.P., MCMILLIAN, M.K., TALAMO, B.R. & CANTLEY, L.C. (1993). Blockade of ATP binding site of P_2 purinoceptors in rat parotid acinar cells by isothiocyanate compounds. *Biochem. Pharmacol.*, **45**, 1936–1940.

TREZISE, D.J., KENNEDY, I. & HUMPHREY, P.P.A. (1993). Characterization of purinoceptors mediating depolarization of rat isolated vagus nerve. *Br. J. Pharmacol.*, **110**, 1055–1060.

VENKOVA, K. & KRIER, J. (1993). Stimulation of lumbar sympathetic nerves evokes contractions of cat colon circular muscle mediated by ATP and noradrenaline. *Br. J. Pharmacol.*, **110**, 1260–1270.

VON KÜGELGEN, I., BÜLTMANN, R. & STARKE, K. (1990). Interaction of adenine nucleotides, UTP and suramin in mouse vas deferens: suramin-sensitive and suramin-insensitive components in the contractile effect of ATP. *Naunyn-Schmied. Arch. Pharmacol.*, **342**, 198–205.

VON KÜGELGEN, I., KURZ, K. & STARKE, K. (1994). P_2-purinoceptor-mediated autoinhibition of sympathetic transmitter release in mouse and rat vas deferens. *Naunyn-Schmied. Arch. Pharmacol.*, **349**, 125–132.

WAUD, D.R. (1976). Analysis of dose-response relationships. In *Advances in General and Cellular Pharmacology*, vol. 1. ed. Narahashi, T. & Bianchi, C.P. pp. 145–178. London: Plenum.

ZIGANSHIN, A.U., HOYLE, C.H.V., BO, X., LAMBRECHT, G., MUTSCHLER, E., BÄUMERT, H.G. & BURNSTOCK, G. (1993). PPADS selectively antagonizes P_{2X}-purinoceptor-mediated responses in the rabbit urinary bladder. *Br. J. Pharmacol.*, **110**, 1491–1495.

(Received March 3, 1994
Revised April 27, 1994
Accepted May 6, 1994)

Br. J. Pharmacol. (1994), **113**, 355–362 © Macmillan Press Ltd, 1994

Characterization of the binding of the first selective radiolabelled histamine H_3-receptor antagonist, [^{125}I]-iodophenpropit, to rat brain

[1]F.P. Jansen, T.S. Wu, H.-P. Voss, [2]H.W.M. Steinbusch, R.C. Vollinga, [3]B. Rademaker, A. Bast & H. Timmerman

Leiden/Amsterdam Center for Drug Research, Department of Pharmacochemistry, Faculty of Chemistry, Vrije Universiteit, De Boelelaan 1083, 1081 HV Amsterdam, The Netherlands

1 The binding of the first selective radiolabelled histamine H_3-receptor antagonist [^{125}I]-iodophenpropit to rat cerebral cortex membranes was characterized.

2 [^{125}I]-iodophenpropit, radiolabelled to a high specific activity of 1900 Ci mmol^{-1}, saturably bound to a single class of sites with a K_D of 0.57 ± 0.16 nM ($n = 4$) and B_{max} of 268 ± 119 fmol mg^{-1} protein.

3 Specific binding at a concentration below 1 nM represented 50 to 60% of total binding.

4 Binding of [^{125}I]-iodophenpropit to rat cerebral cortex membranes was readily displaced by histamine H_3-agonists and antagonists. In contrast, the inhibitory potencies of selective histamine H_1- and H_2-receptor ligands were very low.

5 [^{125}]-iodophenpropit was biphasically displaced by the histamine H_3-receptor antagonists, burimamide and dimaprit, which may indicate the existence of histamine H_3-receptor subtypes. Other histamine H_3-receptor antagonists showed a monophasic displacement.

6 Competition binding curves of H_3-agonists were biphasic and showed a rightward shift upon the addition of the nonhydrolysable GTP analogue, guanosine 5'-*o*-(3-thio) triphosphate (GTPγS; 100 μM) which implicates the interaction of histamine H_3-receptors with G-proteins. The affinities of the H_3-receptor antagonists iodophenpropit, thioperamide and burimamide were not altered by GTPγS.

7 Histamine competition binding curves were shifted to the right by different nucleotides (100 μM) with a rank order of potency GTPγS > Gpp(NH)p, GTP.

8 *In vitro* autoradiographic studies revealed a heterogeneous distribution of [^{125}I]-iodophenpropit binding sites in rat brain, with highest densities observed in specific cerebral cortical areas and layers, the caudate-putamen complex, the olfactory tubercles, the hippocampal formation, the amygdala complex, the hypothalamic area and the mammillary bodies.

9 It is concluded that the histamine H_3-receptor antagonist, [^{125}I]-iodophenpropit, meets the criteria for a suitable radioligand for histamine H_3-receptor binding studies in rat brain.

Keywords: Histamine H_3-receptor binding; radiolabelled H_3-receptor antagonist; [^{125}I]-iodophenpropit; rat cerebral cortex membranes; high affinity; guanine nucleotide shift; G-protein; autoradiography; distribution, histamine H_3-receptor subtypes

Introduction

The histamine H_3-receptor has been characterized as an autoreceptor inhibiting neuronal histamine release in the CNS, and as a heteroreceptor inhibiting the release of various neurotransmitters both in CNS and PNS (Leurs & Timmerman, 1992). Previously, in receptor binding experiments the agonists [^{3}H]-histamine, [^{3}H]-(**R**)α-methylhistamine and [^{3}H]-N$^{\alpha}$-methylhistamine were used to study the molecular pharmacology and distribution of histamine H_3-receptors. These studies suggested the interaction of histamine H_3-receptors with G-proteins. Moreover, from these experiments the presence of subtypes has been suggested (West *et al.*, 1990b). However, the binding profile of the radiolabelled agonists seems to be rather complex. Therefore, the development of radiolabelled histamine H_3-receptor antagonists is of utmost importance. Recently, a new class of highly potent histamine H_3-receptor antagonists has been described (Van der Goot *et al.*, 1992). Its most potent member is clobenpropit (VUF9153) showing a pA_2-value of 9.9 as determined on the electrically contracted guinea-pig intestine. The series allowed the development of the first radiolabelled histamine H_3 receptor antagonist, [^{125}I]-iodophenpropit (Figure 1; Menge *et al.*, 1992). Preliminary results indicated that [^{125}I]-iodophenpropit is a promising tool for histamine H_3-receptor binding experiments (Jansen *et al.*, 1992). The present paper describes the full characterization of [^{125}I]-iodophenpropit as a radioligand for studying histamine H_3-receptors.

Methods

Preparation of rat cerebral cortex membranes

Male Wistar rats (200–250 g, Harlan C.P.B., Zeist, The Netherlands) were killed by decapitation and the brains were rapidly removed. The cerebral cortices were dissected and homogenized in 15 volumes (v/w) of ice-cold Tris-HCl buffer (50 mM Tris-HCl; 5 mM $MgCl_2$, 145 mM NaCl; pH 7.4 at 4°C) using an Ultra-Turrax homogenizer (8 s) and a glass-teflon homogenizer (four up and down strokes) subsequently. All subsequent steps preceding incubation were performed at a temperature of 0 to 4°C. The homogenate was centrifuged

[1] Author for correspondence.
[2] Research Institute Neurosciences, Department of Pharmacology, Faculty of Medicine, Vrije Universiteit, Amsterdam, The Netherlands.
[3] Rephartox bv., Fazantenkamp 83, 3607 CD Maarssen, The Netherlands

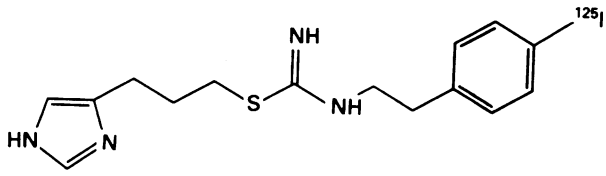


Figure 1 Structure of [^{125}I]-iodophenpropit.

at 800 *g* for 10 min. The pellet was discarded and the supernatant was centrifuged for 20 min at 40,000 *g*. The resulting pellet was resuspended and the last centrifugation step was repeated. The pellet was resuspended in 1.5 volumes (v/w) Tris-HCl buffer and stored at − 80°C. Before each receptor binding experiment the membranes were resuspended in Tris-HCl buffer and were centrifuged for 20 min at 40,000 *g*. Finally, the pellet was resuspended in 7 volumes (v/w) of incubation buffer (50 mM Tris-HCl containing 5 mM $MgCl_2$, 145 mM NaCl; pH 7.4 at 37°C. In some experiments NaCl was omitted).

Receptor binding experiments

Binding experiments were performed at 37°C in the Tris-HCl incubation buffer (pH 7.4) with a total incubation volume of 0.5 ml, using polyethylene tubes. Determinations were performed in triplicate. Drugs (except for thioperamide, see drugs and chemicals) were prepared in incubation buffer. Rat cerebral cortex membranes were incubated for 60 min to reach equilibrium (Jansen *et al.*, 1992). In saturation experiments membranes were incubated with [^{125}I]-iodophenpropit in final concentrations ranging from 0.025 to 3 nM. In competition binding experiments a concentration of 0.25 nM [^{125}I]-iodophenpropit was used. Specific binding was defined as the difference between total binding and binding in the presence of 0.3 μM thioperamide and represented 50 to 60% of total binding. [^{125}I]-iodophenpropit was displaced to the same level by all of the histamine H_3-receptor ligands tested. Moreover, at this level [^{125}I]-iodophenpropit binding was not further displaced upon the addition of 0.1 μM thioperamide.

Incubations were started by the addition of 100 μl membranes (20–60 μg of protein per tube) and were terminated after 60 min by adding 2 ml of ice-cold Tris-HCl buffer (pH 7.4 at 4°C) immediately followed by filtration through Whatman GF/C filters using a Brandel filtration apparatus. Filters were pretreated (for 2 h) with 0.3% polyethyleneimine, reducing filter binding to less than 1% of the total radioactivity added. After filtration of the membranes the filters were washed twice with 2 ml of ice-cold Tris-HCl buffer. The amount of radioactivity bound to the membranes was not reduced by repetition of the washing procedure up to five times. The radioactivity bound to the filters was measured by an LKB gamma counter.

Data analysis

Saturation and competition binding experiments were evaluated using the non-linear curve fitting programme LIGAND (Munson & Rodbard, 1980) on a Macintosh computer. With the aid of this programme binding curves were fitted (unweighed) to a one and a two site model respectively, and statistically tested on the increasing goodness of the fit for a model with additional parameters, based on the 'extra sum of squares' principle (Draper & Smith, 1966) using a probability level of 5%.

Protein assays

Protein concentrations were determined with the Bio-Rad Protein Assay (Bradford, 1976). Bovine serum albumin (BSA) was used as a standard.

Receptor autoradiography

Male Wistar rats (200–250 g, Harlan C.P.B., Zeist, The Netherlands) were killed by decapitation and the brains were removed. Brains were frozen in liquid CO_2. Cryostat sections (14 μm) were mounted on gelatine/chromalum-coated glass slides and stored at − 80°C before use. The brain sections were incubated with 0.3 nM [^{125}I]-iodophenpropit for 60 min at 37°C in 50 mM Tris-HCl buffer containing 145 mM NaCl, 5 mM $MgCl_2$ and 0.25% BSA (pH 7.4 at 37°C). Nonspecific binding was determined by incubation of adjacent sections in the presence of 0.3 μM thioperamide. To stop the incubation the slices were washed twice for 15 min in ice-cold Tris-HCl buffer (50 mM Tris-HCl; 5 mM $MgCl_2$, 145 mM NaCl; pH 7.4 at 4°C) and 15 s in ice-cold distilled water. Sections were dried by a stream of cold air and were exposed to Hyperfilm, (Amersham International, U.K.) for 20 h.

Drugs and chemicals

[^{125}I]-iodophenpropit was labelled to a specific activity of 1900 Ci mmol^{-1} as described by Menge *et al.* (1992). The radiolabelled compound was stored at 4°C in a 1 mM H_2SO_4 solution in ethanol. H_2SO_4 did not affect the pH of the Tris-HCl buffer at the final concentrations of the radioligand used. High performance liquid chromatography (h.p.l.c.) analysis two months after preparation revealed that the radioactivity was almost quantitatively present in one peak with a retention time corresponding to the radioligand.

The following drugs and chemicals were used: thioperamide (Schering Corporation), iodophenpropit dihydrobromide (laboratory stock), clobenpropit dihydrobromide (VUF9153, laboratory stock), impromidine trihydrochloride (SK&F Laboratories), burimamide (SK&F Laboratories), dimaprit dihydrochloride (SK&F Laboratories), histamine dihydrochloride (Sigma), (**R**)α-methylhistamine maleate (gift from Prof. Dr J.-C. Schwartz, Paris), (**S**)α-methylhistamine dihydrobromide (Cookson Chemicals), imetit dihydrobromide (VUF8325, laboratory stock), immepip dihydrobromide (VUF4708; 4-(1*H*-imidazol-4-ylmethyl)piperidine dihydrobromide, laboratory stock), 5'-guanylylimidodiphosphate (Gpp(NH)p) (Sigma), guanosine 5'-o-(3-thio)triphosphate (GTPγS) (Sigma), guanosine 5'-triphosphate (GTP) (Sigma), betahistine dihydrochloride (Solvay Duphar), mepyramine hydrochloride (Sigma), triprolidine hydrochloride (Sigma), amthamine dihydrobromide (laboratory stock), tiotidine (ICI), imidazole (Merck) and polyethylenimine (Aldrich-Chemie). Drugs were dissolved in distilled water or in Tris-HCl buffer except for thioperamide which was diluted in buffer from 1 mM stock solutions prepared in dimethylsulphoxide (DMSO). At the final concentrations used, DMSO did not affect [^{125}I]-iodophenpropit receptor binding.

Statistical analysis

Dissociation constants for agonists in the absence and presence of guanine nucleotides were compared by Student's one tailed, unpaired *t* test. The effect of NaCl on dissociation constants for antagonist was analysed by Student's two tailed, unpaired *t* test. Differences were considered using a probability level of 5%.

Results

[^{125}I]-iodophenpropit saturation binding experiments

Specific binding of [^{125}I]-iodophenpropit (0.025–3 nM) to rat cerebral cortex membranes was saturable (Figure 2a) and yielded linear Scatchard plots. Computer analysis of the saturation binding curves revealed that [^{125}I]-iodophenpropit bound to a single class of sites with a K_D of 0.57 ± 0.16 nM and a B_{max} of 268 ± 119 fmol mg^{-1} of protein ($n = 4$). Hill

coefficients were not significantly different from unity (1.00 ± 0.02). Non-specific binding determined in the presence of 0.3 μM thioperamide was linear with the [^{125}I]-iodophenpropit concentration up to 3 nM. Specific binding at concentrations below 1 nM accounted for 50 to 60% of total binding.

Both dissociation constant and receptor density of the [^{125}I]-iodophenpropit binding sites were unaffected by the non-hydrolysible GTP analogue 5'-guanylylimidodiphosphate (Gpp(NH)p) in a concentration of 100 μM (K_D = 0.55 ± 0.19 nM; B_{max} = 272 ± 101 fmol mg^{-1} protein; n = 4) (Figure 2b).

Competition binding curves of H_3-antagonists

[^{125}I]-iodophenpropit was displaced from rat cerebral cortex membranes by histamine H_3-receptor antagonists (Figure 3). The selective histamine H_3-receptor antagonists, clobenpropit (VUF9153) and iodophenpropit, showed the highest potency with K_D values of 0.9 ± 0.4 nM and 1.0 ± 0.1 nM respectively (Table 1). Omitting sodium chloride from the buffer significantly reduced the affinity of iodophenpropit and thioperamide for [^{125}I]-iodophenpropit binding sites (Table 1). Competition binding curves of clobenpropit, iodophenpropit, thioperamide (K_D = 4.3 ± 1.6 nM) and impromidine (K_D = 51 ± 9 nM) fitted best to a one site model (P > 0.05).

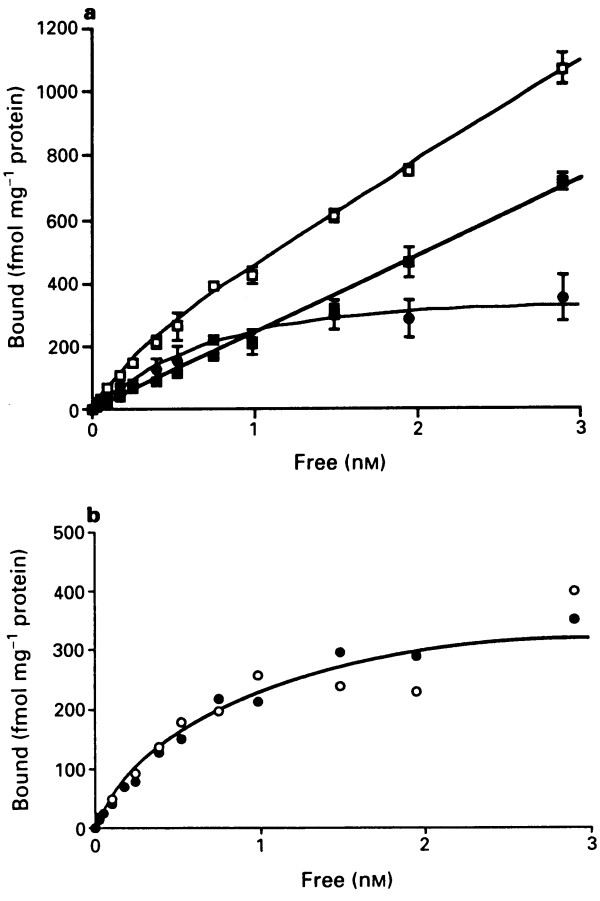


Figure 2 (a) Saturation binding of [^{125}I]-iodophenpropit (0.025–3 nM) to rat cerebral cortex membranes; (□) total binding; (■) non-specific binding; determined by the addition of 0.3 μM thioperamide (●) specific binding. (b) Specific binding of [^{125}I]-iodophenpropit to rat cerebral cortex membranes in the absence (●) and presence (○) of 100 μM Gpp(NH)p. The dissociation constant and receptor density in the absence of Gpp(NH)p were 0.57 ± 0.16 nM and 268 ± 119 fmol mg^{-1} protein, and in the presence of Gpp(NH)p 0.55 ± 0.19 nM and 272 ± 101 fmol mg^{-1} protein respectively (n = 4). Results shown are from one representative experiment with triplciate determinations.

In contrast, competition binding curves of the histamine H_3-receptor antagonists burimamide and dimaprit were significantly better described by a two site model (P < 0.05; Figure 3b). The dissociation constants for the two different sites were 18 ± 9 nM and 725 ± 392 nM for burimamide and 0.42 ± 0.11 μM and 38 ± 37 μM for dimaprit (Table 2). The histamine H_3-receptor antagonist, betahistine, had a K_D value of 131 ± 37 μM (Figure 3a).

Displacement by other ligands

Selective ligands for histamine H_1- (mepyramine and triprolidine) and H_2-receptors (tiotidine and amthamine) and imidazole showed a very low affinity (K_D > 10 μM) towards the [^{125}I]-iodophenpropit binding sites (Table 1).

[^{125}I]-iodophenpropit displacement by H_3-agonists; the effect of guanine nucleotides

Competition binding curves for histamine H_3-receptor agonists were shallow and all fitted a two site model best

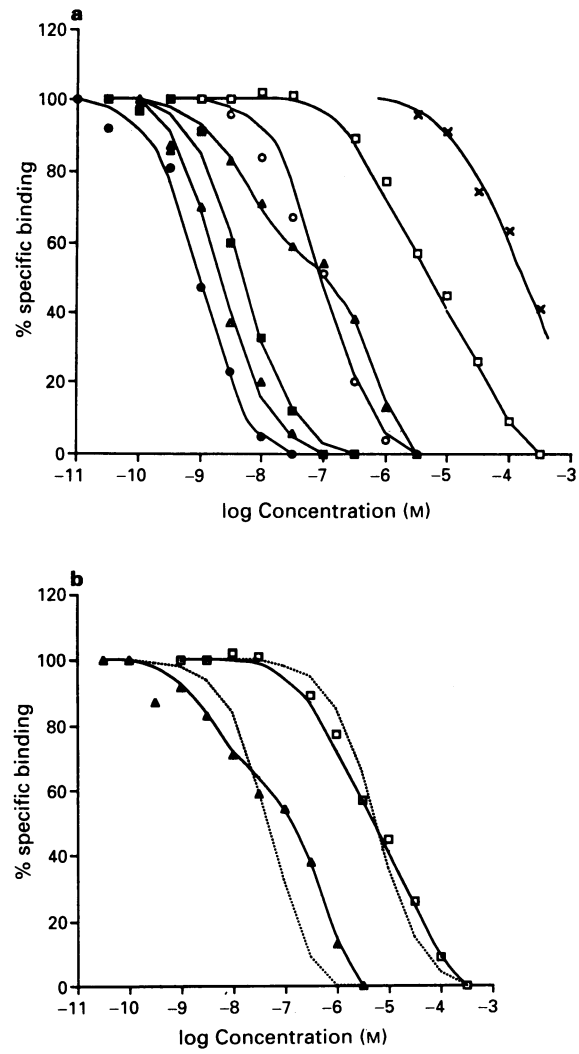


Figure 3 (a) Inhibition of [^{125}I]-iodophenpropit binding (0.25 nM) by histamine H_3-receptor antagonists. (b) Competition binding curves for burimamide and dimaprit compared with the corresponding theoretical one site competition curves (dashed curves). Data are expressed as % specific binding. Specific binding was determined using 0.3 μM thioperamide and represented 50 to 60% of the total binding. Each curve represents a single representative experiment with triplicate determinations. Symbols used: (●) clobenpropit; (△) iodophenpropit; (■) thioperamide; (○) impromidine; (▲) burimamide; (□) dimaprit; (×) betahistine.

($P<0.05$), showing high and low affinity binding sites. The rank order of potency of the five agonists used for the high affinity sites was imetit ($K_H = 2.7 \pm 0.8$ nM), immepip ($K_H = 2.7 \pm 0.5$ nM), (R)α-methylhistamine ($K_H = 3.5 \pm 1.2$ nM)> histamine ($K_H = 38 \pm 10$ nM)>(S)α-methylhistamine ($K_H = 230 \pm 97$ nM) (Table 3).

Upon the addition of GTPγS (100 μM) the competition binding curves of the agonists showed a rightward shift. GTPγS completely abolished the high affinity sites for histamine, (R)α-methylhistamine and (S)α-methylhistamine (curves fitted best to a one site model, $P>0.05$; Table 3, Figure 4). For imetit and the new histamine H_3-receptor agonist, immepip (Vollinga *et al.*, 1994) a significant increase of the high affinity dissociation constant was observed upon addition of GTPγS (Table 3). With respect to competition binding curves for histamine, the nucleotides GTP and Gpp(NH)p at a concentration of 100 μM were less potent than GTPγS. Both GTP and Gpp(NH)p significantly increased the high affinity dissociation constants for histamine (Table 3). GTPγS (100 μM) did not affect the dissociation constants for the histamine H_3-receptor antagonists, iodophenpropit (K_D-value without GTPγS: 1.4 ± 0.4 nM, K_D value with GTPγS: 2.2 ± 0.8 mM, $n = 3$), thioperamide (K_D-value without GTPγS: 1.2 ± 0.4 nM, K_D value with GTPγS: 1.3 ± 0.7 nM, $n = 3$) and burimamide ($K_{D,1}$- and $K_{D,2}$- value without GTPγS: 18 ± 9 nM and 0.7 ± 0.4 μM respectively, $n = 8$; $K_{D,1}$ and $K_{D,2}$ value with GTPγS: 62 ± 44 nM and 3.1 ± 2.8 μM respectively, $n = 3$).

Table 1 Affinities of different ligands towards [^{125}I]-iodophenpropit binding sites on rat cerebral cortex membranes and the effect of NaCl on histamine H_3-receptors antagonist affinity

Ligand	*Tris-buffer* + *$MgCl_2$* (5 mM)	*Tris-buffer* + *$MgCl_2$* (5 mM) + *NaCl* (145 mM)
H_3-antagonists:	(K_D nM)	(K_D, nM)
Clobenpropit	ND	0.93 ± 0.39 (3)
Iodophenpropit	1.7 ± 0.3 (3)	0.97 ± 0.06* (3)
Thioperamide	11 ± 2.3 (7)	4.3 ± 1.6* (7)
Impromidine	107 ± 68 (3)	51 ± 9 (3)
Other ligands:		
Mepyramine	>10,000 (5)	ND
Triprolidine	>10,000 (3)	ND
Tiotidine	>10,000 (4)	ND
Amthamine	>10,000 (2)	ND
Imidazole	>10,000 (2)	ND

All compounds listed were fitted best to a one-site model ($P>0.05$). Values are given as the mean ± s.d. (number of experiments). ND; not determined. *$P<0.05$ as compared with buffer without NaCl.

Distribution of [^{125}I]-iodophenpropit binding sites in rat brain studied by receptor autoradiography

Incubation of rat brain cryostat sections with [^{125}I]-iodophenpropit showed that the radioligand binding sites were heterogeneously distributed (Figure 5a–c). Non-specific binding, defined by incubation of adjacent sections in the presence of 0.3 μM thioperamide, was very low and homogeneously distributed (Figure 5d–f). The highest levels of specific binding were observed in the upper frontal layers and lower temporal layers of the cerebral cortex, the caudate-putamen complex, the olfactory tubercles, the hippocampal formation, the amygdala complex, the substantia nigra, the hypothalamic area and the mammillary bodies. Densities were low in the cerebellum.

Discussion

Recently, we described the preliminary pharmacological characterization of the first radiolabelled histamine H_3-receptor antagonists [^{125}I]-iodophenpropit showing it to be a potential tool for histamine H_3-receptor binding studies (Jansen *et al.*, 1992). In the present study, we describe the full characterization of the binding of [^{125}I]-iodophenpropit to rat brain. [^{125}I]-iodophenpropit meets the basic criteria for a suitable radioligand for receptor binding studies, i.e. high affinity,

Table 2 Affinities of histamine H_3-receptor antagonists discriminating between two [^{125}I]-iodophenpropit binding sites

Antagonist				
Burimamide	$K_{D,1}$ (nM)	R_1 (%)	$K_{D,2}$ (nM)	R_2 (%)
	18 ± 9	54 ± 10	725 ± 392	46 ± 9
Dimaprit	$K_{D,1}$ (μM)	R_1 (%)	$K_{D,2}$ (μM)	R_2 (%)
	0.42 ± 0.11	52 ± 6	38 ± 37	47 ± 6

Values are given as the mean ± s.d. of eight (burimamide) and five (dimaprit) separate experiments with triplicate determinations. $K_{D,1}$ and $K_{D,2}$ are the dissociation constants for the two different binding sites, R_1 and R_2 the corresponding percentages of each site.

Table 3 The effect of guanine nucleotides on the high and low affinity binding sites of histamine H_3-receptor agonists

		High affinity		*Low affinity*	
Agonist:	*Nucleotide*	K_H (nM)	R_H (%)	K_L (μM)	R_L (%)
Histamine	–	38 ± 10	52 ± 4	2.5 ± 0.6	48 ± 4
	GTP	85 ± 35*	51 ± 8	2.5 ± 0.9	49 ± 8
	Gpp(NH)p	137 ± 100*	42 ± 13	3.2 ± 1.5	58 ± 13
	GTPγs	–	–	0.8 ± 0.1*	100**
(R)α-methylhistamine	–	3.5 ± 1.2	52 ± 4	1.2 ± 0.3	48 ± 3
	GTPγs	–	–	0.1 ± 0.1*	100**
(S)α-methylhistamine	–	230 ± 97	39 ± 11	9.5 ± 1.8	61 ± 5
	GTPγs	–	–	12 ± 3.9	100**
Imetit	–	2.7 ± 0.8	59 ± 5	40 ± 12	41 ± 2
	GTPγs	18 ± 10*	52 ± 14	35 ± 20	48 ± 13
Immepip	–	2.7 ± 0.5	63 ± 3	1.0 ± 0.2	37 ± 2
	GTPγs	20 ± 5*	67 ± 5	3.4 ± 3.4	33 ± 8

Values are given as the mean ± s.d. of six (histamine ± GPP(NH)p) or four (remaining) separate experiments with triplicate determinations. The concentrations of GTP, Gpp(NH)p and GTPγS were 100 μM. K_H and K_L correspond to the dissociation constants for the high and low affinity binding sites respectively. R_H and R_L are the percentages of high and low affinity sites.
*$P<0.05$ as compared to value without the nucleotide.
**curve best fitted to a one-site model ($P>0.05$).

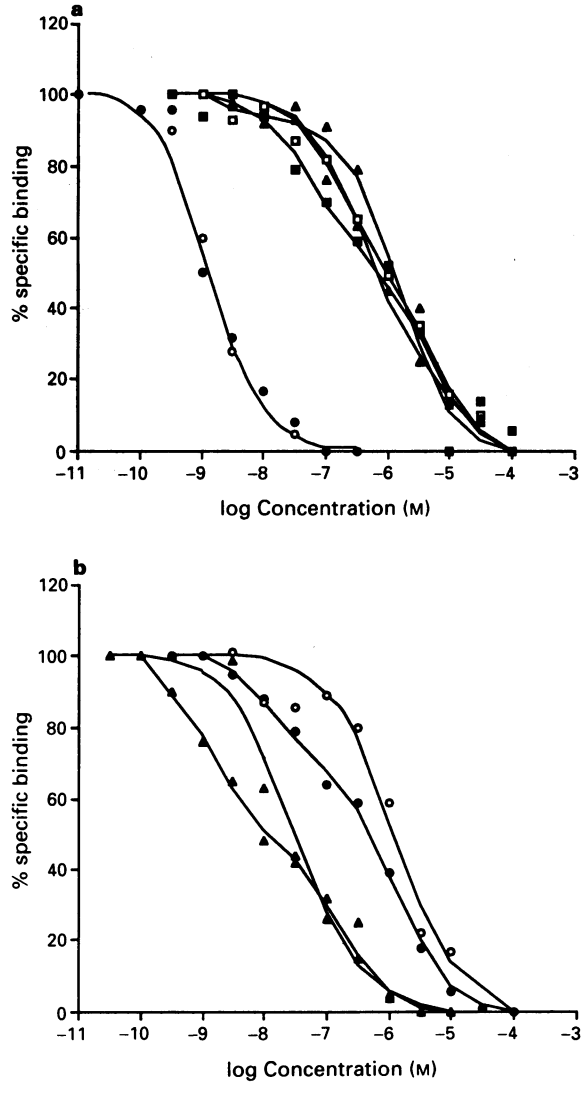


Figure 4 The effect of different nucleotides on displacement of [^{125}I]-iodophenpropit (0.25 nM). (a) The effect of nucleotides on histamine (HA) and thioperamide competition binding curves; (●) thioperamide; (○) thioperamide + GTPγS; (■) HA; (△) HA + GTP; (□) HA + Gpp(NH)p; (▲) HA + GTPγS: (b) The effect of GTPγS on (R) and (S)α-methylhistamine competition binding curves; (▲) (R)α-methylhistamine; (△) (R)α-methylhistamine + GTPγS; (●) (S)α-methylhistamine; (○) (S)α-methylhistamine + GTPγS. Curves displayed are from representative experiments, each point determined in triplicate. The concentration of the nucleotides used was 100 μM.

saturability, reversibility, selectivity and high specific activity. The pK_D value (9.3) observed in saturation binding experiments is close to the pA_2 value (9.6) determined on the guinea-pig intestine. Binding of the radioligand to histamine H_3-receptors was validated by competition binding studies using various selective histamine receptor ligands and by receptor autoradiography.

The binding results obtained with [^{125}I]-iodophenpropit largely correlate to data obtained from receptor binding studies using the radiolabelled agonists [^{3}H]-histamine, [^{3}H]-N^{α}-methylhistamine and [^{3}H]-(R)α-methylhistamine; however, some clear discrepancies also exist. The receptor density found using [^{125}I]-iodophenpropit (268 fmol mg^{-1} protein) was 3 to 8 fold higher than the densities reported using radiolabelled agonists (30 to 80 fmol mg^{-1} protein). The observation that the histamine H_3-receptor antagonists, clobenpropit, iodophenpropit, thioperamide and impromidine displaced [^{125}I]-iodophenpropit according to a one site model is a clear indication that all displaced binding represents histamine H_3-receptors. Considering the variation in chemical structure of the four ligands mentioned, it seems unlikely that the high densities observed using [^{125}I]-iodophenpropit can be explained by binding of the radioligand to an additional high affinity binding component in the membrane preparation for which all these compounds have the same affinity as for the histamine H_3-receptor. Another indication that the specific [^{125}I]-iodophenpropit binding sites represent histamine H_3-receptors is the stereoselective displacement by (R)α-methylhistamine and (S)α-methylhistamine. Moreover in our laboratory, receptor densities of 200 fmol mg^{-1} protein were found using [^{3}H]-N^{α}-methylhistamine (P. Kuyt, personal communication, 1991). Hence, the differences between B_{max}-values obtained with the currently used radiolabelled H_3-agonists compared with the B_{max}-values obtained with [^{125}I]-iodophenpropit might be the result of differences in receptor isolation and incubation procedures.

Displacement of [^{125}I]-iodophenpropit by the histamine H_3-receptor antagonists, burimamide and dimaprit, was shown to be biphasic. This phenomenon may be due to discrimination between subtypes of histamine H_3-receptors by these two compounds. A two site displacement of radiolabelled histamine H_3-agonists by burimamide in rat brain has previously been reported using [^{3}H]-(R)α-methylhistamine (rat cerebral cortex membranes; Arrang *et al.*, 1990) and [^{3}H]-N^{α}-methylhistamine (whole rat brain membranes; West *et al.*, 1990b). However, in another report in which [^{3}H]-(R)α-methylhistamine was used (whole rat brain membranes; West *et al.*, 1990a) burimamide displacement was monophasic. A two site displacement has also been reported for thioperamide (West *et al.*, 1990b), but was not observed in other studies. Variation in the experimental conditions (membrane preparation, composition of the buffer) might account for the discrepancies. Considering the different results, the existence of histamine H_3-receptor subtypes from receptor binding studies needs to be explored further. To validate the existence of possible subtypes, more ligands are needed which clearly discriminate between possible subtypes.

The present study provides evidence for the interaction of histamine H_3-receptors with G-proteins. Displacement of [^{125}I]-iodophenpropit by histamine H_3-receptor agonists was biphasic and was modified by guanine nucleotides. Hence, the two sites found for agonists is probably related to the formation of a ternary complex between the agonist, the receptor and a G-protein rather than discrimination between receptor subtypes by these agonists. The observation that biphasic competition binding curves for the histamine H_3-receptor antagonist, burimamide, was not affected by GTPγS is in accordance with this conclusion. The results obtained with [^{125}I]-iodophenpropit to characterize histamine H_3-receptors were similar to those from binding studies to other G-protein coupled receptors, such as α- (Weinshank *et al.*, 1990) and β-adrenoceptors (Voss *et al.*, 1992), histamine H_1- (Hattori *et al.*, 1991) and histamine H_2-receptors (Ruat *et al.*, 1990), using radiolabelled antagonists. Generally, guanine nucleotides bind to G-proteins, inducing the uncoupling of the G-protein-receptor complex. In a receptor binding study this shows up as a conversion of agonist high affinity binding sites into low affinity binding sites, since the high affinity binding sites represent the binding of an agonist to the receptor – G-protein complex and the low affinity binding sites represent the binding of an agonist to the receptor alone. In our experiments GTPγS completely abolished the high affinity sites for histamine, (R)α-methylhistamine and (S)α-methylhistamine. However, a significant increase of the high affinity dissociation constant of imetit and immepip was observed upon addition of GTPγS. Similar results were described for α_2-adrenoceptors (Weinshank *et al.*, 1990). These observations are different from the generally observed reduction of the ratio between the amount of high and low affinity binding sites by guanine nucleotides. At present, the explanation for these differences remains to be established.

The interaction of histamine H_3-receptors with G-proteins

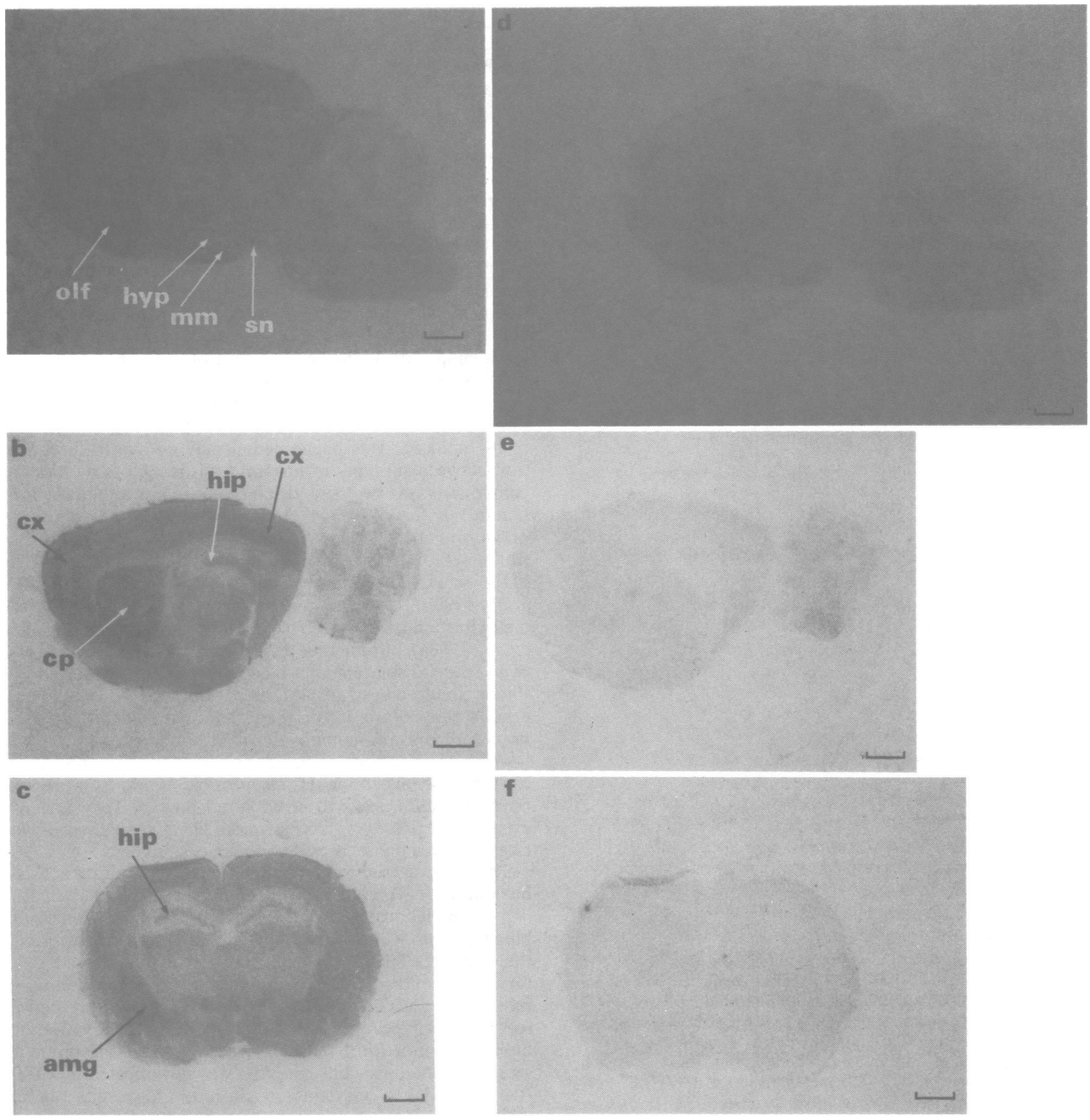


Figure 5 Autoradiographic localization of [^{125}I]-iodophenpropit binding sites in rat brain. On the left side (a to c) total binding is shown using 0.3 nM [^{125}I]-iodophenpropit (a and b: sagittal sections; c: transverse section). On right side (d to f), the corresponding non-specific binding is shown as defined by the inclusion of 0.3 μM thioperamide. Indicated areas: caudate-putamen (cp), hippocampal formation (hip), amygdala complex (amg), substantia nigra (sn), hypothalamic region (hyp), cortex (cx), olfactory tubercles (olf) and mammillary bodies (mm).

has also been indicated by binding studies using the tritium labelled agonists histamine, (**R**)α-methylhistamine and N^{α}-methylhistamine. In 1980, Barbin *et al.* described the high affinity binding of [^{3}H]-histamine to rat brain. Although at that time histamine H_3-receptors were not yet identified, the [^{3}H]-histamine binding sites presumably represented histamine H_3-receptors. In their study, the density of the [^{3}H]-histamine high affinity binding sites was reduced by Gpp(NH)p without altering the affinity. More recently, a reduction of [^{3}H]-N^{α}-methylhistamine binding by GTPγS was observed which may be due both to a reduced density and affinity of [^{3}H]-N^{α}-methylhistamine binding sites (West *et al.*, 1990b). In this last study biphasic displacement of the radiolabelled agonist by thioperamide and burimamide was observed. As the low affinity sites of both antagonists were abolished by GTPγS it was concluded that [^{3}H]-N^{α}-methylhistamine bound to two subtypes of histamine H_3-receptors (H_{3A} and H_{3B}) of which one was not detectable in the presence of GTPγS. Their conclusion is not in agreement with the results of our experiments using [^{125}I]-iodophenpropit, as GTPγS had no effect on displacement curves for burimamide. In another report an effect of guanine nucleotides on [^{3}H]-(**R**)α-methylhistamine binding was observed only when calcium was present in the incubation medium (Arrang *et al.*, 1990). When calcium was included in the buffer saturation curves showed a high and low affinity component, the latter being abolished by Gpp(NH)p. From these rather unexpected results the authors suggested that the low affinity site may be its functional receptor. Reduction of [^{3}H]-N^{α}-methylhistamine binding sites by Gpp(NH)p has also

Table 4 The affinity of histamine H_3-receptor agonists and antagonists for [^{125}I]-iodophenpropit binding sites on rat cerebral cortex compared with their functional potencies

H_3-antagonists:	(pK_D)	(pA_2)
Clobenpropit	9.0	9.9[a]
Iodophenpropit	9.0	9.6[b]
Thioperamide	8.4	8.5[a]
Impromidine	7.3	7.2[c]

	($pK_{D,1}$)	($pK_{D,2}$)	(pA_2)
Burimamide	7.7	6.1	7.2[c]
Dimaprit	6.4	4.4	5.5[c]

H_3-agonists:	(pK_D)	(pD_2)
Histamine	7.4	7.4[c]
(R)α-methylhistamine	8.5	8.4[c]
(S)α-methylhistamine	6.6	6.3[c]
Imetit	8.7	9.3[c]
Immepip	8.6	8.0[d]

The affinities of the various ligands for the [^{125}I]-iodophenpropit binding sites are expressed as $-\log K_D$ ($= pK_D$). The pK_D-value for agonists correspond to their high affinity binding site. The functional potencies of H_3-receptor agonists and antagonists are expressed as pD_2 and pA_2 values respectively.
[a]Determined on guinea-pig intestine (Van Der Goot *et al.*, 1992); [b]Determined on guinea-pig intestine (Jansen *et al.*, 1992); [c]Determined on rat cerebral cortex (Leurs *et al.*, 1992); [d]Determined on guinea-pig jejunum (Vollinga *et al.*, 1994).

been shown by *in vitro* receptor autoradiography (Cumming *et al.*, 1991). Summarizing, various studies using radiolabelled histamine H_3-receptor agonists provided evidence for coupling of the histamine H_3-receptor to a G-protein. However, the binding characteristics of these agonists are complex and results obtained by several authors appear to be to a certain extent controversial.

The affinities of histamine H_3-receptor antagonists largely correlate to the antagonistic activities obtained from functional studies (Table 4). With respect to histamine H_3-receptor agonists, the agonistic activities are closely related to their high affinity binding sites (Table 4). In contrast, in binding studies using radiolabelled agonists, the dissociation constants of histamine H_3-receptor agonists reported are approximately 10 fold lower than corresponding pD_2-values. Hence, the pK_D-values observed in these receptor binding studies may not reflect their affinity for the functional histamine H_3-receptor.

Recently, a detailed description of the distribution of histamine H_3-receptors in rat brain was published using [^{3}H]-(R)α-methylhistamine as a radioligand (Pollard *et al.*, 1993). The distribution of [^{125}]-iodophenpropit binding sites we described in the present study was essentially the same as for [^{3}H]-(R)α-methylhistamine observed by Pollard *et al.* (1993). Histamine H_3-receptors showed a clearly distinct distribution compared to histamine H_1- and H_2-receptors. Moreover, the distribution of histamine H_3-receptors seemed to be distinct from the distribution of histaminergic nerve endings in rat brain (Watanabe *et al.*, 1984). This observation may be explained by the occurrence of the histamine H_3-receptor as a heteroreceptor. The histamine H_3-receptor was first characterized as an autoreceptor inhibiting both synthesis and release of neuronal histamine (Arrang *et al.*, 1983; Van Der Werf *et al.*, 1987). However, several studies have indicated the involvement of histamine H_3-receptors in modulation of the release of other neurotransmitters such as 5-hydroxytryptamine (Fink *et al.*, 1990), noradrenaline (Schlicker *et al.*, 1989) and acetylcholine (Clapham & Kilpatrick, 1992; Vollinga *et al.*, 1992).

In conclusion, [^{125}I]-iodophenpropit binds to rat cerebral cortex membranes with a high affinity, saturability and reversibility. [^{125}I]-iodophenpropit binding sites in rat brain are likely to represent histamine H_3-receptors as the binding is displaced by selective histamine H_3-receptor ligands, in contrast to ligands selective for other receptors. Biphasic displacement of [^{125}I]-iodophenpropit by burimamide and dimaprit may be indicative of the existence of histamine H_3-receptor subtypes. The sensitivity of histamine H_3-receptor agonist competition binding curves to guanine nucleotides confirms the results of previous experiments indicating the interaction of histamine H_3-receptors with G-proteins. The distribution of [^{125}I]-iodophenpropit binding sites in rat brain is heterogeneous and essentially the same as previously reported for the selective histamine H_3-receptor agonist [^{3}H]-(R)α-methylhistamine. [^{125}I]-iodophenpropit is a valuable new tool for studying histamine H_3-receptors.

The authors wish to thank Dr J. Eersels and Dr J.D.M. Herscheid for the synthesis of [^{125}I]-iodophenpropit and Dr W. Menge for the synthesis of histamine H_3-receptor ligands.

References

ARRANG, J.-M., GARBARG, M. & SCHWARTZ, J.-C. (1983). Auto-inhibition of brain histamine release mediated by a novel class (H_3) of histamine receptor. *Nature*, **302**, 832–837.

BARBIN, G., PALACIOS, J.M., RODERGAS, E., SCHWARTZ, J.C. & GARBARG, M. (1980). Characterization of the high-affinity binding sites of [^{3}H]histamine in rat brain. *Mol. Pharmacol.*, **18**, 1–10.

BRADFORD, M.M. (1976). A rapid and sensitive method for the quantitation of microgram quantities of protein utilising the principle of protein-dye binding. *Anal. Biochem.*, **72**, 248–254.

CLAPHAM, J. & KILPATRICK, G.J. (1992). Histamine H_3-receptors modulate the release of [^{3}H]-acetylcholine from slices of rat entorhinal cortex – evidence for the possible existence of H_3-receptor subtypes. *Br. J. Pharmacol.*, **107**, 919–923.

CUMMING, P., SHAW, C. & VINCENT, S.R. (1991). High affinity histamine binding site is the H_3 Receptor – characterization and autoradiographic localization in rat brain. *Synapse*, **8**, 144–151.

DRAPER, N.R. & SMITH, H. (1966). In *Applied Regression Analysis*. New York: Wiley.

FINK, K., SCHLICKER, E., NEISE, A. & GOTHERT, M. (1990). Involvement of presynaptic H_3 receptors in the inhibitory effect of histamine on serotonin release in the rat brain cortex. *Naunyn-Schmied. Arch. Pharmacol.*, **342**, 513–519.

HATTORI, Y., ENDOU, M., GANDO, S. & KANNO, M. (1991). Identification and characterization of histamine H_1- and H_2-receptors in guinea-pig left atrial membranes by [^{3}H]-mepyramine and [^{3}H]-tiotidine binding. *Br. J. Pharmacol.*, **103**, 1573–1579.

JANSEN, F.P., RADEMAKER, B., BAST, A. & TIMMERMAN, H. (1992). The first radiolabeled histamine H_3 receptor antagonist. [^{125}I]iodophenpropit: saturable and reversible binding to rat cortex membranes. *Eur. J. Pharmacol.*, **217**, 203–205.

LEURS, R. & TIMMERMAN, H. (1992). The histamine H_3-receptor: a target for developing new drugs. *Prog. Drug Res.*, **39**, 127–165.

MENGE, W.M.P.B., VAN DER GOOT, H., TIMMERMAN, H., EERSELS, J.L.H. & HERSCHEID, J.D.M. (1992). Synthesis of S-<3-(4(5)-imidazolyl)propyl>,N-<2-(4-(I-125))-iodophenyl)ethyl>isothiourea sulfate (I-125-Iodophenpropit), a new probe for histamine-H_3-receptor binding sites. *J. Label. Compd. Radiopharm.*, **31**, 781–786.

MUNSON, P.J. & RODBARD, D. (1980). A versatile computerized approach for characterization of ligand-binding systems. *Anal. Biochem.*, **107**, 220–239.

POLLARD, H., MOREAU, J., ARRANG, J.-M. & SCHWARTZ, J.-C. (1993). A detailed autoradiographic mapping of histamine-H-3 receptors in rat brain areas. *Neuroscience*, **52**, 169–189.

RUAT, M., TRAIFFORT, E., BOUTHENET, L., SCHWARTZ, J.C., HIRSCHFELD, J., BUSCHAUER, A. & SCHUNACK, W. (1990). Reversible and irreversible labeling and autoradiographic localization of the cerebral histamine H_2-receptor using [^{125}I]iodinated probes. *Proc. Natl. Acad. Sci. U.S.A.*, **87**, 1658–1662.

SCHLICKER, E., FINK, K., HINTERHANER, M. & GOTHERT, M. (1989). Inhibition of noradrenaline release in the rat brain cortex via presynaptic H_3-receptors. *Naunyn-Schmied. Arch. Pharmacol.*, **340**, 633–638.

VAN DER GOOT, H., SCHEPERS, M.J.P., STERK, G.J. & TIMMERMAN, H. (1992). Isothiourea analogues of histamine as potent agonists or antagonists of the histamine H_3 receptor. *Eur. J. Med. Chem.*, **27**, 511–517.

VAN DER WERF, J.F., BAST, A., BIJLOO, G.J., VAN DER VLIET, A. & TIMMERMAN, H. (1987). HA autoreceptor assay with superfused slices of rat brain cortex and electrical stimulation. *Eur. J. Pharmacol.*, **138**, 199–206.

VOLLINGA, R.C., DE KONING, J.T., JANSEN, F.P., LEURS, R., MENGE, W.M.P.B. & TIMMERMAN, H. (1994). A new potent and selective histamine H_3-receptor agonist, 4-(1*H*-imidazol-4-ylmethyl)piperidine. *J. Med. Chem.*, **37**, 332–333.

VOLLINGA, R.C., ZUIDERVELD, O.P., SCHEERENS, H., BAST, A. & TIMMERMAN, H. (1992). A simple and rapid in vitro test system for the screening of histamine H_3 ligands. *Methods Find. Exp. Clin. Pharmacol.*, **14**, 747–751.

VOSS, H.-P., DONNELL, D. & BAST, A. (1992). Atypical molecular pharmacology of a new long-acting β_2-adrenoceptor agonist. TA2005. *Eur. J. Pharmacol.*, **227**, 403–409.

WATANABE, T., TAGUCHI, Y., SHIOSAKA, S., TANAKA, J., KUBOTA, H., TERANO, Y., TOHYAMA, M. & WADA, H. (1984). Distribution of the histaminergic neuron system in the central nervous system of rats; a fluorescent immunohistochemical analysis with histidine decarboxylase as a marker. *Brain Res.*, **295**, 13–25.

WEINSHANK, R.L., ZGOMBICK, J.M., MACCHI, M., ADHAM, N., LICHTBLAU, T., BRANCHEK, A. & HARTIG, P.R. (1990). Cloning, expression, and pharmacological characterization of a human α_{2B}-adrenergic receptor. *Mol. Pharmacol.*, **38**, 681–688.

WEST, R.E., ZWEIG, A., GRANZOW, R.T., SIEGEL, M.I. & EGAN, R.W. (1990a). Biexponential kinetics of (R)-α-[^{3}H]methylhistamine binding to the rat brain histamine receptor. *J. Neurochem.*, **55**, 1612–1616.

WEST, R.E., ZWEIG, S., SHIH, N.-Y., SIEGEL, M.I., EGAN, R.W. & CLARCK, M.A. (1990b). Identification of two H_3-histamine receptor subtypes. *Mol. Pharmacol.*, **38**, 610–613.

(Received October 18, 1993
Revised May 9, 1994
Accepted May 16, 1994)

Br. J. Pharmacol. (1994), **113**, 363–368 © Macmillan Press Ltd, 1994

Sympathetic neurotransmission in the tail artery of aging rats

[1]Eric Thorin, Christine Capdeville-Atkinson, *Bruno Corman & [2]Jeffrey Atkinson

Groupe d'Etude de la Physiopathologie du Vieillissement, Laboratoire de Pharmacologie Cardio-vasculaire, Faculté de Pharmacie de l'Université de Nancy 1, 5 rue Albert Lebrun, 54000 Nancy, and *Département de Biologie Cellulaire et Moléculaire, Centre d'Etudes de Saclay, 91191 Gif sur Yvette, France

1 Age-related changes in noradrenergic neurotransmission in the tail arteries of three rat strains: outbred Wistar (WI/Ico), inbred Wistar (WAG/Rij) and inbred Fischer (F344) have been compared in the present study.

2 The arterial noradrenaline content varied from 5 to 10 ng mg^{-1} wet weight amongst young (3 to 6-month old) representatives of each strain, but did not change with age. As protein content increased in senescent rats (24-month old) by 30–40%, arterial tissue growth would not appear to receive a concomitant increase in sympathetic growth leading to relative, age-related, structural sympathectomy in all strains.

3 The vasoconstrictor response to transmural electrical stimulation was diminished in adult and senescent rats of all strains.

4 As far as could be judged from the increase in noradrenaline release following perfusion with the α-adrenoceptor antagonist, phentolamine (1 μM), the presynaptic α_2-adrenoceptor-mediated inhibition of noradrenaline release was intact in old representatives of all strains.

5 With blockade of the two main systems which control noradrenaline release in the rat tail artery, *viz*, neuronal reuptake with cocaine (4 μM) and presynaptic α_2-adrenoceptors with phentolamine (1 μM), stimulation-evoked release of noradrenaline was similar at all ages and in all strains. This suggests that in the rat tail artery the basic mechanism of neuronal release of noradrenaline is not functionally modified by aging.

6 We conclude that as sympathetic nerve terminals are apparently intact in all three strains of senescent rats used, the age-associated deficit of α-adrenergic control of vascular function is postsynaptic in nature.

Keywords: Noradrenaline; vasoconstriction; rat tail artery; strain of rat; age; electrical stimulation

Introduction

Although the study of the physiology of the aging vascular system in animals is fraught with many difficulties (Bennett & Gardiner, 1988; Vanhoutte, 1988), at first sight the rat would appear to be a good choice for the evaluation of changes in noradrenergic regulation of the vascular system with advancing age in the absence of pathological complications. Thus, for instance, the rat does not develop hypertension with age (Lartaud *et al.*, 1993) and is resistant to atherosclerosis (Gill *et al.*, 1989). Yet experiments carried out in the rat have often given contradictory data (Docherty, 1986, 1990). There are several reasons for this, and Docherty (1990) suggested that the strain of the rat used – generally Fischer 344 or, more recently, Wistar – may be important.

Apart from certain exceptions, such as α_2-adrenoceptor-mediated inhibition of release, noradrenergic neuroeffector function is maintained with advancing age in the Fischer 344 strain (Duckles *et al.*, 1985), which is the strain most frequently used in this type of study. This may not be the case in other strains (Fouda & Atkinson, 1986; Wanstall & O'Donnell, 1988).

The main objective of the current study, therefore, was to ascertain the effect of aging on noradrenergic, neuroeffector mechanisms by comparing age-related changes in different strains of rats (Wistar and Fischer 344). Two Wistar strains were used, the first an outbred Wistar strain (WI/Ico), with which the methodology was developed (Thorin & Atkinson, 1994), and the second an inbred Wistar strain (WAG/Rij) which was used in a recent multicentric study on vascular aging (Heudes *et al.*, 1994; Michel *et al.*, 1994).

Experiments were performed *in vitro* on the richly innervated tail artery (Handa & Duckles, 1987). This artery was used rather than preparations such as the aorta in which structural rather than functional modifications may explain the altered reactivity (Duckles *et al.*, 1985; Docherty, 1990).

Changes in responses to nerve stimulation could arise from a modification of the presynaptic noradrenaline release mechanism(s) and/or of the postsynaptic reactivity to noradrenaline. The technique we used (Thorin & Atkinson, 1994) allows simultaneous measurement of noradrenaline release and vasoconstriction.

Finally, in so-called aging studies, young and adult animals have often been used but truly senescent animals have not always been available. As sexual maturity is attained at 2–3 months and the increase in body weight tails off at around 9 months (Handa & Duckles, 1987; Weihe, 1987), we used 'young' rats aged 3–6 months. Senescent rats were 24-months old, a commonly accepted age for senescence in rats (Docherty, 1990; Wadsworth, 1990). Longevity, as judged from the median length of life, is similar in all 3 strains: 21–29 months in outbred Wistar (Masoro, 1980), 22–29 months in Fischer 344 (Masoro, 1980), and 27 months in Wistar WAG/Rij (Heudes *et al.*, 1994).

In experiments on the Wistar strain which, as stated above, has been less investigated than the Fischer 344 strain, an intermediate age group of 12 months (= adult) was used. The ages of the Fischer 344 rats (3–4 and 24 months) are the same as those taken by Martinez *et al.* (1981) as representative of 'young' and 'aged' rats and include those, 6 and 20 months, suggested by Buchholz *et al.* (1992) as representing the extremes of the greatest age-related difference in noradrenergic function in this strain.

[1]Present address: Department of Pharmacology, University of Vermont, Given Medical Building, Burlington, VT 05405, USA.
[2] Author for correspondence at: Laboratoire de Pharmacologie Cardiovasculaire, Faculté de Pharmacie de l'Université de Nancy 1, 5, rue Albert Lebrun, 54000 Nancy, France.

Four criteria were used for the evaluation of age-related differences in noradrenergic, vascular neuroeffector mechanisms. They were: (1) the density of sympathetic innervation, as indicated by the noradrenaline content of the tail artery relative to wet weight or protein content; (2) the efficiency of the postsynaptic vasoconstrictor mechanism as indicated by the increase in perfusion pressure following transmural nerve stimulation; (3) the efficiency of the α_2-adrenoceptor-mediated inhibition of noradrenaline release, as indicated by the increase in noradrenaline spillover following perfusion with the α-adrenoceptor antagonist phentolamine, and (4) the efficiency of the basic mechanism of neuronal release of noradrenaline, as indicated by the noradrenaline spillover into the perfusate in the presence of the neuronal uptake blocker, cocaine, and phentolamine.

Methods

Animals

Male rats were used in all experiments. The strains and ages used were: (1) outbred Wistar WI/Ico, 3–4 ($n = 10$), 12 ($n = 12$) and 24 months ($n = 14$); (2) inbred Fischer 344, 3–4 ($n = 8$) and 24 months ($n = 8$); and (3) inbred Wistar WAG/Rij, 6 ($n = 9$), 12 ($n = 13$) and 24 ($n = 10$) months. The Wistar WI/Ico and Fischer 344 rats (Iffa-Credo SA, L'Arbresle, France) received food and water *ad libitum*, and were subjected to standard housing and lighting conditions for at least 10 days before each experiment. Twelve-month old Wistar WI/Ico were used in our previous publication which describes the methodology (Thorin & Atkinson, 1994).

The origin, housing and treatment of the Wistar WAG/Rij has been described in detail elsewhere (Heudes *et al.*, 1994).

Anaesthesia, tissue sampling, noradrenaline and protein contents

Under anaesthesia (sodium pentobarbitone, 50 mg kg^{-1}, i.p.), a 1 ml blood sample was taken by aortic puncture (heparin 10 i.u. ml^{-1}) for determination of plasma noradrenaline levels. Following centrifugation (1000 *g*, 4°C, 5 min), perchloric acid (50 µl, 0.3 N) and 3–4, dihydroxybenzylamine (36 nM, internal standard) were added to the plasma (100 µl) which was stored at − 80°C (⩽ 1 week; loss of noradrenaline is undetectable when samples are stored at − 80°C for ⩽ 2 months, unpublished results).

Twice distilled water (500 µl), aluminium oxide (15 mg), and 100 µl of Na_2EDTA (0.13 M) plus $Na_2S_2O_5$ (53 mM) were added to the plasma, and pH adjusted to 8.6 with 0.25 ml of Tris-HCl (2 M, pH 8.8). Samples were shaken at 4°C for 15 min and the supernatant discarded. The alumina was washed 3 times with twice distilled water (2 ml) at 4°C, and noradrenaline eluted with perchloric acid (50 µl, 0.3 N) prior to high performance liquid chromatography. Plasma noradrenaline concentration is expressed as pg ml^{-1}. It should be noted that values are for samples obtained under pentobarbitone anaesthesia.

Samples of the left ventricular myocardium, cerebral cortex, kidney, and 2 segments (1 cm each) of the caudal artery were removed, weighed and stored at − 80°C. Loss of tissue noradrenaline under these conditions is undetectable for at least 2 months (unpublished results). For the determination of tissue noradrenaline levels, samples were homogenized in perchloric acid (510 µl, 0.3 N) containing 3–4 dihydroxybenzylamine as internal standard. After centrifugation at 4°C and 8000 *g* for 30 min, the supernatant was filtered (microfilters 0.45 µm), and 25 µl placed on the chromatographic column. The perchloric acid-soluble protein content of the supernatant was determined; tissue protein content is expressed as µg mg^{-1} wet weight. Tissue noradrenaline content is expressed as ng mg^{-1} wet weight and ng μg^{-1} protein.

For the determination of tissue water content (% w/w) samples were thawed then heated to constant dry weight at 100°C for ⩾ 18 h.

Tail artery perfusion technique

A third caudal artery segment was removed and immediately perfused and superfused at 2 ml min^{-1} in a specially constructed system with modified Krebs-bicarbonate ((mM): NaCl 118, KCl 4.7, $MgCl_2$ 1.2, NaH_2PO_4 1, $CaCl_2$ 2.6, $NaHCO_3$ 25 and glucose 11.1; pH 7.4 ± 0.2, 37 ± 0.2°C) oxgenated with 5% CO_2/95% O_2 (Fouda *et al.*, 1987, 1991; Thorin & Atkinson, 1994). The rat tail artery is a small diameter (451 ± 13 µm) muscular (wall thickness 96 ± 5 µm) artery ($n = 7$, 12 month old WI/Ico rats, unpublished results).

Cocaine (4 µM) was added to inhibit neuronal uptake. This concentration produces maximal blockade of uptake in our preparation (Thorin & Atkinson, 1994). Furthermore as (i) neuronal uptake accounts for ⩾ 90% of the uptake of noradrenaline in the tail artery (Webb *et al.*, 1981), (ii) uptake function is not altered by age (Buchholz & Duckles, 1990), and (iii) a similar concentration (10 µM) has been used in Fischer 344 rat tail arteries (Buchholz & Duckles, 1990), this concentration of cocaine (4 µM) was used in all strains and ages.

The arterial segment was placed under a longitudinal tension of 0.4 g which acted both as a tether and restored the *in vivo* length. Platinum electrodes were placed around the artery at either end of the segment. Segments were perfused and superfused for 30 min prior to electrical stimulation (1 Hz for 4 s, pulse duration 0.2 ms, 5 stimulations, at 5 min intervals for 25 min; pulse generator Alvar SA, Montreuil, France). By the 3rd or 4th stimulation the vasoconstrictor response was stable.

Increases in perfusion pressure (mmHg) following stimulation were measured with a low volume, strain gauge, pressure transducer (Statham P23Db, Statham Ins., Puerto Rico). All pressure values were corrected by the subtraction of the pressure created by the tubing of the perfusion system (= 4 to 6 mmHg) and the basal perfusion pressure created by the resistance of the unstimulated arterial segment (= 10 to 12 mmHg).

Following equilibration, tail artery segments were stimulated (1 Hz, 30 s, square wave pulses, 0.2 ms duration, supramaximal voltage), the frequency of electrical stimulation chosen being approximately half-maximal (Fouda *et al.*, 1987). A relatively low stimulation frequency was used as the effectiveness of presynaptic α_2-adrenoceptor-mediated inhibition of noradrenaline release (see below) is inversely correlated to the intensity of nerve activation (Duckles & Budai, 1990). Furthermore, pressures of ⩽ 160 mmHg were used in order to avoid possible tissue damage (Hynes & Duckles, 1987).

Following 10 min perfusion and superfusion with the α-adrenoceptor antagonist, phentolamine (1 µM), stimulation was repeated. The increase in noradrenaline release following presynaptic α_2-adrenoceptor blockade was expressed as a S2/S1 ratio where S2 represents noradrenaline release in the presence of phentolamine and S1 that in the absence. This high concentration of phentolamine (Fouda *et al.*, 1991) completely abolished the vasoconstrictor response in all strains and ages. Selective α_2-adrenoceptor blockade potentiates vasoconstriction and may modify flow rate at the high pressures developed. This could indirectly modify noradrenaline spillover. This was the reason for preferring a non-specific α-adrenoceptor antagonist to a selective α_2-adrenoceptor antagonist.

As cocaine was present throughout the experiment, noradrenaline spillover into the perfusate, in the presence of the uptake blocker and the antagonist of presynaptic α_2-adrenoceptor-mediated inhibition of noradrenaline release (phentolamine), was taken as an indication of the total neuronal capacity for release.

Noradrenaline release was estimated from noradrenaline spillover into the perfusate, which was collected before stimulation for the measurement of basal noradrenaline release, and then during the 30 s stimulation. Basal release was subtracted from stimulation-induced release. The perfusate was collected over aluminium oxide (15 mg), perchloric acid (0.3 N), 3-4 dihydroxybenzylamine (36 nM), Na_2EDTA (0.13 M) and 53 mM $Na_2S_2O_5$ (53 mM) (4°C, pH 8.6). Samples were shaken (4°C, 15 min), the supernatant discarded, and the alumina washed 3 times with 2 ml of bidistilled water at 4°C. Noradrenaline was eluted with 50 µl of 0.3 N perchloric acid then measured by high performance liquid chromatography.

Fractional noradrenaline release was expressed as pg pg^{-1} per pulse, *viz.* the amount of noradrenaline (pg) collected during the 30 s stimulation period divided by (i) the noradrenaline content of the tail artery (pg) and (ii) the number of pulses.

Drugs

Sodium pentobarbitone was purchased from Sanofi Pharma, Paris, France. Noradrenaline bitartrate, bovine serum albumin, cocaine hydrochloride, 3-4 dihydroxybenzylamine hydrobromide and sodium octyl sulphate, were purchased from Sigma Chemical Company, St. Louis, MO, U.S.A. Aluminium oxide was purchased from Millipore-Waters, Bedford, MA, U.S.A. All other chemicals were purchased from Merck AG, Darmstadt, Germany. Phentolamine was a gift from Ciba Geigy, Basel, Switzerland.

Statistics

Results are expressed as means ± s.e.mean. Significant differences between means were determined by either Scheffe or Student's paired *t*-test. The probability level chosen was $P<0.05$ (*, NS = not significant).

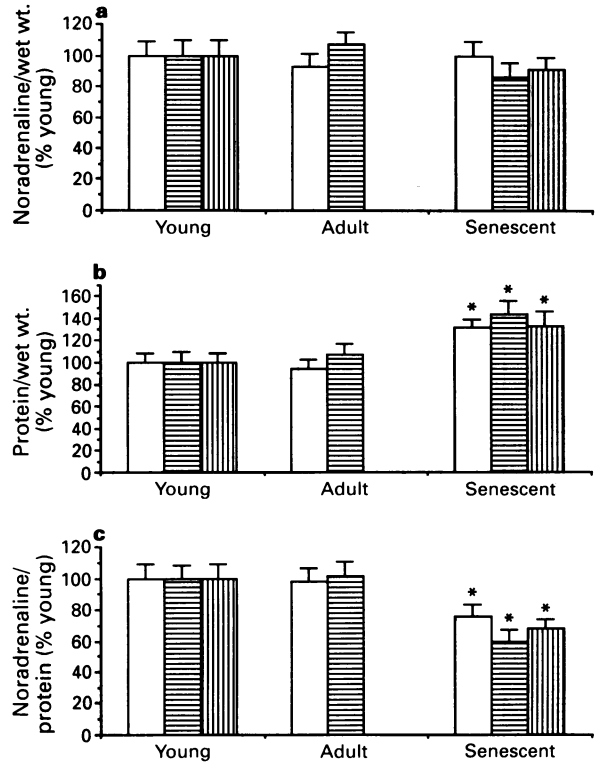


Figure 1 Tail artery noradrenaline content (a: ng ml^{-1} wet weight, c: ng μg^{-1} protein) and acid-soluble protein content (b: µg mg^{-1} wet weight) in Wistar (Wi/Ico: open columns, WAG/Rij: horizontally hatched columns) and Fischer 344 rats (vertically hatched columns) of various ages. For the sake of ease of comparison results are given as percentages of values in young animals which were, for Wi/Ico, WAG/Rij and Fischer 344 respectively: (a) 5.4 ± 0.5, 10.7 ± 1.2, 10.4 ± 1.5; (b) 5.4 ± 0.6, 5.3 ± 0.5, 5.1 ± 0.6; (c) 1.0 ± 0.1, 2.0 ± 0.2, 2.0 ± 0.2. *$P<0.05$ versus young.

Results

Body weight, tissue noradrenaline and protein contents

Body weight tripled in outbred Wistar WI/Ico between the ages of 3–4 and 12 months (young 207 ± 1 g, adult 611 ± 17 g, $P<0.05$) but did not increase thereafter (senescent 600 ± 12 g). In WAG/Rij, the increase was much smaller (young 301 ± 9 g, adult 340 ± 8 g, $P<0.05$); once again there was no further increase in body weight between 12 and 24 months (senescent 347 ± 18 g). Body weight in senescent F344 was double that of young F344 rats (406 ± 8 g versus 199 ± 2 g, $P<0.05$).

Plasma noradrenaline levels increased to a similar extent in senescent animals. Values for WI/Ico were 437 ± 86, 340 ± 29 and 807 ± 66 pg ml^{-1} at 3–4, 12 and 24 months. Values for WAG/Rij were 287 ± 23, 405 ± 30 and 849 ± 76 pg ml^{-1} at 6, 12 and 24 months. Values for F344 were 488 ± 75 and 1017 ± 86 pg ml^{-1} at 3–4 and 24 months.

Tail artery noradrenaline content expressed as ng mg^{-1} wet weight did not vary with age in any of the 3 strains (Figure 1). As soluble protein content increased with age by 30 to 40%, indicating hypertrophy and/or hyperplasia, noradrenaline content expressed as ng μg^{-1} soluble protein decreased by a proportional amount. There were no differences in the tissue water content amongst strains or ages (results not shown).

Left ventricular myocardial noradrenaline and protein contents expressed per mg wet weight decreased with maturity but did not change with age in Wistar rats (Figure 2). The decrease in noradrenaline content relative to protein content was greater in WI/Ico and F344 such that in these two strains – as in the tail artery – noradrenaline content expressed as ng μg^{-1} protein significantly decreased. There were no differences in myocardial water content amongst strains or ages (results not shown).

Renal noradrenaline content was similar in young representatives of all 3 strains (WI/Ico 0.17 ± 0.02, WAG/Rij 0.17 ± 0.01, and F344 0.18 ± 0.02 ng mg^{-1} wet weight, as was protein content (WI/Ico 6.1 ± 0.5, WAG/Rij 5.4 ± 0.4, and F344 6.8 ± 0.4 µg mg^{-1} wet weight). There was no significant change with either maturity or senescence. Cerebral cortex noradrenaline content was similar in young representatives of all 3 strains (WI/Ico 0.17 ± 0.02, WAG/Rij 0.30 ± 0.02, F344 0.28 ± 0.03 ng mg^{-1} wet weight) as was protein content (WI/Ico 1.4 ± 0.02, WAG/Rij 1.7 ± 0.1, F344 2.3 ± 0.1 µg mg^{-1} wet weight). There was no significant change with either maturity or senescence. There were no differences in either renal or cerebral cortical water content amongst strains or ages (results not shown).

Tail artery vasoconstriction and noradrenaline release

Whereas the increase in perfusion pressure following electrical stimulation was lower in adult and senescent rats, noradrenaline release (in the presence of cocaine) was similar at all ages (Figure 3). Inhibition of the presynaptic α_2-adrenoceptor negative feedback control of release, by phentolamine, doubled noradrenaline release (Figure 3). This latter effect was of similar intensity in all strains and at all ages.

Discussion

Body weight, tissue noradrenaline and protein contents

The results for body weight in the 3 strains of rats are in line with more detailed data (Wistar: Weihe, 1987; WI/Ico: Iffa-

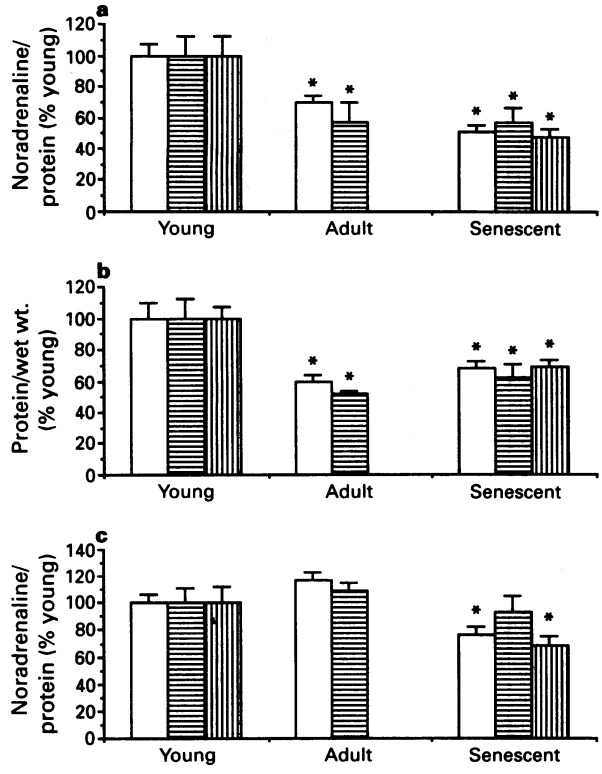


Figure 2 Left ventricular myocardium noradrenaline content (a: ng mg^{-1} wet weight, c: ng μg^{-1} protein) and acid-soluble protein content (b: $\mu g\ mg^{-1}$ wet weight) in Wistar (Wi/Ico: open columns, WAG/Rij: horizontally hatched columns) and Fischer 344 rats (vertically hatched columns) of various ages. For the sake of ease of comparison results are given as percentages of values in young animals which were, for Wi/Ico, WAG/Rij and Fischer 344 respectively: (a) 0.72 ± 0.05, 1.11 ± 0.13, 0.83 ± 0.10; (b) 2.5 ± 0.2, 2.6 ± 0.6, 2.6 ± 0.2; (c) 0.29 ± 0.02, 0.43 ± 0.05, 0.32 ± 0.04. *$P < 0.05$ versus young.

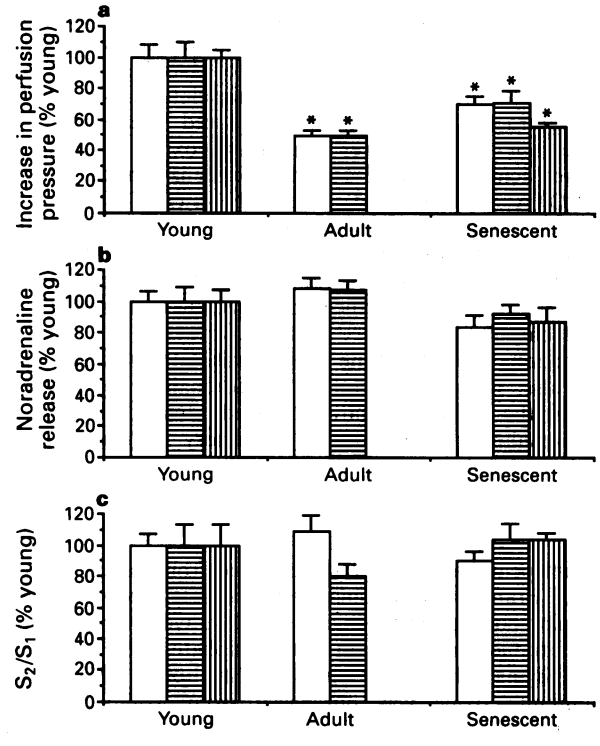


Figure 3 Responses to electrical stimulation in the tail artery of Wistar (Wi/Ico: open columns, WAG/Rij: horizontally hatched columns) and Fischer 344 rats (vertically hatched columns) of various ages. Responses are in (a) increase in perfusion pressure (mmHg); (b) release of noradrenaline (pg pg^{-1} $p^{-1} \times 10^{-6}$); (c) increase in noradrenaline release in the presence of phentolamine (S_2/S_1 ratios). For the sake of ease of comparison results are given as percentages of values in young animals which were, for Wi/Ico, WAG/Rij and Fischer 344 respectively; (a) 128 ± 10, 151 ± 15, 160 ± 9; (b) 4.9 ± 0.3, 2.3 ± 0.2, 2.8 ± 0.4; (c) 2.4 ± 0.2, 2.2 ± 0.3, 2.1 ± 0.3, *$P < 0.05$ versus young.

Credo, 1988; WAG/Rij: Burek, 1978; F344: Masoro, 1980) which show relatively rapid growth up to 8–9 months, with a tailing off thereafter. Thus the young representatives of each strain were still in the growing phase. The Wistar rats reached a stable body weight by 12 months as there was no further increase. The weights of the Fischer 344 rats were in line with those of (approximately) corresponding ages used by Duckles and coworkers (Hynes & Duckles, 1987; Duckles, 1991), and Schmidlin *et al.* (1992).

The senescent WI/Ico was 1.7 times larger than the age-matched WAG/Rij, and 1.5 times larger than the age-matched F344. This may suggest that tail artery dimensions (diameter, wall to lumen ratio, etc.) are different in senescent WI/Ico compared to the two other strains. However, we observed a similar increase in the acid-soluble protein content of the tail artery of all 3 strains of senescent rats. The age-related change in noradrenaline spillover could be due to a change in the length of the diffusion pathway from the synapse to the lumen following wall remodelling. Structural changes would also modify the vasoconstrictor response but it should be noted that we used low levels of sympathetic stimulation at which structural effects on vasoconstriction are less important (Folkow, 1978). If wall remodelling with smooth muscle hypertrophy had occurred in senescent rats, an increased vasoconstrictor response is to be expected, not a decreased response as observed.

Plasma noradrenaline levels increased approximately 2.2 fold with aging (12 to 24 months) but not with maturation (3–4 and 12 months) in Wistar rats. Likewise in senescent Fischer 344 rats, plasma noradrenaline was 2.1 times that of young rats. Many authors have reported that plasma levels of noradrenaline are increased in man (Docherty, 1990), but the methodology used in many reports has been criticised (Bennett & Gardiner, 1988). There are fewer reports in animals but others (Hoffman *et al.*, 1985) have found that plasma noradrenaline levels increase with age in the rat. It should be noted that figures are given for venous levels in man and arterial levels in rats.

An age-related increase in the plasma level of noradrenaline could be due to an increased rate of appearance in the plasma and/or a decreased plasma clearance. As the basic mechanism of neuronal release of noradrenaline does not appear to be modified by aging (see below), and others have reported that noradrenaline reuptake is not modified by age (Buchholz & Duckles, 1990), we would propose, that, although others have stressed the importance of the increased rate of appearance of noradrenaline (Docherty, 1990), a decreased plasma clearance cannot be excluded.

Although there is some evidence that in relatively poorly innervated human (Waterson *et al.*, 1974; Neubauer & Christenson, 1978) and rat (Handa & Duckles, 1987) arteries, noradrenaline content decreases with age, the consensus concerning the richly innervated rat tail artery is that noradrenaline levels are similar in young and senescent animals (Handa & Duckles, 1987; Buchholz & Duckles 1990; Duckles, 1991).

We could find only two exceptions to this rule: the Dawson & Meldrum paper (1992) and one of own previous papers (Fouda & Atkinson, 1986). In both of these studies extremely old rats (up to 30–31 months) were used. It is possible that when dealing with animals whose age is beyond

that of the median length of life (see Introduction) problems of biological variability and selection of survivors become important.

As acid-soluble protein content was greater in the tail artery of senescent rats of all 3 strains the noradrenaline content relative to protein significantly decreased. If we hypothesize that acid-soluble protein represents mainly smooth muscle cells, then arterial tissue growth would not appear to receive a concomitant increase in sympathetic growth leading to 'sympathectomy'. A similar phenomenon has been previously described in the brain microvessels of the Sprague-Dawley rat (Embree *et al.*, 1981).

Changes in the noradrenaline content of the myocardium were more marked than those in the tail artery. There was a decrease in noradrenaline content relative to wet weight in adult and senescent rats. An age-related decrease in noradrenaline content relative to protein was observed in the left ventricular myocardium in two of the strains studied (WI/Ico and F344). This pattern has already been reported in Fischer 344 rats (Martinez *et al.*, 1981; Dawson & Meldrum, 1992; Schmidlin *et al.*, 1992). It is generally assumed that cardiac noradrenergic density declines with age and that this may explain the reduction in stimulation-evoked noradrenaline release (Roberts & Tumer, 1987; Daly *et al.*, 1988; Docherty, 1990).

In our experiments the reduction in noradrenergic innervation as judged from noradrenaline content, would appear to be restricted to cardiovascular tissues as there were no changes in cerebral cortex or kidney. Results in the latter tissue confirm these reported by Eikenburg (1991) in F344 rats. Two other groups have reported a slight (25%) decrease in renal noradrenaline content in senescent F344 rats (Martinez *et al.*, 1981; Dawson & Meldrum, 1992). It should be noted that levels in kidney are 50 times lower than in a richly innervated tissue such as the tail artery, and so in the former, relatively poorly innervated tissue, it would be more difficult to demonstrate statistically any slight change, be it age-related or otherwise.

Tail artery vasoconstriction and noradrenaline release

In all three strains of rats the vasoconstrictor response to electrical stimulation was lower in adult rats but there was no further change with aging. This is in agreement with the majority of previously reported values for blood vessels (Duckles *et al.*, 1985; Fouda & Atkinson, 1986; Hynes & Duckles, 1987; Wanstall & O'Donnell, 1988; Eikenburg, 1991; Atkinson *et al.*, 1994) except the aorta (Tuttle, 1966; Simpkins *et al.*, 1983; Hyland *et al.*, 1987; Moritoki *et al.*, 1988; Wanstall & O'Donnell, 1988). It should be noted, however, that in the latter vessel, there may be a global decrease in reactivity to many agents and not specifically to noradrenaline (Tuttle, 1966; Simpkins *et al.*, 1983; Docherty, 1990).

In our experiments, there was no evidence for an age-related decrease in stimulation-evoked noradrenaline release from the tail artery. Published reports on noradrenaline release are contradictory. In the Fischer 344 rat heart (Daly *et al.*, 1988; Tumer *et al.*, 1990) and the rabbit ear artery (Duckles, 1983) an age-related decrease was observed, whereas in the Fischer 344 rat kidney an increase in noradrenaline release was seen (Eikenburg, 1991). In the Fischer 344 rat tail artery, one group has reported an increase in noradrenaline release which they explained – at least partially – on the basis of a decrease in the sensitivity of the presynaptic α_2-adrenoceptor inhibitory mechanism (Buchholz & Duckles, 1990; Buchholz *et al.*, 1992). Another group reported the opposite, *viz.* that stimulation-evoked noradrenaline release and the efficiency of the presynaptic α_2-adrenoceptor inhibition of release were not modified by age in the Fischer 344 rat tail artery (Dawson & Meldrum, 1992). Our results are in agreement with those of the latter group.

When the two main systems which control noradrenaline release (neuronal uptake and presynaptic α_2-adrenoceptor-mediated inhibition) were blocked (with cocaine and phentolamine, respectively), stimulation-evoked, release of noradrenaline was similar at all ages. A similar result was obtained by the Duckles group (Buchholz & Duckles, 1990) in the Fischer 344 rat tail artery, suggesting that the basic mechanism of neuronal release of noradrenaline is not functionally modified by aging.

In summary, our results are consistent with the hypothesis that vascular noradrenergic nerve terminals are structurally and functionally intact, but, in spite of this the vasoconstrictor response is attenuated. We suggest two explanations for this observation. Firstly, structural changes with increasing medial fibrosis and a decreasing number of small muscle cells (Bouissou *et al.*, 1975) could explain why a muscular artery is less capable of reacting to a noradrenergic stimulus. Secondly, the efficiency of the coupling of the signal transduction mechanism(s) may decline with age (Roberts & Tumer, 1987; Vanhoutte, 1988; Docherty, 1990; Johnston & Wray, 1990). Evidence for such a functional modification has recently been provided by an experiment in Wistar WAG/Rij rat tail arteries in which intracellular calcium (using the fluorescent calcium-sensitive dye, fura-2) and vasoconstriction were measured simultaneously. When stimulated with noradrenaline, arteries from senescent rats showed a diminished vasoconstrictor response with no change in the intracellular calcium signal (Oster *et al.*, 1993).

In conclusion, we suggest that sympathetic nerve terminals are intact in the tail artery of senescent rats, and that the age-associated deficit of α-adrenergic control of vascular function is largely postsynaptic. In studies of age-related changes in noradrenergic vascular regulation in rats, the strain used would appear to be of minor importance.

The authors wish to thank I.R.I.S., Paris for financial support. They especially express their gratitude to Drs Nancy Thibault and Elisabeth Scalbert, of the cardiovascular division of I.R.I.S., Paris for their intellectual and moral support.

References

ATKINSON, J., TATCHUM-TALOM, R. & CAPDEVILLE-ATKINSON, C. (1994). Endothelial function diminishes with age in the mesenteric arterial bed of the normotensive rat. *Br. J. Pharmacol.*, **111**, 1184–1188.

BENNETT, T. & GARDINER, S.M. (1988). Physiological aspects of the aging cardiovascular system. *J. Cardiovasc. Pharmacol.*, **12** (Suppl. 8), S1–S7.

BOUISSOU, H., EMERY, M.C. & SORBARA, R. (1975). Age related changes of the middle cerebral artery and a comparison with the radial and coronary artery. *Angiology*, **26**, 257–268.

BUCHHOLZ, J. & DUCKLES, S.P. (1990). Effect of age on prejunctional modulation of norepinephrine release. *J. Pharmacol. Exp. Ther.*, **252**, 159–164.

BUCHHOLZ, J., TSAI, H., FRIEDMAN, D. & DUCKLES, S.P. (1992). Influence of age on control of norepinephrine release from the rat tail artery. *J. Pharmacol. Exp. Ther.*, **260**, 722–727.

BUREK, J.D. (1978). *Pathology of Aging Rats.* West Palm Beach, FL. U.S.A: CRC Press.

DALY, R.N., GOLDBERG, P.B. & ROBERTS, J. (1988). Effects of age on neurotransmission at the cardiac sympathetic neuroeffector junction. *J. Pharmacol. Exp. Ther.*, **245**, 798–803.

DAWSON, R. & MELDRUM, M.J. (1992). Norepinephrine content in cardiovascular tissues from the aged Fischer 344 rat. *Gerontology*, **38**, 185–191.

DOCHERTY, J.R. (1986). Aging and the cardiovascular system. *J. Auton. Pharmacol.*, **6**, 77–84.

DOCHERTY, J.R. (1990). Cardiovascular responses in ageing: a review. *Pharmacol. Rev.*, **42**, 103–125.

DUCKLES, S.P. (1983). Age-related changes in the adrenergic neuronal function of rabbit vascular smooth muscle. *Neurobiol. Aging*, **4**, 151–156.

DUCKLES, S.P. (1991). Reserpine-induced supersensitivity in rat caudal artery: influence of age. *J. Pharmacol. Exp. Ther.*, **256**, 513–518.

DUCKLES, S.P. & BUDAI, D. (1990). Stimulation intensity as a critical determinant of presynaptic receptor effectiveness. *Trends Pharmacol. Sci.*, **11**, 440–443.

DUCKLES, S.P., CARTER, B.J. & WILLIAMS, C.L. (1985). Vascular adrenergic neuroeffector function does not decline in aged rats. *Circ. Res.*, **56**, 109–116.

EIKENBURG, D.C. (1991). Age-related changes in vascular sympathetic neurotransmission in the rat kidney. *J. Pharmacol. Exp. Ther.*, **259**, 176–181.

EMBREE, L.J., ROUBEIN, I.F., JACKSON, D.W. & ORDWAY, F. (1981). Aging effect on the noradrenaline content of rat brain microvessels. *Expt. Aging Res.*, **7**, 215–224.

FOLKOW, B. (1978). Cardiovascular structural adaptation; its role in the initiation and maintenance of primary hypertension. *Clin. Sci. Mol. Med.*, **55**, 2–25.

FOUDA, A.K. & ATKINSON, J. (1986). Sensitivity to noradrenaline and electrical stimulation decreases with age in the rat tail artery. *Naunyn-Schmied Arch. Pharmacol.*, **334**, 37–39.

FOUDA, A.K., KAUFMANN, A., THORIN, E., HENRION, D., CAPDEVILLE-ATKINSON, C. & ATKINSON, J. (1991). The role of endogenous norepinephrine release in potassium-evoked vasoconstriction of the rat tail artery. *Eur. J. Pharmacol.*, **205**, 63–72.

FOUDA, A.K., MARAZZI, A., BIOLLAT, N., SONNAY, M., GUILLAIN, H. & ATKINSON, J. (1987). Changes in the vascular reactivity of the isolated tail arteries of spontaneous and renovascular hypertensive rats to endogenous and exogenous noradrenaline. *Blood Vessels*, **24**, 63–75.

GILL, T.J., SMITH, G.J., WISSLER, R.W. & KUNZ, H.W. (1989). The rat as an experimental animal. *Science*, **245**, 269–276.

HANDA, R.K. & DUCKLES, S.P. (1987). Influence of age on norepinephrine content in arteries and veins of Fischer 344 rats. *Neurobiol. Aging*, **8**, 511–516.

HOFFMAN, W.E., SEALS, C., MILETICH, D.K. & ALBRECHT, R.F. (1985). Plasma and myocardial catecholamine levels in young and aged rats during halothane anesthesia. *Neurobiol. Aging*, **6**, 117–120.

HEUDES, D., MICHEL, O., CHEVALIER, J., BARIETY, J., EZAN, E., SCALBERT, E., ZIMMERMAN, A. & CORMAN, B. (1994). Effect of chronic angiotensin I converting enzyme inhibition on the aging processes. I. Kidney structure and function. *Am. J. Physiol.*, (in press).

HYLAND, L., WARNOCK, P. & DOCHERTY, J.R. (1987). Age-related alterations in α_1 and β-adrenoceptors mediated responsiveness of rat aorta. *Naunyn-Schmied Arch. Pharmacol.*, **335**, 50–53.

HYNES, M.R. & DUCKLES, S.P. (1987). Effect of increasing age on the endothelium-mediated relaxation of rat blood vessels in vitro. *J. Pharmacol. Exp. Ther.*, **241**, 387–392.

IFFA-CREDO (1988). *Données Biologiques Rat Wistar*. L'Arbresle, France: Iffa-Credo, S.A.

JOHNSON, M.D. & WRAY, A. (1990). Alpha$_1$ adrenergic receptor function in the senescent Fischer 344 rat aorta. *Life Sci.*, **46**, 359–366.

LARTAUD, I., BRAY-DES-BOSCS, L., CHILLON, J.M., ATKINSON, J. & CAPDEVILLE-ATKINSON, C. (1993). *In vivo* cerebrovascular reactivity in Wistar and Fischer 344 rat strains during aging. *Am. J. Physiol.*, **264**, H851–H858.

MARTINEZ, J.L., VASQUEZ, B.J., MESSING, R.B., JENSEN, R.A., LIANG, K.C. & McGAUGH, J.L. (1981). Age-related changes in the catecholamine content of peripheral organs in male and female F344 rats. *J. Gerontol.*, **36**, 280–284.

MASORO, E.J. (1980). Mortality and growth characteristics of rat strains commonly used in aging research. *Exp. Aging Res.*, **6**, 219–233.

MICHEL, J.B., HEUDES, D., MICHEL, O., POITEVIN, P., PHILIPPE, M., SCALBERT, E., CORMAN, B. & LEVY, B.I. (1994). Effect of chronic angiotensin I converting enzyme inhibition on the aging processes: II. Large arteries. *Am. J. Physiol.*, (in press).

MORITOKI, H., TANIOKA, A., MAESHIBA, Y., IWAMOTO, T., ISHIDA, Y. & HIROMASA, A. (1988). Age-associated decrease in histamine-induced vasodilatation may be due to reduction of cyclic GMP formation. *Br. J. Pharmacol.*, **95**, 1015–1022.

NEUBAUER, B. & CHRISTENSEN, N.J. (1978). The decrease in noradrenaline concentration in the posterior tibial artery with age. *Gerontology*, **24**, 299–303.

OSTER, L., THORIN-TRESCASES, N., ROBERT, A. & CAPDEVILLE-ATKINSON, C. (1993). APRIL study: Effect of aging and chronic angiotensin converting enzyme inhibition (ACEI) on intracellular calcium-vasoreactivity coupling. *Proc XV Cong. Int. Ass. Gerontol.*, Budapest, July 1993 (abstract).

ROBERTS, J. & TUMER, N. (1987). Age-related changes in autonomic function of catecholamines. *Rev. Biol. Res. Aging*, **3**, 257–258.

SCHMIDLIN, O., BHARATI, S., LEV, M. & SCHWARTZ, J.B. (1992). Effects of physiological aging on cardiac electrophysiology in perfused Fischer 344 rat hearts. *Am. J. Physiol.*, **262**, H97–H105.

SIMPKINS, J.W., FIELD, P. & RESS, R.J. (1983). Age-related decline in adrenergic responsiveness of the kidney, heart and aorta of male rats. *Neurobiol. Aging*, **4**, 233–238.

THORIN, E. & ATKINSON, J. (1994). Modulation by the endothelium of sympathetic vasoconstriction in an *in vitro* preparation of the rat tail artery. *Br. J. Pharmacol.*, **111**, 351–357.

TUMER, N., RYAN, P.J. & ROBERTS, J. (1990). Action of potassium on neurochemical transmission at the cardiac adrenergic neuroeffector junction with aging. *Mech. Ageing Dev.*, **52**, 87–91.

TUTTLE, R.S. (1966). Age-related changes in the sensitivity of rat aortic strips to norepinephrine and associated chemical and structural alterations. *J. Geront.*, **21**, 510–516.

VANHOUTTE, P.M. (1988). Aging and vascular responses. *J. Cardiovasc. Pharmacol.*, **12** (Suppl. 8), S11–S18.

WADSWORTH, R.M. (1990). Calcium and vascular reactivity in ageing and hypertension. *J. Hypertension*, **8**, 975–983.

WANSTALL, J.C. & O'DONNELL, S.R. (1988). Inhibition of norepinephrine contractions by diltiazem on aorta and pulmonary artery from young and aged rats: influence of alpha-adrenoceptor reserve. *J. Pharmacol. Exp. Ther.*, **245**, 1016–1020.

WATERSON, J.G., FREWIN, D.B. & SOLTYS, J.S. (1974). Age-related differences in catecholamine fluorescence of human vascular tissue. *Blood Vessels*, **11**, 79–85.

WEBB, R.C., VANHOUTTE, P.M. & BOHR, D.F. (1981). Adrenergic neurotransmission in vascular smooth muscle from spontaneously hypertensive rats. *Hypertension*, **3**, 93–103.

WEIHE, W.H. (1987). The laboratory rat. In *The UFAW Handbook on the Care and Management of Laboratory Animals*. ed. Poole, T.B. Burnt Mill, Harlow: Longman Scientific Technical. pp. 309–330.

(Received January 24, 1994
Revised April 28, 1994
Accepted May 25, 1994)

Br. J. Pharmacol. (1994), **113**, 369–374 © Macmillan Press Ltd, 1994

Potent contractile actions of prostanoid EP_3-receptor agonists on human isolated pulmonary artery

Yue-ming Qian, [1]Robert L. Jones, Kam-ming Chan, *Anthony I. Stock & †Jonathan K.S. Ho

Departments of Pharmacology, *Obstetrics and Gynaecology, and †Surgery, Faculty of Medicine, Chinese University of Hong Kong, Shatin, New Territories, Hong Kong

1 In 13 of 15 experiments, prostaglandin E_2 (PGE_2) and sulprostone (a prostanoid EP_1/EP_3-receptor agonist) contracted isolated rings of human pulmonary artery at low concentrations ($\geqslant 5$ and $\geqslant 0.5$ nM respectively). Tissue was obtained from patients undergoing surgery mainly for carcinoma of the lung. Characterization of the receptors involved was complicated by loss of sensitivity to the contractile PGE action over the experimental period. In contrast, contractile responses to KCl, phenylephrine and the specific thromboxane (TP-) receptor agonist, U-46619, did not decrease with time.

2 The relative contractile potencies for seven PGE analogues, measured during the first few hours after setting up the preparations, were as follows: sulprostone > misoprostol = gemeprost $\geqslant$ PGE_2 $\geqslant$ GR 63799X > 17-phenyl-ω-trinor PGE_2 $\geqslant$ 11-deoxy PGE_1. This ranking indicates that an EP_3-receptor is involved.

3 The contractile action of sulprostone was not blocked by the TP-receptor antagonists, EP 169 and GR 32191, and the EP_1-receptor antagonist, AH 6809.

4 In two experiments, PGE_2 (50 nM) reduced basal tone and sulprostone was a weak contractile agent. Phenylephrine-induced tone was also inhibited by PGE_2 ($EC_{50} = 5-20$ nM), 11-deoxy PGE_1 and butaprost (a selective EP_2-receptor agonist); the latter prostanoids were about 2 and 4 times less potent than PGE_2 respectively. Interactions with phenylephrine were different in experiments where PGE_2 alone was contractile: PGE_2 induced contraction superimposed on the phenylephrine response and 11-deoxy PGE_1 induced either further contraction or had no effect. Butaprost produced relaxation at high concentrations; this may not be an EP_2 action since preparations were highly sensitive to relaxant actions of prostacyclin (IP-) receptor agonists (cicaprost and TEI-9063).

5 The study has shown that in the majority of experiments on the human isolated pulmonary artery, the contractile EP_3 system outweighed the relaxant EP_2 system. However, in two experiments the reverse was true. It is not clear to what extent these differences are due to disease processes affecting the tissues. The findings are discussed in relation to the adverse cardiovascular responses occasionally encountered during treatment of postpartum haemorrhage with sulprostone, and more generally to the clinical use of EP-receptor agonists in man.

Keywords: Prostanoid receptors; human pulmonary artery; prostaglandin E_2; sulprostone; misoprostol; gemeprost; cicaprost; TP-receptor antagonists; postpartum haemorrhage; obstetric complications

Introduction

Prostaglandin E_2 (PGE_2) and its analogues have been used therapeutically for their stimulant actions on the pregnant human uterus for some 25 years (Bygdeman *et al.*, 1968; Bygdeman, 1990). The work of Senior and colleagues (1993) clearly indicates that PGE analogues contract human myometrial smooth muscle by activating prostanoid EP_3-receptors. The division of EP-receptors into three subtypes is based largely on *in vitro* smooth muscle measurements and has been recently confirmed by molecular biology techniques (see *Trends Pharmacol. Sci.*, 1994). In general EP_1 and EP_3 subtypes mediate contraction of smooth muscle and EP_2-receptors relaxation.

Sulprostone, which is a highly potent EP_3 agonist, has been recommended for arrest of atonic postpartum haemorrhage due to its excellent tolerance (see Hoppe, 1986). However, the current study originates from observations of severe cardiovascular side effects in two patients receiving intravenous sulprostone for postpartum haemorrhage. Systemic hypotension occurred in the first patient; this is unlikely to have been due to peripheral vasodilatation since sulprostone is almost devoid of EP_2 relaxant activity on vascular smooth muscle (Coleman *et al.*, 1987a,b; Lawrence & Jones, 1992). In the second patient a chest X-ray showed pulmonary congestion (Stock *et al.*, 1994). In this context, the advice sheet on sulprostone (trade name Nalador) contains the warning: 'Do not inject as a bolus (the rapid occurrence of a high plasma level may lead to a critical increase of pressure in the pulmonary circulation)'. The mechanism of the pulmonary hypertension is not known and we therefore decided in the first instance to determine whether sulprostone and other PGE analogues have constrictor actions on human isolated pulmonary vessels, and if so, to identify the prostanoid receptor involved. A preliminary account of our studies has been presented to the British Pharmacological Society (Jones *et al.*, 1994).

Methods

Isolated pulmonary artery preparations

Lung tissue was obtained from 15 Chinese patients undergoing resection of the lung at the Prince of Wales Hospital, Shatin. Twelve of the patients (10 males, 13–76 years; 2 females, 43 and 62 years) had lung cancer and three (one female, 15 years; 2 males, 53 and 58 years) had pulmonary tuberculosis.

Within 10–20 min of lung removal, dissection of sections of pulmonary lobar artery (3–5 mm in diameter) from

[1] Author for correspondence at: Department of Pharmacology, Basic Medical Sciences Building, Chinese University of Hong Kong, Shatin, NT, Hong Kong.

macroscopically healthy areas of a lung lobe was commenced. The tissue was placed in Krebs-Henseleit solution (composition, mM: NaCl 118, KCl 4.7, $MgSO_4$ 1.18, $CaCl_2$ 2.5, KH_2PO_4 1.18, $NaHCO_3$ 25, glucose 10, pH 7.32) at 4–10°C for transport to the laboratory. Adherent tissue, especially that containing tar deposits, was carefully removed. Vessel rings (3–4 mm wide) were cut and suspended in 10 ml organ baths containing the Krebs solution aerated with 95% O_2/5% CO_2 and maintained at 37°C; indomethacin (1 μM) was present throughout the experiments. Washing was by upward displacement and overflow. Tension was recorded with isometric force-displacement transducers (Grass FT03) linked to MacLab recording systems (Chart software version 3.3, data sampling rate = 40 per min). Usually two pairs of matched preparations (i.e. from adjacent portions of an artery) were studied.

Experimental protocols

About 20 min after setting up in the organ bath, each preparation was exposed to a single dose of KCl (40 mM); about 5% of preparations gave weak contractions to KCl and were abandoned. About 1 h after set-up a single priming dose of PGE_2 (50 nM) was applied for 10–15 min.

Agonist potencies Initial experiments showed that sensitivity to the contractile actions of the PGE analogues decayed with time. However, it was not certain that sensitivity would decay in all experiments. Consequently a cross-over design was used in which a cumulative dose-response curve for either PGE_2 or sulprostone was obtained on one preparation concurrently with a cumulative dose-response curve for the test analogue on the matched preparation; these measurements took place between 1.5 and 3 h of setting up the preparations. Responses greater than 80% of the predicted maximum were not obtained in an attempt to reduce tachyphylaxis. After washout each analogue was then retested on the other preparation.

Relaxant effects A stable increase in tone of about 0.7 g was induced by phenylephrine (0.4–2 μM), U-46619 (5–10 nM) or KCl (40 mM). Responses to cumulative doses of prostanoids were then obtained.

Antagonist affinities In the first protocol, one of the matched preparations was treated with antagonist and the other with vehicle for 15 min. Cumulative dose-response curves to the same agonist were then obtained on both preparations. In the second protocol, stable submaximal responses to a particular agonist were obtained on two matched preparations. The antagonist was then added to one preparation and the vehicle to the other; the effects were observed for at least 15 min. All these measurements took place 1.5–3 h after setting up the preparations.

Drugs

The following compounds were gifts: sulprostone and cicaprost (Schering AG, Berlin, Germany); misoprostol (G.D. Searle, U.S.A.); gemeprost (ONO 802; 16,16-dimethyl-*trans*-Δ^2 PGE_1-methyl ester) (Rhone-Poulenc, UK); TEI-9063 (17α,20-dimethyl-$\Delta^{6,6a}$-6a-carba PGI_1) (Teijin, Japan); GR 32191 (9α-(biphenylyl)methoxy-11β-hydroxy-12β-(N-piperidinyl)-ω-octanor-prost-4Z-enoic acid); GR 63799X (13-oxa-13,14-dihydro-16-phenoxy-ω-tetranor PGE_2-4-(benzoylamino) phenyl ester); AH 6809 (6-isopropoxy-9-oxoxanthene-2-carboxylic acid) (Glaxo Group Research, U.K.). EP 169 (*rac* 4a,10a-dihomo-9α,11α-ethano-ω-heptanor-3-oxa-13-phenylthiocarbamoylhydrazino prostanoic acid) was synthesized by Dr N.H. Wilson of the Department of Pharmacology, University of Edinburgh. PGE_2, 17-phenyl-ω-trinor PGE_2, $PGF_{2\alpha}$, fluprostenol (ICI 81008) and U-46619 (15S)-hydroxy-11α,9α-(epoxymethano)prosta-5Z,13E-dienoic acid) were purchased from Cayman Chemicals, U.S.A., and (−)-phenylephrine hydrochloride and indomethacin from Sigma Chemical Co., U.S.A.

Results

Initial observations on the human pulmonary artery

The first three experiments showed that human pulmonary artery preparations were contracted by both PGE_2 and sulprostone (Figure 1a,b). Sensitivity was high initially with threshold effects observed at 1–5 and 0.2–0.5 nM respectively. However, there was a variable loss of sensitivity to the two PGE analogues throughout the experimental period (6–8 h). This took the form of both an increase in the EC_{50} value and a reduction in the maximum response. The phenomenon is illustrated for the whole series of experiments in Figure 2. Contractile responses to KCl, phenylephrine and the specific TP-receptor agonist U-46619 did not decay over the experimental period (data not shown).

Contractile potencies of PGE and PGF analogues

Log concentration-response curves for PGE_2 and five of its analogues, sulprostone, misoprostol, gemeprost, GR 63799X and 17-phenyl-ω-trinor PGE_2 are shown in Figure 3. Relative potencies, expressed as equi-effective molar ratios (PGE_2 = 1.0), are given in Table 1. The data derive only from the first cumulative sequence of doses on each preparation, since the variable loss of sensitivity meant that 'within preparation' estimates of relative potency (see Methods) were potentially subject to considerable error. Sulprostone was the most potent prostanoid and its rates of onset and return to resting tension on washout were always slower than those of the other prostanoids.

$PGF_{2\alpha}$ was only a weak agonist (Figure 3a) and the specific FP-receptor agonist, fluprostenol, produced no effect at concentrations up to 2 μM (2 experiments).

Antagonist studies

In a single experiment, the TP-receptor antagonist, EP 169 (200 nM), added before U-46619 blocked its contractile response, with parallel displacement of the log concentration-response curve to the right (dose-ratio = 41). Assuming reversible, competitive antagonism (Gaddum, 1957), a pA_2 value of 8.3 was obtained (single dose-ratio estimate). The log concentration-response curve to sulprostone was unaffected by this treatment. Similarly in two experiments, a second TP antagonist, GR 32191, at 200 nM failed to affect sulprostone but blocked U-46619 contractions with dose-ratios of 32 and 55, giving a mean pA_2 value of 8.3.

In three separate experiments, EP 169 (200 and 500 nM) and GR 32191 (200 nM) were added following establishment of submaximal responses to sulprostone (10 nM) and U-46619 (2–10 nM). The antagonists abolished the U-46619 response but had minimal or no effect on the sulprostone response; this is illustrated for EP 169 in Figure 4.

The interaction of sulprostone and the EP_1-receptor antagonist, AH 6809, was investigated in a similar manner to that of the TP antagonists. At 5 μM, AH 6809 had no effect on the log concentration-response curve to sulprostone (n = 1) and did not relax preparations already contracted with a submaximal concentration of sulprostone (n = 2). The same stock solutions of AH 6809 were effective in antagonizing the EP_1 contractile actions of 17-phenyl-ω-trinor PGE_2 and gemeprost on the guinea-pig isolated trachea (200 nM EP 169 present); with 2 μM AH 6809, dose-ratios of 50–60 were obtained (n = 3).

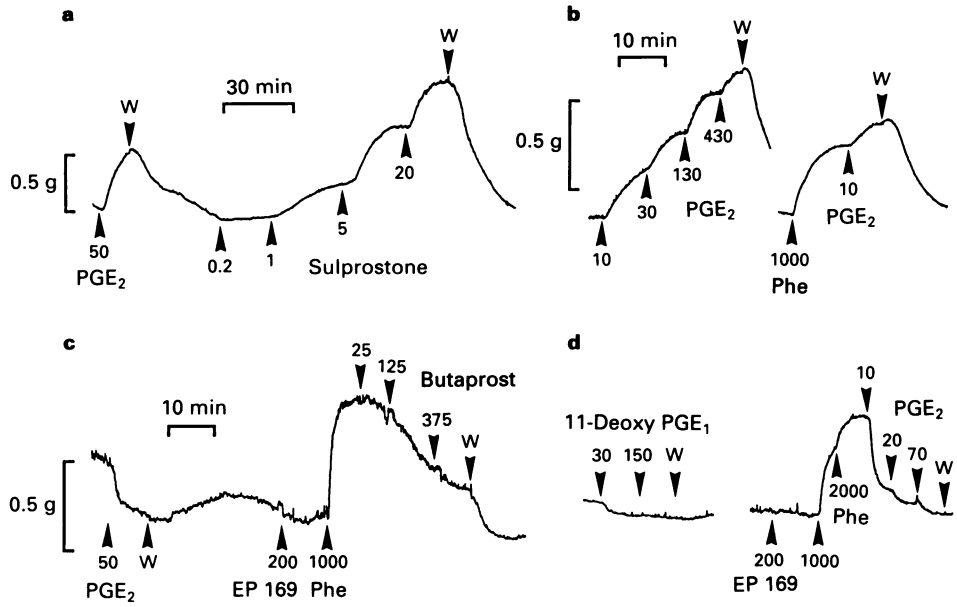


Figure 1 Experimental records showing the actions of prostaglandin E (PGE) analogues on the human isolated pulmonary artery. Records (a) and (b) are from preparations where the priming dose of PGE_2 (50 nM) induced contraction. Records (c) and (d) are from one of only two experiments in which preparations relaxed to the PGE_2 priming dose. W = wash; Phe = phenylephrine; EP 169 is a thromboxane receptor antagonist. Cumulative concentrations (nM) are shown.

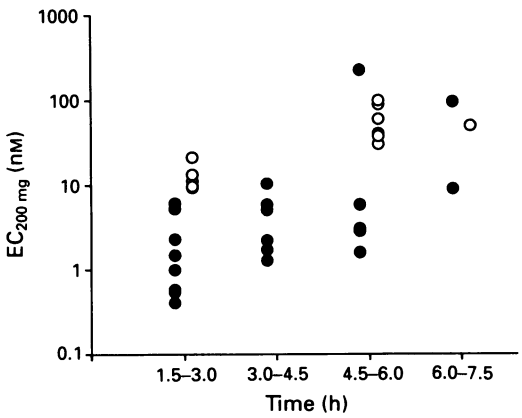


Figure 2 Changes in sensitivity to the contractile actions of sulprostone (●) and prostaglandin E_2 (PGE_2) (○) with time on the human isolated pulmonary artery. The ordinate scale is the concentration of prostanoid required to increase the tension in the preparation by 200 mg.

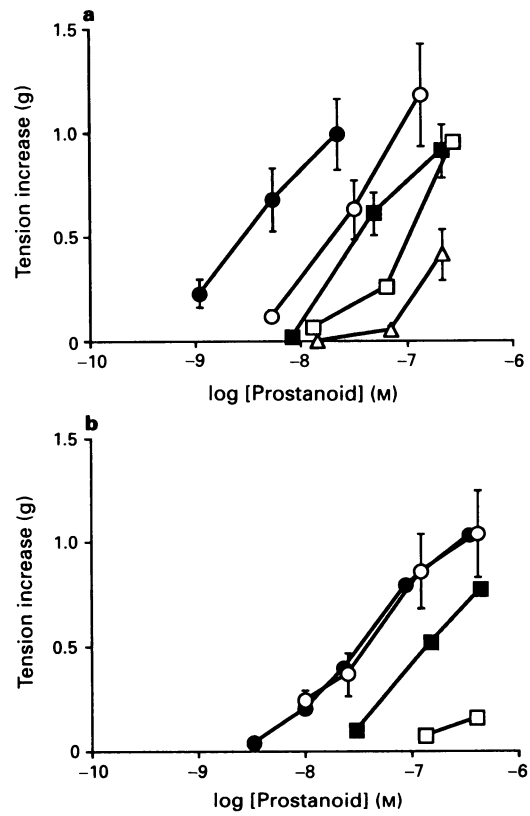


Figure 3 Log concentration-response curves for contractile effects of prostanoids on the human isolated pulmonary artery. Data were obtained between 1.5 and 3 h in experiments where the priming dose of prostaglandin E_2 (PGE_2) produced contraction. Values are mean ± s.e.mean. (a) Sulprostone (●, $n = 8$), misoprostol (○, $n = 4$), GR 63799X (■, $n = 6$), 17-phenyl-ω-trinor PGE_2 (□, mean curve, $n = 2$), $PGF_{2\alpha}$ (△, $n = 3$). (b) PGE_2 (○, $n = 4$), gemeprost (●, mean curve, $n = 2$), 11-deoxy PGE_1 (■, □, individual experiments).

Relaxant actions of prostanoids

The two prostacyclin analogues, cicaprost and TEI-9063, potently inhibited agonist-induced tone on the pulmonary artery preparations (Figure 5a). Relaxant potencies against equi-effective concentrations of phenylephrine (1–2 μM) and U-46619 (5–10 nM) were similar: e.g. cicaprost $IC_{50} = 2.6 \pm 0.5$ nM ($n = 4$) and 2.5 ± 0.5 nM ($n = 3$) respectively. However, the maximum relaxation achieved against KCl was only 65–85%; this is shown for TEI-9063 in an experiment in which the prostacyclin-mimetics were particularly potent (Figure 5a).

There was no evidence from the first 8 experiments that any of the PGE analogues examined were exerting a relaxant EP_2 action. However, we felt it was possible that a strong contractile EP action could mask a weak relaxant action. We therefore addressed this situation in the next 5 experiments by determining the effects of butaprost and 11-deoxy PGE_1 (both of which show moderate potency and selectivity for EP_2-receptors) on phenylephrine-induced tone. In three of the experiments, the PGE_2 priming dose (50 nM) increased tension by about 0.5 g, as found previously. Butaprost had no effect on basal tone at 25 nM but gave slight relaxations

Table 1 Prostanoid EP_3 agonist potencies and EP-receptor selectivities of prostaglandin E (PGE) analogues

PGE analogue	*Equi-effective molar ratio* *Contraction of human pulmonary artery*	*Inhibition of cyclic AMP in human platelets*	*Inhibition of guinea-pig vas deferens*	*EP-receptor selectivity*
PGE_2	1.0 (EC_{50} = 50 nM)	1.0 (IC_{50} = 5.5 nM)	1.0 (IC_{50} = 1.5 nM)	$EP_1 = EP_2 = EP_3$
Sulprostone	0.11	0.40	0.14	$EP_3 > EP_1 \gg EP_2$
Misoprostol	0.70	4.1	0.51	$EP_2 = EP_3 > EP_1$
Gemeprost	0.84*	–	1.0	$EP_3 = EP_1 > EP_2$
GR 63799X	1.5	8.0	0.24	$EP_3 > EP_1 \gg EP_2$
17-Phenyl-ω-trinor PGE_2	3.3*	15	6.3	$EP_1 > EP_3 > EP_2$
11-Deoxy PGE_1	≥4.3*	–	18	$EP_2 > EP_3 > EP_1$
Butaprost	Relaxation only	>140	>1000	$EP_2 \gg EP_1$ / EP_3

Human pulmonary artery data were obtained in the present study; *two experiments only. Human platelet cyclic AMP data are from Matthews & Jones (1993) and guinea-pig vas deferens data from Lawrence *et al.* (1992) .

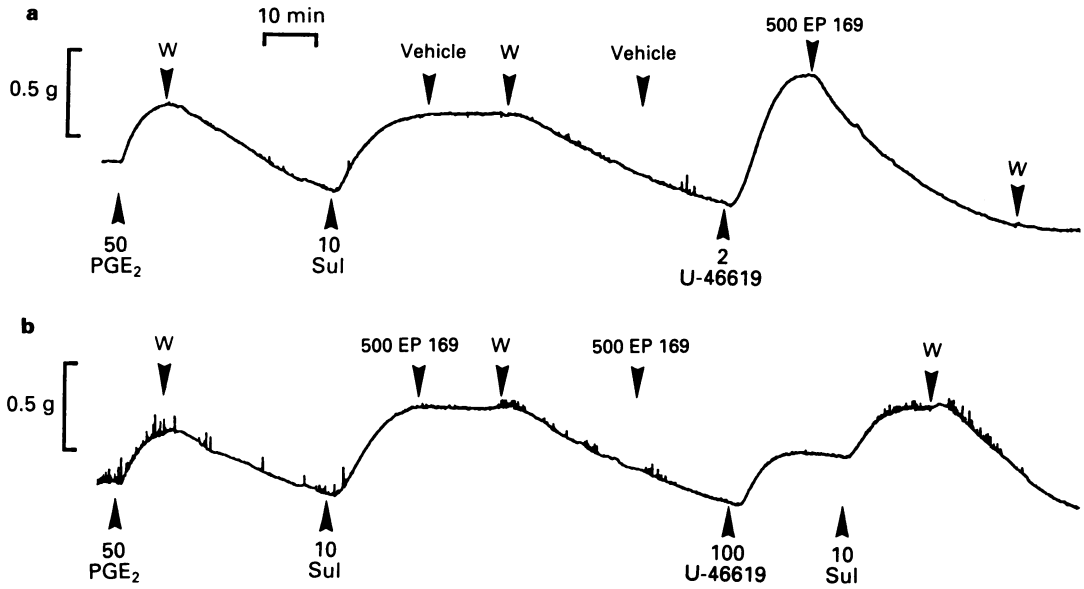


Figure 4 Experimental records showing that the TP-receptor antagonist, EP 169, blocks the contractile action of U-46619, but not that of sulprostone, on the human pulmonary artery. Records (a) and (b) are from matched preparations. Sul = sulprostone, W = wash. Concentrations are in nanomolar.

(0.05–0.15 g) at 125–375 nM. 11-Deoxy PGE_1 (30–450 nM) induced contraction, but its effects were variable (Figure 3b). After production of tone with phenylephrine, PGE_2 gave additional contractions (Figure 1b). Butaprost inhibited tone although the sensitivity of this effect was low and varied to some degree. Relaxation was not seen at 25 nM; on the most sensitive preparation, the IC_{50} value was 350 nM; on the least sensitive preparation, 375 nM butaprost induced 20% relaxation. 11-Deoxy PGE_1 (30–450 nM) had essentially no effect on preparations that were more sensitive to butaprost, whereas in butaprost-insensitive preparations additional contractions were obtained (Figure 5a).

In the other two experiments a quite different picture was seen. PGE_2 (50 nM priming dose), butaprost (125 nM) and 11-deoxy PGE_1 (30 and 150 nM) reduced the resting tone, an effect which was reversed on washing (Figure 1c,d). Phenylephrine-induced tone was also markedly inhibited by PGE_2, butaprost and 11-deoxy PGE_1 (Figures 1c,d and 5b). Butaprost was 3.1 and 4.7 times and 11-deoxy PGE_1 2.4 and 1.9 times less potent than PGE_2. The presence of 200 nM EP 169 had no effect on the response profiles. In both these experiments sensitivity to sulprostone was low, with $EC_{200\,mg}$ values ranging from 32–130 nM early in the experiments.

Discussion

Our studies demonstrate that PGE_2 can either contract or relax the circular smooth muscle of human pulmonary artery preparations. In the majority of experiments the contractile system predominated, with sulprostone being a highly potent contractile agent and butaprost showing only weak relaxant activity. However, in two experiments the balance was reversed; sulprostone was weak and butaprost showed greater relaxant potency. It must be emphasized that all our tissue came from patients with severe lung disease. Clearly there is a possibility that disease processes could have modified the contributions of the opposing receptor systems from those operative in normal lung tissue. However, there is no obvious association between the *in vitro* profile obtained and the patient data available to use.

The contractile PGE action is unlikely to be mediated by FP-receptors, since the potent and specific FP-receptor agonist, fluprostenol (Crossley, 1975; Welburn & Jones, 1978) was inactive. Although $PGF_{2\alpha}$ contracted the preparations, it achieves this by activation of TP-receptors (Norel *et al.*, 1991). Activation of TP-receptors also seemed unlikely since sulprostone has only weak TP-agonist activity on standard

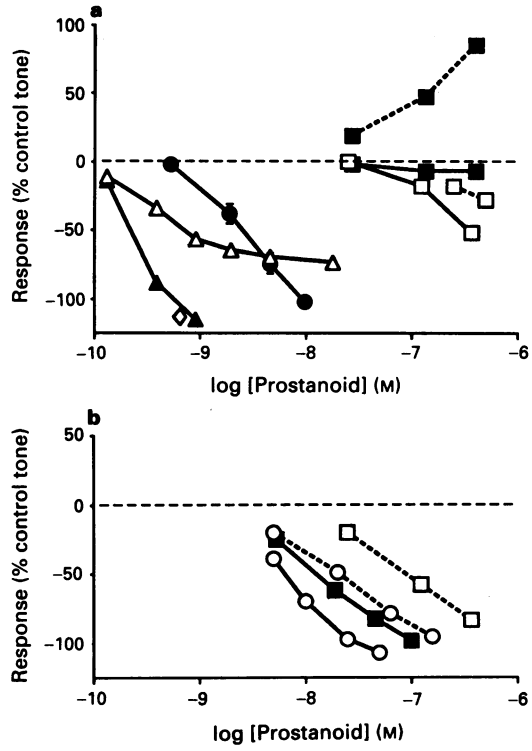


Figure 5 Relaxant effects of prostanoids against induced tone on human isolated pulmonary artery. (a) All preparations gave a contractile response to the prostaglandin E_2 (PGE_2) priming dose. Lower left: cicaprost against phenylephrine (●, $n = 4$) and TEI-9063 against phenylephrine (◇), U-46619 (▲) and KCl (△) in a single experiment. Upper right: 11-deoxy PGE_1 (■) and butaprost (□) against phenylephrine on two preparations (——, - - -) in the same experiment; EP 169 (200 nM) was present. (b) Single experiment in which the priming dose of PGE_2 relaxed basal tone. PGE_2 (○), 11-deoxy PGE_1 (■) and butaprost (□) against phenylephrine in two preparations (——, - - -); EP 169 (200 nM) was present.

TP preparations such as rat aorta (Coleman *et al.*, 1988). Two direct pieces of evidence support this view. First, two potent and specific TP-receptor antagonists did not block the contractile action of sulprostone; EP 169 has a pA_2 range of 8.3–8.8 on standard TP preparations (excluding rabbit tissues which are relatively insensitive to TP antagonists) (Tymkewycz *et al.*, 1991). GR 32191 has been examined previously for block of U-46619 on the human pulmonary artery (Lumley *et al.*, 1989); the reported pA_2 of 8.2 is in agreement with observations in this study. Secondly cross-tachyphylaxis between sulprostone and the TP-receptor agonist, U-46619, was not found. Indeed responses to KCl and phenylephrine were also well maintained throughout the experimental period, thus indicating that the preparations were not generally deteriorating. In general, the agonist actions of PGE analogues are not prone to tachyphylaxis, and this applies to inhibitory (EP_3) actions on the guinea-pig vas deferens (see later).

The most probable mechanism underlying the potent contractile actions of PGE_2 and its analogues is therefore activation of EP_1- and/or EP_3-receptors. The EP_1-receptor can be excluded since the EP_1 antagonist, AH 6809 at 5 μM, did not block the contractile action of sulprostone; given a pA_2 of 6.8 (Coleman *et al.*, 1985) to 7.35 (Lawrence *et al.*, 1992), a dose ratio of 30–110 would be expected. Support for the presence of an EP_3-receptor subtype in the pulmonary artery derives from our measurements of the agonist potencies of the eight PGE analogues examined (Table 1). In particular, sulprostone was found to be more potent than 17-phenyl-ω-trinor PGE_2. This is the situation in the guinea-pig vas deferens, the archetypal EP_3 preparation, whereas the 17-phenyl analogue is more potent on EP_1 preparations such as the guinea-pig trachea and ileum (Lawrence *et al.*, 1992). However it is necessary to emphasize that there is some discrepancy between relative agonist potencies obtained on the guinea-pig vas deferens and those obtained on another EP_3 system, namely inhibition of adenosine 3':5'-cyclic monophosphate (cyclic AMP) accumulation in human washed platelets (Matthews & Jones, 1993). The latter mechanism appears to be involved in the potentiating action of PGE analogues on platelet aggregation induced by ADP, PAF or U-46619. In particular GR 63799X (Bunce *et al.*, 1990) was relatively less potent on the human platelet compared to the vas deferens. Similarly in the present experiments, GR 63799X is somewhat less potent than sulprostone.

Of the other PGE analogues with potent contractile activity on the pulmonary artery, gemeprost (Cervagem) is used for induction of second trimester abortion and for cervical softening prior to surgical termination of first trimester pregnancy (Crowshaw, 1983; Cameron & Baird, 1984b; see Dollery, 1991). Like its close relative, 16,16-dimethyl PGE_2, it is a potent EP_3-agonist on the guinea-pig vas deferens (Table 1) and a potent EP_1-receptor agonist on the guinea-pig trachea ($EC_{50} = 3.8$ nM, 200 nM EP 169 present). Due to its unavailability at the time, gemeprost was not tested on the human platelet cyclic AMP system.

With respect to prostanoid-induced relaxation of the pulmonary artery, we have confirmed earlier reports (Hadhazy *et al.*, 1985; Haye-Legrand *et al.*, 1987) of the potent action of cicaprost, a chemically stable analogue of prostacyclin (Sturzebecher *et al.*, 1986). TEI-9063, an isocarbacyclin analogue with potent inhibitory effects on human platelets (Negishi *et al.*, 1991), was also a potent relaxant agent. Since cicaprost is the most specific of the prostacyclin-mimetics examined to date (Dong *et al.*,1986; Lawrence *et al.*, 1992), we presume these agents are acting on IP-receptors in the pulmonary artery.

On preparations where PGE_2 was contractile, butaprost, a selective EP_2 agonist (Gardiner, 1986), produced relaxation at relatively high concentrations. This effect may be due to activation of EP_2-receptors, but in view of the very high sensitivity of the artery preparations to prostacyclin mimetics, a contribution from IP-receptor activation cannot be ruled out. Stronger evidence for the presence of relaxant EP_2-receptors was obtained in just two experiments. PGE_2 inhibited phenylephrine-induced tone at concentrations of 5 nM and above, and 11-deoxy PGE_1 and butaprost were only about 2 and 4 times less potent. The variable activity of 11-deoxy PGE_1 appears to be due to its ability to activate both contractile EP_3 (Table 1) and relaxant EP_2 systems, coupled with differing sensitivities of the two systems in different preparations in the same experiment and in different experiments. In contrast, butaprost did not contract preparations which contracted well to PGE_2 and sulprostone, since it is essentially devoid of EP_3 agonist activity (Lawrence *et al.*, 1992).

There have been several reports of cardiovascular collapses associated with the use of PGE_2 for obstetric purposes (Cameron & Baird, 1984a; Kilpatrick & Thorburn, 1990). There have also been reports of myocardial infarction (Fliers *et al.*, 1991) and of several deaths associated with the use of sulprostone, usually administered in combination with the progesterone antagonist, mifepristone (Editorial, 1991). If pulmonary hypertension were a causative factor in these incidents, then the balance between EP_2 dilator and EP_3 constrictor actions in the pulmonary circulation may have been weighted towards the latter. In terms of the receptor selectivity of the prostanoid, sulprostone does not have EP_2 dilator activity. Misoprostol does however, and in combination with the progesterone antagonist, mifepristone, is being strongly recommended for termination of early pregnancy (Peyron *et al.*, 1993). In relation to the relative sensitivity of the contractile/relaxant systems in the lung vessels, it would be of great interest to measure this during pregnancy. How-

ever, from both ethical and logistical standpoints, this is unlikely to be possible.

It is also possible that sulprostone has other cardiovascular actions which could accentuate the harmful effects of its direct pulmonary vasoconstrictor action. Thus in preliminary experiments performed by us in the anaesthetized cat, sulprostone ($0.1-1\ \mu g\ kg^{-1}$) induced a sustained rise in arterial blood pressure. An increase in cardiac output secondary to systemic venoconstriction appears a likely mechanism, in view of our observation that sulprostone at concentrations of 10 nM and above contracted circular smooth muscle of the abdominal vena cava of the cat.

Finally it must be borne in mind that EP_3-receptor agonists may have two interactive and potentially dangerous actions in man, the pulmonary vasoconstrictor action reported here and the ability to potentiate platelet aggregation investigated previously by us (Matthews & Jones, 1993).

Gifts of prostanoids from pharmaceutical companies (see Methods) are gratefully acknowledged. This work was supported by a grant from the University and Polytechnic Grants Committee of Hong Kong.

References

BUNCE, K.T., CLAYTON, N.M., COLEMAN, R.A., COLLINGTON, E.W., FINCH, H., HUMPHRAY, J.M., HUMPHREY, P.P.A., REEVES, J.J., SHELDRICK, R.L.G. & STABLES, R. (1990). GR 63799X – a novel prostanoid with selectivity for EP_3 receptors. In *Advances in Prostaglandin, Thromboxane and Leukotriene Research*, Vol. 21. ed. Samuelsson, B., Paoletti, R. & Ramwell, P.W. pp. 379–382. New York: Raven Press.

BYGDEMAN, M. (1990). Non-invasive methods for termination of second trimester pregnancy. *Bailliere's Clin. Obstet. Gynaecol.*, **4**, 351–359.

BYGDEMAN, M., KWON, S.U., MUKHERJEE, T. & WIQVIST, N. (1968). Effect of intravenous infusion of prostaglandin E_1 and E_2 on the pregnant human uterus. *Am. J. Obstet. Gynecol.*, **102**, 317–325.

CAMERON, I.T. & BAIRD, D.T. (1984a). Sudden collapse after intra-amniotic prostaglandin E_2 injection. *Lancet*, **i**, 1046–1047.

CAMERON, I.T. & BAIRD, D.T. (1984b). The use of 16,16-dimethyl-*trans*-Δ^2 PGE_1 methyl ester (gemeprost) vaginal pessaries for the termination of pregnancy in the early second trimester. A comparison with extra-amniotic prostaglandin E_2. *Br. J. Obstet. Gynaecol.*, **91**, 1136–1140.

COLEMAN, R.A., HUMPHRAY, J.M., SHELDRICK, R.L.G. & WHITE, B.P. (1988). Gastric antisecretory prostanoids: actions at different prostanoid receptors. *Br. J. Pharmacol.*, **95**, 724P.

COLEMAN, R.A., KENNEDY, I. & SHELDRICK, R.L.G. (1985). AH6809, a prostanoid EP_1 antagonist. *Br. J. Pharmacol.*, **85**, 273P.

COLEMAN, R.A., KENNEDY, I. & SHELDRICK, R.L.G. (1987a). Evidence for the existence of three subtypes of PGE_2 (EP) sensitive receptors in smooth muscle. *Br. J. Pharmacol.*, **91**, 323P.

COLEMAN, R.A., KENNEDY, I. & SHELDRICK, R.L.G. (1987b). Further evidence for the existence of three subtypes of PGE_2- (EP)-sensitive receptors in smooth muscle. *Br. J. Pharmacol.*, **91**, 407P.

CROSSLEY, N.S. (1975). The synthesis and biological activity of potent, selective luteolytic prostanoids. *Prostaglandins*, **10**, 5–13.

CROWSHAW, K. (1983). Comparison of the pharmacological and biochemical properties of ONO-802 (Cervagem) and the naturally occurring prostaglandins. In *Cervagem. A New Prostaglandin in Obstetrics and Gynaecology*. ed. Karim, S.M.M. pp. 1–14. Lancaster: MTP Press Ltd.

DOLLERY, C. (1991). Gemeprost. In *Therapeutic Drugs*. pp. G10–G12. Edinburgh: Churchill Livingstone.

DONG, Y.J., JONES, R.L. & WILSON, N.H. (1986). Prostaglandin E receptor subtypes in smooth muscle: agonist activities of stable prostacyclin analogues. *Br. J. Pharmacol.*, **87**, 97–107.

EDITORIAL (1991). A death associated with mifepristone/sulprostone. *Lancet*, **337**, 969–970.

FLIERS, E., DUREN, D.R. & VAN ZWIETEN, P.A. (1991). A prostaglandin analogue as a probable cause of myocardial infarction in a young woman. *Br. Med. J.*, **302**, 416.

GADDUM, J.H. (1957). Theories of drug antagonism. *Pharmacol. Rev.*, **9**, 211–218.

GARDINER, P.J. (1986). Characterisation of prostanoid relaxant/inhibitory receptors (Ψ) using a highly selective agonist, TR 4979. *Br. J. Pharmacol.*, **87**, 45–56.

HADHAZY, P., MALOMVOLGYI, B., MAGYAR, K., DEBRECZENI, A. & HUTAS, I. (1985). Species dependent relaxation of intrapulmonary arteries (IPA) of rabbits, dogs and humans by prostacyclin. *Prostaglandins*, **29**, 673–688.

HAYE-LEGRAND, I., BOURDILLAT, B., LABAT, C., CERRINA, J., NOREL, X., BENVENISTE, J. & BRINK, C. (1987). Relaxation of isolated pulmonary muscle preparations with prostacyclin (PGI_2) and its analogs. *Prostaglandins*, **33**, 845–854.

HOPPE, G. (1986). Sulprostone: a therapeutic advance in post-partum haemorrhage. In *2nd Asian Symposium on Prostaglandins and Sulprostone*. pp. 63–73. Asia Pacific Congress Series No 57, Hong Kong: Excerpta Medica Asia Ltd.

JONES, R.L., QIAN, Y.M., CHAN, K.M., STOCK, A. & HO, J.K.S. (1994). Sulprostone is a potent contractile agent on human pulmonary artery in vitro: possible therapeutic implications. *Br. J. Pharmacol.*, **112**, 188P.

KILPATRICK, A.W.A. & THORBURN, J. (1990). Severe hypotension due to intramyometrial injection of prostaglandin E_2. *Anaesthesia*, **43**, 848–849.

LAWRENCE, R.A. & JONES, R.L. (1992). Investigation of the prostaglandin E (EP-) receptor subtype mediating relaxation of the rabbit jugular vein. *Br. J. Pharmacol.*, **105**, 817–824.

LAWRENCE, R.A., JONES, R.L. & WILSON, N.H. (1992). Characterisation of receptors involved in the direct and indirect actions of prostaglandins E and I on the guinea-pig ileum. *Br. J. Pharmacol.*, **105**, 271–278.

LUMLEY, P., WHITE, B.P. & HUMPHREY, P.P.A. (1989). GR 32191, a highly potent and specific thromboxane receptor blocking drug on platelets and vascular smooth muscle *in vitro*. *Br. J. Pharmacol.*, **97**, 783–794.

MATTHEWS, J.S. & JONES, R.L. (1993). Potentiation of aggregation and inhibition of adenylate cyclase in human platelets by prostaglandin E analogues. *Br. J. Pharmacol.*, **108**, 363–369.

NEGISHI, M., HASHIMOTO, H., YATSUNAMI, K., KUROZUMI, S. & ICHIKAWA, A. (1991). TEI-9063, a stable and highly specific prostacyclin analogue for the prostacyclin receptor in mastocytoma P-815 cells. *Prostaglandins*, **42**, 225–237.

NOREL, X., LABAT, C., GARDINER, P.J. & BRINK, C. (1991). Inhibitory effects of BAY u3405 on prostanoid-induced contractions in human isolated bronchial and pulmonary arterial muscle preparations. *Br. J. Pharmacol.*, **104**, 591–595.

PEYRON, R., AUBENY, E., TARGOSZ, V., SILVESTRE, L., RENAULT, M., ELKIK, F., LECLERC, P., ULMANN, A. & BAULIEU, E.E. (1993). Early termination of pregnancy with mifepristone (RU 486) and the orally active prostaglandin misoprostol. *New Engl. J. Med.*, **328**, 1509–1513.

SENIOR, J., MARSHALL, K., SANGHA, R. & CLAYTON, J.K. (1993). *In vitro* characterization of prostanoid receptors on human myometrium at term pregnancy. *Br. J. Pharmacol.*, **108**, 501–506.

STOCK, A.I., JONES, R.L., CHUNG, T. & FUNG, H.Y.M. (1994). Pulmonary oedema in association with an intravenouis infusion of sulprostone. *Acta Obstet. Gynecol. Scand.* (in press).

STURZEBECHER, S., HABEREY, M., MUELLER, B., SCHILLINGER, E., SCHRODER, G., SKUBALLA, W., STOCK, G., VORBRUGGEN, H. & WITT, W. (1986). Pharmacological profile of a novel carbacyclin derivative with high metabolic stability and oral activity in the rat. *Prostaglandins*, **31**, 95–109.

TRENDS PHARMACOL. SCI. (TIPS) (1994). Prostanoid receptors. In *Receptor and Ion Channel Nomenclature Supplement*. ed. Watson, S. & Girdlestone, D. pp. 36–37. Cambridge: Elsevier Trends Journals.

TYMKEWYCZ, P.M., JONES, R.L., WILSON, N.H. & MARR, C.G. (1991). Heterogeneity of thromboxane (TP-) receptors: evidence from antagonist but not agonist potency measurements. *Br. J. Pharmacol.*, **102**, 607–614.

WELBURN, P.J. & JONES, R.L. (1978). A comparison of prostaglandin $F_{2\alpha}$ and three 16-aryloxy analogues on the isolated rabbit jejunum. *Prostaglandins*, **15**, 287–296.

(Received April 5, 1994
Revised May 25, 1994
Accepted May 26, 1994)

Br. J. Pharmacol. (1994), **113**, 375–378 © Macmillan Press Ltd, 1994

Decrease in calcium currents induced by aminoglycoside antibiotics in frog motor nerve endings

R.S. Redman & [1]E.M. Silinsky

Department of Molecular Pharmacology and Biological Chemistry, Searle 8-477, Northwestern University Medical School, 303 E. Chicago Ave., Chicago, IL 60611, U.S.A.

1 The effects of the aminoglycoside antibiotics, streptomycin, neomycin and gentamicin were examined on perineural currents and evoked acetylcholine (ACh) release at frog motor nerve endings.

2 In the standard solutions used previously to measure Ca^{2+} currents, streptomycin reduced the peak amplitude of the Ca^{2+} component of the perineural current.

3 In a solution in which changes in both Ca^{2+} currents and evoked ACh release can be recorded simultaneously, both Ca^{2+} currents and evoked ACh release were reduced by aminoglycosides in the potency order neomycin > streptomycin > gentamicin. This potency sequence is similar to that reported previously for these agents as inhibitors of neurally-evoked contractions of mammalian skeletal muscle.

4 These data suggest that the presynaptic inhibitory effects of aminoglycoside antibiotics at the neuromuscular junction occur as a consequence of a reduction in Ca^{2+} currents in the motor nerve terminal.

Keywords: Aminoglycosides; calcium channels; calcium currents; motor endplate; myaesthenia gravis; neuromuscular junction; neuromuscular transmission; neurotransmitter release; streptomycin; neomycin; gentamicin

Introduction

When certain aminoglycoside antibiotics are used clinically under conditions in which the function of the postjunctional endplate membrane is compromised, synergistic blockade of neuromuscular transmission occurs (Pittinger & Adamson, 1972; Burkett *et al.*, 1979). For example, the release of acetylcholine (ACh) is inhibited by streptomycin, neomycin, kanamycin and gentamicin (for review see Mandell & Sande, 1990); such presynaptic effects have led to the paralysis by these drugs of unanesthetized patients afflicted with myaesthenia gravis (Pittinger & Adamson, 1972), a disorder in which the number of post-junctional ACh receptors is reduced (Lopate & Pestronk, 1990).

The neuromuscular blocking effects of these antibiotics, which may be surmounted by increasing the extracellular Ca^{2+} concentrations (see e.g. Singh *et al.*, 1978), are often ascribed to a reduction in Ca^{2+} entry into the nerve ending (Molgo *et al.*, 1979; Atchison *et al.*, 1988). In contrast, it has also been suggested that these drugs could work by competing with Ca^{2+} for ACh release sites (Fieckers, 1983). This latter suggestion provides a viable alternative interpretation of the data, as the presence of spare Ca^{2+} channels would allow a competitive relationship between *intracellular* Ca^{2+} and aminoglycoside drugs to be reflected in the relationship between *extracellular* Ca^{2+} and the drug (Silinsky, 1981). In an attempt to distinguish between these two possibilities, we thus decided to investigate if streptomycin, neomycin, and gentamicin blocked Ca^{2+} channels under conditions in which simultaneous measurements of Ca^{2+} currents and evoked ACh release (i.e. e.p.ps) may be made. The relative potencies of these agents as inhibitors of Ca^{2+} currents were also evaluated and compared with published data on the potencies of these agents in reducing the neurally-evoked twitch of skeletal muscle.

Methods

Methods for electrophysiological recording and superfusion of solutions were as described previously (Silinsky & Solsona, 1992; Redman & Silinsky, 1993a,b; 1994). Briefly, following immersion anaesthesia, cutaneous pectoris nerve muscle preparations of frog were dissected and superfused with flowing Ringer solution. Neurally-evoked responses (Ca^{2+} currents and e.p.ps) were recorded with conventional electrophysiological equipment (for complete details see Silinsky & Solsona, 1992; Redman & Silinsky, 1993a; 1994). Simultaneous measurements of Ca^{2+} currents and e.p.ps were made after blockade of a proportion of the K^+ channels. For the perineural currents, microelectrodes of 5–15 MΩ resistances filled with normal Ringer solution were positioned under visual control near small axon bundles at the termination of the myelin sheaths and within 50 μm of the intracellular recording electrode used for measuring e.p.ps. For further details of the perineural current waveforms and potential sources of contamination of Ca^{2+} currents at frog motor nerve endings, see Silinsky & Solsona (1992), Mallart (1984), Anderson *et al.* (1988) and Molgo *et al.* (1991).

The Ringer solution contained (mM) NaCl 115, KCl 2, HEPES 2 (pH 7.2–7.4), tubocurarine chloride (4–30 mg l^{-1}), and various concentrations of Ca^{2+}, Mg^{2+}, and the K^+ channel blockers 3,4,diaminopyridine (DAP) and tetraethylammonium (TEA). A modified Ringer solution, which contained $CaCl_2$ 0.9 mM, $MgCl_2$ 10 mM, DAP 100 μM and TEA 250 μM was used for the experiments in which Ca^{2+} currents were measured simultaneously with e.p.ps (Ca^{2+} current Ringer, e.g. Figure 2). These specific concentrations of K^+ channel blockers enabled us to measure changes in ACh release (i.e. e.p.ps) and changes in Ca^{2+} currents simultaneously with minimal complications arising from opposing Ca^{2+}-activated K^+ currents observed in the absence of TEA and without the profound depletion of ACh release seen in the presence of higher concentrations of K^+ channel blockers (see e.g. Anderson *et al.*, 1988). These concentrations of K^+ channel blockers also allowed for the detection of both increases and decreases in Ca^{2+} currents as the extracellular Ca^{2+} concentrations were changed accordingly (Redman & Silinsky, 1993a,b). The mean number of ACh quanta released in response to a nerve impulse (m) was estimated using the tubocurarine method in accordance with the following equation:

$$m = \frac{\text{e.p.p. amplitude}}{\text{m.e.p.p. amplitude}} (1 + 4\ [\text{tubocurarine}]) \qquad (1)$$

[1] Author for correspondence.

where the m.e.p.p. amplitude refers to the mean amplitude of the miniature e.p.ps *in the absence of tubocurarine* and the e.p.p. amplitude reflects the mean e.p.p. amplitude *in the presence of tubocurarine*. Concentrations of tubocurarine are in units of $mg\,l^{-1}$, with the number 4 reflecting the equilibrium affinity of tubocurarine for the ACh receptor in $1\,mg^{-1}$ (see Silinsky, 1981 for further details of this method). In Ca^{2+} current Ringer, the number of ACh quanta released by a nerve impulse as calculated by eqn 1 ranged from 344 to 569 with a mean of 457 ± 23.8 (mean $\pm$ s.e.mean, $n = 22$). Streptomycin, which was pilfered with permission from Dr Chau Wu, was generally used at a concentration of 50 μM. This concentration inhibits evoked ACh release by approximately 50% (Farley *et al.*, 1982) with only minor effects on the postjunctional sensitivity to ACh (Farley *et al.*, 1982; Fieckers, 1983). Neomycin and gentamicin were obtained from Sigma (St. Louis, MO, U.S.A.).

Results

Figure 1 shows perineural recordings of Ca^{2+} currents (upward deflection) under conditions similar to those used by others to measure these currents in frog motor nerve endings (e.g. Figure 4, Molgo *et al.*, 1991). The solution contained TEA 10 mM, DAP 1 mM and Ca^{2+} 8 mM. Note that streptomycin at a concentration found previously to depress evoked ACh release from frog motor nerve by approximately 50% (Farley *et al.*, 1982), reduced the peak of the Ca^{2+} component of the perineural current without changing the Na^+ component. The Ca^{2+} channel blocker, Cd^{2+} (500 μM, Figure 1), further reduced the amplitude of the Ca^{2+} current beyond that produced by streptomycin.

The experimental conditions of Figure 1 are associated with such high levels of ACh output that rapid depletion of available ACh quanta precludes simultaneous measurements of Ca^{2+} currents and evoked ACh release (Anderson *et al.*, 1988). We have found that Ringer solution containing reduced concentrations of TEA, DAP, Ca^{2+} 0.9 mM and Mg^{2+} 10 mM (Ca^{2+} current Ringer, see Methods) permits changes in Ca^{2+} currents to be measured simultaneously with changes in e.p.ps (Redman & Silinsky, 1993a,b); however, this solution produced repetitive firing of the nerves. Figure 2 shows the typical experimental result. Note that streptomycin reduced both the average Ca^{2+} current (a) and e.p.p. (b) measured simultaneously in Ca^{2+} current Ringer. The prejunctional inhibitory effect of streptomycin on ACh release is responsible for the reduction in e.p.p. amplitude by 50% (Farley *et al.*, 1982). (For a discussion of repetitive firing in such solutions, see Silinsky & Solsona, 1992.) Similar results

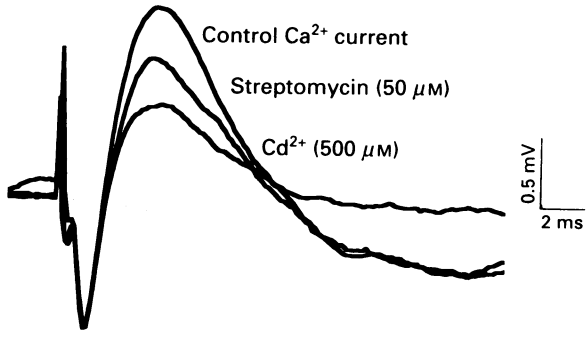


Figure 1 Effects of streptomycin (50 μM) on perineural Ca^{2+} currents in a solution containing Ca^{2+} 8 mM, TEA 10 mM and DAP 1 mM. Streptomycin reduced the Ca^{2+} component of the averaged perineural current ($n = 5$ stimuli) to 66% of the control level. Cd^{2+} further reduced the amplitude of the Ca^{2+} current to 25% of the control level. Stimulation frequency 0.015 Hz. Failure of two traces to return to baseline is due to repetitive firing. For abbreviations, see text.

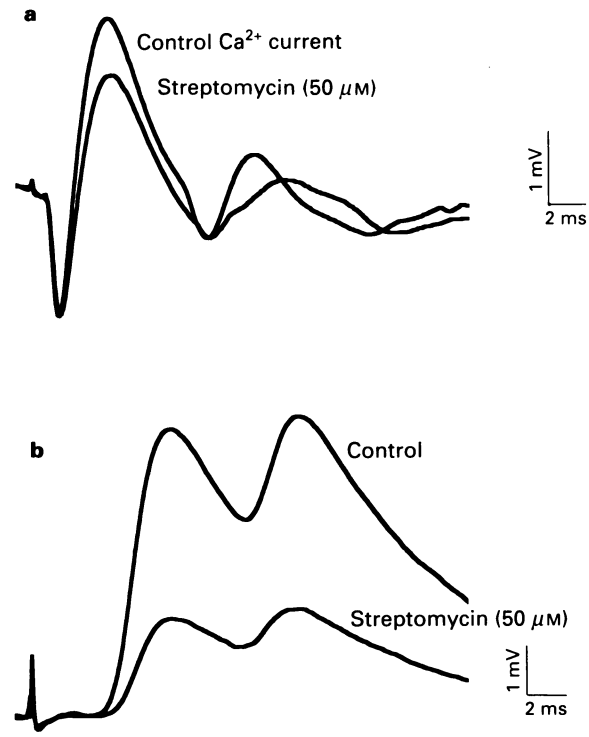


Figure 2 Effects of streptomycin (50 μM) on perineural Ca^{2+} currents (a) and evoked acetylcholine release (e.p.ps, b) as measured simultaneously in Ca^{2+} current Ringer (see Methods). Streptomycin reduced the peak Ca^{2+} component of the averaged perineural current ($n = 3$ stimuli) to 67% of the control and the averaged e.p.p. to 34% of the control. For a discussion of the repetitive firing in the presence of K^+ channel blockade, see Silinsky & Solsona (1992). Stimulation frequency 0.05 Hz.

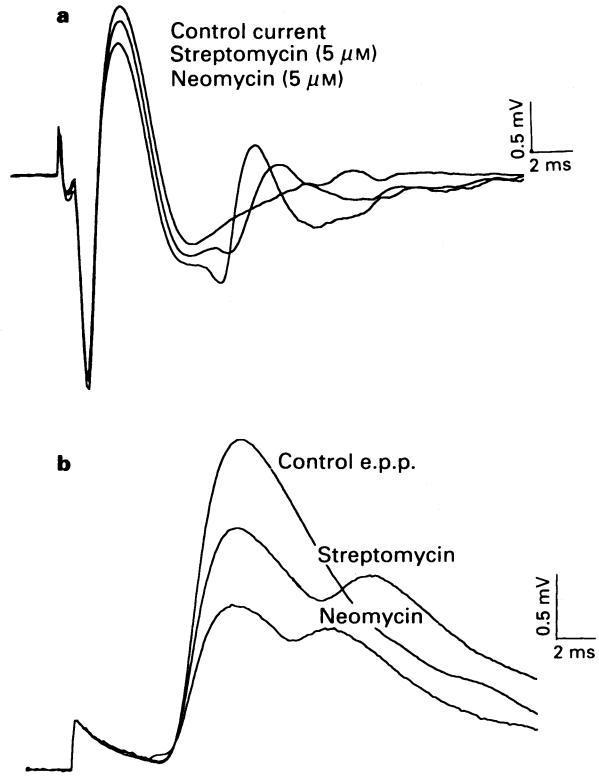


Figure 3 Simultaneous measurements of the effects of streptomycin and neomycin (5 μM) on perineural Ca^{2+} currents (a) and evoked acetylcholine release (b). Streptomycin ($n = 14$ stimuli) was applied first, washed off after a maximal response was obtained (approximately 6 min), followed by the application of neomycin ($n = 12$ stimuli).

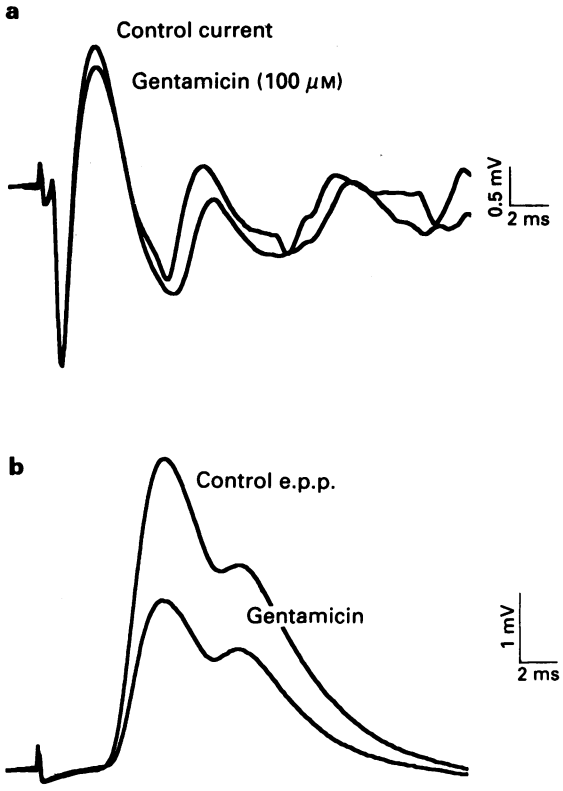


Figure 4 Effects of gentamicin (100 μM) on perineural Ca^{2+} currents (a) and evoked acetylcholine release (b). Gentamicin reduced the Ca^{2+} component of the averaged current ($n = 6$ stimuli) to 85% of the control and the averaged e.p.p. ($n = 12$ stimuli) to 54% of the control.

were observed in 14 other experiments, in which the inhibitory effects of 50 μM streptomycin on ACh release were associated with decreases in Ca^{2+} currents ranging from 66% to 81% of control. This effect of streptomycin on both ACh release and Ca^{2+} currents can be roughly approximated by a reduction in the Ca^{2+} concentration from 0.9 mM to 0.45 mM in the Ca^{2+} current Ringer.

It would appear of interest to compare the relative potencies of different aminoglycoside antibiotics that impair the twitch of the neuromuscular junction with the potencies of these antibiotics in reducing Ca^{2+} currents. Figure 3 compares the effects of 5 μM neomycin and 5 μM streptomycin on both the Ca^{2+} component of the perineural current and in e.p.p. amplitude. Note that 5 μM neomycin produced a 21% reduction in the Ca^{2+} current and a 52% reduction in the e.p.p. amplitude, whereas, streptomycin at the same concentration produced only an 8% reduction in the Ca^{2+} current and a 30% decrease in e.p.p. A similar high potency of neomycin was seen in three other experiments.

Gentamicin, was the least potent of the tested aminoglycoside antibiotics. It began to inhibit neuromuscular transmission only at concentrations $\geqslant 50$ μM. As Figure 4 shows, a concentration of 100 μM was required to produce a 15% reduction in the Ca^{2+} current and a 45% reduction in the e.p.p. amplitude. A similar low potency of gentamicin was observed in four other experiments.

Discussion

These results demonstrate a reduction in Ca^{2+} currents by the aminoglycoside antibiotics, streptomycin, neomycin, and gentamicin. The order of potency of these agents, neomycin > streptomycin > gentamicin on Ca^{2+} currents is the same order as that found for these agents to reduce the neurally-evoked twitches of mammalian muscle (Singh *et al.*, 1978). The results thus suggest that the presynaptic neuromuscular blocking effects of aminoglycoside antibiotics are attributable to a reduction in Ca^{2+} entry through voltage-sensitive Ca^{2+} channels. Preliminary experiments in which streptomycin (50 μM) produces reductions of Ca^{2+} currents and e.p.ps in mouse phrenic nerve-hemidiaphragm preparations in a manner similar to the effects shown in Figure 2 in frog provide support for this suggestion.

The Ca^{2+} current studied in this work is also inhibited by ω-conotoxin and by Cd^{2+} and thus represents the Ca^{2+} current flowing through N-type channels that is responsible for evoked ACh release in frog (Molgo *et al.*, 1991; Silinsky & Solsona, 1992; Redman & Silinsky, 1993a). It is of interest that aminoglycoside antibiotics have been shown previously to inhibit the binding of the Ca^{2+} channel blocker, ω-conotoxin to neuronal membranes (Knaus *et al.*, 1987).

In conclusion, this paper provides the first direct electrophysiological evidence in support of the hypothesis that aminoglycoside antibiotics at therapeutic concentrations, inhibit ACh release from vertebrate motor nerve endings by reducing Ca^{2+} entry through voltage-gated Ca^{2+} channels.

This work was supported by a grant from the NIH (NS 12782).

References

ANDERSON, A.J., HARVEY, A.L., ROWAN, E.G. & STRONG, P.N. (1988). Effects of charbydotoxin, a blocker of calcium-activated potassium channels, on motor nerve terminals. *Br. J. Pharmacol.*, **95**, 1329–1335.

ATCHISON, W.D., ADGATE, L. & BEAMAN, C.M. (1988). Effects of antibiotics on uptake of calcium into isolated nerve terminals. *J. Pharmacol. Exp. Ther.*, **245**, 394–401.

BURKETT, L., BIKHAZI, G.B., THOMAS, K.C., ROSENTHAL, D.A., WIRTA, M.G. & FOLDES, F.F. (1979). Mutual potentiation of the neuromuscular effects of antibiotics and relaxants. *Anesth. Analg.*, **58**, 107–115.

FARLEY, J.M., WU, C.H. & NARAHASHI, T. (1982). Mechanism of neuromuscular block by streptomycin: a voltage clamp analysis. *J. Pharmacol. Exp. Ther.*, **222**, 488–493.

FIECKERS, J.F. (1983). Effects of the aminoglycoside antibiotics, streptomycin, neomycin, on neuromuscular transmission. I. Presynaptic considerations. *J. Pharmacol. Exp. Ther.*, **225**, 487–495.

KNAUS, H.G., STREISSNIG, J., KOZA, A. & GLOSSMAN, H. (1987). Neurotoxic aminoglycoside antibiotics are potent inhibitors of [^{125}I]-omega-conotoxin GVIA binding to guinea-pig cerebral cortex membranes. *Naunyn-Schmied. Arch. Pharmacol.*, **336**, 583–586.

LOPATE, G. & PESTRONK, A. (1993). Autoimmune Myasthenia Gravis. *Hospital Practice*, **28**, 109–131.

MALLART, A. (1984). Presynaptic currents in frog motor endings. *Pflügers Arch.*, **400**, 8–13.

MANDELL, G.L. & SANDE, M.A. (1990). Antimicrobial Agents. In: *Goodman and Gilmans's The Pharmacological Basis of Therapeutics*, ed. Gilman, A.G., Rall, T.W., Nies, A.S. & Taylor, P. pp. 1065–1116. New York: Pergamon Press.

MOLGO, J., LEMEIGNAN, M., UCHIYAMA, T. & LECHAT, P. (1979). Inhibitory effect of kanamycin on evoked transmitter release. Reversal by 3,4-diaminopyridine. *Eur. J. Pharmacol.*, **57**, 93–97.

MOLGO, J., DEL POZO, E., BANOS, J.E. & ANGAUT-PETIT, D. (1991). Changes of quantal transmitter release caused by gadolinium ions at the frog neuromuscular junction. *Br. J. Pharmacol.*, **104,** 133–138.

PITTINGER, C. & ADAMSON, R. (1972). Antibiotic blockade of neuromuscular function. *Annu. Rev. Pharmacol.*, **12,** 169–184.

REDMAN, R.S. & SILINSKY, E.M. (1993a). A selective adenosine antagonist (8-cyclopentyl-1,3,-dipropylxanthine) eliminates both neuromuscular depression and the action of exogenous adenosine by an effect on A_1 receptors. *Mol. Pharmacol.*, **44,** 835–840.

REDMAN, R.S. & SILINSKY, E.M. (1993b). On the simultaneous measurements of calcium currents and acetylcholine release from motor nerve endings. *Soc. Neurosci.*, **19,** 1125 (Abstract).

REDMAN, R.S. & SILINSKY, E.M. (1994). ATP released together with acetylcholine as the mediator of neuromuscular depression at frog motor nerve endings. *J. Physiol.*, **477.1,** 117–127.

SILINSKY, E.M. (1981). On the calcium receptor that mediates depolarization-secretion coupling at cholinergic motor nerve terminals. *Br. J. Pharmacol.*, **73,** 413–429.

SILINSKY, E.M. & SOLSONA, C.S. (1992). Calcium currents at motor nerve endings: absence of effects of adenosine receptor agonists in the frog. *J. Physiol.*, **457,** 315–328.

SINGH, Y.N., HARVEY, A.L. & MARSHALL, I.G. (1978). Antibiotic-induced paralysis of the mouse phrenic nerve-hemidiaphragm preparation and reversibility by calcium and neostigmine. *Anesthesiol.*, **48,** 418–424.

(Received February 14, 1994
Revised May 25, 1994
Accepted June 1, 1994)

Br. J. Pharmacol. (1994), **113**, 379–384 © Macmillan Press Ltd, 1994

Differential inhibition of neuronal calcium entry and [^{3}H]-D-aspartate release by the quaternary derivatives of verapamil and emopamil

[1]R.A. Keith, T.J. Mangano, P.A. DeFeo, *G.E. Ernst & *E.J. Warawa

Depts. of Pharmacology and *Medicinal Chemistry, Zeneca Pharmaceuticals Group, 1800 Concord Pike, Wilmington, DE 19897, U.S.A.

1 Verapamil and emopamil are structurally related phenylalkylamine calcium channel/5-HT$_2$ receptor antagonists that differ in their anti-ischaemic properties in experimental studies. The quaternary ammonium derivatives of these compounds were prepared and tested in assays of neuronal voltage-sensitive calcium channel (VSCC) function to determine whether the compounds act at intra- or extracellular sites.

2 The compounds were tested in K^+-evoked: (1) rat brain synaptosomal $^{45}Ca^{2+}$ influx, (2) release of [^{3}H]-D-aspartate from rat hippocampal brain slices and (3) increase of intracellular calcium in rat cortical neurones in primary culture.

3 Verapamil, emopamil and the emopamil quaternary derivative caused concentration-dependent and comparable (IC_{50} values ~30 μM) inhibition of synaptosomal $^{45}Ca^{2+}$ influx and [^{3}H]-D-aspartate release. The verapamil quaternary derivative was considerably less active in these assays (IC_{50} > 300 μM).

4 The evoked increase of intracellular calcium in cortical neurones was inhibited with the following rank order of potency (IC_{50} value, μM): emopamil (3.6) > verapamil (17) > emopamil quaternary derivative (38) > verapamil quaternary derivative (200).

5 The results suggest that verapamil and emopamil inhibit nerve terminal VSCC function (synaptosomal $^{45}Ca^{2+}$ influx and [^{3}H]-D-aspartate release) by acting at distinct intracellular and extracellular sites, respectively. Verapamil and emopamil may inhibit cell body VSCC function (evoked increase of intracellular calcium in neocortical neurones) by acting at both intracellular and extracellular sites.

6 The different 'sidedness' of action of emopamil and verapamil on nerve terminal VSCC function and/or the preferential inhibition of cell body VSCC function by emopamil may at least partially explain the relatively greater neuroprotective efficacy of emopamil in experimental models of ischaemia.

Keywords: Emopamil; verapamil; voltage-sensitive calcium channel; synaptosomes; fura-2; aspartate release; calcium influx; cortical neurones; quaternary derivatives

Introduction

Emopamil is a phenylalkylamine inhibitor of voltage-sensitive calcium channels (VSCC) and 5-hydroxytryptamine 5-HT$_2$ receptors (Hofmann *et al.*, 1989; Szabo & Hofmann, 1989) that exhibits anti-ischaemic properties in a variety of *in vivo* models (Nakayama *et al.*, 1988; Bielenberg *et al.*, 1989; Lin *et al.*, 1990; Block *et al.*, 1990; Morikawa *et al.*, 1991; Okiyama *et al.*, 1992; Seega & Elger, 1993). Verapamil is chemically similar to emopamil, yet verapamil exhibits considerably less anti-ischaemic efficacy (Hofmann *et al.*, 1989; Lantos *et al.*, 1990; Shirakura *et al.*, 1993). It has been proposed that the limited access of verapamil to the central nervous system could account for its inability to exhibit neuroprotective activity (Szabo, 1989; Defeudis, 1989). Alternatively, differences in potency at 5-HT$_2$ receptors (emopamil is more potent than verapamil) or a difference in the regional vascular selectivity (emopamil exhibits greater cerebrovascular selectivity) may offer pharmacodynamic explanations for the differences in *in vivo* activity. In addition, it has recently been shown that (−)-[^{3}H]-emopamil interacts with a distinct intracellular 'anti-ischaemic' binding site that is found in guinea-pig brain but is most abundant in the liver (Zech *et al.*, 1991; Moebius *et al.*, 1993b). These studies demonstrate that although verapamil and emopamil are chemically similar, their pharmacological properties differ in both quantitative and qualitative aspects. Given the complex pharmacological profile of emopamil, it is difficult to identify the attribute(s) that may be of primary importance in imparting anti-ischaemic efficacy. However, most authors suggest that inhibition of VSCC and/or 5-HT$_2$ receptors are properties that are most probably responsible.

Quaternary derivatives of VSCC antagonists have been used in a variety of physiological preparations to evaluate the relative importance of intra- *vs* extracellular sites in the actions of these compounds. Quaternary derivatives, being permanently charged, are not considered to be capable of crossing hydrophobic cell membranes; therefore, it is assumed that any pharmacological activity of the quaternary derivative is due to affinity at an extracellular site. On the basis of this rationale, several studies investigating the effects of quaternary derivatives have concluded that phenylalkylamines inhibit VSCC activity primarily by acting at an intracellular site (Hescheler *et al.*, 1982; White & Bradford, 1986; Affolter & Coronado, 1986; Cohen *et al.*, 1986; 1987). While the quaternary derivative of verapamil has been evaluated in cardiovascular preparations (Cohen *et al.*, 1986; 1987), neither verapamil nor emopamil quaternary derivatives have been evaluated in neuronal preparations. White & Bradford (1986) showed that D890, the quaternary derivative of methoxyverapamil (D600), was considerably less potent in inhibiting veratridine-induced synaptosomal $^{45}Ca^{2+}$ influx and glutamate release. These observations suggest that phenylalkylamines inhibit VSCC by gaining access to an intracellular site. A complication, however, of studying veratridine-evoked responses is the finding that D600 inhibits neuronal VSCC and voltage-sensitive sodium channels at comparable concentrations (Pauwels *et al.*, 1990).

Although it has been suggested that the anti-ischaemic

[1] Author for correspondence.

actions of emopamil are due to activity at neuronal sites (Bielenberg *et al.*, 1989; Block *et al.*, 1990; Matsumoto *et al.*, 1993), a direct inhibition of neuronal VSCC function by emopamil has not been demonstrated. We recently showed that verapamil inhibits K^+-evoked [^{3}H]-D-aspartate release from hippocampal brain slices and K^+-evoked increases in intracellular calcium in cortical neurones in primary culture (Mangano *et al.*, 1991). The results from this study, as well as earlier studies that found verapamil inhibited K^+-evoked synaptosomal $^{45}Ca^{2+}$ influx (Akerman & Nicholls, 1981; Reynolds *et al.*, 1986; Wei & Chiang, 1986), provided evidence that verapamil inhibits neuronal non-L/non-N-type VSCC. As these K^+-evoked responses are resistant to inhibition by tetrodotoxin, complications from actions at voltage-sensitive sodium channels are not problematic. In the present study, we evaluated the effects of verapamil, emopamil and their quaternary derivatives in several biochemical measures of neuronal VSCC activity in an attempt to investigate the 'sidedness' of action of these compounds in neuronal preparations, and provide additional information on whether pharmacodynamic, instead of, or in addition to pharmacokinetic properties may contribute to the observed differences of *in vivo* neuroprotection observed with verapamil and emopamil.

Methods

K^+-evoked $^{45}Ca^{2+}$ influx into rat synaptosomes

K^+-evoked rat brain synaptosomal $^{45}Ca^{2+}$ influx was determined as described by Lampe *et al.* (1993a) utilizing crude synaptosomes (P2 pellets), isolated as described by Reynolds *et al.* (1986). $^{45}Ca^{2+}$ influx was initiated by the addition of buffer (spiked with approximately 2 mCi ml^{-1} $^{45}Ca^{2+}$) with sufficient K^+ to result in a final concentration of 50 mM K^+. Rapid quenching of the influx, after a 1 s incubation period, was accomplished by adding 3 ml of buffer containing 10 mM Na-EGTA. Samples were immediately filtered through Whatman GF/C glass fibre filters using a Hoefer FH225V filtration unit. Filters were dried for 16 h at 24°C and the retained radioactivity was determined by liquid scintillation counting. Net voltage-dependent $^{45}Ca^{2+}$ uptake was determined as the difference between uptake in 50 mM K^+ and 5 mM K^+. A typical control net calcium influx value was 4.15 ± 0.35 nmol mg^{-1} protein ($n = 5$ experiments, each performed in triplicate). Compounds were equilibrated a minimum of 30 min prior to initiating $^{45}Ca^{2+}$ influx. Data are expressed as the percentage of the net control evoked synaptosomal $^{45}Ca^{2+}$ influx.

K^+-evoked release of [^{3}H]-D-aspartate from rat hippocampal slices

K^+-evoked release of [^{3}H]-D-aspartate from rat hippocampal brain slices was determined as described previously (Keith *et al.*, 1992). Brain slices were superfused with physiological buffer at a rate of 1 ml 6 min^{-1} and exposed to a single 6-min stimulation of buffer containing 75 mM K^+ to evoke [^{3}H]-D-aspartate release. Where indicated, compounds were added 18 min prior to K^+ exposure and remained in the medium throughout the K^+ stimulus. At the conclusion of each experiment, slices from each superfusion chamber were sonicated. The radioactivity present in the collected fractions and the tissue slices was estimated by liquid scintillation counting.

The percentage fractional efflux of tritium was estimated as the fraction of the amount of radioactivity in the superfusate fraction relative to the total amount of radioactivity in the slice at that particular point in time, multiplied by 100. The total amount of evoked tritium release by a K^+ stimulus was estimated by summing the percentage fractional release values over baseline for the four fractions following exposure to K^+. The percentage fractional release of tritium in the fraction before superfusion with K^+ was used as an estimate of baseline release. Results were expressed as the percentage of control total evoked release values obtained from paired brain slice preparations not exposed to drugs. Typical control total evoked release values for the evoked release of [^{3}H]-D-aspartate are $33 \pm 0.3\%$ ($n = 20$).

Cell culture

Primary cultures of rat cortical neurones were prepared by a procedure similar to that described by Dichter (1978). Briefly, cortices were asceptically dissected from Sprague-Dawley foetal rats (17–19 days gestation). Following incubation with 0.08% trypsin, the tissue was triturated, diluted with minimal essential medium (MEM) supplemented with 10% foetal bovine serum and 10% heat-inactivated horse serum, and plated. Cells were plated in 35 mm plates (Fisher) at a density of 750,000 cells per plate. Each 35 mm plate contained a round 25 mm No. 1 cover glass (Erie Scientific) on which plated cells could attach. Culture plates and cover glasses were precoated by incubating them for 3 h with 0.1 mg ml^{-1} poly-L-lysine in 0.01 M borate buffer, pH 8.4, followed by a wash with distilled water. At all times, cultures were maintained at 37°C in a humidified 5% CO_2 atmosphere. Viability of plated cells was typically 80–85% as determined by trypan blue exclusion. Measurements of intracellular calcium were made on cells that were in culture for 14–21 days.

Measurement of intracellular calcium

Measurement of K^+-evoked increase of intracellular calcium was performed on single cortical neurones loaded with fura-2 using a PTI Deltascan 1 alternating channel illumination system attached to a Nikon Diaphot inverted microscope. Methods involved in loading cells with fura-2 and estimation of intracellular calcium have previously been described in detail (Mangano *et al.*, 1991) and are similar to those described by others (Murphy *et al.*, 1987; Thayer *et al.*, 1988; Murphy & Miller, 1989). The cells were perfused at a rate of 2 ml min^{-1} (gravity flow) which allowed for a complete solution exchange in the superfusion system within approximately 10 s. Where indicated, depolarization-induced calcium influx was produced by changing the perfusion solution from one with low K^+ (5.4 mM) to one with high K^+ (50 mM). Typically, a cell received two 1 min K^+ exposures at 16 min intervals. Compounds were added to the superfusion solution 15 min prior to the second K^+ exposure and the results were expressed as the percentage of the maximum increase in intracellular calcium of the first exposure. Under control conditions 50 mM K^+ caused a net increase of intracellular calcium of 920 ± 41 nM ($n = 21$). Control experiments indicated that K^+-evoked increase in intracellular calcium was reproducible as the evoked increase in the second exposure was $97 \pm 2\%$ ($n = 21$) of the initial exposure.

Statistical analyses

The data are expressed as means ± s.e. Statistically significant differences between two means were determined by Student's *t* test for unpaired observations. Significant differences between three or more means were determined by one-way analysis of variance and the Bonferroni modified *t* test as described by Wallenstein *et al.* (1980). IC_{50} values were determined from regression lines of probit-transformed log concentration-response curves. Concentration-response curves were computer-generated based on calculated IC_{50} and slope values.

Materials

Verapamil, tetrodotoxin, veratridine and poly-L-lysine were purchased from Sigma Chemical Co., St. Louis, MO, U.S.A.

Fura-2 AM and the pentapotassium salt of fura-2 were purchased from Molecular Probes, Inc., Eugene, OR, U.S.A. [^{3}H]-D-aspartate and $^{45}Ca^{2+}$ were purchased from NEN Research Products, Boston, MA, U.S.A. Emopamil and the quaternary derivatives of emopamil and verapamil (methiodide salts) were synthesized in the Medicinal Chemistry Department, Zeneca Pharmaceuticals.

Results

Verapamil and emopamil inhibited K^+-evoked synaptosomal $^{45}Ca^{2+}$ influx with statistically equivalent potencies (Figure 1; IC_{50} values = 19 μM and 16 μM, respectively; $P > 0.05$). The quaternary derivative of verapamil was minimally 15 times less potent than verapamil (Figure 1a; $IC_{50} > 300$ μM), whereas quaternary emopamil inhibited synaptosomal $^{45}Ca^{2+}$ influx with a potency that was only 2 fold less than emopamil (Figure 1b; $IC_{50} = 30$ μM for quaternary emopamil; $P < 0.05$ vs emopamil). Although there were small quantitative differences, a similar profile of inhibition was also observed for the phenylalkylamines and their quaternary derivatives against K^+-evoked release of [^{3}H]-D-aspartate from rat hippocampal brain slices. Once again, verapamil and emopamil inhibited K^+-evoked [^{3}H]-D-aspartate release with equivalent potencies (Figure 2; IC_{50} values = 30 and 26 μM, respectively; $P > 0.05$). Quaternary verapamil was considerably less potent than verapamil (Figure 2a; IC_{50} value $\gg 300$ μM), whereas quaternary emopamil was equipotent to emopamil in inhibiting K^+-evoked release of [^{3}H]-D-aspartate (Figure 2b; IC_{50} value = 32 μM for quaternary emopamil; $P > 0.05$ vs emopamil). Thus, there is a high degree of concordance of inhibitory activities of the phenylalkylamines and their quaternary derivatives against synaptosomal $^{45}Ca^{2+}$ influx and hippocampal [^{3}H]-D-aspartate release.

The profile of inhibition of K^+-evoked increase of intracellular calcium in cortical neurones, however, differed from that observed in the $^{45}Ca^{2+}$ flux and [^{3}H]-D-aspartate release studies. Emopamil was approximately 4 times more potent than verapamil in inhibiting K^+-evoked increase of intracellular calcium (Figure 3; IC_{50} values = 3.6 μM and 17 μM, respectively; $P < 0.05$). In addition, the concentration-response curves for both quaternary derivatives were shifted approximately 10 fold to the right relative to each parent compound (Figure 3; IC_{50} values for emopamil and verapamil quaternary derivatives were 38 μM and 200 μM, repectively). Thus, in contrast to the $^{45}Ca^{2+}$ flux and [^{3}H]-D-aspartate release studies, the quaternary derivative of emopamil was substantially less effective than emopamil in inhibiting VSCC function in cortical neurone cell bodies.

Tetrodotoxin (1 μM) abolished the 100 μM veratridine-evoked increase of intracellular calcium in cortical neurones in culture but had no significant effect on any of the K^+-evoked responses measured in the present study (data not shown).

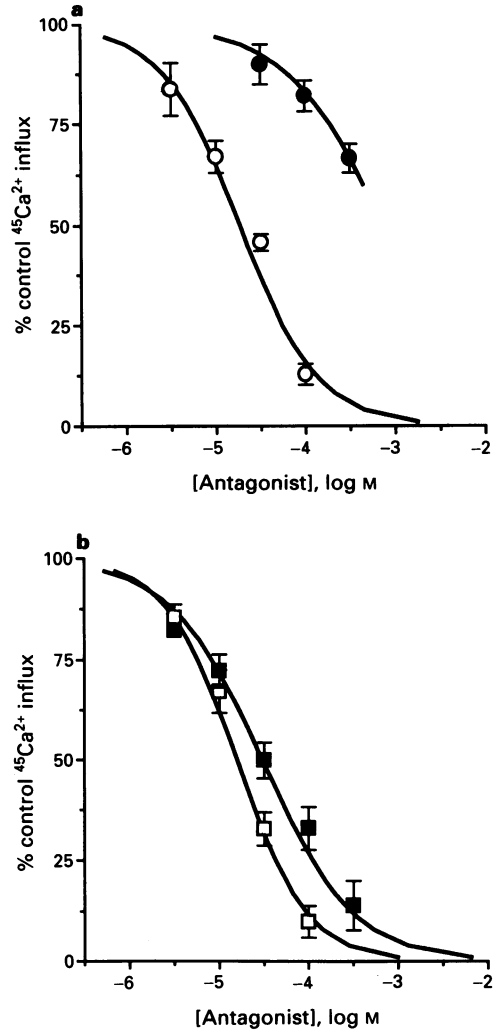


Figure 1 Inhibition of K^+-evoked synaptosomal $^{45}Ca^{2+}$ influx. (a) The verapamil quaternary derivative (●) ($IC_{50} > 300$ μM) was considerably less potent than verapamil (○) ($IC_{50} = 19$ μM). (b) Emopamil (□) ($IC_{50} = 16$ μM) was approximately 2 fold more potent than the quaternary emopamil derivative (■) ($IC_{50} = 30$ μM; $P < 0.05$ vs emopamil). IC_{50} values for verapamil and emopamil were not significantly different ($P < 0.05$). Values represent mean ± s.e. $n = 4-8$ experiments, each performed in triplicate.

Discussion

The observation that a compound exhibits biological activity, coupled with the finding that its quaternized derivative is considerably less active, suggests that the non-quaternized compound crosses the cell membrane and interacts at an intracellular site for activity. Using this rationale, previous studies have concluded that verapamil and closely related phenylalkylamine analogues inhibit VSCC function in both neuronal and cardiovascular biological systems by acting at an intracellular site (Hescheler *et al.*, 1982; Walden *et al.*, 1984; White & Bradford, 1986; Affolter & Coronado, 1986; Cohen *et al.*, 1986; 1987; van Amsterdam *et al.*, 1987). In the present study, we show that the quaternary derivative of verapamil is a substantially less potent inhibitor than verapamil of K^+-evoked synaptosomal $^{45}Ca^{2+}$ influx and K^+-evoked release of [^{3}H]-D-aspartate from hippocampal brain slices. This agrees well with an earlier report by White & Bradford (1986) who showed that the quaternary derivative of methoxyverapamil (D890) was less effective than methoxyverapamil (D600) in inhibiting veratridine-evoked synaptosomal $^{45}Ca^{2+}$ influx and glutamate release. Therefore, the results of the present paper and earlier studies support the contention that verapamil and closely related phenylalkylamines inhibit VSCC function by acting predominantly at an intracellular site. Inasmuch as the results of the present study using K^+-evoked responses agree well with the findings of White & Bradford (1986) where veratridine-evoked responses were studied, it is unlikely that the potential inhibition of voltage-sensitive sodium channels by D600 played a significant role.

From a structural standpoint, emopamil shares the essential chemical backbone of verapamil, with the exception that all methoxy groups are substituted with H. In sharp contrast to verapamil and its quaternary derivative, the quaternary derivative of emopamil was virtually equipotent with emopamil against K^+-evoked $^{45}Ca^{2+}$ influx and [^{3}H]-D-aspartate release, suggesting an extracellular site of action.

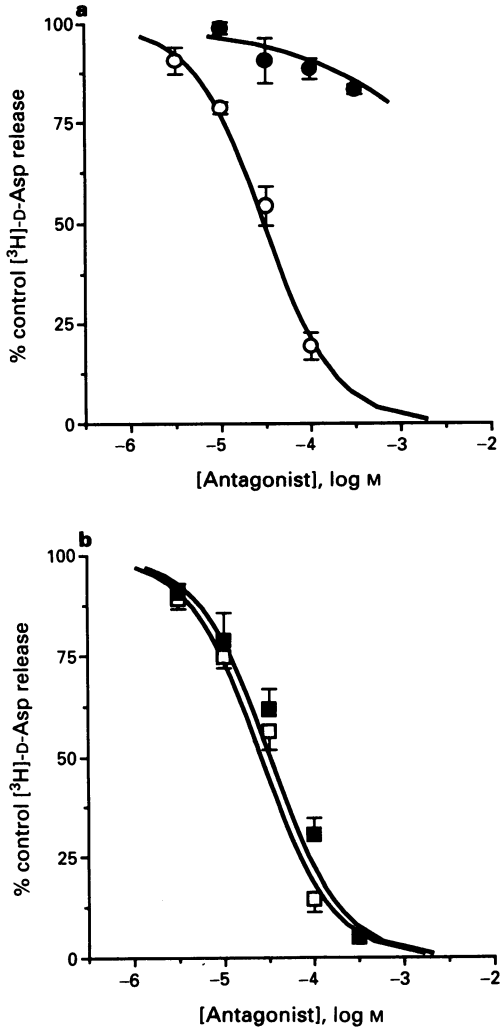


Figure 2 Inhibition of K^+-evoked brain slice [^{3}H]-D-aspartate ([^{3}H]-D-Asp) release. (a) The verapamil quaternary derivative (●) ($IC_{50} \gg 300\ \mu M$) was considerably less potent than verapamil (○) ($IC_{50} = 30\ \mu M$). (b) Emopamil (□) ($IC_{50} = 26\ \mu M$) and quaternary emopamil (■) ($IC_{50} = 32\ \mu M$) were equieffective inhibitors ($P < 0.05$). IC_{50} values for verapamil and emopamil were not significantly different ($P < 0.05$). Values represent mean ± s.e. $n = 3-6$ experiments, each performed in triplicate.

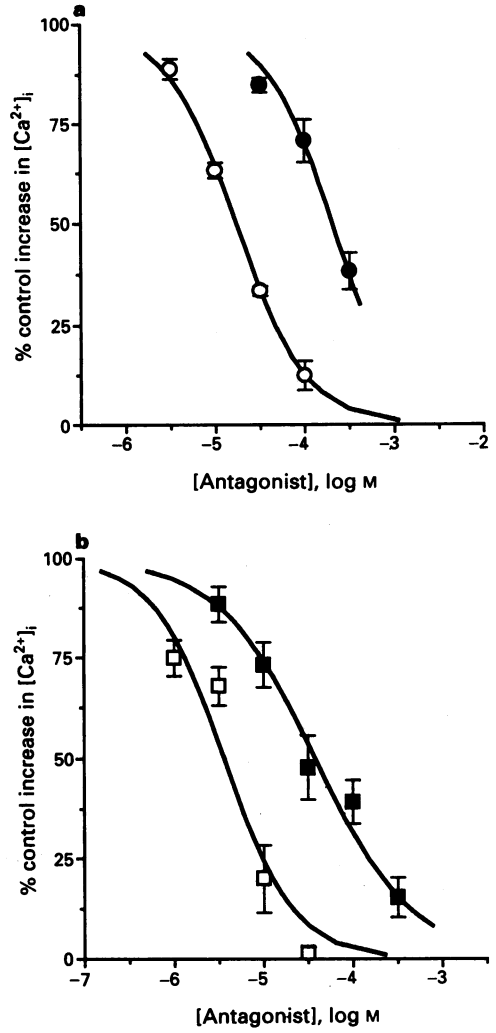


Figure 3 Inhibition of K^+-evoked increase of intracellular calcium ($[Ca^{2+}]_i$) in cortical neurones. (a) The verapamil quaternary derivative (●) ($IC_{50} = 200\ \mu M$) was approximately 10 fold less potent than verapamil (○) ($IC_{50} = 17\ \mu M$). (b) The emopamil quaternary derivative (■) ($IC_{50} = 38\ \mu M$) was approximately 10 fold less potent than emopamil (□) ($IC_{50} = 3.6\ \mu M$). IC_{50} values for verapamil and emopamil were significantly different ($P < 0.05$). Values represent mean ± s.e. $n = 3-4$ cells per point.

Although verapamil and emopamil are phenylalkylamines, the present paper provides evidence that verapamil inhibits neuronal VSCC function by acting at an intracellular site, whereas emopamil acts at a distinct extracellular site. Emopamil, therefore, stands out as an exception to the generally accepted notion that phenylalkylamines inhibit VSCC function by acting at an intracellular site. The major structural difference between emopamil and verapamil is the presence of methoxy groups on verapamil. Thus, the methoxy group appears to be important for activity at the intracellular site, and precludes activity at the extracellular site.

Synaptosomal $^{45}Ca^{2+}$ influx and hippocampal slice [^{3}H]-D-aspartate release represent biochemical measures of nerve terminal calcium entry. The K^+-evoked increase of intracellular calcium in cortical neurones in culture represents a measure of neuronal cell body calcium entry. Inasmuch as these K^+-evoked responses are dependent on the presence of extracellular calcium, and inhibited by selective inhibitors of VSCC (Mangano *et al.*, 1991; Mintz *et al.*, 1992; Lampe *et al.*, 1993b; Keith *et al.*, 1994), it is likely that they represent functional responses of neuronal VSCC. The results of the present study show that the profile of inhibition of nerve terminal VSCC function by verapamil, emopamil and their quaternary derivatives differs from that of neuronal cell body VSCC function. While verapamil and emopamil were equipotent inhibitors of nerve terminal VSCC function, emopamil was 4 times more potent than verapamil in inhibiting cell body calcium entry. In addition, the quaternary derivatives were similarly active relative to the parent compounds *vs* cell body calcium entry, exhibiting approximately 10 fold less potency. Thus, emopamil shows a preferential inhibition of neuronal cell body VSCC relative to verapamil, and quaternization affects the actions of verapamil and emopamil similarly. These results suggest that emopamil and verapamil inhibit neuronal cell body VSCC possibly by acting at both extracellular and intracellular sites.

Emopamil has been shown to be neuroprotective in a variety of experimental ischaemia models (Nakayama *et al.*, 1989; Bielenberg *et al.*, 1989; Lin *et al.*, 1990; Block *et al.*, 1990; Morikawa *et al.*, 1991; Okiyama *et al.*, 1992; Seega & Elger, 1993). While the earlier emopamil literature focused on VSCC inhibition and 5-HT_2 receptor blockade as possible effectors of emopamil's anti-ischaemic efficacy, recent reports suggest that other pharmacological activities may be involved. For example, a unique 22-kD high affinity [^{3}H]-

emopamil 'anti-ischaemic' binding site has been discovered that is prevalent in liver but is also found in brain (Zech *et al.*, 1991; Moebius *et al.*, 1993b). The functional significance of this binding site is unknown. However, the 22-kD binding site is not associated with VSCC, and a number of anti-ischaemic compounds bind with high affinity. Emopamil was also shown to bind with high affinity to a 27-kD binding site that has been classified as a σ_1 receptor subtype localized to the endoplasmic reticulum (Moebius *et al.*, 1993a). In addition, emopamil was shown to cause an insurmountable inhibition of AMPA-induced increases in intracellular calcium in cortical neurones by an AMPA receptor-independent mechanism (Mangano *et al.*, 1992). Both σ ligands and AMPA receptor antagonists have been shown to be neuroprotective (Lobner & Lipton, 1990; Pontecorvo *et al.*, 1991; Sheardown *et al.*, 1993). Therefore, the actions of emopamil at the 22-kD binding site, the σ_1 binding site, and/or inhibition of AMPA receptor responses may contribute to the anti-ischaemic efficacy.

The results of the present paper suggest that a novel interaction with neuronal VSCC could also contribute to the anti-ischaemic efficacy of emopamil. It interacts with an extracellular site to inhibit nerve terminal VSCC responses, whereas verapamil and other phenylalkylamines act at an intracellular site. This extracellular site appears to be distinct from the 22-kD or 27-kD [^{3}H]-emopamil binding site, because those sites have been localized to the endoplasmic reticulum (Zech *et al.*, 1991; Moebius *et al.*, 1993a,b). Emopamil is also an effective inhibitor of cell body VSCC responses, and does so with approximately 4 times the potency of verapamil. Therefore, while emopamil has clearly been shown to exhibit anti-ischaemic properties in experimental models, the factors that contribute to its neuroprotective efficacy may be many, and could include a complex interaction among diverse pharmacodynamic and pharmacokinetic parameters.

The authors thank Ms Carol Thompson and Ms Rebecca Kozel for their expert technical assistance in preparing the cortical neurone preparations.

References

AFFOLTER, H. & CORONADO, R. (1986). Sidedness of reconstituted calcium channels from muscle transverse tubules as determined by D600 and D890 blockade. *Biophys. J.*, **49**, 767–771.

AKERMAN, K.E.O. & NICHOLLS, D.G. (1981). Ca^{2+} transport by intact synaptosomes: the voltage-dependent Ca^{2+} channel and re-evaluation of the role of sodium/calcium exchange. *Eur. J. Biochem.*, **117**, 491–497.

BIELENBERG, G.W., SAUER, D., NUGLISCH, J., BECK, T., ROBERG, C., MENNEL, H.D. & KRIEGLSTEIN, J. (1989). Effects of emopamil on postischemic blood flow and neuronal damage in rat brain. *Naunyn-Schmied. Arch. Pharmacol.*, **339**, 230–235.

BLOCK, F., JASPERS, R.M., HEIM, C. & SONTAG, K.H. (1990). S-Emopamil ameliorates ischemic brain damage in rats: histological and behavioural approaches. *Life Sci.*, **47**, 1511–1518.

COHEN, L., MORGAN, J. & KEZDY, F. (1986). The molecular features of verapamil that promote myocardial enzyme leakage. *Res. Commun. Chem. Pathol. Pharmacol.*, **51**, 379–392.

COHEN, L., VEREAULT, D., WASSERSTROM, J.A., RETZINGER, G.S. & KEZDY, F.J. (1987). Evidence that uncharged verapamil inhibits myocardial contractility. *J. Pharmacol. Exp. Ther.*, **242**, 721–725.

DEFEUDIS, F.V. (1989). The Ca^{2+} channel and 5-HT_2 receptor antagonist (S)-emopamil in cerebral ischaemia. *Trends Pharmacol. Sci.*, **10**, 215–217.

DICHTER, M.A. (1978). Rat cortical neurons in cell culture: culture methods, cell morphology, electrophysiology, and synapse formation. *Brain Res.*, **149**, 279–293.

HESCHELER, J., PELZER, D., TRUBE, G. & TRAUTWEIN, W. (1982). Does the organic calcium channel blocker D600 act from inside or outside on the cardiac cell membrane? *Pflügers Arch.*, **393**, 287–291.

HOFMANN, H.P., RASCHACK, M. & UNGER, L. (1989). (S)-Emopamil, a novel calcium and serotonin antagonist for the treatment of cerebrovascular disorders. 1st Communication: pharmacological profile. *Arzneim.-Forsch./Drug Res.*, **39**, 304–308.

KEITH, R.A., MANGANO, T.J., DEFEO, P.A., HORN, M.B. & SALAMA, A.I. (1992). Actions of neomycin on neuronal L-, N-, and non-L/non-N-type voltage-sensitive calcium channel responses. *J. Mol. Neurosci.*, **3**, 147–154.

KEITH, R.A., MANGANO, T.J. & LAMPE, R.A. (1994). ω-Grammotoxin SIA inhibits ω-Aga-IVA-sensitive/nitrendipine-insensitive K^+-evoked increases of intracellular Ca^{2+} in cortical neurons. *Soc. Neurosci. Abstr.*, (in press).

LAMPE, R.A., DEFEO, P.A., DAVISON, M.D., YOUNG, J., HERMAN, J.L., SPREEN, R.C., HORN, M.B., MANGANO, T.J. & KEITH, R.A. (1993a). Isolation and pharmacological characterization of ω-grammotoxin SIA, a novel peptide inhibitor of neuronal voltage-sensitive calcium channel responses. *Mol. Pharmacol.*, **44**, 451–460.

LAMPE, R.A., MANGANO, T.J., DEFEO, P.A., HORN, M.B. & KEITH, R.A. (1993b). Inhibition of neuronal voltage-sensitive calcium channel responses: effects of synthetic ω-Aga-IVA and synthetic ω-grammotoxin SIA. *Soc. Neurosci. Abstr.*, **19**, 1751.

LANTOS, J., TEMES, G., KELEMEN, D., SAROSI, I. & TOROK, B. Jr. (1990). Influence of protective drugs on the elevation of extracellular potassium ion concentration in the brain during ischaemia. *Acta Physiol. Hung.*, **76**, 49–59.

LIN, B.W., DIETRICH, W.D., BUSTO, R. & GINSBERG, M.D. (1990). (S)-Emopamil protects against global ischemic brain injury in rats. *Stroke*, **21**, 1734–1739.

LOBNER, D. & LIPTON, P. (1990). Sigma-ligands and non-competitive NMDA antagonists inhibit glutamate release during cerebral ischemia. *Neurosci. Lett.*, **117**, 169–174.

MANGANO, T.J., BRITT, M., PULLAN, L.M., THOMPSON, C. & KEITH, R.A. (1992). Insurmountable inhibition of AMPA-induced increase of intracellular calcium in rat cortical neurons by emopamil. *Soc. Neurosci. Abstr.*, **18**, 248.

MANGANO, T.J., PATEL, J., SALAMA, A.I. & KEITH, R.A. (1991). Inhibition of K^+-evoked [^{3}H]-D-aspartate release and neuronal calcium influx by verapamil, diltiazem and dextromethorphan: evidence for non-L/non-N voltage-sensitive calcium channels. *Eur. J. Pharmacol.*, **192**, 9–17.

MINTZ, I.M., VENEMA, V.J., SWIDEREK, K.M., LEE, T.D., BEAN, B.P. & ADAMS, M.E. (1992). P-Type calcium channels blocked by the spider toxin ω-Aga-IVA. *Nature*, **355**, 827–829.

MATSUMOTO, M., SCHELLER, M.S., ZORNOW, M.H. & STRNAT, M.A.P. (1993). Effects of S-emopamil, nimodipine, and mild hypothermia on hippocampal glutamate concentrations after repeated cerebral ischemia in rabbits. *Stroke*, **24**, 1228–1234.

MOEBIUS, F.F., BURROWS, G.G., HANNER, M., SCHMID, E., STRIESSNIG, J. & GLOSSMANN, H. (1993a). Identification of a 27-kda high affinity phenylalkylamine-binding polypeptide as the σ_1-binding site by photoaffinity labeling and ligand-directed antibodies. *Mol. Pharmacol.*, **44**, 966–971.

MOEBIUS, F.F., BURROWS, G.G., STRIESSNIG, J. & GLOSSMANN, H. (1993b). Biochemical characterization of a 22-kDa high affinity antiischemic drug-binding polypeptide in the endoplasmic reticulum of guinea pig liver: potential common target for anti-ischemic drug action. *Mol. Pharmacol.*, **43**, 139–148.

MORIKAWA, E., GINSBERG, M.D., DIETRICH, W.D., DUNCAN, R.C. & BUSTO, R. (1991). Postischemic (S)-emopamil therapy ameliorates focal ischemic brain injury in rats. *Stroke*, **22**, 355–360.

MURPHY, S.N. & MILLER, R.J. (1989). Regulation of Ca^{2+} influx into striatal neurons by kainic acid. *J. Pharmacol. Exp. Ther.*, **249**, 184–193.

MURPHY, S.N., THAYER, S.A. & MILLER, R.J. (1987). The effects of excitatory amino acids on intracellular calcium in single mouse striatal neurons *in vitro*. *J. Neurosci.*, **7**, 4145–4158.

NAKAYAMA, H., GINSBERG, M.D. & DIETRICH, W.D. (1988). (S)-Emopamil, a novel calcium channel blocker and serotonin S_2 antagonist, markedly reduces infarct size following middle cerebral artery occlusion in the rat. *Neurology*, **38**, 1667–1673.

OKIYAMA, K., SMITH, D.H., THOMAS, M.J. & McINTOSH, T.K. (1992). Evaluation of a novel calcium channel blocker, (S)-emopamil, on regional cerebral edema and neurobehavioral function after experimental brain injury. *J. Neurosurg.*, **77**, 607–615.

PAUWELS, P.J., VAN ASSOUW, H.P., PEETERS, L. & LEYSEN, J.E. (1990). Neurotoxic action of veratridine in rat brain neuronal cultures: mechanism of neuroprotection by Ca^{2+} antagonists nonselective for slow Ca^{2+} channels. *J. Pharmacol. Exp. Ther.*, **255**, 1117–1122.

PONTECORVO, M.J., KARBON, E.W., GOODE, S., CLISSOLD, D.B., BOROSKY, S.A., PATCH, R.J. & FERKANY, J.W. (1991). Possible cerebroprotective and *in vivo* NMDA antagonist activities of sigma agents. *Brain Res. Bull.*, **26**, 461–465.

REYNOLDS, I.J., WAGNER, J.A., SNYDER, S.H., THAYER, S.A., OLIVERA, B.M. & MILLER, R.J. (1986). Brain voltage-sensitive calcium channel subtypes differentiated by ω-conotoxin fraction GVIA. *Proc. Natl. Acad. Sci. U.S.A.*, **83**, 8804–8807.

SEEGA, J. & ELGER, B. (1993). Diffusion- and T2-weighted imaging: evaluation of oedema reduction in focal cerebral ischaemia by the calcium and serotonin antagonist levemopamil. *Magn. Reson. Imaging*, **11**, 401–409.

SHEARDOWN, M.J., SUZDAK, P.D. & NORDHOLM, L. (1993). AMPA, but not NMDA, receptor antagonism is neuroprotective in gerbil global ischaemia, even when delayed 24 hours. *Eur. J. Pharmacol.*, **236**, 347–353.

SHIRAKURA, S., KARASAWA, A. & KUBO, K. (1993). Effect of benidipine hydrochloride (KW-3049), on cerebral ischemia induced by bilateral occlusion of the common carotid arteries in rats. *Biol. Pharmacol. Bull.*, **16**, 475–479.

SZABO, L. (1989). (S)-Emopamil, a novel calcium and serotonin antagonist for the treatment of cerebrovascular disorders. 2nd Communication: brain penetration, cerebral vascular and metabolic effects. *Arzneim.-Forsch./Drug Res.*, **39**, 309–314.

SZABO, L. & HOFMANN, H.P. (1989). (S)-Emopamil, a novel calcium and serotonin antagonist for the treatment of cerebrovascular disorders. 3rd Communication: effect on postischemic cerebral blood flow and metabolism, and ischemic neuronal cell death. *Arzneim.-Forsch./Drug Res.*, **39**, 314–319.

THAYER, S.A., STUREK, M. & MILLER, R.J. (1988). Measurement of neuronal Ca^{2+} transients using simultaneous microfluorimetry and electrophysiology., *Pflügers Arch.*, **412**, 216–223.

VAN AMSTERDAM, F.T., HAAS, M. & ZAAGSMA, J. (1987). Dynamic and kinetic differences of the vascular and myocardial effects of calcium antagonists in the rat heart. *J. Cardiovasc. Pharmacol.*, **9**, 570–577.

WALDEN, J., WITTE, O.W., SPECKMANN, E.-J. & ELGER, C.E. (1984). Reduction of calcium currents in identified neurons of Helix pomatia: intracellular injection of D890. *Comp. Biochem. Physiol.*, [C]., **77C**, 211–217.

WALLENSTEIN, S., ZUCKER, C.L. & FLEISS, J.L. (1980). Some statistical methods useful in circulation research. *Circ. Res.*, **47**, 1–9.

WEI, J.W. & CHIANG, D.H. (1986). Effects of calcium antagonists on KCl-evoked calcium uptake by rat cortical synaptosomes. *Gen. Pharmacol.*, **17**, 261–265.

WHITE, E.J. & BRADFORD, H.F. (1986). Participation of intracellular sites in the action of Ca^{2+} channel blockers. *Eur. J. Pharmacol.*, **130**, 243–248.

ZECH, C., STAUDINGER, R., MUHLBACHER, J. & GLOSSMANN, H. (1991). Novel sites for phenylalkylamines: characterisation of a sodium-sensitive drug receptor with (−)-[^{3}H]-emopamil. *Eur. J. Pharmacol-Mol. Pharmacol.*, **208**, 119–130.

(Received February 24, 1994
Revised May 17, 1994
Accepted June 1, 1994)

Br. J. Pharmacol (1994), **113**, 385–388 © Macmillan Press Ltd, 1994

Antiplatelet activities of FK409, a new spontaneous NO releaser

[1]Yasuhiro Kita, Yoshimi Hirasawa, Keizo Yoshida & Kazuhiro Maeda

Department of Pharmacology, New Drug Research Laboratories, Fujisawa Pharmaceutical Co., Ltd., 1-6, 2-chome, Kashima Yodogawa-ku, Osaka 532, Japan

1 We reported that (±)-(E)-ethyl-2-[(E)-hydroxyimino]-5-nitro-3-hexeneamide (FK409) released nitric oxide (NO) spontaneously with a chemiluminescence analyzer. The aim of this study was to compare antiplatelet activities of FK409, a new NO releaser, with those of isosorbide dinitrate (ISDN) *in vivo* and *in vitro*. In order to elucidate the differences in antiplatelet activities between FK409 and ISDN, we compared their modes of action.

2 In *in vitro* experiments, FK409 had a more potent inhibitory effect on rat platelet aggregation induced by adenosine 5'-diphosphate (2.0 μM) than ISDN (IC_{50} = 4.32 ± 0.95 μM and >100 μM respectively).

3 In the rat extracorporeal shunt model (*in vivo* experiments), FK409 suppressed thrombus formation dose-dependently from 0.32 mg kg^{-1}, p.o. and showed the maximum inhibition (52% inhibition vs. vehicle treatment) at 10 mg kg^{-1}, p.o., while ISDN showed no inhibition at 10 mg kg^{-1} and only 17% inhibition at 32 mg kg^{-1}, p.o.

4 FK409 could generate nitrite, which is an oxidative product of NO, much faster than ISDN in phosphate buffer solution and rat plasma during 60-min incubation at 37°C.

5 These data show that FK409 has more potent antiplatelet effects than ISDN, by acting through spontaneously released NO.

Keywords: FK409; isosorbide dinitrate; nitric oxide; antiplatelet activity

Introduction

(±)-(E)-ethyl-2-[(E)-hydroxyimino]-5-nitro-3-hexeneamide (FK409), the chemical structure of which is shown in Figure 1, is a structurally unique vasodilator discovered from the fermentation products of *Streptomyces griseosporeus* (Hino *et al.*, 1989). FK409 produced a potent vasorelaxation mediated by the elevation of guanosine 3':5'-cyclic monophosphate (cyclic GMP) in dog isolated coronary artery (Yamada *et al.*, 1991) and rabbit aorta (Sibata *et al.*, 1991). In addition, the vasorelaxation and the elevation of cyclic GMP were inhibited by methylene blue, an inhibitor of soluble guanylate cyclase. Owing to these facts, although FK409 has no O-NO_2 functional group (unlike organic nitrates) it seems to have a mode of action similar to that of organic nitrates reported by Katsuki *et al.* (1977) and Schultz *et al.* (1977). Previously, it has been reported that organic nitrates showed various pharmacological actions via nitric oxide (NO) (Feelish & Noack, 1987a,b), which is generally accepted as EDRF (Palmer *et al.*, 1987). Recently, we reported that FK409 decomposed and released NO spontaneously in solution (Kita *et al.*, 1994).

It has been shown that the antiplatelet effect of organic nitrates acting via NO (Mellion *et al.*, 1981; Radomski *et al.*, 1987) played an important role in the prevention of acute coronary syndromes such as unstable angina pectoris and acute myocardial infarction (Hjemdahl-Monsen *et al.*, 1986; Fuster *et al.*, 1988). Thus, the antiplatelet action could be an important aspect in the treatment of patients with ischaemic cardiovascular diseases.

The purpose of this study was to evaluate the antiplatelet effects of FK409 in rats; we compared the *in vitro* and *in vivo* effects of FK409 with those of isosorbide dinitrate (ISDN) (Figure 1), which is an organic nitrate and the most popular orally active drug for ischaemic cardiovascular diseases. Additionally we related the differences in the biological potencies of FK409 and ISDN to those of their modes of actions.

[1] Author for correspondence.

Methods

Animals

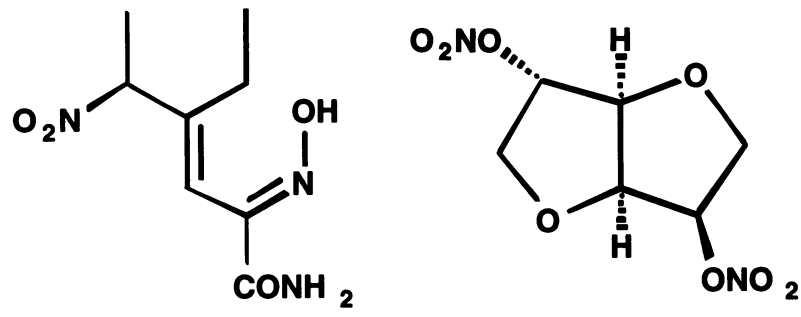
Sprague-Dawley (SD) rats were purchased from Nihon SLC Co. (Sizuoka, Japan). In *in vivo* experiments, rats were fasted for 24 h and given each drug orally, suspended in 0.5% methylcellulose, in a volume of 5 ml kg^{-1}.

In vitro *platelet aggregation*

Male SD rats weighing 240–325 g, were anaesthetized with diethyl ether and blood was collected from the abdominal aorta into plastic vessels containing 2.2% trisodium citrate (10^{-1} volume). Platelet-rich plasma was obtained from the supernatant fraction after centrifugation of blood at 200 *g* for 10 min. The effect of FK409 or ISDN on platelet aggregation was determined by Born's turbidimetric method (Born & Cross, 1968) using an aggregometer (Hema Tracer 801, Niko Bioscience Co., Tokyo, Japan). To 225 μl of platelet-rich plasma in a cuvette, 25 μl of each drug dissolved in Tris-acetate (25 mM) and NaCl (120 mM) buffer adjusted to pH 7.4 or vehicle was added and incubated at 37°C for 2 min. After the incubation, platelet aggregation was induced by the addition of 5 μl of adenosine 5'-diphosphate (ADP; final concentration, 2.0 μM). In order to evaluate platelet aggregation, the maximum increase in light transmission was determined from the aggregation curve for 7 min after the addition of ADP. The effects of each drug were expressed as % inhibition of ADP-induced platelet aggregation compared with vehicle treatment. The IC_{50} value is the drug concentration required to produce 50% inhibition; this was calculated logarithmically for platelet-rich plasma from each rat.

Extracorporeal shunt model

The procedure was performed as described previously (Umetsu & Sanai, 1978). Briefly, male SD rats weighing 325–405 g were anaesthetized with sodium pentobarbitone



FK409 ISDN

Figure 1 Chemical structures of FK409 and ISDN.

(50 mg kg^{-1}, i.p.). A silk thread (5 cm; Tire No. 50, Fujix Co., Osaka, Japan) was placed in the polyethylene tubing (6 cm; Hibiki Size 7, Kunii Co., Tokyo, Japan). Both ends of this tubing were connected to other polyethylene tubing (10 cm; Hibiki Size 4, Kunii Co.). The extracorporeal shunt filled with heparin solution (50 iu ml^{-1}) was introduced between the right carotid artery and the left jugular vein and blood circulation was then established. After 20 min, the blood flow was stopped at the artery side with a pinch cock. Then, the middle tubing was taken away and the thread coated with thrombus was carefully pulled out of the tubing. Immediately, the wet weight of the thrombus was measured. Another new polyethylene tubing containing a silk thread and filled with the heparin solution was inserted between the arterial and venous tubing ends. Blood circulation was re-established by opening the pinch cock. After 20 min, the wet weight of the silk thread was again measured for the second time. Then, the third blood circulation was performed. Thrombus weight was determined by subtracting the weight of a silk thread immersed in heparinized blood from that of the thread coated with thrombus. The total thrombus weight obtained by three blood circulations was taken as a net thrombus weight in one experiment. FK409, ISDN or vehicle was given orally 60 min before the first blood circulation. The effects of each drug were expressed as % inhibition of thrombus formation compared with vehicle treatment.

Nitrite analysis

In the determination of nitrite concentrations in sodium phosphate buffer (0.1 M; PB), FK409 and ISDN were dissolved in PB at 1.5 mM and immediately incubated at 37°C. For the determination of nitrite concentrations in plasma, blood from male SD rats weighing 325–375 g, which had been anaesthetized with ethylether, was collected from the abdominal aorta into plastic vessels containing 4% tripotassium EDTA (40^{-1} volume). Plasma was obtained from the supernatant fraction after centrifugation of blood at 1000 *g* for 15 min. FK409 and ISDN were dissolved in dimethyl sulphoxide at 75 mM and 0.05 ml was added to 2.45 ml of plasma (final drug concentration: 1.5 mM) and immediately incubated at 37°C. Prior to incubation and at various time intervals, the concentrations of nitrite were determined by diazotization. To 0.05 ml of PB or plasma containing drug, 3.95 ml of HCl (0.05 N for plasma and 0.5 N for PB), 0.5 ml of 0.2% sulfanilic acid and 0.5 ml of 0.1% N-(-naphthyl)-ethylenediamine was added subsequently (Bell *et al.* 1963). Absorbance of a purple dye at 548 nm was measured with a spectrophotometer (UV-2200, Shimazu Co., Kyoto, Japan). For the standard curve, sodium nitrite was used under the same experimental conditions.

Drugs

FK409 and ISDN were synthesized by Fujisawa Pharmaceutical Co. (Osaka, Japan). Sodium citrate, ADP and tripotassium EDTA were purchased from Sigma Chemical Co. (St. Louis, MO, USA). Sulfanilic acid and N-(-naphthyl)-ethylenediamine were purchased from Nacalai Tesque Co. (Kyoto, Japan).

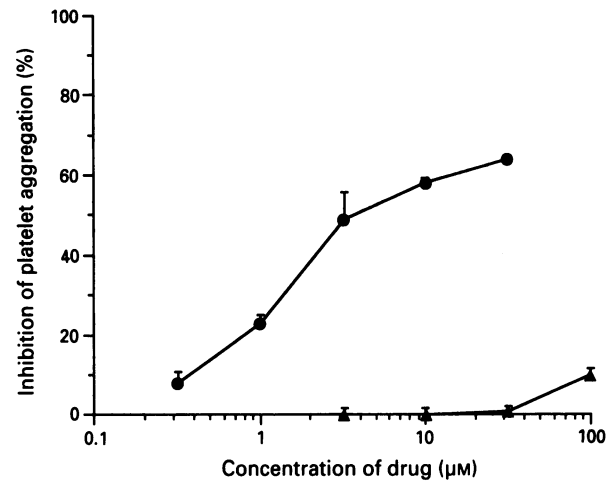


Figure 2 Inhibitory effects of FK409 (●) and ISDN (▲) on platelet aggregation induced by ADP (2.5 μM) in rat platelet-rich plasma. The effects of each drug are expressed as % inhibition of ADP-induced platelet aggregation compared with vehicle treatment. Each value represents the mean + s.e.mean for five experiments.

Results

Effects on in vitro *platelet aggregation*

Figure 2 shows the inhibitory effects of FK409 and ISDN on ADP-induced platelet aggregation in rat platelet-rich plasma. FK409 (0.32–32 μM) dose-dependently suppressed this aggregation. The inhibition value of FK409 at 0.32–32 μM did not reach 100% and was 64% at 32 μM. The IC_{50} value of FK409 was 4.32 ± 0.95 μM. This value is larger than the IC_{50} value (0.75 μM) which we reported in the human platelet-rich plasma test (Kita *et al.*, 1994). ISDN showed only a 10% inhibition of platelet aggregation at 100 μM.

Effects on thrombus formation in the extracorporeal shunt model

To examine *in vivo* antiplatelet action of FK409 and ISDN, we evaluated these drugs in the rat extracorporeal shunt model. Figure 3 shows the effects of FK409 and ISDN on thrombus formation in this model. FK409 (0.32–32 mg kg^{-1}, p.o.) dose-dependently inhibited thrombus formation. FK409 showed maximum inhibition (52%) at 10 mg kg^{-1}, p.o., while

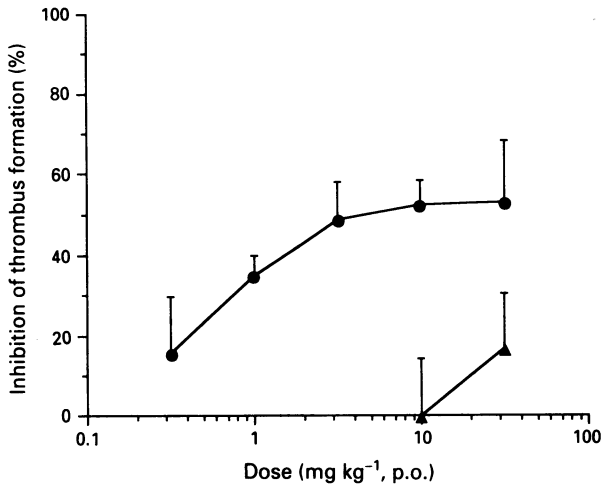


Figure 3 Inhibitory effects of FK409 (●) and ISDN (▲) on thrombus formation in the rat extracorporeal shunt model. The effects of each drug are expressed as % inhibition of thrombus formation compared with vehicle treatment. Each value represents the mean + s.e.mean for six experiments.

ISDN showed no inhibitory effects at 10 mg kg^{-1}, p.o. and produced only 17% inhibition at 32 mg kg^{-1}, p.o.

Nitrite generation in PB and rat plasma

As shown in Figure 4a, FK409 spontaneoulsy generated nitrite which is an oxidative product of NO, while ISDN did not. The concentration of nitrite generated from FK409 was 0.239 ± 0.002 mM after 60-min incubation. The first-order generation of nitrite was observed for FK409, the rate constant being 0.0109 ± 0.0001 min^{-1} (r = 0.972 ± 0.010).

As shown in Figure 4b, ISDN could also generate nitrite time-dependently in rat plasma in contrast to PB. But the nitrite generation from ISDN was much slower than that from FK409 and did not occur in the first order. The concentrations of nitrite generated from FK409 and ISDN were 0.211 ± 0.005 and 0.0069 ± 0.002 mM after 60-min incubation, respectively. The first-order generation of nitrite was observed for FK409, the rate constant being 0.0875 ± 0.0023 min^{-1} (r = 0.997 ± 0.001).

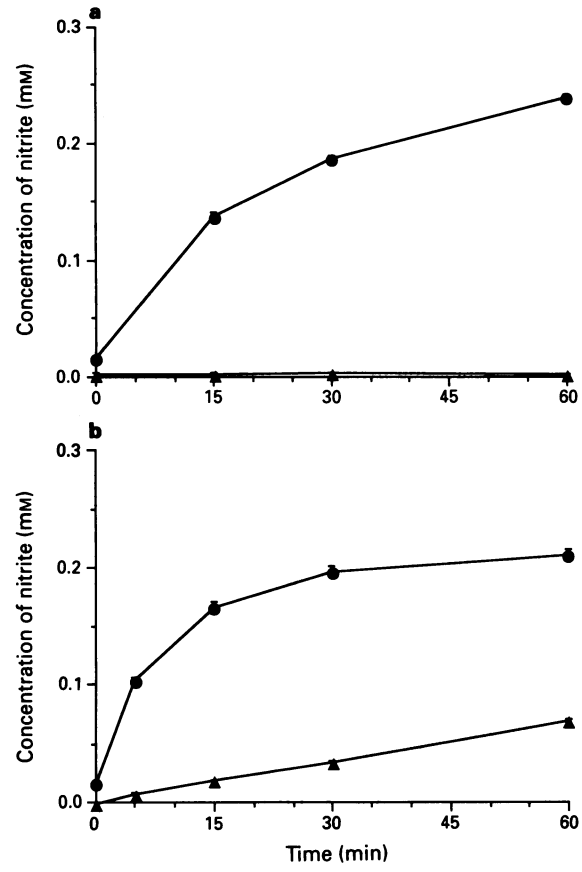


Figure 4 Time-dependent generation of nitrite from FK409 (●) and ISDN (▲) in (a) phosphate buffer solution (pH 7.4) and (b) rat plasma at 37°C. The initial concentration of each drug was 1.5 mM. Each value represents the mean + s.e.mean for three experiments.

Discussion

Organic nitrates such as nitroglycerin (Hampton *et al.*, 1967; Kowey *et al.*, 1981) and ISDN (DeCaterina *et al.*, 1984) have been shown to inhibit platelet aggregation in *in vitro* and *in vivo* experiments. However, in our experiments, ISDN showed very weak inhibitory effects on *in vitro* platelet aggregation and *in vivo* thrombus formation in rats. In comparison with ISDN, FK409 had much more potent antiplatelet effects in both *in vitro* and *in vivo* experiments. However, in both experiments, FK409 inhibited platelet function dose-dependently but could not cause complete inhibition even at maximum doses. In *in vitro* experiments, the inhibition induced by FK409 at 32 μM was almost maximal and was only 64%. In *in vivo* experiments, the inhibitory effect of FK409 on thrombus formation reached a maximum at 10 mg kg^{-1}, p.o. and the inhibition was only 52% at this dose. Interestingly, in contrast with these results in rats, FK409 showed almost complete inhibition (97% inhibition) of platelet aggregation *in vitro* in man at 32 μM and the slope of the concentration-inhibition curve was steeper (Kita *et al.*, 1994). It is not clear why FK409 could not inhibit platelet function completely, in both *in vitro* and *in vivo* experiments in rats, as it did in the human *in vitro* experiments.

Recently, we reported that FK409, in contrast with ISDN, released NO spontaneously with a chemiluminescence analyzer (Kita *et al.*, 1994) and in this paper we have shown that FK409 spontaneoulsy generated nitrite, which is an oxidative product, in PB solution and rat plasma. Taking these data into account the antiplatelet activity of FK409 in our experiments is probably mediated by NO released spontaneously from the compound.

In *in vitro* and *in vivo* experiments, ISDN showed weak inhibition of platelet function at the highest doses (10% inhibition at 100 μM and 17% inhibition at 32 mg kg^{-1}, p.o. respectively). In order to explain the low efficacy of ISDN compared with FK409, we determined the concentrations of nitrite generated from ISDN and FK409 in rat plasma. In contrast with the result in PB, ISDN was able to generate nitrite in rat plasma. Feelish & Noack (1987a,b) reported that organic nitrates such as ISDN showed pharmacological actions via NO released from the compounds. In these reports, the sulphydryl group of cystein was required to biotransform organic nitrates to NO. Recently, it was reported that albumin in plasma catalyzed the denitrification of nitroglycerin in a reaction proceeding by way of its sulphydryl moiety (Chong & Fung., 1990). From these facts, it was considered that ISDN weakly inhibited platelet function in platelet-rich plasma (*in vitro*) and blood (*in vivo*) at the highest doses through being biotransformed to NO by sulphydryl moieties such as cystein contained in serum proteins. The amount of nitrite generated from ISDN during 60-min incubation, however, was much less than that from FK409. These data reflected well the differences in antiplatelet activities between FK409 and ISDN.

In conclusion, we have shown that FK409 has more potent antiplatelet activity than ISDN *in vitro* and *in vivo*. These

beneficial effects of FK409 are mediated by spontaneously released NO, which is considered to be important for the prevention of acute coronary syndromes such as unstable angina pectoris and acute myocardial infarction in patients (Hjemdahl-Monsen *et al.*, 1986; Fuster *et al.*, 1988). The preventive effects of FK409 in experimental animal models with acute coronary syndromes will be evaluated in future work.

References

BELL, F.K., O'NEILL, J.J. & BURGISON, R.M. (1963). Determination of the oil/water distribution coefficients of glyceryl trinitrate and two similar nitrate esters. *J. Pharmacol. Sci.*, **52**, 637–639.

BORN, G.V.R. & CROSS, M.J. (1968). The aggregation of blood platelets. *J. Physiol.*, **168**, 178–195.

CHONG, S. & FUNG, H.-L. (1990). Thiol-mediated catalysis of nitroglycerin degradation by serum proteins. *Drug Metab. Dispos.*, **18**, 61–67.

DECATERINA, R., GIANNESSI, D., CREA, F., CHIERCHIA, S., BERNINI, W., GAZZETTI, P. & L'ABBATE, A. (1984). Inhibition of platelet function by injectable isosorbide dinitrate. *Am. J. Cardiol.*, **53**, 1683–1687.

FEELISCH, M. & NOACK, E. (1987a). Nitric oxide (NO) formation from nitrovasodilators occurs independently of hemoglobin or non-heme iron. *Eur. J. Pharmacol.*, **142**, 465–469.

FEELISCH, M. & NOACK, E. (1987b). Correlation between nitric oxide formation during degradation of organic nitrates and activation of guanylate cyclase. *Eur. J. Pharmacol.*, **139**, 19–30.

FUSTER, V., BADIMON, L., COHEN, M., AMBROSE J.A., BADIMON, J.J. & CHESEBRO, J. (1988). Insight into the pathogenesis of acute ischemic syndromes. *Circulation*, **77**, 1213–1220.

HAMPTON, J.R., HARRISON, A.J., HONOUR, A.J. & MITCHELL J.R.A. (1967). Platelet behavior and drugs used in cardiovascular disease. *Cardiovasc. Res.*, **1**, 101–107.

HINO, N., IWAMI, M., OKAMOTO, M., YOSHIDA, K., HARUTA, H., OKUHARA, M., HOSODA, J., KOHSAK, M., AOKI, H. & IMANAKA, H. (1989). FK409, a novel vasodilator isolated from the acid-treated fermentation broth of *Streptomyces griseosporeus*. I. Taxonomy, fermentation, isolation and physiochemical and biological characteristics. *J. Antibiotics*, **42**, 1578–1583.

HJEMDAHL-MONSEN, C.E., LEWIS, H.D., CAIRNS, J., CHESEBRO, J.H. & FUSTER, V. (1986). Role of antithrombotic therapy in unstable angina, myocardial infarction and sudden death. *J.Am. Coll. Cardiol.*, **8** (Suppl B), 67B–75B.

KATSUKI, S., ARNOLD, W., MITTAL, C. & MURAD, F. (1977). Stimulation of guanylate cyclase by sodium nitroprusside, nitroglycerin and nitric oxide in various tissue preparations and comparison to the effects of sodium azide and hydroxylamine. *J. Cyclic Nucleotide Res.*, **3**, 23–25.

KITA, Y., HIRASAWA, Y., MAEDA, K., NISHIO, E. & YOSHIDA, K. (1994). Spontaneous nitric oxide release accounts for the potent pharmacological actions of FK409. *Eur. J. Pharmacol.*, **257**, 123–130.

KOWEY, P.R., VERRIER, R.L., LOWN, B. & HANDIN, R.I. (1981). The effects of nitroglycerin on intracoronary platelet aggregation and ventricular vulnerability during partial coronary stenosis. *Am. J. Cardiol.*, **47**, 489.

MELLION, B.T., IGNARRO, L.J., OHLSTEIN, E.H., PONTECOROVO, E.G., HYMAN, A.L. & KADOWITZ, P.J. (1981). Evidence for the inhibitory role of guanosine 3',5'-monophosphate in ADP-induced human platelet aggregation in the presence of nitric oxide and related vasodilators. *Blood*, **57**, 946–955.

PALMER, R.M.J., FERRIGE, A.G. & MONCADA, S. (1987). Nitric oxide release accounts for the biological activity of endothelium-derived relaxing factor. *Nature*, **327**, 524–526.

RADOMSKI, M.W., PALMER, R.M.J. & MONCADA, S. (1987). Comparative pharmacology of endothelium-derived relaxing factor, nitric oxide and prostacyclin in platelets. *Br. J. Pharmacol.*, **92**, 181–187.

SCHULTZ, K.D., SCHULTZ, K. & SCHULTZ, G. (1977). Sodium nitroprusside and other smooth muscle relaxants increase cyclic GMP levels in rat ductus deferens. *Nature*, **265**, 750–751.

SIBATA, S., SATAKE, N., SATO, N., MATSUO, M., KOIBUCHI, Y. & HESTER, R.K. (1991). Characteristics of vasorelaxing action of (3E)-4-ethyl-2-hydroximino-5-nitro-3-hexamide FK409, a new vasodilator isolated from microbial sources, in isolated rabbit arteries. *J. Cardiovasc. Pharmacol.*, **17**, 508–518.

UMETSU, T. & SANAI, K. (1978). Effects of 1-methyl-2-mercapto-5-(3-pyridyl)-imidazole (KC-6141), an anti-aggregating compound, on experimental thrombosis in rats. *Thrombos. Haemostas. (Stuttg.)*, **39**, 74–83.

YAMADA, H., YONEYAMA, F., SATOH, K. & TAIRA, N. (1991). Comparison of the effects of the novel vasodilator FK409 with those of nitroglycerin in isolated coronary artery of the dog. *Br. J. Pharmacol.*, **103**, 1713–1718.

(Received February 25, 1994
Revised May 3, 1994
Accepted June 1, 1994)

Br. J. Pharmacol. (1994), **113**, 389–394 © Macmillan Press Ltd, 1994

Up-regulation of [^{3}H]-des-Arg^{10}-kallidin binding to the bradykinin B_1 receptor by interleukin-1β in isolated smooth muscle cells: correlation with B_1 agonist-induced PGI_2 production

[1]J.P. Galizzi, M.C. Bodinier, B. Chapelain, S.M. Ly, L. Coussy, S. Giraud, G. Neliat & T. Jean

CEREP, BP 1, 86600, Celle l'evescault, France

1 Binding of the specific bradykinin B_1 receptor agonist, [^{3}H]-des-Arg^{10}-kallidin (-KD) was investigated in smooth muscle cells (SMC) isolated from rabbit mesenteric arteries (RMA).

2 [^{3}H]-des-Arg^{10}-KD specifically bound to interleukin-1 (IL-1)-treated RMA-SMC in a saturable fashion with an equilibrium dissociation constant (K_D) of 0.3–0.5 nM. The number of binding sites per cell was 20,000–35,000. Kinins inhibited [^{3}H]-des-Arg^{10}-KD binding to RMA-SMC with an order of potency very similar to that observed in typical B_1 specific bioassays: des-Arg^9-bradykinin (BK) $\approx$ KD $\gg\gg$ BK. Furthermore, the B_1 receptor antagonist [Leu^8]des-Arg^9-BK inhibited [^{3}H]-des-Arg^{10}-KD binding with an IC_{50} of 43 nM as expected for its effect at B_1 receptors. The B_2 receptor antagonists, NPC 567 and Hoe 140 only affected [^{3}H]-des-Arg^{10}-KD binding at very high concentrations ($IC_{50} = 0.8\ \mu M$ and $IC_{50} > 10\ \mu M$, respectively).

3 Des-Arg^9-BK (B_1 agonist) and [Hyp^3]Tyr(Me)^8-BK (B_2 agonist) did not induce prostacyclin (PGI_2) production by RMA-SMC. Lipopolysaccharide (LPS) treatment of the cells did not affect the B_1 agonist response whereas IL-1β treatment produced a 7 fold increase in des-Arg^9-BK-stimulated PGI_2 production. IL-1β also stimulated the response to B_2 agonists.

4 Des-Arg^9-BK-induced PGI_2 secretion in IL-1-primed RMA-SMC was mediated by B_1 receptors since it was inhibited by [Leu^8]des-Arg^9-BK ($IC_{50} = 56–73$ nM) but not by Hoe 140. High concentrations of NPC 567 ($IC_{50} = 2.4\ \mu M$) were required to inhibit PGI_2 production induced by B_1 agonists.

5 IL-1-treated RMA-SMC displayed a 5 fold increase in the number of B_1 receptors without modification of the affinity constant, thus establishing a possible relationship between the receptor density and the IL-1-primed B_1 response.

6 LPS treatment of the cells induced a 4 fold increase in B_1 receptor number without modifying PGI_2 secretion. This observation suggests that IL-1 but not LPS, in addition to increase in the number of receptors, signals the cell to permit the coupling of B_1 receptors to the PLA_2/cyclo-oxygenase pathway.

Keywords: [^{3}H]-des-Arg^{10}-kallidin; B_1 receptor; binding; signal transduction

Introduction

Pathophysiological stimuli such as tissue trauma, inflammation, allergy or anoxia, activate tissue or plasma kallikrein which cleaves low and high-molecular weight kininogen into bradykinin (BK) or kallidin (lysBK/KD). BK preferentially acts on B_2 receptors whereas the biological active carboxipeptidase fragments des-Arg^9-BK/des-Arg^{10}-KD activate B_1 receptors. These two receptor types have been distinguished on the basis of their selectivity for agonists and antagonists (Regoli & Barabé, 1980). Stimulation of the B_2 receptor by BK induces a large number of effects which have been extensively reviewed (see for reviews, Regoli *et al.*, 1990a,b; Farmer, 1992; Dray & Perkins, 1993). Under non pathological conditions, a great number of kinin-sensitive tissues display a B_2 kinin specificity whereas B_1 responsiveness is acquired following trauma (Regoli & Barabé, 1980). In a number of smooth muscle preparations, obtained from rabbit vascular tissues (Marceau *et al.*, 1980; Regoli *et al.*, 1981; Bouthillier *et al.*, 1987; Deblois & Marceau, 1987; Pruneau & Bélichard, 1993), human colon (Boschov *et al.*, 1984) or rat duodenum (Couture *et al.*, 1981), the B_1 response increases with the incubation time or after treatment with lipopolysaccharides (LPS). In addition, *in vivo* treatment of rabbits with bacterial extract induces a state of responsiveness in the cardiovascular system (Regoli *et al.*, 1981; Marceau *et al.*, 1984; Deblois *et al.*, 1989). Such a feature has led to the hypothesis that the B_2 receptor might play a more significant role in the earlier stages of inflammatory process whereas B_1 receptor would become more important for the maintenance of the response.

Binding experiments performed on whole pieces of rabbit anterior mesenteric vein (Barabé *et al.*, 1982) have shown that LPS-mediated B_1 sensitization was due to an increase in B_1 receptor expression. IL-1β seems to be a key mediator in LPS-induced B_1 agonist sensitization since it was found to stimulate a number of B_1 responses (Deblois *et al.*, 1988; 1991) and was released *in vitro* by vascular and immune cells upon stimulation by LPS (Libby *et al.*, 1986a,b) or by B_1 agonist (Tiffany & Burch, 1989) and *in vivo* by LPS treatment (Cannon *et al.*, 1989).

Finally, a part of the hypotensive effect of B_1 agonists in LPS-treated rabbit is due to prostaglandin release (Drapeau *et al.*, 1991). The relaxation of dog renal (Rhaleb *et al.*, 1989) and rabbit mesenteric arteries (Churchill & Ward, 1986; Deblois & Marceau, 1987) was inhibited by the cyclo-oxygenase inhibitor, indomethacin. The direct effects of B_1 agonists on prostacyclin (PGI_2) production by IL-1-treated smooth muscle cells has also been described (Levesque *et al.*, 1993).

In order to investigate the interaction of B_1 agonists with the cellular receptors as well as the effects of LPS and IL-1β, the binding of [^{3}H]-des-Arg^{10}-KD was investigated in smooth muscle cells isolated from rabbit superior mesenteric arteries. The treatment of RMA-SMC by LPS or IL-1β strongly increased the number of [^{3}H]-des-Arg^{10}-KD binding sites.

[1] Author for correspondence.

However, IL-1β but not LPS stimulated B_1-induced PGI_2 production. These results suggest that the IL-1-stimulated B_1 agonist response is not solely due to an increase in B_1 receptor expression but depends on IL-1 specific signalling events.

Methods

SMC isolation and cell culture

Rabbit mesenteric artery smooth muscle cells (RMA-SMC) were obtained as described by Ross (1971). Briefly, the superior mesenteric artery was aseptically excised and placed in Dulbecco's modified Eagle's medium (DMEM), 10% foetal calf serum (FCS) and 2% penicillin (100 u ml^{-1})/streptomycin (100 μg ml^{-1}). The artery was dissected free of outer adventitial layers and cut longitudinally. Endothelial lining was removed by gently rubbing the intimal surface with filter paper. Small pieces of tissue were incubated in DMEM, 10% FCS and 1% penicillin/streptomycin. After 6 days, the tissue was removed and adherent cells were cultured until confluence. Then, cells were obtained for the next passage with a brief trypsin (0.05%)-EDTA (0.5 mM) treatment. Their identity as smooth muscle cells was checked by indirect immunofluorescence for α-actin using a monoclonal mouse anti α-actin antibody (1A4). Binding experiments were conducted with the same cells as those used to evaluate PGI_2 production. After the 6th passage, the cells were unable to reach confluence and lost B_1 specific binding sites.

Equilibrium binding studies

In standard equilibrium binding experiments, the cells (3×10^5) were incubated in 500 μl of NaCl 137 mM, KCl 2.7 mM, BSA 0.1%, bacitracin 140 μg ml^{-1}, captopril 20 μM, DTT 0.1 mM and HEPES-Tris 20 mM pH 7.4 (binding buffer), at 4°C in the presence of indicated concentrations of [^{3}H]-des-Arg^{10}-KD. After 4 h incubation, the cells were filtered through polyethyleneimine (0.3%)-treated Whatman GF/C filters, under reduced pressure. The filters were immediately washed twice with 5 ml of cold binding buffer solution without protease inhibitors. For measurement of nonspecific binding, unlabelled des-Arg^9[Leu^8]-BK was included in the medium at a final concentration of 10^{-5} M. Inhibition of [^{3}H]-des-Arg^{10}-KD by different kinins was measured at equilibrium in the presence of 0.35 nM [^{3}H]-des-Arg^{10}-KD.

Measurement of PGI_2 production

PGI_2 was measured as the stable 6-keto-$PGF_{1\alpha}$ with the Cayman assay kit and according to the manufacturer's instructions. The cells were seeded in 96-well plates at 6000 cells/well. Cells at confluence were cultured in the absence or in the presence of LPS (1 μg ml^{-1}) or IL-1β (10 u ml^{-1}) for 20 h in complete culture medium. At the end of the incubation time, the medium was removed, the cells washed once and incubated with 0.15 ml of phosphate buffered saline solution supplemented with 0.5 mg ml^{-1} gelatin and 10 μM of captopril containing the kinin agonist. After 30 min incubation period at 37°C, the supernatants were collected for 6-keto-$PGF_{1\alpha}$ measurement. When used, antagonists were added 30 min before stimulation with the specific agonist.

Materials

[^{3}H]-des-Arg^{10}-KD (60–120 Ci $mmol^{-1}$) was obtained from New England Nuclear (Les Ulis, France). New Zealand white rabbits (2–2.5 kg) were supplied from local sources. DMEM, PBS, penicillin, streptomycin and foetal calf serum (FCS) were obtained from Gibco BRL (Eragny, France). Monoclonal mouse anti α-smooth muscle actin antibodies were from Dako (Trappes, France). Bradykinin and kallidin were from Sigma (La Verpillière, France). des-Arg^9-BK, [Leu^8]des-Arg^9-BK, D-Arg [Hyp^3,D-Phe^7]-BK (NPC 567) and [Hyp^{3}Tyr(Me)^8]-BK were from Bachem (Bubendorf, Switzerland). Hoe 140 (D-Arg-[Hyp^3,Thi^5,D-Tic^7,Oic^8]-BK) was custom-synthesized. IL-1β was obtained from Boehringer (Meylan, France). The Cayman assay kit (PGI_2) was purchased from Interchim (Montluçon, France).

Results

Binding of [^{3}H]-des-Arg^{10}-KD to IL-1-treated RMA-SMC

Preliminary kinetics studies have shown that the binding of [^{3}H]-des-Arg^{10}-KD (0.2–1 nM) to SMC at 4°C reached equilibrium within 4 h. Figure 1 illustrates a typical equilibrium binding experiment of [^{3}H]-des-Arg^{10}-KD to RMA-SMC treated with IL-1β. Specific binding, determined as the difference between total and nonspecific binding, was a saturable function of [^{3}H]-des-Arg^{10}-KD concentration. A Scatchard plot of the data (inset Figure 1) was consistent with the existence of a single class of sites with an average equilibrium dissociation constant (K_D) of 0.3–0.5 nM and an average number of 20,000–35,000 binding sites per cell. The K_D value was not modified when frozen cells were used but the number of binding sites decreased by approximately a factor of 2.5–3.

Effects of kinin agonists and antagonists on [^{3}H]-des-Arg^{10}-KD binding to IL-1-treated RMA-SMC

The inhibition curves of [^{3}H]-des-Arg^{10}-KD binding to IL-1-treated SMC obtained in the presence of increasing concentrations of various kinin agonists are shown in Figure 2a. Kinin agonists inhibited [^{3}H]-des-Arg^{10}-KD binding with a rank order of potency similar to that determined for their activity in B_1 specific biological assays: des-Arg^9-BK (IC_{50} = 7.7 nM) ≈ KD (IC_{50} = 8.2 nM) ≫ BK (IC_{50} = 3800 nM). The selective B_1 antagonist [Leu^8]des-Arg^9-BK also displaced [^{3}H]-des-Arg^{10}-KD binding with a half maximum concentration of

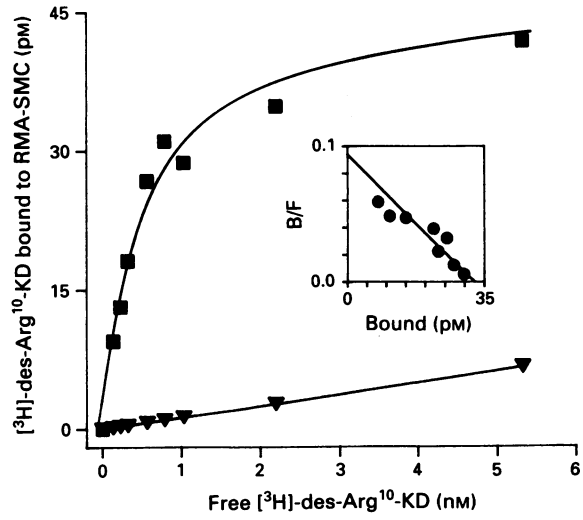


Figure 1 Binding analysis of [^{3}H]-des-Arg^{10}-KD to interleukin-1 (IL-1)-treated rabbit mesenteric artery smooth muscle cells (RMA SMC). Main panel: 3×10^5 cells (passage 5) were incubated at 4°C in 500 μl of binding buffer and in the presence of increasing concentrations of [^{3}H]-des-Arg^{10}-KD without (■, $n = 3$) or with (▼, $n = 3$) 10^{-5} M [Leu^8]des-Arg^9-BK. After 4 h, the cells were filtered under vacuum through GF/C filters and bound radioactivity was measured by a scintillation counter. Inset, Scatchard plot of the specific [^{3}H]-des-Arg^{10}-KD binding component: K_D = 0.35 mM, B_{max} = 35,520 sites/cell (32 pM).

43 nM which is close to the pA_2 measured in rabbit aorta contraction (Regoli *et al.*, 1990b). In addition, the typical specific B_2 antagonists Hoe 140 and NPC 567 inhibited [^{3}H]-des-Arg^{10}-KD binding only at very high concentrations: IC_{50} (Hoe 140) > 10 μM and IC_{50} (NPC 567) = 0.8 μM (Figure 2b). These values are far from those found in B_2-specific bioassays such as the inhibition of BK-mediated rabbit jugular vein contraction which is antagonized by NPC 567 and Hoe 140 with pA_2 values of 8 and 9.2, respectively (Regoli *et al.*, 1990a; Rhaleb *et al.*, 1992).

IL-1 but not LPS stimulates B_1 agonist-induced high level of PGI_2 production by RMA-SMC

Recently, it was shown that B_1 agonist response in rabbit aorta SMC was coupled to PGI_2 production (Levesque *et al.*, 1993). Figure 3a shows that increasing concentrations of the B_1 agonist, des-Arg^9-BK, had no significant effect on PGI_2 production by untreated SMC. LPS (1 μg ml^{-1}) alone did not modify the secretion of prostacyclin measured in the absence or presence of des-Arg^9-BK. Identical results were obtained with 10 μg ml^{-1} of LPS. In contrast, 24 h incubation of SMC with 10 u ml^{-1} of IL-1β markedly enhanced the basal level of PGI_2 from 7 to 19 pg/well. Addition of des-Arg^9-BK produced a 7 fold increase in PGI_2 secretion from 19 to an average of 130 pg/well with a half maximum effect at 20 nM (Exp.1) and 14 nM (Exp.2) (Figure 3a, Exp.2). Indeed, PGI_2 production was mediated by des-Arg^9-BK acting at the B_1 receptor since it was inhibited by the selective B_1 antagonist [Leu^8]Arg^9-BK with an IC_{50} of 73 nM (Figure 3b). The B_2 antagonist, Hoe 140, did not inhibit des-Arg^9-BK-induced PGI_2 production (Figure 3b). As in binding assays, the less specific B_2 antagonist, NPC 567, inhibited PGI_2 production only at the high concentrations: IC_{50} = 2.4 μM.

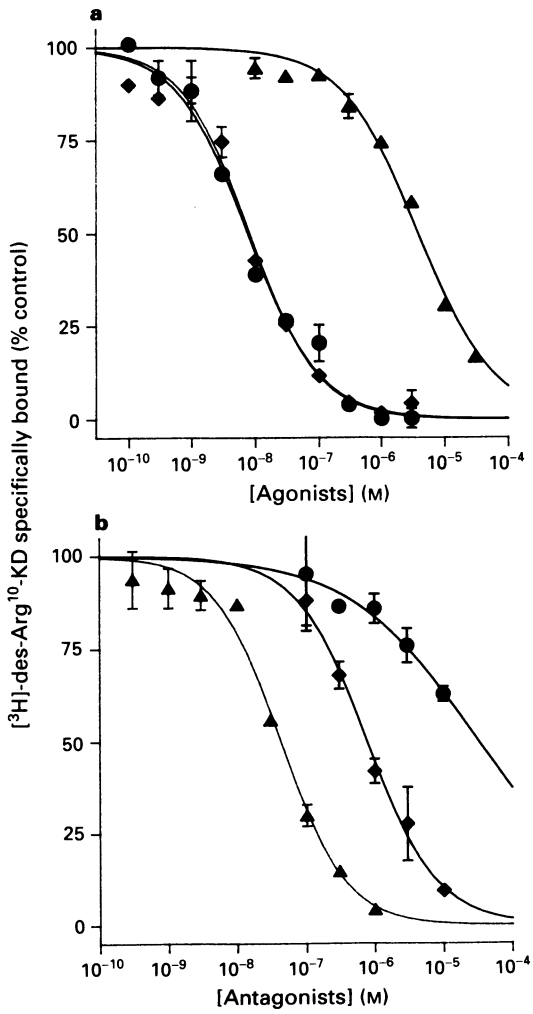


Figure 2 Effects of various kinin derivatives on [^{3}H]-des-Arg^{10}-KD binding to RMA-SMC. IL-1-treated cells (3 × 10^5, 20 h) were incubated at 4°C with 0.35 nM [^{3}H]-des-Arg^{10}-KD in the presence of the indicated concentrations of (a) des-Arg^9-BK (●), kallidin (◆), and bradykinin (▲); (b) [Leu^8]des-Arg^9-BK (▲), NPC 567 (◆) and Hoe 140 (●). After 4 h the cells were filtered as in Figure 1 and the radioactivity was determined; 100% corresponds to the specific binding of [^{3}H]-des-Arg^{10}-KD (1500–2000 d.p.m.) without drugs; values are means ± s.d. of triplicate determinations.

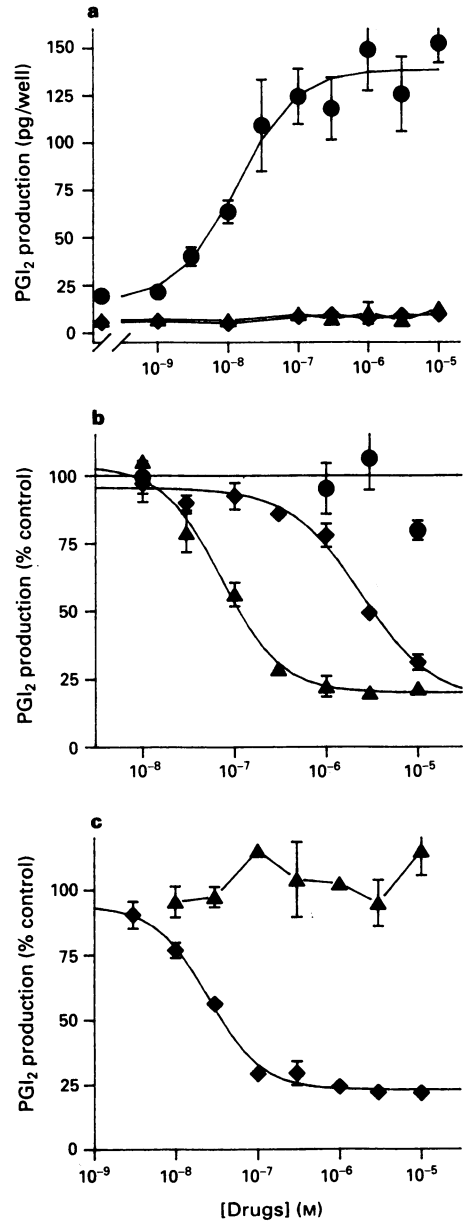


Figure 3 Interleukin 1β (IL-1β) treatment of RMA-SMC enhanced B_1- and B_2-mediated-prostacyclin (PGI_2) secretion. (a) Cells (6000/well) were cultured at confluence in 96 well plates and then incubated without (▲) or with 1 μg ml^{-1} lipopolysaccharide (LPS) (◆) or 10 u ml^{-1} IL-1β (●). After 20 h, the cells were stimulated for 30 min by increasing concentrations of des-Arg^9-BK and the amount of PGI_2 in the supernatant was determined. (b) and (c) IL-1-treated cells were incubated with the indicated concentrations of [Leu^8]des-Arg^9-BK (▲), NPC 567 (◆) or Hoe 140 (●) for 30 min. Then, cells were stimulated for an additional 30 min with (b) the B_1 agonist des-Arg^9-BK (10^{-7} M) or (c) the B_2 agonist [Hyp^3,Tyr(Me)^8]-BK (10^{-8} M). The amount of PGI_2 secreted was measured in the cell supernatant as the stable 6 keto-$PGF_{1\alpha}$ by assay kit as described in Methods. Values are the means ± s.d. of triplicate determinations.

Stimulation of PGI_2 production in IL-1-primed SMC was not restricted to B_1 agonists since it was also found when the B_2 agonist [Hyp^{3}Tyr(Me)^8]-BK was used as stimulating agent. In this case, PGI_2 secretion was blocked by low concentrations of the B_2 specific antagonist, NPC 567 (IC_{50} = 25 nM) but not by the B_1 antagonist, [Leu^8]des-Arg^9-BK up to 10^{-5} M (Figure 3c).

B_1 agonist-induced PGI_2 production in IL-1-treated RMA-SMC is not mediated by nitric oxide

It has recently been proposed that exogenous or endogenous nitric oxide acts on cyclo-oxygenase (COX) to increase the production of prostglandin E_2 (PGE_2) (Salvemini *et al.*, 1993). In this regard, B_1 agonist-induced PGI_2 production in IL-1-treated cells was investigated in the presence of NO inhibitors. Figure 4 shows that neither N^G-nitro-monomethyl-L-arginine (L-NMMA) nor aminoguanidine, the most selective inhibitor of inducible NO synthase, affected the B_1 agonist-induced PGI_2 production by Il-1-treated RMA-SMC. Hence, the difference in LPS and IL-1β-induced PGI_2 secretion was not due to a selective effect of IL-1β on endogenous NO production.

IL-1β and LPS up-regulate [^{3}H]-des-Arg^{10}-KD binding sites in RMA-SMC

After 20 h incubation of RMA-SMC with or without IL-1β, the cells were assessed for [^{3}H]-des-Arg^{10}-KD binding. Figure 5 shows that IL-1 pretreatment of SMC did not modify the equilibrium dissociation constant (K_D(control) = 0.39 nM – K_D (IL-1) = 0.38 nM) but strongly increased the number of binding sites per cell (B_{max}(control) = 6800; 4 pM to B_{max}(IL-1) = 34,300; 23 pM).

LPS, which is already known to induce *de novo* synthesis of specific proteins, increased the number of [^{3}H]-des-Arg^{10}-KD binding sites, (B_{max}(LPS) = 26,200 sites/cell; 17 pM) without significantly modifying the affinity (K_D(LPS) = 0.38 nM). These results suggest that the difference observed in B_1-stimulated PGI_2 production following IL-1 or LPS treatment was not exclusively due to an increase in B_1 receptor expression.

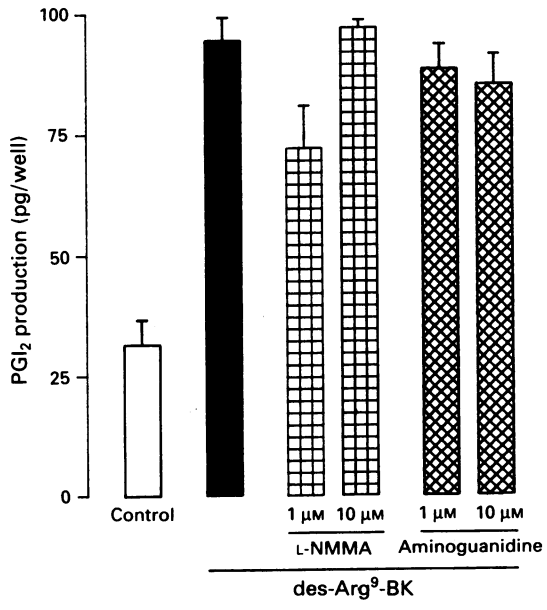


Figure 4 Effects of nitric oxide synthase inhibitors on prostacyclin (PGI_2) production. Cells were cultured at confluence in 96 well plates and then incubated in the presence of 10 u ml^{-1} interleukin-1β (IL-1β). After 20 h, the cells were first incubated without or with L-NMMA or aminoguanidine at the indicated concentrations and then stimulated for 30 min with 10^{-7} M des-Arg^9-BK. PGI_2 production was measured as in Figure 3. Columns are the means ± s.d. of triplicate determinations.

Discussion

In the present study, we describe the characterization of the B_1 receptor as well as its coupling to PGI_2 production in LPS- and IL-1-treated RMA-SMC.

The binding of kinins to the B_1 type receptor has already been described on whole pieces of rabbit mesenteric veins using [^{3}H]-des-Arg^9-BK as a ligand (Barabé *et al.*, 1982). However, as noticed by the authors, such binding experiments suffer from a number of difficulties including the variability from one vein to another and the achievement of binding saturability.

Preliminary experiments revealed that [^{3}H]-des-Arg^{10}-KD bound poorly to isolated RMA-SMC. Since IL-1β has been demonstrated *in vitro* to stimulate the effects of des-Arg^9-BK, [^{3}H]-des-Arg^{10}-KD binding was further investigated in RMA-SMC treated with IL-1β for 20 h. [^{3}H]-des-Arg^{10}-KD was

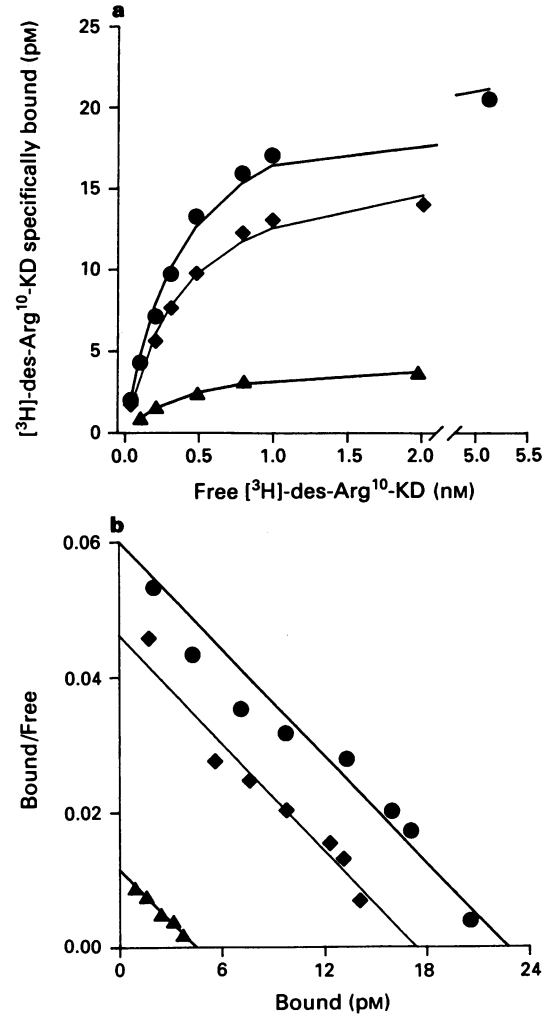


Figure 5 Up-regulation by interleukin-1β (IL-1β) and lipopolysaccharide (LPS) or [^{3}H]-des-Arg^{10}-KD binding sites in RMA-SMC. (a) RMA-SMC at confluence were cultured in the absence (▲, n = 3) or in the presence of 10 u ml^{-1} IL-1β (●, n = 3) or 1 μg ml^{-1} LPS (◆, n = 3). After 20 h, the cells were harvested for saturation binding experiments: 3 × 10^5 cells in 500 μl of binding buffer were incubated at 4°C in the presence of increasing concentrations of [^{3}H]-des-Arg^{10}-KD. After 4 h, the cell bound radioactivity was separated from free by rapid filtration and determined. Nonspecific binding was obtained with 10^{-5} M [Leu^8]des-Arg^9-BK. (b) Scatchard analysis of the specific [^{3}H]-des-Arg^{10}-KD binding component.

found to bind to IL-1-treated SMC in a specific and saturable manner. These binding sites appeared to be physiologically relevant since the K_D value of 0.30–0.5 nM (Figure 1) was comparable to the pD_2 of des-Arg^{10}-KD (8.60) measured in rabbit aortic contraction (Regoli *et al.*, 1990b). Three important observations supported the fact that [^{3}H]-des-Arg^{10}-KD bound to the B_1 receptor type: (i) the agonists des-Arg^9-BK, kallidin and bradykinin inhibited binding with a rank order of potency identical to that determined in B_1 specific bioassays; (ii) the specific B_1 antagonist [Leu^8]des-Arg^9-BK inhibited [^{3}H]-des-Arg^{10}-KD binding with an IC_{50} (43 nM) close to its pA_2 (7.27) measured in rabbit aorta (Regoli *et al.*, 1990b); (iii) the specific B_2 antagonist Hoe 140 had little effect on [^{3}H]-des-Arg^{10}-KD binding.

The role of prostanoid secretion in the relaxation of the rabbit mesenteric arteries following B_1 agonist stimulation has been well established (Churchill & Ward, 1986; Deblois & Marceau, 1987). Isolated RMA-SMC in culture have been demonstrated to release arachidonic acid upon treatment with des-Arg^9-BK (Tropea *et al.*, 1993). Accordingly, des-Arg^9-BK stimulation of the IL-1-primed RMA-SMC produced a 7 fold increase in PGI_2 production as compared to untreated cells. Conversely, LPS treatment did not enhance the response to des-Arg^9-BK. Furthermore des-Arg^9-BK was demonstrated to induce PGI_2 production by interacting at B_1 receptor since B_1 but not B_2 specific antagonists were able to block the des-Arg^9-BK response. The B_2 agonist [Hyp^3]Tyr (Me)^8-BK was also capable of inducing PGI_2 production in IL-1-treated cells, thus demonstrating the existence of functional B_2 receptors in RMA-SMC as already described (Tropea *et al.*, 1993).

In order to gain further insight into the molecular mechanism associated with IL-1 stimulation, the binding of [^{3}H]-des-Arg^{10}-KD was investigated on cells treated with either LPS or IL-1β for 20 h. Saturation binding experiments clearly demonstrated that LPS and IL-1β increased the number of binding sites by a factor of 4 and 5 respectively, without significantly modifying the affinity constant. At first glance, these results suggest that the stimulation of B_1 agonist response by IL-1β might be due to an increase in the number of B_1 binding sites. However, they also point to the fact that an increase in receptor number might not be sufficient to promote B_1-induced PGI_2 release since LPS induced an increase in the number of B_2 receptors without affecting PGI_2 production. Obviously, it is possible that the difference in [^{3}H]-des-Arg^{10}-KD binding sites observed between LPS and IL-1β treatment (26,200 to 34,300 sites/cell) accounts for IL-1-mediated PGI_2 production. Alternatively, IL-1β may act on a downstream event involved in B_1 receptor signalling. For instance, IL-1β has been described as inducing cyclooxygenase type 2 synthesis (COX-2) in endothelial cells (Habib *et al.*, 1993), fibroblasts and macrophages (O'Banion *et al.*, 1992). Although LPS also activates COX-2 synthesis in macrophages, it is possible that in RMA-SMC, COX-2 synthesis would be selectively induced by IL-1β but not by LPS.

Nitric oxide has recently been shown to activate cyclooxygenase activity (Salvemini *et al.*, 1993). Moreover, the induction of nitric oxide synthase in rat lung homogenates from LPS-treated rats was partially inhibited by the IL-1 receptor antagonist (Szabo *et al.*, 1993). However, NO synthase inhibitors did not modify IL-1-mediated PGI_2 production.

Further investigations are needed to confirm that the difference between LPS and IL-1β results from a preferential coupling of IL-1β to COX induction. LPS injection into rabbit induced a sensitization to des-Arg^9-BK as well as an increase in IL-1β plasma concentration (Cannon *et al.*, 1989). LPS also renders vascular cells in culture able to produce IL-1 (Libby *et al.*, 1986a,b). Injection of IL-1β into rabbit enhanced vascular responses to the kinin metabolite, des-Arg^9-BK (Deblois *et al.*, 1991). Thus, the finding that IL-1β greatly stimulates des-Arg^9-BK to produce PGI_2 is in accordance with the notion of IL-1β as a key mediator responsible for the inducing effect.

At present, we do not know if LPS is able to induce IL-1β secretion by RMA-SMC which in turn would produce an increase in [^{3}H]-des-Arg^{10}-KD binding sites and PGI_2 secretion. The observation that LPS is poor inducer of PGI_2 production does not favour this hypothesis. Although LPS does not prime RMA-SMC for B_1 agonist-induced PGI_2 production, the fact that it does increase B_1 receptor number suggests that LPS may be able to prime other B_1-mediated biological effects.

During the preparation of this manuscript a paper was published (Schneck *et al.*, 1994) describing the characterization of B_1 receptor in rabbit isolated aortic cells. The binding affinity for [^{3}H]-des-Arg^{10}-KD was in the same range as reported here but the number of B_1 receptors per cell was very low (680 sites/cell) and did not exceed 4250 sites/cell following EGF treatment.

Thus, the presence of B_1 binding sites in RMA-SMC makes these cells a very attractive model to characterize the molecular features of the receptor and obtain further insight into the mechanisms of its regulation.

We wish to thank Isabelle Bernard, Bernadette Coué and Maryse Vasseur for their expert technical assistance.

References

BARABE, J., BABIUK, C. & REGOLI, D. (1982). Binding of [^{3}H]des-Arg^9-BK to rabbit anterior mesenteric vein. *Can. J. Physiol. Pharmacol.*, **60**, 1551–1555.

BOSCHCOV, P., PAIVA, A.C.M., PAIVA, T.B. & SHIMUTA, S.I. (1984). Further evidence for the existence of two receptor sites for bradykinin responsible for the biphasic effect in the rat isolated duodenum. *Br. J. Pharmacol.*, **83**, 591–600.

BOUTHILLIER, J., DEBLOIS, D. & MARCEAU, F. (1987). Studies on the induction of pharmacological responses to des-Arg^9-bradykinin *in vitro* and *in vivo*. *Br. J. Pharmacol.*, **92**, 257–264.

CANNON, J.G., CLARK, B.D., WINGFIELD, P., SCHMEISSNER, U., LOSBERGER, C., DINARELLO, C.A. & SHAW, A.R. (1989). Rabbit IL-1, cloning, expression, biologic properties and transcription during endotoxemia. *J. Immunol.*, **142**, 2299–2306.

CHURCHILL, L. & WARD, P.E. (1986). Relaxation of isolated mesenteric arteries by des-Arg^9-bradykinin stimulation of B_1 receptors. *Eur. J. Pharmacol.*, **130**, 11–18.

COUTURE, R., MIZRAHI, J., REGOLI, D. & DEVROEDE, G. (1981). Peptides and the human colon: an in vitro pharmacological study. *Can. J. Physiol. Pharmacol.*, **59**, 957–964.

DEBLOIS, D., BOUTHILLIER, J. & MARCEAU, F. (1988). Effect of glucocorticoids, monokines and growth factors on the spontaneously developing responses of the rabbit isolated aorta to des-Arg^9-bradykinin. *Br. J. Pharmacol.*, **93**, 969–977.

DEBLOIS, D., BOUTHILLIER, J. & MARCEAU, F. (1989). Pharmacological modulation of the up-regulated responses to des-Arg^9-bradykinin in vivo and in vitro. *Immunopharmacol.*, **17**, 187–198.

DEBLOIS, D., BOUTHILLIER, J. & MARCEAU, F. (1991). Pulse exposure to protein synthesis inhibitors enhances vascular responses to des-Arg^9-bradykinin: possible role of interleukin-1. *Br. J. Pharmacol.*, **103**, 1057–1066.

DEBLOIS, D. & MARCEAU, F. (1987). The ability of des-Arg^9-bradykinin to relax rabbit isolated mesenteric arteries is acquired during in vitro incubation. *Eur. J. Pharmacol.*, **142**, 141–144.

DRAPEAU, G., DEBLOIS, D. & MARCEAU, F. (1991). Hypotensive effects of Lys-des-Arg^9-bradykinin and metabolically protected agonists of B_1 receptors for kinins. *J. Pharmacol. Exp. Ther.*, **259**, 997–1003.

DRAY, A. & PERKINS, M. (1993). Bradykinin and inflammatory pain. *Trends Neurosci.*, **16**, 99–104.

FARMER, S.G. (1992). Biochemical and molecular pharmacology of kinin receptors. *Annu. Rev. Pharmacol. Toxicol.*, **32**, 511–536.

HABIB, A., CREMINON, C., FROBERT, Y., GRASSI, J., PRADELLES, P. & MACLOUF, J. (1993). Demonstration of an inducible cyclooxygenase in human endothelial cells using antibodies raised against the carboxyl-terminal region of the cyclooxygenase-2. *J. Biol. Chem.*, **268**, 23448–23454.

LEVESQUE, L., DRAPEAU, G., GROSE, J.H., RIOUX, F. & MARCEAU, F. (1993). Vascular mode of action of kinin B_1 receptors and development of a cellular model for the investigation of these receptors. *Br. J. Pharmacol.*, **109**, 1254–1262.

LIBBY, P., ORDOVAS, J.M., AUGER, K.R., ROBBINS, A.H., BIRINYI, L.K. & DINARELLO, C. (1986a). Endotoxin and tumor necrosis factor induce interleukin-1 gene expression in adult human vascular endothelial cells. *Am. J. Pathol.*, **124**, 179–185.

LIBBY, P., ORDOVAS, J.M., BIRINYI, L.K., AUGER, K.R. & DINARELLO, C. (1986b). Inducible interleukin-1 gene expression in human vascular smooth muscle cells. *J. Clin. Invest.*, **78**, 1432, 1438.

MARCEAU, F., BARABE, J., ST-PIERRE, S. & REGOLI, D. (1980). Kinin receptors in experimental inflammation. *Can. J. Physiol. Pharmacol.*, **58**, 536–542.

MARCEAU, F., LUSSIER, A. & ST-PIERRE, S. (1984). Selective induction of cardiovascular responses to des-Arg^9-bradykinin by bacterial endotoxin. *Pharmacol.*, **29**, 70–74.

O'BANION, M.K., WINN, V.D. & YOUNG, D.A. (1992). cDNA cloning and functional activity of a glucocorticoid-regulated inflammatory cyclooxygenase. *Proc. Natl. Acad. Sci. U.S.A*, **89**, 4888–4892.

PRUNEAU, D. & BELICHARD, P. (1993). Induction of bradykinin-mediated relaxation in the isolated rabbit carotid artery. *Eur. J. Pharmacol.*, **239**, 63–67.

REGOLI, D. & BARABE, J. (1980). Pharmacology of bradykinin and related kinins. *Pharmacol. Rev.*, **32**, 1–46.

REGOLI, D.C., MARCEAU, F. & LAVIGNE, J. (1981). Induction of B_1-receptors for kinins in the rabbit by a bacterial lipopolysaccharide. *Eur. J. Pharmacol.*, **71**, 105–115.

REGOLI, D., RHALEB, N.-E., DION, S. & DRAPEAU, G. (1990a). New selective bradykinin receptor antagonists and bradykinin B2 receptors characterization. *Trends Pharmacol. Sci.*, **11**, 156–161.

REGOLI, D., RHALEB, N.-E., DRAPEAU, G. & DION, S. (1990b). Kinin receptor subtypes. *J. Cardiovasc. Pharmacol.*, **15**, S30–S38.

RHALEB, N.E., DION, S., BARABE, J., ROUISSI, N., JUKIC, D., DRAPEAU, G. & REGOLI, D. (1989). Receptor for kinins in isolated arterial vessels of dogs. *Eur. J. Pharmacol.*, **162**, 419–427.

RHALEB, N.E., ROUISSI, N., JUKIC, D., REGOLI, D., HENKE, S., BREIPOHL, G. & KNOLLE, J. (1992). Pharmacological characterization of a new highly potent B_2 receptor antagonist (HOE 140: D-Arg-[Hyp^3,Thi^5,D-Tic^7,Oic^8]bradykinin). *Eur. J. Pharmacol.*, **210**, 115–120.

ROSS, R. (1971). The smooth muscle cell. II. Growth of smooth muscle in culture and formation of elastic fibers. *J. Cell. Biol.*, **50**, 172–186.

SALVEMINI, D., MISKO, T.P., MASFERRER, J.L., SEIBERT, K., CURRIE, M.G. & NEEDLEMAN, P. (1993). Nitric oxide activates cyclooxygenase enzymes. *Proc. Natl. Acad. Sci. U.S.A.*, **90**, 7240–7244.

SCHNECK, K.A., HESS, J.F., STONESIFER, G.Y. & RANSOM, R.W. (1994). Bradykinin B1 receptors in rabbit aorta smooth muscle cells in culture. *Eur. J. Pharmacol.*, **266**, 277–282.

SZABO, C., WU, C.C., GROSS, S.S., THIEMERMANN, C. & VANE, J.R. (1993). Interleukin-1 contributes to the induction of nitric oxide synthase by endotoxin *in vivo*. *Eur. J. Pharmacol.*, **250**, 157–160.

TIFFANY, C.W. & BURCH, R.M. (1989). Bradykinin stimulates tumor necrosis factor and interleukin-1 release from macrophages. *FEBS Lett.*, **247**, 189–192.

TROPEA, M.M., GUMMELT, D., HERZIG, M.S. & LEEB-LUNDBERG, L.M.F. (1993). B_1 and B_2 kinin receptors on cultured rabbit superior mesenteric artery smooth muscle cells: receptor-specific stimulation of inositol phosphate formation and arachidonic acid release by des-Arg^9-bradykinin and bradykinin. *J. Pharmacol. Exp. Ther.*, **264**, 930.

(Received April 25, 1994
Revised June 2, 1994
Accepted June 3, 1994)

Br. J. Pharmacol. (1994), **113**, 395–402 © Macmillan Press Ltd, 1994

Effects of the calcium channel blockers, diltiazem and Ro 40-5967, on systemic haemodynamics and plasma noradrenaline levels in conscious dogs with pacing-induced heart failure

Jinbo Su, Nathalie Renaud, Alain Carayon, Bertrand Crozatier & [1]Luc Hittinger, with the technical assistance of Monique Laplace

I.N.S.E.R.M. U400, Faculté de Médecine, 94010 Créteil Cedex and from Laboratoire de Biochimie Médicale (A.C.), 91 Bld de L'Hôpital, 75634 Paris Cedex 13, France

1 Calcium channel blockers increase cardiovascular morbidity and mortality in patients with left ventricular dysfunction. These adverse effects are probably related to the negative inotropic effect of calcium channel blockers and/or a neurohormonal activation.

2 The present study was designed to examine, in conscious dogs, the acute haemodynamic and sympathetic effects of diltiazem and Ro 40-5967 (a novel calcium channel blocker) in the control state and in heart failure.

3 Thirteen dogs were instrumented with a micromanometer and an aortic catheter. After completion of experiments in the control state, heart failure was induced by right ventricular pacing (250 beats min^{-1}, 3 weeks). Diltiazem and Ro 40-5967 were given intravenously (0.8 mg kg^{-1} and 1.0 mg kg^{-1} respectively). Cardiac output was measured by a thermodilution technique.

4 In the control state, both agents decreased similarly mean aortic pressure with significant increases in heart rate, cardiac output (both +1.0 l min^{-1} and $P<0.001$) and plasma noradrenaline (both +55%) without changes in left ventricular dP/dt_{max}. In heart failure, for matched decreases in mean aortic pressure, neither diltiazem nor Ro 40-5967 changed heart rate significantly; diltiazem decreased cardiac output (−0.3 l min^{-1}, $P<0.02$) and dP/dt_{max} (−14%, $P<0.001$) while Ro 40-5967 still increased cardiac output (+0.3 l min^{-1}, $P<0.02$) although the increased amount was smaller than in the control state. Plasma noradrenaline level was increased more during diltiazem infusion (+120%) than during Ro 40-5967 infusion (+38%, $P<0.001$).

5 Diltiazem and Ro 40-5967 have similar haemodynamic and sympathetic effects in the control state. Heart failure alters haemodynamic and sympathetic responses to both calcium channel blockers but the magnitude of the alteration appears to be different. Diltiazem exerts a depressant effect on cardiac function which cannot be overcome by its vasodilator effect and sympathetic stimulation, while Ro 40-5967 has little effect on cardiac function. These data suggest that novel calcium channel blockers with less depressant effect may not be detrimental in heart failure.

Keywords: Calcium channel blockers; diltiazem; heart failure; left ventricular function; sympathetic system

Introduction

Owing to their peripheral vasodilator and anti-ischaemic actions and to their prevention of intracellular calcium overload, calcium channel blockers had been expected to be useful in the management of heart failure in patients and to improve the haemodynamic and clinical status of patients. However, the results of clinical trials with calcium channel blockers in patients with chronic heart failure have shown that short-term therapy with verapamil (Chew *et al.*, 1981), nifedpine or other dihydropyridines (Brooks *et al.*, 1980; Elkayam *et al.*, 1985; 1990; Barjon *et al.*, 1987) can cause haemodynamic and clinical deterioration; long-term therapy with these agents or diltiazem does not produce significant clinical improvement and may produce adverse effects and increase cardiovascular morbidity and mortality (Muller *et al.*, 1984; Wilcox *et al.*, 1986; the Multicenter Diltiazem Postinfarction Trial Research Group, 1988; Goldstein *et al.*, 1991).

Possible mechanisms for explaining these adverse effects of calcium channel blockers are their depressant effects on cardiac function through the direct negative inotropic action on the myocardium and neurohormonal activation which can produce cellular damage (Packer, 1989; Francis, 1991). A negative inotropic effect has been demonstrated *in vitro* and *in vivo* in normal hearts with calcium channel blockers such as nifedipine and verapamil (Walsh *et al.*, 1981; Millard *et al.*, 1982). Diltiazem appears to exert less negative inotropic effect than other calcium channel blockers in normal animals (Henry, 1980; Walsh *et al.*, 1981; Low *et al.*, 1982; Millard *et al.*, 1992) but it could impair left ventricular function in conscious dogs with volume overload-induced hypertrophied heart (Porter *et al.*, 1983) and in the isolated hypertrophied failing heart (Ezzaher *et al.*, 1991) at a dose which did not affect cardiac function in the control state. It was also shown that some calcium channel blockers increased plasma noradrenaline in normal volunteers and in patients with hypertension (Corea *et al.*, 1979; Cody *et al.*, 1987).

The present study was designed to determine the acute haemodynamic and sympathetic effects of calcium channel blockers in the same chronically instrumented conscious dogs before and after induction of heart failure. Heart failure was produced by chronic rapid right ventricular pacing for two to four weeks. This low-output heart failure model is characterized by ventricular dilatation, ventricular systolic and diastolic dysfunction (Armstrong *et al.*, 1986; Wilson *et al.*, 1987; Shannon *et al.*, 1991; Komamura *et al.*, 1992), alterations in the myocardial β-adrenoceptor system (Calderone *et al.*, 1991; Marzo *et al.*, 1991) and intracellular calcium handing (Perreault *et al.*, 1992) but does not appear to be associated with ischaemia (Wilson *et al.*, 1987). Diltiazem was used in the present study because it appeared to exert less negative inotropic effects than nifedipine and verapamil in

[1] Author for correspondence.

normal animals (Henry, 1980; Walsh *et al.*, 1981; Low *et al.*, 1982; Millard *et al.*, 1982) and because our first goal was to examine the underlying mechanisms of the alteration in cardiac function induced by diltiazem in heart failure. Another goal was to compare the haemodynamic and sympathetic effects of diltiazem with those of a new calcium channel antagonist, Ro 40-5967 which could act through binding sites closely related to verapamil binding sites (Osterrieder & Holck, 1989). We expected that Ro 40-5967 would not depress left ventricular function in heart failure since previous studies in rabbit isolated failing hearts (Ezzaher *et al.*, 1991), in ischaemic *in vivo* canine hearts (Clozel *et al.*, 1989) and in rat hearts with or without heart failure after chronic myocardial infarction (Clozel *et al.*, 1991; Véniant *et al.*, 1991) have demonstrated that Ro 40-5967 has less inotropic effect than other calcium channel blockers.

Methods

Surgery and instrumentation

Thirteen adult mongrel dogs (body weight: 13.5–25.7 kg; avg: 18.3 ± 1.0 kg) were initially sedated with thiopentone sodium (Specia, Paris, France, 15–30 mg kg^{-1}; avg: 18.3 ± 1.4 mg kg^{-1}, i.v.) for intubation. Anaesthesia was then maintained with 1.0% halothane mixed with compressed air. Ventilation was performed with a Harvard ventilator (South Natick, MA, U.S.A.). A left thoracotomy was performed through the fifth intercostal space under sterile conditions. The pericardium was widely opened. Tygon catheters (Norton Plastics and Synthetic Division, Akron, Ohio, U.S.A.) were implanted in the descending aorta and the left atrium. Two chronically implantable pacing leads (No. 8503, Medical Products Division/3M, Ela medical, Montrouge, France) were implanted on the right ventricular free wall. A chronically implantable micromanometer (P7, Konigsberg Instrument, Pasadena, CA, U.S.A.) was inserted into the left ventricular cavity through the left ventricular apex for continuous measurements of left ventricular pressure and left ventricular dP/dt. A drainage tygon catheter was placed in the left thoracic cavity. Wires and catheters were externalized in the interscapular area. The pericardium was left open and the thoracic incision was then repaired in layers. Postoperative care was carried out daily and the dogs were trained to lie on their right side. Ampicillin was given (1 g day^{-1}) for seven days. The animals used in this study were maintained in accordance with the official regulations of the French Ministry of Agriculture.

Experimental protocol

For each dog, experimental protocol consisted of two steps: one before the induction of heart failure (control state) and one after (heart failure).

Experiments in the control state When dogs had fully recovered from surgery after a period of 2 weeks, experiments were performed in the conscious state, dogs lying on their right side. To measure cardiac output, a 5F Swan-Ganz catheter was inserted into the pulmonary artery through the femoral vein under local anaesthesia (1% lignocaine). Two calcium channel antagonists were used in this study. Doses were chosen to produce a decrease of about 10 mmHg of mean aortic pressure in the normal state. Based on the study of Porter *et al.* (1983), diltiazem (0.8 mg kg^{-1}) was given intravenously as a 200 μg kg^{-1} bolus and then followed by continuous infusion (40 μg kg^{-1} min^{-1} for 15 min). Cardiac output was measured with 3–5 injections of 5 ml physiological solution at baseline state and at 5, 10 and 15 min of drug infusion. Ro 40-5967 (1.0 mg kg^{-1}) was administered as a 100 μg kg^{-1} intravenous bolus followed by continuous infusion (60 μg kg^{-1} min^{-1} for 15 min). This dose was shown to produce a significant decrease in mean aortic pressure (Clozel *et al.*, 1989; 1991; Véniant *et al.*, 1991). Similarly, cardiac output was measured at baseline and at 5, 10 and 15 min of drug infusion. Diltiazem and Ro 40-5967 were given in random order on different days separated by at least 24 h.

In order to study the role of left ventricular end-diastolic pressure changes in possible modifications of cardiac function during calcium channel blocker infusions, nitroprusside was intravenously infused (2.0 μg kg^{-1} min^{-1}) to produce similar changes in mean aortic pressure and in left ventricular end-diastolic pressure as those induced by diltiazem. Cardiac output was measured at baseline and during nitroprusside infusion. Nitroprusside was given before diltiazem or Ro 40-5967. The next drug was given when all haemodynamic parameters had returned to their initial levels after a stability period of at least 15 min after nitroprusside infusion.

Experiments in heart failure After completion of studies in the control state, rapid right ventricular pacing was initiated at a rate of 240–260 beats min^{-1}, using a programmable miniature pacemaker (model Medtronic 5320, Medtronic Inc., Minneapolis, Minn, U.S.A.) placed in a pocket of a jacket on the back of the animal. Dogs were examined daily to confirm the continuous pacing. After 2–4 weeks of right ventricular pacing, before any drug infusion, the pacemaker was stopped and the study began after a 15 min period of stability. The same protocol as in the control state was performed. Diltiazem and Ro 40-5967 were given on different days with a separation period of at least 24 h. The same dose of nitroprusside as in the control state was also infused intravenously in heart failure. As in the control state, drug administrations were also in random order.

Data collection and analysis

Absolute values of left ventricular pressure were obtained by calibrating the micromanometer in 37°C water against a Statham P23ID transducer (Gould Inc., Valley View, Ohio, U.S.A.) before implantation. The shift of zero pressure during the study was corrected by comparing left ventricular pressure with left atrial pressure or aortic pressure simultaneously recorded with a Statham pressure transducer. All data were recorded on a multichannel tape recorder (Model 3968A, Hewlett-Packard, Palo Alto, CA, U.S.A.) and on an eight-channel graphic recorder (Model 8800-06, Gould Inc., Valley View, Ohio, U.S.A.) at a paper speed of 50 mm s^{-1}.

Data calculations were performed with a MINC 11-23 computer (Digital Equipment Corp., Marlboro, MA, U.S.A.) after conversion of the signals stored on the magnetic tape recorder. Seven-second long sequences of the signals were analysed at a sampling rate of 200 Hz in each channel. The maximal and minimal rates of left ventricular pressure changes (left ventricular dP/dt_{max} and left ventricular dP/dt_{min}) were obtained by retrograde search for the maximal and minimal values of dP/dt during each cardiac cycle. End diastole was defined as the time point when left ventricular pressure began to rise just after the atrial contraction. End systole was defined as the time point occurring 20 ms before left ventricular dP/dt_{min}. Stroke volume was calculated as the ratio of cardiac output/heart rate.

Plasma noradrenaline assays

To measure arterial plasma noradrenaline levels, blood samples were withdrawn from the aortic catheter at baseline and after 13 min of diltiazem or Ro 40-5967 infusion or after 2 min of nitroprusside infusion in the control state and in heart failure. Plasma noradrenaline was measured according to a procedure described elsewhere (Su *et al.*, 1992). Briefly, plasma noradrenaline concentration was analysed by a liquid chromatography procedure with electrochemical detection. Instrument control, data acquisition, storage and retrieval

function were assessed by a Maxima 820 chromatography Workstation.

Drugs

Diltiazem hydrochloride was synthesized by Laboratoires Synthelabo (Le Plessis-Robinson, France). Ro 40-5967 (chemical structure: (1S,2S)-2-[2-[[3-(benzimidazoly)propyl] metyl-amino]ethyl]-6-fluoro-1,2,3,4-tetrahydro-1-isopropyl-2-naphtyl methoxy-acetate dihydro-chloride) and sodium nitroprusside were obtained from Hoffmann-La Roche (Basel, Switzerland).

Statistical analysis

Values are presented as means ± s.e.mean. All statistic computations were carried out with commercially available software (SuperANOVA V1.11, Abacus Concepts, Berkeley, CA, U.S.A.). One-way analysis of variance for repeated measures was used for intragroup dose interactions. Two-way analysis of variance for repeated measures of same parameters over time was used to compare intergroup drug interactions. After analysis of variance, comparisons between means were performed with contrasts. Statistical significance was defined as $P<0.05$.

Results

Baseline data and changes after induction of heart failure

Baseline haemodynamic parameters and plasma noradrenaline levels were not different before diltiazem and Ro 40-5967 infusions in the control state as well as in heart failure (Tables 1, 2 and 4).

After 2–4 weeks of rapid right ventricular pacing, dogs developed heart failure which was characterized by peripheral signs of congestive heart failure (exertional dyspnoea, ascites) and by haemodynamic changes (Tables 1, 2 and 3). In heart

Table 1 Haemodynamic data at baseline and in response to diltiazem (15 min infusion) in the control state and in heart failure in conscious dogs ($n = 13$)

	Control state		*Heart failure*	
	Baseline	*Response*	*Baseline*	*Response*
Mean aortic pressure (mmHg)	99.8 ± 2.0	89.3 ± 2.0†	82.7 ± 2.0‡	70.3 ± 2.3†
Heart rate (beats min^{-1})	100.0 ± 4.1	136.8 ± 5.8†	131.4 ± 5.5‡	125.4 ± 7.7
LV end-diastolic pressure (mmHg)	7.1 ± 0.9	4.5 ± 0.8*	27.6 ± 1.7‡	19.7 ± 1.7†
LV systolic pressure (mmHg)	130.0 ± 4.0	121.1 ± 3.2†	101.6 ± 2.0‡	90.7 ± 2.6†
LV dP/dt_{max} (mmHg s^{-1})	3635 ± 164	3776 ± 277	1838 ± 80‡	1452 ± 82†
LV dP/dt_{min} (mmHg s^{-1})	−3515 ± 156	−3189 ± 153	−1961 ± 72‡	−1587 ± 83†
Cardiac output (l min^{-1})#	3.45 ± 0.21	4.45 ± 0.30†	2.82 ± 0.18‡	2.30 ± 0.21†
Stroke volume (ml)#	34.9 ± 2.7	34.2 ± 3.3	22.4 ± 6.7‡	19.2 ± 1.7*

#Cardiac output and stroke volume were obtained in 11 dogs. *$P<0.02$ and †$P<0.001$ as compared with corresponding baseline values. ‡$P<0.001$ as compared with the baseline values in the control state.

Table 2 Haemodynamic data at baseline and in response to Ro 40-5967 (15 min infusion) in the control state and in heart failure in conscious dogs ($n = 13$)

	Control state		*Heart failure*	
	Baseline	*Response*	*Baseline*	*Response*
Mean aortic pressure (mmHg)	103.7 ± 1.9	93.3 ± 2.0†	83.1 ± 1.7‡	76.0 ± 1.7†
Heart rate (beats min^{-1})	101.9 ± 5.6	124.6 ± 5.5†	131.1 ± 6.1‡	131.0 ± 4.8
LV end-diastolic pressure (mmHg)	7.9 ± 0.9	6.2 ± 1.0*	28.7 ± 2.0‡	26.8 ± 2.0*
LV systolic pressure (mmHg)	133.7 ± 2.1	126.9 ± 2.9*	101.7 ± 1.5‡	98.0 ± 2.5*
LV dP/dt_{max} (mmHg s^{-1})	3676 ± 172	3907 ± 225	1862 ± 81‡	1800 ± 105
LV dP/dt_{min} (mmHg s^{-1})	−3581 ± 96	−3439 ± 93	−1926 ± 74‡	−1875 ± 92
Cardiac output (l min^{-1})#	3.42 ± 0.25	4.44 ± 0.36†	2.74 ± 0.25‡	2.97 ± 0.32*
Stroke volume (ml)#	35.3 ± 2.3	36.8 ± 3.0	21.4 ± 2.3‡	23.0 ± 2.5

#Cardiac output and stroke volume were obtained in 11 dogs. *$P<0.02$ and †$P<0.001$ as compared with corresponding baseline values. ‡$P<0.001$ as compared with the baseline values in the control state.

Table 3 Haemodynamic data at baseline and in response to nitroprusside (2.0 μg kg^{-1} min^{-1}) in the control state and in heart failure in conscious dogs ($n = 13$)

	Control state		*Heart failure*	
	Baseline	*Response*	*Baseline*	*Response*
Mean aortic pressure (mmHg)	103.1 ± 2.2	89.0 ± 2.0†	84.4 ± 1.9‡	72.8 ± 1.9†
Heart rate (beats min^{-1})	95.5 ± 4.4	126.7 ± 6.1†	134.8 ± 5.2‡	132.2 ± 5.3
LV end-diastolic pressure (mmHg)	8.2 ± 0.9	3.4 ± 1.0†	27.3 ± 2.0‡	18.9 ± 2.5†
LV systolic pressure (mmHg)	133.2 ± 3.0	115.4 ± 2.4†	104.0 ± 2.5‡	95.4 ± 2.2†
LV dP/dt_{max} (mmHg s^{-1})	3669 ± 164	3881 ± 230	1900 ± 101‡	1870 ± 111
LV dP/dt_{min} (mmHg s^{-1})	−3626 ± 145	−3214 ± 138†	−1962 ± 84‡	−1938 ± 97
Cardiac output (l min^{-1})#	3.24 ± 0.23	3.76 ± 0.31*	2.71 ± 0.19‡	3.14 ± 0.27*
Stroke volume (ml)#	35.8 ± 3.2	30.6 ± 2.7†	20.9 ± 2.0‡	24.4 ± 2.2†

#Cardiac output and stroke volume were obtained in 11 dogs. *$P<0.02$ and †$P<0.001$ as compared with corresponding baseline values. ‡$P<0.001$ as compared with the baseline values in the control state.

failure, heart rate and left ventricular end-diastolic pressure increased significantly and mean aortic pressure, left ventricular dP/dt_{max} and cardiac output decreased significantly as compared with those in the control state (Tables 1, 2 and 3). Heart failure was also associated with a significant increase in plasma noradrenaline (Table 4).

Haemodynamic effects of diltiazem in the control state and in heart failure

In the control state, diltiazem decreased significantly mean aortic pressure and increased heart rate and cardiac output without significant changes in left ventricular dP/dt_{max} and in calculated stroke volume (Table 1 and Figure 1). Left ventricular end-diastolic pressure decreased slightly but significantly (Table 1).

After induction of heart failure, diltiazem decreased mean aortic pressure in a similar manner to that observed in the control state but also decreased left ventricular dP/dt_{max}, cardiac output and calculated stroke volume. Heart rate did not change significantly and left ventricular end-diastolic pressure decreased (Table 1 and Figure 1).

Table 4 Plasma noradrenaline concentrations (pmol ml^{-1}) at baseline and in response to calcium channel blockers and nitroprusside in conscious dogs ($n = 10$)

	Control state		*Heart failure*	
	Baseline	*Response*	*Baseline*	*Response*
Diltiazem	0.9 ± 0.2	1.4 ± 0.2*	1.7 ± 0.2‡	3.8 ± 0.4*§
Ro 40-5967	0.9 ± 0.1	1.4 ± 0.3	1.6 ± 0.3†	2.2 ± 0.2*§
Nitroprusside	0.9 ± 0.1	1.7 ± 0.2*	1.6 ± 0.2†	2.4 ± 0.5*§

*$P = 0.05$ as compared with corresponding baseline values in the same state; †$P < 0.01$ and ‡$P < 0.001$ as compared with corresponding baseline values in the control state. §$P < 0.005$ as compared with the corresponding values obtained during diltiazem infusion in the same state.

Haemodynamic effects of Ro 40-5967 in the control state and in heart failure

In the control state, Ro 40-5967 had similar effects to those of diltiazem. It decreased mean aortic pressure with significant increases in heart rate and in cardiac output without significant changes in left ventricular dP/dt_{max}. Calculated stroke volume was increased from 35.3 ± 2.3 ml to 39.2 ± 3.3 ml ($P < 0.02$) 10 min after the onset of infusion but the increase was not significant after 15 min of drug infusion (Table 2). After induction of heart failure, Ro 40-5967 also decreased mean aortic pressure and increased slightly cardiac output without modifications in left ventricular dP/dt_{max} and heart rate. Left ventricular end-diastolic pressure was slightly but significantly reduced (Table 2 and Figure 2). Stroke volume was initially increased from 21.4 ± 2.3 ml to 24.2 ± 3.4 ml ($P < 0.005$) 5 min after the onset of drug infusion but the increase was not statistically significant thereafter. The increase in cardiac output induced by Ro 40-5967 was significantly smaller during heart failure than in the control state and changes in left ventricular dP/dt_{max} were also significantly different under these conditions (Figure 2).

Comparisons of the haemodynamic effects of diltiazem and Ro 40-5967 at matched mean aortic pressure in heart failure

In heart failure, 15 min after the onset of drug infusion, the decrease in mean aortic pressure was 7.1 mmHg with Ro 40-5967 and 12.4 mmHg with diltiazem. To compare the haemodynamic effects of diltiazem with those of Ro 40-5967, in each dog, the time point where the value of mean aortic pressure measured during diltiazem infusion was similar to that at maximal effect of Ro 40-5967 was selected. Haemo-

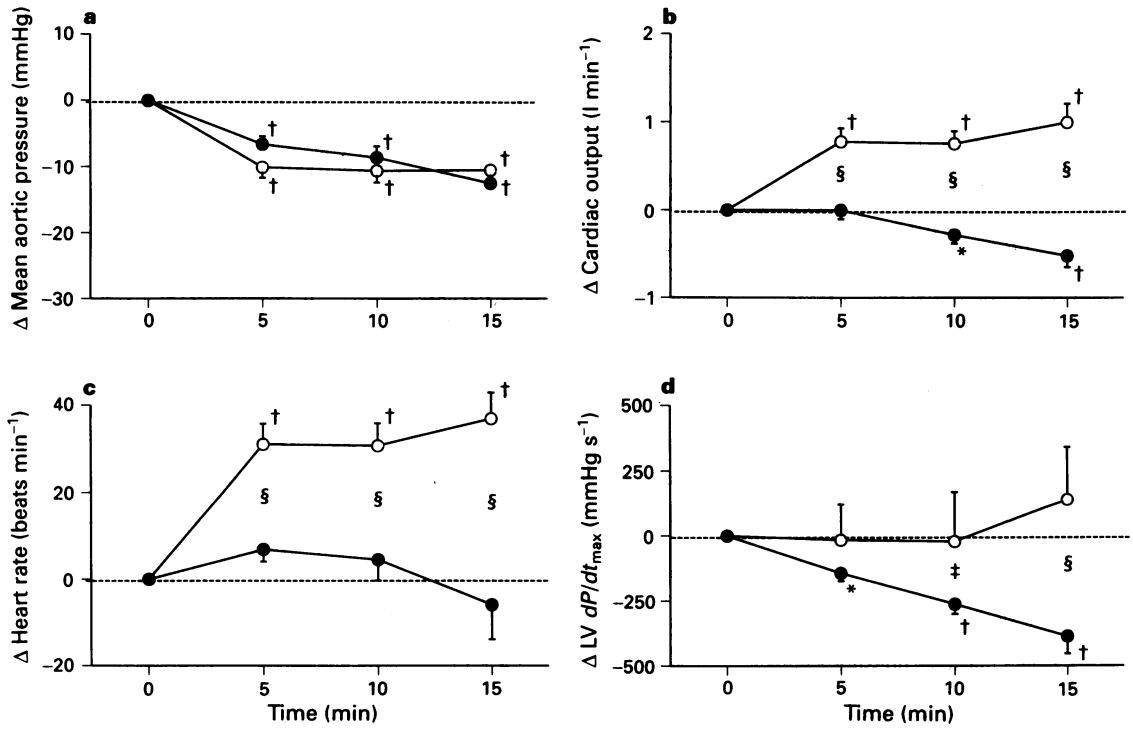


Figure 1 Comparisons of change in haemodynamic parameters ((a) mean aortic pressure; (b) cardiac output; (c) heart rate and (d) LV dP/dt_{max}) in response to diltiazem infusion in the control state (○) and in heart failure (●). LV: left ventricular. Note that, in contrast to the control state, during heart failure, heart rate was not significantly modified and cardiac output and LV dP/dt_{max} decreased. *$P < 0.02$ and †$P < 0.01$ as compared with corresponding baseline values. ‡$P < 0.05$ and §$P < 0.001$ for comparisons between the control state and heart failure.

dynamic parameters at this time point were compared to those at maximal effects of Ro 40-5967. At matched mean aortic pressure and similar heart rate, left ventricular end-diastolic pressure was more reduced by diltiazem than by Ro 40-5967 (Figure 3). Diltiazem decreased left ventricular dP/dt_{max} and cardiac output while Ro 40-5967 increased cardiac output and did not change left ventricular dP/dt_{max} (Figure 3).

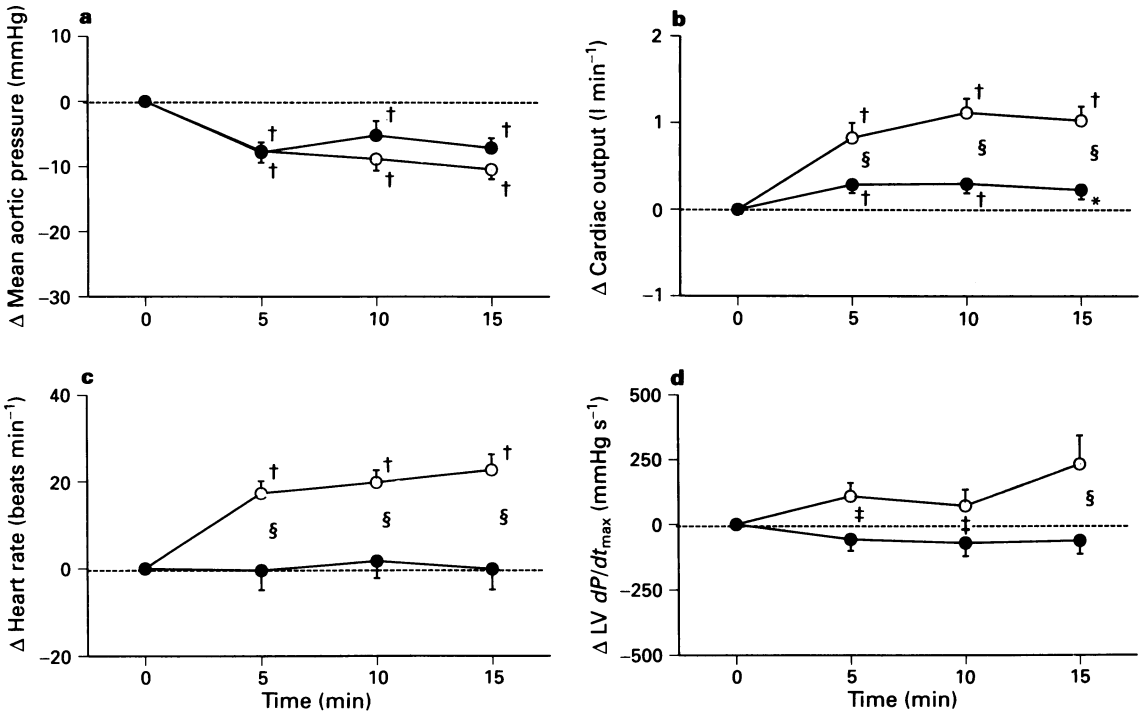


Figure 2 Comparisons of change in haemodynamic parameters ((a) mean aortic pressure; (b) cardiac output; (c) heart rate and (d) LV dP/dt_{max}) in response to Ro 40-5967 infusions in the control state (○) and in heart failure (●). LV: left ventricular. Note that, in heart failure, cardiac output was still significantly increased during Ro 40-5967 infusion although this increase was smaller than in the control state. $*P<0.05$ and $\dagger P<0.01$ as compared with corresponding baseline values. $\ddagger P<0.05$ and $\S P<0.001$ for comparisons between the control state and heart failure.

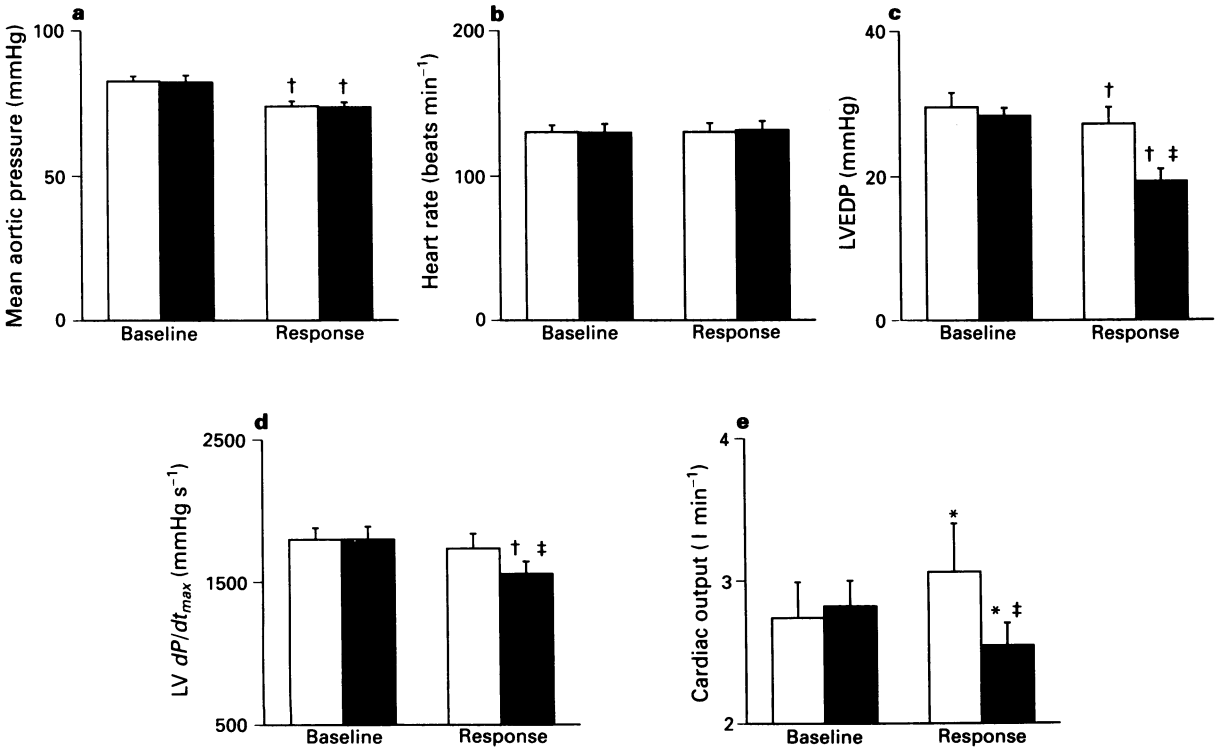


Figure 3 Comparisons of haemodynamic effects (on (a) mean aortic pressure; (b) heart rate; (c) LV end-diastolic pressure; (d) LV dP/dt_{max} and (e) cardiac output) of diltiazem (solid columns) and Ro 40-5967 (open columns) at matched mean aortic pressure in heart failure. LV: left ventricular. $*P<0.02$ and $\dagger P<0.001$ as compared with corresponding baseline value. $\ddagger P<0.001$ as compared with corresponding values obtained during Ro 40-5967 infusion.

Haemodynamic effects of sodium nitroprusside in the control state and in heart failure

Table 3 presents the mean values of haemodynamic parameters at baseline and in response to sodium nitroprusside in the control state and in heart failure. In heart failure, with nitroprusside infusion, although left ventricular end-diastolic pressure was reduced to a similar level as that induced by diltiazem infusion, cardiac output was significantly increased and left ventricular dP/dt_{max} was not changed.

Plasma noradrenaline changes in response to calcium channel blockers and to nitroprusside in the control state and in heart failure

In the control state, both diltiazem and Ro 40-5967 infusions increased plasma noradrenaline by 55% (Table 4). In heart failure, during diltiazem infusion, plasma noradrenaline increased by 120%. In contrast, the increase in plasma noradrenaline level was only 38% during Ro 40-5967 infusion in the same state (Table 4). In the control state, nitroprusside increased plasma noradrenaline to a similar level as that produced by calcium channel blockers (Table 4). In heart failure, nitroprusside increased plasma noradrenaline to a similar level to that produced by Ro 40-5967 and this increase was markedly smaller than that produced by diltiazem (Table 4).

Discussion

Our results showing that diltiazem increased cardiac output and did not modify left ventricular dP/dt_{max} in the control state are in accordance with previous studies (Walsh *et al.*, 1981; Millard *et al.*, 1982; Porter *et al.*, 1983). The increase in cardiac output induced by diltiazem in the control state is, in a large part, due to the increase in heart rate since calculated stroke volumes were not modified during diltiazem infusion. In conscious intact animals, it is impossible to distinguish the direct myocardial effect of a drug from the effects of changes in loading conditions and associated reflex mediated changes. Neural blockade with pharmacological agents is necessary when the direct effects of drugs on the myocardium need to be assessed. Since the major goal of this study was to determine the effects of diltiazem on cardiac function in the intact animal, experiments with neural blockade were not performed and previous studies performed in the control state have shown that, after baroreflex blockade, diltiazem has little negative inotropic effect on the myocardium (Walsh *et al.*, 1981; Millard *et al.*, 1982).

In heart failure, in contrast to the control state, diltiazem impaired cardiac function. The mechanisms involved in the depressed left ventricular function during diltiazem infusion could be modifications of left ventricular filling pressure and/or a direct negative inotropic effect of diltiazem. During diltiazem infusion, left ventricular end-diastolic pressure was decreased significantly. By itself, this decreased left ventricular filling pressure may have been responsible for the decreases in left ventricular dP/dt, cardiac output and stroke volume. However, during sodium nitroprusside infusion, for the same decreases in left ventricular end-diastolic pressure and in mean aortic pressure as those produced by diltiazem, cardiac output increased and left ventricular dP/dt_{max} was not significantly modified. This suggests that impaired cardiac function during diltiazem infusion is probably not related to the modification of left ventricular filling pressure alone but to other mechanisms, particularly a negative inotropic effect of diltiazem on the myocardium. A decreased ventricular function without changes in left ventricular filling pressure was shown in conscious dogs with left ventricular hypertrophy (Porter *et al.*, 1983) and recent data from our laboratory showed a more pronounced negative inotropic effect of diltiazem in rabbit isolated failing heart than in the normal rabbit heart (Ezzaher *et al.*, 1991). Our data extend the results of Porter *et al.* (1983) showing a decreased cardiac function during diltiazem infusion in dogs with left ventricular hypertrophy to a situation of heart failure characterized by a low cardiac output, dilated cardiomyopathy without left ventricular hypertrophy.

Besides the possible direct negative inotropic effect of diltiazem and the changes in left ventricular filling pressure, alterations in cardiac function induced by diltiazem in conscious animals with heart failure may be due to alterations in baroreflex and/or in the myocardial β-adrenergic system. Although the heart failure state of our dogs was moderate, as suggested by the slight decrease in cardiac output and the twofold increase in plasma noradrenaline, baroreflex dysfunction was present. This was indicated by an unchanged heart rate in response to vasodilatation induced by nitroprusside and the calcium channel blockers in heart failure, contrasting with the tachycardia observed in the control state for similar decreases in mean aortic pressure. These results are in accordance with those of a previous study in this model (Wang *et al.*, 1991). Thus, the impaired baroreflex is not able to counteract the direct negative inotropic effect of diltiazem. The decreased heart rate response to vasodilatation in heart failure may also be, in part, due to the alterations in the myocardial β-adrenergic system which are a well recognized characteristic of heart failure. A decreased myocardial β-adrenoceptor density and adenylate cyclase activity and increased G_i protein have been shown in this model (Calderone *et al.*, 1991; Marzo *et al.*, 1991). Thus, even if increased sympathetic activation occurred, as suggested by the increased plasma noradrenaline levels during diltiazem infusion, abnormalities of the myocardial β-adrenoceptor-G protein-adenylate cyclase complex provide little inotropic support (Calderone *et al.*, 1991) and sympathetic stimulation is not sufficient to attenuate the negative inotropic effect of diltiazem. By itself, the activation of the sympathetic system may be deleterious (Francis *et al.*, 1982; Cohn *et al.*, 1984; Swedberg *et al.*, 1990) since it increases intracellular calcium overload (Katz, 1990) and decreases further β-adrenoceptor density and sensitivity to catecholamines (Colucci *et al.*, 1981; Heinsimer & Lefkowitz, 1982). Therefore, calcium channel blockers which induce a lesser sympathetic activation may avoid these adverse effects.

The haemodynamic effects of Ro 40-5967 were different in the control state and in heart failure. Ro 40-5967 did not change heart rate and increased slightly cardiac output in heart failure, contrasting with marked increases in heart rate and in cardiac output in the control state. However, in contrast to diltiazem, Ro 40-5967 infusion had little effect on cardiac function in heart failure, particularly on stroke volume which still tended to increase as in the control state. This may be related to the vascular selective effect of Ro 40-5967 as suggested by an *in vitro* study (Osterrieder & Holck, 1989), to a relatively weak inotropic effect in failing heart (Ezzaher *et al.*, 1991; Clozel *et al.*, 1991) or to a smaller decrease in left ventricular filling pressure than that induced by diltiazem. The effects of Ro 40-5967 in heart failure suggest that all calcium channel blockers may not produce the same effects on cardiac function.

In conclusion, in conscious dogs with moderate heart failure, calcium channel blockers administered acutely do not loose their vasodilator effect, diltiazem impairs cardiac function and this cannot be overcome by its vasodilator effect and by sympathetic activation. These mechanisms may be important in patients with chronic heart failure in whom depressed arterial baroreflex control (Eckberg *et al.*, 1971; Ellenbogen *et al.*, 1989) and decreased catecholamine sensitivity and β-adrenoceptor density have been demonstrated (Bristow *et al.*, 1982). Finally, our results suggest that novel calcium channel blockers with less negative inotropic action may not be detrimental in heart failure.

The authors wish to thank F. Hoffmann-La Roche Ltd (Basel, Switzerland) for the generous supply of Ro 40-5967. The study was supported in part by a grant from Association Française contre les Myophaties, Paris, France and a grant from F. Hoffmann-La Roche Ltd, Basel, Switzerland.

References

ARMSTRONG, P.W., STOPPS, T.P., DORD, S.E. & DE BOLD, A.J. (1986). Rapid ventricular pacing in the dog: pathophysiologic studies of heart failure. *Circulation*, **74**, 1075–1084.

BARJON, J.N., ROULEAU, J.L., BICHET, D., JUNEAU, C. & DE CHAMPLAIN, J. (1987). Chronic renal and neurohumoral effects of the calcium entry blocker nisoldipine in patients with congestive heart failure. *J. Am. Coll. Cardiol.*, **9**, 622–630.

BRISTOW, M.R., GINSBURG, R., MINOBE, W., CUBICCIOTTI, R.S., SAGEMAN, W.S., LURIE, K., BILLINGHAM, M.E., HARRISON, D.C. & STINSON, E.B. (1982). Decreased catecholamine sensitivity and β-adrenergic receptor density in failing human heart. *N. Engl. J. Med.*, **307**, 205–211.

BROOKS, N., CATTELL, M., PIDGEON, J. & BALCON, R. (1980). Unpredictable response to nifedipine in severe cardiac failure. *Br. Med. J.*, **281**, 1324.

CALDERONE, A., BOUVIER, M., LI, K., JUNEAU, C., DE CHAMPLAIN, J. & ROULEAU, J.L. (1991). Dysfunction of the β- and α-adrenergic systems in a model of congestive heart failure. *Circ. Res.*, **69**, 332–343.

CHEW, C.Y.C., HECHT, H.S., COLLETT, J.T., MCALLISTER, R.G. & SINGH, B.N. (1981). Influence of severity of ventricular dysfunction on hemodynamic responses to intravenously administered verapamil in ischemic heart disease. *Am. J. Cardiol.*, **47**, 917–922.

CLOZEL, J.P., BANKEN, L. & OSTERRIEDER, W. (1989). Effects of Ro 40-5967, a novel calcium antagonist, on myocardial function during ischemia induced by lowering coronary perfusion pressure in dogs: comparison with verapamil. *J. Cardiovasc. Pharmacol.*, **14**, 713–721.

CLOZEL, J.P., VÉNIANT, M. & OSTERRIEDER, W. (1991). The structurally novel Ca^{2+} channel blocker Ro 40-5967, which binds to the [^{3}H]desmethoxyverapamil receptor, is devoid of the negative inotropic effects of verapamil in normal and failing rat hearts. *Cardiovasc. Drugs Ther.*, **4**, 731–736.

CODY, R.J., KUBO, S.H., RYMAN, K.S., SHAKNOVICH, A. & LARAGH, J.H. (1987). Systemic and pulmonary hemodynamic responses to nicardipine during graded ergometric exercise in patients with moderate to severe essential hypertension. *J. Am. Coll. Cardiol.*, **10**, 647–654.

COHN, J.N., LEVINE, T.B., OLIVARI, M.T., GARGBERG, V., LURA, D., FRANCIS, G.S., SIMON, A.B. & RECTOR, T. (1984). Plasma norepinephrine as a guide to prognosis in patients with chronic congestive heart failure. *N. Engl. J. Med.*, **311**, 819–823.

COLUCCI, W.S., ALEXANDER, R.W., WILLIAMS, G.H., RUDE, R.E., HOLEMAN, B.L., KONSTAM, M.A., WYNNE, J., MUDGE, G.H. & BRAUNWALD, E. (1981). Decreased lymphocyte beta-adrenergic-receptor density in patients with heart failure and tolerance to the beta-adrenergic agonist pirbuterol. *N. Engl. J. Med.*, **305**, 185–190.

COREA, L., MIELE, N., BENTIVOGLIO, M., BOSCHETTI, E., AGABITI-ROSEI, E. & MUIESAN, G. (1979). Plasma renin activity and plasma epinephrine and norepinephrine in controls and hypertensive patients. *Clin. Sci.*, **57**, 115s–117s.

ECKBERG, D.L., DRABINSKY, M. & BRAUNWALD, E. (1971). Defective cardiac parasympathetic control in patients with heart failure. *N. Engl. J. Med.*, **285**, 877–883.

ELKAYAM, U., WEBER, L., MCKAY, C. & RAHIMTOOLA S. (1985). Spectrum of acute hemodynamic effects of nifedipine in severe congestive heart failure. *Am. J. Cardiol.*, **56**, 560–566.

ELKAYAM, U., AMIN, J., MEHRA, A., VASQUEZ, J., WEBER, L. & RAHIMTOOLA, S.H. (1990). A prospective, randomized, double-blind, crossover study to compare the efficacity and safety of chronic nifedipine therapy with that of isosorbide dinitrate and their combination in the treatment of chronic congestive heart failure. *Circulation*, **82**, 1954–1961.

ELLENBOGEN, K.A., MOHANTY, P.K., SZENTPETERY, S. & THAMES, M.D. (1989). Arterial baroreflex abnormalities in heart failure: reversal after orthotopic cardiac transplantation. *Circulation*, **79**, 51–58.

EZZAHER, A., BOUANANI, N.E.H., SU, J.B., HITTINGER, L. & CROZATIER, B. (1991). Increased negative inotropic effect of calcium-channel blockers in hypertrophied and failing rabbit heart. *J. Pharmacol. Exp. Ther.*, **257**, 466–471.

FRANCIS, G.S., GOLDSMITH, S.R. & COHN, J.N. (1982). Relationship of exercise capacity to resting left ventricular performance and basal plasma norepinephrine levels in patients with congestive heart failure. *Am. Heart. J.*, **10**, 725–731.

FRANCIS, G.S. (1991). Calcium channel blockers and congestive heart failure. *Circulation*, **83**, 336–338.

GOLDSTEIN, R.E., BOCCUZZI, S.J., CRUESS, D., NATTEL, S., THE ADVERSE EXPERIENCE COMMITTEE AND MULTICENTER DILTIAZEM POST-INFARCTION RESEARCH GROUP (1991). Diltiazem increases late-onset congestive heart failure in postinfarction patients with early reduction in ejection fraction. *Circulation*, **83**, 52–60.

HEINSIMER, J.A. & LEFKOWITZ, R.J. (1982). Adrenergic receptors: biochemistry, regulation, molecular mechanism, and clinical implications. *J. Lab. Clin. Med.*, **100**, 641–658,

HENRY, P.D. (1980). Comparative pharmacology of calcium antagonists: nifedipine, verapamil and diltiazem. *Am. J. Cardiol.*, **46**, 1047–1058.

KOMAMURA, K., SHANNON, R.P., PASIPOULARIDES, A., IHARA, T., LADER, A., PATRICK, T.A., BISHOP, S.P. & VATNER, S.F. (1992). Alterations in left ventricular diastolic function in conscious dogs with pacing-induced heart failure. *J. Clin. Invest.*, **89**, 1825–1838.

KATZ, A.M. (1990). Cardiomyopathy of overload. A major determinant of prognosis in congestive heart failure. *N. Engl. J. Med.*, **322**, 100–110.

LOW, R.I., TAKEDA, P., MASON, D.T. & DEMARIA, A.N. (1982). The effects of calcium channel blocking agents on cardiovascular function. *Am. J. Cardiol.*, **49**, 547–553.

MARZO, K.P., FREY, M.J., WILSON, J.R., LIANG, B.T., MANNING, D.R., LANOCE, V. & MOLINOF, P.B. (1991). β-Adrenergic receptor-G protein-adenylate cyclase complex in experimental canine congestive heart failure produced by rapid ventricular pacing. *Circ. Res.*, **69**, 1546–1556.

MILLARD, R.W., LATHROP, D.A., GRUPP, G., ASHRAF, M., GRUPP, I.L. & SCHWARTZ, A. (1982). Differential cardiovascular effects of calcium channel blocking agents: potential mechanisms. *Am. J. Cardiol.*, **49**, 499–506.

MULLER, J.E., TURI, Z.G., PEARLE, D.L., SCHNEIDER, J.F., SERFAS, D.H., MORRISON, J., STONE, P.H., RUDE, R.E., ROSNER, B., SOBEL, B.E., TATE, C., SCHEINER, E., ROBERTS, R., HENNEKENS, C.H. & BRAUNWALD, E. (1984). Nifedipine and conventional therapy for unstable angina pectoria: a randomized, double-blind comparison. *Circulation*, **69**, 728–739.

OSTERRIEDER, W. & HOLCK, M. (1989). In vitro pharmacological profile of Ro 40-5967, a novel Ca^{2+} channel blocker with potent vasodilator but weak inotropic action. *J. Cardiovasc. Pharmacol.*, **13**, 754–759.

PACKER, M. (1989). Pathophysiological and mechanisms underlying the adverse effects of calcium channel-blocking drugs in patients with chronic heart failure. *Circulation*, **80** (Suppl IV), IV59–IV67.

PERREAULT, C.L., SHANNON, R.P., KOMAMURA, K., VATNER, S.F. & MORGAN, J.P. (1992). Abnormalities in intracellular calcium regulation and contractile function in myocardium from dogs with pacing-induced heart failure. *J. Clin. Invest.*, **89**, 932–938.

PORTER, C.B., WALSH, R.A., BADKE, F.R. & O'ROURKE, R.A. (1983). Differential effects of diltiazem and nitroprusside on left ventricular function in experimental chronic volume overload. *Circulation*, **68**, 685–692.

SHANNON, R.P., KOMAMURA, K., STAMBLER, B.S., BIGAUD, M., MANDERS, W.T. & VATNER, S.F. (1991). Alterations in myocardial contractility in conscious dogs with dilated cardiomyopathy. *Am. J. Physiol.*, **260** (Heart Circ. Physiol, **29**), H1903–H1911.

SU, J.B., HITTINGER, L., LE FRANC, P. & CROZATIER, B. (1992). Limited left ventricular inotropic response to exercise in early phase of pressure overload in dogs. *Am. J. Physiol.*, (*Heart Circ. Physiol.*, **32**), H1011–1016.

SWEDBERG, K., ENEROTH, P., KJEKSHUS, J. & WILHELMSEN, L., FOR THE CONSENSUS TRIAL STUDY GROUP (1990). Hormones regulating cardiovasculiar function in patients with severe congestive heart failure and their relation to mortality. *Circulation*, **82**, 1730–1736.

THE MULTICENTER DILTIAZEM POSTINFARCTION TRIAL RESEARCH GROUP (1988). The effect of diltiazem on mortality and reinfarction after myocardial infarction. *N. Engl. J. Med.*, **319**, 385–392.

VÉNIANT, M., CLOZEL, J.P., HESS, P. & WOLFGANG, R. (1991). Ro 40-5967, in contrast to diltiazem, does not reduce left ventricular contractility in rats with chronic myocardial infarction. *J. Cardiovasc. Pharmacol.*, **17**, 277–284.

WALSH, R.A., BADKE, F.R. & O'ROURKE, R.A. (1981). Differential effects of systemic and intracoronary calcium channel blocking agents on global and regional left ventricular function in conscious dogs. *Am. Heart J.*, **102**, 341–350.

WANG, W., CHEN, J.S. & ZUCKER, I.H. (1991). Carotid sinus baroreceptor reflex in dogs with experimental heart failure. *Circ. Res.*, **68**, 1294–1301.

WILCOX, R.G., HAMPTON, J.R., BANKS, D.C., BINKHEAD, J.S., BROOKSBY, I.A.B., BURNS-COX, C.J., HAYES, M.J., JOY, M.D., MALCOM, A.D., MATHER, H.G. & ROWLEY, J.M. (1986). Trial of early nifedipine in acute myocardial infarction: the Trent study. *Br. Med. J.*, **293**, 1204–1208.

WILSON, J.R., DOUGLAS, P., HICKY, W.F., LANOCE, V., FERRARO, N., MUHAMMAD, A. & REICHEK, N. (1987). Experimental congestive heart failure produced by rapid ventricular pacing in the dog: cardiac effects. *Circulation*, **75**, 837–846.

(Received March 14, 1994
Revised June 1, 1994
Accepted June 7, 1994)

Br. J. Pharmacol. (1994), **113**, 403–410 © Macmillan Press Ltd, 1994

Regulation of vascular and gastric smooth muscle contractility by pervanadate

Adebayo Laniyonu, Mahmoud Saifeddine, Sultan Ahmad & [1]Morley D. Hollenberg

Endocrine Research Group, Department of Pharmacology & Therapeutics and Department of Medicine, University of Calgary, Faculty of Medicine, Calgary, AB Canada T2N 4N1

1 The contractile actions of vanadate (VO_4) and pervanadate (PV, peroxide(s) of vanadate) were studied in rat gastric longitudinal muscle strips and in aortic rings. The roles of extracellular sodium and calcium were evaluated and the potential effects of nerve-released agonists were considered. The possibility that these responses were due to the potentiation of tyrosine kinase activity, as a result of PV-mediated tyrosine phosphatase inhibition was explored with the use of tyrosine kinase inhibitors (genistein, tyrphostin) and by Western blot analysis of phosphotyrosyl proteins in PV-treated tissues. The ability of PV to mimic the action of the tyrosine kinase receptor-associated agonist, epidermal growth factor-urogastrone (EGF-Uro), in the gastric preparation was also studied.

2 PV caused concentration-dependent contractions in both gastric and aorta-derived tissues, with a potency that was 1 to 2 orders of magnitude greater than that of VO_4.

3 Although repeated exposure of gastric and aortic tissues to a fixed concentration of VO_4 caused reproducible contractions in both tissues, repeated exposure of gastric tissue to PV caused an increased contractile response plateauing after 3 exposures. In contrast, a single exposure of aortic tissue to PV (20 μM) caused a prolonged desensitization of the tissue to the subsequent contractile actions of PV or other agonists.

4 The contractile responses to PV were unaffected in both preparations by tetrodotoxin, atropine, yohimbine and phenoxybenzamine; and in the aortic preparation, the responses to VO_4 and PV were the same in the presence or absence of a functional endothelium.

5 PV-induced contractions in both tissues were observed in the absence of extracellular sodium but required extracellular calcium and were attenuated by 1 μM nifedipine.

6 In the gastric preparation, the characteristics of the contractile actions of PV paralleled those of EGF-Uro in terms of (1) inhibition by genistein, (2) inhibition by indomethacin and (3) a requirement for extracellular calcium. These response characteristics differed from those of other contractile agonists such as carbachol.

7 In both the gastric and aortic preparations genistein was able to inhibit PV-induced contractions selectively without causing comparable inhibition of KCl-induced contractions. Tyrphostin (AG18) also selectively blocked PV-induced contractions in the gastric, but not in the aortic preparation.

8 In both the gastric and aortic tissue, in step with an increased contractile response, PV caused increases in tissue phosphotyrosyl protein content, as detected by Western blot analysis using a monoclonal antiphosphotyrosine antibody; the increases in phosphotyrosyl protein content were reduced when tissues were treated with PV at the same time as a tyrosine kinase inhibitor.

9 PV, at sub-contractile concentrations, potentiated the contractile action of angiotensin II in both the gastric and aorta tissue.

10 We conclude that the growth factor-mimetic agent, PV, is a much more potent contractile agonist than VO_4 in both vascular and gastric smooth muscle tissue. PV can cause enhanced tissue phosphotyrosyl protein content most likely via the inhibition of tissue protein tyrosine phosphatases. The contractile actions of PV, which require extracelullar calcium and are independent of extracellular sodium, would appear not to be due either to Na^+/Ca^{2+} exchange, promoted by Na^+/K^+-ATPase inhibition or to the inhibition of Ca^{2+}-ATPase and might be best explained by the ability of PV, via tyrosine phosphatase inhibition, to potentiate a tyrosine kinase pathway linked to calcium entry and to the contractile process.

Keywords: Rat aorta; gastric smooth muscle; pervanadate; vanadate; tyrosine kinase; tyrosine phosphatase

Introduction

The role for cellular tyrosine kinases, tyrosine phosphatases and their substrates is most often thought of in the context of cell cycle control and the regulation of cell growth. These processes usually occur over a time course of several hours. Nonetheless, it has become evident over the past 6 to 8 years that so-called 'growth factors', such as epidermal growth factor-urogastrone (EGF-Uro) or platelet-derived growth factor, that act via tyrosine kinase receptor-mediated signal pathways, can acutely regulate vascular and gastric smooth muscle tension (summarized by Berk & Alexander, 1989; Hollenberg, 1994). Data have also been obtained to indicate that tyrosine kinase pathways may also be involved in the regulation of smooth muscle tension by agonists such as angiotensin II, that act via G-protein-coupled receptors (Saifeddine *et al.*, 1992; Yang *et al.*, 1993; Di Salvo *et al.*, 1993b). If the activation of a tyrosine kinase pathway by certain agonists can increase smooth muscle contractility, it can be hypothesized that cellular tyrosine phosphatase activity may act as a counter-regulatory factor to attenuate the actions of such agents. To explore this hypothesis, we considered the use of the insulin-mimetic agent, vanadyl

[1] Author for correspondence.

hydroperoxide (peroxovanadate or pervanadate, PV), that acts in adipocytes (Kadota *et al.*, 1987), T-lymphocytes (O'Shea *et al.*, 1992), granulocytes (Bourgoin & Grinstein, 1992) or platelets (Blake *et al.*, 1993) by augmenting tyrosine kinase activity, presumably due to the inhibition of tyrosine phosphatase (Grinstein *et al.*, 1990; Heffetz *et al.*, 1990; Faure *et al.*, 1992) rather than via the inhibition of Na^+/K^+-ATPase (Dubyak & Kleinzeller, 1980). PV, which is much more potent than vanadate (VO_4) itself (Kadota *et al.*, 1987; Fantus *et al.*, 1989), is believed to be reduced intracellularly to the biologically active insulin-mimetic species. Prior to our study, the effects of PV in smooth muscle systems had not yet been explored.

A number of previous studies have examined the actions of VO_4 in a variety of vascular and non-vascular smooth muscle preparations (e.g. see Shimada *et al.*, 1986 and Sanchez-Ferrer *et al.*, 1988), wherein the effects have been found to vary between tissues and among species (Bhagavan *et al.*, 1993). In brief, VO_4 (1 mM) has been observed to cause a contractile response of variable magnitude in both vascular and non-vascular smooth muscle preparations *via* a mechanism that would appear not to involve the inhibition of Na^+/K^+-ATPase (summarized by Ozaki & Urakawa, 1980, Shimada *et al.*, 1986 and Sanchez-Ferrer *et al.*, 1988). Although it has been suggested that the contractile activity of VO_4 may be via inhibition of sarcolemmal Ca^{2+}-ATPase, causing elevation of intracellular calcium (Sanchez-Ferrer *et al.*, 1988), the ability of VO_4 to potentiate tyrosine kinase activity by inhibiting tyrosine phosphatase has not yet been explored in depth to account for its contractile effects.

Since we had already used tyrosine kinase inhibitors to evaluate a potential role for a tyrosine kinase pathway in the contractile actions of EGF-Uro and angiotensin II in gastric and vascular smooth muscle preparations (Yang *et al.*, 1992; 1993; Saifeddine *et al.*, 1992), we wished to use similar bioassay preparations to study the actions of the tyrosine phosphatase inhibitor, PV. The present study describes the characteristics of the contractile actions of VO_4 and PV in rat gastric longitudinal muscle and aortic ring preparations. Our data illustrate the inhibition of the contractile actions of PV by tyrosine kinase inhibitors (genistein and tyrphostin) and the correlation of PV-induced contractions with increases in tissue phosphotyrosyl protein content that could be attenuated by the tyrosine kinase inhibitors. The results support the hypothesis that PV can cause its effects on smooth muscle tension via the inhibition of a tyrosine phosphatase pathway, so as to potentiate the action of constitutively active tissue tyrosine kinase(s).

Methods

Bioassay procedures

Protocols for the humane treatment of animals, according to the Declaration of Helsinki, and as approved by an institutional committee on animal care were followed in all experiments. After the animals had been killed by cervical dislocation, the thoracic aorta and stomach were removed from male Sprague Dawley albino rats (250–300 g). Tissues were trimmed and aortic rings (either intact, or rubbed free of endothelium) and gastric longitudinal muscle strips were prepared essentially as previously described (Hollenberg *et al.*, 1993). In brief, gastric longitudinal muscle strips (3 × 10 mm) were obtained after trimming the tissue free from all mucosa, by cutting exactly across the visible circular muscle striations, under a dissecting microscope. Both the longitudinal muscle strips and aortic rings (2 × 3 mm) were mounted in a 4 ml organ bath and equilibrated for at least 60 min at 37°C, in a Krebs-Henseleit buffer, pH 7.4 of the following composition (mM): NaCl 115, KCl 4.7, $CaCl_2$ 2.5, $MgCl_2$ 1.2, $NaHCO_3$ 2.5, KH_2PO_4 1.2 and glucose 10.0, gassed continuously with 95% O_2:5% CO_2. In some experiments, sodium was replaced in this buffer by equimolar concentrations of either lithium or choline. To examine responses in the absence of calcium, tissues were switched to a calcium-free buffer, containing 1 mM EGTA 10 min prior to the addition of agonist, after responding to an agonist the tissues were then washed and re-equilibrated in a calcium-containing buffer. Optimal resting tension of both preparations was about 1 mN. Changes in muscle tension were monitored isometrically with either Statham or Gould force-displacement transducers. The presence (or absence) of an intact endothelium in an aortic ring preparation was monitored by evaluating the relaxation response to 1 μM acetylcholine, in a preparation that was precontracted submaximally (EC_{75}) with 0.1 μM noradrenaline. Unless otherwise indicated, tissues were exposed to agonists at 25 min intervals, and were allowed to contract to a plateau tension over a 5 to 10 min period, at which time the tissue was washed three times and re-equilibrated in fresh buffer. The contractile responses of different preparations to VO_4 and PV were normalized by expressing the contractile force as a percentage (% KCl) of the contractile response to 50 mM KCl (3.6 ± 0.5 mN for gastric strips; 1.4 ± 0.1 mN for aortic rings: means ± s.e.mean for $n = 12$). When present, the tyrosine kinase inhibitors (genistein or tyrphostin) were added to the organ bath 15 to 20 min prior to the addition of a contractile agonist. Compounds, as stock solutions, were added to the organ bath (4 ml) and final concentrations were calculated accordingly.

Chemicals and other reagents

Acetylcholine, carbachol, noradrenaline, angiotensin II, sodium vanadate, nifedipine, diltiazam, verapamil, indomethacin, tetrodotoxin and catalase (from bovine liver, 2000 u mg^{-1}) were from Sigma (St. Louis, MO, U.S.A.); genistein was from ICN Biochemicals (Costa Mesa, CA, U.S.A.) and tyrphostin (compound serial No. 23 described by Gazit *et al.*, 1989; also designated AG18) was synthesized according to Gazit *et al.* (1989). Stock solutions of genistein and tyrphostin were prepared in dimethylsulphoxide; the solutions were diluted so that the final concentration of dimethylsulphoxide in the organ bath was ⩽ 0.1% (v/v). This concentration of solvent alone had no effect on the bioassay preparations.

PV was generated essentially as described previously (Kadota *et al.*, 1987) by mixing stock solutions of sodium orthovanadate with an equimolar or molar excess of H_2O_2. After a 15 min period, the reaction was terminated by the addition of catalase (final concentration, 400 u ml^{-1}; 0.2 mg ml^{-1}) to metabolize unreacted H_2O_2. The reaction product, known to contain a number of peroxovanadium coordination compounds was added to the organ bath at least 15 min after initiating the catalase reaction, and within 1 h of preparation, as suggested previously (Kadota *et al.*, 1987; Fantus *et al.*, 1989). The final molarity of PV in the organ bath was calculated on the basis of the original concentration of orthovanadate in the reaction mixture.

Western blot analysis

Gastric longitudinal muscle or aortic ring preparations were mounted in an organ bath for equilibration according to the bioassay procedures described above. Equilibrated tissues were then exposed to PV either with or without pretreatment of the tissues for 20 min with genistein or tyrphostin, as for a contractile bioassay. At a time (about 2–5 min) just prior to the plateau of contraction, tissue was removed from the organ bath, quick-frozen on a solid CO_2-cooled plexiglass plate, chopped with a scalpel and immediately solubilized in 120 μl of boiling sample buffer (Laemmli, 1970), and clarified by centrifugation (microfuge, 2 min at approximately 20,000 *g*) in preparation for polyacrylamide gel electrophoresis (60 × 80 × 1.5 mm, 8% gel) and transfer (1.5 h at

100 V at 4°C) to nitrocellulose (0.45 μM, Bio Rad, Richmond, CA, U.S.A.) for Western blot detection of protein, after blocking the membrane for 1 h at 24°C with 1% w/v gelatin. As an alternative extraction procedure, quick-frozen tissue was placed in 10% trichloroacetic acid, acetone-dried and then solubilized in sample buffer as above, in preparation for gel electrophoresis. Both extraction methods yielded equivalent results. The total protein content of tissue extracts was estimated using the Folin reagent for a 5 to 10 μl aliquot that was first precipitated in 100 μl of 10% w/v trichloroacetic acid and rinsed with 100% ethanol; bovine albumin served as a standard. Equal amounts of protein (50 to 200 μg) were loaded onto the gel for each tissue sample. Monoclonal antiphosphotyrosine antibody (our clone 6D9) was prepared according to Glenney *et al.* (1988), purified by ion exchange chromatography, and used at a concentration of approximately 0.1 μg ml^{-1}. Antibody reacting with immobilized proteins on the Western blot (2.5 h at room temperature) was detected by enhanced chemiluminescence (Amersham, Oakville, Ont. Canada) using horseradish peroxidase-coupled sheep antimouse immunoglobulin G at high dilution (1/50,000 of manufacturers stock reacted with the membrane for 1 h at room temperature). Control experiments demonstrated that the signal yielded by the monoclonal antibody could be neutralized by a phosphotyrosyl hapten (either 5 mM phosphotyrosine or 25 mM phenylphosphate).

Results

Characteristics of the contractile responses to VO_4 and PV

Both VO_4 and PV caused a rapidly developing sustained contraction in both the gastric and aortic tissue assays (Figure 1, a and e). Upon washing the preparations free from VO_4 and PV, tension returned to baseline. The contractile responses caused by either VO_4 or PV in the two tissues were not sensitive to tetrodotoxin (1 μM) and were not blocked by atropine (1 μM), yohimbine (1 μM) or phenoxybenzamine (1 μM) (not shown). Thus, nerve-released neurotransmitters did not appear to play a role. In the aortic preparation, comparable contractile responses to either VO_4 or PV were observed either in the presence or absence of a functional endothelium (not shown).

In some respects, the tissue responses to VO_4 and PV differed. For instance, in the gastric longitudinal muscle tissue, although separate exposures at a fixed concentration of

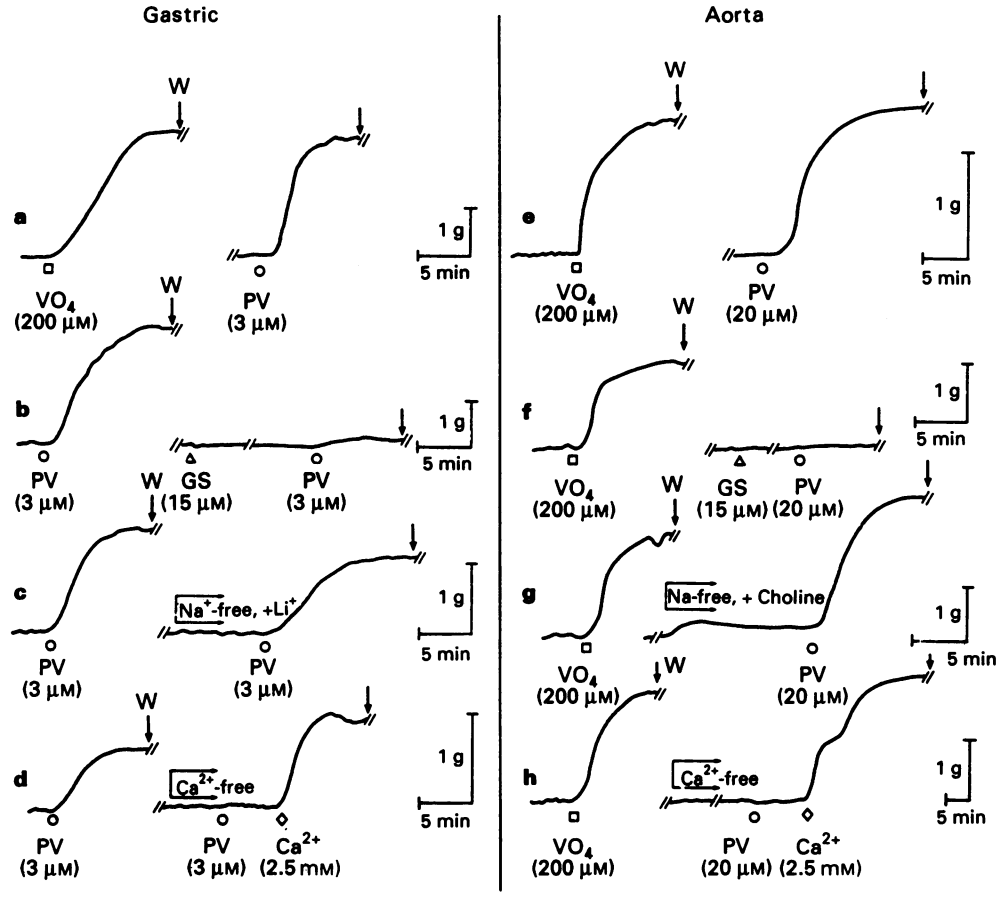


Figure 1 Responses of the gastric longitudinal muscle (LM) and aortic ring preparations to pervanadate (PV): comparison with vanadate (VO_4), effects of genistein and roles of extracellular sodium and calcium. Individual gastric (left: a to d) and aortic (right, e to h) tissue preparations were exposed first either to VO_4 (□, 200 μM) or PV (○, 3 μM) and tension was allowed to reach a plateau level (5–10 min) prior to washing (W, arrows) and re-equilibration. The same tissue was then either treated for 15 min (b and f) with genistein (GS: △, 15 μM) or was changed to a buffer in which sodium ion was replaced either with lithium (tracing c) or with choline (tracing g) or to a calcium-free buffer, containing 1 mM EGTA (tracings d and h). The response to PV (○, 3 μM) was again measured in the presence of 15 μM GS (b and f), in the absence of extracellular sodium (c and g) and in the absence of extracellular calcium (d and h). A contractile response was observed upon replenishing the calcium-free medium with 2.5 mM Ca^{2+} (d and h). Because of the desensitizing action of PV in the aortic tissue, control contractile responses were monitored first with VO_4 (□, 200 μM), prior to challenging each tissue only once with PV (○, 20 μM: tracings e to h). Each tracing (a to h), illustrating the response of an individual tissue preparation, is representative of four or more independently conducted experiments with tissues from four or more separate animals.

VO_4 (e.g. 200 μM) caused a reproducible contraction, without desensitization, repeated exposures of the tissue to a fixed concentration of PV (e.g. 3 μM) resulted in an increased contractile response, that stabilized after the third or fourth contraction. Thus, there appeared to be a 'kindling phenomenon' for PV but not for VO_4 in the gastric preparation. In the aortic tissue, as for the gastric longitudinal muscle tissue, repeated exposure to a fixed concentration of VO_4 caused a reproducible contractile response. However, in the aortic preparation, in contrast to the gastric tissue, concentrations of PV higher than 15 μM caused prolonged and generalized desensitization, in that upon washing the aortic tissue free from PV after the first robust contraction, the tissue became unresponsive for more than 2 h either to a second exposure to PV or to other contractile agonists such as noradrenaline (0.1 μM) or KCl (50 mM). Tissue responsiveness began to return after 3.5 h. These differences in the responses of the two tissues to VO_4 and PV were taken into account in the ensuing studies.

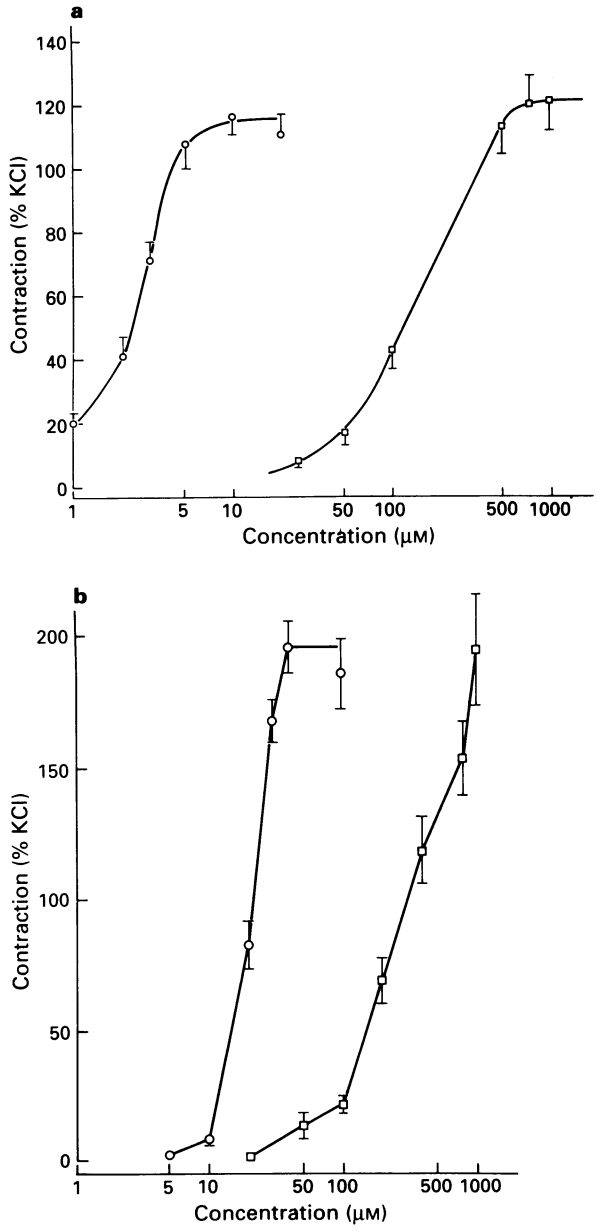


Figure 2 Concentration-effect curves for vanadate (VO_4) and pervanadate (PV). The contractile effects of increasing concentrations of either VO_4 (□) or PV (○) were measured in gastric (a) and aortic (b) preparations as described in the text. Responses in individual tissues are expressed as a percentage (% KCl) of a control response to 50 mM KCl. Values represent the means ± s.e.mean for measurements on 8 to 10 individual tissue preparations.

Concentration-effect curves

Gastric tissue In view of the characteristics of the responses to VO_4, it was possible, with the gastric preparation, to make sequential measurements of the contractile responses to increasing concentrations of VO_4 in individual matched tissue preparations (Figure 2a). The procedure for PV differed however, because of the 'kindling phenomenon' described above. Thus, for the PV concentration-effect curves, the gastric longitudinal muscle tissues were first primed several times with a low concentration of PV (3 μM) until the response had stabilized. At this point, the responsiveness to repeated exposures of either lower or higher concentrations of PV were also observed to be stable and reproducible; the concentration-response measurements for increasing concentrations of PV (Figure 2a) were then done sequentially in the primed tissue preparations.

Aortic tissue In the aortic preparation, the concentration-effect curves for VO_4 were obtained essentially as for the gastric longitudinal muscle preparation, using sequential measurements in individual tissues (Figure 2b). However, for evaluating PV action in the aortic preparation (Figure 2b), each tissue, after responding to a test concentration of KCl (50 mM) and noradrenaline (0.1 μM) (to provide an index of receptor-mediated tissue responsiveness), was subsequently exposed only once to PV. Figure 2 shows the contractile responses of the gastric and aortic preparations to VO_4 and PV expressed as a percentage of the contractile response elicited by 50 mM KCl; equivalent concentration-effect curves (not shown) were obtained when the contractile responses were expressed as a percentage of the responses to noradrenaline (aortic preparation only, 0.1 μM) or angiotensin II (gastric preparation only, 0.1 μM). The concentration-effect curves (Figure 2) showed that PV was approximately one to two orders of magnitude more potent than VO_4 in both tissues. For that reason, the subsequent experiments focused primarily on the contractile actions of PV alone.

Requirements for extracellular sodium and calcium

The contractile response of either the gastric or aortic tissue to PV was observed in the absence of extracellular sodium (Figure 1c and g). Nonetheless, in both the gastric longitudinal muscle and aortic preparations, the contractile

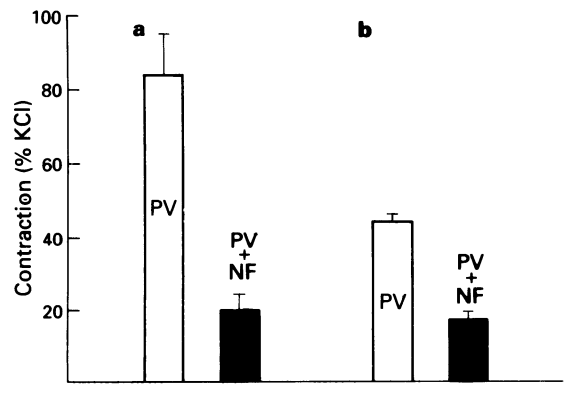


Figure 3 Effect of nifedipine (NF) on the contractile actions of pervanadate (PV). The contractile responses of aortic (a) and gastric (b) tissue preparations to PV were measured either in the absence (open columns) or presence (solid columns) of 1 μM nifedipine. The contractile responses to PV are expressed in each tissue as a percentage (% KCl) of the control contraction elicited by 50 mM KCl. Each histogram shows values for the means ± s.e.mean of measurements on four individual tissue preparations.

actions of PV were dependent on extracellular calcium (Figure 1d and h); a response to PV was not observed upon removal of calcium from the medium, but ensued upon restoring extracellular calcium. In keeping with this result, the calcium channel blocker, nifedipine, markedly attenuated the contractile action of PV in both preparations (Figure 3). Diltiazam and verapamil were much less effective than nifedipine in this regard (not shown).

Parallels between the actions of PV and EGF-Uro in the gastric longitudinal muscle preparation

In view of the ability of PV to mimic the action of a tyrosine kinase-mediated agonist such as insulin, we wondered if the characteristics of the contractile action of PV paralleled those of EGF-Uro in the gastric longitudinal muscle preparation, since EGF-Uro, like insulin, acts via a tyrosine kinase receptor. Because in our hands EGF-Uro did not cause contractions of the aortic tissue, we were not able to assess the parallels between the actions of PV and EGF-Uro in this preparation. As illustrated in Figure 4, there was indeed a parallel between EGF-Uro and PV action in the gastric tissue in terms of (1) the inhibition of the responses by the tyrosine kinase inhibitor, genistein, (2) the sensitivity of the response to indomethacin and (3) a requirement for extracellular calcium. In contrast, the contractile actions of carbachol (1 μM) in the longitudinal muscle preparation were not affected by either genistein or indomethacin and a contractile response to carbachol could be observed in the absence of extracellular calcium (Yang *et al.*, 1992 and data not shown).

Effects of tyrosine kinase inhibitors on contraction and on phosphotyrosyl protein content

We were interested to explore the concentration-range over which the tyrosine kinase inhibitors would affect the contractile actions of PV. As illustrated in Figure 1b and f, and by the concentration-inhibition curves in Figure 5, genistein at concentrations of 15 μM or below was able to attenuate selectively the effects of PV in both the gastric longitudinal muscle and aortic preparations, without causing a comparable inhibition of contractions elicited by KCl. The inhibitory effects were completely reversed upon washing the preparations free from genistein (not shown). The aortic preparation was particularly sensitive to the inhibitory actions of genistein. Tyrphostin was also able to block PV-mediated contractions selectively in the gastric longitudinal muscle preparation (Figure 5) but was unable, at comparable concentrations, to do so in the aortic preparation (not shown).

In view of the known ability of PV to inhibit protein tyrosine phosphatase, thereby potentiating the actions of tissue tyrosine kinases, we analysed, using a Western blot procedure, employing a monoclonal antiphosphotyrosine antibody, the phosphotyrosyl protein content of the gastric longitudinal muscle and aortic tissues after exposure to PV either in the absence or presence of either genistein (gastric and aortic preparations) or tyrphostin (gastric preparation only). As shown in Figure 6, PV, at the same time as it caused a contractile response, caused an increase in the Western blot reactivity of a number of constituents in both

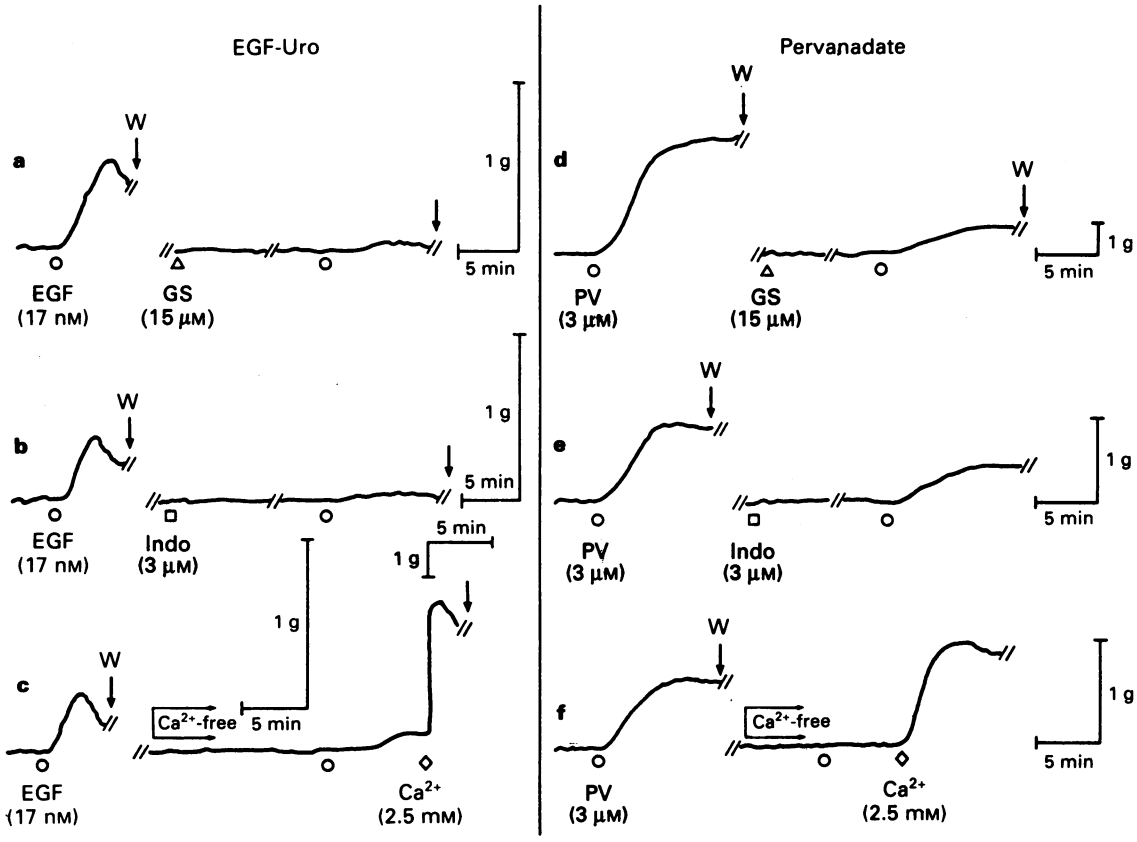


Figure 4 Comparison of the contractile actions of epidermal growth factor-urogastrone (EGF-Uro) and pervanadate (PV) in the gastric longitudinal muscle preparation: effects of genistein (tracings a and d) indomethacin (tracings b and e) and the absence of extracellular calcium (tracing c and f). Tracings for individual tissue preparations are shown, illustrating the responses to EGF-Uro (EGF, 17 nM: a,b,c) or PV (3 μM: d,e,f) either in the absence (before tissue wash, arrow, W) or presence of genistein (tracings a and d, GS: Δ, 15 μM) and indomethacin (tracings b and e, Indo: □, 3 μM). Tissues were treated with either genistein or indomethacin 20 min prior to the addition of EGF-Uro or PV to the organ bath. The effect of switching tissues to a calcium-free buffer containing 1 mM EGTA is also shown (tracings c and f) followed by replenishing the calcium (◇, 2.5 mM) in the continued presence of either EGF-Uro (tracing c) or PV (tracing f). Individual tracings for a single tissue are representative of three or more independently conducted experiments with tissues obtained from different animals.

the gastric and aortic tissues (Figure 6, lanes 1B and 2B); increases were observed prior to the development of maximum tension and were attenuated when the tissues were exposed to PV in the presence of genistein or tyrphostin (Figure 6, lanes 1C and 2C respectively). Genistein (not shown) was also able to reduce but not abolish the PV-mediated increases in gastric longitudinal muscle tissue phosphotyrosyl protein. The PV-mediated increases in tissue phosphotyrosyl protein content were also observed in the absence of extracellular calcium (not shown) under which conditions neither tissue exhibited a contractile response.

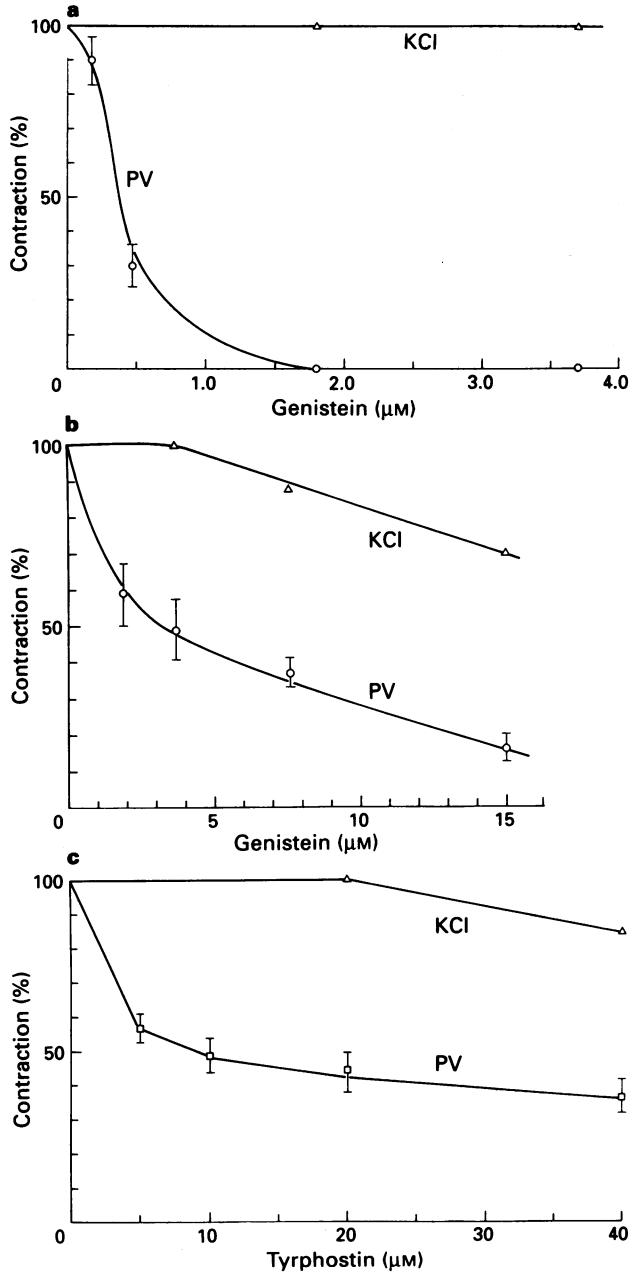


Figure 5 Concentration-effect curves for the inhibition of pervanadate (PV)-mediated contractions by tyrosine kinase inhibitors. The contractile responses to PV (20 μM for aortic tissue, a; 3 μM for gastric longitudinal muscle tissue, b and c) and to 50 mM KCl were measured in individual tissue preparations either in the absence or presence of increasing concentrations of either genistein (a and b) or tyrphostin (c) panel. Tissues were pretreated with genistein or tyrphostin 20 min prior to the addition of PV to the organ bath. The contractile responses of tyrosine kinase inhibitor-treated preparations were then expressed as a percentage (%) of the contraction observed in the absence of inhibitor. (a) Aortic tissue treated with genistein; (b) and (c): gastric tissue treated with either genistein (b) or tyrphostin (c). Values represent the means ± s.e.mean for experiments done with four or more independent tissue preparations.

Potentiation of angiotensin II action

Since our previous work had suggested a role for a tyrosine kinase pathway in the contractile effects of angiotensin (Saifeddine *et al.*, 1992; Yang *et al.*, 1993), we hypothesized that PV, by attenuating tyrosine phosphatase activity, might potentiate the action of angiotensin II. As illustrated in Figure 7, this proved to be the case for both the gastric longitudinal muscle and aortic ring assays, a concentration of PV, which by itself did not cause an appreciable contractile response, shifted the angiotensin II concentration-response curves for both preparations to the left, without affecting the maximum response.

Discussion

The main finding of our study was that PV, which has been found in other systems to be much more potent than VO_4 as an insulin-mimetic inhibitor of phosphotyrosyl phosphatase activity (Fantus *et al.*, 1989; Heffetz *et al.*, 1990; Bourgoin & Grinstein, 1992; O'Shea *et al.*, 1992), was also one to two orders of magnitude more potent than VO_4 in causing contractile responses in gastric and aortic smooth muscle preparations. The contractile responses to PV could not be attributed to the release of neurotransmitter or to the action,

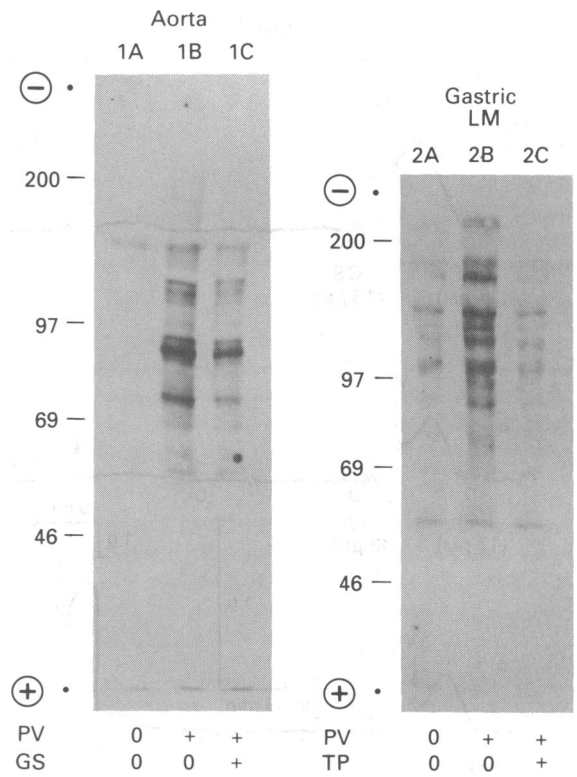


Figure 6 Western blot analysis of phosphotyrosyl proteins in pervanadate (PV)-treated tissues. Aortic (left, lanes 1A, 1B, 1C) and gastric (right, lanes 2A, 2B, 2C) tissues were recovered from the organ bath, as described in Methods, and processed for Western blot analysis. Tissues were either untreated (1A, 2A) or were exposed to PV either in the absence (1B, 2B) or presence of genistein (15 μM, lane 1C) or tyrphostin 80 μM, lane 2C. Molecular weight markers are shown on the left of each blot; the origin (⊕) and buffer front (⊖) are also indicated. The Western blot reaction shown for the monoclonal antiphosphotyrosine antibody was eliminated in the presence of 25 mM phenyl phosphate (not shown).

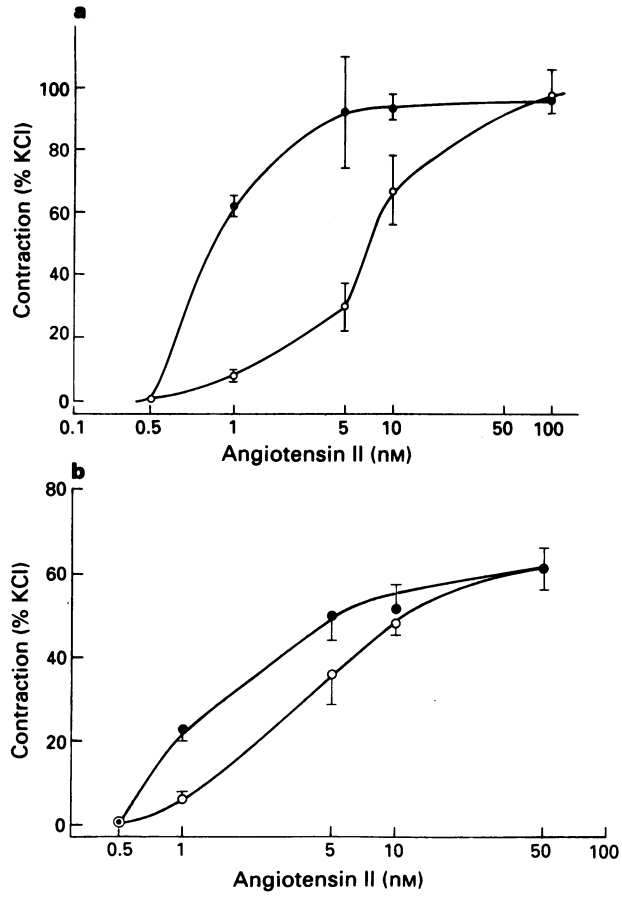


Figure 7 Potentiation of angiotensin II action by pervanadate (PV). The concentration-effect curves for the contractile action of angiotensin II in the gastric (b) and aortic (a) preparations were measured either in untreated tissues (○, control) or tissues that were pretreated with PV (●, 0.5 μM for gastric tissue; 10 μM for aorta tissue) prior to exposing the tissue to increasing concentrations of angiotensin. Values ± s.e.mean representing measurements made on 4 to 6 individual tissue preparations, are expressed as a percentage (% KCl) of the control contractile response in each tissue elicited by 50 mM KCl.

in the aortic preparation, of endothelial cell-released factors. Further, in accord with previous data ruling out a role for Na^+/K^+-ATPase inhibition in the contractile action of VO_4 (summarized by Fox *et al.*, 1983; Shimada *et al.*, 1986 and by Sanchez-Ferrer *et al.*, 1988), our observations that PV could cause its contractile effects in both the aortic and gastric preparations in the absence of extracellular sodium would argue against roles for Na^+/K^+-ATPase inhibition and Na^+/Ca^{2+} exchange in the PV-mediated contractile response. Additionally, there was a requirement for extracellular calcium. This calcium requirement for PV action is in agreement with other work documenting the importance of extracellular calcium for VO_4-induced contractions in rabbit vascular (Fox *et al.*, 1983) and gastric (Candura *et al.*, 1994) smooth muscle preparations. The dependence of the contractile effects on extracellular calcium would argue against the likelihood that PV was acting by inhibiting intracellular Ca^{2+}-ATPase, so as to provide an intracellular source of calcium to regulate the contractile apparatus. As an alternative, in view of the ability of the tyrosine kinase inhibitors to block the contractile action of PV, we suggest that it may be the inhibition of tyrosine phosphatase activity and thus, the potentiation of constitutive tyrosine kinase activity, that may best account for the contractile actions of PV.

One of the hallmarks of the pharmacological actions of VO_4 and PV is the simulation of the tyrosine kinase-mediated effects of insulin on its target tissues (Dubyak & Kleinzeller, 1980; Schechter & Karlish, 1980; Kadota *et al.*, 1987; Fantus *et al.*, 1989), in concert with increased protein tyrosine phosphorylation (Tamura *et al.*, 1984; Heffetz *et al.*, 1990). In a similar vein, our study showed that PV, in parallel with causing tyrosine kinase inhibitor-sensitive increases in tissue phosphotyrosyl protein content, mimicked the contractile action of EGF-Uro in the gastric preparation in terms of a sensitivity towards genistein and indomethacin and a requirement for extracellular calcium. These contractile response characteristics have been found to be typical for the tyrosine kinase-mediated contractile action of EGF-Uro but not for other agonists, such as carbachol, in a number of smooth muscle assay systems including gastric longitudinal muscle (Hollenberg, 1994). Thus, taken together, our data are entirely in keeping with the suggestion above, that the potentiation of a tyrosine kinase-mediated signal transduction pathway can account for the contractile actions of PV in the tissues we have examined.

Our work entirely supports and enlarges upon data that appeared upon completion of our study, demonstrating that VO_4-induced contractions in guinea-pig taenia coli preparations are associated with enhanced protein tyrosine phosphorylation (Di Salvo *et al.*, 1993a). Nonetheless, in our own work, the 1-D gel analysis of the phosphotyrosyl protein profiles of the gastric and aortic tissues exposed to PV in the absence and presence of the tyrosine kinase inhibitors did not single out any individual constituents, for which increased phosphorylation could be correlated directly with a contractile response. A more refined 2-D gel analysis of the phosphoproteins will be required to explore this potential correlation.

As yet, we have no explanation for the qualitative differences between the actions of PV and VO_4 on the gastric and aortic preparations (1) in terms of tissue desensitization (aorta) and (2) in terms of the 'kindling' phenomenon observed in the gastric preparation. Possibly these differences may relate to an increased potency of PV, compared with VO_4, for inhibiting cellular tyrosine phosphatase activity (Fantus *et al.*, 1989; Heffetz *et al.*, 1990; Faure *et al.*, 1992). Further, the differential effects of tyrphostin and the differences in the sensitivities of the two tissues to genistein may point to the involvement of distinct tyrosine kinases in the contractile responses of the two tissues, so as to lead to differences that would be observed upon blocking tyrosine phosphatase action. Alternatively, the differences may reflect a greater ability of PV to affect a variety of other enzyme systems (Bhagavan *et al.*, 1983; Erdmann *et al.*, 1984; Nechay *et al.*, 1986), in addition to the tyrosine phosphatase(s) we believe most likely to be responsible for initiating the rapid contractile response. Thus, although VO_4 and PV are often used interchangeably as probes for assessing the functional significance of tyrosine phosphatase in biological test systems, the two compounds may have distinct and complex actions on other enzyme pathways that may affect tissue responsiveness.

We believe the dependence of the contractile action of PV on extracellular calcium and the ability of PV to potentiate the contractile action of angiotensin II may relate to a role for tyrosine kinase activity in agonist-mediated calcium entry, as suggested by the work of Lee and co-workers (1993). This possibility is also in keeping with the ability of tyrosine kinase inhibitors to modulate voltage-sensitive calcium channels in isolated vascular smooth muscle cells (Wijetunge *et al.*, 1992) and with the ability of angiotensin II to stimulate protein tyrosine phosphorylation in smooth muscle tissue (Tsuda *et al.*, 1991; Huckle *et al.*, 1992; Molloy *et al.*, 1993; Yang *et al.*, 1993). Thus, the putative targets for tyrosine phosphorylation that could regulate tissue contractility might be components associated with the voltage-dependent calcium channel in the plasma membrane and would appear not to involve a downstream regulation of the contractile apparatus *per se*. This suggestion is in accord with our observation that PV-triggered cellular tyrosine phosphorylation, occurring in the absence of extracellular calcium, did

not lead to a contractile response. Thus in summary, our data support the hypothesis that PV causes its contractile effects via the inhibition of a tyrosine phosphatase pathway, thereby amplifying constitutive tyrosine kinase activity, so as to facilitate the calcium entry through voltage-sensitive calcium channels. We believe that such a role for tyrosine phosphorylation/dephosphorylation in the control of smooth muscle tension may be relevant to the action of a variety of G-protein-coupled and growth factor receptor-coupled contractile agonists.

This work was supported in large part by a grant from the Canadian Diabetes Association, supplemented by funds from the Heart and Stroke Foundation of Alberta and the Canadian Medical Research Council. We are indebted to Dr Hwa Lu Chao for the conduct of the Western blot analyses, to Peter Atadja for the synthesis of tyrphostin AG18, and to Dr B.I. Posner for discussions which served as a stimulus for the study of the actions of pervanadate. The secretarial assistance of Ms Louise Mackintosh is gratefully acknowledged.

References

BERK, B.C. & ALEXANDER, R.W. (1985). Vasoactive effects of growth factors. *Biochem. Pharmacol.*, **38**, 219–225.

BHAGAVAN, S. & HOM, G.J. (1983). Physiological and pharmacological properties of vanadium. *Life Sci.*, **33**, 1325–1340.

BLAKE, R.A., WALKER, T.R. & WATSON, S.P. (1993). Activation of human platelets by peroxovandate is associated with tyrosine phosphorylation of PLCγ and formation of inositol phosphates. *Biochem. J.*, **290**, 471–475.

BOURGOIN, S. & GRINSTEIN, S. (1992). Peroxides of vanadate induce activation of phospholipase D in HL-60 cells. *J. Biol. Chem.*, **267**, 11906–11908.

CANDURA, S.M., MANZO, L., MARRACCINI, P., COCCINI, T. & TONINI, M. (1994). Investigation into vanadate-induced potentiation of smooth muscle contractility in the rabbit isolated ileum. *Life Sci.*, **54**, 237–244.

DI SALVO, J., SEMENCHUK, L.A. & LAUER, J. (1993a). Vanadate-induced contraction of smooth muscle and enhanced tyrosine phosphorylation. *Arch. Biochem. Biophys.*, **304**, 386–391.

DI SALVO, J., STEUSLOFF, A., SEMENCHUK, L., SATOH, S., KOLQUIST, K. & PFITZER, G. (1993b). Tyrosine kinase inhibitors suppress agonist-induced contraction in smooth muscle. *Biochem. Biophys. Res. Commun.*, **190**, 968–974.

DUBYAK, G.R. & KLEINZELLER, A. (1980). The insulin-mimetic effects of vanadate in isolated rat adipocytes. *J. Biol. Chem.*, **255**, 5306–5312.

ERDMANN, E., WERDAN, K., KRAWIETZ, W., SCHMITZ, W. & SCHOLZ, H. (1984). Vanadate and its significance in biochemistry and pharmacology. *Biochem. Pharmacol.*, **33**, 945–950.

FANTUS, I.G., KADOTA, S., DERAGON, G., FOSTER, B. & POSNER, B.I. (1989). Pervanadate [peroxide(s) of vanadate] mimics insulin action in rat adipocytes via activation of the insulin receptor tyrosine kinase. *Biochem.*, **28**, 8864–8871.

FAURE, R., BAQUIRAN, G., BERGERON, J.J. & POSNER, B.I. (1992). The dephosphorylation of insulin and epidermal growth factor receptors. Role of endosome-associated phosphotyrosine phosphatase(s). *J. Biol. Chem.*, **267**, 11215–11221.

FOX, A.A.L., BORCHARD, U. & NEUMANN, M. (1983). Effects of vanadate on isolated vascular tissue: biochemical and functional investigations. *J. Cardiovasc. Pharmacol.*, **5**, 309–316.

GAZIT, A., YAISH, P., GILON, C. & LEVITZKI, A. (1989). Tyrphostins I: synthesis and biological activity of protein tyrosine kinase inhibitors. *J. Med. Chem.*, **32**, 2344–2352.

GLENNEY, J.R. Jr., ZOKAS, L. & KAMPS, M.P. (1988). Monoclonal antibodies to phosphotyrosine. *J. Immunol. Methods*, **109**, 277–285.

GRINSTEIN, S., FURUYA, W., LU, D.J. & MILLS, G.B. (1990). Vanadate stimulates oxygen consumption and tyrosine phosphorylation in electropermeabilized human neutrophils. *J. Biol. Chem.*, **265**, 318–327.

HEFFETZ, D., BUSHKIN, I., DROR, R. & ZICK, Y. (1990). The insulinomimetic agents H_2O_2 and vanadate stimulate protein tyrosine phosphorylation in intact cells. *J. Biol. Chem.*, **265**, 2896–2902.

HOLLENBERG, M.D. (1994). The acute actions of growth factors in smooth muscle systems. *Life Sci.*, **54**, 223–235.

HOLLENBERG, M.D., LANIYONU, A.A., SAIFEDDING, M. & MOORE, G.J. (1993). Role of amino- and carboxyl-terminal domains of thrombin receptor-derived polypeptides in biological activity in vascular endothelium and gastric smooth muscle: evidence for receptor subtypes. *Mol. Pharmacol.*, **43**, 921–930.

HUCKLE, W.R., DY, R.C. & EARP, H.S. (1992). Calcium-dependent increase in tyrosine kinase activity stimulated by angiotensin II. *Proc. Natl. Acad. Sci. U.S.A.*, **89**, 8837–8841.

KADOTA, S., FANTUS, I.G., DERAGON, G., GUYDA, H.J., HERSH, B. & POSNER, B.I. (1987). Peroxide(s) of vanadium: a novel and potent insulin-mimetic agent which activates the insulin receptor kinase. *Biochem. Biophys. Res. Commun.*, **147**, 259–266.

LAEMMLI, U.K. (1971). Cleavage of structural proteins during the assembly of the head of bacteriophage T. *Nature*, **227**, 680–685.

LEE, K.-M., TOSCAS, K. & VILLEREAL, M.L. (1993). Inhibition of bradykinin- and thapsigargin-induced Ca^{2+} entry by tyrosine kinase inhibitors. *J. Biol. Chem.*, **268**, 9945–9948.

MOLLOY, C.J., TAYLOR, D.S. & WEBER, H. (1993). Angiotensin II stimulation of rapid protein tyrosine phosphorylation and protein kinase activation in rat aortic smooth muscle cell. *J. Biol. Chem.*, **268**, 7338–7345.

NECHAY, B.R., NANNINGA, L.B., NECHAY, P.S.E., POST, R.L., GRANTHAM, J.J., MACARA, I.G., KUBENA, L.F., PHILLIPS, T.D. & NIELSEN, F.H. (1986). Role of vanadium in biology. *Fed. Proc.*, **45**, 123–132.

O'SHEA, J.J., MCVICAR, D.W., BAILEY, T.L., BURNS, C. & SMYTH, M.J. (1992). Activation of human peripheral blood T lymphocytes by pharmacological induction of protein-tyrosine phosphorylation. *Proc. Natl. Acad. Sci. U.S.A.*, **189**, 10306–10310.

OZAKI, H. & URAKAWA, N. (1980). Effects of vanadate on mechanical responses and Na-K pump in vascular smooth muscle. *Eur. J. Pharmacol.*, **68**, 339–347.

SAIFEDDINE, M., LANIYONU, A.A., YANG, S.-G. & HOLLENBERG, M.D. (1992). Tyrosine kinase inhibitors and the contractile action of angiotensin-II in vascular tissue. *Pharmacol. Commun.*, **1**, 177–184.

SANCHEZ-FERRER, C.F., MARIN, J., LLUCH, M., VALVERDE, A. & SALAICES, M. (1988). Actions of vanadate on vascular tension and sodium pump activity in cat isolated cerebral and femoral arteries. *Br. J. Pharmacol.*, **93**, 53–60.

SCHECHTER, Y. & KARLISH, J.D.K. (1980). Insulin-like stimulation of glucose oxidation in rat adipocytes by vanadyl (IV) ions. *Nature*, **284**, 556–558.

SHIMADA, T., SHIMAMURA, K. & SUNANO, S. (1986). Effects of sodium vanadate on various types of vascular smooth muscles. *Blood Vessels*, **23**, 113–124.

TAMURA, S., BROWN, T.A., WHIPPLE, J.H., FUJITA-YAMAGUCHI, Y., DUBLER, R.E., CHENG, K. & LARNER, J. (1984). A novel mechanism for the insulin-like effect of vanadate on glycogen synthase in rat adipocytes. *J. Biol. Chem.*, **259**, 6650–6658.

TSUDA, T., KAWAHARA, Y., SHII, K., KOIDE, M., ISHIDA, Y. & YOKOYAMA, M. (1991). Vasoconstrictor-induced protein-tyrosine phosphorylation in cultured vascular smooth muscle cells. *FEBS Lett.*, **285**, 44–48.

WIJETUNGE, S., AALKJAER, C., SCHACTER, M. & HUGHES, A.D. (1992). Tyrosine kinase inhibitors block calcium channel currents in vascular smooth muscle cells. *Biochem. Biophys. Res. Commun.*, **189**, 1620–1623.

YANG, S.-G., SAIFEDDINE, M. & HOLLENBERG, M.D. (1992). Tyrosine kinase inhibitors and the contractile action of epidermal growth factor-urogastrone and other agonists in gastric smooth muscle. *Can J. Physiol. Pharmacol.*, **70**, 85–93.

YANG, S.-G., SAIFEDDINE, M., LANIYONU, A.A. & HOLLENBERG, M.D. (1993). Distinct signal transduction pathways for angiotensin-II in guinea pig gastric smooth muscle: differential blockade by indomethacin and tyrosine kinase inhibitors. *J. Pharmacol. Exp. Ther.*, **264**, 958–966.

(Received March 21, 1994
Revised June 6, 1994
Accepted June 7, 1994)

Br. J. Pharmacol. (1994), **113**, 411–418 © Macmillan Press Ltd, 1994

Actions of cromakalim on outward currents of CA1 neurones in hippocampal slices

G. Erdemli & [1]K. Krnjević

Anaesthesia Research Department, McGill University, Montréal, P.Q. Canada

1 Membrane effects of cromakalim (Crom; 50–300 μM) were examined in CA1 neurones recorded mainly by intracellular, single-electrode voltage-clamping in slices (from Sprague-Dawley rats) kept in an interface chamber at 33°C.

2 In 14 cells held at -63 ± 3.5 mV, in the presence of tetrodotoxin, kynurenic acid and (in most cases) bicuculline, bath applied Crom produced no consistent change in holding current (-59 ± 66 pA) or input conductance (G_N) ($-3.9 \pm 5.2\%$).

3 Overall there were no significant changes in instantaneous inward rectification or in Q-current inward relaxations.

4 In 18 out of 22 cells, outward currents, evoked by 0.5 s pulses to voltages > -50 and < -20 mV, were depressed by Crom (by $42 \pm 11\%$, for $n = 22$). Because this effect was consistently seen in Ca current-blocking media, containing either Mn and low Ca, or Cd (and also carbachol), the K channels depressed by Crom were probably of the delayed rectifier (I_{DR}) type.

5 The Crom-control difference current (I_{Crom}), obtained with slow depolarizing ramps, had a biphasic character, inward in the voltage (V) range $> -50 < -20$ mV (where outward currents are depressed by Crom) and tending outward for $V \geqslant -20$ mV.

6 In 10 out of 11 cells, Crom potentiated a D-like, slowly-inactivating outward current (by $88 \pm 31\%$, for $n = 11$).

7 The effects of Crom and of 2 min periods of anoxia were compared in 12 cells: unlike anoxia, Crom produced no consistent increases in G_N; the currents evoked in the same cells by anoxia differed significantly from those evoked by Crom (by 150 ± 60 pA); the directions of current changes induced by Crom and anoxia respectively were not significantly correlated. Crom strongly depressed anoxic outward currents (by $80 \pm 12\%$, $n = 4$).

8 Some Crom-induced effects (increases in D-like current and the outward current elicited at $V \geqslant -20$ mV) were always reversed by tolbutamide (1 mM), but much less consistently by glibenclamide (10–30 μM).

9 In conclusion, the effects of Crom, recorded with intracellular electrodes in CA1 neurones in slices, show little resemblance to the effects of activation of ATP-sensitive K channels.

Keywords: Rat hippocampal slices; delayed rectifier; D-current; K_{ATP}-channels; tolbutamide; glibenclamide; glyburide; anoxia

Introduction

Cromakalim (Crom) has been known for some years as a hypotensive agent. At very low concentrations (<1 μM), it relaxes vascular smooth muscle by activating K conductance (G_K) (Cook & Quast, 1990; Kajioka *et al.*, 1991). More-or-less comparable effects of Crom (but usually at 100 fold higher concentrations) have been seen in several other tissues (Edwards & Weston, 1993); including non-vascular smooth muscle (Allen *et al.*, 1986; Foster *et al.*, 1989); cardiac (Escande *et al.*, 1988; Osterrieder, 1988) and skeletal (Spuler *et al.*, 1989) muscles; insulin-secreting cells (Rorsman & Trube, 1990), as well as some central neurones (Häusser *et al.*, 1991; but cf. Hicks & Henderson, 1992; Sellers *et al.*, 1992).

In keeping with some kind of stabilizing action are several reports that Crom reduces epileptiform discharges of brain tissue, both *in vitro* and *in vivo* (Alzheimer & ten Bruggencate, 1988; Gandolfo *et al.*, 1989; Popoli *et al.*, 1991) and suppresses fluctuations of cytosolic [Ca] in cultured hippocampal cells (Abele & Miller, 1990).

According to most of the recent authors, the effects of Crom are blocked by sulphonylureas and therefore probably mediated by ATP-sensitive K (K_{ATP}) channels (Spruce *et al.*, 1987; Escande *et al.*, 1988; Häusser *et al.*, 1991). However, there is also good evidence that Crom activates Ca-dependent or other K channels (Nakao *et al.*, 1989; Gelband *et al.*, 1989), including some that are not ATP-sensitive (Beech & Bolton, 1989; Carl *et al.*, 1992).

Previous investigators of CA3 neurones in slices from guinea-pigs (Alzheimer & ten Bruggencate, 1988; Alzheimer *et al.*, 1989) or cultured hippocampal neurones from rat embryos (Politi *et al.*, 1989; Politi & Rogawski, 1991) reported widely different effects. In the slices, Crom depressed population spikes and burst firing, but without altering the resting potential or input resistance (Alzheimer & ten Bruggencate, 1988). In a later study (Alzheimer *et al.*, 1989), however, the same group observed a moderate hyperpolarization and a small drop in resistance, ascribed to enhancement of a K-mediated inward rectifier. This effect could be blocked by Cs and Ba, but not by the sulphonylurea tolbutamide (Tolb). In addition, a Ca-dependent slow after-hyperpolarization may have been increased.

By contrast, in cultured neurones, Politi *et al.* (1989) saw no effect on resting membrane properties; but Crom potentiated a slowly-inactivating, delayed rectifier-like outward current, that was activated by large depolarizations and blocked by tetraethylammonium (TEA). In later experiments, this outwardly-rectifying current was shown to be blocked by glibenclamide (Glib) and was stimulated by energy depletion. So Politi & Rogawski (1991) concluded tht the Crom-activated K channels are probably of the classical K_{ATP} type (Ashcroft, 1988).

[1] Author for correspondence at: McIntyre Building No. 1208, 3655 Drummond Street, Montréal, H3G 1Y6, Qué, Canada.

In hippocampal neurones of the CA1 region, brief anoxia elicits a characteristic hyperpolarization (or outward current in voltage-clamp mode), mediated mainly by G_K activation (Krnjević, 1993; Haddad & Jiang, 1993). Whether the anoxic G_K is principally a $G_{K(Ca)}$ activated by cytosolic Ca^{2+}, or K_{ATP} activated by loss of cellular ATP, remains uncertain. Although Glib-binding sites are quite abundant in the hippocampus, especially in CA3 (Mourre *et al.*, 1989; Xia & Haddad, 1991), functional K_{ATP} channels may be present on presynaptic terminals rather than pyramidal cell bodies (Ben-Ari, 1990).

In the present experiments, we looked more closely for any effects of Crom on (a) resting properties, such as membrane current and conductance of CA1 neurones; (b) their voltage-dependent currents; and (c) compared Crom-induced currents and conductance changes with those produced by anoxia in the same cells. A preliminary abstract of some of these findings has appeared (Erdemli & Krnjević, 1993a).

Methods

Sprague-Dawley rats were decapitated under halothane anaesthesia. Transverse hippocampal slices (400 μm) were cut with a McIlwain tissue chopper or a Vibroslicer (Campden Instruments). They were kept for at least 1 h at room temperature, in carbogenated saline (ACSF) of the following composition (in mM): NaCl 124, KCl 3.0, $CaCl_2$ 2.0, $MgCl_2$ 2.0, NaH_2PO_4 1.25, $NaHCO_3$ 26 and glucose 10. They were then transferred to an interface (Haas)-type chamber, kept at 33–34°C. There they were continuously superfused (at 1–2 ml min^{-1}) with carbogenated ACSF, and further oxygenated by a copious flow of carbogen (95% O_2 and 5% CO_2, 1.5 l min^{-1}), appropriately humidified and heated to the bath temperature. For anoxic tests, 95% N_2 and 5% CO_2 were substituted for carbogen, most often for 2 min, and at intervals of not less than 10 min.

Whenever necessary, Ca-currents were suppressed by the following: either a Mn/low Ca ACSF containing (in mM): Mn^{2+} 2.3, Ca^{2+} 0.4, HCO_3^- 11 and no $H_2PO_4^-$; or $H_2PO_4^-$-free ACSF with 100 μM Cd^{2+} added. All drugs were bath-applied: tetrodotoxin (TTX) 1 μM (Qinhuangdao Trading Corp., China); kynurenic acid (1–2 mM); bicuculline methiodide (10 μM); carbachol (carbamyl choline) (20–50 μM) (all from Sigma Inc.); glibenclamide (glyburide, Hoechst Canada) (10–30 μM, from a 10 mM stock solution in dimethylsulphoxide (DMSO)) (Fisher Scientific); tolbutamide (Sigma) 0.5–1 mM, from a 150 mM stock solution in NaOH at pH 13; and cromakalim (gifts from Dr M. Rogawski) 50–300 μM; from stock solutions of 10 mM in 70% (v/v) ethanol or 1 or 10 mM in DMSO.

In general agreement with previous observers (Alzheimer & ten Bruggencate, 1988; Alzheimer *et al.*, 1989; Politi *et al.*, 1989), vehicle control tests showed only marginally significant effects of DMSO (0.1 and 1%) and ethanol (0.7%). DMSO (at both concentrations) somewhat reduced input conductance (by 14.6 ± 3.8%, at V_H − 61 ± 5.9 mV; $n = 14$); but had no significant effect on the holding current nor on the outward currents evoked by pulses to − 40 mV (− 22.5 ± 12.6%) and to − 20 mV (− 12.7 ± 17.9%, $n = 11$). Ethanol (0.7%) also reduced G_N by 10 ± 4.0% ($n = 8$) and did not alter the holding current, but it increased outward currents (at ≈ − 40 mV by 40 ± 12%; $n = 5$) — as reported by others (Carlen *et al.*, 1982; Weiner *et al.*, 1992).

In most experiments, pyramidal layer cells were penetrated with 'sharp' microelectrodes, filled with 3 M KCl (resistances of 60–100 MΩ). Neurones with spikes ⩾ 90 mV were selected for voltage-clamping (by the single electrode) and subsequent tests of Crom and other drugs. For the discontinuous voltage-clamp, the sampling rate was set at 3–5 kHz, and the usual precautions were taken to reduce the electrode time-constant. In order to minimize the effects of junctional potential changes at the bath's ground electrode, a second 3 M KCl microelectrode, placed near the slice, was routinely used as a 'bath probe' reference for the intracellular signals. For current-voltage (I/V) plots, currents were elicited either with 0.5 s depolarizing and hyperpolarizing pulses or with depolarizing voltage ramps (≈ 50 mV s^{-1}). Input conductances (G_N) were given by the slopes of regression lines fitted to the initial ('instantaneous') currents evoked by small hyperpolarizing pulses, in the linear range of the I/V plots.

To minimize indirect or synaptically-mediated effects of drugs, the slices were routinely pretreated with tetrodotoxin (TTX, 1 μM), kynurenic acid (Kyn, 1 mM) and (in most but not all cases) bicuculline (Bic, 10 μM).

Throughout, means are given ± the standard error.

Results

In 14 cells held at − 63 (± 3.5) mV, 10–20 min of superfusion with Crom (50–300 μM in standard ACSF) produced no consistent changes in holding current (ΔI_H) (− 59 ± 66 pA) or G_N (− 3.9 ± 5.2%).

Crom effects on voltage-dependent currents

Inwardly rectifying currents evoked by hyperpolarizing pulses For about half of the cells, the I/V plots showed fast inward rectification, as previously observed in hippocampal neurones (Halliwell & Adams, 1982; Brown *et al.*, 1990), comparable to the K channel-mediated instantaneous rectification (I_{IR}) seen in some other central neurones (Constanti & Galvan, 1983). In 5 out of 10 cells, Crom enhanced this rectification (in agreement with Alzheimer *et al.*, 1989); but overall, the changes were not significant (9.6 ± 23.9%, for $n = 10$). The time-dependent inward rectifier (Q current) (Halliwell & Adams, 1982; Brown *et al.*, 1990) was reduced by Crom in 14 out of 21 cells; but again the overall changes were not significant (− 7.3 ± 7.3%, for $n = 21$).

Outward currents evoked by depolarizing pulses Because of the poor resolution of very fast events, only slowly-inactivating currents were analysed, by measuring the final ('steady-state') values of evoked currents. To avoid loss of voltage control, depolarizing pulses as a rule did not exceed the 0 mV level, from a holding potential (V_H) between ≈ − 80 and − 60 mV. The resulting I/V curves showed the usual outward rectification, evident in the graphs of Figures 1 and 2.

In 10 out of 12 cells, Crom only depressed these outward currents. The effect could be very striking, as in Figure 1a, or less conspicuous, as in Figure 1b. It was most consistent when V was > − 50 mV but < − 30 mV: at − 40 mV, Crom (50–200 μM) depressed net outward currents by 41 (± 18.4)% (for $n = 12$, $P < 0.05$). With greater depolarizations (to ⩾ − 20 mV), the outward currents were also reduced in 5 out of 7 cells, but in the other two they were enhanced. For example, in Figure 1b the outward current was clearly reduced in the range between − 50 and − 30 mV, but at − 20 mV it rose well above the control value. The suppression of outward currents at V > − 50 mV accounts for the inward phase of the Crom difference current, obtained by subtracting control currents from currents recorded in the presence of Crom. This current is also plotted in Figures 1 and 2 (triangles), where it is labelled I_{DIF}. Note the inflexion and upward trend above − 20 mV, which in some neurones led to an outward I_{DIF}.

In no instance could the Crom-induced depression of outward current be reversed by washing with ACSF. Attempts to reverse the effects of Crom with sulphonylureas always resulted in even greater depressions of outward current: Glib (10–20 μM) had a relatively weak action (Figure 1b), reducing the current by 31 ± 16.7% ($n = 7$); but then adding Tolb (0.5–1.5 mM) consistently produced a major further depression (by 54 ± 19%, $P < 0.05$), as well as an inward shift in I_H

(-0.50 ± 0.11 nA) and a $20 \pm 8.8\%$ reduction in G_N (comparable to the changes reported by Godfraind & Krnjević, 1993).

According to Politi *et al.* (1989), Crom potentiates a delayed rectifier-like outward current (I_{DR}). In order to test I_{DR} more selectively, in some experiments Ca currents were suppressed by the use of Mn/low Ca- or Cd-containing ACSF (cf. Storm, 1990). In all five cells recorded in Mn/low Ca medium, Crom induced an inward shift in base line (as in Figure 2a) and strongly depressed net outward currents (near -40 mV, by $59 \pm 15.9\%$, $P<0.025$). Less consistent effects were seen in Cd^{2+} -ACSF (Figure 2b), with some depression in only 3 out of 5 cells: at -40 mV, the mean change was $-29 \pm 15.3\%$ ($n=5$). At $V \geqslant -20$ mV, the results were as variable as before, giving a mean depression of $37 \pm 77.7\%$ ($n=3$).

To narrow the focus on I_{DR}, 20 μM carbachol was also applied in some experiments (in addition to TTX, KYN, BIC, as well as Mn/low/Ca or Cd^{2+}) to eliminate I_M, I_{AHP} and leak currents; carbachol moreover enhances the delayed rectifier of hippocampal neurones (Zhang *et al.*, 1992). The outward current recorded from three cells in this medium was consistently depressed; though in one cell, it was potentiated at $V \geqslant -30$ mV (Figure 2b). In all cases, the Crom-difference current had the same general characteristics as in standard ACSF, showing an inward trend > -50 mV and an outward inflexion near -20 mV (Figure 2).

Overall, in 18 out of 22 cells held at -69.5 ± 3.8 mV, the predominant action of Crom was to depress outward currents elicited by depolarizing pulses to > -50 and < -20 mV (in this range, the outward current was increased in only two cells) — the mean reduction for these 22 cells was by $42 \pm 11\%$ ($P<0.001$). With stronger depolarizations (to $\geqslant -20$ mV), in 4 out of 15 cells Crom enhanced the outward current (e.g. Figures 1 and 2b).

D-current (I_D) This very slowly inactivating outward current (Storm, 1988) can be elicited either by depolarizing steps

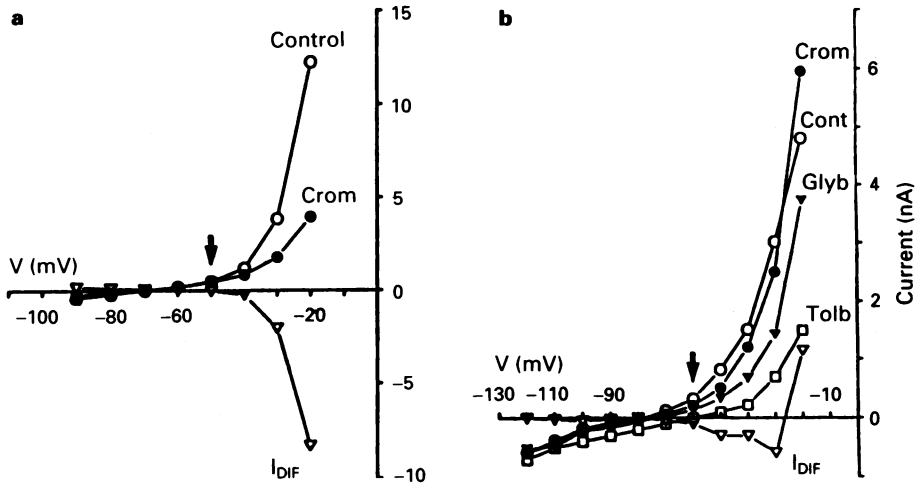


Figure 1 Cromakalim (Crom) depresses outward currents over a wide range of potential, but may enhance currents evoked by large positive pulses (to near 0 mV). *I/V* plots were obtained with 0.5 s pulses from two different CA1 cells: (a), at V_H -50 mV (arrow), in presence of tetrodotoxin and kynurenic acid; (b) at V_H -60 mV, with bicuculline as well. In cell (a) and (b), (○) are initial control data: (●) data obtained after 20–30 min in Crom (100 μM). Difference currents (Crom − control data) are also plotted (▽, I_{Dif}). For cell (b), effects produced by adding glibenclamide (20 μM, ▼), and then tolbutamide (1 mM, □) are also shown.

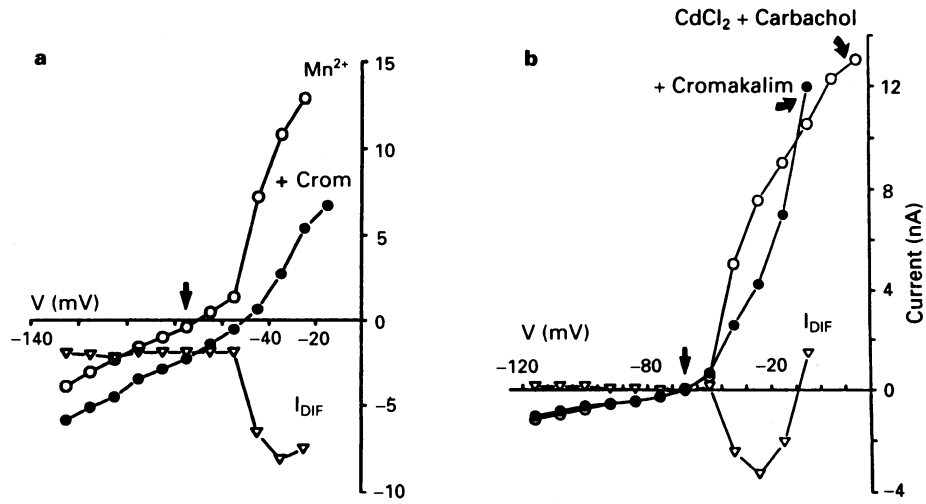


Figure 2 Ca-independent outward current is also depressed by cromakalim (Crom). Two cells were bathed in Ca-current suppressing media: (a) in 2.3 mM Mn^{2+}/0.4 mM Ca^{2+} with tetrodotoxin (TTX), kynurenic acid (Kyn) and bicuculline; and (b) in ACSF containing 100 μM Cd^{2+} and TTX and Kyn, as well as 20 μM carbachol (to reduce outward currents further). In both (a) (V_H -75 mV) and (b) (V_H -55 mV), (○) are initial control; (●) currents recorded in Crom (100 μM); and (Δ), Crom difference currents (I_{Dif}).

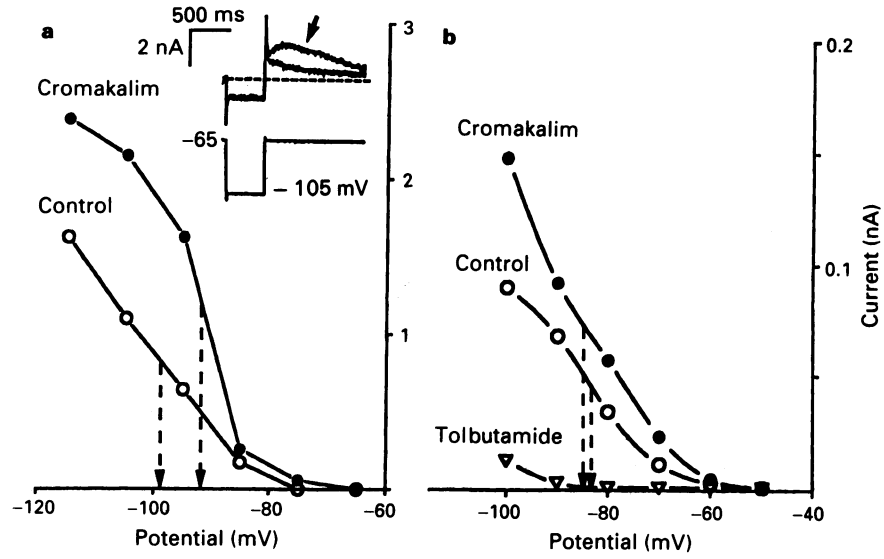


Figure 3 Cromakalim (Crom) enhances a D-like outward current. Two CA1 cells were recorded in presence of tetrodotoxin and kynurenic acid, at V_H − 65 mV (a) and − 50 mV (b). D-like, slowly-inactivating outward currents appeared as rebounds after 0.5 s hyperpolarizing pulses (inset traces in (a) are superimposed responses in control medium and in presence of Crom (arrow)). Steady-state inactivation curves were plotted using data obtained with pulses of various amplitudes before ('control') and during applications of Crom. Dashed vertical lines indicate voltages corresponding to half-observed-peak currents. For cell in (a), control solution also contained 100 μM Cd^{2+} and carbachol (20 μM); and 100 μM Crom was applied in 0.1% DMSO. For cell in (b), 100 μM Crom was in 0.70% ethanol: note that the Crom-potentiated outward current was virtually abolished by 1 mM tolbutamide (▽).

from relatively negative holding potentials ($V_H < -60$ mV), or by large hyperpolarizing pulses from a more positive V_H — after which it appears as a slowly decaying outward current (inset traces in Figure 3a). From such data, steady state inactivation plots can be obtained (Figure 3).

This D-like current was strongly pontentiated by Crom in 10 out of 11 cells. In the presence of Crom (100–200 μM, in most cases from a DMSO stock), the D-like current increased by 88 ± 31.2% ($P<0.025$ for $n=11$). Approximate estimates of half-inactivation potentials showed no significant change (Figure 3) (+ 2.1 ± 1.1 mV, for $n=8$, $P>0.05$) from control values of − 91 ± 4.7 mV. To eliminate a possible involvement of slowly-inactivating Ca-dependent and carbachol-sensitive currents, in four experiments I_D-like currents were recorded in the presence of 100 μM Cd^{2+} and also (in two cases) 20–100 μM carbachol. As is evident in Figure 3a, Crom also enhanced I_D-like current under these more stringent conditions.

In keeping with a recent report that sulphonylureas depress I_D (Crépel *et al.*, 1992) (and as illustrated in Figure 3b) the Crom-enhanced D current was greatly reduced by 1–1.5 mM tolbutamide (by 66 ± 13.2%; $P<0.025$ for $n=6$); though glibenclamide (20–30 μM) was not consistently effective (− 37 ± 20.7%; $P>0.10$ for $n=5$).

Crom effects on currents evoked by voltage ramps

Slow depolarizing ramps (at about 50 mV s^{-1}) were injected into 8 neurones, before and after starting bath-applications of Crom. Typically non-linear, outwardly-rectifying currents were elicited, as illustrated in Figure 4: the linear ramp shown in (a) started from − 90 mV and rose to − 10 mV; it generated the non-linear current trace in (b).

In all 7 cells recorded in regular ACSF, Crom had two main effects: the outward current elicited by the ramp was reduced between ≈ − 50 and − 20 mV, and increased above − 20 mV (Figure 4c). This is seen more easily in Figure 4f where traces (b) and (c) are superimposed; and even better from the difference current (I_{Crom}) in (g), obtained by subtracting trace (b) from trace (c). I_{Crom} was clearly biphasic, turning inward > − 50 mV and then outward > − 30 mV.

All such difference currents showed a zone of reduced outward current (variable in different cells, but mostly within the range − 50 to − 20 mV): thus at V = − 46 ± 3.7 mV, I_{Crom} was consistently inward (− 170 ± 58 pA; for $n=7$, $P<0.05$). But in the 6 cells where the ramps went to a more positive level, the current reversed from inward to outward (Figure 4g and 5d,f): at V = − 18 ± 7.5 mV, I_{Crom} was + 360 ± 127 pA (for $n=6$, $P<0.05$). The addition of Glib (10–20 μM) further depressed the outward current (in the intermediate voltage zone), but had little effect on the net outward I_{Crom} (see Figure 4d and the corresponding difference trace 4h). Tolb caused a steady inward shift in base-line; strongly depressed the total ramp-evoked current, especially at V > − 40 mV; and abolished the outward I_{Crom} (Figure 4e,i).

In two cells recorded in Mn/low Ca medium (and also carbachol in one case), I_{Crom} showed a comparable inward trend but no outward trend at voltages up to + 10 mV.

Comparison of cromakalim- and anoxia-induced changes in membrane properties

In view of previous evidence that Crom and energy-depleting conditions activate a similar current (in cultured hippocampal neurones, Politi & Rogawski, 1991), we compared the currents and conductance changes induced in 12 cells by anoxia and by Crom respectively. Brief anoxia was induced, usually for 2 min by substituting 95% N_2 and 5% CO_2 for carbogen. In these 12 cells, as in the large population reported above, Crom had no consistent effect on G_N (Table 1); whereas anoxia predictably increased G_N, as found by all previous authors (Krnjević, 1993; Haddad & Jiang, 1993). The changes in G_N elicited in individual cells by Crom and by anoxia were not significantly correlated, with regard to their direction ($r=0.486$) and especially their magnitude ($r=0.059$; for both, $P>0.10$).

Although neither Crom nor anoxia generated consistent changes in holding current, the anoxic currents were significantly larger (by 150 ± 60 pA) than the corresponding I_{Crom} (Table 1): also, unlike the latter, the anoxic currents were significantly correlated to V_H (as found previously by Krnjević & Leblond, 1989).

Difference currents were derived from *I/V* data obtained in

the same cell before and during anoxia (10 s before the end of 2 min of anoxia: I_{N2}) or before and during applications of Crom (100–200 μM, for at least 20 min: I_{Crom}). The plots in Figure 5a and b are examples of such difference currents from two cells: I_{N2} (open circles) shows opposite types of rectification, inward for cell (a) and the more usual outward for cell (b); but in both cases I_{N2} reversed near − 80 mV (as is commonly found, Krnjević, 1993). The I_{Crom}'s had no clear reversal potential; they also differed from the corresponding I_{N2}'s: being wholly outward and outwardly rectifying in cell (a); and mainly inward and inwardly rectifying in cell (b). For the second cell, I_{N2} and I_{Crom} were also obtained over a more positive range of V with ramps (Figure 5c and d). I_{Crom} differed from I_{N2} in showing a net inward trend between − 40

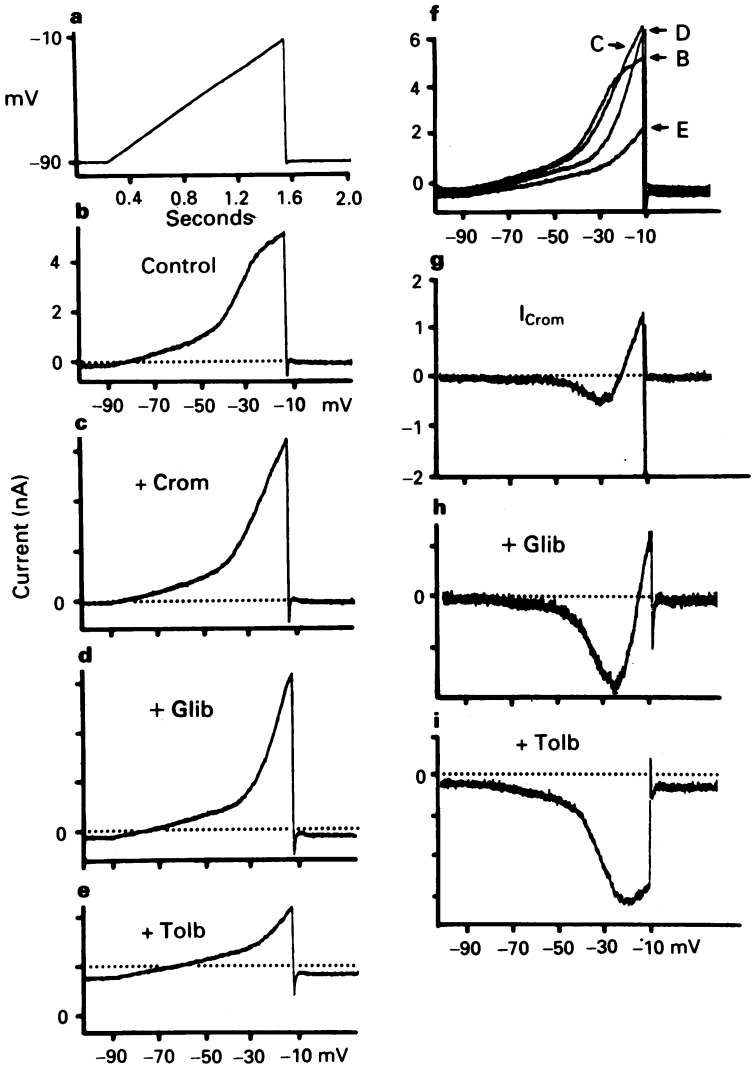


Figure 4 Voltage-dependent effects of cromakalim (Crom) on outward currents evoked by depolarizing voltage ramp. All data were recorded from the same CA1 neurone, in presence of tetrodotoxin, kynurenic acid and bicuculline. Traces (a,b) show the voltage-ramp (from − 90 to ≈ − 10 mV, at ≈50 mV s^{-1}), and the resulting membrane current in control ASCF; (c–e) are the currents elicited by same ramp during subsequent application of Crom (100 μM) (c), after addition of gibenclamide (Glib 20 μM) (d) and then tolbutamide (Tolb, 1 mM) (e). The biphasic effect of Crom (depression of outward current from V < − 20 mV and enhancement > − 20 mV) is shown by the superimposed traces (B) and (C) in (f), and especially by the Crom-control difference current (I_{Crom}) in (g). Glib caused further depression for V < − 20 mV but little change > − 20 mV (f, and (Crom + Glib) − control difference current in h). Tolb produced inward shift in baseline, and strongly depressed outward current over full range of V (f, and (Crom + Glib + Tolb) − control difference current in i).

Table 1 Comparison of effects of anoxia (for 2 min) and bath-applied cromakalim (100 μM) on holding current (I_H) and input conductance (G_H), recorded in same 12 CA1 neurones, at same V_H (− 61 ± 3.5 mV)

	Anoxia	*Cromakalim*	*Anoxia-cromakalim*
Mean I_H change (*pA*)	69.6 (± 62.1)	− 80.0 (± 79.6)	+ 150 (± 60.4)*
Mean G_N change (%)	19.7 (± 5.0) ***	10.0 (± 9.1)	+ 10.6 (± 9.3)
Correlation between V_H and direction of ΔI_H	$r = 0.590$*	$r = 0.353$	

Values are means ± s.e. for $n = 12$
*$P < 0.05$; ***$P < 0.005$.

and − 10 mV. Similarly, I_{Crom} for the third cell (Figure 5f) had a sharp inward component (> − 40 mV) that is wholly lacking in the I_{N2} trace in Figure 5e.

In the presence of Crom, anoxic outward currents became smaller (Figure 6). In 7 cells, the currents diminished by 46 ± 6.8% ($P<0.001$) and the conductance increase by 56 ± 11% ($P<0.005$). Anoxic currents elicited by ramps were also reduced, by 80 ± 12.6% (for $n=4$; $P<0.01$).

Discussion

There is little agreement about the effects of Crom on hippocampal neurones, as reported by different groups, or even the same groups in successive studies. Although we saw no consistent changes in resting membrane properties, in keeping with previous voltage-clamp studies (Alzheimer *et al.*, 1989; Politi *et al.*, 1989), instantaneous rectification was

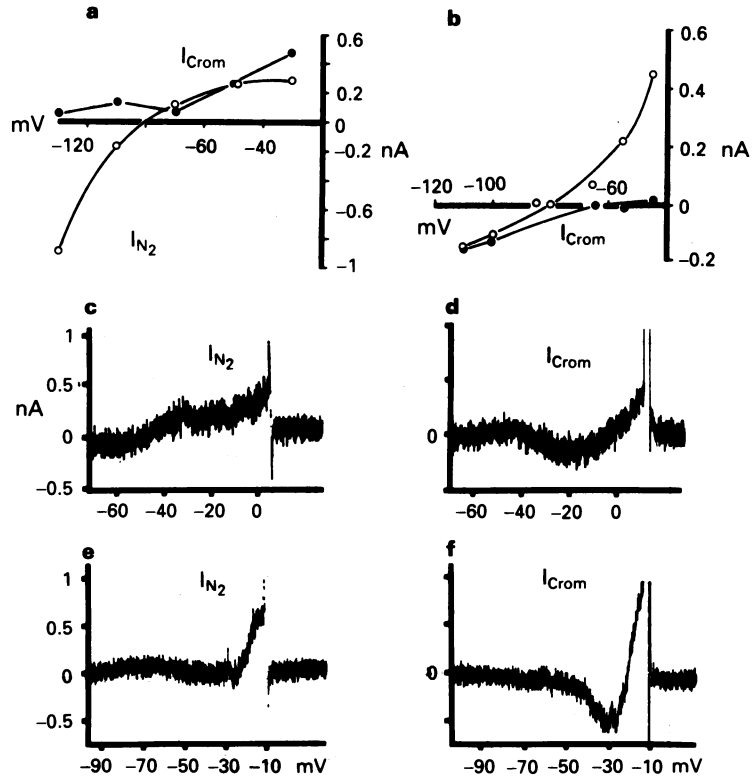


Figure 5 Comparison between anoxic- and cromakalim (Crom) − difference currents (I_{N2} and I_{Crom} respectively) from three CA1 neurones; (a) and (b) were obtained from two cells (in tetrodotoxin (TTX) and kynurenic acid (Kyn)) with brief ± 10 or 20 mV pulses applied at three different V_H's. The difference currents (I_{N2} ○ and I_{Crom} ●) were calculated by subtracting control values from values recorded either near the end of a 2 min period of anoxia or during applications of Crom (for about 20 min). The cell in (b) was also studied with voltage ramps, over a more positive range of V, giving the continuous I_{N2} of (c) and I_{Crom} of (d). Traces in (e) and (f) are I_{N2} and I_{Crom} obtained with comparable ramps from a third cell (in TTX, Kyn and bicuculline).

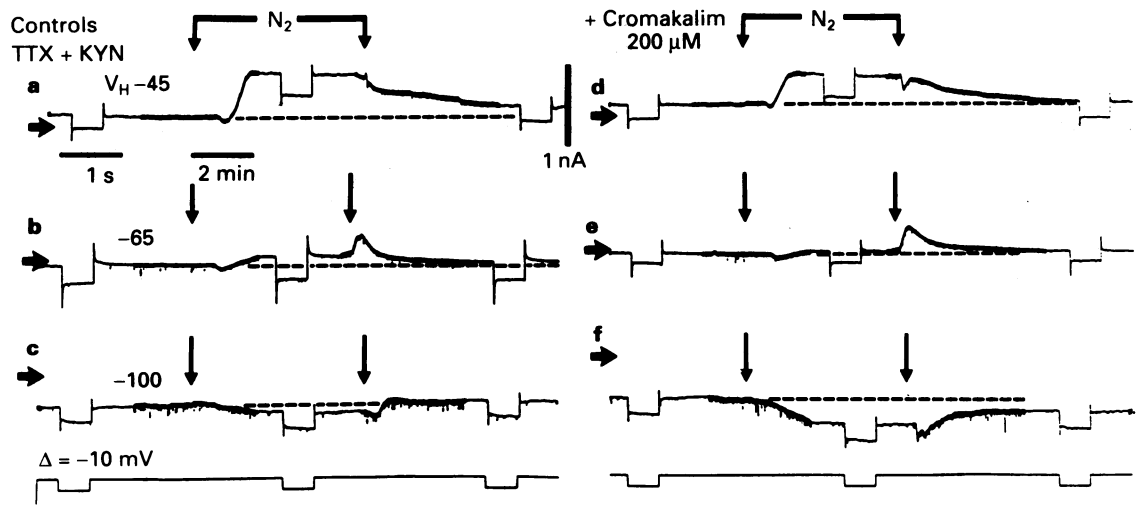


Figure 6 Cromakalim (Crom) depresses outward anoxic current but enhances inward current. Pen recordings were all from same CA1 neurone, in tetrodotoxin (TTX) and kynurenic acid (Kyn). Traces (a–c) are control runs showing effects of 2 min of anoxia (between vertical arrows) observed at V_H's of − 45 (a), − 65 (b) and − 100 mV (c). Note accelerated traces of inward currents evoked by 0.5 s, 10 mV hyperpolarizing pulses (monitored on lowest trace) before anoxia, near peak of anoxic effect, and some min after return of oxygen. Zero current levels are indicated by fat arrows. Traces at right (d–f) are corresponding recordings during Crom application (200 μM), at same V_H's and with similar 2 min anoxic tests.

enhanced in only half of the cells (cf. Alzheimer *et al.*, 1989). Moreover, unlike these authors, who failed to see any suppression of this effect by Tolb, we found Tolb to be a quite potent antagonist. This may be a difference between rat and guinea-pig neurones.

In previous experiments, voltage-dependent outward currents were either unaffected (Alzheimer *et al.*, 1989) or potentiated (Politi *et al.*, 1989; Politi & Rogawski, 1991) by Crom. Our results were mixed: currents elicited by moderate depolarizations (to < -20 mV) were very consistently depressed; larger currents showed both depressions and increases (though in Mn/low Ca solutions increases were very rare).

The simplest explanation for these variable results is that Crom suppresses one type of outward current, but enhances another. In our slices, the Crom-suppressed current appears to predominate for $V < -20$ mV. In guinea-pig slices, if the two currents are about equal in that range of V, Crom would have no effect (as reported by Alzheimer *et al.*, 1989). On the other hand, if only the Crom-potentiated current is present in cultured embryonic cells, only enhancement would be seen (Politi *et al.*, 1989; Politi & Rogawski, 1991). The finding of a GDP-dependent and glibenclamide-sensitive I_{Crom} in hippocampal neurones (Erdemli & Krnjević, 1994a) may explain the observations by Politi & Rogawski (1991) if a comparable (but not GDP-dependent) Crom- and glibenclamide-sensitive current can be elicited in cultured neurones. The use of DMSO and ethanol as vehicles probably contributes another variable. Both solvents produce small but relatively consistent reductions of input conductance, though only ethanol significantly affected (increased) outward currents.

Identity of Crom-suppressed outward current

Because we routinely superfused the slices with TTX and kynurenic acid, the inward I_{Crom} (for $V_H > -30$ mV) cannot be either a voltage-dependent Na- or a glutamate-induced inward current. Nor can it be a Ca-current, being fully evident in Mn low Ca or Cd-containing media. A Cl-inward current would be most prominent at resting (or more negative) V_m: its most likely cause being ongoing GABA-release (and KCl leakage from the microlectrode), it should have been eliminated by bicuculline.

It is therefore reasonable to conclude that Crom indeed suppresses an outward current. Since this effect was regularly observed in Mn and Cd solutions, as well as in the presence of carbachol, the current in question is most like the delayed rectifier (Storm, 1990; Brown *et al.*, 1990). This conclusion is very much in agreement with the finding that diazoxide, another K_{ATP} channel opener, also depresses a delayed rectifier-like outward current (Erdemli & Krnjević, 1993b); as well as preliminary reports that Crom or Crom-analogues inhibit voltage-dependent non-inactivating outward currents in dorsal root ganglia (Owen, 1991) and cultured hippocampal cells (Politi *et al.*, 1993).

Identity of Crom-potentiated outward current

The observation that a D-like current is consistently enhanced by Crom (as well as diazoxide, Erdemli & Krnjević, 1994b) may at least partly account for potentiations of outward current at $V > -30$ mV (seen regularly with ramps). Such enhancement of outward current was less often evident in Mn/low Ca media; which suggests that Crom also potentiates a Ca-dependent K current, as it evidently does in some other types of cells (Nakao *et al.*, 1989; Gelband *et al.*, 1989; Carl *et al.*, 1992).

That a D-like current is enhanced by Crom should not be surprising, because D-currents in CA3 neurones are depressed by sulphonylureas (Crépel *et al.*, 1992). Crom and sulphonylureas have opposite (possibly competitive) actions on K channels of insulin-secreting cells and several kinds of muscle fibres (Cook & Quast, 1990; Kajioka *et al.*, 1991; Edwards & Weston, 1993). In the present experiments, the D-like current was consistently reversed by Tolb but less so by Glib: this may reflect the much lower density of Glib-binding sites in CA1 than CA3 (Mourre *et al.*, 1989; Xia & Haddad, 1991).

Should we therefore conclude that Crom-potentiated currents are classical K_{ATP} currents, as did Politi & Rogawski (1991) regarding the Glib-sensitive outward current potentiated by Crom in cultured cells? Without direct evidence that these channels are ATP-sensitive, it is at least as likely that, at relatively high doses, the sulphonylureas and the channel-openers act on other types of K channels; as shown for some voltage-dependent currents (Reeve *et al.*, 1992; Crépel *et al.*, 1992), as well as the 'non-classical' K_{ATP} current of hypothalamic cells (which is also sensitive to Tolb but not Glib, Ashford *et al.*, 1990,a,b). In hippocampal slices, Tolb especially causes a dramatic reduction of outward current (see Figures 1 and 4; and Godfraind & Krnjević, 1993) that cannot be easily explained by a block of K_{ATP}.

The anticonvulsant action of Crom (Alzheimer & ten Bruggencate, 1988; Gandolfo *et al.*, 1989; Popoli *et al.*, 1991) may thus be mediated by the enhancement of some voltage-dependent outward currents; as well as a possible galanin-like presynaptic action (Ben-Ari, 1990) that might reduce glutamate release.

To recapitulate, of the central neurones studied so far, only some nigral dopaminergic cells have shown the typical actions of Crom: marked hyperpolarization and conductance increase, both antagonized by Glib (Häusser *et al.*, 1991). No remotely comparable effect has been seen in other (non-dopaminergic) nigral cells (Häusser *et al.*, 1991), in hypothalamic neurones (Sellers *et al.*, 1992) or in hippocampal neurones, neither in the previous (Alzheimer & ten Bruggencate, 1988; Politi *et al.*, 1989) nor the present experiments.

Anoxic current and cromakalim

Although I_{Crom} and I_{N2} have some features in common, such as voltage-dependence and outward rectification, the fact that Crom, unlike anoxia, fails to induce a marked conductance increase (at resting V_m), and that I_{Crom} and I_{N2} recorded in individual cells differ sharply argues strongly against a simple identity of these two currents. However, the finding that Crom appears to 'occlude' I_{N2} may indicate some overlap of action, with common activation of certain K channels.

We are grateful to the Medical Research Council of Canada for its financial support; to Dr M. Rogawski (NIH) for several gifts of cromakalim and Hoechst Canada Inc. for a supply of Glyburide (glibenclamide). G.E. was a NATO post-doctoral fellow.

References

ABELE, A.E. & MILLER, R.J. (1990). Potassium channel activators abolish excitotoxicity in cultured hippocampal pyramidal neurons. *Neurosci. Letts.*, **15**, 195–200.

ALLEN, S.L., BOYLE, J.P., CORTIJO, J., FOSTER, R.W., MORGAN, G.P. & SMALL, R.C. (1986). Electrical and mechanical effects of BRL34915 in guinea-pig isolated trachealis. *Br. J. Pharmacol.*, **89**, 395–405.

ALZHEIMER, C. & TEN BRUGGENCATE, G. (1988). Actions of BRL34915 (Cromakalim) upon convulsive discharges in guinea-pig hippocampal slices. *Naunyn-Schmied. Arch. Pharmacol.*, **337**, 429–434.

ALZHEIMER, C. & TEN BRUGGENCATE, G. (1988). Actions of BRL34915 (Cromakalim) upon convulsive discharges in guinea-pig hippocampal slices. *Naunyn-Schmied. Arch. Pharmacol.*, **337**, 429–434.

ALZHEIMER, C., SUTOR, B. & TEN BRUGGENCATE, G. (1989). Effects of cromakalim (BRL34915) on potassium conductances in CA3 neurons of the guinea-pig hippocampus in vitro. *Naunyn-Schmied. Arch. Pharmacol.*, **340**, 465–471.

ASHCROFT, F.M. (1988). Adenosine 5'-triphosphate-sensitive potassium channels. *Annu. Rev. Neurosci.*, **11**, 97–118.

ASHFORD, M.L.J, BODEN, P.R. & TREHERNE, J.M. (1990a). Glucose-induced excitation of hypothalamic neurones is mediated by ATP-sensitive K^+ channels. *Pflügers Arch.*, **415**, 479–483.

ASHFORD, M.L.J., BODEN, P.R. & TREHERNE, J.M. (1990b). Tolbutamide excites rat glucoreceptive ventromedial hypothalamic neurones by indirect inhibition of ATP-K^+ channels. *Br. J. Pharmacol.*, **101**, 531–540.

BEECH, D.J. & BOLTON, T.B. (1989). Properties of the cromakalim-induced potassium conductance in smooth muscle cells isolated from the rabbit portal vein. *Br. J. Pharmacol.*, **98**, 851–864.

BEN-ARI, Y. (1990). Galanine and gibenclamide modulate the anoxic release of glutamate in rat CA3 hippocampal neurons. *Eur. J. Neurosci.*, **2**, 62–68.

BROWN, D.A., GÄHWILER, B.H., GRIFFITH, W.H. & HALLIWELL, J.V. (1990). Membrane currents in hippocampal neurons. *Prog. Brain Res.*, **83**, 141–160.

CARL, A., BOWEN, S., GELBAND, C.H., SANDERS, K.M. & HUME, J.R. (1992). Cromakalim and lemakalim activate Ca^{2+}-dependent K^+ channels in canine colon. *Pflügers Arch.*, **421**, 67–76.

CARLEN, P.L., GUREVICH, N. & DURAND, D. (1982). Ethanol in low doses augments calcium-mediated mechanisms measured intracellularly in hippocampal neurons. *Science*, **215**, 306–309.

CONSTANTI, A. & GALVAN, M. (1983). Fast inward-rectifying current accounts for anomalous rectification in olfactory cortex neurones. *J. Physiol.*, **385**, 153–178.

COOK, N.S. & QUAST, U. (1990). Potassium channel pharmacology. In *Potassium Channels*. ed. Cook, N.S. pp. 181–255. Chichester: Ellis Horwood Limited.

CRÉPEL, V., KRNJEVIĆ, K. & BEN-ARI, Y. (1992). Glibenclamide depresses the slowly inactivating-outward curernt (I_D) in hippocampal neurons. *Can. J. Physiol. Pharmacol.*, **70**, 306–307.

EDWARDS, G. & WESTON, A.H. (1993). The pharmacology of ATP-sensitive potassium channels. *Annu. Rev. Pharmacol. Toxicol.*, **33**, 597–637.

ERDEMLI, G. & KRNJEVIĆ, K. (1993a). Cromakalim actions on membrane currents of CA1 neurons in rat hippocampal slices. *Soc. Neurosci. Abst.*, **19**, 709.

ERDEMLI, G. & KRNJEVIĆ, K. (1993b). Diazoxide suppresses slowly-inactivating outward and inward currents in CA1 hippocampal neurons. *NeuroReport*, **5**, 249–251.

ERDEMLI, G. & KRNJEVIĆ, K. (1994a). Guanosine diphosphate is required for activation of a glyburide, ATP and cromakalim-sensitive outward current in rat hippocampal neurones. *Neuro Report*, **5**, 1362–1364.

ERDEMLI, G. & KRNJEVIĆ, K. (1994b). Effects of diazoxide on CA1 hippocampal neurons in slices. *Abstracts Int. Congress Pharmacol.* (Montreal, July 1994), *Can. J. Physiol. Pharmacol.*, **72**, Suppl. 1, p. 520.

ESCANDE, D., THURINGER, D., LEGUERN, S. & CAVERO, I. (1988). The potassium channel opener cromakalim (BRL34915) activates ATP-dependent K^+ channels in isolated cardiac myocytes. *Biochem. Biophys. Res. Commun.*, **154**, 620–625.

FOSTER, C.D., FUJII, K., KINGDON, J. & BRADING, A.F. (1989). The effect of cromakalim on the smooth muscle of the guinea-pig urinary bladder. *Br. J. Pharmacol.*, **97**, 281–291.

GANDOLFO, G., GOTTESMANN, C., BIDARD, J.-N. & LAZDUNSKI, M. (1989). Subtypes of K^+ channels differentiated by the effect of K^+ channel openers upon K^+ channel blocker-induced seizures. *Brain Res.*, **495**, 189–192.

GELBAND, C.H., LODGE, N.J. & VAN BREEMEN, C. (1989). A Ca^{2+}-activated K^+ channel from rabbit aorta: modulation by cromakalim. *Eur. J. Pharmacol.*, **167**, 201–210.

GODFRAIND, J.M. & KRNJEVIĆ, K. (1993). Tolbutamide suppresses anoxic outward current of hippocampal neurons. *Neurosci. Letts*, **162**, 101–104.

HADDAD, G.G. & JIANG, C. (1993). O_2 deprivation in the central nervous system: on mechanisms of neuronal response, differential sensitivity and injury. *Prog. Neurobiol.*, **40**, 277–318.

HALLIWELL, J.V. & ADAMS, P.R. (1982). Voltage-clamp analysis of muscarinic excitation in hippocampal neurons. *Brain Res.*, **250**, 71–92.

HÄUSSER, M.A., DE WEILLE, J.R. & LAZDUNSKI, M. (1991). Activation by cromakalim of pre- and post-synaptic ATP sensitive K^+ channels in substantia nigra. *Biochem. Biophys. Res. Commun.*, **174**, 909–914.

HICKS, G.A. & HENDERSON, G. (1992). Lack of evidence for coupling of the dopamine D_2 receptor to an adenosine triphosphate-sensitive potassium (ATP-K^+) channel in dopaminergic neurones of the rat substantia nigra. *Neurosci. Letts.*, **141**, 213–217.

KAJIOKA, S., NAKASHIMA, M., KITAMURA, K. & KURIYAMA, H. (1991). Mechanisms of vasodilatation induced by potassium-channel activators. *Clin. Science*, **81**, 129–139.

KRNJEVIĆ, K. (1993). Membrane current activation and inactivation during hypoxia in hippocampal neurons. In *Surviving Hypoxia*. ed. Hochachka, P.W., Lutz, P.L., Sick, T., Rosenthal, M. & van den Thillart, pp. 365–387. Boca Raton, FA. CRC Press.

KRNJEVIĆ, K. & LEBLOND, J. (1989). Changes in membrane currents of hippocampal neurons evoked by brief anoxia. *J. Neurophysiol.*, **62**, 15–30.

MOURRE, C., BEN-ARI, Y., BERNARDI, H., FOSSET, M. & LAZDUNSKI, M. (1989). Antidiabetic sulphonylureas: localization of binding sites in the brain and effects on the hyperpolarization induced by anoxia in hippocampal slices. *Brain Res.*, **486**, 159–164.

NAKAO, K, OKABE, K., KITAMURA, K., KURIYAMA, H. & WESTON, A.H. (1989). Characteristics of cromakalim-induced relaxations in the smooth muscle cells of guinea-pig mesenteric artery and vein. *Br. J. Pharmacol.*, **95**, 795–804.

OSTERRIEDER, W. (1988). Modification of K^+ conductance of heart cell membrane by BRL34915. *Naunyn-Schmied. Arch. Pharmacol.*, **337**, 93–97.

OWEN, D.G. (1991). K^+ channel openers inhibit voltage-activated outward currents in dorsal root ganglion cells. *Soc. Neurosci. Abstr.*, **7**, 778.

POLITI, D.M.T. & ROGAWSKI, M.A. (1991). Glyburide-sensitive K^+ channels in cultured rat hippocampal neurons: activation by cromakalim and energy depleting conditions. *Mol. Pharmacol.*, **40**, 308–315.

POLITI, D.M.T., SUZUKI, S. & ROGAWSKI, M.A. (1989). BRL34915 (cromakalim) enhances voltage-dependent K^+ current in cultured rat hippocampal neurones. *Eur. J. Pharmacol.*, **168**, 7–14.

POLITI, D.M., WERKMAN, T.R. & ROGAWSKI, M.A. (1993). Benzopyran potassium channel openers inhibit voltage-activated outward currents in rat hippocampal neurons. *Soc. Neurosci. Abstr.*, **19**, 708.

POPOLI, P., PEZZOLA, A., SAGRATELLA, S., ZENG, Y.C. & DE CAROLIS, A.S. (1991). Cromakalim (BRL 34915) counteracts the epileptiform activity elicited by diltiazem and verapamil in rats. *Br. J. Pharmacol.*, **104**, 907–913.

REEVE, H.L., VAUGHAN, P.F.T. & PEERS, C. (1992). Glibenclamide inhibits a voltage-gated K current in the human neuroblastoma cell line SH-SY5Y. *Neurosci. Letts.*, **135**, 37–40.

RORSMAN, P. & TRUBE, G. (1990). Biophysics and physiology of ATP-regulated K^+ channels (K_{ATP}). In *Potassium Channels*. ed. Cook, N.S. pp. 96–116. Chichester: Ellis Horwood Ltd.

SELLERS, A.J., BODEN, P.R. & ASHFORD, M.L.J. (1992). Lack of effect of potassium channel openers on ATP-modulated potassium channels recorded from rat ventromedial hypothalamic neurones. *Br. J. Pharmacol.*, **107**, 1068–1074.

SPRUCE, A.E., STANDEN, N.B. & STANFIELD, P.R. (1987). Studies of the unitary properties of adenosine 5'-triphosphate-regulated potassium channels of frog skeletal muscle. *J. Physiol.*, **382**, 213–236.

SPULER, A., LEHMANN-HORN, F. & GRAFE, P. (1989). Cromakalim (BRL 34915) restores in vitro the membrane potential of depolarized human skeletal muscle fibres. *Naunyn-Schmied. Arch. Pharmacol.*, **339**, 327–331.

STORM, J.F. (1988). Temporal integration by a slowly inactivating K^+ current in hippocampal neurons. *Nature*, **336**, 379–381.

STORM, J.F. (1990). Potassium currents in hippocampal pyramidal cells. *Prog. Brain Res.*, **83**, 161–187.

WEINER, J.L., ZHANG, L. & CARLEN, P.L. (1992). Novel ethanol enhancement of the delayed rectifier potassium current in rat hippocampal CA1 neurons. *Soc. Neurosci. Abstr.*, **18**, 1501.

XIA, Y. & HADDAD, G.G. (1991). Major differences in CNS sulfonylurea receptor distribution between the rat (newborn, adult) and turtle. *J. Comp. Neurol.*, **314**, 278–289.

ZHANG, L., WEINER, J.L. & CARLEN, P.L. (1992). Muscarinic potentation of I_K in hippocampal neurons: electrophysiological characterization of the signal transduction pathway. *J. Neurosci.*, **12**, 4510–4520.

(Received February 14, 1994
Revised May 18, 1994
Accepted June 8, 1994)

Br. J. Pharmacol. (1994), 113, 419-424 © Macmillan Press Ltd, 1994

Relaxation of human isolated mesenteric arteries by vasopressin and desmopressin

M.C. Martínez, J.M. Vila, M. Aldasoro, P. Medina, *B. Flor & [1]S. Lluch

Departamento de Fisiología and *Departamento de Cirugía, Universidad de Valencia, 46010 Valencia, Spain

1 The effects of vasopressin and deamino-8-D-arginine vasopressin (DDAVP, desmopressin) were studied in artery rings (0.8-1 mm in external diameter) obtained from portions of human omentum during the course of abdominal operations (27 patients).

2 In arterial rings under resting tension, vasopressin produced concentration-dependent, endothelium-independent contractions with an EC_{50} of 0.59 ± 0.12 nM. The V_1 antagonist $d(CH_2)_5$Tyr(Me)AVP (1 μM) and the mixed V_1-V_2 antagonist desGly-$d(CH_2)_5$D-Tyr(Et)ValAVP (0.01 μM) displaced the control curve to vasopressin to the right in a parallel manner without differences in the maximal responses. In the presence of indomethacin (1 μM) the contractile response to vasopressin was significantly increased ($P<0.01$).

3 In precontracted arterial rings, previously treated with the V_1 antagonist, $d(CH_2)_5$Tyr(Me)AVP (1 μM), vasopressin produced endothelium-dependent relaxation. This relaxation was reduced significantly ($P<0.05$) by indomethacin (1 μM) and unaffected by the V_1-V_2 receptor antagonist desGly-$d(CH_2)_5$D-Tyr(Et)ValAVP (1 μM) or by N^G-nitro-L-arginine methyl ester (L-NAME, 0.1 mM).

4 The selective V_2 receptor agonist, DDAVP, caused endothelium-independent, concentration-dependent relaxations in precontracted arterial rings that were inhibited by the mixed V_1-V_2 receptor antagonist, but not by the V_1 receptor antagonist or by pretreatment with indomethacin or L-NAME.

5 Results from this study suggest that vasopressin is primarily a constrictor of human mesenteric arteries by V_1 receptor stimulation; vasopressin causes dilatation only during V_1 receptor blockade. The relaxation appears to be mediated by the release of vasodilator prostaglandins from the endothelial cell layer and is independent of V_2 receptor stimulation or release of nitric oxide. In contrast, the relaxation induced by DDAVP is largely dependent on stimulation of V_2 receptors.

Keywords: Human mesenteric artery; vasopressin receptors; endothelium; nitric oxide

Introduction

Vasopressin acts directly on vascular smooth muscle to produce vasoconstriction through V_1-receptor activation and promotes reabsorption of water in renal tubular cells through V_2 receptors coupled to adenylate cyclase activation (Michell *et al.*, 1979; Penit *et al.*, 1983). In addition it has been reported that vasopressin induces the release of adrenocorticotrophin through stimulation of V_3 (or V_{1b}) receptors located in the adenohypophysis (Jard *et al.*, 1986).

Further studies of the physiological effects of vasopressin have suggested the existence of V_2 receptors in some vascular beds that could mediate vasodilatation. Administration of either V_2 agonists or vasopressin during V_1 receptor blockade increased blood flow in some vascular beds and decreased peripheral vascular resistance in both man and dogs (Liard & Spadone, 1984; Bichet *et al.*, 1988). In dogs, the mixed V_1-V_2 receptor antagonist $d(CH_2)_5$-D-Tyr(Et)VAVP inhibited the increase in cardiac output and fall in total peripheral resistance induced by the V_2 agonist, 4-valine, 8-D-arginine vasopressin (VDAVP) whereas the V_1 antagonist, $d(CH_2)_5$ Tyr(Me)AVP did not affect these haemodynamic responses (Liard, 1986). Since these effects persisted in anephric dogs (Liard, 1988) it was postulated that V_2-like receptors exist in peripheral vessels. Furthermore, infusion of the V_2 agonist, deamino-8-D-arginine vasopressin (DDAVP, desmopressin) increased plasma adenosine 3':5'-cyclic monophosphate (cyclic AMP) concentration in normal subjects (Bichet *et al.*, 1989) and dogs (Liard, 1992) but a selective V_1 agonist did not. The increase in plasma cyclic AMP levels was prevented by pretreatment with a mixed V_1-V_2 receptor antagonist but was not affected by bilateral nephrectomy. These results suggest that V_2 receptors responsible for the increase in cyclic AMP are extrarenal (Liard, 1992).

Vasopressin produces constriction of isolated mesenteric arteries of the rat (Randall *et al.*, 1988), rabbit and guinea-pig (Vanner *et al.*, 1990). In the human mesenteric arterial bed, vasopressin causes powerful V_1-mediated constriction in isolated mesenteric arteries (Ohlstein & Berkowitz, 1986) and in submucosal arterioles of the intestinal microcirculation (Vanner *et al.*, 1990). However, the possibility that vasopressin and DDAVP cause dilatation in human isolated blood vessels has not been defined. Accordingly, the present investigation was designed to determine directly the *in vitro* vascular response to vasopressin and DDAVP in human mesenteric arteries. Observations were made in the presence and absence of endothelium as well as with selective vasopressin receptor antagonists and inhibitors of cyclo-oxygenase.

Methods

Arterial segments were taken from portions of human omentum during the course of abdominal operations (27 patients, 11 men and 16 women, aged 32-61 years). The arteries were immediately placed in chilled Krebs-Henseleit solution, and rings 3 mm long were cut for isometric recording of tension. The outside diameter of the rings was measured with an ocular micrometer within a Wild M8 zoom microscope (Heerbrugg, Switzerland) and ranged from 0.8 to 1 mm. In approximately 50% of the artery rings the endothelium was removed mechanically by inserting a roughened stainless-steel wire into the lumen and gently rolling the rings on wet filter paper.

[1] Author for correspondence at: Departamento de Fisiología, Facultad de Medicina, Blasco Ibáñez, 17, 46010 Valencia, Spain.

Two stainless steel pins 100 μm in diameter were introduced through the arterial lumen of the ring. One pin was fixed to the wall of the organ bath, while the other was connected to a force-displacement transducer (Grass FT03). Changes in isometric force were recorded on a Grass polygraph (model 7). Each artery ring was set up in a 4 ml bath containing modified Krebs-Henseleit solution of the following composition (mM): NaCl 115, KCl 4.6, $MgCl_2.6H_2O$ 1.2, $CaCl_2$ 2.5, $NaHCO_3$ 25, glucose 1.1 and disodium EDTA 0.01. The solution was equilibrated with 95% O_2 and 5% CO_2 to give a pH of 7.3–7.4. Temperature was held at 37°C. To establish the resting tension for maximal force development, a series of preliminary experiments were performed on rubbed and unrubbed artery rings of similar length and outer diameter which were exposed repeatedly to 60 mM KCl. Basal tension was increased gradually until contractions were maximal. The optimal resting tension was 1 g. The artery rings were allowed to attain a steady level of tension during a 2-h accommodation period before testing. The contractile response to 60 mM KCl was similar in rubbed and unrubbed artery rings (2429 ± 172 versus 2534 ± 265 mg, $P > 0.05$). To study relaxation, artery rings were precontracted with 1–3 μM noradrenaline which gave a contraction ranging from 50 to 70% of contractions produced by 60 mM KCl.

Functional integrity of the endothelium was confirmed routinely by the presence or absence of relaxation induced by acetylcholine (0.1–1 μM) during contraction obtained with noradrenaline (1–3 μM). After each experiment the artery rings were carefully opened flat and stained with $AgNO_3$ to visualize the endothelium. Only results from rings with more than 70% of the endothelium were considered as control rings. Vessels in which the endothelium had been rubbed never showed more than 5% of their intima covered with endothelium.

Concentration-response curves for vasopressin were determined in a cumulative manner and control (in the absence of antagonists) and experimental (in the presence of antagonists) responses were obtained from separate vascular preparations. Vasopressin was applied in cumulative concentrations because preliminary experiments showed that noncumulative additions of vasopressin in these preparations produced similar effects than when vasopressin was applied in a cumulative fashion.

Following the equilibration period, concentration-response curves for vasopressin (0.01 nM–0.1 μM) were obtained in paired rings under resting tension in the absence and presence of either the V_1 antagonist $d(CH_2)_5$Tyr(Me)AVP (0.01 and 1 μM), the V_1–V_2 vasopressin antagonist, desGly-$d(CH_2)_5$D-Tyr(Et)ValAVP (0.01 μM) or indomethacin (1 μM). To check the possibility that DDAVP is an antagonist of the V_1 receptor-mediated contraction, the effects of vasopressin were evaluated in the presence of 0.1 μM DDAVP.

To study vasopressin-induced relaxation, rings were incubated with the V_1 receptor antagonist $d(CH_2)_5$Tyr(Me)AVP and then contracted with 1–3 μM noradrenaline. After a stable contraction was obtained, concentration-response curves to vasopressin were determined in paired rings in the absence and presence of either the V_1–V_2 receptor antagonist desGly-$d(CH_2)_5$D-Tyr(Et)ValAVP (1 μM), indomethacin (1 μM) or L-NAME (0.1 mM). Concentration-response curves to the V_2 agonist DDAVP (0.01 μM–0.1 μM) were also determined from a group of precontracted rings in the absence and in the presence of either the V_1 antagonist, the mixed V_1–V_2 antagonist or indomethacin. As a control for each experimental group, at least 12 artery rings were contracted in a similar way to that described above and left untreated (without DDAVP or vasopressin addition to the bath). In these artery rings less than 10% variability in tension below or above the elevated tension was observed throughout the experiment.

Antagonists were added to the organ bath chambers 15 min before the initiation of cumulative concentration-response curves to agonists. Only one concentration-response curve to vasopressin or DDAVP was obtained in each artery ring.

Drugs

The following drugs were used: noradrenaline hydrochloride, acetylcholine chloride, indomethacin, N^G-nitro-L-arginine methyl ester hydrochloride (L-NAME), arginine vasopressin acetate salt, deamino-Cys D-arginine vasopressin acetate salt (DDAVP, desmopressin), $d(CH_2)_5$Tyr(Me)AVP [(1-(β-mercapto-β,β-cyclopentamethylenepropionic acid) 2-(O-methyl)-tyrosine, 8-arginine) vasopressin], desGly-$d(CH_2)_5$D-Tyr(Et) ValAVP [(1- (β-mercapto-β, β-cyclopentamethylenepropionic acid) 2-(O-ethyl)-D-tyrosine, 4-valine, 8-arginine, 9-desglycine) vasopressin], and sodium nitroprusside dihydrate (Sigma Chemical Co, St. Louis, MO, U.S.A.).

Drugs were prepared and diluted in distilled water except for indomethacin which was dissolved in absolute ethanol and sodium bicarbonate solution (150 mM) and readjusted to pH of 7.4 with HCl prior to use. Stock solutions of the drugs were freshly prepared every day.

Data analysis

EC_{50} values (concentrations of vasopressin producing half-maximal contractions) were determined from individual concentration-response curves by non-linear regression analysis, and from these values the geometric means were calculated. Relaxation was expressed as a percentage of the noradrenaline-induced contraction. All values are expressed as mean ± s.e.mean. In each experimental group n indicates the number of patients. At least 8 artery rings were obtained from each patient. Differences between agonist and antagonist-treated groups were assessed by one-way analysis of variance (ANOVA). Differences between means were identified by t test. Statistical significance was accepted at $P < 0.05$.

Results

Effects of vasopressin in artery rings under resting tension

Vasopressin (0.01 nM–0.1 μM) caused concentration-dependent contractions with an EC_{50} of 0.59 ± 0.12 nM. These contractions were endothelium-independent (Figure 1a). The presence of the V_1 antagonist, ($d(CH_2)_5$Tyr(Me)AVP, 0.01 μM), in the organ bath displaced the control curve for vasopressin 9 fold ($P < 0.05$) to the right in a parallel manner, but differences in the maximal tensions developed were not significant ($P > 0.05$). Increasing the concentration of $d(CH_2)_5$Tyr(Me)AVP to 1 μM further displaced (1525 fold; $P < 0.01$) the control curve for vasopressin (Figure 1a).

Arteries with and without endothelium exposed to 1 μM indomethacin did not show significant changes in resting tension as compared to arteries incubated in Krebs-Henseleit solution. However, the presence of indomethacin increased significantly ($P < 0.01$) both the maximal tension developed and the sensitivity to vasopressin (EC_{50}: 0.14 ± 0.05 nM) of artery rings with and without endothelium (Figure 1b). The mixed V_1–V_2 receptor antagonist desGly-$d(CH_2)_5$D-Tyr(Et) ValAVP (0.01 μM) was also evaluated for its ability to antagonize vasopressin-induced contractions. This compound displaced the control curve for vasopressin 25 fold to the right ($P < 0.05$) in a parallel manner without differences in the maximal response. The presence of the V_2 agonist DDAVP (0.1 μM) did not affect the contractile responses to vasopressin (Figure 1b).

The specificity of the inhibitory effect of $d(CH_2)_5$Tyr (Me)AVP (1 μM) and desGly-$d(CH_2)_5$D-Tyr(Et)ValAVP (0.01 μM) on contractile responses was also studied in artery rings challenged with increasing concentrations of potassium chloride ($n = 3$) or noradrenaline ($n = 3$). The results showed that

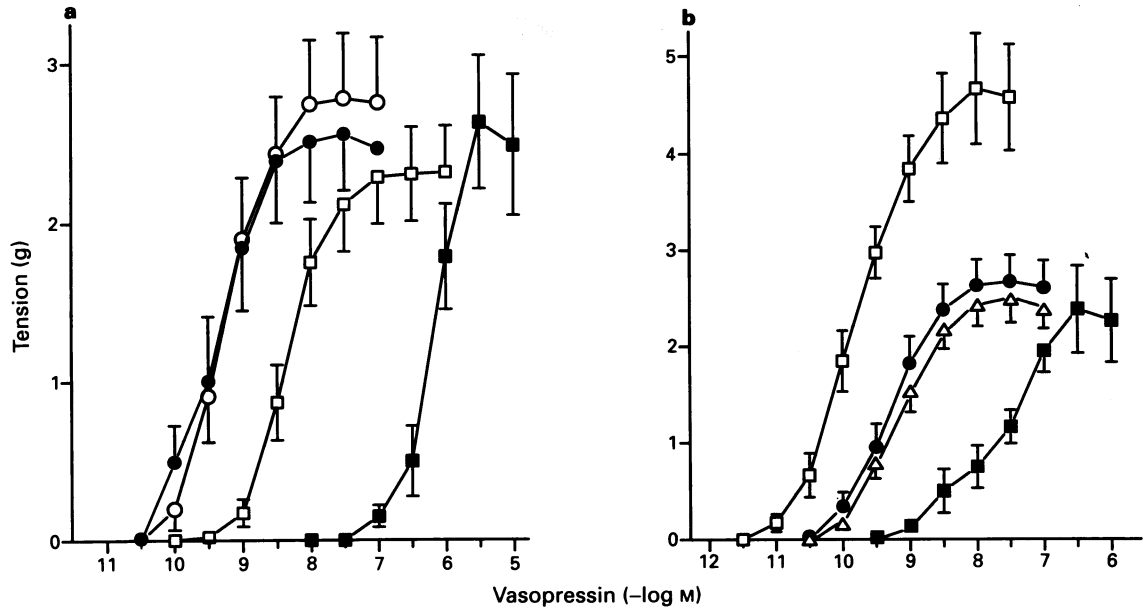


Figure 1 Concentration-response curves for vasopressin determined in human mesenteric arterial rings. (a) Contractile effects of vasopressin in arterial rings with (●) ($n = 5$) and without (○) ($n = 4$) endothelium and in the presence of the V_1 antagonist $d(CH_2)_5Tyr(Me)AVP$ (□, 0.01 μM; ■, 1 μM) ($n = 5$). (b) Responses to vasopressin in the absence (●) ($n = 5$) and presence of indomethacin (□) (1 μM) ($n = 4$), the mixed V_1–V_2 antagonist desGly-$d(CH_2)_5$D-Tyr(Et)ValAVP (■) (0.01 μM) ($n = 4$) or the V_2 agonist DDAVP (△) (0.1 μM) ($n = 4$). Values are means ± s.e.mean.

contractions induced by these agents were not significantly different in the presence of the V_1 or the mixed V_1–V_2 antagonist.

Effects of vasopressin in precontracted artery rings

To determine whether vasopressin induces relaxation in precontracted arteries, increasing concentrations of this peptide were added to rings during submaximal contraction induced by noradrenaline (1–3 μM). Figure 2 shows that vasopressin caused further contractions in precontracted arteries with and without endothelium. In these rings the ability of the smooth muscle to relax was tested by adding 0.1 mM sodium nitroprusside when the maximal contractions had been attained with vasopressin. Under these conditions sodium nitroprusside caused almost complete relaxation of both normal and endothelium-denuded rings.

In artery rings pretreated with the V_1 receptor antagonist ($d(CH_2)_5Tyr(Me)AVP$, 1 μM) and precontracted with noradrenaline (1–3 μM), vasopressin (0.01 nM–0.03 μM) produced concentration-dependent relaxations which were greater ($P < 0.05$) in arteries with endothelium than in endothelium-denuded rings (Figure 3a). At higher concentrations of vasopressin, relaxations changed to contraction, most probably produced by a displacement of the V_1 receptor antagonist from the V_1 receptors.

The mixed V_1–V_2 receptor antagonist desGly-$d(CH_2)_5$D-Tyr(Et)ValAVP (1 μM) was without effect on vasopressin-induced relaxation (Figure 3a). However, the presence of indomethacin (1 μM) reduced significantly ($P < 0.05$) the relaxation induced by vasopressin (Figure 3b). On the other hand, L-NAME (0.1 mM) treatment had no effect on vasopressin-induced relaxation. The same concentration of L-NAME abolished completely the relaxations to acetylcholine (0.1–3 μM) in artery rings with endothelium.

Effects of DDAVP

The selective antidiuretic agonist, DDAVP (0.01 nM–01. μM) did not produce significant changes in the resting tension of mesenteric arteries with ($n = 4$) or without ($n = 4$) endothelium (results not shown). In arteries contracted with

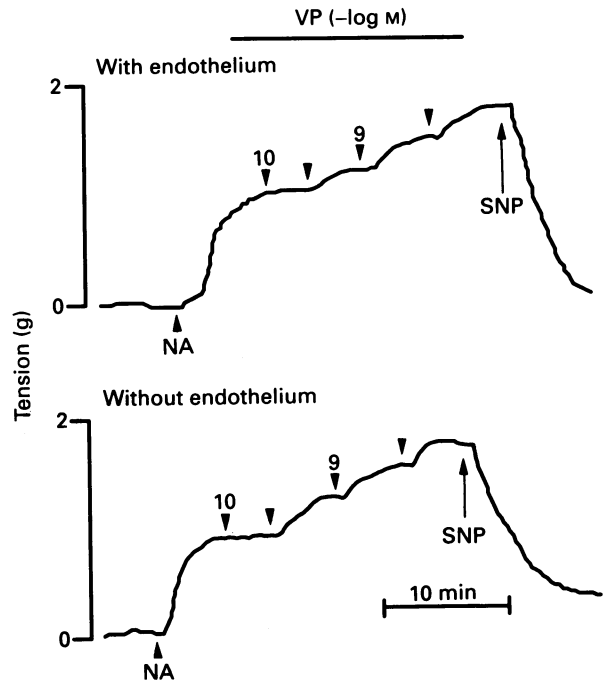


Figure 2 Contractile effects of vasopressin (VP) in arterial rings with and without endothelium precontracted with noradrenaline (NA, 3 μM). Sodium nitroprusside (SNP, 0.1 mM) caused almost complete relaxation of arterial rings.

noradrenaline (1–3 μM), DDAVP caused concentration-dependent relaxations which were similar in the presence and in the absence of endothelium (Figure 4a). Indomethacin (1 μM) did not modify the relaxations induced by DDAVP.

The specific V_1 receptor antagonist ($d(CH_2)_5Tyr(Me)AVP$, 1 μM) did not have a significant effect on DDAVP-induced relaxations (Figure 4b). In contrast, the V_1–V_2 receptor antagonist (desGly-$d(CH_2)_5$D-Tyr(Et)ValAVP, 1 μM) was a

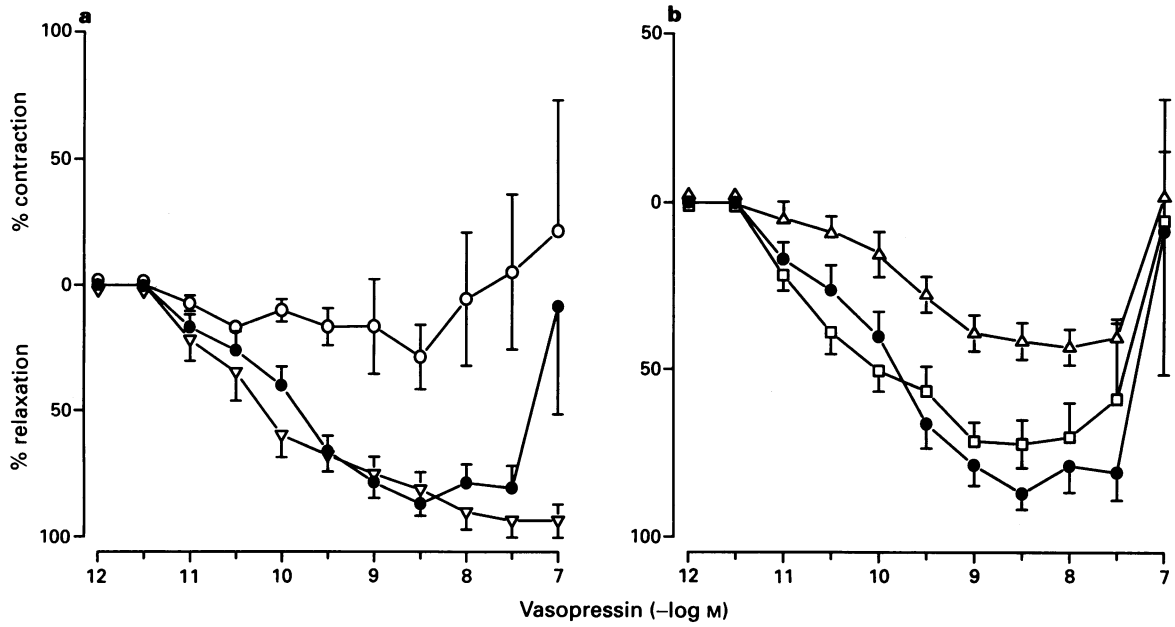


Figure 3 Relaxation to vasopressin of arterial rings treated with the antagonist d(CH_2)$_5$Tyr(Me)AVP (1 μM) and precontracted with noradrenaline (1–3 μM). (a) Concentration-response curves in the presence (●) ($n = 4$) and absence (○) ($n = 4$) of endothelium and in the presence of the V_1–V_2 antagonist desGly-d(CH_2)$_5$D-Tyr(Et)ValAVP (▽) (1 μM) ($n = 4$). (b) Relaxation to vasopressin in the absence (●) and presence of indomethacin (△) (1 μM) ($n = 4$) or N^G-nitro-L-arginine methyl ester (□) (0.1 mM). Values are means ± s.e.mean.

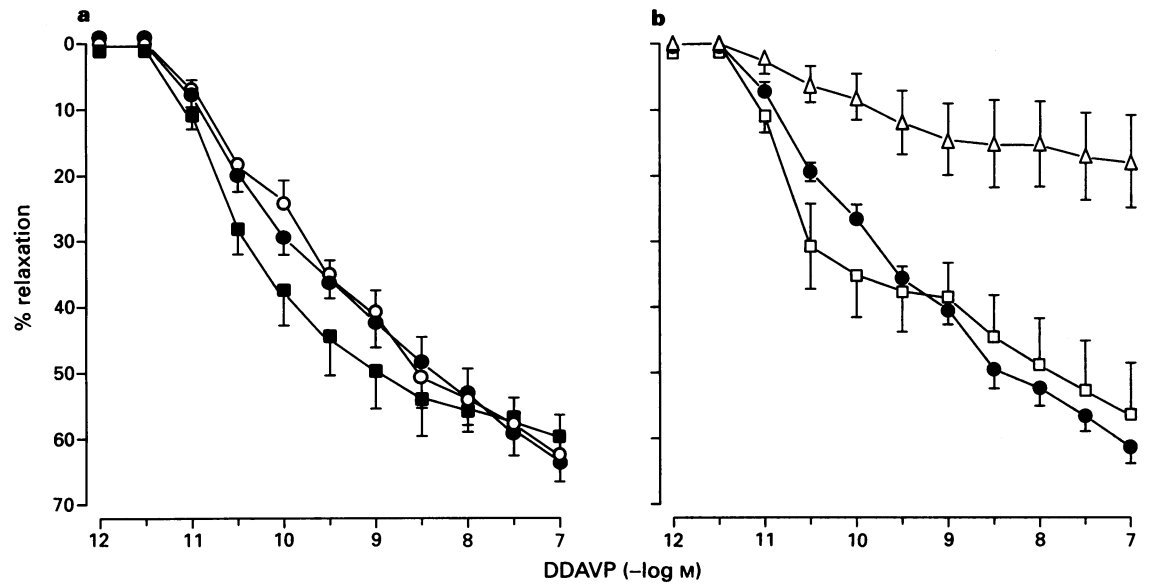


Figure 4 Relaxation to deamino-8-D-arginine vasopressin (DDAVP) of arterial rings precontracted with noradrenaline. (a) Responses to DDAVP in the presence (●) ($n = 4$) and absence (○) ($n = 4$) of endothelium and in the presence of indomethacin (■) (1 μM) ($n = 4$); (b) responses to DDAVP in the absence (●) ($n = 4$) and presence of the V_1–V_2 antagonist, desGly-d(CH_2)$_5$D-Tyr(Et)ValAVP (△) (1 μM) ($n = 4$) or V_1 antagonist d(CH_2)$_5$Tyr(Me)AVP (□) (1 μM) ($n = 4$). Values are means ± s.e.mean.

potent antagonist of DDAVP-mediated relaxation ($P < 0.05$). This antagonist did not affect the relaxations induced by acetylcholine (0.1–3 μM) or sodium nitroprusside (0.01–1 μM).

Discussion

The results of this study confirm previous reports showing that vasopressin is primarily a constrictor of human vascular smooth muscle due to V_1 vasopressin receptor stimulation (Lluch *et al.*, 1984; Ohlstein & Berkowitz, 1986; Martín de Aguilera *et al.*, 1990). Our data also show that the vasopressin-induced contraction is not linked to the presence of an intact endothelium, thus indicating that vasodilator substances secreted by endothelial cells under basal, spontaneous conditions (Martin *et al.*, 1986) do not counteract the effects of vasopressin on smooth muscle cells.

The present investigation demonstrates that vasopressin elicits concentration-dependent relaxation in contracted human mesenteric arteries only during V_1 receptor blockade. Our results also show that DDAVP, a highly specific antidiuretic V_2 receptor agonist (Manning & Sawyer, 1985), induced similar concentration-dependent relaxation to that

observed in response to the combination of vasopressin plus the vasoconstrictor antagonist. In contrast to the results described here, no evidence for the presence of V_2 receptor-mediated dilatation was obtained after application of vasopressin or DDAVP to isolated submucosal arterioles of the intestinal circulation of guinea-pigs, rabbits and humans (Vanner *et al.*, 1990). In addition to regional differences, it is possible that the size of the vessels used may be a factor in the response to DDAVP, as previously reported for vasopressin (Altura, 1975; Takayasu *et al.*, 1993).

In man, vasopressin causes direct, dose-dependent vasodilatation in the forearm, an effect which is augmented by the presence of V_1 receptor blockade (Hirsch *et al.*, 1989). Since infusion of DDAVP induced similar dose-dependent forearm vasodilatation to that observed in response to vasopressin, it was suggested that V_2 receptors were responsible for mediating these effects (Hirsch *et al.*, 1989). The link between V_2 receptor stimulation and cardiovascular effects was reported by Liard (1986) in conscious dogs showing that the V_1-V_2 antagonist d(CH_2)$_5$-D-Tyr(Et)VAVP prevented the increase in cardiac output and fall in total peripheral resistance induced by a specific V_2 agonist. More recent experiments in dogs (Liard, 1994) suggest that V_2 receptor stimulation may trigger the release of nitric oxide since L-NAME, an inhibitor of nitric oxide synthase, attenuates the peripheral vasodilatation induced by injections of DDAVP.

Until now the possibility that vasopressin and DDAVP may dilate mesenteric vessels through V_2 receptors has not been investigated. Efforts to develop a specific V_2 antagonist have been unsuccessful (for review see László *et al.*, 1991). In this respect, all V_2 antagonists have a V_1 antagonistic effect as well (Sawyer & Manning, 1985). We used the mixed V_1-V_2 vasopressin antagonist desGly-d(CH_2)$_5$D-Tyr(Et)Val AVP because it appears to be the most potent *in vitro* antagonist of human vasopressin-stimulated renal adenylate cyclase (Stassen *et al.*, 1984). It also antagonizes exogenous vasopressin-stimulated antidiuresis in conscious water-loaded rats (Kinter *et al.*, 1986). From a theoretical point of view, this analogue would be a highly potent specific vascular V_2 receptor antagonist. In the present experiments the mixed V_1-V_2 antagonist desGly-d(CH_2)$_5$D-Tyr(Et)ValAVP prevented the relaxation induced by DDAVP, whereas the V_1 antagonist d(CH_2)$_5$Tyr(Me)AVP did not. These results suggest that the relaxation observed in response to DDAVP is mediated by a receptor similar to the renal V_2 receptor, a finding similar to that previously reported in dogs (Liard, 1986; 1988). In addition, because indomethacin treatment had little effect on DDAVP-induced relaxation, it is suggested that DDAVP-stimulated vasodilator prostaglandins synthesis under these experimental conditions seems unlikely. This interpretation is in agreement with results from human studies showing that indomethacin treatment did not influence the DDAVP-induced decrease in arterial blood pressure (Hasunuma *et al.*, 1991).

In contrast, the V_1-V_2 antagonist desGly-d(CH_2)$_5$D-Tyr (Et)ValAVP did not show a significant effect on vasopressin-induced relaxation. Therefore it seems unlikely that the relaxant action of vasopressin is mediated by classical V_2 receptors. The reasons for this unexpected finding are not presently known. The V_1-V_2 antagonist desGly-d(CH_2)$_5$D-Tyr(Et)Val AVP exerts potent antagonistic effects on vascular contraction mediated through V_1 receptors. Consequently, it is not established at present what effects might result from the blockade of V_1 receptors. Before we can rule out the intervention of V_2 receptors in the vasopressin-induced relaxation it would seem necessary to design V_2 antagonists that would not block the V_1 receptors. On the other hand, the effects of vasopressin could be indirect, resulting from the release of mediator(s) inducing dilatation. Among the potential nonreceptor mechanisms that could account for the dilatation in response to vasopressin, we have taken into consideration the possible intervention of the endothelial cell layer and the release of prostaglandins.

The vasopressin-induced dilatation after V_1 receptor blockade depends on the presence of an intact endothelium since it was absent in arteries denuded of endothelium. However, this endothelium-dependent relaxation does not involve the intervention of the L-arginine-nitric oxide pathway since L-NAME, a selective inhibitor of nitric oxide synthase, did not inhibit the vasopressin-induced relaxation. Since vasopressin stimulates the synthesis of prostaglandin I_2 by blood vessels (Hassid & Williams, 1983) it might be expected that cyclooxygenase inhibitors can modulate the responses to vasopressin. Our results show that indomethacin inhibits the relaxant effects of vasopressin. This strongly suggests that the effect is largely due to the release of vasodilator prostaglandins from the endothelial cell layer. On the other hand, indomethacin potentiates the vasopressin-induced contraction in arteries with or without endothelium, thus suggesting that relaxant prostaglandins, derived mainly from smooth muscle cells, attenuate the V_1-mediated contractile effect of vasopressin.

We may conclude that the vasopressin receptor mediating contraction in human mesenteric arteries are of the V_1 type. A similar conclusion has been drawn from results obtained in isolated segments of human cerebral arteries (Martín de Aguilera *et al.*, 1990). In view of the specificity and potency of the V_1 antagonist d(CH_2)$_5$Tyr(Me)AVP, it seems appropriate to consider the use of blockade of V_1 receptors in those pathophysiological states characterized by an increased plasma vasopressin level. The physiological significance of the dilatation induced by vasopressin is not readily apparent because of the requirement of the V_1 blockade. Yet these effects may act to counterbalance V_1-mediated vasoconstriction.

In summary, our study shows that vasopressin and DDAVP dilate human mesenteric vessels through different mechanisms. The vasopressin-induced relaxation requires previous blockade of V_1 receptors, appears to be mediated by the release of relaxant prostaglandins and is independent of V_2 receptor stimulation or nitric oxide formation. The effect of DDAVP is largely dependent on stimulation of V_2 receptors predominantly located on smooth muscle cells.

This study was supported by grants from the Ministerio de Sanidad and Dirección General de Investigación Científica y Técnica.

References

ALTURA, B.M. (1975). Dose-response relationships for arginine vasopressin and synthetic analogs on three types of rat blood vessels: Possible evidence for regional differences in vasopressin receptor sites within a mammal. *J. Pharmacol. Exp. Ther.*, **193**, 413–423.

BICHET, D.G., RAZI, M., ARTHUS, M.F., LONERGAN, M., TITTLEY, P., SMILEY, R.K., ROCK, G. & HIRSCH, D.J. (1989). Epinephrine and dDAVP administration in patients with congenital nephrogenic diabetes insipidus. Evidence for a pre-cyclic AMP V_2 receptor defective mechanism. *Kidney Int.*, **36**, 859–866.

BICHET, D.G., RAZI, M., LONERGAN, M., ARTHUS, M.F., PAPUKNA, V., KORTAS, C. & BARJON, J.N. (1988). Hemodynamic and coagulation responses to 1-desamino 8-D-arginine vasopressin in patients with congenital nephrogenic diabetes insipidus. *N. Engl. J. Med.*, **18**, 881–887.

HASSID, A. & WILLIAMS, C. (1983). Vasoconstrictor-evoked prostaglandin synthesis in cultured vascular smooth muscle. *Am. J. Physiol.*, **245**, C278–C282.

HASUNUMA, K., YAMADA, K., TAMURA, Y. & YOSHIDA, S. (1991). Cardiovascular and renin responses to desmopressin in humans: role of prostacyclin and beta-adrenergic systems. *Am. J. Physiol.*, **260,** H1031–H1036.

HIRSCH, A.T., DZAU, V.J., MAJZOUB, J.A. & CREAGER, M.A. (1989). Vasopressin-mediated forearm vasodilatation in normal humans. *J. Clin. Invest.*, **84,** 418–426.

JARD, S., GAILLARD, R.C., GUILLON, G., MARIE, J., SCHOENENBERG, P., MULLER, A.F., MANNING, M. & SAWYER, W.H. (1986). Vasopressin antagonists allow demonstration of a novel type of vasopressin receptor in the rat adenohypophysis. *Mol. Pharmacol.*, **30,** 171–177.

KINTER, L.B., DYTKO, G., ASHTON, D., McDONALD, J., HUFFMAN, W. & STASSEN, F.L. (1986). Discovery and therapeutical utility of vasopressin antagonists in rats. *J. Cardiovasc. Pharmacol.*, **8** (Suppl. 7), S36–S43.

LÁSZLÓ, F.A., LÁSZLÓ, F.J. & DE WIED, D. (1991). Pharmacology and clinical perspectives of vasopressin antagonists. *Pharmacol. Rev.*, **43,** 73–108.

LIARD, J.F. (1986). Cardiovascular effects associated with antidiuretic activity of vasopressin after blockade of its vasoconstrictor action in dehydrated dogs. *Circ. Res.*, **58,** 631–640.

LIARD, J.F. (1988). Effects of a specific antidiuretic agonist on cardiac output and its distribution in intact and anephric dogs. *Clin. Sci.*, **74,** 293–299.

LIARD, J.F. (1992). cAMP and extrarenal vasopressin V_2 receptors in dogs. *Am. J. Physiol.*, **263,** H1888–H1891.

LIARD, J.F. (1994). L-NAME antagonizes vasopressin V_2-induced vasodilatation in dogs. *Am. J. Physiol.*, **266,** H99–H106.

LIARD, J.F. & SPADONE, J.C. (1984). Hemodynamic effects of antagonists of the vasoconstrictor action of vasopressin in conscious dogs. *J. Cardiovasc. Pharmacol.*, **6,** 713–719.

LLUCH, S., CONDE, M.V., DIÉGUEZ, G., LÓPEZ DE PABLO, A.L., GONZÁLEZ, M.C., ESTRADA, C. & GÓMEZ, B. (1984). Evidence for the direct effect of vasopressin on human and goat cerebral arteries. *J. Pharmacol. Exp. Ther.*, **228,** 749–755.

MANNING, M. & SAWYER, W.H. (1985). Development of selective agonists and antagonists of vasopressin and oxytocin. In *Vasopressin.* ed. Schrier, R.W. pp. 131–144. New York: Raven Press.

MARTIN, W., FURCHGOTT, R.F., VILLANI, G.M. & JOTHIANADAN, D. (1986). Depression of contractile responses in the rat aorta by spontaneously released endothelium-derived relaxing factor. *J. Pharmacol. Exp. Ther.*, **237,** 529–538.

MARTÍN DE AGUILERA, E., VILA, J.M., IRURZUN, A., MARTÍNEZ, M.C., MARTÍNEZ CUESTA, M.A. & LLUCH, S. (1990). Endothelium-independent contractions of human cerebral arteries in response to vasopressin. *Stroke*, **21,** 1689–1693.

MICHELL, R.M., KIRK, C.J. & BILLAH, M.M. (1979). Hormonal stimulation of phosphatidylinositol breakdown, with particular reference to the hepatic effects of vasopressin. *Biochem. Soc. Trans.*, **7,** 861–865.

OHLSTEIN, E.H. & BERKOWITZ, B.A. (1986). Human vascular vasopressin receptors: analysis with selective vasopressin receptor antagonists. *J. Pharmacol. Exp. Ther.*, **239,** 737–741.

PENIT, J., FAURE, M. & JARD, S. (1983). Vasopressin and angiotensin II receptors in rat aortic muscle cells in culture. *Am. J. Physiol.*, **244,** E72–E82.

RANDALL, M.D., KAY, A.P. & HILEY, C.R. (1988). Endothelium-dependent modulation of the pressor activity of arginine vasopressin in the isolated superior mesenteric arterial bed of the rat. *Br. J. Pharmacol.*, **95,** 646–652.

SAWYER, W.H. & MANNING, M. (1985). The use of antagonists of vasopressin in studies of its physiological functions. *Fed. Proc.*, **44,** 78–80.

STASSEN, F.L., BERKOWITZ, B.B., HUFFMAN, W.F., WIEBELHAUS, V.D. & KINTER, L.B. (1984). Molecular pharmacology of aquaretic agents. In *Diuretics.* ed. Puschet, J.R. pp. 64–71. Amsterdam: Elsevier.

TAKAYASU, M., KAJITA, Y., SUZUKI, Y., SHIBUYA, M., SUGITA, K., ISHIKAWA, T. & HIDAKA, H. (1993). Triphasic response of rat intracerebral arterioles to increasing concentrations of vasopressin in vitro. *J. Cereb. Blood Flow Metab.*, **13,** 304–309.

VANNER, S., JIANG, M.M., BROOKS, V.L. & SURPRENANT, A. (1990). Characterization of vasopressin actions in isolated submucosal arterioles of the intestinal microcirculation. *Circ. Res.*, **67,** 1017–1026.

(Received May 4, 1994
Revised June 10, 1994
Accepted June 13, 1994)

Br. J. Pharmacol. (1994), **113**, 425–430 © Macmillan Press Ltd, 1994

Effect of acute administration of the 5-HT_{1A} receptor ligand, lesopitron, on rat cortical 5-HT and dopamine turnover

[1]M. Ballarín, A. Carceller & X. Guitart

Neurochemistry Unit, C.N.S. Department, Laboratories Dr. Esteve, Avda. Mare de Deu de Montserrat 221, 08026 Barcelona, Spain

1 The involvement of presynaptic 5-hydroxytryptamine$_{1A}$ (5-HT_{1A}) autoreceptors in the anxiolytic-like properties of lesopitron (E-4424) (2-{4-[4-(4-chloro-1-pyrazolyl)butyl]-1-piperazinyl}pyrimidine) was studied. Brain microdialysis was used to examine the effect of the drug on the release of 5-hydroxytryptamine (5-HT) and its metabolite 5-hydroxyindoleacetic acid (5-HIAA) in the frontal cortex of awake, freely moving rats. Moreover, extracellular cortical 3,4-dihydroxyphenylacetic acid (DOPAC) and homovanillic acid (HVA) were also studied to assess the possible participation of dopaminergic systems.

2 Lesopitron administered at a dose which induces anxiolytic behaviour in rats (30 $\mu g\,kg^{-1}$, i.p.) markedly reduced 5-HT levels (to 45% of the basal value) in cortical perfusates, having no effect on 5-HIAA, DOPAC and HVA. The effects of lesopitron were compared with those produced by the anxiolytic, and structurally related compound, buspirone.

3 Buspirone administered at a dose inducing anxiolytic-like effects in rats (5 $mg\,kg^{-1}$, i.p.) produced a marked decrease in cortical 5-HT levels (to 20% of the basal value), but in contrast to lesopitron, buspirone produced a pronounced increase in cortical DOPAC (to 300% of the basal value) and HVA (to 400% of the basal value) levels. Buspirone administered at a low dose (30 $\mu g\,kg^{-1}$, i.p.) was unable to affect cortical 5-HT levels.

4 To test the hypothesis that the 5-HT decreasing effect of lesopitron could be due to 5-HT_{1A} autoreceptor (somatodendritic)-mediated inhibition of 5-HT neurotransmission, lesopitron was administered locally into the raphe nuclei. Intraraphe administration of 10 μM lesopitron caused a decrease in cortical 5-HT levels (the effect being of the same order as that obtained after systemic injection), with no effect on 5-HIAA, DOPAC and HVA. Raphe 5-HT extracellular levels were not modified after intraraphe administration of lesopitron, indicating the absence of 5-HT reuptake blocking properties.

5 We concluded that lesopitron, at an anxiolytic dose produced a marked inhibition of 5-HT release in the frontal cortex of awake, freely moving rats. This effect was observed after systemic administration as well as after intraraphe administration of the drug, suggesting an agonistic action at raphe 5-HT_{1A} autoreceptors controlling 5-HT release in the projecting areas. In contrast to buspirone, lesopitron treatment had no effect on cortical DOPAC or HVA levels.

Keywords: Lesopitron (E-4424); 5-HT_{1A} receptor; microdialysis; buspirone; anxiolytic

Introduction

Current studies suggest that 5-hydroxytryptaminergic neurotransmission may be involved in the aetiology and treatment of anxiety. Central 5-hydroxytryptamine (5-HT) receptors have been divided into four main classes, named 5-HT_1, 5-HT_2, 5-HT_3 and 5-HT_4 (Peroutka *et al.*, 1990); furthermore several additional 5-HT receptors have been recently cloned, including 5-HT_5, 5-HT_6 and 5-HT_7 receptors (Matthes *et al.*, 1993; Monsma *et al.*, 1993; Shen *et al.*, 1993). The 5-HT_1 class shows extensive heterogeneity (Pedigo *et al.*, 1981) and one of its subtypes, the 5-HT_{1A} receptor, has been particularly implicated in the anxiolytic response (Costall *et al.*, 1992; Amano *et al.*, 1993). 5-HT_{1A} receptors are localized presynaptically on the soma and/or dendrites of 5-hydroxytryptaminergic neurones originating in the raphe nuclei, and postsynaptically on target cells in terminal projection areas (e.g. hippocampus and cortex) (Verge *et al.*, 1985; Pazos & Palacios, 1985).

During the last decade, several nonbenzodiazepine drugs (azaspirones) displaying high affinity and selectivity for the 5-HT_{1A} receptor subtype, including buspirone, gepirone and ipsapirone, have been shown to be clinically effective in the treatment of anxiety (Peroutka, 1985). These drugs, as well as the prototypical 5-HT_{1A} agonist 8-hydroxy-2-(di-n-propylamino)tetralin (8-OH-DPAT) have been shown to inhibit the firing of raphe 5-hydroxytryptaminergic neurones (Van der Maelen *et al.*, 1986; Sprouse & Aghajanian, 1987) and decrease the release of 5-HT in their projecting areas (Sharp *et al.*, 1989; Hutson *et al.*, 1989; Hjorth & Sharp, 1991). These effects have been attributed to activation of presynaptic somatodendritic 5-HT_{1A} autoreceptors. However, an additional involvement of postsynaptic 5-HT_{1A} and/or other 5-HT receptor subtypes (e.g. 5-HT_2) in the anxiolytic response has also been proposed (Schechter *et al.*, 1990; Cowen, 1991; Schreiber & De Vry, 1993).

Lesopitron, a novel pyrimidinyl-piperazine derivate (Figure 1) potently reduces behavioural responses to aversive situations in animal models of anxiety (Costall *et al.*, 1991; 1992; Farré, 1992). Binding studies have shown that, like the structurally related compounds buspirone, ipsapirone and gepirone, lesopitron shows affinity for the 5-HT_{1A} receptor in rat

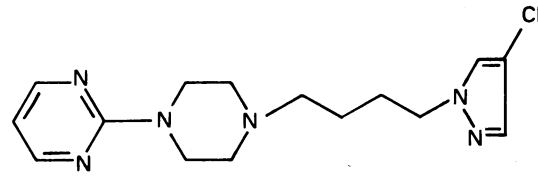


Figure 1 Chemical structure of lesopitron.

[1] Author for correspondence.

brain. Moreover lesopitron shows high selectivity (having no activity at other 5-HT receptors) and specificity (lacking affinity for adrenoceptors, cholinoceptors or benzodiazepine, dopamine, histamine and cholecystokinin receptor sites) (Costall *et al.*, 1992; Farré, 1992).

To assess the participation of somatodendritic 5-HT_{1A} autoreceptors in the anxiolytic properties of lesopitron, we have studied the effects of the drug on the release of 5-HT and its metabolite 5-hydroxyindoleacetic acid (5-HIAA) in the frontal cortex of awake rats using microdialysis. As it is known that activation of dopamine and noradrenaline turnover is an effect shared by the three azaspirones, buspirone, ipsapirone and gepirone (Hamon *et al.*, 1988), the effect of lesopitron on the release of the dopamine metabolites 3,4-dihydroxyphenylacetic acid (DOPAC) and homovanillic acid (HVA) in the same cerebral area was also investigated.

A preliminary account of some of this work was presented to the British Pharmacological Society (Ballarín *et al.*, 1993).

Methods

Brain microdialysis

Male Wistar rats (Interfauna Ibérica, S.A. Sant Feliu de Codines, Spain) weighing 270–300 g, were anaesthesized with chloral hydrate (440 mg kg^{-1}, i.p.) and placed in a stereotaxic frame.

Concentric dialysis probes were made as described previousy (Adell *et al.*, 1989) from 25 G (0.3 mm i.d. × 0.5 mm o.d.) stainless steel tubing (A-M Systems Inc., Everett, U.S.A.). Inlet and outlet cannulae consisted of 0.040 mm i.d. × 0.140 mm o.d. fused silica tubing (Scientific Glass Engineering, Melbourne, Australia). Cuprophan hollow fibres (Gambro GF 80 M) were used for the dialysis membranes (4 mm length).

Probes were implanted into the frontal cortex (3.7 mm anterior to bregma; 3.2 mm lateral to it and 4.4 mm ventral to dura) and/or in the raphe nuclei (7.8 mm posterior to bregma; 0.5 lateral to it and 9.2 mm ventral to dura, according to Paxinos & Watson, 1986). Animals were allowed to recover from surgery, and 18–24 h after implantation, the probes were perfused with artificial cerebrospinal fluid (CSF) (in mM: NaCl 137, KCl 2.4, $CaCl_2$ 1.2, $MgCl_2$ 1.2, Na_2HPO_4 1.4, NaH_2PO_4 0.9 and glucose 7.2, pH 7.4) at a flow rate of 0.25 µl min^{-1} (CMA/100 microinjection pump, Carnegie Medicin, Stockholm) and successive 30 min samples (7.5 µl) were collected. At the end of the experiment brains were removed and frozen for histological verification of dialysis probe placement.

Perfusate analysis

Immediately after collection, samples were analysed for 5-HT, 5-HIAA, DOPAC and HVA, by injecting 7 µl/sample (autoinjector CMA/200 Carnegie Medicin, Stockholm) onto a reversed-phase high performance liquid chromatography (h.p.l.c.-e.d.) system.

The column used was an Ultrasphere 3 µm ODS (4.6 mm × 7.5 mm) (Beckman, U.S.A) and the mobile phase was NaH_2PO_4 150 mM, EDTA 0.5 mM octane-1-sulphonic acid sodium salt 0.2 mM, 12% methanol, pH 3.1 adjusted with phosphoric acid. The flow rate used was 1 ml min^{-1}. The oxidation potential was set at 700 mV vs an Ag/AgCl reference electrode (Hewlett Packard 1048A). The detection limit of the assay for 5-HT was about 1 fmol/injection using a signal-to-noise ratio of 2.

Drug treatment

All reagents used were analytical or h.p.l.c. grade: 5-HT hydrochloride, 5-HIAA, DOPAC and HVA (Sigma Chemical Co., St Louis, MO, U.S.A.); NaCl, KCl, $CaCl_2$, $MgCl_2$, NaH_2PO_4, EDTA (Merck, Germany), octane-1-sulphonic acid sodium salt (Romil Chemicals, GB). 2-{4-[4-(4-Chloro-1-pyrazolyl)butyl]-1-piperazinyl}pyrimidine) (lesopitron) (Lab. Dr Esteve, Barcelona) and buspirone (Lab. Dr Esteve, Barcelona) were administered either through the dialysis probe (dissolved in artificial CSF) or i.p. (dissolved in 0.9% saline, 2 ml kg^{-1} body weight).

Statistical analysis

Dialysate levels of 5-HT, 5-HIAA, DOPAC and HVA were expressed as percentages (mean ± s.e.mean) of the average amount of four samples collected before the administration of the drug (time = 0). Statistical significance ($^*P < 0.05$) between the mean values and saline controls at each time point, was calculated using a two-factor (one between groups, the drug administered, and the other within each group, the time points after administration) repeated measurement analysis of variance. We have used a GLM (General Linear Models) procedure (Hardy, 1989) of the SAS statistical package (SAS Institute Inc., 1989).

Results

Effect of systemic administration of lesopitron and buspirone on 5-HT and 5-HIAA in cortical dialysates

Basal levels of 5-HT and 5-HIAA, measured in frontal cortex dialysates (not corrected for fibre recovery) in awake rats, ranged from 3 to 15 fmol 7 μl^{-1} dialysate and from 3 to 8 pmol 7 μl^{-1} dialysate, respectively. These results were obtained by using artificial CSF as a perfusion medium without addition of a 5-HT uptake blocker.

Peripheral administration of lesopitron (30 µg kg^{-1}, i.p.) (dose with anxiolytic properties) (Costall *et al.*, 1992), caused an immediate reduction in cortical 5-HT levels when compared to saline-treated controls. This effect was significant 90 to 180 min after drug administration, the level decreasing to 45% of the basal value (Figure 2a and Table 1). However, 5-HIAA levels in cortical dialysates were not affected by the drug (Table 1). A high dose of lesopitron (5 mg kg^{-1}, i.p.) decreased cortical 5-HT release to the same extent (to 42% of the basal value; Figure 2a) without affecting 5-HIAA levels (Table 1).

Buspirone (5 mg kg^{-1}, i.p., a dose that produces potential anxiolytic effects in adult rats, Costall *et al.*, 1992) produced a marked reduction of cortical 5-HT levels when compared with saline-treated controls. The effect was significant 60 to 120 min after drug administration, the level decreasing to 24% of the basal value (Figure 2b and Table 1). 5-HIAA levels were unaffected by the drug (Table 1). Moreover, buspirone administered at a low dose (30 µg kg^{-1}, i.p.), had no significant effect on cortical 5-HT levels or 5-HIAA levels (Figure 2b and Table 1).

Effect of systemic administration of lesopitron and buspirone on DOPAC and HVA levels in cortical dialysates

Basal levels of DOPAC and HVA, measured in frontal cortex dialysates (not corrected for fibre recovery) in awake rats, ranged from 100 to 600 fmol 7 μl^{-1} and from 200 to 1000 fmol 7 μl^{-1} respectively. In contrast to lesopitron, which at an anxiolytic-like dose (30 µg kg^{-1}, i.p.) caused no change in DOPAC and HVA cortical levels (Figure 3a,c and Table 1), buspirone (5 mg kg^{-1}, i.p.), caused a pronounced increase in cortical DOPAC (up to 324% of the basal value) (Figure 3b and Table 1) and HVA (up to 388% of the basal value) (Figure 3d and Table 1). These results are in agreement with the reported decreasing 5-HT turnover and increasing dopamine turnover effect of buspirone at anxiolytic doses (Hamon *et al.*, 1988).

Lesopitron, even at doses 100 fold greater than the minimally effective behavioural dose (5 mg kg^{-1}, i.p.), only slightly increased cortical DOPAC and HVA (to 120–130% of basal values) (Figure 3a,c and Table 1).

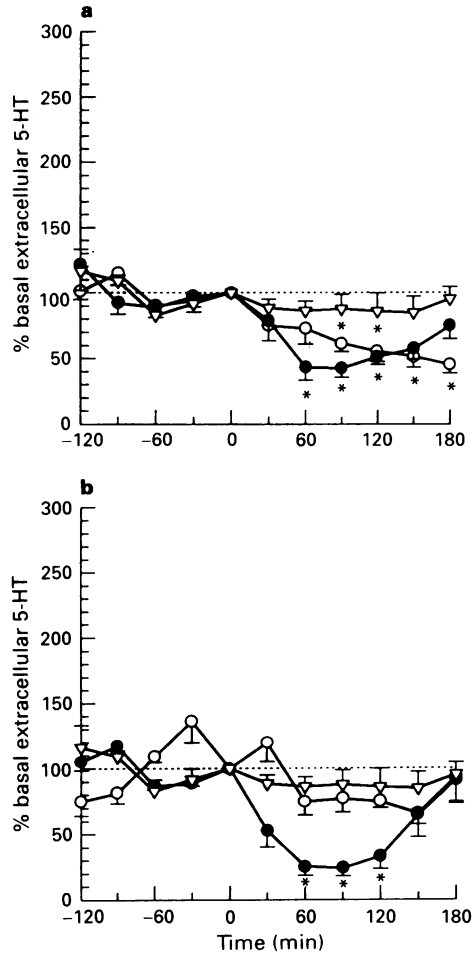


Figure 2 Time-course change in 5-hydroxytryptamine (5-HT) levels in cortical dialysates following (a) lesopitron at different doses: (○) 30 μg kg^{-1}, i.p.; (●) 5 mg kg^{-1}, i.p.; (▽) 0.9% saline 2 ml kg^{-1} and (b) buspirone at different doses: (○) 30 μg kg^{-1}, i.p.; (●) 5 mg kg^{-1}, i.p.; (▽) 0.9% saline 2 ml kg^{-1}. Values are expressed as mean percentages ± s.e.mean, ($n = 6$) of the average amount of four samples collected before injection of the drug ($t = 0$). The dashed line represents 100% baseline level. *$P < 0.05$ compared to saline controls (two-factor repeated-measurement design using GLM procedures of SAS SYSTEM).

Effect of intraraphe perfusion with lesopitron and buspirone on cortical and raphe dialysates

To test the hypothesis that lesopitron decreases 5-HT levels by 5-HT$_{1A}$ autoreceptor (somatodendritic)-mediated inhibition of 5-hydroxytryptaminergic neurotransmission, some rats were implanted with two probes: one close to the dorsal and medial raphe nuclei and the other one in the frontal cortex. Once four basal values were obtained, the artificial CSF perfusing the probe placed in the raphe nuclei, was changed to one containing the drug dissolved in artificial CSF. Perfusion continued for 180 min. During this time, perfusates were collected simultaneously from the raphe nuclei and the frontal cortex.

Cortical dialysates Intraraphe administration of lesopitron 10 μM (without correction for dialysis probe permeability) caused a significant decrease in cortical 5-HT levels (Figure 4a and Table 2) with no effect in 5-HIAA, DOPAC and HVA (Table 2). 5-HT reduction was maximal (to 45% of the basal value) 120 min after starting the administration of the drug (Figure 4a). These results strongly suggest an agonistic action of lesopitron on raphe 5-HT$_{1A}$ autoreceptors modulating 5-HT release in the frontal cortex.

Intraraphe administration of buspirone 100 μM (without correction for dialysis probe recovery) caused a marked decrease in cortical 5-HT release, this was significant from 90 to 180 min after the administration of the drug (Figure 4b and Table 2). 5-HIAA levels were not affected (Table 2) and DOPAC and HVA were only slightly increased (to 120–130% of the basal value) after drug infusion (Table 2).

Raphe dialysates In the raphe nuclei, dialysate basal levels ranged from 10 to 30 fmol 7 μl^{-1} for 5-HT, from 30 to 50 pmol 7 μl^{-1} for 5-HIAA, from 400 to 1500 fmol 7 μl^{-1} for DOPAC and from 600 to 1800 fmol 7 μl^{-1} for HVA. In contrast with the effect on cortical 5-HT release, intraraphe administration of lesopitron (10 μM) failed to affect 5-HT extracellular levels in the raphe nuclei (Figure 4a and Table 2). Raphe 5-HIAA, DOPAC and HVA extracellular levels were also unaffected (Table 2).

Intraraphe buspirone (100 μM) also had no effect on 5-HT raphe levels (Figure 4b and Table 2). Similarly, raphe levels of 5-HIAA, DOPAC and HVA were unaffected (Table 2).

Discussion

The present study demonstrates that systemic administration of lesopitron markedly decreases 5-HT extracellular levels in the frontal cortex of awake freely moving rats. This effect is

Table 1 Comparison of the effects of lesopitron and buspirone administered i.p. at different doses, on the extracellular levels of 5-hydroxytryptamine (5-HT), 5-hydroxyindoleacetic acid (5-HIAA), 3,4-dihydroxyphenylacetic acid (DOPAC) and homovanillic acid (HVA) in the rat frontal cortex

Treatment (mg kg^{-1} i.p.)	*5-HT* (1) (% of basal release)	*5-HIAA* (2) (% of basal release)	*DOPAC* (3) (% of basal release)	*HVA* (4) (% of basal release)
Vehicle Control	87.9 ± 11.0	81.4 ± 3.2	85.8 ± 4.7	92.8 ± 9.8
Lesopitron 0.03	58.7 ± 7.0*	100.0 ± 7.4	96.9 ± 7.1	95.7 ± 7.5
Buspirone 0.03	77.0 ± 10.4	106.5 ± 11.7	104.6 ± 17.1	122.6 ± 17.7
Lesopitron 5.0	42.4 ± 7.0*	79.1 ± 3.0	119.9 ± 17.8	127.5 ± 10.6
Buspirone 5.0	24.0 ± 5.8*	90.7 ± 6.3	324.0 ± 45.8*	388.3 ± 105.6*

The results are expressed as percentages, mean ± s.e.mean ($n = 6$), of the average amount of four samples collected before injection of the drug. The average basal values for each group are: (1) 8.4 ± 1.8 fmol/sample; (2) 4.7 ± 0.6 pmol/sample; (3) 236.4 ± 63.7 fmol/sample and (4) 554.3 ± 88.3 fmol/sample. Values are taken 90 min after injection of the drug (time point of maximum effect for buspirone on 5-HT output, and at which both drugs produce significant changes, see Figure 2a). *$P < 0.05$ compared to vehicle controls (two-factor repeated-measurement design using GLM procedures of SAS system).

also shared by the anxiolytic, structurally related compounds buspirone, ipsapirone and gepirone (Sharp *et al.*, 1989; Routledge *et al.*, 1993). The fact that a 60% reduction of 5-HT release is achieved by a 30 $\mu g\ kg^{-1}$, i.p. dose of lesopitron, while higher doses are needed for buspirone to obtain that effect, is in accordance with the more potent anxiolytic activity showed by lesopitron in animal behavioural tests (Costall *et al.*, 1992).

Our results support electrophysiological data demonstrating that lesopitron inhibits the firing rate of 5-hydroxytrptaminergic neurones in the dorsal raphe nucleus at doses as low as 10 $\mu g\ kg^{-1}$ i.v. through a (−)-tertatolol-sensitive mechanism (Haj-Dahmane *et al.*, 1994). It is then quite plausible that lesopitron can effect cortical 5-HT upon acute administration, at least in part, through activation of somatodendritic 5-HT_{1A} autoreceptors in the raphe nuclei, which mediate inhibition of 5-hydroxytryptaminergic neurotransmission.

Since systemically injected drugs can affect transmitter release by acting on somatodendritic autoreceptors located in

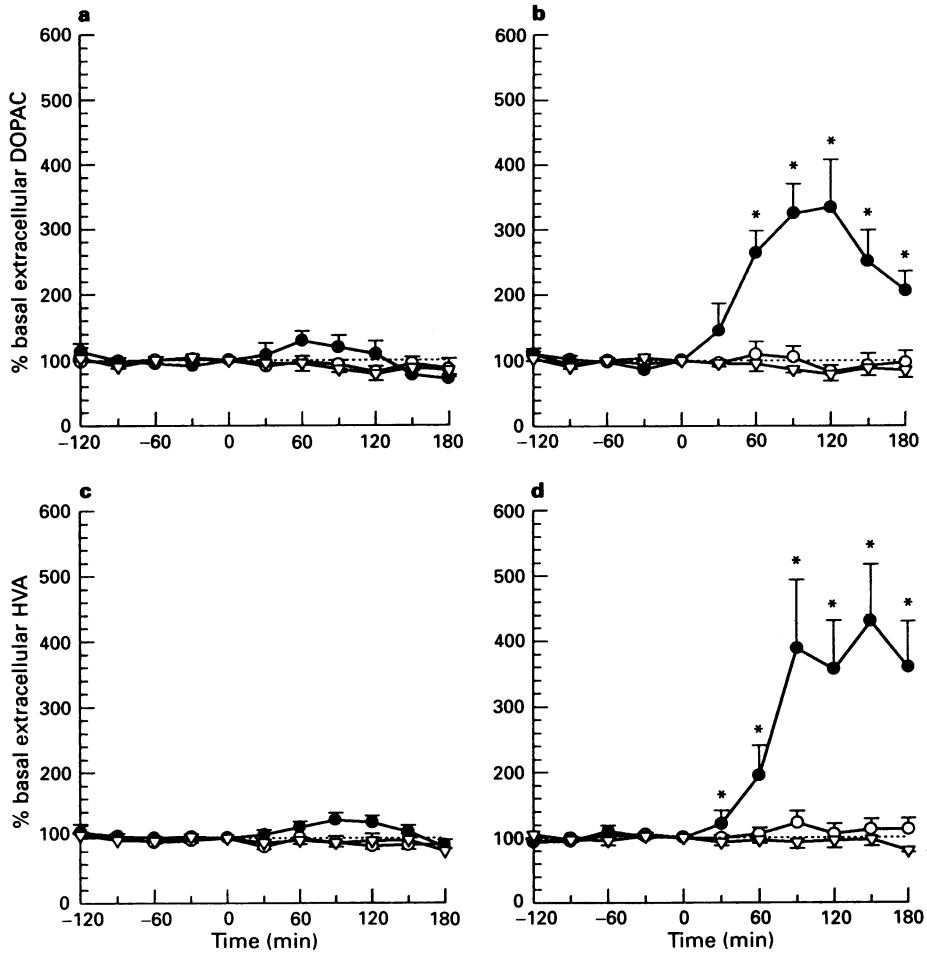


Figure 3 Time-course change in 3,4-dihydroxyphenylacetic acid (DOPAC) and homovanillic acid (HVA) levels in cortical dialysates following (a) (c): lesopitron at different doses (○) 30 $\mu g\ kg^{-1}$, i.p.; (●) 5 $mg\ kg^{-1}$, i.p.; (▽) 0.9% saline 2 $ml\ kg^{-1}$ and (b), (d): buspirone (○) 30 $\mu g\ kg^{-1}$, i.p.; (●) 5 $mg\ kg^{-1}$, i.p.; (▽) 0.9% saline 2 $ml\ kg^{-1}$. Values are mean percentages ± s.e.mean ($n = 6$). See legend to Figure 2 for further details.

Table 2 Comparison of the effects of lesopitron and buspirone administered intraraphe on cortical and raphe perfusate levels of 5-hydroxytryptamine (5-HT), 5-hydroxyindoleacetic acid (5-HIAA), 3,4-dihydroxyphenylacetic acid (DOPAC) and homovanillic acid (HVA)

Treatment (μM i.r)	*Cerebral area*	*5-HT* (1) (% of basal release)	*5-HIAA* (2) (% of basal release)	*DOPAC* (3) (% of basal release)	*HVA* (4) (% of basal release)
Lesopitron	Cortex	45.5 ± 7.5*	85.2 ± 8.6	86.3 ± 8.4	96.1 ± 12.4
	Raphe	95.0 ± 6.5	108.3 ± 4.0	107.8 ± 2.8	111.9 ± 4.2
Buspirone	Cortex	57.1 ± 11.7*	99.9 ± 7.3	112.9 ± 7.0	120.0 ± 2.7
	Raphe	105.2 ± 20.0	116.3 ± 8.7	98.9 ± 5.8	102.6 ± 6.0

Results are expressed as percentages mean ± s.e.mean ($n = 5$) of the average values of four samples taken before perfusion with the drug (basal values). The average basal values for each group are: (1) cortex 5.1 ± 1.4 fmol/sample and raphe 15.2 ± 4.6 fmol/sample; (2) cortex 4.0 ± 0.4 pmol/sample and raphe 34.5 ± 2.3 pmol/sample; (3) cortex 190.0 ± 30.1 fmol/sample and raphe 1100.0 ± 150.0 fmol/sample; (4) cortex 600.2 ± 110.1 fmol/sample and raphe 1230.3 ± 160.0 fmol/sample. Values are taken 120 min after starting drug infusion (time point of which lesopitron produces the maximum effect on 5-HT release and buspirone is close to its maximum effect) and are a mean of five rats. *$P < 0.05$ compared to basal values (two-factor repeated-measurement design using GLM procedures of SAS system).

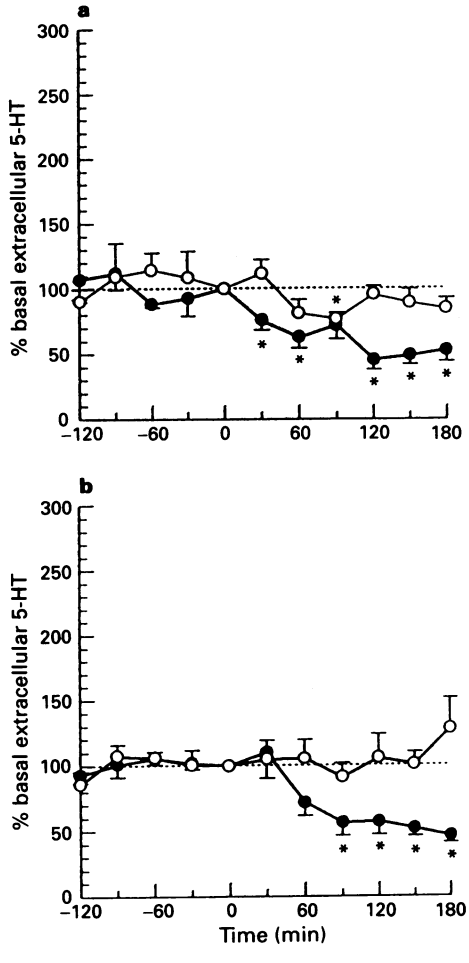


Figure 4 Effect of intraraphe perfusion with CSF containing (a) 10 μM lesopitron and (b) 100 μM buspirone on cortical (●) and raphe (○) 5-hydroxytryptamine (5-HT) dialysate levels. After four samples had been collected to obtain basal values, the artifical CSF was changed (at time 0) to one containing the drug and perfusion continued for 180 min. Results are expressed as percentages (mean ± s.e. mean, $n = 5$) of the average values of the four samples taken before perfusion with the drug (basal values). $^*P < 0.05$ compared to basal values (two-factor repeated-measurement design using GLM procedures of SAS SYSTEM).

the cell body and/or on receptors located on the nerve terminal region, in another group of experiments drugs were administered by local perfusion into the raphe nuclei. Both dorsal and ventral regions were perfused, as the 4 mm dialysis membrane was located in close vicinity to both areas. Comparison between the drug effects following systemic and/or local perfusion, can reveal the contribution of each receptor population. Both routes of administration (lesopitron 30 μg kg^{-1}, i.p. or 10 μM intraraphe) caused a maximal decrease in cortical 5-HT to about 40–50% of controls, indicating that the raphe 5-HT$_{1A}$ population is mainly implicated in lesopitrons activity.

In contrast to its effect on cortical 5-HT levels, intraraphe administration of lesopitron failed to affect 5-HT extracellular levels in the raphe nuclei. It has been shown that extracellular 5-HT in raphe nuclei originates from a cytoplasmic pool and is not dependent on neuronal activity in 5-hydroxytryptaminergic neurones or local activation of 5-HT$_{1A}$ receptors (Adell *et al.*, 1993). It seems plausible that 5-HT output in the raphe nuclei may be regulated by the reuptake process, as *in vivo* blockade with 5-HT uptake inhibitors markedly increases the extracellular 5-HT in this area (Adell & Artigas, 1991). Considering these facts, our results obtained from raphe dialysates suggest that lesopitron, at the doses tested, does not behave as a 5-HT uptake blocker, since direct intraraphe administration (10 μM) failed to affect 5-HT extracellular levels. Moreover our results also suggest that the 5-HT decreasing effect of lesopitron in the frontal cortex is not due to an increase in raphe extracellular 5-HT levels acting on the 5-HT$_{1A}$ autoreceptors, as would be the case in a reuptake blocking situation, and as has been suggested for other compounds (Adell & Artigas, 1991).

Buspirone (100 μM) also failed to affect 5-HT output in raphe nuclei when administered locally into this area. The low influence of buspirone, gepirone and 1-(2-pyrimidinyl)-piperazine (1-PP) on 5-HT uptake into cortical and hippocampal synaptosomes has been described by others (Skolnick *et al.*, 1985). The work of Skolnick *et al.* (1985) suggests that the concentration of buspirone needed to inhibit [^{3}H]-5-HT uptake sites *in vitro*, would not be achieved in rat brain following administration of the minimally effective anti-conflict doses of either buspirone or gepirone.

Lesopitron, as well as buspirone, failed to affect 5-HIAA output. The same effect has been reported with the related compounds, ipsapirone and gepirone (Sharp *et al.*, 1989). However it should be remembered that much of the extracellular 5-HIAA is due to catabolism of unreleased 5-HT and that release and metabolism can be affected differently (Crespi *et al.*, 1990). Thus, changes in the extracellular levels of 5-HIAA do not necessarily indicate corresponding changes in 5-HT release.

Activation of dopamine and noradrenaline turnover constitutes an effect shared by the azaspirones, ipsapirone, gepirone and buspirone (Hamon *et al.*, 1988) that probably takes place through their common metabolite 1-PP (Giral *et al.*, 1987). However, the fact that 1-PP, which has a marked stimulatory effect on catecholaminergic systems, but is without influence on 5-hydroxytryptaminergic neurones (Hamon *et al.*, 1988; Fuller & Perry, 1989; Sharp *et al.*, 1989) has no anxiolytic activity (Young *et al.*, 1987; Amano *et al.*, 1993), and that lesopitron, while having a potent anxiolytic activity in animal tests, has no influence on dopamine metabolites, supports the suggestion that anxiolytic activity does involve mainly 5-hydroxytryptaminergic neurones.

In summary, this study showed that acute administration of lesopitron, at a dose that reduces anxiety-like behaviour, significantly inhibits 5-HT release in the frontal cortex of rats *in vivo*. This effect was obtained after systemic as well as intraraphe administration of lesopitron, suggesting the involvement of raphe 5-HT$_{1A}$ autoreceptors controlling 5-HT release at projecting areas. In contrast with buspirone, lesopitron did not influence cortical dopamine metabolites, indicating that the anxiolytic properties of lesopitron do not appear to be dependent upon an action on dopamine systems.

References

ADELL, A., SARNA, G.S., HUTSON, P.H. & CURZON, G. (1989). An *in vivo* dialysis and behavioural study of the release of 5-HT by *p*-chloroamphetamine in reserpine-treated rats. *Br. J. Pharmacol.*, **97**, 206–212.

ADELL, A. & ARTIGAS, F. (1991). Differential effects of clomipramine given locally or systemically on extracellar 5-hydroxytryptamine in raphe nuclei and frontal cortex. An in vivo microdialysis study. *Naunyn-Schmied. Arch Pharmacol.*, **343**, 237–244.

ADELL, A., CARCELLER, A. & ARTIGAS, F. (1993). In vivo brain dialysis study of the somatodendritic release of serotonin in the raphe nuclei of the rat: effects of 8-hydroxy-2-(Di-n-propylamino)tetralin. *J. Neurochem.*, **60**, 1673–1681.

AMANO, M., GOTO, A., SAKAI, A., ACHIHA, M., HARA, N., TAKAHASHI, N., HARA, C. & OGAWA, N. (1993). Comparison of the anticonflict effect of buspirone and its major metabolite 1-(2-pyrimidinyl)-piperazine (1-PP) in rats. *Jpn. J. Pharmacol.*, **61**, 311–317.

BALLARÍN, M., CARCELLER, A., FARRÉ, A.J. & GUITART, X. (1993). Effect of the acute administration of the 5-HT_{1A} receptor ligand lesopitron on central serotonin and dopamine turnover. *Br. J. Pharmacol.*, **111**, 152P.

COSTALL, B., DOMENEY, A.M., FARRÉ, A.J., KELLY, M.E., MARTINEZ, L. & NAYLOR, R.J. (1992). Profile of action of a novel 5-hydroxytryptamine$_{1A}$ receptor ligand E-4224 to inhibit aversive behaviour in the mouse, rat and marmoset. *J. Pharmacol. Exp. Ther.*, **262**, 90–98.

COSTALL, B., DOMENEY, A.M., KELLY, M.E., MARTINEZ, L., NAYLOR, R.J. & FARRÉ, A.J. (1991). Anxiolitic-like activity in the rat, mouse and monkey of E-4424, a new 5-HT_{1A} receptor ligand. *Serotonin 1991-5-hydroxytryptamine-CNS receptors and brain function.* Birmingham, U.K., July 1991, abst. P. 111.

COWEN, P.J. (1991). Serotonin receptor subtypes: implications for psychopharmacology. *Br. J. Psychiat.*, **159**, 7–14.

CRESPI, F., GARRATT, J.C., SLEIGHT, A.J. & MARSDEN, C.A. (1990). In vivo evidence that 5-hydroxytryptamine (5-HT) neuronal firing and release are not necessarily correlated with 5-HT metabolism. *Neuroscience*, **35**, 139–144.

FARRÉ, A.J. (1992). CNS profile of lesopitron, a new 5-HT_{1A} receptor ligand. *Behav. Pharmacol.*, **3** (Suppl. 1), p. 23 (181).

FULLER, R.W. & PERRY, K.W. (1989). Effects of buspirone and its metabolite 1-(2-pyrimidinyl)piperazine on brain monoamines and their metabolites in rats. *J. Pharmacol. Exp. Ther.*, **248**, 50–56.

GIRAL, P., SOUBRIE, P. & PUECH, A. (1987). Pharmacological evidence for the involvement of 1-(2-pyridinyl)-piperazine (1-PmP) in the interaction of buspirone or gepirone with noradrenergic systems. *Eur. J. Pharmacol.*, **134**, 113–116.

HAJ-DAHMANE, S., JOLAS, T., LAPORTE, A.M., GOZLAN, H., FARRÉ, A.J., HAMON, M. & LANFUMEY, L. (1994). Interactions of lesopitron (E-4424) with central 5-HT_{1A} receptors: in vitro and in vivo studies in the rat. *Eur. J. Pharmacol.*, **255**, 185–196.

HAMON, M., FATTACCINI, C.M., ADRIEN, J., GALLISSOT, M.C., MARTIN, P. & GOZLAN, H. (1988). Alterations of central serotonin and dopamine turnover in rats treated with ipsapirone and other 5-hydroxytryptamine$_{1A}$ agonist with potential anxiolitic properties. *J. Pharmacol. Exp. Ther.*, **246**, 745–752.

HARDY, J. (1989). Repeated-measurement designs: the intricacies of their analysis with the SAS® system. *SAS User's Group International Fourteenth Annual Conference* San Francisco California. April 9–12. pp. 1263–1266.

HJORTH, S. & SHARP, T. (1991). Effect of the 5-HT_{1A} receptor agonist 8-OH-DPAT on the release of 5-HT in dorsal and medial raphe-innervated rat brain regions as measured by in vivo microdialysis. *Life Sci.*, **48**, 1779–1786.

HUTSON, P.H., SARNA, G.S., O'CONNELL, M.T. & CURZON, G. (1989). Hippocampal 5-HT synthesis and release in vivo is decreased by infusion of 8-OHDPAT into the nucleus raphe dorsalis. *Neurosci. Lett.*, **100**, 276–280.

MATTHES, H., BOSCHERT, U., AMLAIKY, N., GRAILHE, R., PLASSAT, J.L., MUSCATELLI, F., MATTEI, M.G. & HEN, R. (1993). Mouse 5-hydroxytryptamine5A and 5-hydroxytryptamine5B receptors define a new family of serotonin receptors: Cloning, functional expression and chromosomal localization. *Mol. Pharmacol.*, **43**, 313–319.

MONSMA, F.J.Jr., SHEN, Y., WARD, R.P., HAMBLIN, M.W. & SIBLEY, D.R. (1993). Cloning and expression of a novel serotinin receptor with high affinity for tricyclic psychotropic drugs. *Mol. Pharmacol.* **43**, 320–327.

PAXINOS, G. & WATSON, C. (1986). *The Rat Brain in Stereotaxic Coordinates.* San Diego: Academic Press.

PAZOS, A. & PALACIOS, J.M. (1985). Quantitative autoradiographic mapping of serotonin receptors in the rat brain: I-serotonin-1-receptors. *Brain Res.*, **346**, 205–230.

PEDIGO, N.N., YAMAMURA, H.J. & NELSON, K.L. (1981). Discrimination of multiple [^{3}H]-5-hydroxytryptamine binding sites by neuroleptic spiperone in the rat brain. *J. Neurochem.*, **36**, 220–226.

PEROUTKA, S.J. (1985). Selective interaction of novel anxiolitics with 5-hydroxytryptamine$_{1A}$ receptors. *Biol. Psychiat.*, **20**, 971–979.

PEROUTKA, S.J., SCHMIDT, A.W., SLEIGHT, A.J. & HARRINGTON, M.A. (1990). Serotonin receptor 'families' in the central nervous system: an overview. *Ann. NY Acad. Sci.*, **600**, 104–113.

ROUTLEDGE, C., GURLING, J., WRIGHT, I.K .& DOURISH, C.T., (1993). Neurochemical profile of the selective and silent 5-HT_{1A} receptor antagonist WAY 100135: an in vivo microdialysis study. *Eur. J. Pharmacol.*, **239**, 195–202.

SAS INSTITUTE INC. (1989). *SAS/STAT® User's Guide.* Version 6, Fourth Edition, Volume 2, Cary, NC: SAS Institute Inc. USA.

SCHECHTER, L.E., BOLAÑOS, F.J., GOZLAN, H., LANFUMEY, L., HAJ-DAHMANE, S., LAPORTE, A.-M., FATACCINI, C.M. & HAMON, M. (1990). Alterations of central serotoninergic and dopaminergic neurotransmission in rats chronically treated with ipsapirone: Biochemical and electrophysiological studies. *J. Pharmacol. Exp. Ther.*, **255**, 1335–1347.

SCHREIBER, R. & DE VRY, J. (1993). 5-HT_{1A} receptor ligands in animal models of anxiety, impulsivity and depression: multiple mechanisms of action? *Prog. Neuro-Psychopharmacol. Biol. Psychiat.*, **17**, 87–104.

SHARP, T., BRAMWELL, S.R. & GRAHAME-SMITH, D.G. (1989). 5-HT1 agonists reduce 5-hydroxytryptamine release in rat hippocampus *in vivo* as determined by brain microdialysis. *Br. J. Pharmacol.*, **96**, 283–290.

SHEN, Y., MONSMA, F.J.Jr., METCALF, M.A., JOSE, P.A., HAMBLIN, M.W. & SIBLEY, D.R. (1993). Molecular cloning and expression of a 5-hydroxytryptamine7 serotonin receptor subtype. *J. Biol. Chem.*, **268**, 18200–18204.

SKOLNICK, P., WEISSMAN, B.A. & YOUDIM, M.B.H. (1985). Monoaminergic involvement in the pharmacological actions of buspirone. *Br. J. Pharmacol.*, **86**, 637–644.

SPROUSE, J.S. & AGHAJANIAN, G.K. (1987). Electrophysiological responses of serotoninergic dorsal raphe neurons to 5-HT_{1A} and 5-HT_{1B} agonists. *Synapse*, **1**, 3–9.

VAN DER MAELEN, C.P., MATHESON, G.K., WILDERMAN, R.C. & PATTERSON, L.A. (1986). Inhibition of the serotoninergic dorsal raphe neurons by systemic and ionotophoretic administration of buspirone, a non-benzodiazepine anxiolytic drug. *Eur. J. Pharmacol.*, **129**, 123–130.

VERGE, D., DAUAL, G., PATEY, A., GOZLAN, H., EL MESTIKAWY, S. & HAMON, M. (1985). Presynaptic 5-HT autoreceptors on serotoninergic cell bodies and/or dendrites but not terminals are of the 5-HT_{1A} subtype. *Eur. J. Pharmacol.*, **113**, 463–464.

YOUNG, R., URBANCIC, A., EMREY, T.A., HALL, P.C. & METCALF, G. (1987). Behavioral effects of several new anxiolytics and putative anxiolytics. *Eur. J. Pharmacol.*, **143**, 361–371.

(Received March 28, 1994
Revised June 5, 1994
Accepted June 13, 1994)

Br. J. Pharmacol. (1994), **113**, 431–438 © Macmillan Press Ltd, 1994

Effects of intrinsic prostaglandins on the spontaneous contractile and electrical activity of the proximal renal pelvis of the guinea-pig

Y. Zhang & [1]R.J. Lang

Department of Physiology, Monash University, Clayton, Victoria 3168, Australia

1 The effects of blocking prostaglandin biosynthesis with indomethacin on the spontaneous electrical and contractile activity recorded in smooth muscle strips of the guinea-pig renal pelvis were examined using standard tension and membrane potential recording techniques.

2 Circumferentially cut strips of proximal renal pelvis contracted more frequently ($4.5 \pm 0.2\ min^{-1}$) than strips cut from the mid region (1.3 ± 0.2; $P < 0.05$, $n = 5$) of the renal pelvis.

3 Indomethacin (1 nM–10 μM) reduced the amplitude and frequency of the contractions of the renal pelvis in a concentration- and time-dependent manner. Contractions were completely abolished in the presence of 30 μM indomethacin.

4 After indomethacin blockade, activation of prostaglandin $F_{2\alpha}$ ($PGF_{2\alpha}$) receptors with dinoprost (1–100 nM) restored the amplitude and frequency of the spontaneous contractions of renal pelvis. Higher concentrations of dinoprost (> 100 nM–3 μM) increased the contraction amplitude of the proximal and mid renal pelvis 1.9 and 1.6 times respectively. The contraction frequency of the mid renal pelvis, but not the proximal pelvis, was also raised above its pre-indomethacin frequency.

5 The spontaneous electrical activity recorded in proximal strips of the renal pelvis was designated to come from three cell types: (i), pacemaker cells (10% of cells recorded), with simple action potentials comprising relatively slow rising and repolarizing phases triggered on top of a slowly-developing pre-potential; (ii), driven cells (75% of cells), with complex action potentials comprising a rapid initial spike, followed by a period of membrane oscillation and a plateau of 0.2–2 s duration; and (iii), intermediate cells (15%) which fired action potentials with an initial rapid and a long plateau phase.

6 Indomethacin (10–30 μM) decreased the amplitude and frequency of the action potentials recorded in driven and intermediate cells. The membrane potential of these cells also depolarized 5 mV to -51.2 ± 2.6 mV ($n = 5$).

7 Dinoprost (300 nM–1.5 μM) increased the rate of action potential discharge, without affecting the membrane potential of driven cells previously exposed to indomethacin (30 μM).

8 These data suggest that the endogenous release of prostaglandins is necessary for the *in vitro* spontaneous contractile activity recorded in the guinea-pig renal pelvis. Blockade of the synthesis of these prostaglandins appears either to modify the ability of the driven regions of the renal pelvis to fire action potentials or to reduce the coupling of these driven regions to their pacemaker cells.

Keywords: Renal pelvis; action potentials; prostaglandins; indomethacin

Introduction

Since the early 1970's, interest has been focused on the autocrine and paracrine actions of locally-generated prostanoids released from a number of hollow organs following distension, mechanical injury, inflammation, bacterial infection or tissue dissection (Smith *et al.*, 1991). In blood vessels (Parkington *et al.*, 1993) and the gastrointestinal tract (Bauer *et al.*, 1985), the net effect of locally-released prostanoids is generally inhibitory, while in the urinary tract they have an overall excitatory action. For example, the prostanoid modulation of reflex micturition, is thought to arise from an excitation of the bladder smooth muscle by distension-released prostanoids, acting upon capsaicin-sensitive sensory and sympthetic nerves (Maggi, 1992). In the upper urinary tract, application of non-steroidal anti-inflammatory drugs, which block prostaglandin synthesis, have been used in the management of renal colic. The pain of renal colic associated with pelviureteral distension arises from the increased pelviureteral pressure and renal blood flow generated after ureteric obstruction. Indomethacin is thought to induce renal vasoconstriction, which, in turn, reduces glomerular capillary pressure and subsequently pelviureteral pressure.

Recently, indomethacin has been shown to have a more direct action on the contractile activity of the upper urinary tract. The amplitude and frequency of the spontaneous contractions of isolated renal pelvic and ureteral strips from sheep (Thulesius & Angelo-Khattar, 1985; Thulesius *et al.*, 1986) and man (Angelo-Khattar *et al.*, 1985; Zwergel *et al.*, 1990) are reduced by indomethacin in a concentration-dependent manner. In the proximal renal pelvis of the rabbit, only the amplitude of the spontaneous contractions decreased in the presence of indomethacin, acetylsalicyclic acid or the prostaglandin antagonist, SC-19220 (Kimoto & Constantinou, 1991); the frequency of their contractions increased. It seems likely that a number of excitatory and inhibitory prostaglandins/cyclo-oxygenase products are being released *in vitro*, the balance of their actions supporting normal pelviureteric peristalsis (Thulesius *et al.*, 1986; Kimoto & Constantinou, 1991). We have investigated the effects of blocking prostanoid synthesis on the spontaneous contractile and electrical activity recorded in the smooth muscle cells of the proximal renal pelvis of the guinea-pig. The amplitude and frequency of these spontaneous contractions were inhibited by indomethacin in a manner correlated with a reduction of the amplitude, duration and frequency of the spontaneous action potentials recorded intracellularly. The decrease in the

[1] Author for correspondence.

frequency of the action potential discharge arose from the increased number of 'failures' of the 'driven' regions of the renal pelvis to fire action potentials upon being invaded by a 'pacemaker' potential. A preliminary account of these results has been presented previously (Zhang *et al.*, 1994).

Methods

Guinea-pigs (300–600 g) (Monash Animal House strain) were stunned, bled and the kidneys excised. The renal pelvis was exposed by careful dissection of the parenchyma and surrounding adipose/connective tissue, opened up longitudinally and the resultant sheet of tissue pinned in a dissecting dish containing pre-oxygenated physiological saline (see below) at 22°C. Circumferentially-cut strips (2 mm wide: 10–15 mm long) were cut from the proximal and mid portions of the renal pelvis and suspended in a 2 ml organ bath (at 35°C). One end of each strip was fixed at the bottom of the organ bath, the other end was attached to a Grass force displacement transducer (Grass FTO3C) connected to a Grass Polygraph (Model 79D).

Electrophysiological recordings

Intracellular recordings were only made from strips (5 mm wide: 5 mm long) of proximal renal pelvis pinned, serosal side up, in a electrophysiological recording chamber on an inverted microscope. Cells were impaled with fine borosilicate glass microelectrodes which had resistances of 50–150 MΩ when filled with 2 M KCl. Membrane potentials were recorded with a standard unity-gain pre-amplifier, stored on a video cassette recorder using a digital data recorder (List VR-10) and later digitized using a Labmaster analog-to digital interface, a personal computer (NEC Powermate 286 Plus) and Axotape 1.1 (Axon Instruments) software. Tests for significant changes of contraction and action potential parameters during an experiment were made with Student's paired *t* tests.

Intramural nerves were stimulated with silver-silver chloride wires placed on either side of the muscle strips and connected to a Grass (S88) stimulator. Stimulating parameters (pulses 0.3 ms in duration, 100–150 V at 20–50 Hz for 1–10 s) were chosen to reduce the likelihood of direct muscle stimulation.

Physiological saline

The bicarbonate buffered physiological saline contained (mM): Na^+ 146, K^+ 5, Ca^{2+} 2.5, Mg^{2+} 1, Cl^- 132, HCO_3^- 25, $H_2PO_4^-$ 1 and glucose 11. This solution had a pH of 7.3–7.4 after being bubbled with 95% O_2:5% CO_2.

Drugs

Dinoprost trometamol (Upjohn), carbachol (carbamylcholine chloride), atropine sulphate, guanethidine sulphate, histamine dihydrochloride, 4-aminopyridine, cyclopiazonic acid, ouabain, tetrodotoxin (TTX) (all Sigma) and tetraethylammonium (TEA; Eastman Kodak) were freshly prepared in distilled water as stock solutions (0.1–10 mM). Indomethacin and nifedipine were dissolved in ethanol. Drugs were diluted with physiological saline to their final concentrations indicated. Solutions were vigorously bubbled before use to restore any changes in pH.

Results

Tension studies

Proximal and mid portions of the renal pelvis developed regular spontaneous contractile activity after 30–60 min equilibration in the organ bath and maintained these contractions for 2–4 h. We have confirmed that the frequency of the spontaneous contractions of the proximal strips of the renal pelvis ($4.5 \pm 0.2\ min^{-1}$) is significantly greater than those recorded in the mid ($1.3 \pm 0.2\ min^{-1}$; $P < 0.05$, $n = 5$ preparations) (Figure 1) or more distal portions of the pelvis (Constantinou *et al.*, 1977; Kimoto & Constantinou, 1991).

In Figure 1a, it can be seen that indomethacin (300 nM–3 μM) induced both a time- and concentration-dependent reduction in the amplitude and frequency of the spontaneous contractions of the proximal and mid portions of the renal pelvis. To quantify the effects of indomethacin (300 nM–30 μM), the amplitude and frequency of the spontaneous contractions were measured after 20 min exposure to each concentration of indomethacin. The amplitude of the contractions of both the proximal and mid renal pelvis were equally affected by indomethacin (300 nM–3 μM) (Figure 1b). The frequency of these contractions, however was only reduced at indomethacin concentrations > 1 μM. When expressed as a fraction of the control, 3 μM indomethacin reduced the frequency of contractions of proximal and mid renal pelvis by 16% and 12% respectively, whereas 10 μM indomethacin induced a 52 and 77% reduction respectively (Figure 1c). Indomethacin, 30 μM, was required to block (within 20 min) the contractions of the renal pelvis completely. Rhythmic contractions, but of reduced amplitude, were restored within 20–30 min following removal of indomethacin from the bathing solution.

Repetitive intrinsic nerve stimulation (50 Hz for 2 s) has a positive inotropic effect on the amplitude and frequency of contraction of both the proximal and mid regions of the renal pelvis (Figure 2a). These positive inotropic effects, which peaked after 30–120 s and slowly declined over 10 min, were still observed after blockade of all spontaneous contractile activity with indomethacin (30 μM) (Figure 2b(i), (ii)). These effects of nerve stimulation were unaffected by the addition of atropine (3 μM) plus guanethidine (3 μM) (Figure 2c) and mostly abolished by the previous application of TTX (3 μM) (Figure 2d) (Maggi *et al.*, 1992; Maggi & Giuliani, 1992).

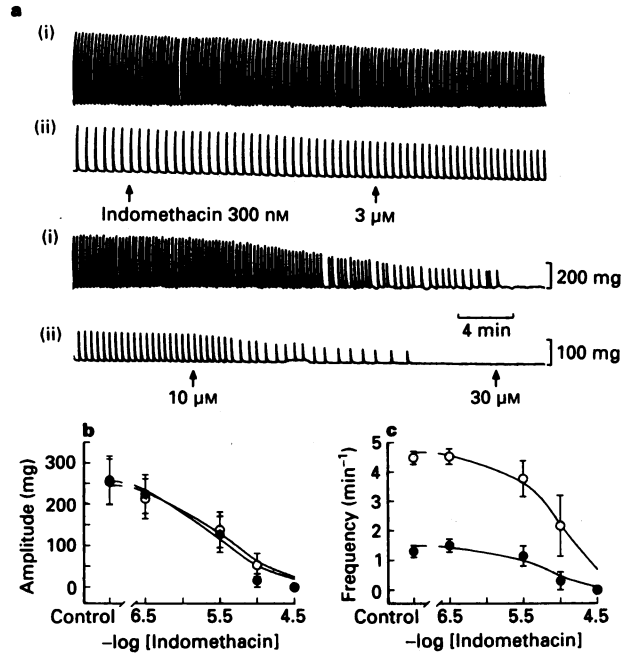


Figure 1 Effects of indomethacin (300 nM–30 μM; ↑) on the amplitude (b) and frequency (c) of the spontaneous contractions generated by circumferentially-cut strips ($n = 5$) of the proximal (a(i), b,c, ○) and mid (a(ii),b,c, ●) renal pelvis of the guinea-pig.

Effects of dinoprost

Addition of dinoprost (1 nM–3 μM), a stable analogue of $PGF_{2\alpha}$ restored the spontaneous contractile activity of the proximal and mid portions of the renal pelvis abolished by indomethacin (30 μM) (Figure 3a). The proximal strips of renal pelvis appeared more sensitive to the action of dinoprost, contractions being activated with dinoprost concentrations >1 nM. In contrast, the mid renal pelvis contracted at dinoprost concentrations >10 nM (Figure 3). Dinoprost (1 nM–3 μM) was equally effective at increasing the contraction amplitude (expressed as % of the maximum induced by dinoprost) of the proximal and mid renal pelvis (Figure 3b). Their averaged maximal contractions to dinoprost (3 μM), however, were significantly larger (425 ± 23 and 327 ± 33 mg respectively) than their control contractions (230 ± 59 and 200 ± 36 mg; $P<0.05$, $n=4$) in the absence of indomethacin. Interpolation of the four individual concentration-response curves showed that the average concentrations of dinoprost to restore the spontaneous contractions of the proximal and mid portions of the renal pelvis to their pre-indomethacin amplitudes were 148 ± 47 and 425 ± 56 nM

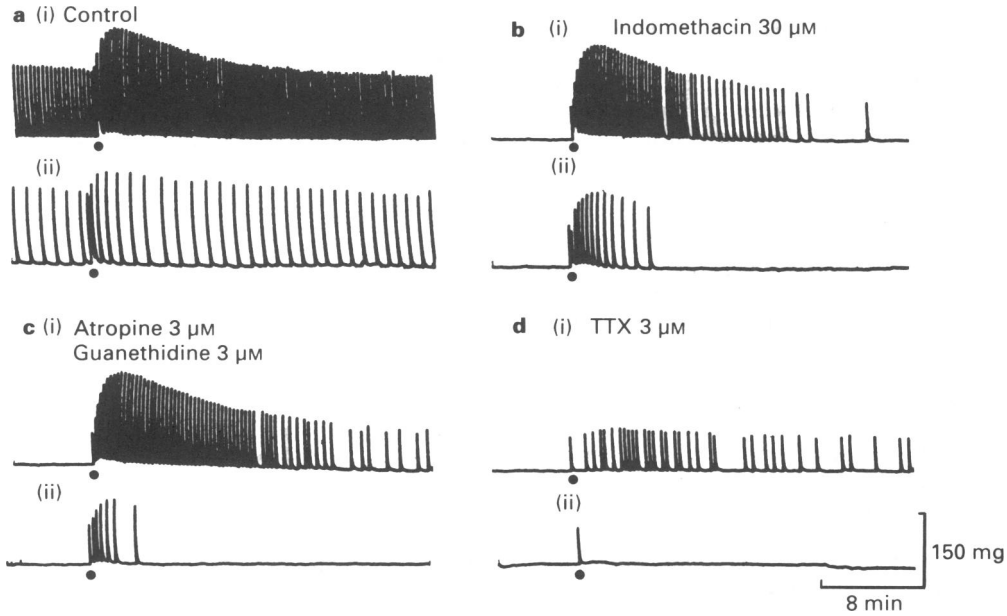


Figure 2 Effects of intramural sensory nerve stimulation (50 Hz for 2 s; ●) on the spontaneous contractile activity of the proximal (i) and mid (ii) renal pelvis of the guinea-pig in the absence (a) and after 20 min exposure (b) to 30 μM indomethacin. These positive inotropic effects of nerve stimulation in the presence of indomethacin were not prevented by atropine (3 μM) + guanethidine (3 μM) (c) but were blocked by tetrodotoxin (TTX 3 μM, d).

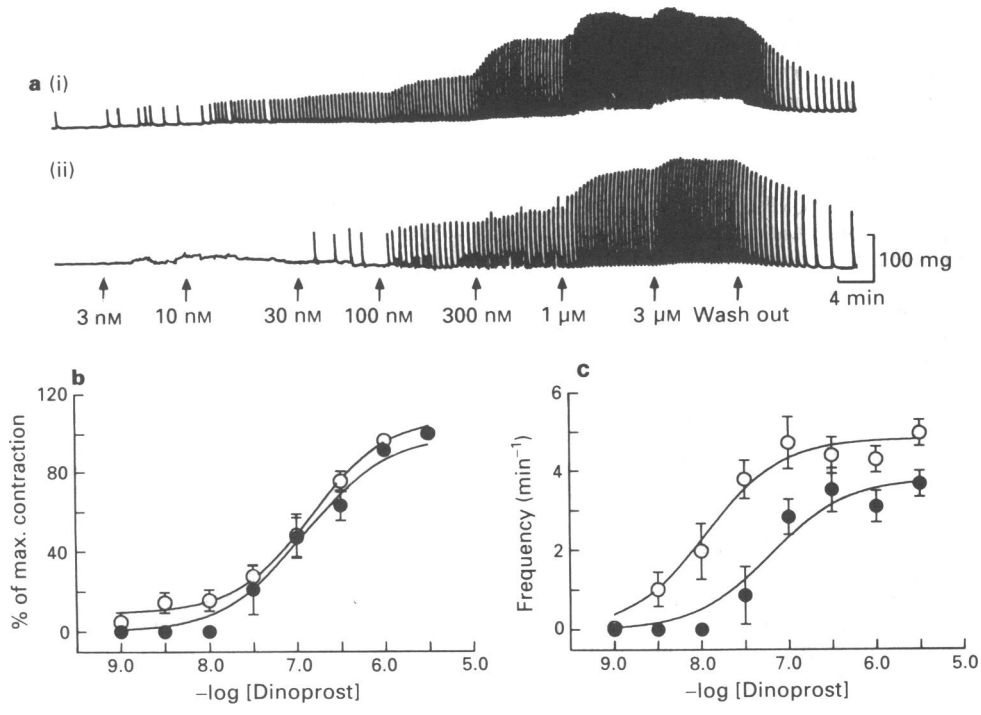


Figure 3 Stimulation of prostaglandin $F_{2\alpha}$ receptors with dinoprost (1 nM–3 μM) induced spontaneous contractions in both proximal (a(i),b,c, ○) and mid (a(ii),b,c, ●) portions of the renal pelvis ($n=4$) previously blocked with indomethacin (30 μM); increasing both their strength (b) and frequency (c) of contraction in a concentration-dependent manner.

respectively ($P<0.05$, $n=4$). The concentrations of dinoprost required to restore the frequency of contraction of the proximal and mid renal pelvis to their pre-indomethacin frequencies were 102 ± 56 and 63 ± 24 nM ($P>0.05$). Higher concentrations (> 100 nM) of dinoprost could not, however, increase the contraction frequency of the proximal strips to a significantly greater extent than the control frequency before the addition of indomethacin (4.5 ± 0.2 min^{-1}; $P>0.05$, $n=4$) (Figure 3c). In contrast, these concentrations of dinoprost (> 100 nM) significantly increased the contraction frequency of the mid renal pelvis to approximately two fold greater than its pre-indomethacin frequency (1.5 ± 0.1 min^{-1}; $P<0.05$, $n=4$) (Figure 3c).

Dinoprost (> 100 nM) also induced a small tonic contraction in the proximal, but not the mid renal pelvis in both the absence and presence of indomethacin ($n=11$). These tonic contractions were 5–40% of the amplitude of the control spontaneous contractions in the absence of indomethacin. Tonic contractions in the presence of indomethacin were also not affected by nifedipine (1 μM) ($n=10$), nicardipine (1 μM) ($n=2$), ouabain (10 μM) ($n=3$) or cyclopiazonic acid (10 μM) ($n=4$), but were blocked by Cd^{2+} (0.5 mM) ($n=5$) or upon removal of Ca^{2+} from the bathing solution ($n=7$) (data not shown). These data suggest that dinoprost may also be triggering an influx of Ca^{2+} through receptor-operated pathways that do not involve dihydropyridine-sensitive Ca^{2+} channels, the Na-K pump or the release of Ca^{2+} from internal stores. Spontaneous contractions of both proximal and mid renal pelvis after indomethacin-induced blockade could also be triggered with the stable PGI analogue, iloprost (100 nM) ($n=3$) and with histamine (10 μM) ($n=1$). Exposure to 20 mM K^+ saline has both positive inotropic and chronotropic effects on the spontaneous contractions of the proximal and mid renal pelvis (Cole *et al.*, 1988); exposure to 100 mM K^+ induced a tonic contraction of 100–130% the amplitude of the spontaneous contractions in control saline. These contractions to high K^+ saline were not affected by 30 μM indomethacin (applied for > 20 min), but were abolished by nifedipine (1 μM) ($n=4$).

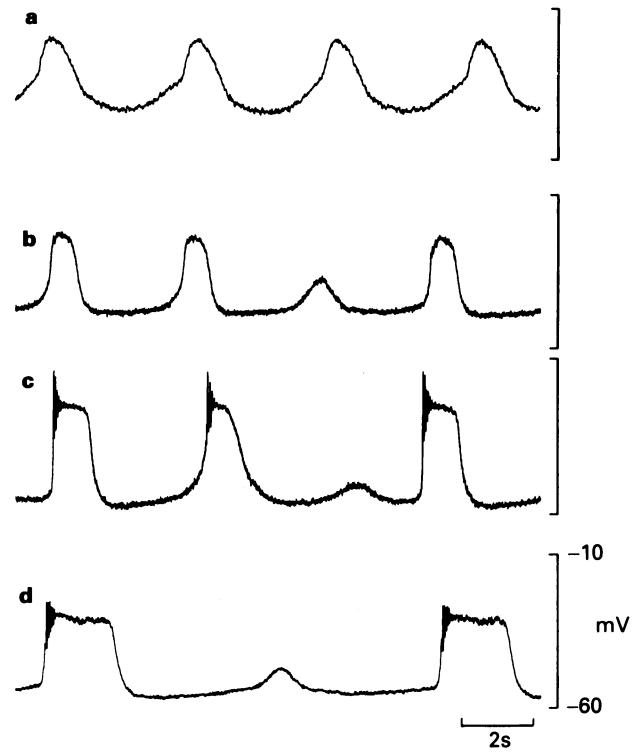


Figure 4 Spontaneous action potentials recorded in strips of proximal renal pelvis were divided into three general types: (a), 10% of cells ($n>100$ cells) had membrane potentials of − 40 to − 45 mV (measured 600 ms before each action potential), fired simple action potentials and were thought as being recorded from 'pacemaker' cells; (c,d), 75% of cells had membrane potentials of − 55 to − 60 mV, fired complex action potentials with a rapidly-rising initial spike which was followed by a period of membrane oscillation and a plateau phase were designated as 'driven' cells; (b), the remaining cells (15%) had action potentials with an initial spike and plateau were designated as 'intermediate' cells.

Microelectrode studies

To date, only a few preliminary electrophysiological recordings have been obtained from the renal pelvis, using the sucrose gap (Zawalinski *et al.*, 1975) or intracellular microelectrode (Golenhofen & Hannappel, 1974; Seki & Suzuki, 1990; Tsuchida & Suzuki, 1992) techniques. We have recently presented an extensive study of the properties of the action potentials recorded in the guinea-pig proximal renal pelvis recorded with intracellular microelectrodes (Zhang & Lang, 1993). Briefly, three types of spontaneous action potential discharge were recorded: (i), 10% of cells ($n>100$) ('pacemaker' cells) had an action potential with a simple 'pacemaker-like' waveform which was triggered on top of a slowly-developing prepotential. These cells had membrane potentials, measured 600 ms preceding a spontaneous event, of − 40 to − 50 mV (− 46 ± 2 mV, $n=7$) (Figure 4a); (ii) 75% of cells ('driven' cells) had more complex action potentials consisting of an initial spike, followed by a period of membrane oscillation and a plateau (0.2–2 s in duration), and membrane potentials of − 55 to − 60 mV (− 58 ± 2 mV, $n=14$) (Figure 4c,d), (iii) the remaining 15% of cells fired action potentials with a single initial spike and plateau and had membrane potentials of about − 45 mV ('intermediate' cells) (Figure 4b) (Zhang & Lang, 1993). Cells from groups (ii) and (iii) had distinct refractory periods, often failing to trigger an action potential 5–20 s after a preceding one. During such failures, the underlying triggering pacemaker potential was revealed (Figure 4b,c,d). Action potentials in all three cell types were blocked upon addition of nifedipine (1–10 μM) (Figure 6a(iv), b(iv)) ($n=6$) or Cd^{2+} (100 nM) ($n=3$), blockers of voltage-operated Ca^{2+} channels.

Effects of indomethacin

Figure 5 illustrates both the time- and concentration-dependent effects of indomethacin (15–30 μM) on the membrane potential and action potentials recorded in a driven cell of the proximal renal pelvis. Both the amplitude and frequency of these action potentials decreased with indomethacin (15–30 μM) (Figure 5a) and this decrease was associated with a time-dependent membrane depolarization of 5 mV to − 51.2 ± 2.6 mV (control membrane potential − 56.8 ± 3.3 mV; $P<0.05$, $n=5$). In five cells, the averaged frequency, initial spike amplitude and half-amplitude duration were respectively 1.6 ± 0.9 min^{-1}, 17.0 ± 7.3 mV and 307 ± 179 ms after a 20 min exposure to indomethacin (30 μM); significantly ($P<0.05$) smaller than their control values of 6.7 ± 1.6 min^{-1}, 34.3 ± 1.2 mV and 1266 ± 307 ms respectively (Figure 5b). The decrease in action potential frequency arose from the increase in 'failures' to fire an action potential, as the frequency of the underlying pacemaker potentials was little affected (Figure 5a(i), (iv) (v)). These effects of indomethacin were reversible after 30 min washout, although the duration and amplitude of the action potentials never fully recovered (data not shown).

Dinoprost, 300 nM and 1.5 μM, significantly increased the rate of action potential discharge to 7.8 ± 2.9 and 14 ± 5.1 min^{-1} respectively in non-pacekmaker cells previously slowed with 30 μM indomethacin (1.6 ± 0.9 min^{-1}; $P<0.05$, $n=5$). In the intermediate cell illustrated in Figure 6a,b, this acceleration of action potential discharge with dinoprost (1.5 μM) was associated with a membrane depolarization of some 10 mV and possibly the recruitment of more than one

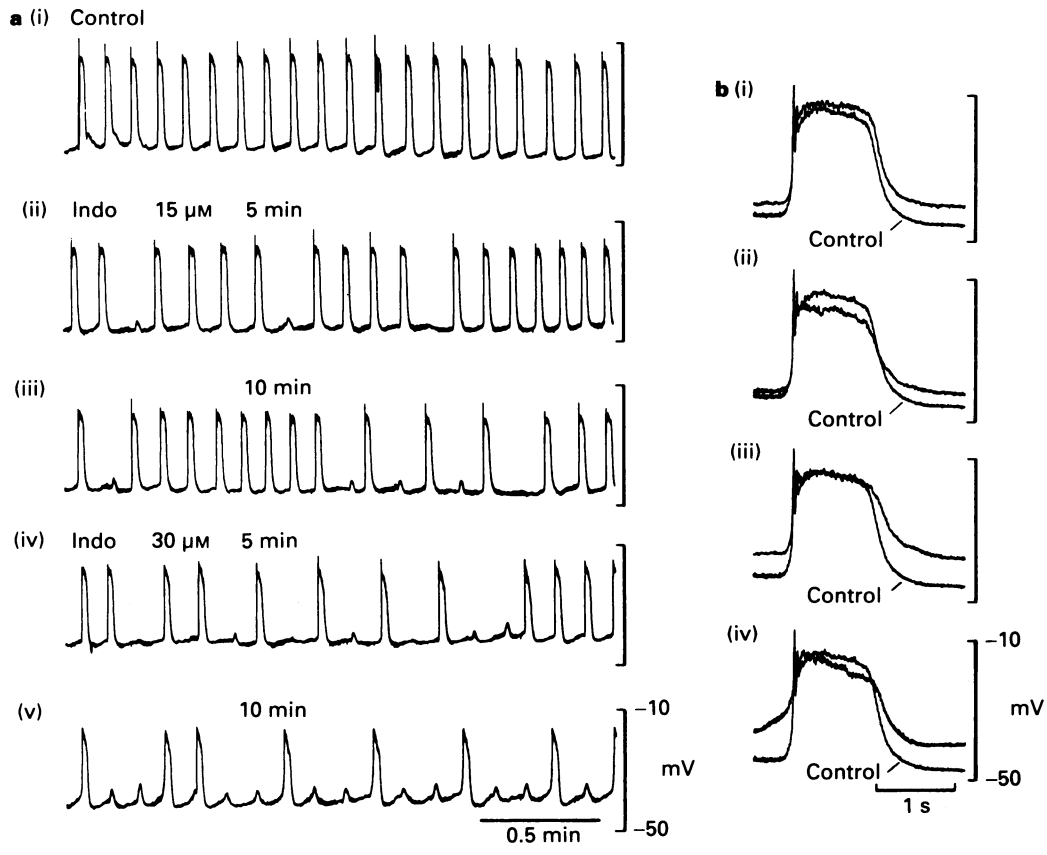


Figure 5 Effects of indomethacin (Indo; 15–30 μM) on the spontaneous action potential recorded in a driven cell of the proximal renal pelvis. Spontaneous action potential discharge became irregular (a(ii),(iii)) with time in indomethacin (15 μM); their frequency of discharge decreasing from 6.7 ± 1.6 to 1.6 ± 0.9 min^{-1} ($P<0.05$, $n=5$) in 30 μM indomethacin (a(iv),(v)). The pacemaker potentials underlying these action potentials could be clearly recorded in the presence of indomethacin, their frequency appeared little affected (a(i),(v)). The change in time course of the action potentials in indomethacin (15–30 μM) has been illustrated by superimposing a control action potential on action potentials recorded after 5 (b(i)) and 10 (b(ii)) min exposure to 15 μM indomethacin and after 5 (b(iii) and 10 (b(iv)) min exposure to 30 μM indomethacin. The averaged initial spike amplitude and half-amplitude duration was respectively 17.0 ± 7.3 mV and 307 ± 179 ms after 30 min exposure to indomethacin (30 μM), compared with their control values of 34.3 ± 1.2 mV and 1266 ± 307 ms ($P<0.05$; $n=5$).

pacemaker potential. In contrast, the membrane potential of driven cells (Figure 6c) was − 51.5 ± 6.7 ($n=3$) and − 49.2 ± 4.2 ($n=5$) respectively after 5 min exposure to 300 nM and 1.5 μM dinoprost (control membrane potential in 30 μM indomethacin of − 51.2 ± 2.6 mV) (Cole *et al.*, 1988).

Nerve stimulation (50 Hz for 2–10 s) also induced action potential discharge in non-pacemaker cells exposed to indomethacin (30 μM) (Figure 7a,b). In the driven cell illustrated in Figure 7, the action potentials initiated upon nerve stimulation (Figure 7b) have been compared with those initiated by dinoprost (1.5 μM; Figure 7c). The action potentials initiated by nerve stimulation were slightly briefer and associated with a membrane after-hyperpolarization (Figure 7b), which was not evident in dinoprost. The increase in the frequency of action potential discharge in the presence or absence of indomethacin were abolished by the previous application of TTX (1.6 μM; $n=6$). Together with the contraction data, it is clear that the mechanisms which control transmitter release are not affected by indomethacin. Also, the mechanism/conductance changes which prevent action potential generation in the presence of indomethacin can be reversed rapidly (within 30 s) upon nerve stimulation or $PGF_{2\alpha}$ receptor activation.

Discussion

The renal pelvis in man and many mammals consists of two morphologically and histochemically distinct types of smooth muscle cells. Typical smooth muscle cells are spindle shaped and grouped into bundles, which branch and interconnect with adjacent bundles, to form a continuous muscle layer from the major and minor calyces to the renal pelvis, the pelviureteric junction and into the ureter. 'Atypical' smooth muscle cells form a thin layer of muscle cells, internal to the typical cells, which extends from the calyceal-renal parenchyma attachment to the pelviureteric junction. Few of these cells appear in the pelviureteric junction and they are generally absent in the proximal ureter. These atypical smooth muscle cells are characterized by their irregular shapes and cell contents, as observed under the electron microscope, and by their lack of non-specific cholinesterase (Gosling & Dixon, 1972; 1974). They have areas of close apposition with other atypical cells and with bundles of typical smooth muscles so that it is likely that they, like the interstitial cells of the gastrointestinal tract, form specialized preferential pathways of electrical conduction. The intrinsic electrical activity of the most proximal atypical cells has been thought to drive the electrical and contractile activity throughout the renal pelvis and therefore ureteric peristalsis (Gosling & Dixon, 1972; 1974; Hannappel & Lutzeyer, 1978).

The nature of the electrical activity in the ureter has been extensively studied using extracellular and intracellular recording techniques (Kuriyama *et al.*, 1967; Kuriyama & Tomita, 1970; Shuba, 1981) and more recently at the whole-cell and single channel current level (Imaizumi *et al.*, 1989; 1990; Lang, 1989; 1990). Recently, we have presented evidence detailing the nature of the ionic conductances underlying the

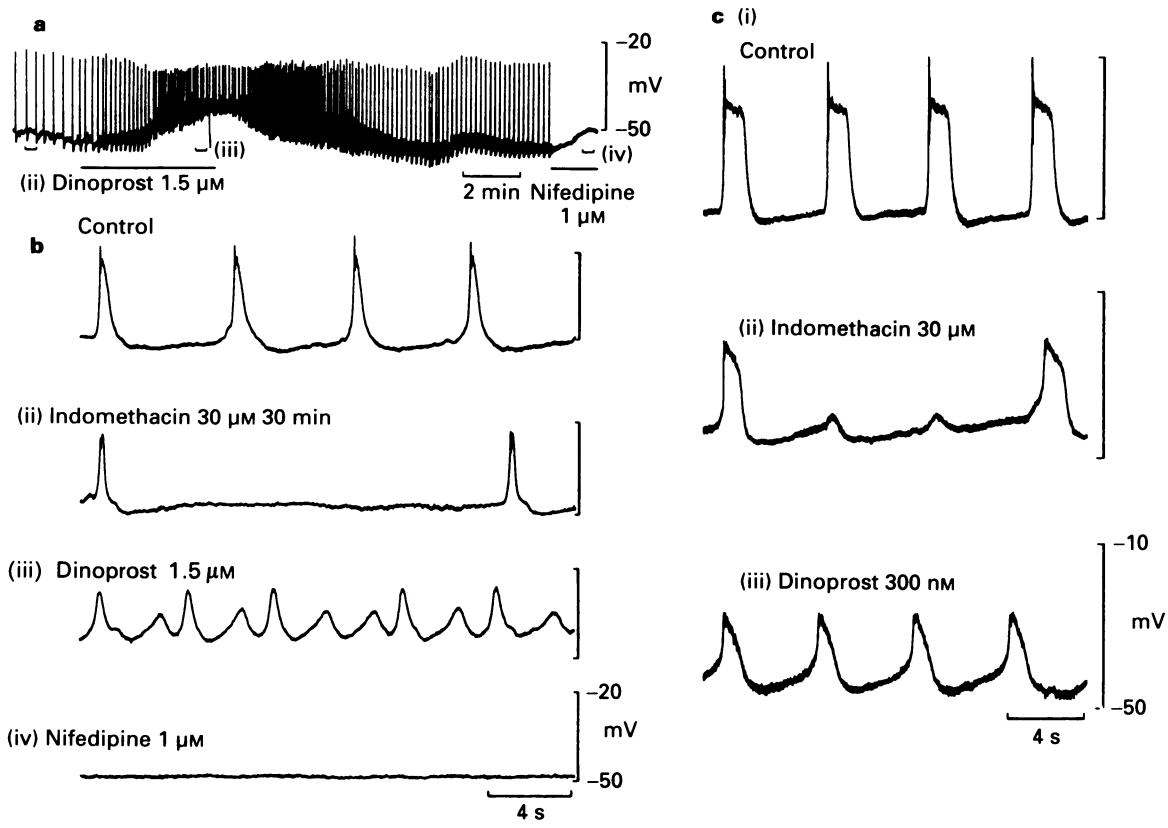


Figure 6 Stimulation of prostaglandin $F_{2\alpha}$ receptors with dinoprost (300 nM–1.5 μM) restores the frequency of action potential discharge in intermediate (a(iii), b(iii)) and driven cells (c(iii)) cells previously reduced by indomethacin (Indo; 30 μM (a(ii), b(ii), c(ii)); the amplitude and half-amplitude duration of the action potentials in dinoprost never fully recovered (b(iii), c(iii)). The intermediate cell illustrated in (a) has been exposed to indomethacin (30 μM) for 30 min. In b(i)–(iv) the action potentials highlighted in (a) have been replotted on an expanded time scale. Note the membrane depolarization in the presence of nifedipine (1 μM) (a(iv),b(iv)).

electrical activity in the renal proximal pelvis (Zhang & Lang, 1993). We have divided the recorded electrical activity into three distinct groupings and have speculated on their physiological roles. The cells with the simple action potentials have been termed 'pacemaker cells', analogous with the heart. These pacemaker action potentials were generally recorded in cells near the urothelial border, suggesting that they were made in atypical cells as has often been proposed (Gosling & Dixon, 1972; 1974; Hannappel & Lutzeyer, 1978). The cells with the longer complex action potentials, similar to those recorded in the ureter (Kuriyama *et al.*, 1967; Kuriyama & Tomita, 1970; Shuba, 1981), have been termed 'driven cells', and are distinguished by their more negative membrane potentials (−55 to −60 mV cf. −45 mV in pacemaker cells). The remaining were designated 'intermediate cells'. We would like to suggest that the pacemaker action potentials were recorded from atypical smooth muscle cells, while the action potentials recorded from intermediate and driven cells were recorded from typical smooth muscle cells which were respectively in close and far electrical contact with a pacemaker region.

In the present experiments, we have demonstrated that the blockade of endogenous prostanoid synthesis leads to an inhibition of both the frequency and amplitude of the spontaneous contractions of the proximal and mid renal pelvis of the guinea-pig. The concentrations of indomethacin (5–30 μM) used in the electrophysiological experiments, while relatively higher than the 50% inhibitory concentrations (IC_{50}) required to block prostaglandin synthesis in homogenates or subcellular fractions of brain, lung, spleen or kidney (0.2–3.7 μM) (Flower, 1974), are comparable to the indomethacin concentrations used to block prostaglandin synthesis in the urinary (Kimoto & Constantinou, 1991; Thulesius & Angelo-Khattar, 1985; Thulesius *et al.*, 1987; Cole *et al.*, 1988) and gastrointestinal tracts (Bauer *et al.*, 1985), perfused lungs and hearts and in rat isolated uteri (Flower, 1974). We felt it important that we maintained our electrode impalements throughout the onset of indomethacin action so that the action potentials recorded in control saline could be directly compared with those in indomethacin. Given the difficulty of maintaining these impalements in spontaneously contracting preparations and the slower onset of action of lower concentrations of indomethacin (>150 min at 1 μM indomethacin) (Angelo-Khattar *et al.*, 1985; Thulesius & Angelo-Khatta, 1985), we chose concentrations of indomethacin (5–30 μM) which produced steady-state blockade within 20 min.

During the onset of indomethacin (10–30 μM) action (Figure 5), the action potentials recorded in driven and intermediate cells reduced in amplitude and duration, consistent with the reduced contraction amplitudes observed with lower concentrations (<1 μM) of indomethacin and with the time-dependent decrease observed with higher concentrations of indomethacin (Figure 1). Final blockade of muscle contraction by indomethacin was associated with a loss of action potential discharge. The membrane depolarization in the presence of indomethacin, we believe, arises from the reduction of the time-dependent K^+ conductances associated with the downstroke and refractory periods of each action potentials. With fewer action potentials of shorter amplitude and duration discharging, these K^+ conductances would have less influence and the membrane potential would therefore be expected to settle closer to its 'true' membrane potential. A similar membrane depolarization to near −40 mV is recorded in driven, intermediate and pacemaker cells when action potential discharge is blocked with nifedipine (1 μM) (Figure

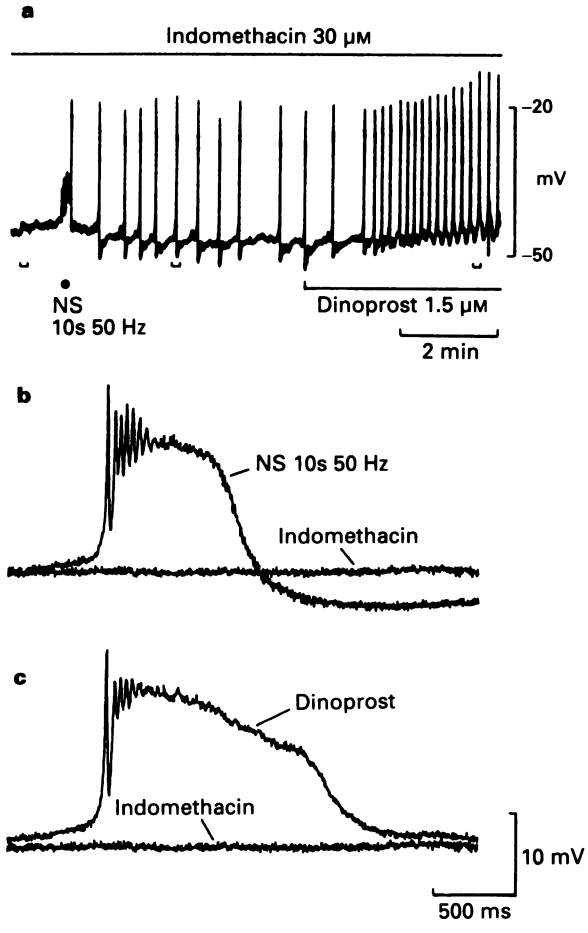


Figure 7 Nerve stimulation (NS; 50 Hz for 10 s) in the presence of indomethacin (30 μM) (a,b) induced action potential discharges of a similar time course to those induced by dinoprost (1.5 μM), except for a larger after-hyperpolarization (a,c). (b,c) are the action potentials highlighted by the brackets in (a) illustrated on an expanded time scale and superimposed on the membrane potential in indomethacin.

6a iv) (Zhang & Lang, 1993). Alternatively, this membrane depolarization in the presence of indomethacin could perhaps suggest that endogenous prostanoids are constantly activating a K^+ conductance, or turning off a Na^+/Cl^- conductance, which helps to maintain the more negative ('diastolic') membrane potential in the driven and intermediate cells. Recently, however, we have demonstrated that an increase in action potentials discharge is associated with the membrane depolarization induced when membrane K^+ conductances are blocked with tetraethylammonium or 4-aminopyridine (2 mM), or when cationic conductances are activated with carbachol (10 μM) (Zhang & Lang, 1993).

What causes failure of action potential discharge in driven cells remains uncertain. The prostanoids may well be sustaining the smooth muscle Ca^{2+} channels in an activatable state, perhaps by shifting the voltage range over which they will open. The loss of this support would reduce the amplitude and duration of the driven action potential which would reduce their associated K^+ conductances leading to membrane depolarization (as discussed above) and further voltage-dependent inactivation of the remaining activatable Ca^{2+} channels. Although, such a decrease in the Ca^{2+} conductance in the presence of indomethacin can be correlated with the time-dependent decrease in the amplitude of the spontaneous contractions, it cannot explain the contractions to raised K^+ concentrations (20–100 mM) in indomethacin. We therefore believe that it is more likely that the prostanoids help to maintain the electrical coupling between pacemaker and driven regions of the renal pelvis. A reduction of this coupling would reduce the likelihood of action potential discharge in a driven cell upon stimulation by a pacemaker potential. The resulting smaller or failed action potentials would, in turn, lead to a more depolarized diastolic membrane potential.

When driven cells failed to discharge an action potential in the presence of indomethacin, the underlying pacemaker trigger was still present at the same frequency as its pre-indomethacin control frequency, suggesting that these pacemaker cells were little affected. As recordings were infrequently made in pacemaker cells (in only nine cells from >100 recorded cells), we have not yet been able to confirm this suggestion directly. Support of this notion, however, comes from the fact that we could not increase the frequency of the spontaneous contractions of the proximal renal pelvis above its intrinsic frequency before indomethacin inhibition. Also, it has been previously demonstrated in the sheep ureter that the frequency of its spontaneous contractions was not quantitatively related to the measured concentrations of the spontaneously-released prostanoids ($PGF_{2\alpha}$, 6-keto-PGF_1 and thromboxane B_2) (Thulesius *et al.*, 1987).

Direct activation of driven cells with applied dinoprost (300 nM–1.5 μM) resulted in a rapid restoration of action potential discharge in a concentration-dependent manner. In only one cell, was this restoration of action potential discharge accompanied with membrane hyperpolarization, as might be expected from the effects of indomethacin. In fact, the membrane potential was unchanged after 5 min exposure to 300 nM dinoprost and depolarized 2 mV in 1.5 μM dinoprost. These small changes in membrane potential are presumably associated with the Ca^{2+}-dependent tonic contractions of the proximal renal pelvis induced by dinoprost (>100 nM) which were insensitive to dihydropyridine Ca^{2+} channel blockers or depletors of internal Ca^{2+} stores. They must also represent a sizable increase in membrane conductance as they could prevent the after-hyperpolarizations usually associated with each action potential (Figure 7).

In conclusion, we have demonstrated that endogenous prostaglandins maintain the smooth muscle contractility of the renal pelvis by maintaining the ability of 'driven' areas to generate action potentials. This may be as a consequence of changes in the membrane conductances in the driven cells, or as a reduction of the coupling between these cells and their pacemaker cells.

Supported by the N.H. & M.R.C. (Australia).

References

ANGELO-KHATTAR, M., THULESIUS, O., NILSSON, T., CHERIAN, T. & JOSEPH, L. (1985). Motility of the human ureter with special reference to the effects of indomethacin. *Scand. J. Urol. Nephrol.*, **19**, 261–265.

BAUER, A.J., REED, J.B. & SANDER, K.M. (1985). Slow wave heterogeneity within the circular muscle of the canine gastric antrum. *J. Physiol.*, **366**, 221–232.

COLE, R.S., FRY, C.H. & SHUTTLEWORTH, K.E. (1988). The action of the prostaglandins on isolated human ureteric smooth muscle. *Br. J. Urol.*, **61**, 19–26.

CONSTANTINOU, C.E., NEUBARTH, J.L. & MENSAH-DWUMAH, M. (1977). Frequency gradient in the autorhythmicity of the pyeloureteral pacemaker system. *Experientia*, **34**, 614–615.

FLOWER, R.J. (1974). Drugs which inhibit prostaglandin biosynthesis. *Pharmacol. Rev.*, **26**, 33–67.

GOLENHOFEN, K. & HANNAPPEL, J. (1974). Electrical activity in different regions of the pyeloureteral system in the guinea-pig. *Experientia*, **S30**, 33.

GOSLING, J.A. & DIXON, J.S. (1972). Structural evidence in support of an urinary tract pacemaker. *Br. J. Urol.*, **44**, 550–560.

GOSLING, J.A. & DIXON, J.S. (1974). Species variation in the location of upper urinary tract pacemaker cells. *Invest. Urol.*, **11**, 418–423.

HANNAPPEL, J. & LUTZEYER, W. (1978). Pacemaker localization in the renal pelvis of the unicalyceal kidney. *In vitro* study in the rabbit. *Eur. Urol.*, **4**, 192–194.

IMAIZUMI, Y., MURAKI, K. & WATANABE, M. (1989). Ionic currents in single smooth muscle cells from the ureter of the guinea-pig. *J. Physiol.*, **411**, 131–159.

IMAIZUMI, Y., MURAKI, K. & WATANABE, M. (1990). Characteristics of transient outward currents in single smooth muscle cells from the ureter of the guinea-pig. *J. Physiol.*, **427**, 301–324.

KIMOTO, Y. & CONSTANTINOU, C.E. (1991). Regional effects of indomethacin, acetylsalicylic acid and Sc-19220 on the contractility of rabbit renal pelvis (pacemaker regions and pelviureteric junction). *J. Urol.*, **146**, 433–438.

KURIYAMA, H., OSA, T. & TOIDA, N. (1967). Membrane properties of the smooth muscle of guinea-pig ureter. *J. Physiol.*, **191**, 225–238.

KURIYAMA, H. & TOMITA, T. (1970). The action potential in the smooth muscle of the guinea-pig taenia coli and ureter studied by the double sucrose-gap method. *J. Gen. Physiol.*, **55**, 147–162.

LANG, R.J. (1989). Identification of the major membrane currents in freshly dispersed single smooth muscle cells of guinea-pig ureter. *J. Physiol.*, **412**, 375–395.

LANG, R.J. (1990). The whole-cell Ca^{2+}-channel current in single smooth muscle cells of the guinea-pig ureter. *J. Physiol.*, **423**, 453–473.

MAGGI, C.A. (1992). Prostanoids as local modulators of reflex micturition. *Pharmacol. Res.*, **25**, 13–20.

MAGGI, C.A. & GIULIANI, S. (1992). Non-adrenergic non-cholinergic excitatory innervation of the guinea-pig isolated renal pelvis: involvement of capsaicin-sensitive primary afferent neurons. *J. Urol.*, **147**, 1394–1398.

MAGGI, C.A., THEODORSSON, E., SANTICIOLI, P. & GIULIANI, S. (1992). Tachykinins and calcitonin gene-related peptide as co-transmitters in local motor responses produced by sensory nerve activation in the guinea-pig isolated renal pelvis. *Neuroscience*, **46**, 549–559.

PARKINGTON, H.C., TARE, M., TONTA, M.A. & COLEMAN, H.A. (1993). Stretch revealed three components in the hyperpolarization of guinea-pig coronary artery in response to acetylcholine. *J. Physiol.*, **465**, 459–476.

SEKI, N. & SUZUKI, H. (1990). Electrical properties of smooth muscle cell membrane in renal pelvis of rabbits. *Am. J. Physiol.*, **259**, F888–F894.

SHUBA, M.F. (1981). Smooth muscle of the ureter: the nature of excitation and mechanisms of action of catecholamines and histamine. In *Smooth Muscle: an Assessment of Current Knowledge*. ed. Bülbring, E., Brading, A.F., Jones, A.W. & Tomita, T. pp. 377–384. London: Edward Arnold.

SMITH, W.L., MARNETT, L.J. & DEWITT, D.L. (1991). Prostaglandin and thromboxane biosynthesis. *Pharmacol. Ther.*, **49**, 153–179.

THULESIUS, O. & ANGELO-KHATTAR, M. (1985). The effect of indomethacin on the motility of isolated sheep ureters. *Acta Pharmacol. Toxicol.*, **56**, 298–301.

THULESIUS, O., ANGELO-KHATTAR, M. & ALI, M. (1987). The effect of prostaglandin synthesis inhibition on motility of the sheep ureter. *Acta Physiol. Scand.*, **131**, 51–54.

THULESIUS, O., UGAILY-THULESIUS, L. & ANGELO-KHATTAR, M. (1986). Generation and transmission of ovine ureteral contractions, with special reference to prostaglandins. *Acta Physiol. Scand.*, **127**, 485–490.

TSUCHIDA, S. & SUZUKI, T. (1992). Pacemaker activity of the pelvicalyceal border recorded by an intracellular glass microelectrode. *Urol. Int.*, **48**, 121–124.

ZAWALINSKI, V.C., CONSTANTINOU, C.E. & BURNSTOCK, G. (1975). Ureteral pacemaker potentials recorded with the sucrose gap technique. *Experientia*, **S31**, 931–933.

ZHANG, Y. & LANG, R.J. (1993). Effects of K^+ and Ca^{2+}-channel blockers on the spontaneous electrical and mechanical activity in the guinea-pig renal pelvis. *Aust. Physiol. Pharmacol. Soc.*, **24**, 167P.

ZHANG, Y., VOGALIS, F. & LANG, R.J. (1994). The effects of intrinsic prostaglandins on the contractile and electrical activity recorded in the guinea-pig renal pelvis. *Proc. Aust. Neurosci. Soc.*, **5**, P121.

ZWERGEL, U.E., ZWERGEL, T.B., NEISIUS, D.A. & ZIEGLER, M. (1990). Effects of prostaglandin synthetase inhibitors on the upper urinary tract. Experimental studies on isolated preparations and urodynamic measurements in man. *Urol. Res.*, **18**, 429–433.

(Received March 21, 1994
Revised June 9, 1994
Accepted June 17, 1994)

Br. J. Pharmacol. (1994), **113**, 439–444 © Macmillan Press Ltd, 1994

Inhibition of glucocorticoid-induced epidermal and dermal atrophy with KH 1060 – a potent 20-epi analogue of 1,25-dihydroxyvitamin D_3

[1]Robert Gniadecki, *Monika Gniadecka & Jørgen Serup

Department of Dermatological Research, Leo Pharmaceutical Products, Industriparken 55, 2750 Ballerup, Denmark, and *Department of Dermatology, Bioengineering and Skin Research Laboratory, University of Copenhagen, Bispebjerg Hospital, Bispebjerg Bakke 23, 2400 Copenhagen, Denmark

1 The possibility of preventing and treating glucocorticoid-induced skin atrophy with KH 1060 (the potent 20-epi-22-oxa-24a-homo-26,27-dimethyl analogue of 1,25-dihydroxyvitamin D_3) was examined in a hairless mouse model.

2 KH 1060 (0.625–6.25 pmol cm^{-2} of skin) applied topically for 7 days together with 2.5 nmol cm^{-2} betamethasone-17-valerate prevented, in a concentration-dependent manner, the development of epidermal, dermal and total skin thinning caused by the glucocorticoid. The effect of KH 1060 on the epidermis occurred at a lower dose than on the dermis, and at doses above 1.25 pmol cm^{-2} KH 1060 caused epidermal hyperplasia.

3 KH 1060 (2.5 pmol cm^{-2}) prevented the development of betamethasone-associated skin atrophy in mice during a long-term (4 weeks) treatment, and reversed established cutaneous glucocorticoid atrophy.

4 Radiolabelling experiments with [^{35}S]-sulphate and [^{3}H]-proline *in vivo* revealed that KH 1060 stimulated the synthesis of sulphated glycosaminoglycans and hydroxyproline in skin treated with betamethasone.

5 These findings strongly suggest that KH 1060 prevents and reverses glucocorticoid-induced skin atrophy by stimulating epidermal proliferation and enhancing synthesis of extracellular matrix in the dermis.

Keywords: Vitamin D-analogues; glucocorticoid-side effects; skin atrophy; murine skin; KH 1060

Introduction

Treatment with glucocorticoids, both topical and systemic, is frequently associated with side effects on the skin, i.e. epidermal atrophy, dermal thinning and fragility, striae, telangiectasia, purpura and impaired wound healing (Jablonska *et al.*, 1979; Lehman *et al.*, 1983; Teillac *et al.*, 1987). These effects are related to the antiproliferative activity of glucocorticoids on epidermal cells (keratinocytes) and fibroblasts and the inhibitory effects on glycosaminoglycan (GAG) and collagen production in the connective tissue of the skin (Bateman, 1989).

Receptors for the vitamin D hormone (1,25-dihydroxyvitamin D_3) have been found recently in a variety of cells present in the skin: keratinocytes, dermal fibroblasts, and endotheliocytes (Walters, 1992). It has been suggested that the vitamin D_3 hormone plays a role in the regulation of keratinocyte growth (Pillai *et al.*, 1988). The receptor-specific effects of 1,25-dihydroxyvitamin D_3 may be elicited by the use of the synthetic analogues of the hormone. One of the most potent analogues is KH 1060, a 20-epi-22-oxa-24a-homo-26,27-dimethyl derivative of 1,25-dihydroxyvitamin D_3 (Binderup *et al.*, 1991). We have recently observed that KH 1060 causes epidermal hyperplasia, dermal thickening, and stimulates GAG synthesis in the skin of hairless mice after topical application (Gniadecki *et al.*, 1994). The effects of KH 1060 were significantly (2–3 times) greater than those of 1,25-dihydroxyvitamin D_3, even when the latter hormone was given in the highest non-lethal concentrations. In this study we have examined whether these stimulatory properties of KH 1060 could be exploited to prevent skin atrophy caused by the topical application of betamethasone-17-valerate.

[1] Author for correspondence.

Methods

Animals and topical application of the drugs

Hairless C3H mice (females, strain *hr/hr* C3H/Tif Bom, wt. approx. 20 g) that are homozygotic mutants in the recessive *hr* locus were used. This mutation causes an abnormal development of the hair club; as a result the hair shaft fails to grow towards the skin surface and becomes buried in the deep dermis forming keratinized cysts (Mann, 1971). Once a day, 50 µl of each drug solution was applied on the back with a micropipette at 3 min intervals, and smeared evenly with gloved finger on approx. 8 cm^2 of the dorsal skin.

The following sets of experiments were performed:
(1) Mice were treated for 1 week with either 2.5 nmol cm^{-2} betamethasone combined with different doses of KH 1060 (0.625–6.25 pmol cm^{-2}) or with 2.5 nmol cm^{-2} betamethasone and the vehicle. Betamethasone at a dose of 2.5 nmol cm^{-2} (i.e. 20 nmol/mouse/day) did not produce systemic effects (cachexia) whereas skin atrophy was consistently observed. A control group was treated only with the vehicle.
(2) Three groups of animals were treated for 4 weeks with: (a) 2.5 nmol cm^{-2} betamethasone with 2.5 pmol cm^{-2} KH 1060, (b) 2.5 nmol cm^{-2} betamethasone with the vehicle, (c) the vehicle.
(3) Mice were treated for 2 weeks with 2.5 nmol cm^{-2} betamethasone to induce skin atrophy. Subsequently animals were divided into two groups and treated for 4 weeks with betamethasone (2.5 nmol cm^{-2}) combined with 2.5 pmol cm^{-2} KH 1060, or vehicle.

Measurement of skin atrophy

Cutaneous atrophy, defined as thinning of the skin, was characterized by four different parameters: (a) skin-fold thickness, (b) total skin thickness measured *in vivo* with

high-frequency high-resolution ultrasound, and (c) epidermal and (d) dermal thickness in histological sections of the skin.

Skin-fold thickness was measured with callipers (Käfer, Germany) on the dorsal skin within the treatment area. This technique is reproducible (in our hands the standard deviation of duplicate measurements was 1.9% of the mean value); however, the results may be influenced by trapping of connective tissue between layers of dermis in the skin-fold.

High frequency ultrasonograph (20 MHz, Dermascan C, Cortex Technology, Hadsund, Denmark) was used to obtain B-mode, cross-sectional images of the treated skin (Serup, 1992). Gain was set from 20 to 45 at 0–30 mm, zoom at the first magnification in the horizontal axis, and the ultrasound velocity at 1580 m s^{-1}. The following skin layers were identified: outer hyperechogenic epidermal entrance echo, dermis with subcutis, underlying low echogenic loose connective tissue, and hyperechogenic muscular fascia. The thickness between the epidermal entrance echo and the low echogenic connective tissue was measured using the 'distance' function of the scanner. Reproducibility of the ultrasound method was slightly lower than that of skin-fold (standard deviation of duplicate measurements was 7.4% of the mean value). However, in contrast to the skin-fold method, the thickness could be determined precisely between anatomical layers of the skin.

For histological evaluation mice were killed by cervical dislocation, the dorsal skin was carefully dissected and stretched to the natural size on the Millipore MF filter. Punch biopsies (diameter 8 mm) were obtained, fixed in 10% buffered formalin, and embedded in paraffin. Five micron thick sections were cut, stained with haematoxylin and eosin, and a representative section of each biopsy was selected for histological studies. The thickness of the epidermis and dermis was measured using a microscope with a micrometer in the eyepiece. The advantage of histometry, compared to the skin-fold and ultrasonography techniques, is the possibility of measurement of epidermal and dermal thickness separately. However, this method suffers from relatively low reproducibility caused by an uneven thickness of the epidermis and dermis (standard deviation of duplicate measurements was approximately 20% of the mean value). Moreover, histometry does not provide reliable information about skin thickness *in vivo* since results are affected by tissue distortion and contraction caused by water and fat removal during histological processing (Gordon, 1990; Kiernan, 1990; Gniadecki *et al.*, 1993; Salmhofer *et al.*, 1993).

All determinations were repeated twice and the mean value was used for subsequent statistical analyses.

Radiolabelling studies

To determine the incorporation of [^{35}S]-sulphate and [^{3}H]-proline into GAGs and hydroxyproline, respectively, mice were treated topically for 7 days on the contralateral sides of the back with 2.5 nmol cm^{-2} betamethasone on one side, and the same dose of betamethasone combined with 0.625, 2.5, and 6.25 pmol cm^{-2} KH 1060 on the other. On the fifth day of treatment 10 μCi of [^{35}S]-sulphate and [^{3}H]-proline were injected intraperitoneally, mice were killed 48 h later and skin punch biopsies were obtained as described above. GAGs were precipitated with 1% cetylpyridinium chloride from skin papain digests according to Schiller *et al.* (1961) and hydroxyproline purified from the skin according to Juva & Prockop (1966). Radioactivity in GAGs and hydroxyproline were determined with a Minaxi 443 (United Technologies, U.S.A.) β scintillation counter.

Serum calcium concentration

Blood was collected from animals in experimental groups 1 and 2 by cardiac puncture, and sera were assayed for calcium concentration using a Hitachi 705 autoanalyser.

Drugs and solutions

KH 1060 [1(S), 3(R)-dihydroxy-20(R)-(4'-hydroxy-4'-ethyl-1'-hexyloxy)-9, 10-seco-pregna-5(Z),7(E),10(19)-triene] (Hansen *et al.*, 1991) was obtained from the Chemical Research Department, Leo Pharmaceutical Products, Denmark. Receptor binding studies of KH 1060 are described elsewhere (Binderup *et al.*, 1991). Betamethasone-17-valerate was purchased from Glaxo (U.S.A.). Solutions of KH 1060 (0.1–1 μM) and betamethasone (0.4 mM) were prepared in a vehicle of 1:1.2 w/w isopropyl alcohol/water mixture buffered with 1 g l^{-1} sodium citrate dihydrate (pH 8.9). [^{35}S]-sulphate and [^{3}H]-proline were purchased from Amersham International (UK).

Statistical analysis

Data are presented as mean ± s.e.mean. The differences between groups were analysed with a *t* test for independent samples, except for the radiolabelling data when a paired *t* test was used. The serial measurements of skin-fold thickness were analysed according to the concept described by Matthews *et al.* (1990): the average changes during treatment were calculated for each mouse after each week of treatment and used as summary measures of the response to the treatment. The summary measures were compared across treatment groups with a two-sample *t* test or tested versus the baseline (no change) with a one-sample *t* test. All *t* tests were two-sided. For the dose-response experiments an analysis of regression was performed with Minitab statistical software (Release 7, Minitab, Inc., State College, U.S.A.). EC_{50} (dose of KH 1060 reducing the response to betamethasone by 50%) was predicted from the regression equations.

Results

Prevention of betamethasone-induced skin atrophy with KH 1060

Effects of 1-week topical treatment with betamethasone

Betamethasone-17-valerate, applied in a dose of 2.5 nmol cm^{-2}, caused significant thinning of the skin: skin-fold thickness and skin thickness measured with ultrasound were

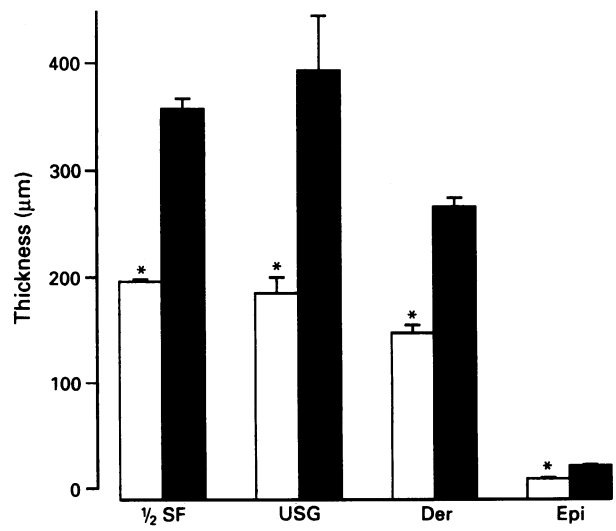


Figure 1 Effect of 2.5 nmol cm^{-2} betamethasone-17-valerate (open columns) and the vehicle (solid columns) on the thickness of total skin (½SF: skin-fold thickness divided by 2; USG: skin thickness determined with the high-frequency ultrasound), dermis (Der), and epidermis (Epi). Drugs were applied topically once a day for 1 week, 5 mice in a group. Each column represents the mean, with s.e.mean. *$P<0.001$ compared with the vehicle group.

decreased compared to the vehicle-treated mice (Figure 1). Both epidermal and dermal thinning were observed histologically after betamethasone application (Figure 1 and 2b). The number of cell layers in the epidermis was reduced to one from 2–3 in the control skin.

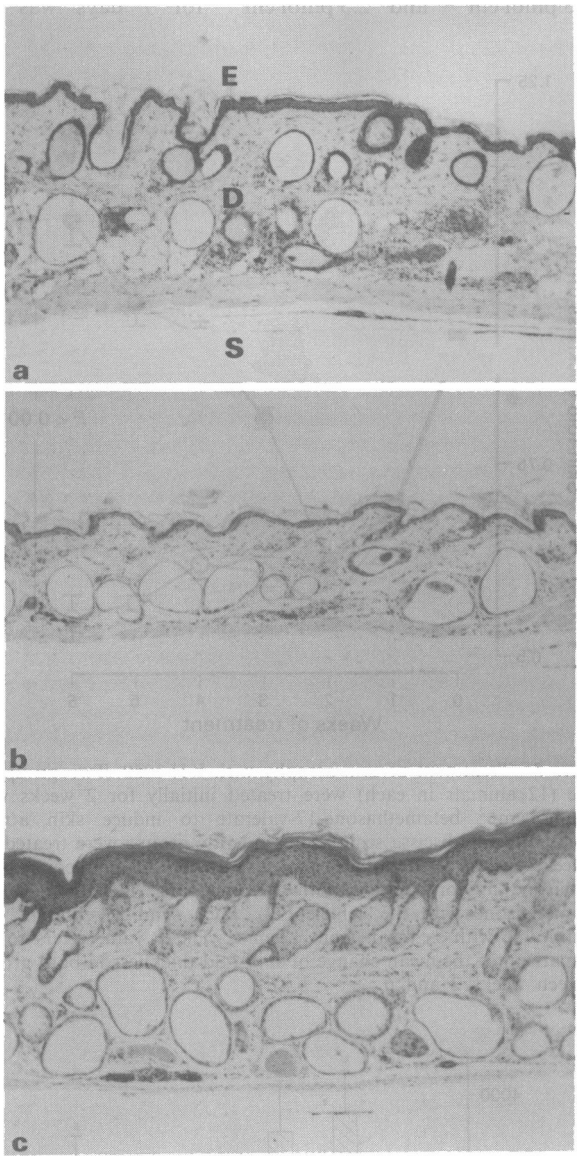


Figure 2 Histological appearance of skin treated for 1 week with the vehicle (a), 2.5 nmol cm^{-2} betamethasone-17-valerate (b), 2.5 nmol cm^{-2} betamethasone-17-valerate and 2.5 nmol cm^{-2} KH 1060 (c). Sections (5 μm, paraffin embedded) were stained with haematoxylin and eosin. Epidermis is marked with E, dermis with D, subcutaneous tissue with S. Bar: 150 μm.

Effects of 1-week treatment with betamethasone and KH 1060
KH 1060 prevented thinning of the skin-fold and the total skin measured with ultrasound in a concentration-dependent manner (EC_{50} = 1.44 ± 0.25 pmol cm^{-2} and 1.94 ± 0.25 pmol cm^{-2}, respectively; Figure 3). The EC_{50} dose of KH 1060 which prevented epidermal thinning was lower than the corresponding value for the dermis (0.62 ± 0.06 pmol cm^{-2} vs 2.19 ± 0.19 pmol cm^{-2}, respectively). Concentrations of KH 1060 above 1.25 pmol cm^{-2} caused epidermal hyperplasia with characteristic features of mitotic activation of basal keratinocytes (Figures 2 and 3).

Effects of 4 week treatment with betamethasone and KH 1060
The anti-atrophic effect of KH 1060 was stable with time: during the 4 week treatment with betamethasone and 2.5 pmol cm^{-2} KH 1060 the drop in skin-fold thickness was prevented (Figure 4). Ultrasonography based measurements of total skin thickness and histometric analysis confirmed the results of skin-fold measurements and revealed that epidermal and dermal thickness was prevented with KH 1060 (Table 1). The histological picture of the skin was similar to that observed after 1 week of treatment.

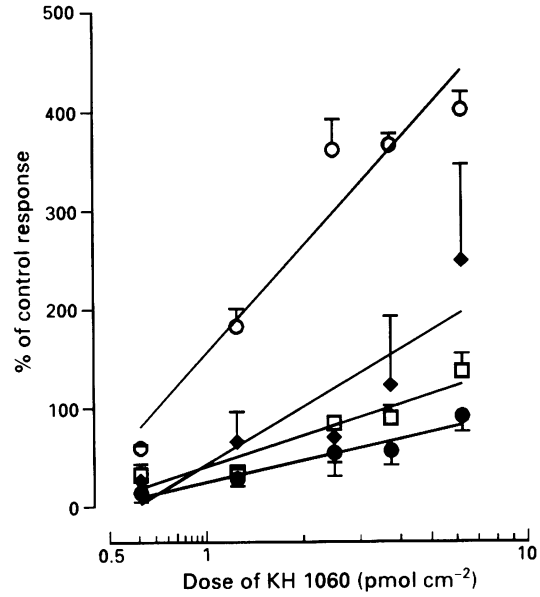


Figure 3 Prevention of skin atrophy induced by betamethasone-17-valerate with KH 1060. Animals were topically treated for 7 days with 2.5 nmol cm^{-2} betamethasone-17-valerate and 0.625–6.25 pmol cm^{-2} KH 1060. Epidermal (○) and dermal (●) thickness was measured histologically, total skin thickness (◆) was evaluated with high-frequency ultrasound, and skin-fold thickness (□) was determined with callipers. Each symbol represents mean ($n = 5$) with s.e.mean (vertical bars). Regression lines are fitted with the least square method.

Table 1 Influence of 2.5 nmol cm^{-2} betamethasone-17-valerate and betamethasone in combination with 2.5 pmol cm^{-2} KH 1060 on epidermal, dermal and total skin thickness in mice

Drugs (topical treatment for 4 weeks)	*Total skin*[a] (μm)	*Epidermis*[b] (μm)	*Dermis*[b] (μm)
Betamethasone	230 ± 20*	9 ± 1*	158 ± 7*
Betamethasone plus KH 1060	390 ± 30**	53 ± 3***	203 ± 15***
Vehicle	410 ± 20	21 ± 2	275 ± 11

[a]Measured with the high-frequency ultrasound
[b]Measured with histometry
*$P < 0.001$ compared to the vehicle
**$P < 0.001$ compared to betamethasone treatment, $P > 0.05$ compared to the vehicle
***$P < 0.01$ compared to the betamethasone and the vehicle groups

Treatment of betamethasone-induced skin atrophy with KH 1060

To investigate whether KH 1060 might not only prevent, but also reverse, pre-existing steroid skin atrophy, skin thinning was produced in mice by the topical application of 2.5 nmol cm^{-2} betamethasone for 2 weeks (Figure 5). Subsequently these mice were treated for 4 weeks either with 2.5 nmol cm^{-2} betamethasone combined with 2.5 pmol cm^{-2} KH 1060 or the same dose of betamethasone with the vehicle. Addition of KH 1060 to betamethasone caused a gradual increase in skin thickness (Figure 5). KH 1060 restored the thickness of both epidermis (62 ± 18 μm vs 6 ± 3 μm in the betamethasone treated group, $P < 0.001$) and dermis (230 ± 29 μm vs 139 ± 19 μm in the betamethasone treated group, $P = 0.02$).

Stimulation of synthesis of sulphated GAGs and hydroxyproline

Both [^{35}S]-sulphate and [^{3}H]-proline incorporation in the betamethasone-treated skin was increased by 2.5 pmol cm^{-2} KH 1060 (Figure 6). KH 1060 at a low dose of 0.625 pmol cm^{-2} did not significantly change the incorporation of the isotopes when compared to the betamethasone treated site. At 6.25 pmol cm^{-2}, KH 1060, the [^{35}S]-sulphate and [^{3}H]-proline labelling were not significantly different from the values obtained with 2.5 pmol cm^{-2} KH 1060.

Effects of KH 1060 on serum calcium

Treatment with KH 1060 at doses of 0.625 pmol cm^{-2}, 1.25 pmol cm^{-2} and 2.5 pmol cm^{-2} for 7 days was not

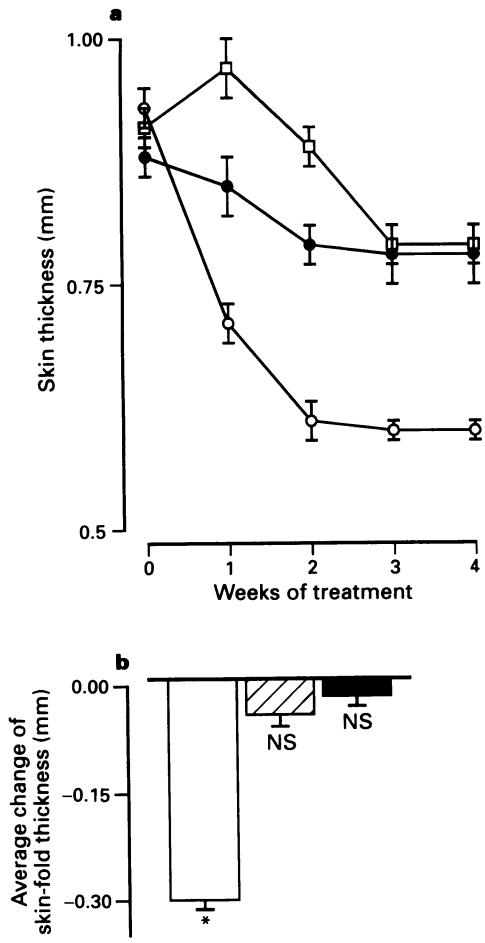


Figure 4 Long-term prevention of betamethasone-induced skin atrophy with KH 1060. (a) Effect of topical treatment with 2.5 nmol cm^{-2} betamethasone (○), betamethasone in combination with 2.5 nmol cm^{-2} KH 1060 (●) and the vehicle (□) on skin-fold thickness in hairless mice. Each symbol represents the mean with s.e.mean from 14 mice. (b) Calculated average changes in skin-fold thickness for the group treated with 2.5 nmol cm^{-2} betamethasone (open columns), betamethasone in combination with 2.5 nmol cm^{-2} KH 1060 (hatched column) and the vehicle (solid column). $*P < 0.001$ vs vehicle and betamethasone + KH 1060 groups (two-sample t test), $P < 0.001$ vs the baseline (one-sample t test). NS: non-significant change vs baseline (one-sample t test).

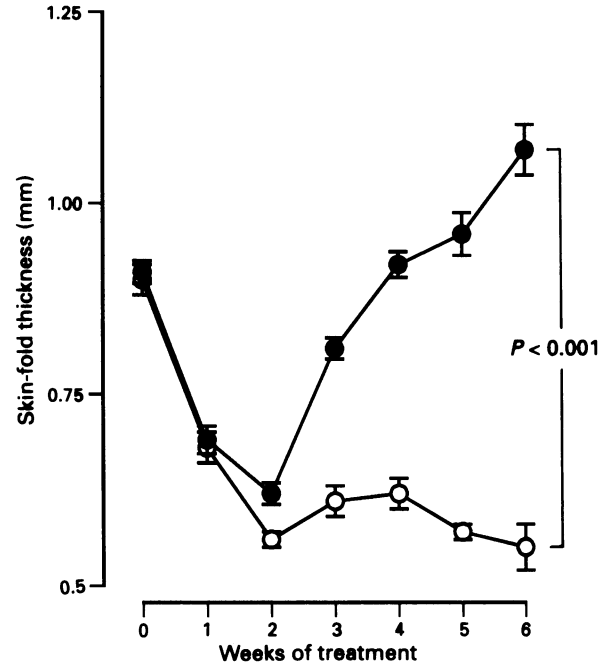


Figure 5 Treatment of skin atrophy with KH 1060. Two groups of mice (12 animals in each) were treated initially for 2 weeks with 2.5 nmol cm^{-2} betamethasone-17-valerate to induce skin atropy (weeks 0–2 on abscissa scale). Subsequently groups were treated for 4 weeks (weeks 2–6 on abscissa scale) with 2.5 nmol cm^{-2} betamethasone in combination with 2.5 pmol cm^{-2} KH 1060 (●) or betamethasone with the vehicle (○). Each symbol represents the mean value with s.e.mean from 12 mice. The P value refers to the comparison of the mean change of skin-fold thickness in both groups between weeks 2 and 6.

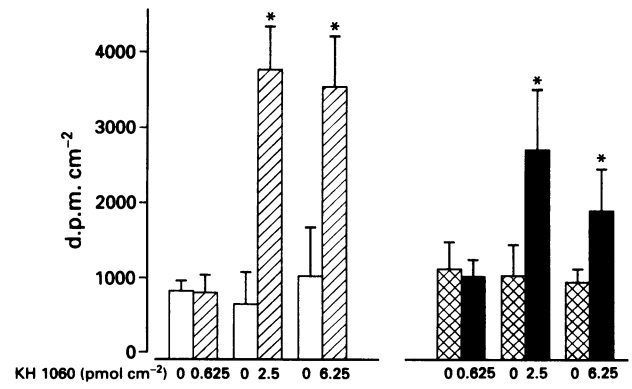


Figure 6 Effect of KH 1060 on incorporation of [^{35}S]-sulphate into glycosaminoglycans and synthesis of hydroxyproline from [^{3}H]-proline in the skin treated with betamethasone-17-valerate. Skin was treated on the contralateral sites of the back with 2.5 nmol cm^{-2} betamethasone and 2.5 nmol cm^{-2} betamethasone and KH 1060 (0.625–6.25 pmol cm^{-2}). Open and hatched columns represent respectively: ^{35}S and ^{3}H-labelling of the control skin treated only with betamethasone-17-valerate. Cross-hatched and solid columns show ^{35}S and ^{3}H labelling in the KH 1060 treated sites, respectively. Each column represents mean ($n = 6$) with s.e.mean. Ordinates: specific radioactivity in disintegrations per minute per cm^2 of the skin. $*P < 0.05$ vs control.

associated with elevation of serum calcium concentrations (2.45 ± 0.36 mM, 2.52 ± 0.42 mM, and 2.6 ± 0.61 mM, respectively vs 2.42 ± 0.39 mM in the control group). However, when higher (3.75 pmol cm^{-2} and 6.25 pmol cm^{-2}) doses of KH 1060 were used hypercalcaemia became evident (2.92 ± 0.43 mM and 3.12 ± 0.49 mM, $P < 0.001$ vs the vehicle). After a 4 week treatment period with 2.5 pmol cm^{-2} KH 1060 and betamethasone, calcaemia was not increased (2.43 ± 0.42 mM vs. 2.42 ± 0.39 mM in the vehicle-treated group).

Discussion

The hairless mouse model has been widely used to examine the atrophogenicity of topical glucocorticoids (van den Hoven *et al.*, 1991; Woodbury & Kligman, 1992). To induce skin atrophy we chose betamethasone-17-valerate, since this drug has been commonly used in clinical practice and has strong atrophogenic properties both in man and in hairless mice (van den Hoven *et al.*, 1991; Korting *et al.*, 1992). In hairless mice treatment with a glucocorticoid induced skin atrophy, which was characterized by thinning of the epidermis and dermis and a drop in the total skin thickness. Epidermal and dermal thickness were measured histometrically. Moreover, to rule out the error induced by tissue shrinkage and distortion during histological processing we measured the thickness of the skin intravitally: with callipers as skin-fold thickness and using ultrasound imaging. All the methods showed consistently that KH 1060 in a concentration-dependent manner was capable of preventing skin atrophy imposed by short term (7 days) treatment with betamethasone. Both epidermal and dermal atrophy were suppressed, however a comparison of EC_{50} values showed that the effect of KH 1060 on the epidermis was observed at lower doses than the effects on the dermis.

Epidermal atrophy during corticosteroid treatment is caused by the direct suppression of keratinocyte proliferation by these hormones (Bateman, 1989; Oikarinen & Autio, 1991). 1,25-dihydroxyvitamin D_3 and its analogues, including KH 1060, regulate keratinocyte proliferation in a complex manner. In the hyperproliferative states, as in psoriasis, and in keratinocyte cell culture, they suppress proliferation, while in normal skin they exert the opposite effect causing epidermal hyperplasia (Hosomi *et al.*, 1983; Bikle, 1992; Lützow-Holm *et al.*, 1992). The histological evaluation of epidermis treated with betamethasone and KH 1060 revealed features of mitotic activation of basal keratinocytes and epidermal hyperplasia. Therefore, it is conceivable that the stimulation of keratinocyte proliferation by KH 1060 was responsible for counteracting the suppressive effects of the glucocorticoid.

Glucocorticoids cause connective tissue damage and dermal thinning principally by inhibiting collagen and GAG synthesis (Saarni *et al.*, 1980; Durant *et al.*, 1986; Bateman, 1989). KH 1060 restored dermal thickness in betamethasone-treated animals, and promoted the incorporation of radiolabelled sulphate in the GAGs and synthesis of hydroxyproline from proline, thus reversing the effect of the glucocorticoid. The labelling was maximal when a 2.5 pmol cm^{-2} concentration of KH 1060 was used. At the higher concentration of 6.25 pmol cm^{-2} a slight decrease in isotope incorporation was observed. This might have been due to a non-specific effect of the systemic hypercalcaemia imposed by KH 1060 at this high concentration. The influence of 1,25-dihydroxyvitamin D_3 and its analogues on the connective tissues has not been fully elucidated. Our recent investigations showed that KH 1060 promotes synthesis of sulphated GAGs and collagen in normal skin, probably by the induction of transforming growth factor $\beta 1$ expression (Gniadecki *et al.*, 1994). It is conceivable that the same mechanism operated during inhibition of corticosteroid-induced dermal atrophy.

To examine whether the effect of KH 1060 was persistent we extended the treatment period to 4 weeks. In this study a single dose of 2.5 pmol cm^{-2} KH 1060 was used, as at this concentration KH 1060 strongly inhibited skin atrophy without the concomitant induction of systemic hypercalcaemia. The results showed that the activity of KH 1060 does not decrease with time. Moreover, treatment with KH 1060 not only protected against epidermal and dermal thinning imposed by betamethasone, but also reversed skin atrophy caused by the 2 weeks pretreatment with the glucocorticoid.

Corticosteroid-induced dermal and epidermal atrophy may be partially inhibited by retinoids (Lesnick *et al.*, 1989; Schwartz *et al.*, 1994). In view of the recent studies which show dependence of vitamin D receptor signalling on the retinoic X receptor (Carlberg *et al.*, 1993) it is conceivable that 1,25-dihydroxyvitamin D_3, and probably the analogue KH 1060, utilise intracellular pathways similar to those of retinoids to stimulate the repair of skin damaged by corticosteroids.

Both glucocorticoids and vitamin D analogues are used in the therapy of psoriasis. It remains to be seen whether these two drugs in combination prevent glucocorticoid-induced dermal atrophy in the patients. It would also be of interest to examine whether vitamin D analogues prevent glucocorticoid epithelial and connective tissue damage in other organs, such as in the gastric mucosa and bone.

The authors wish to thank Dr Signe Birk Jensen from Department of Statistics for her help in data analysis and Mrs Pavla Setina for her technical assistance. Dr Martin Calverley is acknowledged for the linguistic revision of the manuscript.

References

BATEMAN, D.N. (1989). Clinical Pharmacology of topical steroids. In *Pharmacology of the Skin II.* ed. Greaves, M.W. & Shuster, S. pp. 239–249. Berlin: Springer-Verlag.

BIKLE, D.D. (1992). Vitamin D: new actions, new analogs, new therapeutic potential. *Endocr. Rev.*, **13**, 765–784.

BINDERUP, L., LATINI, S., BINDERUP, E., BRETTING, C., CALVERLEY, M. & HANSEN, K. (1991). 20-epi-vitamin D_3 analogues: a novel class of potent regulators of cell growth and immune responses. *Biochem. Pharmacol.*, **42**, 1569–1575.

CARLBERG, C., BENDIK, I., WYSS, A., MEIER, E., STURZENBECKER, L.J., GRIPPO, J.F. & HUNZIKER, W. (1993). Two nuclear signalling pathways for vitamin D. *Nature*, **361**, 657–660.

DURANT, S., DUVAL, D. & HOMO-DELARCHE, F. (1986). Factors involved in the control of fibroblast proliferation by glucocorticoids: a review. *Endocr. Rev.*, **7**, 254–269.

GNIADECKI, R., FULLERTON, A., KEIDING, J. & SERUP, J. (1993). Ultrasound examination of experimental animals. 3rd Conference of the International Society for Ultrasound and the Skin: *Imaging Techniques and the Skin.* Elsinore, Denmark, September 22–25.

GNIADECKI, R., GNIADECKA, M. & SERUP, J. (1994). The effects of KH 1060, a potent 20-epi analogue of the vitamin D_3 hormone, on hairless mouse skin *in vivo*. *Br. J. Dermatol.*, (in press).

GORDON, K.C. (1990). Tissue processing. In *Theory and Practice of Histological Techniques.* ed. Bancroft, J.P. & Stevens, A. pp. 43–59. Edinburgh: Churchill Livingstone.

HANSEN, K., CALVERLEY, M. & BINDERUP, L. (1991). Synthesis and biological activity of 22-oxa vitamin D analogues. In *Vitamin D. Gene Regulation, Structure-Function Analysis and Clinical Application.* ed. Norman, A.W., Bouillon R. & Thomasset, M. pp. 161–162. Berlin, New York: Walter de Gruyter.

HOSOMI, J., HOSOI, J, ABE, E., SUDA, T. & KUROKI, T. (1983). Regulation of terminal differentiation of culture mouse epidermal cells by 1α,25-dihydroxyvitamin D_3. *Endocrinology*, **113**, 1950–1957.

JABLONSKA, S., GRONIOWSKI, M. & DABROWSKI, J. (1979). Comparative evaluation of skin atrophy in man induced by topical corticoids. *Br. J. Dermatol.*, **100**, 193–206.

JUVA, K. & PROCKOP, D.J. (1966). Modified procedure for the assay of ^{3}H or ^{14}C labelled hydroxyproline. *Anal. Biochem.*, **15,** 77–83.

KIERNAN, J.A. (1990). *Histological and Histochemical Methods: Theory and Practice.* pp. 36–48. New York: Pergamon Press.

KORTING, H.C., VIELUF, D. & KERSCHER, M. (1992). 0.25% Prednicarbate cream and the corresponding vehicle induce less skin atrophy than 0.1% Betamethasone-17-valerate cream and 0.05% Clobetasol-17-propionate cream. *Eur. J. Clin. Pharmacol.*, **42,** 159–161.

LEHMAN, P., ZHENG, P., LAVKER, R.M & KLIGMAN, A.M. (1983). Corticosteroid atrophy in human skin. A study by light, scanning, and transmission electron microscopy. *J. Invest. Dermatol.*, **81,** 169–176.

LESNICK, R.H., MEZICK, J.A., CAPETOLA, R. & KLIGMAN, L.H. (1989). Topical all-trans-retinoic acid prevents corticosteroid-induced skin atrophy without abrogating the anti-inflammatory effect. *J. Am. Acad. Dermatol.*, **21,** 186–190.

LÜTZOW-HOLM, C., HUITFELDT, H., BRANDTZAEG, P. & CLAUSTEN, O.P.F. (1992). 1,25 dihydroxyvitamin D_3 and the vitamin D analogue KH 1060 induce hyperproliferation in normal mouse epidermis. *J. Invest. Dermatol.*, **98,** 525 (abstract).

MANN, S.J. (1971). Hair loss and cyst formation in hairless and rhino mutant mice. *Anat. Rec.*, **170,** 485–499.

MATTHEWS, J.N.S., ALTMAN, D.G., CAMPBELL, M.J. & ROYSTON, P. (1990). Analysis of serial measurements in medical research. *Br. Med. J.*, **300,** 230–235.

OIKARINEN, A. & AUTIO, P. (1991). New aspects of the mechanism of corticosteroid-induced dermal atrophy. *Clin. Exp. Dermatol.*, **16,** 416–419.

PILLAI, S., BIKLE, D.D. & ELIAS, P.M. (1988). 1,25-dihydroxyvitamin D production and receptor binding in human keratinocytes varies with differentiation. *J. Biol. Chem.*, **263,** 5390–5395.

SAARNI, H., JALKANEN, M. & HOPSU-HAVU, V.K. (1980). Effects of five anti-inflammatory steroids on collagen and glycosaminoglycan synthesis *in vitro*. *Br. J. Dermatol.*, **103,** 167–173.

SALMHOFER, W., RIEGER, E., SOYER, H.P., SMOLLE, J. & KERL, H. (1993). The influence of skin tension and formalin fixation on sonographic measurement of tumor thickness and correlation with histologic tumor thickness. 3rd Conference of the International Society for Ultrasound and the Skin: *Imaging Techniques and the Skin.* Elsinore, Denmark, Sept. 22–25.

SCHILLER, S., SLOVER, G.A. & DORFMAN, A. (1961). Method for the separation of acid mucopolisaccharides: its application to the isolation of heparin from the skin of rats. *J. Biol. Chem.*, **236,** 983–987.

SCHWARTZ, E., MEZICK, J.A., GENDIMENICO, G.J. & KLIGMAN, L.H. (1994). *In vivo* prevention of corticosteroid-induced skin atrophy by tretinoin in the hairless mouse is accompanied by modulation of collagen, glycosaminoglycan, and fibronectin. *J. Invest. Dermatol.*, **102,** 241–246.

SERUP, J. (1992). Ten years' experience with high-frequency ultrasound examination of the skin: development and refinement of technique and equipment. In *Ultrasound in Dermatology.* ed. Altmeyer, P., el-Gammal, S. & Hoffmann, K. pp. 41–54. Berlin, Heidelberg, New York, London, Paris, Tokyo, Hong-Kong, Barcelona, Budapest: Springer-Verlag.

TEILLAC, D., DE PROST, Y., DEBURE, A., LEVEQUE, J.L., SAINT LEGER, D., ESCOFFIER, C., DUCASSE, M.F., NARET, C. & KREIS, H. (1987). Clinical and biophysical studies of the skin in renal allograft patients. *Clin. Transpl.*, **1,** 195–197.

VAN DEN HOVEN, W.E., VAN DEN BERG, T.P. & KORSTANJE, C. (1991). The hairless mouse as a model for study of local and systemic atrophogenic effects following topical application of corticosteroids. *Acta Derm. Venereol (Stockholm)*, **71,** 29–31.

WALTERS, M.R. (1992). Newly identified actions of the vitamin D endocrine system. *Endocr. Rev.*, **13,** 719–764.

WOODBURY, R. & KLIGMAN, A.M. (1992). The hairless mouse model for assaying the atrophogenicity of topical corticosteroids. *Acta Derm. Venereol. (Stockholm)*, **72,** 403–406.

(Received September 13, 1993
Revised May 29, 1994
Accepted June 16, 1994)

Br. J. Pharmacol. (1994), **113**, 445–450 © Macmillan Press Ltd, 1994

Role of phosphodiesterases III and IV in the modulation of vascular cyclic AMP content by the NO/cyclic GMP pathway

[1]Anita E. Eckly & Claire Lugnier

Université Louis Pasteur de Strasbourg, Laboratoire de Pharmacologie Cellulaire et Moléculaire, CNRS URA 600, B.P. 24,67401 Illkirch, France

1 The effect on cyclic nucleotide contents of selective inhibitors of cyclic nucleotide phosphodiesterase (PDE) isoforms III and IV (respectively SK&F 94120 and rolipram) and their interactions with endothelium and NO have been studied in rat aorta in the presence of indomethacin (10 μM). The participation of NO was assessed by using either N^G-nitro-L-arginine methyl ester (L-NAME) (NO synthase inhibitor: 30 μM) or 3-morpholinosydnonimine (SIN-1, NO donor: 10 μM with SOD 100 units ml^{-1}).

2 The presence of endothelium significantly increased both adenosine 3':5'-cyclic monophosphate (cyclic AMP, 1.7 fold) and guanosine 3':5'-cyclic monophosphate (cyclic GMP, 2.2 fold) contents. Cyclic GMP was largely affected by L-NAME or SIN-1 treatment, this was not the case for cyclic AMP suggesting that the presence of endothelium modified cyclic AMP content in aorta independently of the NO production.

3 In the presence or absence of endothelium, neither SK&F 94120 nor rolipram, alone or combined, significantly modified cyclic GMP content.

4 The PDE III inhibitor significantly affected cyclic AMP content only in non treated aorta without endothelium. In contrast, the PDE IV inhibitor increased cyclic AMP in all conditions. These increases were generally about 2 fold but markedly higher in aorta treated with SIN-1 and superoxide dismutase (SOD, 6 fold). Association of a low concentration of the PDE III inhibitor (5 μM) with the PDE IV inhibitor (30 μM) potentiated the effect of the PDE IV inhibitor on cyclic AMP content, except for aorta without endothelium treated with SIN-1 plus SOD.

5 These data indicate that the presence of the endothelium could increase cyclic AMP content independently of NO and prostacyclin (PGI_2) production. Furthermore, an increase in cyclic GMP content (modulated by NO production) could enhance the cyclic AMP accumulation induced by the PDE IV inhibitor. This result supports the hypothesis that PDE III inhibition by endogenous cyclic GMP may potentiate the effect of PDE IV inhibition on cyclic AMP content. Taken together with our previous studies on relaxation, these results suggest that the NO/cyclic GMP pathway could induce PDE IV-dependent regulation of cyclic AMP via PDE III inhibition.

Keywords: Phosphodiesterases III and IV; nitric oxide; cyclic AMP; cyclic GMP; endothelium; smooth muscle; rat aorta

Introduction

It is now widely accepted that an elevation in the content of cyclic nucleotides induces relaxation of vascular tissue (Bär, 1974; Kukovetz *et al.*, 1981; Murad, 1986; Schoeffter *et al.*, 1987; Lincoln & Cornwell, 1991). The magnitude of adenosine 3':5'-cyclic monophosphate (cyclic AMP) and guanosine 3':5'-cyclic monophosphate (cyclic GMP) accumulation in cells depends upon the rate of their synthesis and their breakdown. The latter is achieved by cyclic nucleotide phosphodiesterases (PDEs) that have been classified into five families (Beavo & Reifsnyder, 1990). It is of particular interest to note that cyclic GMP is not only hydrolyzed by PDEs but can also regulate the activities of some PDEs. Thus, PDE II is stimulated by a micromolar concentration of cyclic GMP whereas PDE III is inhibited by the same range of concentrations of cyclic GMP. PDE IV, is insensitive to cyclic GMP (Beavo & Reifsnyder, 1990). In vascular tissue, these three PDE isozymes are differently distributed between cell types. PDE III and PDE IV are both present in smooth muscle cells (Lugnier *et al.*, 1986; Komas *et al.*, 1991; Lindgren *et al.*, 1991) whereas, in endothelial cells, only the presence of PDE II and PDE IV has been described (Lugnier & Schini, 1990; Souness *et al.*, 1990). Thus, by modulating some PDE activities, cyclic GMP could regulate cyclic AMP metabolism in blood vessels. These observations led to the expectation that some PDEs might be involved in the cyclic GMP/cyclic AMP relationship. It has been reported that an elevation of cyclic GMP by nitrovasodilatators potentiates cyclic AMP increases induced by stimulation of adenylate cyclase in rat aortic smooth muscle (Maurice & Haslam, 1990; Maurice *et al.*, 1991). Elevation of cyclic GMP in vascular smooth muscle could also be related to the presence of endothelium which releases nitric oxide (NO) (Furchgott & Zawadzki, 1980; Palmer *et al.*, 1988). NO can rapidly interact with underlying smooth muscle to activate a cytosolic guanylate cyclase and increase cyclic GMP content (Ignarro *et al.*, 1988). Recently, Komas *et al.* (1991) studied the relaxant effect in rat aorta of PDE III and IV inhibitors, these two PDEs are of particular interest since they preferentially catalyze the hydrolysis of cyclic AMP. It was found that specific inhibitors of PDE III produced an endothelium-independent relaxation, but the relaxant effects of PDE IV inhibitors were dependent on the presence of a functional endothelium and markedly enhanced by cyclic GMP elevating agents or by a PDE III inhibitor. Altogether these results suggest that in rat aorta, cyclic GMP exerts a potentiating effect on cyclic AMP-mediated relaxing action. The mechanism involved is not known but it has been proposed that cyclic GMP increases cyclic AMP by inhibition of PDE III in platelets (Maurice & Haslam, 1990) and vascular preparations (Komas *et al.*, 1991; Jang *et al.*, 1993). The resulting increase in cyclic AMP may therefore allow the control of cyclic AMP level by PDE IV (Muller *et al.*, 1992; Lugnier & Komas, 1993).

[1] Author for correspondence.

The aim of the present work was to study the involvement of PDEs in the modulation of vascular cyclic AMP content by the NO/cyclic GMP pathway. For that purpose, we have investigated the effects of selective PDE III and PDE IV inhibitors (SK&F 94120 and rolipram respectively) on cyclic nucleotide content in rat aorta. The influence of the NO/cyclic GMP pathway on cyclic AMP and cyclic GMP contents was studied on aortic rings with and without endothelium. The NO production was modulated with N^G-nitro-L-arginine methyl ester (L-NAME) which is an inhibitor of NO production or with 3-morpholinosydnonimine (SIN-1) which is a donor of NO in the presence of superoxide dismutase (SOD) which eliminates superoxide ions produced by SIN-1 thus inhibiting the production of peroxynitrite. A preliminary account of some parts of this work has been published in abstract form (Eckly & Lugnier, 1993).

Methods

Preparation of rat aortic rings

Male Wistar rats (400–450 g) were killed by cervical dislocation at 10 h 00 min in order to avoid cyclic nucleotide content variations related to circadian cycles (Lemmer *et al.*, 1986). The thoracic aorta was quickly dissected, cleaned of fat and connective tissues and cut into four rings, 3–4 mm in length. Care was taken to avoid abrasion of the intimal surface of the rings to maintain the integrity of the endothelial layer. In some experiments the intimal surface was subsequently rubbed gently with fine wires. Removal of the endothelium was confirmed by silver nitrate staining (Griffith *et al.*, 1984). The rings were placed (attached with thread without tension) in an organ bath containing 10 ml of Krebs solution at 37°C of the following composition (mM): NaCl 136.9, $NaHCO_3$ 1.19, KCl 2.68, $MgCl_2$ 1.05, $CaCl_2$ 2.5, NaH_2PO_4 0.42, glucose 10. The rings were oxygenated with 95% O_2 and 5% CO_2 to maintain a pH value of 7.4. All experiments were carried out in the presence of 10 μM indomethacin in order to inhibit cyclo-oxygenase activity.

Tissue treatment

Four rings from the same aorta were randomly distributed, precontracted with 1 μM noradrenaline and treated as follows: the first with 0.1% dimethylsulphoxide (DMSO) as drug vehicle; the second with 30 μM SK&F 94120 (PDE III specific-inhibitor); the third with 30 μM rolipram (PDE IV specific-inhibitor) and the last with a combination of 5 μM SK&F 94120 30 μM rolipram. The PDE inhibitors alone or in combination were used in the presence of 0.1% DMSO. These four treatments were carried out in four different conditions: (1) control rings with endothelium; (2) control rings without endothelium; (3) rings with endothelium treated with 30 μM L-NAME; (4) rings without endothelium treated with 10 μM SIN-1 in the presence of 100 units ml^{-1} of SOD.

The aortic rings were first equilibrated for 2 h including washings every 30 min. After 5 min incubation with 1 μM noradrenaline, the rings were treated with PDE inhibitors or drug vehicle for 5 min. When used, SIN-1 was added 2 min before the PDE inhibitors. L-NAME and SOD were added 5 min before noradrenaline. SOD was used in order to avoid the production of peroxynitrite (Gryglewski *et al.*, 1986).

The duration of the incubation with the PDE inhibitors was chosen after preliminary experiments showing that 5 min were necessary for the relaxation response to reach a steady state level. The concentrations of PDE inhibitors were chosen from previous results (Komas *et al.*, 1991), showing that 80% relaxation was attained with 30 μM of PDE inhibitors. Since the presence of a PDE III inhibitor markedly increased PDE IV potency on relaxation (Komas *et al.*, 1991), rolipram (30 μM) was combined with a concentration of SK&F 94120 (5 μM) which did not itself alter the cyclic nucleotide content.

After exposure to the different agents, the tissues were quickly removed from the organ bath and frozen using a clamp precooled in liquid N_2. The preparations were stored at −80°C until the determination of cyclic nucleotide and DNA contents.

Measurement of cyclic nucleotide and DNA contents

Cyclic AMP and cyclic GMP levels were determined in the same aortic ring, by a modified radioimmunoassay (Cailla *et al.*, 1973; 1975). DNA content was assessed by a fluorometric method (Morley & Setaro, 1976). The cyclic nucleotide levels were expressed as fmol μg^{-1} DNA.

Statistical analysis

Data are presented as means ± s.e.mean. Statistical comparisons were performed using Student's *t* test for unpaired data when PDE inhibitor effects were studied on rings originating from the same aorta. Effects of endothelium and NO on cyclic nucleotide contents were analysed by a two-way analysis of variance (ANOVA). The slopes of the regression lines were tested and statistical significance was assumed when $*P<0.05$; $**P<0.01$; $***P<0.001$.

Materials

Noradrenaline bitartrate (Sigma Chemical Co.) was stored as a 10 mM stock solution in buffer containing 7.9 mM Na_2SO_3 and 34 mM HCl and was diluted as required. All other substances were freshly prepared before each experiment. Indomethacin (Sigma Chemical Co.) was dissolved in 0.5% Na_2CO_3. N^G-nitro-L-arginine methyl ester (L-NAME) and superoxide dismutase (SOD) were from Sigma Chemical Co. and were dissolved in Krebs solution. Rolipram and 5-(4-acetamidophenyl)pyrazin-2(1H)-one (SK&F 94120) were obtained as a gift from Schering and Smith Kline & Beecham Research respectively and they were dissolved in 100% DMSO. The NO donor compound, 3-morpholinosydnonimine (SIN-1) was a kind gift of Hoechst-France and was dissolved in 5% glucose.

Results

Effects of endothelium and NO modulating agents on cyclic nucleotide contents in rat aorta

In the control aorta with endothelium (Table 1), the content of cyclic AMP was approximately 3 fold higher than the cyclic GMP content. Pretreatment of aorta with L-NAME

Table 1 Basal cyclic nucleotide contents in rat aorta with and without endothelium

	Cyclic GMP (fmol μg^{-1}	*Cyclic AMP* DNA)
Aorta with endothelium		
Control	14 ± 0.3 ($n = 9$)	39.5 ± 3.1 ($n = 10$)
L-NAME (30 μM)	6.8 ± 1.0*** ($n = 10$)	36.9 ± 4.0 ($n = 8$)
Aorta without endothelium		
Control	6.4 ± 1.9††† ($n = 6$)	23.3 ± 2.5††† ($n = 8$)
SIN-1 (10 μM) + SOD (100 u ml^{-1})	88 ± 19*** ($n = 6$)	30 ± 3.5 ($n = 6$)

Results are the mean ± s.e.mean of *n* experiments (*n* indicated under each cyclic nucleotide value).
***$P<0.001$ in comparison with their control. †††$P<0.001$ in comparison with aorta with endothelium.

reduced the cyclic GMP content by 50%. Cyclic AMP content was not modified by the L-NAME treatment.

In aorta without endothelium (Table 1), the cyclic GMP content was one half that of aorta with endothelium. This cyclic GMP content was similar to that found in the L-NAME pretreated tissue. As expected, addition of SIN-1 in combination with SOD markedly increased cyclic GMP content by 14 fold. Cyclic AMP content in the absence of endothelium was significantly lower (40%) than in the presence of endothelium. SIN-1 plus SOD treatment did not significantly modify cyclic AMP content.

Effects of endothelium on the modulation of cyclic nucleotide contents by PDE III and PDE IV specific inhibitors

In the presence or absence of endothelium, neither SK&F 94120 nor rolipram, alone or combined, significantly modified cyclic GMP content (Figure 1a and c).

In aortae with endothelium (Figure 2a), SK&F 94120 did not alter cyclic AMP content. In contrast, rolipram at the same concentration was able to increase cyclic AMP content (by 1.7 fold). SK&F 94120 in combination with rolipram increased cyclic AMP content by 2.6 fold when compared with 0.1% drug vehicle. This increase was also significantly different from that obtained with rolipram alone.

After removal of the endothelium (Figure 2c), PDE III and PDE IV inhibitors increased cyclic AMP content by 1.7 and 2 fold respectively. Furthermore, addition of SK&F 94120 with rolipram potentiated the effect of rolipram on cyclic AMP content (1.7 fold).

Effects of NO modulating agents on the variation of cyclic nucleotide content by specific inhibitors of PDE III and PDE IV

Even if basal cyclic GMP content (Table 1) was significantly modified by L-NAME and SIN-1 plus SOD, neither rolipram nor SK&F 94120, alone or combined, influenced cyclic GMP levels (Figure 1b and d).

In aortae with endothelium pretreated with L-NAME (Figure 2b), rolipram, but not SK&F 94120 significantly increased cyclic AMP content (1.7 fold in comparison with drug vehicle). This stimulatory effect of rolipram on cyclic AMP content was potentiated by 5 μM SK&F 94120.

In aortae without endothelium, pretreatment with SIN-1 plus SOD (Figure 2d) greatly enhanced the increase in cyclic AMP content induced by rolipram (6 fold). The PDE III inhibitor combined with the PDE IV inhibitor caused a similar increase in cyclic AMP content (5 fold) in comparison with rolipram alone.

Relationship between cyclic GMP and cyclic AMP through inhibition of PDEs

A global analysis of the variations of cyclic AMP content versus cyclic GMP content in rat aortae was performed. This analysis was made for each drug treatment independently of the various conditions modulating NO production.

No significant correlation between cyclic AMP and cyclic GMP contents was observed either in drug vehicle- or in SK&F 94120-treated aortae. This is in contrast to aortae either treated with rolipram alone or in combination with

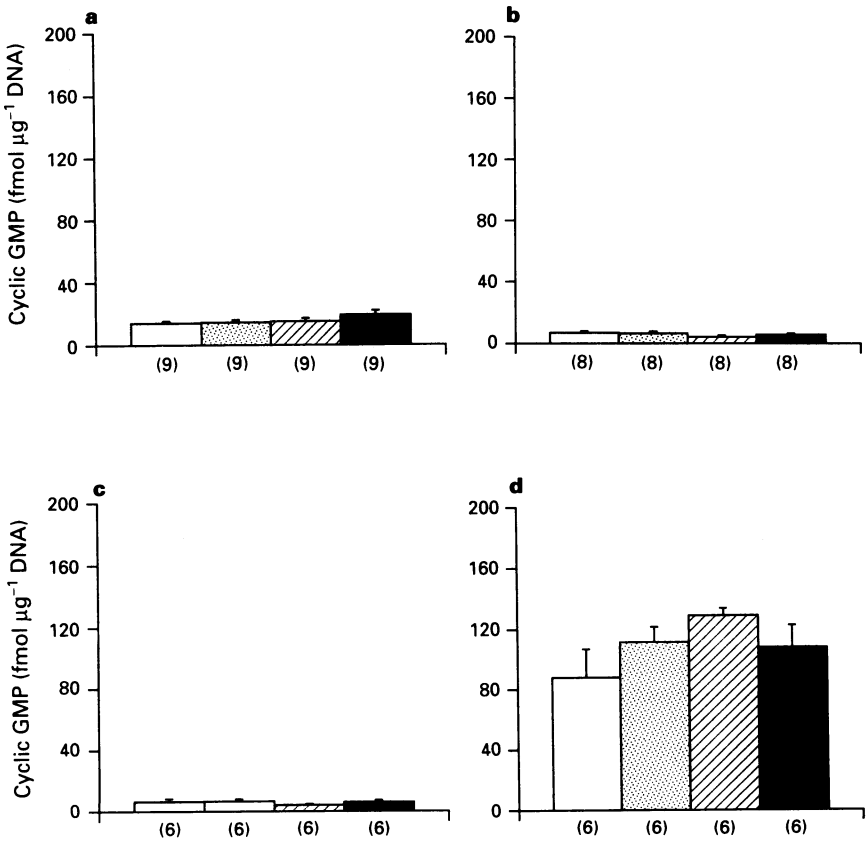


Figure 1 Effects of PDE III and PDE IV inhibitors on cyclic GMP content in control aorta with endothelium (a) or treated with L-NAME (b) and in control aorta without endothelium (c) or treated with SIN-1 plus SOD (d). The rings were incubated in presence of drug vehicle (0.1% DMSO, open columns), PDE III inhibitor (30 μM SK&F 94120, stippled columns), PDE IV inhibitor (30 μM rolipram, hatched columns) or with a combination of the PDE III and PDE IV inhibitors (5 μM SK&F 94120 + 30 μM rolipram, solid columns). The results are expressed as the mean of 6 to 9 experiments (number indicated under the columns) ± s.e.mean. For abbreviations, see text.

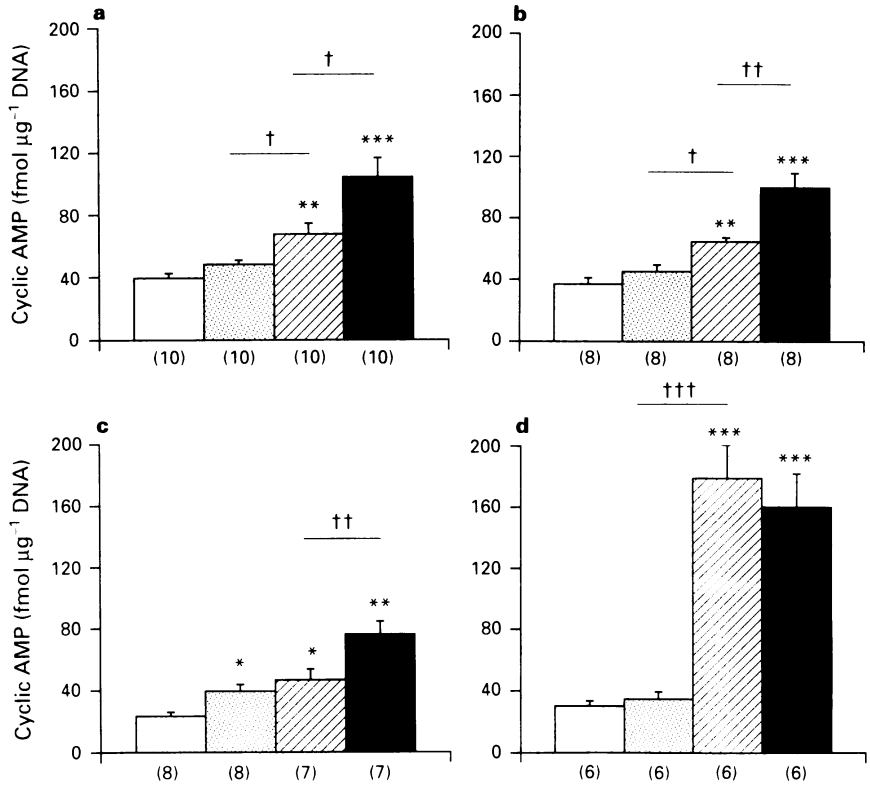


Figure 2 Effects of PDE III and PDE IV inhibitors on cyclic AMP content in control aorta with endothelium (a) or treated with L-NAME (b) and in control aorta without endothelium (c) or treated with SIN-1 plus SOD (d). The rings were incubated in presence of drug vehicle (0.1% DMSO, open columns), PDE III inhibitor (30 µM SK&F 94120, stippled columns), PDE IV inhibitor (30 µM rolipram, hatched columns) or with a combination of 5 µM SK&F 94120 and 30 µM rolipram, (solid columns). The results are expressed as the mean of 6 to 10 experiments (number indicated under the columns) ± s.e.mean. Statistical significance: $\dagger P<0.05$; $\dagger\dagger P<0.01$; $\dagger\dagger\dagger P<0.001$ in comparison with preceding column, and $^{*}P<0.05$; $^{**}P<0.01$; $^{***}P<0.001$ in comparison with aortae incubated with drug vehicle (first column). For abbreviations, see text.

5 µM SK&F 94120 where a significant correlation was obtained between cyclic AMP and cyclic GMP (respectively; $r=0.99$, $P<0.01$ and $r=0.96$, $P<0.05$).

Discussion

The aim of the present study was to determine whether a modification of cyclic GMP could induce a change in cyclic AMP content and to investigate the involvement of PDE III or/and PDE IV in that modulation. The major finding is that inhibition of PDE III by cyclic GMP may be necessary to enhance the effect of PDE IV inhibition on cyclic AMP level. Thus, a mediatory relationship between cyclic GMP and cyclic AMP is possible, occurring through inhibition of PDE III and consequently of PDE IV. Neither the PDE III inhibitor, nor the PDE IV inhibitor, alone or combined, affected cyclic GMP content. This was expected since these two PDEs preferentially hydrolyze cyclic AMP (Beavo & Reifsnyder, 1990).

Considering basal cyclic nucleotide levels, we found that cyclic GMP and cyclic AMP contents were significantly greater in the presence of endothelium than in its absence. It is generally accepted that endothelium increases in cyclic GMP content are due to basal release of NO (for review see Schmidt *et al.*, 1993). However, cyclic AMP increase due to the presence of endothelial cells cannot be related to NO since L-NAME and SIN-1 plus SOD had no effect on basal cyclic AMP content in the rat aorta. This accumulation cannot be attributed to PGI_2 production since indomethacin was used in all experiments. Therefore, the origin of this increase is not known but it could not be ascribed to the endothelial release of NO and PGI_2.

The PDE III inhibitor increased cyclic AMP content in endothelium-free aortae but not in aortae with endothelium. This is in accordance with previous results obtained on vascular preparations without endothelium (Schoeffter *et al.*, 1987) where the PDE III inhibitor, cilostamide, increased cyclic AMP content and induced vascular relaxation. Since cyclic GMP content was higher in whole aortae than in endothelium free-aortae, it might be possible that endogenous cyclic GMP directly inhibited PDE III which could not be further inhibited by SK&F 94120. Similarly the fact that cyclic AMP content is higher in aortae with endothelium could also explain the SK&F 94120 effect. It is well known that the effect of a competitive inhibitor, like SK&F 94120, is dependent on substrate concentration. Thus, an increase in cyclic AMP concentration could displace the PDE III inhibitor from the enzyme and consequently decrease its inhibitory effect. Our previous results showing an endothelium-independent relaxation produced by PDE III inhibitors (Komas *et al.*, 1991) support the role of PDE III in the regulation of cyclic AMP content and in vascular contraction. Additionally, the possibility cannot be excluded that an eventual local cyclic AMP variation could be detected in the whole aorta (Weishaar *et al.*, 1988; Silver *et al.*, 1989; Hohl & Li, 1991). Such a lack of correlation between cyclic AMP content and functional effects has often been reported (Napoli *et al.*, 1980; Vegesna *et al.*, 1986; Hei *et al.*, 1990).

The PDE IV inhibitor was more effective than the PDE III inhibitor in increasing cyclic AMP in our conditions. This is to be expected when using the same concentration of drugs having different K_i values for their respective targets (rolipram K_i value on PDE IV = 0.8 µM, SK&F 94120 K_i value on PDE III = 5 µM; Lugnier & Komas, 1993). The increases induced by rolipram were generally moderate (about 2 fold)

but quite similar to those observed with isoprenaline, forskolin or with other PDE IV inhibitors in different cell types (Reeves *et al.*, 1987; Schoeffter *et al.*, 1987; Anderson & Vinge, 1991).

Since it has been shown that an elevation in cyclic nucleotide content or the presence of a PDE III inhibitor markedly increased PDE IV potency on relaxation (Komas *et al.*, 1991), we added a low concentration of a PDE III inhibitor (which did not alter cyclic nucleotide contents by itself) in the presence of a PDE IV inhibitor. The addition of the PDE III inhibitor potentiated the effect of the PDE IV inhibitor on cyclic AMP content in the majority of conditions. These data are in accordance with those obtained on heart preparations (Gristwood *et al.*, 1986; Klockow *et al.*, 1990; Muller *et al.*, 1990; Shahid & Nicholson, 1990) and human platelets (Andersson & Vinge, 1991). One exception occurred in aortae treated with SIN-1 plus SOD where no potentiation could be obtained. This result might suggest that endogenous cyclic GMP has already inhibited PDE III and prevented the binding of SK&F 94120 on the catalytic domain. Thus the PDE III inhibitor has no further effect on PDE III and consequently on cyclic AMP content which seems already maximal.

One of the most important points of this study is that an increase in cyclic GMP content due to SIN-1 plus SOD treatment was correlated with the increase in cyclic AMP content induced by the PDE IV inhibitor. No similar positive correlation was found when a PDE III inhibitor was used. However, cyclic GMP content induced by basal release of NO from endothelium had no such synergistic effect on cyclic AMP content suggesting that a higher cyclic GMP content is necessary. It has been shown that vasodilator substances, including NO at high doses, can release cyclic AMP in the rat isolated perfused kidney (Heuze-Joubert *et al.*, 1992); we therefore examined the possibility that SIN-1 plus SOD could directly increase cyclic AMP content. Consistent with previous findings (Schini & Vanhoutte, 1989), no accumulation of cyclic AMP was observed here in control rings after SIN-1 plus SOD treatment in comparison with aortae without endothelium.

An important question is how cyclic GMP could modulate the cyclic AMP increasing effect of PDE IV inhibition. It has been previously proposed in platelets (Maurice & Haslam, 1990) and vessels (Komas *et al.*, 1991; Jang *et al.*, 1993) that cyclic GMP could increase cyclic AMP through PDE III inhibition. Moreover, it has been suggested that an increase of cyclic AMP would be necessary for PDE IV functioning (Lugnier & Komas, 1993) since this enzyme has a higher K_m value and a lower V_{max} for cyclic AMP (2 μM; 95 nM $min^{-1} mg^{-1}$) than does PDE III (0.2 μM; 6 μM $min^{-1} mg^{-1}$) (Beavo, 1988). According to this hypothesis, PDE IV would participate in cyclic AMP metabolism only when basal cyclic AMP level is increased. In this condition, inhibition of PDE IV by rolipram leads to a further rise in cyclic AMP (see Figure 3). However, it cannot be excluded that another subcellular mechanism could explain the relationship between cyclic GMP and cyclic AMP. For example, it could be possible that an increase in cyclic GMP acts on PDE IV through phosphorylation by cyclic GMP-dependent protein kinase (PKG). It is well known that some PDE isoenzymes can be phosphorylated (Michaelis & Webley, 1991; Vasta *et al.*, 1992) but, at the present time, no evidence related to PDE IV phosphorylation by PKG supports this hypothesis. Nevertheless, our results show that: (1) the presence of endothelium or the treatment with SIN-1 plus SOD increased basal cyclic GMP indicating stimulation of guanylyl cyclase; (2) a PDE III inhibitor was able to increase cyclic AMP content when basal cyclic AMP level was low, confirming the involvement of PDE III; (3) a PDE III inhibitor potentiated the effect of a PDE IV inhibitor on cyclic AMP content showing a PDE III/PDE IV interactive regulation of cyclic AMP and (4) the NO donor enhanced the effect of PDE IV on cyclic AMP content suggesting the inhibition of PDE III by cyclic GMP. Taken together, these results strengthen the hypothesis that NO/cyclic GMP pathway could induce PDE IV-dependent regulation of cyclic AMP via PDE III inhibition.

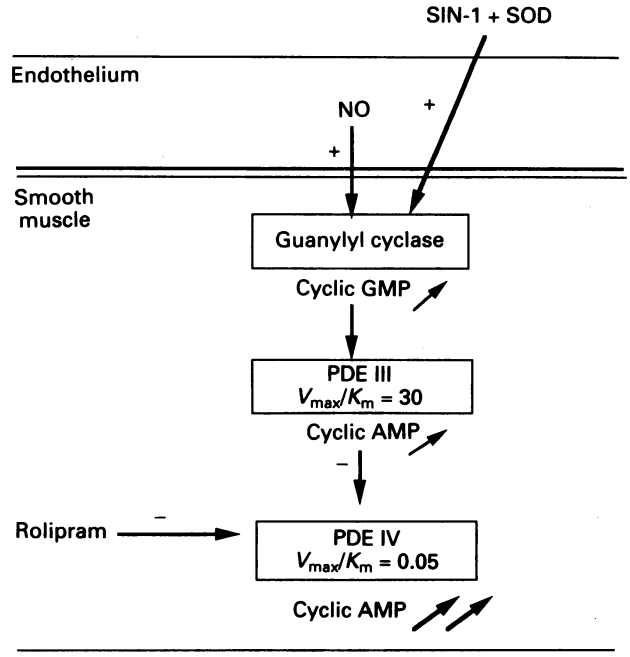


Figure 3 Scheme of hypothetical events by which cyclic GMP modulates cyclic AMP content. In the presence of endothelium, the increase in cyclic GMP levels in vascular smooth muscle (subsequent to endothelial NO production) inhibits PDE III, and the subsequent increase in cyclic AMP levels thereby allows PDE IV (low V_{max}/K_m ratio) to participate in cyclic AMP catabolism. Therefore the specific inhibition of PDE IV increases cyclic AMP content. In the absence of endothelium, similar mechanism could be involved in the presence of NO donor.

In summary, the results of this investigation indicate that an increase in cyclic GMP correlates with the accumulation in cyclic AMP content induced by PDE IV inhibition. This interrelation between cyclic GMP and cyclic AMP depends on the cyclic GMP level that is firstly modulated by NO. Taken together with a previous study performed on the relaxant effect of PDE III and IV inhibition (Komas *et al.*, 1991), these results support our hypothesis suggesting that cyclic GMP enhances cyclic AMP-mediated relaxation through the inhibition of PDE III.

We thank Dr B. Lutz-Bucher for the supply of antibodies, [^{125}I]-cyclic GMP and [^{125}I]-cyclic AMP. We are also grateful to Pr J.-C. Stoclet and Dr R. Miller for their comments on the manuscript. This work was supported by INSERM (920507).

References

ANDERSSON, T.L.G. & VINGE, E. (1991). Interactions between isoprenaline, sodium nitroprusside, and isozyme-selective phosphodiesterase inhibitors on ADP-induced aggregation and cyclic nucleotide levels in human platelets. *J. Cardiovasc. Pharmacol.*, **18**, 237–242.

BÄR, H.P. (1974). Cyclic nucleotides and smooth muscle. In *Adv. Cyclic Nucleotide Res.*, Vol. 4, ed. Greengard, P. & Robinson, G.A. pp. 195–237. New-York: Raven Press.

BEAVO, J.A. (1988). Multiple isozyme of cyclic nucleotide phosphodiesterase. *Adv. Second Messenger Phosphoprotein Res.*, **22**, 1–38.

BEAVO, J.A. & REIFSNYDER, D.H. (1990). Primary sequence of cyclic nucleotide phosphodiesterase isozymes and the design of selective inhibitors. *Trends Pharmacol. Sci.*, **11**, 150–155.

CAILLA, H.L., RACINE-WEISBUCH, M.S. & DELAAGE, M.A. (1973). Adenosine 3',5' cyclic monophosphate assay at 10^{-15} mole level. *Anal. Biochem.*, **56**, 394–407.

CAILLA, H.L., VANNIER, C.J. & DELAAGE, M.A. (1976). Guanosine 3'-5'-cyclic monophosphate assay at 10^{-15} mole level. *Anal. Biochem.*, **70**, 195–202.

ECKLY, A. & LUGNIER, C. (1993). SIN-1 potentiates the effect of rolipram on cAMP content in rat aorta without endothelium. *Endothelium*, **1**, S38.

FURCHGOTT, R.F. & ZAWADZKI, J.V. (1980). The obligatory role of endothelial cells in the relaxation of arterial smooth muscle by acetylcholine. *Nature*, **288**, 373–376.

GRIFFITH, T.M., HENDERSON, A.H., EDWARDS, D.H. & LEWIS, M.J. (1984). Isolated perfused rabbit coronary artery and aortic strip preparations: the role of endothelium-derived relaxant factor. *J. Physiol.*, **351**, 13–24.

GRISTWOOD, R.W. & OWEN, D.A.A. (1986). Effects of rolipram on guinea-pig ventricles in vitro: evidence of an unexpected synergism with SK&F 94120. *Br. J. Pharmacol.*, **87**, 91P.

GRYGLEWSKI, R.J., PALMER, R.M.J. & MONCADA, S. (1986). Superoxide is involved in the breakdown of endothelium-derived relaxing factor. *Nature*, **320**, 454–456.

HEI, Y.-J., MACDONELL, K.L., MCNEILL, J.H. & DIAMOND, J. (1990). Lack of correlation between activation of cyclic AMP-dependent protein kinase and inhibition of contraction of rat vas deferens by cyclic AMP analogs. *Mol. Pharmacol.*, **39**, 233–238.

HEUZE-JOUBERT, I., MENNECIER, P., SIMONET, S., LAUBIE, M. & VERBEUREN, T.J. (1992). Effect of vasodilators, including nitric oxide, on the release of cGMP and cAMP in the isolated perfused rat kidney. *Eur. J. Pharmacol.*, **220**, 161–171.

HOHL, C.M. & LI, Q. (1991). Compartmentation of cAMP in adult canine ventricular myocytes. *Circ. Res.*, **69**, 1369–1379.

IGNARRO, L.J., HARBISON, R.G., WOOD, K.S. & KADOWITZ, P.J. (1986). Activation of purified soluble guanylate cyclase by endothelium-derived factor from intrapulmonary artery and vein: stimulation by acetylcholine, bradykinin and arachidonic acid. *J. Pharmacol. Exp. Ther.*, **237**, 893–900.

JANG, E.K., DAVIDSON, M.M.L., CRANKSHAW, D. & HASLAM, R.J. (1993). Synergistic inhibitory effects of atriopeptin II and isoproterenol on contraction of rat aortic smooth muscle: roles of cGMP and cAMP. *Eur. J. Pharmacol.*, **250**, 477–481.

KLOCKOW, M. (1990). The cAMP specific rolipram inhibited PDE (ROI-PDE) is important for the intracellular cAMP level in myocytes. *Naunyn-Schmied. Arch. Pharmacol.*, **341**, R50.

KOMAS, N., LUGNIER, C. & STOCLET, J.-C. (1991). Endothelium-dependent and independent relaxation of the rat aorta by cyclic nucleotide phosphodiesterase inhibitors. *Br. J. Pharmacol.*, **104**, 495–503.

KUKOVETZ, W.R., GRAIER, W.F. & GROSCHNER, K. (1992). Contribution of agonist-induced hyperpolarization to Ca^{2+} influx and formation of EDRF in vascular endothelial cells. *Jpn. J. Pharmacol.*, **58**, 213P–219P.

LEMMER, B., BISSINGER, H. & LANG, P.H. (1986). Effect of forskolin on cAMP levels in rat heart at different times of day. *ICRS Med. Sci.*, **14**, 1103–1104.

LINCOLN, T.M. & CORNWELL, T.L. (1991). Towards an understanding of the mechanism of action of cyclic AMP and cyclic GMP in smooth muscle relaxation. *Blood Vessels*, **28**, 129–137.

LINDGREEN, S., RASCON, A., ANDERSSON, K.E., MANGANIELLO, V. & DEGERMAN, E. (1991). Selective inhibition of cyclic GMP-inhibited and cyclic GMP-non inhibited cyclic nucleotide phosphodiesterase and relaxation of rat aorta. *Biochem. Pharmacol.*, **42**, 545–552.

LUGNIER, C. & KOMAS, N. (1993). Modulation of vascular cyclic nucleotide phosphodiesterases by cyclic GMP: role in vasodilatation. *Eur. Heart J.*, **14**, 141–148.

LUGNIER, C. & SCHINI, V.B. (1990). Characterization of cyclic nucleotide phosphodiesterases from cultured bovine aortic endothelial cells. *Biochem. Pharmacol.*, **39**, 75–84.

LUGNIER, C., SCHOEFFTER, P., LE BEC, A., STROUTHOU, E. & STOCLET, J.-C. (1986). Selective inhibition of cyclic nucleotide phosphodiesterases of human, bovine and rat aorta. *Biochem. Pharmacol.*, **35**, 1743–1751.

MAURICE, D.H., CRANKSHAW, D. & HASLAM, R.J. (1991). Synergistic actions of nitrovasodilators and isoprenaline on rat aortic smooth muscle. *Eur. J. Pharmacol.*, **192**, 235–242.

MAURICE, D.H. & HASLAM, R.J. (1990). Molecular basis of the synergistic inhibition of platelet function by nitrovasodilators and activators of adenylate cyclase: inhibition of cyclic AMP breakdown by cyclic GMP. *Mol. Pharmacol.*, **37**, 671–681.

MICHAELIS, A.E. & WEBLEY, G.E. (1991). Prostaglandin $F_{2\alpha}$ stimulates cAMP phosphodiesterase via protein kinase C in cultured human granulosa cells. *Mol. Cell. Endocrinol.*, **82**, 207–214.

MORLEY, C.G.D. & SETARO, F. (1976). A modified fluorometric method for the determination of microgram quantities of DNA from cell or tissue cultures. *Anal. Biochem.*, **71**, 313–317.

MULLER, B., LUGNIER, C. & STOCLET, J.-C. (1990). Involvement of rolipram-sensitive cyclic AMP phosphodiesterase in the regulation of cardiac contraction. *J. Cardiovasc. Pharmacol.*, **16**, 796–803.

MULLER, B., STOCLET, J.-C. & LUGNIER, C. (1992). Cytosolic and membrane-bound cyclic nucleotide phosphodiesterases from guinea-pig cardiac ventricles. *Eur. J. Pharmacol.*, **225**, 263–272.

MURAD, F. (1986). Cyclic guanosine monophosphate as a mediator of vasodilatation. *J. Clin. Invest.*, **78**, 1–5.

NAPOLI, S.A., GRUETTER, C.A., IGNARRO, L.B. & KADOWITZ, P.J. (1980). Relaxation of bovine coronary arterial smooth muscle by cyclic GMP, cyclic AMP and analogs. *J. Pharmacol. Exp. Ther.*, **212**, 469–473.

PALMER, R.M.J., REES, D.D., ASHTON, D.S. & MONCADA, S. (1988). L-Arginine is the physiological precursor for the formation of nitric oxide in endothelium-dependent relaxation. *Biochem. Biophys. Res. Commun.*, **153**, 1251–1256.

REEVES, M.L., ENGLAND, P.J. & MURRAY, K.J. (1987). Compartments of cyclic-AMP-dependent protein kinase in perfused guinea-pig hearts. *Biochem. Soc. Trans.*, **15**, 955–956.

SHAHID, M. & NICHOLSON, C.D. (1990). Comparison of cyclic nucleotide phosphodiesterase isoenzymes in rat and rabbit ventricular myocardium: positive inotropic and phosphodiesterase inhibitory effects of Org 30029, milrinone and rolipram. *Naunyn-Schmied. Arch. Pharmacol.*, **342**, 698–705.

SCHINI, V.B. & VANHOUTTE, P.M. (1989). SIN-1 stimulates the production of cyclic GMP but not cyclic AMP in porcine aortic endothelial cells. *J. Cardiovasc. Pharmacol.*, **14**, S91–S94.

SCHMIDT, H.H.W., LOHMANN, S.M. & WALTER, U. (1993). The nitrite oxide and cGMP signal transduction system: regulation and mechanism of action. *Biochim. Biophys. Acta.*, **1178**, 153–175.

SCHOEFFTER, P., LUGNIER, C., DEMESY-WAELDELE, F. & STOCLET, J.-C. (1987). Role of cyclic AMP- and cyclic GMP phosphodiesterases in the control of cyclic nucleotide levels and smooth muscle tone in rat isolated aorta. *Biochem. Pharmacol.*, **36**, 3965–3972.

SILVER, P.J., LEPORE, R.E., O'CONNOR, B., LEMP, B.M., HAMEL, L.T., BENTLEY, R.G. & HARRIS, A.L. (1988). Inhibition of the low Km cyclic AMP phosphodiesterase and activation of the cyclic AMP system in vascular smooth muscle by milrinone. *J. Pharmacol. Exp. Ther.*, **247**, 34–41.

SOUNESS, J.E., DIOCEE, B.K., MARTIN, W. & MOODIE, S.A. (1990). Pig aortic endothelial-cell cyclic nucleotide phosphodiesterases. *Biochem. J.*, **266**, 127–132.

VASTA, V., SMITH, C.J., CALVO, J., BELFRAGE, P. & MANGANIELLO, V.C. (1992). Insulin and isoproterenol induce phosphorylation of the particulate cyclic GMP-inhibited, low Km cyclic AMP phosphodiesterase (cGi PDE) in 3T3-L1 adipocytes. *Biochem. Biophys. Res. Commun.*, **183**, 1070–1075.

VEGESNA, R.V.K. & DIAMOND, J. (1986). Activation of cyclic AMP dependent protein kinase in rabbit aortic rings by prostaglandin E1 and forskolin is accompanied by contraction and relaxation respectively. *Proc. West. Pharmacol. Soc.*, **29**, 303–311.

WEISHAAR, R.E., KOBYLARZ-SINGER, D.C., QUADE, M.M. & KAPLAN, H.R. (1988). Role of cyclic AMP in regulating cardiac muscle contractility: novel pharmacological approaches to modulating cyclic AMP degradation by phosphodiesterase. *Drug Dev. Res.*, **12**, 119–129.

(Received April, 5, 1994
Received June 2, 1994
Accepted June 17, 1994)

Br. J. Pharmacol. (1994), **113**, 451–456 © Macmillan Press Ltd, 1994

Differential potentiation by depolarization of the effects of calcium antagonists on contraction and Ca^{2+} current in guinea-pig heart

Ryo Okuyama, Satomi Adachi-Akahane & [1]Taku Nagao

Department of Toxicology and Pharmacology, Faculty of Pharmaceutical Sciences, University of Tokyo, 7-3-1 Hongo, Bunkyo-ku, Tokyo 113, Japan

1 The effects of elevation of extracellular K^+ concentration ($[K^+]_o$) on the negative inotropic potencies of three representative calcium antagonists, diltiazem, verapamil and nifedipine, were investigated in guinea-pig papillary muscle preparations.

2 The negative inotropic effect of diltiazem was potentiated 110 fold when $[K^+]_o$ was raised from 2.7 mM to 12.7 mM. The effect of verapamil was also potentiated to a lesser extent, but that of nifedipine was not affected.

3 Resting membrane potentials in ventricular muscles were about − 80 mV and − 60 mV in 2.7 mM K^+ and 12.7 mM K^+, respectively.

4 To clarify the mechanism responsible for the differential potentiation of the negative inotropic effects, the blocking actions of the three calcium antagonists on the L-type Ca^{2+} channel current ($I_{Ca(L)}$) were compared at the holding potentials of − 80 mV and − 60 mV by the whole-cell patch-clamp technique.

5 The use-dependent blocking effect of diltiazem on $I_{Ca(L)}$ was enhanced markedly by the change in the holding potential from − 80 mV to − 60 mV. The effect of verapamil was also enhanced to a lesser extent but that of nifedipine was not affected in this range of depolarization.

6 The differential effects of the $[K^+]_o$ elevation on the negative inotropic potencies of the three calcium antagonists are explained by the differences in voltage-dependency of their use-dependent blocking effects on $I_{Ca(L)}$.

7 The properties of diltiazem and verapamil observed in this study may contribute to their protective effects on the ischaemic myocardium, without affecting the normal myocardium.

Keywords: Diltiazem; verapamil; nifedipine; depolarization; papillary muscle; L-type Ca^{2+} channel

Introduction

Representative calcium antagonists, nifedipine, verapamil and diltiazem are used in the treatment of a wide range of cardiovascular diseases. Although the three agents have been demonstrated to bind to the α_1 subunit of the L-type Ca^{2+} channel (Glossmann & Striessnig, 1990), it is known that they show differences pharmacologically in tissue selectivity.

Evidence has been obtained to indicate that calcium antagonists have beneficial effects on the ischaemic myocardium in models of experimental ischaemia (Nagao *et al.*, 1980; Nakamura *et al.*, 1980; Pérez *et al.*, 1980; Reimer & Jennings, 1985). However, in numerous experimental studies investigating the protective effects of calcium antagonists against myocardial ischaemic damage, the results obtained have been divided into positive and negative, depending on the experimental conditions (Kloner & Braunwald, 1987) and calcium antagonists employed. Ichihara and coworkers reported that diltiazem lessened ischaemic myocardial acidosis evoked by coronary occlusion in the canine heart, and that nifedipine did not (Ichihara & Abiko, 1982; Ichihara *et al.*, 1986). No satisfactory explanation has yet been offered to explain such differences in selectivity of calcium antagonists for the ischaemic myocardium. Not only vasodilator effects but also direct effects on the myocardium, e.g. negative inotropic and negative chronotropic effects, may contribute to the protective effects of calcium antagonists on the ischaemic heart.

The effects of calcium antagonists have been reported to be modulated by stimulus frequency and membrane potential (Hondeghem & Katzung, 1984; Taira, 1987; Triggle, 1991). It has been demonstrated that the extracellular K^+ concentration rises to 10–15 mM in the early phase of ischaemia (Wiegand *et al.*, 1979; Hirche *et al.*, 1980). Thus the potencies of the three calcium antagonists may be affected by the alteration of the membrane potential caused by such elevation of the extracellular K^+ concentration. It is also possible that the voltage-dependency of the effects may differ among the calcium antagonists, which would explain the corresponding differences in their effects on the ischaemic heart. Previous electrophysiological studies have shown that the blocking effects of nifedipine, verapamil and diltiazem on the L-type Ca^{2+} channel current ($I_{Ca(L)}$) are potentiated by depolarization of the membrane potential (Ehara & Kaufmann, 1978; Kanaya & Katzung, 1983; Uehara & Hume, 1985). However, quantitative differences in the voltage-dependency of these drugs have not been well investigated. Thus the differences in voltage-dependency among the calcium antagonists are still unclear.

The present study was designed to examine whether elevation of the extracellular K^+ concentration affects the potencies of the calcium antagonists. For this purpose, we compared the negative inotropic effects of nifedipine, verapamil and diltiazem under normal conditions with those under conditions where the extracellular K^+ concentration was raised to 12.7 mM in guinea-pig papillary muscle preparations. Furthermore, we investigated the relationship between the depolarization caused by elevation of the K^+ concentration and the effects of the calcium antagonists on the L-type Ca^{2+} channel current in single ventricular myocytes.

[1] Author for correspondence.

Methods

Force measurements in guinea-pig papillary muscles

Male guinea-pigs weighing 150–370 g were anaesthetized with pentobarbitone (40 mg kg^{-1}, i.p.) and killed by cervical dislocation. The whole heart was rapidly removed and immersed in a normal solution of the following composition (mM): NaCl 136.8, KCl 2.7, $CaCl_2$ 1.8, $MgCl_2$ 1.0, glucose 5.6, $NaHCO_3$ 12, bubbled with 95% O_2 plus 5% CO_2. One papillary muscle was dissected from the left ventricle, and suspended in an organ bath containing the normal solution maintained at 32°C. A resting tension of 0.5 g was applied to the muscle and the preparation was stimulated through a pair of Ag-AgCl electrodes with rectangular pulses (frequency 1 Hz, duration 5 ms, intensity 50% above threshold voltage). The developed tension was measured isometrically by a force transducer. The preparation was allowed to equilibrate for 110 min, the bath solution being changed once at 20 min. Then, the bath solution was exchanged for the normal solution or a high-K^+ solution (KCl concentration 7.7 mM or 12.7 mM). The high-K^+ solution was made by substitution of potassium chloride for the equimolar sodium chloride in the normal solution. Drug administration was started 30 min after this change of the bathing solution. Concentration-response curves were obtained by cumulative application of the drug to the organ bath every 30 min. The potency of the negative inotropic effect was expressed as an IC_{50} value (the concentration of drug required to produce a 50% decrease in the developed tension), which was derived by interpolation of the concentration-response curve.

Measurements of resting membrane potential in ventricular muscles

The whole heart was removed rapidly from male guinea-pigs anaesthetized as described above, and immersed in the normal solution. A small piece of right ventricular muscle was dissected out and fixed in a tissue chamber perfused with the normal solution or the high-K^+ solution at 32°C. An action potential was evoked by rectangular pulses (frequency 1 Hz, duration 5 ms, intensity 50% above threshold voltage).

Resting membrane potentials were recorded via conventional glass micro-electrodes filled with 3 M KCl (resistance 10–20 MΩ). The micro-electrode was coupled via an Ag-AgCl junction to a high-impedance amplifier (MEZ 9201, Nihon Kohden). An Ag-AgCl wire was used as the reference electrode. Data were obtained from the preparations in which the measured resting membrane potentials were stable for over 10 min.

Preparation of single cells

Ventricular myocytes were isolated enzymatically from hearts of male guinea-pigs weighing 200–550 g according to the method described by Cavalié *et al.* (1983). The animals were anaesthetized with pentobarbitone and the ascending aorta was cannulated *in situ* under artificial respiration. The heart was excised and perfused at 37°C by the Langendorff method with collagenase solution for 10–15 min, followed by a high-potassium, Ca^{2+}-free solution (KB solution) for another 10 min. The KB solution (Isenberg & Klockner, 1982) contained (mM): potassium glutamate 70, KCl 25, oxalic acid 10, KH_2PO_4 10, taurine 10, glucose 11, HEPES 10, EGTA 0.5 (pH 7.4, adjusted with KOH). The ventricles were cut into small fragments in KB solution. Ventricular myocytes were dissociated by gentle stirring of the fragments. The dissociated cells were then kept in KB solution at 4°C. The normal Tyrode solution used had the following composition (mM): NaCl 135, KCl 5.4, $MgCl_2$ 1, $CaCl_2$ 1.8, glucose 11, HEPES 5 (pH 7.4). The Ca^{2+}-free Tyrode solution had the same composition as the normal Tyrode solution except for the Ca^{2+} concentration, which was nominally zero. The collagenase solution was made up in Ca^{2+}-free Tyrode solution with 100 units ml^{-1} collagenase (Nitta Gelatine) and 18 μM $CaCl_2$.

The cells were placed in a chamber (0.5 ml capacity) attached to the stage of an inverted microscope (IMT-2, Olympus). The chamber was perfused with external solution of the following composition (mM): NaCl 120, KCl 4, $CaCl_2$ 2, $MgCl_2$ 2, glucose 10, HEPES 5, tetraethylammonium chloride 30 (pH 7.4, adjusted with NaOH). All measurements were carried out at room temperature.

Recording of L-type Ca^{2+} channel currents ($I_{Ca(L)}$) in single isolated ventricular cells

$I_{Ca(L)}$s were recorded using the whole-cell configuration of the patch-clamp technique (Hamill *et al.*, 1981). The tip resistance of the fire-polished microelectrodes was 3–4 MΩ when filled with internal solution of the following composition (mM): KCl 80, CsOH 40, tetraethylammonium chloride 20, MgATP 4, EGTA 10, HEPES 10 (pH 7.4, adjusted with HCl). $I_{Ca(L)}$s were elicited by a voltage-clamp step to 10 mV for 200 ms with a 150 ms prepulse to −40 mV to inactivate the voltage-dependent Na^+ channel current and T-type Ca^{2+} channel current. Transmembrane currents were obtained using a DAGAN 8900 amplifier with a 100 MΩ headstage, low-pass filtered at 1 kHz. Data were recorded on a pen recorder (FBR 252-A, TOA) through an oscilloscope (VC-10, Nihon Kohden), stored on videotape via a 16-bit PCM data processor (PCM-DP 16, Shoshin E.M., sampling rate 44.1 kHz), and then analysed using a software programme called 'C-minus' kindly provided by Dr K. Enomoto (Shimane Medical University) with modification by Dr H. Kasai (University of Tokyo). Command pulses were applied using a computer-operated stimulator (Shoshin E.M. Model OI-8).

After formation of a gigaseal and rupture of the membrane, the $I_{Ca(L)}$, which was activated at 0.067 Hz, was allowed to stabilize for 3–5 min at a holding potential (V_h) of −90 mV. Then the frequency of the stimulation was raised to 1 Hz, and approximately 3 min was allowed in order for $I_{Ca(L)}$ to become stable. The external solution with or without the drug was perfused for another 3–5 min. When $I_{Ca(L)}$ became stable, command pulses were stopped and the cell was rested at V_h −90 mV for 30 s. Then V_h was changed to −80 mV, and a further 10 s rest was followed by stimulation at 1 Hz. V_h was kept at −80 mV for 2 min until $I_{Ca(L)}$ reached the new steady state level. Subsequently, the same protocol was repeated at V_h −90 mV and −60 mV. In control experiments, $I_{Ca(L)}$s were measured in the absence of the drug with the same voltage protocol described above. The recovery from block was confirmed by changing V_h from −60 mV to −90 mV to assess the degree of rundown of $I_{Ca(L)}$. Data showing marked rundown were omitted. At the end of the experiment, leakage current was measured in the presence of 0.2 mM $CdCl_2$, which was subtracted from the recorded current to obtain the peak $I_{Ca(L)}$ amplitude. The peak $I_{Ca(L)}$ amplitude was normalized with the $I_{Ca(L)}$ amplitude at V_h −90 mV immediately before drug application as 100%.

Drugs used

The following drugs were used: (±)-verapamil.HCl (Nacalai Tesque), nifedipine (Sigma). (+)-*cis*-diltiazem was kindly supplied by Tanabe Seiyaku Co.Ltd., Saitama, Japan. Diltiazem and verapamil were dissolved and diluted in distilled water. Nifedipine was dissolved in absolute ethanol at a concentration of 10^{-3} M. Further dilutions of nifedipine were prepared in distilled water. Because of the light-sensitive nature of nifedipine, all experiments were carried out under subdued lighting and the solutions were protected from light.

Statistical analysis

Bonferroni's multiple t test or Student's t test was employed to assess the statistical significance of differences. Differences at $P<0.05$ were considered to be significant. All data in the figures, tables and text are represented as the mean ± s.e. mean.

Results

Effect of extracellular K^+ concentration on the negative inotropic potencies of the calcium antagonists in papillary muscle preparations

Elevation of the extracellular K^+ concentration from 2.7 mM to 12.7 mM reduced the developed tension of papillary muscles to 66.1 ± 6.9% ($n = 6$) and 73.8 ± 6.3% ($n = 18$), respectively, taking the developed tension measured in the normal solution just before the change of the bath solution as 100%. When the bath solution was exchanged with the normal solution, the developed tension did not alter (97.8 ± 2.0%, $n = 18$).

Developed tension of papillary muscles decreased gradually in a time-dependent manner under normal conditions and in the presence of 12.7 mM K^+ in the absence of drugs. When the preparation was treated with vehicle instead of drugs, the developed tension was reduced to about 70% of the initial value 150 min after the first administration of vehicle under both conditions (data not shown). However, the degree of reduction of the developed tension did not differ between the normal and 12.7 mM K^+ conditions, and therefore the time-dependent decrease in the developed tension was not corrected.

Figure 1 shows the concentration-response curves for the negative inotropic effects of diltiazem, verapamil and nifedipine under normal and high-K^+ conditions. The three drugs caused concentration-dependent decreases in developed tension under normal and high-K^+ conditions (Figure 1). The concentration-response curve for diltiazem was shifted markedly to the left by the elevation of extracellular K^+ concentration. Although the concentration-response curve for verapamil was shifted leftward in the presence of 12.7 mM K^+, the degree of potentiation was less than that for diltiazem. The concentration-response curve for nifedipine was unaffected by the elevation of K^+ concentration. IC_{50} values for each drug obtained under the respective conditions, calculated from the concentration-response curves, are shown in Table 1. The rank order of potency of the negative inotropic effect obtained under normal conditions was nifedipine > verapamil > diltiazem. The IC_{50} value for each drug under normal conditions was divided by the IC_{50} value under high-K^+ conditions to obtain the IC_{50} ratio (Table 1), which represents the degree of potentiation of the negative inotropic effects of the drugs caused by the increase of extracellular K^+ concentration. The rank order of the degree of the potentiation was diltiazem > verapamil > nifedipine.

Measurements of resting membrane potentials

Resting membrane potentials in ventricular muscles were measured under normal and high-K^+ conditions. Normal action potentials were evoked by electrical stimulation in each preparation. The mean resting membrane potentials under normal conditions, in the presence of 7.7 mM K^+ and 12.7 mM K^+ were − 82 ± 1 mV, − 67 ± 1 mV and − 59 ± 1 mV, respectively (mean ± s.e.mean of 10 experiments). The results were close to the values reported by other investigators (Nakajima *et al.*, 1976).

In the subsequent $I_{Ca(L)}$ measurements, holding potentials of − 80 mV and − 60 mV were used as the conditions corresponding to normal and 12.7 mM K^+ conditions, respectively, in the papillary muscle preparations.

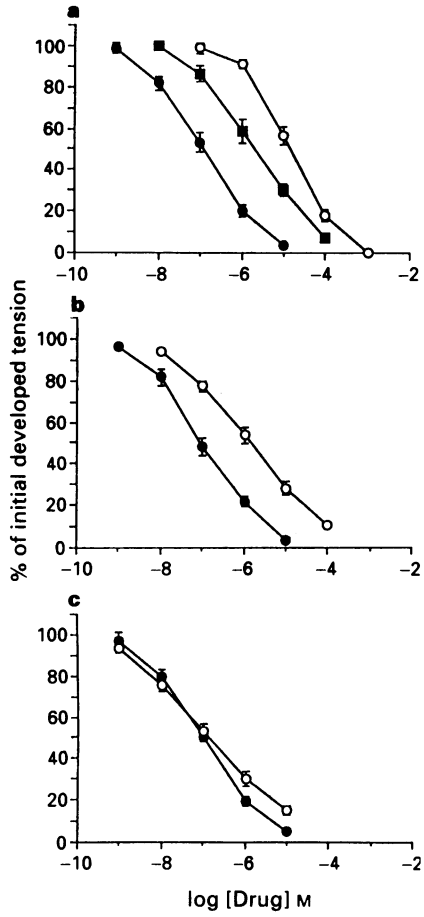


Figure 1 Negative inotropic effects of (a) diltiazem, (b) verapamil and (c) nifedipine on guinea-pig papillary muscles under normal conditions (○) and in 7.7 mM K^+ (■) and 12.7 mM K^+ (●).

Effect of depolarization on the $I_{Ca(L)}$-blocking action of calcium antagonists in single ventricular myocytes

Figure 2 shows typical time courses of $I_{Ca(L)}$ under control conditions (Figure 2a), and in the presence of diltiazem at 3×10^{-6} M (Figure 2b), verapamil at 3×10^{-7} M (Figure 2c) and nifedipine at 3×10^{-8} M (Figure 2d). The drug concentration chosen was that at which the drug suppressed the amplitude of $I_{Ca(L)}$ to about 60% at V_h − 80 mV at a frequency of 1 Hz. Each drug began to block $I_{Ca(L)}$ rapidly after administration, and the effect reached a steady-state within a few minutes. After the change in V_h, stabilization for 2 min allowed the amplitude of $I_{Ca(L)}$ to reach a new steady-state level. In the right-hand panel of Figure 2, the $I_{Ca(L)}$ traces recorded at the times indicated by the arrows in the left-hand panel, at V_h − 60 mV and − 80 mV, are superimposed. Under control conditions, there was little difference between the amplitude of $I_{Ca(L)}$ at V_h − 80 mV and that at V_h − 60 mV (Figure 2a). The blocking effects of diltiazem and verapamil were augmented in a use-dependent manner. In contrast, blockade of $I_{Ca(L)}$ by 3×10^{-6} M diltiazem was markedly enhanced by changing V_h from − 80 mV to − 60 mV (Figure 2b). The blocking effect of 3×10^{-7} M verapamil was also enhanced by the depolarization, but the degree of enhancement was less than that for diltiazem (Figure 2c). The effect of 3×10^{-8} M nifedipine was enhanced only slightly by the depolarization (Figure 2d).

Figure 3 summarizes the amplitudes of $I_{Ca(L)}$ elicited by the first test pulse applied at V_h − 80 mV and − 60 mV after a resting period of 10 s in the presence and absence of drug. None of the calcium antagonists induced any significant tonic block at V_h − 80 mV and − 60 mV.

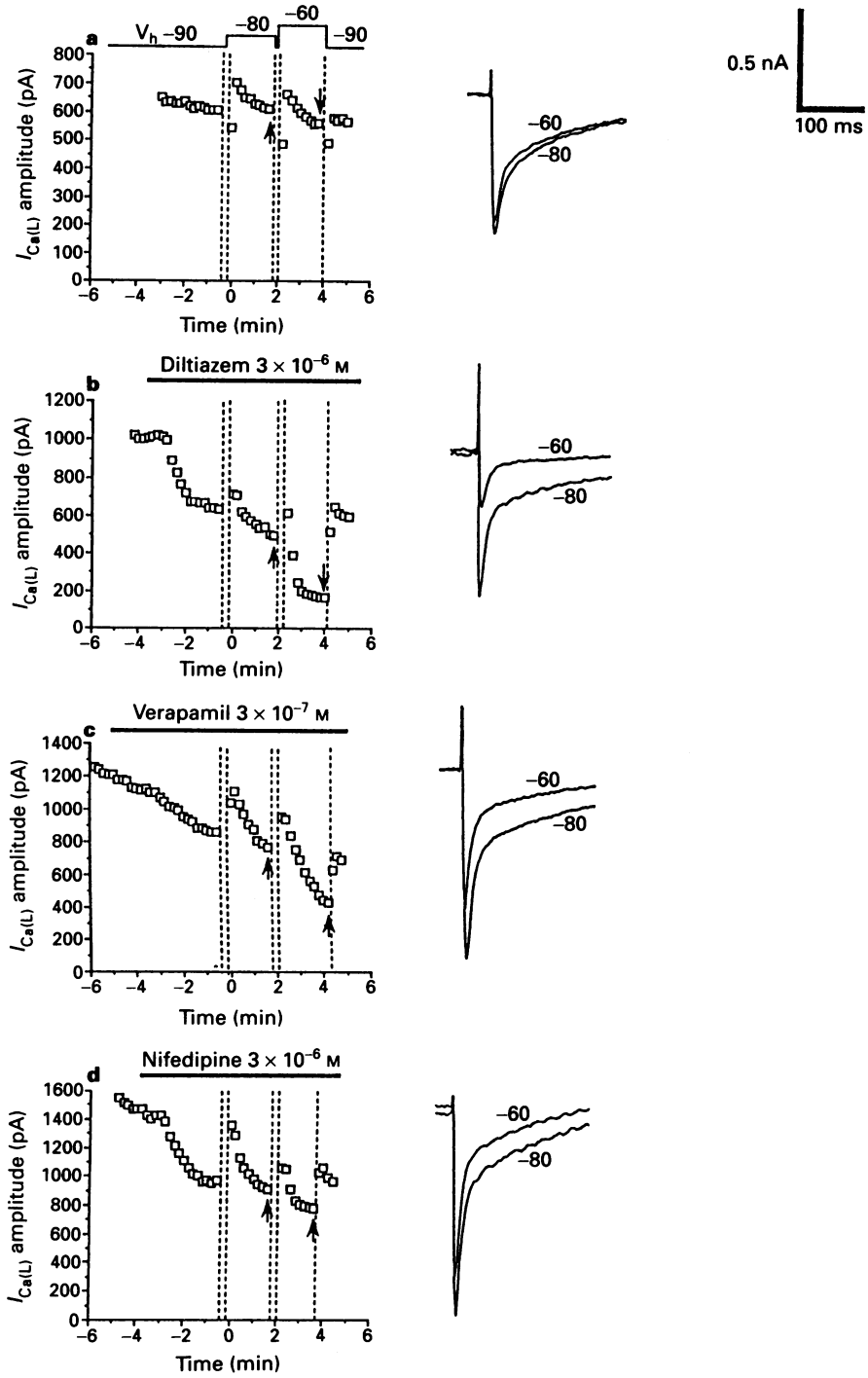


Figure 2 Differential voltage-dependent block of $I_{Ca(L)}$ by the three calcium antagonists. Left panels show typical time courses of peak $I_{Ca(L)}$. Every 12th record of the peak $I_{Ca(L)}$ was plotted. The recordings were made in the normal external solution (a) and in the normal external solution containing (b) 3×10^{-6} M diltiazem, (c) 3×10^{-7} M verapamil, (d) 3×10^{-8} M nifedipine during the period indicated by the horizontal lines. Holding potential (V_h) was changed in turn from -90 to -80, -60 to -90 mV as indicated in (a). During the period indicated by the vertical dashed lines, command pulses were stopped. In the right-hand panel, the superimposed current traces recorded at the times indicated by arrows in the left panels at V_h -80 mV (-80) and V_h -60 mV (-60) are shown.

Figure 4 shows the amplitude of $I_{Ca(L)}$ at the steady-state level about 2 min after the change in V_h. The blocking effects on the amplitude of $I_{Ca(L)}$ shown in Figure 4 represent the sum of tonic blockade and the block accelerated by repetitive channel opening, i.e. 'use-dependent block'. Under control conditions, the amplitude of $I_{Ca(L)}$ was little changed when V_h was changed from -80 mV to -60 mV. In contrast, the blocking effect of diltiazem was markedly enhanced when V_h was depolarized. The effect of verapamil was enhanced significantly, but the degree of enhancement was less than that for diltiazem. The effect of nifedipine was not affected significantly by V_h depolarization.

Discussion

We compared quantitatively the effect of elevation of extracellular K^+ concentration on the negative inotropic effects of three calcium antagonists. In the present study, we focused on the differential modulation of the effects of calcium

Table 1 Effects of elevation of extracellular K^+ concentration upon the negative inotropic potencies of diltiazem, verapamil and nifedipine

	IC_{50} (μM) (pIC_{50})			IC_{50} ratio	
Drug	*Normal*	7.7 mM K^+	12.7 mM K^+	*Normal* / 7.7 mM K^+	*Normal* / 12.7 mM K^+
Diltiazem	16.1 ± 0.41	2.27 ± 0.62	0.145 ± 0.036	7.1	110
	(4.85 ± 0.10)	(5.76 ± 0.15)*	(6.92 ± 0.12)*		
Verapamil	1.93 ± 0.84		0.112 ± 0.043		17
	(5.86 ± 0.15)		(7.05 ± 0.12)†		
Nifedipine	0.185 ± 0.052		0.110 ± 0.016		1.7
	(6.86 ± 0.16)		(6.99 ± 0.06)^{NS}		

IC_{50} (pIC_{50}) values are the mean ± s.e.mean for six experiments. IC_{50} ratio values represent the ratio of normal: 7.7 mM K^+ or normal: 12.7 mM K^+ mean IC_{50}. Individual pIC_{50} values for each drug under high-K^+ conditions were compared statistically with the corresponding pIC_{50} values obtained under normal conditions.
NS = not significantly different; *$P<0.001$, Bonferroni's multiple t test.
†$P<0.001$, Student's t test.

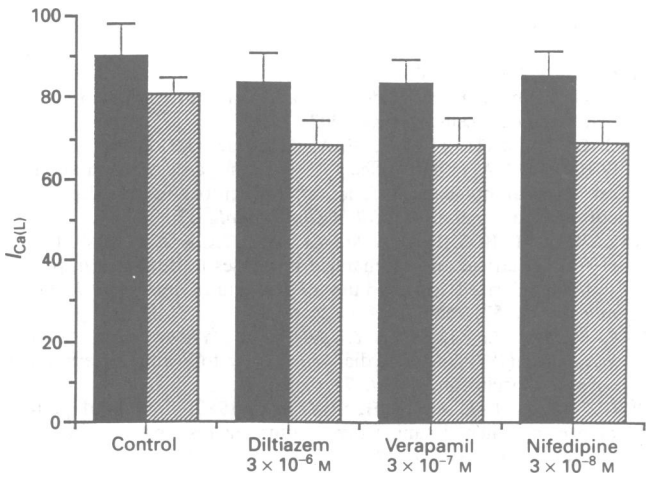


Figure 3 Tonic inhibition of $I_{Ca(L)}$ by 3×10^{-6} M diltiazem, 3×10^{-7} M verapamil and 3×10^{-8} M nifedipine at V_h − 80 mV (solid columns) and V_h − 60 mV (hatched columns). Values are means with s.e.mean for six experiments.

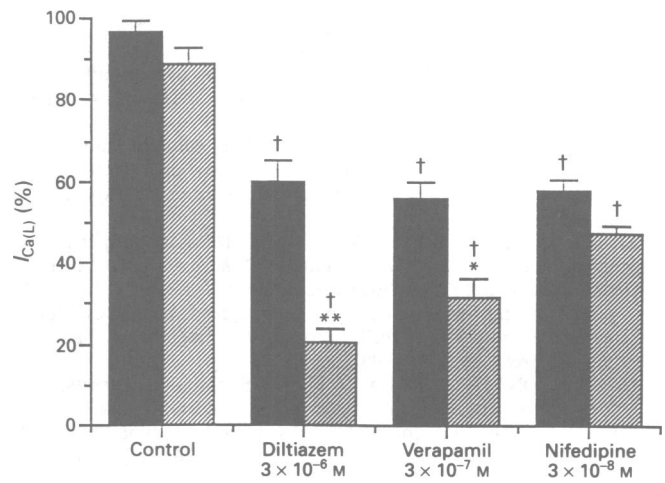


Figure 4 Inhibition of peak $I_{Ca(L)}$ activated at 1 Hz by 3×10^{-6} M diltiazem, 3×10^{-7} M verapamil and 3×10^{-8} M nifedipine at V_h − 80 mV (solid columns) and V_h − 60 mV (hatched columns). Values are means with s.e.mean for six experiments. †$P<0.001$ vs control; *$P<0.01$; **$P<0.001$ vs V_h − 80 mV.

antagonists by the membrane depolarization resulting from elevation of the extracellular K^+ concentration.

One of the most important findings of this study was that the degree of potentiation of the negative inotropic effects resulting from elevation of the extracellular K^+ concentration varied among diltiazem, verapamil and nifedipine.

The recording of $I_{Ca(L)}$ made it clear that the $I_{Ca(L)}$-blocking actions of the three calcium antagonists were differentially augmented by changing V_h from − 80 mV to − 60 mV, corresponding to the respective membrane potentials of the ventricular myocytes under normal and 12.7 mM K^+ conditions. The rank order of augmentation of the $I_{Ca(L)}$-blocking action among the three calcium antagonists agreed well with the rank order of potentiation of their negative inotropic effects induced by elevation of the extracellular K^+ concentration. These results suggest that the differences in voltage-dependency of the $I_{Ca(L)}$-blocking action may be responsible for the differences in potentiation of the negative inotropic effects among the calcium antagonists.

In the recording of $I_{Ca(L)}$, the concentration of each drug was chosen so as to reduce the amplitude of $I_{Ca(L)}$ to approximately 60% at V_h − 80 mV at a frequency of 1 Hz (see Figure 2). The concentration of nifedipine was the lowest; that of verapamil was 10 fold and that of diltiazem was 100 fold higher than that of nifedipine. This concentration ratio was consistent with the relative potencies of the negative inotropic effects of the three drugs under normal conditions in papillary muscles.

In the present study, the component of the $I_{Ca(L)}$-blocking action of the three calcium antagonists that was enhanced by the membrane depolarization was the use-dependent block.

In the present study, nifedipine showed use-dependent block without significant tonic block of $I_{Ca(L)}$, although dihydropyridine has been reported to produce marked tonic block (Lee & Tsien, 1983). One of the possible reasons for this was that nifedipine at 3×10^{-8} M was at a rather low concentration to produce detectable tonic block. Another explanation may be that nifedipine also shows use-dependent block when a stimulus frequency higher than 1 Hz is applied (Uehara & Hume, 1985).

The present findings suggest that the negative inotropic effects of diltiazem and verapamil may be potentiated by an increase of extracellular K^+ concentration under certain ischaemic conditions. Drugs which reduce myocardial contraction locally and decrease oxygen demand are desirable as therapeutic agents for myocardial ischaemia. However, nifedipine, verapamil and diltiazem are known to be far more potent in producing coronary vasodilatation than in producing negative inotropic effects. Himori *et al.* (1976) reported that the doses of diltiazem and verapamil producing a 50% decrease in the developed tension were 5.2 and 3.5 times higher than the doses producing a 100% increase in blood

flow rate, respectively, in canine isolated blood-perfused papillary muscles. Nevertheless, the present results suggest that dilitiazem and verapamil, at doses which produce coronary vasodilatation, can reduce contractile force when extracellular K^+ concentration is elevated. In the case of regional ischaemia, these drugs may preferentially suppress contraction of the ischaemic area at doses producing no effects on normal myocardium. This may partly explain the differential selectivity of the calcium antagonists in the ischaemic heart (see Introduction).

Under ischaemic conditions, various metabolic and ionic changes such as milieu pH changes are known to occur other than elevation of extracellular K^+ concentration. These changes may also affect the potencies of calcium antagonists. Recently, calcium antagonists have been reported to inhibit the mitochondrial Na-Ca antiporter (Cox & Matlib, 1993) and anion channel (Zernig, 1990). Therefore effects of these drugs on mitochondria cannot be disregarded.

In conclusion, the differential potentiation of the negative inotropic effects of the three calcium antagonists by an increase in extracellular K^+ concentration can be explained by the difference in voltage-dependency of the use-dependent block of $I_{Ca(L)}$. The voltage-dependency of the use-dependent effects of diltiazem and verapamil may contribute to their protective effects on the ischaemic myocardium, without affecting the normal myocardium.

We are grategul to Prof. Rikuo Ochi (Juntendo University) for his kind technical advice. Thanks are also extended to Dr Jun-Ichiro Oka for valuable discussion. This work was supported by a Grant-in-Aid for Scientific Research from the Japanese Ministry of Education, Science and Culture.

References

CAVALIÉ, A., OCHI, R., PELZER, D. & TRAUTWEIN, W. (1983). Elementary currents through Ca^{2+} channels in guinea pig myocytes. *Pflügers Arch.*, **398**, 284–297.

COX, D.A. & MATLIB, M.A. (1993). Modulation of intramitochondrial free Ca^{2+} concentration by antagonists of Na-Ca exchange. *Trends Pharmacol. Sci.*, **14**, 408–413.

EHARA, T. & KAUFMANN, R. (1978). The voltage- and time-dependent effects of (−)-verapamil on the slow inward current in isolated cat ventricular myocardium. *J. Pharmacol. Exp. Ther.*, **207**, 49–55.

GLOSSMANN, H. & STRIESSNIG, J. (1990). Molecular properties of calcium channels. *Rev. Physiol. Biochem. Pharmacol.*, **114**, 1–105.

HAMILL, O.P., MARTY, A., NEHER, E., SAKMANN, B. & SIGWORTH, F.J. (1981). Improved patch-clamp techniques for high-resolution current recording from cells and cell-free membrane patches. *Pflügers Arch.*, **391**, 85–100.

HIMORI, N., ONO, H. & TAIRA, N. (1976). Simultaneous assessment of effects of coronary vasodilators on the coronary blood flow and the myocardial contractility by using the blood-perfused canine papillary muscle. *Jpn. J. Pharmacol.*, **26**, 427–435.

HIRCHE, H., FRANZ, C., BÖS, L., BISSIG, R., LANG, R. & SCHRAMM, M. (1980). Myocardial extracellular K^+ and H^+ increase and noradrenaline release as possible cause of early arrhythmias following acute coronary artery occlusion in pigs. *J. Mol. Cell. Cardiol.*, **12**, 579–593.

HONDEGHEM, L.M. & KATZUNG, B.G. (1984). Antiarrhythmic agents: the modulated receptor mechanism of action of sodium and calcium channel-blocking drugs. *Annu. Rev. Pharmacol. Toxicol.*, **24**, 387–423.

ICHIHARA, K. & ABIKO, Y. (1982). Effect of diltiazem, a calcium antagonist, on myocardial pH in ischemic canine heart. *J. Pharmacol. Exp. Ther.*, **222**, 720–725.

ICHIHARA, K., SAKAI, K. & ABIKO, Y. (1986). Effect of nifedipine and niludipine on myocardial pH in the ischemic canine heart. *Arch. Int. Pharmacodyn.*, **280**, 58–73.

ISENBERG, G. & KLOCKNER, U. (1982). Calcium tolerant ventricular myocytes prepared by preincubation in a 'KB medium'. *Pflügers Arch.*, **395**, 6–18.

KANAYA, S. & KATZUNG, B.G. (1983). Effects of diltiazem on transmembrane potential and current of right ventricular papillary muscle of ferrets. *J. Pharmacol. Exp. Ther.*, **228**, 245–251.

KLONER, R.A. & BRAUNWALD, E. (1987). Effects of calcium antagonists on infarcting myocardium. *Am. J. Cardiol.*, **59**, 84B–94B.

LEE, K.S. & TSIEN, R.W. (1983). Mechanism of calcium channel blockade by verapamil, D600, diltiazem and nitrendipine in single dialysed heart cells. *Nature*, **302**, 790–794.

NAGAO, T., MATLIB, M.A., FRANKLIN, D., MILLARD, R.W. & SCHWARTZ, A. (1980). Effects of diltiazem, a calcium antagonist, on regional myocardial function and mitochondria after brief coronary occlusion. *J. Mol. Cell. Cardiol.*, **12**, 29–43.

NAKAJIMA, H., HOSHIYAMA, M., YAMASHITA, K. & KIYOMOTO, A. (1976). Electrical and mechanical responses to diltiazem in potassium depolarized myocardium of the guinea pig. *Jpn. J. Pharmacol.*, **26**, 571–580.

NAKAMURA, M., KIKUCHI, Y., SENDA, Y., YAMADA, A. & KOIWAYA, Y. (1980). Myocardial blood flow following experimental coronary occlusion. *Chest*, **78**, 205–209.

PÉREZ, J.E., SOBEL, B.E. & HENRY, P.D. (1980). Improved performance of ischemic canine myocardium in response to nifedipine and diltiazem. *Am. J. Physiol.*, **239**, H658–H663.

REIMER, K.A. & JENNINGS, R.B. (1985). Effects of calcium-channel blockers on myocardial preservation during experimental acute myocardial infarction. *Am. J. Cardiol.*, **55**, 107B–115B.

TAIRA, N. (1987). Differences in cardiovascular profile among calcium antagonists. *Am. J. Cardiol.*, **59**, 24B–29B.

TRIGGLE, D.J. (1991). Calcium-channel drugs: structure-function relationships and selectivity of action. *J. Cardiovasc. Pharmacol.*, **18**, S1–S6.

UEHARA, A. & HUME, J.R. (1985). Interactions of organic calcium channel antagonists with calcium channels in single frog atrial cells. *J. Gen. Physiol.*, **85**, 621–647.

WIEGAND, V., GÜGGI, M., MEESMANN, W., KESSLER, M. & GREITSCHUS, F. (1979). Extracellular potassium activity changes in the canine myocardium after acute coronary occlusion and the influence of beta-blockade. *Cardiovasc. Res.*, **13**, 297–302.

ZERNIG, G. (1990). Widening potential for Ca^{2+} antagonists: non-L-type Ca^{2+} channel interaction. *Trends Pharmacol. Sci.*, **11**, 38–44.

(Received August 25, 1993
Revised June 3, 1994
Accepted June 16, 1994)

Br. J. Pharmacol. (1994), **113**, 457–462

© Macmillan Press Ltd, 1994

Release of Ca^{2+} from intracellular store in smooth muscle cells of rat portal vein by ATP-induced Ca^{2+} entry

Pierre Pacaud, Guillaume Grégoire & [1]*Gervaise Loirand

Laboratoire de Physiologie, Faculté de médecine Victor Pachon, Université de Bordeaux II, 146 rue Léo Saignat 33076 Bordeaux, France and *INSERM U390, Hopital Arnaud de Villeneuve 34000 Montpellier, France

1 The action of adenosine 5'-triphosphate (ATP, 10 μM) was studied in single patch-clamped smooth muscle cells of rat portal vein where the free internal Ca^{2+} concentration in the cell (Ca_i) was estimated by the emission from the dye indo-1.

2 In the presence of 20 μM gallopamil (D600), a blocker of voltage-dependent Ca^{2+} channels, ATP applied to cells held at a holding potential of − 60 mV evoked a transient inward current and an increase in Ca_i.

3 The rise in Ca_i evoked by ATP was completely suppressed in the absence of external Ca^{2+} although a transient inward current was still observed.

4 ATP-induced responses were not modified by the addition of the inositol 1,4,5-trisphosphate receptor antagonist, heparin (1 mM) in the pipette solution.

5 In the presence of caffeine (5 mM) or ryanodine (100 μM) in the pipette solution, which deplete the intracellular Ca^{2+} store, the ATP-induced Ca_i rise was greatly reduced.

6 Our results suggest that in single cells from rat portal vein, ATP releases Ca^{2+} from intracellular stores without involving $InsP_3$, but via a Ca^{2+} release mechanism activated by Ca^{2+} influx through ATP-gated channels.

Keywords: ATP; intracellular Ca^{2+} store; ryanodine; Ca^{2+}-induced Ca^{2+} release

Introduction

There is considerable evidence that ATP is involved in the control of vascular tone. It mediates both indirect vasodilatation via the endothelium and vasoconstriction by direct stimulation of smooth muscle cells (Kennedy *et al.*, 1985). Sufficient amounts of ATP to activate myocytes could be released locally from damaged endothelial or smooth muscle cells, as well as in the course of intravascular aggregation. In addition, it is well known that ATP is released as an excitatory co-transmitter together with noradrenaline at sympathetic nerve terminals present in smooth muscle tissues (Von Kugelgen & Starke, 1991).

It has been demonstrated in a variety of smooth muscle cells that application of exogenous ATP activates a cation-selective channel (Benham *et al.*, 1987; Benham & Tsien, 1987; Friel, 1988; Xiong *et al.*, 1991; Schneider *et al.*, 1991) and produces a rapid increase in cytosolic Ca^{2+} concentration (Ca_i) (Benham, 1989; Schneider *et al.*, 1991). ATP-induced Ca_i increase could result from stimulation of Ca^{2+} entry either by direct Ca^{2+} permeation through ATP-gated channels (Benham, 1989; Schneider *et al.*, 1991) or indirectly via membrane depolarization and opening of voltage-dependent Ca^{2+} channels (Katsuragi *et al.*, 1990). Furthermore, it has been shown that ATP induces Ca^{2+} release from intracellular stores (Droogmans *et al.*, 1991) probably via the formation of the intracellular second messenger, inositol 1,4,5-trisphosphate ($InsP_3$).

In the present study, by means of simultaneous measurement of membrane currents and Ca_i, we show that ATP releases Ca^{2+} from an intracellular Ca^{2+} store in smooth muscle cells isolated from rat portal vein, without involving the $InsP_3$ receptor. The ATP-induced Ca^{2+} release results from a Ca^{2+}-induced Ca^{2+} release (CICR) mechanism, activated by the influx of Ca^{2+} through a cation channel gated by ATP.

[1] Author for correspondence at present address: Laboratoire de Physiologie, Faculté de médecine Victor Pachon, Université de Bordeaux II, 146 rue Léo Saignat 33076 Bordeaux, France.

Methods

Cell preparation

Wistar rats (150 g) were stunned and then killed by cervical dislocation. The portal vein was cut into several pieces, incubated for 10 min in low-Ca^{2+} (40 μM) physiological saline solution (PSS, composition given below), and then incubated in low-Ca^{2+} PSS containing 1.2 mg ml^{-1} collagenase, 0.5 mg ml^{-1} pronase and 1 mg ml^{-1} bovine serum albumin at 37°C for 20 min. After this, the solution was removed and the pieces of vein were incubated again in a fresh enzyme-free solution and triturated with a fire polished Pasteur pipette to release cells. Cells were stored on glass cover-slips at 4°C in PSS containing 0.8 mM Ca^{2+} at a density of about $1-5 \times 10^4$ cells ml^{-1} and used on the same day. About 80–90% of the cells excluded trypan blue, and contracted in response to various agonists and membrane depolarization.

Membrane current and fluorescence measurements

Voltage clamp and membrane current recordings were made with standard patch-clamp techniques using a Biologic RK400 patch-clamp amplifer. Whole-cell membrane currents were recorded with borosilicate patch pipettes of 1 to 4 MΩ resistance. The series resistances (5–8 MΩ) were not corrected. The liquid junction potentials were corrected with an offset circuit before each experiment. Membrane potential and current records were stored and analysed with an IBM-PC computer.

Measurement of Ca_i was carried out as described previously (Pacaud *et al.*, 1991). Indo-1 (50 μM) was added to the pipette solution, and so entered cells following establishment of the whole-cell recording mode. Cell fluorescence was then monitored in order to follow dye loading, which usually reached a steady state after 1–3 min and recording was started at this point. Ca_i was estimated from the 405/480 ratio (Grynkiewicz *et al.*, 1985).

Results are expressed as the mean ± s.e.mean with n the sample size. Significance was tested by means of Student's t test.

Solutions

The normal physiological saline solution (PSS) contained (in mM): NaCl 130, KCl 5.6, $MgCl_2$ 1, $CaCl_2$ 2, glucose 11, N-[2-hydroxyethyl]piperazine-N'-[2-ethanesulphonic acid] (HEPES) 10, pH 7.4 with NaOH. Ca^{2+}-free PSS was prepared by omitting $CaCl_2$. The basic pipette solution contained (in mM): CsCl 110, NaCl 20, HEPES 10 and was buffered with the addition of approximately 5 mM NaOH. ATP was applied to the recorded cell by pressure ejection from a glass pipette for the period indicated on the records. No change in the holding current was observed during ejection of the physiological saline solution. All experiments were done at room temperature.

Chemicals and drugs

Collagenase was from Worthington, pronase (type E), bovine serum albumin, adenosine 5'-triphosphate disodium salt (ATP), gallopamil hydrochloride (D600) and heparin (from porcine intestinal mucosa; molecular weight, 4000–6000), were purchased from Sigma. Indo-1 (pentasodium salt) and ryanodine were from Calbiochem. Caffeine was from Merck.

Results

ATP induces an inward current and a rise in Ca_i

In the presence of 20 μM D600, application of exogenous ATP (10 μM, 5 s) to a single smooth muscle cell held at a potential of − 60 mV induced a transient inward current and an increase in Ca_i (Figure 1a). The ATP-induced current reached a peak 0.62 ± 0.08 s ($n = 9$) after the onset of the response. The maximal value of ATP-induced Ca_i rise (533 ± 82 nM, $n = 9$) was reached 3.30 ± 0.64 s ($n = 9$) after the peak of the inward current. The absence of inward currents in response to the voltage pulses from − 60 mV to 0 mV attested to the effective blockade of the voltage-dependent Ca^{2+} channels by D600 and thus ruled out the involvement of Ca^{2+} entry through voltage-dependent Ca^{2+} channels in the ATP-induced Ca_i rise.

In nominally Ca^{2+}-free solution, application of ATP (10 μM, 5 s) still induced an inward current whereas no rise in Ca_i was observed (Figure 1b). The absence of inward current and rise in Ca_i in response to membrane depolarization from − 60 mV to 0 mV indicated that no external Ca^{2+} entered the cells. The ATP-induced current recorded under these conditions was significantly shorter (2.11 ± 0.17 s, $n = 8$) than that recorded in 2 mM Ca^{2+}-PSS (3.04 ± 0.22 s, $n = 9$; $P = 0.02$) although the time to peak was not modified (0.67 ± 0.06 s, $n = 8$; $P > 0.5$). This difference was probably due to the presence of the Ca^{2+}-dependent Cl^- current component activated by the rise in Ca_i induced by ATP in the presence of external Ca^{2+} (Pacaud et al., 1992).

ATP activates Ca^{2+} release

Experiments shown in Figure 2 were performed in the absence of voltage-dependent Ca^{2+} channel inhibitors at a Cl^- equilibrium potential of − 45 mV achieved by substituting 105 mM Cs-aspartate for 105 mM CsCl in the pipette solution. In these latter experimental conditions, the Ca^{2+}-dependent Cl^- current at a holding potential of − 60 mV was reduced. Application of ATP to a cell held at − 60 mV evoked a transient inward current accompanied by a rise in Ca_i (Figure 2a). The ATP-induced current did not contain a Cl^- component as the Ca_i threshold for Cl^- current activation was not reached at the time when it was recorded (Pacaud et al., 1992). After the complete decline of the ATP-induced current, Ca_i increased up to a peak and then gradually fell to the resting level. During this delayed Ca_i rise, a small inward Cl^- current was activated. Application of membrane depolarization from − 60 mV to 0 mV a few seconds after Ca_i returned to the resting level induced only a small rise in Ca_i which has been shown to correspond to Ca^{2+} entry through voltage-dependent Ca^{2+} channels (Grégoire et al., 1993); 2 min later, a pair of similar depolarizations was applied (Figure 2b). The first one produced a regenerative Ca_i increase which occurred after the end of the voltage pulse and corresponded to Ca^{2+} release induced by Ca^{2+} entry through voltage-dependent Ca^{2+} channels (Grégoire et al., 1993). This rise in Ca_i activated the Ca^{2+} dependent Cl^- current. The second depolarization of the pair induced only a small rise in Ca_i which declined at the end of the voltage jump. A similar experiment was performed after replacing external Ca^{2+} by Sr^{2+}. Figure 3a clearly shows that under these conditions, the inward current activated by ATP at a holding potential of − 60 mV, was accompanied by only a small change in the fluorescence signal. The maximal increase in fluorescence was obtained 2.28 ± 0.74 s ($n = 4$) after the peak of ATP-induced current and was observed together with a large Cl^- current. After the fluorescence signal had returned to the resting value, voltage-dependent Ca^{2+} channels, known to be permeable to Sr^{2+} (Hess et al., 1986), were activated by membrane depolarization from − 60 mV to 0 mV. This produced a fluorescence increase which declined immediately upon repolarization; 2 min later (Figure 3b), although the Sr^{2+} current evoked by the same depolarization had a similar amplitude, the fluorescence increase was larger and reached a peak 1–2 s after the repolarization. During this phase of regenerative fluorescence rise, ascribed to release from the intracellular Ca^{2+} store (Grégoire et al., 1993), a large Cl^- tail current was activated. A second

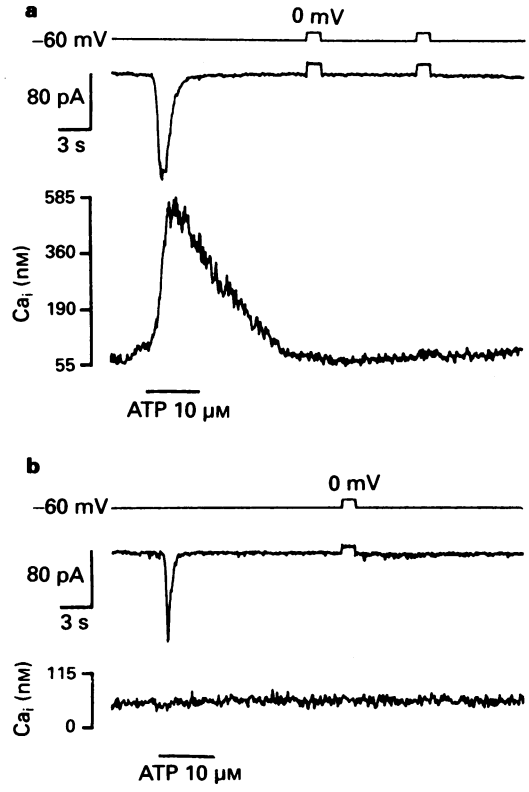


Figure 1 Effects of application of ATP (10 μM, 5 s) on membrane current and Ca_i under voltage-clamp at a holding potential of − 60 mV. Traces show membrane potential (top), membrane current (middle) and Ca_i (bottom). (a) In normal external PSS with 2 mM Ca^{2+} and 20 μM D600, ATP induced a transient inward current and an increase in Ca_i. (b) In the absence of external Ca^{2+}, ATP induced an inward current but no change in Ca_i. Depolarizations to 0 mV show that no Ca^{2+} entry through voltage-dependent Ca^{2+} channels could be evoked in (a) and (b). Traces in (a) and (b) were obtained from two different cells.

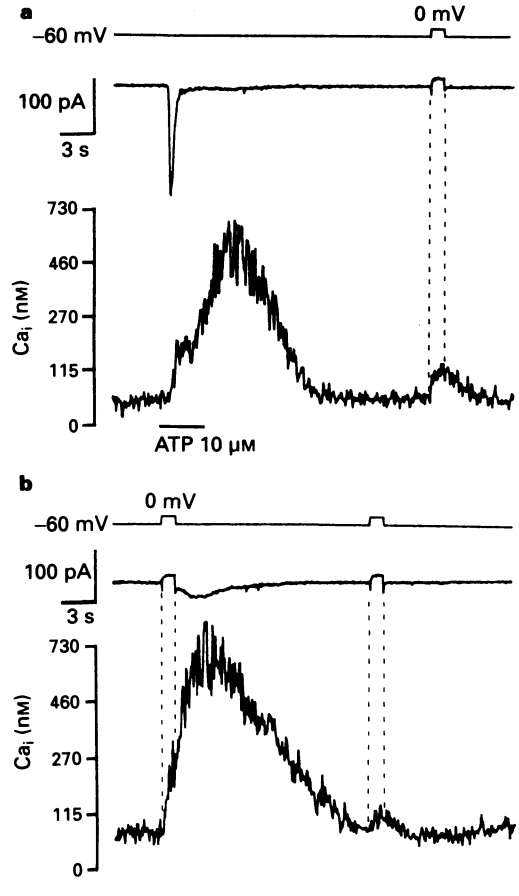


Figure 2 Effects of membrane depolarizations from − 60 mV to 0 mV following ATP (10 μM) application in 2 mM Ca^{2+}-PSS. Traces show membrane potential (top), membrane current (middle) and Ca_i (bottom). (a) Membrane depolarization applied after ATP application induced a small rise in Ca_i. (b) Two minutes later, the first depolarization of a pair produced a regenerative increase in Ca_i which occurred after the end of the voltage step; the second one induced a small increase in Ca_i, similar to that recorded in (a).

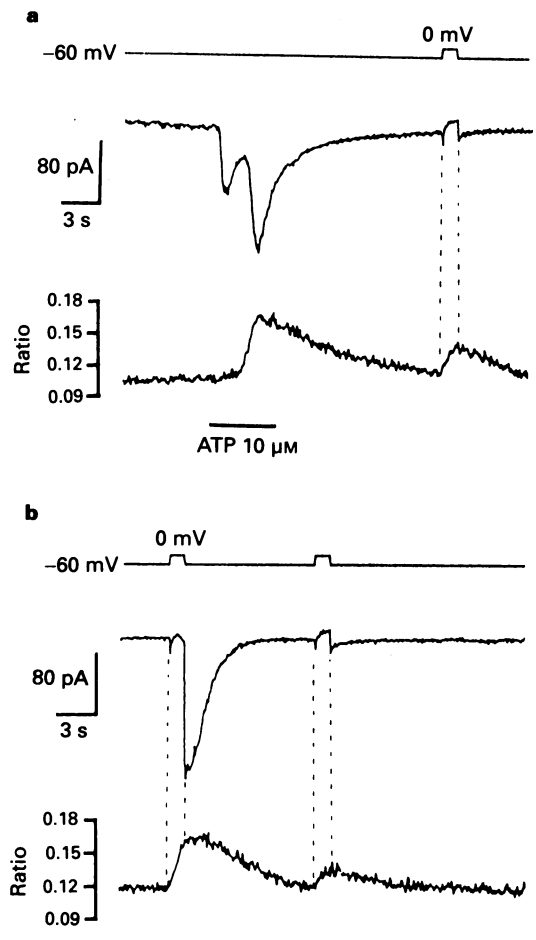


Figure 3 Effects of membrane depolarizations from − 60 mV to 0 mV following ATP (10 μM) application in 2 mM Sr^{2+}-PSS. Traces show membrane potential (top), membrane current (middle) and indo-1 fluorescence expressed as the 405:480 ratio (bottom). (a) ATP induced a transient inward current and a delayed increase in Ca_i which activated a Ca^{2+}-dependent Cl^- current. The depolarization then applied evoked a rise in fluorescence which decayed upon repolarization. (b) Two minutes later, the first depolarization of a pair produced a larger increase in fluorescence, which was maintained after the repolarization and activated a large Cl^- tail current. The second depolarization evoked a smaller rise in fluorescence, insufficient to activate Cl^- current.

depolarization applied immediately after the membrane current and the fluorescence signal had returned to resting values did not produce a regenerative fluorescence rise but only a small and short increase in fluorescence ratio during the voltage pulse.

Does the ATP-induced Ca_i rise contain an $InsP_3$-induced Ca^{2+} release component?

In an attempt to test the possible involvement of $InsP_3$-induced Ca^{2+} release in the ATP-evoked Ca_i rise, heparin (1 mM) a competitive antagonist of $InsP_3$ binding to its receptor (Worley *et al.*, 1987) was added to the pipette solution (Figure 4). This experimental protocol has been shown to inhibit completely the $InsP_3$-induced Ca^{2+} release evoked by noradrenaline application, 5 min after breakthrough into the whole-cell recording mode (Pacaud *et al.*, 1991). Under these conditions, ATP still induced a transient inward current at a holding potential of − 60 mV and a rise in Ca_i. The peak Ca_i reached 515 ± 99 nM ($n = 4$) and thus, was not significantly different from that obtained in the absence of heparin. As described above (Figure 2), only a small and short rise in Ca_i was observed in response to the voltage pulse from − 60 mV to 0 mV applied immediately after ATP application; 30 s later, the same voltage pulse produced a regenerative Ca_i rise, attesting that the Ca^{2+} store was at least partially refilled and that the CICR mechanism remained functional in the presence of heparin.

ATP releases Ca^{2+} by activating ryanodine receptor

To gain further insight into the mechanism through which ATP releases Ca^{2+} from intracellular store, ATP responses were evoked in cells treated with caffeine and ryanodine (Figure 5). Caffeine is known to increase the open probability of the Ca^{2+}-activated Ca^{2+} release channel (Herrmann-Frank *et al.*, 1991). When added to the extracellular solution, caffeine (5 mM) causes a large transient increase in Ca_i, which activates the Ca^{2+}-dependent Cl^- current at a holding potential of − 60 mV (Pacaud *et al.*, 1989). As in Figure 5a, this Ca_i transient can be followed by smaller oscillations. When membrane current and Ca_i decreased to stable levels, application of ATP still produced a large inward current whereas the rise in Ca_i was strongly reduced in amplitude and duration. The maximal Ca_i (235 ± 18 nM, $n = 4$) was reached 0.47 ± 0.03 s ($n = 4$) after the peak inward current induced by ATP, i.e. significantly more rapidly than under control conditions. Application of a pair of depolarization pulses to 0 mV from a holding potential of − 60 mV evoked small rises in Ca_i that reached a peak at the end of the voltage pulse and decayed immediately upon repolarization. The absence of regenerative Ca_i rise in response to the first depolarization of the pair indicated that treatment with

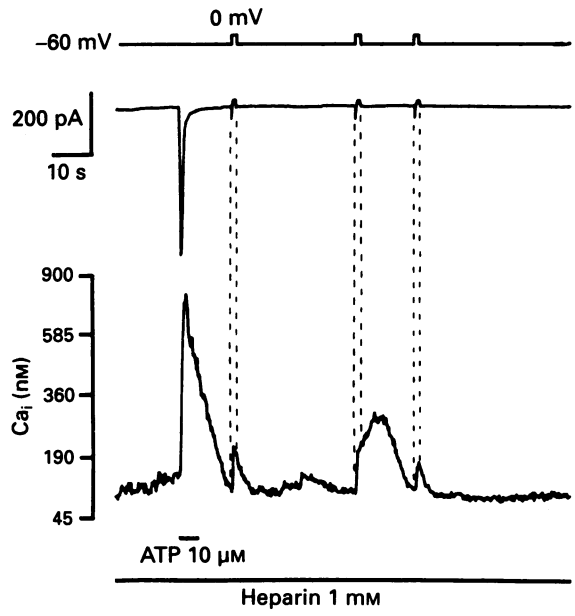


Figure 4 Effect of ATP (10 μM) in cell held at a holding potential of − 60 mV, in the presence of heparin (1 mM) in the pipette solution. Traces show membrane potential (top), membrane current (middle) and Ca_i (bottom). The protocol used was similar to that in Figure 2. ATP was applied 5 min after breakthrough into the whole-cell recording mode. ATP application was followed by a depolarization to 0 mV, then approximately 30 s later, a pair of similar depolarizations was applied.

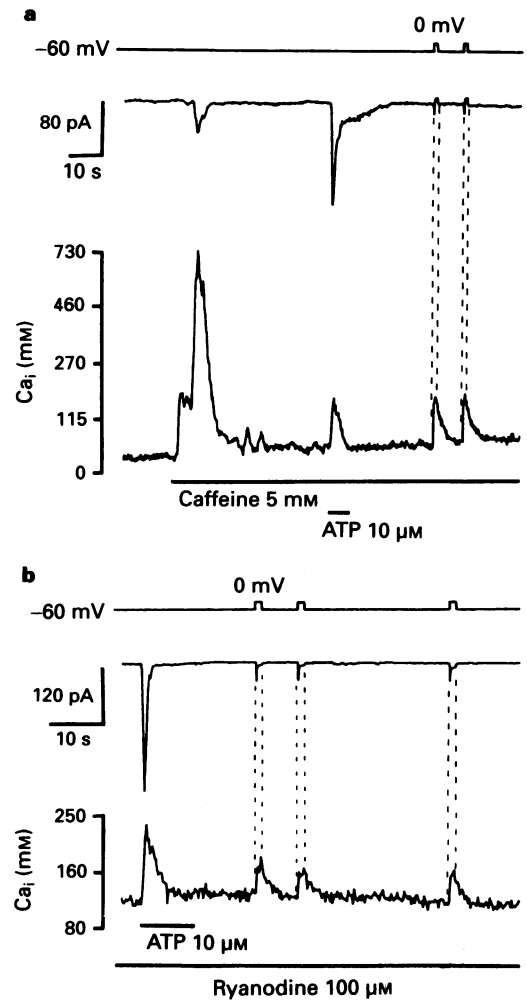


Figure 5 Effect of ATP (10 μM) at a holding potential of − 60 mV in the presence of caffeine or ryanodine. Traces show membrane potential (top), membrane current (middle) and Ca_i (bottom). (a) Extracellular application of caffeine (5 mM) transiently increased Ca_i and activated the Ca^{2+}-dependent Cl^- current. In the continued presence of caffeine, ATP and a pair of depolarizations to 0 mV were successively applied to the cell. (b) Recordings showing the effects of ATP and depolarizations to 0 mV in a cell dialysed with a 100 μM ryanodine-containing pipette solution.

caffeine prevented activation of CICR mechanism (Grégoire *et al.*, 1993).

Ryanodine is also a tool commonly used for the study of CICR and is thought to inhibit CICR by binding to the release channel and stabilizing an open subconductance state (Rousseau *et al.*, 1987). A typical ATP-induced response recorded at a holding potential of − 60 mV in a cell dialysed with a 100 μM ryanodine-containing pipette solution for 5 min is illustrated in Figure 5b. ATP induced an inward current and an increase in Ca_i similar to those evoked in the presence of caffeine. The maximal Ca_i (269 ± 14 nM, $n = 4$) was reached 0.42 ± 0.03 s ($n = 4$) after the peak inward current. Then, each depolarization applied from − 60 mV to 0 mV induced an identical rise in Ca_i. As previously described (Grégoire *et al.*, 1993), the regenerative CICR evoked by membrane depolarization was abolished in the presence of ryanodine.

Discussion

The experiments described in this paper show that application of extracellular ATP in portal vein smooth muscle cells induces a transient current and an increase in Ca_i. These effects of ATP could be explained either by the activation of a Ca^{2+} permeable conductance which causes a rise in Ca_i, or by a Ca^{2+} release from internal Ca^{2+} store which activates a Ca^{2+}-dependent current.

The ATP-induced current is inward at a holding potential of − 60 mV, is not modified by a shift of the Cl^- equilibrium potential, shows fast activation and inactivation, and allows Ca^{2+} influx. These properties are similar to those reported for the non-selective cation current directly gated by ATP in other smooth muscle cells (Friel 1988; Benham, 1989; Schneider *et al.*, 1991).

The ATP-induced Ca_i rise was resistant to voltage-dependent Ca^{2+} channel block but was completely inhibited in the absence of extracellular Ca^{2+}. The Ca^{2+} release component of the Ca_i rise induced by Ca^{2+} entry through voltage-dependent Ca^{2+} channels was abolished when membrane depolarization was applied immediately after the ATP-induced response. A similar result was obtained when extracellular Ca^{2+} was replaced by Sr^{2+}. Because of the indo-1 fluorescence characteristics in the presence of Sr^{2+} (Grégoire *et al.*, 1993), the rise in fluorescence due to Sr^{2+} entry is small and allows a component of Ca^{2+} release, if any, to be observed more easily. Thus, these data suggest that Ca^{2+} or Sr^{2+} entry through ATP-gated cation channels induces a Ca^{2+} release from an intracellular Ca^{2+} store similar to that evoked by Ca^{2+} or Sr^{2+} entry through voltage-dependent Ca^{2+} channels.

In many cell types including smooth muscle cells, the functional effects elicited by exposure to extracellular ATP can be correlated with an ATP-induced mobilization of the intracellular Ca^{2+} store (see Dubyak & El-Moatassim (1993) for review). This Ca^{2+} mobilizing action has been ascribed to ATP-induced stimulation of $InsP_3$ formation, with the generated $InsP_3$ mediating the release of Ca^{2+} (Hoiting *et al.*, 1990; Droogmans *et al.*, 1991). In our experiments, although no Ca_i response at all was recorded in the absence of divalent cations in the external solution, it is possible that a release of Ca^{2+} from the internal store induced by the generation of

$InsP_3$ is involved in the ATP-induced Ca_i rise. It is known that phospholipase C and thus $InsP_3$ formation can be stimulated by Ca^{2+} (Ryo *et al.*, 1987). Thus, a possible amplification of the Ca^{2+} release initially triggered through CICR mechanism could occur as a consequence of $InsP_3$-induced Ca^{2+} release. This hypothesis has been ruled out by the use of heparin: the ATP-induced Ca_i rise was not affected by the presence of heparin in the pipette solution and thus was independent of the activation of the $InsP_3$ receptors.

Treatment with caffeine or ryanodine, known to deplete intracellular stores, leads to a similar and powerful reduction of the ATP-induced Ca_i rise. This is consistent with the involvement of a CICR component in the Ca_i increase produced by ATP. This component, corresponding to the release of Ca^{2+} from an intracellular store activated by Ca^{2+} influx through an ATP-gated channel constitutes the major part of the ATP-induced Ca_i rise in portal vein smooth muscle cells.

We have recently identified, in this cell type, a CICR mechanism that could be initiated by Ca^{2+} entry through voltage-dependent Ca^{2+} channels (Grégoire *et al.*, 1993). The activation of Ca^{2+} release by Ca^{2+} ions that enter the cell through ATP-activated cation channel suggests that, more generally, every Ca^{2+} entry could be amplified by release of Ca^{2+} from intracellular stores. In the case of ATP, results obtained in the presence of ryanodine or caffeine show that the part of the Ca_i rise due to Ca^{2+} entry was small. As membrane currents and Ca_i could be simultaneously recorded in the same cell in response to application of ATP and membrane depolarization, the contribution of Ca^{2+} to the ATP-activated cation current was evaluated (in the presence of caffeine or ryanodine) by comparing the Ca_i rise due to the ATP-gated current with that due to voltage-dependent Ca^{2+} channel currrent (Schneider *et al.*, 1991). Based on this comparison, we estimate that approximately 6% of the ATP-activated cation current is carried by Ca^{2+} ions. This value is very close to that reported by Schneider *et al.* (1991) as they estimated, using the same method, that 5.8% of the ATP-gated channel of myocytes from guinea-pig urinary bladder was carried by Ca^{2+}. This Ca^{2+} entry amplified by a Ca^{2+} release from an intracellular Ca^{2+} store independent of $InsP_3$ generation constitutes a novel mechanism of action. However, effects of ATP in portal vein myocytes would not be independent of those induced by noradrenaline (NA) which is co-liberated at sympathetic nerve terminals. NA has been shown to release Ca^{2+} from an intracellular Ca^{2+} store via activation of the $InsP_3$ receptor (Pacaud *et al.*, 1991) but, in portal vein smooth muscle cells, $InsP_3$-sensitive and ryanodine-sensitive Ca^{2+} stores seem to overlap widely (Grégoire *et al.*, 1993). Thus, responses to NA and ATP, at least for maximal concentrations, might not be additive. For intermediate concentrations, ATP and NA are expected to act in a synergistic manner, because Ca^{2+} released via $InsP_3$ receptor activation during NA stimulation could amplify the CICR activated by ATP and conversely, $InsP_3$ receptor could also be positively regulated by Ca^{2+} released through the ryanodine receptor (Iino & Endo, 1992). Thus, synergistic interaction between different pharmacological receptors can occur not only for agonists that converge on the same intracellular transduction mechanism (Helliwell *et al.*, 1994). This hypothesis remains to be demonstrated; nevertheless, it seems that the vascular neurotransmission is more complex than previously thought.

This work was supported by a grant from the 'Conseil Régional d'Aquitaine' (9203023). We thank Drs R. Marthan and J.P. Savineau for helpful advice in the preparation of this manuscript.

References

BENHAM, C.D. (1989). ATP-activated channels gate calcium entry in single smooth muscle cells dissociated from rabbit ear artery. *J. Physiol.*, **419**, 689–701.

BENHAM, C.D., BOLTON, T.B., BYRNE, N.G. & LARGE, W.A. (1987). Action of extracellular adenosine triphosphate in single smooth muscle cells dispersed from the rabbit ear artery. *J. Physiol.*, **387**, 473–488.

BENHAM, C.D. & TSIEN, R.W. (1987). Receptor-operated, Ca-permeable channels activated by ATP in arterial smooth muscle. *Nature*, **328**, 275–278.

DROOGMANS, G., CALLEWAERT, G., DECLERCK, I. & CASTEELS, R. (1991). ATP-induced Ca^{2+} release and Cl^- current in cultured smooth muscle cells from pig aorta. *J. Physiol.*, **440**, 623–634.

DUBYAK, G.R. & EL-MOATASSIM, C. (1993). Signal transduction via P_2-purinergic receptors for extracellular ATP and other nucleotides. *Am. J. Physiol.*, **265**, C577–C606.

FRIEL, D.D. (1988). An ATP-sensitive conductance in single smooth muscle cells from the rat vas deferens. *J. Physiol.*, **401**, 361–380.

GREGOIRE, G., LOIRAND, G. & PACAUD, P. (1993). Ca^{2+} and Sr^{2+} entry induced Ca^{2+} release from the intracellular Ca^{2+} store in smooth muscle cells of rat portal vein. *J. Physiol.*, **472**, 483–500.

GRYNKIEWICZ, G., POENIE, M. & TSIEN, R.Y. (1985). A new generation of Ca^{2+} indicators with greatly improved fluorescence properties. *J. Biol. Chem.*, **260**, 3440–3450.

HELLIWELL, R.M., WANG, Q., HOGG, R.C. & LARGE, W.A. (1994). Synergistic action of histamine and adenosine triphosphate on the response to noradrenaline in rabbit pulmonary artery smooth muscle cells. *Pflügers Arch.*, **426**, 433–439.

HERRMANN-FRANK, A., DARLING, E. & MEISSNER, G. (1991). Functional characterization of the Ca^{2+}-gated Ca^{2+} release channel of vascular smooth muscle sarcoplasmic reticulum. *Pflügers Arch.*, **418**, 353–359.

HESS, P., LANSMAN, J.B. & TSIEN, R.W. (1986). Calcium channel selectivity for divalent and monovalent cations. Voltage and concentration dependence of single channel current in ventricular heart cells. *J. Gen. Physiol.*, **88**, 293–319.

HOITING, B., MOLLEMAN, A., DUIN, M., DEN HERTOG, A. & NELEMANS, A. (1990). P_2 purinoceptor-mediated inositol phosphate formation in relation to cytoplasmic calcium in DDT_1 MF-2 smooth muscle cells. *Eur. J. Pharmacol.*, **189**, 31–39.

IINO, M. & ENDO, M. (1992). Calcium-dependent immediate feedback control of inositol 1,4,5-trisphosphate induced Ca^{2+} release. *Nature*, **360**, 76–78.

KATSURAGI, T., USUNE, S. & FURUKAWA, T. (1990). Antagonism by nifedipine of contraction and Ca^{2+} influx evoked by ATP in guinea-pig urinary bladder. *Br. J. Pharmacol.*, **100**, 370–374.

KENNEDY, C., DELBRO, D. & BURNSTOCK, G. (1985). P_2-purinoceptors mediate both vasodilatation (via endothelium) and vasoconstriction of the isolated femoral artery. *Eur. J. Pharmacol.*, **107**, 161–168.

PACAUD, P., LOIRAND, G., BARON, A., MIRONNEAU, C. & MIRONNEAU, J. (1991). Ca^{2+} channel activation and membrane depolarization mediated by Cl^- channels in response to noradrenaline in vascular myocytes. *Br. J. Pharmacol.*, **104**, 1000–1006.

PACAUD, P., LOIRAND, G., GREGOIRE, G., MIRONNEAU, C. & MIRONNEAU, J. (1992). Calcium-dependence of the calcium-activated chloride current in smooth muscle cells of rat portal vein. *Pflügers Arch.*, **421**, 125–130.

PACAUD, P., LOIRAND, G., MIRONNEAU, C. & MIRONNEAU, J. (1989). Noradrenaline activates a calcium-activated chloride conductance and increases voltage-dependent calcium current in cultured single cells of a rat portal vein. *Br. J. Pharmacol.*, **97**, 139–146.

ROUSSEAU, E., SMITH, J.S. & MEISSNER, G. (1987). Ryanodine modifies conductance and gating behaviour of single Ca^{2+} release channel. *Am. J. Physiol.*, **253**, C364–C368.

RYO, S.H., CHO, K.S., LEE, K.Y., SUH, P.G. & RHEE, S.G. (1987). Purification and characterization of two immunologically distinct phosphoinositide-specific phospholipase C from bovine brain. *J. Biol. Chem.*, **262**, 12511–12518.

SCHNEIDER, P., HOPP, H.H. & ISENBERG, G. (1991). Ca^{2+} influx through ATP-gated channels increments $[Ca^{2+}]_i$ and inactivates I_{ca} in myocytes from guinea-pig urinary bladder. *J. Physiol.*, **440**, 479–796.

VON KUGELGEN, I. & STARKE, K. (1991). Noradrenaline-ATP co-transmission in the sympathetic nervous system. *Trends Pharmacol Sci.*, **12**, 319–324.

WORLEY, P.F., BARABAN, J.M., SUPATTAPONE, S., WILSON, V.S. & SNYDER, S.H. (1987). Characterization of inositol trisphosphate receptor in brain. Regulation by pH and calcium. *J. Biol. Chem.*, **262**, 12132–12136.

XIONG, Z., KITAMURA, K. & KURIYAMA, H. (1991). ATP activates cationic currents and modulates the calcium current through GTP-binding protein in rabbit portal vein. *J. Physiol.*, **440**, 143–165.

(Received April, 11, 1994
Revised June 13, 1994
Accepted June 20, 1994)

Br. J. Pharmacol. (1994), **113**, 463–470 © Macmillan Press Ltd, 1994

Effects of divalent cations on the potency of ATP and related agonists in the rat isolated vagus nerve: implications for P_2 purinoceptor classification

[1]D.J. Trezise, N.J. Bell, I. Kennedy & P.P.A. Humphrey

Glaxo Institute of Applied Pharmacology, Department of Pharmacology, University of Cambridge, Tennis Court Road, Cambridge CB2 1QJ

1 By use of a 'grease-gap' technique, the depolarizing effects of adenosine 5'-triphosphate (ATP) and ATP analogues on the rat isolated vagus nerve were determined in normal and in Ca^{2+}/Mg^{2+}-free ($+1 \times 10^{-3}$ M ethylenediamine tetraacetic acid) physiological salt solution (PSS).

2 In normal PSS, ATP produced concentration-dependent depolarization responses but the concentration-effect curve to ATP was incomplete and a maximum effect was not achieved. The threshold concentration for depolarization was 1×10^{-5} M and at the highest concentration tested (1×10^{-3} M) the peak amplitude of the response to ATP only amounted to 71% of the depolarization produced by a near maximal response to 5-hydroxytryptamine (5-HT, $.1 \times 10^{-5}$ M).

3 In Ca^{2+}/Mg^{2+}-free PSS, ATP produced depolarization responses at much lower concentrations and of markedly larger amplitude. Under these conditions, the threshold concentration for depolarization was $1-3 \times 10^{-7}$ M and the maximal response to ATP amounted to 526% of the response to 5-HT (1×10^{-5} M) in normal PSS. The concentration-effect curve to ATP was sigmoid, with a defined maximum effect and a mean EC_{50} value of 1.2×10^{-6} M.

4 In contrast to the effects on responses to ATP, the absence of divalent cations in the PSS did not modify the effective concentrations of either α,β-methylene ATP or 5-HT. However, the maximum responses to both α,β-methylene ATP and 5-HT were significantly increased in Ca^{2+}/Mg^{2+}-free PSS.

5 The depolarizing effects of several analogues of ATP were determined in Ca^{2+}/Mg^{2+}-free PSS. ATP-γ-S and 2-methylthioATP were of similar potency to ATP (respective equi-effective molar ratios (EMRs) of 1.9 and 1.3, where ATP = 1) and similar maximum responses were obtained. α,β-Methylene ATP, β,γ-methylene ATP and β,γ-imido ATP were considerably less potent than ATP, analysis yielding mean EMRs of 48.9, 85.0 and 60.0, respectively. Maximum responses to these latter three agonists were not obtained at the highest concentrations tested ($1 \times 10^{-4}-3 \times 10^{-4}$ M). Benzoyl ATP, adenosine 5'-O-(2-thiodiphosphate) and adenosine diphosphate produced only small depolarizing responses at high concentrations ($> 1 \times 10^{-4}$ M). Adenosine monophosphate, adenosine and uridine 5'-triphosphate each had little or no depolarizing effect in Ca^{2+}/Mg^{2+}-free PSS.

6 These data demonstrate that in the absence of divalent cations the excitatory actions of some, but not all, purine nucleotides in the rat vagus nerve are markedly potentiated. In Ca^{2+}/Mg^{2+}-free PSS, the rank order of agonist potencies was ATP = 2-methylthioATP = ATP-γ-S >> α,β-methylene ATP = β,γ-imido ATP = β,γ-methylene ATP. These findings are in stark contrast to our previous observations in normal PSS where the rank order of agonist potencies for these nucleotides was α,β-methylene ATP > ATP-γ-S > β,γ-imido ATP = β,γ-methylene ATP > 2-methylthioATP > ATP.

7 We suggest that the two different rank orders of potency can be explained by differential metabolism involving Ca^{2+}/Mg^{2+}-dependent ectonucleotidases. If so, these data indicate that ATP and 2-methylthioATP are inherently more potent than α,β-methylene ATP as agonists at neuronal P_{2X} purinoceptors in the rat vagus nerve. The possible implications of these findings to the present system for subclassifying P_2 purinoceptors are profound.

Keywords: P_2 purinoceptors; rat vagus nerve; depolarization; ATP; 2-methylthioATP; α,β-methylene ATP

Introduction

The diverse actions of adenosine 5'-triphosphate (ATP) on many physiological systems are mediated via P_2 purinoceptors (see Burnstock, 1990, for review). Evidence from pharmacological studies indicates that P_2 purinoceptors are heterogeneous, and to date, at least five different receptor subtypes termed P_{2X}, P_{2Y}, P_{2T}, P_{2Z} and P_{2U} purinoceptors have been proposed (Burnstock & Kennedy, 1985; Gordon, 1986; O'Connor *et al.*, 1991). This concept of purinoceptor heterogeneity is corroborated by the recent cloning of two genes believed to encode the functional P_{2Y} and P_{2U} receptors (Lustig *et al.*, 1993; Webb *et al.*, 1993). In view of the paucity of available P_2 purinoceptor antagonists, the primary basis on which this classification has been founded is the differential relative agonist potencies of ATP and ATP analogues in different systems. For example, P_{2X} purinoceptor-mediated responses are characterized by the order of agonist potencies of α,β-methylene ATP > β,γ methylene ATP > ATP = 2 methylthioATP, whilst P_{2Y} purinoceptors are characterized by a rank order of potencies of 2 methylthioATP > ATP > α,β-methylene ATP = β,γ methylene ATP (Burnstock & Kennedy, 1985).

Recently, we described the depolarizing actions of ATP on the rat isolated vagus nerve and characterized the receptors mediating this response using a range of ATP analogues (Trezise *et al.*, 1993). Of the agents tested, α,β-methylene ATP was the most potent, whilst ATP and 2-methylthioATP were only weak agonists and on this basis we postulated the

[1] Author for correspondence.

involvement of P_{2X} purinoceptors. In a follow up study, we attempted to elucidate the ionic mechanisms underlying this depolarization by examining the effect of various ion substitutions on responses produced by α,β-methylene ATP (Trezise *et al.*, 1994). Our data showed that these responses, like those mediated via 5-HT_3 receptor activation, depend on Na^+ influx and, thus, provide evidence that the purinoceptor in the vagus nerve activates a cation channel (Trezise *et al.*, 1994). Interestingly, removal of Ca^{2+} and Mg^{2+} from the physiological salt solution produced a large augmentation of α,β-methylene ATP-induced depolarization without markedly changing the EC_{50} value (Trezise *et al.*, 1994). In view of evidence indicating that in some systems removal of divalent cations increases the agonist potency of ATP, for example in rat mast cells (Cockcroft & Gomperts, 1980; Tatham *et al.*, 1988), human fibroblasts (Fine *et al.*, 1989) and in bovine aortic endothelial cells (Motte *et al.*, 1993), we decided to examine whether depolarization responses of the rat vagus nerve produced by ATP as well as other analogues of ATP were differentially affected by removal of divalent cations.

A small part of this work was reported previously to the British Pharmacological Society (Trezise *et al.*, 1994).

Methods

Extracellular recordings of agonist-induced depolarizations were made from segments of rat isolated cervical vagus nerve as previously described (Trezise *et al.*, 1993). Briefly, male AHA Wistar rats (200–270 g) were stunned by a blow to the head, decapitated, and the two cervical vagus nerves rapidly excised. Segments of nerve, approximately 15–20 mm long, were desheathed under a dissecting microscope, and transferred to heated (27°C) two-compartment Perspex baths such that approximately 50% of the nerve lay in the first compartment, while the remainder projected through a greased slot (Dow-Corning high vacuum grease) into the second. The d.c. potential between the two compartments was measured with silver-silver chloride electrodes connected to the preparation through agar-saline/filter paper bridges. Signals were amplified, filtered (0.5 Hz) and displayed on a chart recorder (Lectromed Multitrace 8). Each compartment of the bath was perfused continuously, at a rate of 1–2 ml min^{-1}, with a modified physiological salt solution (PSS; see below for composition), preheated to 27°C and gassed with 95% O_2/5% CO_2. Drugs were applied at known concentrations into the superfusate of the first compartment only.

Experimental protocols

Determination of agonist responses using a single concentration-effect curve protocol In some experiments a single agonist concentration-effect curve only was constructed. Thus, after an initial 30 min equilibration period, the viability of each preparation was assessed by exposure to a near maximal concentration of 5-HT (1×10^{-5} M). Repeated exposures (2–3) to 5-HT (1×10^{-5} M) were performed until reproducible depolarization responses were obtained. After a 30 min wash period, a concentration-effect curve to either ATP, an ATP analogue or 5-HT was constructed non-cumulatively using serially increasing concentrations. Each concentration of agonist was applied for 2–3 min during which time a peak effect was reached. An interval of 45 min was left between each agonist application. In some experiments, after the initial responses to 5-HT, the PSS was changed to one containing no divalent cations (Ca^{2+}/Mg^{2+}-free PSS – see below). This procedure caused a depolarization response in its own right, which was sustained, but further depolarization responses could still be induced (see results). After a further 30 min re-equilibration period in Ca^{2+}/Mg^{2+}-free PSS, a single concentration-effect curve for a given agonist was constructed.

Determination of relative agonist potencies using a two concentration-effect curve protocol In Ca^{2+}/Mg^{2+}-free PSS it was possible to construct two consecutive concentration-effect curves to ATP in the same preparation. In these experiments, an initial 30 min equilibration period was allowed. After this time, the first concentration-effect curve to ATP (3×10^{-7}–1×10^{-4} M) was constructed non-cumulatively by applying serially increasing concentrations of drug for 3 min at 30 min intervals. Following a further 30 min re-equilibration period, a second concentration-effect curve to either ATP or test agonist was constructed as before. One preparation in four served as a time-matched control preparation to monitor any spontaneous changes in sensitivity to ATP during the course of the experimental period.

Analysis of results

The depolarization responses produced by agonists were measured as the peak change (μV) in the d.c. potential between the two compartments. In the single concentration-effect curve protocol experiments, responses to agonists were expressed as a percentage of the response to 5-HT (1×10^{-5} M). In the two concentration-effect curve protocol experiments, relative agonist potencies were determined by expressing all responses as a percentage of the maximum response to ATP obtained from the first concentration-effect curve. Equi-effective molar ratios (EMRs) were obtained by dividing the equi-effective concentration of the test agonist by that of ATP measured at the 50% response level. In some cases where the maximum response to the test agonist did not achieve 50% of the maximum response to ATP measured from the first concentration-effect curve, EMRs were obtained from measurements at the 30% response level. Time-related changes in sensitivity to ATP were corrected for by dividing the test agonist EMR by the equivalent ratio obtained from the control preparation in which consecutive concentration-effect curves to ATP were constructed.

All data are expressed as mean ± s.e.mean or geometric mean with 95% confidence limits where appropriate. Differences between groups were assessed by Student's unpaired *t* test and considered significant when $P < 0.05$.

Drugs and solutions

The composition of the normal physiological salt solution (PSS) was as follows (mM in deionised water): NaCl 118, $NaHCO_3$ 25, KCl 4.7, $MgSO_4.7H_2O$ 0.6, KH_2PO_4 1.2, D-glucose 11.1, $CaCl_2.6H_2O$ 1.3. In some experiments $CaCl_2$ and $MgSO_4$ were omitted and ethylene diaminetetracetic acid (EDTA, 1×10^{-3} M) was added; this is referred to as Ca^{2+}/Mg^{2+}-free PSS. The following drugs were used: 5-hydroxytryptamine creatinine sulphate (5-HT), adenosine 5′-triphosphate disodium salt (ATP), α,β-methylene ATP lithium salt, uridine 5′-triphosphate sodium salt (UTP), β,γ-methylene ATP, 5′-adenylylimidodiphosphate lithium salt (β,γ-imido ATP), adenosine, adenosine 5′-monophosphate (AMP), adenosine 5′-diphosphate sodium salt (ADP), 2′- and 3′-O-(4-benzoylbenzoyl)-ATP (benzoyl ATP), adenosine 5′-O-(2-thiodiphosphate) trilithium salt (ADP-β-s), adenosine 5′-O-(3-thiotriphosphate) (ATP-γ-S), ethylenediaminetetraacetic acid disodium salt (EDTA, all Sigma), 2-methylthioATP tetra sodium salt (Research Biochemicals Incorporated). All drugs were dissolved and diluted to the required concentration in the appropriate PSS, and stored on ice.

Results

Comparison of the effects of ATP in normal PSS and in Ca^{2+}/Mg^{2+}-free PSS

In normal PSS, ATP (1×10^{-5}–1×10^{-3} M) produced concentration-related, depolarization responses of the rat vagus

nerve. The threshold concentration of ATP for depolarization was 1×10^{-5} M and at the highest concentration tested (1×10^{-3} M) the amplitude of the response to ATP only amounted to $70.6 \pm 7.8\%$ ($n = 6$) of the response to 5-HT (see Figures 1a, 2a and 5). A maximal response to ATP was not obtained at a concentration of 1×10^{-3} M and thus an EC_{50} value could not be determined. The effects of higher concentrations were not determined due to the possible complicating factor of significant chelation of divalent cations by ATP (Bartfai, 1979).

Changing the perfusate from normal PSS to Ca^{2+}/Mg^{2+}-free PSS produced a sustained depolarization response which was $300.0 \pm 40.1\%$ ($n = 4$) of the response to 5-HT (1×10^{-5} M). In this Ca^{2+}/Mg^{2+}-free PSS, there was a marked decrease in the threshold concentration of ATP required for depolarization ($1-3 \times 10^{-7}$ M; Figure 1b). The

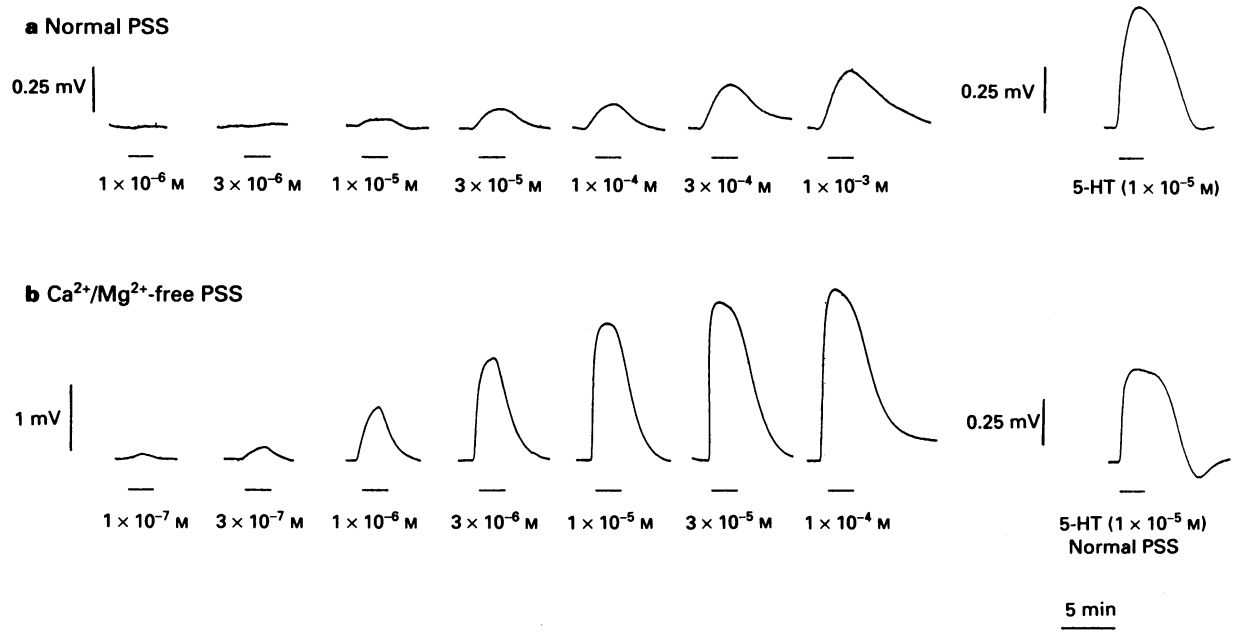


Figure 1 Discontinuous records of the effect of adenosine 5'-triphosphate (ATP) on extracellularly recorded membrane potentials in the rat isolated vagus nerve in (a) normal physiological salt solution (PSS) and (b) Ca^{2+}/Mg^{2+}-free PSS. An upward deflection indicates depolarization of the nerve trunk, calibrated in mV. Each concentration of drug was perfused for the time period indicated by the solid horizontal bar; 45 min was left between agonist applications. Note the marked differences in the potency and absolute amplitude of responses to ATP under the two experimental conditions. For comparison the near maximal depolarization response of each preparation to 5-hydroxytryptamine (5-HT, 1×10^{-5} M) in normal PSS is shown.

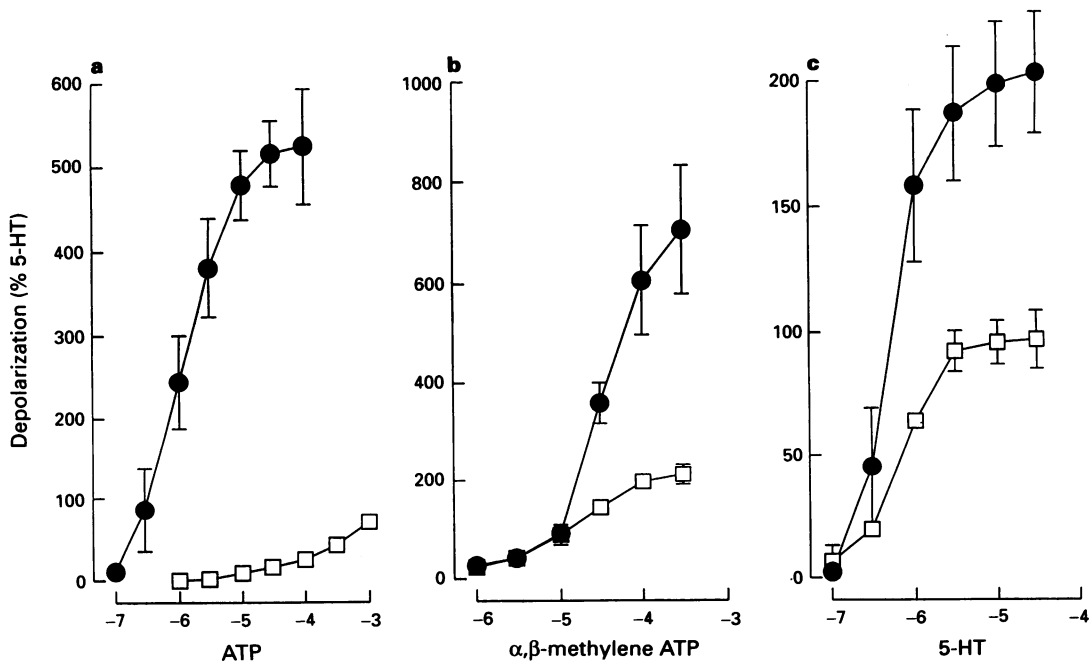


Figure 2 Comparison of depolarizing responses of the rat isolated vagus nerve produced by (a) adenosine 5'-triphosphate (ATP), (b) α,β-methylene ATP and (c) 5-hydroxytryptamine (5-HT) in either normal physiological salt solution (PSS, □) or in Ca^{2+}/Mg^{2+}-free PSS (●). Each point represents the mean with s.e.mean of n determinations ($n = 4-10$). The abscissa scales show the log molar concentration of drug and the ordinate scale the depolarizing response expressed as a percentage of the depolarization evoked by 5-HT (1×10^{-5} M) in normal PSS in the same preparation (see methods).

concentration-effect curve to ATP was complete, with a clearly defined maximum response at a concentration of 1×10^{-4} M and a mean EC_{50} value of 1.19×10^{-6} M (0.27–5.20), $n = 4$. The mean maximum amplitude of the response to ATP in Ca^{2+}/Mg^{2+}-free PSS was 525.6 ± 68.0% ($n = 4$) of the response to 5-HT (1×10^{-5} M), measured in normal PSS in the same preparation (Figure 2a). In normal PSS, when a sustained depolarization response (301.3 ± 23.4% of the 5-HT response) was induced by KCl (6×10^{-3} M added), the amplitude of the depolarization response to ATP (3×10^{-4} M) was not affected (control 53.7 ± 4.3%, test 46.9 ± 9.0%, $n = 4$).

Comparison of the effects of α,β-methylene ATP in normal PSS and in Ca^{2+}/Mg^{2+}-free PSS

In normal PSS, α,β-methylene ATP (10^{-6}–3×10^{-4} M) produced concentration-dependent depolarization responses with a mean EC_{50} value of 1.18×10^{-5} M (0.90–1.61) and a maximal response that amounted to 190.1 ± 15.0% ($n = 10$) of the initial response to 5-HT (1×10^{-5} M). The amplitude of depolarization responses to α,β-methylene ATP was significantly increased in Ca^{2+}/Mg^{2+}-free PSS; the response at the highest concentration tested was 727.1 ± 127.4% ($n = 5$) of the initial response to 5-HT (1×10^{-5} M), determined in normal PSS ($P < 0.05$; Figure 2b). Although, in the absence of a clearly defined maximum response, a true EC_{50} value could not be calculated, there was no apparent change in the concentrations of α,β-methylene ATP required to produce depolarization in Ca^{2+}/Mg^{2+}-free PSS compared to normal PSS. Similarly, the concentrations required for depolarization by both β,γ-methylene ATP and β,γ-imido ATP were not modified by removal of divalent cations, although an increase in the amplitude of responses was observed (data not shown).

Comparison of the effects of 5-HT in normal PSS and in Ca^{2+}/Mg^{2+}-free PSS

In normal PSS, 5-HT (1×10^{-7}–3×10^{-5} M) produced concentration-dependent depolarization responses with a mean EC_{50} value of 6.7×10^{-7} M (4.4–10.0) and a maximal response that was 96.7 ± 2.0% ($n = 5$) of the initial response to 5-HT (1×10^{-5} M). The amplitude of depolarization responses to 5-HT were significantly increased in Ca^{2+}/Mg^{2+}-free PSS; the mean maximum response was 204.0 ± 25.0% ($n = 5$) of the initial response to 5-HT (1×10^{-5} M), determined in normal PSS ($P < 0.05$; Figure 2c). However, there was no significant change in the sensitivity to 5-HT, such that in Ca^{2+}/Mg^{2+}-free PSS the mean EC_{50} value was 7.6×10^{-7} M (2.4–23.7).

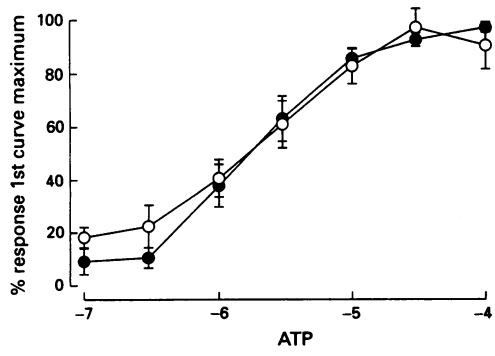


Figure 3 Reproducibility of concentration-effect curves to adenosine 5'-triphosphate (ATP) for depolarizing responses of the rat isolated vagus nerve in Ca^{2+}/Mg^{2+}-free physiological salt solution. First curve (●), second curve (○). Each point represents the mean with s.e.mean of n determinations ($n = 8$). The abscissa scale shows the log molar concentration of ATP and the ordinate scale the depolarizing response expressed as a percentage of the maximum response to ATP determined from the respective first concentation-effect curve.

Determination of relative potencies of purinoceptor agonists in Ca^{2+}/Mg^{2+}-free PSS

Reproducibility of concentration-effect curves to ATP In order to determine relative purinoceptor agonist potencies a two concentration-effect curve protocol was adopted (see Methods). With this protocol depolarization responses to ATP were found to be reproducible (Figure 3); the mean concentration-ratio between the first and second concentration-effect curves was 1.07 (0.45–2.53), $n = 8$. There was no statistically significant difference in the maximum responses obtained to ATP from the first and second concentration-effect curves.

Effects of ATP analogues 2-MethylthioATP and ATP-γ-S (both 1×10^{-7}–3×10^{-4} M) both produced concentration-related depolarization responses of the rat vagus nerve in Ca^{2+}/Mg^{2+}-free PSS (see Figure 4a, 4b and 5). The mean maximum response to each agent (second concentration-effect curve) was not statistically significantly different from the corresponding maximum response to ATP in the control preparation (ATP control 81.8 ± 9.3%, 2-methylthioATP 87.1 ± 8.8%, $n = 4$; ATP control 90.1 ± 10.3%, ATP-γ-S 95.6 ± 7.5%, $n = 5$). Both agonists were approximately equipotent with ATP (mean corrected EMRs of 1.3 (0.3–6.4) and 1.9 (0.8–4.4), for 2-methylthioATP and ATP-γ-S, respectively).

α,β-Methylene ATP, β,γ-methylene ATP, and β,γ-imido ATP (each 1×10^{-6}–3×10^{-4} M) were less potent agonists than ATP. The mean corrected EMRs were as follows: α,β-methylene ATP 48.8 (29.7–80.2), $n = 8$; β,γ-methylene ATP 85.0 (52.0–138.8), $n = 9$; β,γ-imido ATP 60.0 (37.6–96.0), $n = 6$. Under these experimental conditions, the response to α,β-methylene ATP at the highest concentration tested (3×10^{-4} M) was smaller than the maximum response to ATP (see Figure 4c). In contrast, in the single concentration-effect curve studies the response to α,β-methylene ATP was somewhat larger than the maximum response to ATP (Figures 2a and b). This variability could reflect the differences in the experimental protocols used, but is more likely to be explained by normal biological variation. Since a clearly defined maximum for α,β-methylene ATP was not obtained in either series of experiments one cannot make a quantitative comparison of the relative maxima *vis-a-vis* that of ATP.

Benzoyl ATP and ADP-β-S (both 1×10^{-6}–1×10^{-4} M) produced only small depolarizing responses at the highest concentrations tested and, thus, EMRs were not determined (see Figure 4d). The peak amplitude of the depolarization response to benzoyl ATP (1×10^{-4} M) and ADP-β-S (1×10^{-4} M) was 30.3 ± 8.7% ($n = 4$) and 28.9 ± 12.0% of the maximal response to ATP, respectively ($n = 5$).

ADP, AMP or adenosine (all 1×10^{-6}–1×10^{-4} M) had no marked effect on membrane potential in Ca^{2+}/Mg^{2+}-free PSS. The peak amplitude of the responses to each of these agents at the highest concentration tested (1×10^{-4} M) was 13.7 ± 8.0% ($n = 4$), 3.9 ± 2.7% ($n = 5$) and 0.5 ± 0.5% ($n = 4$) of the maximal response to ATP, respectively. UTP was without effect at concentrations up to 1×10^{-3} M ($n = 4$).

Discussion

The major finding of the present study was that removal of divalent cations had differential effects on the depolarizing actions of ATP, certain ATP analogues and of 5-HT in the rat isolated vagus nerve. A marked increase in potency (i.e. lowering of the threshold concentration and the EC_{50} value) of ATP, 2-methylthioATP and ATP-γ-S was observed when Mg^{2+} and Ca^{2+} ions were removed. In contrast, the potencies of α,β-methylene ATP, β,γ-methylene ATP and β,γ-imido ATP were not affected by divalent cations. In addition, for

all of the agonists, removal of divalent cations produced an increase in the maximum response (i.e. augmentation). The precise mechanisms underlying these processes of potentiation and augmentation have not been investigated directly in this study. However, the fact that some but not all, agonists were potentiated, whilst the effects of all agonists tested were augmented suggests that the mechanisms involved are distinct.

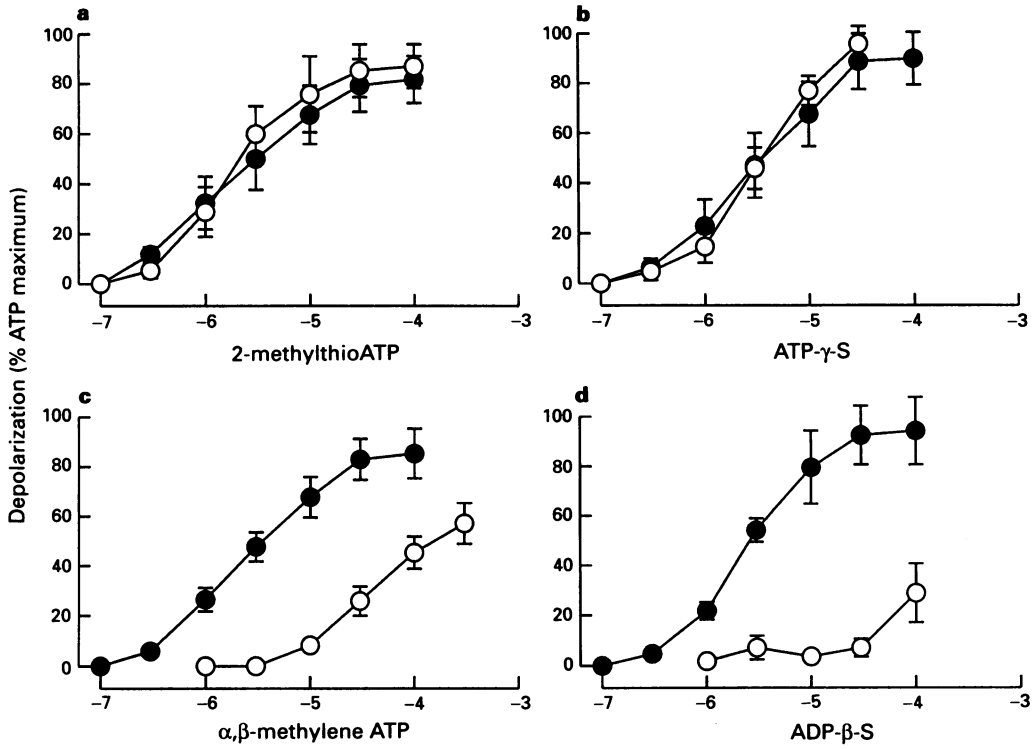


Figure 4 Comparison of the depolarizing effects of adenosine-5-triphosphate (ATP) with (a) 2-methylthio ATP, (b) ATP-γ-S, (c) α,β-methylene ATP and (d) ADP-β-S on the rat isolated vagus nerve in Ca^{2+}/Mg^{2+}-free physiological salt solution. In each panel the time-matched control responses to ATP are represented by (●) and the responses to test agonist by (○). Each point represents the mean with s.e.mean of n determinations ($n = 4-8$). The abscissa scales show the log molar concentration of drug and the ordinate scale the depolarizing response expressed as a percentage of the maximum response to ATP determined from the first concentration-effect curve.

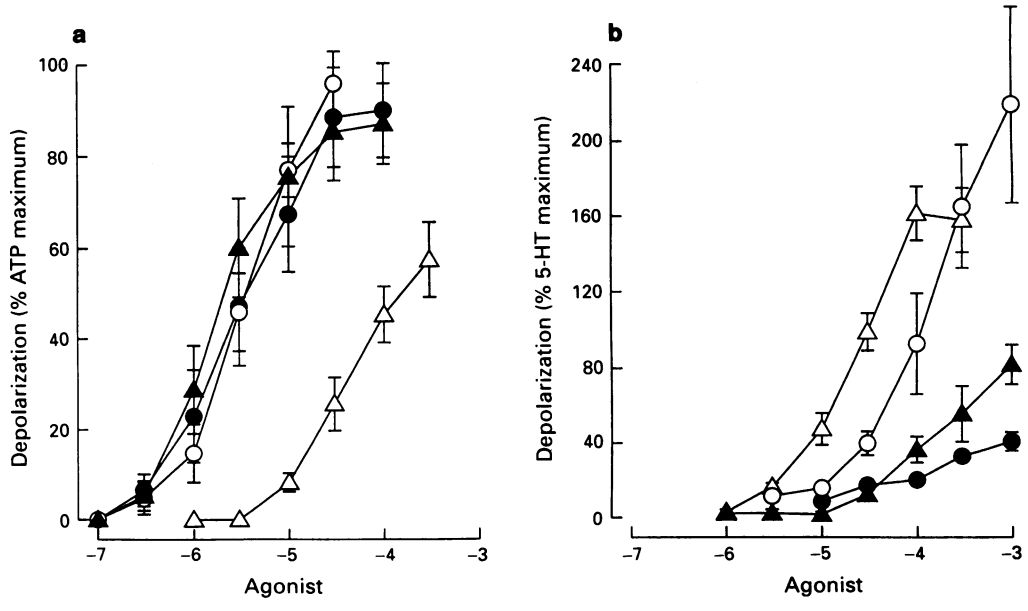


Figure 5 Comparison of the depolarizing effects of adenosine-5'-triphosphate (ATP) and ATP analogues on the rat isolated vagus nerve in (a) Ca^{2+}/Mg^{2+}-free PSS and (b) normal PSS (some data from Trezise *et al.*, 1993). In each panel the depolarization responses to ATP (●), ATP-γ-S (○), 2-methylthioATP (▲) and α,β-methylene ATP (△) are shown. Each point represents the mean with s.e.mean of n determinations ($n = 4-9$). The abscissa scales show the log molar concentration of drug and the ordinate scale the depolarizing response expressed either as a percentage of the maximum response to ATP determined from the first concentration-effect curve (a) or as a percentage of the depolarization response to 5-hydroxytryptamine (5-HT, 1×10^{-5} M) (b). Note the marked differences in the potencies of ATP, ATP-γ-S, and 2-methylthioATP, but not α,β-methylene ATP, in the absence and presence of divalent cations.

The augmentation of depolarization responses of the rat vagus nerve induced by ATP and the ATP analogues tested was not restricted to purines in that depolarization responses evoked by 5-HT were also augmented. It has previously been shown by use of a 'sucrose-gap' recording technique that depolarization responses of the rat internal carotid nerve, induced by 5-HT, are augmented by removal of divalent cations (Nash & Wallis, 1981). The mechanism underlying this phenomenon does not appear to be related to the change in membrane potential observed when divalent cations were removed since in this study we have shown that a similar depolarization response produced by increasing the extracellular K^+ concentration did not augment the response to ATP. Evidence from studies on single cells is consistent with these observations from whole nerve preparations that divalent cations reduce both ATP- and 5-HT-induced membrane currents. In neurones isolated from sensory and parasympathetic cardiac ganglia of the rat, the amplitude of depolarization responses induced by ATP are markedly reduced when the extracellular concentration of divalent cations is increased (Krishtal & Marchenko, 1984; Krishtal *et al.*, 1988a; Bean *et al.*, 1990; Fieber & Adams, 1991). Similarly, whole cell currents induced by 5-HT in rat dorsal root and rabbit nodose ganglion neurones are attenuated by Ca^{2+} and Mg^{2+} (Robertson & Bevan, 1991; Peters *et al.*, 1993). There are several possible explanations for these inhibitory effects of divalent cations including channel block or an effect on desensitization, but, at least in the case of ATP, an action at or close to the ion channel itself seems probable since the single channel conductance measured in membrane patches is also markedly increased on removal of divalent cations (Krishtal *et al.*, 1988a; Bean *et al.*, 1990).

In addition to the augmentation of responses to ATP, removal of divalent cations also markedly increased its potency, causing a large leftward shift of the concentration-effect curve and a decrease in the EC_{50} value. In contrast, the potencies of α,β-methylene ATP, β,γ-methylene ATP, β,γ-imidoATP and 5-HT in causing depolarization remained unchanged (see Figures 2 and 5). One possible explanation for the increase in potency of ATP could be that in the absence of divalent cations a greater proportion of ATP exists in an active ATP^{4-} form. In physiological salt solutions ATP^{4-} forms complexes primarily with Mg^{2+} and Ca^{2+}, and also to a much lesser extent with Na^+, K^+ and H^+. The proportion of these various complexes depends on the temperature, pH and ionic composition of the solution and the concentration of ATP (Bartfai, 1979; see Lustig *et al.*, 1992). By manipulating these factors it is possible to vary the concentration of complexed and uncomplexed ATP in a given solution. Using this approach, evidence has been obtained that certain purinoceptors preferentially recognise the ionised, tetrabasic form of ATP (ATP^{4-}; Cockcroft & Gomperts, 1980; Tatham *et al.*, 1988; Fine *et al.*, 1989; Lustig *et al.*, 1992; Motte *et al.*, 1993). It would seem that ATP^{4-} also has agonist effects in the vagus nerve in that ATP produced marked responses in the absence of Ca^{2+} and Mg^{2+}. It is difficult, however, to assess precisely the contribution (if any) that the increase in the concentration of ATP^{4-} that occurs on removal of divalent cations may have made to the increase in potency of ATP. It can be estimated (Cockcroft & Gomperts, 1980) that the maximum increase in the ATP^{4-} concentration when divalent cations are omitted, compared to normal PSS, is 23 fold, for the range of ATP concentrations that we tested. However, since the nature of the concentration-effect curves for ATP were very different in normal PSS and Ca^{2+}/Mg^{2+}-free PSS (see Figure 2a) a quantitative estimate of the difference in potency could not be made. Nevertheless, there was a 50–100 fold difference in the threshold concentrations for the depolarization response to ATP under these different conditions suggesting that an increase in the concentration of ATP^{4-} when divalent cations are omitted cannot be the sole explanation for the increase in potency of ATP.

A more plausible explanation for the increase in potency of ATP is that in the whole nerve preparation removal of Ca^{2+} and Mg^{2+} prevents the metabolic breakdown of ATP by cell surface ectonucleotidase enzymes. It is well established that Ca^{2+}/Mg^{2+}-dependent isoforms of ectonucleotidase exist and that the preferred substrate for the enzyme in many cases is ATP complexed with Mg^{2+} (see Nagy, 1986 for review). The finding that responses to 2-methylthioATP, another nucleotide susceptible to metabolic breakdown (Welford *et al.*, 1986), were also markedly potentiated in Ca^{2+}/Mg^{2+}-free PSS is consistent with this hypothesis. Conversely, the methylene- and imido-analogues of ATP, α,β-methylene ATP, β,γ-methylene ATP and β,γ-imido ATP, were not potentiated in Ca^{2+}/Mg^{2+}-free PSS, which adds further support to this idea since these simple modifications to the ATP molecule have been shown to confer resistance to ectonucleotidases (Cusack & Hourani, 1984; Hourani *et al.*, 1985; Welford *et al.*, 1986; 1987). ATP-γ-S was also potentiated in Ca^{2+}/Mg^{2+}-free PSS. Although there is evidence to suggest that this nucleotide is resistant to metabolism in endothelial cells (Cusack *et al.*, 1983) and in certain visceral smooth muscles (Welford *et al.*, 1986; 1987), in frog skeletal muscle low concentrations of ATP-γ-S ($< 10\ \mu M$) are broken down as rapidly as ATP (Cascalheira & Sebastião, 1992). Taken together, these findings of differential modification of the potencies of ATP and ATP analogues suggest that removal of divalent cations from the PSS might increase the potency of ATP by preventing the influence of metabolizing enzymes.

In normal PSS, the rank order of agonist potencies for depolarizing the rat vagus nerve was α,β-methylene ATP > ATP-γ-S > β,γ-methylene ATP = β,γ-imido ATP > 2-methylthioATP ≥ ATP (Trezise *et al.*, 1993; see Figure 5). This profile is similar to that described for the P_{2X} purinoceptor subtype (Burnstock & Kennedy, 1985). In contrast, in Ca^{2+}/Mg^{2+}-free PSS, the rank order of agonist potencies was ATP = 2-methylthioATP = ATP-γ-S > α,β-methylene ATP ≥ β,γ-methylene ATP = β,γ-imido ATP, a profile more consistent with the involvement of a P_{2Y} purinoceptor (Burnstock & Kennedy, 1985). Thus, using this range of nucleotides in the rat vagus nerve, it is possible to demonstrate profiles of agonist potencies that resemble either the P_{2X} or the P_{2Y} purinoceptor subtype, simply by modifying the composition of the PSS. Since it seems highly unlikely that a fundamental change in the nature of the receptor structure could have occurred simply by removal of divalent cations this finding demands an alternative explanation (see below).

In the present study, 2-methylthioATP was a very potent agonist in the absence of divalent cations. This agent is believed to be a selective agonist for P_{2Y}, compared to P_{2X}, purinoceptors (Burnstock & Kennedy, 1985; Cusack, 1993). This might suggest the involvement of P_{2Y} purinoceptors, and not P_{2X} purinoceptors, in mediating depolarization of the rat vagus nerve. However, it would be difficult to argue that P_{2Y} purinoceptors are involved since ADP-β-S and ADP, other potent P_{2Y} purinoceptor agonists (Martin *et al.*, 1985; Berrie *et al.*, 1989; Boyer *et al.*, 1989), were only weak agonists in Ca^{2+}/Mg^{2+}-free PSS. The weak activity of UTP, ADP and benzoyl ATP, even in the absence of divalent cations, suggests that P_{2U}, P_{2T} or P_{2Z} purinoceptors are not involved (see Cusack, 1993). One could propose the involvement of a further purinoceptor subtype to explain the data in this study but given the profound effect of divalent cations on the potency of ATP this would seem imprudent. In attempting to arrive at an explanation, we have therefore assumed that all of the purine agonists are acting predominantly at a common receptor, believed to be of the P_{2X} type (see below).

Under the present purinoceptor classification system, P_{2X} purinoceptors are described as ligand-gated cation channels, whilst P_{2Y} purinoceptors utilise G-protein coupling for signal transduction (Kennedy, 1990; see Bean, 1992 and Dubyak & El-Moatassim, 1993 for reviews). The P_{2X} purinoceptor has yet to be characterized structurally but a P_{2Y} receptor gene, however, has recently been cloned (Webb *et al.*, 1993). The

P_{2Y} receptor protein that this gene encodes contains seven helical transmembrane domains, as would be expected for a G-protein-linked receptor. Although there is yet no structural proof that the P_{2X} purinoceptor forms part of a channel, there is good functional data, analogous to that obtained for the nicotinic and the 5-HT_3 receptor, to indicate that this is the case. Thus, in rat nodose ganglion (vagal) neurones there is convincing evidence that ATP opens cation channels (Krishtal & Marchenko, 1984; Krishtal *et al.*, 1988a; Bean, 1990). We have confirmed the dependence of the purinoceptor-mediated depolarization response of the equivalent whole nerve preparation on extracellular monovalent cations (Trezise *et al.*, 1994). The extremely short latency of onset (<50 ms) of the response to ATP in single cells (Krishtal *et al.*, 1988a; Bean, 1990; Fieber & Adams, 1991) precludes the involvement of any known G-protein-coupled receptor system and suggests that these cation channels are directly ligand-gated. Thus, on a transductional basis and by implication structural, the purinoceptor(s) on the vagus nerve would be classified as a P_{2X} purinoceptor.

Interestingly, in experiments on single cells, several workers have previously shown that ATP, and in some studies 2-methylthioATP, are more potent agonists than α,β-methylene ATP in causing depolarization via the opening of ligand-gated cation channels (e.g. rat vas deferens, Friel, 1988; rabbit ear artery, Benham & Tsien, 1987; guinea-pig bladder, Inoue & Brading, 1990; rat superior cervical ganglion neurones, Cloues *et al.*, 1993; rat parasympathetic neurones; Allen & Burnstock, 1990; Fieber & Adams, 1991; rat nucleus solitarii neurones, Ueno *et al.*, 1992). However, in the corresponding whole tissue preparations, ATP and 2-methylthioATP are less potent agonists than α,β-methylene ATP (e.g. guinea-pig bladder, Inoue & Brading, 1990; rabbit ear artery, O'Connor *et al.*, 1990; rat vagus nerve, Trezise *et al.*, 1993). Our findings of different rank orders of potencies for ATP, 2-methylthioATP and α,β-methylene ATP in the absence and presence of divalent cations may offer some explanation for this paradox. In studies on single cells in which drugs are applied very rapidly, the metabolism of ATP and of other hydrolysable agonists is likely to be negligible within the period that the response is measured (latency of onset 10–50 ms). In contrast, in whole cells where diffusion is limiting, metabolism may become the rate limiting event and the most metabolically stable compounds will appear the most potent. Therefore, it might be anticipated that measurement of agonist potencies in whole preparations in the absence of divalent cations will prevent agonist metabolism and provide a much more reliable measurement of purinoceptor agonist potency, and moreover, one that is consistent with studies on single cells. In our experiments in Ca^{2+}/Mg^{2+}-free PSS, the threshold concentration and potency (EC_{50} value 1.19×10^{-6} M) of ATP, and the rank order of potency of ATP analogues, were remarkably similar to values estimated from studies on single rat nodose ganglion neurones (Krishtal *et al.*, 1988a; Bean *et al.*, 1990). Confirmation of this hypothesis (or otherwise) awaits the availability of compounds which will selectively inhibit ectonucleotidase enzymes.

In conclusion, the results of the present study suggest that ATP and 2-methylthio ATP are much more potent agonists at the putative P_{2X} purinoceptor in the vagus nerve than was first thought. Given the susceptibility of these agents to metabolic breakdown, it may be difficult to classify these receptors operationally unless more metabolically stable and selective agonists can be identified. As such agonists are chemically not readily accessible, more emphasis will need to be given to the search for potent and selective antagonists. Nevertheless, the findings of this study are important in as much as they suggest that ATP and 2-methylthioATP are actually considerably more potent than α,β-methylene ATP at P_{2X} purinoceptors in the rat vagus nerve. If so, these findings will have profound implications for the classification of P_2 purinoceptors.

References

ALLEN, T.G.J. & BURNSTOCK, G. (1990). The actions of adenosine 5'-triphosphate on guinea-pig intracardiac neurones in culture. *Br. J. Pharmacol.*, **100**, 269–276.

BARTFAI, T. (1979). Preparation of metal-chelate complexes and the design of steady-state kinetic experiments involving metal nucleotide complexes. In *Advances in Cyclic Nucleotide Research*, Vol. 10, ed. Brooker, G., Greengard, P. & Robinson, G.A. pp. 219–242. New York: Raven Press.

BEAN, B.P. (1992). Pharmacology and electrophysiology of ATP-activated ion channels. *Trends Pharmacol. Sci.*, **13**, 87–90.

BEAN, B.P., WILLIAMS, C.A. & CEELAN, P.W. (1990). ATP-activated channels in rat and bullfrog sensory neurones: current voltage relation and single channel behaviour. *J. Neurosci.*, **10**, 11–19.

BENHAM, C.D. & TSIEN, R.W. (1987). A novel receptor-operated Ca^{2+}-permeable channel activated by ATP in smooth muscle. *Nature*, **328**, 275–278.

BERRIE, C.P., HAWKINS, P.T., STEPHENS, L.R., HARDEN, T.K. & DOWNES, C.P. (1989). Phosphatidylinositol 4,5-biphosphate hydrolysis in turkey erythrocytes is regulated by P_{2Y} purinoceptors. *Mol. Pharmacol.*, **35**, 526–532.

BOYER, J.,L., DOWNES, C.P. & HARDEN, T.K. (1989). Kinetics and activation of phospholipase C by P_{2Y} purinergic agonists and guanine nucleotides. *J. Biol. Chem.*, **264**, 884–890.

BURNSTOCK, G. (1990). Purinergic mechanisms. *Ann. N.Y. Acad. Sci.*, **603**, 1–17.

BURNSTOCK, G. & KENNEDY, C. (1985). Is there a basis for distinguishing two types of P_2-purinoceptor? *Gen. Pharmacol.*, **16**, 433–440.

CASCALHEIRA, J.F. & SEBASTIÃO, A. (1992). Adenine nucleotide analogues, including γ-phosphate-substituted analogues, are metabolised extracellularly in innervated frog sartorius muscle. *Eur. J. Pharmacol.*, **222**, 49–59.

CLOUES, R., JONES, S. & BROWN, D.A. (1993). Zn^{2+} potentiates ATP-activated currents in rat sympathetic neurons. *Pflügers Arch.*, **424**, 152–158.

COCKCROFT, S. & GOMPERTS, B.D. (1980). The ATP^{4-} receptor of rat mast cells. *Biochem. J.*, **188**, 789–798.

CUSACK, N.J. (1993). P_2 receptor: subclassification and structure-activity relationships. *Drug Dev. Res.*, **28**, 244–252.

CUSACK, N.J. & HOURANI, S.M.O. (1984). Some pharmacological and biochemical interactions of the enantiomers of adenylyl 5'-(β,γ-methylene)-diphosphonate with the guinea-pig urinary bladder. *Br. J. Pharmacol.*, **82**, 155–159.

CUSACK, N.J., PEARSON, J.D. & GORDON, J.L. (1983). Stereoselectivity of ectonucleotidases on vascular endothelial cells. *Biochem. J.*, **214**, 975–981.

DUBYAK, G.R. & EL-MOATASSIM, C. (1993). Signal transduction via P_2-purinergic receptors for extracellular ATP and other nucleotides. *Am. J. Physiol.*, **265**, C577–C606.

FIEBER, L.A. & ADAMS, D.J. (1991). Adenosine triphosphate-evoked currents in cultured neurones dissociated from rat parasympathetic cardiac ganglia. *J. Physiol.*, **434**, 239–256.

FINE, J., COLE, P. & DAVIDSON, J.S. (1989). Extracellular nucleotides stimulate receptor-mediated calcium mobilization and inositol phosphate production in human fibroblasts. *Biochem. J.*, **263**, 371–376.

FRIEL, D.D. (1988). An ATP-sensitive conductance in single smooth muscle cells from the rat vas deferens. *J. Physiol.*, **401**, 361–380.

GORDON, J.L. (1986). Extracellular ATP: effects, sources and fate. *Biochem. J.*, **233**, 309–319.

HOURANI, S.M.O., WELFORD, L.A. & CUSACK, N.J. (1985). L-AMP-PCP, an ATP receptor agonist in guinea-pig bladder, is inactive on taenia coli. *Eur. J. Pharmacol.*, **108**, 197–200.

INOUE, R. & BRADING, A.F. (1990). The properties of the ATP-induced depolarisation and current in single cells isolated from the guinea-pig urinary bladder. *Br. J. Pharmacol.*, **100**, 619–625.

KENNEDY, C. (1990). P_1- and P_2-purinoceptor subtypes – an update. *Arch. Int. Pharmacodyn.*, **303**, 30–50.

KRISHTAL, O.A. & MARCHENKO, S.M. (1984). ATP-activated ionic conductance in the somatic membrane of mammalian sensory ganglionic neurones. *Neurofiziologiya*, **16**, 327–336.

KRISHTAL, O.A., MARCHENKO, S.M. & OBUKHOV, A.G. (1988a). Cationic channels activated by extracellular ATP in rat sensory neurons. *Neuroscience*, **27**, 995–1000.

KRISHTAL, O.A., MARCHENKO, S.M., OBUKHOV, A.G. & VOLKOVA, T.M. (1988b). Receptors for ATP in rat sensory neurones: the structure-function relationship for ligands. *Br. J. Pharmacol.*, **95**, 1057–1062.

LUSTIG, K.D., SHIAU, A.K., BRAKE, A.J. & JULIUS, D. (1983). Expression cloning of an ATP receptor from mouse neuroblastoma cells. *Proc. Natl. Acad. Sci. U.S.A.*, **90**, 5113–5117.

LUSTIG, K.D., SPORTIELLO, M.G., ERB, L. & WEISMAN, G.A. (1992). A nucleotide receptor in vascular endothelial cells is specifically activated by the fully ionised forms of ATP and UTP. *Biochem. J.*, **284**, 733–739.

MARTIN, W., CUSACK, N.J., CARLETON, J.S. & GORDON, J.L. (1985). Specificity of P_2-purinoceptor that mediates endothelium-dependent relaxation of the pig aorta. *Eur. J. Pharmacol.*, **108**, 295–299.

MOTTE, S., PIROTTON, S. & BOEYNAEMS, J.M. (1993). Evidence that a form of ATP uncomplexed with divalent cations is the ligand of P_{2y} and nucleotide/P_{2u} receptors on aortic endothelial cells. *Br. J. Pharmacol.*, **109**, 967–971.

NAGY, A. (1986). Enzymatic characteristics and possible role of synaptosomal ecto-adenosine triphosphatase from mammalian brain. In *Cellular Biology of Ectoenzymes*. ed. Kreutzberg, G.W., Redington, M. & Zimmerman, H. Berlin Heidelberg: Springer-Verlag.

NASH, H.L. & WALLIS, D.I. (1981). Effects of divalent cations on responses of a sympathetic ganglion to 5-hydroxytryptamine and 1, 1-dimethyl-4-phenyl piperazinium. *Br. J. Pharmacol.*, **73**, 759–772.

O'CONNOR, S.E., DAINTY, I.A. & LEFF, P. (1991). Further subclassification of ATP receptors based on agonist potencies. *Trends Pharmacol Sci.*, **12**, 137–141.

O'CONNOR, S.E., WOOD, B.E. & LEFF, P. (1990). Characterization of P_{2x}-receptors in rabbit isolated ear artery. *Br. J. Pharmacol.*, **101**, 640–644.

PETERS, J.A., MALONE, H.M. & LAMBERT, J.J. (1993). An electrophysiological investigation of the properties of 5-HT_3 receptors of rabbit nodose ganglion neurones in culture. *Br. J. Pharmacol.*, **110**, 665–676.

ROBERTSON, B. & BEVAN, S. (1991). Properties of 5-hydroxytryptamine3 receptor-gated currents in adult rat dorsal root ganglion neurones. *Br. J. Pharmacol.*, **102**, 272–276.

TATHAM, P.E.R., CUSACK, N.J. & GOMPERTS, B.D. (1988). Characterisation of the ATP^{4-} receptor that mediates permeabilisation of rat mast cells. *Eur. J. Pharmacol.*, **147**, 13–21.

TREZISE, D.J., BELL, N.J. & HUMPHREY, P.P.A. (1994). Ionic dependence of depolarising responses evoked by α,β-methylene ATP in the rat isolated vagus nerve. *Br. J. Pharmacol.*, **112**, 405P.

TREZISE, D.J., KENNEDY, I. & HUMPHREY, P.P.A. (1993). Characterisation of purinoceptors mediating depolarisation of rat isolated vagus nerve. *Br. J. Pharmacol.*, **110**, 1055–1060.

UENO, S., HARATA, N., INOIE, K. & AKAIKE, N. (1992). ATP-gated current in nucleus tractus solitarii neurons. *J. Neurophysiol.*, **68**, 778–785.

WEBB, T.E., SIMON, J., KRISHEK, B.J., BATESON, A.N., SMART, T.G., KING, B.F., BURNSTOCK, G. & BARNARD, E.A. (1993). Cloning and functional expression of a brain G-protein-coupled receptor. *FEBS Lett.*, **324**, 219–225.

WELFORD, L.A., CUSACK, N.J. & HOURANI, S.M.O. (1986). ATP analogues and the guinea-pig taenia coli: a comparison of the structure-activity relationships of ectonucleotidases with those of the P_2 purinoceptor. *Eur. J. Pharmacol.*, **129**, 217–224.

WELFORD, L.A., CUSACK, N.J. & HOURANI, S.M.O. (1987). The structure-activity relationships of ectonucleotidases and of excitatory P_2 purinoceptors: evidence that dephosphorylation of ATP analogues reduces pharmacological potency. *Eur. J. Pharmacol.*, **141**, 123–130.

(Received February 24, 1994
Revised May 12, 1994
Accepted June 20, 1994)

Br. J. Pharmacol. (1994), **113**, 471–478 © Macmillan Press Ltd, 1994

Inhibitory effect of strychnine on acetylcholine receptor activation in bovine adrenal medullary chromaffin cells

Gemma A.J. Kuijpers, Leoncio A. Vergara, [1]Soledad Calvo & [2]*Gal Yadid

Laboratory of Cell Biology and Genetics, National Institute of Diabetes, Digestive and Kidney Diseases, National Institutes of Health, Bethesda, MD, U.S.A. and *Dept. of Life Sciences, Bar-Ilan University, Israel

1 Strychnine, which is known as a potent and selective antagonist of the inhibitory glycine receptor in the central nervous system, inhibits the nicotinic stimulation of catecholamine release from bovine cultured adrenal chromaffin cells in a concentration-dependent (1–100 μM) manner. At 10 μM nicotine, the IC_{50} value for strychnine is approximately 30 μM. Strychnine also inhibits the nicotine-induced membrane depolarization and increase in intracellular Ca^{2+} concentration.

2 The inhibitory action of strychnine is reversible and is selective for nicotinic stimulation, with no effect observed on secretion elicited by a high external K^+ concentration, histamine or angiotensin II.

3 Strychnine competes with nicotine in its effect, but does not modify the apparent positive cooperativity of the nicotine binding sites. In the absence of nicotine, strychnine has no effect on catecholamine release. Glycine does not affect catecholamine release nor the inhibitory action of strychnine on this release.

4 These results suggest that strychnine interacts with the agonist binding site of the nicotinic acetylcholine receptor in chromaffin cells, thus exerting a pharmacological effect independently of the glycine receptor.

Keywords: Strychnine; acetylcholine; glycine; nicotine; glycine receptor; chromaffin, secretion; nicotinic ACh receptor

Introduction

The convulsive alkaloid, strychnine, has been established as a specific antagonist of the postsynaptic receptor for the inhibitory neurotransmitter, glycine, in the central nervous system (Curtis *et al.*, 1971; Young & Snyder, 1973; Fostholm & Rotter, 1985). The strychnine recognition site appears to be located on the 48 kDa subunit of the glycine receptor (Graham *et al.*, 1983; Pfeiffer *et al.*, 1984), which has significant structural and amino acid sequence homology with the nicotinic acetylcholine receptor polypeptide family (Grenningloh *et al.*, 1987).

In addition to its interaction with the glycine receptor, strychnine has been shown to interfere with cholinergic transmission. Several decades ago it was demonstrated that strychnine has a depressant effect on the response of the superior cervical ganglion and the neuromuscular junction to nerve impulses and to acetylcholine (ACh) (Lanari & Luco, 1939; Alving, 1961; Landau, 1967).

More recently, it was found that strychnine inhibits nicotine-activated currents in a recombinant insect α_7 acetylcholine receptor subunit expressed in oocytes (Marshall *et al.*, 1990), as well as in the functionally expressed rat brain α_7 nicotinic ACh receptor (Seguela *et al.*, 1993). The function of native chick ciliary ganglion α_7 ACh receptor is also inhibited by strychnine (Zhang *et al.*, 1994). Furthermore, strychnine inhibits the ACh-induced electrophysiological response of chick cochlear hair cells mediated by a novel cholinoceptor (Fuchs & Murrow, 1992). Strychnine also inhibits the binding of α-bungarotoxin to native and homomeric chick α_7 neuronal ACh receptor (Anand *et al.*, 1993), and to the cholinoceptor of *Aplysia* ganglionic neurones and rat brain neurones (Ono & Salvaterra, 1981). The antagonistic effects of strychnine on cholinoceptor, i.e., nicotinic receptor activation may be explained by a structural similarity of the nicotine and strychnine molecules (Beers & Reich, 1970).

The chromaffin cell has been extensively studied as a cholinergic neurosecretory system, and activation of the nicotinic receptor in these cells leads to the Ca^{2+}-dependent exocytotic release of catecholamines, adenosine triphosphate (ATP), chromogranins and enkephalins (Livett, 1984). Recently, Yadid *et al.* (1989, 1993) showed that bovine adrenal medullary chromaffin cells possess a high affinity [^{3}H]-strychnine binding site. These authors also showed that glycine and milacemide, a glycine prodrug, can evoke catecholamine release from slices of adrenal medullary tissue and from freshly isolated chromaffin cells (Yadid *et al.*, 1991; 1992).

These data led us to examine the effects of strychnine and glycine in the bovine chromaffin cell in more detail, and search for an interaction of strychnine with the nicotinic receptor in these cells.

Methods

Cell preparation and cell culture

Bovine adrenal glands were obtained from the slaughterhouse and kept on ice for ca. 60 min. Chromaffin cells were isolated from the adrenal medulla by three successive collagenase perfusions and purification on a Percoll gradient essentially as described by Kuijpers *et al.* (1989). Cells were cultured in a 1:1 mixture of Dulbecco's modified Eagle's medium (DMEM) and Ham's F-12 nutrient medium (Sigma Chem. Co., St. Louis, MO, U.S.A.), buffered with 15 mM HEPES and 21 mM $NaHCO_3$, containing 10% foetal bovine serum (Biofluids, Rockville, MD, U.S.A.) and antibiotics (penicillin, 100 units ml^{-1}, streptomycin, 100 μg ml^{-1}, Fungizone, 250 ng ml^{-1}). Cells were cultured at a density of 0.5×10^6 cells cm^{-2} in 24-well culture plates (Costar Corp., Cambridge, MA, U.S.A.), and they attached to the plates within a few hours after plating. Since DMEM contains 0.3 mM glycine, in some studies on the effects of glycine, cells were cultured in glycine-free Minimal Essential Medium Eagle's (EMEM) medium (Biofluids), containing 10% dialyzed foetal bovine serum.

[1] Present address: Department of Pharmacology, Faculty of Medicine, University of Alicante, Spain.
[2] Author for correspondence at present address: Bar Ilan University, Ramat Gan, Israel 55900.

For intracellular calcium and membrane potential studies, cells were cultured on round coverslips (diameter, 25 mm) or in tissue culture dishes (diameter, 35 mm), respectively, in the absence of Fungizone, for 3–5 days.

Secretion studies

After 3–7 days of culture, cells were taken from the incubator and washed four to six times with a physiological salt solution (standard release medium, SRM) containing (mM): NaCl 150, KCl 5.6, $MgCl_2$ 1, NaH_2PO_4/Na_2HPO_4 1.5, $CaCl_2$ 2.2, glucose 10, HEPES 10 and 0.25% BSA (pH 7.35) over a 30–45 min time period. After washing, cells were incubated in SRM with the appropriate additions. Incubations were carried out by replacing SRM solutions completely for each experimental period. Cells were stimulated with nicotine or other agonists, or with K^+ for 10 min. Stimulation with K^+ was carried out by replacing 47.4 mM NaCl in the medium with 47.4 mM KCl. After stimulation the medium containing secreted catecholamines was removed from the well and diluted in concentrated acetic acid (final concentration of acetic acid, 10%). The cells were then lysed in 10% acetic acid and all samples were stored at −70°C until analysis of catecholamine content by the trihydroxyindole (THI) method. In one experiment samples were stored in 0.4% perchloric acid (PCA), and catecholamine analysis was performed by high performance liquid chromatography (h.p.l.c.) as well as by the THI method, as described below.

All experiments were done at room temperature.

Catecholamine analysis

Catecholamines were determined using a modification of the original THI method (von Euler & Floding, 1955; Kelner *et al.*, 1985). Standards were solutions of adrenaline in the appropriate diluent. In one experiment, catecholamines and DOPAC were also measured by h.p.l.c. For the THI method, catecholamines were converted to fluorescent trihydroxyindole products by potassium ferricyanide and measured in a spectrofluorometer with excitation set at 412 nm and emission at 523 nm.

For h.p.l.c., samples were filtered through 45 μm pore filters, diluted and injected into an h.p.l.c. apparatus coupled to an electrochemical detector. Separation of catecholamines was achieved by reverse phase liquid chromatography through a 5 μm column (4.6 mm i.d. × 250 mm) (Altex Ion Pair Ultrasphere C-18) with a column temperature of 30°C. Mobile phase consisted of 2.1 l water, 3.2 g Na-HEPES, 0.2 g EDTA, 16 ml triethylamine, 12 ml 85% *o*-phosphoric acid (all h.p.l.c. grade chemicals from Fisher Scientific, Fairlawn, NJ. U.S.A.) and 60 ml acetonitrile (Burdick & Jockson, Muskegon, MI, U.S.A.). Electrochemical detection was carried out with an EiCOM CB-100 analytical cell and a Waters 460 detector. The oxidation potential was set between 0.64 and 0.67 V. The mobile phase was pumped at 0.8 ml min^{-1}.

Intracellular calcium measurements

Chromaffin cells plated on coverslips were loaded with 5 μM indo-1 acetoxymethyl ester (Indo-1/AM) in a Krebs solution (KRB) for 120 min at room temperature. A stock solution of Indo-1/AM (1 mM) was previously prepared in anhydrous dimethylsulphoxide (DMSO) containing 20% Pluronic F127. The composition of KRB was (mM): NaCl 140, KCl 5, $CaCl_2$ 2.6, $MgCl_2$ 1, $NaHCO_3$ 5, glucose 5 and Na-HEPES 5 (pH 7.4). Coverslips were mounted on the stage of an inverted Diaphot-TMD microscope (Nikon, Inc.), and excited with a super high pressure mercury light source (Nikon, Inc.) and 340 nm filter. Emitted light was measured simultaneously at 410 nm and 485 nm by two separate photomultiplier tubes using the Nikon dual photometry system. Data were collected using the FastInCA programme developed at the Center for Image Analysis (College of Medicine, University of Cincinnati, Cincinnati, OH, U.S.A.) in collaboration with Nikon, Inc.

Membrane potential recording

The membrane potential was measured by the nystatin-perforated patch clamp technique (Horn & Marty, 1988). The composition of the pipette solution was (mM): KCl 70, K-aspartate 70, $MgCl_2$ 1, NaCl 10, K-HEPES 10 and nystatin 0.25 mg ml^{-1}, pH 7.2. The bath was continuously perfused with KRB at a rate of 5 ml min^{-1}. Nicotine and/or strychnine were added to the perfusion solution at the appropriate times. A signal was recorded using the EPC-7 patch clamp amplifier in current clamp mode, and the data were digitized on line using a TL-1 DMA interface and the Axotape programme (Axon Instruments, Foster City, CA, U.S.A.).

Drugs used

Nicotine (free base), histamine dihydrochloride, glycine (free base), and angiotensin II (human) were obtained from Sigma Chemical Co., St. Louis, MO, U.S.A. Oxotremorine-M (oxotremorine methiodide) was obtained from Research Biochemicals Inc., Natick, MA, U.S.A.

Data and statistical analysis

Results on catecholamine secretion obtained by the THI method were expressed as percentage of total cellular catecholamine content of the start of the experiment, or as percentage of control or maximal response. Within an experiment, incubations were always done in triplicate and the results were averaged. The data shown are averages with s.e.mean of n individual experiments. Results from one experiment obtained by h.p.l.c. were expressed as picogram of catecholamine per supernatant sample volume, and given as averages with s.e.mean of three determinations. Statistical analysis was carried out by Student's two-tailed t test for paired measurements, or a two-way analysis of variance (ANOVA).

Results

Bovine cultured chromaffin cells released 11–32% of their total catecholamine content upon stimulation with a nicotine concentration causing maximal release (10 μM). Basal, unstimulated, catecholamine release varied between 0.1 and 1.8% of the total cell content. Strychnine (1–100 μM) induced a dose-dependent inhibition of nicotine-stimulated catecholamine release. At a nicotine concentration of 10 μM, the inhibition by strychnine ranged from 18% at 10 μM strychnine to 88% at 100 μM strychnine, with an IC_{50} value for strychnine of approximately 30 μM (Figure 1). Strychnine concentrations up to 100 μM did not affect a non-receptor-mediated secretory response, caused by membrane depolarization due to elevation of the extracellular K^+ concentration from 5.6 mM to 53 mM (Figure 1). Strychnine did not affect the basal release of catecholamines.

The effect of strychnine on nicotine-stimulated catecholamine release was very rapid and the extent of the inhibition induced by 35 μM strychnine was not significantly different for strychnine preincubation times in the range of 0–120 s (Figure 2). The effect was also reversible, since repeated washing of the cells with SRM after a 2 min incubation with 35 μM strychnine fully restored the subsequent secretory response of the cells to nicotine (Figure 2). Analysis of the various catecholamines adrenaline, noradrenaline, dopamine, 5-HT (5-hydroxytryptamine) and the dopamine metabolite DOPAC (3,4-dihydroxyphenylacetic acid) by h.p.l.c. showed that strychnine inhibits the nicotine-stimulated release of all these amines, albeit to different extents, with inhibition being

most profound in the case of adrenaline (82%) and least in the case of noradrenaline (28%) (Figure 3).

The dose-response curves relating nicotine concentration to secretory response in the presence and absence of strychnine are shown in Figure 4. This figure clearly shows that the effect of strychnine on catecholamine release is competitive, and that the strychnine-induced inhibition can be overcome by increasing the nicotine concentration. The nicotine concentration at which half maximal secretion occurs is shifted by strychnine (30 μM) from ca. 5 μM to ca. 15 μM. Analysis of the dose-response curves revealed that the Hill coefficient for nicotine-stimulated catecholamine release is 2.55 ± 0.50 (average ± s.e.mean, $n = 3$), and is not changed significantly by strychnine (10–30 μM) (Table 1). Strychnine also inhibited competitively the secretion induced by the cholinoceptor agonist, oxotremorine-M (Oxo-M) (Figure 5). At 100 μM Oxo-M, the IC_{50} value for strychnine was approximately

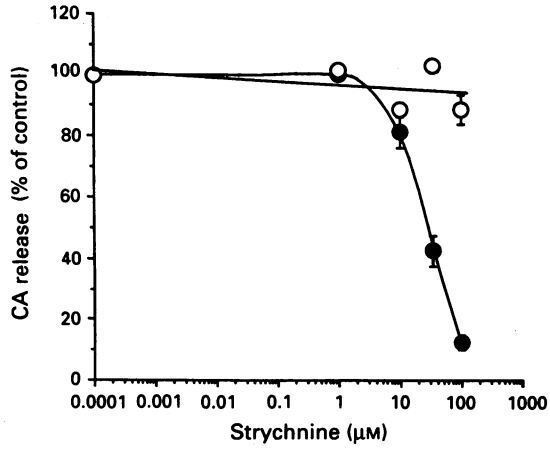


Figure 1 Effect of strychnine (1–100 μM) on catecholamine (CA) release stimulated by nicotine (10 μM) (●) and K^+ (53 mM) (○) from chromaffin cells. Data are expressed as percentage of control release in the absence of strychnine, and are averages ± s.e.mean of 2–9 (nicotine) and 1–3 (K^+) experiments. All data represent net release, i.e., basal release was subtracted from total release to give the response to agonist alone. Basal CA release was 0.78 ± 0.14% (average ± s.e.mean, $n = 13$) of total cellular CA content at the start of the incubation. Control release was, for nicotine (10 μM): 17.7 ± 2.2% of total cellular CA, and for K^+ (53 mM): 6.4 ± 0.5% of total CA ($n = 12$ and $n = 4$, respectively). Curves are significantly different from each other ($P < 0.001$, ANOVA). For all experiments, the total cellular catecholamine content varied between 30 and 100 nmol/10^6 cells.

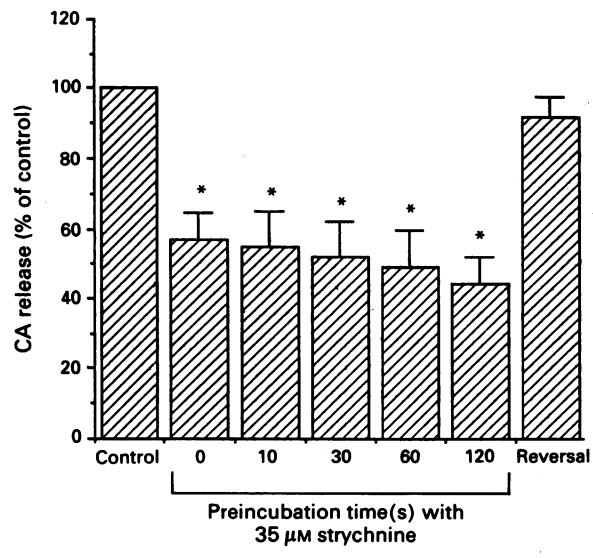


Figure 2 Effect of preincubation time(s) with strychnine on nicotine-stimulated catecholamine (CA) release. Cells were preincubated with strychnine (35 μM) for the indicated period of time, and then stimulated with nicotine (10 μM). The response was expressed as a percentage of control release induced by nicotine alone. Data given are average ± s.e.mean of four experiments. The reversal indicates CA release of cells in response to nicotine (10 μM), after they had been preincubated with strychnine (35 μM) for 120 s and then washed 5–8 times with SRM (5 min total). Basal secretion was 0.66 ± 0.08% of total cellular CA, and control release stimulated by nicotine was 14 ± 4% of total CA ($n = 4$). *Significant difference from control ($P < 0.001$, Student's t test). Effects of different preincubation times (0–120 s) were not significantly different from each other.

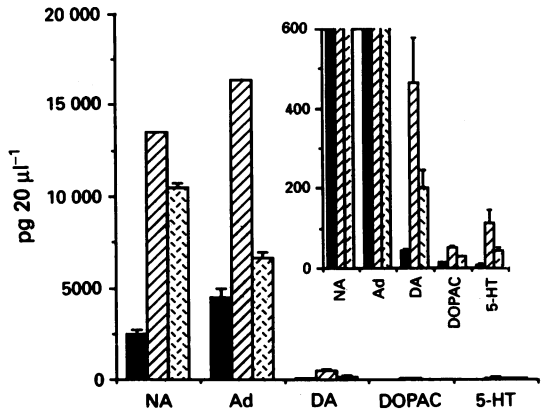


Figure 3 Effect of strychnine on catecholamine and catecholamine metabolite secretion, NA = noradrenaline; Ad = adrenaline; DA = dopamine; DOPAC = 3,4-dihydroxyphenylacetic acid; 5-HT = 5-hydroxytryptamine. Cells were incubated with SRM (solid columns), nicotine (2 μM) (hatched columns) or nicotine in the presence of strychnine (30 μM) (stippled columns). Samples of the cell media from three different wells, collected after 10 min of incubation, were assayed by h.p.l.c. and electrochemical detection. The data are given as pg 20 μl^{-1} cell medium (mean ± s.e.mean; $n = 3$). Insert shows same graph, but at smaller abscissa scale. The total cellular catecholamine contents of the differently treated cells were: (control, SRM) 62.6 ± 2.7, (nicotine) 55.8 ± 0.9, and (nicotine + strychnine) 63.7 ± 0.5 nmol/10^6 cells ($n = 3$).

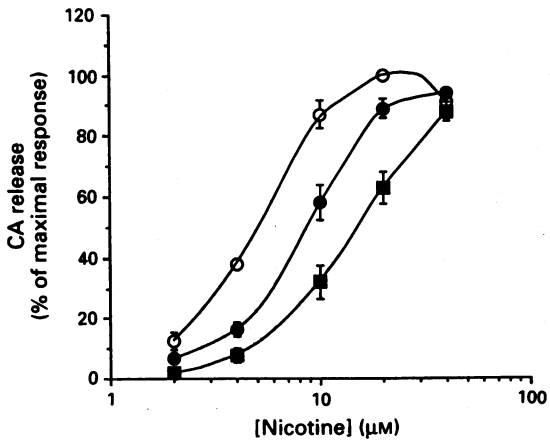


Figure 4 Effect of strychnine on dose-response curves for nicotine-stimulated catecholamine (CA) release from chromaffin cells. Cells were incubated with nicotine alone (○) or with nicotine in the presence of 10 μM strychnine (●) or 30 μM strychnine (■). Data given are averages ± s.e.mean of three experiments. Results are expressed as percentage of the maximal response with 20 μM nicotine (17.6 ± 3.2% of total cellular CA). Basal secretion was 0.84 ± 0.27% of total cellular CA ($n = 3$). The control response is significantly different from the response in the presence of 10 μM strychnine ($P < 0.005$, ANOVA), and the latter is significantly different from the response in the presence of 30 μM strychnine ($P < 0.01$, ANOVA).

Table 1 Effect of strychnine on Hill coefficient for nicotine-stimulated catecholamine release from bovine chromaffin cells

Nicotine (control)	*Nicotine + strychnine* (10 μM)	*Nicotine + strychnine* (30 μM)
2.55 ± 0.50	2.31 ± 0.33	2.48 ± 0.44

Hill coefficients are calculated for catecholamine release response elicited by nicotine (2–20 μM) (control) or nicotine (2–20 μM) + strychnine (10 and 30 μM).

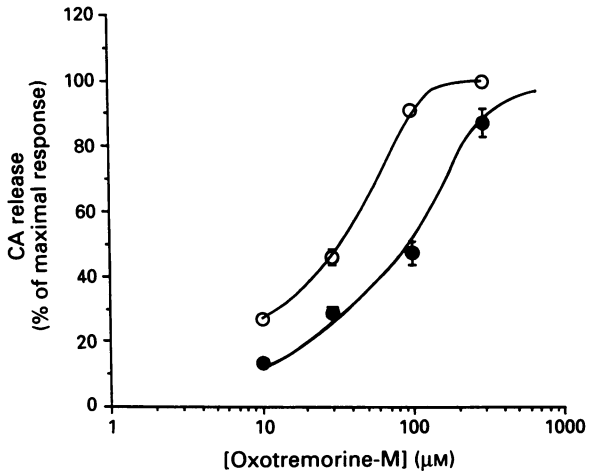


Figure 5 Effect of strychnine on dose-response curves for oxotremorine-M (Oxo-M)-stimulated catecholamine (CA) release. Cells were incubated with Oxo-M alone (○) or with Oxo-M in the presence of strychnine (35 μM) (●). Data given are averages ± s.e.mean of 2–4 experiments. Results are expressed as percentage of maximal secretion with 300 μM Oxo-M (15.3 ± 3.0%). Basal secretion was 1.05 ± 0.25% of total CA ($n = 4$). Control response is significantly different from response in presence of 35 μM Oxo-M ($P < 0.01$, ANOVA).

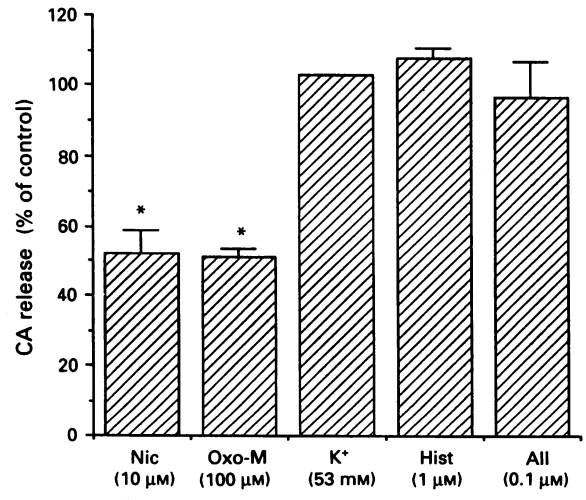


Figure 6 Effect of strychnine on catecholamine (CA) release induced by various agonists. Agonists were used at the concentrations indicated. Cells were washed, and then incubated with agonist in the absence or presence of strychnine (35 μM). Data are given as percentage of control release induced by the agonist in the absence of strychnine and are averages ± s.e.mean of n experiments. Control release was: nicotine (Nic) (10 μM): 15.2 ± 2.3% ($n = 8$); oxotremorine-M (Oxo-M) (100 μM): 12.3 ± 3.2% ($n = 3$); K^+ (53 mM): 4.99 ($n = 1$); angiotensin II (AII) (0.1 μM): 1.22 ± 0.06% ($n = 4$); histamine (Hist) (1 μM): 2.26 ± 0.40% ($n = 3$). *Significant difference from control ($P < 0.001$, Student's t test).

35 μM. Half maximal secretion occurs at ca. 35 μM Oxo-M in the absence of strychnine, and at ca. 90 μM in the presence of 35 μM strychnine.

In order to investigate the selectivity of the inhibitory effect of strychnine, we measured the catecholamine release of chromaffin cells in response to various agonists, in the absence and presence of strychnine (Figure 6). As described above, strychnine (1–100 μM) had no effect on secretory stimulation induced by depolarization of the cell membrane. Moreover, strychnine did not inhibit the catecholamine release induced by histamine (1 μM) or angiotensin II (0.1 μM) (Figure 6).

Glycine (0.1–1 mM) did not affect the inhibition of cholinoceptor-stimulated release by strychnine (35 μM). Moreover, glycine (1–1000 μM) did not have a significant effect on basal catecholamine release but it did slightly potentiate the nicotine-stimulated catecholamine release. In the latter study, cells were cultured in glycine-free EMEM medium (data not shown).

In order to localize the effect of strychnine in the cascade of events involved in receptor-activated catecholamine secretion, we studied the nicotine-induced changes in intracellular calcium concentration ($[Ca^{2+}]_i$) and membrane potential. Under resting conditions, $[Ca^{2+}]_i$ was 110 ± 9 nM (average ± s.e.mean, $n = 11$) and increased to 237 ± 36 nM ($n = 11$) upon stimulation of the cells by 10 μM nicotine (Figure 7a,b). After removal of the agonist from the cell medium, $[Ca^{2+}]_i$ gradually returned to resting values. When a second pulse of nicotine was applied in the presence of 40 μM strychnine, the response was significantly reduced to 61 ± 5% ($n = 7$) of the first response in the absence of strychnine (t test, $P < 0.05$) (Figure 7a). This effect of strychnine was reversible, as shown by the recovery of the response following a third exposure of the cells to nicotine alone, to 82 ± 2% ($n = 7$) of the first response. In control experiments, in which the cells were repeatedly stimulated with 10 μM nicotine in the absence of strychnine, the response of the cells to the second application of nicotine was similar to the first response (97 ± 1%; $n = 4$) (Figure 7b). Strychnine did not affect the basal level of $[Ca^{2+}]_i$ (Figure 7a).

Nicotine (10 μM) also induced a rapid depolarization of the cell membrane followed by a slower recovery phase (Figure 8a). The response of the membrane potential to nicotine was totally reversible. Up to four repetitive stimulations of a cell, separated by 3 min intervals, elicited similar responses, as shown in Figure 8b and no desensitization was evident under our experimental conditions. When strychnine (40 μM) was added simultaneously with nicotine during the second stimulation, the depolarizing response was significantly reduced (Figure 8a). This effect of strychnine was fully reversible, as a total recovery of the response was attained following a third stimulation of the cell with nicotine alone, shortly after washout of the strychnine from the medium (Figure 8a). Strychnine (40 μM) did not affect the resting membrane potential. The inhibitory effect of strychnine was very rapid, since the extent of the inhibition was the same after preincubation of the cell with strychnine for zero and 2 min (data not shown).

Discussion

In this study, we have obtained evidence that strychnine can interact with the peripheral nicotinic acetylcholine receptor expressed in adrenal medullary chromaffin cells. Strychnine blocks nicotine- and oxotremorine-M-stimulated catecholamine secretion from chromaffin cells, but does not affect non-cholinoceptor stimulation by agonists such as histamine and angiotensin II, or by elevation of the extracellular K^+ concentration. These results suggest that the inhibitory action of strychnine is specific for acetylcholine receptor activation. The reversibility of the strychnine effect suggests that the inhibitory action is mediated through a cellular receptor.

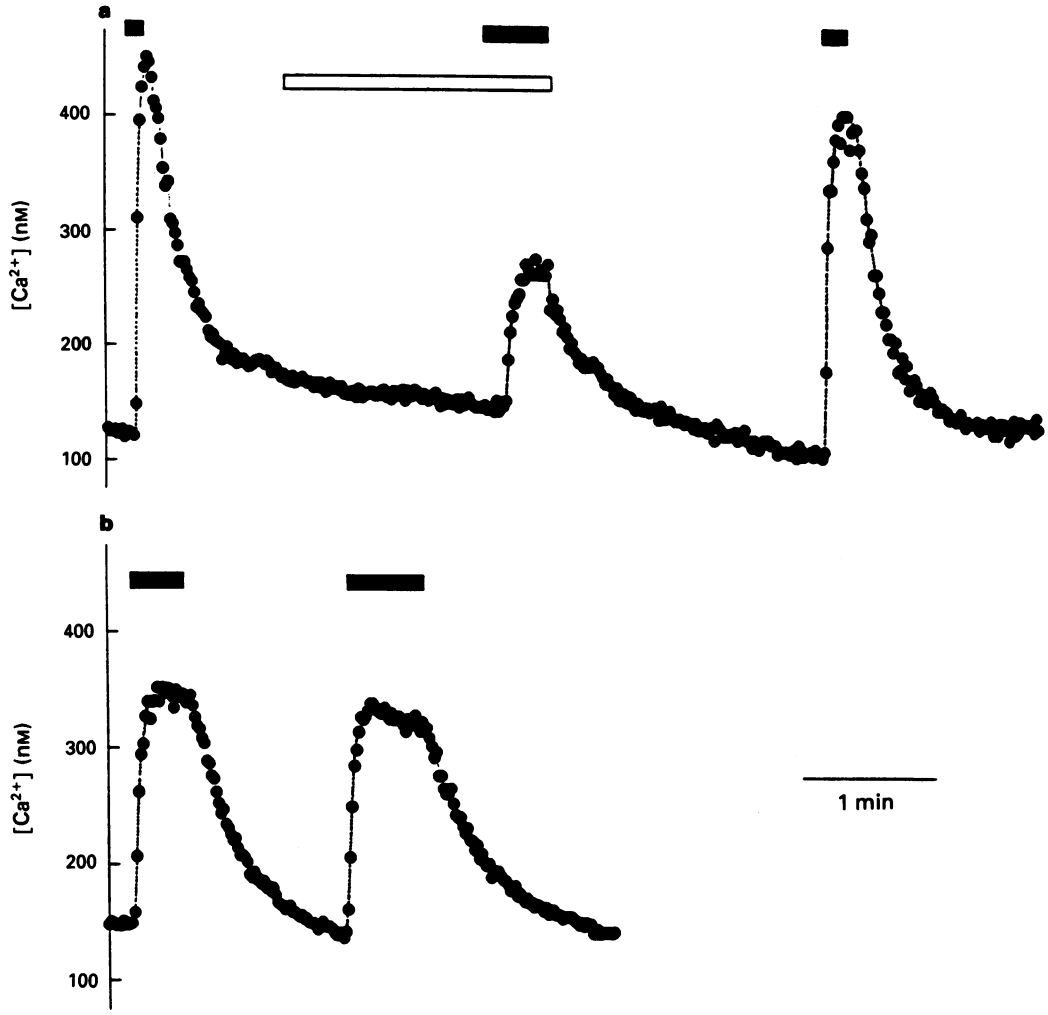


Figure 7 Effect of strychnine on intracellular Ca^{2+} transients in response to nicotine stimulation. Cells were (a) incubated with nicotine (10 μM), followed by nicotine + strychnine (40 μM), and then nicotine again, or (b) incubated with nicotine, followed by nicotine alone again. Preincubation time with strychnine was 80 s. Results shown are from single experiments, and are representative for 7 (a) and 4 (b) experiments. Solid bars indicate application of nicotine, open bars indicate application of strychnine.

The competitiveness of the effect with cholinoceptor agonists indicates that strychnine may interact with the ACh binding site itself, or with a site distal but very close to the receptor, thereby reducing its apparent affinity for cholinoceptor agonists. The rapid and reversible inhibition by strychnine of the increase in membrane potential and $[Ca^{2+}]_i$ induced by nicotine, is in agreement with the results obtained in the secretion studies, and supports the conclusion that strychnine interferes with an early step in the nicotinic acetylcholine receptor mediated cell stimulation.

The results of our study are in accordance with the older findings that strychnine and ACh can act in an antagonistic manner. Bonnet (1938) showed that in crayfish peripheral ganglia, ACh antagonizes the paralytic effects of strychnine. Similarly, Lanari & Luco (1939), Alving (1961) and Landau (1967) demonstrated that strychnine has a curare-like, depressant action on the sympathetic superior cervical ganglion and the neuromuscular junction stimulated by ACh or nerve stimulation.

The inhibition of the Oxo-M-induced catecholamine release by strychnine can be interpreted in light of recent findings by Shirvan *et al.* (1991), that in the chromaffin cell the nicotinic ACh receptor is activated by the otherwise muscarinic agonist Oxo-M. Shirvan *et al.* (1991) argued that nicotine and Oxo-M occupy different sites on this unique cholinoceptor. Our results indicate that these two sites cannot be distinguished in our study, since nicotine- and Oxo-M-stimulated CA release appear to be about equally sensitive to inhibition by strychnine.

The Hill coefficient for the nicotine-induced secretory response is 2.55. This suggests a positive cooperativity between the nicotine (ACh) binding sites at the nicotinic ACh receptor on chromaffin cells. Hill coefficients of 1.5–2.7 have been found in skeletal muscle fibres (Maelicke, 1984), and have been taken to indicate a positive cooperativity between two or more agonist binding sites at the ACh receptor. The lack of an effect of strychnine on the Hill coefficient thus suggests that strychnine, although interfering with the secretory response elicited by nicotine via an effect on its binding site, does not affect the apparent cooperative interaction between the ACh binding sites.

Our h.p.l.c. measurements suggest that strychnine induces a differential inhibition of the cholinoceptor mediated release of various catecholamines from chromaffin cells. In particular, the release of noradrenaline is reduced to a much lesser extent than the release of adrenaline. The latter finding may be due to a difference in sensitivity between the ACh receptors on adrenaline-and noradrenaline-containing cells.

The lack of an effect of glycine on catecholamine release contradicts previous findings from other laboratories (Yadid *et al.*, 1991; 1992), that glycine can induce the release of catecholamines in the absence of other agonists. This discrepancy could be due to the different ways in which the cells were prepared. In this study we used isolated chromaffin

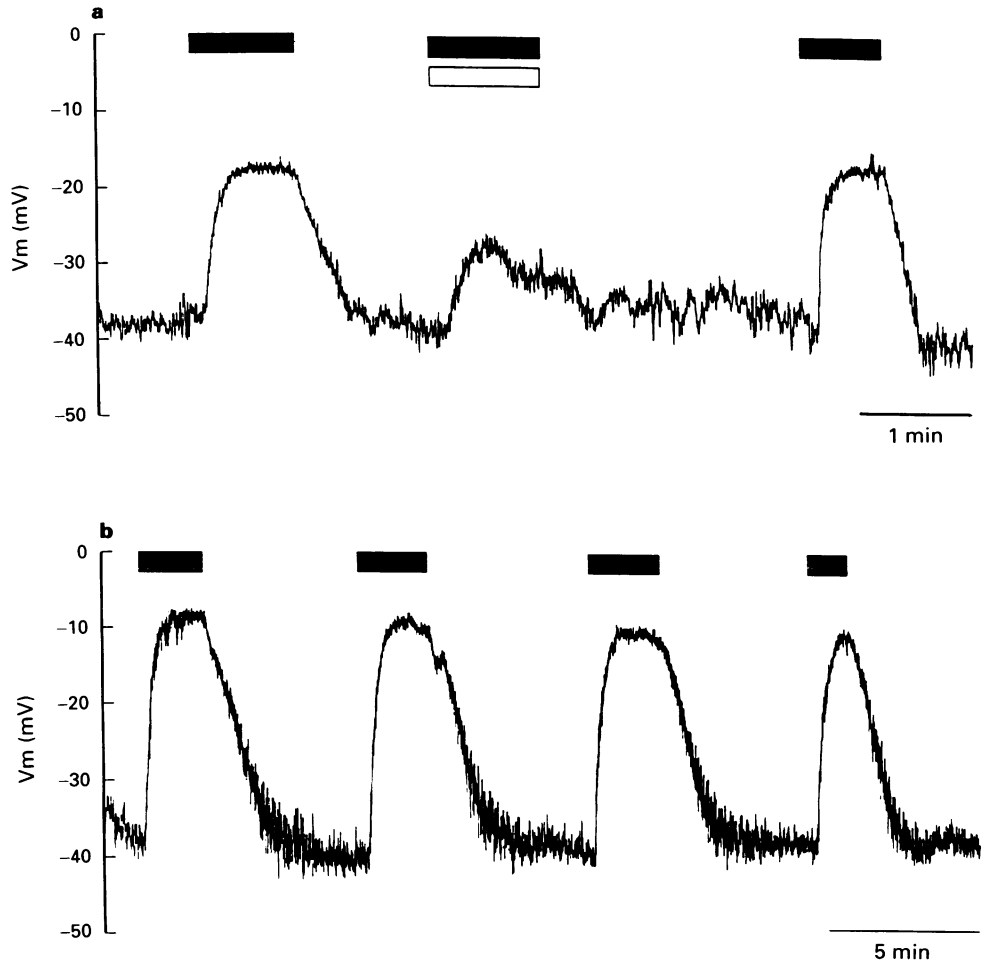


Figure 8 Effect of strychninė on membrane potential elevation induced by nicotine. Cells were (a) activated by nicotine (10 μM), followed by nicotine (10 μM) + strychnine (40 μM), and then nicotine (10 μM) again, or (b) repeatedly activated by nicotine (10 μM). Results shown are from single experiments, and are representative for three experiments. Solid bars indicate application of nicotine, open bars indicate application of strychnine.

cells, which were cultured for 3–7 days, whereas in the experiments of Yadid *et al.* (1991, 1992) freshly isolated chromaffin cells or slices of adrenal medulla were used. The exposure of the cells to serum or other factors during the cell culture might affect the expression of a functional strychnine-sensitive glycine receptor in our cells. At any rate, the absence of an effect of glycine on the inhibitory effect of strychnine reported in this study, suggests that strychnine exerts its effect through a direct blockade of the nicotinic acetylcholine receptor.

The inhibitory effect we describe occurs at relatively high, micromolar concentrations of strychnine. Blockade of cholinergic transmission at the sympathetic ganglion and neuromuscular junction has also been reported to take place in the concentration range of 10–80 μM (Lanari & Luco, 1939), 2–130 μM (Landau, 1967) or 20–100 μM (Alving, 1961). At these concentrations the drug is likely to have its lethal effect through paralysis of the neuromuscular junctions (Wall *et al.*, 1955). However, the concentration needed to inhibit a cholinoceptor-mediated response appears to depend on what type of ACh receptor is studied. In a recent study, it was found that 0.1 μM strychnine blocks the nicotine-activated current in a recombinant insect α-like nervous system ACh receptor expressed in oocytes (Marshall *et al.*, 1990). Also, an IC_{50} value of 0.35 μM was reported for strychnine inhibition of the current response to nicotine of a functionally expressed rat brain homooligomeric α_7 nicotinic receptor (Seguela *et al.*, 1993). In chick cultured ciliary ganglion neurones, containing native α_1 ACh receptors, Zhang *et al.* (1994) found that 1–10 μM strychnine inhibits the rapid and slow component of the nicotinic response. Moreover, in a novel cholinoceptor from chick isolated cochlear hair cells (Fuchs & Murrow, 1992), strychnine blocks the ACh response for 80–100% at concentrations of 0.3–3 μM.

With respect to binding to the nicotinic ACh receptor, K_i values for strychnine, reflecting its ability to compete with α-bungarotoxin (αBuTX) binding, of 5.4 and 6.9 μM have been reported for native brain α_7 receptor and α_7 homomers expressed in oocytes, respectively (Anand *et al.*, 1993). Similarly, K_i values of 6.8 μM and 2.2 μM have been reported for the cholinoceptor in *Aplysia* ganglia and rat brain membranes (Ono & Salvaterra, 1981). However, strychnine appears to be a more potent competitive inhibitor of αBuTX binding in central nervous tissue than in peripheral tissue (Schmidt & Raferty, 1974; Ono & Salvaterra, 1981). Taken together, these results are in accordance with our findings that strychnine, at micromolar concentrations, can competitively antagonize nicotinic receptor responses.

The K_d values reported in studies on the binding of strychnine to the glycine receptor are in the nanomolar range (Young & Snyder, 1973; 1974; Marvizon *et al.*, 1986; Yadid *et al.*, 1989). However, the concentration of strychnine needed to inhibit a functional glycine receptor-mediated response appears to be in the range of 1–10 μM (Mercuri *et al.*, 1990; Ito & Cherubini, 1991; Droge & Tao, 1993), or even 10–100 μM (Wu *et al.*, 1992). This discrepancy may partly be explained by the fact that the K_d values found in binding studies can be several orders of magnitude smaller than

suggested by dose-response studies under physiological conditions (Maelicke & Prinz, 1983; Paul *et al.*, 1993). Thus, the effects of strychnine in cholinoceptor systems can occur at similar concentrations as in glycine receptor systems.

Apart from its interaction with the glycine receptor, strychnine has been shown, although less effectively, to interfere with GABA-mediated neuronal inhibition (Curtis *et al.*, 1968; 1971; Davidoff *et al.*, 1969; Safronov *et al.*, 1989). In addition, interactions between bicuculline, a specific $GABA_A$ receptor antagonist, and specific [^{3}H]-strychnine binding have been observed (Goldinger & Muller, 1980; Marvizon *et al.*, 1986).

It has been suggested that strychnine can affect membrane ion permeability changes (Phillis & York, 1967; De Groat, 1970; Curtis *et al.*, 1971; Freeman, 1972). Indeed, recent studies have shown that at high micromolar concentrations (10–300 μM), strychnine can block a number of ion channels, e.g., K^+ and Na^+ channels in nervous tissues (Shapiro, 1977a,b; Cahalan & Almers, 1979; Yamamoto, 1986), and Ca^{2+} channels in brain and heart muscle (Ramos, 1974; O'Neill & Bolger, 1990). The fact that the inhibitory effect of strychnine on nicotine-stimulated catecholamine release, described in this paper, is competitive with nicotine, and the fact that K^+-stimulated release is unaffected, however, argues against a blockade of non-receptor coupled ion channels as the mechanism for the inhibition.

In conclusion, the results of our study demonstrate that strychnine specifically inhibits nicotine-stimulated catecholamine secretion from chromaffin cells, most likely by competitively antagonizing the activation of the chromaffin cell nicotinic ACh receptor by its agonists. The chemical similarities between the nicotine and strychnine molecules (Beers & Reich, 1970), as well as the homology between the well-characterized strychnine-binding subunit on the inhibitory glycine receptor and nicotinic acetylcholine receptor polypeptides (Greeningloh *et al.*, 1987), are in accordance with the hypothesis that strychnine can bind to the nicotinic ACh receptor, either at or close to the agonist binding site. Since nicotinic ACh receptors are thought to be members of a gene family of ligand-gated ionotropic receptors including neuronal and muscle nicotinic receptors, $GABA_A$ receptors, and glycine receptors (Grenningloh *et al.*, 1987; Schofield *et al.*, 1987), and since strychnine can interfere with the physiological events mediated through any of these receptor proteins, we suggest that strychnine interacts with an allosteric site common to the ion channel forming transmitter receptors.

We thank Dr H.B. Pollard for helpful discussion during the course of this work, and for critically reading the manuscript.

References

ALVING, B.O. (1961). The action of strychnine at cholinergic junctions. *Arch. Int. Pharmacodyn. Ther.*, **131**, 123–150.

ANAND, R., PENG, X. & LINDSTROM, J. (1993). Homomeric and native α_7 acetylcholine receptors exhibit remarkably similar but non-identical pharmacological properties, suggesting that the native receptor is a heteromeric protein complex. *FEBS Lett.*, **327**, 241–246.

BEERS, W.H. & REICH, E. (1970). Structure and activity of acetylcholine. *Nature*, **228**, 917–922.

BONNET, V. (1938). Action of strychnine and acetylcholine on neuronic rhythmicity in crustaceans. *Compt. Rend. Soc. Biol.*, **127**, 804–806.

CAHALAN, M.D. & ALMERS, W. (1979). Block of sodium conductance and gating current in squid giant axons poisoned with quaternary strychnine. *Biophys. J.*, **27**, 57–74.

CURTIS, D.R., DUGGAN, A.W. & JOHNSTON, G.A.R. (1971). The specificity of strychnine as a glycine antagonist in the mammalian spinal cord. *Exp. Brain Res.*, **12**, 547–565.

CURTIS, D.R., HOSLI, L. & JOHNSTON, G.A.R. (1968). A pharmacological study of the depression of spinal neurones by glycine and related amino acids. *Exp. Brain Res.*, **6**, 1–18.

DAVIDOFF, R.A., APRISON, M.H. & WERMAN, R. (1969). The effects of strychnine on the inhibitory effects of glycine and γ-aminobutyric acid. *Int. J. Neuropharmacol.*, **8**, 191–194.

DE GROAT, W.C. (1970). The effects of glycine, GABA and strychnine on sacral parasympathetic preganglionic neurones. *Brain Res.*, **18**, 542–544.

DROGE, M.H. & TAO, Y. (1993). Glycine effects on in vitro motor pattern generation in mouse spinal cord. *Neurosci. Lett.*, **158**, 139–142.

VON EULER, U.S. & FLODING, I. (1955). A fluorometric method for differential estimation of adrenaline and noradrenaline. *Acta Physiol. Scand.*, **33**, (Suppl. 118), 45–56.

FOSTHOLM, A. & ROTTER, A. (1985). Glycine receptor distribution in mouse CNS: autoradiographic localization of [^{3}H]strychnine binding sites. *Brain Res. Bull.*, **15**, 473–486.

FREEMAN, A.R. (1972). Axon membrane effects of inhibitory synaptic blocking agents. *Fed. Proc.*, **31**, 333.

FUCHS, P.A. & MURROW, B.W. (1992). A novel cholinergic receptor mediates inhibition of chick cochlear hair cells. *Proc. R. Soc. B.*, **248**, 35–40.

GOLDINGER, A. & MULLER, W.E. (1980). Stereospecific interaction of bicuculline with specific [^{3}H]-strychnine binding to rat spinal cord synaptosomal membranes. *Neurosci. Lett.*, **16**, 91–95.

GRAHAM, D., PFEIFFER, F. & BETZ, H. (1983). Photoaffinity labelling of the glycine receptor of the rat spinal cord. *Eur. J. Biochem.*, **131**, 519–525.

GRENNINGLOH, G., RIENITZ, A., SCHMITT, B., METHFESSEL, C., ZENSEN, M., BEYREUTHER, K., GUNDELFINGER, E.D. & BETZ, H. (1987). The strychnine-binding subunit of the glycine receptor shows homology with nicotinic acetylcholine receptor. *Nature*, **328**, 215–220.

HORN, R. & MARTY, A. (1988). Muscarinic activation of ionic currents measured by a new whole-cell recording method. *J. Gen. Physiol.*, **92**, 145–159.

ITO, S. & CHERUBINI, E. (1991). Strychnine-sensitive glycine responses of neonatal rat hippocampal neurones. *J. Physiol.*, **440**, 67–83.

KELNER, K.L., LEVINE, R.A., MORITA, K. & POLLARD, H.B. (1985). A comparison of trihydroxyindole and HPLC/electrochemical methods for catecholamine measurement in adrenal chromaffin cells. *Neurochem. Int.*, **7**, 373–378.

KUIJPERS, G.A.J., ROSARIO, L. & ORNBERG, R.L. (1989). Role of intracellular pH in secretion from adrenal medullar chromaffin cells. *J. Biol. Chem.*, **264**, 698–705.

LANARI, A. & LUCO, J.V. (1939). The depressant action of strychnine on the superior cervical sympathetic ganglion and on skeletal muscle. *Am. J. Physiol.*, **126**, 277–282.

LANDAU, E.M. (1967). The effect of strychnine on the neuromuscular junction of the rat. *Life Sci.*, **6**, 2515–2517.

LIVETT, B.G. (1984). Adrenal medulary chromaffin cells in vitro. *Physiol. Rev.*, **64**, 1103–1161.

MAELICKE, A. (1984). Biochemical aspects of cholinergic excitation. *Angew. Chem. Int. Ed. Engl.*, **23**, 195–221.

MAELICKE, A. & PRINZ, H. (1983). The acetylcholine receptor-ion channel complex: Linkage between binding and response. In *Modern Cell Biology*, Vol. 1 (Satir, B.H., series ed.), pp. 171–197. New York: Alan R. Liss, Inc.

MARSHALL, J., BUCKINGHAM, S.D., SHIGAI, R., LUNT, G.G., GOOSEY, M.W., DARLISON, M.G., SATTELLE, D. & BARNARD, E. (1990). Sequence and functional expression of a single α-subunit of an insect nicotinic acetylcholine receptor. *EMBO J.*, **9**, 4391–4398.

MARVIZON, J.C.G., VAZQUEZ, J., CALVO, M.G., MAYOR, F., RUIZ-GOMEZ, A., VALDIVIESO, F. & BENAVIDES, J. (1986). The glycine receptor: pharmacological studies and mathematical modelling of the allosteric interaction between the glycine- and strychnine-binding sites. *Mol. Pharmacol.*, **30**, 590–597.

MERCURI, N.B., CALABRESI, P. & BERNARDI, G. (1990). Effects of glycine on neurons in the rat substantia nigra zona compacta: In vitro electrophysiological study. *Synapse*, **5**, 190–200.

O'NEILL, S.K. & BOLGER, G.T. (1990). The effects of strychnine on the regulation of voltage-dependent calcium channels by dihydropyridines in brain and heart. *Pharmacol. Biochem. Behav.*, **35**, 833–840.

ONO, J.K. & SALVATERRA, P.M. (1981). Snake α-toxin effects on cholinergic and non cholinergic responses of Aplysia Californica neurons. *J. Neurosci.*, **1**, 259–270.

PAUL, I., BASILE, A.S., ROJAS, E., YOUDIM, M.B.H., DE COSTA, B., SKOLNICK, P., POLLARD, H.B. & KUIJPERS, G.A.J. (1993). Sigma receptors modulate nicotinic receptor function in adrenal chromaffin cells. *FASEB J.*, **7**, 1171–1178.

PFEIFFER, F., SIMLER, R., GRENNINGLOH, G. & BETZ, H. (1984). Monoclonal antibodies and peptide mapping reveal structural similarities between the subunits of the glycine receptor of the spinal cord. *Proc. Natl. Acad. Sci. U.S.A.*, **81**, 7224–7227.

PHILLIS, J.W. & YORK, D.H. (1967). Strychnine block of neural and drug-induced inhibition in the cerebral cortex. *Nature*, **216**, 922–923.

RAMOS, J.G. (1974). On the mechanism of strychnine spikes. *Acta Physiol. Lat. Am.*, **24**, 124–133.

SAFRONOV, B.V., BAEV, K.V., BATUEVA, I.V., RUSIN, K.I. & SUDEREVSKAYA, E.I. (1989). Peculiarities of receptor-channel complexes for inhibitory mediators in the membranes of lamprey spinal cord neurons. *Neurosci. Lett.*, **102**, 82–86.

SCHMIDT, J. & RAFERTY, M.A. (1974). The cation sensitivity of the acetylcholine receptor from Torpedo californica. *J. Neurochem.*, **23**, 617–623.

SCHOFIELD, P.R., DARLISON, M.G., FUJITA, N, BURT, D.R., STEPHENSON, F.A., RODRIGUEZ, H., RHEE, L.M., RAMACHANDRAN, J., REALE, V., GLENCORSE, T.A., SEEBURG, P.H. & BARNARD, E.A. (1987). Sequence and functional expression of the $GABA_A$ receptor shows a ligand-gated receptor super-family. *Nature*, **328**, 221–227.

SEGUELA, P., WADICHE, J, DINELEY-MILLER, K., DANI, J.A. & PATRICK, J.W. (1993). Molecular cloning, functional properties, and distribution of rat brain α_7: a nicotinic cation channel highly permeable to calcium. *J. Neurosci.*, **13**, 596–604.

SHAPIRO, B.I. (1977a). Effects of strychnine on the potassium conductance of the frog node of ranvier. *J. Gen. Physiol.*, **69**, 897–914.

SHAPIRO, B.I. (1977b). Effects of strychnine on the sodium conductance of the frog node of ranvier. *J. Gen. Physiol.*, **69**, 915–926.

SHIRVAN, M.H., POLLARD, H.B. & HELDMAN, E. (1991). Mixed nicotinic and muscarinic features of cholinergic receptor coupled secretion in bovine chromaffin cells. *Proc. Natl. Acad. Sci. U.S.A.*, **88**, 4860–4864.

WALL, P.D., MCCULLOCH, W.S., LETTVIN, J.Y. & PITTS, W.H. (1955). Effects of strychnine with special reference to spinal afferent fibres. *Epilepsy*, **4**, 29–39.

WU, W., ZISKIND-CONHAIM, L. & SWEET, M. (1992). Early development of glycine- and GABA-mediated synapses in rat spinal cord. *J. Neurosci.*, **12**, 3935–3945.

YADID, G., MAOR, G., YOUDIM, M.B.H., SILBERMAN, M. & ZINDER, O. (1993). Autoradiographic localization of strychnine-sensitive glycine receptor in bovine adrenal medulla. *Neurochem. Res.*, **18**, 1051–1055.

YADID, G., YOUDIM, M.B.H. & ZINDER, O. (1989). High affinity strychnine binding to adrenal medulla chromaffin cell membranes. *Eur. J. Pharmacol.*, **175**, 365–366.

YADID, G., ZINDER, O. & YOUDIM, M.B.H. (1991). Effect of the prodrug milacemide (2-N-pentylaminoacetamide) on catecholamine secretion from isolated adrenal chromaffin cells. *Br. J. Pharmacol.*, **104**, 760–764.

YADID, G., ZINDER, O. & YOUDIM, M.B.H. (1992). Preferred release of epinephrine by glycine from adrenal chromaffin cells. *Eur. J. Pharmacol.*, **221**, 389–391.

YAMAMOTO, D. (1986). Dynamics of strychnine block of single sodium channels in bovine chromaffin cells. *J. Physiol.*, **370**, 95–407.

YOUNG, A.B. & SNYDER, S.H. (1973). Strychnine binding associated with receptor of central nervous system. *Proc. Natl. Acad. Sci. U.S.A.*, **70**, 2832–2836.

YOUNG, A.B. & SNYDER, S.H. (1974). Strychnine binding in rat spinal cord membranes associated with the glycine synaptic receptor: cooperativity of glycine interactions. *Mol. Pharmacol.*, **10**, 790–809.

ZHANG, Z., VIJAYARAGHAVAN, S. & BERG, D.K. (1994). Neuronal acetylcholine receptors that bind α-bungarotoxin with high affinity function as ligand-gated ion channels. *Neuron*, **12**, 167–177.

(Received March 9, 1994
Revised June 2, 1994
Accepted June 20, 1994)

Br. J. Pharmacol. (1994), **113**, 479–484 © Macmillan Press Ltd, 1994

Modulation by neuropeptide Y of parasympathetic nerve-evoked nasal vasodilatation via Y_2 prejunctional receptor

[1]J. Silvain Lacroix, Lesley G. Ulman & Erica K. Potter

Prince of Wales Medical Research Institute, Prince of Wales Hospital, Randwick, 2031, Sydney, NSW, Australia

1 In pentobarbitone anaesthetized dogs, preganglionic stimulation of the superior cervical sympathetic nerve (15 V, 1 ms, 10 Hz) induced marked reduction of nasal arterial blood flow, whereas parasympathetic nerve stimulation (5 V, 1 ms, 10–30 Hz) evoked frequency-dependent vasodilatation.

2 Sympathetic nerve stimulation for 3 min at 10 Hz evoked significant ($P<0.05$) and prolonged attenuation of the vasodilator response to subsequent parasympathetic stimulation. Pretreatment with phentolamine (0.5 mg kg^{-1} h^{-1}), propranolol (1 mg kg^{-1}) and atropine (0.5 mg kg^{-1}) reduced the vasoconstrictor effect of sympathetic stimulation by $35 \pm 4\%$ whereas the parasympathetic nerve-evoked vasodilatation was not significantly modified. Atropine-resistant parasympathetic vasodilatation remained significantly attenuated for more than 30 min after non-adrenergic sympathetic nerve-evoked vasoconstriction.

3 Vasodilator effects of exogenous vasoactive intestinal polypeptide and peptide histidine isoleucine and vasoconstrictor effects of exogenous neuropeptide Y (NPY) and the NPY analogue [Leu^{31}, Pro^{34}] NPY (Y_1-receptor agonist, 8 nmol kg^{-1}), were not altered by adrenoceptor antagonists and atropine whereas the effects of exogenous noradrenaline and acetylcholine were virtually abolished. Attenuation of parasympathetic-evoked vasodilatation could be mimicked by exogenous NPY (8 nmol kg^{-1}) and the NPY analogue, N-acetyl [Leu^{28}, Leu^{31}] NPY 24–36 (Y_2-receptor agonist, 20 nmol kg^{-1}) but not by exogenous Y_1-receptor agonist. The Y_2-receptor agonist did not show significant vasoconstrictor action.

4 It is concluded that sympathetic nerve stimulation attenuates parasympathetic vasodilatation via NPY release acting on prejunctional Y_2 receptors.

Keywords: Blood flow; sympathetic; parasympathetic, non-adrenergic non-cholinergic; neuropeptide Y (NPY); Y_1 receptor agonist; Y_2 receptor agonist

Introduction

The nasal mucosa is densely innervated by efferent sympathetic and parasympathetic nerves involved in the regulation of local blood flow and mucus secretion (Eccles & Wilson, 1974). Stimulation of the nasal parasympathetic nerve, i.e. the vidian nerve, causes atropine-sensitive nasal secretion most likely mediated by acetylcholine (ACh, Eccles & Wilson, 1973) and vasodilatation (Tschalussow, 1913) via atropine-resistant mechanisms (Eccles & Wilson, 1973; Malm, 1973). Vasoactive intestinal polypeptide (VIP) is a potent vasodilator agent (Malm *et al.*, 1980) co-localized with ACh in postganglionic parasympathetic neurones supplying exocrine glands and blood vessels in the nasal mucosa (Uddman *et al.*, 1978). VIP is released during parasympathetic stimulation and could be the mediator of the non-cholinergic nasal vasodilatation observed upon stimulation of the vidian nerve in cats (Lundberg *et al.*, 1981). The peptide with N-terminal histidine (H) and C-terminal isoleucine (I) amide (PHI: Tatemoto, 1984) co-exists with VIP in nasal parasympathetic neurones (Lundberg *et al.*, 1984) and have vasodilator action on airway vasculature (Widdicombe, 1990). Both VIP and PHI may be considered as candidates for the atropine-resistant parasympathetic vasodilatation elicited by nerve stimulation (Lundberg *et al.*, 1984).

Electrical stimulation of the preganglionic fibres to the superior cervical sympathetic ganglion reduces nasal mucosa blood flow (Änggård & Edwall, 1974; Eccles, 1978). Noradrenaline (NA) is considered to be the classical mediator of nasal vasoconstrictor effects in postganglionic perivascular sympathetic nerves (Änggård & Densert 1974; Lacroix, 1989). Recent immunohistochemical studies as well as functional observations have suggested that both adrenergic and non-adrenergic mechanisms may occur in the peripheral sympathetic control of several vascular beds (Lundberg *et al.*, 1989) including the nasal mucosa (Lacroix, 1989). One candidate for non-adrenergic effects is neuropeptide Y (NPY), a 36 amino acid peptide that is colocalized with noradrenaline (NA) in sympathetic postganglionic perivascular nerves in several organs including the nasal mucosa in various species (Lundberg *et al.*, 1982; Lacroix *et al.*, 1990). In the cardiovascular system, NPY induces vasoconstriction via postjunctional receptors (Potter, 1985). In addition, NPY inhibits its own release as well as other neurotransmitter release such as NA (Edvinsson, 1988) and ACh (Revington *et al.*, 1990; Warner & Levy, 1990) by acting on prejunctional receptors (see Lundberg *et al.*, 1990). NPY probably acts via at least two subtypes of receptors, Y_1 and Y_2, which show differences in sensitivity to various NPY analogues *in vitro* (Wahlestedt *et al.*, 1986; Fuhlendorff *et al.*, 1990). Postjunctional NPY receptors have been called Y_1 receptors and prejunctional receptors have been called Y_2 receptors (Wahlestedt *et al.*, 1986; Lundberg *et al.*, 1988). By means of functional experiments *in vivo* combined with binding studies *in vitro*, NPY analogues have recently been developed. The Y_1-selective analogue [Leu^{31},Pro^{34}] NPY has the same vasopressor effect as NPY in rats and shares similar binding *in vitro* to various cell lines expressing only Y_1 receptor (Herzog *et al.*, 1992). In contrast, the recently developed Y_2-receptor agonist N-acetyl [Leu^{28}, Leu^{31}] NPY 24–36, mimics the action of NPY in inhibiting cardiac vagal action (a Y_2-receptor-mediated interaction) but has no pressor effect (a Y_1-receptor action) (Potter *et al.*, 1994).

We have recently shown that sympathetic nerve stimulation as well as exogenous NPY, attenuates the vasodilator response to subsequent parasympathetic nerve stimulation in the nasal mucosa of cats via non-adrenergic and non-

[1] Author for correspondence at Laboratory of Experimental Rhinology, Clinic of Otorhinolaryngology, University Hospital CH-1211 Geneva 14, Switzerland.

cholinergic mechanisms (Lacroix et al., 1994). The purpose of the present study was to evaluate possible interactions between sympathetic and parasympathetic nerves in the control of canine nasal mucosa blood flow. In order to characterize further the mechanisms underlying these interactions, parasympathetic-nerve evoked vasodilatation was also studied in the presence of exogenous NPY and the Y_1 and Y_2 receptor agonists, [Leu^{31}, Pro^{34}] NPY and N-acetyl [Leu^{28}, Leu^{31}] NPY 24–36, respectively.

Methods

Experiments were performed on twelve adult mixed breed dogs of either sex weighing between 4 and 9 kg. These experiments were approved by the institutional animal care and ethics committee. The dogs were anaesthetized with pentobarbitone sodium (35 mg kg^{-1}, i.v.). The trachea was cannulated low in the neck and the animals were artifically ventilated. A catheter connected to a Statham P23AC blood pressure transducer was placed in a femoral artery for systemic blood pressure monitoring. Another catheter was inserted in a femoral vein for administration of compounds and further doses of anaesthetic as required (0.5–1 ml of a 1-in-5 dilution of pentobarbitone). The left cervical vagus nerve was dissected high in the neck, the vagal sheath was removed and then the sympathetic nerve was easily separated from the vagal trunk. In some animals the sympathetic nerve was traced to the superior cervical sympathetic ganglion (Berridge & Roach, 1986). The left zygomatic arch was removed and the vidian nerve and the sphenopalatine ganglion were exposed by a procedure similar to the one described by Eccles & Wilson (1973). The proximal portion of the cervical sympathetic nerve as well as the cut peripheral end of the parasympathetic nerve was placed on bipolar platinum electrodes connected to a Grass S 88 stimulator (Grass Instruments, Quincy, U.S.A.). The identification of the cervical sympathetic nerve was confirmed by observing dilatation of the pupil with its electrical stimulation. The preganglionic parasympathetic nature of the vidian nerve was confirmed by the inhibition of vasodilatation evoked by its electrical stimulation after administration of chlorisondamine (2 mg kg^{-1}, i.v.). The left external carotid artery was dissected up to the internal maxillary artery. The main arterial branches located beyond to the superficial temporal artery were ligated as described previously by Lacroix et al. (1988), a procedure which leaves the internal maxillary artery flow supplying only the nasal mucosa. The superficial temporal artery was cannulated for selective injection of agents into the main nasal arterial blood supply. The nasal arterial blood flow was recorded with a transonic flow probe (3SB454) placed around the internal maxillary artery and connected to a T206 ultrasonic blood flowmeter (Transonic System Inc., NY, U.S.A.). All parameters were continuously recorded on a Grass polygraph model 7C in all experiments. The animals were allowed a 1 h intervention-free period following completion of surgery.

Experimental protocol

Group 1 ($n = 8$) Solutions of ACh (5.5×10^{-11} to 5.5×10^{-8} mol), VIP (3×10^{-11} to 3×10^{-9} mol), PHI (3.3×10^{-11} to 1.6×10^{-8} mol) and NA (6×10^{-11} mol to 6×10^{-8} mol) were infused into the superficial temporal artery over a period of 15 s. The administration of saline alone had no measurable effect. An interval of 5 min was allowed between successive injections. Fifteen minutes after the completion of the ACh, VIP, PHI and NA injections, parasympathetic nerve stimulations (5 V, 5 ms) were performed at continuous frequencies of 10, 20 and 30 Hz for 10 s. Each stimulation was performed 3 min after the blood flow in the internal maxillary artery returned to base line from the preceeding stimulation. Sympathetic nerve stimulation (15 V, 5 ms) was then performed continuously at 10 Hz for 3 min. Parasympathetic nerve stimulations were repeated 5 min, 30 min and then 1 h after sympathetic nerve stimulation. This entire protocol was repeated after pretreatment with the α-adrenoceptor antagonist, phentolamine (0.5 mg kg^{-1} h^{-1}), the β-adrenoceptor antagonist, propranolol (1 mg kg^{-1}) and the parasympathetic muscarinic receptor blocker, atropine (0.5 mg kg^{-1}), all delivered by local intra-arterial (i.a.) injection. Stimulations of the parasympathetic nerve were also performed 5 min, 30 min and 1 h after the administration of exogenous NPY (8 nmol kg^{-1}) dissolved in 5 ml of saline and infused into the femoral vein for 1 min.

Group 2 ($n = 4$) The parasympathetic nerve was stimulated at 10, 20 and 30 Hz in animals under control conditions and after pretreatment with phentolamine, propranolol and atropine (same doses as above). Parasympathetic nerve stimulations were repeated 5 min, 30 min and 1 h after the i.v. administration of the NPY analogue, [Leu^{31}, Pro^{34}] NPY (Y_1-receptor agonist, 8 nmol kg^{-1}), Ninety minutes later, parasympathetic nerve stimulation was also performed after the i.v. infusion of the NPY analogue, N-acetyl [Leu^{28}, Leu^{31}] NPY 24–36 (Y_2-receptor agonist, 20 nmol kg^{-1}).

Analysis of results

Changes of the nasal arterial blood flow were expressed in terms of vascular resistance in the maxillary artery (R_{ma}), obtained by dividing the driving mean arterial blood pressure in the femoral artery by the peak value of the blood flow volume rate in the maxillary artery. Before each experiment a zero flow in the maxillary artery was obtained by clamping the artery downstream to the transonic probe for 30 s. The durations of the responses were given in s and calculated from the end of the electrical stimulation until return to former basal values. All data are presented as mean ± standard error of the mean (s.e.mean). Statistical differences were evaluated by one way ANOVA test.

Drugs used

The following drugs were used: pentobarbitone sodium (Nembutal, Boehringer Ingelheim, Germany), acetylcholine (ACh, acetylcholine chloride, Sigma, U.S.A.), VIP (Peninsula, U.S.A.) and PHI (porcine PHI-27, Bachem, U.S.A.); phentolamine (Regitine, Ciba-Geigy, Switzerland), propranolol (Inderal, ICI, UK), atropine (atropine sulphate, Astra, Sweden), NA (Levophed, Winthrop, Australia) and NPY (h-NPY, Novabiochem Switzerland); the Y_2-receptor agonist, N-acetyl [Leu28, Leu31] NPY 24–36 and the Y_1-receptor agonist, [Leu^{31}, Pro^{34}] NPY (AusPep, Australia); chlorisondamine (Ecolid, Ciba-Geigy, Switzerland).

All solutions were freshly prepared before each experiment by dissolving the compounds in sterile 0.9% w/v NaCl.

Results

The basal blood flow in the internal maxillary artery of the dog was 8.5 ± 2 ml min^{-1} kg^{-1}. After section of both sympathetic and parasympathetic nerves on the left side the homolateral nasal arterial flow was 9.7 ± 2.5 ml min kg^{-1} (representing a 14% increase). The femoral arterial blood pressure was not modified by the section of the sympathetic or the parasympathetic nerves.

Electrical stimulation of the parasympathetic nerve induced frequency-dependent reductions of the R_{ma} (Figure 1a) whereas the BP was not significantly modified (not shown). Parasympathetic stimulation at 10 Hz increased the blood flow from 9.7 ± 2.5 ml min^{-1} kg^{-1} to 11.35 ± 1.8 ml min^{-1} kg^{-1} representing a reduction in R_{ma} of 16.8 ± 2% (Figure 1a). During stimulation at 30 Hz the blood flow increased to 13.4 ± 1.8 ml min^{-1} kg^{-1} correspnding to a R_{ma} reduction of

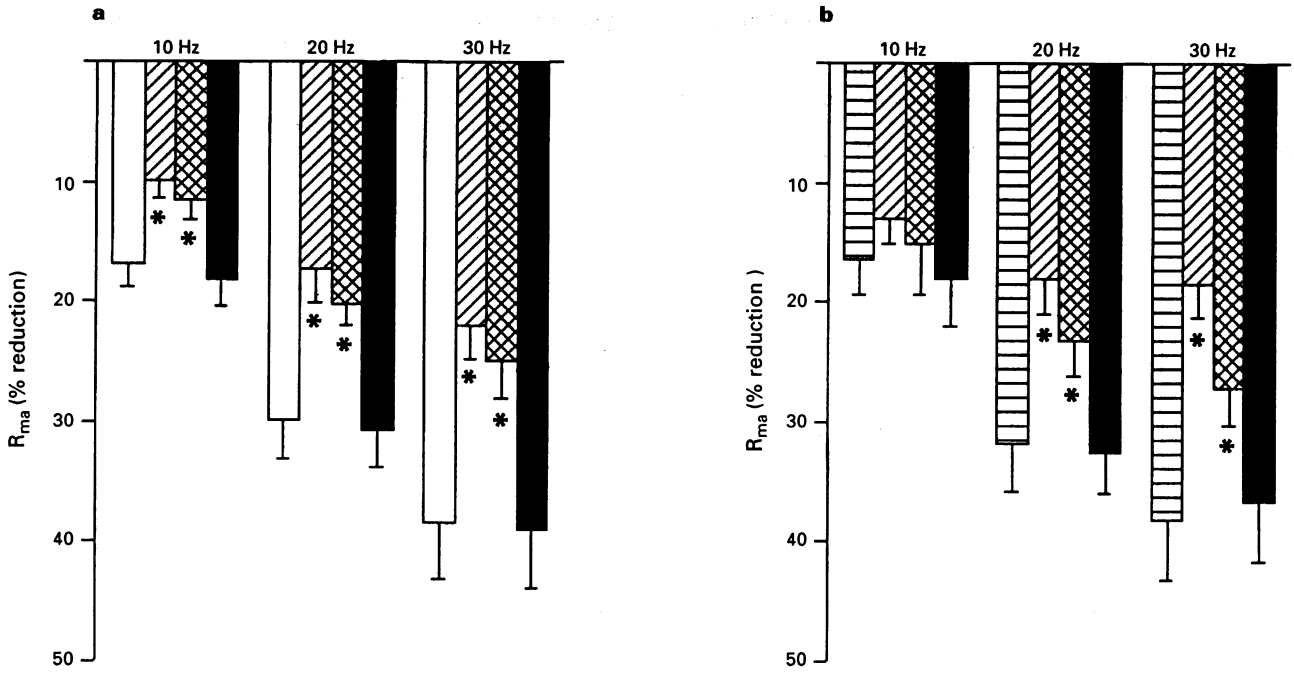


Figure 1 Effects of parasympathetic nerve stimulation (5 V, 5 ms) at different frequencies on the vascular resistance in the internal maxillary artery (R_{ma}) of the dog (a) under control conditions (open column) and (b) after pretreatment with phentolamine (0.5 mg kg^{-1} h^{-1}), propranolol (1 mg kg^{-1}) and atropine (0.5 mg kg^{-1}) (horizontally hatched column). The effects of the same parasympathetic stimulations are also shown just after sympathetic nerve stimulation (15 V, 5 ms, 10 Hz, 3 min) (diagonally hatched column), 30 min after sympathetic stimulation (cross hatched column) and 1 h later (solid column). $n = 8$, $^*P < 0.05$ when compared to control (one way ANOVA test).

38.5 ± 4.7% (Figure 1a). The blood flow increase lasted for 43 ± 5 s after stimulation at 10 Hz and 78 ± 8.2 s after 30 Hz stimulation.

Sympathetic nerve stimulation at 10 Hz for 3 min reduced the blood flow in the maxillary artery by 57.5 ± 7% lasting more than 7 min. The vasodilator responses evoked by electrical stimulations of the parasympathetic nerve were attenuated by an average 40% ($P < 0.05$) after sympathetic nerve stimulation at 10 Hz for 3 min (Figure 1a). Thirty minutes after the SNS the vasodilatation evoked by the stimulation of the parasympathetic nerve was still reduced by 23 ± 5% (Figure 1a). One hour after the completion of the SNS, the vasodilator effect of parasympathetic nerve stimulation was not significantly different in magnitude to that before sympathetic stimulation (Figure 1a and 3a).

After combined pretreatment with phentolamine, propranolol and atropine the driving mean arterial blood pressure was reduced by 18 ± 6%. In parallel, the blood flow in the internal maxillary artery was reduced by the same magnitude so the R_{ma} was not significantly modified. The vascular effects of exogenuous NA and ACh were virtually abolished in pretreated animals (not shown). The peak of the vasodilator responses to parasympathetic nerve stimulation was not significantly different from that observed before the administration of the adrenoceptor blockers and atropine (Figure 1). In contrast the responses were slower in onset and prolonged by 55% (Figure 3b).

After adrenoceptor blockade, the vasoconstriction evoked by sympathetic stimulation at 10 Hz for 3 min was reduced by an average 35% when compared to control (Figure 3b). The subsequent atropine-resistant vasodilatation evoked by parasympathetic nerve stimulation at 20 Hz and 30 Hz was reduced by more than 40% ($P < 0.05$) (Figure 1b). Thirty minutes after the sympathetic nerve stimulation, the vasodilatation evoked by the stimulation of the parasympathetic nerve was still reduced by 28 ± 5% (Figure 1b). After 1 h, the effects of parasympathetic stimulations were similar in magnitude to those before the sympathetic stimulation (Figure 1b and 3b).

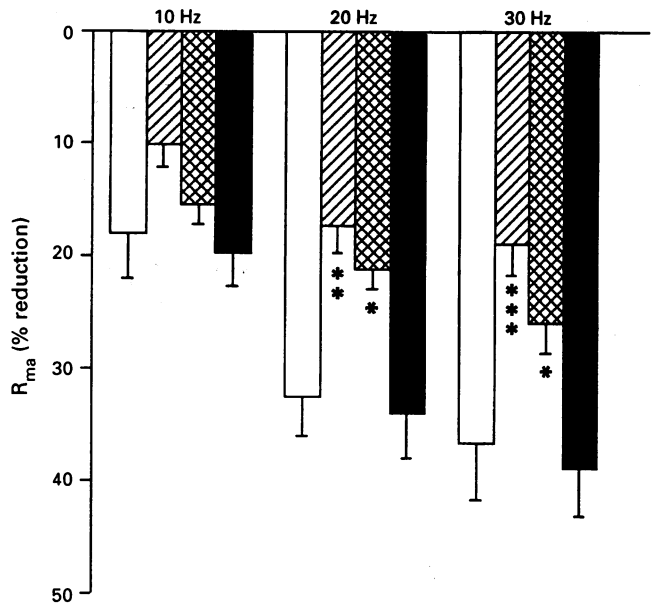


Figure 2 Effects of parasympathetic nerve stimulation (5 V, 5 ms) at different frequencies on the vascular resistance in the internal maxillary artery (R_{ma}) of the cat pretreated with phentolamine (0.5 mg kg^{-1} h^{-1}), propranolol (1 mg kg^{-1}) and atropine (0.5 mg kg^{-1}) (open column), just after the administration of exogenous neuropeptide Y) (NPY, 8 nmol kg^{-1}, i.v.) (diagonally hatched column), 30 min after the administration of NPY (cross hatched column) and 1 h later (solid column). $n = 8$, $^*P < 0.05$ and $P < 0.01$ when compared to the first column (one way ANOVA test).

The administration of exogenous NPY (8 nmol kg^{-1}, i.v.) increased arterial blood pressure by 25 ± 7 mmHg lasting 7.4 ± 1.8 min. In parallel the blood flow in the internal maxillary artery was reduced by 43 ± 8%. Atropine-resistant

vasodilatations evoked by parasympathetic stimulations at 20 and 30 Hz were reduced by more than 45% ($P<0.05$) after the administration of exogenous NPY (Figure 2 and 3c). The vasodilatation induced by parasympathetic stimulation at 20 and 30 Hz remained significantly reduced ($P< 0.05$) 30 min after the administration of exogenous NPY (Figure 2). One hour after the completion of the NPY infusion, stimulation of the parasympathetic fibres evoked increases in nasal blood flow similar in magnitude to those before the NPY administration (Figure 2 and 3c).

The infusion of the putative Y_1 receptor agonist, [Leu^{31}, Pro^{34}] NPY increased femoral blood pressure by

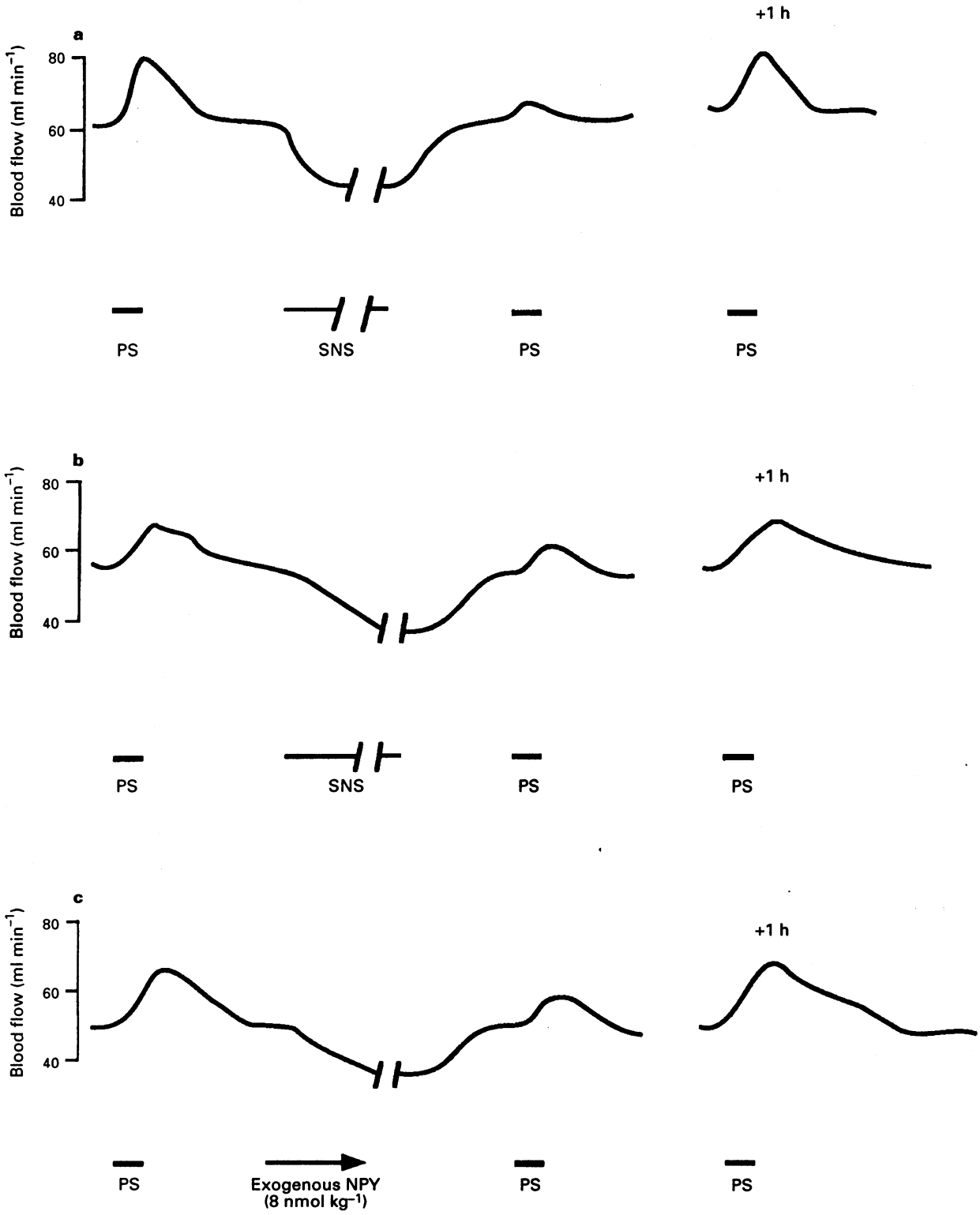


Figure 3 Recording from an anaesthetized dog showing changes in blood flow in the internal maxillary artery upon stimulation of the parasympathetic nerve (PS, 5 V, 5 ms) at 30 Hz for 10 s, during sympathetic nerve stimulation (SNS, 15 V, 5 ms, for 3 min) and the effect of subsequent parasympathetic stimulations. Note that 1 h later, the effect of the parasympathetic stimulation is of the same magnitude as that before sympathetic nerve stimulation: (a) under control conditions, (b) after pretreatment with phentolamine (0.5 mg kg^{-1} h^{-1}), propranolol (1 mg kg^{-1}) and atropine (0.5 mg kg^{-1}). In (c) the vasoconstrictor effect of exogenous NPY (8 nmol kg^{-1}, i.v.) is similar to the sympathetic stimulation shown in (b) as well as the inhibition of the subsequent parasympathetic vasodilatation. Time scale is given by the PS stimulation for 10 s.

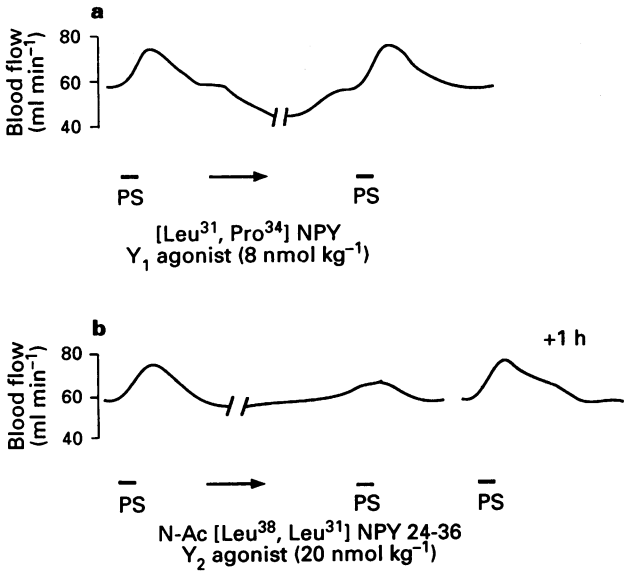


Figure 4 Recording from an anaesthetized dog showing changes in blood flow in the internal maxillary artery upon stimulation of the parasympathetic nerve (PS, 5 V, 5 ms) at 30 Hz for 10 s after pretreatment with phentolamine (0.5 mg kg^{-1} h^{-1}), propranolol (1 mg kg^{-1}) and atropine (0.5 mg kg^{-1}). In (a) the vasoconstrictor effect of the NPY analogue [Leu^{31}, Pro^{34}] NPY (Y_1-receptor agonist, 8 nmol kg^{-1}) is similar to those of exogenous NPY shown in Figure 3c but has no influence on the subsequent parasympathetic vasodilatation. In (b) the administration of the NPY analogue N-acetyl [Leu^{28}, Leu^{31}] NPY 24–36 (Y_2-receptor agonist, 20 nmol kg^{-1}) has no significant vasoconstrictor effect. However, the subsequent parasympathetic vasodilatation is reduced. One hour later, the effect of the parasympathetic stimulation is of the same magnitude as that before the administration of the Y_2-receptor agonist. Time scale is given by the PS stimulation for 10 s.

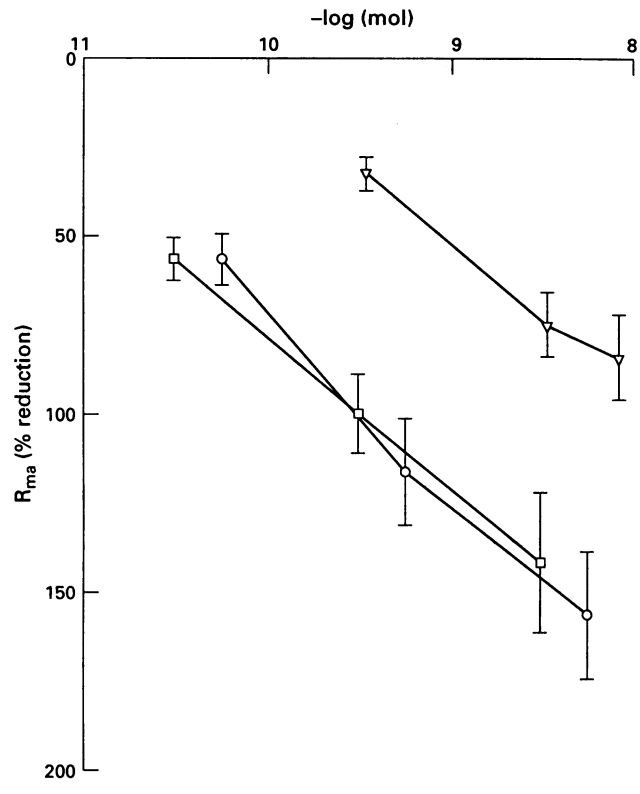


Figure 5 Effects of local intra arterial-injection of acetylcholine (Δ), vasoactive intestinal polypeptide (O) and peptide histidine isoleucine (□) on the vascular resistance in the internal maxillary artery (R_{ma}) of the dog.

23 ± 2.8 mmHg lasting more than 7 min (not shown). In parallel, the nasal mucosa blood flow was reduced by an average of 20% (Figure 4a). The vasodilator response to parasympathetic nerve stimulation was not modified after the administration of [Leu^{31}, Pro^{34}] NPY (Figure 4a).

Both blood pressure and nasal blood flow remained unchanged after the infusion of the NPY analogue, N-acetyl [Leu^{28}, Leu^{31}] NPY 24–36 (Figure 4b). However, the vasodilator responses to parasympathetic nerve stimulation at 10, 20 and 30 Hz were significantly reduced by an average 50% ($P<0.05$) after the administration of the Y_2-receptor agonist (Figure 4b). Thirty minutes later the response to parasympathetic nerve stimulation remained significantly reduced (not shown). One hour after the infusion of the Y_2-receptor agonist, the vasodilatations evoked by the parasympathetic stimulations remained smaller but were not significantly different in magnitude from those obtained before the infusion of the Y_2-receptor agonist (Figure 4b).

Local intra-arterial injections of ACh, VIP and PHI evoked dose-dependent reductions of the R_{ma} (Figure 5) without significant modification of the arterial blood pressure. On a molar basis the rank order potency was VIP > PHI ACh >. Exogenous NA induced dose-dependent increases in R_{ma} (not shown). The vasodilator effect of ACh was rapid whereas those of VIP and PHI were slow in onset and long lasting (not shown). The effects of ACh and NA were abolished after pretreatment with the α-adrenoceptor blockers and atropine whereas the vasodilator effects of VIP and PHI persisted (not shown).

Discussion

The results of the present study show that sympathetic nerve stimulation attenuates subsequent parasympathetic nerve-evoked nasal vasodilatation in anaesthetized dogs. Similar interactions between the sympathetic and parasympathetic system in the vascular control of the nasal mucosa have been recently described in cats (Lacroix *et al.*, 1994).

In dogs *in vivo*, NPY released upon strong sympathetic nerve stimulation, inhibits ACh release from postganglionic parasympathetic nerve and reduces vagal effectiveness at the heart (Potter, 1988; Revington *et al.*, 1990; Warner & Levy, 1990). Similar mechanisms may be involved in the inhibitory interactions which occur between sympathetic and parasympathetic nasal perivascular nerves during their successive activation. According to the observations reported here, it is likely that sympathetically released NPY attenuates cholinergic vasodilatation in the dog nasal mucosa under control conditions.

Parasympathetically-evoked vasodilatation was not modified after pretreatment with adrenoceptor blockers and atropine, suggesting the involvement of non-adrenergic non-cholinergic mechanisms. As reported earlier by Malm *et al.* (1980), the atropine-resistant nasal vasodilatation evoked by stimulation of the vidian nerve could be mimicked by exogenous VIP and to a lesser extent by PHI. Since VIP is present in perivascular postganglionic parasympathetic neurones in the nasal mucosa (Uddman *et al.*, 1978) and VIP is released during parasympathetic stimulation (Lundberg *et al.*, 1981), this neuropeptide is a probable candidate for mediator of the non-adrenergic, non-cholinergic parasympathetic vasodilatation observed in the present study.

After the administration of both adrenoceptor and cholinoceptor antagonists, the attenuation of the parasympathetic vasodilatation remained intact, whereas the effects of both NA and ACh were abolished. The recently developed NPY analogue, N-acetyl [Leu^{28}, Leu^{31}] NPY 24–36, has functional specificity for the prejunctional Y_2 receptor since it attenuates cardiac vagal action without a significant postjunctional Y_1-mediated pressor effect (Potter *et al.*, 1994). In the present study, the attenuation of the atropine-resistant

parasympathetic vasodilatation was mimicked by both NPY and the Y_2-receptor agonist, N-acetyl [Leu^{28}, Leu^{31}] NPY 24–36. In agreement with a recent report by Potter *et al.* (1994) this new NPY analogue has no pressor effects in dogs. In contrast, the Y_1-receptor agonist, [Leu^{31}, Pro^{34}] NPY, has shown similar vasopressor effects to exogenous NPY but has no influence on the parasympathetic nerve-evoked vasodilatation. Taken together, these observations strongly suggest that sympathetically released NPY has a prolonged inhibitory effect on parasympathetic vasodilatation via prejunctional Y_2 receptors.

In conclusion, the present observations show that sympathetic nerve stimulation and exogenous NPY have long-lasting inhibitory effects on parasympathetic nerve-evoked vasodilatation in the dog nasal mucosa. These sympathetic-parasympathetic interactions could be mimicked by N-acetyl [Leu^{28}, Leu^{31}] NPY 24–36, a specific Y_2-receptor agonist, suggesting that NPY attenuates parasympathetic vasodilatation by an action on Y_2 presynaptic NPY receptors.

The present study was supported by the National Health and Medical Research Council of Australia and the National Heart foundation of Australia. J.S.L.'s work is supported by a Scholar Award from the Swiss National Fund for Scientific Research (32-31964.91) and grant (32-37872.93). We thank Margaret Smith-White and Nicole Spinks for expert technical assistance and Prof. Ian McCloskey for his helpful comments throughout this study.

References

ÄNGGÅRD, A. & DENSERT, O. (1974). Adrenergic innervation of the nasal mucosa of the cat. A histological and physiological study. *Acta Otolaryngol.* (Stockholm), **78,** 232–241.

ÄNGGÅRD, A. & EDWALL, L. (1974). The effect of sympathetic nerve stimulation on the tracer disappearance rate and local blood content in the nasal mucosa of the cat. *Acta Otolaryngol.* (Stockholm), **77,** 131–139.

BERRIDGE, T.L. & ROACH, A.G. (1986). Characterization of α-adrenoceptors in the vasculature of the canine nasal mucosa. *Br. J. Pharmacol.*, **88,** 345–354.

ECCLES, R. (1978). The domestic pig as an experimental model for studies of the nasal cycle. *Acta Otalaryngol.* (Stockholm), **85,** 431–436.

ECCLES, R. & WILSON, H. (1973). The parasympathetic secretory nerves of the nose of the cat. *J. Physiol.*, **230,** 213–223.

ECCLES, R. & WILSON, H. (1974). The autonomic innervation of the nasal blood vessels of the cat. *J. Physiol.*, **238,** 549–560.

EDVINSSON, L. (1988). The effets of neuropeptide Y on the circulation. *ISI Atlas of Sciences: Pharmacol.*, **2,** 359.

FUHLENDORFF, J., GETHER, U., AAKERLUND, L., LANGELAND-JOHENSEN, N., TØGERSON, H., MELBERG, S.G., OLSEN, U.B., THASTRUP, O. & SCHWARTZ, T.W. (1990). [Leu^{31}, Pro^{34}] Neuropeptide Y: a specific Y_1 receptor agonist. *Proc. Natl. Acad. Sci. U.S.A.*, **87,** 182–185.

HERZOG, H., HORT, Y.J., BALL, H.J., HAYES, G., SHINE, J., SELBIE, L.A. (1992). Cloned human neuropeptide Y receptor couples to two different second messenger systems. *Proc. Natl. Acad. Sci. U.S.A.*, **89,** 5794–5798.

LACROIX, J.S. (1989). Adrenergic and non-adrenergic mechanisms in sympathetic vascular control of the nasal mucosa. *Act Physiol. Scand.*, **136** (Suppl 581), 1–63.

LACROIX, J.S., ST JÄRNE, P., ÄNGGÅRD, A. & LUNDBERG, J.M. (1988). Sympathetic vascular control of the pig mucosa (1): increased resistance and capacitance vessels responses upon stimulation with irregular bursts compared to continuous impulses. *Acta Physiol. Scand.*, **132,** 83–90.

LACROIX, J.S., ÄNGGÅRD, A., HÖKFELT, T., O'HARE, J., FAHRENKRUG, J. & LUNDBERG, J.M. (1990). Neuropeptide Y: presence in sympathetic and parasympathetic innervation of the nasal mucosa. *Cell Tissue Res.*, **259,** 119–128.

LACROIX, J.S., ULMAN, L.G. & POTTER, E.K. (1994). Sympathetic and parasympathetic interaction in vascular control of the nasal mucosa in cats. *J. Physiol.*, (in press).

LUNDBERG, J.M., ÄNGGÅRD, A., EMSON, P., FAHRENKRUG, J. & HÖKFELT, T. (1981). Vasoactive intestinal polypeptide and cholinergic mechanisms in cat nasal mucosa: Studies on choline acetyltransferase and release of vasoactive intestinal polypeptide. *Proc. Natl. Acad. Sci. U.S.A.*, **78,** 5255–5259.

LUNDBERG, J.M., FAHRENKRUG, J., HÖKFELT, T., MARTLING, C.R., LARSSON, O., TATEMOTO, K. & ÄNGGÅRD, A. (1984). Coexistence of peptide HI (PHI) and VIP in nerves regulating blood flow and bronchial smooth muscle tone in various mammals including man. *Peptides*, **5,** 593–606.

LUNDBERG, J.M., FRANCO-CERECEDA, A., HEMSEN, A., LACROIX, J.S. & PERNOW, J. (1990). Pharmacology of noradrenaline and neuropeptide tyrosine (NPY)- mediated sympathetic cotransmission. *Fundam. Clin. Pharmacol.*, **4,** 373–391.

LUNDBERG, J.M., HEMSEN, A., LARSSON, O., RUDEHILL, A., SARIA & FREDHOLM, B.A. (1988). Neuropeptide Y receptor in pig spleen: binding characteristics, reduction of cyclic AMP formation and calcium antagonist inhibition of vasoconstriction. *Eur. J. Pharmacol.*, **145,** 21.

LUNDBERG, J.M., PERNOW, J. & LACROIX, J.S. (1989). Neuropeptide Y: sympathetic co-transmitter and modulator *News Physiol. Sci.*, **4,** 13–17.

LUNDBERG, J.M., TERENIUS, L., HÖKFELT, T., MARTLING, C.R., TATEMOTO, K., MUTT, V., POLAK, J., BLOOM, S.R. & GOLDSTEIN, M. (1982). Neuropeptide Y (NPY)-like immunoreactivity in peripheral noradrenergic nerves and effects of NPY on sympathetic function. *Acta Physiol. Scand.*, **116,** 477–480.

MALM, L. (1973). Stimulation of sympathetic nerve fibres to the nose in cats. *Acta Otolaryngol.* (Stockholm), **75,** 519–526.

MALM, L., SUNDLER, F. & UDDMAN, R. (1980). Effects of vasoactive intestinal peptide (VIP) on resistance and capacitance vessels in nasal mucosa. *Acta Otolaryngol.* (Stockholm), **90,** 304–308.

POTTER, E.K. (1985). Prolonged non-adrenergic inhibition of cardiac vagal action following sympathetic stimulation: neuromodulation by neuropeptide Y? *Neurosci. Lett.*, **54,** 117.

POTTER, E.K. (1988). Neuropeptide Y as an autonomic neurotransmitter., *Pharmacol. Ther.*, **37,** 251.

POTTER, E.K., BARDEN, J.A., MCCLOSKEY, M.J.D., SELBIE, L.A., TSENG, A., HERZOG, H. & SHINE, J. (1994). A novel neuropeptide Y analog, N-acetyl [Leu^{28}, Leu^{31}] NPY 24–36, with functional specificity for the presynaptic (Y2) receptor. *Eur. J. Pharmacol.*, (in press).

REVINGTON, M., POTTER, E.K. & MCCLOSKEY, D.I. (1990). Prolonged inhibition of cardiac vagal action following sympathetic stimulation and galanin in anaesthetized cats. *J. Physiol.*, **431,** 495–503.

TATEMOTO, K. (1984). PHI – a new brain – gut peptide. *Peptides*, **5,** 151–154.

TSCHALUSSOW, M.A. (1913). Die Innervation der Gefässe der Nasenschleimhaut. *Pflügers Arch.*, **151,** 523–542.

UDDMAN, R., ALUMETS, J., DENSERT, O., HÅKANSSON, R. & SUNDLER, F. (1978). Occurrence and distribution of VIP nerves in the nasal mucosa and tracheobronchial wall. *Acta Otolaryngol.* (Stockholm), **85,** 443–448.

WAHLESTEDT, C., YANAIHARA, N. & HÅKANSSON, R. (1986). Evidence for different pre- and post-junctional receptors for neuropeptide Y and related peptides. *Regul. Peptides*, **13,** 307–318.

WARNER, M.R. & LEVY, M.N. (1990). Role of neuropeptide Y neural control of the heart. *J. Cardio Electrol.*, **1,** 80–91.

WIDDICOMBE, J.G. (1990). The non-adrenergic, non-cholinergic system and airways vasculature. *Arch. Int. Pharmacodyn.*, **303,** 83–90.

(Received December 23, 1993
Revised April 1, 1994
Accepted June 30, 1994)

Br. J. Pharmacol. (1994), **113**, 485–495 © Macmillan Press Ltd, 1994

Modulation of 5-HT release in the guinea-pig brain following long-term administration of antidepressant drugs

[1]Pierre Blier & Claude Bouchard

Neurobiological Psychiatry Unit, Department of Psychiatry, McGill University, 1033, Pine Avenue West, Montréal, Québec, Canada H3A 1A1

1 The aims of the present study were to determine whether long-term 5-hydroxytryptamine (5-HT) reuptake blockade and inhibition of type-A monoamine oxidase (MAO-A) lead to an enhancement of the electrically evoked release of tritium from guinea-pig brain slices preloaded with [^{3}H]-5-HT, and to assess the sensitivity of the terminal 5-HT_{1D} autoreceptor, the α_2-adrenoceptor also located on 5-HT terminals, and the 5-HT_3 receptor that modulates 5-HT release following these two types of antidepressant treatments.

2 The electrically evoked release of tritium was significantly enhanced following a 21-day treatment with the 5-HT reuptake blocker, paroxetine and the reversible MAO-A inhibitor, befloxatone, in preloaded slices of the hypothalamus, hippocampus and frontal cortex 48 h after removal of the osmotic minipumps used to deliver the drugs.

3 The inhibitory effect of the terminal 5-HT autoreceptor agonist, 5-methoxytryptamine, on the evoked release of tritium was attenuated in slices of the hypothalamus, hippocampus, but not frontal cortex, following the paroxetine treatment. In the befloxatone group, the effectiveness of 5-methoxytryptamine was unaltered in the same brain structures.

4 The sensitivity of the α_2-adrenoceptor on 5-HT terminals, assessed using UK 14.304, was attenuated in hypothalamus, hippocampus, but not frontal cortex slices prepared from befloxatone-treated guinea-pigs and preloaded with [^{3}H]-5-HT. The paroxetine treatment did not alter the sensitivity of this α_2-adrenoceptor in the hypothalamus.

5 The sensitivity of the α_2-adrenoceptor on noradrenaline terminals, also assessed using UK 14.304, was not altered in hippocampus and hypothalamus slices preloaded with [^{3}H]-noradrenaline following the long-term befloxatone treatment.

6 In frontal cortex slices, [^{3}H]-5-HT uptake was no longer significantly attenuated after a 21-day treatment with paroxetine, whereas it was still markedly inhibited in hypothalamus slices. The enhancing effect of paroxetine on the evoked release of [^{3}H]-5-HT in the superfusion medium was no longer evident in frontal cortex slices of the paroxetine group. These data indicate that long-term 5-HT reuptake blockade desensitized the 5-HT transporter in the frontal cortex.

7 The capacity of the 5-HT_3 receptor agonist, 2-methyl-5-HT, to enhance the electrically evoked release of tritium was not altered in hypothalamus, hippocampus, and frontal cortex slices prepared from befloxatone-treated guinea-pigs, but was significantly attenuated in the paroxetine group also treated for 21 days. Following a 2-day paroxetine treatment, the enhancing effect of 2-methyl-5-HT on tritium release was unaltered in frontal cortex slices.

Keywords: 5-HT reuptake blockade; monoamine oxidase inhibition; 5-HT autoreceptor; α_2-adrenoceptors; 5-HT_3 receptors; [^{3}H]-5-HT release; [^{3}H]-noradrenaline release

Introduction

By use of *in vivo* electrophysiological techniques, long-term administration of antidepressant treatments has been shown to increase 5-hydroxytryptamine (5-HT) neurotransmission in the rat hippocampus (Blier & de Montigny, 1994). In the case of electroconvulsive shocks and tricyclic antidepressant (TCA) drugs, this enhancement was attributable to an enhanced responsiveness of the postsynaptic 5-HT_{1A} receptors (Chaput *et al.*, 1991). Long-term administration of TCA drugs has also been shown to induce a progressive increase of the responsiveness of postsynaptic neurones to microiontophoretically-applied 5-HT in other rat brain regions, such as the amygdala, lateral geniculate nucleus and facial motor nucleus via 5-HT receptors which have not yet been fully characterized (de Montigny & Aghajanian, 1978; Menkes *et al.*, 1980; Wang & Aghajanian, 1980; Menkes & Aghajanian, 1981). Selective 5-HT reuptake inhibitors (SSRI) and monoamine oxidase inhibitors (MAOI), in contrast, produce the same net effect on 5-HT neurotransmission but by enhancing the function of 5-HT neurones (Blier & de Montigny, 1994). Both types of drugs produce an initial decrease of 5-HT neuronal firing activity, which plays an important role in controlling 5-HT release in terminal fields, which is followed by a gradual recovery as a result of the desensitization of their somatodendritic 5-HT_{1A} autoreceptors. This normalized firing activity in the presence of an increased neuronal concentration of 5-HT resulting from sustained MAO inhibition could explain, at least in part, the enhancement of 5-HT neurotransmission by MAOI. While the SSRI do not increase the tissue concentration of 5-HT, as MAOI do, they produce a desensitization of the terminal 5-HT autoreceptor, which exerts a potent negative feedback influence on 5-HT release, thus allowing a greater release of 5-HT per action potential.

The present studies were undertaken to determine whether 5-HT release is also increased in brain regions other than the hippocampus following long-term treatment with an SSRI and a MAOI, and to elucidate further the mechanisms by which these two types of drugs enhance 5-HT release. Three receptors were studied: the terminal 5-HT autoreceptor, the α_2-adrenoceptor located on 5-HT terminals, which also inhibits 5-HT release (see Starke *et al.* for a review, 1989), and finally the 5-HT_3 receptor that is not located on 5-HT

[1] Author for correspondence.

terminals but exerts a positive feedback influence on 5-HT release (Galzin & Langer, 1991; Blier & Bouchard, 1993; Blier *et al.*, 1993). The experiments were carried out in guinea-pigs for two reasons. First, their terminal 5-HT autoreceptors are of the 5-HT_{1D} subtype, as in man, whereas they are of the 5-HT_{1B} subtype in rats (Hoyer & Middlemiss, 1989; Galzin *et al.*, 1992). Second, the MAO isozyme ratio of the A and B subtypes in guinea-pig is similar to that found in man but different from that in the rat, at least in the basal ganglia (Azzaro *et al.*, 1985).

Methods

Treatments

Male guinea-pigs were implanted, under halothane anaesthesia, with an osmotic minipump (Alza, Palo Alto, CA, U.S.A.) which delivered the SSRI, paroxetine (10 mg kg^{-1}, day^{-1}; SmithKline Beecham, Harlow, England), the reversible and selective type A MAOI, befloxatone (0.75 mg kg^{-1} day^{-1}; Delalande, Rueil-Malmaison, France), or the vehicle used to dilute these two drugs (50:50 ethanol and water). After 21 days, the minipumps were removed under halothane anaesthesia and the *in vitro* release experiments were carried out 48 h later to allow elimination of drugs.

Superfusion experiments

The guinea-pigs, weighing 300–400 g at the time of the experiments, were killed by decapitation and their brains rapidly removed and dissected on an ice-cold glass plate. Slices from the hypothalamus, hippocampus, or frontal cortex of 0.4 mm thickness were prepared with a McIlwain chopper and incubated for 30 min at 37°C in Krebs solution containing 20 nM [^{3}H]-5-HT creatinine sulphate (specific activity 1.1 TBq $mmol^{-1}$; NEN Research Products, Mississauga, Canada), 100 nM [^{3}H]-5-HT in one series of experiments, or 100 nM [^{3}H]-noradrenaline (specific activity 543 GBq $mmol^{-1}$), and bubbled with a mixture of 95% O_2:5% CO_2. The composition of the Krebs solution in mmol l^{-1} concentrations were: NaCl 118, KCl 4.7, $CaCl_2$ 1.3, $MgCl_2$ 1.2, NaH_2PO_4 1, $NaHCO_3$ 25, glucose 11.1, Na_2EDTA 0.004 and ascorbic acid 0.11. At the end of the incubation period, one hypothalamic slice, three slices of the hippocampus, or two slices of frontal cortex were transferred into separate glass chambers and superfused continuously at a rate of 0.5 ml min^{-1} with Krebs solution maintained at 37°C and saturated with O_2/CO_2. Nineteen consecutive 4-min fractions were collected starting 52, 60 or 90 min after the beginning of superfusion for the hypothalamus, hippocampus, and frontal cortex slices, respectively. The slices were stimulated twice for 2 min, 8 min (S_1) and 44 min (S_2) after the end of the washing period. The electrical field generated in the chambers between two platinum electrodes (2 cm apart) had a voltage drop of about 10 V. The following stimulation parameters were used to elicit [^{3}H]-5-HT and [^{3}H]-NA release in hypothalamic slices: 20 mA, 2 ms, 3 Hz for 2 min. In the experiments carried out with hippocampus and frontal cortex slices, the following parameters were used: 30 mA, 2 ms, 3 Hz for 2 min. This frequency of stimulation was chosen because it is within the range of the firing rate of 5-HT and noradrenergic neurones recorded in freely-moving cats (Jacobs, 1986). The first stimulation period (S_1) was always used as control and the drugs were added 8 or 20 min before S_2 and remained present until the end of the superfusion. At the end of the experiments, the slices were solubilized in 0.5 ml of Soluene 350 (Packard Instruments, Downers grove, II, U.S.A.) and the radioactivity in the slices and superfusate samples was determined by liquid scintillation spectrometery. The amount of tritium released per 4-min sample was expressed as a fraction of the total tissue tritium content at the beginning of the respective collection period. The overflow of tritium produced by the electrical stimulation was calculated as the total increase in radioactivity above the basal outflow of tritium determined in the sample immediately preceding the start of stimulation (sp_1 or sp_2). In order to assess the drug-induced changes of electrically-evoked overflow of radioactivity, S_2/S_1 ratios were calculated. The sp_2/sp_1 ratios were also calculated to determine whether the drugs had altered the basal outflow of radioactivity. The amount of tritium released by electrical stimulation in rat brain slices under these conditions provides a reliable estimate of the release of tritiated or endogenous 5-HT (Baumann & Waldmeier, 1981; Moret & Briley, 1990b; Blier & Bouchard, 1993).

In order to detect treatment effects, concentration-effect curves were constructed by studying simultaneously in the same superfusion apparatus five chambers with slices prepared from a control and five chambers with slices from a treated guinea-pig with the same drug concentration. One to three pairs of guinea-pigs from the same arrival (which were implanted with the minipump on the same day and then housed in the same cages) were used for each drug concentration. This experimental design was deemed optimal to minimize the problem of inter-experimental variations, as indicated by the differences between the control groups, which are inherent to such superfusion studies.

Determination of [^{3}H]-5-HT uptake

For determination of *in vitro* [^{3}H]-5-HT uptake, hypothalamus and frontal cortex slices were prepared as for the superfusion experiments. They were incubated for 3 min at 37°C and continuously bubbled with 5% CO_2:95% O_2. Following this stabilization period, [^{3}H]-5-HT was added to final concentration of 20 nM in all the experiments with the exception of one series in which 100 nM was used. After a 3 min incubation period, uptake was terminated by transferring the slices to 5 ml of ice cold Krebs solution and they were then solubilized in 0.5 ml Soluene 350. Radioactivity in the slices and the incubation medium was determined by liquid spectroscopy. Parallel experiments were carried out at 0°C as control for passive diffusion. The amount of tritium actively captured by the tissue (C_A) was calculated according to the formula: $C_A = C_T - C_P$ where C_T and C_P are the tissue/medium ratios of [^{3}H]-5-HT at 37°C (total) and 0°C (passive), respectively. The percentage inhibition was calculated by comparing the C_A values obtained in the slices prepared from the control and treated guinea-pigs.

The following drugs were used: 2-methyl-5-HT, 5-carboxamidotryptamine (5-CT), UK 14.304 (5-bromo-6-[2-imidazoline-2-ydaminol-quinoxaline]), idazoxan, (Research Biochemicals, Natick, MA, U.S.A.), 5-methoxytryptamine (5-MeOT; Sigma, St-Louis, MO, U.S.A.), paroxetine, methiothepin, S-zacopride and befloxatone.

The means for the spontaneous and evoked fractional releases were compared with Student's two-tailed *t* test. The concentration-effect curves were compared using a three-factor analysis of variance (independent variables: agonist concentration, treatment and animal; dependent variable: S_2/S_1 ratios for the individual chambers). The tissue-medium ratios of radioactivity were compared in the control and treated groups to determine the *t* values. Probability (*P*) values smaller than 0.05 were considered as significant.

Results

Effects of long-term paroxetine and befloxatone administration on tritium release

The electrically evoked release of tritium in the absence of any drug in S_1 was significantly enhanced following the 21-day treatment with paroxetine by 35%, 25% and 31% in the hypothalamus, hippocampus and frontal cortex, respectively, when compared to controls processed in parallel in the same

experiments (Figure 1). The spontaneous outflow of radioactivity in the sample immediately preceding this first period of stimulation (sp_1), was slightly but significantly decreased by 9% in the hypothalamic and hippocampal slices prepared from the paroxetine treated guinea-pigs as compared to the controls (Table 1). These alterations were unlikely to have resulted from the residual 5-HT reuptake blockade following the 48 h washout for two reasons. First, when paroxetine was

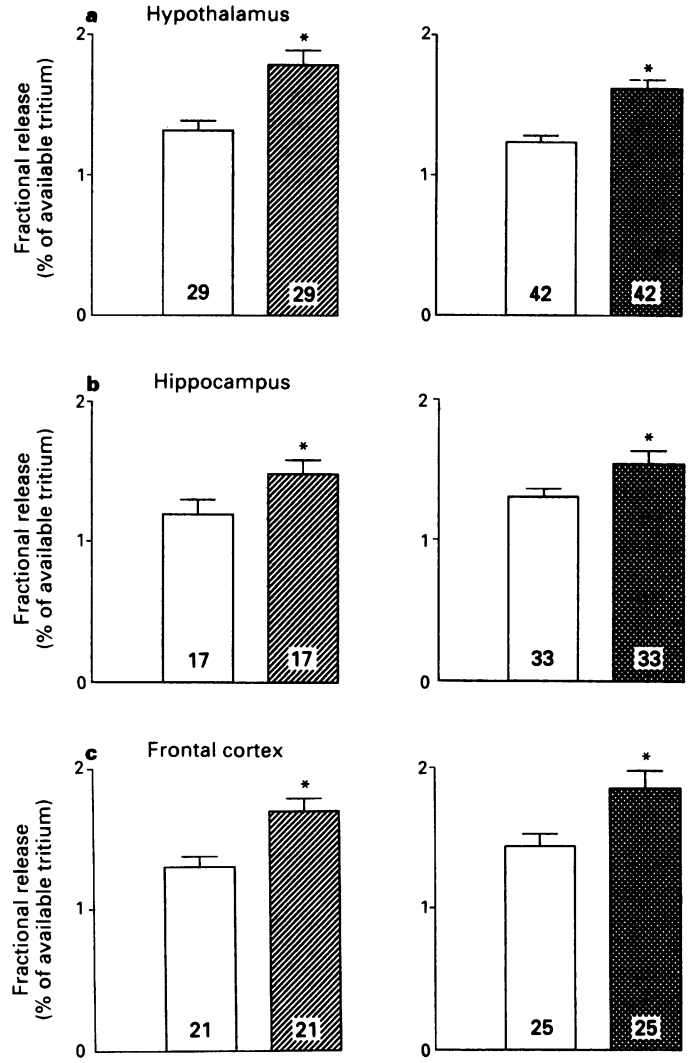


Figure 1 Effect of long-term administration of paroxetine (10 mg kg^{-1} day^{-1} for 21 days) and of befloxatone (0.75 mg kg^{-1} day^{-1} for 21 days) on the electrically stimulated tritium overflow in slices prepared from various regions of the guinea-pig brain and preloaded with [^{3}H]-5-HT. These drugs were administered using osmotic minipumps implanted subcutaneously and removed 48 h before the animals were killed. Ordinates: fraction of the total radioactivity released by 360 pulses (20 mA in hypothalamic and 30 mA in hippocampal and frontal cortex slices, 2 ms, 3 Hz) in the first period of stimulation before the introduction of any drug in the superfusate. Experiments were always carried out in pairs of guinea-pigs, a control and a treated one, processed in parallel in the same superfusion apparatus. The figures within the columns refer to the number of animals studied, and for each animal four to five chambers were used. Open columns, control; hatched columns, paroxetine; cross-hatched columns, befloxatone. *$P<0.05$ when compared with the corresponding control value.

Table 1 Effect of long-term administration of paroxetine or befloxatone on the spontaneous outflow of tritium from guinea-pig brain slices preloaded with [^{3}H]-5-HT[1]

	Hypothalamus	*Hippocampus*	*Frontal cortex*
Control	1.20 ± 0.03% (29)	1.12 ± 0.06% (17)	0.82 ± 0.02% (21)
Paroxetine	1.09 ± 0.03%* (29)	1.04 ± 0.04%* (17)	0.76 ± 0.03% (21)
Control	1.18 ± 0.02% (42)	1.16 ± 0.03% (33)	0.87 ± 0.04% (25)
Befloxatone	1.27 ± 0.02%* (42)	1.28 ± 0.04%* (33)	0.88 ± 0.03% (25)

[1]Percentage of total tissue tritium content present in the slices in the 4-min sample of superfusate collected immediately before the first period of electrical stimulation. The experiments were carried out 48 h after a 21-day treatment with paroxetine (10 mg kg^{-1} day^{-1}, s.c.) or befloxatone (0.75 mg kg^{-1} day^{-1}, s.c.). No drug was present in the superfusate. The figures given in parentheses refer to the number of guinea-pigs studied, and for each animal four to five chambers were studied.
*$P<0.05$ when compared to the controls processed in parallel in the same experiments.

introduced 20 min before S_2 in controls, it produced a significant increase in the spontaneous outflow of tritium from hypothalamic slices ($sp_2/sp_1 = 0.88 \pm 0.02$, $n = 6$, in the presence of 1 μM paroxetine versus 0.79 ± 0.01, $n = 29$, in the absence of paroxetine). Second, when [^{3}H]-5-HT uptake was determined with the same concentration of [^{3}H]-5-HT as that used in the superfusion experiments (20 nM), it was not significantly altered in hypothalamic slices 48 h after a 21-day treatment (Figure 8). The total tissue content of radioactivity at the end of the experiments was not significantly altered in the slices prepared from guinea-pigs treated with paroxetine compared with the controls (data not shown).

In the slices prepared from guinea-pigs treated with befloxatone for 21 days, the electrically evoked release of tritium was also significantly enhanced by 30%, 18% and 29% in the hypothalamus, hippocampus and frontal cortex, respectively, when compared to controls processed in parallel (Figure 1). The spontaneous outflow of radioactivity (sp_1) was slightly but significantly enhanced by 9% and 10% in the hypothalamus and hippocampus, respectively, but unchanged in frontal cortex slices prepared from befloxatone-treated guinea-pigs (Table 1). These modifications of basal outflow and evoked overflow of tritium release are not likely to be attributable to residual inhibition of MAO-A since the introduction of befloxatone (0.1 μM) 20 min before S_2 decreased in hippocampal slices both the electrically evoked release of tritium ($S_2/S_1 = 0.56 \pm 0.06$, $n = 8$, versus the control condition $S_2/S_1 = 1.06 \pm 0.07$, $n = 10$) and the spontaneous outflow of radioactivity ($sp_2/sp_1 = 0.67 \pm 0.02$, $n = 8$ versus controls, 0.80 ± 0.02, $n = 10$). The total tissue content of radioactivity at the end of the experiments was not significantly altered in the slices prepared from guinea-pigs treated with befloxatone than from the controls (data not shown).

Assessment of the responsiveness of the terminal 5-HT autoreceptor

In order to assess the sensitivity of the terminal 5-HT autoreceptor following a 21-day treatment with paroxetine or befloxatone, concentration-effect curves were constructed using the potent 5-HT_1 agonist, 5-CT (1–100 nM). In the paroxetine group, there was an attenuation of the capacity of 5-CT to inhibit the electrically evoked release of tritium from preloaded hypothalamic slices, whereas in the befloxatone group there was no difference versus the control groups (Figure 2). These results indicate that the paroxetine, but not the befloxatone treatment, produced a desensitization of the terminal 5-HT autoreceptor in the hypothalamus. However, given the marked inhibition of 5-CT already present at concentrations as low as 1 and 3 nM, another 5-HT autoreceptor agonist, 5-MeOT, was used. 5-MeOT produced a more gradual inhibitory effect of the electrically evoked release of tritium in hypothalamic slices over a concentration-range of three orders of magnitude (Figure 3). In the paroxetine group, there was again an attenuation of the inhibitory effect of 5-MeOT on the electrically evoked release of tritium. This attenuation was greater than that obtained with 5-CT. Consistent with the results obtained with 5-CT, the inhibitory effect of 5-MeOT was unaltered in the befloxatone group. In order to demonstrate further the attenuated function of the terminal 5-HT autoreceptor following the long-term paroxetine treatment, the efficacy of the 5-HT autoreceptor antagonist, methiothepin, was examined in hypothalamic slices prepared from control and treated guinea-pigs. The rationale for this approach was that if indeed the paroxetine, but not the befloxatone, treatment desensitized the 5-HT autoreceptor, then blocking it should produce a smaller effect in the treated group. At a 0.3 μM concentration, methiothepin did in fact produce a lesser enhancement of the evoked release of tritium in hypothalamic slices prepared from the paroxetine-treated guinea-pigs than in those from the control group. ($S_2/S_1 = 2.04 \pm 0.10$, $n = 5$, vs controls 2.52 ± 0.07, $n = 5$). However, in the befloxatone-treated guinea-pigs, the effect of methiothepin was unaltered ($S_2/S_1 = 1.76 \pm 0.15$, $n = 4$, vs controls 1.62 ± 0.08, $n = 5$).

In hippocampal slices, there was a small, albeit significant, attenuation of the inhibitory effect of 5-MeOT on the electrically evoked release of tritium in the paroxetine group, while befloxatone treatment did not have such an effect (Figure 3b). As with hypothalamic slices, the enhancing effect of 0.3 μM methiothepin was significantly less pronounced in the paroxetine group ($S_2/S_1 = 2.11 \pm 0.08$, $n = 10$) than in the control group ($S_2/S_1 = 2.62 \pm 0.21$, $n = 10$). As was also the case for hypothalamic slices, in hippocampal slices prepared from befloxatone-treated guinea-pigs, the enhancing effect of

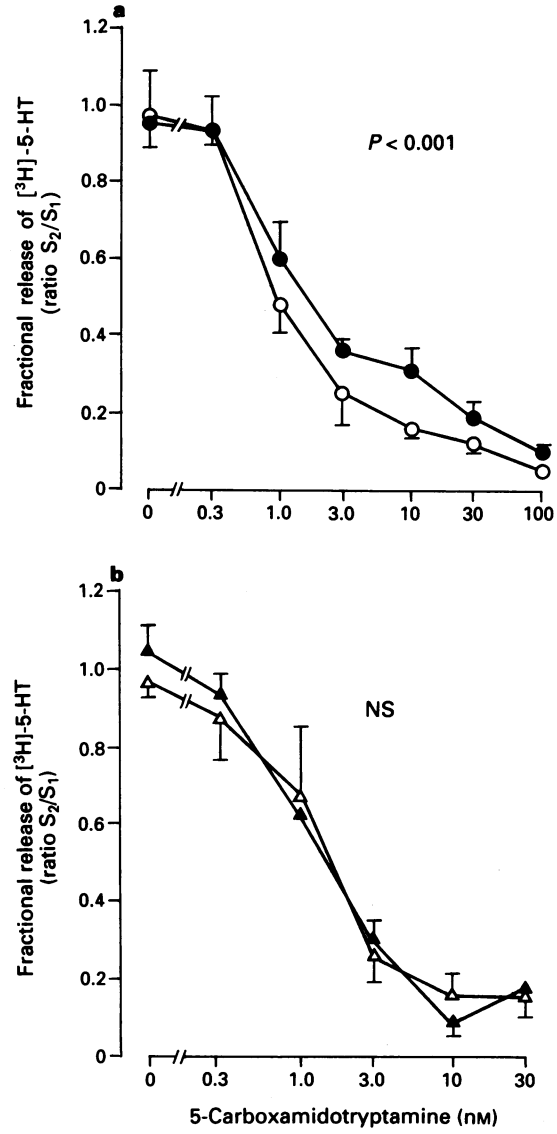


Figure 2 Inhibition produced by the 5-HT autoreceptor agonist 5-carboxamidotryptamine of the evoked release of tritium elicited by electrical stimulation in preloaded hypothalamus slices prepared from control (open symbols) and treated (solid symbols) guinea-pigs with paroxetine (a) or befloxatone (b) for 21 days. The experiments were carried out 48 h after removal of the osmotic minipump used to deliver the drugs. Ordinates: fraction of the total tissue radioactivity released by 360 pulses (30 mA, 2 ms, 3 Hz). Values are expressed as the ratio (S_2/S_1) obtained between the second period of stimulation in the presence of the agonist (S_2) and the first one carried out in the absence of the agonist (S_1). Each point represents the mean ± s.e. of the results obtained with superfusion chambers in the same experiments in pairs of control and treated guinea-pigs. The level of statistical significance, calculated using analysis of variance, between the curves obtained in the control and the treated groups is indicated in the graphs; NS indicates a $P > 0.05$.

0.3 μM methiothepin remained unaltered (control: S_2/S_1 = 2.48 ± 0.20, $n = 5$; befloxatone: $S_2/S_1 = 2.50 \pm 0.20$, $n = 4$).

In frontal cortex slices prepared from paroxetine-treated guinea-pigs, although there was a significant difference in the inhibitory effect of 0.1 μM 5-MeOT on the electrically evoked release of tritium, analysis of the concentration-effect curves did not yield a statistically significant difference between the control and the paroxetine group. As with hypothalamic and hippocampal slices prepared from befloxatone-treated guinea-pigs, the inhibitory effect of 5-MeOT was also unaltered in frontal cortex slices (Figure 3c).

Assessment of the responsiveness of the α_2-adrenoceptor located on 5-HT terminals

Since the inhibition of MAO-A by befloxatone increases brain noradrenaline concentration and since acute 5-HT reuptake blockade attenuates the capacity of the α_2-adreno-

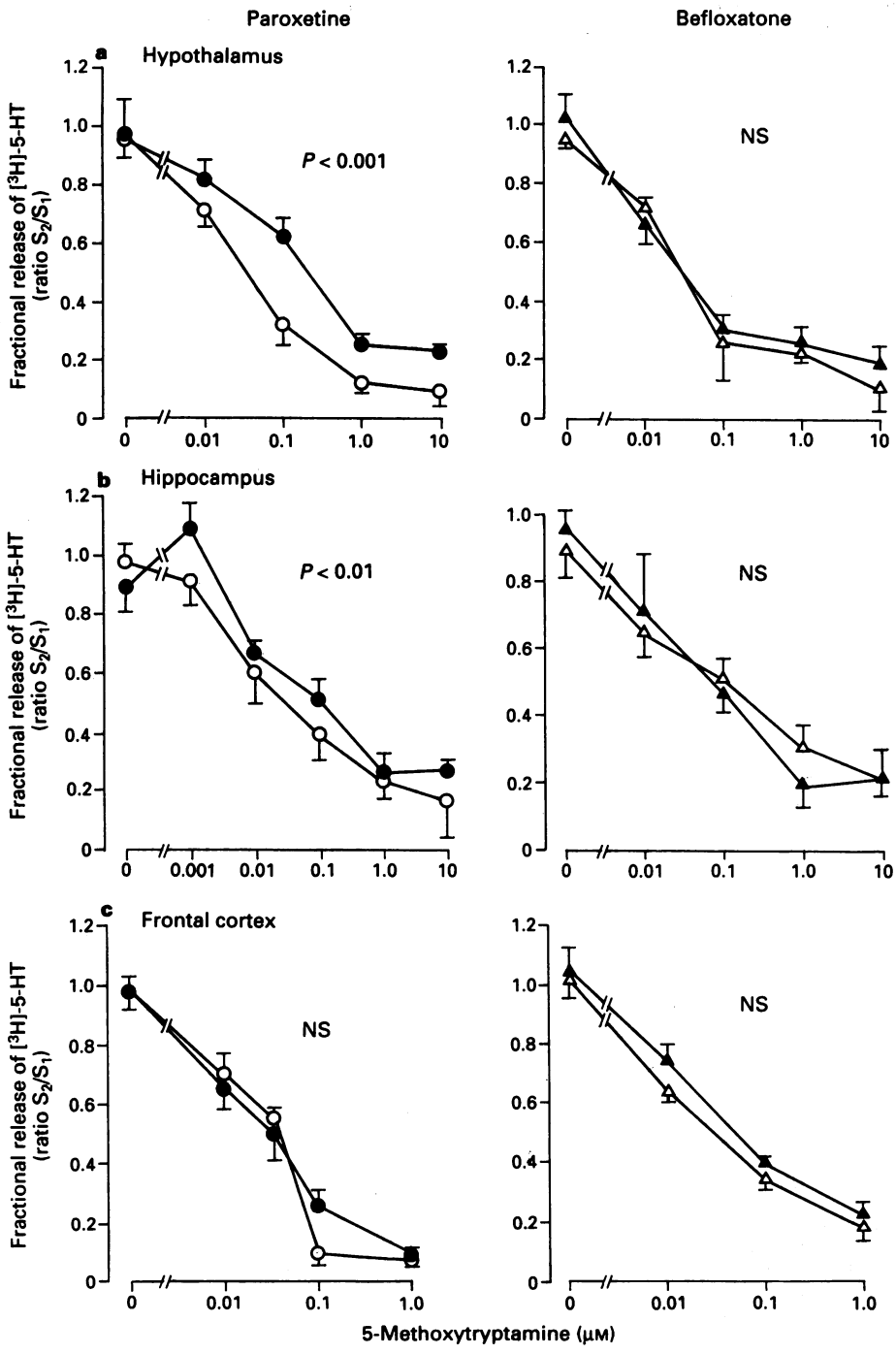


Figure 3 Inhibition produced by the 5-HT autoreceptor agonist, 5-methoxytryptamine, of the evoked release of radioactivity elicited by electrical stimulation in preloaded hypothalamic, hippocampal, and frontal cortex slices prepared from control (open symbols) and treated guinea-pigs (solid symbols) paroxetine or befloxatone for 21 days. The experiments were carried out 48 h after removal of the osmotic minipump used to deliver the drugs. Ordinates: fraction of the total tissue radioactivity released by 360 pulses (20 mA for hypothalamus and 30 mA for hippocampus and frontal cortex slices, 2 ms, 3 Hz). Values are expressed as the ratio (S_2/S_1) obtained between the second period of stimulation in the presence of the agonist (S_2) and the first one carried out in the absence of the agonist (S_1). Each point represents the mean ± s.e. of the results obtained with superfusion chambers in the same experiments in pairs of control and treated guinea-pigs. The level of statistical significance, calculated by analysis of variance, between the control and curves obtained in the treated group is indicated in the graphs; NS indicates a $P > 0.05$.

ceptor to decrease 5-HT release (Blier *et al.*, 1990), it was deemed crucial to examine the sensitivity of the α_2-adrenoceptor following a long-term treatment with drugs which were shown to alter its degree of activation, or its function, when given acutely. In addition, the function of this α_2-adrenoceptor was also examined using the α_2-adrenoceptor antagonist, idazoxan. In hypothalamic slices, the inhibitory effect of the α_2-adrenoceptor agonist, UK 14.304, on the electrically-evoked release of tritium was identical in the control group and in the group treated for 21 days with paroxetine (Figure 4a). In contrast, the inhibitory effect of UK 14.304 was significantly attenuated in the befloxatone group, as was the enhancing effect of a 1 μM concentration of the α_2-adrenoceptor antagonist, idazoxan (Figures 4b and 6). In hippocampal slices, the inhibitory effect of UK 14.304 on the electrically evoked release of tritium was also reduced in the befloxatone group (although statistical significance was not quite reached; Figure 5a), but the enhancing effect of 1 μM idazoxan was similar in both groups (Figure 6). In frontal cortex slices, neither the inhibitory effect of UK 14.304 nor the effect of 1 μM idazoxan was significantly altered by the befloxatone treatment (Figures 6 and 7).

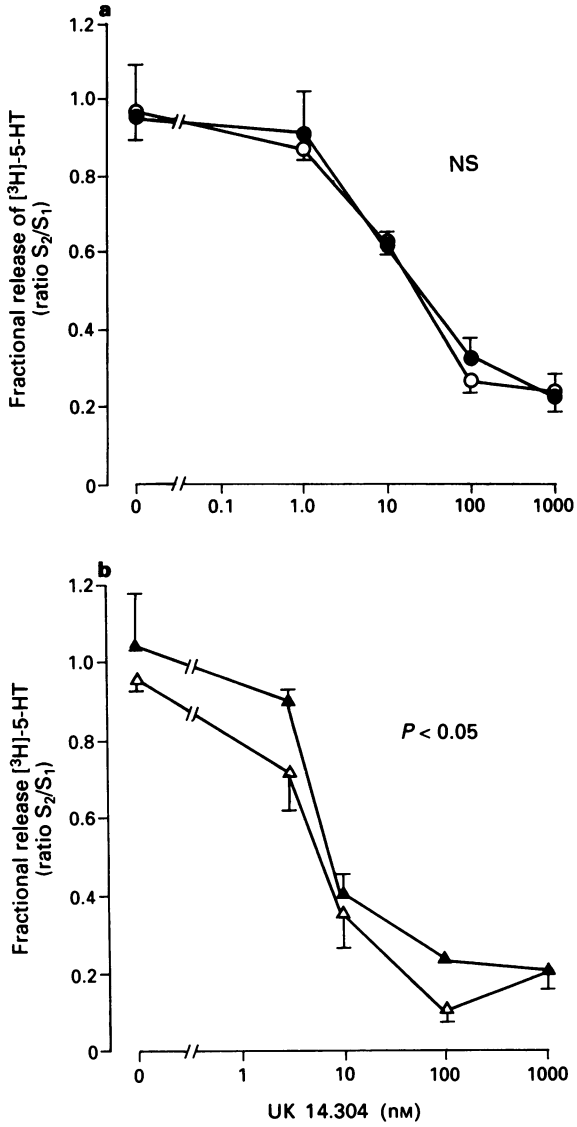


Figure 4 Inhibition produced by the α_2-adrenoceptor agonist, UK 14.304, of the evoked release of radioactivity elicited by electrical stimulations in preloaded hypothalamic slices prepared from control (open symbols) and treated (solid symbols) guinea-pigs with paroxetine (a) or befloxatone (b) for 21 days. The experiments were carried out 48 h after removal of the osmotic minipump used to deliver the drugs. Ordinates: fraction of the total tissue radioactivity released by 360 pulses (30 mA, 2 ms, 3 Hz). Values are expressed as the ratio (S_2/S_1) obtained between the second period of stimulation in the presence of the agonist (S_2) and the first one carried out in the absence of the agonist (S_1). Each point represents the mean ± s.e. of the results obtained with superfusion chambers in the same experiments in pairs of control and treated guinea-pigs. The level of statistical significance, calculated by analysis of variance, between the control and the curves obtained in the treated group is indicated in the graphs; NS indicates a $P > 0.05$.

Assessment of the sensitivity of the α_2-adrenoceptor located on NA terminals following long-term befloxatone administration

Since the long-term befloxatone treatment induced a desensitization of the α_2-adrenoceptor located on 5-HT terminals in the hypothalamus, the sensitivity of the α_2-adrenoceptor on noradrenaline terminals was then investigated in the hypothalamus and hippocampus to determine whether a sustained increase of endogenous NA could also alter the responsiveness of the latter presynaptic α_2-adrenoceptor. The concentration-effect curves of the UK 14.304-induced inhibition of the electrically evoked release of tritium in hippocampal and hypothalamic slices preloaded with [^{3}H]-NA were identical in the control and the befloxatone group (Figure 5b; data not shown for hypothalamic slices). It is noteworthy that in hippocampal slices, the evoked release of tritium and the spontaneous outflow of radioactivity were significantly enhanced in four pairs of controls and befloxatone-treated guinea-pigs (control: $S_1 = 1.56 \pm 0.06\%$, befloxatone: $S_1 = 1.92 \pm 0.16\%$; control: $sp_1 = 0.80 \pm 0.05\%$, befloxatone: $sp_1 = 0.98 \pm 0.05\%$) and the tissue content of radioactivity decreased (control: 108 ± 6 nCi, befloxatone: 86 ± 4 nCi). In hypothalamic slices, none of these parameters were significantly altered (data not shown).

Determination of [^{3}H]-5-HT uptake and of the function of the 5-HT transporter

Using a final concentration of 20 nM [^{3}H]-5-HT for incubation, uptake was determined in control and paroxetine-treated guinea-pigs. Following a 2-day treatment with paroxetine, [^{3}H]-5-HT uptake was inhibited by approximately 50% in hypothalamic and frontal slices, with the minipump delivering the drug at the time the guinea-pigs were killed, when compared to control slices processed in parallel in the same experiments (Figure 8). There was still a significant attenuation of the degree of [^{3}H]-5-HT uptake in hypothalamic slices after the 21-day paroxetine treatment when the animals were killed with the minipump in place, but it was smaller than that observed after the 2-day treatment. This could be attributable, in part, to the fact that the guinea-pigs received more than 10 mg kg^{-1} day^{-1} of paroxetine at the beginning of the treatment and less at the end of the 21-day period since the dose was based on the mean weight of the animal during this period. The decreasing dose of paroxetine that the guinea-pigs were receiving during the 21-day treatment could not, however, explain the lack of significant inhibition of [^{3}H]-5-HT uptake in frontal cortex (Figure 8). Furthermore, the [^{3}H]-5-HT uptake values obtained after the 21-day treatment with paroxetine were nearly identical whether or not the pump was in the animal delivering the drug (Figure 8). These results suggest that the 5-HT transporter had desensitized during the 21-day treatment, at least in the frontal cortex, as previously described in the rat brain subjected to the same treatment (Piñeyro *et al.*, 1994). In these previous experiments, the desensitization of the transporter was evidenced by incubating the slices with a 100 nM, but not with a 20 or a 5 nM concentration of [^{3}H]-5-HT after a 48 h washout period. This was probably attributable to the 5-HT transporters being more saturated at the 100 nM concentration. Under the latter condition in the present experiments, there was a significant inhibition of the uptake of [^{3}H]-5-HT

(23 ± 4%, $P = 0.002$) in frontal cortex slices prepared from five paroxetine-treated guinea-pigs (after a 48 h washout period) when compared to five controls processed at the same time.

In a final series of experiments, the effect of 1 μM paroxetine on the evoked release of [^{3}H]-5-HT was examined in frontal cortex slices to provide further functional evidence for the attenuated efficacy of the 5-HT transporter. The enhancing effect of paroxetine, introduced 20 min before S_2, was significantly attenuated in the paroxetine group (S_2/S_1 = 1.12 ± 0.07, $n = 10$) when compared to the controls (S_2/S_1 = 1.46 ± 0.11, $n = 15$). In contrast, 1 μM paroxetine altered the S_2/S_1 ratios in hypothalamic slices neither in the control

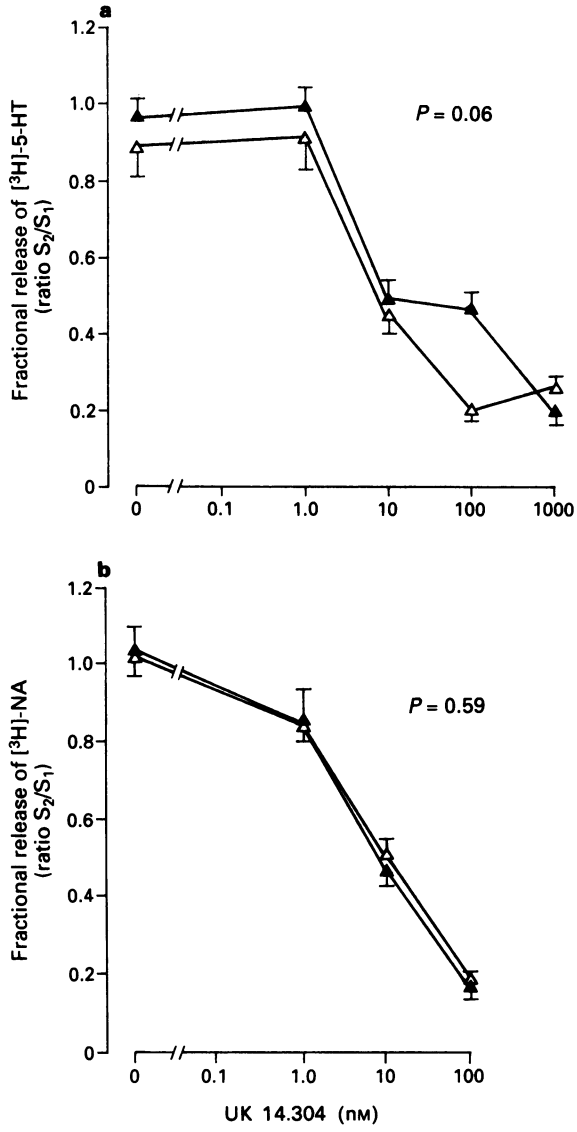


Figure 5 Inhibition produced by the α_2-adrenoceptor agonist, UK 14.304, of the evoked release of radioactivity elicited by electrical stimulations in hippocampal slices preloaded with either [^{3}H]-5-HT (a) or [^{3}H]-noradrenaline ([^{3}H]-NA) (b) in controls (Δ) and guinea-pigs treated with befloxatone for 21 days (▲). The experiments were carried out 48 h after removal of the osmotic minipump used to deliver the drugs. Ordinates: fraction of the total tissue radioactivity released by 360 pulses (30 mA, 2 ms, 3 Hz). Values are expressed as the ratio (S_2/S_1) obtained between the second period of stimulation in the presence of the agonist (S_2) and the first one carried out in the absence of the agonist (S_1). Each point represents the mean ± s.e. of the results obtained with superfusion chambers in the same experiments in pairs of control and befloxatone-treated guinea-pigs. The level of statistical significance, calculated by analysis of variance, between the control and the curves obtained in the treated group is indicated in the graphs.

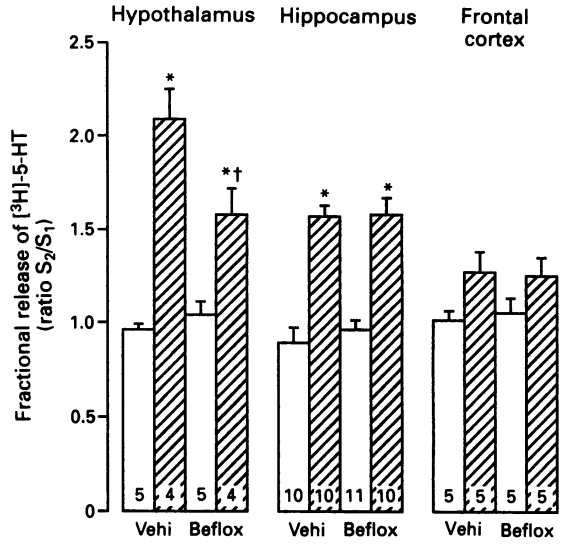


Figure 6 Effect of the α_2-adrenoceptor antagonist, idazoxan, on the evoked release of radioactivity elicited by electrical stimulations in preloaded hypothalamic hippocampal, and frontal cortex slices prepared from control and treated guinea-pigs with befloxatone for 21 days. The experiments were carried out 48 h after removal of the osmotic minipump used to deliver the drug. Open columns, control; hatched columns, idazoxan, 1 μM before S_2. Ordinates: fraction of the total tissue radioactivity released by 360 pulses (30 mA, 2 ms, 3 Hz). Values are expressed as the ratio (S_2/S_1) obtained between the second period of stimulation in the presence of the antagonist (S_2) and the first one carried out in the absence of the antagonist (S_1). Values are expressed as mean ± s.e. of the results obtained in the same experiments with control and treated guinea-pigs. *$P < 0.05$ when compared with the corresponding control value; †$P < 0.05$ when compared to the value obtained with idazoxan in the control group.

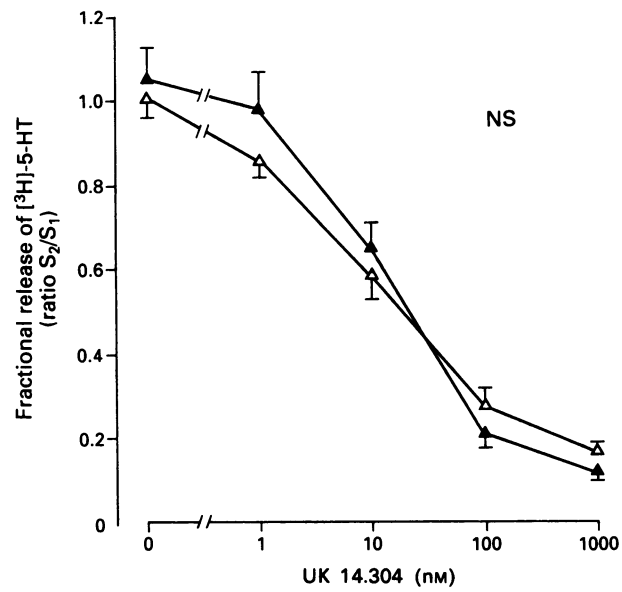


Figure 7 Inhibition produced by the α_2-adrenoceptor agonist, UK 14.304, of the evoked release of radioactivity elicited by electrical stimulations in preloaded frontal cortex slices prepared from control (Δ) and treated guinea-pigs (▲) with befloxatone for 21 days. The experiments were carried out 48 h after removal of the osmotic minipump used to deliver the drugs. Ordinates: fraction of the total tissue radioactivity released by 360 pulses (30 mA, 2 ms, 3 Hz). Values are expressed as the ratio (S_2/S_1) obtained between the second period of stimulation in the presence of the agonist (S_2) and the first one carried out in the absence of the agonist (S_1). Each point represents the mean ± s.e. of the results obtained with superfusion chambers in the same experiments with control and treated guinea-pigs. The level of statistical significance, calculated by analysis of variance, between the control and the curves obtained in the treated group is indicated in the graphs; NS indicates a $P > 0.05$.

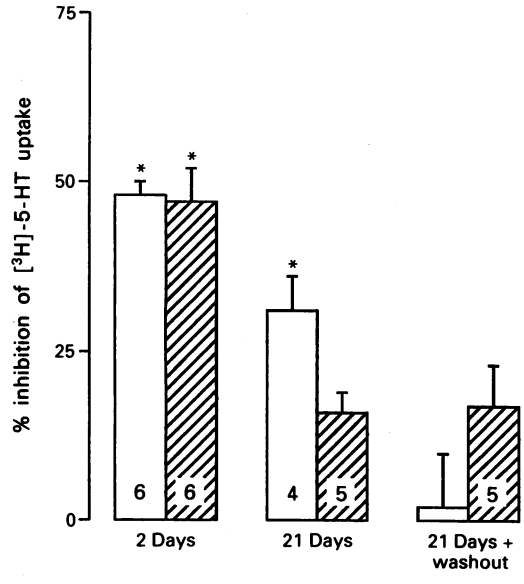


Figure 8 Inhibition of [^{3}H]-5-HT uptake in hypothalamus (open columns) and frontal cortex (hatched columns) slices of guinea-pigs during and following the administration of the 5-HT reuptake blocker, paroxetine. Paroxetine was administered via an osmotic minipump implanted subcutaneously which delivered 10 mg kg^{-1} day^{-1}. Inhibition of [^{3}H]-5-HT uptake was determined by incubating the slices with 20 nM [^{3}H]-5-HT for 3 min. The percentage inhibition was calculated by comparing the tissue/medium ratios of radioactivity in the control and the treated groups. The figures given in the histograms refer to the number of pairs of guinea-pigs studied: a control and a treated one done in quintuplets. Five pairs were tested in the 21 days + washout condition for the hypothalamus. The washout period consisted of removing the minipump for 48 h prior the experiment. *$P<0.05$, when compared to the tissue-medium ratios obtained in the controls processed in parallel in the same experiments.

(0.97 ± 0.12, $n = 4$) nor in the paroxetine group (0.95 ± 0.06, $n = 5$).

Assessment of the sensitivity of the 5-HT$_3$ receptor which enhances the evoked release of 5-HT

The 5-HT$_3$ receptors which modulate 5-HT release desensitize rapidly *in vitro* (Galzin & Langer, 1991; Blier & Bouchard, 1993). The sensitivity of the latter receptors was therefore also studied following long-term treatment with paroxetine and befloxatone. As previously reported by Galzin & Langer (1991) and our group (Blier & Bouchard, 1993), the 5-HT$_3$ receptor agonist, 2-methyl-5-HT, produced a concentration-dependent increase of the electrically-evoked release of tritium in the hypothalamic, hippocampal and frontal cortex slices prepared from control guinea-pigs (Figure 9). In slices prepared from paroxetine-treated guinea-pigs following a 48 h wash-out period, there was a significant attenuation of the enhancing effect of 2-methyl-5-HT on the evoked release of tritium in all three brain regions (Figure 9). In order to determine whether this desensitization induced by paroxetine supervenes only following long-term 5-HT reuptake blockade, the effect of 2-methyl-5-HT was studied in frontal cortex slices prepared from guinea-pigs treated for 2 days with paroxetine, also following a 48-h washout period: the enhancing effect of 2-methyl-5-HT was unchanged (Figure 10). In contrast with the results obtained with the 21-day treatment with paroxetine, the enhancing effect of 2-methyl-5-HT was unaltered following a 21-day treatment with befloxatone (Figure 9). Given the unmodified responsiveness of this 5-HT$_3$ receptor in befloxatone-treated animals, we then assessed whether an enhanced activation of this receptor could contribute in frontal cortex slices to the enhanced [^{3}H]-5-HT release consistently observed in the befloxatone group. To this end, the 5-HT$_3$ antagonist S-zacopride (0.1 μM) was superfused, starting 8 min before S_2. In the control as well as in the befloxatone group, this antagonist did not significantly alter [^{3}H]-5-HT release (control: $S_2/S_1 = 1.11 \pm 0.06$, $n = 5$; befloxatone: $S_2/S_1 = 1.11 \pm 0.09$, $n = 5$), thus indicating that under these *in vitro* conditions, this 5-HT$_3$ receptor is not tonically activated.

Discussion

The results of the present study indicate that long-term 5-HT reuptake blockade and type A-MAO inhibition lead to enhanced 5-HT release (Figure 1). In the case of paroxetine, this effect appears to be due to an attenuation of the capacity of the terminal 5-HT autoreceptor to inhibit 5-HT release in the hypothalamus and hippocampus. This is suggested by the lesser effectiveness of the 5-HT autoreceptor antagonist, methiothepin, to increase [^{3}H]-5-HT release and by the attenuation of the inhibitory effect of the 5-HT receptor agonist, 5-MeOT (Figure 3), following a long-term paroxetine treatment. It is conceivable that the attenuated effect of 5-MeOT might have been due to competition of this exogenous agonist with endogenous 5-HT, the availability of which was increased by the paroxetine treatment. However, 5-HT release was enhanced to a similar level in the befloxatone group in the hypothalamic and hippocampal slices and yet, the effectiveness of 5-MeOT was not altered following the befloxatone treatment (Figures 1 and 3). This desensitization of the terminal 5-HT autoreceptor in the guinea-pig hypothalamus is fully consistent with that observed in the study of Moret & Briley (1990a) using the same *in vitro* methodology in hypothalamic slices prepared from rats treated with the SSRI, citalopram. Similarly, previous results obtained using *in vivo* electrophysiological techniques in our laboratory indicated the capacity of the terminal 5-HT autoreceptor to desensitize in the rat hippocampus following a 2 to 3 week treatment with SSRI, including paroxetine (Chaput *et al.*, 1986; 1991; Blier *et al.*, 1988). Taken together, these results show that the terminal 5-HT autoreceptor in the hypothalamus and hippocampus, whether it be of the 5-HT$_{1B}$ subtype in the rat brain or of the 5-HT$_{1D}$ subtype in the guinea-pig brain, desensitizes following long-term 5-HT reuptake blockade.

In frontal cortex slices, however, the evoked [^{3}H]-5-HT release was increased despite the absence of a desensitization of the terminal 5-HT autoreceptor (Figures 1 and 3). The most likely explanation for this enhanced release is a down-regulation of the 5-HT transporter (Figure 8). Indeed, it has been reported that following a 21-day treatment with paroxetine, there was a 60% decrease in the B_{max} value for the 5-HT transporter in the rat frontal cortex, using [^{3}H]-paroxetine as a ligand, after a 48 h washout period (Piñeyro *et al.*, 1994). This decrease in the density of [^{3}H]-5-HT uptake sites could be attributed to a decrease in their mRNA level as documented by Lesch *et al.* (1993). Since, in the present experiments the addition of 1 μM paroxetine in the superfusate did not increase the electrically evoked release of tritium in frontal cortex slices in the paroxetine, it may be assumed that a decreased number of 5-HT transporter sites was the underlying cause of the 31% increase in [^{3}H]-5-HT release (Figure 1c). This, raises the possibility that such a down-regulation of the 5-HT transporter may have contributed to the enhancement of the electrically evoked [^{3}H]-5-HT release observed in hypothalamic and hippocampal slices following the long-term treatment. In the guinea-pig and rat hypothalamus, a complete blockade of 5-HT reuptake does not alter the evoked release of [^{3}H]-5-HT (Passarelli *et al.*, 1987; Blier & Bouchard, 1993; present results). It may thus be concluded that this enhanced 5-HT release in the hypothalamus was entirely attributable to the desensitization of the 5-HT autoreceptor. In the hippocampus, however,

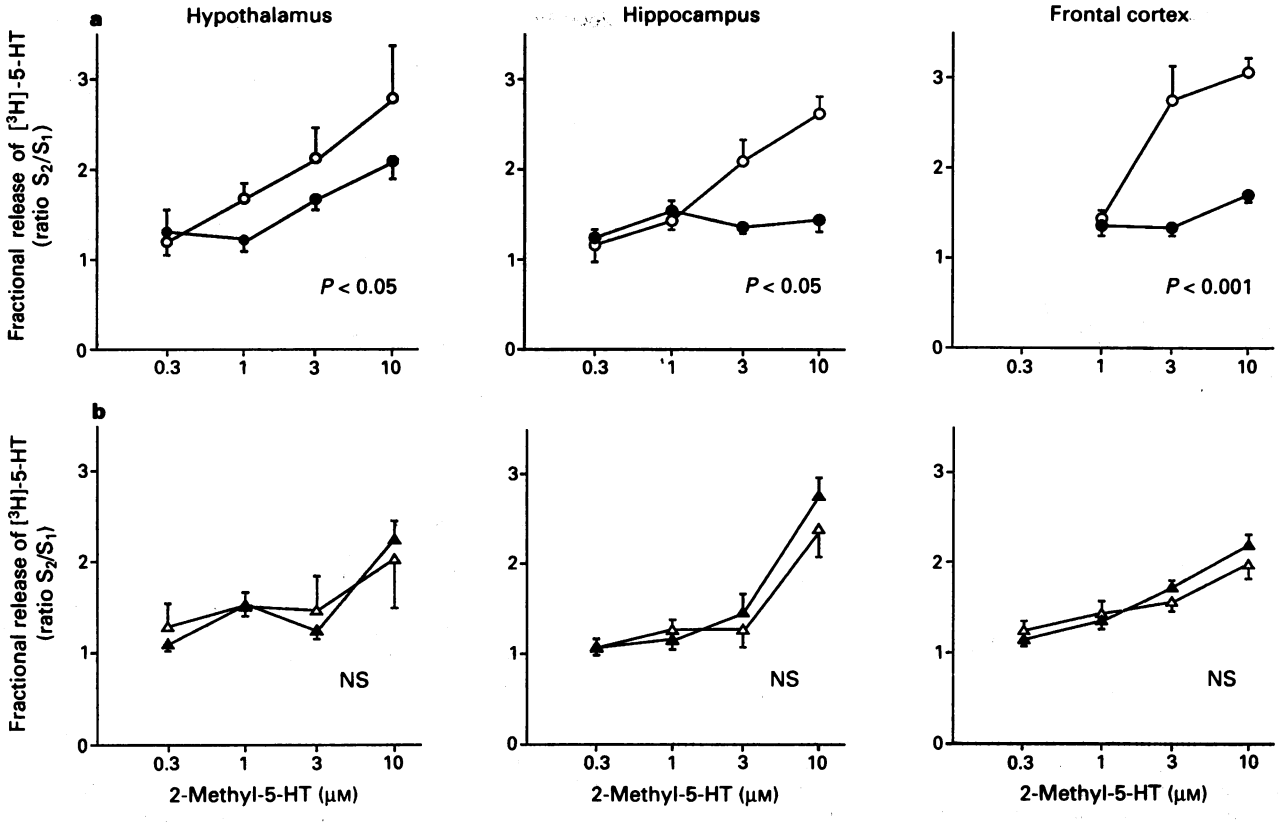


Figure 9 Enhancement produced by the 5-HT_3 receptor agonist, 2-methyl-5-HT, of the evoked release of radioactivity elicited by electrical stimulations in preloaded hypothalamic, hippocampal, and frontal cortex slices prepared from control (open symbols) and treated guinea-pig (filled symbols) with paroxetine (a) or befloxatone (b) for 21 days. The experiments were carried out 48 h after removal of the osmotic minipump used to deliver the drugs. Ordinates: fraction of the total tissue radioactivity release by 360 pulses (20 mA for hypothalamus and 30 mA for hippocampus and frontal cortex slices, 2 ms, 3 Hz). Values are expressed as the ratio (S_2/S_1) obtained between the second period of stimulation in the presence of the agonist introduced 8 min before S_2 and the first one carried out in the absence of the agonist (S_1). Each point represents the mean ± s.e. of the results obtained with superfusion chambers in the same experiments with control and treated guinea-pigs. The level of statistical significance, calculated by analysis of variance, between the control and the curves obtained in the treated group is indicated in the graphs; NS indicates a $P > 0.05$.

5-HT reuptake blockade does lead to enhanced [^{3}H]-5-HT collected in the superfusate (Blier & Bouchard, 1993). Therefore, based on this acute effect of paroxetine and on the down-regulation of the 5-HT transporter reported in the rat hippocampus following long-term paroxetine administration (Piñeyro *et al.*, 1994), the contribution of such an alteration of the 5-HT transporter to the enhancement of [^{3}H]-5-HT release observed in this brain region cannot be ruled out. It is noteworthy that an upregulation of the 5-HT reuptake sites was recently reported to occur in the rat brain following long-term fluoxetine administration (Hrdina & Vene, 1993). However, these results were obtained with a single concentration of [^{3}H]-paroxetine.

In the case of the befloxatone treatment, the enhanced [^{3}H]-5-HT release after a 48-h washout period is not likely to result from residual inhibition of MAO-A activity since the activity of the enzyme is back to normal 24 h after a supramaximal dose of befloxatone (Curet *et al.*, 1992), consistent with the fact that endogenous 5-HT levels in the rat brain return to normal within 24 h after a supramaximal dose of befloxatone (Curet *et al.*, 1992), and that the content of tritium in the slices prepared from the treated and control guinea-pigs remained unaltered (present study). In the hypothalamus and the hippocampus, the enhancement of the evoked release of [^{3}H]-5-HT was possibly due to a desensitization of the α_2-adrenoceptor on 5-HT terminals, as previously documented in the rat hippocampus (Mongeau *et al.*, 1994). Indeed, when maximally activated by the α_2-adrenoceptor agonist UK 14.304, this presynaptic receptor produces the same degree of inhibition (> 80%) of the electrically-evoked release of [^{3}H]-5-HT as that mediated by the 5-HT autoreceptor (Figures 1, 2 and 5), consistent with previous results obtained in the rat brain (Blier & de Montigny, 1994). Furthermore, since the α_2-adrenoceptor antagonist, idazoxan, enhances the electrically evoked release of [^{3}H]-5-HT, this α_2-heteroreceptor appears to be tonically activated in the guinea-pig brain as also appears to be the case in the rat and the human brain (Raiteri *et al.*, 1990; Galzin *et al.*, 1992; Feuerstein *et al.*, 1993; Mongeau *et al.*, 1993). The possibility that, in the hypothalamus, the α_2-heteroreceptor plays a significant role in the enhancement of [^{3}H]-5-HT release in the befloxatone group is further supported by the observation that the α_2-adrenoceptor antagonist, idazoxan, exerted a smaller enhancing effect on the evoked release of [^{3}H]-5-HT from slices prepared from befloxatone-treated guinea-pigs.

In frontal cortex slices, however, neither the inhibitory effect of UK 14.304 nor the enhancing effect of idazoxan was significantly altered following the befloxatone treatment (Figures 6 and 7). Yet, the electrically evoked release of [^{3}H]-5-HT was enhanced to the same degree (30%) as in the hypothalamic slices. Taken together, these results suggest that 48 h following a 21-day treatment with befloxatone, the releasable pool of 5-HT may still be enhanced despite the total concentration of 5-HT in the brain being back to normal. It is interesting to note that the degree of enhancement of [^{3}H]-5-HT release was smaller in the hippocampus (+ 18%) than in the hypothalamus (+ 30%). This could well result from a greater inhibitory tonus by endogenous and tritiated noradrenaline on the α_2-adrenoceptors on 5-HT

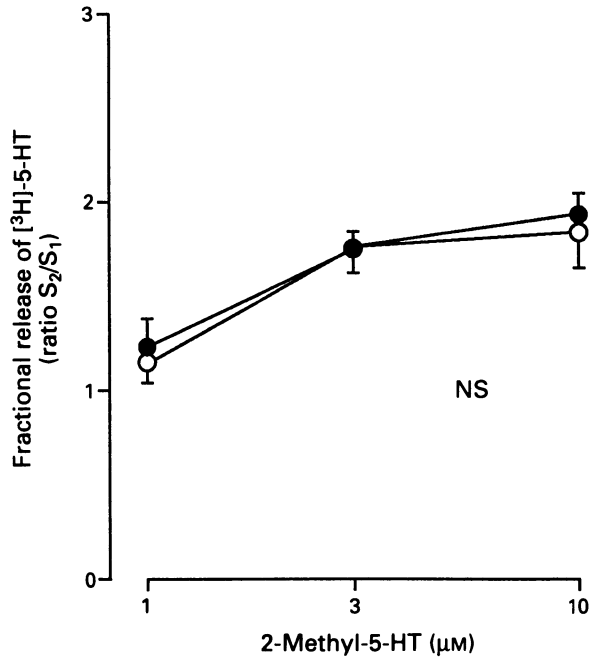


Figure 10 Enhancement produced by the 5-HT_3 receptor agonist, 2-methyl-5-HT, of the evoked release of radioactivity elicited by electrical stimulations in frontal cortex slices prepared from control (○) and treated guinea-pigs (●) with paroxetine for 2 days. The experiments were carried out 48 h after removal of the osmotic minipump used to deliver the drug. Ordinates: fraction of the total tissue radioactivity release by 360 pulses (30 mA, 2 ms, 3 Hz). Values are expressed as the ratio (S_2/S_1) obtained between the second period of stimulation in the presence of the agonist introduced 8 min before S_2 and the first one carried out in the absence of the agonist (S_1). Each point represents the mean ± s.e. of the results obtained with chambers in the same experiments with control and treated guinea-pigs. The level of statistical significance, calculated by analysis of variance, between the control and the curves obtained in the treated animals is indicated in the graphs; NS indicates a $P>0.05$.

terminals in the hippocampus than in the hypothalamus as suggested by the observation that the electrically evoked release of [^{3}H]-noradrenaline was enhanced in the former but not in the latter structure. This enhanced [^{3}H]-noradrenaline release could also explain why the enhancing effect of idazoxan on [^{3}H]-5-HT release was not attenuated in hippocampal slices prepared from befloxatone-treated guinea-pigs, and also the clear trend toward a desensitization of the α_2-adrenoceptor on 5-HT terminals. Indeed, it is expected that, through α_2-autoreceptor antagonism, idazoxan further enhanced noradrenaline release thus resulting in an increased activation of α_2-adrenoceptor on 5-HT terminals in the hippocampus.

Following long-term MAO-A inhibition, the α_2-adrenoceptor on 5-HT terminals was desensitized in the hypothalamus whereas, in the same structure, the α_2-autoreceptor remained normosensitive. It seems that the terminal 5-HT autoreceptor also would not desensitize as a consequence of sustained agonist occupation because long-term administration of befloxatone did not produce this adaptative phenomenon. Since the paroxetine treatment induced a desensitization of the 5-HT autoreceptor, it is nevertheless possible that these two drugs do not alter the concentration of 5-HT in the biophase of the 5-HT autoreceptor to the same extent. Another possibility to account for this differential adaptive capacity would be that sustained blockade of the 5-HT transporter results in an alteration of signal transduction from the 5-HT autoreceptor sites.

The results of this study indicate that the 5-HT_3 receptors which enhance [^{3}H]-5-HT release were desensitized following the paroxetine, but not the befloxatone, treatment (Figure 9). Since it was demonstrated that this receptor is not located on 5-HT terminals at least in the hypothalamus (Blier *et al.*, 1993), it is unlikely that this desensitization resulted from a functional interaction between the 5-HT transporter and this 5-HT_3 receptor. Rather, it appears that 5-HT reuptake blockade and MAO-A inhibition do not alter the level of 5-HT to the same degree in the biophase of this 5-HT_3 receptor. Since this receptor exerts a positive feedback role on 5-HT release and since it is desensitized following long-term paroxetine administration, it cannot contribute to the enhancement of [^{3}H]-5-HT release observed in this treatment group. 5-HT_3 receptors, in the area postrema and/or on vagal afferents, are believed to mediate nausea and emesis following administration of chemotherapeutic agents because these side effects can be blocked with selective 5-HT_3 antagonists. Since 5-HT reuptake blockers can enhance the availability of 5-HT at all 5-HT receptor subtypes, it is thus possible that the nausea they often produce is the result of enhanced activation of 5-HT_3 receptors. In support of this possibility, we have recently provided evidence that the nausea produced by the administration of SSRI in man can be blocked by cisapride (Bergeron & Blier, 1994), a benzamide derivative with moderate affinity for 5-HT_3 receptors, which blocks the enhancement of the electrically evoked release of [^{3}H]-5-HT produced by 2-methyl-5-HT in preloaded slices of the guinea-pig brain. If the 5-HT_3 receptors which mediate nausea and emesis had characteristics similar to those which can modulate 5-HT release, then their desensitization observed after the 21-day, but not the 2-day, treatment with paroxetine could explain the well-known disappearance of nausea following prolongation of a treatment with SSRI in man.

In conclusion, long-term 5-HT reuptake blockade leads to an enhancement of the evoked [^{3}H]-5-HT release which can be attributable, at least in the hypothalamus and hippocampus, to a desensitization of the terminal 5-HT_{1D} autoreceptor. It can be presumed that in depressed patients, long-term administration of an SSRI also produces a desensitization of the terminal 5-HT_{1D} autoreceptor and results in an enhanced 5-HT release. The possibility that the ensuing increased 5-HT neurotransmission is responsible for the antidepressant response is supported by the reappearance of depressive symptoms observed after tryptophan depletion in patients successfully treated with the SSRI fluvoxamine or fluoxetine (Delgado *et al.*, 1990; 1992). In the frontal cortex, other factors such as the down-regulation of the 5-HT transporter may account for this enhanced release. Inhibition of type-A MAO also produces an enhancement of the evoked [^{3}H]-5-HT release which could result from a desensitization of α_2-heteroreceptors, at least in the hypothalamus. Other factors, such as the increase in the releasable pool of 5-HT, may also contribute to this effect of MAOI. Again it can be presumed that an enhancement of 5-HT neurotransmission is important in the therapeutic response produced by MAOI in depressed patients because tryptophan depletion, as well as 5-HT synthesis inhibition, produced a rapid relapse in remitted patients treated with an MAOI (Shopsin *et al.*, 1976; Delgado *et al.*, 1990).

Supported by the Medical Research Council of Canada Grant no. MA-11014 and Scholarship to P.B., the Fonds de la Recherche en Santé du Québec, and Centre de Recherche Delalande. We would like to thank T. Vo and L. Caillé for their help with the statistical analyses, and H. Cameron for secretarial assistance.

References

AZZARO, A.J., KING, J., KOTZUK, J., SCHOEPP, D.D., FROST, J. & SCHOCHET, S. (1985). Guinea pig striatum as a model of human dopamine distribution: the role of monoamine oxidase isozyme ratio, localization and affinity for substrate in synaptic dopamine metabolism. *J. Neurochem.*, **45**, 949–956.

BAUMANN, P.A. & WALDMEIER, P.C. (1981). Further evidence for negative feedback control of serotonin release in the central nervous system. *Naunyn-Schmied. Arch. Pharmacol.*, **317**, 36–43.

BERGERON, R. & BLIER, P. (1994). Cisapride for the treatment of nausea produced by selective serotonin reuptake inhibitors. *Am. J. Psychiat.*, **151**, 1084–1086.

BLIER, P. & BOUCHARD, C. (1993). Functional characterization of a 5-HT_3 receptor which modulates the release of 5-HT in the guinea-pig brain. *Br. J. Pharmacol.*, **108**, 13–22.

BLIER, P., CHAPUT, Y. & DE MONTIGNY, C. (1988). Long-term 5-HT reuptake blockade, but not monoamine oxidase inhibition, decreases the function of terminal 5-HT autoreceptors: an electrophysiological study in the rat brain. *Naunyn-Schmied. Arch. Pharmacol.*, **337**, 246–254.

BLIER, P. & DE MONTIGNY, C. (1994). Current advances and trends in the treatment of depression. *Trends Pharmacol. Sci.*, **15**, 220–226.

BLIER, P., GALZIN, A.-M. & LANGER, S.Z. (1990). Interaction between serotonin uptake inhibitors and alpha-2 adrenergic heteroreceptors in the rat hypothalamus. *J. Pharmacol. Exp. Ther.*, **254**, 236–244.

BLIER, P., MONROE, P.J., BOUCHARD, C., SMITH, D.C. & SMITH, D.J. (1993). 5-HT_3 receptors which modulate [^{3}H]-5-HT release in the guinea pig hypothalamus are not autoreceptors. *Synapse*, **15**, 143–148.

CHAPUT, Y., DE MONTIGNY, C. & BLIER, P. (1986). Effects of a selective 5-HT reuptake blocker, citalopram, on the sensitivity of 5-HT autoreceptors: electrophysiological studies in the rat. *Naunyn-Schmied. Arch. Pharmacol.*, **33**, 342–349.

CHAPUT, Y., DE MONTIGNY, C. & BLIER, P. (1991). Pre- and post-synaptic modifications of the serotonin system by long-term administration of antidepressant treatments: an *in vivo* electrophysiological study in the rat. *Neuropsychopharmacol.*, **5**, 219–229.

CURET, O., DAMOISEAU, G. & AUBIN, N. (1992). Biochemical profile of befloxatone, a new reversible MAO-A inhibitor. *Clin. Neuropharmacol.*, **15** (Suppl. 1B), 424.

DE MONTIGNY, C. & AGHAJANIAN, G.K. (1978). Tricyclic antidepressants: long-term treatment increases responsitivity of rat forebrain neurons to serotonin. *Science*, **202**, 1303–1306.

DELGADO, P.L., CHARNEY, D.S., PRICE, L.H., AGHAJANIAN, G.K., LANDIS, H. & HENINGER, G.R. (1990). Serotonin function and the mechanism of antidepressant action: reversal of antidepressant-induced remission by rapid depletion of plasma tryptophan. *Arch. Gen. Psychiatry*, **47**, 411–418.

DELGADO, P.L., MILLER, H.L., SALOMON, R.M., LICINIO, J., PRICE, L.H., HENINGER, G.R. & CHARNEY, D.S. (1992). The mechanism of antidepressant action in depression. *Soc. Neurosci.*, Abst 18, p. 727.

FEUERSTEIN, T.J., MUTSCHLER, A., LUPP, A., VAN VILTHOVEN, V., SCHLICKER, E. & GÖTHERT, M. (1993). Endogenous noradrenaline activates α_2-adrenoceptors on serotonergic nerve endings in human and rat neocortex. *J. Neurochem.*, **61**, 474–480.

GALZIN, A.M. & LANGER, S.Z. (1991). Modulation of 5-HT release by presynaptic inhibitory and facilitatory 5-HT receptors in brain slices. *Adv. Biosci.*, **82**, 59–62.

GALZIN, A.M., POIRIER, M.F., LISTA, A., CHODKIEWIECZ, J.P., BLIER, P., RAMDINE, R., LOO, H., ROUX, F.X., REDONDO, A. & LANGER, S.Z. (1992). Characterization of the 5-hydroxytryptamine autoreceptor modulating the release of [^{3}H]-5-hydroxytryptamine in slices of the human neocortex. *J. Neurochem.*, **59**, 1293–1301.

HRDINA, P.D. & VENE, T.B. (1993). Chronic fluoxetine treatment upregulates 5-HT uptake sites and 5-HT_2 receptors in rat brain: an autoradiographic study. *Synapse*, **14**, 324–331.

HOYER, D. & MIDDLEMISS, D.K. (1989). The pharmacology of terminal 5-HT autoreceptors in mammalian brain: evidence for species differences. *Trends Pharmacol. Sci.*, **10**, 130–132.

JACOBS, B.L. (1986). Single unit activity of brain monoamine-containing neurons in freely moving animals. *N.Y. Acad. Sci.*, **473**, 70–77.

LESCH, K.P., AUKLAKH, C.S., WOLOZIN, B.J., TOLLIVER, T.J., HILL, J.L. & MURPHY, D.L. (1993). Regional brain expression of serotonin transporter mRNA and its regulation by reuptake inhibiting antidepressants. *Mol. Brain Res.*, **17**, 31–35.

MENKES, D.B. & AGHAJANIAN, G.K. (1981). α_1-Adrenoceptor-mediated responses in the lateral geniculate nucleus are enhanced by chronic antidepressant treatment. *Eur. J. Pharmacol.*, **74**, 27–35.

MENKES, D.B., AGHAJANIAN, G.K. & MCCALL, R.B. (1980). Chronic antidepressant treatment enhances α-adrenergic and serotonergic responses in the facial nucleus. *Life Sci.*, **27**, 45–55.

MONGEAU, R., BLIER, P. & DE MONTIGNY, C. (1993). *In vivo* electrophysiological evidence for a tonic inhibitory action of endogenous norepinephrine on α_2-adrenergic heteroreceptors on 5-hydroxytryptamine terminals in the rat hippocampus. *Naunyn Schmied. Arch. Pharmacol.*, **347**, 266–272.

MONGEAU, R., DE MONTIGNY, C. & BLIER, P. (1994). Electrophysiological evidence for desensitization of α_2-adrenoceptors on 5-HT terminals following long-term treatment with drugs that increase noradrenaline synaptic availability. *Neuropsychopharmacol.*, **10**, 41–51.

MORET, C. & BRILEY, M. (1990a). Serotonin autoreceptor subsensitivity and antidepressant activity. *Eur. J. Pharmacol.*, **180**, 351–356.

MORET, C. & BRILEY, M. (1990b). Modulation by drugs of the release of total tritium and ^{3}H5-HT from rat hypothalamic slices. *Naunyn-Schmied. Arch. Pharmacol.*, **341**, 398–403.

PASSARELLI, F., GALZIN, A.-M. & LANGER, S.Z. (1987). Interaction between neuronal uptake inhibitors and presynaptic serotonin autoreceptors in rat hypothalamic slices: comparison of K^+ and electrical depolarization. *J. Pharmacol. Exp. Ther.*, **242**, 1056–1063.

PIÑEYRO, G., BLIER, P., DENNIS, T. & DE MONTIGNY, C. (1994). Desensitization of the neuronal 5-HT reuptake carrier following its long-term blockade. *J. Neurosci.*, **14**, 3036–3047.

RAITERI, M., MAURA, G., FOLGHERA, S., CAVAZZANI, P., ANDRIOLI, G.C., SCHLICKER, E., SCHALNUS, R. & GÖTHERT, M. (1990). Modulation of 5-hydroxytryptamine release by presynaptic inhibitory α_2-adrenoceptors in the human cerebral cortex. *Naunyn-Schmied. Arch. Pharmacol.*, **342**, 508–512.

SHOPSIN, B., FRIEDMAN, E. & GERSHON, S. (1976). Parachlorophenylalanine reversal of tranylcypyromine effects in depressed patients. *Arch. Gen. Psychiatry*, **33**, 811–819.

STARKE, K., GÖTHERT, M. & KILBINGER, H. (1989). Modulation of neurotransmitter release by presynaptic autoreceptors. *Physiol. Rev.*, **69**, 864–969.

WANG, R.Y. & AGHAJANIAN, G.K. (1980). Enhanced sensitivity of amygdaloid neurons to serotonin and norepinephrine by antidepressant treatment. *Comm. Psychopharmacol.*, **4**, 83–90.

(Received May 31, 1994
Accepted June 13, 1994)

Br. J. Pharmacol. (1994), **113**, 496–498 © Macmillan Press Ltd, 1994

Effect of nitric oxide gas on the generation of nitric oxide by isolated blood vessels: implications for inhalation therapy

Rachel J. Kiff, David W. Moss & [1]Salvador Moncada

Wellcome Research Laboratories, Beckenham, Kent, BR3 3BS

1 We have investigated, using rat aortic rings, whether exogenous nitric oxide (NO) gas affects the activity or expression of the inducible, Ca^{2+}-independent NO synthase.

2 Incubation of rings with lipopolysaccharide (LPS, *S.typhosa*) for 6 h resulted in a gradual loss of tissue tone, a time-dependent reduction in constrictor response to phenylephrine and significant expression and activity of Ca^{2+}-independent NO synthase.

3 Following incubation of LPS-treated rings with NO gas, the expression of inducible NO synthase mRNA was still observed, although the enzyme activity was significantly reduced and there was no reduction in the response to phenylephrine.

4 Therefore, NO gas can inhibit the action but not the induction of an NO synthase likely to play a role in inflammatory states such as adult respiratory distress syndrome (ARDS).

5 These observations may explain the rebound phenomenon observed in some ARDS patients following inhalation therapy with NO gas.

Keywords: Inducible nitric oxide synthase; adult respiratory distress syndrome; inhibition; NO; isolated blood vessels

Introduction

The acute pulmonary arterial hypertension of adult respiratory distress syndrome (ARDS) has, until recently, been treated by infusion of vasodilators such as prostacyclin (Jones *et al.*, 1987), nitroprusside or glyceryl trinitrate (Naeije *et al.*, 1982) that also cause systemic vasodilatation and hypotension. Inhalation of NO gas for up to 53 days, however, reduces pulmonary-artery hypertension and improves oxygen exchange in ARDS patients without causing systemic vasodilatation (Rossaint *et al.*, 1993). Recent studies have shown that higher concentrations (> 10 p.p.m.) are less effective than lower concentrations (ED_{50} ~ 100 p.p.b.) (Gerlach *et al.*, 1993b) and that a rebound deterioration of arterial oxygenation, sometimes accompanied by pulmonary vasoconstriction, can occur on cessation of inhalation (Gerlach *et al.*, 1993a).

In the rat cerebellum, the murine macrophage cell line, J774, and bovine aortic endothelial cells, endogenous or exogenously-applied NO reduces NO synthase activity (Rogers & Ignarro, 1992; Assreuy *et al.*, 1993; Buga *et al.*, 1993). Such modulatory effects of NO on the enzyme that produces it may explain the rebound vasoconstriction observed in patients after long-term inhalation of NO. We have now investigated whether exogenously-applied NO gas can inhibit the expression or activity of NO synthase induced by lipopolysaccharide (LPS) in rat isolated aortic rings.

Methods

Organ bath studies

The tone of endothelium-denuded rat thoracic aortic rings, suspended in organ baths, was studied as described previously (Rees *et al.*, 1990). LPS (100 ng ml^{-1}) was added to the organ bath 15 min before the tissues were contracted submaximally (ED_{90}) with a concentration of phenylephrine determined previously from a cumulative dose-response curve (0.1–1 μM). At 2, 4 and 6 h after addition of LPS ($n = 6$ for each time), the tissues were washed to remove phenylephrine, allowed to equilibrate and the initial concentration of phenylephrine re-applied to monitor the sensitivity of the tissues to this vasoconstrictor. In some experiments, when the contraction induced by the initial concentration of phenylephrine had reached a plateau, the tissues were bubbled constantly with NO gas (five volumes per million (v.p.m.) in nitrogen, 200 cm^3 min^{-1}) as well as with 95% O_2: 5% CO_2. At 2, 4 and 6 h ($n = 6$ for each time) after treatment with LPS, the NO administration was stopped, the tissues were washed and their responsiveness to phenylephrine re-assessed. In other experiments, the NO gas was interrupted for a period of 15 min at 2, 4 and 6 h after LPS administration and the spontaneous restoration of tone was monitored ($n = 4$).

Assay of NO synthase

Adhering fat and connective tissue were trimmed from rat freshly isolated thoracic aortae and the endothelium was removed. Tissues were incubated for 6 h with LPS (100 ng ml^{-1}) at 37°C in Krebs solution gassed with 95% O_2:5% CO_2 in the presence or absence of NO gas (5 v.p.m.). Some LPS-treated tissues were incubated with the protein synthase inhibitor, cycloheximide (10 μM) for 6 h. Six aortae were subjected to each treatment and the tissues were pooled, freeze-clamped with liquid nitrogen and stored at − 70°C. Thawed tissues were cut into pieces in HESD buffer (20 mM HEPES pH 7.8, 0.1 mM EDTA, 0.2 M sucrose, 5 mM dithiothreitol) plus protease inhibitors (leupeptin and soya bean trypsin inhibitor, 10 μg ml^{-1} and pepstatin, 1 μg ml^{-1}) and maintained at 4°C. CHAPS (20 mM) was added to the homogenate and mixed for 20 min. The homogenate was centrifuged at 10,000 *g* for 20 min at 4°C and the supernatant removed.

NO synthase was assayed by the formation of [U-^{14}C]-citrulline from L-[U^{14}C]-arginine (Palmer & Moncada, 1989); 50 μl of supernatant was incubated for 20 min at 37°C with 1.57 μM L-[U-^{14}C]-arginine, 3 μM L-arginine, 125 μM NADPH, 10 μM tetrahydrobiopterin, 2.5 mM $CaCl_2$, 10 μg ml^{-1} calmodulin and 0.5 mg ml^{-1} bovine serum albumin in a total volume of 100 μl 20 mM HEPES buffer. The reaction was stopped by addition of 1.5 ml Dowex-50W resin and 5 ml H_2O. Radioactivity in the fractions containing

[1] Author for correspondence.

[U-^{14}C]-citrulline was determined by liquid scintillation counting. Enzyme assays were performed in triplicate for each treatment group. The limit of detection for the assay was 1 pmol min^{-1} mg^{-1} protein.

Polymerase chain reaction (PCR) of NO synthase mRNA

Rings of endothelium-denuded thoracic aortae were freeze-clamped with liquid nitrogen and stored at − 70°C either immediately after preparation or after exposure for 6 h to LPS (100 ng ml^{-1}) at 37°C in Krebs solution in the presence or absence of NO gas (5 v.p.m.). Poly A$^+$ mRNA was extracted from the frozen tissues with a Fast Track kit (Invitrogen). Random-primed reverse transcription of mRNA to cDNA and PCR were performed using a Gene-Amp RT-PCR-kit (Perkin Elmer Cetus) according to the manufacturer's instructions. The following conditions were employed for amplification: denature 96°C, 35 s; anneal 55°C, 2 min; extend 72°C, 3 min for 35 cycles, using oligonucleotide primers specific for either endothelial or inducible NO synthase.

The primer sequences were as follows: iNOS, sense: 5′ ATT TGG TCT AGA AGT GCA AAG TCT GAG ACA TGG CTT 3′; antisense: 5′ ACC ACT GGA TCC TGC CGA TGC AGC GAG GGG CAT TCC 3′; eNOS, sense: 5′ CAG TGT CCA ACA TGC TGC TGG AAA TTG 3′; antisense: 5′ TAA AGG TCT TCT TCC TGG TGA TGC 3′. The expected size of PCR product using endothelial NO synthase primers was 485 base pairs and that using inducible NO synthase was 650 base pairs. PCR products were resolved by 1% agarose gel electrophoresis.

Materials

LPS (Difco), sucrose and $CaCl_2$ (BDH), NADPH (Boehringer Mannheim), L-[U-^{14}C]-arginine (Amersham), tetrahydrobiopterin (Dr B. Schircks Laboratories, Switzerland) and NO gas (BOC Special Gases) were obtained as indicated. All other chemicals were obtained from Sigma.

Statistics

Results are expressed as mean ± s.e.mean for (n) separate experiments. Student's unpaired t test was used to determine the significance of differences between means and $P<0.05$ was taken as statistically significant.

Results

Organ bath studies

Aortic rings incubated with LPS and contracted with phenylephrine lost tone gradually over 6 h. Administration of NO gas caused a rapid loss of tone that reached a plateau within 15 min, with no evidence of tachyphylaxis over a 6 h period. Cessation of the NO gas for 15 min every 2 h restored the tone to levels observed prior to exposure to NO, an effect that was rapidly reversed (within 5 min) on re-exposure (Figure 1a). The contraction to a fixed concentration of phenylephrine was reduced in a time-dependent manner after administration of LPS. NO gas prevented this loss in sensitivity in LPS-treated rings, so that there was no difference in the maximum force of contraction to phenyleph-

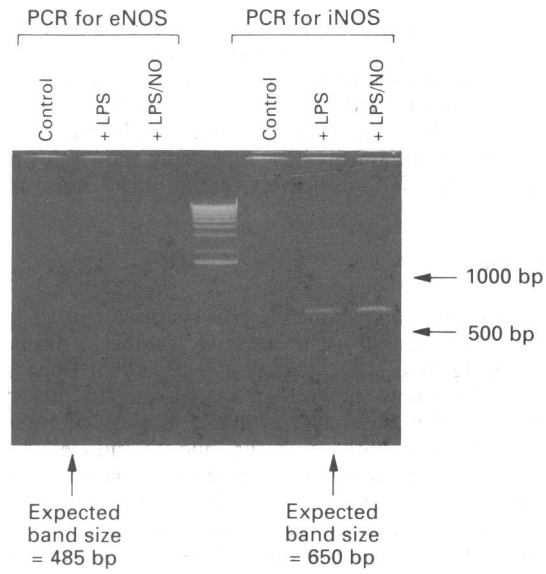


Figure 2 Polymerase chain reaction (PCR) of NO synthase mRNA, isolated from untreated aortic rings (Control) and those treated for 6 h with LPS or LPS and NO gas. Oligonucleotide primers specific for either endothelial (eNOS) or inducible (iNOS) enzyme were used. The first three lanes are PCR products using eNOS, the last three lanes are those using iNOS specific primers and the centre lane is a molecular weight ladder.

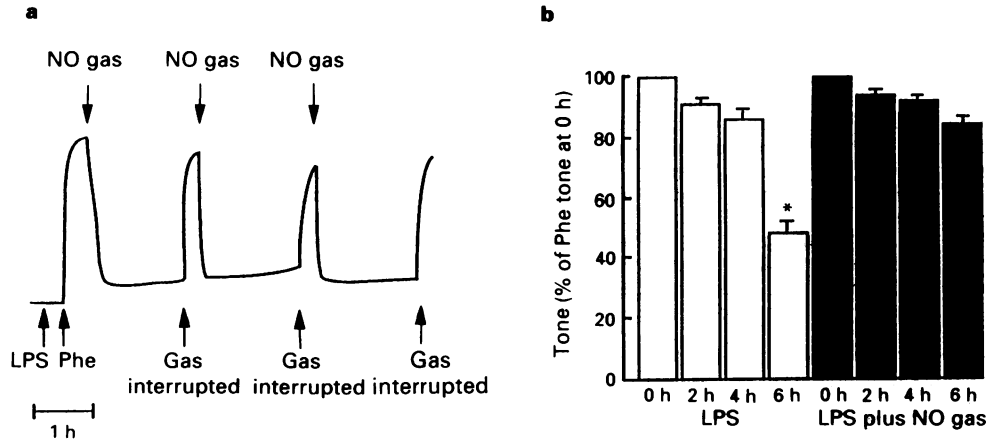


Figure 1 (a) Reversibility of the vasodilatation induced by prolonged exposure to nitric oxide (NO) gas. Endothelium-denuded rat aortic rings were treated with lipopolysaccharide (LPS, 100 μg ml^{-1}) and precontracted with phenylephrine (Phe). NO gas was bubbled into the organ bath, causing vasodilatation. Interruption of exposure to NO gas for 15 min every 2 h restored the tissue tone to that observed prior to treatment with NO. Trace representative of four experiments. (b) The contraction induced by phenylephrine (Phe) 2, 4 and 6 h after the induction of NO synthase by LPS, in the absence and presence of NO gas. Each column is the mean ± s.e.mean of six separate experiments. *$P<0.05$ versus phenylephrine tone at 0 h.

rine at 2, 4 and 6 h in the tissues treated with NO (Figure 1b).

NO synthase assays

There was no significant generation of NO at 0 h (1.12 ± 0.59 pmol min^{-1} mg^{-1} protein); however, after 6 h incubation with LPS, significant Ca^{2+}-independent generation of NO was observed (21.48 ± 0.27 pmol min^{-1} mg^{-1} protein, $P < 0.05$ versus the control tissues). This was abolished by pretreatment with cycloheximide (10 μM, 1.31 ± 0.35 pmol min^{-1} mg^{-1} protein) and by the presence of NO gas throughout the 6 h incubation (2.78 ± 0.33 pmol min^{-1} mg^{-1} protein).

PCR of NO synthase

PCR analysis showed that mRNA for endothelial NO synthase was absent both in freshly-prepared endothelium-denuded aortic rings and in those exposed to LPS for 6 h (Figure 2). In contrast, mRNA for inducible NO synthase, although absent from untreated tissues, was present in those which had been treated with LPS, both in the presence and absence of NO (Figure 2). Previous nucleotide sequence analysis of PCR fragments have repeatedly shown this primer pair to amplify iNOS exclusively (unpublished observations).

Discussion

Both constitutive and inducible NO synthase can be modulated by NO acting as a negative feedback mechanism (Rogers & Ignarro, 1992; Assreuy *et al.*, 1993; Buga *et al.*, 1993). We have now shown that NO gas directly inhibits the activity of LPS-induced NO synthase in rings of rat aorta. LPS induces NO synthase in the smooth muscle of aortic rings, causing a gradual loss of phenylephrine-induced tone (Rees *et al.*, 1990). Exposure to NO gas, however, produced a rapid loss of tone which was constant over a period of 6 h, with no evidence of tachyphylaxis. This is consistent with the lack of tachyphylaxis observed after inhalation of NO for up to 53 days (Rossaint *et al.*, 1993). Removal of the NO gas resulted in rapid restoration of the tissue tone to that originally induced by phenylephrine. Furthermore, the sensitivity to a fixed dose of phenylephrine, tested after washing out phenylephrine from the tissue, remained constant in the presence of NO. These results indicate an absence of NO production in those tissues exposed to NO gas. This was confirmed by our finding that the activity of the NO synthase in rings incubated with LPS was significantly inhibited by NO gas as well as by cycloheximide. Since mRNA for the inducible NO synthase was observed in rings incubated with LPS, both in the presence and absence of NO gas, it appears that NO gas inhibits the NO synthase at a post-transcription level, possibly by direct enzyme inhibition.

A low concentration of inhaled NO has been shown to be critical for a positive clinical effect. However, even when NO was used in the parts per billion range, a step-wise weaning-off procedure was required to prevent a marked deterioration of arterial oxygenation and enhancement of vascular resistance on termination of inhalation (Gerlach *et al.*, 1993a). Our results, obtained from tissues exposed to a concentration of NO gas comparable to those administered to patients with ARDS, support our previous results (Assreuy, 1993) and those of Gerlach *et al.* (1993a) which suggest that continuous exposure to NO gas may inhibit endogenous NO synthase, resulting in dependence on exogenous NO. Inhibition of basal continuous release of NO in the vasculature leads to selective hypersensitivity to the vasodilator actions of NO donors, an effect which has been attributed to up-regulation of the soluble guanylate cyclase. A decrease in basal release of NO also results in enhanced responsiveness to vasocontrictors (Moncada *et al.*, 1991). Furthermore, prolonged treatment of rabbits with the NO donor, molsidomine, results in reduced endothelium-dependent relaxation, which suggests a decreased synthesis of endogenous NO (Bult *et al.*, 1990). If a similar phenomenon occurs in the lung, then inhibition of endogenous NO synthesis by NO gas will lead to dependence on its actions, so that its withdrawal will leave the pulmonary circulation, and probably the airways, more susceptible to the action of constrictor agents, a phenomenon that could account for the reported clinical observations.

We wish to thank Annie Higgs and Pam Smith for their help in the preparation of this manuscript.

References

ASSREUY, J., CUNHA, F.Q., LIEW, F.Y. & MONCADA, S. (1993). Feedback inhibition of nitric oxide synthase activity by nitric oxide. *Br. J. Pharmacol.*, **108**, 833–837.

BUGA, G.M., GRISCAVAGE, J.M., ROGERS, N.E. & IGNARRO, L.J. (1993). Negative feedback regulation of endothelial cell function by nitric oxide. *Circ. Res.*, **73**, 808–812.

BULT, H., BUYSSENS, N., DE MEYER, G.R.Y., JORDAENS, F.H. & HERMAN, A.G. (1990). Effects of chronic treatment with a source of exogenous nitric oxide on the release of endothelium-derived relaxing factor by aortae from normal and hypercholesterolaemic rabbits. In *Nitric oxide from L-Arginine: a Bioregulatory System.* ed. Moncada, S. & Higgs, E.A. pp. 101–106. Amsterdam: Elsevier Science Publishers.

GERLACH, H., PAPPERT, D., LEWANDOWSKI, K., ROSSAINT, R. & FALKE, K.J. (1993a). Long-term inhalation with evaluated low doses of nitric oxide for selective improvement of oxygenation in patients with adult respiratory distress syndrome. *Intensive Care Med.*, **19**, 443–449.

GERLACH, H., ROSSAINT, R., PAPPERT, D. & FALKE, K.J. (1993b). Time course and dose-response of nitric oxide inhalation for systemic oxygenation and pulmonary hypertension in patients with adult respiratory distress syndrome. *Eur. J. Clin. Invest.*, **23**, 499–502.

JONES, D.K., HIGENBOTTAM, T.W. & WALLWORK, J. (1987). Treatment of primary pulmonary hypertension with intravenous epoprostenol (prostacyclin). *Br. Heart J.*, **57**, 270–278.

MONCADA, S., REES, D.D., SCHULZ, R. & PALMER, R.M.J. (1991). Development and mechanism of a specific supersensitivity to nitrovasodilators after inhibition of vascular nitric oxide synthesis in vivo. *Proc. Natl. Acad. Sci. U.S.A.*, **88**, 2166–2170.

NAEIJE, R., MELOT, C., MOLS, P. & HALLEMANS, R. (1982). Effects of vasodilators on hypoxic pulmonary vasoconstriction in normal man. *Chest*, **82**, 404–410.

PALMER, R.M.J. & MONCADA, S. (1989). A novel citrulline-forming enzyme implicated in the formation of nitric oxide by vascular endothelial cells. *Biochem. Biophys. Res. Commun.*, **158**, 348–352.

REES, D.D., CELLEK, S., PALMER, R.M.J. & MONCADA, S. (1990). Dexamethasone prevents the induction of endotoxin of a nitric oxide synthase and the associated effects on vascular tone: an insight into endotoxin shock. *Biochem. Biophys. Res. Commun.*, **173**, 541–547.

ROGERS, N.E. & IGNARRO, L.J. (1992). Constitutive nitric oxide synthase from cerebellum is reversibly inhibited by nitric oxide formed from L-arginine. *Biochem. Biophys. Res. Commun.*, **189**, 242–249.

ROSSAINT, R., FALKE, K.J., LOPEZ, F., SLAMA, K., PISON, U. & ZAPOL, W.M. (1993). Inhaled nitric oxide for the adult respiratory distress syndrome. *New Engl. J. Med.*, **328**, 399–405.

(Received May 12, 1994
Revised June 13, 1994
Accepted June 21, 1994)

Br. J. Pharmacol (1994), **113**, 499-507 © Macmillan Press Ltd, 1994

Blockade by ifenprodil of high voltage-activated Ca^{2+} channels in rat and mouse cultured hippocampal pyramidal neurones: comparison with N-methyl-D-aspartate receptor antagonist actions

[1]John Church, *Elizabeth J. Fletcher, Keith Baxter & *John F. MacDonald

Department of Anatomy, University of British Columbia, 2177 Wesbrook Mall, Vancouver, B.C., Canada V6T 1Z3 and *Department of Physiology, University of Toronto, 1 King's College Circle, ON., Canada M5S 1A8

1 The block by ifenprodil of voltage-activated Ca^{2+} channels was investigated on increases in intracellular free calcium concentration ($[Ca^{2+}]_i$) evoked by 50 mM K^+ (high-$[K^+]_o$) in Fura-2-loaded rat hippocampal pyramidal neurones in culture and on currents carried by Ba^{2+} ions (I_{Ba}) through Ca^{2+} channels in mouse cultured hippocampal neurones under whole-cell voltage-clamp. The effects of ifenprodil on voltage-activated Ca^{2+} channels were compared with its antagonist actions on N-methyl-D-aspartate- (NMDA) evoked responses in the same neuronal preparations.

2 Rises in $[Ca^{2+}]_i$ evoked by transient exposure to high-$[K^+]_o$ in our preparation of rat cultured hippocampal pyramidal neurones are mediated predominantly by Ca^{2+} flux through nifedipine-sensitive Ca^{2+} channels, with smaller contributions from nifedipine-resistant, ω-conotoxin GVIA-sensitive Ca^{2+} channels and Ca^{2+} channels sensitive to crude funnel-web spider venom (Church *et al.*, 1994). Ifenprodil (0.1-200 μM) reversibly attenuated high-$[K^+]_o$-evoked rises in $[Ca^{2+}]_i$ with an IC_{50} value of 17 ± 3 μM, compared with an IC_{50} value of 0.7 ± 0.1 μM for the reduction of rises in $[Ca^{2+}]_i$ evoked by 20 μM NMDA. Tested in the presence of nifedipine 10 μM, ifenprodil (1-50 μM) produced a concentration-dependent reduction of the dihydropyridine-resistant high-$[K^+]_o$-evoked rise in $[Ca^{2+}]_i$ with an IC_{50} value of 13 ± 4 μM. The results suggest that ifenprodil blocks Ca^{2+} flux through multiple subtypes of high voltage-activated Ca^{2+} channels.

3 Application of the polyamine, spermine (0.25-5 mM), produced a concentration-dependent reduction of rises in $[Ca^{2+}]_i$ evoked by high-$[K^+]_o$. The antagonist effects of ifenprodil 20 μM on high-$[K^+]_o$-evoked rises in $[Ca^{2+}]_i$ were attenuated by spermine 0.25 mM but not by putrescine 1 or 5 mM. In contrast, spermine 0.1 mM increased rises in $[Ca^{2+}]_i$ evoked by NMDA and enhanced the ifenprodil (5 μM) block of NMDA-evoked rises in $[Ca^{2+}]_i$.

4 Similar results were obtained in mouse cultured hippocampal pyramidal neurones under whole-cell voltage-clamp. Ifenprodil attenuated both the peak and delayed whole-cell I_{Ba} with an IC_{50} value of 18 ± 2 μM, whilst it attenuated steady-state NMDA-evoked currents with an IC_{50} of 0.8 ± 0.2 μM. Block of I_{Ba} by ifenprodil 10 μM was rapid in onset, fully reversible and occurred without change in the current-voltage characteristics of I_{Ba}. The ifenprodil block of I_{Ba} was enhanced on membrane depolarization and was weakly dependent on the frequency of current activation. Spermine 0.1 mM potentiated control NMDA-evoked currents but attenuated I_{Ba}. In agreement with the microspectrofluorimetric studies, co-application of spermine produced a small enhancement of the inhibitory effect of ifenprodil 10 μM on NMDA-evoked responses whereas the reduction of I_{Ba} by ifenprodil 10 μM in the presence of spermine was less than expected if the inhibitory effects of ifenprodil and spermine on I_{Ba} were simply additive.

5 The results indicate that ifenprodil blocks high voltage-activated Ca^{2+} channels in rat and mouse cultured hippocampal pyramidal neurones. Although the Ca^{2+} channel blocking actions of ifenprodil are observed at higher concentrations than those associated with NMDA antagonist activity, Ca^{2+} channel blockade may contribute, at least in part, to the established neuroprotective and anticonvulsant properties of the compound.

Keywords: Ifenprodil; voltage-activated calcium channels; N-methyl-D-aspartate (NMDA); polyamines; cultured hippocampal pyramidal neurones

Introduction

The phenylethanolamine, ifenprodil, has been employed in the treatment of human cerebrovascular disease (Otomo & Kodama, 1976). Recent interest has centred on its activity as an antagonist of the N-methyl-D-aspartate (NMDA) subtype of glutamate receptor as the functional basis for both its neuroprotective and anticonvulsant actions (reviewed by Wong & Kemp, 1991; Carter *et al.*, 1991). Although NMDA receptor-mediated events undoubtedly play a role in the pathogenesis of neurodegenerative and convulsive phenomena, Ca^{2+} flux through voltage-activated Ca^{2+} channels is also an important contributing factor (see Heinemann & Hamon, 1986; Siesjö & Bengtsson, 1989). It is therefore of interest that ifenprodil blocks Ca^{2+} channel-mediated responses in vascular smooth muscle, a property thought to underlie its vasorelaxant effects (Honda & Sakai, 1987; Honda *et al.*, 1988).

In this study we examined the ability of ifenprodil to block high voltage-activated (HVA) Ca^{2+} channels in rat and mouse cultured hippocampal neurones and compared this effect with its NMDA receptor antagonist actions in the same neuronal preparations. Because ifenprodil has been reported to interact with the polyamine modulatory site on the NMDA receptor-channel complex (Ransom & Stec, 1988; Schoemaker *et al.*, 1990; Carter *et al.*, 1991; Williams *et al.*, 1991) and, in turn, polyamines interact with voltage-activated

[1] Author for correspondence.

Ca^{2+} channels (reviewed by Scott *et al.*, 1993; see also Pullan *et al.*, 1990; Schoemaker, 1992; Herman *et al.*, 1993), we also investigated the ability of polyamines to modulate the HVA Ca^{2+} channel and NMDA receptor antagonist actions of ifenprodil. We find that ifenprodil can block neuronal HVA Ca^{2+} channels, an action which is modified to a limited extent by spermine. Although the concentrations of ifenprodil required to block HVA Ca^{2+} channels are more than 10 times higher than those required to attenuate NMDA-evoked responses in the same neurones, the Ca^{2+} channel blocking properties of this compound may contribute to its established neuroprotective and anticonvulsant actions.

Methods

Fluorescent dye studies

Details of the methods employed have been described previously (Church *et al.*, 1994). In brief, hippocampal pyramidal neurones were obtained from 18-day-old foetal Wistar rats, maintained in culture for 9–14 days, and loaded with the membrane-permanent form of Fura-2 (Grynkiewicz *et al.*, 1985). Coverslips were then placed in a chamber at 20–24°C and superfused at 1.5 ml min^{-1} with a solution containing (mM): NaCl 136.5, KCl 3, NaH_2PO_4 1.5, $MgSO_4$ 1.5, D-glucose 10, $CaCl_2$ 2, N-2-hydroxyethylpiperazine-N'-2-ethanesulphonic acid (HEPES) 10, tetrodotoxin (TTX) 0.0005 (final pH 7.35–7.4). In experiments employing NMDA, Mg^{2+} was omitted and 2 μM glycine added. Both NMDA (20 μM) and high-$[K^+]_o$ solutions (50 mM, by substitution for NaCl) were administered in 1 ml aliquots to the inflow of the perfusion chamber and allowed to remain in contact with the neurones for 20 s before wash-out. Test compounds were applied by superfusion; their effects were expressed as the percentage change of the peak response to an excitant during their administration, in relation to the peaks of the control and recovery responses obtained before and after their administration, respectively.

Cytoplasmic free calcium concentrations ($[Ca^{2+}]_i$) were measured by the dual excitation fluorescence ratio method on an Attofluor Digital Fluorescence Microscopy System (Atto Instruments Inc.; Carl Zeiss Canada Ltd.). Fluorescence intensity measurements were obtained from multiple neurone somata simultaneously and raw intensity data at each excitation wavelength (334 and 380 nm) were corrected for background prior to calculation of the ratio. The *in situ* calibration method was used to convert fluorescence ratios into $[Ca^{2+}]_i$. During exposure to 10 μM Br-A23187, calibration parameters (R_{max}, R_{min} and β) were obtained in the presence (2 mM) and absence (nominally zero-Ca^{2+} solution in the presence of 100 μM ethylene glycol-*bis*(β-aminoethyl ether) *N,N,N',N'*-tetraacetic acid (EGTA)) of Ca^{2+}. The published K_D value of 135 nM (at 20°C) was employed (Grynkiewicz *et al.*, 1985).

Statistical results are reported as mean ± s.e. mean, where *n* refers to the total number of neurones from which observations were made under each experimental condition. Each experiment was performed on at least three different neuronal cultures. Averaged data points were fitted to a standard logistic equation (see Church *et al.*, 1994) to derive IC_{50} values (the concentration of test compound resulting in a 50% inhibition of the control responses). Statistical analysis was performed by Student's *t* test, $P < 0.05$ being considered significant.

Electrophysiological studies

Dissociated mouse hippocampal pyramidal neurones grown in culture were used for whole-cell recordings using conventional voltage-clamp techniques, as previously described (MacDonald *et al.*, 1989; Church *et al.*, 1994). Cultures were used at 7–14 days following plating. Recordings were performed at 20–24°C.

Prior to the investigation of excitatory amino acid-evoked responses, cultures were rinsed with an extracellular solution containing (mM): NaCl 140, $CaCl_2$ 1.3, KCl 5.4, HEPES 25, glucose 33, TTX 0.0001 and glycine 0.003 (unless otherwise indicated) at a final pH of 7.35–7.4. Patch electrodes constructed from thin-walled borosilicate glass were filled with a solution containing (mM): CsF 110, CsCl 10, HEPES 10 and EGTA 10, adjusted to pH 7.35–7.4 with 1 M CsOH. The membrane holding potential (V_h) was −60 mV unless otherwise indicated in the text. Control currents were evoked by 5 s applications of 60 μM NMDA, 60 μM kainate and 30 μM (**RS**)-α-amino-3-hydroxy-5-methylisoxazole-4-propionic acid (AMPA).

For recording voltage-activated Ca^{2+} channel currents, an intracellular solution was used of composition (mM): CsCl

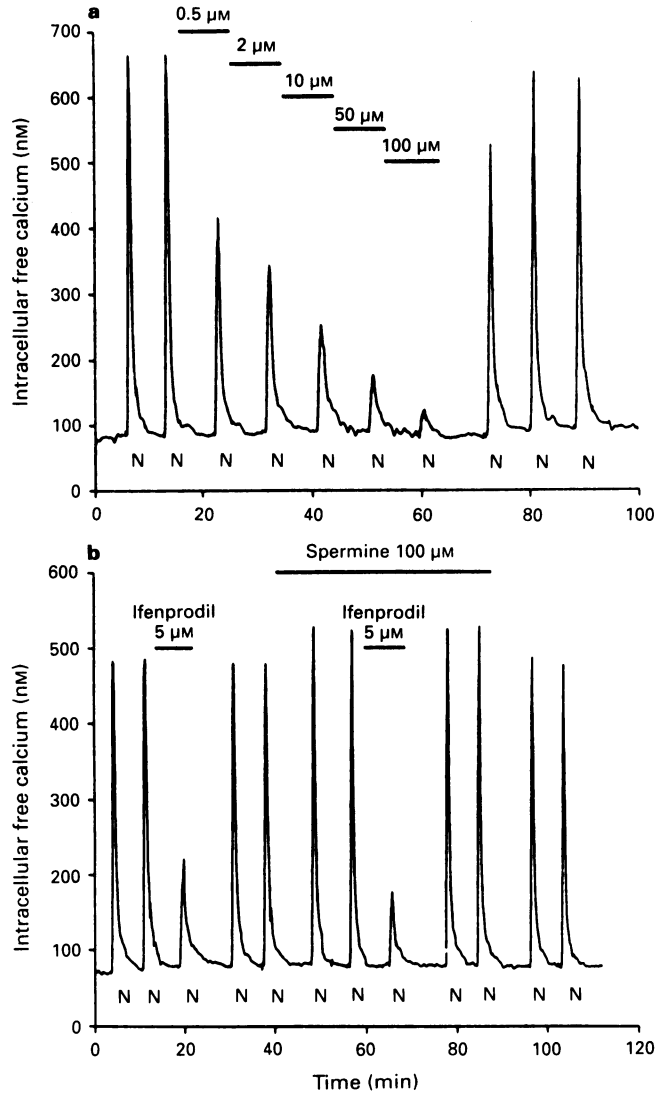


Figure 1 Ifenprodil inhibits NMDA-evoked rises in $[Ca^{2+}]_i$. (a) The effects of ifenprodil 0.5–100 μM, applied for the periods indicated by the bars above the trace, on NMDA- (N) evoked rises in $[Ca^{2+}]_i$. A concentration-dependent reduction of NMDA-evoked responses is seen. The record is a mean of data obtained from 14 neurones simultaneously. (b) The effects of ifenprodil 5 μM, applied in the absence and presence of spermine 100 μM for the periods indicated by the bars above the trace, on NMDA- (N) evoked rises in $[Ca^{2+}]_i$. The record is a mean of data obtained from 10 neurones simultaneously. In these neurones, ifenprodil 5 μM produced a 64% reduction in NMDA-evoked rises in $[Ca^{2+}]_i$. Spermine 100 μM potentiated the NMDA-evoked responses by 12% and increased the magnitude of the block of NMDA-evoked responses by ifenprodil 5 μM to 77%.

110, TEA 10, EGTA 10 and HEPES 10, to which was added Mg-ATP 2, phosphocreatine 50, creatine phosphokinase 50 iu and GTP 2 (final pH 7.35–7.4; final osmolarity 310 mOsm) to retard run-down of the whole-cell currents (MacDonald *et al.*, 1989). The support solution was kept on ice for the duration of the experiment to prevent degradation of its components and was not used for periods longer than 5 h. After attaining the whole-cell patch configuration the standard extracellular solution (see above) was changed to one containing (mM): NaCl 140, CsCl 5, $BaCl_2$ 5, $MgCl_2$ 1, HEPES 25 and glucose (pH 7.35–7.4, 330 mOsm). The concentration of TTX was increased to 0.3–0.6 μM and extracellular KCl was replaced with CsCl to block, respectively, voltage-activated Na^+ and K^+ channels. The series resistance and capacitance of the electrode were compensated for (Axopatch 1B, Axon Instruments), whilst that of the membrane was only partially achieved due to the difficulty of clamping neurones with extensive processes. Leak currents were estimated in the presence of extracellular solution with 100 μM cadmium added. Barium currents (I_{Ba}) flowing through voltage-activated Ca^{2+} channels were evoked by 250 ms voltage-steps from a V_h of −80 mV to a test potential (V_t) of −10 mV at 20 s intervals. Other protocols adopted are detailed in the text. Ifenprodil was perfused over the neurone and I_{Ba} activated until steady-state block was attained. For construction of concentration-inhibition plots the concentration of ifenprodil was sequentially increased to achieve full block before recovery was attempted in order to minimize the possible error contributed by run down of I_{Ba}. Cells which displayed less than 50% recovery of control current amplitude were excluded from analysis.

All solutions were applied to neurones from a 3-barrelled perfusion system allowing for rapid (<50 ms) application to the entire neurone under voltage-clamp. The IC_{50} values, EC_{50} values (the concentration of NMDA evoking a response 50% that of maximum) and percentage reductions of control responses are expressed as mean ± s.e. mean, with n the number of neurones tested. IC_{50} values were estimated by fitting data points to the same logistic equation as in the fluorescent dye experiments (see above).

Sources and handling of compounds

Compounds were obtained from Sigma Chemical Co., with the exceptions of ifenprodil tartrate, TTX, AMPA (Research Biochemicals Inc.) and Fura-2 AM (Molecular Probes Inc.). Stock solutions of ifenprodil (1 or 5 mM in distilled water) and nifedipine (10 mM in ethanol) were made up fresh each day from the solid, stored in glass vials and diluted in perfusion medium immediately prior to use. Ifenprodil stock solutions were briefly sonicated to ensure solubilization of the compound. The highest concentration of ethanol in final working solutions was 0.1%, which in control experiments had no effect on responses. Nifedipine-containing solutions

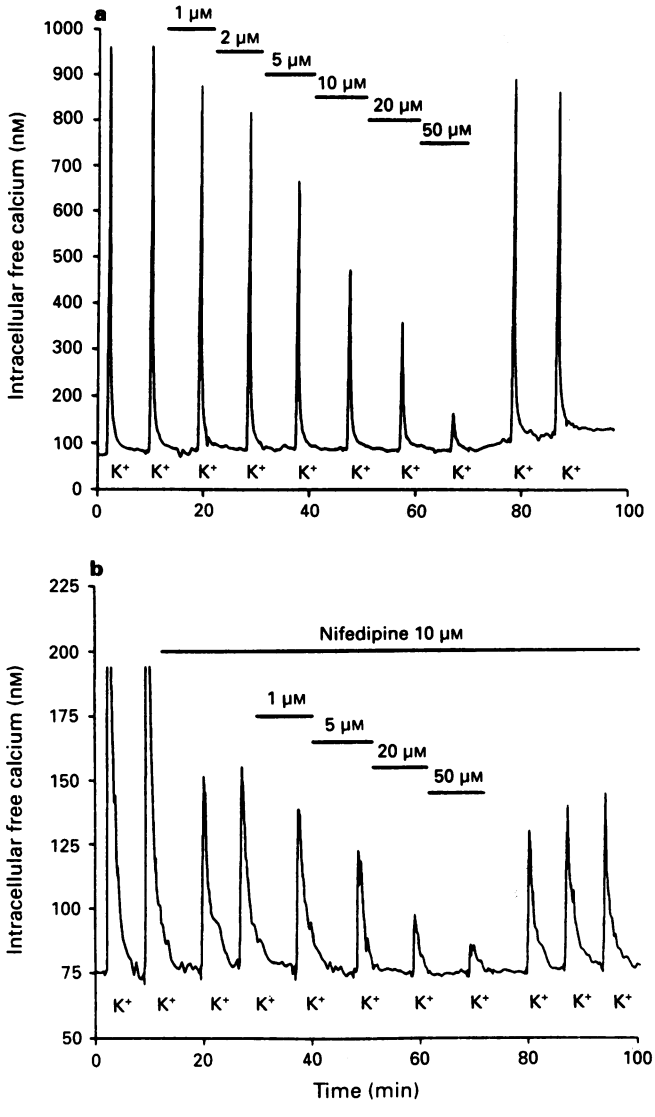


Figure 2 Ifenprodil inhibits rises in $[Ca^{2+}]_i$ evoked by high-$[K^+]_o$. (a) The effects of ifenprodil 1–50 μM, applied for the periods indicated by the bars above the trace, on rises in $[Ca^{2+}]_i$ evoked by 50 mM K^+ (K^+). A concentration-dependent reduction of high-$[K^+]_o$-evoked responses is seen. The record is a mean of data obtained from 39 neurones simultaneously. (b) Ifenprodil produces a concentration-dependent reduction of nifedipine-resistant high-$[K^+]_o$-evoked rises in $[Ca^{2+}]_i$. Under control conditions (first and second responses; peaks truncated for convenience in figure preparation), 50 mM K^+ (K^+) evoked large rises in $[Ca^{2+}]_i$ which were reduced by 80% by nifedipine 10 μM (third and fourth responses). Co-application of ifenprodil 1–50 μM, for the periods indicated by the bars above the trace, produced a concentration-dependent reduction of the nifedipine-resistant residual response. The record is a mean of data obtained from 9 neurones simultaneously.

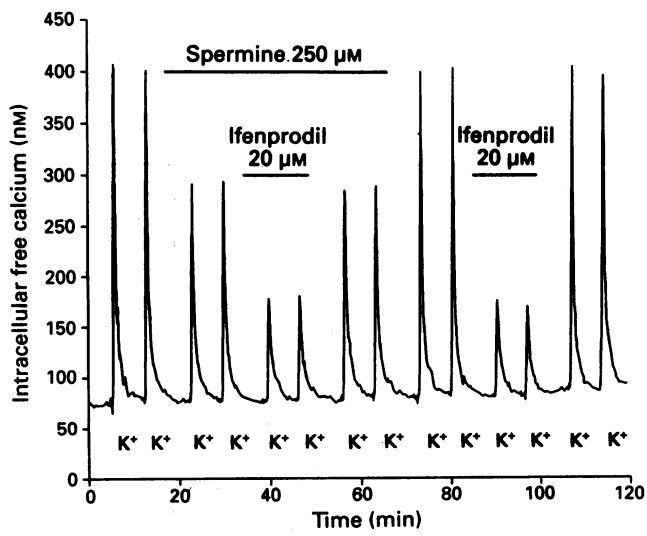


Figure 3 The polyamine, spermine, attenuates high-$[K^+]_o$-evoked rises in $[Ca^{2+}]_i$ and reduces the inhibitory effect of ifenprodil. Spermine 250 μM, applied for the period indicated by the bar above the trace, reduced high-$[K^+]_o$-evoked rises in $[Ca^{2+}]_i$ by 33%. Ifenprodil 20 μM, co-applied with spermine, reduced high-$[K^+]_o$-evoked rises in $[Ca^{2+}]_i$ by 52% from control values established in the presence of spermine. Following recovery from spermine application, ifenprodil 20 μM produced a 69% depression of high-$[K^+]_o$-evoked rises in $[Ca^{2+}]_i$. The record is a mean of data obtained from 8 neurones simultaneously.

were handled in the manner described previously (Church et al., 1994).

Results

Fluorescent dye studies

Ifenprodil block of NMDA-evoked responses Ifenprodil (0.02–100 μM) produced a concentration-dependent reduction of rises in $[Ca^{2+}]_i$ evoked by NMDA, with an apparent IC_{50} value of 0.7 ± 0.1 μM ($n > 75$ at each concentration tested; Figure 1). At the highest concentration tested (100 μM) ifenprodil produced an incomplete inhibition of NMDA-evoked responses (88 ± 0.4% reduction; $n = 177$), as previously reported in rat cultured hippocampal pyramidal neurones (Legendre & Westbrook, 1991) and in *Xenopus* oocytes expressing NR1A/NR2B heteromeric NMDA receptors (Wiliams, 1993). The polyamine, spermine (100 μM), potentiated NMDA-evoked responses by 13 ± 2% ($n = 95$, reviewed by Williams et al., 1991; see also Rock & MacDonald, 1992; Araneda et al., 1993; Benveniste & Mayer, 1993) and increased the potency of ifenprodil as an antagonist of NMDA-evoked rises in $[Ca^{2+}]_i$ (Figure 1b).

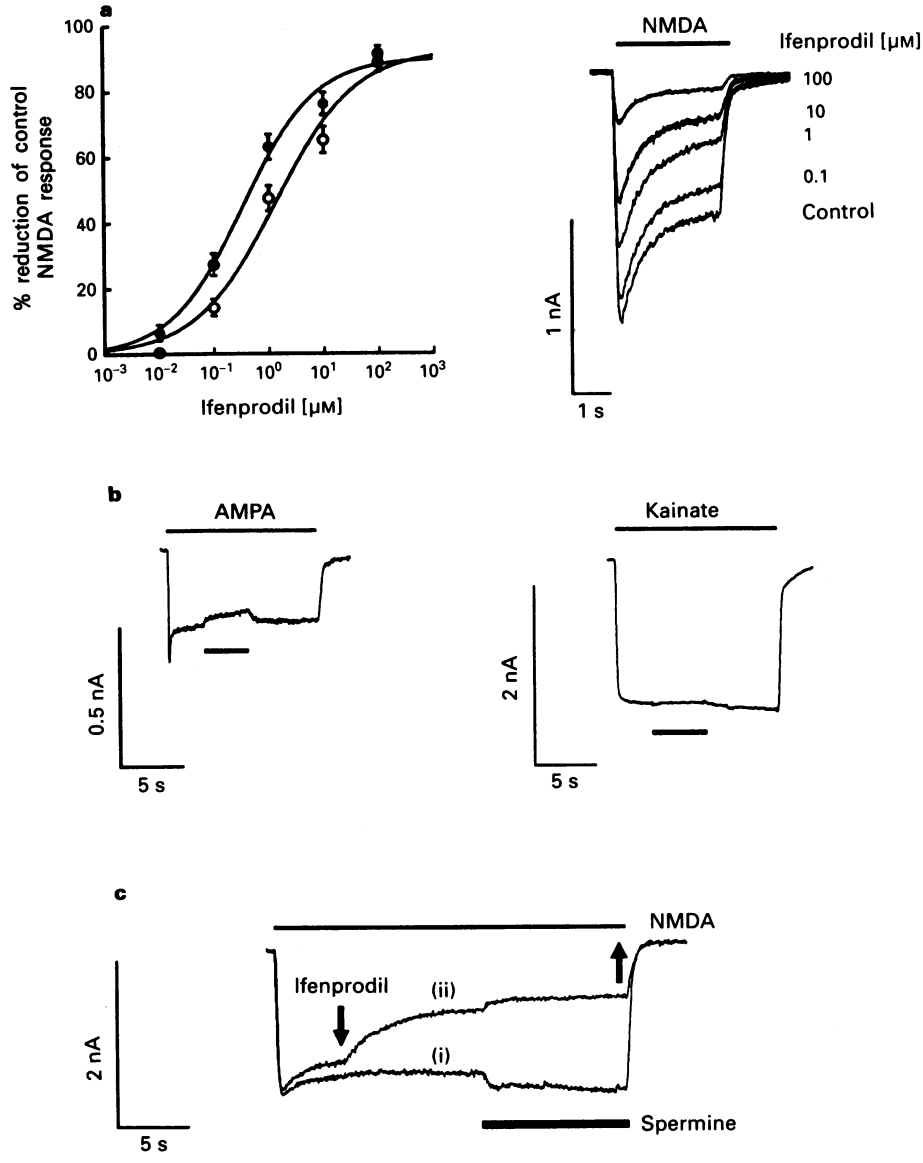


Figure 4 Ifenprodil block of amino acid-evoked currents in voltage-clamped neurones. (a) To left: dose-inhibition plot indicates the mean ± s.e. mean percentage reduction by ifenprodil of the control steady-state (●) and peak (○) components of NMDA-evoked currents for 7 neurones at a V_h of −60 mV. The respective IC_{50} values for the ifenprodil block of the peak and steady-state components of the NMDA-evoked response were 2.8 ± 0.9 and 0.8 ± 0.2 μM. Abscissa scale: ifenprodil concentration in μM. Ordinate scale: % reduction of control NMDA-evoked response. To right: sample traces indicate block of control NMDA-evoked currents (NMDA 60 μM; applied for the period indicated by the bar above the trace) by increasing concentrations of ifenprodil (0.1–100 μM) as indicated to right. On wash in control solution there was recovery to 75% of control (not shown). Calibration: current amplitude in nA; time in s. (b) On the same neurone currents evoked by AMPA (30 μM) and kainate (60 μM), applied for the periods indicated by the bars above the traces, were attenuated by 23% and 4%, respectively, on co-application of 100 μM ifenprodil (applied for the periods indicated by the bars below the traces). Calibration: current amplitude in nA; time in s. (c) On a different neurone the interaction of ifenprodil and spermine on NMDA-evoked responses is highlighted. Prolonged application of NMDA (bar above trace) evoked a control current (trace (i)) that was potentiated on co-application of spermine (100 μM; bar below trace). On a subsequent NMDA-evoked response in the same neurone (trace (ii)) ifenprodil 10 μM (applied between arrows) produced an approximately 50% block of control. Co-application of spermine (100 μM) increased the ifenprodil-induced block to more than 60%. The action of ifenprodil was reversed on wash in control solution (not shown). Calibration: current amplitude in nA; time in s.

Thus, ifenprodil 5 μM produced a 61 ± 1% reduction in NMDA-evoked rises in $[Ca^{2+}]_i$ which, on the same neurones, increased to a 72 ± 1% reduction in the presence of spermine 100 μM ($n = 95$; $P < 0.001$, Student's paired t test).

Ifenprodil block of high-$[K^+]_o$-evoked responses We have previously shown that, under our experimental conditions, rises in $[Ca^{2+}]_i$ evoked by the transient application of 50 mM K^+-containing medium are largely a consequence of Ca^{2+} flux through nifedipine-sensitive HVA Ca^{2+} channels, with smaller components reflecting Ca^{2+} flux through both nifedipine-resistant, ω-conotoxin GVIA- (ω-CgTx) sensitive channels and channels resistant to both nifedipine and ω-CgTx but sensitive to crude funnel-web spider venom (Church *et al.*, 1994). The contribution of endogenously-released glutamate to the observed responses appears to be minimal (see Church *et al.*, 1994). Ifenprodil (0.1–200 μM) produced a concentration-dependent reduction of the rise in $[Ca^{2+}]_i$ evoked by high-$[K^+]_o$, with an apparent IC_{50} value of 16.9 ± 3.0 μM ($n > 50$ at each concentration tested; Figure 2a). The effect was rapid in onset and reversible, except at concentrations ≥ 100 μM when recovery was slow and often incomplete. At the highest concentration tested (200 μM), ifenprodil reduced rises in $[Ca^{2+}]_i$ evoked by 50 mM K^+ by 98 ± 0.3% ($n = 81$), a result otherwise achieved in our experimental preparation only by omitting Ca^{2+} from the external medium or by the combined addition of nifedipine, ω-CgTx and crude funnel-web spider venom to Ca^{2+}-containing medium (see Church *et al.*, 1994). The latter finding suggests that ifenprodil is able to block Ca^{2+} flux through both nifedipine-sensitive and nifedipine-resistant HVA Ca^{2+} channels. To examine more closely the actions of ifenprodil against dihydropyridine-resistant HVA Ca^{2+} channels, it was applied in the presence of a maximally-effective concentration of nifedipine (10 μM; see Church *et al.*, 1994). Nifedipine 10 μM produced an 80 ± 1% reduction ($n = 101$) of high-$[K^+]_o$-evoked rises in $[Ca^{2+}]_i$; co-application of ifenprodil 1–50 μM reduced the residual nifedipine-resistant response in a concentration-dependent manner with an apparent IC_{50} of 12.6 ± 3.7 μM ($n > 90$ at each concentration tested; Figure 2b).

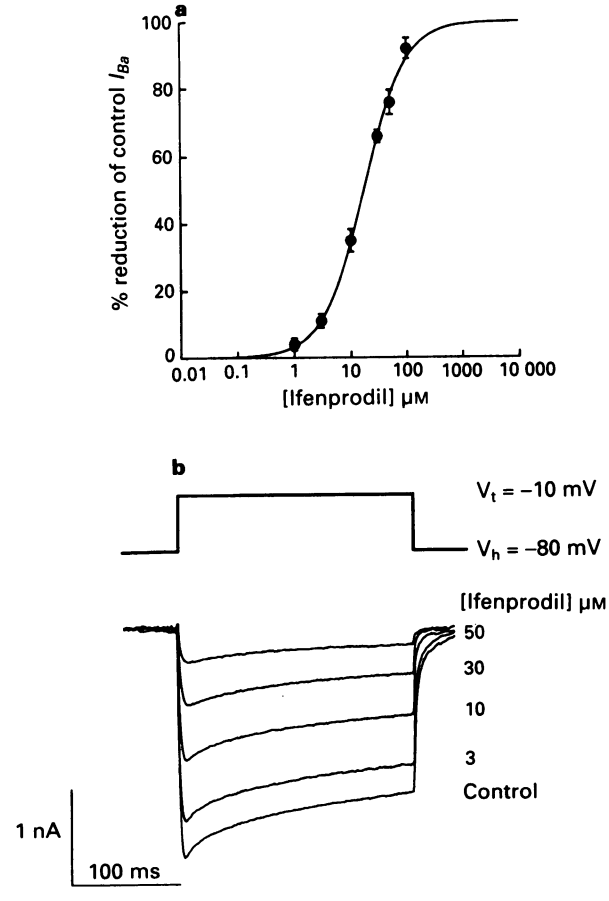


Figure 5 Ifenprodil blocks HVA I_{Ba} in hippocampal neurones. (a) Concentration-inhibition plot for ifenprodil as an antagonist of I_{Ba} evoked on a voltage step from a V_h of −80 mV to a V_t of −10 mV. Data points indicate mean ± s.e. mean for 8 neurones tested. Abscissa scale: concentration of ifenprodil in μM. Ordinate scale: % reduction of control I_{Ba}. (b) Sample traces of the ifenprodil block of control I_{Ba} evoked by the voltage step indicated above trace. Concentration of ifenprodil applied is indicated to the right of traces. Complete recovery was obtained (not shown). Calibration: current amplitude in nA; time in ms.

Ifenprodil may act, at least in part, at a polyamine-sensitive modulatory site on the NMDA receptor-channel complex to produce functional NMDA antagonism (see Introduction). Because polyamines also modulate the activity of neuronal L- and N-type HVA Ca^{2+} channels (Pullan *et al.*, 1990; Schoemaker, 1992; Scott *et al.*, 1993), we examined the effects of spermine and putrescine on high-$[K^+]_o$-evoked rises in $[Ca^{2+}]_i$ in both the absence and presence of ifenprodil 20 μM. Spermine alone, applied at 0.25, 0.5, 1 and 5 mM, produced a concentration-dependent reduction of high-$[K^+]_o$-evoked rises in $[Ca^{2+}]_i$; the respective percentage inhibitions from control values were 32 ± 1% ($n = 87$), 39 ± 2% ($n = 29$), 46 ± 2% ($n = 66$), and 64 ± 2% ($n = 46$). In contrast to a recent study on NE-115 mouse neuroblastoma cells (Herman *et al.*, 1993) putrescine, applied at 1 and 5 mM, also produced reductions in high-$[K^+]_o$-evoked rises in $[Ca^{2+}]_i$, although it was less effective than spermine in this regard (1 ± 1%, $n = 109$ and 27 ± 2%, $n = 34$ reductions by 1 and 5 mM putrescine, respectively). Spermine, but not putrescine, attenuated the inhibitory action of ifenprodil 20 μM against high-$[K^+]_o$-evoked rises in $[Ca^{2+}]_i$ (Figure 3). Thus ifenprodil 20 μM, applied in the absence or presence of spermine 0.25 mM, reduced high-$[K^+]_o$-evoked rises in $[Ca^{2+}]_i$ by 63 ± 1% and 54 ± 2%, respectively ($n = 70$, $P < 0.001$, Student's paired t test). Applied in the absence or presence of putrescine, ifenprodil 20 μM produced 66 ± 2 and 64 ± 2% (putrescine 1 mM; $n = 47$, not significant, Student's paired t test), and 65 ± 3 and 63 ± 2% (putrescine 5 mM; $n = 18$, not significant, Student's paired t test), reductions in high-$[K^+]_o$-evoked rises in $[Ca^{2+}]_i$ respectively.

Electrophysiological studies

Ifenprodil block of NMDA-evoked responses Superfusion of ifenprodil (0.1–100 μM) produced a reversible block of the steady-state currents evoked on 5 s applications of NMDA with an IC_{50} value of 0.80 ± 0.19 μM and a Hill coefficient of 0.53 ± 0.05 ($n = 7$; Figure 4a), comparable to the values reported by Legendre & Westbrook (1991) for the high affinity component of ifenprodil block of NMDA-evoked currents in rat cultured hippocampal pyramidal neurones. The NMDA antagonist action of ifenprodil (1 μM) was not competitive, producing a non-parallel shift in the NMDA concentration-response plot with a 50 ± 3% ($n = 5$) reduction of the maximum NMDA-evoked response without a change in the EC_{50} value for NMDA (data not shown). Antagonism of NMDA-evoked responses by ifenprodil (1 μM) was unaffected by changes in V_h over the range −100 mV to +60 mV ($n = 5$; not shown; see Legendre & Westbrook, 1991; Williams, 1993) and channel activation was not required for the development of block by ifenprodil. Ifenprodil inhibition of the steady-state component of the NMDA-evoked response was greater than that of the peak, as evidenced by the approximately 4 fold difference between the IC_{50} values for the two components (see Figure 4a). The IC_{50} value for the peak component was 2.8 ± 0.9 μM with a Hill coefficient 0.54 ± 0.06 ($n = 7$). The block of the steady-state NMDA-evoked responses by ifenprodil was not significantly altered on elevating the extracellular glycine con-

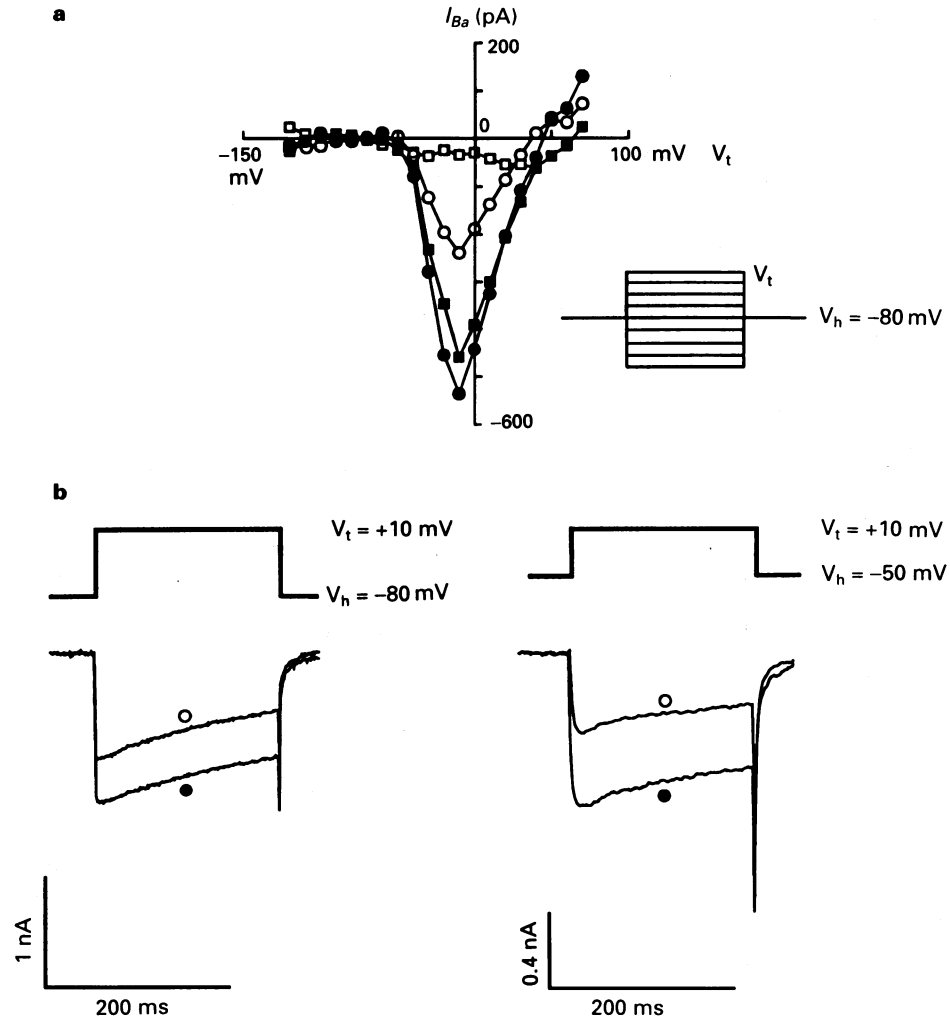


Figure 6 Voltage-dependence of ifenprodil block of I_{Ba}. (a) Ifenprodil does not affect the current-voltage relationship for I_{Ba}. Traces indicate the amplitude of I_{Ba} evoked on a 200 ms step from a V_h of -80 mV to V_t as indicated on abscissa scale. Control currents (●) were reduced by 10 (○) and 100 (□) μM ifenprodil with recovery (■) to control levels on wash. (b) On a second neurone, ifenprodil 10 μM (○) produced 43 and 50% reductions, respectively, of control I_{Ba} (●) evoked on voltage steps to +10 mV from a V_h of -80 mV (left) and -50 mV (right) as indicated above traces. Calibration: current amplitude in nA; time in ms.

centration; ifenprodil, 10 μM, reduced NMDA-evoked responses by 47 ± 5% and 47 ± 6% in the presence of 1 and 10 μM glycine, respectively (n = 6; not significant, Student's paired *t* test; see Legendre & Westbrook, 1991). The differential effect of ifenprodil on the peak and steady-state components of NMDA-evoked currents (see above) was also unaffected on elevation of the extracellular glycine concentration. Ifenprodil 100 μM attenuated kainate- and AMPA-evoked responses by, respectively, 20 ± 7% ($n = 6$) and 44 ± 6% ($n = 5$; Figure 4b), in contrast to its reported selectivity for NMDA at this concentration (Legendre & Westbrook, 1991). Superfusion with 100 μM spermine potentiated NMDA-evoked responses by 22 ± 6% (range 0–70%; $n = 17$; Figure 4c). The effect appeared to be optimal as lower concentrations of spermine (10 or 50 μM; $n = 4$ at each concentration) produced no additional potentiation and elevating the concentration above 100 μM resulted in attenuation of the control NMDA-evoked currents (see Williams *et al.*, 1991; cf. Rock & MacDonald, 1992). Irrespective of the amplitude of the polyamine-evoked potentiation of NMDA-evoked currents, the percentage reduction of control NMDA responses by ifenprodil 10 μM was increased on co-application of 100 μM spermine. In 14 out of 17 neurones tested there was a 50 ± 4% reduction of NMDA-evoked responses by 10 μM ifenprodil, which increased to a 64 ± 3% reduction of the new control response in the presence of 100 μM spermine ($P < 0.02$, Student's paired *t* test; Figure 4c). In the remaining 3 neurones no change in the inhibitory effect of ifenprodil was observed.

Ifenprodil block of I_{Ba} Inward barium currents evoked on voltage steps from a V_h of -80 mV to a V_t of -10 mV were concentration-dependently blocked by ifenprodil (0.1–100 μM). Ifenprodil reduced both the peak and delayed (240 ms following onset of the voltage step) components of I_{Ba} with an IC_{50} value of 17.8 ± 2.0 μM and a Hill coefficient of 1.2 ± 0.1 ($n = 8$; Figure 5), a value similar to that seen in the fluorescent dye studies for reduction of high-$[K^+]_o$-evoked rises in $[Ca^{2+}]_i$. The action of ifenprodil was rapid in onset and fully reversible on wash in control solution. At the highest concentrations tested (50 and 100 μM) there was almost complete attenuation of the whole-cell I_{Ba}, which we have shown previously to be comprised of both nifedipine-sensitive and nifedipine-resistant, ω-CgTx-sensitive components (Church *et al.*, 1994). Furthermore, in agreement with the microspectrofluorimetric studies (see above), ifenprodil 10 μM produced similar reductions of both the control I_{Ba} and that current remaining in the presence of a maximally-effective concentration (10 μM) of nifedipine (respec-

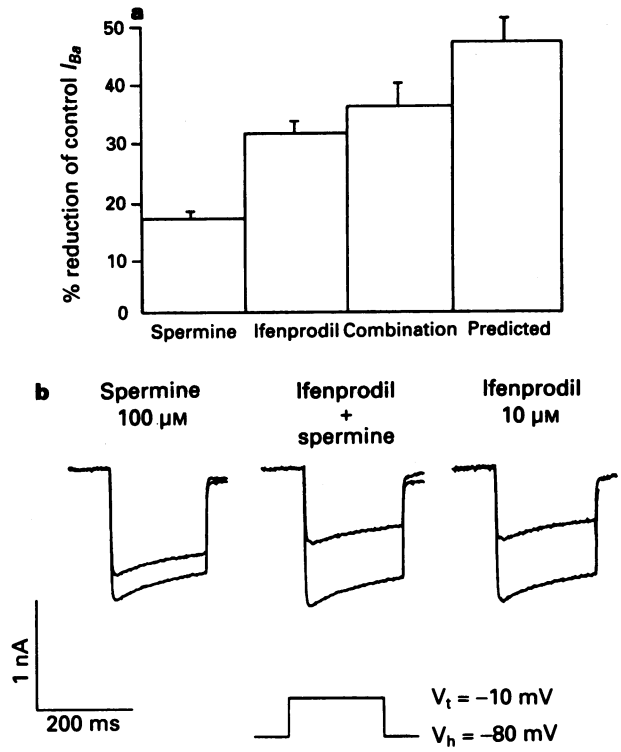


Figure 7 Interaction of the spermine and ifenprodil block of I_{Ba}. (a) Histogram indicates mean ± s.e. mean of the % reduction of control I_{Ba} by 100 μM spermine, 10 μM ifenprodil or a combination of the two on 8 neurones. An estimate of the predicted effect (the sum of the % reductions for spermine and ifenprodil) is shown at far right. Ordinate scale: % reduction of control I_{Ba}. (b) Sample traces of the I_{Ba} evoked following a 200 ms voltage step from a V_h of −80 mV to a V_t of −10 mV. Spermine (100 μM) reduced the I_{Ba} by 27%, which on co-application of 10 μM ifenprodil increased to a 48% block. Following wash, and recovery to control levels (not shown), application of 10 μM ifenprodil alone resulted in a 41% reduction of I_{Ba}. Calibration bars: current amplitude in nA; time in ms.

tively 38 ± 4% and 36 ± 4% reductions of I_{Ba} in the 5 neurones tested).

Ifenprodil 10 μM did not alter the current-voltage relationship for I_{Ba} ($n = 4$; Figure 6a) but an increase in the percentage reduction of the control I_{Ba} was observed when V_h was decreased from −80 mV to −50 mV (31 ± 3% and 53 ± 3% reduction, respectively, of controls in 10 neurones tested; $P < 0.05$, Student's paired t test; Figure 6b). The percentage block of I_{Ba} by ifenprodil, 10 μM, was also increased from 35 ± 3% to 46 ± 3% ($n = 10$) when the frequency of current activation was increased from 0.05 Hz to 0.2 Hz (not shown).

In agreement with previous studies (see Scott *et al.*, 1993), spermine attenuated HVA Ca^{2+} channel currents. Superfusion with 100 μM spermine produced a reversible 16 ± 3% reduction (range 8–27%, $n = 7$) of the control I_{Ba}. Superfusion of the same neurones with 10 μM ifenprodil produced a 33 ± 3% reduction (range 20–45%) of I_{Ba} which increased to a 37 ± 5% reduction (range 22–53%) during co-application of spermine 100 μM. The latter value is less than might be expected if the inhibitory effects of ifenprodil and spermine were additive (computed mean of combination, 48 ± 4%; see Figure 7).

Discussion

Ifenprodil blocks high-$[K^+]_o$-evoked rises in $[Ca^{2+}]_i$ and HVA Ca^{2+} channel currents in cultured hippocampal pyramidal neurones. The Ca^{2+} channel blocking action of ifenprodil described in the present study adds another element to the diverse pharmacological profile of this compound, which encompasses interactions with the NMDA receptor-channel complex and σ binding sites (see below), as well as α-adrenoceptors (Honda *et al.*, 1988; Chenard *et al.*, 1991). The concentrations of ifenprodil effective at blocking neuronal HVA Ca^{2+} channels are similar to those which attenuate responses mediated by voltage-activated Ca^{2+} channels in smooth muscle (e.g. Adeagbo & Magbagbeola, 1985; Honda & Sakai, 1987; Honda *et al.*, 1988). Although the mechanism whereby ifenprodil blocks HVA Ca^{2+} channels remains unclear, some aspects of this action (i.e. voltage- and frequency-dependence) are reminiscent of the effect of dihydropyridines such as nifedipine (see Bertolino & Llinás, 1992). In contrast to nifedipine, however, ifenprodil is able to block completely I_{Ba} and high-$[K^+]_o$-evoked rises in $[Ca^{2+}]_i$ in our neuronal preparations (see Church *et al.*, 1994). In this regard, ifenprodil shows similarities to the phenylalkylamine (e.g. verapamil) and piperazine (e.g. flunarizine) classes of Ca^{2+} channel blockers, which can also inhibit Ca^{2+} flux through dihydropyridine-insensitive Ca^{2+} channels (e.g. Mangano *et al.*, 1991; Tytgat *et al.*, 1991; Bowman *et al.*, 1993). Interestingly, ifenprodil has been found to inhibit KCl-stimulated $^{45}Ca^{2+}$ uptake into rat brain synaptosomes (a dihydropyridine- and ω-CgTx-resistant response; see Mintz *et al.*, 1992) at concentrations associated in the present study with dihydropyridine-insensitive HVA Ca^{2+} channel blockade (Honda *et al.*, 1989).

Polyamines have been suggested to act as modulators of neuronal L- and N-type HVA Ca^{2+} channels (reviewed by Scott *et al.*, 1993). For example, spermine allosterically inhibits [^{3}H]-nitrendipine binding to L-type Ca^{2+} channels in rat cortical membranes with an EC_{50} value of 260 μM (Schoemaker, 1992) and inhibits the binding of [^{125}I]-ω-CgTx to N-type Ca^{2+} channels in rat hippocampal synaptosomes with an IC_{50} value of 9 μM (Pullan *et al.*, 1990). In the present experiments, spermine inhibited high-$[K^+]_o$-evoked rises in $[Ca^{2+}]_i$ and I_{Ba}, a result in accordance with previous voltage-clamp data obtained in dorsal root ganglion neurones (Scott *et al.*, 1993). However, in contrast to the differing potencies of spermine as a modulator at L- and N-type HVA Ca^{2+} channels (see above), in the present experiments ifenprodil appeared equally efficacious as a blocker of HVA Ca^{2+} channel-mediated responses recorded in either the presence or absence of nifedipine. It seems unlikley that ifenprodil modulates HVA Ca^{2+} channel activity in a manner completely analogous to polyamines, although some overlap of their site(s) of action may exist, given the ability of spermine (but not putrescine) to modulate the Ca^{2+} channel blocking action of ifenprodil.

Ifenprodil has nanomolar affinity for σ binding sites in the central nervous system, the pharmacological profile of which is similar to that of σ_2, rather than σ_1, sites (see Benavides *et al.*, 1992; Hashimoto & London, 1993). Although binding studies have suggested a possible association of σ receptors with voltage-activated Ca^{2+} channels (Rothman *et al.*, 1991) and a variety of other σ ligands also block neuronal HVA Ca^{2+} channels (Church & Fletcher, unpublished observations; also Mangano *et al.*, 1991; Netzer *et al.*, 1993), the affinities of these compounds for σ binding sites are much higher than the concentrations associated with their HVA Ca^{2+} channel blocking actions. The Ca^{2+} channel blocking properties of ifenprodil are therefore unlikely to be mediated via interactions with σ binding sites.

The potency and mechanism of the NMDA antagonist action of ifenprodil has been extensively investigated (reviewed by Carter *et al.*, 1991; Wong & Kemp, 1991) and it was not our intention to replicate the data here. Nevertheless, in our hands, ifenprodil attenuated NMDA-evoked responses at concentrations that are in good agreement with a previous study on rat cultured hippocampal neurones (IC_{50} for block of high affinity component = 0.75 μM; Legendre & Westbrook, 1991). In addition, ifenprodil antagonism of NMDA-evoked

responses did not involve interactions with the agonist or strychnine-insensitive glycine binding sites and the absence of use- and voltage-dependency of the ifenprodil block argues against an open-channel blocking mechanism (see Legendre & Westbrook, 1991). Binding profiles employing [^{3}H]-dizocilpine indicate that ifenprodil may act as a closed-channel blocker (Reynolds & Miller, 1989); electrophysiological correlates of this mechanism could include the ifenprodil-induced modal shift in NMDA channel gating (Legendre & Westbrook, 1991) and, as observed here, its higher affinity for the steady-state (i.e. predominantly desensitized) component of the NMDA-evoked response. Indeed, the observed potentiation of the ifenprodil block by spermine highlights the sensitivity of the ifenprodil block to the state of activation of the NMDA receptor-channel complex and argues against a simple competitive interaction between these two ligands (see Reynolds & Miller, 1989; Bakker *et al.*, 1991). Finally, molecular cloning techniques have revealed the heterologous nature of NMDA receptors (Moriyoshi *et al.*, 1991; Monyer *et al.*, 1992) and studies on recombinant heteromeric NMDA receptors have indicated that they differ in their sensitivity to, and mechanism of antagonism by, ifenprodil (Williams, 1993) and polyamines (Durand *et al.*, 1992). Although it is likely that the NMDA-evoked responses observed in the present study are a composite of activation of a mixed population of NMDA receptors, it is of interest that the IC_{50} value for NMDA antagonism by ifenprodil and the absence of use- and voltage-dependency of the ifenprodil block (but not its insensitivity to glycine) is similar to the reported effects of ifenprodil at NR1A/NR2B, rather than NR1A/NR2A, receptors (see Williams, 1993).

The ability of ifenprodil to block multiple subtypes of HVA Ca^{2+} channels may play a role in its neuroprotective and anticonvulsant actions. In particular, the ability of ifenprodil to block dihydropyridine-insensitive HVA Ca^{2+} channels may be associated with reduced excitatory transmitter release (see Bertolino & Llinás, 1992; Luebke *et al.*, 1993), as has been shown for compounds such as dextromethorphan (Annels *et al.*, 1991; Mangano *et al.*, 1991; Netzer *et al.*, 1993) and flunarizine (Tytgat *et al.*, 1991; Bowman *et al.*, 1993; Cousin *et al.*, 1993), both of which also possess neuroprotective and anticonvulsant efficacy *in vivo* (e.g. Deshpande & Wieloch, 1986; Prince & Feeser, 1988; Czuczwar *et al.*, 1992; Löscher & Hönack, 1993). In addition, ifenprodil has been reported to be only 3 fold lower in potency as an antagonist of audiogenic seizures in genetically epilepsy-prone rats than dizocilpine (De Sarro & De Sarro, 1993), despite the fact that dizocilpine is at least 80 fold more potent as an NMDA antagonist than ifenprodil when assessed under voltage-clamp conditions (see MacDonald *et al.*, 1991). The discrepancy between the NMDA antagonist potencies of ifenprodil and dizocilpine compared with their similar anticonvulsant activities might reflect, at least in part, the more pronounced Ca^{2+} channel blocking actions of ifenprodil compared to dizocilpine (IC_{50} for block of Ca^{2+} channel current by dizocilpine in dissociated guinea-pig CA1 pyramidal neurones = 63 μM; ffrench-Mullen & Rogawski, 1992).

Software for the analysis of the microspectrofluorimetric data was developed by Dr K. Abdel-Hamid, to whom we are grateful. The study was supported by Operating Grants from the Medical Research Council of Canada to J.C. and J.F.M. J.C. is a Scholar of the British Columbia Health Research Foundation and E.J.F. is a Fellow of the Medical Research Council of Canada.

References

ADEAGBO, A.S.O. & MAGBAGBEOLA, A.O. (1985). Pharmacological actions of ifenprodil in the rat isolated anococcygeus muscle. *J. Pharm. Pharmacol.*, **37**, 833–835.

ANNELS, S.J., ELLIS, Y. & DAVIES, J.A. (1991). Non-opioid antitussives inhibit endogenous glutamate release from rabbit hippocampal slices. *Brain Res.*, **564**, 341–343.

ARANEDA, R.C., ZUKIN, R.S. & BENNETT, M.V.L. (1993). Effects of polyamines on NMDA-induced currents in rat hippocampal neurones: a whole-cell and single-channel study. *Neurosci. Lett.*, **152**, 107–112.

BAKKER, M.H.M., MCKERNAN, R.M., WONG, E.H.F. & FOSTER, A.C. (1991). [^{3}H]MK-801 binding to N-methyl-D-aspartate receptors solubilized from rat brain: effects of glycine site ligands, polyamines, ifenprodil and desipramine. *J. Neurochem.*, **57**, 39–45.

BENAVIDES, J., PENY, B., ALLEN, J. & SCATTON, B. (1992). Pharmacological characterization of in vivo [^{3}H]ifenprodil binding sites in the mouse brain. *J. Pharmacol. Exp. Ther.*, **260**, 896–901.

BENVENISTE, M. & MAYER, M.L. (1993). Multiple effects of spermine on N-methyl-D-aspartic acid receptor responses of rat cultured hippocampal neurones. *J. Physiol.*, **464**, 131–163.

BERTOLINO, M. & LLINÁS, R.R. (1992). The central role of voltage-activated and receptor-operated calcium channels in neuronal cells. *Annu. Rev. Pharmacol. Toxicol.*, **32**, 399–421.

BOWMAN, D., ALEXANDER, S. & LODGE, D. (1993). Pharmacological characterization of the calcium channels coupled to the plateau phase of KCl-induced intracellular free Ca^{2+} elevation in chicken and rat synaptosomes. *Neuropharmacology*, **32**, 1195–1202.

CARTER, C., BENAVIDES, J., DANA, C., SCHOEMAKER, H., PERRAULT, G., SANGER, D. & SCATTON, B. (1991). Non-competitive NMDA receptor antagonists acting on the polyamine site. In *Excitatory Amino Acid Antagonists*. ed. Meldrum, B.S. pp. 130–163. Oxford: Blackwell Scientific Publications.

CHENARD, B.L., SHALABY, I.A., KOE, B.K., RONAU, R.T., BUTLER, T.W., PROCHNIAK, M.A., SCHMIDT, A.W. & FOX, C.B. (1991). Separation of α_1-adrenergic and N-methyl-D-aspartate antagonist activity in a series of ifenprodil compounds. *J. Med. Chem.*, **34**, 3085–3090.

CHURCH, J., FLETCHER, E.J., ABDEL-HAMID, K. & MACDONALD, J.F. (1994). Loperamide blocks high-voltage-activated calcium channels and N-methyl-D-aspartate-evoked responses in rat and mouse cultured hippocampal pyramidal neurons. *Mol. Pharmacol.*, **45**, 747–757.

COUSIN, M.A., NICHOLLS, D.G. & POCOCK, J.M. (1993). Flunarizine inhibits both calcium-dependent and -independent release of glutamate from synaptosomes and cultured neurones. *Brain Res.*, **606**, 227–236.

CZUCZWAR, S.J., GASIOR, M., JANUSZ, W. & KLEINROK, Z. (1992). Influence of flunarizine, nicardipine and nimodipine on the anticonvulsant activity of different antiepileptic drugs in mice. *Neuropharmacology*, **31**, 1179–1183.

DE SARRO, G.B. & DE SARRO, A. (1993). Anticonvulsant properties of non-competitive antagonists of the N-methyl-D-aspartate receptor in genetically epilepsy-prone rats: comparison with CPPene. *Neuropharmacology*, **32**, 51–58.

DESHPANDE, J.K. & WIELOCH, T. (1986). Flunarizine, a calcium entry blocker, ameliorates ischemic brain damage in the rat. *Anesthesiology*, **64**, 215–224.

DURAND, G.M., GREGOR, P., ZHENG, X., BENNETT, M.V.L., UHL, G.R. & ZUKIN, R.S. (1992). Cloning of an apparent splice variant of the rat N-methyl-D-aspartate receptor NMDAR1 with altered sensitivity to polyamines and activators of protein kinase C. *Proc. Natl. Acad. Sci. USA*, **89**, 9359–9363.

FFRENCH-MULLEN, J.M.H. & ROGAWSKI, M.A. (1992). Phencyclidine block of calcium current in isolated guinea-pig hippocampal neurones. *J. Physiol.*, **456**, 85–105.

GRYNKIEWICZ, G., POENIE, M. & TSIEN, R.Y. (1985). A new generation of Ca^{2+} indicators with greatly improved fluorescence properties. *J. Biol. Chem.*, **260**, 3440–3450.

HASHIMOTO, K. & LONDON, E.D. (1993). Further characterization of [^{3}H]ifenprodil binding to σ receptors in rat brain. *Eur. J. Pharmacol.*, **236**, 159–163.

HEINEMANN, U. & HAMON, B. (1986). Calcium and epileptogenesis. *Exp. Brain Res.*, **65**, 1–10.

HERMAN, M.D., REUVENY, E. & NARAHASHI, T. (1993). The effect of polyamines on voltage-activated calcium channels in mouse neuroblastoma cells. *J. Physiol.*, **462**, 645–660.

HONDA, H. & SAKAI, Y. (1987). The mode of action of ifenprodil tartate in isolated canine cerebral and femoral arteries. *Arch. Int. Pharmacodyn.*, **285**, 211–225.

HONDA, H., SAKAI, Y., IWATA, T., OHBA, S., KANEZUKA, T. & IRINO, O. (1988). Effects of ifenprodil tartrate on α-adrenoceptors and Ca^{2+} movement in isolated canine saphenous veins. *Arch. Int. Pharmacodyn.*, **292**, 112–121.

HONDA, H., SHIBUYA, T. & SALAFSKY, B. (1989). Effects of ifenprodil tartrate on calcium flux in arteries and brain synaptosomes. *Proc. West. Pharmacol. Soc.*, **32**, 155–158.

LEGENDRE, P. & WESTBROOK, G.L. (1991). Ifenprodil blocks N-methyl-D-aspartate receptors by a two-component mechanism. *Mol. Pharmacol.*, **40**, 289–298.

LÖSCHER, W. & HÖNACK, D. (1993). Differences in anticonvulsant potency and adverse effects between dextromethorphan and dextrorphan in amygdala-kindled and non-kindled rats. *Eur. J. Pharmacol.*, **238**, 191–200.

LUEBKE, J.I., DUNLAP, K. & TURNER, T.J. (1993). Multiple calcium channel types control glutamatergic synaptic transmission in the hippocampus. *Neuron*, **11**, 895–902.

MACDONALD, J.F., BARTLETT, M.C., MODY, I., PAHAPILL, P., REYNOLDS, J.N., SALTER, M.W., SCHNEIDERMAN, J.H. & PENNEFATHER, P.S. (1991). Actions of ketamine, phencyclidine and MK-801 on NMDA receptor currents in cultured mouse hippocampal neurones. *J. Physiol.*, **432**, 483–508.

MACDONALD, J.F., MODY, I. & SALTER, M.W. (1989). Regulation of N-methyl-D-aspartate receptors revealed by intracellular dialysis of murine neurones in culture. *J. Physiol.*, **414**, 17–34.

MANGANO, T.J., PATEL, J., SALAMA, A.I. & KEITH, R.A. (1991). Inhibition of K^+-evoked [^{3}H]D-aspartate release and neuronal calcium influx by verapamil, diltiazem and dextromethorphan: evidence for non-L/non-N voltage-sensitive calcium channels. *Eur. J. Pharmacol.*, **192**, 9–17.

MINTZ, I.M., VENEMA, V.J., SWIDEREK, K.M., LEE, T.D., BEAN, B.P. & ADAMS, M.E. (1992). P-type calcium channels blocked by the spider toxin ω-Aga-IVA. *Nature*, **355**, 827–829.

MONYER, H., SPRENGEL, R., SCHOEPFER, R., HERB, A., HIGUCHI, M., LOMELI, H., BURNASHEV, N., SAKMANN, B. & SEEBURG, P.H. (1992). Heteromeric NMDA receptors: molecular and functional distinction of subtypes. *Science*, **256**, 1217–1221.

MORIYOSHI, K., MASU, M., ISHI, T., SHIGEMOTO, R., MIZUNO, N. & NAKANISHI, S. (1991). Molecular cloning and characterization of the rat NMDA receptor. *Nature*, **354**, 31–37.

NETZER, R., PFLIMIN, P. & TRUBE, G. (1993). Dextromethorphan blocks N-methyl-D-aspartate-induced currents and voltage-operated inward currents in cultured cortical neurons. *Eur. J. Pharmacol.*, **238**, 209–216.

OTOMO, E. & KODAMA, R. (1976). Double blind study of FX-505 (ifenprodil) on cerebrovascular disease. *Clin. Eval.*, **4**, 419–458.

PRINCE, D.A. & FEESER, H.R. (1988). Dextromethorphan protects against cerebral infarction in a rat model of hypoxia-ischemia. *Neurosci. Lett.*, **85**, 291–296.

PULLAN, L.M., KEITH, R.A., LAMONTE, D., STUMPO, R.J. & SALAMA, A.I. (1990). The polyamine spermine affects ω-conotoxin binding and function at N-type voltage-sensitive calcium channels. *J. Auton. Pharmacol.*, **10**, 213–219.

RANSOM, R.W. & STEC, N.L. (1988). Cooperative modulation of [^{3}H]MK-801 binding to the N-methyl-D-aspartate receptor-ion channel complex by L-glutamate, glycine, and polyamines. *J. Neurochem.*, **51**, 830–836.

REYNOLDS, I.J. & MILLER, R.J. (1989). Ifenprodil is a novel type of N-methyl-D-aspartate receptor antagonist: interaction with polyamines. *Mol. Pharmacol.*, **36**, 758–765.

ROCK, D.M. & MACDONALD, R.L. (1992). The polyamine spermine has multiple actions on N-methyl-D-aspartate receptor single-channel currents in cultured cortical neurons. *Mol. Pharmacol*, **41**, 83–88.

ROTHMAN, R.B., REID, A., MAHBOUBI, A., KIM, C.-H., DE COSTA, B.R., JACOBSON, A.E. & RICE, K.C. (1991). Labeling by [^{3}H]1,3-Di(2-tolyl)guanidine of two high affinity binding sites in guinea pig brain: evidence for allosteric regulation by calcium channel antagonists and pseudoallosteric modulation by σ ligands. *Mol. Pharmacol.*, **39**, 222–232.

SCHOEMAKER, H. (1992). Polyamines allosterically modulate [^{3}H]nitrendipine binding to the voltage-sensitive calcium channel in rat brain. *Eur. J. Pharmacol.*, **225**, 167–169.

SCHOEMAKER, H., ALLEN, J. & LANGER, S.Z. (1990). Binding of [^{3}H]ifenprodil, a novel NMDA antagonist, to a polyamine-sensitive site in the rat cerebral cortex. *Eur. J. Pharmacol.*, **176**, 249–250.

SCOTT, R.H., SUTTON, K.G. & DOLPHIN, A.C. (1993). Interaction of polyamines with neuronal ion channels. *Trends Neurosci.*, **16**, 153–160.

SIESJÖ, B.K. & BENGTSSON, F. (1989). Calcium fluxes, calcium antagonists, and calcium-related pathology in brain ischemia, hypoglycemia, and spreading depression: a unifying hypothesis. *J. Cereb. Blood Flow Metabol.*, **9**, 127–140.

TYTGAT, J., PAUWELS, P.J., VEREECKE, J. & CARMELIET, E. (1991). Flunarizine inhibits a high-threshold inactivating calcium channel (N-type) in isolated hippocampal neurons. *Brain Res.*, **549**, 112–117.

WILLIAMS, K. (1993). Ifenprodil discriminates subtypes of the N-methyl-D-aspartate receptor: selectivity and mechanisms at recombinant heteromeric receptors. *Mol. Pharmacol.*, **44**, 851–859.

WILLIAMS, K., ROMANO, C., DICHTER, M.A. & MOLINOFF, P.B. (1991). Modulation of the NMDA receptor by polyamines. *Life Sci.*, **48**, 469–498.

WONG, E.H.F. & KEMP, J.A. (1991). Sites for antagonism on the N-methyl-D-aspartate receptor channel complex. *Annu. Rev. Pharmacol. Toxicol.*, **31**, 401–425.

(Received March 23, 1994
Revised May 9, 1994
Accepted June 1, 1994)

Br. J. Pharmacol (1994), **113**, 508–512 © Macmillan Press Ltd, 1994

Role of kinins in anaphylactic-induced bronchoconstriction mediated by tachykinins in guinea-pigs

Fabio L.M. Ricciardolo, *†Jay A. Nadel, Paul D. Graf, [2]Claude Bertrand, Shigemi Yoshihara & [1]Pierangelo Geppetti

Cardiovascular Research Institute and the Departments of *Medicine and †Physiology, University of California San Francisco, California, U.S.A.

1 In the present study, we have investigated the role of kinins in allergen-induced bronchoconstriction.

2 Anaesthetized guinea-pigs were sensitized to ovalbumin, ventilated artificially, pretreated with atropine (1.4 μmol kg^{-1}, i.v.) and total pulmonary resistance (R_L) measured. In preliminary studies in the presence of the neutral endopeptidase inhibitor, phosphoramidon (4.5 μmol kg^{-1}, i.v.), the bradykinin B_2 receptor antagonist Hoe 140 (0.1 μmol kg^{-1}, i.v.) completely abolished the increase in R_L following aerosolized bradykinin (1 mM, 40 breaths), but had no effect on the increase in R_L following aerosolized neurokinin A (NKA, 10 μM, 40 breaths). On the other hand, a combination of the NK_1 (CP-96,345, 2 μmol kg^{-1}, i.v.) and NK_2 (SR 48968, 0.3 μmol kg^{-1}, i.v.) tachykinin receptor antagonists abolished completely the increase in R_L produced by NKA and partially inhibited the increase in R_L produced by bradykinin. These results confirm previous studies that suggest that bradykinin induces the release of tachykinins from sensory nerves in guinea-pig airways.

3 Aerosolized ovalbumin (0.5%, 5 breaths) increased R_L in sensitized guinea-pigs pretreated with atropine (1.4 mmol kg^{-1}, i.v.), an effect that began within 2 min and reached a maximum within 5 min; R_L remained above baseline at 20 min. Pretreatment with the bradykinin B_2 receptor antagonist, Hoe 140, decreased the bronchoconstrictor effect of ovalbumin markedly at 10 to 20 min. In the presence of phosphoramidon (4.5 μmol kg^{-1}, i.v.) the inhibition induced by Hoe 140 was apparent earlier and remained over the 20 min period of study.

4 Pretreatment with a combination of NK_1 (CP-96,345) and NK_2 (SR 48968) tachykinin receptor antagonists also markedly inhibited ovalbumin-induced bronchoconstriction; addition of the bradykinin B_2 receptor antagonist to the NK_1 and NK_2 tachykinin receptor antagonists had no additional inhibitory effect on antigen-induced bronchoconstriction.

5 These findings confirm that activation of sensory nerves to release tachykinins in guinea-pig airways contribute to antigen-induced bronchoconstriction, and provide evidence that tachykinin release is due to kinins generated during the allergic response.

Keywords: Kinins; tachykinins; receptors; neurogenic inflammation; allergen challenge; bronchoconstriction; sensory nerves; Hoe 140; SR 48968; CP-96,345.

Introduction

Stimulation of a subpopulation of sensory nerves causes the release of neuropeptides, including the tachykinins substance P (SP) and neurokinin A (NKA), from their peripheral terminals. This release produces a series of effects collectively referred to as 'neurogenic inflammation', which in the airways includes plasma extravasation and bronchconstriction (Lundberg & Saria, 1983; Lundberg *et al.*, 1984; Barnes, 1986; Nadel, 1991). Plasma extravasation and bronchconstriction are effects produced by exposure to antigen in sensitized animals. Recently, we showed that tachykinins released from sensory nerve endings (via activation of NK_2 and NK_1 tachykinin receptors) play an important role in antigen-induced plasma extravasation and bronchoconstriction in sensitized guinea-pigs (Bertrand *et al.*, 1993a,b). As there is no evidence that the antigen-antibody complex *per se* activates sensory nerves, we reasoned that mediators released from tissue, inflammatory cells or plasma may be involved in the antigen-evoked stimulation of sensory nerves.

Kinins, including bradykinin, derived from a plasma precursor, and kallidin released from a tissue precursor, have been proposed to take part in the allergic inflammatory response because increased kinin levels have been detected in immediate and late phase reactions in experimental animals (Erjefalt *et al.*, 1993) and in man (Christiansen *et al.*, 1992). Bradykinin antagonists have been found to reduce the late bronchial response (Abraham *et al.*, 1991) and the hyperresponsiveness (Farmer *et al.*, 1992) that occurs after exposure to antigen. Bradykinin potently stimulates primary sensory neurones (Kaufman *et al.*, 1980) and releases neuropeptides from their peripheral endings in different tissues, including the airways (Geppetti *et al.*, 1988; Saria *et al.*, 1988; Geppetti, 1993). Kinins released upon exposure to antigen play an important role in the activation of sensory nerves, which contribute substantially to the antigen-evoked plasma extravasation in guinea-pigs (Bertrand *et al.*, 1993d).

In the present study, we investigated whether bronchoconstriction in response to antigen and mediated by activation of sensory nerves is due to release of kinins. To test this hypothesis, we used Hoe 140, a selective and potent peptide antagonist of B_2 bradykinin receptors (Hock *et al.*, 1991), because this compound completely prevents the bronchoconstriction evoked by aerosolized or intravenously injected bradykinin in guinea-pigs (Wirth *et al.*, 1993). The effect of Hoe 140 on antigen-induced bronchoconstriction was compared to the effect produced by the combination of nonpeptide antagonists of NK_2 (SR 48968) (Emonds-Alt *et al.*, 1992) and NK_1 (CP-96,345) (Snider *et al.*, 1991) tachykinin recep-

[1] Author for correspondence at present address: Laboratory of Clinical Pharmacology and Institute of Internal Medicine IV, University of Florence, Viale Pieraccini 6, 50139 Florence, Italy.
[2] Present address: Ciba-Geigy A.G., Pulmonary Pharmacology, Pharma Division, R-1056.2.15, CH-4002, Basel, Switzerland.

tors. The combination of NK_1 and NK_2 tachykinin receptor antagonists was used because this combination is necessary to block completely the bronchoconstriction induced by tachykinins released by capsaicin in guinea-pigs *in vivo* (Bertrand *et al.*, 1993c). Some experiments were performed in animals pretreated with phosphoramidon, because previous studies (Bertrand *et al.*, 1993a,b) showed that blockade of neutral endopeptidase (NEP) activity by phosphoramidon increases the sensory nerve-mediated responses to antigen.

Methods

Animals

Male Hartley guinea-pigs (Simonsen Laboratories Inc., Gilroy, CA, U.S.A) that weighed 250–300 g at the time of housing, were used in this study. They were kept in a temperature-controlled environment with standard laboratory food and water freely available.

Sensitization procedure

Animals were sensitized according to a protocol described previously (Dunn *et al.*, 1988; Bertrand *et al.*, 1993a). Sensitization consisted of two separate injections of 70 mg ovalbumin (Grade V) in 1.5 ml 0.9% NaCl intraperitoneally, with an interval of one week between the injections. The animals were studied two weeks after the second injection. Non-sensitized (control) animals were injected twice with 1.5 ml 0.9% NaCl.

Measurement of total pulmonary resistance (R_L)

Animals were anaesthetized using sodium pentobarbitone (45 mg kg^{-1}, i.p.; Anthony Product Corp., Arcadia, CA, U.S.A.) and then ventilated artificially with a tracheal cannula, using a constant-volume ventilator (model 683; Harvard Apparatus Co., Inc., South Natick, MA, U.S.A.) at a frequency of 80 breaths min^{-1}. The tidal volume was adjusted to maintain normal arterial blood gases as described previously (Dusser *et al.*, 1988). Airflow was monitored continuously with a pneumotachograph (A. Fleisch, Medical Inc., Richmond, VA, U.S.A.) connected to a differential pressure transducer (model DP45; Validyne Engineering Corp., Northrige, CA, U.S.A.). A fluid-filled polyethylene catheter was introduced into the oesophagus to measure the oesophageal pressure as an approximation of pleural pressure. Intratracheal pressure was measured with a polyethylene catheter inserted into a short tube connecting the tracheal cannula to the pneumotachograph. The transpulmonary pressure (defined as the pressure difference between the intratracheal and oesophageal pressures) was measured with a differential pressure transducer (model DP7; Validyne Engineering Corp.). Output signals representing transpulmonary pressure and airflow were amplified with an amplifier (model CD19; Validyne Engineering Corp.) and recorded on a polygraph recorder (model 1508 B Visicorder; Honeywell, Inc., Denver, CO, U.S.A.). R_L was calculated as described previously (Dusser *et al.*, 1988). The right jugular vein and the left carotid artery were cannulated to permit administration of drugs and to withdraw a sample of blood for arterial blood gas measurement.

Experimental design

Baseline R_L remained stable for at least 2 h, and no significant changes were produced by aerosols (5 breaths or 40 breaths) or i.v. injection (1 ml kg^{-1}) of 0.9% NaCl after a stabilization period of 30 min. Aerosols of saline or antigen (ovalbumin 0.5%; 5 breaths) were generated by an ultrasonic nebulizer (model 25, DeVilbiss, Somerset, PA) and were delivered into the airways by the respirator via the tracheal cannula (aerosol delivery rate, 0.2 ml min^{-1}). All animals were pretreated with atropine (1.4 μmol kg^{-1}, i.v., 15 min before the stimulus). Phosphoramidon (4.5 μmol kg^{-1}, i.v.) was given 5 min before the stimulus.

Drugs

Ovalbumin, atropine and histamine were obtained from Sigma Chemical (St. Louis, MO, U.S.A.). Phosphoramidon, bradykinin and NKA were purchased from Peninsula Laboratories, Inc. (Belmont, CA, U.S.A.). CP-96,345 ((2S,3S) cis-2-(diphenylmethyl)-N-((2-methoxy-phenyl)-methyl)-1-azabicyclo[2.2.2]octan-3-amine) and SR 48968 (S)-N-methyl-N([4-(-acetyl-amino-4-phenylpiperidino)-2-(3,4dichlorophenylbutyl] benzamide) were kindly provided by Dr J.A. Lowe III (Pfizer Inc, Groton, CT, U.S.A.) and Dr X. Emonds-Alt (Sanofi Recherche, Montpellier, France), respectively. Hoe 140 (D-Arg-[Hyp^3,$This^5$,D-Tic^7,Oic^8]-bradykinin) was a kind gift of Dr F.J. Hock (Hoechst AG, Frankfurt, Germany). Drugs were dissolved in 0.9% saline or in dimethyl sulphoxide (Hoe 140 and SR 48.968). Further dilutions were made in 0.9% saline.

Statistical analysis

Values in the text and figures are the mean ± standard error of the mean (s.e.mean). Statistical comparisons were performed by a one way analysis of variance and Dunnett's test or bilateral unpaired Student's *t* test, when appropriate. In all cases, a P value of less than 0.05 was considered significant.

Results

Aerosolized bradykinin (1 mM, 40 breaths) increased R_L approximately 2 fold above baseline value, and the bradykinin B_2 receptor antagonist Hoe 140 (0.1 μmol kg^{-1}, i.v., 15 min before the stimulus) abolished the bronchoconstriction completely (Figure 1b) in guinea-pig pretreated with atropine (1.4 μmol kg^{-1}) and phosphoramidon (4.5 μmol kg^{-1}). A combination of NK_2 (SR 48968, 0.3 μmol kg^{-1}, i.v., 15 min before the stimulus) and NK_1 (CP-96,345, 2 μmol kg^{-1} i.v., 5 min before the stimulus) tachykinin receptor antagonists decreased the bradykinin-induced increase in R_L by approximately 60% (Figure 1b). Aerosolized NKA (10 μM, 40 breaths) increased R_L more than 3 fold above baseline value, an effect that was not changed by pretreatment with Hoe 140 (0.1 μmol kg^{-1}, i.v.), but was abolished completely by the combination of NK_2 (SR 48968, 0.3 μmol kg^{-1} i.v.) and NK_1 (CP-96,345, 2 μmol kg^{-1} i.v.) tachykinin antagonists (Figure 1a).

Aerosols of the vehicle of ovalbumin (0.9% NaCl, 5 breaths) did not increase R_L significantly over the 20 min period of study in guinea-pigs sensitized to ovalbumin (data not shown). However, aerosolized ovalbumin (0.5%, 5 breaths) increased R_L approximately 2 fold above baseline value in the sensitized guinea-pigs: the increase in R_L was evident within 2 min after exposure, reached a maximum within 5 min, and R_L was still increased above baseline after 20 min (Figure 2a). Pretreatment with the bradykinin B_2 receptor antagonist Hoe 140 (0.1 μmol kg^{-1}, i.v.) decreased the bronchoconstrictor effect of aerosolized ovalbumin at 10, 15 and 20 min after the delivery of ovalbumin. When the guinea-pigs were pretreated with phosphoramidon (4.5 μmol kg^{-1}, i.v.), a selective inhibitor of NEP, the increase in R_L after inhalation of ovalbumin was not significantly greater than the increase obtained in the absence of phosphoramidon (Figure 2a,b). In the presence of phosphoramidon Hoe 140 still decreased markedly the ovalbumin-induced increase in R_L (Figure 2b): a significant inhibition by Hoe 140 of the ovalbumin-induced bronchoconstriction was found as early as 3 min and remained at 20 min (Figure 2b).

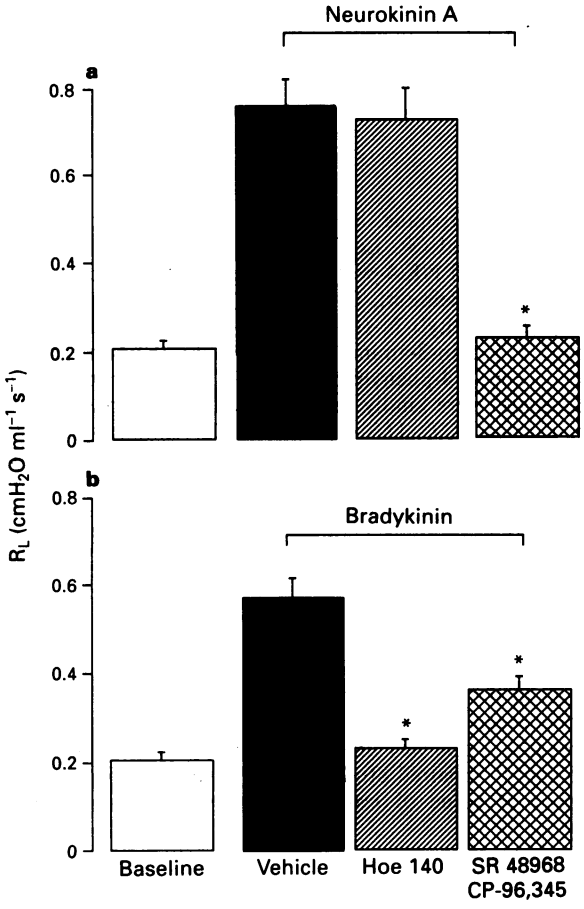


Figure 1 Effect of the bradykinin B_2 receptor antagonist (Hoe 140; 0.1 μmol kg^{-1}, i.v., given 15 min before the stimulus) (hatched column), or the combination of tachykinin NK_2 (SR 48968; 0.3 μmol kg^{-1}, i.v., given 15 min before stimulus) and NK_1 (CP-96,345; 2 μmol kg^{-1}, i.v., given 5 min before stimulus) receptor antagonists (cross-hatched column) on the maximal increase in total pulmonary resistance (R_L evoked) by aerosolized bradykinin (b) or aerosolized neurokinin A (a). Animals were pretreated with phosphoramidon (4.5 μmol kg^{-1}, i.v., given 5 min before stimulus) and atropine (1.4 μmol kg^{-1}, i.v., given 15 min before stimulus). Vehicle (filled columns) indicates animals pretreated with the vehicle of Hoe 140 and SR 48968 (10% dimethyl sulphoxide in 0.9% saline) 15 min before the stimulus. Baseline (open columns) indicates values measured before the beginning of the aerosolization of the stimulus. Each column is the mean ± s.e.mean of at least 5 experiments. $^*P<0.01$ versus control.

In another series of experiments in the presence of phosphoramidon, we studied the effect of adding Hoe 140 to the tachykinin receptor antagonists SR 48968 (0.3 μmol kg^{-1}, i.v.) and CP-96,345 (2 μmol kg^{-1}, i.v.): the increase in R_L produced by aerosolized ovalbumin was decreased significantly by pretreatment with the combination of SR 48968 and CP-96,345 (Figure 3). In animals whose pretreatment included SR 48968 and CP-96,345 plus Hoe 140, no further reduction in the ovalbumin-induced effects occurred compared to the inhibitory effects of the NK_2 and NK_1 tachykinin antagonists alone (Figure 3).

Discussion

The major finding in the present study is that a selective bradykinin B_2 receptor antagonist decreases markedly oval-

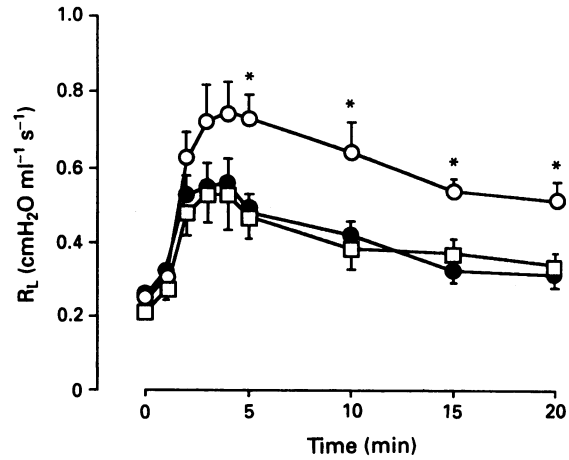


Figure 3 Effect of the combination of antagonists on NK_2 (SR 48968, 0.3 μmol kg^{-1}, i.v., 15 min before stimulus) and NK_1 (CP-96,345, 2 μmol kg^{-1}, i.v., 5 min before stimulus) tachykinin receptor (●) or the combination of these two antagonists plus the bradykinin B_2 receptor antagonist, Hoe 140 (0.1 μmol kg^{-1}, i.v., 15 min before stimulus) (□), on the increase in total pulmonary resistance (R_L) evoked by aerosolized ovalbumin (0.5%, 5 breaths) in sensitized guinea-pigs. Anaesthetized animals were pretreated with atropine (1.4 μmol kg^{-1}, i.v., 15 min before stimulus) and phosphoramidon (4.5 μmol kg^{-1}, i.v., 5 min before stimulus). Controls (○) received the vehicle of Hoe 140 and SR 48968 (10% dimethyl sulphoxide in 0.9% saline) 15 min before the stimulus. Each point is the mean ± s.e.mean of 7 experiments. $^*P<0.05$ versus control.

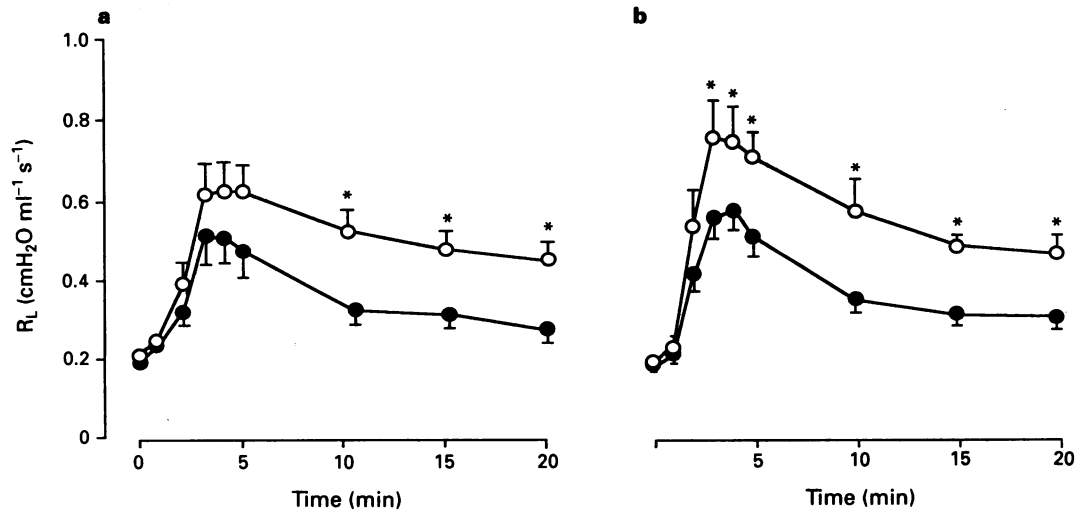


Figure 2 Effect of Hoe 140 (0.1 μmol kg^{-1}, i.v., 15 min before the stimulus) (●) and its vehicle (10% dimethyl sulphoxide in 0.9% saline) (○) on the increase in total pulmonary resistance (R_L) evoked by aerosolized ovalbumin (0.5%, 5 breaths) in sensitized guinea-pigs. Experiments were performed in the absence (a) or in the presence of phosphoramidon (4.5 μmol kg^{-1}, i.v., 5 min before stimulus) (b). Each point is the mean ± s.e.mean of 8 experiments. $^*P<0.05$ vs. Hoe 140.

bumin-induced bronchoconstriction in sensitized guinea-pigs, thus implicating kinins in this allergic response. Present and previous (Wirth *et al.*, 1993) findings show that B_2 bradykinin receptors mediate bradykinin-induced bronchoconstriction in guinea-pigs. Bradykinin is known to be released into bronchoalveolar lavage fluid in both sensitized guinea-pigs (Erjefalt *et al.*, 1993) and in asthmatic human subjects (Christiansen *et al.*, 1992) after inhalation of antigen, adding credibility to the present finding that a bradykinin B_2 antagonist inhibits antigen-induced bronchoconstriction to a considerable extent.

The present studies also provide data on the importance of tachykinins in the antigen-induced bronchoconstriction in guinea-pigs. These results, which confirm previous findings (Bertrand *et al.*, 1993b), indicate that a combination of NK_1 and NK_2 receptor antagonists inhibit considerably antigen-induced bronchoconstriction in sensitized guinea-pigs. Furthermore, present results provide evidence that kinins released into airways as a result of antigen-antibody interactions and the subsequent release of tachykinins from the sensory nerves in the airways acts as a 'cascade' to produce allergic bronchoconstriction. This conclusion is based on the following: first, bradykinin is known to stimulate sensory nerves and to release sensory neuropeptides from several tissues, including airways (Geppetti, 1993). When bradykinin is applied topically to the airways, most of its effects are mediated by the stimulation of sensory nerves with the subsequent release of tachykinins. In the present studies, bradykinin-induced bronchoconstriction was markedly attenuated by pretreatment with NK_1 and NK_2 receptor antagonists, confirming previous studies in which capsaicin pretreatment was used to deplete tachykinins from sensory nerves (Ichinose *et al.*, 1990). Second, in the present study, pretreatment with a combination of NK_1 and NK_2 receptor antagonists markedly reduced antigen-induced bronchoconstriction. Furthermore, addition of a bradykinin B_2 receptor antagonist to the tachykinin antagonists did not further reduce antigen-induced bronchoconstriction.

From these results, we suggest the following sequence of events: the antigen-antibody response in airways causes the release of mediators, including kinins. The kinins activate sensory nerves to release tachykinins which act on their receptors on airway smooth muscle. Of course, one might hypothesize that the opposite sequence occurs (i.e., that antigen-antibody interactions in airways cause sensory nerves to release tachykinins, with the subsequent release of kinins). Several pieces of information mitigate against this sequence: first, to our knowledge, tachykinins are not reported to release kinins in any tissue. Second, in the present study, tachykinin (NKA)-induced bronchoconstriction was not inhibited by pretreatment with a bradykinin B_2 receptor antagonist.

Ovalbumin also increases vascular permeability in airways in sensitized guinea-pigs, and a similar cascade of antigen-antibody interaction is hypothesized leading to kinin activation in airways, which in turn causes the release of tachykinins from sensory nerves, which act on receptors in the postcapillary venules to increase vascular permeability (Bertrand *et al.*, 1993d). Thus, in guinea-pigs, similar cascades involving kinin activation and tachykinin release appear to play a role in both antigen-induced airway smooth muscle contraction and plasma extravasation.

We showed previously that phosphoramidon, an NEP inhibitor, potentiates the mild bronchoconstriction induced by an aerosol of 0.1% ovalbumin, but not the marked response induced by a higher dose of ovalbumin (0.5%) (Bertrand *et al.*, 1993b). The present results showing that bronchoconstriction induced by 0.5% ovalbumin was not increased by blockade of NEP are in agreement with these previous data. However, NEP appears to be involved in the break down of kinins and/or tachykinins which are released after the inhalation of 0.5% ovalbumin and which mediate the bronchoconstriction in response to this dose of antigen. This conclusion is suggested by the observation that inhibition of ovalbumin-induced bronchoconstriction by Hoe 140 is evident earlier in animals pretreated with phosphoramidon than in animals not pretreated with phosphoramidon.

If the present mechanisms found in guinea-pigs also exist in human subjects, we suggest that bradykinins and/or tachykinin receptor antagonists may be of value in reducing symptoms in allergic states where kinins and tachykinins appear to be involved in the pathophysiological responses.

Supported in part by Program Project HL-24136 from the National Institute of Health.

References

ABRAHAM, W.M., BURCH, R.M., FARMER, S.G., SIELCZAK, M.W., AHMED, A. & CORTES, A. (1991). A bradykinin antagonist modifies allergen-induced mediator release and late bronchial responses in sheep. *Am. Rev. Respir. Dis.*, **143**, 787–796.

BARNES, P.J. (1986). Asthma as an axon reflex. *Lancet*, **i**, 242–245.

BERTRAND, C., GEPPETTI, P., BAKER, J., YAMAWAKI, I. & NADEL, J.A. (1993a). Role of neurogenic inflammation in antigen-induced vascular extravasation in guinea-pig trachea. *J. Immunol.*, **150**, 1479–1485.

BERTRAND, C., GEPPETTI, P., GRAF, P.D., FORESI, A. & NADEL, J.A. (1993b). Involvement of neurogenic inflammation in antigen-induced bronchoconstriction in guinea-pigs. *Am. J. Physiol.*, **265**, L507–L511.

BERTRAND, C., NADEL, J.A., GRAF, P.D. & GEPPETTI, P. (1993c). Capsaicin increases airflow resistance in guinea pigs *in vivo* by activating both NK_2 and NK_1 tachykinin receptors. *Am. Rev. Respir. Dis.*, **148**, 909–914.

BERTRAND, C., NADEL, J.A., YAMAWAKI, I. & GEPPETTI, P. (1993d). Role of kinins in the vascular extravasation evoked by antigen and mediated by tachykinins in guinea-pig trachea. *J. Immunol.*, **151**, 4902–4907.

CHRISTIANSEN, S.C., PROUD, D., SARNOFF, R.B., JUERGENS, U., COCHRANE, C.G. & ZURAW, B.L. (1992). Elevation of tissue kallikrein and kinin in the airways of asthmatic subjects after endobronchial allergen challenge. *Am. Rev. Respir. Dis.*, **145**, 900–905.

DUNN, C.J., ELLLIOTT, G.A., OOSTVEEN, J.A. & RICHARDS, I.M. (1988). Development of a prolonged eosinophil-rich inflammatory leukocyte infiltration in the guinea-pig asthmatic response to ovalbumin inhalation. *Am. Rev. Respir. Dis.*, **137**, 541–547.

DUSSER, D.J., UMENO, E., GRAPH, P.D., DJOKIC, T.D., BORSON, D.B. & NADEL, J.A. (1988). Airway neutral endopeptidase-like enzyme modulates tachykinin-induced bronchoconstriction *in vivo*. *J. Appl. Physiol.*, **65**, 2585–2591.

EMONDS-ALT, X., VILAIN, P., GOULAOUIC, P., PROIETTO, V., VAN BROECK, D., ADVENIER, C., NALINE, E., NELIAT, G., LE FUR, G. & BRELIERE, J.C. (1992). A potent and selective non-peptide antagonist of the neurokinin A (NK_2) receptor. *Life Sci.*, **50**, 101–106.

ERJEFALT, I., GREIFF, L., ALKNER, U. & PERSSON, C.G.A. (1993). Allergen-induced biphasic plasma exudation responses in guinea-pig large airways. *Am. Rev. Respir. Dis.*, **148**, 695–701.

FARMER, S.G., WILKINS, D.E., MEEKER, S.A., SEEDS, E.A.M. & PAGE, C.P. (1992). Effects of bradykinin receptor antagonists on antigen-induced respiratory distress, airway hyperresponsiveness and eosinophilia in guinea-pigs. *Br. J. Pharmacol.*, **107**, 653–659.

GEPPETTI, P. (1993). Sensory neuropeptide release by bradykinin: mechanisms and pathophysiological implications. *Regul. Pept.*, **47**, 1–23.

GEPPETTI, P., MAGGI, C.A., PERRETTI, F., FRILLI, S. & MANZINI, S. (1988). Simultaneous release by bradykinin of substance P- and calcitonin gene-related peptide immunoreactivities from capsaicin-sensitive structures in guinea-pig heart. *Br. J. Pharmacol.*, **94**, 288–290.

HOCK, F.J., WIRTH, K., ALBUS, U., LINZ, W., GERHARDS, H.J., WIEMER, G., HENKE, S.T., BREIPOHL, G., KÖNIG, W., KNOLLE, J. & SCHÖLKENS, B.A. (1991). Hoe 140 a new potent and long acting bradykinin-antagonist: *in vitro* studies. *Br. J. Pharmacol.*, **102**, 769–773.

ICHINOSE, M., BELVISI, M.G. & BARNES, P.J. (1990). Bradykinin induced bronchoconstriction in guinea-pig *in vivo*: role of neural mechanisms. *J. Pharmacol. Exp. Ther.*, **253**, 594–599.

KAUFMAN, M.P., COLERIDGE, H.M., COLERIDGE, J.C.G. & BAKER, D.G. (1980). Bradykinin stimulates afferent vagal C-fibers in intrapulmonary airways of dogs. *J. Appl. Physiol.*, **48**, 511–517.

LUNDBERG, J.M., HÖKFELT, T., MARTLING, C.-R., SARIA, A. & CUELLO, C. (1984). Substance P-immunoreactive sensory nerves in the lower respiratory tract of various mammals including man. *Cell Tissue Res.*, **235**, 251–261.

LUNDBERG, J.M. & SARIA, A. (1983). Capsaicin-induced desensitization of airway mucosa to cigarette smoke, mechanical and chemical irritants. *Nature*, **302**, 251–253.

NADEL, J.A. (1991). Neutral endopeptidase modulates neurogenic inflammation. *Eur. Respir. J.*, **4**, 745–754.

SARIA, A., MARTLING, C.-R., YAN, Z., THEODORSSON-NORHEIM, E., GAMSE, R. & LUNDBERG, J.M. (1988). Release of multiple tachykinins from capsaicin-sensitive sensory nerves in the lung by bradykinin, histamine, dimethylphenyl, piperazinium, and vagal nerve stimulation. *Am. Rev. Respir. Dis.*, **137**, 1330–1335.

SNIDER, M.R., CONSTANTINE, J.W., LOWE III, A.J., LONGO, K.P., LEBEL, W.S., WOODY, H.A., DROZDA, S.E., DESAI, M.C., VINICK, F.J., SPENCER, R.W. & HESS, H. (1991). A potent nonpeptide antagonist of the substance P (NK-1) receptor. *Science*, **351**, 435–437.

WIRTH, K.J., GEHRING, D. & SCHOLKENS, B.A. (1993). Effect of Hoe 140 on bradykinin-induced bronchoconstriction in anaesthetized guinea-pigs. *Am. Rev. Respir. Dis.*, **148**, 702–706.

(Received February 7, 1994
Revised May 9, 1994
Accepted June 1, 1994

Br. J. Pharmacol. (1994), **113**, 513-521 © Macmillan Press Ltd, 1994

Differential effects of the PAF receptor antagonist UK-74,505 on neutrophil and eosinophil accumulation in guinea-pig skin

[1]M.J. Sanz, V.B. Weg, D.T. Walsh, T.J. Williams & [2]S. Nourshargh

Department of Applied Pharmacology, National Heart & Lung Institute, Dovehouse Street, London SW3 6LY

1 The effect of the dihydropyridine, platelet activating factor (PAF) receptor antagonist, UK-74,505, on leucocyte accumulation and oedema formation in guinea-pig skin was investigated. The inflammatory reactions studied were elicited by exogenous mediators, a passive cutaneous anaphylactic (PCA) reaction and zymosan particles.

2 Leucocyte accumulation and oedema formation were measured as the local accumulation of i.v. administered ^{111}In-labelled neutrophils or eosinophils together with ^{125}I-labelled albumin. UK-74,505 was either administered i.v. or used to pretreat the radiolabelled leucocytes *in vitro* prior to their last wash and injection into recipient animals.

3 *In vitro*, UK-74,505 inhibited PAF-induced elevations in cytoplasmic levels of Ca^{2+} ($[Ca^{2+}]_i$) in fura-2-loaded guinea-pig neutrophils and eosinophils with IC_{50} values of 10^{-9} M and 7×10^{-9} M respectively. Neutrophils and eosinophils pretreated with 10^{-7} M and 10^{-6} M UK-74,505 respectively, and maintained at 37°C, were unresponsive to PAF for the 4 h period investigated.

4 *In vivo*, using 2 h test periods, i.v. UK-74,505 (0.5 and 2.5 mg kg^{-1}) inhibited the accumulation of ^{111}In-neutrophils, ^{111}In-eosinophils and oedema formation induced by intradermal PAF, but had no effect on responses elicited by leukotriene B_4 (LTB_4) and zymosan-activated plasma (ZAP, used as a source of C5a des Arg). UK-74,505 (2.5 mg kg^{-1}) was also without an effect on responses induced by a PCA reaction but significantly suppressed the ^{111}In-eosinophil accumulation following the intradermal administration of zymosan particles. The ^{111}In-neutrophil accumulation induced by zymosan particles was not, however, affected by UK-74,505.

5 In a second series of *in vivo* experiments, ^{111}In-leucocytes were pretreated *in vitro* with UK-74,505 prior to their last wash and injection into recipient animals. Radiolabelled neutrophils, and eosinophils were pretreated with 10^{-7} M and 10^{-6} M UK-74,505 respectively, concentrations previously shown to block the leucocyte responses to PAF *in vitro* for up to 4 h. The *in vitro* pretreatment of the cells with the PAF antagonist, whilst not affecting the responses to intradermally-injected PAF, suppressed the ^{111}In-eosinophil accumulation response induced by zymosan particles.

6 The results of this study indicate that PAF is not involved in neutrophil accumulation, eosinophil accumulation and oedema formation induced by LTB_4, ZAP and a PCA reaction. Endogenous PAF does, however, appear to have a role in zymosan-induced eosinophil accumulation but not neutrophil accumulation, suggesting the existence of different inflammatory pathways in the induction of neutrophil and eosinophil accumulation *in vivo*. Furthermore, while leucocyte accumulation induced by exogenous PAF does not appear to involve leucocyte PAF receptors, the mechanism by which endogenous PAF mediates the zymosan-induced eosinophil accumulation appears dependent on the expression of PAF receptors on eosinophils.

Keywords: PAF; PAF receptor antagonist; UK-74,505; neutrophil accumulation; eosinophil accumulation; oedema formation; passive cutaneous anaphylactic (PCA) reaction; zymosan; inflammation; guinea-pig skin

Introduction

The interaction of leucocytes with the microvasculature, triggered by inflammatory stimuli, constitutes a characteristic feature of an inflammatory response essential to host defence following infection or injury. This response is regulated by the coordinated expression and/or activation of leucocyte and endothelial cell adhesion molecules (Springer, 1990). Neutrophils are the predominant leucocytes to arrive at sites of acute inflammation, capable of defending the host against bacterial infections. Neutrophils are also intimately associated with oedema formation (Wedmore & Williams, 1981a) and the recruitment of other phagocytic leucocytes such as monocytes (Doherty *et al.*, 1988; Territo *et al.*, 1989). As with neutrophils, eosinophils are also involved in host defence but appear to have a specialized role in the control of inflammatory reactions induced by helminthic parasites (Kay, 1985). If inappropriately or excessively activated, neutrophils and eosinophils can also mediate tissue damage and contribute to the development of inflammatory disease states. In this respect, neutrophils have been implicated in the pathogenesis of disorders including adult respiratory distress syndrome (ARDS) and myocardial infarction (reviewed in Malegh & Gallin, 1987), whilst eosinophils are predominantly associated with allergic inflammatory disorders such as asthma and atopic dermatitis (reviewed in Kay, 1985).

PAF, a potent lipid mediator with a wide profile of biological activities such as bronchoconstriction, microvascular leakage and platelet aggregation, is a potent chemoattractant and activator of leucocytes (reviewed in Braquet *et al.*, 1987). By acting on specific cell surface receptors (Hanahan, 1986; Kroegel *et al.*, 1989b), PAF can stimulate neutrophils and eosinophils *in vitro* inducing chemotaxis, adhesion and degranulation (Hanahan, 1986; Wardlaw *et al.*, 1986; Kimani *et al.*, 1988; Czarnetzki & Csato, 1989; Kroegel *et al.*, 1989a). In addition to activating cells directly, PAF can act as a priming agent for eosinophils (Blom *et al.*, 1992;

[1] Present address: Departamento de Farmacologia, Facultad de Farmacia, Universidad de Valencia, C/Vincent Andres Estelles s/n, 46100 Burjassot (Valencia), Spain
[2] Author for correspondence.

Zoratti et al., 1992). In vivo, intradermal administration of PAF causes neutrophil and eosinophil accumulation and oedema formation in a number of species including guinea-pigs (Faccioli et al., 1991), horses (Foster et al., 1992a,b), and rabbits (Wedmore & Williams, 1981b; Humphrey et al., 1982; Colditz & Movat, 1984a). In man, intradermal PAF induces eosinophil accumulation in atopic subjects (Henocq & Vargaftig, 1988).

The availability of specific PAF receptor antagonists has allowed direct investigations into the pathophysiological roles of this mediator. In animal models, PAF antagonists provide protection against allergic disorders, airway hyperreactivity, shock, ischaemia-induced tissue damage and several other inflammatory conditions (Braquet et al., 1989b; Page & Abbot, 1989). UK-74505, a dihydropyridine PAF receptor antagonist, is a highly selective, potent and long-acting inhibitor of PAF-induced responses (Alabaster et al., 1991). This compound has been shown to inhibit PAF-induced bronchoconstriction in guinea-pigs, PAF-induced oedema in rat and rabbit skin (Alabaster et al., 1991; Pons et al., 1993), platelet accumulation and oedema formation in an Arthus reaction in rabbit skin (Pons et al., 1993). Further, in conscious dogs, UK-74,505 caused complete inhibition of PAF-induced whole blood aggregation ex vivo for at least 14 h (Alabaster et al., 1991). When orally administered, UK-74,505 blocked airway obstruction in response to aerosolized antigen in actively sensitized guinea-pigs (Watson et al., 1991) and bronchoconstriction and changes in blood neutrophil counts following aerosolized PAF in man (O'Connor et al., 1991).

The aim of the present study was to investigate the effect of i.v. UK-74,505 on the accumulation of neutrophils and eosinophils, and oedema formation in guinea-pig skin. The inflammatory reactions investigated were elicited by the exogenous administration of PAF, LTB_4 and ZAP, or by endogenously-released mediators in response to zymosan particles and in a PCA reaction. In addition, we demonstrated that UK-74,505 has a long duration of action in inhibiting PAF-induced stimulation of guinea-pig neutrophils and eosinophils in vitro, as previously found with rabbit and dog platelets (Parry et al., 1990; Alabaster et al., 1991; Pons et al., 1993). This property of UK-74,505 enabled us to block PAF receptors on ^{111}In-leucocytes in vitro before their i.v. injection, thus allowing an investigation into the role of neutrophil and eosinophil PAF receptors in the process of leucocyte accumulation in vivo.

Methods

Animals

Female ex-breeder Dunkin–Hartley guinea-pigs (800–900 g) and female Dunkin–Hartley guinea-pigs (300–400 g) were purchased from Harlan Olac, Bicester, Oxon.

Preparation of guinea-pig zymosan-activated plasma

Guinea-pig zymosan activated plasma (ZAP) was used as a source of C5a des Arg. Heparinized plasma was incubated with zymosan (5 mg ml^{-1}) for 30 min at 37°C. Zymosan was removed by centrifugation (2 × 10 min at 2500 g). ZAP was chromatographed on Sephadex G-25M columns, to remove low molecular weight substances, and stored in aliquots at − 20°C.

Generation of guinea-pig antiserum for the passive cutaneous anaphylactic reaction

The PCA antiserum was prepared as previously described (Weg et al., 1991). Briefly, guinea-pigs were immunized by s.c. injection of 0.2 mg BGG in 0.2 ml Freund's complete adjuvant. Animals were boosted by similar injections of antigen in incomplete adjuvant on day 21. Animals were exsanguinated and serum prepared on day 30. Aliquots were stored at − 20°C.

Isolation and purification of guinea-pig peritoneal eosinophils

Guinea-pig peritoneal eosinophils were isolated and purified as previously described (Faccioli et al., 1991). Briefly, ex-breeder guinea-pigs received 4–5 i.p. injections of 1 ml of horse serum at 2 day intervals. Peritoneal cells were collected by lavage 24 h after the last injection and purified over a discontinuous Percoll gradient (1.080, 1.085, 1.090, 1.095 and 1.100 g ml^{-1}). The purity of the cells was 98.1 ± 0.7% for $n = 7$ preparations, the contaminating cells being predominantly mononuclear leucocytes.

Isolation and purification of guinea-pig peritoneal neutrophils

Guinea-pig neutrophils were obtained by a modification of the method described by Bokoch & Gilman (1984). Animals were injected i.p. with 15 ml of 5% sodium caseinate. The peritoneal exudate was collected 16 h later in 30 ml of heparinized saline. Neutrophils were purified using the Percoll gradient described above for eosinophils. The prepared neutrophils were greater than 98% pure, contaminating cells being mononuclear cells.

Measurement of intracellular Ca^{2+} levels using fura-2

Neutrophil and eosinophil intracellular Ca^{2+} levels ($[Ca^{2+}]_i$) were measured by monitoring the fluorescence of cells loaded with the calcium indicator fura-2 (Grynkiewicz et al., 1985). As previously described (Nourshargh et al., 1992), neutrophils or eosinophils (10^7 cells ml^{-1}) were incubated with fura-2 acetoxymethyl ester (2.5 μM) in Ca^{2+}/Mg^{2+}-free PBS for 30 min at 37°C. After two washes the cells were finally resuspended at 10^6 cells ml^{-1} in Ca^{2+}/Mg^{2+}-free PBS containing 10 mM HEPES, 0.25% BSA and 10 mM glucose (pH 7.4). Aliquots were dispensed in quartz cuvettes and the extracellular Ca^{2+} levels adjusted to 1 mM with $CaCl_2$. Changes in fluorescence were monitored with a Perkin Elmer LS50 fluorescence spectrophotometer fitted with a thermostatically controlled cell holder incorporating an electronic stirrer and maintained at 37°C by a water circulator. Fluorescence readings were taken at excitation wavelengths 340 nm and 380 nm and emission wavelength 510 nm. The $[Ca^{2+}]_i$ (nM) was calculated using the ratio of the two fluorescence readings using a K_d value of 224 nM. Responses were allowed to develop for 3 min and data were expressed as maximal increase in $[Ca^{2+}]_i$ over the basal levels.

^{111}In-labelling of guinea-pig peritoneal neutrophils and eosinophils

Guinea-pig neutrophils and eosinophils were radiolabelled with ^{111}In as previously described (Faccioli et al., 1991; Teixeria et al., 1993). Briefly, the cells ($2–3 \times 10^7$ in 1 ml of Hanks' solution), were incubated with $^{111}InCl_3$ (approximately 100 μCi in 10 μl) chelated with 2-mercaptopyridine-N-oxide (40 μg in 0.1 ml of 50 mM PBS, pH 7.4) for 15 min at room temperature. The labelled leucocytes were then washed twice and finally resuspended for i.v. injection in Hanks' solution (10^7 leucocytes ml^{-1}) pH 7.3 containing 10% cell-free citrated guinea-pig plasma. In some experiments, cells were treated with UK-74,505 before their last wash, as described below. Supernatant aliquots were collected during washes and after the final suspension in order to assess labelling efficiency which was greater than 80% for both cell types. At the end of the 2 h in vivo test period, free ^{111}In levels in plasma were less than 10%.

Pretreatment of guinea-pig neutrophils and eosinophils with UK-74,505

^{111}In-labelled or unlabelled cells were pretreated with UK-74,505 before their last wash. At this point, the cell pellet was resuspended in 2 ml of Hanks' solution and split into 2 aliquots of 1 ml. UK-74,505 was added to one aliquot and the other aliquot was used as a control. The cells were treated with UK-74,505 for a period of 15 min at final concentrations of 10^{-7} M for neutrophil suspensions and 3×10^{-7} M or 10^{-6} M for eosinophil suspensions.

Measurement of ^{111}In-leucocyte accumulation and plasma protein leakage in guinea-pig skin

Guinea-pigs were sedated (Hypnorm, 0.2 ml, i.m.) and their dorsal skin shaved. ^{111}In-eosinophils (5×10^6 cells) or ^{111}In-neutrophils (5×10^6 cells) were injected i.v. together with ^{125}I-HSA via an ear vein. When necessary, UK-74,505 or its vehicle was administered i.v. 10 min before the cells. Five minutes after administration of ^{111}In-labelled cells, the agents under investigation, freshly prepared in sterile saline containing 0.1% BSA from stock solutions, were injected i.d. in 0.1 ml volumes into the back skin. The PCA reaction was elicited by local antigen (BGG) challenge of skin sites previously sensitized (20–24 h before i.v. radiolabelled leucocytes and albumin) with an IgG-rich anti-BGG antiserum (50 µl, 1/50 dilution) as previously described (Weg *et al.*, 1991; 1993). Each test was performed in duplicate sites according to a balanced site injection plan. After 2 h, the animals were anaesthetized with i.p. Sagatal and a 3 ml blood sample was collected into heparin by cardiac puncture. The animals were then killed by an overdose of Sagatal, the dorsal skin removed, and the skin sites punched out with a 17 mm diameter punch. Skin, blood and plasma samples were counted in a 5-head gamma counter with automatic spill-over and cross-talk correction (Canberra Packard Ltd, Pangbourne, Berks). The ^{111}In counts per cell were determined and used to express neutrophil or eosinophil accumulation in each skin site in terms of labelled leucocytes. Exudate volumes were expressed in terms of microlitres of plasma by dividing skin sample ^{125}I counts by ^{125}I counts in 1 µl of plasma.

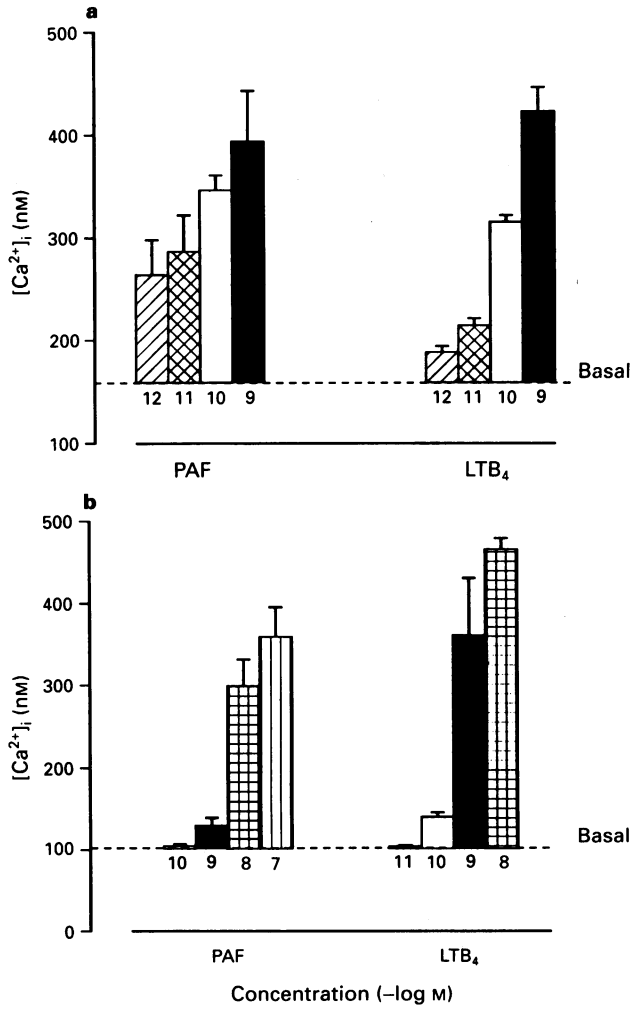


Figure 1 Elevations in $[Ca^{2+}]_i$ in guinea-pig neutrophils and eosinophils induced by platelet activating factor (PAF) and leukotriene B_4 (LTB_4). Responses are for (a) guinea-pig neutrophils and (b) guinea-pig eosinophils. Results are expressed as increase in $[Ca^{2+}]_i$ over the basal and are mean ± s.e.mean for $n = 4$ experiments. Basal $[Ca^{2+}]_i$ for neutrophils and eosinophils were 159.0 ± 9.5 nM ($n = 4$) and 101.7 ± 18.1 nM ($n = 4$) respectively.

Materials

Bovine serum albumin (<0.1 ng LPS mg^{-1}, BSA), sodium caseinate, PAF, zymosan, and bovine γ-globulin (BGG) were purchased from Sigma Chemical Co, Poole, Dorset. LTB_4 was from Cascade Biochem Ltd, Reading, Berkshire. ^{125}I-human serum albumin (^{125}I-HSA, 20 mg ml^{-1} albumin in sterile isotonic saline, 50 µCi ml^{-1}) and $^{111}InCl_3$ (2 mCi in 0.2 ml sterile pyrogen free of 0.04 N HCl) were from Amersham International, Amersham, Buckinghamshire. Sagatal (pentobarbitone sodium, 60 mg ml^{-1}) was from May and Baker, Dagenham, Essex. Hypnorm (0.315 mg ml^{-1} fentanyl citrate and 10 mg ml^{-1} fluanisone) was from Janssen Pharmaceutical Ltd, Grove, Oxford. Freund's complete and incomplete adjuvant were from Difco Laboratories, West Molesey, Surrey. Fura-2 acetoxymethyl ester was from Cambridge Bioscience, Cambridge. Percoll and Sephadex G-25M (PD-10) columns were from Pharmacia Fine Chemicals, Uppsala, Sweden. Horse serum, sterile Hanks' balanced salt solution, (10 × HBSS) and HEPES were from Gibco BRL, Paisley. The PAF receptor antagonist, UK-74,505 (4-(2-chlorophenyl)-1,4-dihydro-3-ethoxycarbonyl-6-methyl-2-[4-(2-methylimidazol[4,5-c]pyrid-1-yl)phenyl]-5-[N-(2-pyridylcarbamoyl)pyridine]), initially dissolved in 0.1 N HCl and diluted in saline, was a gift from Dr M.J. Parry, Pfizer Central Research, Sandwich, Kent.

Statistical analysis

All data are presented as the mean ± s.e.mean of the indicated number of animals (*in vivo*) or experiments (*in vitro*). Statistical significance was assessed by two way analysis of variance. *P* values less than 0.05 were considered to be significant.

Results

Effect of UK-74,505 on stimulated elevations in neutrophil and eosinophil $[Ca^{2+}]_i$

The potency and duration of action of UK-74,505 on PAF-induced guinea-pig neutrophil and eosinophil activation, as measured by elevations in $[Ca^{2+}]_i$ using fura-2, was investigated *in vitro*.

Guinea-pig peritoneal neutrophils loaded with fura-2 were found to have a basal $[Ca^{2+}]_i$ of 159.0 ± 95 nM ($n = 4$ experiments). On stimulation with PAF or LTB_4 the cells exhibited a rapid and dose-dependent increase in $[Ca^{2+}]_i$. Generally, responses peaked within about 30 s and returned to the basal level after about 2 to 3 min (traces not shown). The order of potency of the agonists appeared to be PAF > LTB_4 (Figure 1a).

Guinea-pig peritoneal eosinophils exhibited a basal $[Ca^{2+}]_i$ of 101.7 ± 18.1 nM ($n = 4$ experiments). As compared to neutrophils, guinea-pig eosinophils were less responsive to the two agonists (Figure 1b). Furthermore, the order of potency of the stimuli differed for eosinophils in that it appeared to be $LTB_4 > PAF$. The time-course of stimulated changes in eosinophil $[Ca^{2+}]_i$ induced by PAF and LTB_4 were similar to the responses obtained with neutrophils.

Based on the above results, in subsequent experiments assessing the effect of UK-74,505, submaximal concentrations of the two agonists were chosen to stimulate the cells, i.e. 10^{-10} M PAF and LTB_4 for stimulating neutrophils and 10^{-8} M PAF and 10^{-9} M LTB_4 for stimulating eosinophils. UK-74,505 incubated with the leucocytes for 2 min prior to their stimulation, inhibited the PAF-induced increase in $[Ca^{2+}]_i$ in both cell types in a dose-dependent manner (Figure 2). The effect of UK-74,505 was specific for PAF in that the responses elicited by LTB_4 were not affected. The calculated IC_{50} values of the antagonist in inhibiting the PAF-induced elevations in $[Ca^{2+}]_i$ in neutrophils and eosinophils were 10^{-9} M and 7×10^{-9} M respectively. With both cell types the basal $[Ca^{2+}]_i$ was not significantly altered after the addition of UK-74,505 (e.g. for neutrophils, basal $[Ca^{2+}]_i$ was 121 ± 8 nM and 115 ± 12 nM for control and 10^{-7} M UK-74,505-treated cells respectively, $n = 4$ preparations; for eosinophils, basal $[Ca^{2+}]_i$ was 108 ± 11 nM and 117 ± 8 nM for control and 10^{-6} M UK-74,505-treated cells respectively, $n = 4$ preparations).

Having established the potency and specificity of UK-74,505 in suppressing PAF-stimulated $[Ca^{2+}]_i$ elevations in the leucocytes, the duration of action of the antagonist was investigated. Guinea-pig neutrophils and eosinophils pretreated for 15 min with 10^{-7} M and 10^{-6} M UK-74,505 respectively, washed and resuspended in fresh buffer (and kept at 37°C) were totally unresponsive to PAF up to 4 h after the treatment of the cells (Figure 3). With respect to the eosinophils, lower concentrations of the antagonist, e.g. 3×10^{-7} M, failed to maintain a total inhibition of the PAF response during the 4 h test period (Figure 3). The effect of UK-74,505 at concentrations of 10^{-7} M and 10^{-6} M, on neutrophils and eosinophils respectively, were specific for PAF (Figure 3). With neutrophils, concentrations greater than 10^{-7} M of the antagonist appeared to have a small inhibitory effect on LTB_4-induced responses (results not shown).

Effect of intravenous UK-74,505 on ^{111}In-leucocyte accumulation and oedema formation induced by PAF, LTB_4 and ZAP in guinea-pig skin

Intradermal PAF induced accumulation of ^{111}In-neutrophils, ^{111}In-eosinophils and oedema formation in guinea-pig skin over a 2 h *in vivo* test period (Figure 4). At the dose used (10^{-9} mol per site), PAF appeared to be very effective in inducing plasma protein leakage. LTB_4 (5×10^{-10} mol per site) induced a larger eosinophil accumulation response than PAF, whilst being inactive in causing neutrophil accumulation and oedema formation. ZAP (100%) was an effective stimulus with respect to all three inflammatory events.

Based on a previous study (Pons *et al.*, 1993), UK-74,505 was initially administered i.v. at a dose of 0.5 mg kg^{-1}. At this dose, UK-74,505 significantly inhibited leucocyte accumulation and oedema formation induced by PAF, but

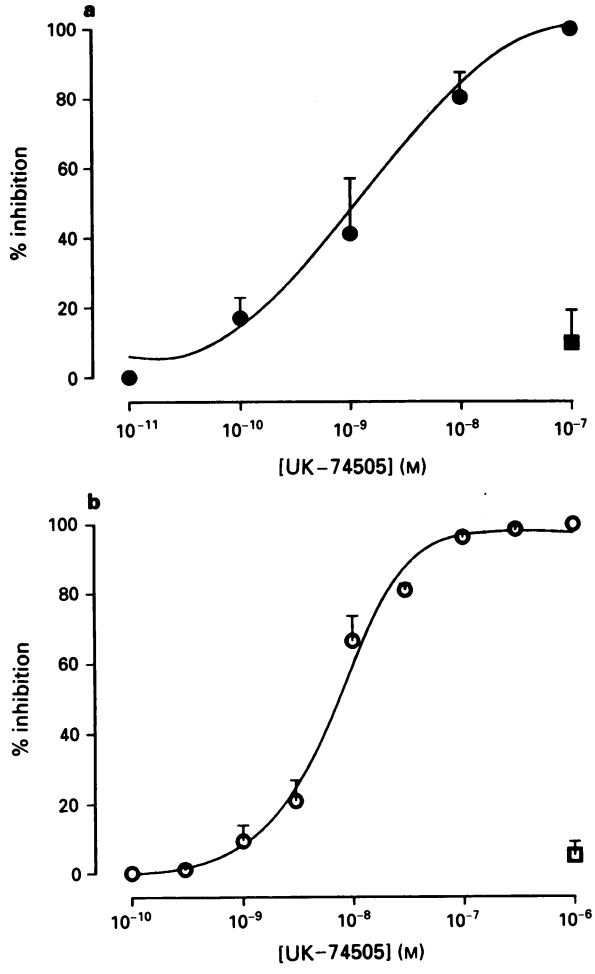


Figure 2 Effect of UK-74,505 on elevations in $[Ca^{2+}]_i$ induced by platelet activating factor (PAF) and leukotriene B_4 (LTB_4) in guinea-pig neutrophils and eosinophils. UK-74,505 was added to leucocyte suspensions 2 min prior to stimulation. Basal $[Ca^{2+}]_i$ was not significantly different before and after addition of UK-74,505. Results are expressed as percentage inhibition of increases in $[Ca^{2+}]_i$ in (a) guinea-pig neutrophils stimulated with PAF (10^{-10} M, ●) or LTB_4 (10^{-10} M, ■), and (b) guinea-pig eosinophils stimulated with PAF (10^{-8} M, ○) or LTB_4 (10^{-9} M, □). Results are the mean ± s.e.mean of $n = 4$ preparations.

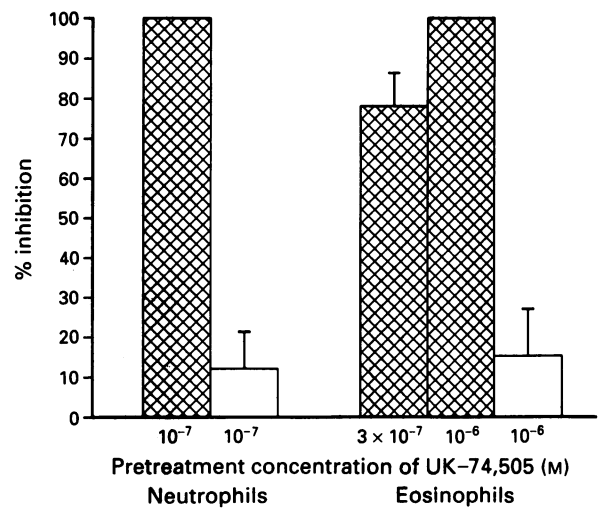


Figure 3 Maintenance of the inhibitory effect of UK-74,505 on elevations in $[Ca^{2+}]_i$ induced by platelet activating factor (PAF) (cross hatched columns) and leukotriene B_4 (LTB_4) (open columns) in guinea-pig neutrophils and eosinophils. Leucocytes were pretreated with UK-74,505 for a period of 15 min at concentrations of 10^{-7} M for neutrophils and 3×10^{-7} M or 10^{-6} M for eosinophils. The cells were then washed and kept at 37°C in a water bath. The responsiveness of the leucocytes, after a 4 h incubation period, with respect to stimulated elevations in $[Ca^{2+}]_i$ was assessed. Results show percentage inhibition of neutrophil responses elicited by PAF (10^{-10} M) and LTB_4 (10^{-10} M) and eosinophil responses elicited by PAF (10^{-8} M) and LTB_4 (10^{-9} M). Results are expressed as mean ± s.e.mean for $n = 3$–4 experiments.

had no effect on the inflammatory responses elicited by LTB_4 and ZAP (data not shown). A larger dose of the antagonist, 2.5 mg kg^{-1}, gave a similar profile of results (Figure 4).

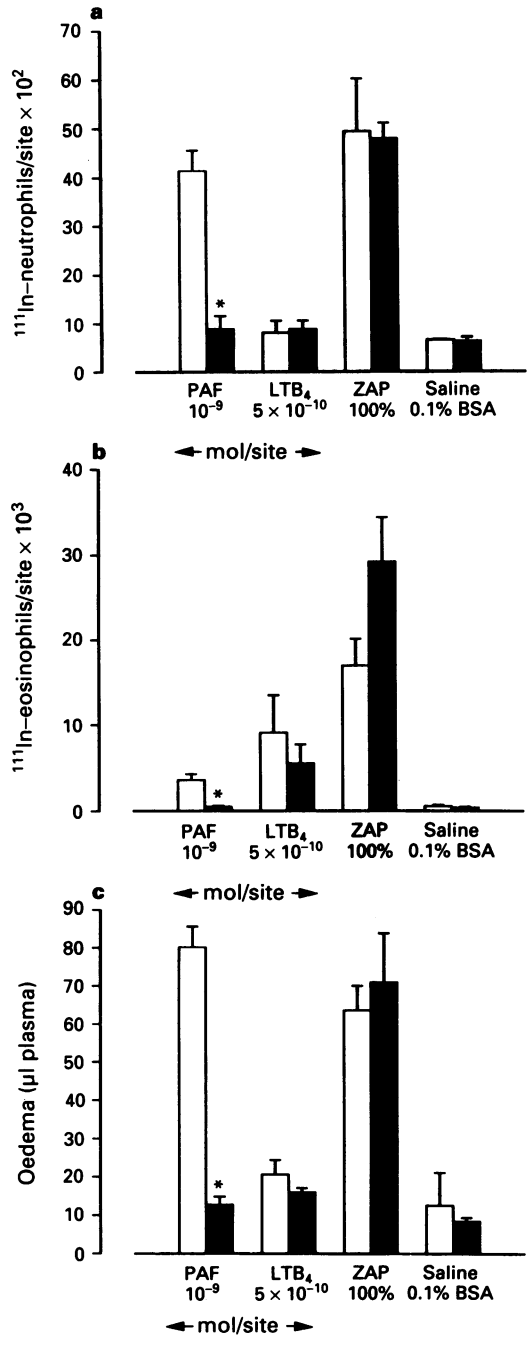


Figure 4 Effect of i.v. administration of UK-74,505 on (a) ^{111}In-neutrophil accumulation (b) ^{111}In-eosinophil accumulation and (c) oedema formation induced by platelet activating factor (PAF), leukotriene B_4 (LTB_4) and zymosan-activated plasma (ZAP) in guinea-pig skin. Guinea-pigs received an i.v. injection of either vehicle (open columns) or 2.5 mg kg^{-1} UK-74,505 (solid columns) followed 10 min later by the i.v. injection of labelled cells and ^{125}I-HSA; 5 min later, PAF (10^{-9} mol per site), LTB_4 (5×10^{-10} mol per site) and ZAP (100%) were administered by i.d. injections. After 2 h, the animals were killed and cell accumulation and plasma protein leakage were measured. (a) Results are expressed as number of ^{111}In-neutrophils per site per 5×10^6 cells injected and presented as mean ± s.e.mean of responses in $n = 6$ animals. (b) Results are expressed as number of ^{111}In-eosinophils per site per 5×10^6 cells injected and presented as described above for $n = 6$ experiments. (c) Results are expressed as µl of plasma (oedema formation) for $n = 6$ experiments. Significant differences from control are indicated by $^*P < 0.01$.

Effect of intravenous UK-74,505 on ^{111}In-leucocyte accumulation and oedema formation induced by a PCA reaction in guinea-pig skin

Injection of antigen (BGG, 0.01–1 µg per site) into sensitized sites resulted in pronounced and dose-dependent accumula-

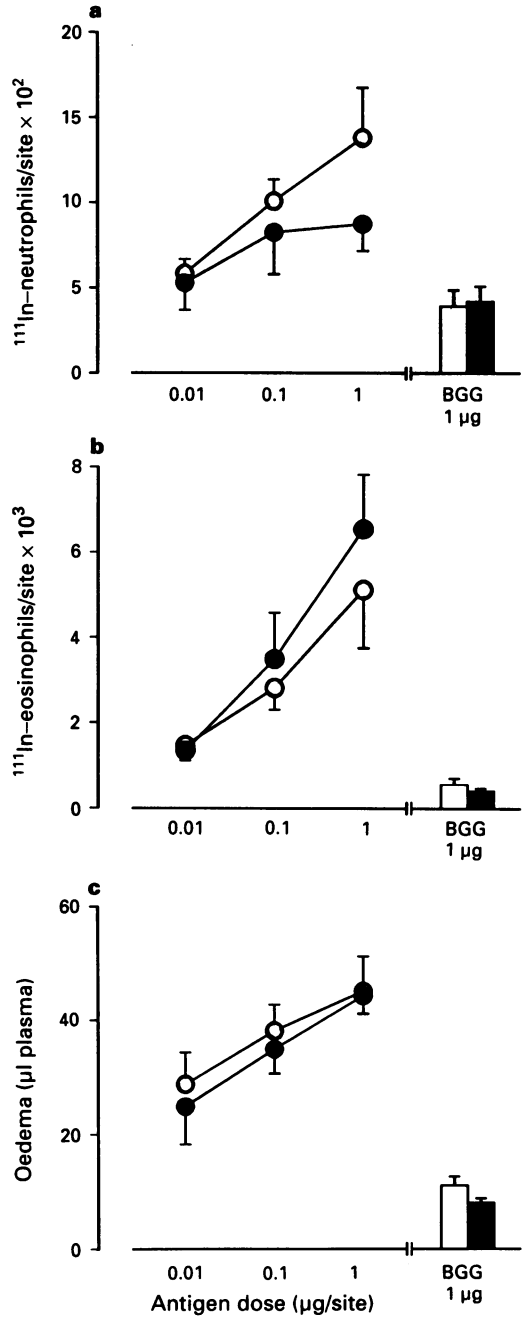


Figure 5 Effect of i.v. UK-74,505 on inflammatory responses induced by a passive cutaneous anaphylactic (PCA) reaction. To elicit the PCA reaction, antigen (BGG) was administered intradermally into previously sensitized sites. The doses of BGG used were 0.01, 0.1 and 1 µg per site. Animals received an i.v. dose of either vehicle or 2.5 mg kg^{-1} UK-74,505 10 min before the i.v. administration of labelled cells and ^{125}I-HSA. BGG or saline was injected i.d. 5 min later. Responses obtained in control and UK-74,505-treated animals are represented by open and solid symbols/columns respectively. (a) Results are expressed as number of ^{111}In-neutrophils per site per 5×10^6 cells injected and presented as mean ± s.e.mean of responses in $n = 6$ animals. (b) Results are expressed as number of ^{111}In-eosinophils per site per 5×10^6 cells injected and presented as described above for $n = 6$ animals. (c) Results are expressed as µl of plasma (oedema formation) and presented as mean ± s.e.mean of responses obtained in $n = 6$ animals.

tion of ^{111}In-neutrophils (Figure 5a) and ^{111}In-eosinophils (Figure 5b) in guinea-pig skin, while BGG alone induced a very small response. Plasma protein leakage in PCA reaction sites was also dependent on the dose of BGG (Figure 5c). Although ^{111}In-leucocyte accumulation and oedema formation appeared reduced in animals treated with i.v. UK-74,505 (0.5 mg kg^{-1}), as compared with controls, this inhibition was not statistically significant at any of the antigen doses tested (data not shown). A larger dose of UK-74,505, 2.5 mg kg^{-1}, was also without a significant effect on the inflammatory responses elicited by the PCA reaction (Figure 5).

Effect of in vitro *pretreatment of neutrophils and eosinophils with UK-74,505 on leucocyte accumulation in guinea-pig skin*

The following series of experiments were designed to investigate the role of PAF receptors expressed on the cell surface of leucocytes in the process of leucocyte accumulation *in vivo*. Based on the findings from the *in vitro* experiments, radiolabelled guinea-pig neutrophils and eosinophils were treated with UK-74,505 at concentrations of 10^{-7} M and 10^{-6} M respectively prior to their last wash and injection into recipient animals. This procedure was previously shown to block the leucocyte PAF responses for up to 4 h.

While i.v. UK-74,505 (2.5 mg kg^{-1}) almost totally inhibited the PAF-induced leucocyte accumulation, the *in vitro* pretreatment of ^{111}In-neutrophils and ^{111}In-eosinophils with UK-74,505 failed to alter their accumulation in response to exogenously administered PAF (Figure 6). However, pretreatment of ^{111}In-eosinophils with UK-74,505 partially inhibited their accumulation in response to i.d. zymosan particles (100 μg per site, Figure 7). Intravenous UK-74,505 (2.5 mg kg^{-1}) inhibited the zymosan-induced accumulation of ^{111}In-eosinophils to the same extent (52 ± 11% inhibition for $n = 6$ pairs, $P < 0.05$, Figure 7). Neither procedures of i.v. administration or *in vitro* pretreatment significantly affected the zymosan-induced ^{111}In-neutrophil accumulation. The small level of oedema induced by zymosan particles was also significantly suppressed by i.v. 2.5 mg kg^{-1} UK-74,505 (6.6 ± 2.7 and 3.7 ± 0.8 μl plasma above saline levels in control and UK-74,505-treated animals respectively, means ± s.e.mean for $n = 6$ pairs of animals, $P < 0.05$).

Discussion

In the present study we have used the specific and highly potent PAF antagonist, UK-74,505 to investigate the role of PAF in the accumulation of neutrophils and eosinophils and the corresponding oedema in guinea-pig skin. The avid binding of UK-74,505 to receptors enabled us to investigate the effect of selectively blocking PAF receptors on neutrophils and eosinophils on their accumulation *in vivo*.

The potency and duration of action of UK-74,505 on neutrophil and eosinophil stimulation was investigated *in vitro* using elevations in $[Ca^{2+}]_i$ in fura-2-loaded leucocytes as a measure of cell activation. UK-74,505 inhibited PAF-

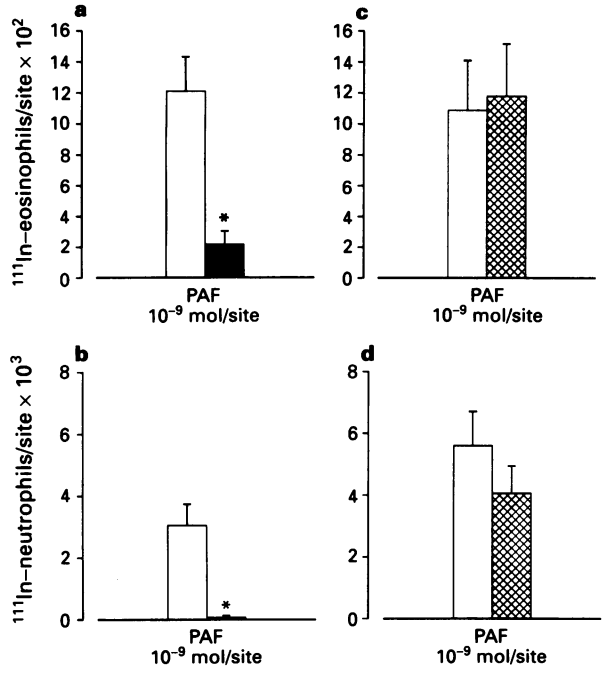


Figure 6 Effect of (a,b) i.v. UK-74,505 and (c,d) *in vitro*-pretreatment with UK-74,505 on ^{111}In-neutrophil accumulation and ^{111}In-eosinophil accumulation induced by platelet activating factor (PAF) in guinea-pig skin. (a,b) Guinea-pigs received an i.v. injection of either vehicle (open columns) or 2.5 mg kg^{-1} UK-74,505 (solid columns) followed 10 min later by the i.v. injection of labelled cells. (c) Guinea-pigs were injected with control ^{111}In-neutrophils (open columns) or ^{111}In-neutrophils pretreated with UK-74,505 (10^{-7} M for 15 min, cross hatched columns), as described in the Methods section. (d) Guinea-pigs were injected with control ^{111}In-eosinophils (open columns) or ^{111}In-eosinophils pretreated with UK-74,505 (10^{-6} M for 15 min, cross hatched columns). Five min after administration of labelled cells, PAF (10^{-9} mol per site) was injected i.d. After 2 h, the animals were killed and the cell accumulation measured as described in Methods. Results are expressed as number of ^{111}In-leucocytes per site per 5×10^6 cells injected and presented as mean ± s.e.mean of responses obtained after subtraction of saline/BSA values in $n = 6$ pairs. Significant differences from control are indicated by $^*P < 0.01$.

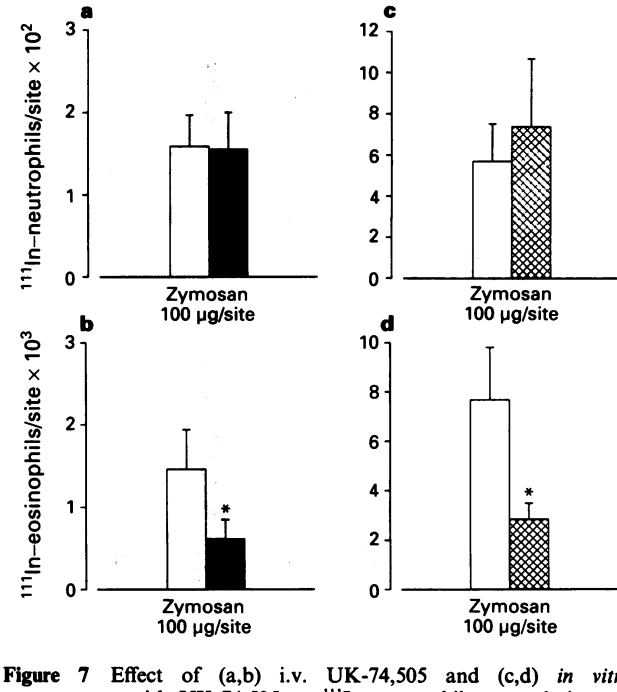


Figure 7 Effect of (a,b) i.v. UK-74,505 and (c,d) *in vitro*-pretreatment with UK-74,505 on ^{111}In-neutrophil accumulation and ^{111}In-eosinophil accumulation induced by zymosan particles (100 μg per site) in guinea-pig skin. (a,b) Guinea-pigs received an i.v. injection of either vehicle (open columns) or 2.5 mg kg^{-1} UK-74,505 (solid columns) followed 10 min later by the i.v. injection of labelled cells. (c) Guinea-pigs were injected with control ^{111}In-neutrophils (open columns) or ^{111}In-neutrophils pretreated with UK-74,505 (10^{-7} M for 15 min, cross hatched columns), as described in the Methods section. (d) Guinea-pigs were injected with control ^{111}In-eosinophils (open columns) or ^{111}In-eosinophils pretreated with UK-74,505 (10^{-6} M for 15 min, cross hatched columns). Five min after administration of labelled cells, zymosan (100 μg per site) was injected i.d. After 2 h, the animals were killed and the cell accumulation measured as described in Methods. Results are expressed as number of ^{111}In-leucocytes per site per 5×10^6 cells injected and presented as mean ± s.e.mean of responses obtained after subtraction of saline/BSA values in $n = 5$–6 pairs. Significant differences from control are indicated by $^*P < 0.05$.

induced elevations in cytoplasmic levels of Ca^{2+} in guinea-pig neutrophils and eosinophils in a dose-dependent manner. Further, as we previously found with rabbit platelets (Pons *et al.*, 1993), UK-74,505 was long acting and guinea-pig neutrophils and eosinophils pretreated with UK-74,505 remained unresponsive to PAF for the 4 h period investigated. This effect of UK-74,505 was selective as the antagonist did not affect elevations in $[Ca^{2+}]_i$ induced by LTB_4. These results also demonstrate that the increases in $[Ca^{2+}]_i$ induced by LTB_4 in neutrophils and eosinophils are not dependent on the generation of PAF.

In vivo, intravenous UK-74,505 blocked the cell accumulation and oedema formation induced by PAF, but had no effect on the responses induced by LTB_4 or ZAP. These experiments demonstrated the selectivity of the antagonist *in vivo* and suggest that, in this model, PAF does not act as a secondary mediator in the induction of oedema and leucocyte accumulation elicited by LTB_4 and C5a. PAF has however been implicated in a number of allergic inflammatory reactions and using the hetrazepine PAF antagonist, WEB 2086, we have previously investigated the role of endogenous PAF in inducing ^{111}In-eosinophil accumulation (Weg *et al.*, 1992) and oedema formation (Weg *et al.*, 1991) in a model of type I hypersensitivity, the PCA reaction. It was found that while WEB 2086 alone had no effect, a combination with an antihistamine and a LTD_4 receptor antagonist, totally suppressed the oedema formation in this model. However, WEB 2086 alone or in combination failed to affect eosinophil accumulation during guinea-pig PCA (Weg *et al.*, 1992). Since UK-74,505 is a more potent and long lasting antagonist, the role of PAF was reassessed in this model by the use of this compound.

Intradermal injection of antigen into sensitized sites led to a dose-dependent accumulation of ^{111}In-eosinophils and ^{111}In-neutrophils and oedema formation. Pretreatment of guinea-pigs with UK-74,505 had no effect on leucocyte accumulation or oedema formation in this model, strongly suggesting that endogenously released PAF is not playing a major role in the guinea-pig PCA. It is possible that the level of PAF produced, on its own, is not sufficient to affect cell accumulation, but together with histamine and LTD_4 can contribute to increased plasma leakage (Weg *et al.*, 1991; 1992). In contrast to the oedema response, the mediators involved in the induction of neutrophil and eosinophil accumulation in the guinea-pig PCA reaction remain unknown. These mediators may be mast cell derived such as interleukin-3 (IL-3), IL-4, IL-5, GM-CSF (Plaut *et al.*, 1989; Wodnar-Filipowicz *et al.*, 1989), tumour necrosis factor α (TNFα) (Gordon *et al.*, 1990) and IL-8 (Möller *et al.*, 1993), all of which have been implicated in the process of leucocyte accumulation (Nourshargh, 1993).

The avid binding of UK-74,505 to PAF receptors enabled us to address the importance of PAF receptors on eosinophils and neutrophils in the process of PAF-induced leucocyte accumulation *in vivo*. ^{111}In-eosinophils and ^{111}In-neutrophils, with their PAF receptors blocked by pre-incubation with UK-74,505, were administered i.v. to guinea-pigs. In contrast to the inhibitory effect of i.v. UK-74,505 *in vitro* pretreatment of the labelled leucocytes with the PAF antagonist had no effect on the cell accumulation induced by intradermal PAF. These results suggest that leucocytes are not the primary target in the process of PAF-induced neutrophil and eosinophil accumulation in guinea-pig skin. One possible explanation is that exogenous PAF induces oedema formation and leucocyte accumulation by acting on PAF receptors on endothelial cells rather than on leucocytes. Indeed, PAF can act on endothelial cells *in vitro* to enhance the permeability of endothelial cell monolayers to macromolecules (Handley *et al.*, 1984), cause changes in their cytoskeletal structure (Bussolino *et al.*, 1987) and increase their adhesiveness for neutrophils (Zimmerman *et al.*, 1992). In addition, with respect to neutrophil accumulation *in vivo*, Colditz & Movat (1984b) demonstrated that skin sites in the rabbit can be specifically desensitized to PAF by a previous intradermal injection of the phospholipid suggesting that PAF acts on endothelial cells or adjacent tissue cells to induce neutrophil accumulation.

The *in vitro* pretreatment of leucocytes with UK-74,505 resulted in an inhibition of ^{111}In-eosinophil, but not ^{111}In-neutrophil, accumulation in response to intradermal zymosan particles, consistent with the effects obtained with i.v. UK-74,505. These results indicate that endogenously generated PAF is involved in the zymosan-induced eosinophil accumulation and that PAF mediates this response via activation of eosinophil PAF receptors. Whether the zymosan-induced PAF generation is mediated directly or via the generation of a secondary mediator is as yet unknown. The initial stimulus involved in the recruitment of both neutrophils and eosinophils, following the intradermal injection of zymosan particles, is very likely to be the complement derived chemoattractant C5a (Jose *et al.*, 1983). However, since UK-74,505 had no effect on the leucocyte accumulation induced by ZAP, activation of the complement cascade does not appear to be a sufficient stimulus for the generation of endogenous PAF. It is possible that once at the site of inflammation, eosinophils release an array of mediators through the process of phagocytosis (Burke *et al.*, 1990) which may then stimulate endothelial cells to express PAF (Braquet *et al.*, 1989a; Zimmerman *et al.*, 1992). The interaction of endothelial cell-associated PAF with PAF receptors on the eosinophil may then lead to activation and up-regulation of adhesion molecules on the eosinophil thus facilitating the process of eosinophil infiltration into the tissue. Whilst *in vitro*, endothelial cell associated PAF is involved in neutrophil adhesion and migration (Zimmerman *et al.*, 1990, Watanabe *et al.*, 1991; Kuijpers *et al.*, 1992), the lack of effect of UK-74,505 on the neutrophil accumulation response in the present study suggests the existence of other mechanisms. In rabbit skin, the zymosan-induced neutrophil accumulation and oedema formation is totally inhibited by an anti-C5a antibody (Jose & Williams, 1987). In addition, since zymosan can stimulate IL-8 generation *in vivo* (Beaubien *et al.*, 1990; Collins *et al.*, 1991) and IL-8 release from neutrophils *in vitro* (Bazzoni *et al.*, 1991; Au *et al.*, 1994) this potent neutrophil chemoattractant may be amplifying the zymosan-induced neutrophil accumulation and therefore masking any possible inhibitory effects of the PAF antagonist. Although human IL-8 can also induce eosinophil accumulation in guinea-pig skin, this is not a potent effect (Collins *et al.*, 1993).

In conclusion, PAF does not appear to be involved in eosinophil accumulation, neutrophil accumulation and oedema formation induced by LTB_4, ZAP and a PCA reaction. However, our results indicate that PAF has a role in eosinophil accumulation but not neutrophil accumulation, induced by zymosan particles, suggesting the existence of different inflammatory pathways in the induction of neutrophil and eosinophil accumulation *in vivo*. Furthermore, the results suggest that whilst leucocyte PAF receptors do not appear to mediate neutrophil and eosinophil accumulation induced by exogenous PAF, the eosinophil PAF receptors play an important role in eosinophil accumulation induced by endogenously generated PAF in response to zymosan particles.

This work was supported by The Wellcome Trust, National Asthma Campaign and Conselleria de Cultura, Educacion y Ciencia (Generalitat Valencia).

References

ALABASTER, V.A., KEIR, R.F., PARRY, M.J. & DE SOUZA, R.N. (1991). UK-74,505, a novel and selective PAF antagonist, exhibits potent and long lasting activity in vivo. In *New Drugs for Asthma Therapy*. ed. Anderson, G.P., Chapman, I.P. & Morley, J. pp. 221–227. Basle: Birkhauser Verlag.

AU, B.-T., WILLIAMS, T.J. & COLLINS, P.D. (1994). Role of the CD11b/CD18 receptor and platelet activating factor in the regulation of interleukin-8 release from zymosan-stimulated human neutrophils. *Br. J. Pharmacol.*, **112**, 21P.

BAZZONI, F., CASSATELLA, M.A., ROSSI, F., CESKA, M., DEWALD, B. & BAGGIOLINI, M. (1991). Phagocytosing neutrophils produce and release high amounts of the neutrophil-activating peptide 1/interleukin 8. *J. Exp. Med.*, **173**, 771–774.

BEAUBIEN, B.C., COLLINS, P.D., JOSE, P.J., TOTTY, N.F., WATERFIELD, M.D., HSUAN, J. & WILLIAMS, T.J. (1990). A novel neutrophil chemoattractant generated during an inflammatory reaction in the rabbit peritoneal cavity in vivo: purification, partial amino acid sequence and structural relationship to interleukin 8. *Biochem. J.*, **271**, 797–801.

BLOM, M., TOOL, A.T.J., ROOS, D. & VERHOEVEN, A.J. (1992). Priming of human eosinophils by platelet-activating factor enhances the number of cells able to bind and respond to opsonized particles. *J. Immunol.*, **149**, 3672–3677.

BOKOCH, G.M. & GILMAN, A.G. (1984). Inhibition of receptor-mediated release of arachidonic acid by Pertusis toxin. *Cell*, **39**, 301–308.

BRAQUET, P., TOUQUI, L., SHEN, T.Y. & VARGAFTIG, B.B. (1987). Perspectives in platelet-activating factor research. *Pharmacol. Rev.*, **39**, 97–145.

BRAQUET, P., HOSFORD, D., BRAQUET, M., BOURGAIN, R. & BUSSOLINO, F. (1989a). Role of cytokines and platelet-activating factor in microvascular immune injury. *Int. Arch. Allergy Appl. Immunol.*, **88**, 88–100.

BRAQUET, P., PAUBERT-BRAQUET, M., KOLTAI, M., BOURGAIN, R., BUSSOLINO, F. & HORSFORD, D. (1989b). Is there a case for PAF antagonists in the treatment of ischemic states. *Trends Pharmacol. Sci.*, **10**, 23–30.

BURKE, L.A., CREA, S.E.G., WILKINSON, J.R.W., ARM, J.P., SPUR, B.W. & LEE, T.H. (1990). Comparison of the generation of platelet-activating factor and leukotriene C_4 in human eosinophils stimulated by unopsonized zymosan and by the calcium ionophore A23187: the effects of nedocromil sodium. *J. Allergy Clin. Immunol.*, **85**, 26–35.

BUSSOLINO, F., CAMUSSI, G., AGLIETTA, M., BRAQUET, P., BOSIA, A., PESCARMONA, G., SANAVIO, F., D'URSO, N. & MARCHISIO, P.C. (1987). Human endothelial cells are targets for platelet-activating factor. I. Platelet-activating factor induces changes in cytoskeleton structures. *J. Immunol.*, **139**, 2439–2446.

COLDITZ, I.G. & MOVAT, H.Z. (1984a). Kinetics of neutrophil accumulation in acute inflammatory lesions induced by chemotaxins and chemotaxinogens. *J. Immunol.*, **133**, 2169–2173.

COLDITZ, I.G. & MOVAT, H.Z. (1984b). Desensitization of acute inflammatory lesions to chemotaxins and endotoxin. *J. Immunol.*, **133**, 2163–2168.

COLLINS, P.D., JOSE, P.J. & WILLIAMS, T.J. (1991). The sequential generation of neutrophil chemoattractant proteins in acute inflammation in the rabbit in vivo: relationship between C5a and a protein with the characteristics of IL-8. *J. Immunol.*, **146**, 677–684.

COLLINS, P.D., WEG, V.B., FACCIOLI, L.H., WATSON, M.L., MOQBEL, R. & WILLIAMS, T.J. (1993). Eosinophil accumulation induced by human interleukin-8 in the guinea-pig in vivo. *Immunology*, **79**, 312–318.

CZARNETZKI, B.M. & CSATO, M. (1989). Comparative studies of human eosinophil migration towards platelet-activating factor and leukotriene B_4. *Int. Arch. Allergy Appl. Immunol.*, **88**, 191–193.

DOHERTY, D.E., DOWNEY, G.P., WORTHEN, G.S., HASLETT, C. & HENSON, P.M. (1988). Monocyte retention and migration in pulmonary inflammation. *Lab. Invest.*, **59**, 200–213.

FACCIOLI, L.H., NOURSHARGH, S., MOQBEL, R., WILLIAMS, F.M., SEHMI, R., KAY, A.B. & WILLIAMS, T.J. (1991). The accumulation of ^{111}In-eosinophils induced by inflammatory mediators in vivo. *Immunology*, **73**, 222–227.

FOSTER, A., CUNNINGHAM, F. & LEES, P. (1992). PAF: A putative mediator of allergic skin disease in the horse. *Clin. Exp. Allergy*, **22**, 129.

FOSTER, A.P., CUNNINGHAM, F.M. & LEES, P. (1992). Inflammatory effects of platelet activating factor (PAF) in equine skin. *Equine Vet. J.*, **24**, 208–214.

GORDON, J.R., BURD, P.R. & GALLI, S.J. (1990). Mast cells as a source of multifunctional cytokines. *Immunol. Today*, **11**, 458–464.

GRYNKIEWICZ, G., POENIE, M. & TSIEN, R.Y. (1985). A new generation of Ca^{2+} indicators with greatly improved fluorescence properties. *J. Biol. Chem.*, **260**, 3440–3450.

HANAHAN, D.J. (1986). Platelet-activating factor: a biologically active phosphoglyceride. *Annu. Rev. Biochem.*, **55**, 483–509.

HANDLEY, D.A., ARBEENY, C.M., LEE, M.L., VAN VALEN, R.G. & SAUNDERS, R.N. (1984). Effect of platelet activating factor on endothelial permeability to plasma macromolecules. *Immunopharmac.*, **8**, 137–143.

HENOCQ, E. & VARGAFTIG, B.B. (1988). Skin eosinophilia in atopic patients. *J. Allergy Clin. Immunol.*, **81**, 691–695.

HUMPHREY, D.M., MCMANUS, L.M., SATOUCHI, K., HANAHAN, D.J. & PINCKARD, R.N. (1982). Vasoactive properties of acetyl glyceryl ether phosphocholine and analogues. *Lab. Invest.*, **46**, 422–427,

JOSE, P.J., FORREST, M.J. & WILLIAMS, T.J. (1983). Detection of the complement fragment C5a in inflammatory exudates from the rabbit peritoneal cavity using radioimmunoassay. *J. Exp. Med.*, **158**, 2177–2182.

JOSE, P.J. & WILLIAMS, T.J. (1987). Suppression of acute inflammatory responses by anti-C5a antibodies. *Complement*, **4**, 175 (Abstr).

KAY, A.B. (1985). Eosinophils as effector cells in immunity and hypersensitivity disorders. *Clin. Exp. Immunol.*, **62**, 1–12.

KIMANI, G., TONNESEN, M.G. & HENSON, P.M. (1988). Stimulation of eosinophil adherence to human vascular endothelial cells in vitro by platelet-activating factor. *J. Immunol.*, **140**, 3161–3166.

KROEGEL, C., YUKAWA, T., DENT, G., VENGE, P., CHUNG, K.F. & BARNES, P.J. (1989a). Stimulation of degranulation from human eosinophils by platelet-activating factor. *J. Immunol.*, **142**, 3518–3526.

KROEGEL, C., YUKAWA, T., WESTWICK, J. & BARNES, P.J. (1989b). Evidence for two platelet activating factor receptors on eosinophils: dissociation between PAF-induced intracellular calcium mobilization, degranulation and superoxide anion generation in eosinophils. *Biochem. Biophys. Res. Commun.*, **162**, 511–521.

KUIJPERS, T.W., HAKKERT, B.C., HART, M.H.L. & ROOS, D. (1992). Neutrophil migration across monolayers of cytokine-prestimulated endothelial cells: a role for platelet-activating factor and IL-8. *J. Cell Biol.*, **117**, 565–572.

MALEGH, H.L. & GALLIN, J.I. (1987). Neutrophils in human diseases. *N. Engl. J. Med.*, **317**, 687–694.

MÖLLER, A., LIPPERT, U., LESSMANN, D., KOLDE, G., HAMANN, K., WELKER, P., SCHADENDORF, D., ROSENBACH, T., LUGER, T. & CZARNETZKI, B.M. (1993). Human mast cells produce IL-8. *J. Immunol.*, **151**, 3261–3266.

NOURSHARGH, S. (1993). Mechanisms of neutrophil and eosinophil accumulation in vivo. *Am. Rev. Respir. Dis.*, **148**, S60–S64.

NOURSHARGH, S., PERKINS, J.A., SHOWELL, H.J., MATSUSHIMA, K., WILLIAMS, T.J. & COLLINS, P.D. (1992). A comparative study of the neutrophil stimulatory activity in vitro and pro-inflammatory properties in vivo of 72 amino acid and 77 amino acid IL-8. *J. Immunol.*, **148**, 106–111.

O'CONNOR, B.J., RIDGE, S.M., CHEN-WORSDELL, Y.M., UDEN, S., BARNES, P.J. & CHUNG, K.F. (1991). Complete inhibition of airway and neutrophil responses to inhaled platelet activating factor (PAF) by an oral PAF antagonist, UK-74,505. *Am. Rev. Respir. Dis.*, **143**, 156A.

PAGE, C. & ABBOT, A. (1989). PAF: new antagonist, new roles in disease and a major role in reproductive biology. *Trends Pharmacol. Sci.*, **10**, 255–257.

PARRY, M.J., ALABASTER, V.A., CHEESEMAN, H.E., DE SOUZA, R.N. & KEIR, R.F. (1990). In vitro and in vivo profile of UK-74,505: a novel, highly potent and selective dihydropyridine PAF antagonist. *J. Lipid Mediators*, **2**, 181.

PLAUT, M., PIERCE, J.H., WATSON, C.J., HANLEY-HYDE, J., NORDAN, R.P. & PAUL, W.E. (1989). Mast cell lines produce lymphokines in response to cross-linkage of Fc epsilon RI or to calcium ionophores. *Nature*, **339**, 64–67.

PONS, F., ROSSI, A.G., NORMAN, K.E., WILLIAMS, T.J. & NOURSHARGH, S. (1993). Role of platelet-activating factor in platelet accumulation in rabbit skin: effect of the novel long-acting PAF antagonist, UK-74,505. *Br. J. Pharmacol.*, **109**, 234–242.

SPRINGER, T.A. (1990). Adhesion receptors of the immune system. *Nature*, **346**, 425–434.

TEIXEIRA, M.M., WILLIAMS, T.J. & HELLEWELL, P.G. (1993). E-type prostaglandins enhance local oedema formation and neutrophil accumulation but suppress eosinophil accumulation in guinea pig skin. *Br. J. Pharmacol.*, **110**, 416–422.

TERRITO, M.C., GANZ, T., SELSTED, M.E. & LEHRER, R. (1989). Monocyte-chemotactic activity of defensins from human neutrophils. *J. Clin. Invest.*, **84**, 2017–2020.

WARDLAW, A.J., MOQBEL, R., CROMWELL, O. & KAY, A.B. (1986). Platelet-activating factor. A potent chemotactic and chemokinetic factor for human eosinophils. *J. Clin. Invest.*, **78**, 1701–1706.

WATANABE, M., YAGI, M., OMATA, M., HIRASAWA, N., MUE, S., TSURUFUJI, S. & OHUCHI, K. (1991). Stimulation of neutrophil adherence to vascular endothelial cells by histamine and thrombin and its inhibition by PAF antagonists and dexamethasone. *Br. J. Pharmacol.*, **102**, 239–245.

WATSON, J.W., SHOWELL, H.J. & FREIERT, K.W. (1991). The PAF receptor antagonist UK-74,505 but not WEB-2086 blocks the airway obstructive response to aerosolized antigen in actively sensitized boosted guinea pigs. *Am. Rev. Respir. Dis.*, **143**, 154A.

WEDMORE, C.V. & WILLIAMS, T.J. (1981a). Control of vascular permeability by polymorphonuclear leukocytes in inflammation. *Nature*, **289**, 646–650.

WEDMORE, C.V. & WILLIAMS, T.J. (1981b). Platelet-activating factor (PAF), a secretory product of polymorphonuclear leukocytes, increases vascular permeability in rabbit skin. *Br. J. Pharmacol.*, **74**, 916–917P.

WEG, V.B., WATSON, M.L., CORDEIRO, R.S.B. & WILLIAMS, T.J. (1991). Histamine, leukotriene D_4 and platelet activating factor in guinea pig passive cutaneous anaphylaxis. *Eur. J. Pharmacol.*, **204**, 157–163.

WEG, V.B., WATSON, M.L., FACCIOLI, L.H. & WILLIAMS, T.J. (1992). [^{111}In]-eosinophil accumulation during passive cutaneous anaphylaxis in the guinea pig. *Br. J. Pharmacol.*, **105**, 127P.

WEG, V.B., WILLIAMS, T.J., LOBB, R.R. & NOURSHARGH, S. (1993). A monoclonal antibody recognising very late activation antigen-4 (VLA-4) inhibits eosinophil accumulation in vivo. *J. Exp. Med.*, **177**, 561–566.

WODNAR-FILIPOWICZ, A., HEUSSER, H. & MORONI, C. (1989). Production of the haemopoietic growth factors GM-CSF and interleukin-3 by mast cells in response to IgE receptor-mediated activation. *Nature*, **339**, 150–152.

ZIMMERMAN, G.A., MCINTYRE, T.M., MEHRA, M. & PRESCOTT, S.M. (1990). Endothelial cell-associated platelet-activating factor: a novel mechanism for signaling intercellular adhesion. *J. Cell Biol.*, **110**, 529–540.

ZIMMERMAN, G.A., PRESCOTT, S.M. & MCINTYRE, T.M. (1992). Endothelial cell interactions with granulocytes: tethering and signaling molecules. *Immunol. Today*, **13**, 93–100.

ZORATTI, E.M., SEDGWITK, J.B., BATES, M.E., VRTIS, R.F., GEIGER, K. & BUSSE, W.W. (1992). Platelet-activating factor primes human eosinophil generation of superoxide. *Am. J. Respir. Cell Mol. Biol.*, **6**, 100–106.

(Received April 15, 1994
Revised May 23, 1994
Accepted June 1, 1994)

Br. J. Pharmacol. (1994), **113**, 522–526 © Macmillan Press Ltd, 1994

Inhibition by SR140333 of NK_1 tachykinin receptor-evoked, nitric oxide-dependent vasodilatation in the hamster cheek pouch microvasculature *in vivo*

[1]Judith M. Hall & Susan D. Brain

Pharmacology Group, Biomedical Sciences Division, King's College London, Manresa Road, London SW3 6LX

1 This study investigated tachykinin-evoked vasodilatation in the microvasculature of the hamster cheek pouch *in vivo*. Arterioles and venules were observed by intravital microscopy with video recording, and vasodilatation and constriction, defined as changes in blood vessel diameter, measured by image analysis. All agents were applied topically by superfusion. None of the agents tested had a significant effect on venule diameter.

2 When arterioles were preconstricted (by ca. 50%) with endothelin-1 present in the superfusing medium, substance P (0.3–30 nM) was a potent vasodilator, being 10 fold more active than both neurokinin A and the NK_1 receptor-selective agonist, substance P methyl ester. The NK_2 receptor-selective agonist, [β-Ala^8]-NKA(4-10)(0.1–10 μM) was active only at high concentrations, and the NK_3 receptor-selective agonist senktide (0.1–10 μM) was virtually inactive ($n = 8$ hamsters). Dilatation evoked by tachykinins and analogues was rapid in onset (<0.5 min) and readily reversible.

3 At low concentrations (1–10 nM), the non-peptide tachykinin NK_1 receptor antagonist SR140333 ((S)1-{2-[3(3,4-dichlorophenyl)-1-(3-iso-propoxyphenylacetyl)piperidin-3-yl]ethyl}-4-phenyl-1-azoniabicyclo[2.2.2]octone, chloride) had no effect on the diameter of preconstricted arterioles *per se*, but potently inhibited dilator responses to substance P methyl ester (apparent pK_B 9.9 ± 0.2; $n = 5$ hamsters, $n = 10$ estimates). SR140333 (10 nM) did not inhibit submaximal dilator responses evoked by human alpha calcitonin gene-related peptide (αCGRPh; 1.0 nM; $P > 0.05$; $n = 5$).

4 The nitric oxide synthase inhibitor N^G-nitro-L-arginine methyl ester (L-NAME; 10 μM) caused a 51.3 ± 5.4% arteriolar constriction. In the presence of L-NAME, submaximal vasodilator responses to substance P (10–100 nM) and carbachol (0.1–1.0 μM) were significantly attenuated ($n = 5$ hamsters; $P < 0.05$) as compared to responses obtained in preparations that were preconstricted to a similar extent by endothelin-1 (48.0 ± 5.6%). L-NAME (10 μM) was without effect on submaximal vasodilator responses to αCGRPh (0.1 nM) or sodium nitroprusside (10 nM) ($n = 5$ hamsters; $P > 0.05$).

5 We conclude that tachykinin-evoked arteriolar vasodilatation in the hamster cheek pouch is mediated via NK_1 receptor activation and depends, at least in part, on the release of nitric oxide. The NK_1 receptors mediating vasodilatation can be blocked by topical application of SR140333; which may therefore be useful in the investigation of the role of NK_1 receptors in neurogenic inflammation in the microvasculature.

Keywords: Cheek pouch (hamster); substance P; neurokinin; tachykinin; NK_1-receptor; nitric oxide; microvasculature; SR140333; L-NAME; vasodilatation

Introduction

Peripherally released sensory neuropeptides, including the tachykinin, substance P and calcitonin gene-related peptide (CGRP), have been shown to have potent effects in the vasculature in a number of species including man (see Holzer, 1992). In the microvasculature, CGRP has been clearly demonstrated to cause long-lasting vasodilatation in many preparations, such as the hamster cheek pouch (Brain *et al.*, 1985; Raud *et al.*, 1991; Hall & Brain, 1993); and has been shown to mediate the increased blood flow resulting from sensory nerve stimulation by capsaicin in rabbit skin (Hughes & Brain, 1991), and by capsaicin and saphenous nerve stimulation in rat skin (Escott & Brain, 1993). Studies with the non-peptide tachykinin NK_1 receptor antagonists, CP-96,345 and RP67580, have established that tachykinins act via NK_1 receptors on post-capillary venules to increase microvascular permeability leading to oedema formation (e.g. Garret *et al.*, 1992; Lembeck *et al.*, 1992; see Holzer, 1992; Hall, 1994). In the hamster cheek pouch, Gao and coworkers (1993) have recently demonstrated inhibition by CP-96,345 of capsaicin and substance P-evoked plasma extravasation. These studies provide further evidence for a role for NK_1 receptors in the microvasculature.

A role for tachykinins as arteriolar dilators in the microvasculature, however, is not well documented. Substance P has been found by intravital microscopy (Persson *et al.*, 1991; Raud *et al.*, 1991) and laser-Doppler flowmetry (Andrews & Helme, 1989; Kerezoudis *et al.*, 1993; Lam & Ferrell, 1993) to cause transient arteriolar dilatation, and the higher activity of substance P as compared to neurokinins A and B has led to the suggestion that arteriolar dilatation results, at least in part, from NK_1 receptor stimulation (see Lam & Ferrell, 1993). Confirmation of NK_1-receptor evoked arteriolar dilatation, however, requires evidence from studies with receptor-selective antagonists. There are few published studies involving the use of antagonists in the microvasculature. Limited examples include inhibition of the substance P-evoked increase in blood flow in the rat hind knee joint by the NK_1 receptor antagonist, CP-96,345 (Lam & Ferrell, 1993), and inhibition of substance P methyl ester-evoked dilatation in guinea-pig pial arterioles by the peptide NK_1 receptor antagonist, GR82334 (Beattie *et al.*, 1993).

The aim of the present study was to use intravital microscopy to carry out a quantitative investigation of the tachykinin receptors mediating vasodilatation in the hamster cheek pouch *in vivo*. We described here the effects of tachykinin receptor-selective agonists and the recently des-

[1] Author for correspondence.

cribed non-peptide NK_1 receptor antagonist, SR140333 (Emonds-Alt *et al.*, 1993) on NK_1 receptor-mediated vasodilatation in the microvasculature. We confirm that NK_1 receptors mediate tachykinin-evoked arteriolar vasodilatation in the microvasculature, and demonstrate a role for nitric oxide in basal and NK_1 receptor-mediated arteriolar dilatation. We suggest that the novel non-peptide NK_1 receptor antagonist, SR140333, may be a valuable tool in investigating the role of NK_1 receptors in neurogenic inflammation since it is active following topical application, and unlike several other non-peptide NK_1 receptor antagonists, does not appear to have effects, such as ion channel blockade, unrelated to tachykinin receptor antagonism (Emonds-Alt *et al.*, 1993).

A preliminary account of this work has been communicated at the meeting of the European Neuropeptide Club, Strasbourg, France, April 1994 (Hall *et al.*, 1994).

Methods

Tissue preparation

Male golden (Syrian) hamsters (90–160 g) were anaesthetized with sodium pentobarbitone (Sagatal 50 mg kg^{-1}, i.p.) and anaesthesia was maintained with 15 mg kg^{-1} pentobarbitone as required. A single layer of vascular membrane was prepared as described by Duling (1973) with some modifications (Brain, 1989). Briefly, the hamster was placed on a specially designed stage with a central depressed well, the right cheek pouch was gently everted and placed in the well and pinned to a silicon rubber ring encircling a window. A single vascular layer was dissected out keeping an intact blood supply, and all connective tissue was removed. The tissue was superfused with Krebs-bicarbonate solution (composition mM: NaCl 120, KCl 47, $MgCl_2$ 0.12, $CaCl_2$ 0.18, glucose 10, $NaHCO_3$ 23) at a rate of 4 ml min^{-1} and the Krebs solution, warmed to 35°C, was gassed with 5% CO_2 in air. An area of microvasculature was selected which allowed an arteriole and adjacent venule (each between 20 and 40 μm in diameter) to be viewed concomitantly. The microvessels were observed with a Leiz dialux microscope having a 27 × salt-water dipping objective and 10 × eye pieces. Diameters of microvessels were measured using a computerised imaging and data analysis system (Kompira Ltd, Strathclyde, U.K.). In all experiments, unless stated otherwise, arterioles were preconstricted (by ca. 50%) with endothelin-1 (usually 30–300 pM) superfused 20 min before, and throughout, the experiment. All agents were applied to the cheek pouch topically by superfusion. Following application of dilator agents, vessel diameters were measured at 30 s, 1 min and every min thereafter until a maximal dilatation was obtained. In all studies, both arteriole and venule diameters were monitored concomitantly.

Tachykinin receptor studies

Up to five tachykinins and analogues (substance P, neurokinin A, substance P methyl ester, [β-Ala^8]-NKA(4-10) and Succ-[Asp^6,Me-Phe^8]-SP(6-11) (senktide)) were applied to each cheek pouch using a cumulative-dosing protocol with a random order of peptides between hamsters. Maximal dilator responses to tachykinins developed within 1–2 min of drug application, so each concentration of peptide was applied for 2 min. In experiments with SR140333, following determination of a control concentration-response curve to substance P methyl ester, concentration-responses curves were obtained every 20 min in the presence of increasing concentrations of SR140333 (1, 3 and 10 nM; 10 min incubation see Emonds-Alt *et al.*, 1993; test hamsters). In a separate series of experiments investigating the reproducibility of agonist responses, full cumulative concentration-response curves were obtained every 20 min for substance P methyl ester for 2.5 h (the duration of the longest experiment). In a separate series of experiments, SR140333 (10 nM) was tested against submaximal responses to human alpha CGRP (αCGRPh; 1 nM). Substance P (100 nM) and neurokinin A (100 nM) were also tested for effects on basal blood vessel diameter in cheek pouches that were not superfused with endothelin-1.

Nitric oxide studies

Preparations were superfused with Krebs solution containing N^G-nitro-L-arginine methyl ester (L-NAME; 10 μM) or endothelin-1 (at concentrations to give equivalent vasoconstriction). Submaximal responses were obtained to carbachol (0.1–1.0 μM), substance P (10 nM–100 nM), αCGRPh (0.1 nM) and sodium nitroprusside (10 nM) using a 20 min dose-cycle and a randomized order of dosing. Responses to carbachol and substance P were maximal within 2 min whereas those to αCGRPh and sodium nitroprusside were maximal after 3 min, so these agents were applied for 2 and 3 min respectively.

Source of drugs

Drugs were obtained as follows: sodium pentobarbitone (Sagatal; Rhône Mérieux Ltd, U.K.), human endothelin-1, substance P, neurokinin A, substance P methyl ester, [β-Ala^8]-NKA(4-10), senktide, bradykinin (Bachem, U.K.). Carbamylcholine chloride (carbachol), N^G-nitro-L-arginine methyl ester, sodium nitroprusside (Sigma, U.K.). SR140333 ((S)1-{2-[3(3,4-dichlorophenyl)-1-(3-iso-propoxyphenylacetyl)piperidin-3-yl] ethyl}-4-phenyl-1-azoniabicyclo[2.2.2]octone, hydrochloride) was a gift from Drs Brelière and Emonds-Alt, Sanofi Recherche, France. All salts were of analytical grade and were obtained from B.D.H., U.K. Senktide and [β-Ala^8]-NKA(4-10) were dissolved in dimethyl sulphoxide, all other peptides and other agents were dissolved in distilled water. Peptides were stored at −20°C.

Expression of results and statistical analysis

Vasodilatation was calculated as % maximal increase in arteriolar diameter (when compared with basal or preconstricted tone). Data from individual experiments were combined, and results are expressed as mean ± s.e.mean of experiments carried out in at least 4 hamsters for each study. One experiment only was carried out in each hamster. Tests for significant differences between means were made using Student's paired or unpaired *t* tests as appropriate. The apparent pK_B values were determined from individual dose-ratios using the Gaddum-Schild equation $pK_B = -\log K_B = \log(x\text{-}1) - \log[A]$; where x is the dose-ratio and [A] the antagonist concentration.

Results

Tachykinin receptor studies

In the absence of endothelin-1 in the superfusing Krebs solution, substance P (100 nM) and neurokinin A (100 nM) gave small, reversible arteriolar dilator responses (by 12.2 ± 2.6% and 14.6 ± 5.6% respectively; $n = 7$). In preparations where arterioles were preconstricted with endothelin-1, all tachykinins and analogues produced a rapid, concentration-related and rapidly reversible arteriolar dilatation, but were without significant effect on venule diameter. The relative activities of the various peptides, however, differed markedly. Thus, substance P was the most potent dilator being approximately 10 fold more active than both neurokinin A and the NK_1 receptor-selective agonist, substance P methyl ester. The NK_2 receptor-selective agonist [β-Ala^8]-NKA(4-10) was active only at high concentrations, and the NK_3 receptor-selective agonist, senktide, was vir-

tually inactive (Figure 1). In experiments with no antagonist, the lateral position and maximal response of the log concentration-response curve to substance P methyl ester did not change with time (2.5 h; $n = 4$; data not shown).

In cheek pouches superfused with endothelin-1, SR140333 (1–10 nM) had no effect on arteriolar diameter *per se*, but caused a concentration-related shift to the right of the log concentration-response curve of the NK_1 receptor-selective agonist, substance P methyl ester (Figure 2). The position of the log concentration-response curve to substance P methyl ester in control hamsters did not change with time ($n = 4$; data not shown). A full kinetic analysis of these data was not carried out (see Discussion); however, for the purpose of comparison, an estimate of antagonist potency (apparent pK_B) was determined. The apparent pK_B was estimated as 9.9 ± 0.2 ($n = 10$ estimates; $n = 5$ hamsters). SR140333 (10 nM) did not inhibit submaximal responses to αCGRPh ($n = 4$; $P > 0.05$; Figure 2), and in these latter experiments as a control, SR140333 (10 nM) significantly inhibited submaximal responses to substance P methyl ester ($n = 4$; $P < 0.01$; Figure 2).

Nitric oxide studies

Superfusion of the cheek pouch with L-NAME (10 μM) caused a gradual arteriolar constriction which stabilized after approximately 20 min at $51.3 \pm 5.4\%$ reduction in arteriole diameter. Control preparations were superfused with endothelin-1 to a similar degree of constriction (by $48.0 \pm 5.6\%$). Concentrations of substance P that caused significant dilatation in endothelin-1 constricted preparations gave markedly reduced dilator responses in preparations superfused with L-NAME (Figure 3). Dilator responses to carbachol were similarly significantly smaller when measured in the presence of L-NAME, whereas submaximal vasodilator responses to αCGRPh (Figure 3) and sodium nitroprusside (not shown) were similar in both groups of hamsters.

Discussion

This study demonstrates that tachykinin-evoked arteriolar vasodilatation in the hamster cheek pouch microvasculature results from NK_1 receptor stimulation, and is dependent, at least in part, on the release of nitric oxide. Further, endogenous nitric oxide release contributes to basal arteriolar tone in the hamster cheek pouch microvasculature. The recently described non-peptide tachykinin NK_1 receptor antagonist, SR140333, is a high affinity and selective antagonist when applied topically in this preparation.

NK_1 receptors

Tachykinin receptors are divided into three types, NK_1, NK_2 and NK_3 (see Guard & Watson, 1991; Maggi *et al.*, 1992, for reviews). In the vasculature, NK_1 receptors account for the majority of reported effects of tachykinins (see Holzer, 1992; Hall, 1994). Consistent with this, in the present study on tachykinin-evoked arteriolar dilatation, the relative activities of the endogenous tachykinins and receptor-selective analogues, and the high affinity of the NK_1 receptor-selective antagonist, SR140333, indicate the involvement of NK_1 receptors in vasodilatation. Thus, as previously described (Raud *et al.*,1991), substance P caused arteriolar dilatation and, in this present study, was found to be 10 fold more potent than neurokinin A. The NK_1 receptor-selective agonist, substance P methyl ester, was also a potent arteriolar vasodilator whereas the NK_2 receptor agonist, [β-Ala^8]-NKA(4-10) was only weakly active at high concentrations and the NK_3 selective agonist senktide was virtually inactive. The vasodilator effect seen with high concentrations of [β-Ala^8]-NKA(4-10) is likely to result from an interaction

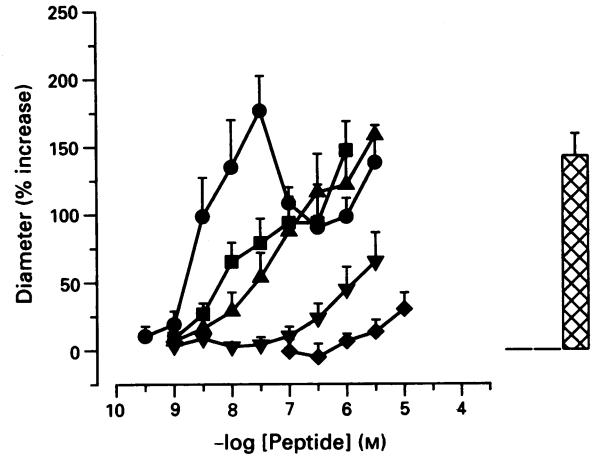


Figure 1 Log concentration-response curves showing vasodilator responses for tachykinins and analogues in the hamster cheek pouch. Arterioles were preconstricted by ca. 50% by endothelin-1, and arteriolar dilatation is expressed as % increase from this preconstricted level. Tachykinins and analogues were applied by superfusion at each concentration for 2 min and results are shown for substance P (●), neurokinin A (▲), substance P methyl ether (■), [β-Ala^8]-NKA(4-10) (▼) and senktide (◆). For comparison, the vasodilator response to sodium nitroprusside (100 nM; cross-hatched column) is shown. Responses are mean ± s.e.mean for experiments carried out on 8 hamsters.

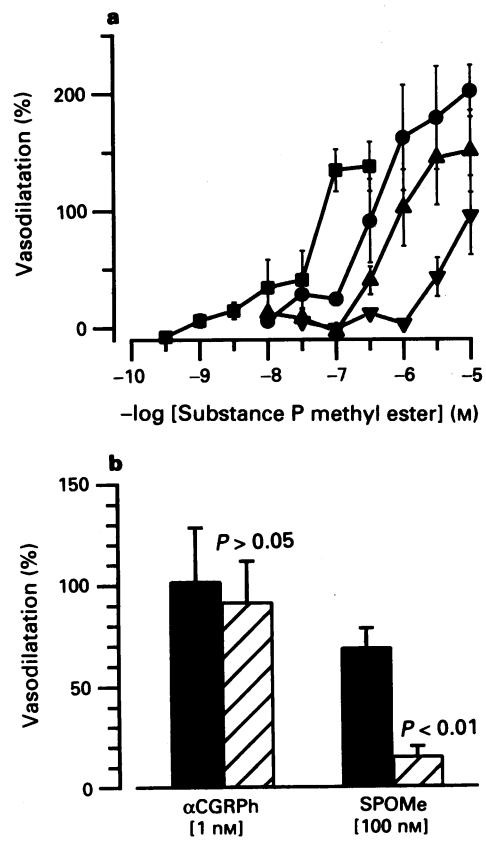


Figure 2 SR140333 selectively inhibits NK_1 receptor-mediated vasodilatation in hamster cheek pouch. In (a), concentration-response curves were obtained for substance P methyl ester either in the absence (■) or presence of SR140333 at 1 nM (●), 3 nM (▲) or 10 nM (▼). Selectivity of SR140333 for NK_1 receptor-mediated vasodilatation is shown in (b). Submaximal vasodilator responses to human alpha calcitonin gene-related peptide (αCGRPh; 1 nM) are unaffected by SR140333 whereas responses to substance P methyl ester (SPOMe, 100 nM) are significantly inhibited. Solid columns show control vasodilator responses; hatched columns, responses obtained in the presence of SR140333 (10 nM). Mean responses ± s.e.mean as shown for 4–5 hamsters.

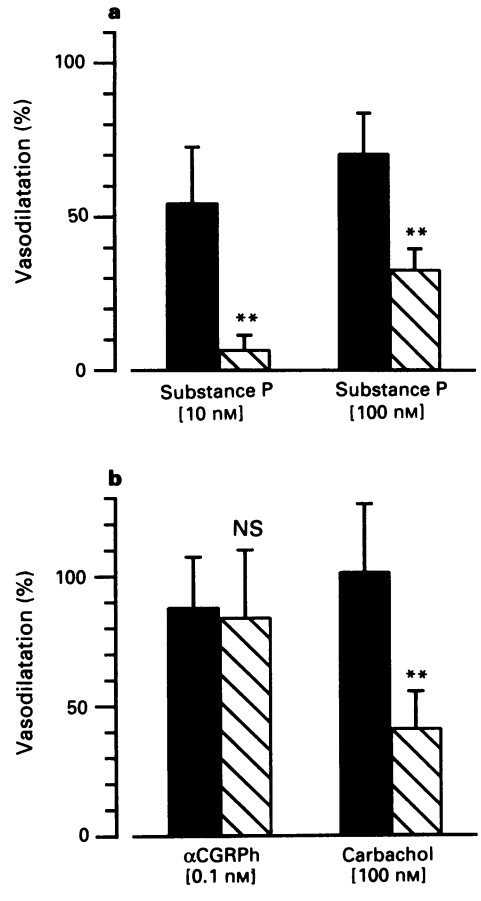


Figure 3 N^G-nitro-L-arginine methyl ester (L-NAME) inhibits vasodilator responses to substance P in hamster cheek pouch microvasculature. L-NAME (10 μM) produced a 51.3 ± 5.4% reduction in basal arteriole diameter. Vasodilator responses obtained in the presence of L-NAME (10 μM; hatched columns) are compared with those obtained in preparations preconstricted to a similar degree (48.0 ± 5.6%) by endothelin-1 (solid columns). In (a) L-NAME significantly inhibited vasodilator responses to substance P (10 and 100 nM), and in (b), vasodilator responses to carbachol (100 nM) were similarly inhibited whereas vasodilator responses to human alpha calcitonin gene-related peptide (α-CGRPh; 0.1 nM) were similar in both groups of hamsters. Responses are shown as mean ± s.e.mean for 5 hamsters. $^{**}P<0.05$.

of this agonist with NK_1 receptors as we have previously suggested in other preparations *in vitro* (Hall *et al.*, 1993b).

The involvement of NK_1 receptors in evoking arteriolar vasodilatation in the hamster cheek pouch was confirmed by our studies with the recently described non-peptide receptor antagonist, SR140333 (Emonds-Alt *et al.*, 1993; Jung *et al.*, 1994). Topical application of SR140333 inhibited arteriolar dilator responses to the NK_1 receptor-selective agonist, substance P methyl ester in a concentration-related manner, but was without effect on submaximal vasodilator responses evoked by αCGRPh. In our experiments on the hamster cheek pouch, we did not think it appropriate to analyse the nature of the antagonism in detail since these experiments were carried out *in vivo*. Further, in the guinea-pig ileum *in vitro*, we found the antagonism of responses to substance P methyl ester by high antagonist concentrations was apparently non-competitive (unpublished observations), possibly as a result of its very high affinity; as also reported by Emonds-Alt *et al.* (1993). However, a comparison of apparent pK_B values indicates that the affinity of SR140333 in the hamster cheek pouch (apparent pK_B 9.9) is similar to its affinity in the guinea-pig ileum (apparent pK_B 9.4; Hall *et al.*, 1994). The antagonist therefore does not appear to distinguish between hamster and guinea-pig NK_1 receptors (see Hall *et al.*, 1993a).

Our results demonstrating NK_1 receptor-mediated arteriolar dilatation in the hamster cheek pouch are consistent with studies in the microvasculature of other species. Thus, topically applied substance P was found to increase blood flow in rat knee joint and this was partially inhibited by the NK_1 receptor antagonist, CP-96,345 (Lam & Ferrell, 1993). In guinea-pig pial arterioles, perivascular administration of the NK_1 receptor-selective agonist, substance P methyl ester, caused vasodilatation, an effect inhibited by the NK_1 receptor antagonist GR82334 (Beattie *et al.*, 1993), and the vasodilatation resulting from nerve stimulation in rat cremaster skeletal muscle microvasculature was inhibited by a tachykinin receptor antagonist (Brock & Joshua, 1993). It should be noted, however, that evidence for the involvement of endogenous tachykinins to sensory nerve-evoked blood flow is limited; and, at least in rat and rabbit skin, evidence favours a role for CGRP (Hughes & Brain, 1991; Delay-Goyet *et al.*, 1992; Escott & Brain, 1993). For example, the NK_1 receptor antagonist, RP67580, does not inhibit the increased blood flow in skin evoked by stimulation of the saphenous nerve in the rat (Delay-Goyet *et al.*, 1992), though the increased blood flow is inhibited by the CGRP receptor antagonist, $CGRP_{8-37}$ (Escott & Brain, 1993). However, basal blood flow in rat extrapulmonary airways is increased by capsaicin, an effect mimicked by substance P, but not CGRP (Piedimonte *et al.*, 1992) suggesting a role for tachykinins in blood flow control in this tissue.

Mechanism of NK_1 receptor evoked vasodilatation

Vasodilator responses to substance P were significantly inhibited by the nitric oxide synthase inhibitor, L-NAME (10 μM), which itself produced a ca. 50% basal arteriolar constriction. This suggests that NK_1 receptor activation results in the release of nitric oxide which is responsible for the observed arteriolar vasodilatation. Nitric oxide-dependent arteriolar vasodilatation has previously been demonstrated in large blood vessels in response to NK_1 receptor activation (see Holzer, 1992; Hall, 1994), in substance P-evoked vasodilatation in certain rat oral microvessels (Kerezoudis *et al.*, 1993), and in substance P and neurokinin A-evoked vasodilatation in rabbit tenuissimus muscle microvasculature (Persson *et al.*, 1991). The observation that L-NAME significantly reduced basal arteriolar diameter in the hamster cheek pouch suggests that tonic release of nitric oxide contribute to basal arteriolar tone, as has been reported previously in rat skin (Lawrence & Brain, 1992), and in other microvasculature beds including the rat gastric mucosa (Tepperman & Whittle, 1992).

In conclusion, we have demonstrated that NK_1 receptor stimulation in the hamster cheek pouch results in arteriolar dilatation. The dilator effect of tachykinins was inhibited by the nitric oxide synthase inhibitor, L-NAME, which also reduced arteriolar diameter in this preparation. These results are consistent with the idea that in certain microvascular beds, endogenous tachykinins, in addition to CGRP, could potentially contribute to neurogenic vasodilatation of arterioles; and that in the case of the tachykinins, such neurogenic vasodilatation may be mediated via nitric oxide release. The possible contribution of the tachykinins to control of blood flow is of interest in that it is well established that the tachykinins act to increase microvascular permeability at the post-capillary venule, leading to oedema formation. The present study therefore indicates that tachykinins can potentially contribute to neurogenic inflammation by more than one NK_1 receptor-mediated acute pro-inflammatory mechanism. SR140333 inhibited NK_1 receptor-mediated vasodilatation, and since this antagonist is active following topical application *in vivo*, it may be a valuable tool with which to investigate the role of NK_1 receptors in neurogenic inflammatory processes.

We thank Drs Brelière and Emonds-Alt, Sanofi Recherche, Montpellier, France for the gift of SR140333 and Dr Ian K.M. Morton for preparing the figures. This study was supported by the Wellcome Trust.

References

ANDREWS, P.V. & HELME, R.D. (1989). Tachykinin-induced vasodilatation in rat skin measured with a laser-Doppler flowmeter: evidence for receptor-mediated effects. *Regul. Pept.*, **25**, 267–275.

BEATTIE, D.T., STUBBS, C.M., CONNER, H.E. & FENIUK, W. (1993). Neurokinin-induced changes in pial artery diameter in the anaesthetized guinea-pig. *Br. J. Pharmacol.*, **108**, 146–149.

BRAIN, S.D. (1989). The direct observation of arteriolar constriction by endothelin in vivo. *Eur. J. Pharmacol.*, **160**, 401–403.

BRAIN, S.D., WILLIAMS, T.J., TIPPINS, J.R., MORRIS, H.R. & MACINTYRE, I. (1985). Calcitonin gene-related peptide is a potent vasodilator. *Nature*, **313**, 54–56.

BROCK, J.W. & JOSHUA, I.G. (1993). Neural release of substance P causes dilation of arterioles in rat striated muscle. *Regul. Pept.*, **43**, 65–71.

DELAY-GOYET, P., SATOH, H. & LUNDBERG, J.M. (1992). Relative involvement of substance P and CGRP mechanisms in antidromic vasodilation in the rat skin. *Acta Physiol. Scand.*, **146**, 537–538.

DULING, B.R. (1973). The preparation and use of the hamster cheek pouch for studies of the microcirculation. *Microvasc. Res.*, **5**, 423–429.

EMONDS-ALT, X., DOUTREMEPUICH, J.-D., HEAULME, M., NELIAT, G., SANTUCCI, V., STEINBERG, R., VILAIN, P., BICHON, D., DUCOUX, J.-P., PROIETTO, V., VAN BROECK, D., SOUBRIE, P., LE FUR, G. & BRELIERE, J.-C. (1993). In vitro and in vivo biological activities of SR 140333, a novel potent tachykinin NK_1 receptor antagonist. *Eur. J. Pharmacol.*, **250**, 403–413.

ESCOTT, K.J. & BRAIN, S.D. (1993). Effect of a calcitonin gene-related peptide antagonist ($CGRP_{8-37}$) on skin vasodilatation and oedema induced by stimulation of the rat saphenous nerve. *Br. J. Pharmacol.*, **110**, 772–776.

GAO, X.-P., ROBBINS, R.A., SNIDER, R.M., LOWE III, J., RENNARD, S.I., ANDIN, P. & RUBINSTEIN, I. (1993). NK_1 receptors mediate tachykinin-induced increase in microvascular clearance in hamster cheek pouch. *Am. J. Physiol.*, **265**, H593–H598.

GARRET, C., CARRUETTE, A., FARDIN, V., MOUSSAOUI, S., PEYRONEL, J.-F., BLANCHARD, J.-C. & LADURON, P.M. (1991). Pharmacological properties of a potent and selective nonpeptide substance P antagonist. *Proc. Natl. Acad. Sci. U.S.A.*, **88**, 10208–10212.

GUARD, S. & WATSON, S.P. (1991). Tachykinin receptor types: classification and membrane signalling mechanisms. *Neurochem. Int.*, **18**, 149–165.

HALL, J.M. (1994). Receptor function in the periphery. In *The Tachykinin Receptors*. ed. Buck, S.H. & Totowa, N.J., Chapter 17. New Jersey, U.S.A.: Humana Pres Inc.

HALL, J.M. & BRAIN, S.D. (1993). Quantification of the vasodilator effects of CGRP, amylin and [$Cys(ACM)^{2,7}$]-hCGRP on the microvasculature of the hamster cheek pouch in vivo. *Neuropeptides*, **24**, P52.

HALL, J.M., BUTT, S. & BRAIN, S.D. (1994). SR140333 inhibits NK_1-receptor mediated vasodilation in hamster cheek pouch microvasculature. *Neuropeptides*, **26**, 39.

HALL, J.M., CAULFIELD, M.P., WATSON, S.P. & GUARD, S. (1993a). Receptor subtypes or species homologues: relevance to drug discovery. *Trends Pharmacol. Sci.*, **14**, 376–383.

HALL, J.M., MITCHELL, D. & MORTON, I.K.M. (1993b). Tachykinin receptors mediating responses to sensory nerve stimulation and exogenous tachykinins and analogues in the rabbit isolated iris sphincter. *Br. J. Pharmacol.*, **109**, 1008–1013.

HOLZER, P. (1992). Peptidergic sensory neurons in the control of vascular functions: mechanisms and significance in the cutaneous and splanchnic vascular beds. *Rev. Physiol. Biochem. Pharmacol.*, **121**, 49–146.

HUGHES, S.R. & BRAIN, S.D. (1991). A calcitonin gene-related peptide (CGRP) antagonist ($CGRP_{8-37}$) inhibits microvascular responses induced by CGRP and capsaicin in skin. *Br. J. Pharmacol.*, **104**, 738–742.

JUNG, M., CALASSI, R., MARUANI, J., BARNOUIN, M.C., SOUILHAC, J., PONCELET,M., GUEUDET, C., EMONDS-ALT, X., SOUBRIE, P., BRELIERE, J.-C. & LE FUR, G. (1994). Neuropharmacological characterization of SR 140333, a non-peptide antagonist of NK_1 receptors. *Neuropharmacology*, **33**, 167–179.

KEREZOUDIS, N.P., OLGART, L. & EDWALL, L. (1993). Differential effects of nitric oxide synthesis inhibition on basal blood flow and antidromic vasodilation in rat oral tissues. *Eur. J. Pharmacol.*, **241**, 209–219.

LAM, F.Y. & FERRELL, W.R. (1993). Effects of interactions of naturally-occurring neuropeptides on blood flow in the rat knee joint. *Br. J. Pharmacol.*, **108**, 694–699.

LAWRENCE, E. & BRAIN, S.D. (1992). Responses to endothelins in the rat cutaneous microvasculature: a modulatory role of locally-produced nitric oxide. *Br. J. Pharmacol.*, **106**, 733–738.

LEMBECK, F., DONNERER, J., TSUCHIYA, M. & NAGAHISA, A. (1992). The non-peptide tachykinin antagonist, CP-96,345, is a potent inhibitor of neurogenic inflammation. *Br. J. Pharmacol.*, **105**, 527–530.

MAGGI, C.A., PATACCHINI, R., ROVERO, P. & GIACHETTI, A. (1993). Tachykinin receptors and tachykinin receptor antagonists. *J. Auton. Pharmacol.*, **13**, 23–93.

PERSSON, M.G., HEDQVIST, P. & GUSTAFSSON, L.E. (1991). Nerve-induced tachykinin-mediated vasodilatation in skeletal muscle is dependent on nitric oxide formation. *Eur. J. Pharmacol.*, **205**, 295–301.

PIEDIMONTE, G., HOFFMAN, J.I.E., HUSSEINI, W.K., HISER, W.L. & NADEL, J.A. (1992). Effect of neuropeptides released from sensory nerves on blood flow in the rat airway microcirculation. *J. Appl. Physiol.*, **72**, 1563–1570.

RAUD, J., LUNDEBERG, T., BRODDA-JANSEN, G., THEODORSSON, E. & HEDQVIST, P. (1991). Potent anti-inflammatory action of calcitonin gene-related peptide. *Biochem. Biophys. Res. Commun.*, **180**, 1429–1435.

TEPPERMAN, B.L. & WHITTLE, B.J.R. (1992). Endogenous nitric oxide and sensory neuropeptides interact in the modulation of the rat gastric microcirculation. *Br. J. Pharmacol.*, **105**, 171–175.

(Received April 25, 1994
Revised May 25, 1994
Accepted June 2, 1994)

Br. J. Pharmacol. (1994), **113**, 527–535 © Macmillan Press Ltd, 1994

Block of the delayed rectifier current (I_K) by the 5-HT_3 antagonists ondansetron and granisetron in feline ventricular myocytes

[1]F.G. de Lorenzi, T.R. Bridal & W. Spinelli

Wyeth-Ayerst Research, Cardiovascular and Diabetes Division, CN 8000, Princeton, NJ 08543 U.S.A.

1 We investigated the effects of two 5-HT_3 antagonists, ondansetron and granisetron, on the action potential duration (APD) and the delayed rectifier current (I_K) of feline isolated ventricular myocytes. Whole-cell current and action potential recordings were performed at 37°C with the patch clamp technique.

2 Ondansetron and granisetron blocked I_K with a K_D of 1.7 ± 1.0 and 4.3 ± 1.7 μM, respectively. At a higher concentration (30 μM), both drugs blocked the inward rectifier (I_{K1}).

3 The block of I_K was dependent on channel activation. Both drugs slowed the decay of I_K tail currents and produced a crossover with the pre-drug current trace. These results are consistent with block and unblock from the open state of the channel.

4 Granisetron showed an intrinsic voltage-dependence as the block increased with depolarization. The equivalent voltage-dependency of block (δ) was 0.10 ± 0.04, suggesting that granisetron blocks from the intracellular side at a binding site located 10% across the transmembrane electrical field.

5 Ondansetron (1 μM) and granisetron (3 μM) prolonged APD by about 30% at 0.5 Hz. The prolongation of APD by ondansetron was abolished at faster frequencies (3 Hz) showing reverse rate dependence.

6 In conclusion, the 5-HT_3 antagonists, ondansetron and granisetron, are open state blockers of the ventricular delayed rectifier and show a clear class III action.

Keywords: Myocardium; potassium channels; delayed rectifier; inward rectifier; action potential duration; class III effect

Introduction

Ondansetron and granisetron are two 5-HT_3 receptor antagonists that are used clinically to prevent nausea and vomiting induced by chemotherapy (Aapro, 1991). In addition, preclinical studies suggest that this class of compounds might have clinically useful anxiolytic and antipsychotic actions (Costall *et al.*, 1990). Several studies have also shown that 5-HT_3 antagonists of different chemical structure have significant electrophysiological effects in cardiac muscle. Prolongation of the QT_c electrocardiographic interval in anaesthetized laboratory animals has been reported with tropisetron (Hof *et al.*, 1993), ondansetron and zatosetron (Williams *et al.*, 1991). The effects of tropisetron (ICS 205–930), an indole, have further been examined in cellular electrophysiological studies in guinea-pig papillary muscle, where tropisetron prolonged action potential duration at 30% and 70% of repolarization (APD_{30} and APD_{70}) (Scholtysik, 1987). However, in sheep Purkinje fibres, tropisetron did not have any significant effect on APD_{90} and did shorten APD_{50} (Williams *et al.*, 1985). In a study in guinea-pig ventricular myocytes at concentrations that were high compared to the therapeutic range, tropisetron showed both class I and class III antiarrhythmic actions and blocked potassium, sodium, and calcium currents (Scholtysik *et al.*, 1988). Although tropisetron has been reported to have antiarrhythmic effects in several animal models (Williams *et al.*, 1985; Coker *et al.*, 1986; Hof *et al.*, 1993), a clinical study found limited antiarrhythmic activity in patients with ventricular arrhythmias (Morganroth & McGinn, 1988), while a second clinical report suggested that granisetron might produce serious disturbances of cardiac rhythm, including ventricular arrhythmias and cardiac arrest (Ballard *et al.*, 1992).

In this study, we report that both ondansetron, a carbazole, and granisetron, an indazole, prolonged APD in cat ventricular myocytes. In voltage clamp studies, we examined the effects of both compounds on the delayed rectifier (I_K) and inward rectifier (I_{K1}) potassium currents, as block of these channels is known to delay repolarization. The aim of this study was, first, to investigate the mechanism by which ondansetron and granisetron prolong APD, and, second, to characterize the mechanism of this block. These results could be useful in developing new class III antiarrhythmic agents and in understanding the mechanisms of block of I_K channels.

[1] Author for correspondence.

Methods

Cell preparation

Ventricular myocytes were isolated from the myocardium of pentobarbitone-anaesthetized cats weighing 2–4 kg, according to a modification of the method described by Silver *et al.* (1983). Briefly, the hearts were isolated and perfused on a Langendorf apparatus with nominally Ca^{2+}-free Krebs-Henseleit (KH) solution at 37°C for 4 min. The KH contained (in mM): NaCl 130, KCl 4.8, $MgSO_4$ 1.2, NaH_2PO_4 1.2, $NaHCO_3$ 25, dextrose 12.5. The pH was 7.35–7.40 when equilibrated with 95% O_2:5% CO_2. The hearts were then enzymatically digested for 12–15 min with a nominally Ca^{2+}-free KH containing 0.7 mg ml^{-1} of type II collagenase (197/u mg^{-1}; Worthington, Freehold, NJ, U.S.A.). The ventricular tissue was dissected from the atria, minced, and then passed through a 200 μm pore nylon mesh. The filtrate was centrifuged at 720 r.p.m. for 1–2 min. Afterwards, the pellet was re-suspended in Ca^{2+}-free KH. The process was repeated two more times and the pellet then re-suspended in KH containing 2% bovine serum albumin (BSA) and 100 μM Ca^{2+}. The cells were allowed to equilibrate for 5 min at 37°C under a 95% O_2:5% CO_2 gas curtain. The Ca^{2+} concentration was raised after 5 min to 0.5 mM. The ventricular myocytes were plated in 35 mm Petri dishes and stored under controlled

humidified 95% O_2:5% CO_2 atmosphere. The myocytes were used within 8 h of isolation.

Current and voltage recordings

Potassium currents were recorded with the patch-clamp technique in the whole-cell configuration. For recording of transmembrane action potentials the voltage clamp amplifier was switched to the current clamp mode. Action potentials were elicited by 10–15 ms long depolarizing current pulses delivered through the microelectrode. The patch electrodes were made of Kimax-51, a borosilicate glass from Kimble (Toledo, OH, U.S.A.), of 1.5 mm outside diameter. They were pulled on a Narashige vertical puller (Narashige PP-83, Tokyo, Japan) by the 2-stage method. The pipette solution contained (in mM): K-aspartate 145, NaCl 5, $MgCl_2$ 1, EGTA 10, HEPES 5, ATP·Mg 5, phosphocreatine-Na_2 5, pH ajusted to 7.2 with KOH. Electrodes had a resistance of 3–5 MΩ when measured in the bath solution. The external medium was a modified Tyrode solution of the following composition (in mM): NaCl 138, KCl 4, $CaCl_2$ 2, $MgCl_2$ 0.5, $NaHCO_3$ 24, dextrose 5.5. The solution was aerated with 95% O_2:5% CO_2 and the pH was 7.35–7.40. Recordings were performed with a List EPC-7 amplifier (List-Medical, Darmstadt, Germany) coupled either to a Basic-Fastlab (Indec Systems; Sunnyvale, CA, U.S.A.) or pClamp (Axon Instruments, Foster City, CA, U.S.A.) data acquisition and analysis software. Signals were low-pass filtered with a corner frequency of 3 kHz. The reference zero potential was adjusted in the bath solution before forming the seal. The pipette-cell membrane seals showed a resistance greater than 2 GΩ. Capacitance was optimally compensated. Series resistance was 3.54 ± 0.31 MΩ (14 cells), producing for a 100 pA current a 0.35 mV uncertainty on the potential. Data were sampled at 0.5–1.0 kHz, except for the I_{K1} experiments (2 kHz) and the studies of recovery from block (4 kHz).

Data analysis

The delayed rectifier current was analysed from outward tail currents elicited upon repolarization to the holding potential (− 45 mV) from various conditioning potentials (− 45 mV to + 45 mV). Two pulse durations were used, 250 ms and 2500 ms, the former being more relevant to the duration of an action potential and the latter allowing a more complete activation. Concentration-response curves were constructed from the percentages of unblocked tail currents. The concentration-response data were curve-fitted according to the relationship:

$$Y = Y_{max}\text{-}[(Y_{max} - Y_{min})/(1 + (K_D/A)^H)] \quad (1)$$

where Y_{max} and Y_{min} are the theoretical maximum and minimum values of the function. A is the concentration of antagonist (ondansetron or granisetron), K_D the dissociation constant, and H the Hill coefficient. The parameter Y_{max} was set at 100%; Y_{min}, K_D and H were left free during computation.

Activation curves were analysed with a Boltzmann distribution according to the following equation:

$$I = I_{max}/[1 + \exp(V_{1/2}\text{-}V)/k] \quad (2)$$

where I is the recorded tail amplitude and V is the test potential. The potential, V, is the independent variable. The maximum current (I_{max}), the voltage of half activation ($V_{1/2}$), and the slope factor (k) were left free during computation.

The voltage-dependence of block was analysed with a Boltzmann distribution, according to the following equation (Woodhull, 1973):

$$1\text{-}Y = A/(A + (K_D \cdot \exp(-z\delta V/KT)) \quad (3)$$

where K_D is the theoretical dissociation constant at 0 mV, z the charge number, K the Boltzmann constant, T the absolute temperature, and δ the fractional equivalent voltage-dependency. Other variables are as above. K_D and δ were the computed parameters, V was the independent variable.

A non-linear least squares iterative algorithm based on the Gauss-Newton iterative solution method was used to estimate the variables of the equations. The programme was written by Dr K. Goldberg at Wyeth-Ayerst Research and was run on a HP-9836 computer. Uncertainty on computed parameters was assessed from their asymptotic variance. The decay of tail currents was fitted to exponential functions using a nonlinear iterative procedure (Axon Instruments pCLAMP clampfit programme).

Student's t test (paired and unpaired) was used for statistical comparisons. The level of significance was set at $P < 0.05$. Values are expressed as mean ± s.e.mean.

Determination of pK_a and partition coefficients

The values of pK_a were determined by Mr D. Herold (Ancillary Services, Wyeth-Ayerst Research) using a Sirius PCA 101 titrator (Sirius Analytical Instruments Ltd., East Sussex, UK). Octanol/phosphate buffer (pH = 7.4) partition coefficients were determined by Mr J.M. Kulishoff, Jr., (Ancillary Services, Wyeth-Ayerst Research) by high performance liquid chromatography (h.p.l.c.) analysis.

Drugs

Hydrochloride salts of ondansetron (Glaxo Group Research Ltd., Greenford, Middlesex, UK) and granisetron (Smith-Kline Beecham Pharmaceuticals, Betchworth, Surrey, UK) were dissolved in distilled water. Experiments were performed in the presence of nisoldipine (300 nM), which was predissolved in 70% ethanol for a final vehicle concentration of 0.1%. Nisoldipine was a gift from Miles Inc. (West Haven, CT, U.S.A.). All experiments were conducted at 37°C.

Animal care

Animals were cared for and used in accordance with the Animal Welfare Act as amended. Protocols were examined and approved by the Institutional Animal Care Use Committee (IACUC).

Results

Prolongation of action potential duration

Control action potential duration (APD) of cat ventricular myocytes during pacing at 0.5 Hz at 37°C was 456 ± 34 ms (9 cells). Superfusion with ondansetron (1 μM) and granisetron (3 μM) produced a marked lengthening of APD_{90} (Figure 1), from 479 ± 23 to 625 ± 44 ms with ondansetron ($n = 5$) and from 427 ± 71 to 575 ± 117 ms with granisetron ($n = 4$). With ondansetron, APD_{90} returned to pre-drug values after 5 min in drug-free Tyrode solution. With granisetron, the effect was not totally reversible even after prolonged washout: after 15 min, APD_{90} was 478 ± 90 ms. Neither ondansetron nor granisetron affected action potentional amplitude or resting membrane potential. Resting potential values for the ondansetron and granisetron groups were − 78 ± 2 and − 73 ± 3 mV before drug exposure, − 78 ± 3 and − 74 ± 5 mV in presence of drug, and − 78 ± 3 and − 74 ± 5 mV after washout, respectively. Amplitude was 130 ± 4 and 127 ± 3 mV in pre-drug, 129 ± 4 and 123 ± 5 mV in presence of drug and 128 ± 4 and 124 ± 6 mV in washout, respectively. The results of these studies show that ondansetron and granisetron have a clear class III effect.

Block of the delayed rectifier (I_K) current

The mechanism of action of ondansetron and granisetron was examined by studying their effects on the delayed

rectifier current. Under control conditions (Figure 2a and c), depolarization steps from −45 to +45 mV elicited, immediately after the capacitive transient, rapidly decaying transient outward currents (I_{to}), which were followed by slowly developing outward currents. Upon repolarization to −45 mV, each trace was followed by a slowly decaying outward current tail. These tail currents have been shown to represent the deactivation of the delayed rectifier current (Noble & Tsien, 1969), and a measurement of their peak amplitude in reference to holding current provides an estimate of the I_K current activated during the depolarizing step. Conditions were adjusted to minimize inward currents that are normally activated by such depolarizing steps. The fast inward Na^+ current (I_{Na}) was inactivated by holding the cell at a depolarized potential (−45 mV), while the L-type Ca^{2+} current was almost totally blocked by 300 nM nisoldipine in Tyrode solution. After a 6 min exposure to 10 μM ondansetron (Figure 2d) and a 5 min exposure to 10 μM granisetron (Figure 2b), the amplitude of tail currents was significantly reduced. After granisetron, the holding current became less positive by about 70 pA. In 4 similar studies at 10 μM, the holding current was reduced by 52 ± 12 pA. The effects on tail current amplitude and holding current were reversed upon drug washout (not shown). Ondansetron did not affect holding current. Despite the profound block of tail currents, the effect of both compounds on the time-dependent current that developed during the depolarizing step was variable. Previous studies have shown that this current is variable in size and in drug sensitivity among myocytes (Follmer & Colatsky, 1990; Spinelli *et al.*, 1993).

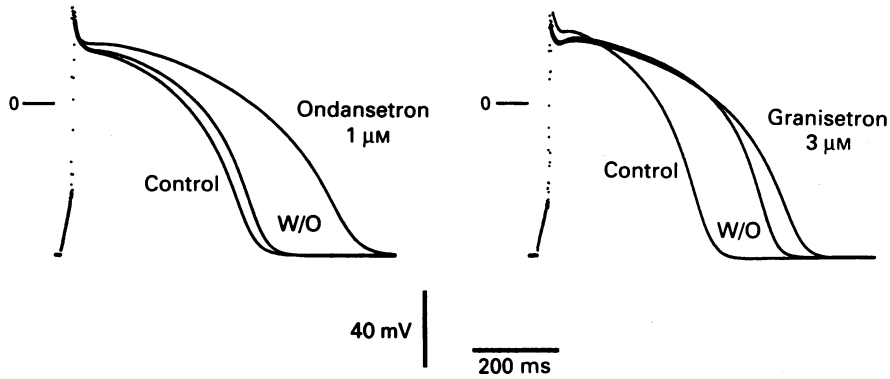


Figure 1 Effects of ondansetron and granisetron on the transmembrane action potential of cat ventricular myocytes. Each tracing represents an average of 10 action potentials obtained at steady-state from two different cells. Temperature: 37°C; stimulation rate: 0.5 Hz.

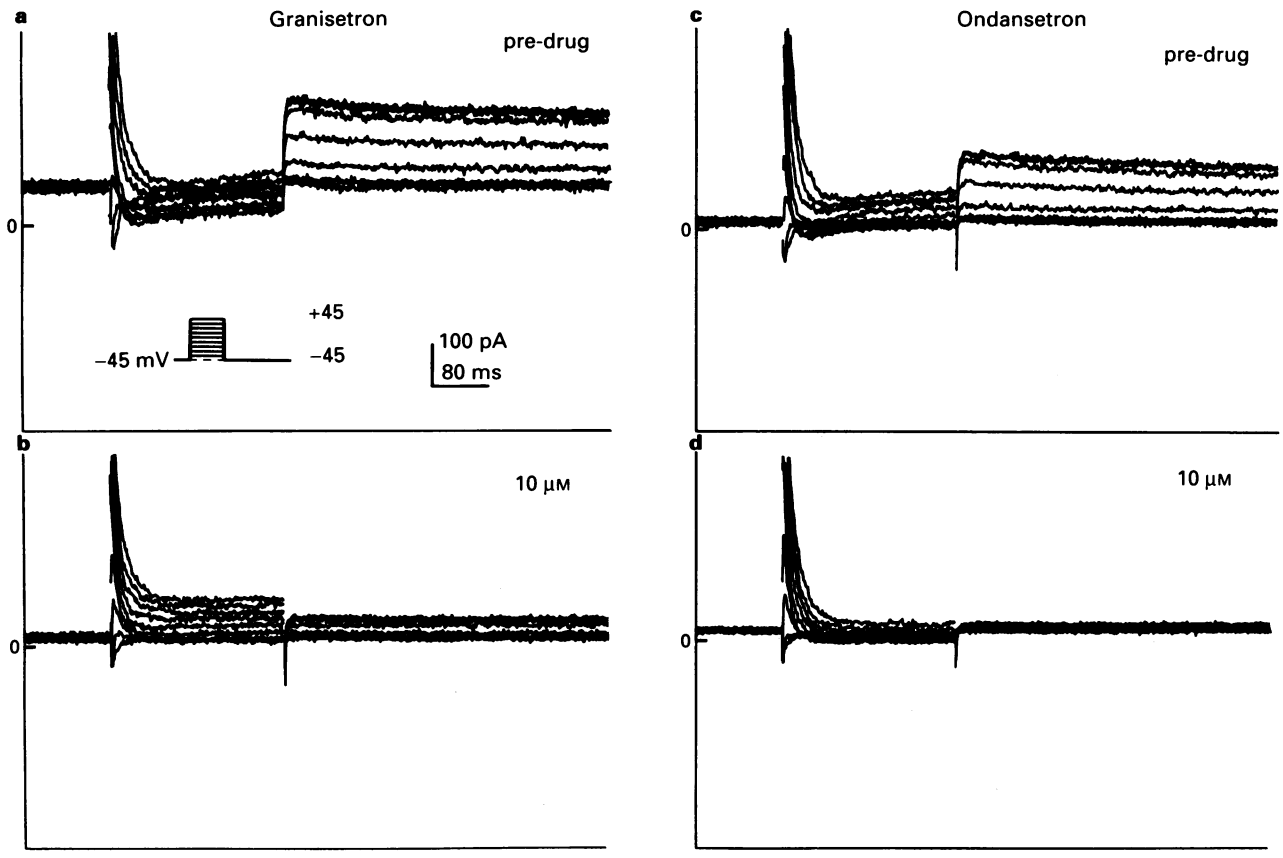


Figure 2 Effect of granisetron and ondansetron on the delayed rectifier tail currents in two different myocytes. The voltage protocol is shown in (a); step duration: 250 ms. Panels (a) and (c), pre-drug condition. Panels (b) and (d), after a 5 to 6 min exposure to 10 μM of either drug. Nisoldipine (300 nM) was present to block $I_{Ca\text{-}L}$. All experiments performed at 37°C.

For these reasons, in this study we only describe the effects of ondansetron and granisetron on I_K tail currents.

Activation parameters

The drug effect on the voltage-dependent activation of the delayed rectifier was studied from the amplitude of tail currents at − 45 mV following step depolarizations to test potentials between − 35 and + 45 mV. Figure 3b and d show the effects of ondansetron (1 μM, $n = 5$) and granisetron (3 μM, $n = 4$) on the activation curves obtained with 2500 ms-long test pulses. These drug concentrations were selected because they produced similar prolongation of APD and similar inhibition of tail currents (see below). Previous studies had also shown that maximum tail current amplitude did not further increase after 5000 ms pulses, showing that a 2500 ms pulse produces full activation (Spinelli *et al.*, 1993). With both compounds, the voltage-dependent activation of tail currents was well fitted by the Boltzmann function. Maximum pre-drug current at maximum activation (I_{max}) was 155 ± 3 and 202 ± 3 pA for the cells treated with granisetron and ondansetron, respectively. Despite the different maximum currents, the pre-drug parameters of activation were similar for both groups. Ondansetron (1 μM, Figure 3b) reduced the current at maximum activation to 63 ± 2% of the pre-drug value. The drug shifted $V_{1/2}$ by 2.7 ± 0.9 mV in the negative direction (from − 10.1 ± 0.7 to − 12.8 ± 1.2 mV) without affecting the slope factor (k: from 8.5 ± 0.6 to 9.1 ± 1.0 mV). After a 10 min washout, $V_{1/2}$ returned to the pre-drug value (− 10.4 ± 1.0 mV) and I_{max} recovered to 90 ± 2% of the pre-drug value. Granisetron (3 μM; Figure 3d) had similar effects, reducing I_{max} to 57 ± 2% and shifting $V_{1/2}$ by 6.4 ± 1.1 mV (from − 8.3 ± 0.5 to − 14.7 ± 1.9 mV), without altering the slope factor (k: from 7.7 ± 0.6 to 6.9 ± 1.6 mV). The effect of granisetron was reversed to a lesser degree even after prolonged washout (10–15 min): I_{max} recovered to 77 ± 1.6% of pre-drug value and $V_{1/2}$ returned to − 10.1 ± 0.9 mV.

The activation of I_K tail currents in the same groups of cells was also studied with 250 ms-long test pulses, a duration more relevant to the duration of action potentials. The resulting tail currents were, at full activation, 10 to 20 pA smaller in amplitude than those observed after 2500 ms-long depolarization steps (Figure 3a and c). Again, although pre-drug I_{max} were different between the two groups (146 ± 3 pA for ondansetron and 187 ± 4 pA for granisetron), the activation parameters were similar. Both compounds reduced I_{max} to a similar extent and shifted the activation curve $V_{1/2}$ in the negative direction by 3.1 ± 1.0 mV for ondansetron and by 5.3 ± 0.7 mV for granisetron (from 4.2 ± 0.9 to 1.1 ± 0.5 mV and from 4.7 ± 0.9 to − 0.6 ± 0.6 mV, respectively) without affecting the slope factors.

Comparison of activation curves obtained after 2500 ms-long (Figure 3b,d) and 250 ms-long steps (Figure 3a,c) reveals that I_{max} values at 250 ms are only slightly lower, both in controls and in presence of drugs. The percentage of block at each voltage is similar at both durations. These results suggest that: (1) the currents activated with the shorter step protocol (250 ms) were close to full activation, and that: (2) the amount of block did not vary between 250 ms and 2500 ms. However, the activation curves obtained with the longer pulse protocol showed a significant shift to the left indicating that more current was activated at more negative test potentials. This observation is quantified by a 12 mV shift of $V_{1/2}$ values in the negative direction with the 2500 ms protocol.

Concentration-response relationships

The concentration-response curves for block of the I_K tail current are shown in Figure 4. The data are presented as percentage of pre-drug amplitude after 2500 ms depolariza-

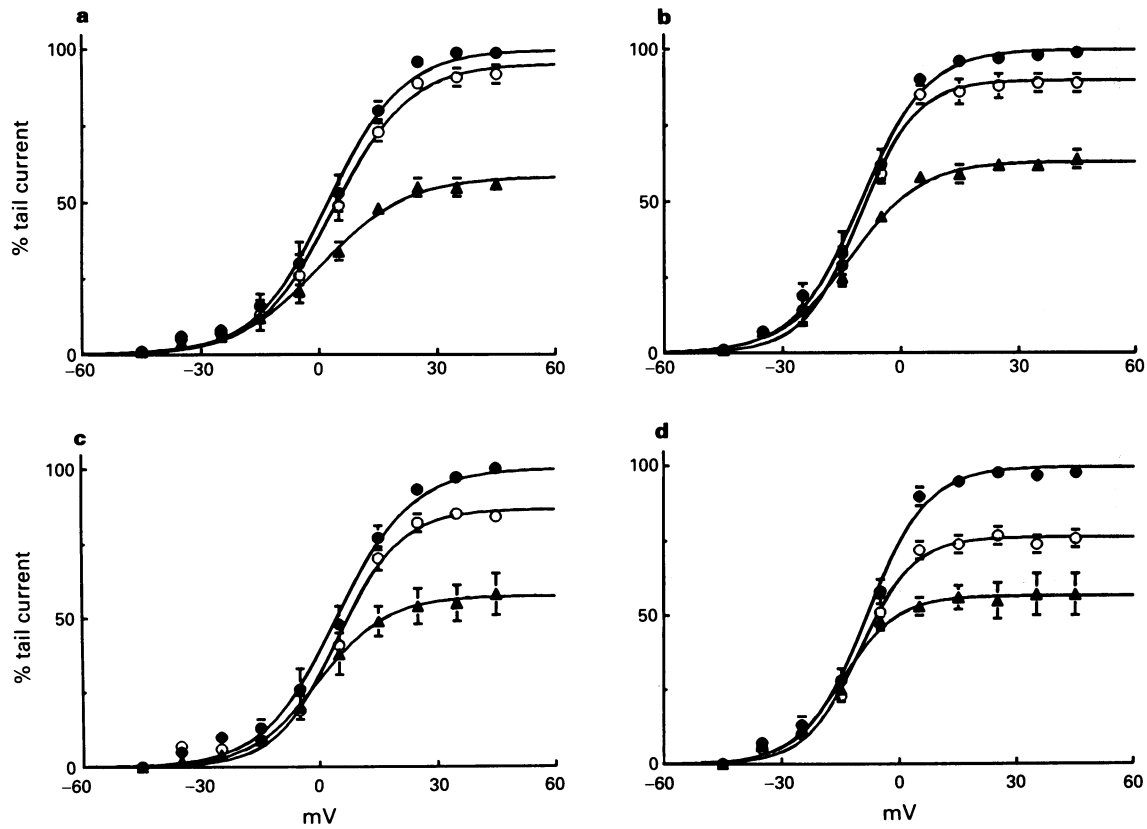


Figure 3 Effects of ondansetron (1 μM, a,b) and granisetron (3 μM, c,d) on the voltage-dependent activation of I_K tail currents: (●) pre-drug controls; (▲) in presence of drug; (○) washout. Two conditioning pulse durations were used for each cell: 250 ms (a,c) and 2500 ms (b,d). All curves normalized to maximum activation (I_{max}) in pre-drug condition.

tions to + 35 mV. The potential and duration of the test pulse were chosen to insure that tail current amplitude reached steady state (see above). Drug concentrations were applied in a cumulative way and each concentration was superfused for 5 to 8 min before the effect on tail currents was measured; this time interval was sufficient to reach a steady-state effect. The data were curve-fitted according to the general equation for receptor occupancy (eq. 1, see Methods). The dissociation constants were estimated to be 1.7 ± 1.0 μM for ondansetron ($n = 13$) and 4.3 ± 1.7 μM ($n = 8$) for granisetron. The Hill coefficients were not significantly different, and were 0.64 ± 0.33 and 0.78 ± 0.37 for ondansetron and granisetron, respectively. The effects of both compounds were not totally reversed by a 10–15 min washout for ondansetron and a 15–25 min washout for granisetron. In summary, ondansetron and granisetron showed good efficacy as blockers of I_K tail currents. Ondansetron was about 2.5 times more potent than granisetron, with both drugs showing similar Hill coefficients.

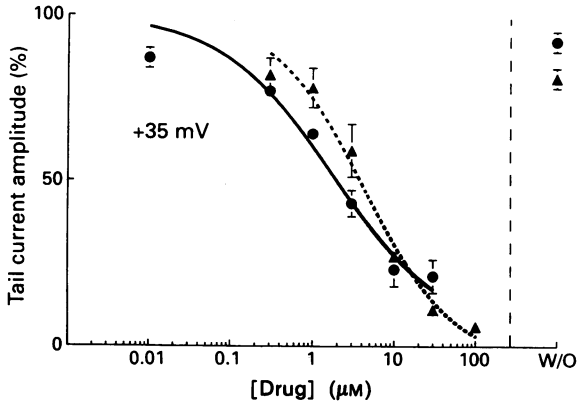


Figure 4 Concentration-response relationships were obtained from the amplitude of tail currents following a 2500 ms-long pulse at + 35 mV. The block of I_K is reversible upon washout (W/O). Each point represents an average of 3 to 9 cells. Ondansetron (●) 13 cells; granisetron (▲), 8 cells.

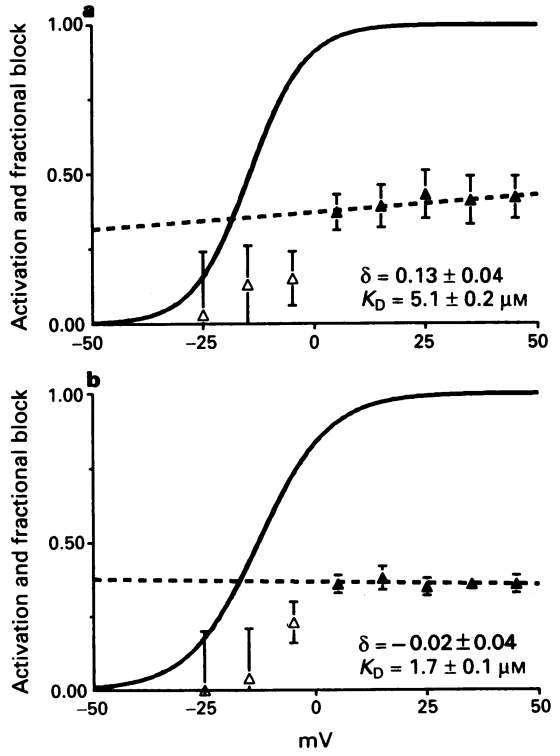


Figure 5 Normalized pre-drug activation curve (solid line) and fractional block (broken line, eq. 3) by granisetron (3 μM; a) and ondansetron (1 μM; b) illustrating the dependence of the block on the activation process and voltage. Only granisetron showed an intrinsic voltage dependence. K_D: dissociation constant at 0 mV; δ: equivalent voltage-dependency, as calculated from eq. 3.

Activation-dependence of block

Analysis of the activation curves showed that little block is observed at voltages more negative than − 5 mV and that block increases with stronger depolarizations, suggesting that the block might be dependent on channel activation. To analyse this phenomenon, the amplitude of the tail current at each potential in the presence of drug is normalized to the amplitude obtained in pre-drug conditions ($I_{drug}/I_{control}$) (Figure 5a and b). With both drugs, the initial degree of block (shown by unfilled symbols) increased steeply in the voltage range of channel activation, until it reached a plateau level at potentials more positive than + 5 mV (shown by filled symbols), when full activation was obtained. A similar profile of block was observed at all drug concentrations (not shown) and it is consistent with the view that ondansetron and granisetron blocked the channel while in the open state.

With granisetron, the degree of block showed a further limited but clear increase between + 5 and + 45 mV, a voltage range where all channels are in the open state. Although the increase of block exhibited a shallow slope, it was observed at all concentrations and it could not be explained by channel gating as it was observed at voltages and at a time (2500 ms) where the activation process had already reached a maximum. Thus, these results were suggestive of a limited, intrinsic, voltage-dependent component in the block by granisetron. Considering that granisetron is a weak base ($pK_a = 9.6$) and thereby most of its molecules will bear a positive charge at physiological pH, it is possible that the voltage-dependency might result from the effect of the transmembrane electric field on the positively charged granisetron molecule. To quantify the voltage sensitivity of the block, the fractional block at full activation was fitted using a Boltzmann distribution function (Woodhull, 1973). The data obtained with 3 μM granisetron (Figure 5a) yielded an equivalent voltage-dependency (δ) of about 0.13, which means that the positively charged molecule is subject to 13% of the transmembrane electric field at its site of action. The computed dissociation constant for 0 mV was 5.1 ± 0.2 μM.

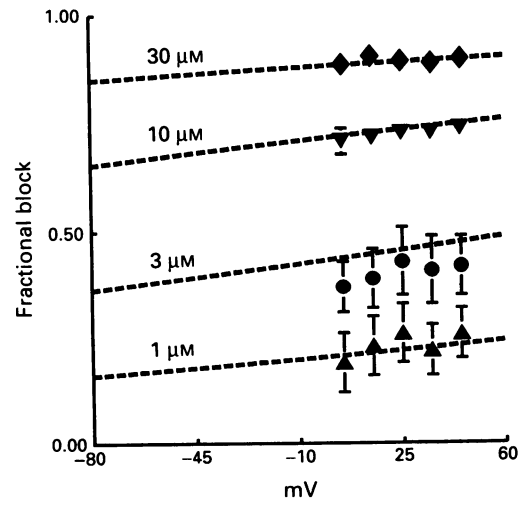


Figure 6 Voltage- and concentration-dependence of I_K block by granisetron showing the best simultaneous fit using eq. 3 for the indicated concentrations. Compared parameters: equivalent voltage-dependency, δ = 0.10 ± 0.04, and dissociation constant at 0 mV, K_D = 3.9 ± 0.7 μM. The lines represent the constrained fit.

This voltage-dependence was consistently observed at various concentrations. The best simultaneous fit of all the data sets obtained is shown in Figure 6. It yielded an equivalent voltage-dependency of 0.10 ± 0.04 and a dissociation constant for 0 mV of 3.9 ± 0.7 μM, in fair agreement with the previously calculated K_D.

Ondansetron is a much weaker base than granisetron, with a pK_a of 7.4, and thus at physiological pH only 50% of the molecules will be positively charged. Over the entire range of concentrations studied, we did not observe any indication of voltage dependency in its blocking action. The results with 1 μM are shown in Figure 5b.

Recovery from block

Analysis of the tail currents showed that the time course of decay was considerably slowed in the presence of drug. This could result from channels that unblock after repolarization and thus contribute to the conductance of outward current before they completely deactivate. Kinetic analysis of this phenomenon is difficult in cat myocytes under normal conditions because the decay of control tail currents at depolarized voltages (e.g. − 40 mV) is very slow and does not allow a reliable estimate of the deactivation time constant. To accelerate the decay of the tail current, 0.2 mM $CdCl_2$ was added to the Tyrode solution. Addition of Cd^{2+} has been shown to speed the decay of I_K tail currents (Follmer *et al.*, 1992b) without affecting their sensitivity to blockers of the delayed rectifier (Colatsky *et al.*, 1994).

The tail current decay was usually well fitted by a single exponential function, but some cells (6 out of 16) showed a second smaller and slower exponential component. In these cases, only the first component describing the fast initial decay of I_K was analysed. The smaller currents of the late phase are of undetermined nature and could include a second component of I_K, or a contamination by electrogenic transporters or other currents. Figure 7a shows the effect of 1 μM ondansetron on the decay of a tail current elicited on repolarization to − 60 mV following a 1000 ms conditioning step at + 40 mV. In the presence of drug, τ increased from 444 ms to 653 ms and the tail current in the presence of drug crossed the control trace after 600 ms. A rounding and delay of the peak of the tail (of about 20 ms) also occurred. In 7 myocytes, τ increased from 242 ± 50 ms to 337 ± 76 ms (+ 39%). These changes of time course are consistent with the view that open channels can release drug upon repolarization and then become available to conduct outward current before they deactivate. Similar results were obtained with granisetron (3 μM) in 9 cells, where τ increased at − 60 mV, from 256 ± 50 ms to 327 ± 52 ms (+ 28%). A significant delay of the peak current (> 8 ms) was observed with both drugs in 9 out of 16 cells and averaged 21 ± 3 ms. In the remaining cells, the delay was too small to be clearly measured against the background noise of the current trace. Figure 7b and c show that the deactivation of tail currents was voltage-dependent. Both drugs slowed the decay of the tail currents and the slowing, in percentage, seemed to decrease with depolarization.

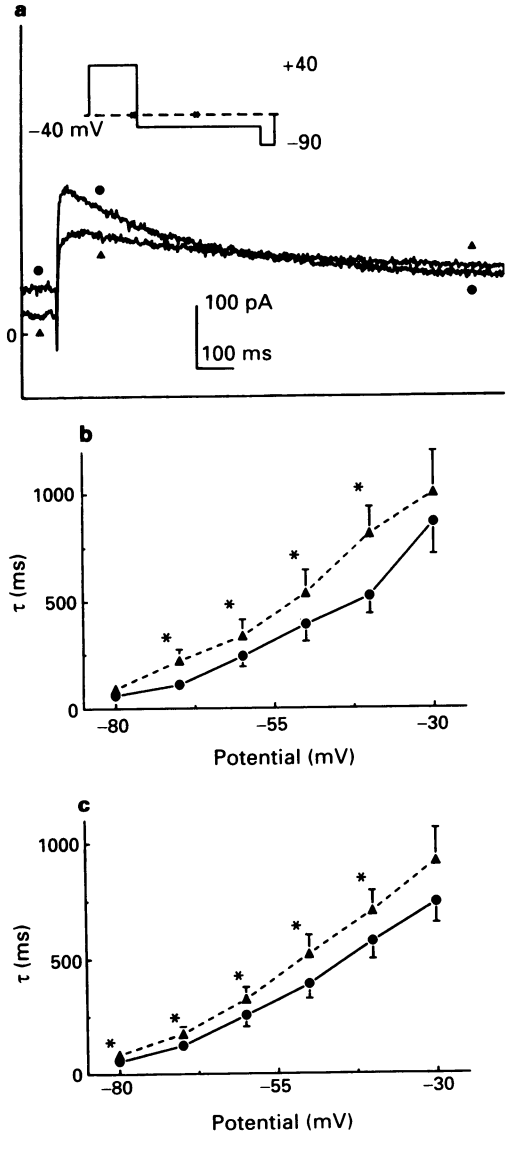


Figure 7 (a) Effects of ondansetron (1 μM) on the rate of decay of I_K tail current. Both ondansetron and granisetron (not shown) consistently induced a slowing of the decay and a crossover with the pre-drug current trace. Control (●); ondansetron (▲). In the example, τ increased from 444 to 653 ms. Tail currents recorded at − 60 mV, after a 1000 ms conditioning pulse. The time window displayed is indicated by the two stars in the protocol. (b) and (c) Time constants of tail decay as a function of voltage. Ondansetron (b) (7 cells) and granisetron (c) (9 cells); $^*P < 0.05$ (paired Student's *t* test).

Frequency dependence of APD prolongation

The prolongation of APD was studied as a function of the frequency of stimulation. Frequency was increased from 0.3–0.5 to 3 Hz and then returned to 0.3–0.5 Hz to verify the stability of the preparation. Figure 8 shows the results from four cells. Ondansetron was chosen because its action in blocking I_K tails did not show intrinsic voltage-dependence and thus the results can be interpreted solely in terms of kinetics of block. Prolongation of APD by ondansetron (1 and 2 μM) was abolished at 3 Hz. Such a decrease of efficacy in prolonging APD by other class III agents has been termed 'reverse use dependence' (Hondeghem & Snyders, 1990).

Effects on the inward rectifier (I_{K1}) current

Since the inward rectifier, I_{K1}, is known to contribute to the late phase of repolarization (Giles & Imaizumi, 1988), we examined whether ondansetron and granisetron block I_{K1}. Ondansetron (1 μM) had no detectable effects on holding current at − 80 mV, reversal potential, or whole-cell conductance from − 100 to − 25 mV, a voltage-range where I_{K1} is predominant. The block of I_K is apparent at more positive voltages (Figure 9). Similar results were obtained in 3 more cells. Similarly, granisetron at 3 μM, an equipotent concentration for blocking the delayed rectifier, did not have any significant effect (not shown). These results are consistent with the lack of effect on the resting potential observed with both compounds at these concentrations in the current-clamp studies. At a higher concentration, ondansetron (10 μM) did not have any detectable effect either ($n = 3$, not shown). However, both ondansetron and granisetron at 30 μM produced a significant block of I_{K1} as shown by the decrease of

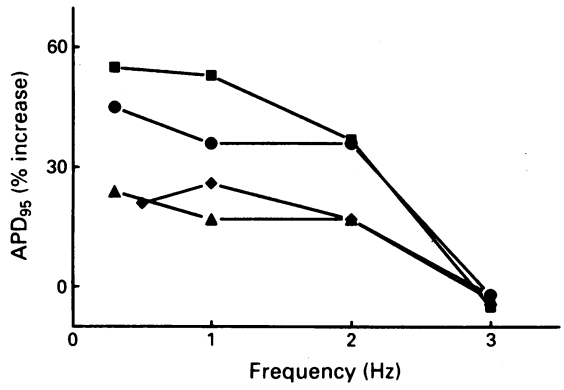


Figure 8 Frequency-dependency of APD prolongation by ondansetron (▲; ◆: 1 μM; ●, ■: 2 μM) in four myocytes. Experimental points represent an average of 6 to 15 action potentials recorded at steady-state.

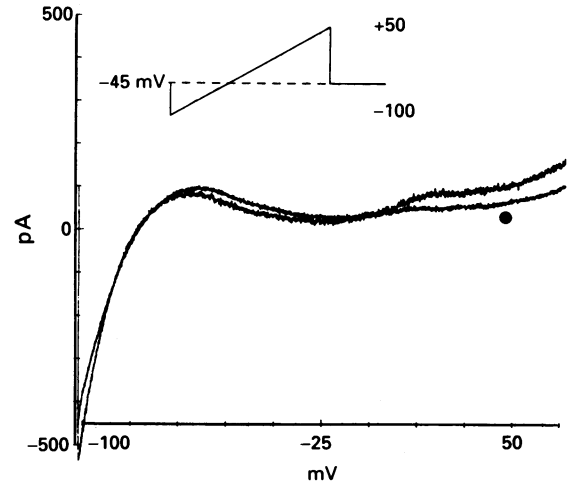


Figure 9 Effects of ondansetron (1 μM) on the quasi steady state current-voltage relationship in one myocyte. Ondansetron had little effect from − 100 to − 25 mV, a voltage range where the inward rectifier current, I_{K1}, is predominant. (●) current in presence of drug; voltage ramp, 3.34 mV s^{-1}.

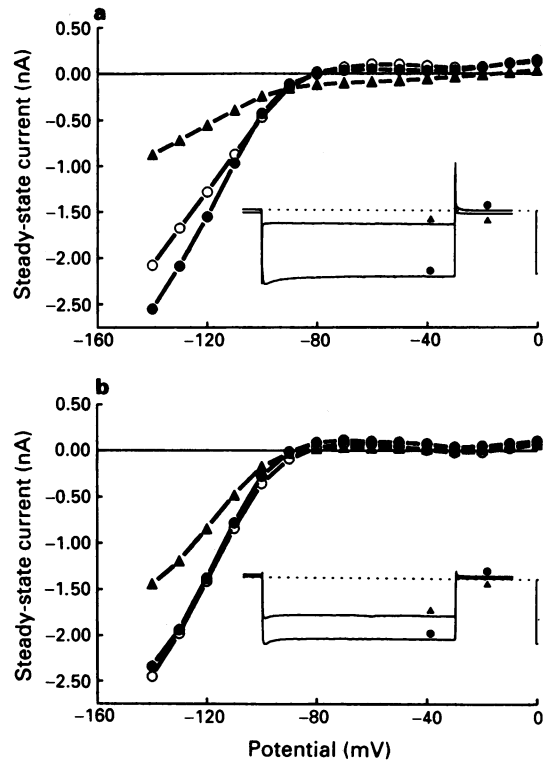


Figure 10 Effects of granisetron (a) and ondansetron (b) on I_{K1} in two different myocytes: (●) pre-drug; (▲) 30 μM drug; (○) washout. Current amplitude was measured at the end of 500 ms-long test pulse stepped from a holding potential of − 80 mV. Granisetron decreased the whole-cell inward conductance from 55 nS to 16 nS, while ondansetron decreased it from 55 nS to 34 nS. Insets show original current tracings recorded at − 140 mV; scale bars 2500 pA.

inward current at voltages more negative than − 90 mV (Figure 10). To quantify this effect, whole-cell conductance was measured between − 130 and − 100 mV, a range of potentials where membrane conductance is mostly determined by g_{K1}. Membrane conductance decreased from 45 ± 6 to 28 ± 4 nS ($n = 4$) with ondansetron, and from 40 ± 7 to 9 ± 2 nS ($n = 4$) with granisetron. The effect of ondansetron was almost completely reversible after 10 min washouts, while the effect of granisetron was only partially reversed after 20–30 min washouts. Granisetron was considerably more potent than ondansetron, as shown by the larger decrease of membrane conductance and by the important shift of the zero current potential to more depolarized potentials (from − 82 ± 2 mV to − 44 ± 8 mV).

Discussion

In cat ventricular myocytes, depolarizing voltage steps produced a small, gradually developing outward current that comprises the delayed rectifier (I_K) and other not yet identified conductances. Previous studies have shown that the outward currents obtained during the test potentials were variable in size and kinetic profile among myocytes (Spinelli *et al.*, 1993). Upon repolarization, each outward current trace was followed by a slowly decaying current tail. The tail currents were larger than the currents elicited during the depolarizing pulse, which is consistent with the high degree of inward rectification shown by I_K in cat ventricular myocytes (Follner *et al.*, 1992b). Tail currents increased with depolarization and reached full activation at positive potentials both after 250 and 2500 ms-long pulses. The longer pulses (2500 ms) activated larger tail currents at less positive potentials, which resulted in a 12 mV shift of the $V_{1/2}$ of the activation function. Nevertheless, maximum tail amplitude after 250 ms pulses was 90% of the maximum amplitude observed after 2500 ms pulses.

These results are consistent with the view that I_K in cat ventricular myocytes consists of a single, rapidly activating component similar to I_{Kr} of guinea-pig myocytes (Sanguinetti & Jurkiewicz, 1990). In agreement with this view, previous studies have shown the tail currents are abolished by WAY-123398 and E-4031, two specific blockers of I_K, even after very long pulses (5 s), whereas the time-dependent currents are only modestly affected even by very high drug concentrations (Follmer & Colatsky, 1990; Spinelli *et al.*, 1993). A single, rapidly activating, I_K has also been reported in rabbit ventricle (Carmeliet, 1992). Because of uncertainty on the nature of the conductances activated during the depolarizing pulse, and the difficulty of measuring small changes of current, in this study we decided to report only the results obtained with tail currents.

In voltage clamp studies, ondansetron and granisetron reversibly blocked I_K tail currents elicited after 2500 ms-long steps to + 35 mV with an estimated K_D of 1.7 ± 1.0 μM and 4.3 ± 1.7 μM, respectively. In current clamp experiments, ondansetron (1 μM) and granisetron (3 μM) prolonged APD_{90} by 30 ± 7% and 32 ± 8% without affecting other parameters of the transmembrane potential. Using a voltage clamp pro-

tocol that roughly approximated the voltage and duration of the plateau of an action potential (250 ms-long steps to + 15 mV), ondansetron and granisetron, at these same concentrations, blocked I_K tail currents by 41 ± 5% and 38 ± 4% without affecting the inward rectifier current. Thus, the class III effect observed in these studies is consistent with a block of the delayed rectifier current. At a significantly higher concentration (30 μM), both compounds blocked the inward rectifier. Granisetron was more potent than ondansetron and some blocking effect was evident at 10 μM, as indicated by a negative shift of holding current at − 45 mV.

Analysis of the activation curves permits a few conclusions regarding the mechanism of block of I_K. In the presence of the drug, the degree of block tracked the voltage-dependent activation of tail currents, suggesting that both 5-HT_3 antagonists blocked channels in the open state. Also, in the presence of the drug, the normalized activation curves were shifted in the hyperpolarized direction. The apparent negative voltage shift of the gating process may represent a voltage-dependent modulation of I_K that is distinct from voltage-dependence of block and is consistent with the hypothesis that the drug blocks the I_K channel in a given state (Hille, 1978; Carmeliet, 1993). Alternatively, the voltage shift may result from the block of a second component of I_K that is activated at more positive potentials. Finally, analysis of block at voltages where full activation has been attained revealed a modest increase of the amount of block with granisetron which is suggestive of an intrinsic voltage-dependent component of block.

Open-state block of the cardiac delayed rectifier has been reported with quinidine (Furukawa *et al.*, 1989), flecainide and encainide (Colatsky *et al.*, 1990; Follmer *et al.*, 1992a), dofetilide (Carmeliet, 1992), and almokalant (Carmeliet, 1993). Voltage-dependency of open-state block has been observed in a few studies. The block of the cloned human potassium channel HK2 by quinidine was voltage-dependent and was associated with an equivalent voltage-dependency of 0.19 (Snyders *et al.*, 1992). Block of the Shaker K^+ channel by tetraethylammonium (TEA) showed an equivalent voltage-dependency of 0.15 (Yellen *et al.*, 1991). Granisetron ($pK_a = 9.6$) is over 99% in the charged form at physiological pH. As for quinidine and TEA, our results are consistent with the hypothesis that the positively charged granisetron blocks the channel from the intracellular side of the membrane. In this case, the block by a positively charged molecule should increase in a voltage-dependent manner and δ, the equivalent voltage-dependency, can be interpreted to represent the fraction of the membrane electric field that the molecule must penetrate to reach the binding site. A similar effect was not observed with ondansetron. The reason for this difference is unclear. At physiological pH, ondansetron ($pK_a = 7.4$) is about 50% in the uncharged form. It is possible that the receptor for the charged molecule is outside the electric field of the membrane or that the block is due to the uncharged form. Due to the different proportion of the uncharged form, ondansetron is significantly more lipid soluble than granisetron. The octanol/buffer (pH = 7.4) partition coefficient for ondansetron is 1.70 compared to 0.73 for granisetron. Thus, ondansetron might also interact with the receptor via a hydrophobic pathway that is not available for the charged granisetron molecule. The higher lipophilicity of ondansetron might explain the faster and generally more complete washout observed with this molecule.

Changes in the time course of deactivation of the tail currents are also consistent with open channel block and unblock. If a significant fraction of channels are blocked and the rate of unblock is comparable to the rate of decay of the tail, the channels that become unblocked should transiently conduct outward current before closing and induce an apparent slowing of tail deactivation. This should result in a crossover with the control current, and, potentially, in a delay of the raising phase. The results obtained were consistent with this view, showing crossover of tail currents and a significant increase of τ with both ondansetron and granisetron. Significant delays of the peak current were observed, indicating that the unblock process affected the rate of raise of the tail current. This indicated that the rate of unblock was relatively slow, on the order of the rate of deactivation of the channels, but fast enough to induce a significant increase in outward current approximately within the first 20 ms. The observed changes in time course are similar to those reported for the block of the delayed rectifier by quaternary ammonium ions in the squid axon (Armstrong, 1971), by quinidine in rabbit (Furukawa *et al.*, 1989) and cloned human channels (Snyders *et al.*, 1992), and by class Ic antiarrhythmic drugs in cat ventricular myocytes (Follmer & Colatsky, 1990). Our results showed an appreciable contribution of open-state unblock to the tail current decay, but we cannot rule out the possibility that some trapping occurred in rested channels, as demonstrated with almokalant, a class III antiarrhythmic agent (Carmeliet, 1993).

Neuronal 5-HT_3 receptors are associated with an ion channel permeable to Na^+ and K^+ and showing a slightly higher selectivity for K^+ (Malone *et al.*, 1991). Thus, it is not surprising that 5-HT_3 antagonists can affect myocardial ion channels. Previous studies with various 5-HT_3 antagonists in whole animals have reported increases of ventricular refractoriness and prolongation of the QT interval of the ECG (Williams *et al.*, 1991), and some indication of antiarrhythmic effect (Williams *et al.*, 1985; Hof *et al.*, 1993). The data presented are consistent with open-state block and unblock of I_K by both ondansetron and granisetron. This profile of action should result in a use-dependent block of I_K. The amount of block after 250 and 2500 ms steps was similar, suggesting that a steady-state had been achieved after 250 ms and that, consequently, the τ of block should be less than 200 ms. The rates of unblock were not directly investigated. Fast block and slow unblock of I_K have been reported for quinidine and dofetilide (Furukawa *et al.*, 1989; Carmeliet, 1992). Such a profile is not considered favourable as steady-state block may be obtained at low rates of stimulation and no further increase of block would be obtained at faster rates (Carmeliet, 1993). The duration of the action potential is the resultant of several different conductances. Thus, it is not possible to translate directly changes at the level of the I_K channel in frequency-dependent effects on APD (Carmeliet, 1993; Spinelli *et al.*, 1993). In current clamp experiments, ondansetron behaved like dofetilide and quinidine in that the prolongation of APD was considerable at slow rates of stimulation and very limited at fast rates. A prolongation of APD characterized by reverse rate dependency could potentially carry the risk of proarrhythmic effects during a period of bradycardia. However, the concentrations required to block I_K (1–5 μM) are about 50 fold higher than the concentrations at which 5-HT_3 receptors are inhibited (Malone *et al.*, 1991), leaving an acceptable safety margin in therapy. Although metabolic phenotype and co-medication may affect this safety margin, present clinical experience with ondansetron does not show significant cardiovascular adverse effects (Markham & Sorkin, 1993).

The authors wish to thank Dr T.J. Colatsky for his continuous support, useful comments, and careful review of the manuscript.

References

AAPRO, M.S. (1991). 5-HT_3 receptor antagonists: an overview of their present status and future potential in cancer therapy-induced emesis. *Drugs*, **42**, 551–568.

ARMSTRONG, C.M. (1971). Interaction of tetraethylammonium ion derivatives with the potassium channels of giant axons. *J. Gen. Physiol.*, **58**, 413–437.

BALLARD, H.S., BOTTINO, G., & BOTTINO, J. (1992). Ondansetron and chest pain. *Lancet*, **340**, 1107.

CARMELIET, E. (1992). Voltage- and time-dependent block of the delayed K^+ current in cardiac myocytes by dofetilide. *J. Pharmacol. Exp. Ther.*, **262**, 809–817.

CARMELIET, E. (1993). Use-dependent block and use-dependent unblock of the delayed rectifier K^+ current by almokalant in rabbit ventricular myocytes. *Circ. Res.*, **73**, 857–868.

COKER, S.J., DEAN, H.G., KANE, K.A. & PARRATT, J.R. (1986). The effects of ICS 205-930, a 5-HT antagonist, on arrhythmias and catecholamine release during canine myocardial ischaemia and reperfusion. *Eur. J. Pharmacol.*, **127**, 211–218.

COLATSKY, T.J., FOLLMER, C.H. & STARMER, C.F. (1990). Channel specificity in antiarrhythmic drug action: mechanism of potassium channel block and its role in suppressing and aggravating cardiac arrhythmias. *Circulation*, **82**, 2235–2242.

COLATSKY, T.J., SPINELLI, W. & FOLLMER, C.H. (1994). Molecular mechanisms of potassium channel block by antiarrhythmic drugs. In *Electropharmacological Control of Cardiac Arrhythmias*. ed. Singh, B.N., Wellens, H.J.J. & Hiraoka, M. pp. 247–253. Mount Kisco, NY: Futura Publishing Company Inc.

COSTALL, B., NAYLOR, R.J. & TYERS, M.B. (1990). The psychopharmacology of 5-HT$_3$ receptors. *Pharmacol. Ther.*, **47**, 181–202.

FOLLMER, C.H. & COLATSKY, T.J. (1990). Block of the delayed rectifier potassium current, I_K, by flecainide and E-4031 in cat ventricular myocytes. *Circulation*, **82**, 289–293.

FOLLMER, C.H., CULLINAN, C.A. & COLATSKY, T.J. (1992a). Differential block of cardiac delayed rectifier current by class Ic antiarrythmic drugs: evidence for open channel block and unblock. *Cardiovasc. Res.*, **26**, 1121–1130.

FOLLMER, C.H., LODGE, N.J. CULLINAN, C.A. & COLATSKY, T.J. (1992b). Modulation of the delayed rectifier, I_K, by cadmium in cat ventricular myocytes. *Am. J. Physiol.*, **262**, C75–C83.

FURUKAWA, T., TSUJIMURA, Y., KITAMURA, K., TANAKA, H. & HABUCHI, Y. (1989). Time- and voltage-dependent block of the delayed K^+ current by quinidine in rabbit sinoatrial and atrioventricular nodes. *J. Pharmacol. Exp. Ther.*, **251**, 756–763.

GILES, W.R. & IMAIZUMI, Y. (1988). Comparison of potassium currents in rabbit atrial and ventricular cells. *J. Physiol.*, **405**, 123–145.

HILLE, B. (1978). Local anesthetic action on inactivation of the Na channel in nerve and skeletal muscle: possible mechanisms for antiarrhythmic agents. In *Biophysical Aspects of Cardiac Muscle*. ed. Morand, M., pp. 55–74. New York, NY: Academic Press Inc.

HOF, R.P., HOF, A., NOVOSEL, D. & ZIERHUT, W. (1993). Antiarrhythmic and hemodynamic effects of tropisetron in anesthetized rabbits. *J. Cardiovasc. Pharmacol.*, **22**, 499–505.

HONDEGHEM, L.M. & SYNDERS, D.J. (1990). Class III antiarrhythmic agents have a lot of potential but a long way to go: reduced effectiveness and dangers of reverse use dependence. *Circulation*, **81**, 686–690.

MALONE, H.M., PETERS, J.A. & LAMBERT, J.J. (1991). Physiological and pharmacological properties of 5-HT$_3$ receptors – a patch clamp-study. *Neuropeptides*, **19**, (Suppl.) 25–30.

MARKHAM, A. & SORKIN, E.M. (1993). Ondansetron: an update of its therapeutic use in chemotherapy-induced and postoperative nausea and vomiting. *Drugs*, **45**, 931–952.

MORGANROTH, J. & MCGINN, C. (1988). Antiarrhythmic effect of a 5-hydroxytryptamine M-receptor antagonist, ICS 205-930. *Am. J. Cardiol.*, **61**, 470–471.

NOBLE, D. & TSIEN, R.W. (1969). Outward membrane currents activated in the plateau range of potentials in cardiac Purkinje fibres. *J. Physiol.*, **200**, 205–231.

SANGUINETTI, M.C. & JURKIEWICZ, N.K. (1990). Two components of cardiac delayed rectifier K^+ current: differential sensitivity to block by class III antiarrhythmic agents. *J. Gen. Physiol.*, **96**, 195–215.

SCHOLTYSIK, G. (1987). Evidence for inhibition by ICS 205-930 and stimulation by BRL 34915 of K^+ conductance in cardiac muscle. *Naunyn-Schmied. Arch. Pharmacol.*, **335**, 692–696.

SCHOLTYSIK, G., IMOTO, Y., YATANI, A. & BROWN, A.M. (1988). 5-hydroxytryptamine antagonist ICS 205-930 blocks cardiac potassium, sodium and calcium currents. *J. Pharmacol. Exp. Ther.*, **245**, 773–778.

SILVER, L.H., HEMWALL, E.L., MARINO, T.A. & HOUSER, S.R. (1983). Isolation and morphology of calcium-tolerant feline ventricular myocytes. *Am. J. Physiol.*, **245**, H891–H896.

SNYDERS, D.J., KNOTH, K.M., ROBERDS, S.L. & TAMKUN, M.M. (1992). Time-, voltage-, and state-dependent block by quinidine of a cloned human cardiac potassium channel. *Mol. Pharmacol.*, **41**, 322–330.

SPINELLI, W., MOUBARAK, I.F., PARSONS, R.W. & COLATSKY, T.J. (1993). Cellular electrophysiology of WAY-123,398, a new class III antiarrhythmic agent: specificity of I_K block and lack of reverse use dependence in cat ventricular myocytes. *Cardiovasc. Res.*, **27**, 1580–1591.

WILLIAMS, F.M., ROTHAUL, A.L., KANE, K.A. & PARRATT, J.R. (1985). Antiarrhythmic and electrophysiological effects of ICS 205-930, an antagonist of 5-hydroxytryptamine at peripheral receptors. *J. Cardiovasc. Pharmacol.*, **7**, 550–555.

WILLIAMS, P.D., COHEN, M.L. & TURK, J.A. (1991). Electrocardiographic effects of zatosetron and ondansetron, two 5HT$_3$ receptor antagonists, in anesthetized dogs. *Drug Dev. Res.*, **24**, 277–284.

WOODHULL, A.M. (1973). Ionic blockage of sodium channels in nerve. *J. Gen. Physiol.*, **61**, 687–708.

YELLEN, G., JURMAN, M.E., ABRAMSON, T. & MACKINNON, R. (1991). Mutations affecting internal TEA blockade identify the probable pore-forming region of a K^+ channel. *Science*, **251**, 939–942.

(Received February 15, 1994
Accepted June 6, 1994)

Br. J. Pharmacol. (1994), **113**, 536–540 © Macmillan Press Ltd, 1994

Inhibition of the glutamate transporter and glial enzymes in rat striatum by the gliotoxin, αaminoadipate

Gethin J. McBean

Department of Biochemistry, University College, Belfield, Dublin 4, Ireland

1 The effect of the gliotoxic analogue of glutamate, αaminoadipate, on the high affinity transport of D-[^{3}H]-aspartate into a crude striatal P_2 preparation, and on the activity of two enzymes of which glutamate is the substrate has been examined.

2 The L-isomer of αaminoadipate competitively inhibited the transport protein, with a K_i value of 192 μM, whereas the D-isomer of αaminoadipate was ineffective. The potent convulsant, L-methionine-*S*-sulphoximine, was also without effect on the activity of the gluatmate transport protein.

3 L-αAminoadipate was a competitive inhibitor of both glutamine synthetase, and γ-glutamylcysteine synthetase, with K_i values of 209 μM and 7 mM respectively. Once again, the D-isomer of αaminoadipate was a far weaker inhibitor of either enzyme.

4 The results are discussed in terms of the mechanism of action of αaminoadipate in causing toxicity of glial cells.

Keywords: glutamate transport; glutamine synthetase; γ-glutamylcysteine synthetase; αaminoadipate; glial cell; toxicity

Introduction

Several analogues of the excitatory transmitter, L-glutamate, have been shown to be extremely potent neurotoxins after either direct injection into the brain, or during incubation of tissue slices or cell cultures *in vitro* (McBean & Roberts, 1985; Meldrum & Garthwaite, 1990). αAminoadipate (αAA) is a structural analogue of glutamate which, in contrast to most other glutamate-like compounds, is toxic to glial cells. Injection of DL-αAA into the retina of rats results in marked, but transient, morphological damage to Muller (glial) cells, without any change in the morphological integrity of the surrounding neurones (Olney *et al.*, 1971). Similarly, intracerebral application of the compound into the striatum of adult rats causes a significant reduction in the activity of the glial enzyme, glutamine synthetase, at 6 h after the injection, with a return to normal levels of activity by 24 h after the lesion, whereas neuronal cells are unaffected by this treatment at either time (McBean, 1990).

Studies on the stereospecificity of the effects of αAA have shown that the 'active component', in terms of its gliotoxicity, is the L-isomer (Olney *et al.*, 1980), which is also a weak neuroexcitant (McLennan & Hall, 1978). The D-isomer, on the otherhand, which is an N-methyl-D-aspartate (NMDA) receptor antagonist, is not gliotoxic and may actually be neuroprotective (Olney *et al.*, 1980).

Little is known of how L-αAA causes toxicity to glial cells, but since this compound is the most effective gliotoxin identified (Olney *et al.*, 1971), it is unlikely that excitation of neuronal glutamate receptors alone could account for its toxic potency. One component of the action of L-αAA may be an inhibition of cystine transport into glial cells, which could contribute to a reduction in the quantity of glutathione available for protection of tissue against free radical-induced cell damage (Kato *et al.*, 1993). However, there are several other aspects of glutamate metabolism in glial cells which, if disrupted by L-αAA, could provide an alternative mechanism for causing the toxic effects of this compound. This paper describes a series of experiments in which the effects of both the racemate and separate isomers of αAA were assessed on the activity of the plasma-membrane glutamate transporter, and on two enzymes, glutamine synthetase and γ-glutamylcysteine synthetase, both of which are associated with the glial cell metabolism of glutamate (Meister & Tate, 1979; Norenberg & Martinez-Hernandez, 1979). In the case of the glutamate transporter, the non-metabolizable analogue of glutamate, D-aspartate, was used to measure the rate of glutamate transport.

[1] Author for correspondence.

Methods

High-affinity sodium-dependent transport of D-[^{3}H]-aspartate into crude striatal synaptosomes

Rats were killed by cervical dislocation, and the brains rapidly removed and placed on ice. A 5% (w/v) homogenate of the striatum was prepared using 0.32 M sucrose in 50 mM Tris-HCl, pH 7.4. Following centrifugation at 3,200 r.p.m. for 5 min, the supernatant was removed and re-centrifuged at 12,000 r.p.m. for 12 min. The pellet was washed once in Tris-sucrose, and re-precipitated by centrifugation as before at 12,000 r.p.m. The final pellet (P_2) was re-suspended in Tris-sucrose and maintained on ice until the transport assay.

D-[^{3}H]-aspartate transport

A tube containing 975 μl of Krebs bicarbonate medium (contents, in mM: NaCl 109.6, KCl 4.7, KH_2PO_4 1.2, $MgSO_4$ 1.2, $NaHCO_3$ 25, $CaCl_2$ 2.5 and glucose 11.5), pH 7.4 and 25 μl P_2 was pre-incubated at 25°C for 5 min and the reaction started by the addition of 25 μl D-[^{3}H]-aspartate (final specific activity 0.125 μCi nmol^{-1}). The concentration of D-aspartate used ranged from 0.39 μM to 1.95 μM (experiments prior to this study having established that the sodium-dependent high affinity transport of D-aspartate had a K_m of 10 μM, and a V_{max} of 35 nmol mg^{-1} protein 4 min^{-1}). The incubation was continued for 4 min and was terminated by centrifugation at 10,000 r.p.m. in a microcentrifuge. The pellet was washed once in Tris-sucrose and extracted overnight with 200 μl sodium dodecyl sulphate. The quantity of radioactivity present was determined by liquid scintillation spectroscopy. Sodium-free Krebs medium was used to assess the sodium-dependency of the transport.

Glutamine synthetase

Rat striata were homogenized in 0.1 M sodium acetate, pH 7.4, centrifuged at 1,200 *g*, and the supernatant used for the assay. The γ-glutamyl-transfer activity of the enzyme was measured according to the method of Wellner & Meister (1966), in which 150 mM glutamine (unless otherwise stated) was added as substrate, in the presence of 0.1 mM ATP, 200 mM hydroxylamine and 33 mM $MnCl_2$. The quantity of γ-glutamylmono-hydroxamate (GHA) formed at 37°C over 20 min was determined spectrophotometrically at 500 nm.

γ-Glutamylcysteine synthetase

Samples of whole rat brain were homogenized in 9 volumes of ice-cold 0.15 M KCl, containing 0.5 mM mercaptoethanol and 1 mM $MgCl_2$, and then subjected to partial purification by ammonium sulphate fractionation. The activity of the enzyme was determined at 37°C during 30 min incubation of 100 μl samples of the purified homogenate by the method of Richman *et al.* (1973), using 2 mM glutamate (unless otherwise stated) and 10 mM α-aminobutyrate (replacing cysteine) as substrates in the presence of 20 mM $MgCl_2$ and 5 mM ATP in a final volume of 0.5 ml. Incubation of the samples was continued for 30 min at 37°C and terminated by the addition of 0.5 ml 10% trichloroacetic acid. Following centrifugation, the quantity of inorganic phosphate in the supernatant was determined by colourimetric assay. Protein determinations were performed on each set of tissue preparation by the method of Markwell *et al.* (1978).

The results in each table are expressed as the mean ± s.e.mean of the number of observations indicated. Statistical analysis of each set of data was by Student's unpaired *t* test, and the difference between means was regarded as significant at *P* values of less than 0.05.

L-Methionine-*S*-sulphoximine and αaminoadipate were purchased from the Sigma Chemical Co., Poole, Dorset. D-[^{3}H]-aspartate (specific activity 25 Ci mmol^{-1}) was provided by Radiochemical Centre, Amersham, Bucks. All other chemicals and reagents were bought from either BDH, Ltd., England, or Sigma.

Results

The effects of αaminoadipate on D-[^{3}H]-aspartate transport

Samples of crude P_2 were incubated at 25°C for 4 min in the presence of 0.39 μM D-[^{3}H]-aspartate. Addition of L-αAA to the incubation medium resulted in a dose-dependent reduction in the rate of sodium-dependent D-[^{3}H]-aspartate transport from 1.53 ± 0.17 nmol mg^{-1} protein 4 min^{-1} to 1.16 ± 0.12 nmol mg^{-1} protein 4 min^{-1} with 100 μM L-αAA, and 0.53 ± 0.07 nmol mg^{-1} protein 4 min^{-1} with 500 μM L-αAA, as shown in Table 1. DL-αAA was a weaker inhibitor of D-[^{3}H]-aspartate transport, since the effect of adding 500 μM DL-αAA to the incubation mixture resulted in only a 41% reduction in the rate of D-[^{3}H]-aspartate transport (0.90 ± 0.14 nmol mg^{-1} protein 4 min^{-1}). The D-isomer of αAA showed a minimal effect on the high-affinity uptake of D-[^{3}H]-aspartate, and L-methionine-*S*-sulphoximine (MSO) was also ineffective as an inhibitor of the glutamate transporter. L-αAA proved to be a competitive inhibitor of the transport protein, as shown in Figure 1, with a K_i value of 192 μM.

The effect of αaminoadipate on the acitivity of glutamine synthetase in striatal homogenates

Once again, the L-isomer of αAA was the more potent inhibitor of glutamine synthetase, and a dose-dependent inhibition of the enzyme was observed following co-incubation of the substrate with L-αAA (Table 2)·. Although D-αAA was markedly less effective than L-αAA, inhibition of the activity of glutamine synthetase was observed, at high concentrations, as shown in Table 2, where 1 mM D-αAA reduced the activity of the enzyme to 55% control (15.4 ± 1.6

Table 1 Inhibition of D-[^{3}H]-aspartate transport into a striatal P_2 preparation by αaminoadipate (αAA) and L-methionine-*S*-sulphoximine (MSO)

Inhibitor	*Concentration* (μM)	*Transport* (nmol mg^{-1} protein 4 min^{-1})	*(% of control)*
Control		1.53 ± 0.17	
L-αAA	100	1.16 ± 0.12	76
	500	0.53 ± 0.07	37**
DL-αAA	100	1.04 ± 0.09	78
	500	0.90 ± 0.14	59**
D-αAA	100	1.26 ± 0.11	83
	500	1.19 ± 0.14	78
MSO	100	1.52 ± 0.16	99
	500	1.35 ± 0.17	88

Mean ± s.e.mean of at least 4 independent observations, measured in triplicate. *$P<0.05$ vs control; **$P<0.01$ vs control.

Table 2 Inhibition of striatal glutamine synthetase by αaminoadipate (αAA) and L-methionine-*S*-sulphoximine (MSO)

Inhibitor	*Concentration* (μM)	*Activity* (nmol GHA mg^{-1} protein min^{-1})	*(% of control)*
Control		27.7 ± 2.6	
L-αAA	200	14.5 ± 1.2	52**
	1000	7.2 ± 0.6	26**
DL-αAA	200	15.4 ± 1.6	55**
	1000	9.6 ± 0.6	35**
D-αAA	200	26.0 ± 2.4	94
	1000	15.4 ± 1.6	55**
MSO	200	3.2 ± 0.4	11***
	1000	0.7 ± 0.2	3***

Mean ± s.e.mean of at least 3 independent observations, measured in triplicate. *$P<0.02$ vs control; **$P<0.01$ vs control; ***$P<0.001$ vs control.

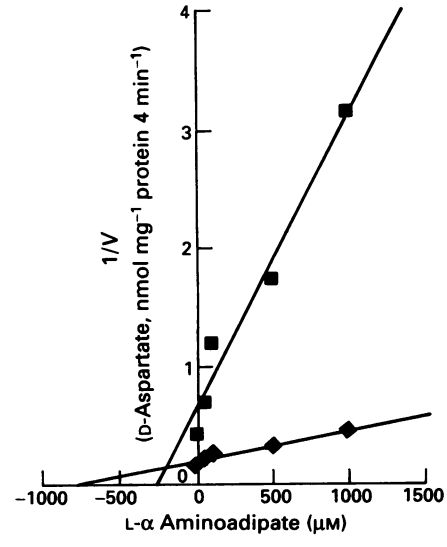


Figure 1 Dixon plot showing inhibition of D-[^{3}H]-aspartate transport by L-αaminoadipate, at 0.39 μM (■) and 1.95 μM aspartate (◆). The results are the mean of at least 3 independent observations, measured in triplicate.

nmol GHA formed mg^{-1} protein min^{-1}). As expected, MSO was an extremely potent inhibitor of the enzyme, and only 11% of the control activity of the enzyme remained after incubation with 200 μM MSO.

L-αAA was a competitive inhibitior of glutamine synthetase, with respect to the substrate, glutamine, with a K_i value of 109 μM, as shown in Figure 2.

Inhibition of γ-glutamylcysteine synthetase by L-αaminoadipate and L-methionine-S-sulphoximine

αAA proved to be a weak competitive inhibitor of γ-glutamylcysteine synthetase (Table 3), although, once again, the L-isomer of αAA was the most potent form of the compound: in the presence of 10 mM L-αAA the activity of the enzyme was reduced to 67% control (0.179 ± 0.013 μmol Pi mg^{-1} protein min^{-1}). A 10 mM concentration of MSO gave an almost total inhibition in the activity of the enzyme. Kinetic analysis (Figure 3) indicated that L-αAA competes with glutamate, as does MSO, but the K_i for inhibition of this enzyme by L-αAA is considerably higher (7 mM) than that for inhibition of glutamine synthetase. Inhibition of γ-glutamylcysteine synthetase by L-αAA was independent of any variation in the concentration of the second substrate, αaminobutyrate (results not shown).

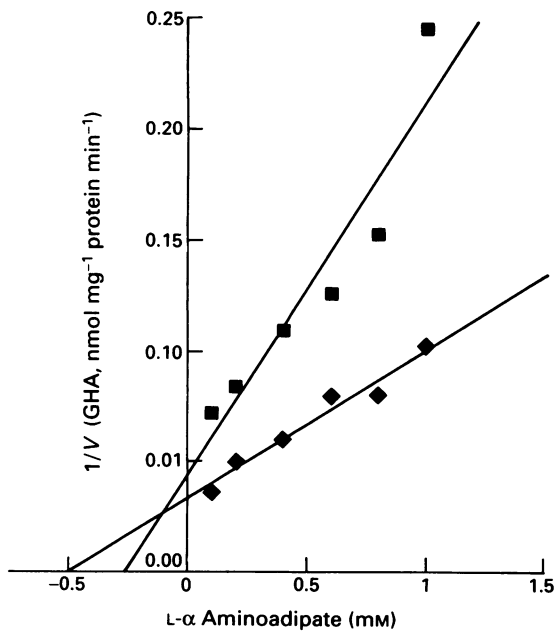


Figure 2 Graph showing competitive inhibition of glutamine synthetase activity by L-αaminoadipate, at 200 μM (■) and 300 μM (◆) glutamine. Each point is the mean of at least 3 independent observations, measured in duplicate.

Table 3 Inhibition of γ-glutamylcysteine synthetase by L-αaminoadipate and L-methionine-*S*-sulphoximine

Inhibitor	*Concentration* (mM)	*Activity* (μmol Pi mg^{-1} protein 30 min^{-1})	*(% of control)*
None		0.264 ± 0.017	
L-αAA	2.5	0.234 ± 0.012	89
L-αAA	10	0.179 ± 0.013	67*
D-αAA	10	0.273 ± 0.014	103
MSO	10	0.023 ± 0.004	8.7**

Mean ± s.e.mean of 4 independent observations, measured in duplicate. *$P<0.02$; **$P<0.001$.

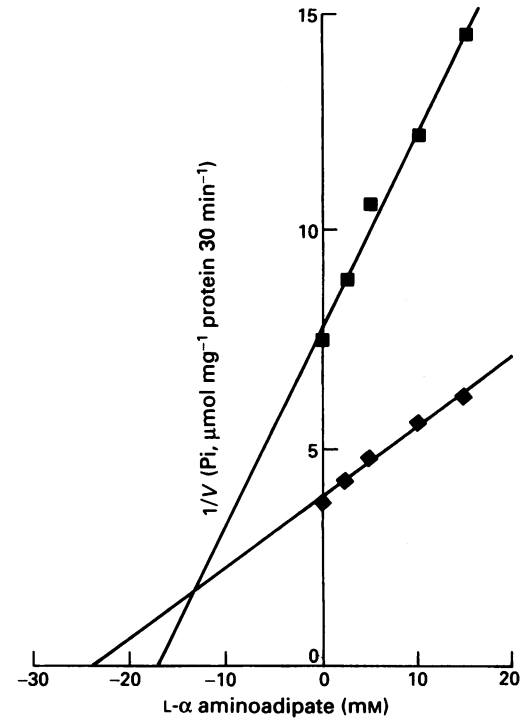


Figure 3 Dixon plot showing inhibition of γ-glutamylcysteine synthetase by L-αaminoadipate, at 0.5 mM (■) and 2.0 mM glutamate (◆). Each point is the mean of 2 independent observations, measured in duplicate.

Discussion

The results described in this paper clarify several aspects of the mechanism of gliotoxicity by αAA. Firstly, in each of the parameters of glutamate transport and metabolism tested, it is the L-isomer which is by far the most active form of αAA. The same stereospecificity of αAA was reported by Olney *et al.* (1980), who presented evidence showing that the L-isomer was the most toxic form of αAA to retinal Muller cells after application *in vivo*, and a similar order of potency of the various forms of αAA was observed more recently by Kato *et al.* (1993) in experiments in which the effects of αAA on the glutathione content of carp retina was measured.

The second aspect of the toxicity of αAA which is clarified by the results presented in this paper is the question of the glial-cell specificity. As the L-isomer of αAA is no more than a weak excitant of neuronal glutamate receptors (McLennan & Hall, 1978), the toxicity of this compound is much more likely to be mediated by a direct effect on glial cells themselves. The glutamate high-affinity, sodium-dependent, transporter is located on both neuronal and glial cells in the brain (Drejer *et al.*, 1982), and is responsible for the rapid removal of glutamate from the synaptic cleft following activation of excitatory pathways and release of the neurotransmitter (Nicholls & Attwell, 1990). Both immunocytochemical localization experiments and *in situ* hybridization studies with mRNA coding for GLAST and GLT-1 glutamate transporters have revealed a glial localization for these transport proteins (Danbolt *et al.*, 1992; Pines *et al.*, 1992; Storck *et al.*, 1992) and recent evidence has shown that at least one of these transporters may be regulated physiologically by protein kinase C-mediated phosphorylation of the protein (Casado *et al.*, 1993). Studies on neuronal and glial cells in culture have indicated that the glial site of transport is predominant (Drejer *et al.*, 1982), which could explain why L-αAA, acting primarily through inhibition of the glutamate transporter, would initially cause a disruption of glutamatergic activity in glial cells. The same rationale has been offered by Kato *et al.* (1993) to explain the glial-cell

specificity of L-αAA in inhibiting the cystine/glutamate exchanger in retinal Muller cells, and similarly, the potent glycolytic inhibitor, fluorocitrate, acts preferentially on glial cells at low concentrations (Paulsen *et al.*, 1987). It has been noted previously (McBean, 1990) that during incubation of striatal slices with DL-αAA, at high concentrations of the toxin (for example, superfusion for 40 min with 1 mM), neuronal cells also become affected and die. Indeed, one of the most potent inhibitors of glutamate transport known, DL-*threo*-3(OH) aspartate, caused neuronal degeneration in the striatum after intracerebral injection (McBean & Roberts, 1985). There are two possible reasons for this spread of toxicity to neuronal cells with high concentrations of DL-αAA: firstly, with increasing concentrations of the toxin, neuronal transport of glutamate would also be inhibited, and secondly, the eventual outcome of prolonged inhibition of either glial or neuronal transport would be an elevation in glutamate concentrations in the synaptic cleft, activation of post-synaptic receptors, and a process of disruption of glutamatergic function akin to that proposed to occur in ischaemia (Nicholls & Attwell, 1990).

Although the question of whether L-αAA is a substrate, as well as an inhibitor, of the high-affinity glutamate transport has not been addressed directly in this series of experiments, previous work by Huck *et al.* (1984) had indicated that in cultures at least, L-αAA is actively accumulated into glial cells before its toxic effects are observed. It is highly probable, therefore, that L-αAA gains access into striatal glial cells by means of the glutamate transporter.

As in the case of the glutamate transport protein, L-αAA is also the active isomer which competitively inhibits the activity of glutamine synthetase, with a comparable K_i value to that of the inhibition of transport, although the degree of inhibition of this enzyme is greater at a given concentration of the toxin than for the glutamate transporter. In this case, however, the D-isomer does have some inhibitory activity, and this is in agreement with some of the original work on glutamine synthetase by Wellner *et al.* (1966), in which it was shown that both the L- and D-isomers of αAA are not only inhibitors, but also substrates of the enzyme. This observation may explain the third feature of αAA toxicity: the transience of αAA effects. It has been noted that in experiments *in vivo* (Olney *et al.*, 1980; McBean, 1990), morphological changes to glial cells, and a reduction in the activity of the glial marker enzyme, glutamine synthetase, are apparent at 6, but not 24 h, after intraretinal or intrastriatal injections, respectively. As αAA is a substrate for glutamine synthetase, it is reasonable to assume that this would account for the gradual decline in its toxic potency.

To what extent, then, does inhibition of glutamine synthetase by L-αAA contribute to the toxicity of this compound? MSO is a much more potent inhibitor of glutamine synthetase than is either isomer of αAA, and is, moreover, an irreversible inhibitor of this enzyme (Cooper *et al.*, 1983). Intracerebral injection of MSO is well-known to cause convulsions, which are due to an elevation in ammonia levels, rather than an alteration in glutamate concentration *per se* (Cooper *et al.*, 1983). DL-αAA, on the otherhand, which does not cause convulsions after intra-striatal injection (McBean, 1990) would not, presumably, have the same disruptive influence on ammonia levels, because it is a substrate of the enzyme. The similarity between the K_i values of both the transport of D-[^{3}H]-aspartate and this enzyme would imply that the concentration of L-αAA inside the glial cell would be sufficient to inhibit the enzyme, but the precise implication of this, as regards a disruption in glutamate metabolism, needs further investigation.

It is not surprising that L-αAA also inhibits γ-glutamylcysteine synthetase in addition to glutamine synthetase, as there are many mechanistic similarities between these two enzymes: γ-glutamylcysteine synthetase is, like glutamine synthetase, found in glial cells (Meister & Tate, 1976) and both reactions proceed via an enzyme-bound γ-glutamylphosphate intermediate, before entry of the second substrate (ammonia for glutamine synthetase; and cysteine for γ-glutamylcysteine synthetase). However, it is unlikely that the direct inhibition of γ-glutamylcysteine synthetase by L-αAA contributes much to the overall toxicity of this compound in glial cells, for the following reasons: firstly, L-αAA is a far less effective inhibitor of γ-glutamylcysteine synthetase than of glutamine synthetase, as the differences in the magnitude of the K_i for each enzyme testifies (see Figures 2 and 3). Secondly, it is the intracellular concentration of cysteine that regulates the activity of the enzyme, not glutamate, with which L-αAA competes (Meister & Tate, 1976).

γ-Glutamylcysteine synthetase is the rate-limiting enzyme of the γ-glutamyl cycle, which is responsible for maintaining glutathione levels in cells (Meister & Tate, 1976). There is currently much interest in the role of glutathione in the brain in preventing damage to cells by oxidative stress (Pellmar *et al.*, 1993). It has previously been shown that L-αAA in the retina leads to a reduction in GSH concentration (Kato *et al.*, 1993), and the same observation has been made using incubation of striatal slices with L-αAA (McBean, unpublished results). Inhibition of a cystine transporter by L-αAA may provide a possible mechanism for depletion of glutathione, but given the very slow rate of this transporter (V_{max}: 8.3 nmol 5 mg^{-1} tissue 15 min^{-1}; Kato *et al.*, 1993), it is debatable whether the supply of cysteine for the synthesis of glutathione would be enormously depleted by inhibition of this transporter alone. γ-Glutamyltranspeptidase activity, for instance, is also closely linked to the transport of cysteine across cell membranes (Hanigan & Rickets, 1993). It could be argued that inhibition of the glutamate transporter by L-αAA might produce a secondary effect on cystine transport, because these transport systems must inevitably be interlinked. In this context, it is worth noting that one mechanism of glutamate toxicity which operates via a disruption of cystine/cysteine transport is probably only apparent in young animals in which the glutamate transporter is not yet fully developed (Coyle & Puttfarcken, 1993).

In conclusion, these results confirm the stereospecificity of the glial cell toxicity of αAA, as it is the L-isomer that is the more effective inhibitor of both the transport of glutamate and of glutamine synthetase and γ-glutamylcysteine synthetase. Furthermore, the preference of L-αAA for glial cells is best explained by the relatively higher incidence of the transporter on these cells, compared to neurones (Drejer *et al.*, 1982) and also because glutamine synthetase is exclusively localized to glial cells, although the most relevant effect of L-αAA toxicity in glial cells is probably inhibition of the plasma membrane glutamate transporter. This study also highlights the importance of glial cells in maintaining the integrity of the surrounding neurones, and indicates that a disruption of glutamate metabolism in these cells, as opposed to neurones, is sufficient to cause a toxic reaction in the CNS. Further work will be aimed at analysing the impact of toxins like L-αAA on the free-radical detoxification mechanisms in the brain, and of how closely glutamate metabolism is linked to the production of anti-oxidants, such as glutathione.

The support of the Health Research Board of Ireland for part of this work is gratefully acknowledged.

References

CASADO, M., BENDAHAN, A., ZAFRA, F., DANBOLT, N.C., ARAGON, C., GIMENEZ, C. & KANNER, B.I. (1993). Phosphorylation and modulation of brain glutamate transporter by protein kinase C. *J. Biol. Chem.*, **268**, 27313–27317.

COOPER, A.J.L., VERGARA, F. & DUFFY, T.E. (1983). Cerebral glutamine synthetase. In *Glutamate, Glutamine and GABA in the Central Nervous System* ed. Hertz, L., Kvamme, E., McGeer, E.G. & Schousboe, A. pp. 77–93. New York: Alan R. Liss Inc.

COYLE, J.T. & PUTTFARCKEN, P. (1993). Oxidative stress, glutamate and neurodegenerative disorders. *Science*, **262**, 689–695.

DANBOLT, N.C., STORM-MATHISEN, J. & KANNER, B.I. (1992). An (Na^+-K^+) coupled L-glutamate transporter purified from rat brain is located in glial cell processes. *Neuroscience*, **51**, 295–310.

DREJER, J., LARSSON, O.M. & SCHOUSBOE, A. (1982). Characterisation of L-glutamate and L-glutamine uptake into, and release from, astrocytes and neurones cultured from different brain regions. *Expl. Brain Res.*, **47**, 259–269.

HANIGAN, M.H. & RICKETS, W.A. (1993). Extracellular glutathione is a source of cysteine for cells that express γ-glutamyltranspeptidase. *Biochemistry*, **32**, 6302–6306.

HUCK, S., GRASS, F. & HORTANGL, H. (1984). The glutamate analogue, α-aminoadipic acid is taken up by astrocytes before exerting its giotoxic effects *in vitro*. *J. Neurosci.*, **4**, 2650–2657.

KATO, S., ISHITA, S., SUGAWARA, K. & MAWATARI, K. (1993). Cystine/glutamate antiporter expression in retinal Muller glial cells: implications for DL-alpha-aminoadipate toxicity. *Neurosci.*, **57**, 473–482.

MARKWELL, M., HAAS, S.M., BIEBER, L. & TOLBERT, N. (1978). A modification of the Lowry procedure to simplify protein determination in membrane and lipoprotein samples. *Analyt. Biochem.*, **87**, 206–210.

MCBEAN, G.J. (1990). Intrastriatal injection of DL-α aminoadipate reduces kainate toxicity *in vitro*. *Neurosci.*, **34**, 225–234.

MCBEAN, G.J. & ROBERTS, P.J. (1985). Neurotoxicity of L-glutamate and DL-*threo*-3-hydroxyaspartate in the rat striatum. *J. Neurochem.*, **44**, 247–254.

MCLENNAN, H. & HALL, J.G. (1978). The action of D-α-aminoadipate on excitatory amino acid receptors of rat brain. *Brain Res.*, **149**, 541–545.

MEISTER, A. & TATE, S.S. (1976). Glutathione and related γ-glutamyl compounds: biosynthesis and utilisation. *Annu. Rev. Biochem.*, **45**, 559–604.

MELDRUM, B. & GARTHWAITE, J. (1990). Excitatory amino acid neurotoxicity and neurodegenerative disease. *Trends Pharmacol. Sci.*, **11**, 379–387.

NICHOLLS, D. & ATTWELL, D. (1990). The release and uptake of excitatory amino acids. *Trends Pharmacol. Sci.*, **11**, 462–468.

NORENBERG, M.D. & MARTINEZ-HERNANDEZ, A. (1979). Fine structural localisation of glutamine synthetase in astrocytes of rat brain. *Brain Res.*, **161**, 301–310.

OLNEY, J.W., DEGUBAREFF, T. & COLLINS, J.F. (1980). Stereospecificity of the gliotoxic and anti-neurotoxic actions of alpha-aminoadipate. *Neurosci. Lett.*, **19**, 278–282.

OLNEY, J.W., HO, O.L. & REE, V. (1971). Cytotoxic effects of acidic and sulphur-containing amino acids on the infant mouse nervous system. *Expl. Brain Res.*, **14**, 61–67.

PAULSEN, R.A., CONTESTABILE, A., VILANI, L. & FONNUM, F. (1987). An *in vivo* model for studying function of brain tissue temporarily devoid of glial cell metabolism. *J. Neurochem.*, **48**, 1377–1385.

PELLMAR, T.C., RONEY, D. & LEPINSKI, D.L. (1992). Role of glutathione in repair of free radical damage in hippocampus *in vitro*. *Brain Res.*, **583**, 194–200.

PINES, G., DANBOLT, N.C., BJORAS, M., KHANG, Y., BENDAHAN, A., EIDE, L., KOEPSELL, H., STORM-MATHISEN, J. & KANNER, B.I. (1992). Cloning and expression of a rat brain glutamate transporter. *Nature*, **360**, 464–467.

RICHMAN, R.G., ORLOWSKI, M. & MEISTER, A. (1973). Inhibition of γ-glutamylcysteine synthetase by L-methionine-S-sulphoximine. *J. Biol. Chem.*, **268**, 6684–6690.

STORCK, T., SCHULTE, S., HOFMANN, K. & STOFFAL, W. (1992). Structure, expression and functional analysis of a Na+-dependent glutamate/aspartate transporter from rat brain. *Proc. Natl. Acad. Sci. U.S.A.*, **89**, 10955–10959.

WELLNER, V.P. & MEISTER, A. (1966). Binding of adenosine triphosphate and adenosine diphosphate by glutamine synthetase. *Biochemistry*, **5**, 872–879.

WELLNER, V.P., ZOUKIS, M. & MEISTER, A. (1966). Activity of glutamine synthetase toward the optical isomers of αaminoadipic acid. *Biochemistry*, **5**, 3509–3514.

(Received March 18, 1994
Revised June 6, 1994
Accepted June 10, 1994)

Br. J. Pharmacol. (1994), **113**, 541–549 © Macmillan Press Ltd, 1994

Peptide histidine isoleucine-like immunoreactivity release from the rat gastric fundus

[1]Diego Currò, Paolo Preziosi, Enzo Ragazzoni & Giovanni Ciabattoni

Institute of Pharmacology, Catholic University School of Medicine, L.go F. Vito, 1, I-00168 Rome, Italy

1 Longitudinal muscle strips from the rat gastric fundus were subjected to *in vitro* electrical field stimulation (EFS) under non-adrenergic non-cholinergic (NANC) conditions to study the release of peptide histidine isoleucine-like immunoreactivity (PHI-LI) and the correlation between PHI-LI release and NANC relaxation.

2 Different radioimmunoassay (RIA) systems employing C-terminal- and N-terminal-specific anti-PHI sera were used to determine the relative contributions of PHI and its C-terminally extended forms, peptide histidine glycine (PHI-Gly) and peptide histidine valine [PHV(1–42)], to the PHI-LI released by the rat gastric fundus.

3 In the presence of atropine (1 μM) and guanethidine (5 μM), EFS (120 mA, 1 ms, 0.25–32.0 Hz, trains of 2 min) induced frequency-dependent relaxations of 5-hydroxytryptamine (3 μM) pre-contracted strips.

4 EFS at frequencies of 8–32 Hz evoked significant increases in PHI-LI outflow. The increases in PHI-LI outflow evoked by 16-Hz EFS were abolished by tetrodotoxin (3 μM) and by a calcium-free medium, indicating an active release process from intramural nerves.

5 The EFS-induced release of PHI-LI measured with the N-terminal-specific antiserum was significantly greater than that detected with the C-terminal-specific antisera.

6 Sephadex G-25 gel permeation chromatographic analysis was performed on the PHI-LI released in response to 32-Hz EFS. A C-terminal-specific antiserum revealed one peak co-eluting with the rat PHI standard. When PHI-LI was measured with the N-terminal-specific antiserum, two peaks were found that co-eluted with the rat PHV(1–42) and rat PHI-Gly/PHI standards, respectively.

7 The present data suggest that the extended forms of PHI are the primary components of the PHI-LI released by NANC inhibitory neurones in the rat gastric fundus and support a NANC inhibitory neurotransmitter role for PHI and its extended forms in this tissue.

Keywords: Peptide histidine isoleucine (PHI); peptide histidine glycine (PHI-Gly); peptide histidine valine [PHV(1–42)]; rat gastric fundus; non-adrenergic non-cholinergic (NANC); relaxation

Introduction

Peptide histidine isoleucine (PHI) is a 27-amino-acid peptide (P) with an N-terminal histidine (H) and a C-terminal isoleucine (I). It was originally isolated from porcine small intestine and shows remarkable sequence homology with vasoactive intestinal polypeptide (VIP), sharing 13 amino-acid residues in identical positions (Tatemoto & Mutt, 1981). PHI and VIP are co-synthesized from the same precursor molecule (Itoh *et al.*, 1983) and co-localize in the neurones of various tissues (Yanaihara *et al.*, 1983; Bishop *et al.*, 1984; Christofides *et al.*, 1984; Lundberg *et al.*, 1984a; Fahrenkrug *et al.*, 1985), including the rat gastric fundus (Ekblad *et al.*, 1985). The two peptides have also been shown to produce similar biological effects, such as stimulation of pancreatic (Dimaline & Dockray, 1980; Holst *et al.*, 1987), intestinal (Anagnostides *et al.*, 1983) and hormonal secretions (Samson *et al.*, 1983; Szecówka *et al.*, 1983; Grunditz *et al.*, 1986), vasodilatation (Lundberg & Tatemoto, 1982; Lundberg *et al.*, 1984a; Suzuki *et al.*, 1984; Bardrum *et al.*, 1986) and relaxation of genitourinary (Bardrum *et al.*, 1986; Blank *et al.*, 1986), bronchial (Lundberg *et al.*, 1984a; Ellis & Farmer, 1989) and gastrointestinal (Biancani *et al.*, 1989; Nurko *et al.*, 1989; D'Amato *et al.*, 1990) smooth muscles. They are also co-released in response to parasympathetic nerve stimulation (Lundberg *et al.*, 1984b; Holst *et al.*, 1987; Yasui *et al.*, 1987; Ohta *et al.*, 1990). These findings strongly support the hypothesis that VIP and PHI act as co-transmitters.

Non-adrenergic non-cholinergic (NANC) inhibitory innervation is responsible for receptor relaxation of the gastric fundus during food intake (Abrahamsson, 1986). Under *in vitro* NANC conditions, electrical field stimulation (EFS) of rat gastric fundus strips causes relaxation (Heazell, 1977), which can be reduced by peptidases (De Beurme & Lefebvre, 1987; Kamata *et al.*, 1988; D'Amato *et al.*, 1992a; Boeckxstaens *et al.*, 1992), anti-VIP and anti-PHI sera (Kamata *et al.*, 1988; De Beurme & Lefebvre, 1988; D'Amato *et al.*, 1990; Li & Rand, 1990) and nitric oxide (NO)-synthase inhibitors (Li & Rand, 1990; Boeckxstaens *et al.*, 1991; 1992; D'Amato *et al.*, 1992a). Nitric oxide (Boeckxstaens *et al.*, 1991), VIP and PHI (D'Amato *et al.*, 1990; Lefebvre *et al.*, 1991) all cause relaxation of the smooth muscle of the rat gastric fundus. Moreover, EFS of rat gastric fundus strips has been shown to elicit the release of VIP (D'Amato *et al.*, 1992b) and of a vasorelaxant substance(s) that is biologically similar to NO (Boeckxstaens *et al.*, 1991). Therefore, NO (or an NO-releasing substance), VIP and PHI are considered to be putative neurotransmitters released by NANC neurones in this tissue.

The aim of this study was to determine whether PHI release could be induced by EFS in the rat gastric fundus. If so, PHI would fulfil both the 'identity of action' and 'detectable release' criteria for a neurotransmitter. Two C-terminal-extended forms of PHI, peptide histidine glycine (PHI-Gly) and peptide histidine valine [PHV(1–42)], co-localize with PHI in a number of rat tissues, including the stomach, where they account for 65% of the detectable PHI-like immunoreactivity (PHI-LI) (Cauvin *et al.*, 1989b) and produce biological effects identical to those of PHI (Lefebvre *et al.*, 1991). We, therefore, used radioimmunoassay (RIA) systems employing C-terminal- and N-terminal-specific antisera to

[1] Author for correspondence.

determine whether PHI or its extended forms are preferentially released by the rat gastric fundus.

Methods

General

Male and female Wistar rats weighing 150–250 g were fasted overnight with free access to water. The animals were killed by decapitation and exsanguinated. A mid-line abdominal incision was made, and the gastric fundus was removed and immediately placed in Krebs solution at room temperature. One or two longitudinal muscle strips (3 × 20 mm) were prepared from each fundus, according to the method of Vane (1957). The strips were immediately transferred to organ baths or glass tubes (see below) containing Krebs solution, which was maintained at a constant temperature of 37°C and bubbled with a 95% O_2:5% CO_2 mixture. Under these conditions, the pH of the solution was 7.4. Different strips were used for functional and release experiments (see below). In both cases, the composition of the Krebs solution was as follows (mM): NaCl 118.5, KCl 4.8, $CaCl_2$ 1.9, KH_2PO_4 1.2, $MgSO_4$ 1.2, $NaHCO_3$ 25 and glucose 10.1

Functional experiments

The strips were suspended between two parallel platinum electrodes (20 mm long, 4 mm wide, 5 mm apart) inside 5 ml organ baths and connected to auxotonic transducers (Harvard smooth muscle) under a 1 g load. Smooth-muscle activity, magnified 5–10 times, was recorded with Rikadenki R-01 single-pen recorders. For these experiments, the bath solution also contained atropine 1 μM and guanethidine 5 μM. Strip tone was induced with 5-hydroxytryptamine (5-HT) 3 μM to enable recording of NANC relaxations. After a 60-min equilibration period, during which the bath solution was changed every 10 min, the strips were stimulated with rectangular, bipolar electrical pulses of constant duration (1 ms) and amplitude (120 mA) delivered with a Palmer Bioscience 6012 Stimulator linked in series with a Basile Biological Research Apparatus constant-current unit. The pulse train duration was 2 min; frequencies ranged from 0.25–32.0 Hz. After equilibration, the bath solution was changed every 5 min between trains of EFS.

Release experiments

Each strip was mounted under a 1 g load between two parallel platinum electrodes (20 mm long, 3.5 mm wide, 3 mm apart) inside a 4 ml silanized glass tube containing 2 ml of the Krebs solution plus atropine 1 μM, guanethidine 5 μM, 5-HT 3 μM, bovine serum albumin (BSA) 50 mg l^{-1}, bacitracin 30 mg l^{-1} and aprotinin 100,000 kallikrein inhibitor units (KIU) l^{-1}. Additional experiments were performed to determine whether 5-HT had any effect on the evoked release of PHI-LI (see Experimental protocols below). After a 60-min equilibration period (during which the strip was transferred, every 10 min, to a different tube containing fresh solution), the strip was subjected to 2 min incubations (in different tubes) before, during and after the EFS described above. After each incubation, the solution was collected on ice and stored at − 20°C. At the end of each experiment, the strip was blotted and weighed. The samples were extracted with ethanol 2:1 (v/v), centrifuged at 2,000 *g* for 30 min at 4°C, vacuum-dried in a Speedvac Evaporator linked with a Savant refrigerated condensation trap and kept at − 20°C until assayed. Recovery of known amounts of PHI, added to the solution and extracted and dried in the same manner as the samples, was almost 100%.

PHI measurement

PHI-LI was measured by RIA using three different anti-PHI sera. Serum R8403 (N-terminal-specific) and R8801 (C-terminal-specific), raised against synthetic porcine PHI (14–27) and PHI(1–15), respectively, were kindly supplied by Prof. Dr N. Yanaihara. The third antiserum, R01, was obtained from New Zealand white rabbits immunized with synthetic porcine PHI (pPHI) which had been coupled to human serum albumin (HSA) with carbodiimide. Lyophilized pPHI (0.5 mg) was added to HSA (1.15 mg in 0.575 ml) and 1-ethyl-3-(3-dimethyl-aminopropyl) carbodiimide hydrochloride (5 mg in 0.5 ml), both dissolved in 0.25 M phosphate buffer, pH 7.4. The reaction mixture was stirred overnight at 4°C, and the conjugate was then dialysed against distilled water for 24 h at 4°C. The final yield of the coupling reaction, assessed by adding a trace amount of [^{125}I]-pPHI to the reaction mixture, averaged 40%. The conjugate was emulsified with a double volume of complete Freund's adjuvant and injected subcutaneously at multiple sites on the backs of two 6-week-old New Zealand rabbits at 3-week intervals. Each rabbit received 30 nmol of pPHI in each of the three initial injections and half this amount in each booster immunization. The rabbits were bled 15 days after the third injection and after each booster injection. The cross-reactivity of the antiserum with several other peptides and pPHI analogues was tested by adding up to 1 μg/tube corticotrophin-releasing factor (CRF), gastric inhibitory peptide (GIP), glucagon, growth hormone-releasing factor (GRF), helodermin, peptide histidine methionine (PHM), pPHI(14–27), rat PHI (rPHI), rat PHI-Gly (rPHI-Gly), rat PHV(1–42) [rPHV (1–42)], sauvagine, secretin, urotensin I and VIP.

Production and characterization of anti-pPHI sera R8403 and R8801 have been described previously (Yanaihara *et al.*, 1984; Yasui *et al.*, 1987). We tested their cross-reactivities with rPHI-Gly and rPHV(1–42). R8403 showed full immunological recognition of both C-terminal-extended forms of PHI, while R8801 cross-reactivity with these peptides was lower than 0.01%.

Iodinated pPHI was prepared using the chloramine T method and purified on a Sep Pak C18 cartridge, according to a slightly modified version of the method described by Fahrenkrug (1984). The column was eluted with a step-wise gradient of methanol from 0 to 80%. For each step, three 1-ml fractions were collected. Ten microlitres of each fraction were counted in a γ-counter and the radioactive peak fractions were pooled and used as labelled antigen in the RIA systems.

The RIA was performed in a buffer containing 10 mM sodium phosphate, NaCl 154 mM, ethylene diamine tetraacetic acid (EDTA) 25 mM, thimerosal 0.01%, BSA 0.5% and Tween 20 0.03%, pH 7.2. The diluent for sera contained aprotinin 500 KIU ml^{-1}. The dried samples were reconstituted with buffer and concentrated five fold in the RIA systems employing R8403 and R8801 sera and 10 fold in the assay performed with our serum R01. Krebs solution, extracted and reconstituted in the same manner, was used to assess non-specific binding and for calculation of standard curves. The pH of the concentrated Krebs solution was 7.9, while the final pH of the incubation medium in the RIA system at 4°C was 7.2. The anti-pPHI sera were used at final dilutions of 1:320,000 (R8403), 1:800,000 (R8801) and 1:80,000 (R01) to obtain approximately 40% binding of the iodinated peptide. The RIAs were performed as follows: an initial incubation was carried out at 4°C in disposable plastic tubes containing 0.1 ml of anti-pPHI serum, 0.1 ml of sample or standard solution and 0.1 ml of buffer. After 24 h, 0.1 ml of [^{125}I]-pPHI (5,000 c.p.m./tube) was added and the incubation was continued at 4°C for 48 h. Separation of free from bound pPHI was achieved by adding 0.1 ml of anti-rabbit goat serum, diluted 1:20, and 0.5 ml of a 6.6% polyethylene glycol solution. After a 2 h incubation at 4°C, the tubes were centrifuged at 3,000 *g* for 1 h at 4°C, the supernatant was

discarded and the pellet was counted in a γ-counter. The standard curves ranged from 1.95 to 1,000 pg/tube of rPHI. Each sample was assayed in duplicate; PHI-LI measurements with sera R8403 and R8801 were performed in the same sample.

Since the PHI-LI levels were not influenced by the wet weight of the tissues within the range 112–167 mg (137.7 ± 4.6 mg), the results were expressed as pg per fraction. The total evoked PHI-LI release was calculated by subtracting the basal values from each value observed during and after the EFS and summing the differences. For each experiment, these sums are reported as absolute values (pg).

Experimental protocols

EFS frequency-response curves Strip relaxation and PHI-LI release induced by isolated EFS at increasing frequencies (0.25–32.0 Hz) were studied. In functional experiments, strips were allowed to recover basal tone prior to subsequent EFS. In the release experiments, the interval between stimulations was increased progressively from 10 to 60 min as higher frequencies were used. All relaxations were expressed as both amplitudes and areas under the curves (estimated using the trapezoidal rule for planar area). The results are shown as percentages of the maximal response (to 32 Hz) obtained in each strip.

Effect of 5-HT on PHI-LI release Two strips from each fundus were subjected to EFS at 1, 4 and 16 Hz, the first in the normal incubation medium, the second in the same solution without 5-HT, 3 μM. PHI-LI was measured in the incubation medium before, during and after each EFS with antisera R8403 and R8801.

Effects of tetrodotoxin and calcium-free Krebs solution Relaxations and PHI-LI release elicited by EFS, 16-Hz, were measured before and after 15 min incubation with tetrodotoxin (TTX) 3 μM. Sixty minutes elapsed between the pre- and post-TTX stimulations. In the functional experiments, the post-TTX relaxation was expressed as a percentage of the first.

The influence of calcium removal from the incubation medium was tested only on EFS-induced PHI-LI release, since this experimental condition abolished smooth muscle tone and made it impossible to evaluate the mechanical responses. PHI-LI release was measured in response to EFS (16 Hz) delivered before and after 30 min incubation in calcium-free Krebs solution containing an equimolar concentration of Mg^{2+}. Sixty minutes elapsed between the two determinations.

Effect of thiorphan on PHI-LI release Two strips from each fundus were subjected to EFS at 32 Hz, the first in the normal incubation medium, the second in the same medium with 1 μM thiorphan, a neutral endopeptidase inhibitor. PHI-LI was measured in the medium before, during and after EFS with antisera R8403 and R8801.

Gel permeation chromatography The chromatographic study of the PHI-LI released in response to EFS was performed on a 1 × 100 cm column containing Sephadex G-25 fine gel. The column was equilibrated and eluted with the buffer used for the RIA at a flow rate of 5 ml h^{-1}. The PHI-LI used in this analysis was obtained by stimulating four strips at 32 Hz and pooling the 2-ml fractions collected during the EFS and the 4-min period that followed it. The resulting sample (24 ml) was concentrated on two Sep Pak C18 cartridges, each equilibrated with 10 ml of a 10 mM HCl-10% CH_3CN solution and eluted with 4 ml of a 50% CH_3CN in 10 mM HCl solution. The eluates were vacuum-dried, reconstituted with buffer in a total volume of 1 ml and loaded onto the top of the column. A small amount of dextran blue was added to calculate the void volume (Vo). PHI-LI was measured in 0.5 ml collection fractions with antisera R8403 and R8801.

Drugs used

Atropine sulphate, BSA, chloramine T, guanethidine sulphate, human CRF, human GRF, HSA, 5-HT creatinine sulphate, polyethylene glycol, porcine GIP, porcine glucagon, pPHI, porcine secretin, sauvagine, tetrodotoxin, thimerosal, DL-thiorphan, urotensin I (Sigma, St Louis, MO, U.S.A.); aprotinin (Lepetit, Milan, Italy); bacitracin (Lusofarmaco, Milan, Italy); complete Freund's adjuvant (Difco Laboratories, Detroit, MI, U.S.A.); 1-ethyl-3-(3-dimethyl-aminopropyl) carbodiimide hydrochloride (Calbiochem, La Jolla, CA, U.S.A.); EDTA (Carlo Erba, Milano, Italy); helodermin, pPHI(14–27) (Novabiochem, Laufelfingen, Switzerland); Na ^{125}I (Amersham, Buckinghamshire, U.K.); PHM, rPHI, VIP (Bachem, Bubendorf, Switzerland); Sephadex G-25 fine gel (Pharmacia, Uppsala, Sweden). rPHI-Gly and rPHV(1–42) were kindly supplied by Prof. Dr P. Robberecht.

Statistical analysis

The results were evaluated by means of Dunnett's test for multiple comparisons with a control. All values are reported as mean ± s.e.mean. $P<0.05$ was considered statistically significant.

Results

Antiserum characterization and RIA system performance

The anti-pPHI serum produced in our laboratory (R01) proved highly specific and capable of recognizing the C-terminus of PHI. Its cross-reactivity was <0.01% with rPHV(1–42), CRF, GIP, glucagon, GRF, helodermin, sauvagine, urotensin

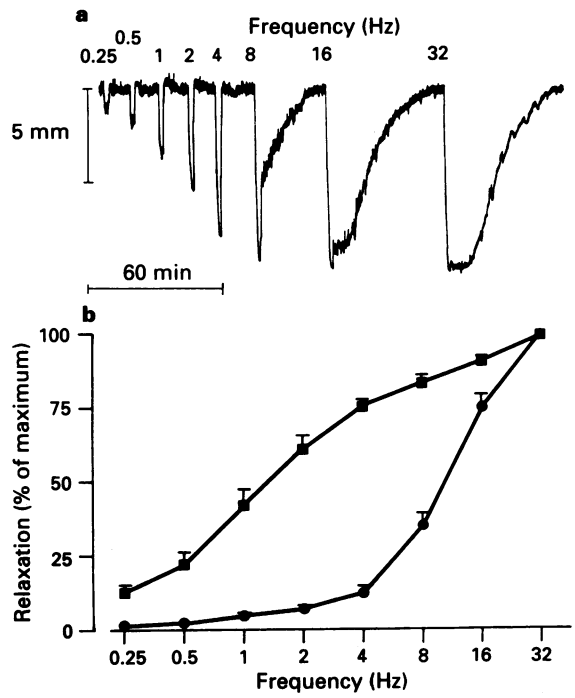


Figure 1 Relaxation of longitudinal muscle strips from the rat gastric fundus induced by electrical field stimulation (0.25–32.0 Hz, 120 mA, 1 ms, pulse trains of 2 min). (a) Representative tracing from one muscle strip. (b) Mean results ± s.e.mean based on responses of 12 strips. Relaxations were measured as peak amplitude (■) and as area under the curve (●) and are expressed as percentages of the maximal relaxation induced with 32-Hz EFS in each strip.

I and VIP; 0.2% with secretin; 0.94% with rPHI-Gly and PHM, and 100% with pPHI(14–27) and rPHI.

The IC_{50} of the standard curve from the RIA system employing serum R01 averaged 85.3 ± 1.9 pg/tube, and non-specific binding of the labelled ligand was less than 3%. The intra-assay ($n = 4$) and inter-assay ($n = 5$) coefficients of variation were ± 2.4% and ± 2.3% at the lowest level of standard (1.95 pg/tube) and ± 6.4% and ± 12.0% at the highest level of standard (1,000 pg/tube), respectively. The lowest concentration that could be measured with 95% confidence (i.e., 2 s.d. at zero) was 1.95 pg/tube. The detection limit was thus 1.95 pg ml^{-1} of the original sample, since each dried 1 ml sample was reconstituted in 0.1 ml in the RIA system.

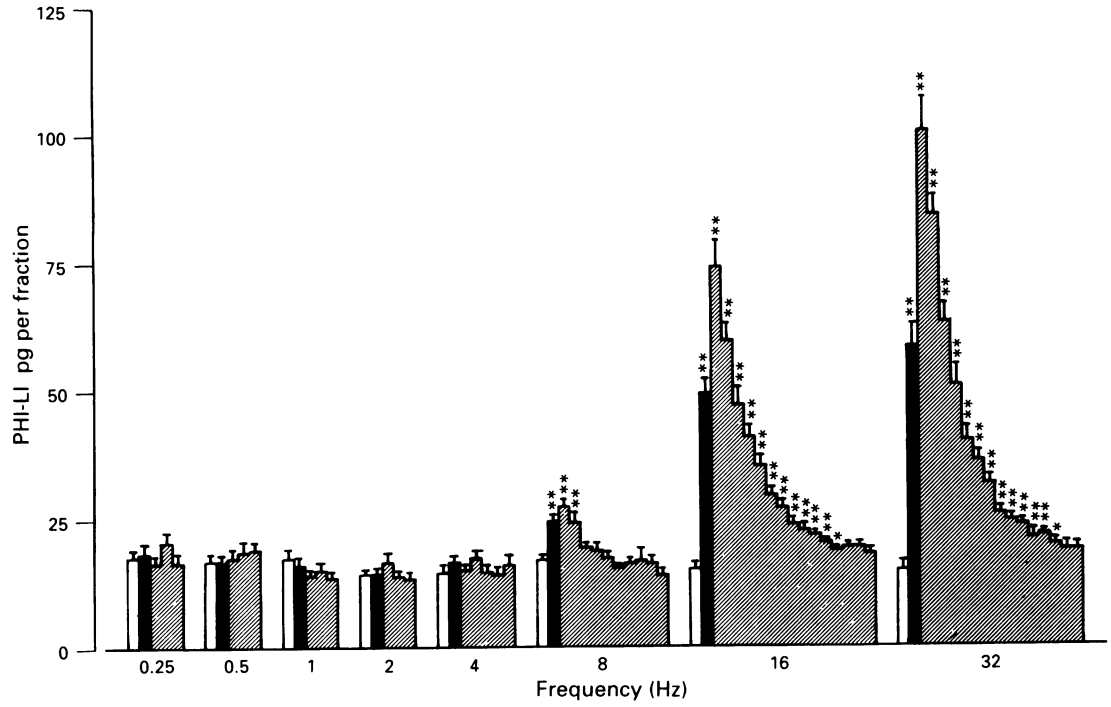


Figure 2 Peptide histidine isoleucine-like immunoreactivity (PHI-LI) concentrations measured with anti-pPHI serum R8403 in the incubation medium of longitudinal muscle strips of the rat gastric fundus before (open columns), during (solid columns) and after (hatched columns) electrical field stimulation (0.25–32.0 Hz, 120 mA, 1 ms, pulse trains of 2 min). Each column represents mean PHI-LI with s.e.mean found in 2-min collection fractions from 13 strips. Values significantly different from baseline levels: $*P<0.05$; $**P<0.01$.

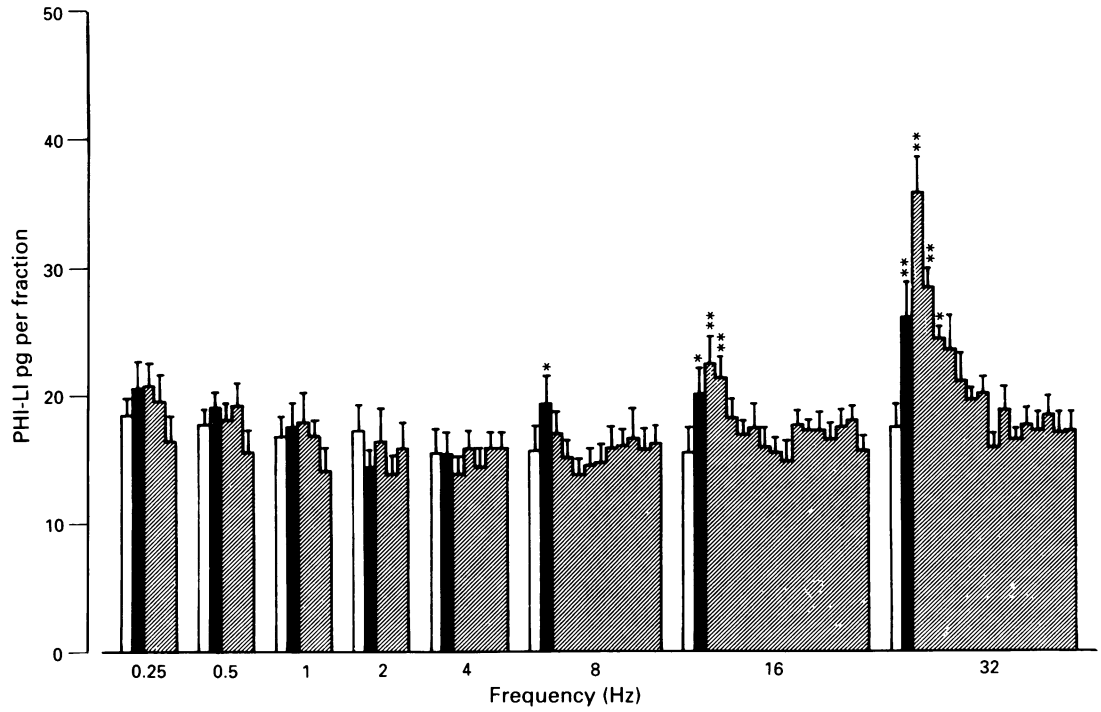


Figure 3 Peptide histidine isoleucine-like immunoreactivity (PHI-LI) concentrations measured with anti-pPHI serum R8801 in the incubation medium of longitudinal muscle strips of the rat gastric fundus before (open columns), during (solid columns) and after (hatched columns) electrical field stimulation (0.25–32.0 Hz, 120 mA, 1 ms, pulse trains of 2 min). Each column represents mean PHI-LI (s.e.mean shown by vertical lines) found in 2 min collection fractions from 13 strips. Values significantly different from baseline levels: $*P<0.05$; $**P<0.01$.

EFS frequency-response curves

Figure 1 shows an actual tracing, as well as the mean results, from the functional experiments. Within the range of 0.25–32.0 Hz, EFS elicited frequency-dependent NANC relaxations characterized by two distinct phases, which were well evident when higher frequencies were used. The initial relaxation, which began immediately after the initiation of EFS, developed rapidly to a near-maximal level. The second phase was characterized by a slight additional decrease in tone, which occurred much more gradually. At frequencies of 2 Hz or less, recovery of basal tone was almost immediate; the recovery period increased progressively thereafter to a maximum of about 1 h after 32-Hz EFS. Consequently, the frequency-response curves calculated on the basis of the amplitude are different from those based on the area under the curve (Figure 1).

EFS at frequencies of 8–32 Hz evoked statistically significant, frequency-dependent increases of PHI-LI outflow into the incubation medium (Figures 2, 3, 4). Although the basal (pre-EFS) levels of PHI-LI outflow measured with the three antisera were essentially the same, the increases detected with the N-terminal-specific serum R8403 were significantly greater than those measured with antiserum R8801 or R01, both of which are C-terminal-specific. In addition, in assays based on R8403, PHI-LI levels increased during the 2-min EFS, but peak release was consistently observed during the initial 2-min post-EFS period. This level then gradually decreased, reaching essentially basal values 6 min after EFS at 8 Hz, 26 min after 16-Hz EFS and 28 min after 32-Hz EFS (Figure 2). PHI-LI measured with either R8801 or R01 also peaked shortly after stimulation (except with 8-Hz EFS), but the recovery to basal levels was achieved much more rapidly after cessation of EFS (2, 6 and 8 min, respectively, after EFS at 8, 16 and 32 Hz) (Figures 3, 4).

Table 1 shows the mean total EFS-evoked PHI-LI release measured with the three antisera. The mean release observed with R8801 was not significantly different from that measured with serum R01, while both were significantly lower than that measured with R8403. The mean total release values observed in the R8801 assays following EFS at 8, 16 and 32 Hz were 15.5 ± 4.3%, 8.4 ± 1.2% and 12.3 ± 0.8% ($n = 13$), respectively, of those measured in the R8403 assays. An identical pattern was displayed by serum R01. The relationship between the total evoked PHI-LI release found with R8403 and strip relaxation is shown in Figure 5.

Effect of 5-HT on PHI-LI release

In the absence of 5-HT, the pattern of PHI-LI release produced by EFS was similar to that described above. There was no release in response to 1- or 4-Hz EFS, and the total

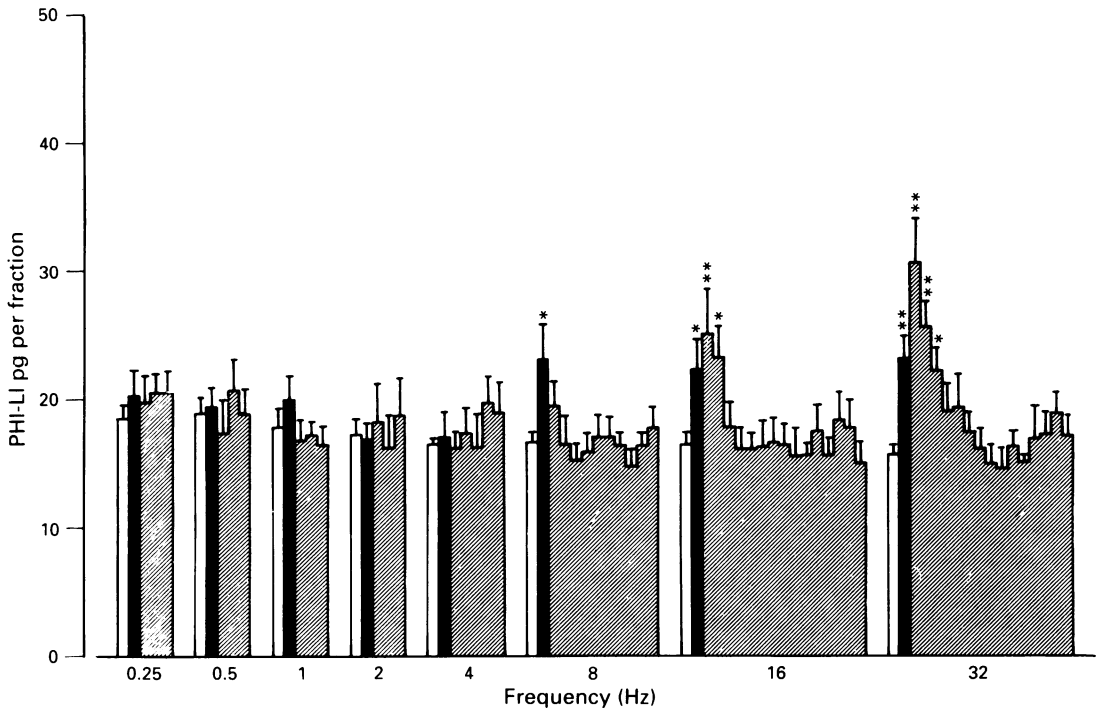


Figure 4 Peptide histidine isoleucine-like immunoreactivity (PHI-LI) concentrations measured with anti-pPHI serum R01 in the incubation medium of longitudinal muscle strips of the rat gastric fundus before (open columns), during (solid columns) and after (hatched columns) electrical field stimulation (0.25–32.0 Hz, 120 mA, 1 ms, pulse trains of 2 min). Each column represents mean PHI-LI with s.e.mean found in 2-min collection fractions from seven strips. Values significantly different from baseline levels: $*P<0.05$; $**P<0.01$.

Table 1 Total PHI-LI release from the rat gastric fundus detected by three different anti-pPHI sera in response to EFS

EFS frequency (Hz)	*R8403*	*R8801*	*R01*
		Total PHI-LI released (pg)	
8	34.8 ± 5.4	4.0 ± 0.8*	4.3 ± 0.9*
16	289.2 ± 19.5	24.3 ± 4.4*	25.0 ± 6.4*
32	430.3 ± 9.0	52.6 ± 3.1*	42.6 ± 6.2*

Numbers are means ± s.e.mean of 13 experiments for antisera R8403 and R8801 and seven experiments for antiserum R01; $*P<0.001$ vs R8403.

release evoked by 16-Hz EFS was no different from that induced in the control strips exposed to 5-HT: 289.6 ± 32.6 vs 291.4 ± 32.4 pg ($n = 4$) as measured by R8403 and 32.8 ± 8.9 vs 32.4 ± 8.1 pg ($n = 4$) with R8801, in the absence and presence of 5-HT, respectively.

Effects of TTX and calcium-free Krebs solution

In this series of experiments, responses were evaluated to a single frequency (16 Hz) EFS and PHI-LI release was measured only with antisera R8403 and R8801. The addition of 3 μM TTX had no effect on basal strip tone, but completely abolished the relaxant response to 16-Hz EFS ($n = 8$). Neither TTX nor the calcium-free Krebs solution influenced basal outflow of PHI-LI, but both abolished the response to EFS (Figure 6).

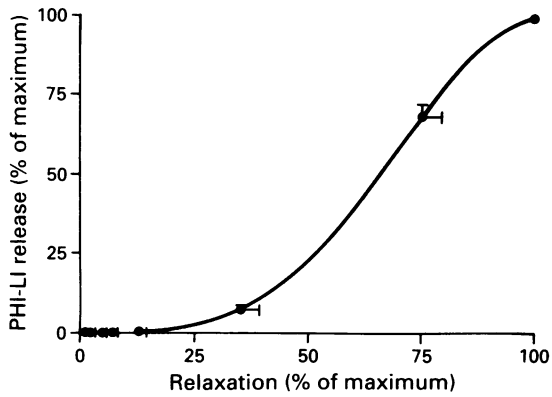


Figure 5 Relationship between relaxation (expressed as area under the curve) and total evoked peptide histidine isoleucine-like immunoreactivity (PHI-LI) release (calculated by subtracting the basal value from the value observed in each 2-min collection fraction during and after the stimulation and adding the differences) measured with anti-pPHI serum R8403. Data are expressed as percentage of maximal values and given as means ± s.e.mean from 12 strips for the relaxation and 13 strips for the release.

Effect of thiorphan on PHI-LI release

Thiorphan 1 μM had no effect on the EFS-induced PHI-LI release measured with antisera R8403 or R8801.

The total release evoked with 32-Hz EFS in control strips and in those incubated with thiorphan were 461.4 ± 22.5 and 454.9 ± 27.7 pg, respectively, when measured with R8403, and 67.8 ± 8.5 and 55.8 ± 12.2 pg, respectively, when measured with R8801 ($n = 4$).

Gel permeation chromatography

Figure 7 shows the gel filtration profile of the PHI-LI released in response to 32-Hz EFS and detected with R8403 or R8801. R8801 revealed a single immunoreactive peak that co-eluted with the synthetic rPHI standard, while R8403 detected two peaks, the first co-eluting with the synthetic rPHV(1–42) standard and the second in the same positions as the synthetic rPHI-Gly and rPHI standards. The first peak revealed by R8403 represented 50.1% of the total immunoreactivity measured with this antiserum, while the single peak detected with R8801 was only 38.8% of the total immunoreactivity measured with the N-terminal-specific antiserum. This value (38.8%) is quite similar to the ratio of the PHI-LI measured by R8801 and that revealed by R8403 (37.7 ± 3.1) in samples from the release experiments corresponding to the factions pooled for the chromatographic analysis (2 min during EFS plus the following 4 min). The second peak disclosed

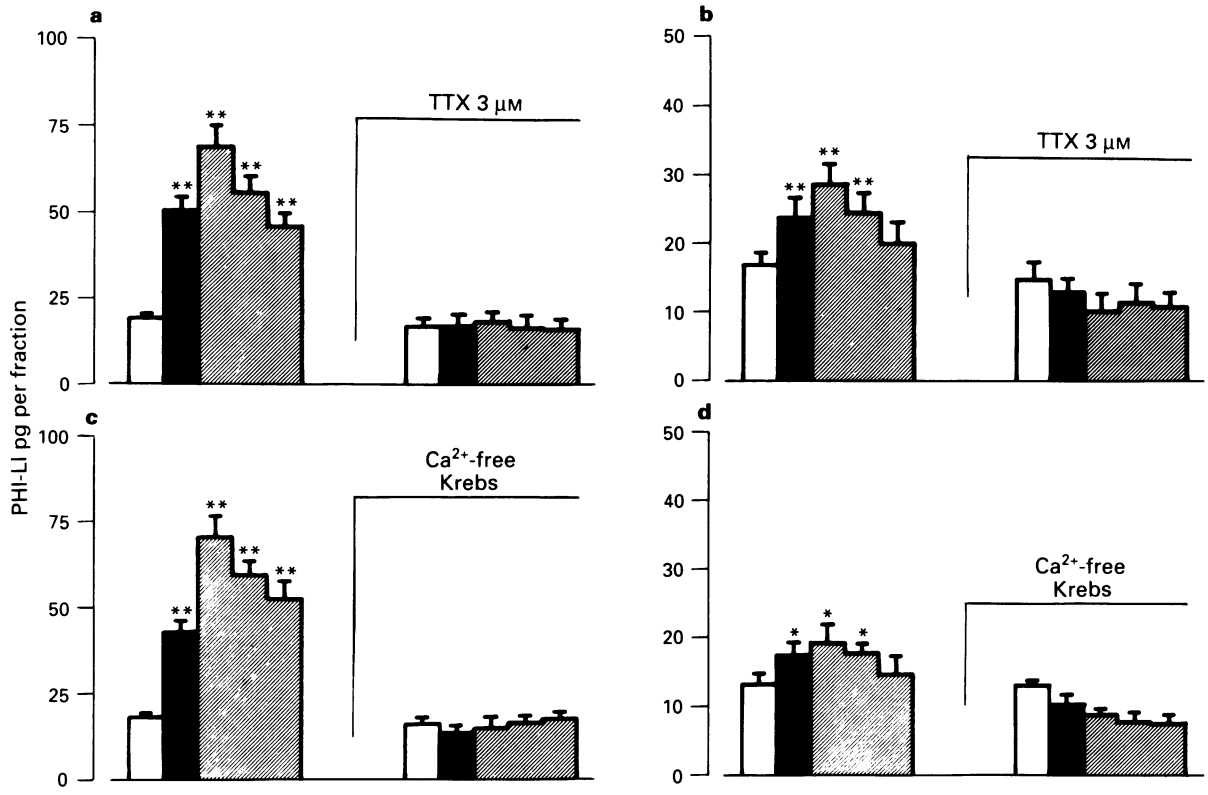


Figure 6 Release of peptide histidine isoleucine-like immunoreactivity (PHI-LI) from longitudinal muscle strips of rat gastric fundus induced by electrical field stimulation (16 Hz, 120 mA, 1 ms, pulse trains of 2 min) before and after addition of 3 μM tetrodotoxin (a, b) and before and after strip incubation with a calcium-free medium (c, d). Each column represents mean with s.e.mean PHI-LI measured with anti-pPHI serum R8403 (a, c) or anti-pPHI serum R8801 (b, d) in 2-min collection fractions from six strips. Open, solid and hatched columns, as in Figures 2, 3 and 4, refer to fractions collected before, during and after electrical stimulation. Values significantly different from baseline values: $*P < 0.05$; $**P < 0.01$.

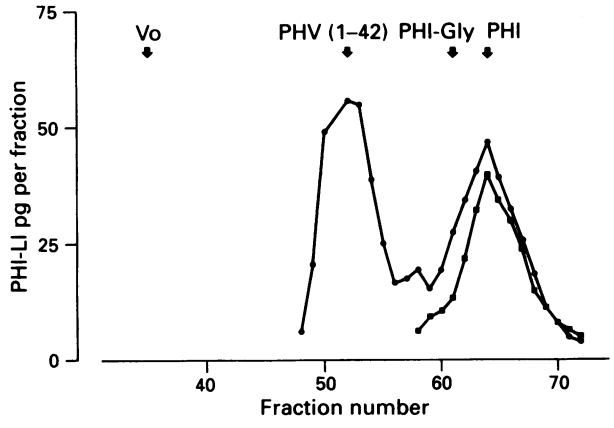


Figure 7 Sephadex G-25 gel filtration chromatographic profiles of the PHI-LI released by longitudinal muscle strips from the rat gastric fundus that were subjected to 32-Hz EFS (fractions of the incubation medium collected during and after EFS of four strips were pooled for this analysis). PHI-LI was detected with anti-pPHI serum R8403 (●) and with anti-pPHI serum R8801 (■). Arrows indicate the elution positions of dextran blue (Vo), synthetic rPHV (1–42), synthetic rPHI-Gly and synthetic rPHI.

by R8403, which appeared before and was larger than that detected by R8801, is probably due to the superimposition of an early, small peak representing PHI-Gly and a later, larger peak produced by PHI. In fact, when the R8801 peak is subtracted from the second peak detected by R8403, the result suggests a small peak co-eluting with the synthetic rPHI-Gly standard and representing the remaining 11.1% of the total PHI-LI.

Discussion

NANC inhibitory neurones are responsible for both the receptive and adaptive relaxations that occur in the proximal third of the stomach. There was initially a great deal of controversy about the identity of the neurotransmitters released by these neurones, but, until a few years ago, VIP and ATP were considered to be the most likely candidates. However, Bult *et al.* (1990) have recently demonstrated that NO acts as an inhibitory NANC neurotransmitter at the ileo-colonic junction, and Li & Rand (1990) have provided evidence that it plays an identical role in the rat gastric fundus. It currently appears that the NANC relaxation to EFS in the rat gastric fundus involves two components: a nitrergic component that is primarily responsible for the relaxation observed with low-frequency or short-duration EFS, and a peptidergic component that is mainly responsible for the relaxation induced by EFS at high frequencies or long duration (Li & Rand, 1990; D'Amato *et al.*, 1992a,b; Boeckxstaens *et al.*, 1992; Currò *et al.*, 1992). VIP is still considered as the most likely candidate for the peptidergic component, but there are also reasons to believe that PHI participates in this response, as follows: (a) both rat and porcine PHI (rPHI and pPHI) relax the smooth muscle of the rat gastric fundus, although they are about 2 and 30 times less potent than VIP; therefore, rPHI, which differs from pPHI for two amino-acid residues in the sequence, is approximately 15 times more potent than pPHI in relaxing the rat gastric fundus, although its potency in this respect is still half of that displayed by VIP (Lefebvre *et al.*, 1991); (b) electrically induced NANC relaxation in this tissue is reduced by a specific anti-pPHI serum (D'Amato *et al.*, 1990); (c) two C-terminally extended forms of rPHI, rPHI-Gly and rPHV(1–42), relax the rat gastric fundus, although their potencies are 4 and 3 fold less, respectively, than that of rPHI. These findings mean that PHI and its extended forms fulfil the 'identity of action' criterion for putative neurotransmitters in this NANC system. The results described here demonstrate that EFS of the rat gastric fundus elicits the release of PHI-LI through a TTX-sensitive, calcium-dependent mechanism, which means that PHI and its extended forms also satisfy the 'detectable release' criterion for inhibitory NANC neurotransmitters in this tissue.

The finding that significantly increased PHI-LI release is evoked only at EFS frequencies of 8 Hz or higher is consistent with the idea that PHI and VIP may act as co-transmitters in the rat gastric fundus, since the same pattern of release has been observed for VIP-LI in this tissue (D'Amato *et al.*, 1992b). These two peptides are also co-released in the dog gastric corpus in response to vagal stimulation (Ohta *et al.*, 1990). Our data support the hypothesis that VIP and PHI are primarily involved in the NANC relaxation elicited by high frequency EFS. With this type of stimulation, recovery to basal tone is more gradual than that observed after low frequency EFS. This gradual recovery is also observed when exogenously applied PHI and VIP are removed from the bath medium (results not shown). Therefore, there is a good correlation between the time course of the mechanical responses and the time course of the release of PHI-LI and VIP-LI elicited in these muscle strips by high frequency EFS. Moreover, peptidases and anti-VIP sera primarily inhibit the NANC relaxations provoked by high frequency EFS, while those induced by low frequencies of stimulation are mainly attenuated by NO-synthase inhibitors (Li & Rand, 1990; Boeckxstaens *et al.*, 1992).

PHI-LI release was measured under the same experimental conditions used in the functional study in order to correlate this release as closely as possible with the intensity of evoked relaxation. The question arose, however, as to whether the substances used to unravel the NANC relaxation, in particular 5-HT, might have exerted modulatory effects on PHI-LI release. This possibility was excluded in separate experiments conducted in the absence and presence of 5-HT.

The existence of C-terminally extended forms of PHI or PHM was first suggested for human neuroblastoma cells (Hoshino *et al.*, 1984) and later for porcine stomach (Yiangou *et al.*, 1985). In the latter study, an N-terminal-specific anti-pPHI serum revealed levels of PHI-LI that were 2–4 times higher than those measured by a C-terminal-specific antiserum. Subsequent gel-permeation chromatographic analysis of these extracts revealed a PHI-LI component that eluted before PHI itself and reacted exclusively with an N-terminal-specific antiserum. Similar chromatographic profiles were observed for stomach extracts from cats, rats and man. This larger molecular form of PHI was later found in the nasal mucosa and genitourinary tissue from various species (Yiangou *et al.*, 1986), in the gastrointestinal tracts of dogs (Yasui *et al.*, 1987), in human adrenal phaeochromocytoma (Yiangou *et al.*, 1987) and in rat small intestine (Cauvin *et al.*, 1989b) and characterized as PHV(1–42). A third extended form of PHI, isolated from rat small intestine, was characterized as PHI-Gly (Cauvin *et al.*, 1989a). In the present study, the total EFS-induced PHI-LI release revealed by the C-terminal-specific antisera was approximately 12% of that measured by the N-terminal-specific antiserum, regardless of the stimulation frequency used. Since the former sera (R8801 and R01) do not recognize rPHI-Gly or rPHV(1–42), it is reasonable to assume that PHI-LI detected by these sera represents PHI itself. In contrast, serum R8403 showed full cross-reactivity with both rPHI-Gly and rPHV(1–42), and the immunoreactivity revealed by this serum represents the total produced by PHI and its extended forms. These data suggest that PHI itself accounts for only a small portion (12%) of the PHI-LI observed with EFS. It is also possible, however, that at least part of the PHI released under these circumstances undergoes cleavage by endogenous peptidase(s) (such as neutral endopeptidase, which has been described in the rat gastric fundus; Bunnett *et al.*, 1993) that are not inhibited by aprotinin or bacitracin. This might give rise to

N-terminal fragments that are fully recognized by serum R8403 with short C-terminal fragments that fail to react with sera R8801 or R01. This may provide an alternative explanation for the low levels of PHI-LI detected by the C-terminal-specific antisera. However, the addition of thiorphan, which selectively inhibits neutral endopeptidase, had no effect on the amounts of PHI-LI recovered with either the C- or the N-terminal-specific antisera, which excludes PHI degradation by this peptidase and weakens the above mentioned peptidase-degradation hypothesis. The chromatographic data clearly identify both PHV(1–42) and PHI as components of the PHI-LI released in response to EFS and strongly suggest the presence of PHI-Gly as well. A distinct peak corresponding to the PHI-Gly standard could not be obtained, but the second peak detected by serum R8403 was somewhat earlier and larger than that revealed by serum R8801. It is possible that this R8403 peak contains a small peak that represents PHI-Gly, as well as a larger one produced by PHI itself. In fact, when the R8801 peak is subtracted from the second peak detected by R8403, the remainder is a small peak that co-elutes with the synthetic PHI-Gly standard. The samples used for this analysis were composed of fractions that were collected during EFS and the 4-min period that followed it and, for this reason, the relative proportions of PHI, PHI-Gly and PHV(1–42) in the total PHI-LI released in response to EFS (measured in fractions collected up to 30 min after stimulation) could not be determined. The higher PHI/total PHI-LI ratio in the pool used for chromatographic analysis, with respect to that found in the total (30 min) PHI-LI release measured in the release experiments, is a result of these differences in sampling time. Nevertheless, our data strongly suggest that PHV(1–42) is the predominant molecular form released by the rat gastric fundus in response to EFS.

Using chromatographic separation, Cauvin *et al.* (1989b) found that PHI-Gly, PHV(1–42) and PHI accounted for 32%, 33% and 36%, respectively, of the total PHI-LI detected in tissue extracts of rat stomach. The fact that the PHI/total PHI-LI ratio reported by these authors (1:3) is somewhat higher than that observed in the present study (1:8) is probably due to the fact that the tissue extracts used in the former study were obtained from the stomach as a whole. This ratio has, in fact, been shown to be lower in the gastric fundus (1:7) than it is in the antrum (1:3) (Yiangou *et al.*, 1986), and the former ratio is quite similar to the one that we have reported for our fundus strips.

The concentration of exogenous rPHI and its extended forms that elicited a strip relaxation comparable to that produced with 32-Hz EFS was approximately 30 nM (data not shown). The total PHI-LI detected with serum R8403 during and after EFS at this frequency was about 430 pg. Considering the volume of the incubation medium and the molecular weights of rPHI and its extended forms, this figure translates into a concentration of 0.07 nM, i.e. approximately 400 times lower than the concentration of exogenous rPHI required to produce the same biological effect. However, the PHI-LI concentration produced at the neuromuscular junction during nerve stimulation is much higher than that measured in the incubation medium, and it would be more appropriate to compare this concentration with that of exogenous rPHI. It is also important to remember that the EFS-induced relaxation is not mediated exclusively by PHI-related peptides, since VIP is also released in response to this stimulus.

In conclusion, the present data demonstrate that PHI-LI release occurs in response to activation of intramural neurones of rat gastric fundus and support the NANC inhibitory neurotransmitter role for PHI and its extended forms in this tissue.

Supported by National Research Council (CNR), targeted project 'Prevention and control of disease factors', subproject 2. The authors are indebted to Prof. Dr N. Yanaihara (Laboratory of Bioorganic Chemistry, Shizuoka College of Pharmacy, Shizuoka, Japan) for the generous gift of the anti-pPHI sera R8403 and R8801, to Prof. Dr P. Robberecht (Department of Biochemistry and Nutrition, University of Brussels, Belgium) for providing us with rPHI-Gly and rPHV (1–42), and to Mrs M. Kent for editorial help in preparing the manuscript.

References

ABRAHAMSSON, H. (1986). Non-adrenergic non-cholinergic nervous control of gastrointestinal motility patterns. *Arch. Int. Pharmacodyn.*, **280** (Suppl.), 50–61.

ANAGNOSTIDES, A.A., MANOLAS, K., CHRISTOFIDES, N.D., YIANGOU, Y., WELBOURN, R.B., BLOOM, S.R. & CHADWICK, V.S. (1983). Peptide histidine isoleucine (PHI). A secretagogue in porcine intestine. *Dig. Dis. Sci.*, **28**, 893–896.

BARDRUM, B., OTTESEN, B. & FAHRENKRUG, J. (1986). Peptides PHI and VIP: comparison between vascular and nonvascular smooth muscle effect in rabbit uterus. *Am. J. Physiol.*, **251**, E48–E51.

BIANCANI, P., BEINFELD, M.C., HILLEMEIER, C. & BEHAR, J. (1989). Role of peptide histidine isoleucine in relaxation of cat lower esophageal sphincter. *Gastroenterology*, **97**, 1083–1089.

BISHOP, A.E., POLAK, J.M., YIANGOU, Y., CHRISTOFIDES, N.D. & BLOOM, S.R. (1984). The distributions of PHI and VIP in porcine gut and their co-localisation to a proportion of intrinsic ganglion cells. *Peptides*, **5**, 255–259.

BLANK, M.A., BROWN, J.R., HUNTER, J.C., BLOOM, S.R. & TYERS, M.B. (1986). Effects of VIP and related peptides and Gila monster venom on genitourinary smooth muscle. *Eur. J. Pharmacol.*, **132**, 155–161.

BOECKXSTAENS, G.E., PELCKMANS, P.A., BOGERS, J.J., BULT, H., DE MAN, J.G., OOSTERBOSCH, L., HERMAN, A.G. & VAN MAERCKE, Y.M. (1991). Release of nitric oxide upon stimulation of nonadrenergic noncholinergic nerves in the rat gastric fundus. *J. Pharmacol. Exp. Ther.*, **256**, 441–447.

BOECKXSTAENS, G.E., PELCKMANS, P.A., DE MAN, J.G., BULT, H., HERMAN, A.G. & VAN MAERCKE, Y.M. (1992). Evidence for a differential release of nitric oxide and vasoactive intestinal polypeptide by nonadrenergic noncholinergic nerves in the rat gastric fundus. *Arch. Int. Pharmacodyn.*, **318**, 107–115.

BULT, H., BOECKXSTAENS, G.E., PELCKMANS, P.A., JORDAENS, F.H., VAN MAERCKE, Y.M. & HERMAN, A.G. (1990). Nitric oxide as an inhibitory non-adrenergic non-cholinergic neurotransmitter. *Nature*, **345**, 346–347.

BUNNETT, N.W., WU, V., STERNINI, C., KLINGER, J., SHIMOMAYA, E., PAYAN, D., KOBAYASHI, R. & WALSH, J.H. (1993). Distribution and abundance of neutral endopeptidase (EC 3.4.24.11) in the alimentary tract of the rat. *Am. J. Physiol.*, **264**, G497–G508.

CAUVIN, A., VANDERMEERS, A., VANDERMEERS-PIRET, M.-C., RATHE, J., ROBBERECHT, P. & CHRISTOPHE, J. (1989a). Peptide histidine isoleucinamide (PHI)-(1–27)-Gly as a new major form of PHI in the rat small intestine. *Endocrinology*, **125**, 1296–1302.

CAUVIN, A., VANDERMEERS, A., VANDERMEERS-PIRET, M.-C., ROBBERECHT, P. & CHRISTOPHE, J. (1989b). Variable distribution of three molecular forms of peptide histidine isoleucinamide in rat tissues: identification of the large molecular form as peptide histidine valine-(1–42). *Endocrinology*, **125**, 2645–2655.

CHRISTOFIDES, N.D., POLAK, J.M. & BLOOM, S.R. (1984). Studies on the distribution of PHI in mammals. *Peptides*, **5**, 261–266.

CURRÒ, D., MONTUSCHI, P. & PREZIOSI, P. (1992). Role of endogenous nitric oxide in the non-adrenergic non-cholinergic (NANC) relaxation of the rat gastric fundus. *Pharmacol. Res.*, **26** (Suppl. 1), 208.

D'AMATO, M., CURRÒ, D., CIABATTONI, G. & LEFEBVRE, R.A. (1990). Is peptide histidine isoleucine an inhibitory nonadrenergic noncholinergic neurotransmitter in the rat gastric fundus? *Arch. Int. Pharmacodyn.*, **303**, 216–231.

D'AMATO, M., CURRÒ, D. & MONTUSCHI, P. (1992a). Evidence for dual components in the non-adrenergic non-cholinergic relaxation in the rat gastric fundus: role of endogenous nitric oxide and vasoactive intestinal polypeptide. *J. Auton. Nerv. Syst.*, **37**, 175–186.

D'AMATO, M., CURRÒ, D., MONTUSCHI, P., CIABATTONI, G., RAGAZZONI, E. & LEFEBVRE, R.A. (1992b). Release of vasoactive intestinal polypeptide from the rat gastric fundus. *Br. J. Pharmacol.*, **105**, 691–695.

DE BEURME, F.A. & LEFEBVRE, R.A. (1987). Influence of α-chymotrypsin and trypsin on the non-adrenergic non-cholinergic relaxation in the rat gastric fundus. *Br. J. Pharmacol.*, **91**, 171–177.

DE BEURME, F.A. & LEFEBVRE, R.A. (1988). Vasoactive intestinal polypeptide as possible mediator of relaxation in the rat gastric fundus. *J. Pharm. Pharmacol.*, **40**, 711–715.

DIMALINE, R. & DOCKRAY, G.J. (1980). Actions of a new peptide from porcine intestine (PHI) on pancreatic secretion in the rat and turkey. *Life Sci.*, **27**, 1947–1951.

EKBLAD, E., EKELUND, M., GRAFFNER, H., HÅKANSON, R. & SUNDLER, F. (1985). Peptide-containing nerve fibers in the stomach wall of rat and mouse. *Gastroenterology*, **89**, 73–85.

ELLIS, J.L. & FARMER, S.G. (1989). Effects of peptidases on non-adrenergic, non-cholinergic inhibitory responses of tracheal smooth muscle: a comparison with effects on VIP- and PHI-induced relaxation. *Br. J. Pharmacol.*, **96**, 521–526.

FAHRENKRUG, J. & PEDERSEN, J.H. (1984). Development and validation of a specific radioimmunoassay for PHI in plasma. *Clin. Chim. Acta*, **143**, 183–192.

FAHRENKRUG, J., BEK, T., LUNDBERG, J.M. & HÖKFELT, T. (1985). VIP and PHI in cat neurons: co-localization but variable tissue content possible due to differential processing. *Regul. Pept.*, **12**, 21–34.

GRUNDITZ, T., HÅKANSON, R., HEDGE, G., RERUP, C., SUNDLER, F. & UDDMAN, R. (1986). Peptide histidine isoleucine amide stimulates thyroid hormone secretion and coexists with vasoactive intestinal polypeptide in intrathyroid nerve fibers from laryngeal ganglia. *Endocrinology*, **118**, 783–790.

HEAZELL, M.A. (1977). A non-adrenergic inhibitory innervation in the rat stomach. *Arch. Int. Pharmacodyn.*, **226**, 109–117.

HOLST, J.J., FAHRENKRUG, J., KNUHTSEN, S., JENSEN, S.L., NIELSEN, O.V., LUNDBERG, J.M. & HÖKFELT, T. (1987). VIP and PHI in the pig pancreas: coexistence, corelease and cooperative effects. *Am. J. Physiol.*, **252**, G182–G189.

HOSHINO, M., YANAIHARA, C., OGINO, K., IGUCHI, K., SATO, H., SUZUKI, T. & YANAIHARA, N. (1984). Production of VIP- and PHM (human PHI)-related peptides in human neuroblastoma cells. *Peptides*, **5**, 155–160.

ITOH, N., OBATA, K., YANAIHARA, N. & OKAMOTO, H. (1983). Human preprovasoactive intestinal polypeptide contains a novel PHI-27-like peptide, PHM-27. *Nature*, **304**, 547–549.

KAMATA, K., SAKAMOTO, A. & KASUYA, Y. (1988). Similarities between the relaxations induced by vasoactive intestinal peptide and by stimulation of the non-adrenergic non-cholinergic neurons in the rat stomach. *Naunyn-Schmied. Arch. Pharmacol.*, **338**, 401–406.

LEFEBVRE, R.A., SAS, S. & CAUVIN, A. (1991). Relaxant effect of rat PHI, PHI-Gly and PHV(1–42) in the rat gastric fundus. *Peptides*, **12**, 271–274.

LI, C.G. & RAND, M.J. (1990). Nitric oxide and vasoactive intestinal polypeptide mediate non-adrenergic, non-cholinergic inhibitory transmission to smooth muscle of the rat gastric fundus. *Eur. J. Pharmacol.*, **191**, 303–309.

LUNDBERG, J.M. & TATEMOTO, K. (1982). Vascular effects of the peptides PYY and PHI: comparison with APP and VIP. *Eur. J. Pharmacol.*, **83**, 143–146.

LUNDBERG, J.M., FAHRENKRUG, J., HÖKFELT, T., MARTLING, C.-R., LARSSON, O., TATEMOTO, K. & ÄNGGÅRD, A. (1984a). Co-existence of peptide HI (PHI) and VIP in nerves regulating blood flow and bronchial smooth muscle tone in various mammals including man. *Peptides*, **5**, 593–606.

LUNDBERG, J.M., FAHRENKRUG, J., LARSSON, O. & ÄNGGÅRD, A. (1984b). Corelease of vasoactive intestinal polypeptide and peptide histidine isoleucine in relation to atropine-resistant vasodilation in cat submandibular salivary gland. *Neurosci. Lett.*, **52**, 37–42.

NURKO, S., DUNN, B.M. & RATTAN, S. (1989). Peptide histidine isoleucine and vasoactive intestinal polypeptide cause relaxation of opossum internal anal sphincter via two distinct receptors. *Gastroenterology*, **96**, 403–413.

OHTA, T., ITO, S. & OHGA, A. (1990). Co-release of PHI and VIP in dog stomach by peripheral and central vagal stimulation. *Br. J. Pharmacol.*, **100**, 231–236.

SAMSON, W.K., LUMPKIN, M.D., MCDONALD, J.K. & MCCANN, S.M. (1983). Prolactin-releasing activity of porcine intestinal peptide (PHI-27). *Peptides*, **4**, 817–819.

SUZUKI, Y., MCMASTER, D., LEDERIS, K. & RORSTAD, O.P. (1984). Characterization of the relaxant effects of vasoactive intestinal peptide (VIP) and PHI on isolated brain arteries. *Brain Res.*, **322**, 9–16.

SZECOWKA, J., LINS, P.E., TATEMOTO, K. & EFENDIC, S. (1983). Effects of porcine intestinal heptacosapeptide and vasoactive intestinal polypeptide on insulin and glucagon secretion in rats. *Endocrinology*, **112**, 1469–1473.

TATEMOTO, K. & MUTT, V. (1981). Isolation and characterization of the intestinal peptide porcine PHI (PHI-27), a new member of the glucagon-secretin family. *Proc. Natl. Acad. Sci. U.S.A.*, **78**, 6603–6607.

VANE, J.R. (1957). A sensitive method for the assay of 5-hydroxytryptamine. *Br. J. Pharmacol.*, **12**, 344–349.

YANAIHARA, N., NOKIHARA, K. & YANAIHARA, C. (1983). Immunocytochemical demonstration of PHI and its co-existence with VIP in intestinal nerves of the rat and pig. *Arch. Histol. Jpn.*, **46**, 575–581.

YANAIHARA, N., YANAIHARA, C., NOKIHARA, K., IGUCHI, K., FUKATA, S., TANAKA, M., YAMAMOTO, Y. & MOCHIZUKI, T. (1984). Immunochemical study on PHI/PHM with use of synthetic peptides. *Peptides*, **5**, 247–254.

YASUI, A., NARUSE, S., YANAIHARA, C., OZAKI, T., HOSHINO, M., MOCHIZUKI, T., DANIEL, E.E. & YANAIHARA, N. (1987). Co-release of PHI and VIP by vagal stimulation in the dog. *Am. J. Physiol.*, **253**, G13–G19.

YIANGOU, Y., CHRISTOFIDES, N.D., BLANK, M.A., YANAIHARA, N., TATEMOTO, K., BISHOP, A.E., POLAK, J.M. & BLOOM, S.R. (1985). Molecular forms of peptide histidine isoleucine-like immunoreactivity in the gastrointestinal tract. Nonequimolar levels of peptide histidine isoleucine and vasoactive intestinal peptide in the stomach explained by the presence of a big peptide histidine isoleucine-like molecule. *Gastroenterology*, **89**, 516–524.

YIANGOU, Y., REQUEJO, F., POLAK, J.M. & BLOOM, S.R. (1986). Characterization of a novel prepro VIP derived peptide. *Biochem. Biophys. Res. Commun.*, **139**, 1142–1149.

YIANGOU, Y., DI MARZO, V., SPOKES, R.A., PANICO, M., MORRIS, H.R. & BLOOM, S.R. (1987). Isolation, characterization and pharmacological actions of peptide histidine valine 42, a novel prepro-vasoactive intestinal peptide-derived peptide. *J. Biol. Chem.*, **262**, 14010–14013.

(Received January 4, 1994
Revised June 6, 1994
Accepted June 8, 1994)

Br. J. Pharmacol. (1994), **113**, 550–554 © Macmillan Press Ltd, 1994

Cooling effects on nitric oxide production by rabbit ear and femoral arteries during cholinergic stimulation

N. Fernández, L. Monge, A.L. García-Villalón, J.L. García, B. Gómez & [1]G. Diéguez

Departamento de Fisiología, Facultad de Medicina, Universidad Autónoma, Arzobispo Morcillo 1, 28029 Madrid, Spain

1 Ear (cutaneous) and femoral (deep) arteries from rabbit were perfused at 37°C and 24°C (cooling) and the production of nitrite, as an index of nitric oxide production, was measured under basal conditions and cholinergic stimulation.

2 In both types of arteries under control conditions, the basal production of nitrite was similar at 24°C and 37°C. Compared with the control conditions, the basal production of nitrite was significantly lower in ear and femoral arteries without endothelium or treated with N^G-nitro-L-arginine methyl ester (L-NAME, 10^{-4} M) but it was similar in those treated with atropine (10^{-6} M).

3 At 37°C, methacholine (10^{-7}–10^{-5} M) increased the production of nitrite in ear and femoral arteries; this increase persisted during 30–60 min and was practically abolished by L-NAME (10^{-4} M), atropine (10^{-6} M), or removal of the endothelium. In ear arteries the total nitrite production to activation with methacholine was higher at 24°C than at 37°C due to this production persisted increased for a longer period (> 150 min), whereas in femoral arteries it was lower at 24°C than at 37°C.

4 It is suggested that: (a) the endothelium of rabbit ear and femoral arteries produce nitric oxide under basal conditions, which is increased by cholinergic stimulation, and (b) cooling potentiates endothelial nitric oxide production to cholinergic stimulation in cutaneous arteries, whereas it inhibits this production in deep arteries.

Keywords: Skin arteries; temperature; endothelium; nitrite; femoral arteries; cholinergic stimulation; NO

Introduction

The main function of the cutaneous circulation is body thermoregulatory function, and it appears that cooling affects reactivity of cutaneous vessels to vasoactive stimuli (Vanhoutte & Flavahan, 1986). Also it becomes apparent that nitric oxide is a relaxant factor that produces a basal vasodilator tone and is involved in the response of different vascular beds to vasoactive stimuli (Moncada *et al.*, 1991). Nitric oxide is synthesized in the endothelium from L-arginine and this synthesis can be stimulated by several types of stimuli, including cholinoceptor agonists, and is inhibited by L-arginine analogues (Moncada *et al.*, 1991).

In rabbit ear artery, considered as a cutaneous blood vessel (Patton & Wallace, 1978; Roberts & Zygmunt, 1984; Harker & Vanhoutte, 1988), we have recently observed that cooling increases the relaxation to cholinergic stimulation (Monge *et al.*, 1993) and reduces the contraction to endothelin-1 (Monge *et al.*, 1991) and to adrenergic activation (García-Villalón *et al.*, 1992) probably by endothelium-dependent mechanisms. In these three studies (Monge *et al.*, 1991; 1993; García-Villalón *et al.*, 1992) we suggested that these effects of cooling are specific for cutaneous vessels since they were not present in the femoral artery (a deep vessel), and that they might be related to an increased release of endothelial nitric oxide.

The present study was performed to determine the effects of cooling on nitric oxide production by cutaneous and non cutaneous arteries measuring the production of nitrite in rabbit central ear and femoral arteries at 37°C and 24°C (cooling) under basal conditions and after cholinergic stimulation. Currently, there is not a completely satisfactory technique to measure the production of nitric oxide by vessels, mainly due to the very short life of this radical. Nitric oxide is quickly oxidized to form nitrite (Marletta *et al.*, 1988) and determination of nitrite production has been used as an indirect measurement of nitric oxide production (Ignarro *et al.*, 1990; Bereta *et al.*, 1992).

[1] Author for correspondence.

Methods

Forty-eight New Zealand White rabbits either sex, weighing 2–2.5 kg, were killed by i.v. injection of sodium pentobarbitone (Sigma, 100 mg kg^{-1}). The two central ear and the two femoral arteries were dissected free and each artery was cut to a length of 6 cm (ear arteries) or 4 cm (femoral arteries). The two ear and the two femoral arteries were then cannulated with a polyethylene tubing and each pair of arteries was placed inside a small chamber and perfused in series with Krebs-Henseleit solution (composition mM: NaCl 115, KCl 4.6, KH_2PO_4 1.2, $MgSO_4$ 1.2 $CaCl_2$ 2.5, $NaHCO_3$ 25, glucose 11.1 equilibrated with 95% oxygen and 5% CO_2 to give a pH of 7.3–7.4). The total volume of the perfusion system and perfusion chamber was 0.2 ml. The perfusion was carried out with a peristaltic pump (Minipuls 3, Gilson Medical), and the chamber containing each pair of arteries was placed inside an organ bath at 37°C or 24°C (cooling).

First, the arteries were washed with the Krebs-Henseleit solution during 15 min at a rate of 0.5 ml min^{-1} and then they were continuously perfused at a rate of 2 ml h^{-1}. After an equilibration period of 30 min, 1 ml-samples of the perfusate were collected every 30 min in separate assay tubes kept on ice. Three samples were collected under basal conditions and another five samples after adding methacholine (10^{-7}–10^{-5} M) to the perfusion solution; the first sample after methacholine was taken 30 min after adding this drug. The effects of methacholine (10^{-7}–10^{-5} M) on nitrite production were determined in intact ear and femoral arteries at 37°C and 24°C. Also, the effects of methacholine (10^{-5} M) were determined at 37°C in ear and femoral arteries without endothelium, or treated with the inhibitor of nitric oxide synthase N^G-nitro-L-arginine methyl ester (L-NAME, 10^{-4} M) (Moore *et al.*, 1990; Rees *et al.*, 1990) or with atropine (10^{-6} M). Endothelium removal was accomplished by rubbing the vessel lumen with a roughened steel rod. L-NAME or atropine were added to the medium at the beginning of perfusion, and maintained throughout the experiment. To test if basal nitrite release changed throughout the experimental period, three preparations at 37°C and 24°C were

used to measure nitrite production during 4 h in intact, non-treated ear and femoral arteries.

Nitrite content of each sample was assayed in duplicate by the Griess reaction (Rider & Melon, 1946). Briefly, two 0.45 ml-aliquots were taken from the perfusate sample and each of them was incubated with 50 µl of Griess reagent at room temperature for 15 min (final concentration: 0.5% sulphanilamide/0.05% naphthylenediamine dihydrochloride (Merck) in 2% H_3PO_4). The peak absorbance at 540 nm was measured with a Schimadzu u.v.-160 spectrophotometer using a reference cuvette containing Griess reagent and identical Krebs-Henseleit solution to that used for the arterial perfusion. Nitrite concentration was determined with dilutions of sodium nitrite in Krebs-Henseleit solution. Background nitrite levels were determined in Krebs-Henseleit solution passing through a polyethylene tube exposed to identical experimental conditions except contact with arteries, and subtracted from the values determined in the experimental preparation.

To determine whether our experimental procedure alters the functional capability of the arteries, we performed a few experiments where we measured the level of oxygenation in the perfusate during 4 h of perfusion and recorded the *in vitro* reactivity of arteries after this perfusion. After ear and femoral arteries were mounted in the perfusion system we collected samples of the perfusate after passing through the arteries every 30 min during 4 h and measured gases content and pH by standard electrometric methods (Radiometer ABL 300, Copenhagen, Denmark). This was made in four preparations of ear and femoral arteries at 37°C (two preparations under control and two preparations treated with 10^{-6} M methacholine), and in another two preparations of ear and femoral arteries at 24°C. After this test, these same arteries were removed from the perfusion system, cut in segments 2 mm long and mounted in a set up for isometric tension recording at 37°C as described elsewhere (Monge *et al.*, 1993). In this preparation, the contraction of the arteries under basal conditions to potassium choride (50 mM), and the relaxation to methacholine (10^{-7}–10^{-5} M) and to sodium nitroprusside (10^{-6}–10^{-4} M) after precontraction with endothelin-1 (10^{-9}–10^{-8} M) were recorded.

Data analysis

The production of nitrite by each pair of arteries (two ear and two femoral arteries) obtained in each sample was expressed in pmol 30 min^{-1}. The effects of methacholine on nitrite production under the different conditions were evaluated as the peak increment (maximal level obtained after stimulation over the basal production) and as the total increment (the total amount of nitrite over the basal production obtained in the five samples recorded after stimulation). The basal production was considered as the average of the nitrite content in the three samples obtained before applying methacholine. To compare the effects of methacholine in arteries at 37°C and 24°C, and in arteries with and without endothelium or treated with L-NAME or atropine at 37°C, an analysis of variance followed by the Dunnet's test was applied to the data. In each case, $P<0.05$ was considered statistically significant.

Drugs used were: methacholine chloride, N^G-nitro-L-arginine methyl ester hydrochloride (L-NAME) and atropine sulphate, all from Sigma. All drugs were dissolved in isotonic saline (NaCl 0.9%) with ascorbic acid 1% M to prevent oxidation of the drugs.

Results

At 37°C, the amount of nitrite released under basal conditions (three samples during 90 min) averaged 46 ± 2 pmol 30 min^{-1} (ear arteries, $n = 16$) and 52 ± 2 pmol 30 min^{-1} (femoral arteries, $n = 16$). In three control preparations of ear and femoral arteries the spontaneous release of nitrite diminished slowly throughout a period of 4 h (these results are not shown, but the time course of this production was

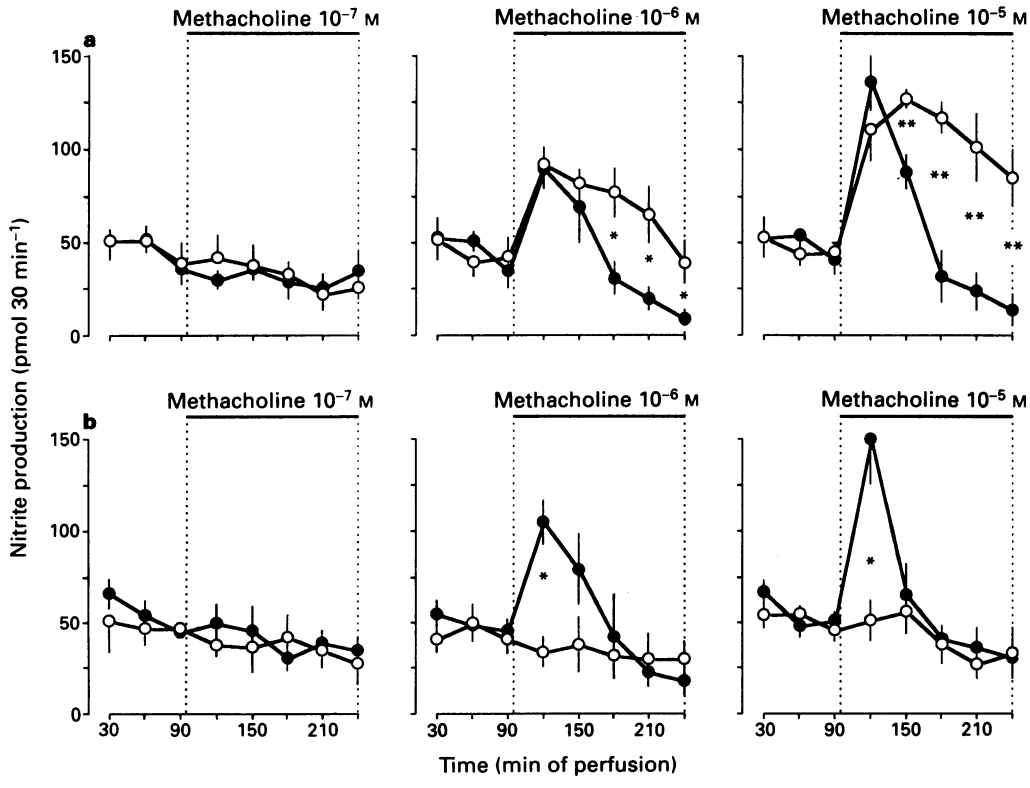


Figure 1 Production of nitrite by rabbit central ear (a) and femoral (b) arteries before and during stimulation with methacholine (10^{-7}–10^{-5} M) at 37°C (●) and at 24°C (○). Values are means ± s.e. Statistically significant difference between 37°C and 24°C; *$P<0.05$; **$P<0.01$.

similar to that exhibited by the arteries that were treated with 10^{-7} M methacholine, Figure 1).

Methacholine (10^{-7}–10^{-5} M), added to the perfusion solution, provoked a concentration-dependent, transient increase of nitrite production over the basal production that was comparable in ear and femoral arteries at 37°C; this increment for 10^{-6} and 10^{-5} M methacholine was evident during 30–60 min (Figure 1 and Table 1). In the presence of atropine (10^{-6} M) the basal production of nitrite in ear ($n = 3$) and femoral ($n = 3$) arteries was not significantly different from that obtained in non-treated arteries, but the increase in nitrite production induced by 10^{-5} M methacholine was reduced by 90% (Figure 2). In the presence of L-NAME (10^{-4} M) the levels of basal production of nitrite in both types of arteries were about 40% of those found in non-treated arteries, and the increase in nitrite production caused by 10^{-5} M methacholine in ear ($n = 5$) and femoral ($n = 5$) arteries was also reduced by about 90% (Figure 2). Both ear ($n = 3$) and femoral ($n = 3$) arteries without endothelium released an amount of nitrite that was not significantly different from background levels, both under basal conditions and after addition of 10^{-5} M methacholine.

At 24°C (cooling) the basal production of nitrite was comparable to that at 37°C, both in ear (46 ± 2 vs 46 ± 2 pmol 30 min^{-1}, $n = 12$, $P > 0.05$) and femoral (48 ± 3 vs 52 ± 2 pmol 30 min^{-1}, $n = 12$, $P > 0.05$) arteries. In ear arteries during cooling, methacholine (10^{-7}–10^{-5} M) also increased nitrite production over the basal release in a concentration-dependent way, but the total increment was consistently higher than at 37°C (Figure 1 and Table 1). Although in these arteries the peak increment of nitrite production at 24°C was similar to that at 37°C, the increment was more prolonged (> 150 min) (Figure 1) so that the total increment of nitrite production induced by methacholine (10^{-6}–10^{-5} M) was higher at 24°C. On the contrary, in femoral arteries at 24°C, methacholine (10^{-7}–10^{-5} M) did not modify significantly the release of nitrite with regard to basal production, so that the effect of this drug in these particular arteries was lower at 24°C than at 37°C (Figure 1 and Table 1).

In our experimental conditions the values for P_{O_2}, P_{CO_2} and pH measured in the perfusate collected after passing through ear and femoral arteries were similar at 37° and 24°C, both in the arteries treated or non treated with 10^{-6} M methacholine. These values for P_{O_2}, P_{CO_2} and pH in ear arteries averaged 188 ± 7 mmHg, 38 ± 4 mmHg and 7.32 ± 0.010 mmHg, respectively, and in femoral arteries they averaged 199 ± 7 mmHg, 39 ± 4 and 7.30 ± 0.009, respectively, throughout the perfusion period. After this test, the arteries were removed from the perfusion system and cut in segments 2 mm in length for isometric tension recording at 37°C. In these arteries (eight segments) under basal conditions, potassium chloride (50 mM) produced contraction of ear (1.86 ± 0.16 g) and of femoral arteries (3.43 ± 0.43 g). After contraction with endothelin-1 the arteries (eight segments) exhibited concentration-dependent relaxation to methacholine (10^{-7}–10^{-5} M, the maximal relaxation with regard to the active tone was 71 ± 5% for ear arteries and 64 ± 7% for femoral arteries) and to sodium nitroprusside (10^{-6}–10^{-4} M, the maximal relaxation was 74 ± 4% for ear arteries and 73 ± 6% for femoral arteries). No major differences were observed between the contractcion or relaxation responses of ear and femoral arteries that had been perfused at 37°C or 24°C, or that had been treated or not treated with 10^{-6} M methacholine during perfusion.

Table 1 Total increases in nitrite production (pmol) in rabbit ear and femoral arteries during 150 min of stimulation with methacholine at 37°C and 24°C (cooling)

	Ear artery		*Femoral artery*	
Methacholine (M)	*37°C*	*24°C*	*37°C*	*24°C*
10^{-7}	5 ± 3 (6)	2 ± 2 (3)	13 ± 6 (6)	3 ± 4 (3)
10^{-6}	72 ± 14 (5)	147 ± 20* (4)	79 ± 16 (5)	21 ± 12* (4)
10^{-5}	130 ± 21 (5)	305 ± 27** (5)	118 ± 19 (5)	25 ± 19** (5)

In parentheses, number of experiments. Values are means ± s.e. Statistically significant difference between 37°C and 24°C; *$P < 0.05$; **$P < 0.01$.

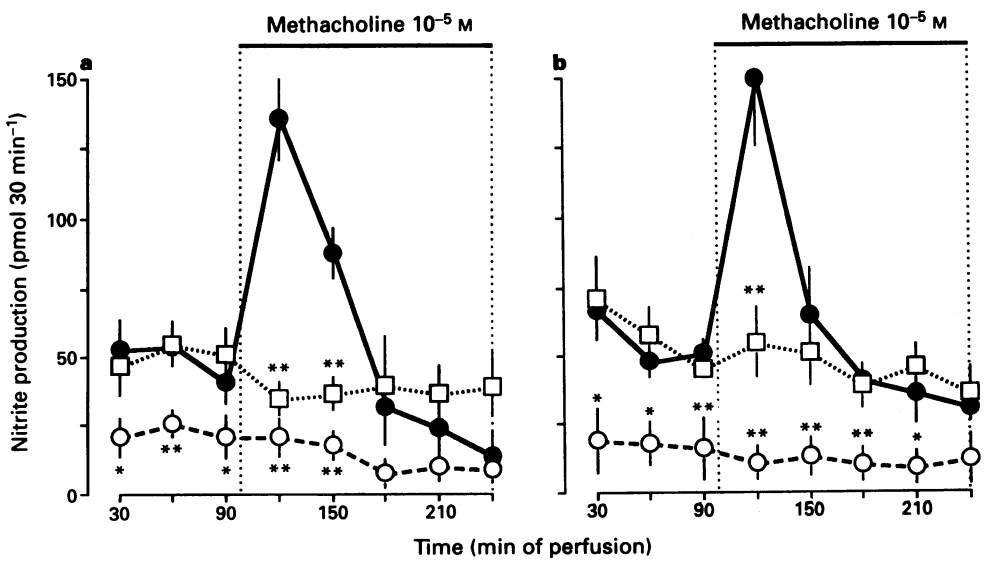


Figure 2 Production of nitrite by rabbit central ear (a) and femoral (b) arteries before and during stimulation with 10^{-5} M methacholine at 37°C in control conditions (●) and in the presence of 10^{-4} M N^G-nitro-L-arginine methyl ester (○) or 10^{-6} M atropine(□). Values are means ± s.e. Statistically significant difference between the control and treatment with N^G-nitro-L-arginine methyl ester or atropine; *$P < 0.05$; **$P < 0.01$.

Discussion

In this study we have evaluated the effects of cooling on the production of nitric oxide in cutaneous and non-cutaneous arteries under basal conditions and when they were stimulated with methacholine. Nitric oxide production was evaluated indirectly by measuring nitrite content in the perfusate of rabbit ear (cutaneous) and femoral (non cutaneous) arteries exposed to 37°C and moderate cooling (24°C). Nitrite production seems to increase when the release of nitric oxide is augmented in perfused arteries (Ignarro *et al.*, 1987), cultured endothelial cells (Bereta *et al.*, 1992) and whole organs (Ignarro *et al.*, 1990). Also, nitrite production can be blocked by inhibitors of the enzyme, nitric oxide synthase (Ignarro *et al.*, 1991; Schultz *et al.*, 1991), suggesting that the nitrite measured in these preparations is mostly produced from nitric oxide metabolism, and therefore measurements of nitrite production can be taken as an index of the nitric oxide release from vessels. In the present study we measured the levels of Po_2, Pco_2 and pH in the perfusate during the period of arterial perfusion, and after this period we also evaluated the reactivity of the perfused arteries. The results of these experiments suggest that the experimental procedure used in our study provides a good oxygenation of the arteries and mostly preserves the functional capability of the arteries to contract and to relax. The contraction to potassium chloride as well as the relaxation to cholinergic stimulation and to sodium nitroprusside of the arteries after perfusion was comparable to that determined for the same type of arteries in a previous study from our laboratory (Monge *et al.*, 1993).

Both ear and femoral arteries under basal conditions produced nitrite, and this production was lower in the arteries without endothelium or treated with L-NAME. The arteries treated with atropine, however, exhibited a basal nitrite production similar to that found in non treated arteries. These results suggest that the endothelium of these arteries releases nitric oxide, which might be independent of muscarinic receptors under basal conditions. The basal release of nitrite diminished slowly throughout the experimental period and this was similar in ear and femoral arteries at both 37°C and 24°C. The reason for this feature is unclear. A possible deterioration of the preparations during the perfusion could be reasonably excluded as the experimental conditions do not seem to alter the functional capability of the arteries as indicated above.

The cholinoceptor agonist, methacholine, increased the production of nitrite in ear and femoral arteries over the basal release in a concentration-dependent way, and it was blocked by L-NAME, suggesting that the increase in nitrite production by methacholine is mostly due to an increment in the production of nitric oxide. In addition, the results with methacholine in arteries without endothelium or treated with atropine suggest that the increase in nitric oxide production induced by this drug takes place in the endothelium and is mostly caused by activation of endothelial muscarinic receptors. This feature agrees with the idea generally accepted that cholinoceptor stimulation increases the release of nitric oxide by the endothelium (Moncada *et al.*, 1991). At 37°C, in ear and femoral arteries stimulated with methacholine the production of nitrite reached a maximal peak followed by a decrease, returning to basal levels 90 min after stimulation, in spite of the fact that arteries were still exposed to methacholine.

Although it is accepted that cooling specifically alters the response of cutaneous arteries to some types of vasoactive stimuli (Vanhoutte & Flavahan, 1986), very little is known about the role played by the endothelium in vascular reactivity at low temperature (Karaki & Nagase, 1987; Bodelsson *et al.*, 1989). This could be of particular interest in cutaneous vessels as they have a thermoregulatory function. We have recently reported that cooling reduces the contraction to endothelin-1 (Monge *et al.*, 1991) or adrenergic activation (García-Villalón *et al.*, 1992), and at the same time it increases the relaxation to cholinergic stimulation (Monge *et al.*, 1993) in ear (cutaneous) but not in femoral (deep) arteries from rabbits. In these studies we suggested that these effects of cooling on the contraction and relaxation are specific for cutaneous vessels and hypothesized that they could be related to an increased release of endothelial nitric oxide in the stimulated arteries during cooling (Monge *et al.*, 1991; 1993; García-Villalón *et al.*, 1992) The results found in the present study are consistent with the hypothesis previously proposed (Monge *et al.*, 1993) in the sense that in ear arteries, but not in femoral arteries the release of endothelial nitric oxide to cholinoceptor stimulation is potentiated during cooling. In ear arteries methacholine produced a peak increment in nitrite production that was similar at 37°C and 24°C, but the increment in this production consistently persisted for a longer period at 24°C than at 37°C. Therefore, although the peak increment in nitrite production was comparable at both temperatures, the total amount of nitrite, and consequently that of nitric oxide, released by ear arteries during activation with methacholine was higher at 24°C than at 37°C. In femoral arteries methacholine did not mostly affect the basal release of nitrite during cooling, thus the effects of cholinoceptor stimulation on release of nitric oxide in these particular arteries is lower at 24°C than at 37°C, which clearly contrasts with that found in ear arteries. The facilitated production of nitrite (and consequently of nitric oxide) in cutaneous arteries to methacholine at 24°C could be related to a more prolonged effectiveness of cholinoceptor stimulation and/or to an increased function of metabolic pathway for nitric oxide synthesis in these arteries during cooling. Cooling might augment the sensitivity of endothelial cholinoceptors to cholinoceptor agonists or the postreceptorial mechanisms involved in nitric oxide synthesis in cutaneous arteries. Although these results are consistent with the increased cholinoceptor relaxation of ear arteries observed during cooling (Monge *et al.*, 1993), the comparison of the present results with those in the arterial relaxant response must be cautious, because the effects of cooling on the nitrite production by ear arteries when they were activated with methacholine required a relatively long period to be observed, whereas the time-course of the vascular relaxant response to cholinoceptor stimulation is much shorter. With regard to femoral arteries, our study shows that the production of nitrite in these arteries after cholinoceptor stimulation was reduced by cooling. This observation apparently does not correlate well with previous experiments where we found that the *in vitro* relaxation of femoral arteries to cholinoceptor activation was not affected by cooling (Monge *et al.*, 1993). This apparent discrepancy might be related to the different methods used, and it is possible that although cooling can decrease the production of nitric oxide this reduction is not sufficient to decrease the relaxation of femoral arteries to cholinoceptor stimulation during cooling. It is apparent, however, that the effects of cooling on cutaneous (ear) and deep (femoral) arteries to produce nitric oxide after cholinoceptor stimulation are different. This difference might be related to a different behaviour of endothelial cholinoceptors and of the metabolic pathway for nitric oxide synthesis in cutaneous and deep arteries during cooling.

In conclusion, if the production of nitrite is a reliable index of nitric oxide production, the present results indicate that cooling potentiates the production of nitric oxide from the endothelium of cutaneous arteries, but not of deep arteries, when they are stimulated. These effects of cooling would explain, at least in part, the reduced contraction to endothelin-1 (Monge *et al.*, 1991) and adrenergic activation (García-Villalón *et al.*, 1992) and the increased relaxation to cholinoceptor stimulation (Monge *et al.*, 1993) of cutaneous arteries during cooling. Moreover, other endothelial factors,

in addition to nitric oxide, such as prostanoids of hyperpolarizing factor cannot be excluded as co-mediators in the effects of cooling on the functional response of cutaneous vessels.

The authors are grateful to Mrs M.E. Martínez and H. Fernández-Lomana for technical assistance. This work was supported, in part, by FIS (92/0289; 93/0338), CICYT (93/0085) and CAM (109/91).

References

BERETA, M., BERETA, J., COHEN, S. & COHEN, M.C. (1992). Low density lipoprotein accumulation of nitrites in murine brain endothelial cell cultures. *Biochem. Biophys. Res. Commun.*, **186**, 315–320.

BODELSSON, M., ARNEKLO-NOBIN, B. & TORNEBRANDT, K. (1989). Cooling augments contractile response to 5-hydroxytryptamine via an endothelium-dependent mechanism. *Blood Vessels*, **26**, 347–359.

GARCÍA-VILLALÓN, A.L., MONGE, L., MONTOYA, J.J., GARCÍA, J.L., FERNÁNDEZ, N., GÓMEZ, B. & DIÉGUEZ, G. (1992). Cooling and adrenergic response of rabbit ear and femoral artery: role of the endothelium. *Br. J. Pharmacol.*, **106**, 727–732.

HARKER, C.T. & VANHOUTTE, P.M. (1988). Cooling the central ear artery of the rabbit: myogenic and adrenergic responses. *J. Pharmacol. Exp. Ther.*, **245**, 89–93.

IGNARRO, L.J., BUGA, G.M., WOOD, K.S., BYRNS, R.E. & CHAUDHURI, G. (1987). Endothelium-derived relaxing factor produced and released from artery and vein is nitric oxide. *Proc. Natl. Acad. Sci. U.S.A.*, **84**, 9265–9269.

IGNARRO, L.J., BUSH, P.A., BUGA, G.M, WOOD, K.S., FUKUTO, J.M. & RAJFER, J. (1990). Nitric oxide and cyclic GMP formation upon electrical field stimulation cause relaxation of corpus cavernosum smooth muscle. *Biochem. Biophys. Res. Commun.*, **170**, 843–850.

KARAKI, H. & NAGASE, H. (1987). Low temperature augments the endothelium-dependent relaxation in isolated rat aorta. *Eur. J. Pharmacol.*, **142**, 129–132.

MARLETTA, M.A., YOON, P.S., IYENGAR, R., LEAF, C.D. & WISHNOK, J.S. (1988). Macrophage oxidation of L-arginine to nitrite and nitrate: nitric oxide is an intermediate. *Biochemistry*, **27**, 8706–8711.

MONCADA, S., PALMER, R.M. & HIGGS, E.A. (1991). Nitric oxide: physiology, pathophysiology, and pharmacology. *Pharmacol. Rev.*, **42**, 109–142.

MONGE, L., GARCÍA-VILLALÓN, A.L., MONTOYA, J.J., GARCÍA, J.L., GÓMEZ, B. & DIÉGUEZ, G. (1991). Response of rabbit ear artery to endothelin-1 during cooling. *Br. J. Pharmacol.*, **104**, 609–612.

MONGE, L., GARCÍA-VILLALÓN, A.L., MONTOYA, J.J., GARCÍA, J.L., FERNÁNDEZ, N., GÓMEZ, B. & DIÉGUEZ, G. (1993). Role of the endothelium in the response to cholinoceptor stimulation of rabbit ear and femoral arteries during cooling. *Br. J. Pharmacol.*, **109**, 61–67.

MOORE, P.K., AL-SWAYEH, O.A., CHONG, N.W.S., EVANS, R.A. & GIBSON, A. (1990). L-N^G-nitro-arginine (L-NOARG), a novel, L-arginine-reversible inhibitor of endothelium-dependent vasodilatation in vitro. *Br. J. Pharmacol.*, **99**, 408–412.

PATTON, J.N. & WALLACE, W.F.M. (1978). Responses of isolated rabbit ear arteries to intra- and extraluminal L- and D-noradrenaline in the temperature range 37–3°C. *Ir. J. Med. Sci.*, **147**, 313–317.

REES, D.D., PALMER, R.M.J., SCHULZ, R., HODSON, H.F. & MONCADA, S. (1990). Characterization of three inhibitors of endothelial nitric oxide synthase *in vitro* and *in vivo*. *Br. J. Pharmacol.*, **101**, 146–152.

RIDER, B.F. & MELON, M.G. (1946). Colorimetric determination of nitrites. *Ind. Eng. Chem.*, **18**, 96–99.

ROBERTS, M.F. & ZYGMUNT, A.C. (1984). Reflex and local thermal control of rabbit ear blood flow. *Am. J. Physiol.*, **246**, R979–R984.

SCHULTZ, P.J., TAYEH, M.A., MARLETTA, M.A. & RAIJ, L. (1991). Synthesis and action of nitric oxide in rat glomerular mesangial cells. *Am. J. Physiol.*, **261**, F600–F606.

VANHOUTTE, P.M. & FLAVAHAN, N.A. (1986). Effects of temperature on alpha-adrenoceptor in limb veins: role of receptor reserve. *Fed. Proc.*, **45**, 2347–2354.

(Received April 18, 1994
Revised June 2, 1994
Accepted June 16, 1994)

Br. J. Pharmacol. (1994), **113**, 555–563 © Macmillan Press Ltd, 1994

Trichloroethanol potentiation of γ-aminobutyric acid-activated chloride current in mouse hippocampal neurones

[1]Robert W. Peoples & Forrest F. Weight

Laboratory of Molecular and Cellular Neurobiology, National Institute on Alcohol Abuse and Alcoholism, National Institutes of Health, Bethesda, MD 20892, U.S.A.

1 The action of 2,2,2-trichloroethanol on γ-aminobutyric acid (GABA)-activated Cl^- current was studied in mouse hippocampal neurones in tissue culture by use of whole-cell patch-clamp recording.

2 Trichloroethanol increased the amplitude of currents activated by 1 μM GABA or 0.1 μM muscimol. Trichloroethanol, 1–25 mM, potentiated current activated by 1 μM GABA in a concentration-dependent manner with an EC_{50} of 3.0 ± 1.4 mM and a maximal response (E_{max}) of 576 ± 72% of control.

3 Trichloroethanol potentiated currents activated by GABA concentrations $< 10\,\mu M$, but did not increase the amplitude of currents activated by concentrations of GABA $\geq 10\,\mu M$. Despite marked potentiation of currents activated by low concentrations of GABA, trichloroethanol did not significantly alter the EC_{50}, slope, or E_{max} of the GABA concentration-response curve.

4 Trichloroethanol, 5 mM, potentiated GABA-activated current in neurones in which ethanol, 10–500 mM, did not. The effect of trichloroethanol was not altered by the putative ethanol antagonist, Ro 15-4513. Trichloroethanol did not potentiate currents activated by pentobarbitone.

5 In the absence of exogenous GABA, trichloroethanol at concentrations ≥ 2.5 mM activated a current that appeared to be carried by Cl^- as its reversal potential changed with changes in the Cl^- gradient and as it was inhibited by the $GABA_A$ antagonists, bicuculline methiodide and picrotoxin.

6 Since trichloroethanol is thought to be the active metabolite of chloral hydrate and other chloral derivative anaesthetics, potentiation of the GABA-activated current in central nervous system neurones by trichloroethanol may contribute to the sedative/hypnotic effects of these agents.

Keywords: $GABA_A$ receptor; trichloroethanol; anaesthetic; hippocampal neurones; chloride current; membrane ion current; alcohol; receptor modulation; neurotransmitter receptor

Introduction

A number of sedative/hypnotic agents have been found to enhance the action of γ-aminobutyric acid (GABA) at the $GABA_A$ receptor subtype in the CNS. Despite great structural diversity, benzodiazepines (Haefely *et al.*, 1975; Choi *et al.*, 1977; MacDonald & Barker, 1978), barbiturates (Nicoll *et al.*, 1975; Ransom & Barker, 1975), anaesthetic steroids (Harrison & Simmonds, 1984; Majewska *et al.*, 1986), ethanol (Nestoros, 1980; Suzdak *et al.*, 1986b; Mehta & Ticku, 1988), and inhalational anaesthetics (Gage & Robertson, 1985; Nakahiro *et al.*, 1989; Jones *et al.*, 1992) have all been reported to enhance $GABA_A$ receptor-mediated cellular responses. As GABA is believed to be the predominant inhibitory neurotransmitter in the brain, enhancement of central GABAergic transmission may mediate or contribute to the CNS depression produced by these agents.

Trichloroethanol is the principal active metabolite of chloral derivative sedative/hypnotic agents, such as chloral hydrate, and is believed to be responsible for the pharmacological effects of these agents (Breimer, 1977; Rall, 1990). Although chloral derivatives have been widely used both clinically and experimentally, the cellular mechanism of action of chloral derivatives or their active metabolite, trichloroethanol, has not been established. Previous studies in the periphery have found that α-chloralose can activate a Cl^- current in frog dorsal root ganglion neurones (Ishizuka *et al.*, 1989), and that trichloroethanol decreases the amplitude and prolongs the duration of acetylcholine-mediated currents at the neuromuscular junction (Pennefather & Quastel, 1980; Sterz *et al.*, 1981). Recently, trichloroethanol has been reported to potentiate $5\text{-}HT_3$ receptor-activated current in nodose ganglion neurones (Lovinger & Zhou, 1993), to increase the amplitude and duration of $GABA_A$-receptor-mediated currents evoked in response to pressure application of GABA in hippocampal neurones in culture and to prolong inhibitory postsynaptic currents between hippocampal neurones in culture or in brain slices (Lovinger *et al.*, 1993). The present study was performed in order to characterize the effect of trichloroethanol on the $GABA_A$ receptor-ion channel complex. Some of the results presented here have been reported previously in preliminary form (Peoples & Weight, 1991).

[1] Author for correspondence at: Laboratory of Molecular and Cellular Neurobiology, National Institute on Alcohol Abuse and Alcoholism, National Institutes of Health, 12501 Washington Ave., Rockville, MD 20852, U.S.A.

Methods

Cultures of hippocampal neurones grown on glial feeder layers were prepared from 15–17 day foetal mice essentially as described by Forsythe & Westbrook (1988). Neurones were maintained in medium containing 95% MEM, 5% heat-inactivated equine serum, and a serum supplement (final concentrations in $\mu g\,ml^{-1}$: corticosterone 4, insulin 10, progesterone 1, putrescine 320, selenium 1, transferrin 200 and triiodothyronine 2); this medium was given half-changes weekly. Neurones were cultured for 1–4 weeks prior to use in experiments.

Patch-clamp recording of whole-cell currents was performed in hippocampal neurones at 25°C using a List EPC-7 or an Axopatch-1D patch-clamp amplifier. Electrodes with tip resistances of 2–5 MΩ were used; series resistances of 3–10 MΩ were compensated by 40–80%. Neurones were superfused at 1–2 $ml\,min^{-1}$ in an extracellular medium containing (in mM): NaCl 150, KCl 5, $CaCl_2$ 2.5, $MgCl_2$ 2, HEPES 10, glucose 10, tetrodotoxin 0.0002–0.001, pH was adjusted to 7.4 with NaOH and osmolality to 340

mosmol kg^{-1} with sucrose. Unless stated otherwise, the patch-pipette contained (in mM): CsCl 140, $MgCl_2$ 2, Mg_4ATP 2, BAPTA 10, HEPES 10, pH was adjusted to 7.4 with CsOH and osmolality to 310 mosmol kg^{-1} with sucrose. Drug solutions were prepared in extracellular medium and in most experiments were applied to neurones by gravity flow using a linear multi-barrel pipette array (diameter of each pipette $\sim$200 μm) placed within 100 μm of the cell body. Cells were constantly bathed in extracellular medium flowing from one barrel (flow rate $\sim$3 μl s^{-1}), and drug solutions were applied by opening a valve connected to another barrel and moving the barrel array so that the desired solution superfused the cell. In some experiments, drug solutions were applied by gravity flow from a single large-bore pipette (diameter $\sim$100 μm) placed within 100 μm of the cell body. Concentrations of agonists producing receptor desensitization (e.g., GABA concentrations $>$1 μM) were applied at intervals of 3–5 min to allow for full recovery from desensitization; low concentrations of agonists were applied at intervals of at least 90 s. Data were displayed on a digital oscilloscope (Nicolet 1090-IIIA) and recorded on a chart recorder (Gould 2400S); in most cases data were also filtered at 2 kHz, digitized at 1–5 kHz and stored on a microcomputer.

Statistical analysis of concentration-dependent data was performed using the nonlinear curve-fitting programme ALLFIT (DeLean *et al.*, 1978). Values reported from concentration-response analysis are those obtained by fitting the data to the logistic equation

$$y = ((E_{max}-E_{min})/(1 + (x/EC_{50})^{-n})) + E_{min},$$

where x and y are concentration and response, respectively, E_{min} is the minimal response, E_{max} is the maximal response, EC_{50} is the half-maximal concentration, and n is the slope factor. Time constants of decay were calculated by fitting data to a single exponential function using the programme NFIT. Statistical comparisons were performed using Student's *t* tests or analyses of variance (in some cases followed by Student's Newman-Keuls ranges tests), as noted. Average values are reported as the mean ± s.e.

Results

Trichloroethanol potentiation of GABA- and muscimol-activated current

Figure 1 illustrates potentiation of currents activated by GABA or muscimol by trichloroethanol. In a typical neurone, 1 μM GABA activated an inward current that was potentiated over fourfold by 2.5 mM trichloroethanol (Figure 1a). Application of 2.5 mM trichloroethanol in the absence of GABA activated only a very small inward current (20 pA).

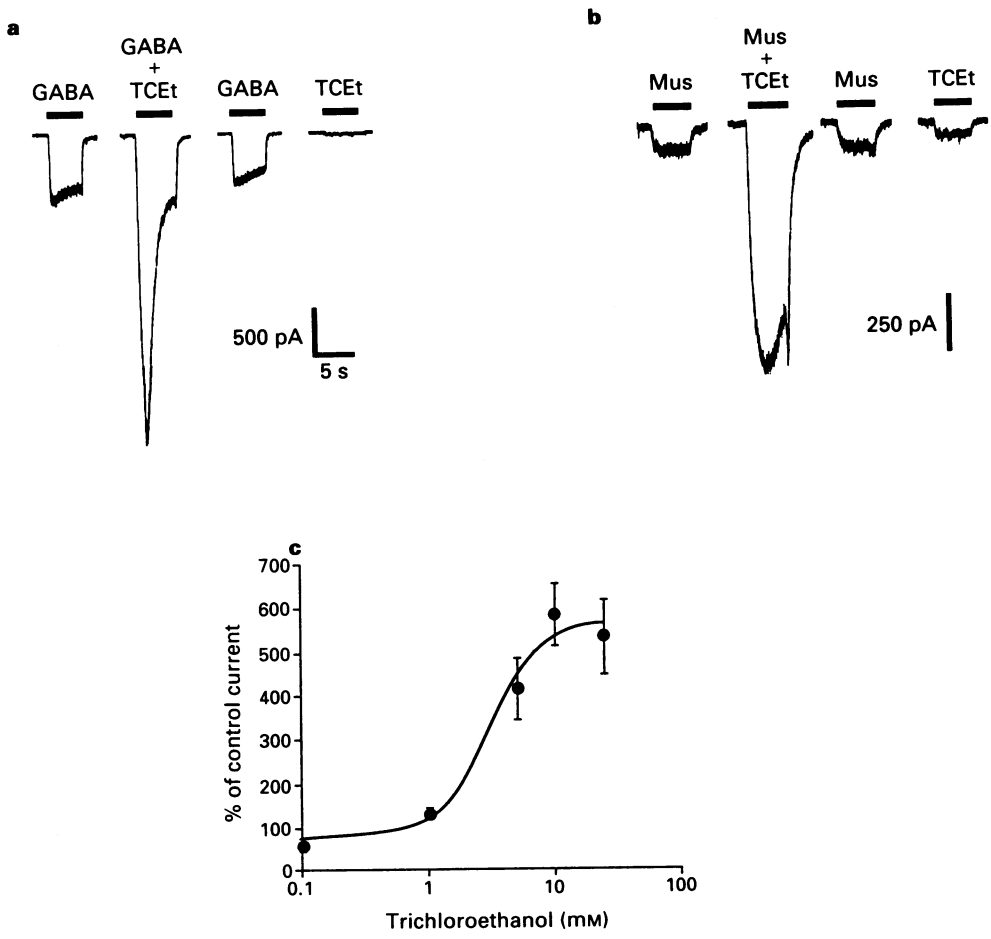


Figure 1 Trichloroethanol potentiation of current activated by GABA agonists. (a) Records of current activated by 1 μM GABA and its potentiation by 2.5 mM trichloroethanol (TCEt). Record at far right shows effect of 2.5 mM trichloroethanol alone (without added GABA). (b) Records of current activated by 0.1 μM muscimol (Mus) and its potentiation by 5 mM trichloroethanol (TCEt). Record at far right shows effect of 5 mM trichloroethanol alone (without added muscimol). Records in (a) and (b) are from different hippocampal neurones. Membrane holding potential was − 50 mV. Solid bar above each record indicates time of agonist and/or drug application, as labelled. (c) Concentration-response curve for potentiation by trichloroethanol of current activated by 1 μM GABA. Each data point is mean ± s.e. of at least 6 neurones voltage-clamped at − 50 mV. The curve shown is the best fit of the data to the logistic equation described in the Methods; the EC_{50} for trichloroethanol was 3.0 ± 1.4 mM, the slope factor was 2.1, and the E_{max} was 576 ± 72% of control.

Trichloroethanol, 1–50 mM, increased the amplitude of currents activated by 0.1–2.5 μM GABA in all neurones tested ($n = 72$). Trichloroethanol also enhanced current activated by the $GABA_A$-selective agonist, muscimol (Figure 1b). In this neurone, 0.1 μM muscimol or 5 mM trichloroethanol, alone, activated small, nondesensitizing currents, whereas the same concentrations of muscimol and trichloroethanol in combination activated a current that was over six times greater than the sum of the individual currents. On average, 5 mM trichloroethanol increased the amplitude of current activated by 0.1 μM muscimol by 569 ± 149% (paired t test, $P < 0.05$; $n = 4$). The enhancement of GABA-activated current amplitude by trichloroethanol exhibited a clear concentration-dependence (Figure 1c). The EC_{50} for trichloroethanol enhancement of current activated by 1 μM GABA was 3.0 ± 1.4 mM, the slope factor was 2.1, and the maximal effect was 576 ± 72% of control.

Dependence of trichloroethanol potentiation on GABA concentration

Figure 2a shows records of currents activated by various concentrations of GABA and their modulation by trichloroethanol in a hippocampal neurone. In this neurone, 5 mM trichloroethanol increased the amplitude of currents activated by 0.25 μM or 2.5 μM GABA by 1150% and 61%, respectively. In contrast, 25 μM GABA activated a large, rapidly-desensitizing current in this neurone that was 86% of control in the presence of 5 mM trichloroethanol.

Figure 2b shows the concentration-response curves for GABA-activated ion current in the absence and presence of 5 mM trichloroethanol. GABA-activated current exhibited a clear concentration-dependence between 1 and 100 μM GABA. The average maximal current activated by GABA in these neurones was 2566 ± 133 pA, the EC_{50} for GABA was 15.4 ± 2.2 μM, and the slope factor was 1.4 ± 0.3. In the presence of trichloroethanol, the average maximal current was 2259 ± 164 pA, the EC_{50} for GABA was 12.2 ± 2.8 μM, and the slope factor was 1.0 ± 0.3; these values did not differ significantly from those of the control GABA concentration-response curve (analysis of variance, $P > 0.05$).

Figure 2c illustrates the dependence of trichloroethanol potentiation of GABA-activated current on GABA concentration. Trichloroethanol, 5 mM, augmented the currents activated by 0.1, 0.25, 1 and 2.5 μM GABA (580 ± 196, 639 ± 142, 514 ± 246, and 300 ± 72% of control, respec-

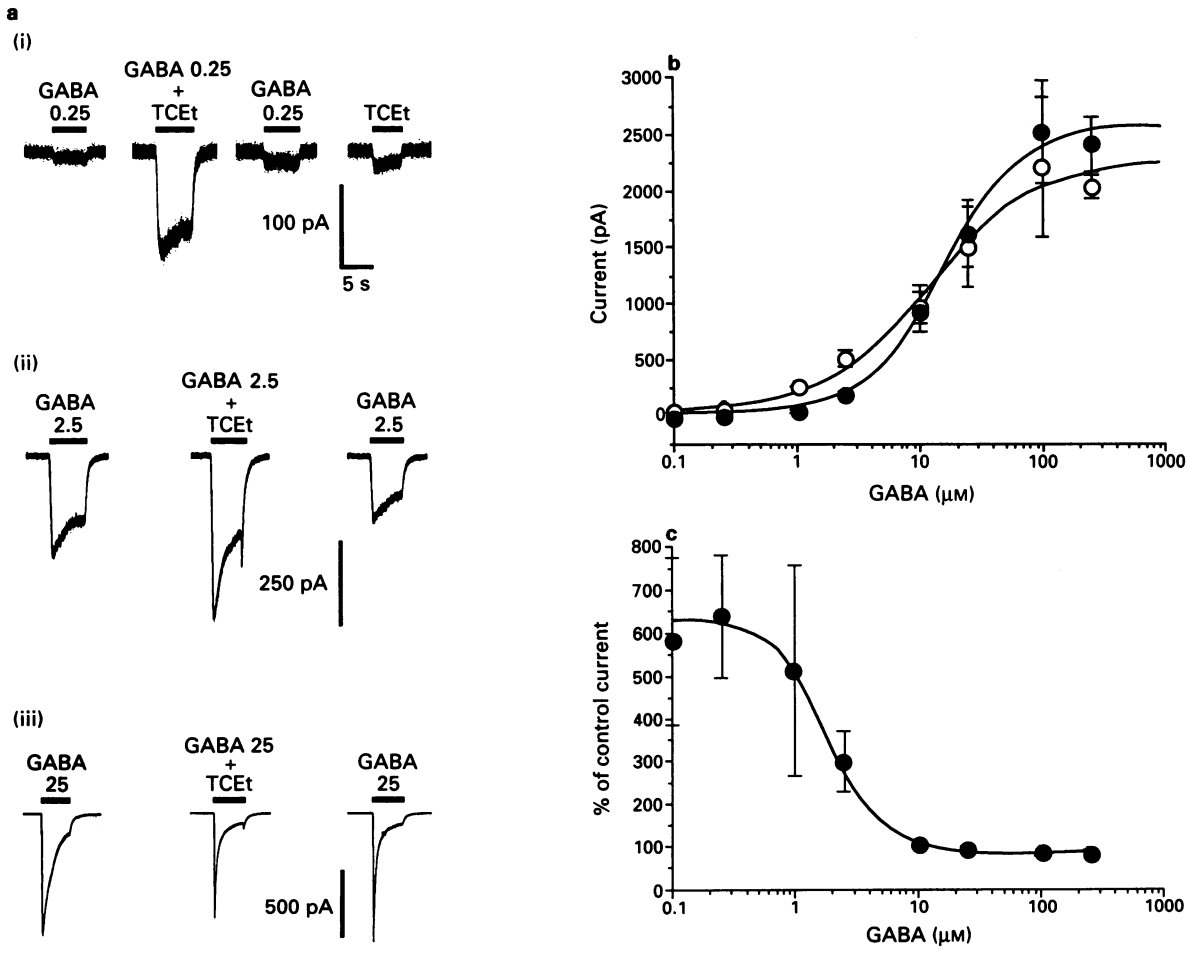


Figure 2 Dependence of trichloroethanol potentiation upon GABA concentration. (a) Records of current activated by 0.25 μM (i), 2.5 μM (ii), and 25 μM (iii) GABA in the absence and presence of 5 mM trichloroethanol (TCEt) in a hippocampal neurone. Record at far right in (i) shows effect of 5 mM trichloroethanol alone (without added GABA). Membrane holding potential was − 10 mV. Solid bar above each record indicates time of agonist and/or drug application, as labelled. (b) Concentration-response curves for GABA-activated current in the absence (●) and presence (○) of 5 mM trichloroethanol. Each data point is the mean ± s.e. of 4–6 neurones. Membrane holding potential was − 10 mV. The curves shown were fitted to the data using the logistic equation described in the Methods. The E_{max} of GABA was 2566 ± 133 pA, the EC_{50} was 15.4 ± 2.2 μM, and the slope factor was 1.4. In the presence of 5 mM trichloroethanol, the E_{max} of GABA was 2259 ± 164 pA, the EC_{50} was 12.2 ± 2.8 μM, and the slope factor was 1.0. These values in the presence of trichloroethanol did not differ significantly from those of the control GABA concentration-response curve (analysis of variance, $P > 0.05$). (c) Plot of potentiation of GABA-activated current by 5 mM trichloroethanol as a function of GABA concentration. Trichloroethanol significantly enhanced currents activated by 0.1, 0.25, 1 and 2.5 μM GABA (repeated measures analysis of variance, $P < 0.05$). The curve shown is the best fit of the data to the logistic equation given in the Methods. Data points are means ± s.e. of 4–6 neurones; error bars not visible are smaller than the size of the symbols.

tively; repeated measures analysis of variance, $P<0.05$), but did not affect the currents activated by 10, 25, 100 and 250 μM GABA (107 ± 10, 94 ± 6, 87 ± 6, 86 ± 6% of control, respectively; repeated measures analysis of variance, $P>0.05$). The lack of a potentiating effect of trichloroethanol on currents activated by GABA at concentrations of 10 μM or greater was also observed when a maximally effective concentration of trichloroethanol, 25 mM, was tested. Trichloroethanol, 25 mM, significantly reduced the amplitude of current activated by 10 μM GABA (2311 ± 366 vs 1344 ± 342 pA in the absence and the presence of trichloroethanol, respectively; paired t test, $P<0.05$; $n=4$) and 25 μM GABA (3518 ± 599 vs 1800 ± 670 pA in the absence and the presence of trichloroethanol, respectively; paired t test, $P<0.05$; $n=4$). In addition, trichloroethanol did not significantly alter the rate of decay of current activated by 10 μM GABA (time constants: 1335 ± 185 vs 1093 ± 225 ms in the absence and presence of 5 mM trichloroethanol, respectively; paired t test, $P>0.1$; $n=5$) and 25 μM GABA (time constants: 787 ± 185 vs 736 ± 70 ms in the absence and presence of 5 mM trichloroethanol, respectively; paired t test, $P>0.5$; $n=6$).

Comparison of ethanol and trichloroethanol effects on GABA-activated current

Ethanol has been reported to enhance responses mediated by $GABA_A$ receptors in the CNS (Nestoros, 1980; Suzdak *et al.*, 1986b; Mehta & Ticku, 1988), although there have also been reports that ethanol does not affect GABA responses in some preparations (Gage & Robertson, 1985; Barker *et al.*, 1987; Harrison *et al.*, 1987; White *et al.*, 1990). We compared the effects of ethanol and trichloroethanol on GABA-activated current in the same neurones. In order for the comparison to be valid, we chose to use an anaesthetic concentration of trichloroethanol (see Discussion) and concentrations of ethanol below, in, and above the anaesthetic range (60–100 mM; Little, 1991). Figure 3a shows records of ion current evoked by GABA in the absence and presence of trichloroethanol or ethanol in a hippocampal neurone. In this cell, the amplitude of current activated by 1 μM GABA was enhanced by 5 mM trichloroethanol (274% of control), but was not affected by 100 or 500 mM ethanol (116 and 111% of control, respectively). Figure 3b illustrates that 10–500 mM ethanol did not affect the average amplitude of current activated by 1 μM GABA (analysis of variance and Student's Newman-Keuls ranges test, $P>0.05$; $n=6$). In contrast, in the same neurones, the average current activated by 1 μM GABA in the presence of 5 mM trichloroethanol was 310 ± 76% of control (analysis of variance and Student's Newman-Keuls ranges test, $P<0.01$; $n=6$).

Effect of the putative ethanol antagonist, Ro 15-4513

The augmentation by ethanol of responses mediated by $GABA_A$ receptors has been reported to be antagonized by the imidazodiazepine partial-inverse agonist Ro 15-4513 (ethyl 8-azido-5,6-dihydro-5-methyl-6-oxo-4H-imidazo-[1,5-a][1,4] benzodiazepine-3-carboxylate) (Suzdak *et al.*, 1986a; Harris *et al.*, 1988). Figure 4 illustrates that the enhancement

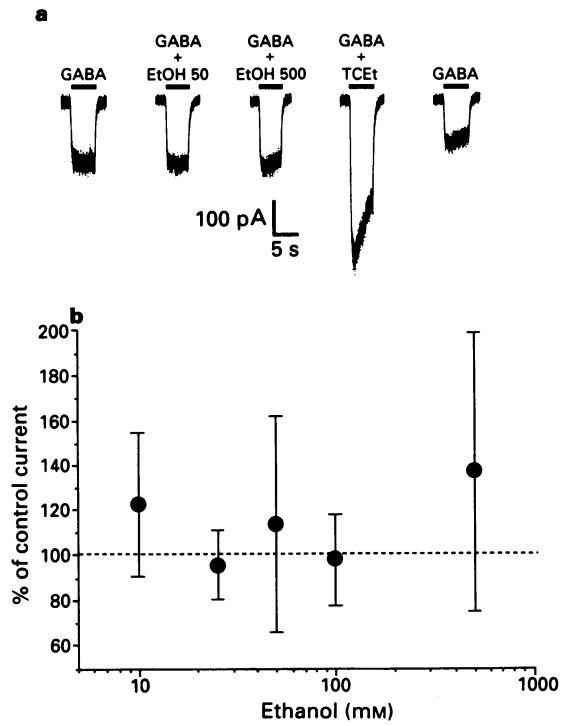


Figure 3 Comparison of the effects of ethanol and trichloroethanol on GABA-activated current in the same neurones. (a) Records of ion current activated by 1 μM GABA in the absence and presence of 50 mM ethanol (EtOH 50), 500 mM ethanol (EtOH 500), or 5 mM trichloroethanol (TCEt) in a single hippocampal neurone voltage-clamped at − 50 mV. Similar results were obtained in 5 other neurones tested. (b) Concentration-response for ethanol effect on current activated by 1 μM GABA. Data are means ± s.e. of 6 neurones voltage-clamped at − 50 mV. Ethanol at concentrations from 10 to 500 mM did not significantly affect GABA-activated current (analysis of variance and Student's Newman-Keuls ranges test, $P>0.05$). In the same neurones, in the presence of 5 mM trichloroethanol, current activated by 1 μM GABA was 310 ± 76% of control (analysis of variance and Student's Newman-Keuls ranges test, $P<0.01$).

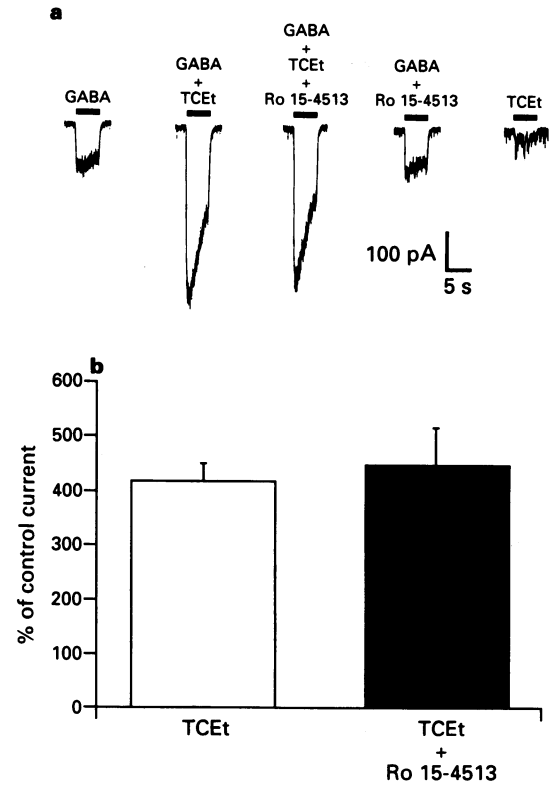


Figure 4 Effect of putative ethanol antagonist, Ro 15-4513, on trichloroethanol potentiation of GABA-activated current. (a) Records of current activated by 1 μM GABA in the absence and presence of 2.5 mM trichloroethanol (TCEt) and 1 μM Ro 15-4513, as labelled. Membrane holding potential was − 50 mV. (b) Comparison of average effect of 2.5 mM trichloroethanol (TCEt) on current activated by 1 μM GABA, plotted as percentage of control GABA-activated current, in the absence and presence of 1 μM Ro 15-4513, as labelled. Results are means ± s.e. of 5 neurones. Membrane holding potential was − 50 mV. There was no significant difference between the effect of trichloroethanol in the absence or presence of Ro 15-4513 (paired t test, $P>0.5$).

of GABA-activated current by trichloroethanol was similar in the presence of 1 μM Ro 15-4513. Ro 15-4513 at this concentration did not alter the amplitude of the GABA-activated current. On average, the enhancement of GABA-activated current by trichloroethanol did not differ significantly in the absence and presence of 1 μM Ro 15-4513 (414 ± 32 vs 444 ± 71% of control, respectively; paired t test, $P > 0.5$; $n = 5$).

Effect of trichloroethanol on pentobarbitone-activated current

The $GABA_A$ receptor-ionophore complex can be activated in the absence of exogenous GABA by barbiturate anaesthetics at high concentrations (Mathers & Barker, 1980; Schulz & MacDonald, 1981). To assess whether trichloroethanol enhances pentobarbitone-activated current in a manner similar to GABA-activated current, current was activated by pentobarbitone in the absence and presence of trichloroethanol. Unlike the GABA-activated current, the current activated by low concentrations of pentobarbitone (10 and 100 μM) was not potentiated by trichloroethanol (repeated measures analysis of variance, $P > 0.05$, $n = 4$). In addition, the concentration-response curve for pentobarbitone-activated current was not significantly altered by 5 mM trichloroethanol (Figure 5). In the absence of trichloroethanol, pentobarbitone had an EC_{50} of 428 ± 38 μM, an E_{max} of 1305 ± 59 pA, and a slope factor of 1.5 ± 0.2, whereas in the presence of trichloroethanol, pentobarbitone had an EC_{50} of 441 ± 45 μM, an E_{max} of 1073 ± 53 pA, and a slope factor of 1.7 ± 0.3; these values did not differ significantly (analysis of variance; $P > 0.05$).

Ionic basis and pharmacology of current activated by trichloroethanol

As noted above, at concentrations of 2.5 mM or greater, trichloroethanol activated an inward current in the absence of exogenous GABA. We studied the ionic basis of the current activated by trichloroethanol by altering the ionic content of the patch-pipette solution, which dialyzes the interior of the neurones under study. The top set of records in Figure 6a illustrates that when CsCl was in the patch-pipette solution, the trichloroethanol-activated current was inward at a holding potential of − 20 mV and outward at + 20 mV. In contrast, when the patch-pipette solution contained Cs methanesulphonate in place of CsCl, the trichloroethanol-activated current was outward at both − 20 and + 20 mV (Figure 6a, bottom traces).

The graph in Figure 6b plots the average amplitude of currents activated by 25 mM trichloroethanol as a function of membrane holding potential in neurones internally dialyzed with a solution containing CsCl (open circles) or Cs methanesulphonate (closed circles). The reversal potential of trichloroethanol-activated current was − 0.8 mV when CsCl was in the patch-pipette solution, but shifted to − 50.6 mV when CsCl was replaced with Cs methanesulphonate in the intracellular solution. The reversal potential of GABA-activated current was − 46.0 mV when the recording pipette contained Cs methanesulphonate (not shown).

Figure 7 shows that current activated by trichloroethanol was reversibly inhibited by the $GABA_A$ antagonists, bicuculline methiodide (Figure 7a) or picrotoxin (Figure 7b). The average amplitude of the current activated by 10 mM trichloroethanol was 73 ± 18 pA under control conditions, and − 8 ± 5 pA in the presence of 50 μM bicuculline methiodide (paired t test, $P < 0.005$; $n = 6$ cells). The inhibition of trichloroethanol-activated current by picrotoxin was more gradual in onset but produced a similar degree of inhibition: the steady-state amplitude of the current activated by 25 mM trichloroethanol was 38 ± 16 pA under control conditions, and − 3 ± 5 pA in the presence of 100 μM picrotoxin (paired t test, $P < 0.05$; $n = 6$ cells). In 5 of 12 cells tested, 10 or 25 mM trichloroethanol in the presence of $GABA_A$ receptor antagonists induced a small-amplitude (5–30 pA) outward current (as indicated by the negative values above).

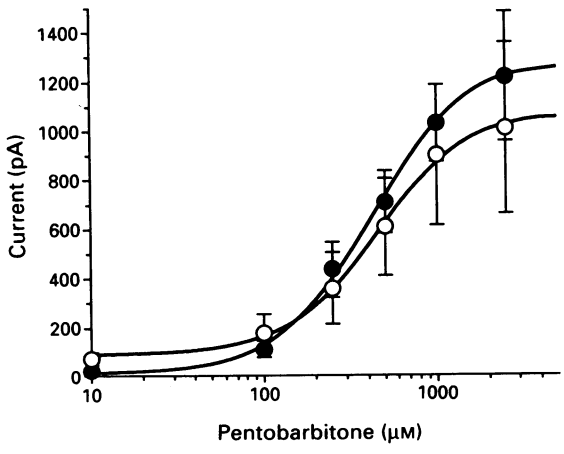


Figure 5 Effect of trichloroethanol on pentobarbitone-activated current. Concentration-response curves for pentobarbitone-activated current, without added GABA, in the absence (●) and presence (○) of 5 mM trichloroethanol. In the absence of trichloroethanol, pentobarbitone had an EC_{50} of 428 ± 38 μM, an E_{max} of 1305 ± 59 pA, and a slope factor of 1.5 ± 0.2, and in the presence of trichloroethanol, pentobarbitone had an EC_{50} of 441 ± 45 μM, an E_{max} of 1073 ± 53 pA, and a slope factor of 1.7 ± 0.3; these values were not significantly different (analysis of variance; $P > 0.05$). The curves shown are the best fits of the data to the logistic equation given in the methods. Data points are means ± s.e. of 4 neurones. Membrane holding potential was − 10 mV.

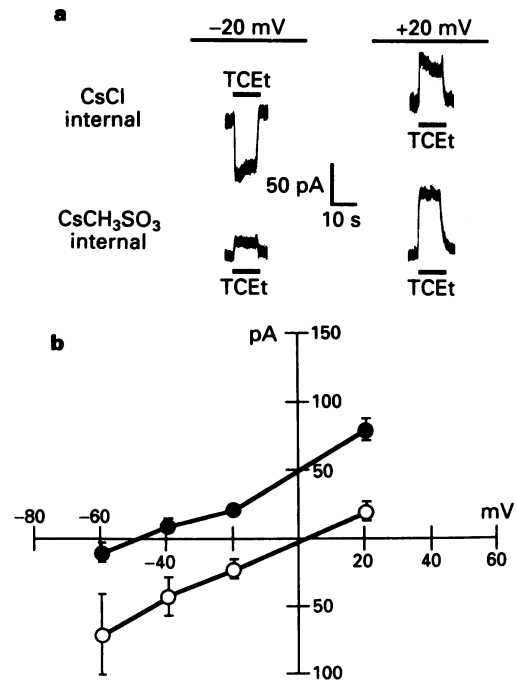


Figure 6 Effect of intracellular Cl^- concentration on trichloroethanol-activated current. (a) Records of current activated by 25 mM trichloroethanol (TCEt) in neurones internally perfused with solutions containing CsCl (upper traces) or Cs methanesulphonate ($CsCH_3SO_3$) (lower traces) at holding potentials of − 20 mV and + 20 mV, as indicated. The Cl^- concentration in the $CsCH_3SO_3$ recording pipette solution was 4 mM. (b) Current-voltage plot for trichloroethanol-activated current in neurones internally perfused with a solution containing CsCl (○) or $CsCH_3SO_3$ (●). Data points are the means ± s.e. obtained from 4 neurones. Note that the reversal potential of the trichloroethanol-activated current with $CsCH_3SO_3$ in the patch-pipette was approximately 50 mV negative to the reversal potential with CsCl in the patch-pipette.

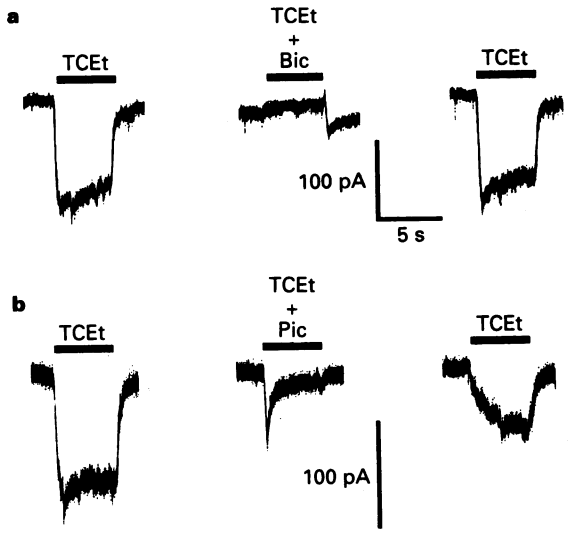


Figure 7 Effect of $GABA_A$ antagonists on trichloroethanol-activated current. (a) Records of current activated by 10 mM trichloroethanol (TCEt) in the absence and presence of 50 μM bicuculline methiodide (Bic). (b) Records of current activated by 25 mM trichloroethanol (TCEt) in the absence and presence of 100 μM picrotoxin (Pic). Records in (a) and (b) are from different neurones; holding potential of neurones was − 50 mV.

Discussion

In this investigation, we found that trichloroethanol could potentiate ion current activated by GABA or the $GABA_A$ agonist muscimol in cultured hippocampal neurones. Trichloroethanol increased the amplitude of the current activated by 1 μM GABA in a concentration-dependent manner, with an EC_{50} of 3 mM and an E_{max} of 576% of control. These results are in accord with the observations of Lovinger *et al.* (1993), who reported that 0.2–10 mM trichloroethanol increased the amplitude and duration of current activated by pressure application of GABA in cultured hippocampal neurones and prolonged inhibitory postsynaptic currents in hippocampal neurones in culture or in brain slices. However, this action of trichloroethanol appears to differ from the actions of other sedative/hypnotic agents on the $GABA_A$ receptor. Other sedative/hypnotic or anaesthetic agents that modulate $GABA_A$ responses, including benzodiazepines (Choi *et al.*, 1981; Little, 1984, Yu *et al.*, 1988), barbiturates (Barker & Ransom, 1978; Akaike *et al.*, 1985), ethanol (Mehta & Ticku, 1988), and hypnotic steroids (Harrison & Simmonds, 1984; Morrow *et al.*, 1988; 1990) in most cases shift the concentration-response curves for $GABA_A$ agonists to the left without altering the maximal response, suggesting an increase in the affinity of the receptor for agonist. Studies on $GABA_A$ receptors expressed in *Xenopus* oocytes suggest that volatile anaesthetics may also act by shifting the concentration-response curve for the $GABA_A$ receptor to the left (Lin *et al.*, 1993). In some cases, barbiturates (Higashi & Nishi, 1982; Yu *et al.*, 1988; Horne *et al.*, 1993), benzodiazepines (Biscoe & Duchen, 1985), and anaesthetic steroids (Horne *et al.*, 1993) have also been reported to increase the maximal response to $GABA_A$ agonists. In the present study, however, enhancement of GABA-evoked ion current by trichloroethanol was observed only at concentrations of GABA < 10 μM, with the result that trichloroethanol did not significantly alter either the EC_{50} or the E_{max} of the GABA concentration-response curve. There are several possible reasons for the preferential action of trichloroethanol at low agonist concentrations. First, increasing agonist concentrations in the presence of trichloroethanol may result in a very rapid onset of receptor desensitization that attenuates the amplitude of GABA-activated current. Second, trichloroethanol may enhance the rate of agonist-activated channel opening from the closed state, but not from the desensitized state. Thus, trichloroethanol might augment currents activated by low GABA concentrations, at which many of the ion channels are in the closed, non-desensitized state, but would not augment currents activated by higher GABA concentrations, when many of the channels are in the closed, desensitized state. This mechanism has been proposed to explain the potentiation of $5\text{-}HT_3$ receptor-mediated current by trichloroethanol in nodose ganglion neurones (Lovinger & Zhou, 1993). Third, the $GABA_A$ receptor-ion channel complex can enter into multiple open states, depending upon the concentration of GABA (MacDonald *et al.*, 1989). The selectivity of trichloroethanol for currents activated by low GABA concentrations may be due to a preferential action of trichloroethanol upon a kinetic substate of the receptor favoured at low GABA concentrations.

The observation in the present study that trichloroethanol did not potentiate currents activated by concentrations of GABA at or above 10 μM might seem to render implausible an effect of trichloroethanol on GABAergic synaptic currents, since GABA concentrations in the synapse appear to approach the millimolar range (Maconochie *et al.*, 1994). Enhancement of inhibitory postsynaptic currents by trichloroethanol has been demonstrated, however, in hippocampal neurones both in culture and in brain slices (Lovinger *et al.*, 1993). At least two explanations for this apparent discrepancy are possible. As mentioned previously, an effect of trichloroethanol to enhance currents activated by high concentrations of GABA may have been obscured in the present study by attenuation of peak current due to rapid desensitization. Alternatively, trichloroethanol could act primarily during the falling phase of the postsynaptic current, following the decline in the GABA concentration below the threshold for potentiation. Thus, trichloroethanol would have little or no effect on the peak amplitude of the postsynaptic current, when the synaptic concentration of GABA is high, but would prolong the falling phase of the current, when the synaptic concentration of GABA is low. These predicted results agree well with the observation that trichloroethanol increases the duration, but not the peak amplitude, of GABA-mediated postsynaptic currents (Lovinger *et al.*, 1993).

If the potentiation of GABA-activated current by trichloroethanol results from a general conformational alteration of the $GABA_A$ receptor-ionophore complex, one would expect that current would also be augmented if the channel were activated by an agent acting at another site. Our observation that trichloroethanol did not enhance pentobarbitone-activated current in the absence of exogenous GABA suggests that the action of trichloroethanol on the channel protein does not involve such a conformational change. The observation that trichloroethanol did not enhance pentobarbitone-activated current at a concentration that markedly enhanced GABA-activated current also implies that trichloroethanol does not modulate the function of the pentobarbitone site in a manner similar to its action at the GABA site.

The enhancement of GABA-mediated responses by volatile anaesthetic agents has been attributed to elevation of intracellular Ca^{2+}, as the effect was not observed when the neurones were dialyzed internally with a solution containing 11 mM BAPTA and 1 mM Ca^{2+}, which was calculated to buffer intracellular free Ca^{2+} to 10–100 nM (Mody *et al.*, 1991). In the present study, despite using an intracellular solution containing 10 mM BAPTA and no added Ca^{2+} (calculated intracellular free Ca^{2+} concentration < 1 nM), we observed a potentiation of GABA-activated current of over five fold by trichloroethanol. Thus, trichloroethanol does not appear to enhance GABA-activated current by elevating intracellular Ca^{2+}.

Benzodiazepines, barbiturates, and ethanol do not augment GABA responses in all central neurones (Study &

Barker, 1981; Biscoe & Duchen, 1985; Aguayo, 1990). Variation among neurones in sensitivity to modulation of $GABA_A$ receptor function by these sedative/hypnotic agents has been attributed to variation in the subunit composition of the receptor and/or in the biochemical state of the receptor by processes such as phosphorylation. Different combinations of $GABA_A$ receptor subunits yield receptors that differ in their functional properties, including sensitivity to modulation by barbiturates, benzodiazepines, and anaesthetic steroids (Levitan *et al.*, 1988; Pritchett *et al.*, 1989; Sigel *et al.*, 1990; Verdoorn *et al.*, 1990; Horne *et al.*, 1993), and perhaps also to ethanol (Lüddens *et al.*, 1990; Wafford *et al.*, 1991; Korpi *et al.*, 1993). In addition, Leidenheimer *et al.* (1993) recently reported that the phosphorylation state of the $GABA_A$ receptor-ion channel complex influences its sensitivity to modulation by benzodiazepines and barbiturates. Our observation that trichloroethanol potentiated GABA-activated current in all neurones tested may indicate that the determinants of the $GABA_A$ receptor responsible for sensitivity to trichloroethanol are less stringent than those responsible for its sensitivity to other modulators.

In addition to the potentiation of GABA-activated current, we found that trichloroethanol concentrations $\geqslant 2.5$ mM activated a current in the absence of exogenous GABA. The observations that the reversal potential for this current shifted when the intracellular Cl^- concentration was changed and that this shift was coincident with the shift in reversal potential of GABA-activated current, suggest that the trichloroethanol-activated current is carried predominantly by Cl^-. In addition, the antagonism of this current by either bicuculline or picrotoxin suggests that the trichloroethanol-activated Cl^- current involves GABA-gated ion channels. Whether the current activated by trichloroethanol in the absence of exogenous GABA results from a direct stimulation of the $GABA_A$ receptor-ionophore complex or from potentiation of low concentrations of endogenous GABA is not clear. The observation that the $GABA_A$ competitive antagonist, bicuculline, inhibits the trichloroethanol-activated current could be interpreted as support for the latter hypothesis. However, it remains possible that bicuculline inhibits the trichloroethanol-activated current not by displacing endogenous GABA bound to the receptor, but by stabilizing the receptor-ionophore complex so that it is less sensitive to activation by trichloroethanol. It is of interest to note that barbiturates and hypnotic steroids also activate a Cl^- current in the absence of exogenous GABA (Mathers & Barker, 1980; Schulz & MacDonald, 1981; Higashi & Nishi, 1982; Jackson *et al.*, 1982; Akaike *et al.*, 1985; Majewska *et al.*, 1986; Barker *et al.*, 1987), and that these currents are also antagonized by bicuculline and picrotoxin (Higashi & Nishi, 1982; Akaike *et al.*, 1985; Majewska *et al.*, 1986; Barker *et al.*, 1987).

GABA is now considered to be the major inhibitory neurotransmitter in the mammalian brain, and the major presynaptic inhibitory neurotransmitter in the spinal cord (Barker & Owen, 1986; Roberts, 1986; McCormick, 1989). Previous studies have shown that benzodiazepines, barbiturates, hypnotic steroids, and inhalational anaesthetics can potentiate inhibitory synaptic responses in brain and presynaptic inhibition in spinal cord, and it has been suggested that potentiation of GABA-mediated synaptic responses may contribute to the sedative/hypnotic actions of those agents (Nicoll, 1972; Nicoll *et al.*, 1975; Majewska *et al.*, 1986; Jones *et al.*, 1992; Tanelian *et al.*, 1993). In contrast, the cellular actions of chloral derivative anaesthetics have been less well characterized. Chloral anaesthetics are rapidly metabolized *in vivo* to trichloroethanol, which is believed to be responsible for the CNS effects of these agents (Rall, 1990). We estimate the anaesthetic concentration of trichloroethanol to be in the range of 2–5 mM, based on data from Breimer (1977), Owen & Taberner (1980), and Pringle *et al.* (1981). Our observations that trichloroethanol could potentiate GABA-activated current in all neurones studied, and that the EC_{50} for this effect was 3 mM, suggest that potentiation of GABA-mediated responses may contribute to the sedative/hypnotic actions of chloral derivative anaesthetics.

In addition to potentiating GABA-activated current, we have also found that trichloroethanol can inhibit ion currents activated by excitatory amino acids (Peoples *et al.*, 1990). Given the important role of excitatory amino acid neurotransmitters in regulating excitability in the CNS (Mayer & Westbrook, 1987; Collingridge & Lester, 1989), both inhibition of excitatory amino acid-mediated responses and potentiation of GABA-mediated responses in the CNS by chloral derivatives may contribute to their sedative/hypnotic actions.

We thank Drs David Lovinger and Geoffrey White for discussion of the research, and Stephen McCort, Ashish Dugar, and Anna Vasquez for technical assistance.

References

AGUAYO, L.G. (1990). Ethanol potentiates the $GABA_A$-activated Cl^- current in mouse hippocampal and cortical neurons. *Eur. J. Pharmacol.*, **187**, 127–130.

AKAIKE, N., HATTORI, K., INOMATA, N. & OOMURA, Y. (1985). γ-Aminobutyric-acid- and pentobarbitone-gated chloride currents in internally perfused frog sensory neurones. *J. Physiol.*, **360**, 367–386.

BARKER, J.L., HARRISON, N.L., LANGE, G.D. & OWEN, D.G. (1987). Potentiation of γ-aminobutyric-acid-activated chloride conductance by a steroid anaesthetic in cultured rat spinal neurones. *J. Physiol.*, **386**, 485–501.

BARKER, J.L. & OWEN, D.G. (1986). Electrophysiological pharmacology of GABA and diazepam in cultured CNS neurons. In *Benzodiazepine/GABA Receptors and Chloride Channels: Structural and Functional Properties*. ed. Olsen, R.W. & Venter, J.C. pp. 135–165. New York: Alan R. Liss.

BARKER, J.L. & RANSOM, B.R. (1978). Pentobarbitone pharmacology of mammalian central neurones grown in tissue culture. *J. Physiol.*, **280**, 355–372.

BISCOE, T.J. & DUCHEN, M.R. (1985). Actions and interactions of GABA and benzodiazepines in the mouse hippocampal slice. *Q. J. Exp. Physiol.*, **70**, 313–328.

BREIMER, D.D. (1977). Clinical pharmacokinetics of hypnotics. *Clin. Pharmacokinet.*, **2**, 93–109.

CHOI, D.W., FARB, D.H. & FISCHBACH, G.D. (1977). Chlordiazepoxide selectively augments GABA action in spinal cord cell cultures. *Nature*, **269**, 342–344.

CHOI, D.W., FARB, D.H. & FISCHBACH, G.D. (1981). Chlordiazepoxide selectively potentiates GABA conductance of spinal cord and sensory neurons in cell culture. *J. Neurophysiol.*, **45**, 621–631.

COLLINGRIDGE, G.L. & LESTER, R.A.J. (1989). Excitatory amino acid receptors in the vertebrate central nervous system. *Pharmacol. Rev.*, **40**, 143–210.

DELEAN, A., MUNSON, P.J. & RODBARD, D. (1978). Simultaneous analysis of families of sigmoidal curves: application to bioassay, radioligand assay, and physiological dose-response curves. *Am. J. Physiol.*, **235**, E97–E102.

FORSYTHE, I.D. & WESTBROOK, G.L. (1988). Slow excitatory postsynaptic currents mediated by *N*-methyl-D-aspartate receptors on cultured mouse central neurones. *J. Physiol.*, **396**, 515–533.

GAGE, P.W. & ROBERTSON, B. (1985). Prolongation of inhibitory postsynaptic currents by pentobarbitone, halothane and ketamine in CA1 pyramidal cells in rat hippocampus. *Br. J. Pharmacol.*, **85**, 675–681.

HAEFELY, W., KULCSAR, A., MÖHLER, H., PIERI, L., POLC, P. & SCHAFFNER, R. (1975). Possible involvement of GABA in the central actions of benzodiazepines. *Adv. Biochem. Psychopharmacol.*, **14**, 131–151.

HARRIS, R.A., ALLAN, A.M., DANIELL, L.C. & NIXON, C. (1988). Antagonism of ethanol and pentobarbital actions by benzodiazepine inverse agonists: neurochemical studies. *J. Pharmacol. Exp. Ther.*, **247**, 1012–1017.

HARRISON, N.L., MAJEWSKA, M.D., HARRINGTON, J.W. & BARKER, J.L. (1987). Structure-activity relationships for steroid interaction with the γ-aminobutyric acid$_A$ receptor complex. *J. Pharmacol. Exp. Ther.*, **241**, 346–353.

HARRISON, N.L. & SIMMONDS, M.A. (1984). Modulation of the GABA receptor complex by a steroid anaesthetic. *Brain Res.*, **323**, 287–292.

HIGASHI, H. & NISHI, S. (1982). Effect of barbiturates on the GABA receptor of cat primary afferent neurones. *J. Physiol.*, **332**, 299–314.

HORNE, A.L., HARKNESS, P.C., HADINGHAM, K.L., WHITING, P. & KEMP, J.A. (1993). The influence of the γ_{2L} subunit on the modulation of responses to GABA$_A$ receptor activation. *Br. J. Pharmacol.*, **108**, 711–716.

ISHIZUKA, S., SIKDAR, S.K., YASUI, S., OYAMA, Y. & AKAIKE, N. (1989). α-Chloralose opens the chloride channel of frog isolated sensory neurons. *Brain Res.*, **498**, 181–184.

JACKSON, M.B., LECAR, H., MATHERS, D.A. & BARKER, J.L. (1982). Single channel currents activated by γ-aminobutyric acid, muscimol and (−)-pentobarbital in cultured mouse spinal neurons. *J. Neurosci.*, **2**, 889–894.

JONES, M.V., BROOKS, P.A. & HARRISON, N.L. (1992). Enhancement of γ-aminobutyric acid-activated Cl^- currents in cultured rat hippocampal neurones by three volatile anaesthetics. *J. Physiol.*, **449**, 279–293.

KORPI, E.R., KLEINGOOR, C., KETTENMANN, H. & SEEBURG, P.H. (1993). Benzodiazepine-induced motor impairment linked to point mutation in cerebellar GABA$_A$ receptor. *Nature*, **361**, 356–359.

LEIDENHEIMER, N.J., WHITING, P.J & HARRIS, R.A. (1993). Activation of calcium-phospholipid-dependent protein kinase enhances benzodiazepine and barbiturate potentiation of the GABA$_A$ receptor. *J. Neurochem.*, **60**, 1972–1975.

LEVITAN, E.S., SCHOFIELD, P.R., BURT, D.R., RHEE, L.M., WISDEN, W., KÖHLER, M., FUJITA, N., RODRIGUEZ, H.F., STEPHENSON, A. & DARLISON, M.G. (1988). Structural and functional basis for GABA$_A$ receptor heterogeneity. *Nature*, **335**, 76–79.

LIN, L.-H., WHITING, P. & HARRIS, R.A. (1993). Molecular determinants of general anesthetic action: role of GABA$_A$ receptor structure. *J. Neurochem.*, **60**, 1548–1553.

LITTLE, H.J. (1984). The effects of benzodiazepine agonists, inverse agonists and Ro 15-1788 on the responses of the superior cervical ganglion to GABA *in vitro*. *Br. J. Pharmacol.*, **83**, 57–68.

LITTLE, H.J. (1991). Mechanisms that may underlie the behavioural effects of ethanol. *Prog. Neurobiol.*, **36**, 171–194.

LOVINGER, D.M. & ZHOU, Q. (1993). Trichloroethanol potentiation of 5-hydroxytryptamine$_3$ receptor-mediated ion current in nodose ganglion neurons from the adult rat. *J. Pharmacol. Exp. Ther.*, **265**, 771–776.

LOVINGER, D.M., ZIMMERMAN, S.A., LEVITIN, M., JONES, M.V. & HARRISON, N.L. (1993). Trichloroethanol potentiates synaptic transmission mediated by γ-aminobutyric acid$_A$ receptors in hippocampal neurons. *J. Pharmacol. Exp. Ther.*, **264**, 1097–1103.

LÜDDENS, H., PRITCHETT, D.B., KÖHLER, M., KILLISCH, I., KEINÄNEN, K., MONYER, H., SPRENGEL, R. & SEEBURG, P.H. (1990). Cerebellar GABA$_A$ receptor selective for a behavioral alcohol antagonist. *Nature*, **346**, 648–651.

MACDONALD, R.L. & BARKER, J.L. (1978). Benzodiazepines specifically modulate GABA mediated postsynaptic inhibition in cultured mammalian neurones. *Nature*, **271**, 563–564.

MACDONALD, R.L., ROGERS, C.J. & TWYMAN, R.E. (1989). Kinetic properties of the GABA$_A$ receptor main conductance state of mouse spinal cord neurones in culture. *J. Physiol.*, **410**, 479–499.

MACONOCHIE, D.J., ZEMPEL, J.M. & STEINBACH, J.H. (1994). How quickly can GABA$_A$ receptors open? *Neuron*, **12**, 61–71.

MAJEWSKA, M.D., HARRISON, N.L., SCHWARTZ, R.D., BARKER, J.L. & PAUL, S.M. (1986). Steroid hormone metabolites are barbiturate-like modulators of the GABA receptor. *Science*, **232**, 1004–1007.

MATHERS, D.A. & BARKER, J.L. (1980). (−)Pentobarbital opens ion channels of long duration in cultured mouse spinal neurons. *Science*, **209**, 507–509.

MAYER, M.L. & WESTBROOK, G.L. (1987). The physiology of excitatory amino acids in the vertebrate central nervous system. *Prog. Neurobiol.*, **28**, 197–276.

MCCORMICK, D.A. (1989). GABA as an inhibitory neurotransmitter in human cerebral cortex. *J. Neurophysiol.*, **62**, 1018–1027.

MEHTA, A.K. & TICKU, M.K. (1988). Ethanol potentiation of GABAergic transmission in cultured spinal cord neurons involves γ-aminobutyric acid$_A$-gated chloride channels. *J. Pharmacol. Exp. Ther.*, **246**, 558–564.

MODY, I., TANELIAN, D.L. & MACIVER, M.B. (1991). Halothane enhances tonic neuronal inhibition by elevating intracellular calcium. *Brain Res.*, **538**, 319–323.

MORROW, A.L., PACE, J.R., PURDY, R.H. & PAUL, S.M. (1990). Characterization of steroid interactions with γ-aminobutyric acid receptor-gated chloride ion channels: evidence for multiple steroid recognition sites. *Mol. Pharmacol.*, **37**, 263–270.

MORROW, A.L., SUZDAK, P.D. & PAUL, S.M. (1988). Benzodiazepine, barbiturate, ethanol and hypnotic steroid hormone modulation of GABA-mediated chloride ion transport in rat brain synaptoneurosomes. *Adv. Biochem. Psychopharmacol.*, **45**, 247–261.

NAKAHIRO, M., YEH, J.Z., BRUNNER, E. & NARAHASHI, T. (1989). General anesthetics modulate GABA receptor channel complex in rat dorsal root ganglion neurons. *FASEB J.*, **3**, 1850–1854.

NESTOROS, J.N. (1980). Ethanol specifically potentiates GABA-mediated neurotransmission in feline cerebral cortex. *Science*, **209**, 708–710.

NICOLL, R.A. (1972). The effects of anaesthetics on synaptic excitation and inhibition in the olfactory bulb. *J. Physiol.*, **223**, 803–814.

NICOLL, R.A., ECCLES, J.C., OSHIMA, T. & RUBIA, F. (1975). Prolongation of hippocampal inhibitory postsynaptic potentials by barbiturates. *Nature*, **258**, 625–627.

OWEN, B.E. & TABERNER, P.V. (1980). Studies on the hypnotic effects of chloral hydrate and ethanol and their metabolism *in vivo* and *in vitro*. *Biochem. Pharmacol.*, **29**, 3011–3016.

PENNEFATHER, P. & QUASTEL, D.M.J. (1980). Actions of anesthetics on the function of nicotinic acetylcholine receptors. In *Molecular Mechanisms of Anesthesia* (*Progress in Anesthesiology*, Vol. 2). ed. Fink, B.R. pp. 45–58. New York: Raven Press.

PEOPLES, R.W., LOVINGER, D.M. & WEIGHT, F.F. (1990). Inhibition of excitatory amino acid currents by general anesthetic agents. *Soc. Neurosci. Abstr.*, **16**, 1017.

PEOPLES, R.W. & WEIGHT, F.F. (1991). Modulation of amino acid-activated ion currents by trichloroethanol. *Third IBRO World Congress of Neurosci. Abstr.*, **3**, 63.

PRINGLE, M.J., BROWN, K.B. & MILLER, K.W. (1981). Can the lipid theories of anesthesia account for the cutoff in anesthetic potency of homologous series of alcohols? *Mol. Pharmacol.*, **19**, 49–55.

PRITCHETT, D.B., SONTHEIMER, H., SHIVERS, B.D., YMER, S., KETTENMANN, H., SCHOFIELD, P.R. & SEEBURG, P.H. (1989). Importance of a novel GABA$_A$ receptor subunit for benzodiazepine pharmacology. *Nature*, **338**, 582–585.

RALL, T.W. (1990). Hypnotics and sedatives; ethanol. In *The Pharmacological Basis of Therapeutics*. ed. Gilman, A.G., Rall, T.W., Nies, A.S. & Taylor, P. pp. 345–382. Elmsford, New York: Pergamon Press.

RANSOM, B.R. & BARKER, J.L. (1975). Pentobarbital modulates transmitter effects on mouse spinal neurones grown in tissue culture. *Nature*, **254**, 703–705.

ROBERTS, E. (1986). GABA: the road to neurotransmitter status. In *Benzodiazepine/GABA Receptors and Chloride Channels: Structural and Functional Properties*. ed. Olsen, R.W. & Venter, J.C. pp. 1–39. New York: Alan R. Liss.

SCHULZ, D.W. & MACDONALD, R.L. (1981). Barbiturate enhancement of GABA-mediated inhibition and activation of chloride ion conductance: correlation with anticonvulsant and anesthetic actions. *Brain Res.*, **209**, 177–188.

SIGEL, E., BAUR, R., TRUBE, G., MÖHLER, H. & MALHERBE, P. (1990). The effect of subunit composition of rat brain GABA$_A$ receptors on channel function. *Neuron*, **5**, 703–711.

STERZ, R., HERMES, M, PEPER, K. & BRADLEY, R.J. (1981). Effects of halogenated derivatives of ethanol on the nicotine acetylcholine receptor. *Brain Res.*, **230**, 434–438.

STUDY, R.E. & BARKER, J.L. (1981). Diazepam and (−)-pentobarbital: fluctuation analysis reveals different mechanisms for potentiation of γ-aminobutyric acid responses in cultured central neurons. *Proc. Natl. Acad. Sci. U.S.A.*, **78**, 7180–7184.

SUZDAK, P.D., GLOWA, J.R., CRAWLEY, J.N,. SCHWARTZ, R.D., SKOLNICK, P. & PAUL, S.M. (1986a). A selective imidazobenzodiazepine antagonist of ethanol in the rat. *Science*, **234**, 1243–1247.

SUZDAK, P.D., SCHWARTZ, R.D., SKOLNICK, P. & PAUL, S.M. (1986b). Ethanol stimulates γ-aminobutyric acid receptor-mediated chloride transport in rat brain synaptoneurosomes. *Proc. Natl. Acad. Sci. U.S.A.*, **83**, 4071–4075.

TANELIAN, D.L., KOSEK, P., MODY, I. & MACIVER, M.B. (1993). The role of the $GABA_A$ receptor/chloride channel complex in anesthesia. *Anesthesiol.*, **78**, 757–776.

VERDOORN, T.A., DRAGUHN, A., YMER, S., SEEBURG, P.H. & SAKMANN, B. (1990). Functional properties of recombinant rat $GABA_A$ receptors depend upon subunit composition. *Neuron*, **4**, 919–928.

WAFFORD, K.A., BURNETT, D.M., LEIDENHEIMER, N.J., BURT, D.R., WANG, J.B., KORUJI, P., DUNWIDDIE, T.V., HARRIS, R.A. & SIKELA, J.M. (1991). Ethanol sensitivity of the $GABA_A$ receptor expressed in Xenopus oocytes requires 8 amino acids contained in the γ_{2L} subunit. *Neuron*, **7**, 27–33.

WHITE, G., LOVINGER, D.M. & WEIGHT, F.F. (1990). Ethanol inhibits NMDA-activated current but does not alter GABA-activated current in an isolated adult mammalian neuron. *Brain Res.*, **507**, 332–336.

YU, O., CHIU, T.H & ROSENBERG, H.C. (1988). A comparison of the effects of midazolam and pentobarbital on the dose-response of GABA-gated Cl^- influx in rat brain microsacs. *Brain Res.*, **451**, 376–380.

(Received January 4, 1994
Revised May 25, 1994
Accepted June 16, 1994)

Br. J. Pharmacol. (1994), **113**, 564–568 © Macmillan Press Ltd, 1994

Reduction by N^G-nitro-L-arginine of H_2O_2-induced endothelial cell injury

[1]Shun-ichi Shimizu, Masaki Nomoto, *Toshinori Yamamoto & Kazutaka Momose

Department of Pharmacology and *Clinical Pharmacy, School of Pharmaceutical Sciences, Showa University, 1-5-8 Hatanodai, Shinagawa-ku, Tokyo 142, Japan

1 The effects of three analogues of N^G-nitro-L-arginine (L-NOARG) and N^G-monomethyl-L-arginine (L-NMMA), inhibitors of nitric oxide (NO) synthase, on hydrogen peroxide (H_2O_2)-induced endothelial cell injury were studied.

2 Endothelial cell injury was assessed by measuring the release of intracellular lactate dehydrogenase (LDH) and ^{51}Cr.

3 Addition of H_2O_2 (250–1,000 μM) to endothelial cells induced the release of LDH dose-dependently. The release of LDH was reduced by pretreatment with N^G-nitro-L-arginine methyl ester (L-NAME, 10^{-4}–4×10^{-3} M), L-NOARG (10^{-4}–4×10^{-3} M) and N^G-nitro-L-arginine benzyl ester (L-NABE, 10^{-4}–4×10^{-3} M), inhibitors of NO synthase.

4 L-NOARG analogues also reduced H_2O_2-induced ^{51}Cr release from endothelial cells, while L-NMMA had no effect.

5 The protective effect of L-NAME was not reversed by addition of L-arginine (L-Arg, 1–10 mM).

6 Both L-NAME and L-NMMA completely inhibited L-Arg metabolism to L-citrulline coupled with NO synthesis.

7 These findings suggest that L-NOARG analogues but not L-NMMA reduced H_2O_2-induced endothelial cell injury, and that these effects may not be related to inhibition of NO production.

Keywords: Endothelial cells; N^G-nitro-L-arginine; N^G-nitro-L-arginine methyl ester; N^G-nitro-L-arginine benzyl ester; N^G-monomethyl-L-arginine methyl ester; L-arginine; hydrogen peroxide; cytotoxicity

Introduction

Reactive oxygen species have been implicated in the development of many diseases such as ischaemia-reperfusion injury (Granger, 1988) and inflammation (Fantone & Ward, 1982; Henson & Johnston, 1987). Although the mechanism of cell death induced by reactive oxygen species has not been determined in detail, they are known to cause lipid peroxidation (Bus *et al.*, 1974), DNA strand breakage (Brawn & Fridovich, 1981; Spragg, 1991) and a variety of changes in proteins (Freeman & Crapo, 1982). It is generally accepted that hydroxyl radicals, a highly reactive form of oxygen, are responsible for the oxidant injury. It has been proposed that the hydroxyl radical is derived from superoxide anion or hydrogen peroxide (H_2O_2) in the presence of iron (iron-catalyzed HaberWeiss (Fenton) reaction). Beckman *et al.* (1990) suggested that generation of hydroxyl radicals via the Haber-Weiss pathway may be limited *in vivo* and they proposed that nitric oxide (NO) reacts with superoxide anion in pathological states to produce cytotoxic species such as peroxynitrite and hydroxyl radicals. Moreover, Noronha-Dutra *et al.* (1993) have shown that NO reacts with H_2O_2 to produce singlet oxygen, a highly reactive form of oxygen. NO may exert cytotoxic effects in the presence of reactive oxygen species. Therefore, the role of NO in the process of pathogenesis has been studied. In these studies, NO synthase inhibitors have been used widely (Dawson *et al.*, 1992; Matheis *et al.*, 1992; Patel *et al.*, 1993).

Vascular endothelial cells generate NO via a Ca^{2+}/calmodulin-dependent constitutive enzyme which catalyzes the conversion of L-arginine to L-citrulline (Mayer *et al.*, 1989; Förstermann *et al.*, 1991; Pollock *et al.*, 1991; Schmidt *et al.*, 1992). Vascular endothelial cells are one of the major biological targets of oxygen radical species produced by activated neutrophils and macrophages. Thus, vascular endothelial cells may be exposed to NO and reactive oxygen species simultaneously. Therefore, we investigated the role of NO in H_2O_2-induced endothelial cell injury. In the present study, we found differences in effect between N^G-nitro-L-arginine analogues (L-NOARG analogues) and N^G-monomethyl-L-arginine (L-NMMA), inhibitors of NO synthase, on H_2O_2-induced endothelial cell injury. L-NOARG analogues but not L-NMMA reduce H_2O_2-induced endothelial cell injury and this protective effect may not be related to the inhibition of NO production.

Methods

Endothelial cell culture

Fresh bovine thoracic aortae obtained from an abattoir were kept in phosphate buffered saline (pH 7.4) with penicillin (200 u ml^{-1}) and streptomycin (200 μg ml^{-1}). Aortae were trimmed free of adhering fat and connective tissue, and washed with phosphate buffered saline. Endothelial cells were obtained by scraping the luminal surface with a razor blade (Shasby & Shasby, 1986), and were cultured in minimal essential medium (MEM) containing penicillin (100 u ml^{-1}), streptomycin (100 μg ml^{-1}) and 10% foetal calf serum (FCS). Cells were finally grown on Cytodex 3 microcarrier beads (Pharmacia).

Endothelial cells were characterized by microscopic observation and incorporation of acetylated low density lipoprotein labelled with 1,1′-dioctadecyl-1-3,3,3′3′-tetramethylindocarbocyanine perchlorate (McGuire & Orkin, 1987). Cells at 6 and 7 passages were used for the experiments.

Lactate dehydrogenase (LDH) release

Confluent endothelial cells on microcarrier beads were washed five times with Krebs solution (pH 7.4) containing (mM): NaCl 118.5, KCl 4.74, $CaCl_2 \cdot 2H_2O$ 2.5, $MgSO_4 \cdot 7H_2O$

[1] Author for correspondence.

1.18, KH_2PO_4 1.18, $NaHCO_3$ 2.5, glucose 11 and N-2-hydroxyethylpiperazine-N'-2-ethanesulphonic acid (HEPES) 10. Cells (50 µl of microcarrier beads, approximately 1×10^6 cells) were then treated with various concentrations of H_2O_2 (250–1,000 µM) at 37°C in 0.5 ml of Krebs solution. LDH activity was determined in cell supernatants and cell fractions of endothelial cells solubilized in 2% Triton X-100 (Thies & Autor, 1991). The percentage of the total LDH activity (supernatant fraction + cell fraction) released into the supernatant fraction was then calculated.

^{51}Cr release

Confluent endothelial cells on microcarrier beads (approximately 1.4×10^7 cells) were radioactively labelled with 18.5 MBq of $Na_2{}^{51}CrO_4$ (Amersham) in 5 ml of culture medium for 16 h at 37°C. This medium was removed and cells were washed five times with Krebs solution. Cells (50 µl of microcarrier beads, approximately 1×10^6 cells) were then exposed to H_2O_2 (500 µM) at 37°C in 0.5 ml of Krebs solution for 3 h, after which time 200 µl of cell-free medium was recovered to determine ^{51}Cr radioactivity (supernatant fraction). The remaining cells were solubilized by addition of 500 µl of 2% Triton X-100, and 200 µl of medium was recovered to determine ^{51}Cr radioactivity (cell fraction). The percentage of the total ^{51}Cr radioactivity (supernatant fraction + cell fraction) released into the superatant fraction was calculated.

Measurement of L-arginine metabolism

Confluent cells on microcarrier beads were transferred to culture medium containing neither L-arginine nor FCS for 24 h prior to the experiment to deplete L-arginine (L-Arg) content. L-Arg-depleted cells were washed 5 times with Krebs solution. The washed cells (100 µl of microcarrier beads, approximately 2×10^6 cells) were incubated at 37°C in 290 µl of Krebs solution containing 37 kBq L-[^{3}H]-arginine (2.29 TBq mmol^{-1}) for 5 min, after which time 10 µl of ionomycin (final concentration of 10^{-6} M) was added and the reaction began. The reaction was terminated with 10 µl of perchloric acid (final concentration of 2%), and after 30 min the reaction mixture was sonicated (5 s) and centrifuged for 10 min at 3,000 r.p.m. [^{3}H]-citrulline formation was determined by high performance liquid chromatography (h.p.l.c.) by a modified version of the method of Rees *et al.* (1990). The supernatant was applied to h.p.l.c. using an ODS-80Ts (4.6 mm i.d. × 150 mm, Tosoh Co., Japan) with a mobile phase of 25 mM sodium acetate (pH 4.35) containing 15 mM sodium hexane sulphonate, and radioactivity in each fraction containing [^{3}H]-citrulline was determined with a liquid scintillation spectrometer.

Materials

N^G-nitro-L-arginine (L-NOARG), N^G-nitro-L-arginine methyl ester (L-NAME), N^G-nitro-L-arginine benzyl ester (L-NABE), N^G-monomethyl-L-arginine acetate salt (L-NMMA) and N^G-nitro-D-arginine methyl ester (D-NAME) were obtained from Sigma Chemical Co. (St. Louis, MO, U.S.A.). H_2O_2 (30% solution) was obtained from Wako Chemicals (Japan). Minimal essential medium was obtained from Gibco Laboratories (Grand Island, NY, U.S.A.). Foetal calf serum was purchased from Boehringer Mannheim. L-[2,3,4,5-^{3}H]-arginine monohydrochloride (2.29 TBq mmol^{-1}) was purchased from Amersham. All other reagents were of the highest grade commercially available.

Statistical analysis

Results are expressed as mean ± s.e.mean of n observations. For multiple comparisons, either Duncan's or Dunnett's test was used. A paired t test was used in those experiments where only two groups were being compared. In all cases, a P value of less than 0.05 was considered statistically significant.

Results

Effects of L-arginine and nitric oxide inhibitors on H_2O_2-induced endothelial cell injury

Endothelial cell injury was assessed by measuring the release of intracellular LDH. Addition of H_2O_2 (250–1,000 µM) to endothelial cells caused LDH release in a dose-dependent manner after a delay of approximately 1 h (Figure 1).

Figure 2 shows the effects of L-NOARG, L-NAME and L-NABE (all at 10^{-6}–4×10^{-3} M), inhibitors of NO synthase, on H_2O_2-induced endothelial cell injury. Pretreatment of cells with all L-NOARG analogues reduced H_2O_2-induced LDH release from endothelial cells. The order of protective effect was as follows: L-NABE > L-NAME = L-NOARG. However, the D-enantiomer of NAME had no effect (data not shown).

The effects of L-Arg, L-NMMA and L-NOARG analogues on H_2O_2-induced ^{51}Cr release from endothelial cells, another marker of cell injury, are shown in Figure 3. Treatment with L-Arg (2 mM) or L-NMMA (1 mM) had no effect, while L-NOARG (1 mM), L-NAME (1 mM) and L-NABE (1 mM) reduced H_2O_2-induced ^{51}Cr release.

Thus, three L-NOARG analogues, but not L-NMMA, reduced H_2O_2-induced endothelial cell injury. Further results are referred to the effect of L-NAME.

Effects of L-arginine on the protective effect of N^G-nitro-L-arginine methyl ester

L-NAME (10^{-6}–4×10^{-3} M) was added to endothelial cell cultures in the presence of various concentrations of L-Arg (1–10 mM), and H_2O_2-induced endothelial cell injury was assessed. L-Arg at no concentration investigated affected the reduction of H_2O_2-induced LDH release by L-NAME (Figure 4).

Effect of nitric oxide synthase inhibitors on nitric oxide synthesis

To determine the effects of L-NMMA and L-NAME on NO synthase activity we used L-citrulline (L-Cit) formation from L-Arg as a marker for NO synthesis. Ionomycin-stimulated L-Cit formation was inhibited by L-NAME and L-NMMA in a dose-dependent manner, with maximum inhibition at concentrations in excess of 10^{-5} and 10^{-3} M, respectively (Figure 5).

Discussion

L-NOARG analogues and L-NMMA are known to be NO synthase inhibitors. Recently, Frew *et al.* (1993) reported that L-NOARG blocks basal and agonist-stimulated production of NO, while L-NMMA blocks basal production but not agonist-stimulated production of NO in rat aortae. However, there have been reports that L-NMMA inhibits agonist-stimulated production of NO in many tissues and cells including rat thoracic aortae (Rees *et al.*, 1990), bovine aortic endothelial cells (Ishii *et al.*, 1990) and rabbit thoracic aortae (Zembowicz *et al.*, 1993). Previously, we reported that the Ca^{2+} ionophore ionomycin-stimulated NO synthesis in endothelial cells can be determined by measurement of L-citrulline (L-Cit) formation from L-Arg (Shimizu *et al.*, 1993). In the present study, both L-NAME and L-NMMA inhibited L-Cit formation from L-Arg coupled with NO synthase in endothelial cells. Thus, both L-NOARG analogues and L-NMMA acted as inhibitors of NO synthesis.

We found that L-NOARG analogues reduced H_2O_2-induced endothelial cell injury. Surprisingly, despite its inhibition of L-Arg metabolism, L-NMMA did not reduce H_2O_2-induced endothelial cell injury. Inhibition of NO synthase by L-NOARG analogues is reversible (Mayer *et al.*, 1993), and can be reversed by L-Arg (Ishii *et al.*, 1990; Mayer *et al.*, 1993; Frew *et al.*, 1993). However, the protective effect of L-NAME was neither reversed in the presence of L-Arg nor increased in the presence of L-NMMA (data not shown), and thus may not involve the inhibition of NO production.

It is generally accepted that highly reactive hydroxyl radicals (·OH) formed via the iron-catalyzed Haber-Weiss (Fenton) reaction, are responsible for oxidant-induced injury of endothelial cells (Todoki *et al.*, 1992). We have observed inhibition of H_2O_2-induced endothelial cell injury by pretreatment with N-(2-mercaptopropionyl)-glycine and 1,3-dimethyl-2-thiourea, ·OH scavengers, and dipyridyl, an iron chelator (data not shown). Therefore, ·OH was responsible for H_2O_2-induced endothelial cell injury. Recently, NO has been shown to react with superoxide anion and H_2O_2 to produce highly cytotoxic such as peroxynitrite, ·OH and singlet oxygen (Beckman *et al.*, 1990; Hogg *et al.*, 1992; Noronha-Dutra *et al.*, 1993). However, addition of L-Arg to endothelial cells did not affect H_2O_2-induced endothelial cell injury. Moreover, carboxy-PTIO, a NO scavenger (Akaike *et al.*, 1993), also showed no effect on H_2O_2-induced endothelial cell injury (data not shown). Thus, under our conditions, NO could not be responsible for H_2O_2-induced endothelial injury. Recently, it was suggested that L-NMMA functions as an alternative substrate for NO synthase, and produces NO and L-Cit (Olken & Marletta, 1993). Frew *et al.* (1993) showed that pretreatment with L-NMMA reduces the ability of L-NOARG to inhibit acetylcholine-induced relaxation in rat aortae, but that the effects of L-NAME were not affected by

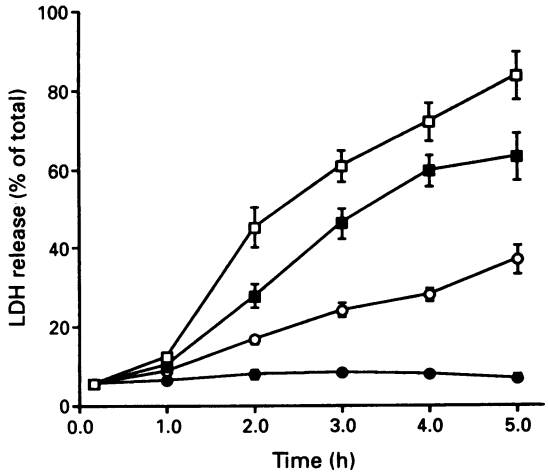


Figure 1 Time course and concentration-response curves of lactate dehydrogenase (LDH) release from endothelial cells exposed to H_2O_2. Cells were incubated in the presence of various concentrations of H_2O_2 (control, ●; 250, ○; 500 ■ and 1,000 μM □) at 37°C. At the indicated times after addition of the H_2O_2, the percentage of the total LDH released into the medium was determined. Results are the means ± s.e.mean of three different experiments performed in triplicate.

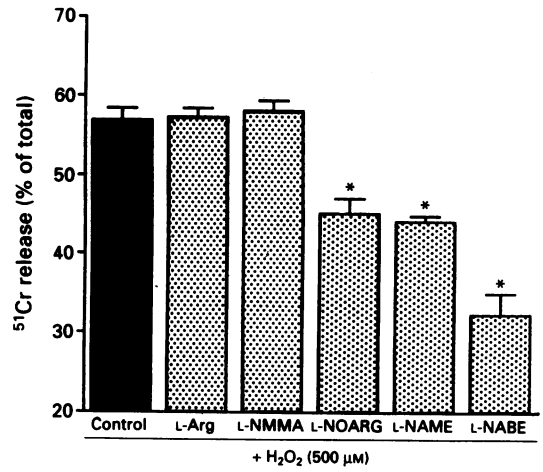


Figure 3 Effects of L-arginine (L-Arg), N^G-monomethyl-L-arginine (L-NMMA), N^G-nitro-L-arginine (L-NOARG), N^G-nitro-L-arginine methyl ester (L-NAME) and N^G-nitro-L-arginine benzyl ester (L-NABE) on H_2O_2-induced ^{51}Cr release from endothelial cells. Cells were pretreated with Krebs solution (control), L-Arg (1 mM), L-NMMA (1 mM), L-NOARG (1 mM), L-NAME (1 mM) or L-NABE (1 mM) for 10 min at 37°C, followed by incubation with H_2O_2 (500 μM) for 3 h at 37°C. Results are the means ± s.e.mean of four different experiments performed in triplicate. *Significantly different from cells treated with H_2O_2 alone (control, $P<0.05$).

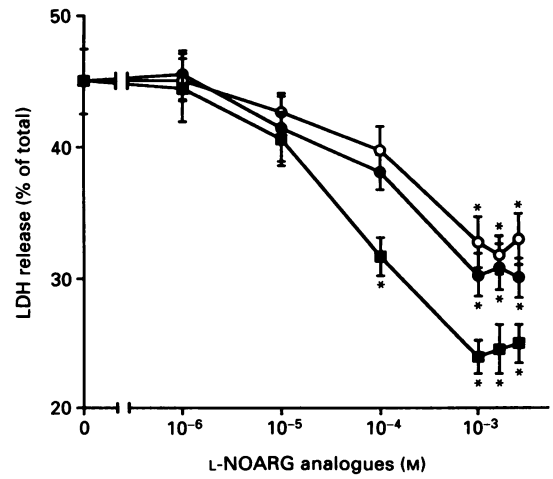


Figure 2 Effects of N^G-nitro-L-arginine analogues on H_2O_2-induced lactate dehydrogenase (LDH) release from endothelial cells. Cells were pretreated with N^G-nitro-L-arginine methyl ester (L-NAME, 10^{-6}–4×10^{-3} M, ○), N^G-nitro-L-arginine (L-NOARG, 10^{-6}–4×10^{-3} M, ●) or N^G-nitro-L-arginine benzyl ester (L-NABE, 10^{-6}–4×10^{-3} M, ■) for 10 min at 37°C, followed by incubation with H_2O_2 (500 μM) for 3 h at 37°C. Results are the means ± s.e.mean of four different experiments performed in triplicate. *Significantly different from cells treated with H_2O_2 alone ($P<0.05$).

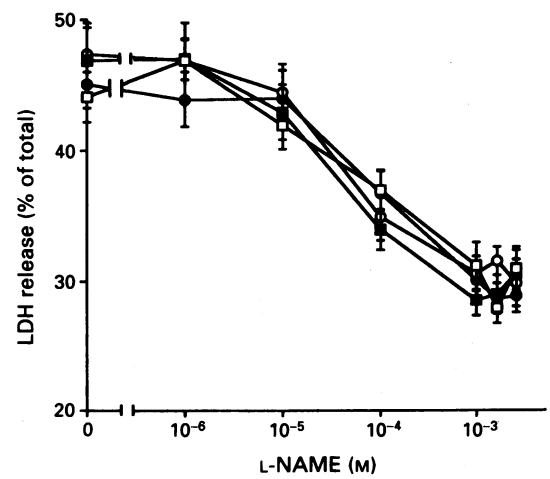


Figure 4 Effect of L-arginine (L-Arg) on the protective effect of N^G-nitro-L-arginine methyl ester. Cells were pretreated with N^G-nitro-L-arginine methyl ester (L-NAME, 10^{-6}–4×10^{-3} M) in the presence of L-Arg (0 ●; 1 ○; 5 ■; 10 mM □) for 10 min at 37°C, followed by incubation with H_2O_2 (500 μM) for 3 h at 37°C. Results are the means ± s.e.mean for four different experiments performed in triplicate.

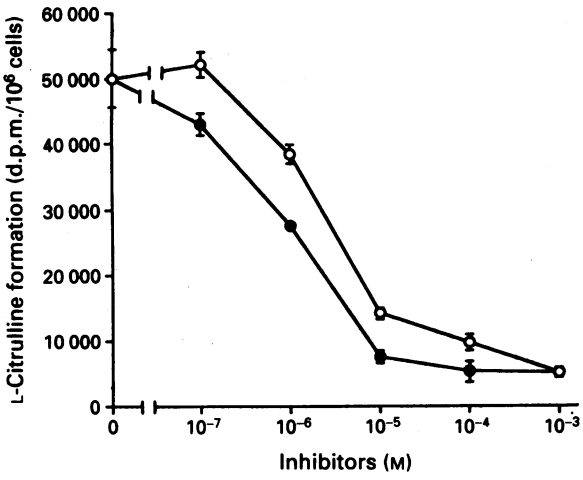


Figure 5 Effects of N^G-nitro-L-arginine methyl ester (L-NAME) and N^G-monomethyl-L-arginine (L-NMMA) on L-citrulline formation from L-arginine induced by ionomycin. Cells were incubated for 4 min at 37°C in the presence of ionomycin (10^{-6} M), and L-NAME (10^{-7}–10^{-3} M, ●) or L-NMMA (10^{-7}–10^{-3} M, ○) were added 10 min before a supplement of ionomycin. Results are the means ± s.e.mean for triplicate assays.

simultaneous addition of L-NMMA (data not shown). This result also suggests that NO may not be responsible for H_2O_2-induced endothelial cell injury. From these results, L-NOARG analogues may reduce cell injury without inhibition of NO production.

NO synthase generates NO from L-Arg in the presence of Ca^{2+}/calmodulin, NADPH, and tetrahydrobiopterin (H_4 biopterin) in vascular endothelial cells and brain (Mayer *et al.*, 1989; Förstermann *et al.*, 1991; Pollock *et al.*, 1991; Schmidt *et al.*, 1992). However, NO synthase also generates H_2O_2 from molecular oxygen at low concentrations of L-Arg and H_4biopterin (Mayer *et al.*, 1991; Heinzel *et al.*, 1992). Both L-NOARG and L-NAME have been shown to block the substrate-independent generation of H_2O_2, whereas L-NMMA has no effect on this reaction. When we investigated the effects of L-NOARG analogues on H_2O_2-induced endothelial cell injury, L-Arg was not supplemented in the medium, and the H_4biopterin content of endothelial cells may be lowered by addition of H_2O_2. Moreover, we reported previously, that addition of H_2O_2 to endothelial cells increases intracellular Ca^{2+} concentration (Saito *et al.*, 1993). Therefore, addition of H_2O_2 to endothelial cells may stimulate NO synthase to produce H_2O_2. Accordingly, it is possible that L-NOARG analogues block the L-Arg-independent generation of H_2O_2 by NO synthase and consequently reduce H_2O_2-induced endothelial cell injury. However, addition of L-Arg, even at a high concentration (10 mM), did not alter the protective effects of L-NOARG analogues. Although the mechanism is not clear, we speculate that intracellular L-Arg contents were lowered by H_2O_2, probably by inhibition of the incorporation of L-Arg into cells. A detailed study will be required to test this hypothesis.

In conclusion, we have shown that despite the similar inhibition by L-NOARG analogues and L-NMMA of L-Cit formation from L-Arg coupled with NO production, L-NOARG analogues reduced H_2O_2-induced endothelial cell injury, while L-NMMA did not. The effects of L-NOARG analogues may be independent of NO production.

References

AKAIKE, T., YOSHIDA, M. MIYAMOTO, Y., SATO, K., KOHNO, M., SASAMOTO, K., MIYAZAKI, K., UEDA, S. & MAEDA, H. (1993). Antagonistic action of imidazolineoxyl N-oxides against endothelium-derived relaxing factor/·NO through a radical reaction. *Biochemistry*, **32**, 827–832.

BECKMAN, J.S., BECKMAN, T.W., CHEN, J., MARSHALL, P.A. & FREEMAN, B.A. (1990). Apparent hydroxyl radical production by peroxynitrite: implications for endothelial injury from nitric oxide and superoxide. *Proc. Natl. Acad. Sci. U.S.A.*, **87**, 1620–1624.

BRAWN, K. & FRIDOVICH, I. (1981). DNA strand scission by enzymically generated oxygen radicals. *Arch. Biochem. Biophys.*, **206**, 414–419.

BUS, J.S., AUST, S.D. & GIBSON, J.E. (1974). Superoxide- and singlet oxygen-catalyzed lipid peroxidation as a possible mechanism for paraquat (methyl viologen) toxicity. *Biochem. Biophys. Res. Commun.*, **58**, 749–755.

DAWSON, D.A., KUSUMOTO, K., GRAHAM, D.J., MCCULLOCH, J. & MACRAE, I.M. (1992). Inhibition of nitric oxide synthesis does not reduce infarct volume in a rat model of focal cerebral ischaemia. *Neurosci. Lett.*, **142**, 151–154.

FANTONE, J.C. & WARD, P.A. (1982). Role of oxygen-derived free radicals and metabolites in leukocyte-dependent inflammatory reactions. *Am. J. Pathol.*, **107**, 397–418.

FÖRSTERMANN, U., POLLOCK, J.S., SCHMIDT, H.H.H.W., HELLER, M. & MURAD, F. (1991). Calmodulin-dependent endothelium-derived relaxing factor/nitric oxide synthase activity is present in the particulate and cytosolic fractions of bovine aortic endothelial cells. *Proc. Natl. Acad. Sci. U.S.A.*, **88**, 1788–1792.

FREEMAN, B.A. & CRAPO, J.D. (1982). Biology of disease. Free radicals and tissue injury. *Lab. Invest.*, **47**, 412–426.

FREW, J.D., PAISLEY, K. & MARTIN, W. (1993). Selective inhibition of basal but not agonist-stimulated activity of nitric oxide in rat aorta by N^G-monomethyl-L-arginine. *Br. J. Pharmacol.*, **110**, 1003–1008.

GRANGER, D.N. (1988). Role of xanthine oxidase and granulocytes in ischemia-reperfusion injury. *Am. J. Physiol.*, **255**, H1269–H1275.

HEINZEL, B., JOHN, M., KLATT, P., BÖHME, E. & MAYER, B. (1992). Ca^{2+}/calmodulin-dependent formation of hydrogen peroxide by brain nitric oxide synthase. *Biochem. J.*, **281**, 627–630.

HENSON, P.M. & JOHNSTON, R.B. (1987). Tissue injury in inflammation. Oxidants, proteinases, and cationic proteins. *J. Clin. Invest.*, **79**, 669–674.

HOGG, N., DARLEY-USMAR, V.M., WILSON, M.T. & MONCADA, S. (1992). Production of hydroxyl radicals from the simultaneous generation of superoxide and nitric oxide. *Biochem. J.*, **281**, 419–424.

ISHII, K., CHANG, B., KERWIN, J.F., HUANG, Z. & MURAD, F. (1990). N^{ω}-Nitro-L-arginine: a potent inhibitor of endothelium-derived relaxing factor formation. *Eur. J. Pharmacol.*, **176**, 219–223.

MATHEIS, G., SHERMAN, M.P., BUCKBERG, G.D., HAYBRON, D.M., YOUNG, H.H. & IGNARRO, L.J. (1992). Role of L-arginine-nitric oxide pathway in myocardial reoxygenation injury. *Am. J. Physiol.*, **262**, H616–H620.

MAYER, B., JOHN, M., HEINZEL, B., WERNER, E.R., WACHTER, H., SCHULTZ, G. & BÖHME, E. (1991). Brain nitric oxide synthase is a bioprotein- and flavin-containing multi-functional oxido-reductase. *FEBS Lett.*, **288**, 187–191.

MAYER, B., SCHMIDT, K., HUMBERT, P. & BÖHME, E. (1989). Biosynthesis of endothelium-derived relaxing factor: a cytosolic enzyme in porcine aortic endothelial cells Ca^{2+}-dependently converts L-arginine into an activator of soluble guanylyl cyclase. *Biochem. Biophys. Res. Commun.*, **164**, 678–685.

MAYER, B., SCHMID, M., KLATT, P. & SCHMIDT, K. (1993). Reversible inactivation of endothelial nitric oxide synthase by N^G-nitro-L-arginine. *FEBS Lett.*, **333**, 203–206.

MCGUIRE, P.G. & ORKIN, R.W. (1987). Isolation of rat aortic endothelial cells by primary explant techniques and their phenotypic modulation by defined substrata. *Lab. Invest.*, **57**, 94–105.

NORONHA-DUTRA, A.A., EPPERLEIN, M.M. & WOOLF, N. (1993). Reaction of nitric oxide with hydrogen peroxide to produce potentially cytotoxic singlet oxygen as a model for nitric oxide-mediated killing. *FEBS Lett.*, **321**, 59–62.

OLKEN, N.M. & MARLETTA, M.A. (1993). N^G-Methyl-L-arginine functions as an alternate substrate and mechanism-based inhibitor of nitric oxide synthase. *Biochemistry*, **32**, 9677–9685.

PATEL, V.C., YELLON, D.M., SINGH, K.J., NEILD, G.H. & WOOLFSON, R.G. (1993). Inhibition of nitric oxide limits infarct size in the *in situ* rabbit heart. *Biochem. Biophys. Res. Commun.*, **194**, 234–238.

POLLOCK, J.S., FÖRSTERMANN, U., MITCHELL, J.A., WARNER, T.D., SCHMIDT, H.H.H.W., NAKANE, M. & MURAD, F. (1991). Purification and characterization of particulate endothelium-derived relaxing factor synthase from cultured and native bovine aortic endothelial cells. *Proc. Natl. Acad. Sci. U.S.A.*, **88**, 10480–10484.

REES, D.D., PALMER, R.M.J., SCHULZ, R., HODSON, H.F. & MONCADA, S. (1990). Characterization of three inhibitors of endothelial nitric oxide synthase *in vitro* and *in vivo*. *Br. J. Pharmacol.*, **101**, 746–752.

SAITO, Y., SHIMIZU, S., KANBE, K., YAMAMOTO, T. & MOMOSE, K. (1993). Effect of hydrogen peroxide on NO biosynthesis in aortic endothelial cells. *Jpn. J. Pharmacol.*, **61** (Suppl. 1), 72P.

SCHMIDT, H.H.H.W., POLLOCK, J.S., NAKANE, M., FÖRSTERMANN, U. & MURAD, M. (1992). Ca^{2+}/calmodulin-regulated nitric oxide synthase. *Cell Calcium*, **13**, 427–434.

SHASBY, D.M. & SHASBY, S.S. (1986). Effect of calcium on transendothelial albumin transfer and electrical resistance. *J. Appl. Physiol.*, **60**, 71–79.

SHIMIZU, S., YAMAMOTO, T. & MOMOSE, K. (1993). Inhibition by methylene blue of the L-arginine metabolism to L-citrulline coupled with nitric oxide synthesis in cultured endothelial cells. *Res. Commun. Chem. Pathol. Pharmacol.*, **82**, 35–48.

SPRAGG, R.G. (1991). DNA strand break formation following exposure of bovine pulmonary artery and aortic endothelial cells to reactive oxygen products. *Am. J. Respir. Cell. Mol. Biol.*, **4**, 4–10.

THIES, R.L. & AUTOR, A.P. (1991). Reactive oxygen injury to cultured pulmonary artery endothelial cells: mediation by poly (ADP-ribose)polymerase activation causing NAD depletion and altered energy balance. *Arch. Biochem. Biophys.*, **286**, 353–363.

TODOKI, K., OKABE, E., KIYOSE, T., SEKISHITA, T. & ITO, H. (1992). Oxygen free radical-mediated selective endothelial dysfunction in isolated coronary artery. *Am. J. Physiol.*, **262**, H806–H812.

ZEMBOWICZ, A., HATCHETT, R.J., JAKUBOWSKI, A.M. & GRYGLEWSKI, R.J. (1993). Involvement of nitric oxide in the endothelium-dependent relaxation induced by hydrogen peroxide in the rabbit aorta. *Br. J. Pharmacol.*, **110**, 151–158.

(Received April 22, 1994
Revised May 31, 1994
Accepted June 16, 1994)

Br. J. Pharmacol. (1994), **113**, 569–575 © Macmillan Press Ltd, 1994

Developmental changes in ANP-stimulated guanylyl cyclase activity enhanced by ATP in rat lung membrane fractions

P. Charoonroje, [1]Y. Tokumitsu & Y. Nomura

Department of Pharmacology, Faculty of Pharmaceutical Scienes Hokkaido University, Sapporo, 060 Japan

1 ANP (atrial natriuretic peptides)- or ANP/ATP-stimulated guanylyl cyclase activities were compared in adult (2 month old) and neonatal (5–7 day old) rat lung membrane fractions.

2 The enzyme activities of both membranes depended on the incubation time and ATP concentration: although the activities of both membranes were similar after a short incubation time (4 min), those in adult membranes were lower than those of neonatal membranes after longer incubation times (10 and 30 min) or at lower concentrations of ATP.

3 ANP/ATPγS-stimulated guanylyl cyclase activities, which were much higher than ANP/ATP-stimulated activites, were similar in both membranes.

4 ATPase activity of adult membranes was higher than that of neonatal membranes, suggesting that hydrolysis of ATP leads to a decrease of ANP/ATP-guanylyl cyclase activity in adult membranes. Triton X-100 enhanced and diminished ANP/ATP-stimulated guanylyl cyclase activities of adult and neonatal membranes, respectively, and thereby abolished the adult/neonatal difference in the membrane response to ATP.

5 ANP-stimulated activities of both membranes were much more activated by pre-incubation with ATPγS than those induced by simultaneous addition of ATPγS. The former activities were decreased to levels of the latter by Triton X-100. The latter activities were not affected by Triton X-100.

6 The present results suggested that conformation of lung plasma membranes is related to activation of the ANP receptor/guanylyl cyclase system.

Keywords: Atrial natriuretic peptide; ATP; guanylyl cyclase; rat lung membranes; developmental change

Introduction

Atrial natriuretic peptide (ANP) synthesized in atrial cardiocytes and released into the circulation evokes a variety of physiological responses. Some of the physiological actions of ANP are mediated via production of guanosine 3′:5′-cyclic monophosphate (cyclic GMP) by the activation of membrane-bound guanylyl cyclase (Atlas & Laragh, 1986; Chinkers *et al.*, 1989; Inagami, 1989; Pandey & Singh, 1990). Recently, enhancement of guanylyl cyclase by ATP was demonstrated (Kurose *et al.*, 1987; Chang *et al.*, 1990; Gazzano *et al.*, 1991; Marala *et al.*, 1991; Chamienia & Johns, 1992; Lebowitz *et al.*, 1992), and coexistence of ANP receptors and guanylyl cyclase was identified in membranes prepared from various mammalian tissues and cells (Kuno *et al.*, 1986; Pual *et al.*, 1987; Takayanagi *et al.*, 1987; Meloche *et al.*, 1988). However, little is known about the definitive biochemical mechanism of the ATP action.

ANP receptors coupled to guanylyl cyclase are in abundance in lung plasma membranes of mammals (Lad & White, 1979; Inomata *et al.*, 1987; Imamura *et al.*, 1988). The function of lung is greatly changed after birth, and hence it is interesting to investigate how effects of ATP on ANP-stimulated guanylyl cyclase activity are changed during development. In the present study, we examined changes of ANP-stimulated guanylyl cyclase activity during the course of development by using lung plasma membranes from adult and neonatal rats. The results obtained show that there are large differences in incubation time-dependency and ATP effect on ANP-stimulated guanylyl cyclase activities between adult and neonatal rat lung membranes.

[1] Author for correspondence.

Methods

Preparation of rat lung plasma membranes

Male rats of a Wistar strain, adult (2 month old) and neonate (5–7 day old) were used. Each lung was minced in 0.25 M sucrose-1 mM EDTA-20 mM HEPES buffer (pH 7.5) containing aprotinin (50 u ml^{-1}) and homogenized with polytron and subsequently Teflon homogenizer. Homogenates were centrifuged for 5 min at 600 *g* and the supernatant was centrifuged for 30 min at 25000 *g*. Pellets were washed, resuspended with 0.25 M sucrose: 1 mM EDTA: 20 mM HEPES buffer (pH 7.5), and stored at −80°C until use as crude plasma membrane fractions.

Measurement of guanylyl cyclase activity

Crude plasma membrane fractions (40–50 μg protein) were suspended in the assay medium of a final volume of 0.3 ml containing 20 mM HEPES buffer (pH 7.5), 0.25 mM GTP, 0.4 mM IBMX, 3 mM $MgCl_2$, 0.5 nM EDTA, 5 mM creatine phosphate, 30 u ml^{-1} creatine phosphokinase, and 0.1% bovine serum albumin (BSA) and incubated with ANP at 30°C. ANP was added at 500 nM unless otherwise noted. Reaction was terminated by addition of 0.03 ml of 1 N HCl. The amount of cyclic GMP produced by guanylyl cyclase was measured by radioimmnoassay as described previously (Honma *et al.*, 1977) and assessed as guanylyl cyclase activity.

Measurement of ATPase activity

Crude plasma membrane fractions (40–50 μg protein) were suspended in 20 mM HEPES buffer (pH 7.5) containing 3 mM $MgCl_2$, 0.5 mM EDTA, 0.1% BSA, and various doses of ATP in a final volume of 0.3 ml and incubated at 30°C. Reaction was terminated by addition of 0.03 ml of 3 N $HClO_4$. To 1 ml of the deproteinized supernatant were added

2 ml of 1.25% ammonium molybdate in 0.15 N H_2SO_4, and a further 3 ml of 0.08% *p*-aminonaphthol sulphonic acid reagent described by Fiske & Subbarow (1925). Samples were allowed to stand for 30 min at 30°C and measured at 750 nm. The amount of inorganic phosphate released by hydrolysis of ATP was assessed as ATPase activity.

[^{35}S]-adenosine 5'-(3-thio) triphosphate binding to crude plasma membrane fractions

Crude plasma membrane fractions (40–50 μg protein) were suspended with 20 mM HEPES buffer (pH 7.5) containing 100 mM NaCl, 3 mM $MgCl_2$, 0.5 mM EDTA, and various doses of [^{35}S]-adenosine 5'-(3-thio)-triphosphate ([^{35}S]-ATPγS) in a final volume of 0.3 ml and incubated at 30°C for 30 min. The measurement of non-specific binding was carried out by the addition of unlabelled ATPγS at a concentration of 250 μM under similar conditions.

Treatment of crude plasma membrane fractions with Triton X-100

Crude plasma membrane fractions (40–50 μg protein) were incubated with or without ATP or ATPγS in the presence or absence of 0.1% Triton X-100 in the medium for assay of guanylyl cyclase. In the case of pretreatment of membranes with ATPγS, membrane fractions (40–50 μg protein) were pre-incubated with 200 μM ATPγS at 37°C for 5 min in 20 mM HEPES buffer (pH 7.4) containing 0.25 M sucrose, 3 mM $MgCl_2$, 0.5 mM EDTA, and 0.1% BSA in a final volume of 0.2 ml. After pre-incubation, the medium for assay of guanylyl cylcase was added into the pre-incubated membrane suspensions and guanylyl cyclase activities were measured in the presence or absence of 0.1% Triton X-100 under similar conditions to those described above.

Measurement of plasma membrane fluidity

The degree of fluidity of the nonpolar regions of biological membranes has been estimated by the introduction of a highly efficient hydrocarbon fluorophore, 1,6-diphenyl 1,3,5-hexatriene (DPH) which is localized in the hydrophobic regions of biological membranes. The fluorescence polarization of the DPH in the rat lung membranes was measured as follows. Two μl of 1 mM DPH solution in tetrahydrofuran were added to the lung membrane suspension (100 μg protein) in 2 ml of 25 mM HEPES buffer (pH 7.5) containing 145 mM NaCl, and 4 mM KCl in a cuvette. After the membrane suspension containing DPH was stirred for 15 min at 25°C, the polarization of the DPH fluorescence was measured as described previously (Nomura & Kurihara, 1987). The following relationship was employed to obtain the polarization (P) of the DPH fluorescence:

$$P = (I_\eta - I_l)/(I_\eta + I_l)$$

Here I_η and I_l represent the fluorescence intensity parallel to, and perpendicular to the plane of polarization of the excitation beam, respectively. The emission of DPH was excited at 360 nm and monitored at 430 nm through a 390-nm cut-off filter. The molar ratio of DPH was used for measurement of the fluorescence polarization.

Plasma membrane proteins

Proteins were measured by the method of Lowry *et al.* (1951).

Materials

Cyclic GMP assay kits and aprotinin were provided by Yamasa Shoyu (Japan) and Hoechst Japan, respectively. ANP, ATP, ATPγS, creatine phosphate, creatine phosphokinase, 3-isobutyl-1-methylxanthine (IBMX), and bovine serum albumin (BSA) were purchased from Sigma (USA). 1,6-Diphenyl 1,3,5-hexatriene (DPH) was from Tokyo Chemical Ind. (Japan).

Analysis of data

Scatchard plots of equilibrium binding of [^{35}S]-ATPγS were analyzed by a nonlinear least-squares curve-fitting procedure with a one-site or two-site model using the modified LIGAND programme (Munson & Rodbard, 1980). Statistical differences were analyzed by Student's *t* test.

Results

Effects of ATP on ANP-stimulated guanylyl cyclase activities and its incubation time-dependency

ANP slightly activated guanylyl cyclase of adult and neonatal rat lung membranes in a concentration-dependent manner, and its action was markedly enhanced in both membranes by simultaneous addition of 100 μM ATP (Figure 1). There was no significant difference in the enzyme activities between adult and neonatal membranes under the conditions incubated at 30°C for 3 min. ATP itself had no effect on guanylyl cyclase activity.

Figure 2 shows the time course for ANP-stimulated guanylyl cyclase activities of adult and neonatal lung membranes with or without 100 μM ATP. Stimulation of guanylyl cyclase activity by ANP in adult membranes reached a maximal level at 4 min. In contrast, the enzyme activity of neonatal membranes continued to increase up to incubation time 10 min, resulting in 2 fold that of adult membranes at incubation times 10 min and 30 min (Figure 2a). The enzyme activities enhanced by addition of 100 μM ATP were increased time-dependently in both membranes. However, as in the absence of ATP at the incubation times 10 min and 30 min, enzyme activity of adult membranes was one-half that of neonatal membranes (Figure 2b).

The dose-dependent effects of ATP on ANP-stimulated guanylyl cyclase activities were examined at various incubation times in adult and neonatal lung membranes (Figure 3). ATP enhanced ANP-stimulated guanylyl cyclase in a concentration-dependent manner in both membranes. ANP-stimulated guanylyl cyclase activities of adult and neonatal

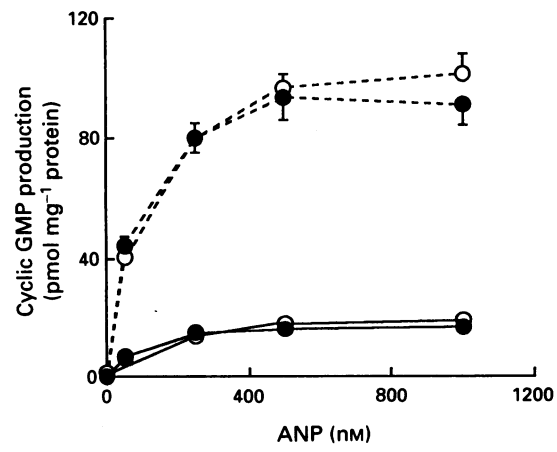


Figure 1 Effects of ATP on ANP-stimulated guanylyl cyclase activities in plasma membrane fractions of adult and neonatal rat lungs. Crude plasma membranes were incubated with indicated concentrations of ANP for 3 min in the presence (dashed lines) and absence (solid lines) of ATP (100 μM). Measurement of guanylyl cyclase activity was carried out as described in the Methods. Adult (●); neonate (○). Values are means ± s.e.mean of five separate experiments. For abbreviations in this and other legends, see text.

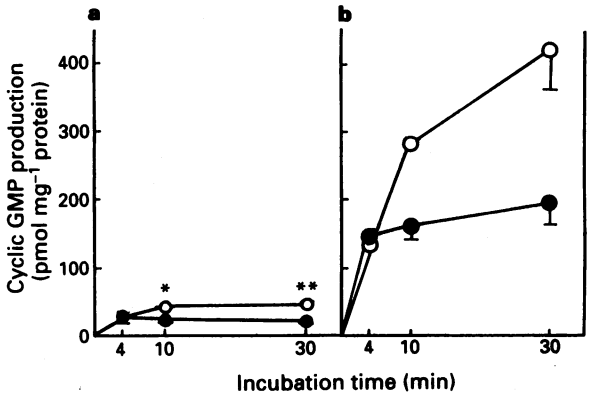


Figure 2 Effects of incubation times and ATP addition on ANP-stimulated guanylyl cyclase in plasma membrane fractions of adult and neonatal rat lungs. Crude plasma membranes were incubated for indicated incubation times in the presence (b) and absence (a) of ATP (100 μM). Measurement of guanylyl cyclase activity was carried out as described in the Methods. Adult (●); neonate (○). Values are means ± s.e.mean of five separate experiments. $*P<0.05$; $**P<0.01$.

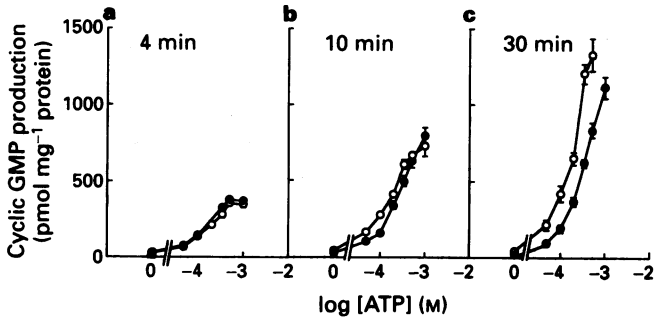


Figure 3 Relationship between incubation time and ATP concentration in ANP-stimulated guanylyl cyclase activities of plasma membrane fractions of adult and neonatal rat lungs. Crude plasma membranes were incubated with indicated concentrations of ATP for 4 min (a), 10 min (b), and 30 min (c). Measurement of guanylyl cyclase activity was carried out as described in the Methods. Adult (●); neonate (○). Values are means ± s.e.mean of four separate experiments.

membranes at incubation time of 4 min were similar at all ATP concentrations tested (Figure 3a). In contrast, at incubation time 10 min, the enzyme activities of neonatal membranes were significantly higher than those of adult membranes at concentrations of ATP below 300 μM (see Figure 2). Concentrations of ATP above 500 μM enhanced the enzyme activities of both membranes to a similar extent, and hence there was no significant difference in the enzyme activities between the two membranes (Figure 3b). After an incubation time of 30 min, the enzyme activities of neonatal membranes were always significantly higher than those of adult membranes at all ATP concentrations tested (Figure 3c).

Relationship between ATP effect on ANP-stimulated guanylyl cyclase activity and ATPase activity

The amount of ATP-binding to adult and neonatal lung membranes was measured using various concentrations of ATPγS. Scatchard plots of the data are shown in Figure 4. The analysis of the binding data in both membranes exhibited curvilinear plots, indicating that two classes of ATP-binding sites (high affinity with a small number and low affinity with a large number) exist in rat lung membranes. The values of K_d and B_{max} for ATPγS binding are shown in

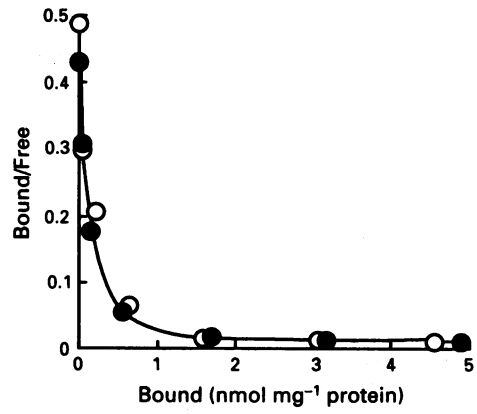


Figure 4 Scatchard plot analysis of [^{35}S]-ATPγS binding to plasma membrane fractions in adult and neonatal rat lungs. Crude plasma membranes were incubated with various concentrations of [^{35}S]-ATPγS and [^{35}S]-ATPγS binding activity to each membrane was measured as described in Methods. Adult (●); neonate (○).

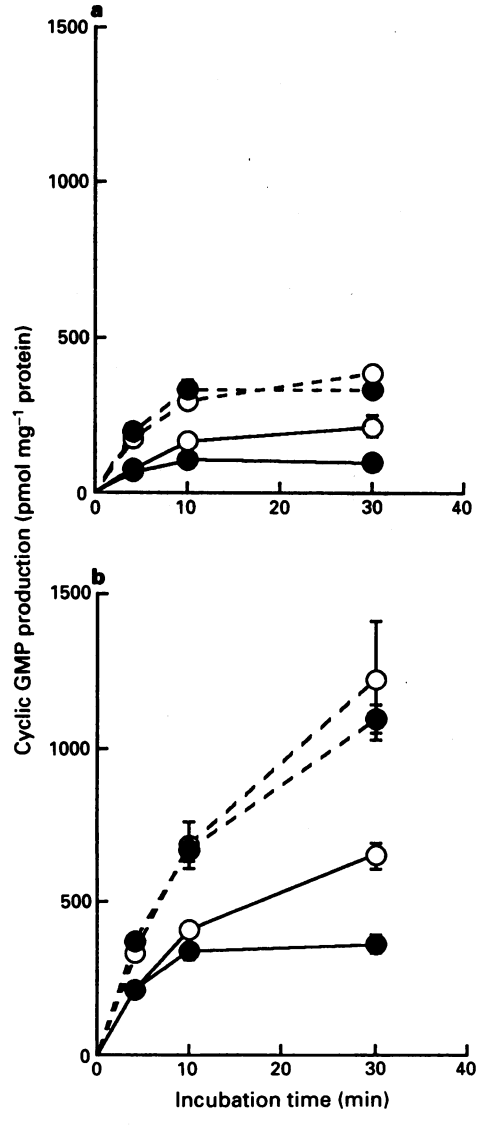


Figure 5 Comparison of effects of ATP and ATPγS on ANP-stimulated guanylyl cyclase activities in plasma membrane fractions of adult and neonatal rat lungs. Crude plasma membranes were incubated for indicated incubation times with (a) ATP or ATPγS at 50 μM and (b) ATP or ATPγS at 200 μM. Measurement of guanylyl cyclase activity was carried out as described in the Methods. Adult (●); neonate (○); ATP (solid lines); ATPγS (dashed lines). Values are means ± s.e.mean of four separate experiments.

Table 1 The values of K_d and B_{max} of [^{35}S]-adenosine 5'-(3-thio)triphosphate ([^{35}S]-ATPγS) binding to lung membrane fractions

	High affinity binding		*Low affinity binding*	
	K_d (μM)	B_{max} (pmol mg^{-1} protein)	K_d (μM)	B_{max} (nmol mg^{-1} protein)
Adult	2.25 ± 0.30	664.5 ± 45.7	373.4 ± 28.5	8.10 ± 0.20
Neonate	2.54 ± 0.15	789.7 ± 100.1	448.5 ± 54.2	8.71 ± 0.15

The activities of [^{35}S]-ATPγS binding to lung membranes of adult and neonate were measured as described in Methods. Values are means ± s.e.mean of five separate experiments.

Table 1. There were no significant differences in K_d values or B_{max} values between adult and neonatal membranes.

ANP-stimulated guanylyl cyclase activities enhanced by ATP were compared with those enhanced by non-hydrolyzable ATPγS in adult and neonatal membranes (Figure 5). The effects of 50 μM and 200 μM ATPγS on the enzyme activities of both membranes were larger than those of 50 μM and 200 μM ATP, respectively. In addition, ANP/ATPγS activated guanylyl cyclase of both membranes to a similar extent. These results raised the possibility that the difference in the ATP effect on ANP-stimulated guanylyl cyclase activities between adult and neonatal membranes is explained by the difference in the ATP hydrolytic activity of the two membrane preparations. To test this possibility, ATPase activities of adult and neonatal lung membranes were compared (Figure 6). ATPase activation depended on ATP concentrations. The order of the efficacy of ATPase activities was adult > neonate at incubation time 4 min at all ATP concentrations tested. At incubation times 10 min and 30 min, the efficacies in both membranes were similar at low concentrations of ATP, but higher in adult than neonate at high concentrations of ATP. These results suggest that the hydrolysis of ATP in part contributes to the smaller ATP effect on guanylyl cyclase in adult membranes. The degree of the ATP effects on ANP-stimulated guanylyl cyclase activities was, however, similar in both membranes at incubation time of 4 min. In addition, at incubation times at 10 min, ANP/ATP-stimulated guanylyl cyclase activity of adult membranes was lower than that of neonatal membranes. Hence, there is a possibility that other factor(s) besides ATPase affects the ATP effect on guanylyl cyclase activity.

Effects of Triton X-100 on guanylyl cyclase activities

There is evidence that some detergents perturb the interaction between ATP and guanylyl cyclase (Kurose *et al.*, 1987; Chang *et al.*, 1990). Hence, we examined effects of 0.1% Triton X-100 on ANP/ATP-stimulated guanylyl cyclase activities at various incubation times in adult and neonatal lung membranes (Figure 7). Addition of 0.1% Triton X-100 diminished the enzyme activity in neonatal membranes and enhanced the activity in adult membranes. As a result of the opposite actions of Triton X-100, the magnitude of the stimulatory effect of ANP/ATP on the enzyme activities became similar in both membranes. Effects of pre-incubation with ATPγS on ANP-stimulated guanylyl cyclase activities of both membranes were compared with those of simultaneous addition of ATPγS in the presence or absence of Triton X-100 (Figure 8). Pre-incubation with 200 μM ATPγS caused much more elevation of ANP-stimulated guanylyl cyclase activities compared to those with simultaneous addition of ANP and 200 μM ATPγS (see Figure 5b). Addition of Triton-X-100, however, almost completely abolished the enhanced effects of pre-incubation with ATPγS. The resulting activities were similar to those induced by simultaneous addition of ATPγS in both membranes. On the other hand, guanylyl cyclase activation by simultaneous addition of ANP and ATPγS was not affected by Triton X-100 in either membrane (see Figure 4b).

It is known that plasma membrane fluidity affects the membrane-related reactions, regulation of intracellular metabolism, and membrane-bound enzymes (Singer & Nicholson, 1972; Shinitzky & Inbar, 1976; Freedman, 1981). It is possible that membrane fluidity of lung membranes affects the ANP/ATP-stimulated guanylyl cyclase activity. Accordingly, the membrane fluidity of adult and neonatal lung membranes was observed by measuring fluorescence polariza-

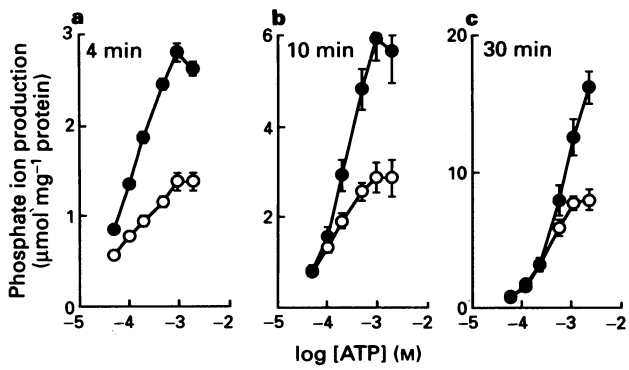


Figure 6 ATPase activities in plasma membrane fractions of adult, and neonatal rat lungs. Crude plasma membranes were incubated with indicated concentrations of ATP for 4 min (a), 10 min (b), and 30 min (c). Inorganic phosphates released by ATPase were measured as described in the Methods. Adult (●); neonate (○). Values are means ± s.e.mean of four separate experiments.

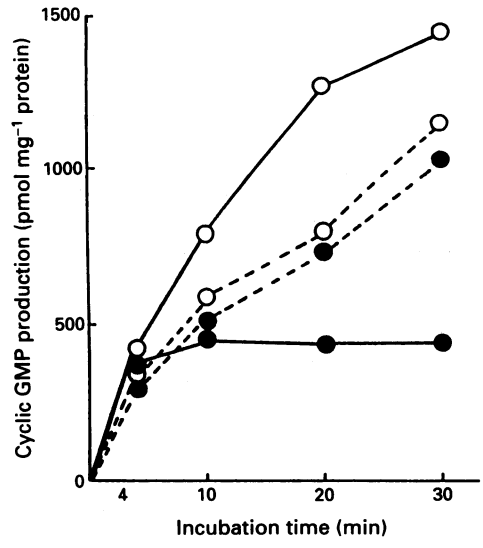


Figure 7 Effects of Triton X-100 treatment on ANP/ATP-stimulated guanylyl cyclase activities in plasma membrane fractions of adult and neonatal rat lungs. Crude plasma membranes were incubated with simultaneous addition of ANP (0.5 μM) and ATP (100 μM) in the presence (dashed lines) and absence (solid lines) of 0.1% Triton X-100 for indicated incubation times. Measurement of guanylyl cyclase activity was carried out as described in the Methods. Adult (●); neonate (○).

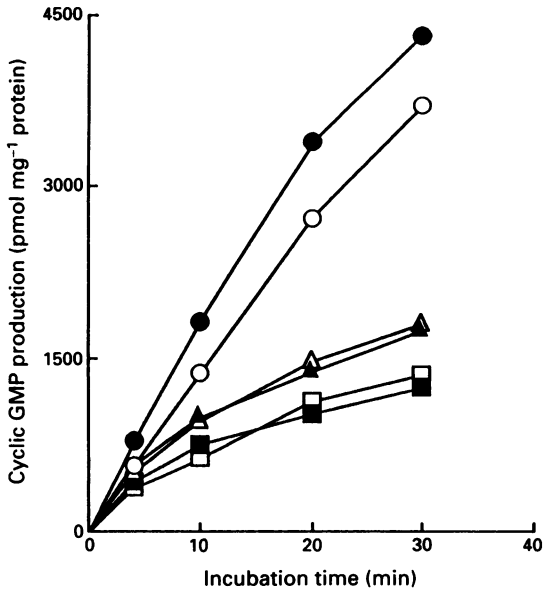


Figure 8 Effects of Triton X-100 on ANP/ATPγS-stimulated guanylyl cyclase activity of plasma membrane fractions of adult (closed symbols) and neonatal (open symbols) rat lungs. Crude plasma membranes were pre-incubated for 5 min with (circles and triangles) or without (squares) ATPγS (200 μM). Thereafter ATPγS (200 μM) was added to the membrane suspensions without ATPγS (squares). All the membrane suspensions containing ATPγS and ANP were used for the measurement of guanylyl cyclase activity according to the Methods in the presence (triangles and squares) and absence (circles) of Triton X-100 for indicated incubation times.

Table 2 Fluorescence polarization of lung membrane fractions

	Fluorescence polarization
Adult	0.2443 ± 0.0018
Neonate	0.2176 ± 0.0009

The groups are significantly different from each other at $P<0.001$. Measurement of fluorescence polarization in lung membranes of adult and neonate is described in Methods. Values are means ± s.e.mean of six separate experiments.

tion of DPH-membrane suspension. As shown in Table 2, the order of the fluorescence polarization was adult > neonate, indicating that the order of magnitude of membrane fluidity was neonate > adult.

Discussion

Developmental changes of ANP-receptor/guanylyl cyclase system were studied using plasma membrane fractions prepared from adult (2 month old) and neonatal (5–7 day old) rat lungs. ANP slightly activated guanylyl cyclase and its activity was markedly enhanced by addition of ATP in both membranes. ATPγS caused much greater enhancement of ANP-stimulated guanylyl cyclase than ATP. ATP and ATPγS had no effect on basal guanylyl cyclase activity of rat lung membranes, in agreement with observations by Marala *et al.* (1991), and in disagreement with observations by other investigators (Kurose *et al.*, 1987; Chang *et al.*, 1990; Gazzano *et al.*, 1991). The stimulatory effects of ATP analogues on basal guanylyl cyclase activities were dependent on Mg^{2+} concentration in incubation medium (Gazzano *et al.*, 1991). The Mg^{2+} concentration and membrane preparation used in our experiments may not be suitable for activation of basal guanylyl cyclase by ATP.

ANP- or ANP/ATP-stimulated guanylyl cyclase activity of adult membranes was approximately one-half that of neonatal membranes when the incubation time was prolonged (10–30 min). The lower enzyme activity of adult membranes was restored to the level of neonatal membranes by addition of increasing ATP concentrations, but fell again with prolongation of incubation time. In contrast, addition of ATPγS exerted a similar degree of activation of ANP-stimulated guanylyl cyclase in both membranes. There was no significant difference in the ability of ATPγS binding between the membranes. ATPase activity of adult membranes was higher than that of neonatal membranes. These results suggest that an increase in ATP hydrolysis decreases the effect of ATP on guanylyl cyclase activity. There was, however, not always an inverse correlation between the incubation time- and ATP concentration-dependent ATPase activities and guanylyl cyclase activities in both membranes. For example, the response of guanylyl cyclase to ANP was similar in both membranes regardless of the presence of ATP, while ATPase activity of adult membranes was already higher than that of neonatal membranes at the early incubation time of 3–4 min. In addition, Kurose *et al.* (1987) reported that ADP and ADPβS also enhanced ANP-stimulated guanylyl cyclase, but their efficacies were only about half that of ATP. These results raised the possibility that other factor(s) besides ATPase affect(s) the ATP effect on guanylyl cyclase.

More recent studies (Leitman *et al.*, 1986; Fuller *et al.*, 1988; Pandey *et al.*, 1988; Chang *et al.*, 1989; Chinkers *et al.*, 1989; Lowe *et al.*, 1989; Schulz *et al.*, 1989; Uchida *et al.*, 1989) using the co-purification of ANP receptor/guanylyl cyclase and molecular cloning, demonstrated that there are three distinct ANP receptor molecules with different molecular weight in various mammalian tissues: types A- and B-receptors are preferentially activated by ANP and BNP (brain natriuretic peptide), and by CNP (clearance natriuretic peptide), respectively. Both receptors are coupled to guanylyl cyclase. Type C-receptors without guanylyl cyclase are related to clearance of excess of ANP, BNP and CNP which are coupled to the adenylyl cyclase/cyclic AMP signal transduction system through inhibitory GTP-binding protein (Anand-Srivastava *et al.*, 1990). Co-purified ANP receptor/guanylyl cyclase which retained ANP-binding characteristics, however, could not be stimulated by ANP, suggesting that some components essential for guanylyl cyclase activation were lost during the purification procedure or that the regulatory domain of the enzyme was labile (Pual *et al.*, 1987; Takayanagi *et al.*, 1987; Meloche *et al.*, 1988).

It was demonstrated that allosteric nucleotide-binding sites for ATP participate in the activation of ANP-stimulated guanylyl cyclase (Kurose *et al.*, 1987; Singh *et al.*, 1988; Chinkers & Garbers, 1989; Marala *et al.*, 1991). In addition, Kurose *et al.* (1987) demonstrated that adenosine analogues, ADP, ADPβS, or AppNHp but not UTP, CTP, and AMP also enhanced ANP-stimulated guanylyl cyclase, although they produced smaller effects than ATP itself. These results suggested that ATP or ATPγS activated guanylyl cyclase via best occupation of the allosteric site(s). The present study showed that there are two classes of ATP-binding sites on plasma membranes of rat lung from Scatchard analysis of ATPγS binding. Therefore, the protein kinase-like domain appears to contain ATP-binding sites.

Particulate guanylyl cyclase activities were enhanced by some detergents due to the unmasking of receptor binding domains (Lad & White, 1979; Garbers & Radnay, 1981; Meloche *et al.*, 1988). In addition, Chang *et al.* (1990) and Gazzano *et al.* (1991) suggested that the effects of ATPγS on stimulating ANP-dependent guanylyl cyclase activity are exerted via the action of accessory proteins or non-protein cofactor which is susceptible to membrane washing and detergents, and is stabilized by ATPγS. The present study showed that Triton X-100 brought about stimulation in adult

membranes and suppression in neonatal membranes of ANP/ATP-stimulated guanylyl cyclase activities, thereby resulting in the abolition of the difference in the responsiveness between the different membranes. In contrast, ATPγS pre-incubation caused much more elevation of ANP-stimulated guanylyl cyclase activities compared with that produced by simultaneous addition of ATPγS. The markedly elevated activities were, however, decreased by Triton X-100 to levels induced by simultaneous addition of ATPγS in both membranes.

The above results, together with results observed by previous investigators suggested the following two possibilities. There exist modulatory factor(s) regulated by ATP. The factor(s) is more abundant in adult membranes than in neonatal membranes, and exhibits time-dependent inhibitory effects on ANP- or ANP/ATP-stimulated guanylyl cyclase activity. The inhibitory effect is counteracted by non-hydrolyzable ATPγS, and the ATPγS effect is not affected by Triton X-100. Another possibility is that conformation of plasma membranes is related to activation of the ANP receptor/guanylyl cyclase system. The guanylyl cyclase activities of membranes were only slightly activated by ANP alone, but markedly activated by ANP/ATP or ANP/ATPγS. The active conformation of the membranes is stabilized by ATPγS pre-incubation and this effect is abolished by Triton X-100. No direct evidence is yet available to support our hypotheses, and the mechanism of actions of Triton X-100 on ANP/ATP-dependent guanylyl cyclase activity cannot be clearly explained. In any case, it seems premature to conclude that Triton X-100 diminishes ANP/ATP-stimulated guanylyl cyclase activity simply by denaturation of the enzyme.

The degree of fluorescence polarization of neonatal membranes was lower than that of adult membranes, indicating that membrane fluidity of neonatal membranes was higher than that of adult membranes. This fact may imply that an essential component for the activation of guanylyl cyclase embedded in the membranes becomes more exposed, and thereby contributes to the enhanced response to ANP (Freedman, 1981).

Weil *et al.* (1986) reported that plasma concentrations of ANP are elevated during the first 2–4 days of human life and decline rapidly, suggesting that the enormous changes which were related to elevated pulmonary arterial pressure occurred in the circulation after birth. The phenomenon that plasma ANP concentration is high in neonates may contribute to an increase in ANP/ATP-dependent cyclic GMP production of neonatal rat lung membranes. Therefore, the characteristics of guanylyl cyclase in adult and neonatal lung membranes should be examined from different aspects.

References

ANAND-SRIVASTAVA, M.B., SAIRAM, M.R. & CANTIN, M. (1990). Ring-deleted analogs of atrial natriuretic factor inhibit adenylate cyclase/cAMP system. *J. Biol. Chem.*, **265**, 8566–8572.

ATLAS, S.A. & LARAGH, J.H. (1986). Atrial natriuretic peptide: a new factor in hormonal control of blood pressure and electrolyte homeostasis. *Annu. Rev. Med.*, **37**, 397–414.

CHAMIENIA, A.L. & JONES, E.J. (1992). The influence of changes in perfusion pressure and angiotensin II on the renal excretory responses to atrial natriuretic peptides. *Eur. J. Pharmacol.*, **218**, 319–325.

CHANG, C.-H., KOHSE, K.P., CHANG, B., HIRATA, M., JIANG, B., DOUGLAS, J.E. & MURAD, F. (1990). Characterization of ATP-stimulated guanylate cyclase activation in rat lung membranes. *Biochim. Biophys. Acta*, **1052**, 159–165.

CHANG, M.-S., LOWE, D.G., EWIS, M., HELLMISS, R., HEN, E. & GOEDDEL, D.V. (1989). Differential activation by atrial and brain natriuretic peptides of two different receptor guanylate cyclases. *Nature*, **341**, 68–72.

CHINKERS, M. & GARBERS, D.L. (1989). The protein kinase domain of the ANP receptor is required for signalling. *Science*, **245**, 1392–1394.

CHINKERS, M., GARBERS, D.L., CHANG, M.-S., LOWE, D.G., CHIN, H., GOEDDEL, D.V. & SCHULZ, S. (1989). A membrane form of guanylate cyclase is an atrial natriuretic peptide receptor. *Nature*, **338**, 78–83.

FISKE, C.H & SUBBAROW, Y. (1925). The colorimetric determination of phosphorus. *J. Biol. Chem.*, **66**, 375–400.

FREEDMAN, R.B. (1981). Membrane-bound enzymes. In *Membrane Structure*, ed. Finean, J.B. & Michell, R.H. pp. 161–214. New York: Elsevier.

FULLER, F., PORTER, J.G., ARFSTEN, A.E., MILLER, J., SCHILLING, J.W., SCARBOUGH, R.M., LEWICKI, J.A. & SCHENK, D.B. (1988). Atrial natriuretic peptide clearance receptor. *J. Biol. Chem.*, **263**, 9395–9401.

GARBERS, D.L. & RADNAY, E.W. (1981). Characteristics of the soluble and particulate forms of guanylate cyclase. *Adv. Cyclic Nucleotide Res.*, **14**, 241–254.

GAZZANO, H., WU, H.I. & WALDMAN, S.A. (1991). Adenine nucleotide regulation of particulate guanylate cyclase from rat lung. *Biochim. Biophys. Acta*, **1077**, 99–106.

HONMA, M., SATOH, T., TAKEZAWA, J. & UI, M. (1977). An ultra sensitive method for the simultaneous determination of cyclic AMP and cyclic GMP in small-volume samples from blood and tissue. *Biochem. Med.*, **18**, 257–273.

IMAMURA, T., OHNUMA, N. & IWASA, F. (1988). Protective effect of alpha-human ANP on chemical-induced pulmonary edema. *Life Sci.*, **42**, 403–414.

INAGAMI, T. (1989). Atrial natriuretic factor. *J. Biol. Chem.*, **264**, 3043–3046.

INOMATA, N., OHNUMA, N. & FURUYA, M. (1987). Alpha-human atrial natriuretic peptide (α-hANP) presents pulmonary edema induced by arachidonic acid treatment in isolated perfused lungs from guinea pig. *Jpn. J. Pharmacol.*, **44**, 211–214.

KUNO, T., ANDRESEN, J.W., KAMISAKI, Y., WALDMAN, S.A., CHANG, L.Y., SAHEKI, S., LEITMAN, D.C., NAKANE, M. & MURAD, F. (1986). Co-purification of an atrial natriuretic factor receptor and particulate guanylate cyclase from rat lung. *J. Biol. Chem.*, **261**, 5817–5823.

KUROSE, H., INAGAMI, T. & UI, M. (1987). Participation of adenosine 5'-triphosphate in the activation of membrane-bound guanylate cyclase by the atrial natriuretic factor. *FEBS Lett.*, **219**, 375–379.

LAD, P.J. & WHITE, A.A. (1979). Effect of alamethicin, gramicidin S and melittin upon the particulate guanylate cyclase from rat lung. *Biochim. Biophys. Acta*, **570**, 198–208.

LEBOWITZ, M.R., MOSES, A.M. & SCHEIMAN, S.J. (1992). Effects of atrial natriuretic peptides on metabolism of arginine vasopressin by isolated perfused rat kidney. *Am. J. Physiol.*, **263**, R273–R278.

LEITMAN, D.C., ANDERSEN, J.W., KUNO, T., KAMISAKI, Y., CHANG, J.-K. & MURAD, F. (1986). Identification of multiple binding sites for atrial natriuretic factor by affinity crosslinking in cultured endothelial cells. *J. Biol. Chem.*, **261**, 11650–11655.

LOWE, D.G., CHANG, M.-S., HELLMISS, R., CHEN, E., SINGH, S., GARBERS, D.L. & GOEDDEL, D.V. (1989). Human atrial natriuretic peptide receptor defines a new paradigm for second messenger signal transduction. *EMBO J.*, **8**, 1377–1384.

LOWRY, O.H., ROSEBROUGH, N.J., FARR, A.L. & RANDALL, R.J. (1951). Protein measurement with the folin phenol reagent. *J. Biol. Chem.*, **193**, 266–275.

MARALA, R.B., SITARAMAYYA, A. & SHARMA, R.K. (1991). Dual regulation of atrial natriuretic factor-dependent guanylate cyclase activity by ATP. *FEBS Lett.*, **281**, 73–76.

MELOCHE, S., MCNICOLL, N., LIU, B., ONG, H. & DELEAN, A. (1988). Atrial natriuretic factor R1 receptor from bovine adrenal zona glomerulosa: purification, characterization, and modulation by amiloride. *Biochemistry*, **27**, 8151–8158.

MUNSON, P. & RODBARD, D. (1980). LIGAND: a versatile computerized approach for characterization of ligand binding system. *Anal. Biochem.*, **107**, 220–239.

NOMURA, T. & KURIHARA, K. (1987). Liposomes as a model for olfactory cells: changes in membrane potential in response to various odorants. *Biochemistry*, **26**, 6135–6140.

PANDEY, K.N., PAVLON, S.N. & INAGAMI, T. (1988). Identification and characterization of three distinct atrial natriuretic factor receptor. *J. Biol. Chem.*, **263**, 13406–13413.

PANDEY, K.N. & SINGH, S. (1990). Molecular cloning and expression of murine guanylate cyclase/atrial natriuretic factor receptor cDNA. *J. Biol. Chem.*, **265**, 12342–12348.

PUAL, A.K., MARALA, R.B., JAISWAL, R.K. & SHARMA, R.K. (1987). Coexistence of guanylate cyclase and atrial natriuretic factor receptor in a 180 kD protein. *Science*, **235**, 1224–1226.

SCHULZ, S., SINGH, S., BELLET, R.A., SINGH, G., TUBB, D.J., CHIN, H. & GARBERS, D.L. (1989). The primary structure of a plasma membrane guanylate cyclase demonstrates diversify within this new receptor family. *Cell*, **58**, 1155–1162.

SHINITZKY, M. & INBAR, M. (1976). Microviscosity parameters and protein mobility in biological membranes. *Biochim. Biophys. Acta*, **433**, 133–149.

SINGER, S.J. & NICHOLSON, G.L. (1972). The fluid model of the structure of cell membranes. *Science*, **175**, 720–731.

SINGH, S., LOWE, D.G., THORPE, D.S., RODRIGNEZ, H., KUANG, W.J., DANGOTT, L.J., CHINKERS, M., GOEDDEL, D.V. & GARBERS, D.L. (1988). Membrane guanylate cyclase is a cell surface receptor with homology to protein kinases. *Nature*, **334**, 708–712.

TAKAYANAGI, R., INAGAMI, T., SNAJDAR, R.M., INADA, T., TAMURA, M. & MISONO, K.S. (1987). Two distinct forms of receptors for atrial natriuretic factor in bovine adrenocortical cells. *J. Biol. Chem.*, **262**, 12104–12113.

UCHIDA, K., MIZUNO, T., SHIMONAKA, M., SUGIURA, N., NARA, K., LING, N., HAGIWARA, H. & HIROSE, S. (1989). Purification and properties of active atrial natriuretic peptide receptor (type C) from bovine lung. *Biochem. J.*, **263**, 671–678.

WEIL, J., BIDLINGMAIER, F., DOHLEMANN, C., KUHNEL, U., STROM, T. & LANG, R.E. (1986). Comparison of plasma ANP levels in healthy children from birth to adult and in children with cardiac disease. *Pediatr. Res*,. **20**, 1328–1331.

(Received July 13, 1993
Revised March 25, 1994
Accepted April 25, 1994)

Br. J. Pharmacol. (1994), **113**, 576–580 © Macmillan Press Ltd, 1994

The effects of aldose reductase inhibition with ponalrestat on changes in vascular function in streptozotocin diabetic rats

Donna J. Otter & [1]Russell Chess-Williams

Department of Biomedical Science, University of Sheffield, Sheffield S10 2TN

1 The responses of rat isolated aortae to vasoconstrictor and vasodilator agents have been studied in 14-day streptozotocin-diabetic rats. The effects of treatment with the aldose reductase inhibitor, ponalrestat, on these responses have also been investigated.

2 Maximum contractile responses and aortic sensitivity to phenylephrine were significantly enhanced in 14-day diabetic aortae.

3 In contrast, endothelium-dependent relaxations to carbachol were depressed in diabetic rats, whilst endothelium-independent relaxations to forskolin and sodium nitroprusside were unchanged.

4 Pretreatment with ponalrestat (25 mg kg^{-1}, daily) prevented both the enhanced maximum contractile responses to phenylephrine and the depressed endothelium-dependent relaxations to carbachol in aortae from 14-day diabetic rats. Ponalrestat however, had no effect on the reduced phenylephrine EC_{50} values observed in tissues from diabetic animals.

5 It is concluded that ponalrestat prevents the depression of endothelium-dependent aortic relaxations induced by diabetes of 14 days duration, suggesting that the polyol pathway is involved in these vascular changes. Ponalrestat does not prevent the increase in aortic sensitivity to α_1-adrenoceptor agonists.

Keywords: Aldose reductase; diabetes mellitus; aorta; α-adrenoceptor; endothelium-dependent relaxation; nitric oxide; ponalrestat; forskolin

Introduction

Diabetes mellitus is associated with several cardiovascular complications, predisposing the patient to diseases such as hypertension, atherosclerosis and thrombosis (Christlieb *et al.*, 1976). This may be due in part, to altered responsiveness of blood vessels to neurotransmitters and hormones (Weidmann *et al.*, 1979). Studies of vascular α-adrenoceptor responsiveness are contradictory with reports of increased (Agrawal *et al.*, 1987; Taylor *et al.*, 1993), decreased (Turlapaty *et al.*, 1980; Cameron & Cotter, 1992) and unchanged (Fulton *et al.*, 1991) vascular α-adrenoceptor responsiveness and receptor density in diabetes.

In addition to changes in vascular smooth muscle function, endothelial alterations have also been documented. However, results are again contradictory. Several studies report impaired endothelium-dependent relaxation (Kamata *et al.*, 1989; Cameron & Cotter, 1992; Taylor *et al.*, 1993), but there have been reports of unchanged (Head *et al.*, 1987; Mulhern & Docherty, 1989) and also enhanced (White & Carrier, 1986) endothelium-dependent relaxation responses induced by diabetes.

In tissues which are insulin-independent for glucose transport, e.g. endothelium (Dvornik, 1978), hyperglycaemia is known to activate the polyol pathway resulting in sorbitol accumulation (Gabbay, 1973). Aldose reductase, the first enzyme in this pathway, has been identified in many tissues susceptible to damage in diabetes, and inhibitors of this enzyme have been shown to be effective in the prevention of diabetic neuropathy (Carrington *et al.*, 1991), reduction of diabetic albuminuria and retinal complications (McCaleb *et al.*, 1991) and reversal of diabetic cataracts (Beyer-Mears & Cruz, 1985).

Few studies have examined the effects of aldose reductase inhibition on diabetes-induced alterations of the cardiovascular system. Ponalrestat has been shown to prevent the decrease in muscarinic receptor density in diabetic rat atria (Kofo-Abayomi & Lucas, 1987) and we have also found this compound prevents the diabetes-induced changes in cardiac β-adrenoceptor sensitivity and receptor density (Austin & Chess-Williams, 1991). In vascular tissue, Cameron & Cotter (1992) have shown prevention of impaired endothelium-dependent relaxation with nitromethane but Taylor *et al.* (1994) have recently reported that ponalrestat treatment does not prevent the depression of endothelium-mediated relaxations of mesenteric arteries from diabetic rats.

In man endothelium-dependent relaxations are depressed (Saenz de Tejada *et al.*, 1989; McVeigh *et al.*, 1992) and we have observed a similar depression in aortae from 14 day streptozotocin diabetic rats. The present study investigates the effects of treatment with ponalrestat on these endothelium-dependent relaxations in diabetic and control rats.

Methods

Pretreatment of animals

Male Wistar rats (230–270 g) were given a single intraperitoneal injection of streptozotocin (STZ, 65 mg kg^{-1}) dissolved in 0.01 M citrate buffer (pH 4.5). Age-matched control rats received citrate buffer alone. Animals were fed normal rat chow and water *ad libitum*. Blood glucose was measured with glucose-sensitive BM glycaemie 1-44 test strips (Boehringer Mannheim) and a Glucochek S.C. (Medistron Limited). STZ-treated animals with blood glucose levels greater than 15 nM were considered diabetic and used in the study. Animals to be pretreated with ponalrestat (Statil, I.C.I.) received the initial intraperitoneal injection of streptozotocin or vehicle and the following day the animals were given an oral dose of ponalrestat (25 mg kg^{-1}). Oral dosing via gavage was continued daily for 2 weeks.

Fourteen days after the induction of diabetes, animals were killed by exsanguination, thoracic aortae rapidly excised, and the adherent fat and connective tissue removed. Segments, approximately 3 mm in length were cut from the aortae and carefully cut longitudinally to form strips. The strips were then mounted in 30 ml organ baths containing Krebs-bicarbonate solution (composition in mM: NaCl 118.4, KCl

[1] Author for correspondence.

4.7, $NaHCO_3$ 25, glucose 11.7, $MgSO_4$ 1.2, $KHPO_4$ 1.2 and $CaCl_2$ 1.9) and gassed with 5% CO_2 in O_2 at 37°C. Isometric tension developed by the circular smooth muscle was recorded via Lectromed UF1 force transducers on a Lectromed M19 chart recorder. Tissues were equilibrated for 60 min under a resting tension of 1 g, with several changes of bathing medium. Cumulative concentration-response curves were then obtained to phenylephrine. Separate tissues were precontracted with phenylephrine (1.1 μM) and relaxation responses obtained to carbachol (0.1–30 μM), forskolin (1 μM) and sodium nitroprusside (300 nM).

Drugs

(−)-Phenylephrine hydrochloride, carbamylcholine chloride, forskolin, sodium nitroprusside and streptozotocin were obtained from Sigma (St. Louis, U.S.A.). Ponalrestat (I.C.I 128436, Statil; MK538, prodiax) was a gift from Zeneca pharmaceuticals, Macclesfield, Cheshire.

Statistics

Drug-induced changes in tension were plotted as a percentage of the maximum change for each concentration-response curve. Individual EC_{50} values (molar concentration producing half-maximal response) were determined and geometric mean EC_{50} values with 95% confidence limits calculated. Differences in mean EC_{50} values were analysed by Analysis of Variance and Student's modified *t* test (Newman-Keuls) applied to individual logarithmic values. Responses were also plotted as a percentage of the precontraction to phenylephrine. Differences in mean responses were analysed by Analysis of Variance and Student's modified *t* test. Differences with a *P* value of 0.05 or less were considered significant.

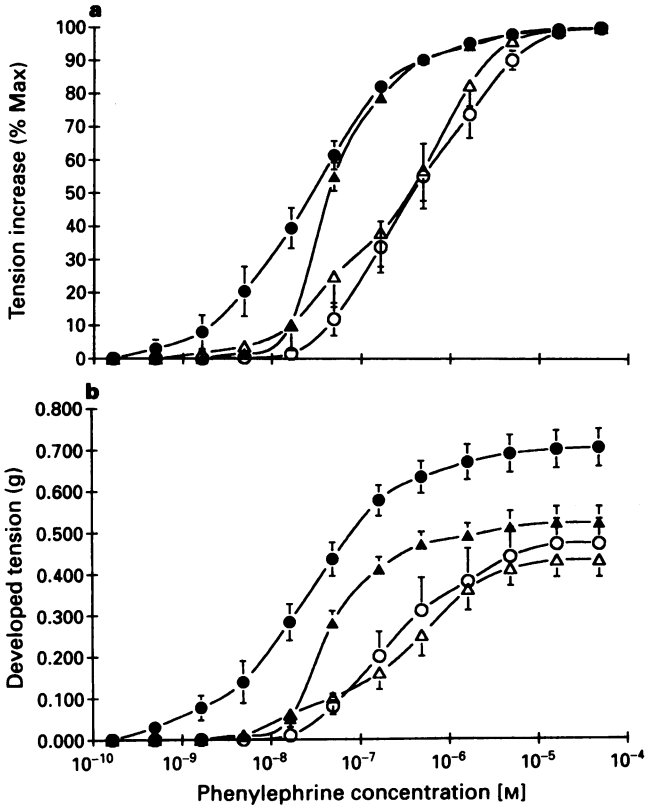


Figure 1 Mean ($n \geq 8$) cumulative concentration-response curves to phenylephrine of aortae from non-diabetic (○), diabetic (●), ponalrestat-treated non-diabetic (△) and ponalrestat-treated diabetic animals (▲). Responses are plotted as (a) mean responses as a percentage of individual maximum responses and (b) the mean tensions developed (± s.e.mean) for each concentration of phenylephrine.

Results

The pretreatment of animals with streptozotocin resulted in the development of symptoms characteristic of diabetes i.e. polydipsia, polyphagia and polyuria. In addition, rats suffered a significant weight loss (18.3 ± 3.4 g) over the 14 day period compared with a weight gain of 60.5 ± 7.9 g for control animals. Blood glucose levels were also elevated (> 16 mM) relative to control animals (8.1 ± 1.1 mM). Treatment of diabetic rats with ponalrestat did not alleviate weight loss (23.3 ± 9.3 g) or the rise in blood glucose levels (> 18 mM). Ponalrestat treatment of control animals did not affect weight gain (66.0 ± 3.8 g) or blood glucose levels (9.4 ± 0.4 mM) over 14 days.

Contractile responses of isolated aortae

Diabetes of 14-days duration enhanced α_1-adrenoceptor-mediated responses of aortae to phenylephrine. The maximum developed tensions were significantly ($P<0.01$) increased in diabetic aortae, whilst concentration-response curves were shifted to the left, resulting in significantly ($P<0.001$) reduced EC_{50} values (Table 1, Figure 1).

Ponalrestat treatment of control animals did not affect responses to phenylephrine, but ponalrestat treatment of diabetic animals significantly ($P<0.05$) reduced the maximum tensions developed to phenylephrine (Table 1, Figure 1). The values for these ponalrestat-treated diabetic animals were then not significantly different from values for control or ponalrestat-treated control rats. However, the diabetes-induced reduction in phenylephrine EC_{50} values was not prevented by ponalrestat and remained significantly reduced in diabetic animals compared with values for control or ponalrestat-treated control animals.

Table 1 Responses of aortae to phenylephrine and carbachol

	Control	*Diabetic*	*Ponalrestat-treated control*	*Ponalrestat-treated diabetic*
Phenylephrine				
Maximum developed tension (g)	0.47 ± 0.06	0.70 ± 0.05**	0.43 ± 0.04	0.52 ± 0.04*
Mean EC_{50} (nM)	401	10.0***	214.9	45.9**
	(161–995)	(4.0–2.1)	(60.0–768.9)	(35.1–60.2)
Carbachol				
Maximum relaxation (g)	0.43 ± 0.03	0.29 ± 0.02***	0.38 ± 0.03	0.38 ± 0.06
Maximum relaxation (%)	78.2 ± 4.4	60.2 ± 4.3**	76.1 ± 7.4	76.3 ± 5.6*
Mean EC_{50} (μM)	0.89	1.31	1.20	1.25
	(0.61–1.29)	(1.05–1.64)	(0.82–1.88)	(0.80–1.80)

Geometric mean ($n \geq 8$) EC_{50} values (with 95% confidence limits) and maximum responses (± s.e.mean) to phenylephrine and carbachol. Relaxation responses to carbachol were recorded following precontraction with 1.1 μM phenylephrine. Responses are expressed as the maximal relaxation in g and also as a percentage of the precontraction to phenylephrine.
*$P<0.05$ relative to diabetics. **$P<0.01$; *** $P<0.001$ relative to controls.

Relaxation responses of isolated aortae

In tissues precontracted with phenylephrine, carbachol induced concentration-related relaxations which were dependent on the presence of an intact endothelium. In aortae from diabetic animals, the relaxation responses were depressed compared with controls (Figure 2a). Maximum relaxation responses were significantly ($P<0.001$) reduced in diabetics compared with controls (Table 1) and this reduction was still observed when responses were expressed as a percentage of the phenylephrine precontraction ($P<0.01$) (Figure 2b). Carbachol EC_{50} values were not significantly different between control and diabetic animals (Table 1).

Maximal relaxations obtained to forskolin (1 μM) were significantly ($P<0.01$) greater in aortae from diabetic animals compared with controls (Table 2). However, this was due to the larger precontraction obtained to phenylephrine in aortae from diabetic animals (0.65 ± 0.1 g) compared with controls (0.43 ± 0.1 g). When responses were expressed as a percentage of the precontraction, responses to forskolin were similar in control and diabetic tissues (Table 2). Similar results were obtained with nitroprusside (300 nM), maximum responses to this agent being similar in aortae from control and diabetic animals when responses were expressed as a percentage of the precontraction to phenylephrine (Table 2).

Relaxation responses to carbachol, whether expressed in absolute tension or as a percentage of the precontraction to phenylephrine, were similar in tissues from ponalrestat-treated control and ponalrestat-treated diabetic animals (Figure 2, Table 1). The values for ponalrestat-treated animals, both diabetic and non-diabetic, were also similar to those for untreated control animals. However, maximum relaxations to carbachol of tissues from ponalrestat-treated diabetic rats were significantly greater than those for tissues from untreated diabetic animals (Table 1). Ponalrestat treatment did not affect carbachol EC_{50} values in any of the animal groups studied.

Relaxation responses to forskolin and nitroprusside were similar in tissues from ponalrestat-treated control and ponalrestat-treated diabetic rats and these were not significantly different from the values obtained for control non-diabetic and diabetic animals (Figure 2).

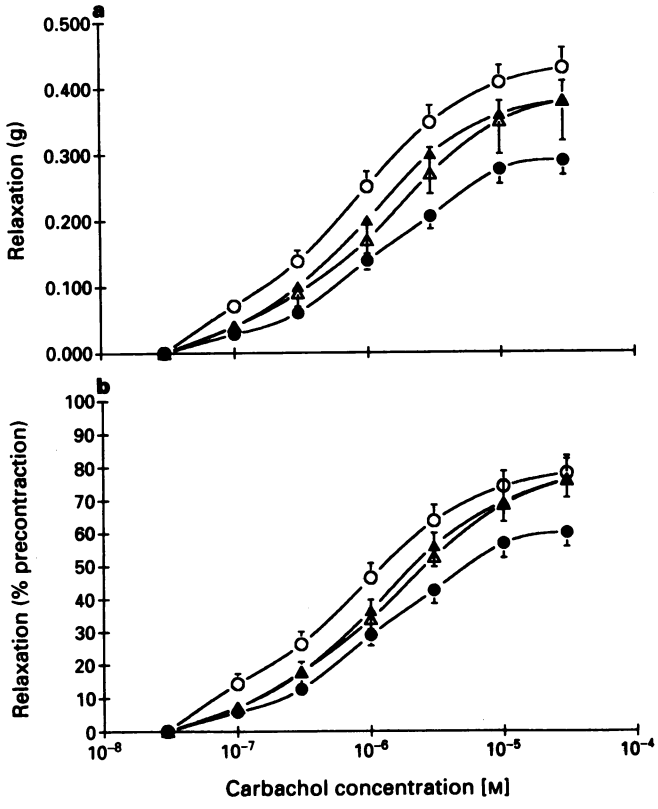


Figure 2 Mean ($n \geq 4$) cumulative concentration-response curves to carbachol of aortae from non-diabetic (○), diabetic (●), ponalrestat-treated non-diabetic (△) and ponalrestat-treated diabetic animals (▲). Responses are plotted as (a) relaxation in g, and (b) a percentage of the phenylephrine precontraction.

Discussion

In the present study aortae from rats with 14-day streptozotocin-induced diabetes demonstrated enhanced α-adrenoceptor-mediated vasoconstrictions and depressed endothelium-dependent relaxations. Treatment with ponalrestat prevented some but not all of these vascular changes.

The enhanced vasoconstrictor responses to phenylephrine were exhibited as a change in both sensitivity (decrease in EC_{50}) and responsiveness (increase in maximum response). Ponalrestat prevented the latter but not the former effect suggesting that two mechanisms were operating to increase aortic responses to phenylephrine in diabetes, only one of which involves the polyol pathway. An increase in the maximum responses to noradrenaline and phenylephrine has been reported by other investigators (Agrawal *et al.*, 1987; White & Carrier, 1988). The reduced endothelial-mediated effects observed in diabetic animals may provide an explanation for the effect of diabetes on the maximum responses to phenylephrine. The contractile responses of vascular tissues with intact endothelium can be inhibited by simultaneous nitric oxide release (Martin *et al.*, 1986). If this is reduced in diabetes, as observed in the present study, responses to contractile agents such as phenylephrine may be enhanced. In support of this hypothesis, ponalrestat was found to prevent both the depressed endothelial-mediated relaxation responses to carbachol and the increased maximal responses to phenylephrine. In contrast, the change in sensitivity (decreased EC_{50} values) to phenylephrine in aortae from diabetic rats was not affected by aldose reductase pretreatment, suggesting that a different mechanism may be operating. This suggestion is supported by the report that maximal responses

Table 2 Relaxation responses of aortae to forskolin and nitroprusside

	Control	*Diabetic*	*Ponalrestat-treated control*	*Ponalrestat-treated diabetic*
Forskolin				
Maximum relaxation (g)	0.46 ± 0.04	0.69 ± 0.07**	0.55 ± 0.05	0.62 ± 0.05
Maximum relaxation (%)	111.4 ± 6.2	107.5 ± 1.9	108.28 ± 3.0	113.1 ± 5.4
Nitroprusside				
Maximum relaxation (g)	0.26 ± 0.03	0.59 ± 0.09***	0.48 ± 0.05*	0.51 ± 0.05*
Maximum relaxation (%)	101.8 ± 3.9	101.6 ± 4.6	107.34 ± 5.3	105.9 ± 3.1

Geometric mean ($n \geq 7$) EC_{50} values (with 95% confidence limits) and mean maximum responses (± s.e.mean) to forskolin (1 μM) and nitroprusside (300 nM). Responses are expressed as the relaxation in g and also as a percentage of the initial precontraction to phenylephrine.
*$P<0.05$; **$P<0.01$; *** $P<0.001$ relative to controls.

and sensitivity of isolated aortae to noradrenaline and methoxamine are enhanced in diabetes when tissues have an intact endothelium but in denuded tissues only sensitivity is increased in diabetes (Harris & MacLeod, 1988).

Taylor *et al.* (1994) have also found ponalrestat to be ineffective in preventing the reduction in EC_{50} values for noradrenaline-induced contractile responses of mesenteric arteries from the diabetic rat. Possible mechanisms which may be operating to increase aortic sensitivity to α_1-adrenoceptor agonists include an alteration in calcium handling as observed in the hearts of diabetic animals (Heygler *et al.*, 1987). The α_1-adrenoceptor-mediated responses of the rat aorta are at least partially coupled to the influx of extracellular calcium (Macleod & McNeill, 1985). Alternatively, a diabetes-induced reduction in sympathetic tone to the vasculature may increase vascular α-adrenoceptor density. Such a change in sympathetic nerve activity has been proposed to explain the increase in β-adrenoceptor sensitivity and receptor density observed in 2-week diabetic rat hearts (Austin & Chess-Williams, 1991). The mechanisms involved in the sensitivity changes were not investigated in the present study, but they would appear to be specific for the α-adrenoceptor since previous studies reporting increased α-adrenoceptor responsiveness have found responses to 5-hydroxytryptamine and calcium to be unaltered in diabetic animals (Agrawal *et al.*, 1987; Harris & MacLeod, 1988).

The depressed endothelium-dependent relaxations to carbachol observed in the present study agree with reports from other laboratories using streptozotocin-diabetic rats (Kamata *et al.*, 1989; Cameron & Cotter, 1992) and spontaneously diabetic rats (Durante *et al.*, 1988). In addition, endothelium-dependent relaxations are impaired in human diabetes (Saenz de Tejada *et al.*, 1989; McVeigh *et al.*, 1992). The cause of this depression is unknown but in the present study the relaxation responses of the smooth muscle to forskolin, a direct activator of adenylate cyclase (Seamon & Daley, 1983), were unchanged suggesting that there was no general depression of relaxation responses. Furthermore, responses to nitroprusside, a nitric oxide donor, were not affected by the diabetic state and suggest that the responsiveness of vascular smooth muscle to guanosine 3′:5′-cyclic monophosphate (cyclic GMP) was unaffected and the defect in endothelium-dependent relaxations to carbachol exists at the level of nitric oxide synthesis and/or release. The elevation in responses to forskolin and nitroprusside when the data were expressed in absolute values (i.e. g) was solely due to the increased precontraction induced by phenylephrine in tissues from diabetic animals and the effect was not seen when the data were expressed as a percentage of the precontraction values. Relaxation responses to carbachol were depressed in aortae from diabetic animals whichever method was used to express the results.

There have been suggestions that increased production of vasoconstrictor arachidonic acid metabolites is responsible for impaired endothelium-dependent relaxation in diabetes (Tesfamariam *et al.*, 1990). Although the present study cannot rule this out, a number of reports have shown that blocking the action of these substances in aortae does not prevent impaired endothelium-mediated responses (Pieper & Gross, 1988; Hattori *et al.*, 1991). Furthermore, in our preliminary studies we found that indomethacin (10 μM) failed to inhibit responses to carbachol, and relaxations were depressed in aorta from diabetic rats even in the presence of indomethacin (unpublished data). N^G-monomethyl-L-arginine (L-NMMA, 50 μM) was also found to inhibit responses equally in aortae from control and diabetic animals whilst methylene blue (10 μM) virtually abolished responses to carbachol in both experimental groups. These data indicate that relaxation responses to carbachol were mediated via nitric oxide.

The most probable explanation for the reduced relaxation responses would appear to be an alteration in the vascular endothelium resulting in reduced synthesis, release and/or breakdown of EDRF (NO). Indeed endothelial damage has been reported in diabetes (Moore *et al.*, 1985), although others have found functional changes without apparent endothelium damage (Hattori *et al.*, 1991). The beneficial effects of ponalrestat on the diabetes-induced changes in relaxation in the present study imply that the polyol pathway is involved in the functional defect, at least in larger capacitance vessels. Recent reports however, suggest that this protective effect may not be exerted on smaller resistance vessels, since ponalrestat treatment did not reverse the diabetes-induced defect in endothelium-dependent relaxations in perfused mesenteric vessels (Taylor *et al.*, 1994). If proved correct, this may limit the usefulness of aldose reductase inhibitors in preventing diabetic neuropathy which, at least in experimental models of diabetes mellitus, has been shown to be preceded by reductions in nerve blood flow (Stevens *et al.*, 1994).

A number of mechanisms may explain the role of the polyol pathway in endothelial dysfunction (see Cameron & Cotter, 1992). When the polyol pathway flux is high, glucose is diverted through the pentose phosphate shunt (Dvornik, 1987), which requires three molecules of ATP for each molecule of glucose (Davidson & Murphy, 1985) and this can produce an ATP deficit. Since agonist-stimulated NO release requires energy (Griffith *et al.*, 1986) nitric oxide production may be limited. Alternatively, free radicals may be involved in the endothelial dysfunction. Reduced glutathione (GSH) and superoxide dismutase (SOD) levels in diabetes have been reported (Loven *et al.*, 1986), possibly caused by reductions in NADPH and NAD^+ due to the increased flux through the polyol pathway. The reduction in GSH and SOD would render cells less able to cope with oxidative stress, as seen in the reports of increased sensitivity to superoxide damage (Pieper & Gross, 1988) and increased accumulation of superoxide anions in diabetes (Hattori *et al.*, 1991). Superoxide ions break down nitric oxide (Gryglewski *et al.*, 1986) and it has been reported that SOD can restore impaired endothelium-dependent relaxation to normal (Hattori *et al.*, 1991). In our laboratory however, SOD potentiates carbachol relaxations in both diabetic and control tissues. Relaxations to carbachol, even when experiments were performed in the presence of SOD (30 units ml^{-1}), were still significantly reduced in aortae from diabetic rats (92.7 ± 8.0% of the precontraction) compared to controls (121.0 ± 8.8%).

In conclusion, the present study demonstrates enhanced α-adrenoceptor contractile responses and depressed endothelium-dependent relaxations in aortae from 14 day streptozotocin diabetic rats. The increase in vascular α_1-adrenoceptor sensitivity was independent of the change in endothelial function. Ponalrestat proved to be beneficial in the prevention of these functional changes implicating the involvement of the polyol pathway in diabetes-induced alterations in endothelium-dependent relaxations.

References

AGRAWAL, D.K., BHIMJI, S. & MCNEILL, J.H. (1987). Effect of chronic experimental diabetes on vascular smooth muscle function in rabbit carotid artery. *J. Cardiovasc. Pharmacol.*, **9**, 584–593.

AUSTIN, C.E. & CHESS-WILLIAMS, R. (1991). Diabetes-induced changes in cardiac β-adrenoceptor responsiveness: effects of aldose reductase inhibition with ponalrestat. *Br. J. Pharmacol.*, **102**, 478–482.

BEYER-MEARS, A. & CRUZ, E. (1985). Reversal of diabetic cataract by sorbinil, an aldose reductase inhibitor. *Diabetes*, **34**, 15–21.

CAMERON, N.E. & COTTER, M.A. (1992). Impaired contraction and relaxation in aorta from streptozotocin-diabetic rats: role of polyol pathway. *Diabetologia*, **35**, 1011–1019.

CARRINGTON, A.L., ETTLINGER, C.B., CALCUTT, N.A. & TOMLINSON, D.R. (1991). Aldose reductase inhibition with imirestat, effects on impulse conduction and insulin-stimulation of Na^+/K^+-adenosine triphosphatase activity in sciatic nerves of STZ-diabetic rats. *Diabetologia*, **34**, 397–401.

CHRISTLIEB, A.R., JANKA, H., KRAUS, B., GLEASON, R.E., ICASAS-CABRAL, E.A., AIELLO, L.M., CABRAL, B.V. & SOLANO, A. (1976). Vascular reactivity to Angiotensin II and to norepinephrine in diabetic subjects. *Diabetes*, **25**, 268–274.

DAVIDSON, W.S. & MURPHY, D.G. (1985). Aldehyde reductases and their involvement in muscular dystrophy. In *Enzymology of Carbonyl Metabolism 2: Aldehyde Dehydrogenase, Aldo-keto Reductase, and Alcohol Dehydrogenase.* ed. Flynn, T.G. & Weiner, H. pp. 251–263. New York: A.R. Liss Inc.

DURANTE, W., SEN, A.K. & SUNAHARA, F.A. (1988). Impairment of endothelium-dependent relaxation in aortae from spontaneously diabetic rats. *Br. J. Pharmacol.*, **94**, 463–468.

DVORNIK, D. (1987). Hyperglycaemia in the pathogenesis of diabetic complications. In *Aldose Reductase Inhibition. An Approach to the Prevention of Diabeteic Complications.* ed. Porte, D. pp. 69–151. New York: Biomedical Information Corporation.

DVORNIK, D. (1978). Chronic complications of diabetes. *Annu. Rep. Med. Chem.*, **13**, 159–166.

FULTON, J.R., HODGSON, W.C., SIKORSKI, B.W. & KING, R.G. (1991). Attenuated responses to endothelin-1, KCl and $CaCl_2$, but not noradrenaline, of aortae from rats with streptozotocin-induced diabetes mellitus. *Br. J. Pharmacol.*, **104**, 928–932.

GABBAY, K.H. (1973). The sorbitol pathway and the complications of diabetes. *New Engl. J. Med.*, **288**, 831–836.

GRIFFITH, T.M., EDWARDS, D.H., NEWBY, A.C., LEWIS, M.J. & HENDERSON, A.H. (1986). Production of endothelium-derived relaxant factor is dependent on oxidative phosphorylation and extracellular calcium. *Cardiovasc. Res.*, **20**, 7–12.

GRYGLEWSKI, R.J., PALMER, R.M.J. & MONCADA, S. (1986). Superoxide anion is involved in the breakdown of endothelium-derived vascular relaxing factor. *Nature*, **320**, 454–456.

HARRIS, K.H. & MACLEOD, K.M. (1988). Influence of endothelium on contractile responses of arteries from diabetic rats. *Eur. J. Pharmacol.*, **153**, 55–64.

HATTORI., Y., KAWASAKI, H., ABE, K. & KANNO, M. (1991). Superoxide dismutase recovers altered endothelium-dependent relaxation in diabetic rat aorta. *Am. J. Physiol.*, **261**, H1086–H1094.

HEAD, R.J., LONGHURST, P.A., PANEK, R.L. & STITZEL, R.E. (1987). A contrasting effect of the diabetic state upon the contractile responses of aortic preparations from the rat and rabbit. *Br. J. Pharmacol.*, **91**, 275–286.

HEYGLER, C.E., PRAKASH, A. & MCNEILL, J.H. (1987). Alterations in sarcolemmal Ca2+ pump activity during diabetes mellitus. *Am. J. Physiol.*, **252**, H540–H544.

KAMATA, K., MIYATA, N. & KASUYA, Y. (1989). Impairment of endothelium-dependent relaxation and changes in levels of cGMP in aorta from STZ-induced diabetic rats. *Br. J. Pharmacol.*, **97**, 614–618.

KOFO-ABAYOMI, A. & LUCAS, P.D. (1987). Muscarinic receptor density is reduced in diabetic rat atria, an effect prevented by the aldose reductase inhibitor, Statil. *J. Pharm. Pharmacol.*, **39**, 1019–1021.

LOVEN, D., SCHEDL, H., WILSON, H., DAABEES, T.T., STEGINK, L.D., DIEKUS, T.T. & OBERLEY, L. (1986). Effect of insulin and oral glutathione or glutathione levels and superoxide dismutase activities in organs of rats with streptozotocin-induced diabetes. *Diabetes*, **35**, 503–507.

MACLEOD, K.M. & MCNEILL, J.H. (1985). The influence of chronic experimental diabetes on contractile responses of rat isolated blood vessels. *Can. J. Physiol. Pharmacol.*, **63**, 52–57.

MARTIN, W., FURCHGOTT, R.F., VILLANI, G.M. & JOTHIANANDAN, D. (1986). Depression of contractile responses in rat aorta by spontaneously released endothelium-derived relaxing factor. *J. Pharmacol. Exp. Ther.*, **237**, 529.

MCCALEB, M.L., MCKEAN, M.L., HOHMAN, T.C., LAVER, N. & ROBISON, W.G. (1991). Intervention with the aldose reductase inhibitor, tolrestat, in renal and retinal lesions of STZ-diabetic rats. *Diabetologia*, **34**, 695–701.

MCVEIGH, G.E., BRENNAN, G.M., JOHNSTON, G.D., MCDERMOTT, B.J., MCGRATH, L.T., HENRY, W.R., ANDREWS, J.W. & HAYES, J.R. (1992). Impaired endothelium-dependent and independent vasodilation in patients with type 2 (non-insulin-dependent) diabetes mellitus. *Diabetologia*, **35**, 771–776.

MOORE, S.A., BOHLEN, H.G., MILLER, B.G. & EVAN, A.P. (1985). Cellular and vessel wall morphology of cerebral cortical arterioles after short term diabetes in adult rats. *Blood Vessels*, **22**, 265–277.

MULHERN, M. & DOCHERTY, J.R. (1989). Effects of experimental diabetes on the responsiveness of rat aorta. *Br. J. Pharmacol.*, **97**, 1007–1012.

PIEPER, G.M. & GROSS, G.J. (1988). Oxygen free radicals abolish endothelium-dependent relaxation in diabetic rat aorta. *Am. J. Physiol.*, **255**, H825–H833.

SAENZ DE TEJADA, I., GOLDSTEIN, I., AZADZOI, K., KRANE, R.J. & COHEN, R.A. (1989). Impaired neurogenic and endothelium-mediated relaxation of penile smooth muscle from diabetic men with impotence. *New Engl. J. Med.*, **320**, 1025–1030.

SEAMON, K.B. & DALEY, J.W. (1983). Forskolin, cyclic AMP and cellular physiology. *Trends Pharmacol. Sci.*, **4**, 120–123.

STEVENS, E.J., CARRINGTON, A.L. & TOMLINSON, D.R. (1994). Nerve ischaemia in diabetic rats: time-course of development, effect of insulin treatment plus comparison of streptozotocin and BB models. *Diabetologia*, **37**, 43–48.

TAYLOR, P.D., WICKENDEN, A.D., MIRRLEES, D.J. & POSTON, L. (1994). Endothelial functon in the isolated perfused mesentery and aorta of rats with streptozotocin-induced diabetes: effect of treatment with the aldose reductase inhibitor ponalrestat. *Br. J. Pharmacol.*, **111**, 42–47.

TESFAMARIAM, B., BROWN, M.L., DEYKIN, D. & COHEN, R.A. (1990). Elevated glucose promotes generation of endothelium-derived vasoconstrictor prostanoids in rabbit aorta. *J. Clin. Invest.*, **85**, 929–932.

TURLAPATY, P.D.M.V., LUM, G. & ALTURA, B.M. (1980). Vascular responsiveness and serum biochemical parameters in alloxan diabetes mellitus. *Am. J. Physiol.*, **239**, E412–E421.

WEIDMANN, P., BERETTA-PICCOLI, C., GLUCK, Z., KEUSCH, G., MUJAGIC, M., GRIMM, M., MEIER, A. & ZIEGLER, W.H. (1979). Sodium-volume factor, cardiovascular reactivity and hypotensive mechanism of diuretic therapy in mild hypertension associated with diabetes mellitus. *Am. J. Med.*, **67**, 779–784.

WHITE, R.E. & CARRIER, G.O. (1986). Supersensitivity and endothelium dependency of histamine-induced relaxation in mesenteric arteries isolated from diabetic rats. *Pharmacology*, **33**, 34–38.

WHITE, R.E. & CARRIER, G.O. (1988). Enhanced vascular α-adrenergic neuroeffector system in diabetes: importance of calcium. *Am. J. Physiol.*, **255**, H1036–H1042.

(Received February 3, 1994
Revised May 9, 1994
Accepted June 16, 1994)

Br. J. Pharmacol. (1994), **113**, 581–587 © Macmillan Press Ltd, 1994

Characterization of prostanoid receptors on rat neutrophils

[1]Helen Wise & Robert L. Jones

Department of Pharmacology, The Faculty of Medicine, The Chinese University of Hong Kong, Shatin, New Territories, Hong Kong

1 The effects of various prostanoid agonists have been compared on the increase in intracellular free calcium ($[Ca^{2+}]_i$) and the aggregation reaction of rat peritoneal neutrophils induced by N-formyl-L-methionyl-L-leucyl-L-phenylalanine (FMLP).

2 Prostaglandin E_2 (PGE_2) and the specific IP-receptor agonist, cicaprost, both inhibited the FMLP-induced increase in $[Ca^{2+}]_i$ (IC_{50} 33 nM and 18 nM respectively) and the FMLP-induced aggregation reaction (IC_{50} 5.6 nM and 7.9 nM respectively). PGD_2, $PGF_{2\alpha}$, and the TP-receptor agonist, U 46619, were inactive at the highest concentration tested (1 μM).

3 The EP_1-receptor agonist, 17-phenyl-ω-trinor PGE_2, and the EP_3-receptor agonists, GR 63799X and sulprostone, had no inhibitory effect on FMLP-stimulated rat neutrophils.

4 PGE_1 (EP/IP-receptor agonist) and iloprost (IP-receptor agonist) inhibited the FMLP-induced increase in $[Ca^{2+}]_i$ with IC_{50} values of 34 nM and 38 nM respectively. The EP_2-receptor agonists, butaprost and misoprostol (1 μM), inhibited both FMLP-stimulated $[Ca^{2+}]_i$ and aggregation. However another EP_2-receptor agonist, AH 13205, was inactive in both assays.

5 Prostanoid receptors present on rat neutrophils were further characterized by measuring [^{3}H]-adenosine 3′:5′-cyclic monophosphate ([^{3}H]-cyclic AMP) accumulation. Only those agonists capable of stimulating [^{3}H]-cyclic AMP accumulation were able to inhibit both FMLP-stimulated $[Ca^{2+}]_i$ and aggregation.

6 These results indicate that rat neutrophils possess inhibitory IP and EP-receptors; the relative potencies of PGE_2, misoprostol and butaprost are those expected for the EP_2-receptor subtype. No evidence for DP, FP, TP or EP_1 and EP_3-receptors was obtained.

Keywords: Prostaglandin E_2; prostacyclin; prostanoid receptors; cyclic AMP accumulation; intracellular free calcium; FMLP-stimulated aggregation; rat peritoneal neutrophils

Introduction

Neutrophils play a major role in the body's defence against infection and trauma and contribute towards pathophysiological conditions such as adult respiratory distress syndrome (ARDS) (Winder *et al.*, 1993), myocardial infarction and rheumatoid arthritis (Carlos & Harlan, 1990). Neutrophils can be recruited to areas of local inflammation in response to a variety of chemotactic stimuli such as N-formyl-L-methionyl-L-leucyl-L-phenylalanine (FMLP), platelet-activating factor (PAF), complement fragment C5a, and leukotriene B_4 (LTB_4). Activation of neutrophils by chemotactic factors results in degranulation, NADPH oxidase-catalysed superoxide (O_2^-) production, and a variety of other cellular responses (De Togni *et al.*, 1984; Rossi, 1986).

Neutrophil responses can be modulated by prostaglandins (Gryglewski & Salvemini, 1992) with prostaglandins having both pro- and anti-inflammatory roles (Goodwin, 1991; Kitsis *et al.*, 1991; Phipps *et al.*, 1991). Prostaglandins have been shown to have inhibitory effects on neutrophil responses *in vivo* (Fantone *et al.*, 1981) and *in vitro* (Fantone & Kinnes, 1983; Ham *et al.*, 1983; De Togni *et al.*, 1984; Kato *et al.*, 1986; Gryglewski *et al.*, 1987; Ney & Schrör, 1989; 1991; Nagata *et al.*, 1992). Prostaglandins inhibit only responses mediated by direct receptor activation and do not inhibit phorbol ester or A23187-induced responses (Fantone & Kinnes, 1983; De Togni *et al.*, 1984; Ney & Schrör, 1991).

Since adenosine 3′:5′-cyclic monophosphate (cyclic AMP) also inhibits neutrophil function and is thought to provide negative feedback control of neutrophil activation (De Togni *et al.*, 1984; Verghese *et al.*, 1985; Nagata *et al.*, 1992; Nielsen *et al.*, 1992), it is presumed that the prostaglandin-mediated effects may also be due to elevated neutrophil cyclic AMP resulting from activation of prostaglandin receptors. PGE_1 and PGE_2 have been shown to be consistently effective in inhibiting human neutrophil responses and recent evidence suggests that their effect is mediated via an EP_2-receptor (Armstrong & Talpain, 1992; Wheeldon & Vardey, 1993) which is coupled positively to adenylyl cyclase (Coleman *et al.*, 1990). In contrast, it has been reported that stimulation of EP_3-receptors (which are negatively coupled to adenylyl cyclase) by sulprostone leads to potentiation of opsonized zymosan-induced release of LTB_4 from human neutrophils (Wheeldon & Vardey, 1993) and directly stimulates chemotaxis (Armstrong, 1992).

The aim of the present study therefore was to characterize the major prostanoid receptors present on rat neutrophils, and to examine the EP-receptor in more detail. The effects of a comprehensive range of prostanoid receptor-selective agonists have been tested for potentiation or inhibition of neutrophil function, as measured by changes in FMLP-stimulated $[Ca^{2+}]_i$ and aggregation. These same agonists were also tested for effects on the production of cyclic AMP.

Methods

Preparation of neutrophils

Male, Sprague-Dawley rats fed *ad libitum* and weighing 190–230 g were used throughout this study. Peritoneal neutrophils were elicited by intraperitoneal injection of 3 ml of NIH thioglycollate broth (0.26 g ml^{-1}) 19 h prior to harvesting the cells (Fisker *et al.*, 1990). The rats were killed by cervical dislocation, and the leucocytes collected from the peritoneal cavity by lavage with 40 ml of ice-cold HEPES-

[1] Author for correspondence.

buffered saline (HBS:composition, mM: NaCl 145, KCl 5, $MgCl_2$ 1, HEPES acid, 10, pH 7.55) supplemented with glucose (10 mM) and bovine serum albumin (1%, w/v). The cells were centrifuged at 20°C for 10 min at 300 *g*, and washed once in the same buffer. The cell suspension was then layered over Ficoll-paque and centrifuged at 20°C for 20 min at 700 *g* in a swing-out rotor. The resulting cell pellet contained 89 ± 1% neutrophils (assessed microscopically using Wright's stain). The main contaminating cell types were mononuclear leukocytes (Fisker *et al.*, 1990). The viability of cells in the final cell pellet was 94 ± 1% as judged by the Trypan blue exclusion test ($n = 19$).

Neutrophil aggregation

Neutrophil aggregation was measured with a Chrono-log platelet aggregometer set at 37°C and 800 r.p.m. (Ford-Hutchinson & Evans, 1988). The cells were resuspended in HBS supplemented with glucose (10 mM) to a cell density of 5×10^6 cells ml^{-1}. The aggregometer was adjusted to record 0% light transmission with unstimulated neutrophils and 100% transmission with 2.5×10^6 cells ml^{-1}. The cell suspension (500 µl) was incubated in siliconized cuvettes for 1 min with the addition of $CaCl_2$ (1 mM). Test drugs (5 µl) were then added for 2 min followed by FMLP (16 nM). Maximal aggregation was defined as the maximal change in light transmission during the 1–2 min following addition of FMLP and is expressed in arbitrary units (mm deflection of pen recorder). Control responses to FMLP alone were tested regularly throughout the course of each experiment.

Measurement of cytosolic free calcium concentration $[Ca^{2+}]_i$

$[Ca^{2+}]_i$ was measured by resuspending the cells in HBS supplemented with glucose (10 mM), $CaCl_2$ (1 mM) and bovine serum albumin (1%, w/v), to a cell density of 6×10^6 cells ml^{-1} (McCarthy *et al.*, 1989). The cell suspension was incubated with fura-2 acetoxy methyl ester (1 µM) for 30 min at 37°C, then the cells were washed and resuspended in the same medium to a cell density of 2×10^6 cells ml^{-1}. The cell suspension was kept at room temperature until required, and could be kept for at least 5 h after loading without substantial leakage of fura-2 from the cells, increase in basal $[Ca^{2+}]_i$, or decrease in responsiveness to FMLP. In all experiments, a control sample of cells was not incubated with dye; these cells were used to measure autofluorescence.

Samples (0.7 ml) of cell suspension were centrifuged in a Hettich microfuge for 30 s at 11,000 *g* and then resuspended to 1 ml with HBS containing glucose (10 mM) and $CaCl_2$ (1 mM). Fura-2 fluorescence of neutrophil suspensions (510 nm emission) was determined at 37°C with constant stirring, using a Hitachi F-4010 fluorescence spectrophotometer. $[Ca^{2+}]_i$ was measured as the ratio of fura-2 fluorescence at excitation wavelengths of 340 and 380 nm according to the method of Grynkiewicz *et al.* (1985). Cells were incubated for 1 min before the addition of test drug ($\leq$ 10 µl) which was followed after 2 min with FMLP (1 nM). The FMLP-induced change in $[Ca^{2+}]_i$ was calculated as the maximal change in $[Ca^{2+}]_i$ during the 30 s following addition of FMLP. Control responses to FMLP alone were tested regularly throughout the course of each experiment. The various concentrations of prostanoids tested were added in a random sequence. There were no detectable solvent effects for any of the compounds tested.

Measurement of [^{3}H]-cyclic AMP accumulation

Cyclic AMP production was assayed by measuring the conversion of [^{3}H]-ATP to [^{3}H]-cyclic AMP according to Barber *et al.* (1980). Rat neutrophils were incubated with [^{3}H]-adenine (10 µCi ml^{-1}) for 60 min at 37°C in buffer (HBS supplemented with glucose (10 mM), $CaCl_2$ (1 mM) and bovine serum albumin (1%, w/v)) at a cell density of 3×10^7 cells ml^{-1}. Labelled cells were washed and incubated at 1×10^7 cells ml^{-1} in buffer containing the type IV phosphodiesterase (PDE) inhibitor, rolipram (0.1 mM), indomethacin (3 µM) and adenosine deaminase (1 u ml^{-1}). After 10 min incubation at 37°C, test drugs were added for a further 10 min when the reaction was terminated by the addition of ice-cold 7.5% trichloroacetic acid.

[^{3}H]-ATP was separated from [^{3}H]-cyclic AMP by column chromatography according to Salomon *et al.* (1974). [^{14}C]-cyclic AMP (10,000 d.p.m.) was added to each sample prior to column elution to correct for the percentage recovery of the columns. The levels of [^{3}H]-cyclic AMP and [^{14}C]-cyclic AMP were determined by liquid scintillation counting. Results are expressed as either (1) relative to the basal activity represented by [^{3}H]-cyclic AMP generated in the absence of exogenous stimuli, or (2) relative to the response to cicaprost (0.1 µM).

Data analysis

EC_{50} values (concentration of FMLP producing 50% of maximal response) and IC_{50} values (concentration of test compound producing 50% inhibition of maximal response) were calculated using the four-parameter logistic curve fitting programme ALLFIT (De Lean *et al.*, 1978). Results are expressed as means with standard error of the mean of (n) experiments. Statistical analysis was performed using Student's unpaired t test.

Materials

FMLP, fura-2 acetoxy methyl ester, PGD_2, PGE_2, $PGF_{2\alpha}$, neutral alumina (type WN-3), and imidazole were supplied by the Sigma Chemical Co. (U.S.A.). PGE_1, 17-phenyl-ω-trinor PGE_2 and U 46619 (15S)-hydroxy-11α,9α-(epoxymethano)prosta-5Z,13E-dienoic acid) were purchased from Cayman Chemicals (U.S.A.). NIH thioglycollate broth was purchased from Difco (U.S.A.) and Ficoll-paque from Pharmacia (Sweden). 8-[^{3}H]-adenine (specific activity 27 Ci $mmol^{-1}$) and [adenine-U-^{14}C]-cyclic AMP (specific activity 278 mCi $mmol^{-1}$) were purchased from Amersham International (U.K.). Dowex AG 50W-XA (200–400 mesh) was purchased from Bio-Rad (U.S.A.). The gifts of prostanoids are gratefully acknowledged: AH 13205 (*trans*-2-[4-(1-hydroxyhexyl)phenyl]-5-oxocyclopentaneheptanoic acid) and GR 63799X (13-oxa-13,14-dihydro-16-phenoxy-ω-tetranor-PGE_2-4-(benzoylamino)phenyl ester; Glaxo, U.K.); cicaprost, iloprost, rolipram and sulprostone (Schering AG, Germany); butaprost (Bayer, U.K.); misoprostol (Searle, U.S.A.), and MB 28767 (*rac* 15S-hydroxy-9-oxo-16-phenoxy-ω-tetranor-prost-13E-enoic acid; Rhone-Poulenc, U.K.).

Results

FMLP-induced neutrophil aggregation

The addition of FMLP to suspensions of neutrophils produced a rapid concentration-dependent increase in aggregation which was maximal at 60 nM. The EC_{50} value for FMLP was 18.0 ± 3.4 nM ($n = 5$).

Effect of prostanoids on FMLP-induced aggregation

When tested at 1 µM, none of the fourteen compounds tested had any direct effect of neutrophil aggregation. However, at the same concentration, PGE_1, PGE_2, butaprost, misoprostol, MB 28767, iloprost and cicaprost all significantly inhibited aggregation stimulated by FMLP (16 nM) (Table 1).

PGE_2 and cicaprost produced a concentration-dependent inhibition of FMLP-stimulated aggregation with maximal inhibition of approximately 50–60% (Figure 1). IC_{50} values

for PGE_2 and cicaprost were 5.6 and 7.9 nM respectively. PGD_2, $PGF_{2\alpha}$, and U 46619 had no effect on FMLP-mediated responses at 0.1 nM to 1 μM (Figure 1); sulprostone was similarly inactive (data not shown). Inclusion of indomethacin (3 μM) to inhibit any endogenous production of prostanoids had no effect on the concentration-response curve for PGE_2 (data not shown) and was therefore not routinely included in this series of experiments.

Effect of FMLP on rat neutrophil $[Ca^{2+}]_i$

In the presence of external calcium (1 mM), FMLP caused a rapid, concentration-dependent increase in $[Ca^{2+}]_i$ which decayed to about 40% of its peak value within 1 min, after which the decay was much slower (Figure 2). A maximally effective concentration of FMLP (10 nM) increased $[Ca^{2+}]_i$ by 297 ± 45 nM, from a basal level of 26 ± 1 nM, with an EC_{50} of 1.17 ± 0.08 nM ($n = 3$).

Table 1 Effects of prostanoid agonists on the FMLP-stimulated responses of rat neutrophils

Prostanoid	*Receptor specificity*	*Aggregation (% control)*	*$[Ca^{2+}]_i$ rise (% control)*
PGE_2	EP	38 ± 4***	46 ± 5***
Cicaprost	IP	57 ± 1***	61 ± 5***
PGD_2	DP	99 ± 6	100 ± 6
$PGF_{2\alpha}$	FP	95 ± 12	98 ± 5
U 46619	TP	105 ± 4	99 ± 8
Iloprost	IP/EP_1	58 ± 6***	56 ± 3***
PGE_1	EP/IP	52 ± 5***	60 ± 8***
17-Phenyl-ω-trinor PGE_2	EP_1	86 ± 8	99 ± 5
AH 13205	EP_2	101 ± 8	99 ± 3
Butaprost	EP_2	73 ± 7***	78 ± 5*
Misoprostol	EP_2/EP_3	48 ± 5***	63 ± 7**
GR 63799X	EP_3	103 ± 5	87 ± 6
MB 28767	EP_3/TP	76 ± 7**	101 ± 3
Sulprostone	EP_3/EP_1	101 ± 8	102 ± 4

Prostanoids (1 μM) were added 2 min before an EC_{50} concentration of FMLP. Results are expressed as % control response (means ± s.e.mean, $n = 4$–7). For the aggregation experiments, the control response to FMLP (16 nM) was 16.3 ± 0.7 mm ($n = 13$). For the calcium experiments, the control response to FMLP (1 nM) was 126 ± 8 nM increase in $[Ca^{2+}]_i$ ($n = 20$). *$P<0.05$, **$P<0.01$, ***$P<0.001$, compared to FMLP alone.

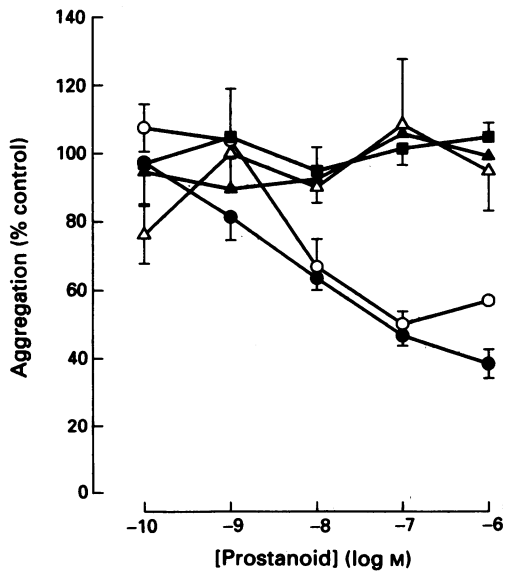


Figure 1 The effects of prostanoid receptor agonists on FMLP-induced neutrophil aggregation. Rat neutrophils were incubated for 2 min with test compound prior to the addition of an EC_{50} concentration of FMLP (16 nM). Control response to FMLP (16 nM) = 100 ± 6%, representing an aggregation response of 20.3 ± 0.7 mm ($n = 13$). Data shown are means with s.e.mean of 4 to 6 separate determinations: PGE_2 (●); cicaprost (○); U 46619 (■); PGD_2 (▲); $PGF_{2\alpha}$ (△).

Effect of prostanoid agonists on the FMLP $[Ca^{2+}]_i$ response

None of the fourteen compounds tested had any direct effect on rat neutrophil $[Ca^{2+}]_i$ over the concentration range 0.1 nM to 1 μM. However, several of the prostanoids tested influenced the subsequent response to a half-maximally effective concentration of FMLP (1 nM) added 2 min after the test compound (Figures 2 and 3).

At concentrations of 1 nM, or less, PGE_1, PGE_2, the PGI_2-mimetics, cicaprost and iloprost, butaprost (an EP_2-selective agonist) and misoprostol (an EP_2/EP_3-receptor agonist) tended to enhance the increase in $[Ca^{2+}]_i$. However, this enhancement was relatively small and rarely reached the level of statistical significance. In contrast, at concentrations greater than 10 nM, PGE_1, PGE_2, cicaprost and iloprost all inhibited the response to FMLP with maximal inhibition at approximately 44% of the control response ($P<0.001$ compared with the control response). The inhibitory phase of all four concentration-response curves were virtually superimposable, producing IC_{50} values of 33, 18, 34 and 38 nM for PGE_2, cicaprost, PGE_1 and iloprost respectively.

Butaprost and misoprostol also produced a statistically significant inhibition of the FMLP-stimulated response at 1 μM ($P<0.05$). All inhibitory activities correlated well with inhibition of aggregation ($r = 0.885$, $P<0.01$) except that MB 28767 had no effect on FMLP-stimulated $[Ca^{2+}]_i$ (Table 1).

The concentration-response curves for the EP_3-selective agonists, GR 63799X and MB 28767, and the EP_3/EP_1-receptor agonist, sulprostone, tended to lie above the control response line, with the facilitation of the FMLP response by GR 63799X (1 nM) being statistically significant ($P<0.05$). The thromboxane A_2-mimetic, U 46619, PGD_2, $PGF_{2\alpha}$ and the EP_2-receptor agonist, AH 13205, had no effect on the FMLP-induced increase in $[Ca^{2+}]_i$. The EP_1-selective agonist 17-phenyl-ω-trinor PGE_2 (Lawrence & Jones, 1992) produced a slight increase in response at 1 nM whilst being without effect at all other concentrations tested.

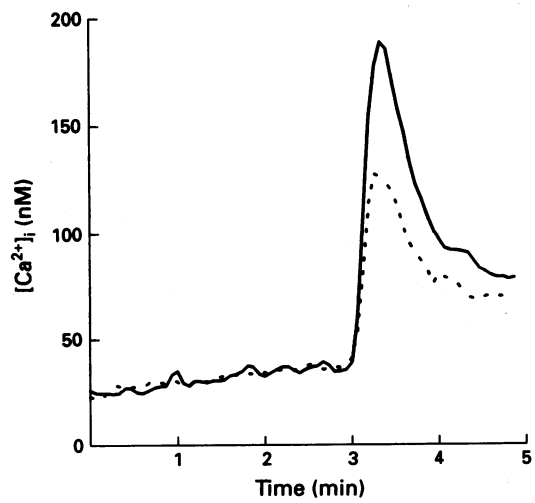


Figure 2 The effect of PGE_2 on FMLP-induced increase in rat neutrophil $[Ca^{2+}]_i$. Results shown are the typical responses of fura-2-loaded neutrophils to buffer (solid line) or PGE_2 (1 μM; dashed line) added at $t = 1$ min followed by FMLP (1 nM) at $t = 3$ min.

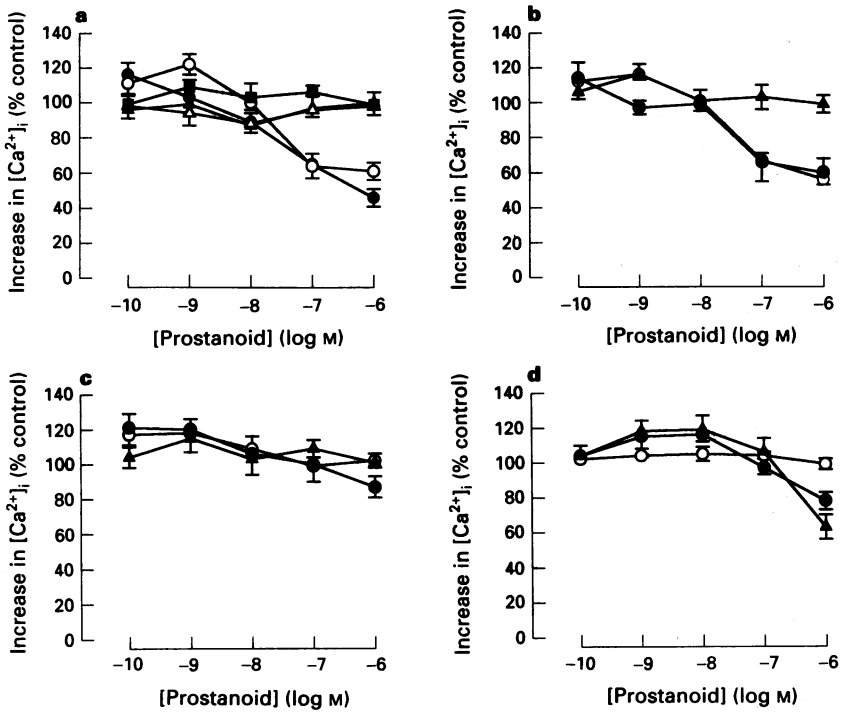


Figure 3 The effects of prostanoid receptor agonists on FMLP-induced increase in rat neutrophil $[Ca^{2+}]_i$. Control response to FMLP (1 nM) = 100 ± 7% (n = 20). Basal $[Ca^{2+}]_i$ was 21 ± 2 nM, and the increase in $[Ca^{2+}]_i$ due to FMLP (1 nM) was 126 ± 8 nM (n = 20). Data shown are means with s.e.mean of 5 to 7 separate determinations. (a) PGE_2 (●); cicaprost (○); U 46619 (■); PGD_2 (▲); $PGF_{2\alpha}$ (△); (b) PGE_1 (●); iloprost (○); 17-phenyl-ω-trinor PGE_2 (▲); (c) GR 63799X (●); sulprostone (○); MB 28767 (▲); (d) Butaprost (●); misoprostol (▲); AH 13205 (○).

[^{3}H]-cyclic AMP accumulation

PGE_2 and cicaprost produced a concentration-dependent increase in [^{3}H]-cyclic AMP accumulation, with cicaprost being approximately 10 fold more potent than PGE_2 (Figure 4a). PGD_2, $PGF_{2\alpha}$, and U 46619 had no effect on adenylyl cyclase activity at 0.1 nM to 1 μM (Figure 4a). Of the EP-receptor selective drugs tested, 17-phenyl-ω-trinor PGE_2 and sulprostone were without effect at 0.1 nM to 1 μM, whilst butaprost produced a 2 fold increase in [^{3}H]-cyclic AMP accumulation at 1 μM (Figure 4b).

To determine if any of our selected compounds had EP_3-like activity, we incubated the cells with 1 μM test drug in the presence and absence of an adenylyl cyclase stimulant to look for inhibition of adenylyl cyclase activity. Cicaprost (0.1 μM) was chosen to activate adenylyl cyclase as it was considerably more effective (237 ± 25% control, n = 6) than either forskolin (100 μM, 133 ± 27% control, n = 4) or isoprenaline (1 μM, 186 ± 11% control, n = 4). When tested alone, PGE_2, PGE_1, iloprost, butaprost and misoprostol all increased [^{3}H]-cyclic AMP accumulation (Figure 5a,b), with the response to PGE_2, PGE_1 and iloprost being statistically significant ($P < 0.05$). None of the remaining eight compounds had any effect alone. GR 63799X, MB 28767 and sulprostone, i.e. the EP_3-receptor agonists, all failed to inhibit cicaprost-stimulated [^{3}H]-cyclic AMP accumulation. Sulprostone was tested further at 0.1 nM to 1 μM and had no effect on the response to cicaprost (data not shown). Similarly none of the remaining compounds tested at 1 μM had any inhibitory effect on the response to cicaprost (Figure 5).

Discussion

In this investigation we have characterized the prostanoid receptors present on rat neutrophils by using a mixture of functional and biochemical assays, and a wide range of prostanoid agonists of varying receptor selectivity. The primary response of neutrophils to activation by FMLP is the rapid elevation of $[Ca^{2+}]_i$ (McCarthy *et al.*, 1989) closely followed by adherence to, and migration across, the endothelial cell layer (Winder *et al.*, 1993). Neutrophils stimulated by chemotactic factors undergo a transient change in surface properties that permits the cells to adhere more readily to surfaces such as endothelial cells, and to each other (Hoffstein *et al.*, 1982). Neutrophil aggregation *in vitro* has therefore been used in the present study as a measure of the adhesion response.

Of the five major prostanoid agonists (PGE_2, cicaprost, PGD_2, $PGF_{2\alpha}$, and U 46619) that define the EP, IP, DP, FP and TP-receptors (Coleman *et al.*, 1990), only PGE_2 and cicaprost inhibited FMLP-stimulated elevation of $[Ca^{2+}]_i$ and aggregation. The log concentration-response curves for each agent in the two assays were parallel. Other prostaglandins with IP-agonist activity, i.e. PGE_1 and iloprost, were also similarly potent in inhibiting FMLP-stimulated elevation of $[Ca^{2+}]_i$ with IC_{50} values of approximately 36 nM.

PGE_2 and IP-receptor agonists such as PGI_2 and beraprost have also been reported to be equipotent in inhibiting FMLP-induced chemotaxis in rat neutrophils (Kainoh *et al.*, 1990). Cicaprost is considerably more specific than iloprost as an IP-receptor agonist (Dong *et al.*, 1986, Armstrong *et al.*, 1989), and its profile in our experiments indicates the presence of IP-receptors on the rat neutrophil. Our observations therefore confirm the presence of both EP and IP-receptors capable of inhibiting rat neutrophil function and contrast with the relative lack of potency of IP-receptor agonists in assays of human neutrophil function (Hecker *et al.*, 1990, Wheeldon & Vardey, 1993). Our data also confirm the observations of Ham *et al.* (1983) who noted that rat neutrophils were unresponsive to PGD_2, which was in marked contrast to the high potency of DP-receptor agonists in inhibiting opsonized zymosan-induced release of LTB_4 from human neutrophils (Wheeldon & Vardey, 1993).

In this present paper we show that at the level of the initial response to FMLP, i.e. the elevation of $[Ca^{2+}]_i$, prostaglandin

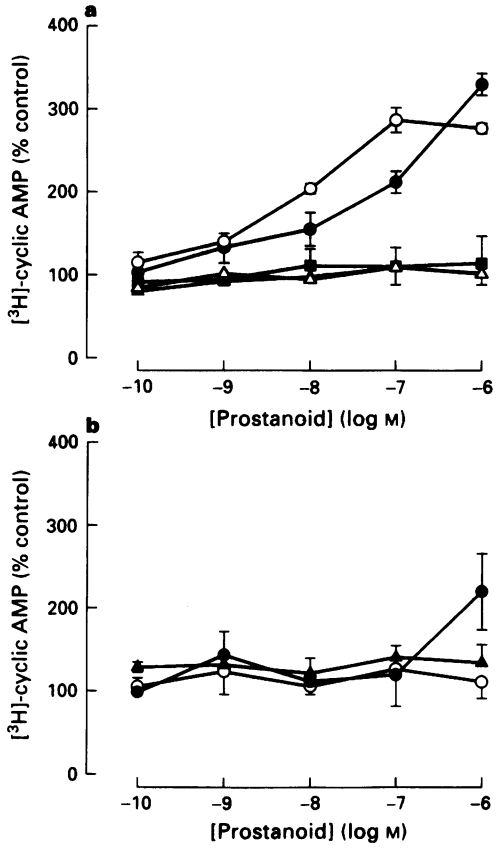


Figure 4 The effects of prostanoid receptor agonists on [^{3}H]-cyclic AMP accumulation in the presence of rolipram (0.1 mM), indomethacin (3 μM) and adenosine deaminase (1 u ml^{-1}). Rat neutrophils were incubated for 10 min before the addition of test compound for a further 10 min. Data represent the means with s.e.mean of 3 experiments performed in triplicate. (a) PGE_2 (●); cicaprost (○); U 46619 (■); PGD_2 (▲); $PGF_{2\alpha}$ (△); (b) Butaprost (●); 17-phenyl-ω-trinor PGE_2 (▲); sulprostone (○).

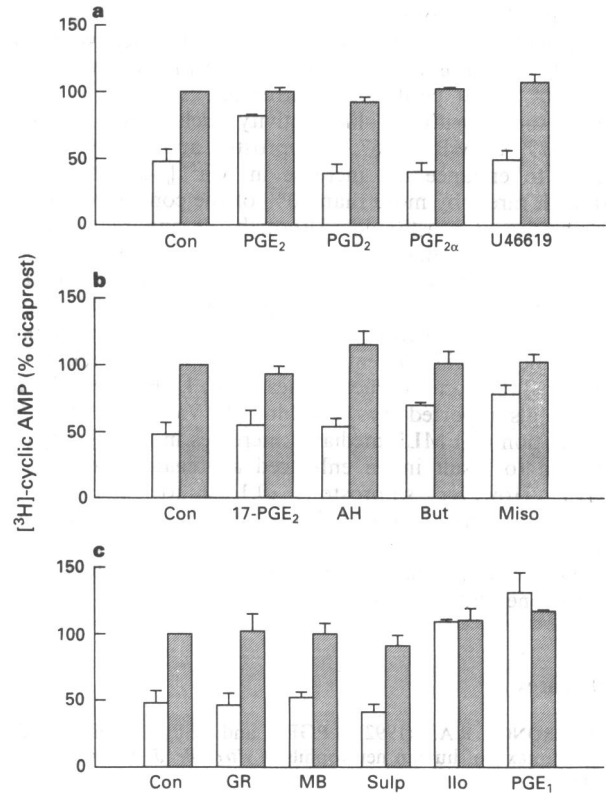


Figure 5 The effects of prostanoid receptor agonists on [^{3}H]-cyclic AMP accumulation stimulated by cicaprost. Rat neutrophils were incubated in the presence of rolipram (0.1 mM), indomethacin (3 μM) and adenosine deaminase (1 u ml^{-1}) for 10 min before the addition of test compound (1 μM), in the presence (hatched columns) and absence (open columns) of cicaprost (0.1 μM). The reaction was stopped after a further 10 min. Data represent the means with s.e.mean of 3 experiments performed in triplicate. Cicaprost (0.1 μM) elevated [^{3}H]-cyclic AMP levels to 223 ± 38% control ($n = 3$). Abbreviations: Con (control), 17-PGE_2 (17-phenol-ω-trinor PGE_2), AH (AH13205), But (butaprost), Miso (misoprostol), GR (GR 63799X), MB (MB 28767), Sulp (sulprostone) and Ilo (iloprost).

analogues active at the EP_2-receptor, e.g. PGE_1, PGE_2, butaprost and misoprostol, all have an inhibitory action. This is unlikely to be due to any cytotoxic effect since there was no obvious fura-2 loss from the cells on the addition of prostanoids. These same compounds, tested at 1 μM, also inhibited the aggregation response to FMLP, thus identifying an inhibitory role for EP_2-receptors in rat neutrophils. MB 28767 was the only compound tested which inhibited FMLP-stimulated aggregation yet had no effect on FMLP-stimulated $[Ca^{2+}]_i$. MB 28767 has previously been shown to exhibit EP_2-like activity by relaxing rabbit jugular vein with an equi-effective molar ratio of approximately 400 when compared with PGE_2 (Lawrence & Jones, 1992). Therefore it is probable that we are able to detect an EP_2-like effect of MB 28767 due to the relatively high sensitivity of the aggregation assay to PGE_2 (IC_{50} 5.6 nM) when compared with the sensitivity of the calcium assay to PGE_2 (IC_{50} 33 nM).

In the same study by Lawrence & Jones (1992), the relaxant potency of butaprost on the rabbit jugular vein was found to be surprisingly weak (about 700 and 80 times less than PGE_2 and misoprostol respectively) and this led to the first suggestion of the existence of subtypes of the EP_2-receptor. In our present study, the EP_2-selective agonist AH 13205 (Nias *et al.*, 1993) at 1 μM had no effect on FMLP-mediated activation of the rat neutrophil or on the accumulation of [^{3}H]-cyclic AMP. In contrast, AH 13205 was only 16 fold less potent than PGE_2 in inhibiting opsonized zymosan-induced release of LTB_4 from human neutrophils (Wheeldon & Vardey, 1993). More recently AH 13205 has been used to distinguish the EP_2-receptor from a recently identified subtype, the EP_4-receptor, present in pig saphenous vein where AH 13205 was reported to be 11,000 fold less potent than PGE_2 (Coleman *et al.*, 1994). It is conceivable that AH 13205 may have shown an effect in our study at a higher concentration, but we chose to limit the concentration of compounds tested to 1 μM in order to maintain their specificity of action. Since in the present study the potency of butaprost is much closer to that of misoprostol, it is probable that our results support the presence of conventional EP_2-receptors.

The inhibitory action of prostaglandins on neutrophils is considered to be due to stimulation of cyclic AMP production since chemoattractants such as FMLP indirectly elevate intracellular cyclic AMP levels as part of a negative regulatory system (Verghese *et al.*, 1985), and prostaglandin-induced inhibition of neutrophil function tends to be paralleled by increases in cyclic AMP (Ney & Schrör, 1991). We have found that only those compounds which stimulated adenylyl cyclase activity were able to inhibit FMLP-stimulated $[Ca^{2+}]_i$ and neutrophil aggregation. Whilst the drugs which can elevate neutrophil [^{3}H]-cyclic AMP clearly inhibit neutrophil activity and might be considered as anti-inflammatory, one rarely observes more than 60% inhibition of any measure of neutrophil function (see also Wheeldon & Vardey, 1993). Clearly there are important regulators of neutrophil function other than adenylyl cyclase.

The lack of effect of prostaglandins alone in stimulating an increase in $[Ca^{2+}]_i$ and aggregation also suggests the lack of

prostaglandin receptors directly coupled to phospholipase C. In particular, the lack of effect of the EP_1-selective agonist 17-phenyl-ω-trinor PGE_2 would indicate the absence of EP_1-receptors on rat peritoneal neutrophils.

Prostanoids with EP_3-like activity such as PGE_1, PGE_2, GR 63799X, MB 28767, misoprostol and sulprostone all tended to enhance the increase in $[Ca^{2+}]_i$ due to FMLP, although rarely by more than 20% of the control response in the absence of prostanoid. Although the apparent potentiation of FMLP-mediated increases in $[Ca^{2+}]_i$ by various prostanoids is relatively small and rarely reached a level of statistical significance, the response could not be attributed to an artifact of the experimental design and was of a similar magnitude as the potentiation by sulprostone (1 μM) of opsonized zymosan-induced release of LTB_4 from human neutrophils reported by Wheeldon & Vardey (1993). Any potentiation of FMLP-mediated increases in $[Ca^{2+}]_i$ might be expected to result in an enhanced aggregatory response to FMLP. However, sulprostone (0.1 nM to 1 μM) had no potentiating effect on FMLP-mediated neutrophil aggregation. Activation of EP_3-receptors would also be expected to inhibit adenylyl cyclase activity. GR 63799X, MB 28767 or sulprostone did not inhibit cicaprost-stimulated [^{3}H]-cyclic AMP accumulation, thus providing further evidence for the lack of EP_3-receptors on rat neutrophils. It is not clear at present why low concentrations of EP_3 and some EP_2-receptor agonists appeared to facilitate FMLP-mediated increase in $[Ca^{2+}]_i$. The absence of specific receptor antagonists clearly hampers the interpretation of the results here.

In conclusion, we have shown that the ability of FMLP to increase $[Ca^{2+}]_i$ and to stimulate an aggregation response in rat neutrophils is not affected by DP, FP or TP-receptor agonists, but can be inhibited by EP and IP-receptors agonists. The lack of DP-receptors and the presence of functionally active IP-receptors contrast with reported studies on human neutrophils. Rat neutrophils appear to lack EP_1-receptors whilst possessing an EP_2 or EP_2-like receptor which appears to mediate the inhibitory effect of PGE_2. We have found no evidence for an EP_3-receptor capable of facilitating the chemotaxic responses of rat neutrophils.

The authors would like to acknowledge the excellent technical support provided by Mr Kevin Chow Bing Shui. This project was supported by UPGC Grant SP-92/90.

References

ARMSTRONG, R.A. (1992). PGE_2 and EP_3 agonists induce chemotaxis of human neutrophils *in vitro*. *Br. J. Pharmacol.*, **105**, 45P.

ARMSTRONG, R.A. & TALPAIN, E. (1992). Characterisation of the PGE receptor on human promyelocytic leukemia (HL-60) cells differentiated with dimethylsulfoxide into neutrophil-like cells. *Br. J. Pharmacol.*, **107**, 91P.

ARMSTRONG, R.A., LAWRENCE, R.A., JONES, R.L., WILSON, N.H. & COLLIER, A. (1989). Functional and ligand binding studies suggest heterogeneity of platelet prostacyclin receptors. *Br. J. Pharmacol.*, **97**, 657–668.

BARBER, R., RAY, K.P. & BUTCHER, R.W. (1980). Turnover of adneosine 3',5'-monophosphate in WI-38 cultured fibroblasts. *Biochemistry*, **19**, 2560–2567.

CARLOS, T.M. & HARLAN, J.M. (1990). Membrane proteins involved in phagocyte adherence to endothelium. *Immunological Rev.*, **114**, 5–28.

COLEMAN, R.A., GRIX, S.P., HEAD, S.A., LOUTTIT, J.B., MALLETT, A. & SHELDRICK, R.L.G. (1994). A novel inhibitory prostanoid receptor in piglet saphenous vein. *Prostaglandins*, **47**, 151–168.

COLEMAN, R.A., KENNEDY, I., HUMPHREY, P.P.A., BUNCE, K. & LUMLEY, P. (1990). Prostanoids and their receptors. In *Comprehensive Medicinal Chemistry*, Vol. 3, *Membranes and their Receptors*. ed. Hansch, C., Sammes, P.G. & Taylor, J.B. pp. 643–676. Oxford: Pergamon Press.

DE LEAN, A., MUNSON, P.J. & RODBARD, D. (1978). Simultaneous analysis of families of sigmoidal curves: application to bioassay, radioligand assay and physiological dose-response curves. *Am. J. Physiol.*, **235**, E97–E102.

DE TOGNI, P., CABRINI, G. & DI VIRGILIO, F. (1984). Cyclic AMP inhibition of fMet-Leu-Phe-dependent metabolic response in human neutrophils is not due to its effect on cytosolic Ca^{2+}. *Biochem. J.*, **224**, 629–635.

DONG, Y.J., JONES, R.L. & WILSON, N.H. (1986). Prostaglandin E receptor subtypes in smooth muscle: agonist activities of stable prostacyclin analogues. *Br. J. Pharmacol.*, **87**, 97–107.

FANTONE, J.C., KUNKEL, S.L. & WARD, P.A. (1981). Suppression of human polymorphonuclear function after intravenous infusion of prostaglandin E1. *Prostaglandins Med.*, **7**, 195–198.

FANTONE, J.C. & KINNES, A.D. (1983). Prostaglandin E_1 and prostaglandin I_2 modulation of superoxide production by human neutrophils. *Biochem. Biophys. Res. Commun.*, **113**, 506–512.

FISKER, S., KUDAHL, K. & SONNE, O. (1990). Isolation of rat peritoneal mononuclear and polymorphonuclear leucocytes on discontinuous gradients of Nycodez. *J. Immunol. Methods*, **133**, 31–38.

FORD-HUTCHINSON, A.W. & EVANS, J.F. (1988). Neutrophil aggregation and chemokinesis assays. *Methods in Enzymology*, **162**, 72–78.

GOODWIN, J.S. (1991). Are prostaglandins proinflammatory, antiinflammatory, both or neither? *J. Rheumatol.*, **18** (Suppl. 28), 26–29.

GRYGLEWSKI, R.J., SZCZEKLIK, A. & WANDZILAK, M. (1987). The effect of six prostaglandins, prostacyclin and iloprost on generation of superoxide anions by human polymorphonuclear leukocytes stimulated by zymosan or formyl-methionyl-leucyl-phenylalanine. *Biochem. Pharmacol.*, **36**, 4209–4213.

GRYGLEWSKI, R.J. & SALVEMINI, D. (1992). Modulation of polymorphonuclear leukocyte function by prostaglandins and nitric oxide. In: *Prostacyclin: New Perspectives for Basic Research and Novel Therapeutic Indications*. ed. Rubanyi, G.M. & Vane, J. pp. 59–92. Amsterdam: Elsevier Science Publishers.

GRYNKIEWICZ, G., PEONIE, M. & TSIEN, R.Y. (1985). A new generation of Ca^{2+} indicators with greatly improved fluorescence properties. *J. Biol. Chem.*, **260**, 3440–3450.

HAM, E.A., SODERMAN, D.D., ZANETTI, M.E., DOUGHERTY, H.W., MCCAULEY, E. & KUEHL, F.A. Jr. (1983). Inhibition by prostaglandins of leukotriene B4 release from activated neutrophils. *Proc. Natl. Acad. Sci. U.S.A.*, **80**, 4349–4353.

HECKER, G., NEY, P. & SCHRÖR, K. (1990). Cytotoxic enzyme release and oxygen centered radical formation in human neutrophils are selectively inhibited by E-type prostaglandins but not by PGI_2. *Naunyn-Schmied. Arch. Pharmacol.*, **341**, 308–315.

HOFFSTEIN, S.T., FRIEDMAN, R.S. & WEISSMANN, G. (1982). Degranulation, membrane addition, and shape change during chemotactic factor induced aggregation of human neutrophils. *J. Cell Biol.*, **95**, 234–241.

KAINOH, M., IMAI, R., UMETSU, T., HATTORI, M. & NISHIO, S. (1990). Prostacyclin and beraprost sodium as suppressors of activated rat polymorphonuclear leukocytes. *Biochem. Pharmacol.*, **39**, 477–484.

KATO, H., ISHITOYA, J. & TAKENAWA, T. (1986). Inhibition of inositol phospholipids metabolism and calcium mobilization by cyclic AMP-increasing agents and phorbol ester in neutrophils. *Biochem. Biophys. Res. Commun.*, **139**, 1272–1278.

KITSIS, E.A., WEISSMANN, G. & ABRAMSON, S.B. (1991). The prostaglandin paradox: additive inhibition of neutrophil function by aspirin-like drugs and prostaglandin E_1 analogue misoprostol. *J. Rheumatol.*, **18**, 1461–1465.

LAWRENCE, R.A. & JONES, R.L. (1992). Investigation of the prostaglandin E (EP-) receptor subtype mediating relaxation of the rabbit jugular vein. *Br. J. Pharmacol.*, **105**, 817–824.

MCCARTHY, S.A., HALLAM, T.J. & MERRITT, J.E. (1989). Activation of protein kinase C in human neutrophils attentuates agonist-stimulated rises in cytosolic free Ca^{2+} concentration by inhibiting bivalent-cation influx and intracellular Ca^{2+} release in addition to stimulating Ca^{2+} efflux. *Biochem. J.*, **264**, 357–364.

NAGATA, S., KEBO, D.K., KUNKEL, S. & GLOVSKY, M.M. (1992). Effect of adenylate cyclase activators on C5a-induced human neutrophil aggregation, enzyme release and superoxide production. *Int. Arch, Allergy Immunol.*, **97**, 194–199.

NEY, P. & SCHRÖR, K. (1989). E-Type prostaglandins but not iloprost inhibit platelet activating factor-induced generation of leukotriene B_4 by human polymorphonuclear leukocytes. *Br. J. Pharmacol.*, **96**, 186–192.

NEY, P. & SCHRÖR, K. (1991). PGD_2 and its mimetic ZK 110.841 are potent inhibitors of receptor-mediated activation of human neutrophils. *Eicosanoids*, **4**, 21–28.

NIALS, A.T., VARDEY, C.J., DENYER, L.H., THOMAS, M., SPARROW, S.J., SHEPHERD, G.D. & COLEMAN, R.A. (1993). AH 13205, a selective prostanoid EP_2-receptor agonist. *Cardiovasc. Drug Rev.*, **11**, 165–179.

NIELSEN, C.P., BAYER, C., HODSON, S. & HADJOKAS, N. (1992). Regulation of the respiratory burst by cyclic 3′,5′-AMP, an association with inhibition of arachidonic acid release. *J. Immunol.*, **149**, 4036–4040.

PHIPPS, R.P., STEIN, S.H. & ROPER, R.L. (1991). A new view of prostaglandin E regulation of the immune response. *Immunol. Today*, **12**, 349–351.

ROSSI, F. (1986). The O_2^--forming NADPH oxidase of the phagocytes: nature, mechanisms of activation and function. *Biochem. Biophys. Acta.*, **853**, 65–89.

SALOMON, Y., LONDOS, C. & RODBELL, M. (1974). A highly sensitive adenylate cyclase assay. *Anal. Biochem.*, **58**, 541–548.

VERGHESE, M.W., FOX, K., MCPHAIL, L.C. & SYNDERMAN, R.J. (1985). Chemoattractant-elicited alterations of cAMP levels in human polymorphonuclear leukocytes require a Ca^{2+}-dependent mechanism which is independent of transmembrane activation of adenylate cyclase. *J. Biol. Chem.*, **260**, 6769–6775.

WHEELDON, A. & VARDEY, C.J. (1993). Characterization of the inhibitory prostanoid receptors on human neutrophils. *Br. J. Pharmacol.*, **108**, 1051–1054.

WINDER, A.C.J., MULLEN, P.G., FOWLER, A.A. & SUGERMAN, H.J. (1993). Role of the neutrophil in adult respiratory distress syndrome. *Br. J. Surg.*, **80**, 10–17.

(Received March 22, 1994
Revised May 16, 1994
Accepted May 20, 1994)

Br. J. Pharmacol. (1994), **113**, 588–592 © Macmillan Press Ltd, 1994

Inhibitory transmitter action of calcitonin gene-related peptide in guinea-pig ureter via activation of glibenclamide-sensitive K channels

[1]Paolo Santicioli & Carlo Alberto Maggi

Pharmacology Department, A. Menarini Pharmaceuticals, Via Sette Santi 3, 50131, Florence, Italy

1 In single sucrose gap, electrical field stimulation (EFS, 1–5 Hz) produced graded hyperpolarization of the membrane of the guinea-pig ureter smooth muscle, which was blocked by tetrodotoxin (0.3 μM) or *in vitro* capsaicin desensitization (3 μM for 15 min). Capsaicin itself produced a transient hyperpolarization of the membrane on its first application.

2 Superfusion with human α calcitonin gene-related peptide (CGRP, 30–300 mM) likewise produced a transient hyperpolarization of the membrane, mimicking the neurogenic inhibitory junction potential (i.j.p.). The hyperpolarization by CGRP was unaffected by tetrodotoxin, indicating a postjunctional site of action.

3 Both the EFS-evoked i.j.p. and the CGRP-induced hyperpolarization were inhibited by the CGRP receptor antagonist, CGRP(8–37) (0.3–3 μM) which did not affect the hyperpolarization produced by the K_{ATP} channel opener, cromakalim (0.3 μM).

4 The K_{ATP} channel blocker, glibenclamide (1 μM) blocked both the EFS-evoked i.j.p. and the CGRP-induced hyperpolarization.

5 When evoked in a low K medium (1.2 mM, KCl being replaced by an equimolar amount of NaCl), the EFS-evoked i.j.p. and the CGRP-induced hyperpolarization were both markedly enhanced, consistent with the idea that opening of K channels underlies both responses.

6 The present findings provide direct electrophysiological evidence for a neurotransmitter role of CGRP, released from the peripheral endings of capsaicin-sensitive primary afferent neurones, in the guinea-pig ureter. The action of both exogenous and endogenous CGRP involves the activation of glibenclamide-sensitive (K_{ATP}) potassium channels.

Keywords: Guinea-pig ureter; calcitonin gene-related peptide (CGRP); efferent function of sensory nerves; potassium channel openers; glibenclamide

Introduction

Calcitonin gene-related peptide (CGRP), a 37 amino acid neuropeptide, is widely distributed in the mammalian peripheral nervous system, principally stored in the peripheral endings of capsaicin-sensitive primary afferent neurones (Yamamoto & Tohyama, 1989 for review). Nerve fibres containing CGRP-like immunoreactivity (CGRP-LI) are widely distributed to various viscera, including the upper urinary tract (Su *et al.*, 1986); the application of depolarizing stimuli produces the release of CGRP-LI from afferent neurones in the mammalian ureter (Santicioli *et al.*, 1988; Maggi *et al.*, 1990; 1992b). The suggestion has been advanced that CGRP acts as an inhibitory neuromuscular transmitter in the guinea-pig ureter, where it may suppress latent pacemakers and prevent antiperistaltic waves of contraction to produce backflow of urine toward the kidney (Maggi & Giuliani, 1991; Maggi *et al.*, 1992a). The inhibitory action of CGRP on the evoked motility of the guinea-pig ureter is produced through the simulation of specific receptors densely distributed over the smooth muscle layers (Sann *et al.*, 1993) and is selectively blocked by a CGRP receptor antagonist, the C-terminal fragment CGRP(8–37) (Maggi & Giuliani, 1991).

In a recent study (Maggi *et al.*, 1994) we presented evidence that activation of glibenclamide-sensitive potassium channels (K_{ATP} channels, Cook & Quast, 1990 for review) provides a powerful mechanism for regulation of motility of the ureter by producing membrane hyperpolarization and preventing the activation of latent pacemakers by depolarizing stimuli. Since CGRP has been shown to activate K_{ATP} channels in arterial smooth muscle (Standen *et al.*, 1989), it appears of interest to know whether this effector mechanism may underlie the action of CGRP in the ureter.

By using a single sucrose gap technique, we have now obtained electrophysiological evidence that endogenous CGRP produces inhibitory junction potentials (i.j.ps) in the guinea-pig ureter and that opening of glibenclamide-sensitive K channels is the effector mechanism for this type of neuromuscular peptidergic transmission.

Methods

Male albino guinea-pigs, weighing 250–300 g were stunned and bled. A segment of distal ureter (1.5 cm in length) was excised and placed in oxygenated and warmed (95% O_2 and 5% CO_2, pH 7.4 at 37°C) Krebs solution. The composition of Krebs solution was (mmol l^{-1}): NaCl 119, $NaHCO_3$ 25, KH_2PO_4 1.2, $MgSO_4$ 1.5, KCl 4.7, $CaCl_2$ 2.5 and glucose 11. A single sucrose gap, modified as described in detail by Artemenko *et al.* (1982) and Hoyle (1987) was used to investigate changes in membrane potential in response to electrical stimulation. The ureters were superfused with oxygenated Krebs solution at a rate of 1 ml min^{-1}. The temperature of the solution was kept constant at 35 ± 0.5°C.

Depolarizing square wave pulses (1–5 Hz for 10 s, 0.15–0.2 ms pulse width, 30–40 V) were delivered by means of a GRASS S 88 stimulator coupled with a GRASS SIU5 stimulus isolation unit. Tetrodotoxin (0.3 μM) was applied for 10 min before EFS. *In vitro* capsaicin-desensitization was produced by superfusion with 3 μM capsaicin for 15 min followed by 15 min washout. In each preparation, two

[1] Author for correspondence.

stimulation cycles at various frequencies were performed before and after drug treatment. The hyperpolarization by CGRP was evoked by 15 s superfusion with the stated CGRP concentration. In some experiments, a low-K (1.2 mM) Krebs solution was prepared by replacing KCl with an equimolar amount of NaCl.

Statistical analysis of data was performed by means of Student's 2 tailed t test for paired data. A probability <0.05 was considered statistically significant.

Drugs used were: human αCGRP and human αCGRP (8–37) from Peninsula; glibenclamide and capsaicin from Sigma; tetrodotoxin from Sankyo.

Results

Electrical field stimulation (EFS) produced by applying train of pulses at a frequency of 1–5 Hz (pulse width 0.15–0.2 ms, 30–40 V) for 10 s produced graded hyperpolarizing responses which started within 4–9 s and peaked 15–20 s from the onset of stimulation (Figure 1). The peak amplitude and rate of hyperpolarization (mV s^{-1}) were linearly correlated to the frequency of stimulation. The hyperpolarization produced by EFS could be evoked for several consecutive stimulation cycles at 15–30 min intervals from each other. The evoked hyperpolarization was abolished by 0.3 μM tetrodotoxin (Figure 1) indicating its dependence upon transmitter release from intramural nerves (inhibitory junction potentials, i.j.p.). The parameters of i.j.p. activated by EFS are given in Table 1.

Application of capsaicin (3 μM) evoked a prompt and transient hyperpolarization (1.32 ± 0.31 mV, peak at 26 ± 3 s from capsaicin application, $n = 4$) followed by a transient depolarization (1.43 ± 0.2 mV, peak at 171 ± 24 s from capsaicin application, $n = 4$). A second application of 3 μM capsaicin, 15 min later failed to affect membrane potential indicating complete desensitization. In capsaicin-desensitized ureters, EFS was unable to evoke i.j.ps, indicating their dependence from transmitter(s) release from the peripheral endings of capsaicin-sensitive afferents (Figure 1).

Since CGRP is a powerful inhibitor of motility of the ureter, we next examined whether exogenous CGRP mimics the hyperpolarization produced by EFS. Superfusion with human αCGRP (CGRP, 30–300 nM for 15 s, Figure 2) produced a concentration-dependent hyperpolarization mimicking the nerve-mediated i.j.ps. The hyperpolarizing effect of CGRP (100 nM) observed in the presence of tetrodotoxin (0.3 μM) was unchanged as compared to controls (0.93 ± 0.21 and 0.88 ± 0.25 mV, NS, $n = 4$), indicating a postjunctional site of action.

The CGRP receptor antagonist, CGRP(8–37) (0.3–3 μM) had no effect on its own, indicating total lack of agonist activity but prevented, in a concentration-dependent manner, the hyperpolarization produced by exogenously applied CGRP (Figure 2) and the EFS-evoked i.j.ps (Figure 3). The degree of inhibition produced by CGRP(8–37) was inversely related to the concentration of the agonist (in the case of exogenous CGRP, Figure 2) or to the frequency of stimulation (in the case of the EFS-evoked i.j.p., Figure 3), consistent with the competitive nature of its antagonism at CGRP receptors (Chiba *et al.*, 1989; Maggi *et al.*, 1991).

In control experiments, CGRP(8–37) (3 μM) did not affect the hyperpolarization produced by 0.3 μM cromakalim (0.68 ± 0.07 and 0.65 ± 0.11 mV, $n = 3$). On the other hand, the K_{ATP} channel blocker, glibenclamide (0.3–1 μM), which blocks the hyperpolarization induced by cromakalim in the guinea-pig ureter (Maggi *et al.*, 1994), suppressed the hyperpolarization produced by CGRP (Figure 2) and the EFS-evoked i.j.p. (Figure 3), providing evidence for the involvement of K_{ATP} channels in the hyperpolarization produced by endogenous CGRP.

Further evidence that CGRP acts as a K channel opener in the ureter, was obtained by examining the effect of a low-K Krebs solution on the hyperpolarization produced by exogenous CGRP and on the CGRP-mediated i.j.p. produced by EFS. In fact the hyperpolarization produced by cromakalim, leading to K outflow via glibenclamide-sensitive K_{ATP} channels, was enhanced when the transmembrane K chemical gradient was increased. Data shown in Figures 2 and 3 indicate that the EFS-evoked i.j.ps and the hyperpolarization produced by exogenous CGRP were both markedly potentiated when elicited in a low-K Krebs solution.

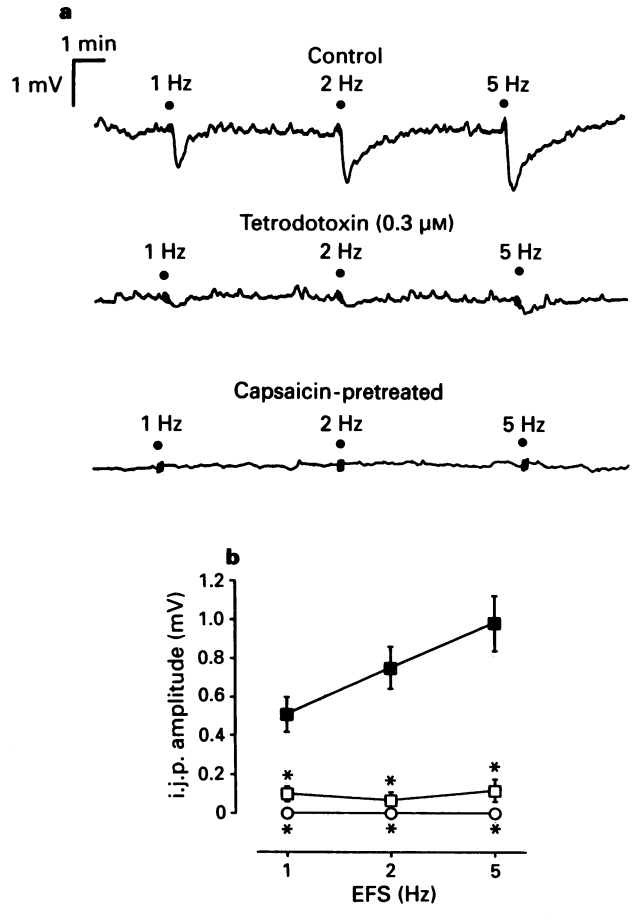


Figure 1 (a) Frequency-dependent inhibitory junction potentials (i.j.p.) evoked by electrical field stimulation (EFS) in the smooth muscle of the guinea-pig ureter and their inhibition by tetrodotoxin or capsaicin-pretreatment. (b) EFS-evoked i.j.p. in the guinea-pig ureter (controls, ■, $n = 10$) and the effect of tetrodotoxin (0.3 μM, □, $n = 6$) or *in vitro* capsaicin-pretreatment (○, $n = 4$). *Significantly different from control, $P<0.05$.

Table 1 Parameters of the inhibitory junction potential produced by electrical field stimulation in the guinea-pig ureter

	Frequency of stimulation		
Parameter	1 Hz	2 Hz	5 Hz
Latency (s)	7.36 ± 0.29	5.90 ± 1.59	4.73 ± 0.28
T_{max} (s)	17.1 ± 0.58	18.5 ± 1.05	19.8 ± 0.90
$T_{50\%}$ (s)	14.7 ± 1.5	17.0 ± 1.7	22.6 ± 2.22
Amplitude (mV)	0.46 ± 0.06	0.61 ± 0.07	0.83 ± 0.10
Rate (mV s^{-1})	0.031 ± 0.003	0.033 ± 0.004	0.043 ± 0.006

Each value is mean ± s.e.mean of ten experiments
T_{max} = time to achieve maximal hyperpolarization
T_{50}% = time to recover 50% of hyperpolarization
Rate = rate of hyperpolarization.

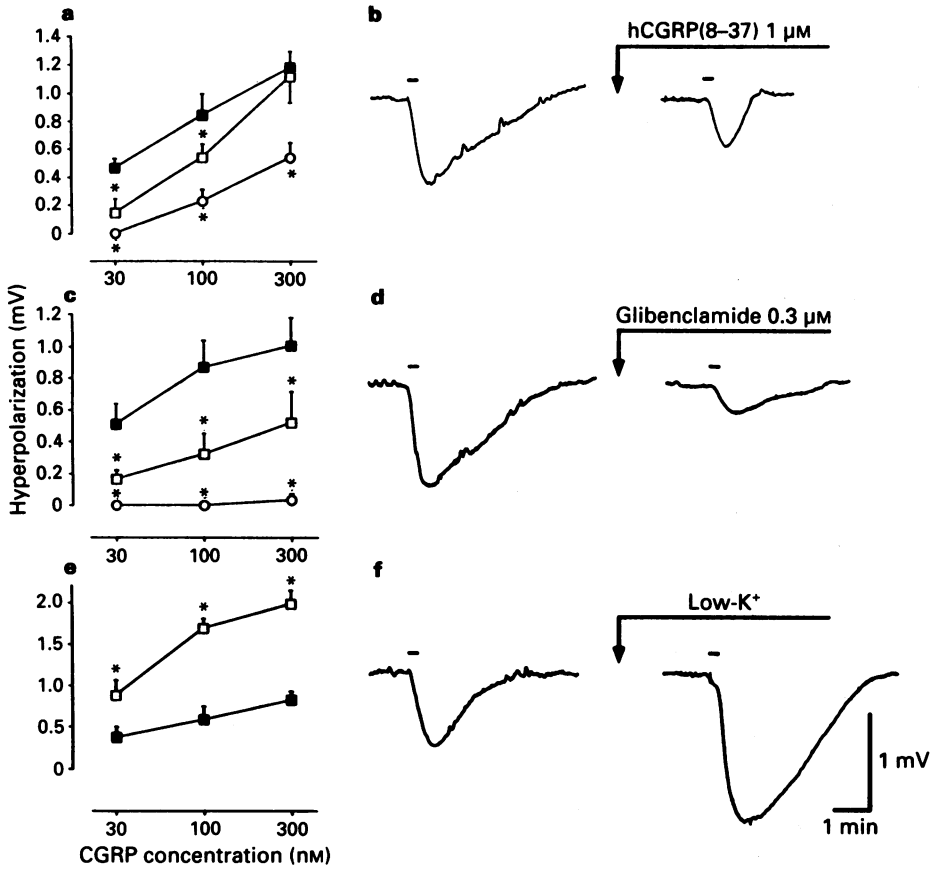


Figure 2 Calcitonin gene-related peptide (CGRP)-induced hyperpolarization of the smooth muscle of the guinea-pig ureter and its modification by the CGRP receptor antagonist human αCGRP(8–37) (a and b), glibenclamide (c and d) or by a low-K Krebs solution (e and f). (a) Control (■), $n=7$; hCGRP(8–37) 1 μM, (□), $n=4$ and 3 μM, (○), $n=3$. (c) Control (■), $n=8$; glibenclamide 0.3 μM (□), $n=4$, 1 μM (○), $n=4$. (e) Control (■), $n=4$; low-K Krebs solution (□), $n=4$. In each panel * indicates values which are significantly different from control, $P<0.05$. In (b), (d) and (f) the responses to 100 nM CGRP is shown before and after hCGRP(8–37), glibenclamide or in a low K Krebs solution. Horizontal bars mark the application of 100 nM CGRP.

Discussion

The dense plexus of CGRP-containing nerves present in the guinea-pig ureter represents the peripheral terminals of primary afferent neurones sensitive to the actions of capsaicin (Su *et al.*, 1986). These primary afferent neurones are thought to exert a dual, sensory and 'efferent' function, the latter being accomplished through the release of sensory neuropeptides (such as CGRP) in an efferent manner (Maggi & Meli, 1988, for review). A marked release of CGRP occurs in the guinea-pig ureter in response to various depolarizing stimuli, including capsaicin itself, electrical stimulation of intramural nerves and bradykinin (Santicioli *et al.*, 1988; Maggi *et al.*, 1990; 1992b). Under physiological conditions, the mammalian ureter does not display any spontaneous electrical or mechanical activity, being normally excited, through electromechanical coupling, by waves of excitation arising from the renal pelvis pacemaker (Weiss, 1992, for review). Latent pacemakers in the ureter may however be excited in non-physiological conditions (e.g. stones, bacterial infections) to produce antiperistaltic waves of contractions which induce urine backflow toward the kidney (Weiss, 1992). CGRP does not affect the quiescent ureter but produces a powerful suppression of evoked motility by activating specific receptors expressed in the smooth muscle layers (Maggi & Giuliani, 1991; Sann *et al.*, 1993). In a previous study we demonstrated the ability of endogenous CGRP, released from primary afferent nerves to suppress background motility of ureter sustained by chemical excitation of latent pacemakers (Maggi & Giuliani, 1991). By using the competitive CGRP receptor antagonist, CGRP(8–37) (Chiba *et al.*, 1989; Dennis *et al.*, 1989; Maggi *et al.*, 1991), we have now obtained evidence that CGRP receptors are junctionally activated to mediate a neurogenic hyperpolarization of ureter smooth muscle produced by stimulation of peripheral endings of capsaicin-sensitive afferents.

Although CGRP receptors have not yet been cloned, indirect evidence suggests that they belong to the superfamily of G-protein coupled receptors (Poyner, 1992, for review). Exogenous CGRP has been reported to activate a class of ATP-sensitive K channels (K_{ATP}) in e.g. arterial smooth muscle (Standen *et al.*, 1989) which are also activated by the K channel opener, cromakalim and blocked by the sulphonylurea-type antidiabetic agent, glibenclamide. The ATP-sensitive K channels have a role in regulating insulin release from pancreatic β cells and appear also to be present in neurones, cardiac cells and smooth muscles (Cook & Quast, 1990; Ashcroft & Ashcroft, 1990). However, the association of this effector system with neurotransmission in normal tissues has never been demonstrated. Since the K_{ATP} channel agonist, cromakalim, produces a glibenclamide-sensitive hyperpolarization of the guinea-pig ureter smooth muscle (Maggi *et al.*, 1994), the activation of this mechanism would be a likely explanation for the hyperpolarization produced by CGRP in the ureter.

The present findings indicate that cromakalim- and glibenclamide-sensitive K channels are junctionally activated by endogenous CGRP released from capsaicin-sensitive primary afferents. The membrane hyperpolarization produced by activation of K_{ATP} channels is capable of suppressing the

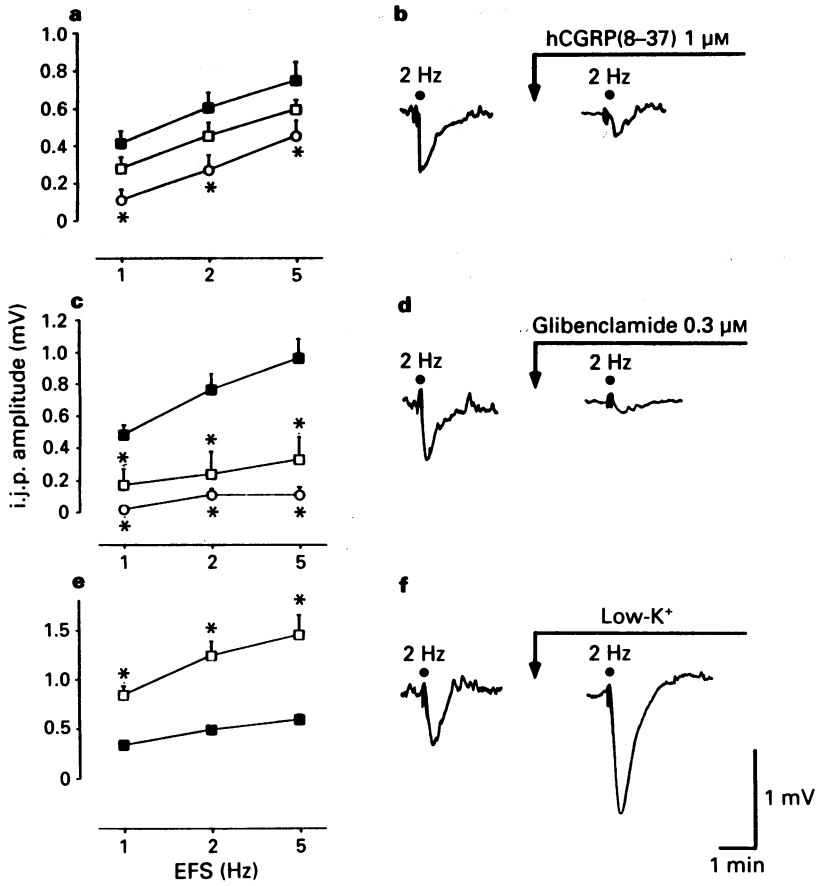


Figure 3 EFS-induced inhibitory junction potentials (i.j.p.) in the smooth muscle of the guinea-pig ureter and its modification by the calcitonin gene-related peptide (CGRP) receptor antagonist CGRP(8–37) (a and b), glibenclamide (c and d) or by a low-K Krebs solution (e and f). (a) Control, (■), $n = 8$; hCGRP(8–37) 0.3 μM (□), $n = 3$ and 1 μM (○), $n = 5$. (c) Control (■), $n = 8$; glibenclamide 0.3 μM (□), $n = 4$; 1 μM (○), $n = 4$. (e) Control (■), $n = 5$; low-K Krebs solution (□), $n = 5$. In each panel * indicates values which are significantly different from control, $P < 0.05$. In (b), (d) and (f) the response to EFS at 2 Hz (train duration 10 s) is shown before and after hCGRP(8–37), glibenclamide or in a low K Krebs solution.

evoked motility sustained by depolarization of latent pacemakers in the ureter (Maggi *et al.*, 1994). This mechanism may provide the basis through which locally released CGRP suppresses latent pacemakers and prevents antiperistalsis in the ureter. From the present findings it also appears that peptidergic neurotransmission in the peripheral nervous system is not necessarily confined to high frequencies of nerve stimulation (Lundberg & Hokfelt, 1983), since a CGRP-mediated response was readily demonstrated here at low frequency stimulation (10 pulses at 1 Hz).

References

ARTEMENKO, D.P., BURY, V.A., VLADIMIROVA, I.A. & SHUBA, M.F. (1982). Modification of the single sucrose-gap method. *Physiol. Zhurn.*, **28**, 374–380.

ASHCROFT, S.J.H. & ASHCROFT, F.M. (1990). Properties and functions of ATP-sensitive K channels. *Cell. Signalling*, **2**, 197–214.

CHIBA, T., YAMAGUCHI, A., YAMATANI, T., NAKAMURA, A., MORISHITA, T., INUI, T., FUKASE, M., NODA, T. & FUJITA, T. (1989). CGRP receptor antagonist hCGRP (8–37). *Am. J. Physiol.*, **256**, E331–335.

COOK, N.S. & QUAST, U. (1990). Potassium channel pharmacology. In *Potassium Channels*. ed. pp. 181–258. Cook, N.S. Chichester, England: Ellis Horwood.

DENNIS, T., FOURNIER, A., ST PIERRE, S. & QUIRION, R. (1989). Structure-activity profile of calcitonin gene-related peptide in peripheral and brain tissue. Evidence for receptor multiplicity. *J. Pharmacol. Exp. Ther.*, **251**, 718–725.

HOYLE, C.H.V. (1987). A modified single sucrose gap-junction potentials and electrotonic potentials in gastrointestinal smooth muscle. *J. Pharmacol. Methods*, **18**, 219–226.

LUNDBERG, J.M. & HOKFELT, T. (1983). Coexistence of peptides and classical neurotransmitters. *Trends Neurosci.*, **6**, 325–333.

MAGGI, C.A., CHIBA, T. & GIULIANI, S. (1991). Human α-calcitonin gene-related peptide (8–37) as an antagonist of exogenous and endogenous calcitonin gene-related peptide. *Eur. J. Pharmacol.*, **192**, 85–88.

MAGGI, C.A. & GIULIANI, S. (1991). The neurotransmitter role of CGRP in the rat and guinea-pig ureter: effect of a CGRP antagonist and species-related differences in the action of omega conotoxin on CGRP release from primary afferents. *Neurosci.*, **43**, 261–271.

MAGGI, C.A., GIULIANI, S., DEL BIANCO, E., GEPPETTI, P., THEODORSSON, E. & SANTICIOLI, P. (1992a). CGRP in the regulation of urinary tract motility. *Ann. New York Acad. Sci.*, **657**, 328–343.

MAGGI, C.A. & MELI, A. (1988). The sensory-efferent function of capsaicin-sensitive sensory neurons. *Gen. Pharmacol.*, **19**, 1–43.

MAGGI, C.A., SANTICIOLI, P., DEL BIANCO, E. & GIULIANI, S. (1992b). Local motor responses to bradykinin and bacterial chemotactic peptide FMLP in the guinea-pig isolated renal pelvis and ureter. *J. Urology*, **148**, 1944–1950.

MAGGI, C.A., GIULIANI, S. & SANTICIOLI, P. (1994). Effect of cromakalim and glibenclamide on spontaneous and evoked motility of the guinea-pig isolated renal pelvis and ureter. *Br. J. Pharmacol.*, **111**, 687–694.

MAGGI, C.A., TRAMONTANA, M,. CECCONI, R. & SANTICIOLI, P. (1990). Neurochemical evidence for the involvement of N-type calcium channels in transmitter secretion from peripheral endings of sensory nerves in guinea-pigs. *Neurosci. Lett.*, **114**, 203–206.

POYNER, D.R. (1992). CGRP: multiple actions, multiple receptors. *Pharmacol. Ther.*, **56**, 23–51.

SANN, H., ROSSLER, W., HAMMER, K. & PIERAU, F.R.K. (1992). SP and CGRP in the ureter of chicken and guinea-pig: distribution, binding sites and possible functions. *Neuroscience*, **49**, 699–713.

SANTICIOLI, P., MAGGI, C.A., GEPPETTI, P., DEL BIANCO, E., THEODORSSON, E. & MELI, A. (1988). Release of CGRP-LI from organs of the genitourinary tract in rats. *Neurosci. Lett.*, **92**, 197–201.

STANDEN, N.B., QUAYLE, J.M., DAVIES, N.W., BRAYDEN, J.E., HUANG, Y. & NELSON, T.M. (1989). Hyperpolarizing vasodilators activate ATP-sensitive K channels in arterial smooth muscle. *Science*, **245**, 177–180.

SU, H.C., WHARTON, J., POLAK, J.M., MULDERRY, P.K., GHATEI, M.A., GIBSON, S.J., TERENGHI, G., MORRISON, J.F.B., BALLESTA, J. & BLOOM, S.R. (1986). CGRP immunoreactivity in afferent neurons supplying the urinary tract: combined retrograde tracing and immunohistochemistry. *Neuroscience*, **18**, 727–747.

WEISS, R.M. (1992). Physiology and pharmacology of renal pelvis and ureter. In *Campbell's Urology*, ed. Walsh, P.C., Retik, A.B., Stamey, T.A. & Vaughan, E.D. Volume I, pp. 113–144. Philadelphia PA: W.B. Saunders Co.

YAMAMOTO, A.I. & TOHYAMA, M. (1989). CGRP in the nervous tissue. *Prog. Neurobiol.*, **33**, 335–395.

(Received January 19, 1994
Revised May 18, 1994
Accepted June 20, 1994)

Br. J. Pharmacol. (1994), **113**, 593–599 © Macmillan Press Ltd, 1994

A distinctive electrophysiological signature from the Peyer's patches of rabbit intestine

[1]D.J. Brayden & *A.W. Baird

Elan Corporation Research Institute, Trinity College Dublin, Dublin 2, and *Department of Pharmacology, University College Dublin, Blackrock, Co. Dublin, Ireland

1 Rabbit small intestinal segments containing Peyer's patches (PP) were examined in Ussing chambers using short-circuit current (I_{sc}) recording. By comparison with control small intestinal mucosal segments, rabbit PP-containing epithelia exhibited decreased basal I_{sc}, increased transepithelial resistance (TER) and unchanged potential difference (PD).

2 Carbachol caused a decrease in I_{sc} in rabbit PP epithelia. Forskolin, dibutyryl cyclic GMP, histamine and the calcium ionophore, A23187, were without effect. In contrast, control epithelial segments of rabbit intestine responded to carbachol and forskolin with an increased I_{sc}, indicative of electrogenic chloride secretion. The EC_{50} for carbachol was approximately 2 μM in both types of epithelia. Methacholine also caused an outward current in rabbit PP epithelia which had similar properties to that of carbachol. The effect of the cholinomimetics on rabbit PP was basolateral-sided, reversible, and sensitive to low concentrations of the general muscarinic cholinoceptor blockers, atropine, scopolamine and also to the M_1 cholinoceptor blocker, pirenzepine.

3 The I_{sc} response to cholinomimetics in rabbit PP was insensitive to bumetanide, amiloride, TEA, barium, acetazolamide, piroxicam and omeprazole, but was attenuated in the presence of ouabain. Using bilaterally-substituted solutions, the carbachol effect on rabbit PP I_{sc} was abolished in chloride/bicarbonate-free, but not in chloride-free solutions, suggestive of stimulation of electrogenic bicarbonate absorption by the agent. Substitution for sodium abolished both the basal current and the I_{sc} response to carbachol. Part of the effect of carbachol on PP I_{sc} appeared to be mediated by submucosal neurones because addition of tetrodotoxin reduced the effect by 60%.

4 As microfold (M) epithelial cells predominate in the PP of the rabbit, the unusual phenotype of cholinomimetic-induced outward current may be used as an electrophysiological marker for these potential sites of oral vaccine delivery, and in particular it may also be of use as a marker for rabbit M cells.

Keywords: Rabbit Peyer's patches; Ussing chamber; carbachol; M cells

Introduction

Peyer's patches (PP) represent concentrations of lymphoid tissue which are distributed throughout mammalian intestine. Functions of these gut-associated lymphoepithelial tissues (GALT) include sampling of lumenal nutrients, bacteria and viral particles. The PP are composed of a specialized follicle-associated epithelium (FAE) overlying lymphoid follicular domes (Owen & Jones, 1974). The FAE are sites of intestinal antigen presentation to T lymphocytes which in turn invaginate into the basolateral pocket of the main epithelial cell type of the FAE, i.e. the microfold or M-cell (for review, see Ho *et al.*, 1990).

In marked comparison to the absorptive/secretory columnar epithelial cells of adjoining intestinal tissue, M cells are almost devoid of lysosomes which means that intracellular proteolysis is reduced. The unusual pocket shape of these cells means that peptides only have to travel a short distance from the apical to the basolateral membrane by comparison with adjacent columnar epithelia. Thus intact macromolecules may be delivered across the epithelial barrier. Furthermore, absorbed antigen is also presented to the thoracic duct of the lymphatic system and thus can avoid the first pass effect caused by drainage into the hepatic portal vein (Kreuter, 1991).

PP of the intestine are a potential target site for peptide absorption (Keljo & Hamilton, 1983; Ducroc *et al.*, 1983). Recent research has focused on specific targeting processes for peptides with the PP. Particulate uptake by rabbit PP was demonstrated to be efficient for negatively charged liposomes (Tomizawa *et al.*, 1993), and also for latex microparticles (Lefevre *et al.*, 1985; Pappo & Ermak, 1989; Jepson *et al.*, 1993), the site appearing to be localized to the M-cell. Indeed there is some evidence that nanoparticles are specifically absorbed by porcine PP using endocytosis (Scherer *et al.*, 1993). While the absorptive capacity of PP may be low even for particles of small size and ideal polymer composition (Ebel, 1990), such a property could be preferable for localized vaccine delivery rather than for delivery of peptides. Recently, M cells were stimulated to secrete monoclonal IgA into the intestine in order to bind a single surface epitope on enteric pathogens and thereby to provide localized immunity (Neutra & Kraehenbuhl, 1993).

Although the epithelium of PP is structurally continuous with the epithelial cells which regulate absorption and secretion of electrolytes and water, there is little information regarding the ion transport characteristics of these specialised structures. The present study explores features of PP-containing intestinal segments by comparing their ion transport parameters with that of adjacent normal epithelia. Tissues obtained from rabbit were examined by the short-circuit current method in a classic Ussing chamber. An unusual distinctive electrophysiological response to carbachol is described. The response may derive from M cells, the predominant cell type of rabbit PP (Pappo *et al.*, 1988).

Methods

Isolation of PP segments from rabbit small intestine

Male and female New Zealand White rabbits (2–3 kg) were killed by intravenous pentobarbitone sodium injection (150

[1] Author for correspondence.

mg kg^{-1}). The intestine from duodenum to terminal ileum was removed and placed in oxygenated Krebs-Henseleit solution. Fresh solution was used to irrigate the lumen in order to remove debris. Up to 10 PP were located in the region from jejunum to terminal ileum. The area of the rabbit PP used for studies was approximately 1.2 cm^2. Upon location of the patch, the intestinal segment was slipped over plastic pipettes where the PP was clearly delineated against the background of a light source. The gut was opened along the line of mesentery attachment in order that the PP remained entire. PP-containing segments and adjacent epithelial (control) segments of epithelia were stripped of associated smooth muscle (Cuthbert & Margolius, 1982).

Short-circuit current recording in Ussing chamber

Rabbit epithelium with or without PP were mounted in Ussing chambers of window areas of 1.13 cm^2. Measurements of potential difference (PD) (apical side negative), transepithelial resistance (TER) and I_{sc} were made as decribed previously (Cuthbert & Margolius, 1982) using a DVC 1000 Dual Voltage Clamp (World Precision Instruments, U.K.). The voltage was clamped intermittently to 1 mV and the current required was used to calculate TER by applying the Ohmic relationship.

Solutions

The Krebs-Henseleit (KH) solution used to bath the tissues had the following composition (mM): NaCl 117, KCl 4.7, $MgSO_4$ 1.2, KH_2PO_4 1.2, $NaHCO_3$ 25, $CaCl_2$ 2.5 and glucose 11.1. The pH was 7.4 when equilibrated with a mixture of 95% O_2:5% CO_2. Chloride-free KH contained (mM): sodium gluconate 117, potassium gluconate 4.7, and $CaSO_4$ 2.5, as substitutes for NaCl, KCl and $CaCl_2$ respectively, and was equilibrated with 95% O_2:5% CO_2 at a pH of 7.4. Chloride/bicarbonate-free KH contained these substitutions and in addition HEPES acid 10, and Tris base 10, in place of $NaHCO_3$. This solution was bubbled with 95% O_2 which maintained pH at 7.4. Sodium-free KH contained (mM): N-methyl D-glucamine chloride (NMDG) 117, HEPES acid 10, Tris base 10, KCl 4.7, $MgCl_2$ 1.2, KH_2PO_4 1.2, $CaCl_2$ 2.5 and glucose 11.1. The pH was 7.4 when equilibrated with O_2. All solutions were within an osmolarity range of 270–290 mOsmol l^{-1}.

Drugs and chemicals

Forskolin and A23187 were obtained from Calbiochem. Carbachol, methacholine, scopolamine, tetrodotoxin, histamine, dibutryl cyclic GMP, amiloride, bumetanide, pirenzepine, tetraethylammonium (TEA), histamine, ouabain, piroxicam and barium chloride were obtained from the Sigma Chemical Co (UK). Diamox-TM (acetazolamide) was supplied by Lederle Labs (UK). Omeprazole was a gift from Astra-Hassle (Sweden). All other chemicals were reagent grade. Drugs were added in a volume that comprised no more than 1% of the total volume of the Ussing chamber/glass reservoirs.

Statistics

Student's *t* test (paired or unpaired as applicable) was used to test for significance. $P<0.05$ was considered significant.

Results

Basal electrical parameters of rabbit PP epithelia

The basal parameters of PP epithelia compared to control adjacent segments are given in Table 1. There was a statistically higher TER and statistically lower basal I_{sc} in PP epithelia while the PD was similar to controls.

Table 1 Basal electrophysiological parameters from rabbit PP-containing epithelia and intestinal controls

	PP	*Control*
TER (Ω cm^2)	137.7 ± 7.9 (37)*	26.9 ± 3.0 (10)
PD (mV)	−2.0 ± 0.2 (37)	−2.5 ± 0.4 (10)
I_{sc} (μA cm^{-2})	16.5 ± 1.5 (37)*	90.2 ± 8.6 (10)

Numbers in parentheses indicate number of segments examined.
*$P<0.001$, unpaired *t* test. Values are mean ± s.e.mean 30 min after mounting in the Ussing chamber. PP = Peyer's patch epithelium. Numbers in parentheses are segments taken from 12 rabbits for PP and 6 rabbits for control intestines.
PD = potential difference; TER = transepithelial resistance.

Pharmacological responses in rabbit PP epithelia

Basolateral additions of carbachol caused a concentration-dependent decrease in I_{sc} in voltage-clamped rabbit PP (Figure 1a). Such an effect may be due to stimulation of outward current (cation secretion and/or anion absorption) or, alternatively, inhibition of inward current (anion secretion and/or cation absorption). The mean net reduction in I_{sc} in response to 10 μM carbachol was -5.8 ± 0.6 μA cm^{-2} ($n = 32$).

In contrast, carbachol stimulated a predominant inward I_{sc} in control rabbit intestine (Figure 1c). The I_{sc} increase in response to 10 μM carbachol was 34.9 ± 5.5 μA cm^{-2} ($n = 8$, $P<0.001$). Responses to carbachol were biphasic, in control preparations; a transient reduction in I_{sc} followed by a sustained net I_{sc} increase (Figure 1c). From the concentration-response curves (Figure 1b,d) the EC_{50} values were not different (approximately 2 μM; $n = 4$ in each case).

Responses to carbachol in rabbit PP preparations were basolateral-sided; no effects were observed after apical additions. A second response could be achieved in the same preparation after washing (Figure 2a). Atropine pretreatment (0.1 μM; added basolaterally) virtually abolished the carbachol effect on I_{sc}. When added at the plateau of the I_{sc} response to carbachol, atropine caused the current to return to basal levels ($n = 6$, see Figure 1a,c). Similar results were obtained with scopolamine ($n = 3$, Figure 2a). Methacholine (MCh; 10 μM; basolateral) mimicked the response of rabbit PP tissue to carbachol. The reduction in I_{sc} produced by MCh was reversed by pirenzepine, an M_1-selective muscarinic receptor antagonist (Figure 2b).

Histamine (10 μM) and A23187 (1 μM), which are shown to elevate intracellular calcium and to increase I_{sc} in intestinal epithelial cells (Wasserman *et al.*, 1988; Wong *et al.*, 1989), were without effect on I_{sc} in rabbit PP epithelia ($n = 3$ for each agent). In the presence of histamine and A23187, responses to carbachol in rabbit PP were not different from untreated controls ($n = 3$, results not shown). Results from these preliminary experiments indicate that elevation of intracellular free calcium does not contribute to cholinomimetic-stimulated outward current in rabbit PP.

Forskolin (10 μM) had a modest effect on I_{sc}, giving a net mean increase of 1.6 ± 0.5 μA cm^{-2} in rabbit PP ($n = 6$). By comparison, forskolin stimulated a net I_{sc} increase of 57.0 ± 12.8 μA cm^{-2} ($n = 6$, $P<0.001$) in control rabbit intestine (Figure 3). In the presence of forskolin the characteristic carbachol response was maintained in both types of tissue.

Dibutyryl cyclic GMP (1 mM) added bilaterally to voltage-clamped rabbit PP was without effect ($n = 3$). Moreover, I_{sc} responses to carbachol were not modified in the presence of

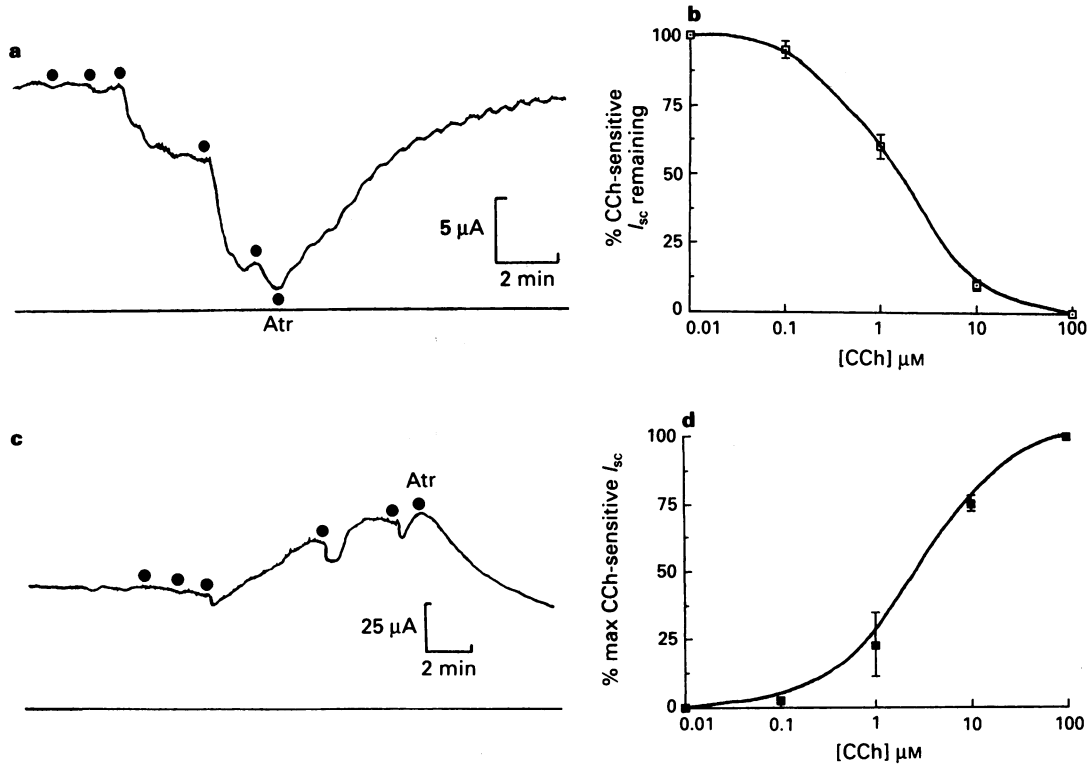


Figure 1 Short-circuit current responses of rabbit PP and intestinal epithelia to carbachol (CCh). In (a) and (c) CCh was added in log concentration steps from 0.01 to 100 μM to a PP and control intestinal epithelium respectively. The horizontal bar indicates zero μA in each case. The plot of percentage CCh-sensitive I_{sc} remaining versus concentration is shown for PP (b) and the plot of percentage maximum CCh-sensitive I_{sc} versus concentration is shown for control epithelia (d). $n = 4$ experiments for each plot. The EC_{50} for CCh was approximately 2 μM in each preparation. Note that the outward current was reversed by atropine (Atr, 0.1 μM) in PP epithelium (a) and that the inward current was reversed by atropine in control rabbit intestine (c).

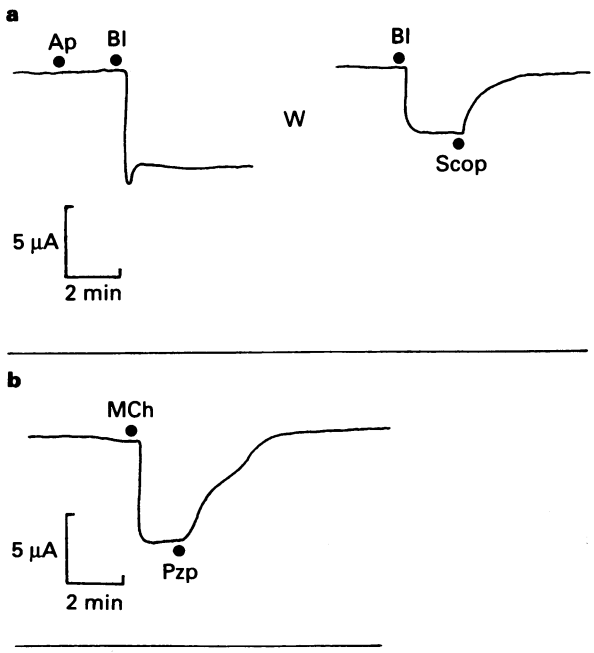


Figure 2 Carbachol I_{sc} responses in rabbit PP epithelia are sided and reversible. In (a) carbachol was added first to the apical (Ap) side without result and then to the basolateral side (Bl) where a decrease in I_{sc} was noted. Upon washing (W), the response to basolateral additions of carbachol was re-established and was inhibited by scopolamine (Scop, 0.1 μM). Example is typical of 4 experiments. In (b) a response is shown to basolateral addition of methacholine (MCh, 10 μM), followed by a reversing of the response with pirenzepine (Pzp, 0.1 μM), also added to the basolateral side. Example is typical of 4 experiments. Horizontal lines indicate zero μA.

dibutyryl cyclic GMP, suggesting that cyclic GMP plays little part in ion transport responses to cholinoceptor agonists (Figure 4). In contrast, in the rabbit small intestine cyclic GMP is well-known as the powerful intracellular mediator of the electrogenic chloride secretory action stimulated by heat stable enterotoxin (Field *et al.*, 1978).

Ionic basis of the basal I_{sc}

The following inhibitors were without effect on basal I_{sc} in rabbit PP tissue: bumetanide (200 μM), amiloride (0.1 mM), barium (3 mM), tetraethyl ammonium chloride (3 mM), piroxicam (10 μM), ouabain (1 μM) and omeprazole (0.1 mM). At least 4 separate experiments were carried out using bilateral additions of each agent. The only manoeuvre tested which abolished or reduced the basal I_{sc} was replacement of KH with sodium-free solution. In 6 paired experiments sodium-free solution abolished basal I_{sc}, reduced PD and increased TER with respect to controls (Table 2).

Ionic basis of the carbachol-stimulated I_{sc} *in rabbit PP*

The carbachol-evoked outward current was not altered by pretreatment with bumetanide (200 μM; serosal) or amiloride (0.1 mM; mucosal) which inhibit the Na/K/2Cl cotransporter and the Na/H exchanger respectively. Bilateral addition of the potassium channel blockers, barium (3 mM) or tetraethyl ammonium chloride (3 mM), was without effect on carbachol responses in rabbit PP. The results with these inhibitors are summarized in Table 3.

In 6 paired preparations from 6 different rabbits, serosal incubation with 1 μM ouabain for 30 min inhibited by 60% the outward current stimulated by carbachol in rabbit PP. The mean control value for the CCh-stimulated I_{sc} was -3.6 ± 0.7 μA cm^{-2} while the mean value for the ouabain-

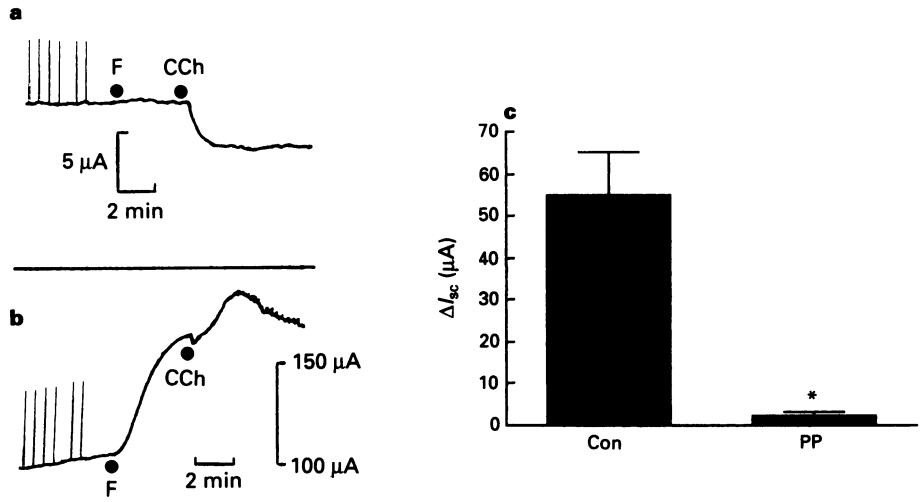


Figure 3 I_{sc} responses of rabbit PP and control intestinal epithelia to forskolin. In (a) and (b) forskolin (F, 10 μM) was added to the basolateral side of PP and control epithelia respectively. The responses for forskolin are pooled in (c), where $P<0.002$ ($n=6$). In each case carbachol (CCh, 10 μM) was added as a second agent in order to demonstrate pharmacological responsiveness and to define the tissue segment. The horizontal line indicates zero μA for recording (a).

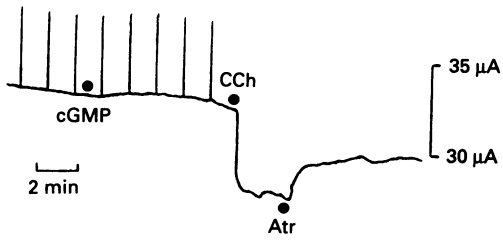


Figure 4 Absence of dibutyryl-cyclic GMP I_{sc} response in rabbit PP epithelium. 1 mM dibutyryl-cyclic GMP (cGMP) was added bilaterally followed by basolateral addition of carbachol (CCh, 10 μM) and atropine (Atr, 0.1 μM). The presence of cyclic GMP had no effect on the subsequent I_{sc} responses to carbachol.

Table 2 Effects of sodium-free solution on electrophysiological parameters from rabbit PP-containing epithelia and intestinal controls

	KH	*Na-free solution*
TER (Ω cm²)	168.0 ± 7.8 (6)	265.2 ± 31.3 (6)*
PD (mV)	−1.1 ± 0.2 (6)	0.0 ± 0.1 (6)**
I_{sc} (μA cm⁻²)	11.3 ± 3.3 (6)	0.6 ± 0.8 (6)*
ΔI_{sc} after CCh	−3.6 ± 0.7 (6)	0.0 ± 0.0 (6)**

Numbers in parentheses indicate number of segments examined.
For comparison each PP came from a different rabbit and was paired. *$P<0.05$, **$P<0.005$, paired t test. Basal values are mean ± s.e.mean 30 min after mounting in the chamber. TER = transepithelial resistance; PD = potential difference.

pretreated tissues was -1.1 ± 0.77 μA cm^{-2} ($P<0.05$). Ion substitution experiments were performed in order to help identify the charge-carrying ion(s) responsible for the carbachol-stimulated I_{sc}. Replacement of chloride in the bath solutions had no effect on carbachol responses (Table 4) confirming the result with bumetanide. In contrast, responses were inhibited by 50% in chloride/bicarbonate-free KH ($P<0.001$). TER values were maintained throughout chloride/bicarbonate substitution experiments, indicating that the integrity of the tissue was not compromised. Likewise, there were no statistical differences in basal electrical parameters in these substituted solutions. The large effect of chloride/bicarbonate-free KH on the carbachol response implied that bicarbonate absorption may contribute to the outward I_{sc}. Incubation with acetazolamide (0.45 mM) in either KH or in chloride-free KH was without effect on responses to subsequent challenge with carbachol ($n=4$, paired in each case). In 6 paired preparations from 6 rabbits, sodium-free solution caused abolition of subsequent responses to carbachol (Table 2). The increased TER values obtained in sodium-free solution indicated that the tissues were still viable.

Incubation with the inhibitor of Na/H ATPase, omeprazole (0.1 mM), was without effect on subsequent I_{sc} responses to carbachol in rabbit PP. In 4 paired preparations the mean responses were -4.2 ± 0.9 μA cm^{-2} (Control) and -3.6 ± 1.0 μA cm^{-2} (Test). These values were not statistically different. The indirect evidence thus indicates that bicarbonate absorption stimulated by carbachol does not appear to be linked to proton secretion.

The possibility that prostaglandins might be involved in the mediation of the CCh-stimulated I_{sc} was investigated by preincubation of 6 paired PP tissues from 6 rabbits with piroxicam (10 μM) for 30 min. The mean control value for the CCh-stimulated I_{sc} was -3.6 ± 0.7 μA cm^{-2} while the mean value for the piroxicam-pretreated tissues was -4.0 ± 1.2 μA cm^{-2} (NS).

Neuronal involvement in the carbachol response in rabbit PP

Acetylcholine stimulates chloride secretion in small intestinal epithelium of rabbit both by a direct effect on intestinal epithelial tissues and also by an indirect effect mediated by cholinergic neurones in the lamina propria (Diener *et al.*, 1988). In rabbit PP, tetrodotoxin, an inhibitor of neuronal sodium conductance, reduced the carbachol stimulated outward current on average by 60.1% in 5 paired experiments on adjacent patches from the same animal for each experiment (Figure 5a–c). Thus, the cholinoceptor response can be estimated as 39.9% due to a direct effect on the patch-containing epithelium. These results are comparable with those of Diener *et al.* (1988), in which tetrodotoxin also substantially reduced the I_{sc} response in rabbit intestine to a number of secretagogues. The effects of tetrodotoxin were not reversible. However, unchanged TER measurements indicated that attenuation of the I_{sc} response to carbachol was not due to toxicity.

Table 3 The effects of ion transport inhibitors on the I_{sc} response to carbachol in rabbit PP epithelia

	ΔI_{sc} *in response to CCh*
Control	$-5.78 \pm 0.56\ \mu A\ cm^{-2}$ (32)
Bumetanide	$-7.05 \pm 0.78\ \mu A\ cm^{-2}$ (4)
Amiloride	$-6.46 \pm 0.77\ \mu A\ cm^{-2}$ (3)
Barium	$-5.90 \pm 0.65\ \mu A\ cm^{-2}$ (3)
TEA	$-5.56 \pm 0.40\ \mu A\ cm^{-2}$ (3)
Ouabain	$-1.11 \pm 0.77\ \mu A\ cm^{-2}$ (6)*

Numbers in parentheses indicate number of segments examined. Values are mean ± s.e.mean for the peak reduction in I_{sc} 2 min after addition of 10 μM carbachol. The concentrations and side of addition of the inhibitors are given in the text. Inhibitors were present for at least 15 min before addition of carbachol. *$P<0.05$, unpaired.

Table 4 The effects of substituted Krebs-Henseleit solutions on the I_{sc} response to carbachol in rabbit PP epithelia

	ΔI_{sc} *after CCh*
Normal KH	$-6.20 \pm 0.90\ \mu A\ cm^{-2}$ (16)
Cl-free KH	$-6.94 \pm 0.82\ \mu A\ cm^{-2}$ (10)
Cl/HCO_3-free KH	$-1.01 \pm 0.56\ \mu A\ cm^{-2}$ (10)*
Na-free KH	$0.00 \pm 0.00\ \mu A\ cm^{-2}$ (6)*

Numbers in parentheses indicate number of segments examined. **$P<0.005$, unpaired t test. Values are mean ± s.e.mean for the peak reduction in I_{sc} 2 min after addition of 10 μM carbachol.

Discussion

The objective of this investigation was to compare basal and stimulated electrophysiological parameters of PP-derived intestinal epithelial tissues from the rabbit with adjacent, histologically normal intestinal controls. To our knowledge this is the first study describing transepithelial ion transport processes in PP-containing epithelium of the intestine. The basal electrical characteristics of control rabbit small intestine compare favourably with those obtained in previous studies (Smith & Field, 1980), respectively. Measurements made with PP tissues indicated that the basal I_{sc} was lower, and the TER was higher than the corresponding controls. Even with the higher TER, the PP regions should be classified as leaky epithelia (Frizzell & Schultz, 1972). The lower basal I_{sc} in the PP may be a consequence of activity of a smaller number of columnar epithelial cells which are identical to those in adjacent (control) tissue or, alternatively, of distinct populations of cells which contribute to basal I_{sc} in PP. Of the range of inhibitors used, amiloride, bumetanide, barium, TEA, piroxicam or ouabain all failed to inhibit the basal I_{sc}. Replacement of sodium abolished basal I_{sc} and increased TER, indicating that maintenance of the current is sodium-dependent and not due to voltage offset.

In response to established secretagogues, control ileal tissues behaved in a predictable manner with inward current responses to carbachol, A23187 and histamine, which were accounted for by electrogenic chloride secretion as previously reported (Bolton & Field, 1977; Frizzell, 1977). During treatment of PP epithelia with cholinomimetics we discovered a characteristic outward I_{sc} in response to carbachol and methacholine. No inward current was detected. These cholinomimetics caused a sided, reversible, receptor-dependent decrease in I_{sc}, which may or may not be identical to the cholinergic-induced transient outward I_{sc} reported in mouse colonic studies (Sagmanligil & Levin, 1993). Of importance is that carbachol caused a predominantly inward I_{sc} in control intestine, as reported here and in the latter study.

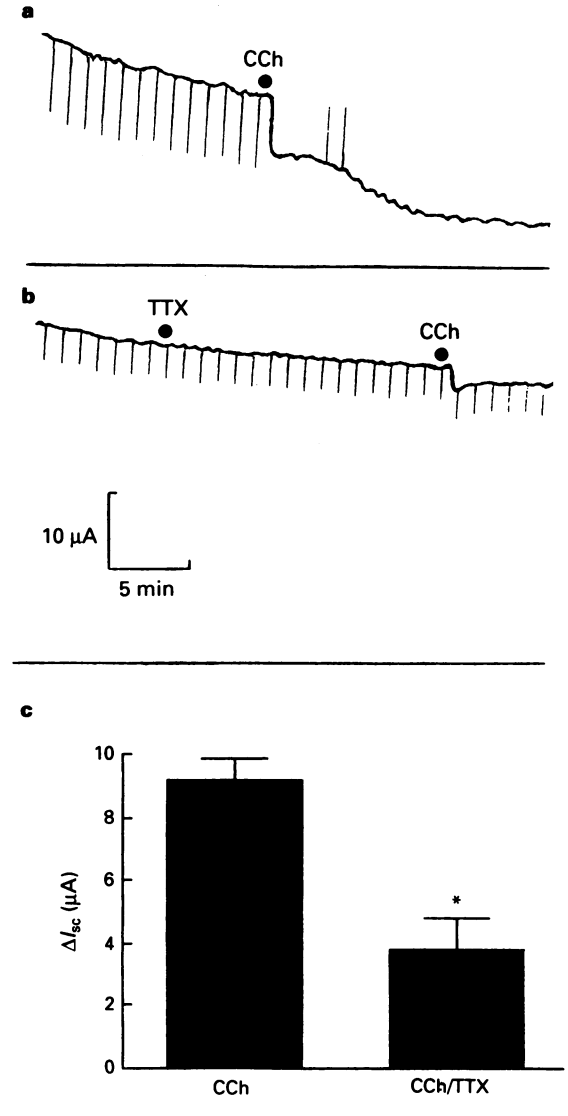


Figure 5 Tetrodotoxin inhibited the carbachol-stimulated outward current in rabbit PP epithelium. In (a) a typical PP response to carbachol (CCh, 10 μM) is shown. In (b) a PP-containing epithelium from the same segment of the same rabbit was pretreated with tetrodotoxin (TTX, 1 μM basolateral) followed by CCh. In (c) the pooled responses are shown from 5 paired preparations using the same protocol. $P<0.02$, paired.

The carbachol response in rabbit PP did not appear to be mediated by calcium because the I_{sc} was unresponsive to A23187 and to histamine, agents known to increase intracellular Ca^{2+} in intestinal epithelia (Wong *et al.*, 1989; Wasserman *et al.*, 1988). Another likely candidate as mediator of the electrogenic process in response to muscarinic activation is cyclic GMP. Unlike carbachol, the dibutryl ester of cyclic GMP had no effect on I_{sc} and, moreover, did not prevent subsequent responses to carbachol. Previous studies on T84 cells showed that occlusivity in the I_{sc} response demonstrates the presence of a common intracellular pathway, while synergy indicates separate intracellular pools (Cartwright *et al.*, 1985; Brayden *et al.*, 1993). According to this model, the lack of occlusivity between cyclic GMP and the carbachol response (and the lack of effect of cyclic GMP on I_{sc} *per se*) indicates that cyclic GMP is not involved in the action of carbachol in rabbit PP epithelia.

Ouabain inhibition of the outward I_{sc} response in PP implicated participation of the Na/K ATPase on the basolateral membrane. Electrogenic chloride transport processes did not contribute to the I_{sc} response to carbachol in

PP as shown by the failure of serosal bumetanide and of chloride-free solution to alter the response. Sodium transport did not contribute to the outward I_{sc}, as shown by the lack of effect of mucosal amiloride in concentrations high enough to inhibit Na/H exchange. The inhibition of the outward I_{sc} by sodium-free solutions is difficult to interpret since the Na/K ATPase may also be blocked under such conditions. Electrogenic potassium absorption did not make a major contribution as seen by the lack of effect of mM concentrations of serosal barium and TEA.

When chloride/bicarbonate-free solution was substituted for KH, the carbachol-induced I_{sc} was indeed reduced. As the basal electrical parameters were similar in the two solutions, it seems that the reduced effect of carbachol in the substituted solution was specifically related to the absence of bicarbonate and not to loss of cellular integrity. Bicarbonate substitution alone was not investigated since this leaves the possibility of the stressed tissue reversibly switching to chloride transport, as has been shown already for rabbit colon in the case of adenosine (Grasl & Turnheim, 1984). However, as acetazolamide was without effect on the outward current, our working hypothesis is that carbachol stimulates bicarbonate absorption which is carbonic anhydrase-independent. It is known that carbonic anhydrase inhibitors do not alter transport of bicarbonate derived from metabolism (Hopfer & Liedtke, 1987). Similarly, the lack of effect of omeprazole suggests the bicarbonate absorption stimulated by carbachol in PP appears to be proton-independent. The assumption was made that these inhibitors can reach their enzyme binding sites in this system.

Tetrodotoxin, which blocks neuronal sodium channels but does not alter electrogenic chloride secretion in intestinal epithelia (Hubel, 1978), attenuated the outward current response to carbachol in PP. Thus, carbachol may have distinct, additive indirect actions on mucosal nerves and direct effects on epithelial cells (Diener *et al.*, 1988). TTX-sensitive carbachol-induced outward I_{sc} has been reported in colon from rat (Nzegwu & Levin, 1990) and mouse (Sagmanligil & Levin, 1993).

In this study, the neuronal component may mask direct epithelial effects of carbachol. In the presence of tetrodotoxin the residual response to carbachol was only 2–3 $\mu A\,cm^{-2}$, not enough upon which to carry out quantitative research. Thus, we cannot discern what degree of muscarinic receptor involvement in the carbachol response is divided between the PP epithelial cells and the pre- and postsynaptic myenteric neurones.

The majority of cells in PP of the rabbit are of the M cell type (Pappo *et al.*, 1988). Features include truncated microvilli on the apical membrane, low levels of intracellular lysosomes (Owen, 1977) and high levels of vimentin (Jepson *et al.*, 1992). M cells are ideal candidates for oral peptide targeting because they appear to have bioadhesive properties for peptide-encasing polymers, namely latex microspheres (Lefèvre *et al.*, 1985; Pappo & Ermak, 1989), and cyanoacrylate nanoparticles (Scherer *et al.*, 1993). More importantly, the basolateral side of the M cells opens to the lymphatic system rather than to the hepatic portal vein. As PP make up as much as 1% of the total absorptive area of the intestine of the rabbit, it would be useful to specifically target the M cells using markers such as negative staining for alkaline phosphatase (Owen & Bhalla, 1983), mannan coated microspheres (Tomizawa *et al.*, 1993) or with monoclonal antibodies to apical membrane surface antigens (Pappo *et al.*, 1991).

Many of the characteristics of rabbit PP appear to have common features with those of human PP (Cornes, 1965). It is not unlikely that the carbachol response located in rabbit PP in this study may be used as new electrophysiological marker for the M cell. The carbachol-stimulated outward I_{sc} may be of use as a marker for characterization of primary cultures of subtypes of cells which make up the PP epithelium.

References

BOLTON, J.E. & FIELD, M. (1977). Ca^{2+} ionophore-stimulated ion secretion in rabbit ileal mucosa: relation to actions of cyclic AMP and carbamylcholine. *J. Membr. Biol.*, **35**, 159–174.

BRAYDEN, D.J., KROUSE, M.E., LAW, T. & WINE, J.J. (1993). Stilbenes stimulate T84 Cl^- secretion by elevating Ca^{2+}. *Am. J. Physiol.*, **264**, G325–G333.

CARTWRIGHT, C.A., MCROBERTS, J.A., MANDEL, K.G. & DHARMSATHAPHORN, K. (1985). Synergistic action of cyclic AMP and calcium-mediated chloride secretion in a colonic epithelial cell line. *J. Clin. Invest.*, **76**, 1837–1842.

CORNES, J.S. (1965). Number, size and distribution of Peyer's patches in the human small intestine. 1. Development of Peyer's patches. *Gut*, **6**, 225–233.

CUTHBERT, A.W. & MARGOLIUS, H.A. (1982). Kinins stimulate net chloride secretion by the rat colon. *Br. J. Pharmacol.*, **75**, 587–598.

DIENER, M., BRIDGES, R.J., KNOBLOCK, S.F. & RUMMEL, W. (1988). Indirect effects of bradykinin on ion transport in rat colon descendens: mediated by prostaglandins and enteric neurons. *Naunyn-Schmied. Arch. Pharmacol.*, **337**, 69–73.

DUCROC, R., HEYMAN, M., BEAUFRERE, B. & MORGAT, J.L. (1983). Horseradish peroxidase transport across rabbit jejunum and Peyer's patches in vitro. *Am. J. Physiol.*, **245**, G54–G58.

EBEL, J.P. (1990). A method for quantifying peptide absorption from the mouse small intestine. *Pharm. Res.*, **7**, 848–851.

FIELD, M., GRAF, H.L., LAIRD, W.J. & SMITH, P.L. (1978). Heat stable enterotoxin of E. Coli: in vitro effects of guanylate cyclase activity, cyclic GMP concentration, and ion transport in small intestine. *Proc. Natl. Acad. Sci. U.S.A.*, **75**, 2800–2804.

FRIZZELL, R.A. (1977). Active chloride secretion by rabbit colon: calcium-dependent stimulation by ionophore A23187. *J. Membr. Biol.*, **35**, 175–187.

FRIZZELL, R.A. & SCHULTZ, S.G. (1972). Ionic conductance of the extracelular shunt pathway in rabbit ileum. *J. Gen. Physiol.*, **59**, 318–346.

GRASL, M. & TURNHEIM, K. (1984). Stimulation of electrolyte secretion in rabbit colon by adenosine. *J. Physiol.*, **346**, 93–110.

HO, N.F.H., DAY, J.S., BARSUHN, C.L., BURTON, P.S. & RAUB, T.J. (1990). Biophysical model approaches to mechanistic transepithelial studies of peptides. *J. Controlled Release*, **11**, 3–24.

HOPFER, U. & LIEDTKE, C.M. (1987). Proton and bicarbonate transport mechanisms in the intestine. *Annu. Rev. Physiol.*, **49**, 51–68.

HUBEL, K.A. (1978). The effects of electrical field stimulation and tetrodotoxin on ion transport by the isolated rabbit ileum. *J. Clin. Invest.*, **62**, 1039–1047.

JEPSON, M.A., MASON, C.M., BENNETT, M.K., SIMMONS, N.L. & HIRST, B.H. (1992). Co-expression of vimentin and cytokeratins in M cells of rabbit intestinal lymphoid follicle-associated epithelium. *Histochem. J.*, **24**, 33–39.

JEPSON, M.A., SIMMONS, N.L., SAVIDGE, T.C., JAMES, P.S. & HIRST, B.H. (1993). Selective binding and transcytosis of latex microspheres by rabbit intestinal M cells. *Cell Tissue Res.*, **271**, 399–405.

KELJO, J.J. & HAMILTON, J.R. (1983). Quantitative determination of macromolecular transport rate across intestinal Peyer's patches. *Am. J. Physiol.*, **244**, G637–G644.

KREUTER, J. (1991). Peroral administration of nanoparticles. *Advanced Drug Deliv. Rev.*, **7**, 71–86.

LEFEVRE, M.E., JOEL, D.D. & SCHIDLOVSKY, G. (1985). Retention of ingested latex particles in Peyer's patches of germfree and conventional mice. *Proc. Soc. Exp. Biol. Med.*, **179**, 522–528.

NEUTRA, M.R. & KRAEHENBUHL, J.P. (1993). The role of transepithelial transport by M cells in microbial invasion and host defense. *J. Cell Sci.*, Suppl. **17**, 209–217.

NZEGWU, H.C. & LEVIN, R.J. (1990). Dietary restriction increases secretion in rat distal colon induced by secretagogues acting via calcium but not by cyclic AMP. *Proc. Nutr. Soc.*, **49**, 178A.

OWEN, R.L. (1977). Sequential uptake of horseradish peroxidase by lymphoid follicle epithelium of Peyer's patches in normal unobstructed mouse intestine: an ultrastructural study. *Gastroenterology*, **72**, 440–451.

OWEN, R.L. & BHALLA, D.K. (1983). Cytochemical analysis of alkaline phosphatase and esterase activities and of lectin-binding and anionic sites in rat and mouse Peyer's patch M cells. *Am. J. Anat.*, **168**, 199–212.

OWEN, R.L. & JONES, A.L. (1974). Epithelial specialization within human Peyer's patches: an ultrastructural study of intestinal lymphoid follicles. *Gastroenterology*, **66**, 189–203.

PAPPO, J. & ERMAK, T.H. (1989). Uptake and translocation of fluorescent latex particles by rabbit Peyer's patch follicle epithelium: a quantitative model for M cell uptake. *Clin. Exp. Immunol.*, **76**, 144–148.

PAPPO, J., ERMAK, T.H. & STEGER, H.J. (1991). Monoclonal antibody-directed targeting of fluorescent microspheres to Peyer's patch M cells. *Immunology*, **73**, 277–280.

PAPPO, J., STEGER, H.J. & OWEN, R.C. (1988). Differential adherence of epithelium overlying gut-associated lymphoid tissue: an ultrastructural study. *Lab. Invest.*, **58**, 692–697.

SAGMANLIGIL, V. & LEVIN, R.J. (1993). Electrogenic ion secretion in proximal, mid and distal colon from fed and starved mice. *Comp. Biochem. Physiol.*, **106C**, 449–456.

SCHERER, D., MOOREN, F.C., KINNE, R.K.H. & KREUTER, J. (1993). In vitro permeability of PBCA nanoparticles through porcine small intestine. *J. Drug Targeting*, **1**, 21–27.

SMITH, P.L. & FIELD, M. (1980). In vitro anti-secretory effect of trifluoperazine and other neuroleptics in rabbit and human small intestine. *Gastroenterology*, **78**, 1545–1553.

TOMIZAWA, H., ARAMAKI, Y., FUJII, Y., HARA, T., SUZUKI, N., YACHI, K., KIKUCHI, H. & TSUCHIYA, S. (1993). Uptake of phosphatidylserine liposomes by rat Peyer's patches following intraluminal administration. *Pharm. Res.*, **10**, 549–552.

WASSERMAN, S.I., BARRETT, K.E., HUOTT, P.A., BEUERLEIN, G., KAGNOFF, M.F. & DHARMSATHAPHORN, K. (1988). Immune-related intestinal Cl^- secretion. 1. Effect of histamine on the T84 cell line. *Am. J. Physiol.*, **254**, C53–C62.

WONG, S.M.E., LINDEMAN, R.P., PARANGI, S. & CHASE Jr., H.S. (1989). Role of calcium in mediating action of carbachol in T84 cells. *Am. J. Physiol.*, **257**, C976–C985.

(Received March 7, 1994
Revised May 12, 1994
Accepted May 27, 1994)

Br. J. Pharmacol. (1994), **113**, 600–606 © Macmillan Press Ltd, 1994

Block of human voltage-sensitive Na^+ currents in differentiated SH-SY5Y cells by lifarizine

N.A. Brown, [1]J.A. Kemp & [2]G.R. Seabrook

Merck Sharp & Dohme Research Laboratories, Neuroscience Research Centre, Terlings Park, Eastwick Road, Harlow, Essex CM20 2QR

1 The ability of lifarizine (RS-87476) to block human voltage-sensitive Na^+ channel currents was studied by use of whole cell patch clamp recording from differentiated neuroblastoma cells (SH-SY5Y).

2 The Na^+ conductance in differentiated SH-SY5Y cells (24.0 ± 2.4 nS, $n = 11$) was half-maximally activated by 10 ms depolarizations to -37 ± 2 mV and was half-maximally inactivated by predepolarizing pulses of 200 ms duration to -86 ± 3 mV ($n = 11$).

3 At low stimulus frequencies (0.1 to 0.33 Hz) voltage-dependent sodium currents were completely blocked, in a concentration-dependent manner, by extracellular application of either tetrodotoxin ($EC_{50} = 4 \pm 1$ nM, $n = 12$) or by lifarizine ($EC_{50} = 783 \pm 67$ nM, $n = 9$). The onset of block by lifarizine ($\tau = 91 \pm 14$ s at 10 μM) was considerably slower than that of tetrodotoxin ($\tau = 16 \pm 3$ s at 100 nM).

4 Lifarizine (1 μM) reduced the peak sodium conductance in each cell (from 26.4 ± 2.0 nS to 15.1 ± 2.7 nS, $n = 4$) without changing the macroscopic kinetics of sodium current activation or inactivation ($V_{\frac{1}{2}} = -35 \pm 1$ mV and -87 ± 4 mV respectively, $n = 4$). Similarly, lifarizine (1 μM) did not affect the reversal potential of the macroscopic sodium current ($+14 \pm 5$ mV in control and $+16 \pm 2$ mV in 1 μM lifarizine; $n = 4$) or reactivation time-constant ($\tau = 14.0 \pm 4.4$ ms).

5 Block of the sodium channel open state by tetrodotoxin (30 nM) did not prevent the inhibition caused by a subsequent application of lifarizine (3 μM). In contrast the depression caused by lifarizine was readily reversible after pretreatment of cells with the local anaesthetic, lignocaine (10 mM).

6 These data demonstrate that lifarizine is a use- and voltage-dependent antagonist of human voltage-sensitive sodium currents. The slow kinetics and pharmacology of the block by lifarizine indicate that access of this drug to the channel is more restricted than that of tetrodotoxin and may involve an allosteric site or state of the channel that is also regulated by local anaesthetics.

Keywords: SH-SY5Y cells; lifarizine; tetrodotoxin; lignocaine; sodium channel; ion channel blockers

Introduction

Activation of voltage-sensitive sodium channels is necessary for the initiation and propagation of action potentials within nerve cells (Hodgkin & Huxley, 1952). Consequently agents that modulate sodium channel function have profound effects upon neuronal excitability. There are at least five distinct toxin binding sites on neuronal voltage-sensitive sodium channels (Catterall, 1992). The functional effects of these toxins include block of the channel pore by tetrodotoxin, the reduction of time-dependent inactivation by batrachotoxin, and the shift in voltage-dependence caused by alkaloid neurotoxins (reviewed in Hille, 1984; Catterall, 1992). Non-neuronal tissues including cardiac and epithelial cells also have sodium channels; however, the pharmacology of these channels is distinct from that of most neurones. These differences presumably relate to the diversity of sodium channel subtypes that have been cloned from mammalian tissues (Noda *et al.*, 1986; Kayano *et al.*, 1988; George *et al.*, 1992a,b; Gellens *et al.*, 1992).

Present therapies for epilepsy and ischaemic stroke are either not ideal due to side-effects, or are non-existent. Despite the differences in aetiology of these conditions both involve an abnormal neuronal hyperexcitability that is associated with the activation of voltage-sensitive sodium channels, and/or calcium influx via voltage-sensitive calcium channels and neurotransmitter-gated ion channels. Indeed the actions of several clinically effective anticonvulsant agents such as carbamazepine, phenytoin, and lamotrigine are believed to be attributable to their block of Na^+ channels (Matsuki *et al.*, 1984; McLean & MacDonald, 1986; Goa *et al.*, 1993). The characteristic voltage- and use-dependence of sodium channel block is thought to underlie their efficacy and tolerability as anticonvulsants, in that the degree of ion channel block only becomes significant during periods of sustained depolarizations and high-frequency firing (e.g. Matsuki *et al.*, 1984; McLean & MacDonald, 1986).

Ion channel blockers such as the Na^+ channel antagonists, lamotrigine and lifarizine (RS-87476) are also neuroprotective in animal models of ischaemia (Kucharczyk *et al.*, 1991; Alps, 1992; Meldrum *et al.*, 1992). However, it is not clear whether the beneficial effects of lifarizine are mediated by blocking sodium or calcium channels, or indeed by actions on both channel types. *In vitro* studies have shown that lifarizine blocks sodium currents in mouse neuroblastoma cells (Sheridan *et al.*, 1991) and can antagonize responses to calcium channel activators in smooth muscle preparation at micromolar concentrations (Fraser & Spedding, 1991). The mechanism by which lifarizine reduces sodium currents is not fully understood, but in mouse neuroblastoma cell lines does not appear to involve a change in sodium channel activation kinetics (Sheridan *et al.*, 1991). Whether the effects of lifarizine involve changes in sodium channel inactivation, as is evident with local anaesthetics, has yet to be determined. Consequently, in this study we examined the ability and mechanism by which lifarizine reduced voltage-sensitive sodium currents in differentiated neuroblastoma cells. Furthermore, as it is known that there are several structurally and pharmacologically distinct types of sodium channel types between species and tissues we used SH-SY5Y cells which are of human neural origin.

[1] Present address: Hoffman La Roche A.G., Pharma Division, Preclinical Research, CNS Department, CH-4002, Basle, Switzerland.
[2] Author for correspondence.

Methods

Cell culture and differentiation procedures

SH-SY5Y cells were grown in tissue culture in a medium that contained Dulbecco's Modified Eagles Medium (GIBCO), 10% foetal calf serum, 2 mM L-glutamine (Geneticin), and were plated on poly-L-lysine coated coverslips. Cells were differentiated for 3 to 5 days using retinoic acid as previously described (Palman *et al.*, 1984; Seward & Henderson, 1990).

Whole cell patch clamp recording

Whole cell patch clamp recordings were made using borosilicate glass microelectrodes (Clark Electromedical Instruments), as previously described (Caeser *et al.*, 1993), with a pipette solution that contained (in mM); CsFl 120, NaCl 10, CsCl 10, HEPES 10, EGTA 10, and $CaCl_2$ 0.5, adjusted to pH 7.3 with CsOH. Cells were perfused at a rate of 1 to 2 ml min^{-1} with an extracellular solution that contained (in mM): NaCl 135, glucose 10, HEPES 10, tetraethylammonium 10, EGTA 1, KCl 5, and $MgCl_2$ 4, pH 7.4, at 22°C. Drugs were applied via the superfusion system. Cells were voltage-clamped at either -80 mV or -100 mV and sodium currents were elicited by 10 ms depolarizing pulses to > -50 mV at a frequency of 0.033 to 3 Hz. Currents were amplified with an Axopatch 200 patch clamp amplifier (Axon Instruments), and captured on line via a CED1401 interface (Cambridge Electronic Design) which was connected to a Compaq 386 microcomputer. Steady-state leak currents were subtracted with the amplifier, and voltage-step leak currents by the CED voltage-clamp analysis software. Boltzman functions were used to describe to voltage-dependence of sodium current activation and inactivation (e.g. Hille, 1984). Data are expressed as the mean ± s.e.mean.

Drugs

Drugs were applied in the superfusion medium in known concentrations, reaching the recording chamber after a delay of 20–30 s. The following drugs were used: Lifarizine (piperazine 1-[diphenyl-methyl]-4-[2-(4-methyl-phenyl)-5-methyl imidazol-4-yl)methyl] trihydrochloride) was synthesized at Merck Sharp & Dohme Research Laboratories, lignocaine and tetrodotoxin was purchased from Sigma.

Results

Kinetics of sodium channel activation and inactivation

Sodium currents in differentiated SH-SY5Y cells were activated by depolarizing pulses to > -50 mV, and exhibited time-dependent inactivation that was dependent upon the holding membrane potential (Figure 1a). Under these recording conditions the macroscopic Na^+ current reversal potential was $+14 \pm 5$ mV ($n = 4$). The voltage-dependence of Na^+ currents in differentiated SH-SY5Y cells was determined from fits to Boltzman functions. Na^+ currents were half-maximally activated by depolarizations to -37 ± 2 mV with a steepness of 4.5 ± 0.4 mV per e-fold change in membrane potential ($n = 11$; Figure 1) and half-maximally inactivated by 200 ms predepolarizing pulses to -86 ± 3 mV with 8.7 ± 0.5 mV per e-fold change in membrane potential. The peak sodium conductance in control conditions determined from the maximum of the Boltzman function fitted to the inactivation curves was 24 ± 2 nS ($n = 11$).

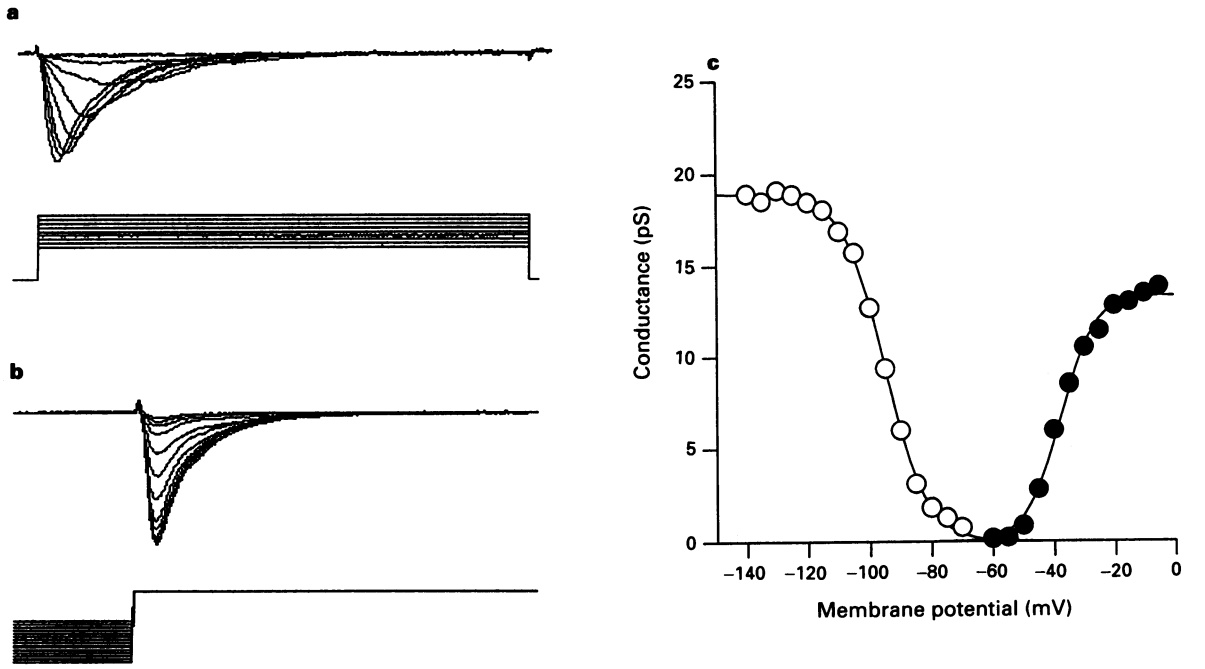


Figure 1 Voltage-dependent activation and inactivation of sodium currents in a differentiated SH-SY5Y cell. (a) Activation protocol depicting a family of superimposed sodium currents (upper traces) elicited by 10 ms depolarizations of 5 mV increments between -60 to -20 mV from a resting membrane potential of -100 mV (lower traces). (b) Inactivation protocol depicting a family of superimposed sodium currents elicited (upper traces) elicited by a depolarization to -20 mV from a variable prepulse potential increasing from -140 to -70 mV at 5 mV increments (lower traces). (c) The peak sodium current at each test potential (activation curve, ●) or prepulse potential (inactivation curve, ○) was used to calculate the whole cell sodium conductance for each membrane potential. Boltzman functions fitted to these data (solid lines) were used to calculate the half-maximal potentials for activation and inactivation (see methods). The maximal conductance during the activation protocol in this cell was lower than that during the inactivation protocol because at a holding potential of -100 mV, the sodium current was already partly inactivated.

Block by tetrodotoxin, lignocaine and lifarizine

At low stimulus frequencies (0.1 Hz) voltage-dependent sodium currents in SH-SY5Y cells were completely blocked, in a concentration-dependent manner, by extracellular application of either tetrodotoxin ($EC_{50} = 4 \pm 1$ nM, $n = 12$) or by lifarizine ($EC_{50} = 783 \pm 67$ nM, $n = 9$). Sodium currents in these cells were also antagonized in a concentration-dependent manner by the local anaesthetic, lignocaine ($EC_{50} = 295 \pm 37$ μM, $n = 8$). Block of sodium currents by lifarizine (1 μM) was voltage-dependent in that the percentage inhibition was greater at a holding potential of − 80 mV (60 ± 3%, $n = 3$) than at − 100 mV (41 ± 4%, $n = 8$). No change in the rate of time-dependent inactivation of the macroscopic current was seen with lifarizine (Figure 2). The onset of block by a maximal concentration of lifarizine ($\tau = 91 \pm 14$ s at 10 μM, $n = 3$) was 5 fold slower than that of tetrodotoxin ($\tau = 16 \pm 3$ s at 100 nM; Figure 3). Although the depression caused by lifarizine was not accentuated by short duration increases in the frequency of depolarizations (15 events at 0.3, 1 and 3 Hz) sustained increases in the stimulus frequency did accentuate the extent of block by submaximally effective concentrations (Figure 3). Block of sodium currents by pretreatment with the open channel blocker TTX (30 nM) did not prevent the depression caused by the subsequent addition of lifarizine (3 μM; $n = 3$; Figure 4). Consistent with this, the block of sodium currents by lifarizine did not require sodium current activation. In cells that were voltage-clamped at − 100 mV and exposed to lifarizine (3 μM) for > 3 min in the absence of stimulation, complete block of the whole cell current elicited by a single pulse to − 20 mV was observed ($n = 3$). In contrast to the lack of interaction between lifarizine and tetrodotoxin, the depression caused by the local anaesthetic, lignocaine (10 mM), was readily reversible after pretreatment of cells with lifarizine (3 μM). Thus this local anaesthetic either occludes or modifies the site or state of the channel to which lifarizine binds. Although readily reversible, the time constant of recovery from block with lignocaine (control $\tau = 63 \pm 25$ s, $n = 3$) was slower following co-application of lifarizine (152 ± 28 s, $n = 5$).

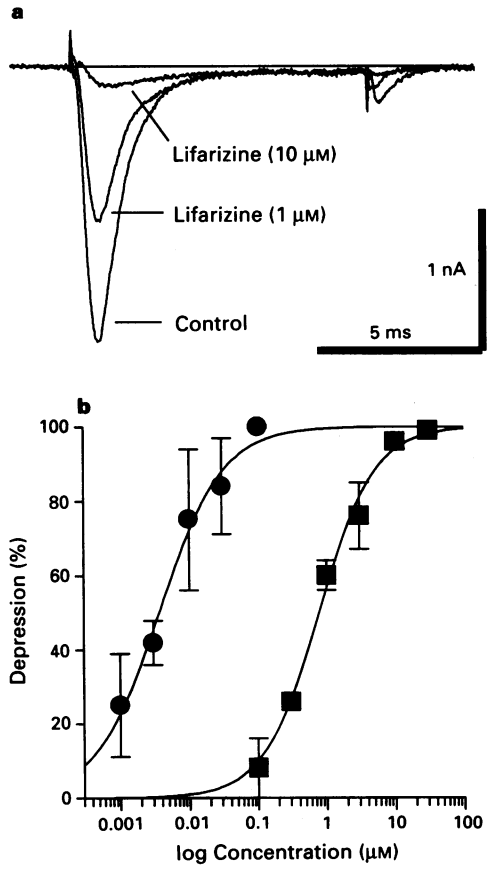


Figure 2 Depression of sodium currents by tetrodotoxin and lifarizine. (a) Superimposed sodium currents elicited by step depolarization from − 100 to − 20 mV in control conditions and the presence of lifarizine (1, 10 μM). (b) Concentration-effect relationship for the inhibition of sodium currents by tetrodotoxin (●) and lifarizine (■) evoked by stepping from a holding membrane potential of − 80 mV to − 20 mV at a stimulus frequency of 0.1 Hz. Solid lines represent the fit of a single-site logistic equation to the data. Each point represents the mean ± s.e.mean from 3 to 8 cells. The half-maximally effective concentration for tetrodotoxin was 4 nM (Hill slope = 0.94 ± 0.11), and for lifarizine was 783 nM (Hill slope = 1.07 ± 0.09).

Effects on voltage-dependence and reactivation kinetics

Lifarizine (1 μM) reduced the peak sodium conductance in each cell (from 26.4 ± 2.0 nS to 15.1 ± 2.7 nS, $n = 4$) without changing the macroscopic kinetics of sodium current activation ($V_{\frac{1}{2}} = -35 \pm 1$ mV, 6.1 ± 0.7 mV/e-fold change in membrane potential, $n = 4$), or inactivation ($V_{\frac{1}{2}} = 87 \pm 4$ mV, 9.8 ± 0.8 mV/e-fold change in membrane potential, $n = 4$). Similarly, lifarizine (1 μM) did not affect the reversal potential of the macroscopic sodium current (+ 16 ± 2 mV at 1 μM). To test whether lifarizine was reducing the rate at which sodium currents recovered from time-dependent inactivation, a twin pulse protocol was used to determine the rate of sodium current reactivation (Figure 4). Na^+ currents were elicited with increasing time intervals after a 7 ms prepulse to − 20 mV (P_1), and the amplitude of the sodium current in the 2nd pulse (P_2) was expressed as a fraction of the control current (P_2/P_1). The reactivation time-constant of the sodium current in the presence of 1 μM lifarizine ($\tau = 14.0 \pm 4.4$ ms) was not significantly different from control ($\tau = 15.9 \pm 2.6$ ms, $n = 4$).

Discussion

SH-SY5Y cells are a neuroblastic subclone of the SK-N-SH cell line that was originally isolated from human metastatic neuroblastoma tissue (Bielder *et al.*, 1973; Ross *et al.*, 1983). When differentiated with retinoic acid, these cells exhibit several features characteristic of neurones (Palman 1984; Morton *et al.*, 1992) including voltage-dependent Na^+, Ca^{2+} and K^+ currents (Seward & Henderson 1990; Toselli *et al.*, 1991; Morton *et al.*, 1992; Forsythe *et al.*, 1992). Although the calcium currents expressed by these cells have been extensively characterized, little is known about the biophysical or pharmacological properties of their sodium currents. Therefore in the present study the voltage-dependence of the macroscopic Na^+ conductance in differentiated SH-SY5Y cells was determined and the effects of tetrodotoxin and lifarizine studied.

The Na^+ conductance in differentiated SH SY5Y cells was half-maximally activated by depolarizations to − 37 mV and half-maximally inactivated by predepolarizing pulses to − 86 mV. This voltage-dependence was identical to that described for Na^+ currents in the human neuroblastoma IMR 32 cell line (Ginsborg *et al.*, 1991). At least four types of sodium channel α-subunit cDNA's have been cloned from rat brain: types I, II IIa and III (reviewed in Catterall, 1992). Structural homologues of these subunits are also found in human tissue. Type A human sodium channel alpha subunits are 97% homologous with the rat type II cDNA sequence (Ahmed *et al.*, 1992). When transiently expressed in Chinese hamster ovary cells these channels are activated at similar membrane potentials ($V_{\frac{1}{2}} = -24$ mV) to currents recorded from SH-SY5Y and IMR32 cells. However, the potential for half-maximal inactivation of channels formed by HBA α

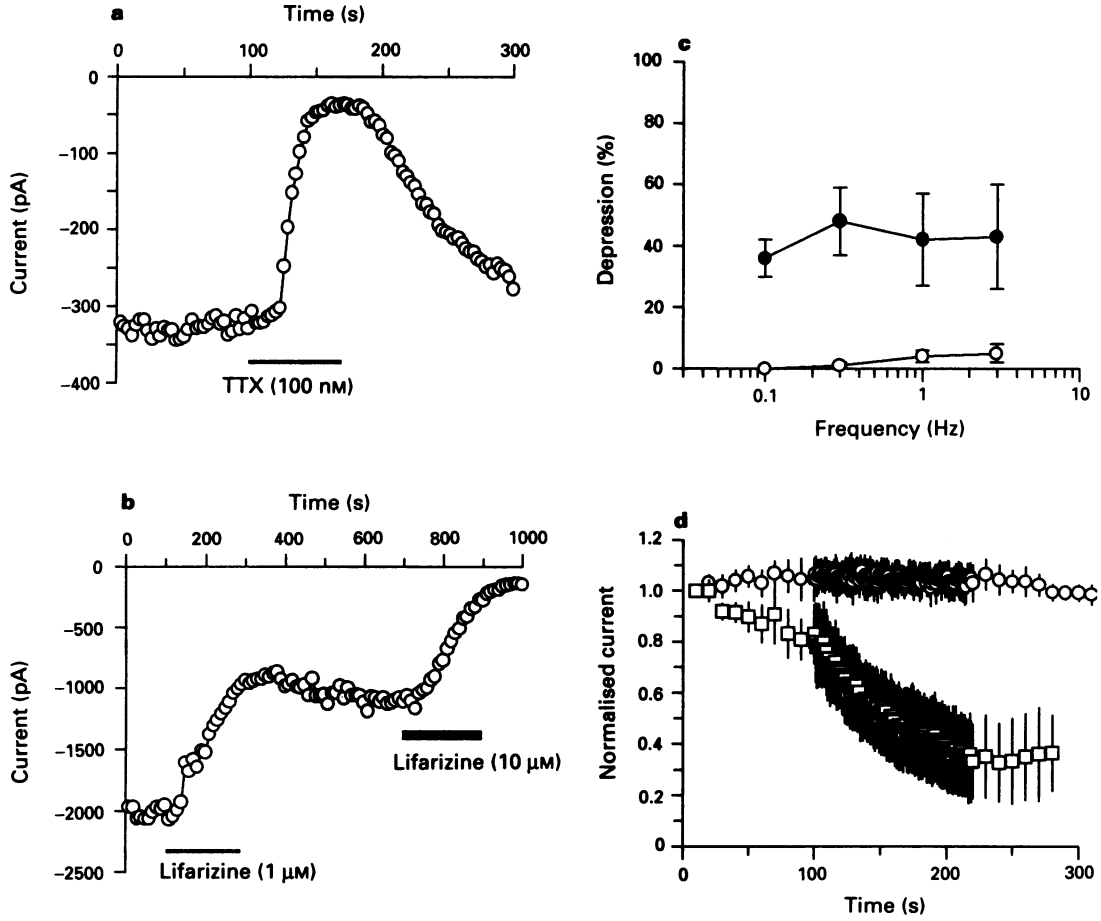


Figure 3 Comparison between the rate of onset of block by lifarizine and tetrodotoxin, and its use-dependence. (a) Reversible depression caused by tetrodotoxin (100 nM) applied for the duration of the horizontal bar. Each point represents the peak sodium current flowing during a 10 ms pulse from − 100 to − 20 mV at a stimulus frequency of 0.1 Hz. (b) Depression of sodium currents by lifarizine (1 and 10 μM) at a stimulus frequency of 0.033 Hz. Note change in scale. The inhibition caused by lifarizine had a 5 fold slower on-rate compared to tetrodotoxin and was not readily reversible despite prolonged wash-off periods of > 30 min. (c) Increasing the stimulus frequency from 0.1 to 3 Hz for 15 events did not increase the percentage depression caused by submaximally-effective concentrations of lifarizine (1 μM). Data represent the effects in control conditions (○) and after application of lifarizine (●). Each point represents data from 3 to 9 cells. (d) The apparent lack of use-dependence was due to the slow on-rate of lifarizine, in that the percentage depression was accentuated by sustained increases in the stimulus frequency. Cells were voltage-clamped at − 100 mV and sodium currents were elicited by depolarizations to − 20 mV at 0.1 Hz. Raising the stimulus frequency to 1 Hz in control conditions (○) did not affect the sodium current amplitude. After equilibration for > 2 min in lifarizine (1 μM) this protocol was repeated (□). Increasing the stimulus frequency increased the percentage block to approximately 40% of the original amplitude in lifarizine at 0.1 Hz. Values are normalised to either the first event in control conditions, or the first event after equilibration in lifarizine which alone produces ca. 40% depression in amplitude. Data are the mean ± s.d. from 3 cells.

subunits is 50 mV less negative than that found in differentiated SH-SY5Y cells ($V_{\frac{1}{2}}$'s = − 37 and − 86 mV respectively). Sodium channels are composed of a pore forming α subunit and one or more β subunits (Catterall, 1992). Differences between the voltage-dependence of the HBA α subunit and endogenous channels in human neuroblastoma cells may reflect the absence of one/more of these regulatory subunits. Indeed when the β1 subunit of rat brain sodium channels was co-expressed with α subunit cDNA this resulted in both a negative shift in the voltage-dependence of inactivation and an increase in the rate of time-dependent inactivation (Isom *et al.*, 1992). Although there are differences between the biophysical properties of the α and αβ1 sodium channel complexes, the majority of toxin binding sites reside on the sodium channel α subunit (Catterall, 1992). Consequently studies concerning drug interactions with the sodium channel alpha subunit are believed to be predictive of their effects on endogenous sodium channel function (e.g. Ragsdale *et al.*, 1993).

Several models have been proposed to account for the way in which drugs can block sodium channels. The most notable of these include the Strichartz-Courtney model, Hille's modulated receptor model, and the guarded receptor hypothesis which have been used to explain the kinetics of sodium channel block by local anaesthetics (reviewed in Hille, 1984; Grant, 1991). Although these models do not directly consider the effects of toxins that act at other receptor sites they have provided an important framework around which the actions of novel drugs can be tested.

Batrachotoxin, a lipid soluble toxin from the Columbian arrow-poison frog, modifies the gating kinetics of sodium channels by shifting the voltage-dependence of activation at more negative values and by slowing the rate of channel inactivation (Tanguy & Yeh, 1988). Although lifarizine displaces [^{3}H]-batrachotoxin binding (IC_{50} 120 nM; Kucharczyk *et al.*, 1991) it is probably via an allosteric effect because lifarizine had minimal effects on sodium channel kinetics in SH-SY5Y cells. Local anaesthetics also displace [^{3}H]-batrachotoxin binding to sodium channels through an action at a site distinct from that of tetrodotoxin (e.g. McNeal *et*

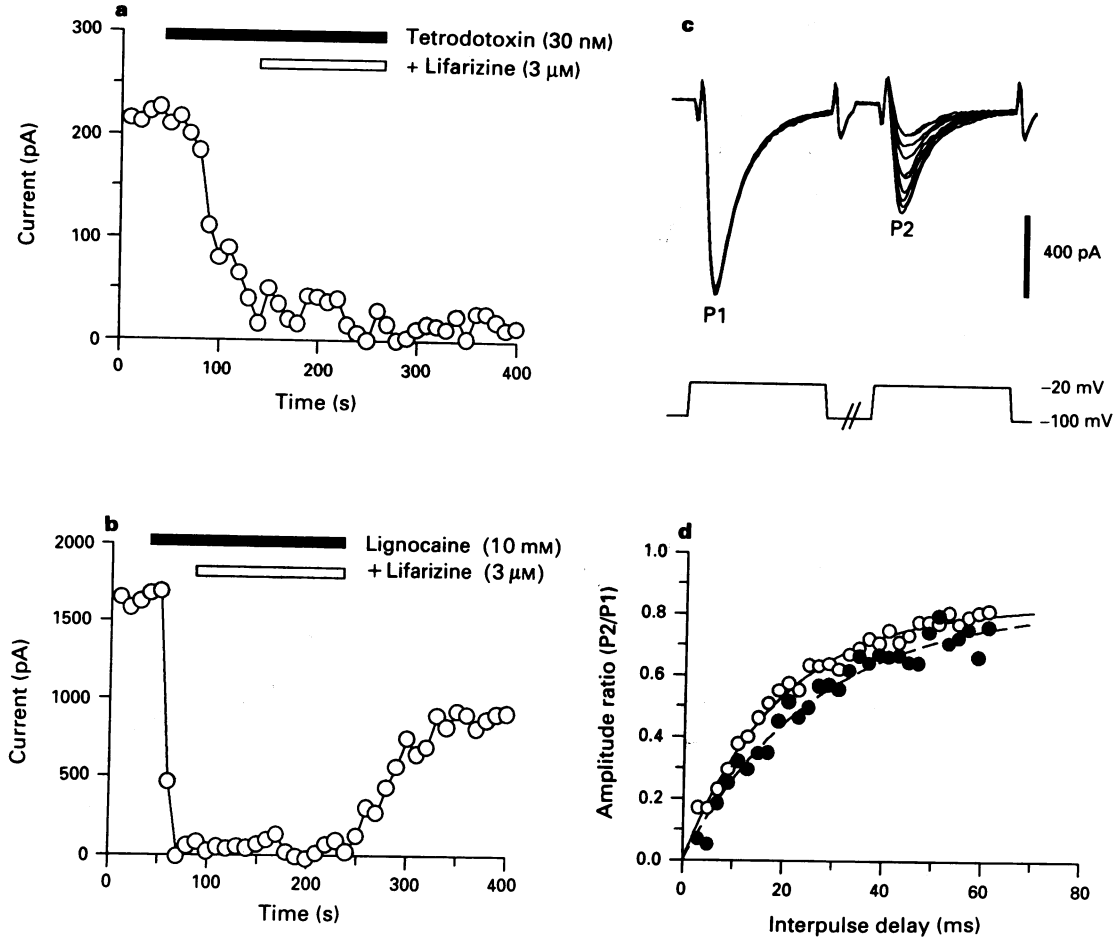


Figure 4 Effect of the open channel blocker, tetrodotoxin and the sodium channel modulator, lignocaine, on the time course of block by lifarizine and its effect on the recovery of sodium currents from time-dependent inactivation. (a) Inhibition of sodium currents by tetrodotoxin (30 nM) and by co-application of lifarizine (3 μM). Block of the conducting open channels with tetrodotoxin was readily reversible. Treatment with TTX did not preclude the inhibition by lifarizine, as depicted by the lack of recovery following coapplication of both antagonists. (b) Inhibition of sodium currents by lignocaine (10 mM) and by co-application of lifarizine (3 μM). Block of the channels by lignocaine was readily reversible. Treatment with lignocaine prevented the subsequent inhibition by lifarizine, as depicted by the recovery following coapplication of both antagonists. Each point represents the peak sodium current elicited by depolarization from − 100 to − 20 mV. Drugs were applied for the duration of the horizontal bar. (c) Na^+ currents were elicited with increasing time-intervals after a 7 ms prepulse from − 100 mV to − 20 mV (P1), and the amplitude of the sodium current in the 2nd pulse (P2) was expressed as a fraction of the control current (P2/P1). The voltage steps are represented by the lower traces. (d) Time-course of the recovery from time-dependent inactivation in an individual cell in control conditions (○) and presence of 1 μM lifarizine (●). The reactivation time-constant of the sodium current in the presence of 1 μM lifarizine ($\tau = 14.0 \pm 4.4$ ms) was not significantly different from control ($\tau = 15.9 \pm 2.6$ ms, $n = 4$).

al., 1985). Evidence for this hypothesis stems from the observation that charged quaternary local anaesthetics such as QX-314 are not readily lipid soluble and are only weakly effective if applied extracellularly (Frazier *et al.*, 1970) whereas lipid soluble local anaesthetics such as lignocaine are equally effective if applied intra- or extra-cellularly and thus presumably acts via the lipid phase associated with the channel (Hille, 1977).

Block of sodium currents by local anaesthetics exhibits both 'tonic', and 'voltage-sensitive' components. The voltage-sensitivity may either be a direct effect on ligand binding or may indirect by virtue of the voltage-dependence of channel opening. Courtney (1975) introduced the concept of use-dependent block to account for the mechanism of action of local anaesthetics and hypothesized that the use-dependence of block was due to the stabilization of the inactivated state of the channel. Hille (1977) further proposed the local anaesthetics bind to a single receptor site and suggested that the kinetics of block were determined by the ability of the drug to interact with either the resting, open or inactivated state of the channel. This modulated receptor hypothesis implied that receptor-occupied channels do not conduct and consequently the voltage-dependence of the remaining unmodified sodium current should remain unaltered. Consistent with this theory, block of sodium currents by lifarizine in SH-SY5Y cells did not involve a change in the voltage-dependence of the sodium currents. However in contrast to the actions of local anaesthetics and antiarrythmics which slow the rate of recovery from time-dependent inactivation and may cause a negative shift in the voltage-dependence of inactivation (Hille 1977; Ragsdale *et al.*, 1991) lifarizine did not alter the reactivation rates or inactivation kinetics of the macroscopic sodium current in SH-SY5Y cells.

To determine whether the effect of lifarizine was mediated by a similar site to that regulated by local anaesthetics, the use-dependence of block by lifarizine and its interaction with fast onset Na^+ channel antagonists was examined. Both tetrodotoxin and lignocaine can block neuronal sodium channels in a use-dependent manner i.e. the amount of depression caused by submaximal concentrations of these agents is accentuated by stimulus frequencies of $\geqslant 1$ Hz (e.g. Caeser *et al.*, 1993). In contrast to the effects of these channel blockers the depression caused with lifarizine was not accentuated by high stimulus frequencies under a similar experimental

paradigm (15 events at 0.1 to 3 Hz). However, this apparent lack of use-dependence was partly due to the very slow on-rate of lifarizine compared to TTX in that sustained increases in the stimulus frequency (> 1 min at 1 Hz) did accentuate the block by lifarizine (Figure 3d).

In contrast to the modulated receptor theory of local anaesthetic action, the guarded receptor model (Grant, 1991) assumes that ion channel blockers gain access to their receptor only once the channel has been opened and places more emphasis on the effects of drugs on channel activation rather than inactivation. However, this model cannot account for the inhibition of sodium currents by lifarizine because block by lifarizine did not require channel activation and was not prevented by pretreatment with the open channel blocker, tetrodotoxin. In contrast to the lack of interaction between lifarizine and tetrodotoxin, the depression caused by the local anaesthetic, lignocaine, was readily reversible after pretreatment of cells with lifarizine. Consequently this local anaesthetic either occludes or modifies the site or state of the channel to which lifarizine binds.

It is likely that block of sodium channels involves at least two kinetically discrete states. Drugs that block the conducting state of the open channel such as tetrodotoxin impart use-dependence (B1), whereas drugs that block non-conducting states may cause tonic block that lack use-dependence (B2). Whether the B1 and B2 blocked states occur via a single receptor as proposed by the modulated receptor hypothesis (Hille, 1977) or from effects at two distinct receptor sites is not clear. However, this notion of bimodal block can explain how compounds like lifarizine can inhibit sodium currents without modifying the voltage-dependence or reactivation kinetics of Na^+ currents in human neuroblastoma cells.

The slow on-rate and limited use-dependence seen with lifarizine indicate that this compound may have a poor anticonvulsant profile *in vivo*. Nevertheless the kinetics of sodium channel block by lifarizine, in addition to effects on other ion channel species, could be more suitable for a neuroprotective agent (Kucharczyk *et al.*, 1991). Whether the sustained mild hypotensive effects and tachycardia caused by lifarizine are a consequence of effects on peripheral sodium, or other ion channels, remains to be determined.

We are grateful for the excellent technical support provided by Jan Myers, and to Graham Showell for the synthesis of lifarizine.

References

AHMED, C.M.I., WARE, D.H., LEE, S.C., PATTEN, C.D., FERRER-MONTIEL, A.V., SCHNIDER, A.F., MCPHERSON, J.D., WAGNER-MCPHERSON, C.B., WASMUTH, J.J., EVANS, G.A. & MONTAL, M. (1992). Primary structure, chromosomal localisation, and functional expression of a voltage-gated sodium channel from human brain. *Proc. Natl. Acad. Sci. U.S.A.*, **89**, 8220–8224.

ALPS, B.J. (1992). Drugs acting on calcium channels: potential treatment for ischaemic stroke. *Br. J. Clin. Pharmacol.*, **34**, 199–206.

BIELDER, J.L., HELSON, L. & SPENGLER, B.A. (1973). Morphology and growth, tumorigenicity, and cytogenetics of human neuroblastoma cells in continuous culture. *Cancer Res.*, **33**, 2643–2652.

CAESER, M., SEABROOK, G.R. & KEMP, J.A. (1993). Block of voltage-dependent sodium currents by the substance P receptor antagonist (±)-CP-96,345, in neurones cultured from rat cortex. *Br. J. Pharmacol.*, **109**, 918–924.

CATTERALL, W.A. (1992). Cellular and molecular biology of voltage-gated sodium channels. *Physiol. Rev.*, **72**, S15–S48.

COURTNEY, K.R. (1975). Mechanism of frequency-dependent inhibition of sodium currents in frog myelinated nerve by lidocaine derivative GEA 968. *J. Pharmacol. Exp. Ther.*, **195**, 225–236.

FORSYTHE, I.D., LAMBERT, D.G., MAHORSKI, S.R. & LINDSELL, P. (1992). Elevation of cytosolic calcium by cholinoceptor agonists in SH-SY5Y human neuroblastoma cell: estimation of the contribution of voltage-dependent currents. *Br. J. Pharmacol.*, **107**, 207–214.

FRASER, S. & SPEDDING, M. (1991). RS-87476, a novel neuroprotective agent, antagonises the effects of calcium channel activators in guinea-pig taenia. *Br. J. Pharmacol.*, **104**, 156P.

FRAZIER, D.T., NARAHASHI, T. & YAMADA, Y. (1970). The site of action and active form of local anaesthetics. Experiments with quaternary compounds. *J. Pharmacol. Exp. Ther.*, **171**, 45–51.

GELLENS, M.E., GEORGE, A.L., CHEN, L., CHAHINE, M., HORN, R., BARCHI, R.L. & KALLEN, R.G. (1992). Primary structure and functional expression of the human cardiac tetrodotoxin-insensitive voltage-dependent sodium channel. *Proc. Natl. Acad. Sci. U.S.A.*, **89**, 554–558.

GEORGE, A.L., KNITTLE, T.J. & TAMKUN, M.M. (1992a). Molecular cloning of an atypical voltage-gated sodium channel expressed in human heart and uterus: evidence for a distinct gene family. *Proc. Natl. Acad. Sci. U.S.A.*, **89**, 4893–4897.

GEORGE, A.L., KOMISAROF, J., KALLEN, R.G. & BARCHI, R.L. (1992b). Primary structure of the adult human skeletal muscle voltage-dependent sodium channel. *Ann. Neurol.*, **21**, 131–137.

GINSBORG, B.L., MARTIN, R.J. & PATMORE, L. (1991). On the sodium and potassium currents of a human neuroblastoma cell line. *J. Physiol.*, **434**, 121–129.

GOA, K.L., ROSS, S.R. & CHRISP, P. (1993). Lamotrigine – a review of its pharmacological properties and clinical efficacy in epilepsy. *Drugs*, **46**, 152–176.

GRANT, A.O. (1991). Models of drug interaction with the sodium channel. *Clin. Invest. Med.*, **14**, 447–457.

HILLE, B. (1977). Local anaesthetics: hydrophyllic and hydrophobic pathways for the drug-receptor interaction. *J. Gen. Physiol.*, **69**, 475–496.

HILLE, B. (1984). *Ionic Channel of Excitable Membranes*, p. 426. Massachusetts: Sinauer Assoc. Inc.

HODGKIN, A.L. & HUXLEY, A.F. (1952). Currents carried by sodium and potassium ions through the membrane of the giant axon of *Loligo*. *J. Physiol.*, **116**, 449–472.

ISOM, L.L. DE JONGH, K.S., PATTON, D.E., REBER, B.F.X., OFFORD, J., CHARBONNEAU, H., WALSH, K., GOLDIN, A.L. & CATTERALL, W.A. (1992). Primary structure and functional expression of the β1 subunit of the rat brain sodium channel. *Science*, **256**, 839–842.

KAYANO, T., NODA, M., FLOCKERZI, V., TAKAHASHI, H. & NUMA, S. (1988). Primary structure of rat brain sodium channel III deduced from the cDNA sequence. *FEBS Letters*, **228**, 187–194.

KUCHARCZYK, J., MINTOROVITCH, J., MOSELEY, M.E., ASGARI, H.S., SEVICK, R.J., DERUGIN, N. & NORMAN, D. (1991). Ischemic brain damage: reduction by sodium-calcium ion channel modulator RS-87476. *Radiology*, **179**, 221–227.

MATSUKI, N., QUANDT, F.N., TEN EICK, R.E. & YEH, J.Z. (1984). Characterisation of the block of sodium channels by phenytoin in mouse neuroblastoma cells. *J. Pharmacol. Exp. Ther.*, **228**, 523–530.

MCCLEAN, M.J. & MACDONALD, R.L. (1986). Carbamazepine and 10,11-epoxycarbamazepine produce use- and voltage-dependent limitation of rapidly firing action potentials of mouse central neurons in cell culture. *J. Pharmacol. Exp. Ther.*, **238**, 727–738.

MCNEAL, E.T., LEWANDOWSKI, G.A., DALY, J.W. & CREVELING, C.R. (1985). [^{3}H]batrachotoxin A 20α-benzoate binding to voltage-sensitive sodium channels: a rapid and quantitative assay for local anesthetic activity in a variety of drugs. *J. Med. Chem.*, **28**, 381–388.

MELDRUM, B.S., SWAN, J.H., LEACH, M.J., MILLAN, M.H., GWINN, R., KADOTA, K., GRAHAM, S.H., CHEN, J. & SIMON, R.P. (1992). Reduction of glutamate release and protection against ischemic brain damage by BW 1003C87. *Brain Res.*, **593**, 1–6.

MORTON, A.J., HAMMOND, C., MASON, W.T. & HENDERSON, G. (1992). Characterisation of the L- and N-type calcium channels in differentiated SH-SY5Y neuroblastoma cells: calcium imaging and single channel recording. *Mol. Brain Res.*, **13**, 53–61.

NODA, M., IKEDA, T., SUZUKI, H., TAKESHIMA, H., TAKAHASHI, T., KUNO, M. & NUMA, S. (1986). Expression of functional sodium channels from cloned cDNA. *Nature*, **322**, 826–828.

PALMAN, S., RUUSALA, A.I., ABRAHAMSSON, L., MATTSSON, M.E.K. & ESSCHER, T. (1984). Retinoic acid differentiation of cultured human neuroblastoma cells: comparison with phorbol ester-induced differentiation. *Cell Diff.*, **14**, 135–144.

RAGSDALE, D.S., NUMANN, R., CATTERALL, W.A. & SCHEUER, T. (1993). Inhibition of Na^+ channels by the novel blocker PD-85,639. *Mol. Pharmacol.*, **43**, 949–954.

RAGSDALE, D.S., SCHEUER, T. & CATTERALL, W.A. (1991). Frequency and voltage-dependent inhibition of type IIA Na^+ channels, expressed in a mammalian cell line, by local anesthetic, antiarrhythmic, and anticonvulsant drugs. *Mol. Pharmacol.*, **40**, 756–765.

ROSS, R.A., SPENGLER, B.A. & BIELDER, J.L. (1983). Coordinate morphological and biochemical interconversion of human neuroblastoma cells. *J. Natl. Cancer Inst.*, **71**, 741–747.

SEWARD, E.P. & HENDERSON, G. (1990). Characterisation of two-components of the N-like, high-threshold-activated calcium current in differentiated SH-SY5Y cells. *Pflügers Arch.*, **417**, 223–230.

SHERIDAN, R.D., PATMORE, L. & SPEDDING, M. (1991). The novel neuroprotective agent, RS-87476, potently inhibits sodium currents in mouse neuroblastoma. *Br. J. Pharmacol.*, **104**, 25P.

TANGUY, J. & YEH, J.Z. (1988). Batrachotoxin uncouples gating charge immobilization from fast Na inactivation in squid giant axons. *Biophys. J.*, **54**, 719–730.

TOSELLI, M., MASETTO, S., ROSSI, P. & TAGLIETTI, V. (1991). Characterisation of a voltage-dependent calcium current in the human neuroblastoma cell line SH-SY5Y during differentiation. *Eur. J. Neurosci.*, **3**, 514–522.

(Received January 10, 1994
Revised April 11, 1994
Accepted June 1, 1994)

Br. J. Pharmacol. (1994), **113**, 607–613 © Macmillan Press Ltd, 1994

Bradykinin B_2 receptors and coupling mechanisms in the smooth muscle of the guinea-pig taenia caeci

Julie L. Field, Semal K. Butt, [1]Ian K.M. Morton & Judith M. Hall

Pharmacology Group, Biomedical Sciences Division, King's College London, Chelsea, London SW3 6LX

1 In the smooth muscle of the guinea-pig taenia caeci, bradykinin produces a relaxation followed by a contraction. In the presence of hexamethonium and guanethidine, both these phases of the response were insensitive to tetrodotoxin (100 nM), ω-conotoxin GVIA (100 nM) and ibuprofen (1 μM), suggesting that they are due to a direct action on the smooth muscle.

2 The B_1 receptor-selective agonist, [des-Arg^9]-BK (1-100 μM), was inactive in the taenia caeci, and the B_1 receptor-selective antagonist, [Leu^8,des-Arg^9]-BK (1–10 μM), did not inhibit either phase of the bradykinin-induced response. The B_2 receptor-selective antagonist, D-Arg-[Hyp^3,Thi^5,D-Tic^7,Oic^8]-BK (Hoe 140) (30–300 nM), inhibited both the bradykinin-induced relaxation and contraction with a similar affinity (apparent pK_B estimates of 8.5 ± 0.1 and 8.4 ± 0.1 respectively).

3 In a depolarizing high-K^+-solution, bradykinin produced concentration-related contractions, though of diminished magnitude; but no relaxation was observed in such media. In Krebs solution, the Ca^{2+}-activated K^+-channel blocker, apamin (10 nM), abolished relaxant responses. These observations suggest that contraction results both from membrane potential-dependent, and membrane potential-independent, mechanisms; whereas relaxant responses result entirely from membrane potential-dependent mechanisms. Contractile responses obtained in the high K^+-solution were inhibited by D-Arg-[Hyp^3,Thi^5,D-Tic^7,Oic^8]-BK with an apparent pK_B value of 8.4 ± 0.1.

4 In a Ca^{2+}-free, EGTA-containing medium, relatively high concentrations of bradykinin (> 100 nM) produced transient contractions, suggesting that a component of the contractile response results from release of Ca^{2+} from an intracellular store. This intracellular Ca^{2+} store could be refilled in the presence of extracellular Ca^{2+}. The B_1 receptor antagonist, [Leu^8,des-Arg^9]-BK (10 μM), did not inhibit this bradykinin-induced contraction, whereas the B_2 receptor antagonist, D-Arg-[Hyp^3,Thi^5,D-Tic^7,Oic^8]-BK (100 nM) markedly attenuated it ($P < 0.001$; $n = 6$).

5 Bradykinin (10 nM–100 μM) significantly elevated tissue levels of total [^{3}H]-inositol phosphates in the presence of Li^+, after incubation with *myo*-[^{3}H]-inositol. The B_1 receptor-selective agonist, [des-Arg^9]-BK (100 μM) did not stimulate [^{3}H]-inositol phosphate formation, and the B_1 receptor-selective antagonist, [Leu^8,des-Arg^9]-BK, did not inhibit the formation of [^{3}H]-inositol phosphates in response to a sub-maximal concentration of bradykinin (10 μM; $P > 0.05$). Two B_2 receptor antagonists, D-Arg-[Hyp^3,D-Phe^7]-BK and D-Arg-[Hyp^3,Thi^5,D-Tic^7,Oic^8]-BK, inhibited bradykinin-induced accumulation of total [^{3}H]-inositol phosphates with apparent pK_B estimates of 5.4 ± 0.3 and 8.4 ± 0.1, respectively.

6 These data suggest that in the guinea-pig taenia caeci, the five aspects of the action of bradykinin studied (the relaxant and the contractile elements of the biphasic mechanical response, the contractile response in a depolarizing high-K^+ solution medium and zero-Ca^{2+} media, and stimulation of phosphatidylinositol turnover), all result from activation of B_2 receptors. A possible causal relationship is suggested between these B_2 receptor-mediated membrane potential-dependent, and -independent events, and their roles in excitation contraction coupling.

Keywords: Bradykinin receptors; bradykinin B_2 receptors; bradykinin receptor antagonists; bradykinin receptor mechanisms; taenia caeci (guinea-pig); electromechanical coupling; pharmacomechanical coupling; phosphatidylinositol turnover; Ca^{2+}-activated K^+-channel; apamin

Introduction

Bradykinin receptors have been divided into two types, designated B_1 and B_2 (see Regoli & Barabé, 1980; see Hall, 1992). In isolated smooth muscle preparations, activation of these receptors leads to relaxation and/or contraction; and these responses may result from a direct action on the smooth muscle, or involve the release of other mediators (see Hall, 1992). Two signal transduction pathways have been linked to bradykinin receptor activation in smooth muscle, phosphatidylinositol hydrolysis (see Hall, 1992; Marsh & Hill, 1992; Ransom *et al.*, 1992) and eicosanoid biosynthesis (Bramley *et al.*, 1990; see Burch, 1990; Farmer & Burch, 1992 and Hall, 1992).

In the guinea-pig taenia caeci, bradykinin produces a biphasic response consisting of a fast relaxation followed by a slow contraction (Carter *et al.*, 1986). This is in contrast to the fast monophasic contractions seen in this preparation with a number of spasmogens including carbachol, substance P and histamine (Hall *et al.*, 1986; Hall & Morton, 1991a). Stimulation of one bradykinin receptor type could cause both phases of the response; or alternatively, the two phases could result from activation of two distinct receptor types. Additionally, one or both phases may follow release of neuronally-derived mediators or cyclo-oxygenase products. The aim of this study was to examine these possibilities by determining the involvement of cyclo-oxygenase and neuronal-derived mediators and the nature of the receptors and coupling-mechanisms involved in each component of the biphasic response to bradykinin in the guinea-pig taenia caeci. To this end, experiments included functional tissue-contractility studies, measurement of phosphatidylinositol hydrolysis, and determination of the affinities of the B_1 and B_2 bradykinin receptor antagonists, [Leu^8,des-Arg^9]-BK (Regoli & Barabé, 1980) and D-Arg-[Hyp^3,Thi^5,D-Tic^7,Oic^8]-BK (Hock *et al.*, 1991), respectively.

[1] Author for correspondence.

Preliminary accounts of these results have been communicated to the British Pharmacological Society (Hall *et al.*, 1991; Field *et al.*, 1992a).

Methods

Tissue preparation

Two of the three available taenia caeci longitudinal muscle strips were dissected from the caecum of male, Dunkin-Hartley guinea-pigs (450–800 g), killed by stunning and exsanguination.

Isolated tissue studies

Segments of taenia caeci were mounted in 2 ml organ baths, by use of a micrometer-controlled isometric assembly that allowed precise length adjustment, with an initial resting tension of 500 mg. In taenia caeci preparations which developed spontaneous tone, a biphasic response to bradykinin was observed: only such tissues were used in this study. Tension was measured by means of Grass FT03B force-displacement transducers coupled to JJ Instruments CR342 potentiometric flat-bed recorders following d.c. amplification, or Grass model 7E polygraphs. Responses to bradykinin were normally compared with carbachol, as a control, in the same preparation; so allowing normalization of tension in terms of maximum individual tensions developed with carbachol.

All experiments, unless otherwise stated, were carried out in Krebs solution (composition (mM): NaCl 118, KCl 4.6, $MgSO_4$ 1.15, $NaHCO_3$ 25, $CaCl_2$ 2.5, KH_2PO_4 1.2, glucose 10), maintained at 37°C and oxygenated with 95% O_2:5% CO_2. The Krebs solution contained atropine, mepyramine, cimetidine, guanethidine, (all at 1 μM) and hexamethonium (10 μM). In experiments to test for the involvement of neuronal activity or production of prostanoids in the responses to bradykinin, full concentration-response curves were compared in the presence and absence of tetrodotoxin (100 nM), ω-conotoxin GVIA (100 nM) or ibuprofen (1 μM). In experiments with apamin, tissues were incubated with this channel-blocker (10 nM) for at least 10 min.

Experiments in high-K^+ media

In experiments in which responses in the absence of membrane potential were studied, after equilibration in Krebs solution, tissues were transferred to a high-K^+ medium (composition (mM): K_2SO_4 107, Na_2SO_4 2.5, $MgCl_2$ 1.15, $KHCO_3$ 16, $CaCl_2$ 5, KCl 5, Na phosphate buffer 0.4, glucose 10; see Jenkinson & Morton, 1967a,b), maintained at 37°C and oxygenated with 95% O_2:5% CO_2. Bradykinin responses were compared, throughout, with those to carbachol in the same preparations. This high-K^+ medium, based on impermeant SO_4^{2-}, has been shown in the taenia caeci preparation to prevent swelling with time (Durbin & Jenkinson, 1961) which is otherwise observed with KCl media, and allows responses and changes in ion permeability to be studied over relatively long periods (Jenkinson & Morton, 1967a,b). However, for comparison, some control experiments were also made testing bradykinin responses at various times after exposure (5, 10, 15 and 20 min) to a high-K^+ medium with 30 mM KCl substituted for NaCl in the Krebs solution, where there was an initial contracture and subsequent fall in tension.

Experiments in reduced-Na^+ medium

Taenia preparations were mounted in Krebs solution, and then contractility was tested in a modified Krebs medium containing 75, 50 and 25 mM Na^+; where reduced Na^+ was replaced with equimolar tris-HCl buffer (Brading *et al.*, 1980). In one series, full concentration-response curves to bradykinin were obtained; and in another, comparison was made between matched submaximal concentrations of bradykinin (1 μM), carbachol (100 nM), and KCl (30 mM).

Antagonists pK_B estimates for responses in Krebs and high-K^+ media

In both normal Krebs and high-K^+ media, concentration-response curves to bradykinin were obtained using sequential dosing in a randomized block-design, with responses compared with those obtained in the presence of bradykinin receptor antagonist (test preparation), or no antagonist (concurrent-control preparation). A 12 min bradykinin dose-cycle was used in conjunction with a 10 min antagonist pre-test incubation period. In studies with high-K^+ medium, tissues were first placed in Krebs solution and responses obtained to bradykinin and carbachol. Responses were normalized in each preparation in terms of the maximal carbachol contraction obtained in Krebs solution, and the estimates are shown as means ± s.e.mean.

Experiments in Ca^{2+}-free medium

Submaximal contractile responses to bradykinin (10 μM) were obtained in Krebs solution, and in a modified-Krebs Ca^{2+}-free medium (Ca^{2+} replaced by equimolar Mg^{2+}, with 1 mM EGTA) for 3 min. To refill Ca^{2+}-stores, tissues were placed in a modified Krebs depolarizing-medium containing 5 mM Ca^{2+} and 30 mM K^+, for 15 min. In experiments to determine the receptor type involved in these contractions, individual preparations were tested with single applications of bradykinin (10 μM) in Ca^{2+}-free Krebs medium, each challenge after a 15 min period in the modified Krebs Ca^{2+}-containing medium to refill stores. After stabilization of responses, preparations were re-tested with bradykinin (10 μM) in the presence of either the B_1 receptor antagonist [Leu^8,des-Arg^9]-BK (10 μM) or the B_2 receptor antagonist D-Arg-[Hyp^3,Thi^5,D-Tic^7,Oic^8]-BK (100 nM); or no antagonist (controls).

Phosphatidylinositol hydrolysis

The methodology was adapted from Berridge *et al.* (1982) (see Hall & Morton, 1991a). Briefly, cross-chopped (350 × 350 μm) tissues were washed twice in Krebs solution (composition as above, but omitting atropine) at 37°C, then incubated under 95% O_2:5% CO_2 with cleaned *myo*-[2-^{3}H]-inositol (844 GBq mol^{-1}) for 1 h at 37°C in a shaking water-bath, followed by washing and resuspension in Krebs solution. Tissue aliquots (40 μl) were transferred to vials containing Li^+ (12 mM) and agonist, with or without antagonist, in Krebs solution to a final volume of 250 μl under 95% O_2:5% CO_2. Tubes were incubated at 37°C for 30 min in a shaking water-bath. The reaction was terminated by addition of 940 μl of chloroform:methanol:HCl (100:200:2,v:v:v)(0.1 M HCl), followed by 300 μl each of chloroform and distilled water and centrifugation (1000 *g* for 5 min). A 800 μl aliquot of the aqueous phase was applied with 8 ml of water to a Dowex-formate anion-exchange column (AG1-X8 resin, Biorad Laboratories, California, U.S.A.). The inositol phosphates were eluted with 6 ml 800 mM ammonium formate: 100 mM formic acid after removal of [^{3}H]-inositol and other labelled impurities, by 2 × 8 ml washes with 5 mM sodium tetraborate: 60 mM ammonium formate. The [^{3}H]-inositol phosphate eluate was collected and the samples counted by liquid scintillation spectrometry after addition of Liquiscint (National Diagnostics, U.K) and vortexing. No attempt was made to separate the inositol phosphates and therefore results are described as total [^{3}H]-inositol phosphates ([^{3}H]-IPs). The lipid (400 μl) was removed and left overnight before counting these samples as above. To allow for variation in absolute amounts of tissue samples, results were normalized

with respect to sample lipid content, and are expressed as the % maximal carbachol-induced accumulation of total [^{3}H]-inositol phosphates (see Hall & Morton, 1991a). This normalization procedure was valid only if the agonists do not increase incorporation of ^{3}H into lipids, and under these conditions neither carbachol (Hall & Morton, 1991a), nor bradykinin (bradykinin 118 ± 26% of basal control 100%; $P > 0.05$; $n = 8$), increased ^{3}H incorporation into the lipid fraction.

Materials

Agents were obtained as follows: carbamylcholine chloride (carbachol), atropine sulphate, tetrodotoxin, ω-conotoxin GVIA, ibuprofen and hexamethonium bromide (Sigma, UK), mepyramine maleate (May & Baker, UK), cimetidine (Smith, Kline & French, UK), guanethidine sulphate (Ciba, UK), bradykinin, D-Arg-[Hyp^3,D-Phe^7]-BK (Bachem, UK). D-Arg-[Hyp^3,Thi^5,D-Tic^7,Oic^8]-BK (Hoe 140) was a kind gift from Dr A. Hallett, Sandoz Institute for Medical Research, London. All salts were of analytical grade and were obtained from B.D.H., U.K. All drugs were dissolved in distilled water (except ibuprofen in 5% Na_2CO_3), and peptides were stored deep frozen.

Expression of results and statistical analysis

In all experiments, apparent pK_B estimates and their s.e.mean were obtained from individual dose-ratio estimates (x) between responses in test and control preparations, by calculation from the Gaddum-Schild equation, $pK_B = -\log_{10} K_B = \log_{10}(x\text{-}1) - \log_{10}[A]$, where [A] is the antagonist concentration. In functional experiments in Krebs solution, some depression of the maximal contractile response to bradykinin was observed with high concentrations of D-Arg-[Hyp^3,Thi^5,D-Tic^7,Oic^8]-BK, so affinity estimates were taken from individual dose-ratios only where no depression was evident (see Field *et al.*, 1992b). Affinity estimates are referred to throughout as apparent pK_B values, since there was no full Schild analysis to test for competition. Tests for statistical significance were made using Student's *t* test for two independent-samples, or paired-samples, as appropriate. EC_{50} estimates are shown with 95% confidence limits.

Results

Functional studies

The taenia caeci preparations used in this study had a moderate degree of natural tone where, as shown in Figure 1, a typical response to bradykinin is bisphasic with an immediate initial relaxant phase (EC_{50} 1.3 (0.8–2.0 μM); followed by a delayed second contractile phase (EC_{50} 0.1 (0.05–0.2) μM) which is markedly slow as compared with the fast monophasic contractile responses to carbachol in the same tissue. In preparations with greater or lesser degrees of tone, the relaxant or contractile phases, respectively, are relatively enhanced (data not shown). Both the relaxant and contractile components of the response to bradykinin appear to be mediated through a direct action on smooth muscle cells since the responses were unaffected by tetrodotoxin, ω-conotoxin (both 100 nM) or ibuprofen (1 μM) ($n = 4$–6; data not shown). The Ca^{2+}-activated K^+-channel blocker, apamin (10 nM), completely blocked the relaxant phase without affecting the contractile phase (data not shown; Carter *et al.*, 1986).

The B_1 receptor-selective agonist, [des-Arg^9]-BK (1-100 μM), was inactive and the B_1 receptor-selective antagonist, [Leu^8,des-Arg^9]-BK (1–10 μM), did not inhibit either the relaxation or contraction in response to bradykinin (1 nM–10 μM; data not shown). The B_2 receptor antagonist, D-Arg-[Hyp^3,Thi^5,D-Tic^7,Oic^8]-BK (30–300 nM), potently antagonized both the relaxant and contractile phases of the biphasic response with apparent pK_B estimates of 8.4 ± 0.2 and 8.4 ± 0.1 ($n = 12$ for both phases; Figure 2, Table 1).

Experiments in Ca^{2+}-free medium

Bradykinin (10 μM) produced a transient monophasic contractile response in Ca^{2+}-free EGTA-containing medium which, on first challenge, was 37.5 ± 5.2% ($n = 20$) of the control bradykinin contractile response obtained in normal Krebs solution (see Figure 3a). This contractile response decreased with repeated applications of bradykinin in the Ca^{2+}-free medium (Figure 3a), but could be restored if tissues were incubated in a modified depolarizing (30 mM K^+) Ca^{2+}-containing (5 mM) Krebs medium to refill stores (Figure 3a). In experiments to determine the type of bradykinin receptor involved in contractile responses that are independent of external-Ca^{2+}, preparations were tested in the absence, and then the presence, of the B_1 receptor-selective

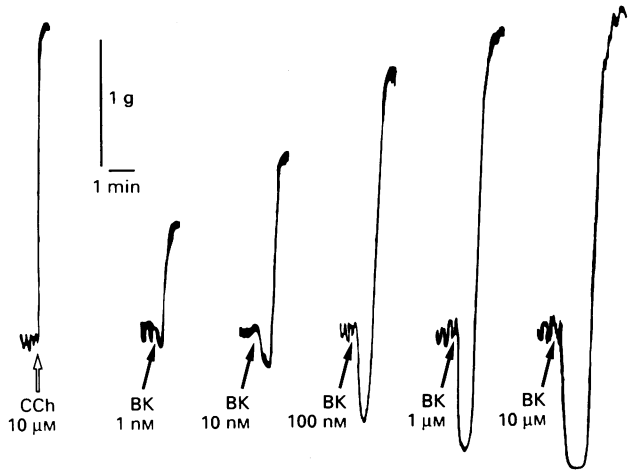


Figure 1 Typical biphasic concentration-related isometric tension records for bradykinin (BK) in the guinea-pig isolated taenia caeci preparation, compared to the fast monophasic contractile response to carbachol (CCh). The preparation was mounted in Krebs solution at 37°C. This figure is representative of > 12 experiments.

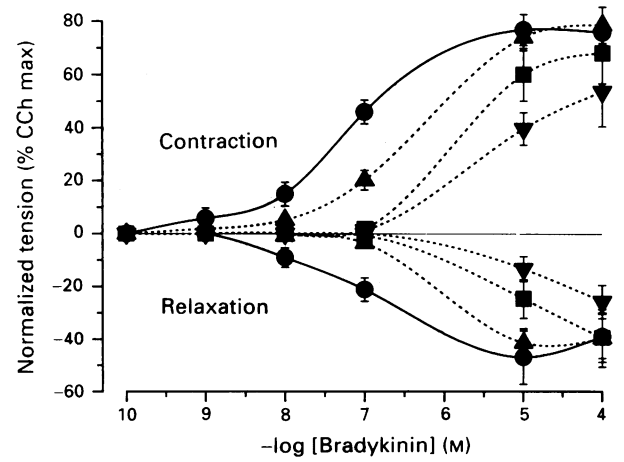


Figure 2 Log concentration-response curves for the biphasic responses to bradykinin in the guinea-pig taenia caeci and their antagonism by D-Arg-[Hyp^3,Thi^5,D-Tic^7,Oic^8]-BK. The upper section represents bradykinin-induced contraction, and the lower, bradykinin-induced relaxation; with both responses shown in terms of normalized tension, as % of maximal responses to carbachol in individual preparations. Curves are control (●), or in the presence of antagonist at 30 nM (▲), 100 nM (■), and 300 nM (▼). Each point is the mean (± s.e.mean) from 9–12 preparations.

Table 1 Affinity estimates for D-Arg-[Hyp^3,Thi^5,D-Tic^7, Oic^8]-BK against bradykinin

System	*Response*	*Medium*	pK_B *(s.e.mean; n)*
Functional	Contraction	Krebs medium	8.4 (0.1; 12)
Functional	Relaxation	Krebs medium	8.5 (0.1; 12)
Functional	Contraction	High-K^+ medium	8.4 (0.1; 7)
Biochemical	Phosphatidylinositol hydrolysis	Krebs medium	8.4 (0.1; 4)

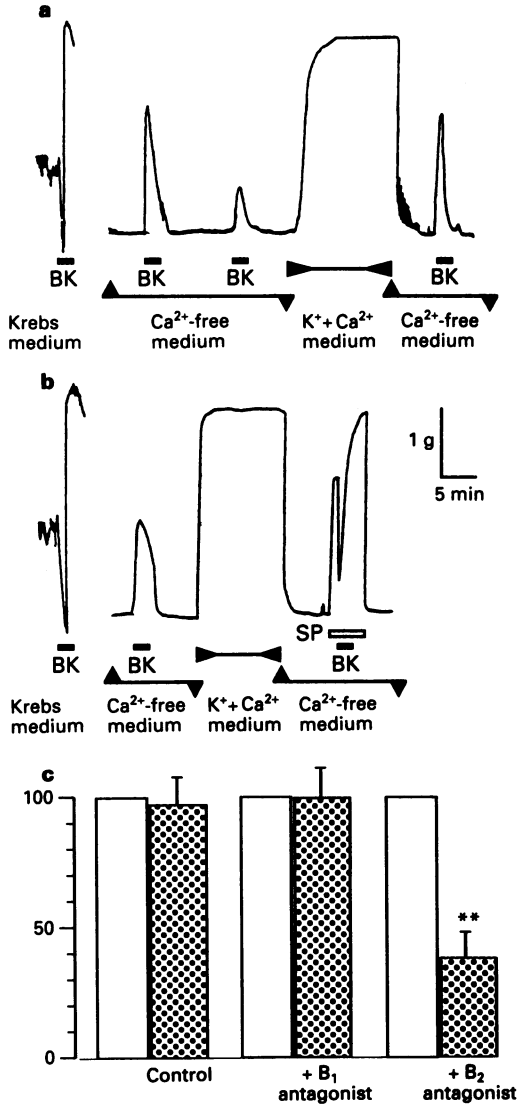


Figure 3 Mechanical responses to bradykinin (10 μM) were tested in a zero-Ca^{2+} medium. In (a), typical responses with isometric recording at 37°C, are shown in normal Krebs solution, followed by responses to bradykinin in the Ca^{2+}-free medium (see Methods) that diminish on re-challenge; and then a restored response after a third challenge in the Ca^{2+}-free medium, following 15 min incubation in a Ca^{2+}-store refilling-medium (5 mM Ca^{2+}, 30 mM K^+; see methods). In (b) a similar protocol is shown, except after Ca^{2+}-store refilling a contracture is induced with substance P (SP, 10 μM) before addition of bradykinin (10 μM) in order to demonstrate a relaxant phase in the action of the latter. In (c) the receptor type involved in contractions in the Ca^{2+}-free medium is tested by including a B_1 receptor-selective antagonist ([Leu^8,des-Arg^9]-BK; 10 μM) or a B_2 receptor-selective antagonist (D-Arg-[Hyp^3,Thi^5,D-Tic^7,Oic^8]-BK (100 nM) in the Ca^{2+}-free medium during re-challenge after Ca^{2+}-store refilling, with a third group acting as control: there was a significant attenuation of bradykinin responses (compared with the control level of 100%) after blockade of B_2 (**$P<0.001$; $n=6$), but not B_1, receptors.

antagonist, [Leu,^{8},des-Arg^9]-BK (10 μM) or the B_2 receptor-selective antagonist, D-Arg-[Hyp^3,Thi^5,D-Tic^7,Oic^8]-BK (100 nM), and compared with appropriate concurrent controls (Figure 3c). The B_1 receptor antagonist was without effect ($P>0.05$), whereas the B_2 receptor antagonist markedly attenuated these responses ($P<0.001$); controls showed no significant change in response ($P>0.05$) on re-testing. No relaxant responses were seen in this Ca^{2+}-free medium, where there is no natural tone; but when transient contractions were induced by application of substance P (10 μM), relaxant responses could be demonstrated (Figure 3b).

Experiments in reduced-Na^+ medium

Contractile responses to bradykinin were attenuated in reduced-Na^+ media, showing, with 75, 50 and 25 mM Na^+, a progressive rightward shift of the log concentration-response curves with some depression of maximum (data not shown). In experiments with matched responses to carbachol (100 nM) and KCl (30 mM), responses to bradykinin (1 μM) were reduced: at these Na^+ concentrations to 63.6 ± 7.2%, 48.3 ± 5.6% and 39.1 ± 4.3%, respectively, of the bradykinin

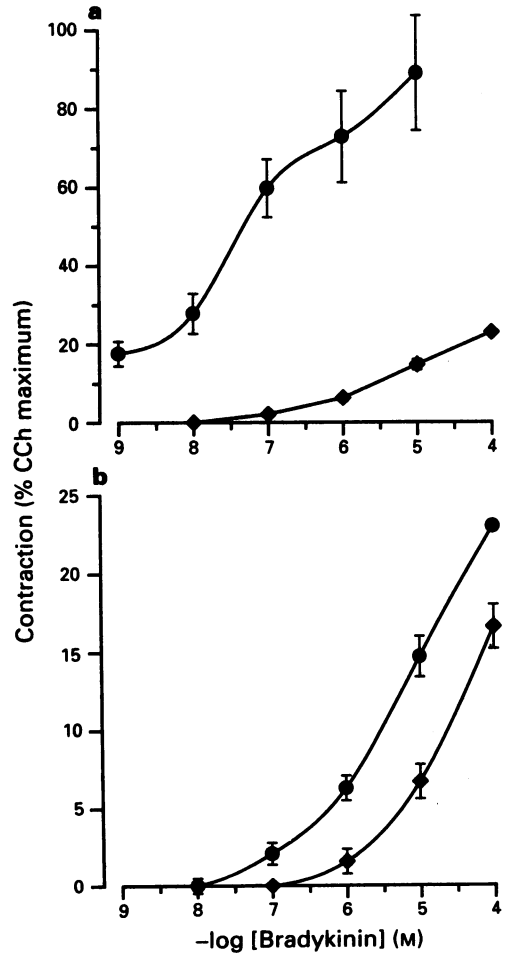


Figure 4 Bradykinin-induced contractile responses in Krebs solution and a high-K^+ medium, and antagonism of responses under the latter conditions by D-Arg-[Hyp^3,Thi^5,D-Tic^7,Oic^8]-BK. (a) Shows log concentration-response curves produced by bradykinin in Krebs solution (●), as compared with those after incubation of the preparation in the high-K^+ depolarizing medium (◆); (b) shows, in the high-K^+ medium, the shift to the right of the responses curves in the presence of antagonist: control (●), and in the presence of 30 nM D-Arg-[Hyp^3,Thi^5,D-Tic,Oic^8]-BK (◆), Each point is the mean (± s.e.mean) taken from 4–6 experiments. Note rescaling of abscissae in (b).

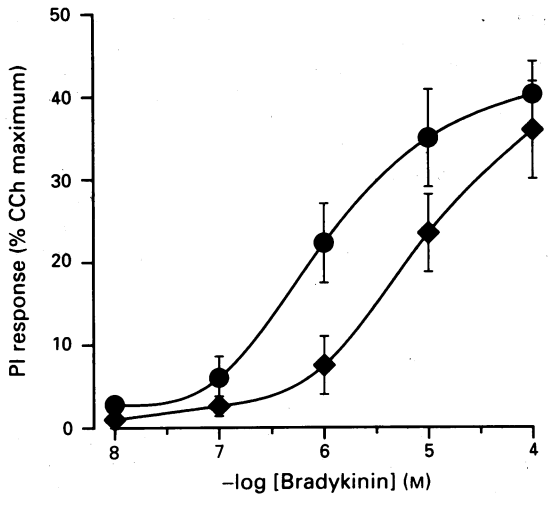


Figure 5 Phosphatidylinositol (PI) hydrolysis studies in the guinea-pig taenia caeci. Log concentration-response curves for bradykinin-stimulated [^{3}H]-inositol phosphate formation, in the absence (●), and the presence (◆), of D-Arg-[Hyp^3,Thi^5,D-Tic^7,Oic^8]-BK (30 nM). Each point is the mean (± s.e.mean) taken from 4 experiments.

control; whereas responses to the control spasmogens were not significantly reduced (data not shown; $P>0.05$). Preparations in low-Na^+ media showed little tone, and relaxant responses were not seen; but when bradykinin was added during the tonic phase of a carbachol pre-contraction, a relaxant action could then be demonstrated (data not shown).

Experiments in high-K^+ media

In a K_2SO_4-based depolarizing high-K^+ medium, carbachol and bradykinin (10 nM–100 μM) produced reliable and reproducible concentration-related contractile responses, though of greatly diminished magnitude as compared to that observed in Krebs solution (Figure 4). Under these conditions, the contractions observed with the maximum achievable concentration of bradykinin (100 μM) were reduced to 25.5% of the bradykinin maximum in Krebs solution, or some 19.0% of the carbachol Krebs control (cf. 43% for carbachol, itself, under these conditions; Hall & Morton, 1991a). No relaxation was observed in response to bradykinin, either in this K_2SO_4– based medium, or a medium where KCl was part-substituted for the NaCl of Krebs medium (30 mM), even when in the initial stage of the K^+-contracture when there was considerable tone: however, contractions could always be elicited (data not shown). The log concentration-response curve for bradykinin contraction in the K_2SO_4-based high-K^+ medium was shifted to the right in the presence of D-Arg-[Hyp^3,Thi^5,D-Tic^7,Oic^8]-BK (30 nM) (Figure 4), giving an apparent pK_B of 8.4 ± 0.1 ($n=4$) (Table 1).

Phosphatidylinositol hydrolysis studies

Bradykinin produced a concentration-related increase in tissue levels of total [^{3}H]-IPs with an EC_{50} value of 0.97 (0.83–1.11) μM ($n=8$) (Figure 5). The maximum increase in accumulation of [^{3}H]-IPs by bradykinin (100 μM) was 340 ± 20% relative to basal levels. For comparison, the maximum accumulation of [^{3}H]-IPs in response to carbachol (1 mM) was 804 ± 62% ($n=8$) relative to basal levels.

The B_1 receptor-selective agonist [des-Arg^9]-BK (1 mM) did not significantly elevate total [^{3}H]-IPs over basal ($n=4$; $P>0.05$), and the B_1 receptor antagonist [Leu^8,des-Arg^9]-BK (3 μM) failed to inhibit total [^{3}H]-IPs accumulation stimulated by a sub-maximal concentration (10 μM) of bradykinin ($P>0.05$; $n=4$) (not shown). In contrast, the B_2 receptor antagonists D-Arg-[Hyp^3,D-Phe^7]-BK and D-Arg-[Hyp^3,Thi^5,D-Tic^7,Oic^8]-BK produced parallel rightward shifts of the bradykinin log concentration-response curve, with apparent pK_B estimates of 5.4 ± 0.3 and 8.4 ± 0.1 ($n=4$), respectively (Table 1). The inhibitory effect of D-Arg-[Hyp^3,Thi^5,D-Tic^7,Oic^8]-BK was selective for bradykinin, since the antagonist (1 μM) did not inhibit basal, nor (100 μM) carbachol-induced, [^{3}H]-IPs accumulation ($P>0.05$, data not shown).

Discussion

This study provides evidence that bradykinin receptors with indistinguishable recognition properties mediate the relaxant and contractile phases of the bradykinin-induced response in the guinea-pig taenia caeci under normal conditions: further, these same properties are shown by the receptors mediating bradykinin-induced hydrolysis of inositol phospholipids, as well as those evoking contractions in a high-K^+ depolarizing-medium and in a Ca^{2+}-free medium. The receptors involved in these five responses are not B_1 receptors, since the B_1-selective agonist, [des-Arg^9]-BK, was inactive in all experiments and the B_1-selective antagonist [Leu^8,des-Arg^9]-BK did not inhibit any facets of the responses to bradykinin. In contrast, the B_2 antagonist D-Arg-[Hyp^3,Thi^5,D-Tic^7,Oic^8]-BK, inhibited all types of bradykinin response with a similar affinity (pK_B 8.4–8.5; Table 1). This antagonist, and several related [D-Phe^7]-BK antagonists, were also able to displace [^{3}H]-bradykinin in competition binding experiments in the taenia caeci (Field *et al.*, 1992c). The affinity of D-Arg-[Hyp^3,Thi^5,D-Tic^7,Oic^8]-BK (and related B_2 antagonists; Field *et al.*, 1988; 1992b,c) for the guinea-pig taenia caeci receptor, is similar to that in other guinea-pig preparations, though lower than its affinity at B_2 receptors in several other species (Field *et al.*, 1992b,c). These observations support the existence of species-homologues of the B_2 receptor (see Hall, 1992; Hall *et al.*, 1993). These receptors in the guinea-pig taenia caeci are likely to be present on the smooth muscle cells, since tetrodotoxin and ω-conotoxin, and cyclo-oxygenase inhibitors, did not inhibit bradykinin responses; further these experiments were carried out in Krebs solution containing autonomic blockers and histamine receptor antagonists.

Regarding the mechanism of contraction, it was of interest that bradykinin B_2 receptor-induced contractile responses were considerably attenuated in the high-K^+ medium, suggesting that an important component of the bradykinin response depends on membrane potential-dependent events (electromechanical coupling), such as depolarization and calcium-entry via voltage-sensitive channels. Electromechanical coupling-mechanisms for bradykinin were not studied in detail here, but there is some evidence from this preparation suggesting a contribution from Na^+-entry to depolarization: from electrophysiological observations (Aarsen & Van Caspel-De Bruyn, 1970), $^{24}Na^+$-permeability determinations (Morton *et al.*, 1987), and functional experiments (present study).

The bradykinin B_2 receptor-mediated response remaining in high-K^+ depolarizing conditions must result from membrane potential-independent mechanisms (pharmaco-mechanical coupling); for example, release of intracellular Ca^{2+}. Further, the observation that bradykinin B_2 receptor stimulation could still produce transitory contractions in the absence of extracellular Ca^{2+}, indicates that bradykinin is indeed able to release Ca^{2+} from intracellular stores. It may well be relevant that a recent study in bovine tracheal smooth muscle cells, which quantified intracellular Ca^{2+} by direct imaging with fura-2, demonstrated a bradykinin-induced B_2 receptor antagonist-sensitive Ca^{2+}-elevation. This corresponded to a graded-influx of Ca^{2+} in the presence of extracellular Ca^{2+}. In contrast, in the absence of extracellular Ca^{2+}, there was Ca^{2+}-release; but this was essentially quantal

and resulted in lower levels of intracellular Ca^{2+} (Marsh & Hill, 1993). As a possible mechanism for Ca^{2+}-release in the taenia caeci, the role of the phosphatidylinositol hydrolysis transduction-pathway in the mobilization of Ca^{2+} from intracellular stores is particularly well established, and its involvement in bradykinin receptor-mediated signalling has been described in a number of cell types (see Burch, 1990, Farmer & Burch, 1992 and Hall, 1992). Recently, a role has been claimed for this pathway in contraction by bradykinin of smooth muscle of the gut (Ransom *et al.*, 1992), and airways (Marsh & Hill, 1992; 1992). In the present study, bradykinin caused a concentration-related increase in accumulation of total [^{3}H]-IPs: further, this was antagonized by the B_2 antagonists, D-Arg-[Hyp^3,Thi^5,D-Tic^7,Oic^8]-BK and D-Arg-[Hyp^3,D-Phe^7]-BK with the same affinity (pK_B 8.4 and 5.4, respectively) as for the functional responses (Table 1, Field *et al.*, 1992b). These data are compatible with the same receptor being involved in these functional and biochemical aspects of the action of bradykinin, and may indicate a causal relationship.

It is the presence of an initial relaxant component in the normal functional responses to bradykinin in the taenia caeci which distinguishes bradykinin from spasmogens such as carbachol, substance P and histamine, which give only a fast contraction (Hall & Morton 1986; 1991a; Hall *et al.*, 1986). In fact, biphasic responses to bradykinin have been reported in a number of other cell types (see Hall, 1992), and the present study was prompted, in part, by the description in NG108-15 cells (Higashida & Brown, 1986) of an initial apamin-sensitive hyperpolarization followed by a slower, phorbol ester mimicked, depolarization phase. The present study showed that the initial relaxant phase with bradykinin is mediated via B_2 receptors with the same properties as those for the contractile phase, since D-Arg-[Hyp^3,Thi^5,D-Tic^7,Oic^8]-BK showed a concentration-related antagonism, again yielding an apparent pK_B of 8.4 (Table 1). The relaxation phase is abolished by a low concentration of apamin (this study; Gater *et al.*, 1985; Carter *et al.*, 1986), indicating that it is caused by the opening of Ca^{2+}-activated K^+-channels: a proposal supported by ion-flux and electrophysiological studies. Thus, in depolarized taenia caeci preparations, bradykinin caused an apamin-sensitive increase in K^+-permeability (measured as efflux of ^{86}Rb in a medium containing 121 mM $KMeSO_4$; Gater *et al.*, 1985). Similarly, in the rat duodenum, we have demonstrated that B_2 receptors also mediate apamin-sensitive relaxation, and an apamin-sensitive increase in K^+-permeability (Hall & Morton, 1991b). In the guinea-pig taenia caeci, we found that relaxant responses to bradykinin depended on electromechanical coupling-mechanisms, in as much as that in high-K^+ depolarizing-media, where hyperpolarization cannot mediate responses, relaxant responses to bradykinin are abolished. In normal Krebs solution, electrophysiological studies have demonstrated an initial apamin-sensitive hyperpolarization associated with a membrane conductance increase (Den Hertog *et al.*, 1988). This Ca^{2+}-dependent hyperpolarization, through opening of K^+-channels, is independent of extracellular Ca^{2+}, and is supposed to use Ca^{2+} mobilized from an intracellular store (Den Hertog *et al.*, 1988). The observations from the present study do not contribute direct evidence regarding the origin of this Ca^{2+}; but do support an intracellular source for the Ca^{2+} contributing both to relaxation and contraction since both these actions of bradykinin could be demonstrated in zero-Ca^{2+} media. The hypothesis may be advanced that a common B_2 receptor, acting through the polyphosphoinositide pathway, is responsible for a release of intracellular Ca^{2+} which contributes to electrophysiological or mechanical events.

A question raised by this study is the mechanism of the divergence observed in the receptor-coupling processes in the taenia caeci. One group of receptors (e.g. muscarinic M_3, tachykinin NK_1 and histamine H_1) elicit simple monophasic contractions (both in normal and high-K^+ media), and activate the polyphosphoinositide pathway (Hall & Morton, 1986; Hall *et al.*, 1986; Gardner *et al.*, 1988; Hall & Morton, 1991a). The second group, which includes α_1-adrenoceptors and P_{2Y}-purinoceptors (Jenkinson & Morton, 1967a; Banks *et al.*, 1979; Den Hertog *et al.*, 1985; Nelemens & Den Hertog, 1987; O'Connor *et al.*, 1991) also activate the polyphosphoinositide pathway, but nevertheless cause an initial relaxation associated with opening of apamin-sensitive Ca^{2+}-activated K^+-channels. The bradykinin B_2 receptor-effector mechanism bears more resemblance to the latter group, though the initial relaxation is quickly followed by contraction. Further work is needed to explain this divergence. A speculative possibility is that it arises at the G protein level, so that different stores of Ca^{2+} are mobilized, or ion channels modulated.

In conclusion, our data show that in the smooth muscle of the guinea-pig taenia caeci, activation of bradykinin B_2 receptors causes a biphasic mechanical response. This response is due to a direct action of the smooth muscle and does not depend on the release of neuronally-derived mediators or prostanoids. Although the full sequence of events leading to the biphasic responses cannot be determined from these experiments, the hypothesis advanced is that receptor-induced stimulation of phosphatidylinositol hydrolysis leads to Ca^{2+}-mobilization from intracellular stores which contributes to responses. The initial relaxant phase involved membrane potential-dependent mechanisms, *viz.* those involving the opening of Ca^{2+}-activated K^+-channels and hyperpolarization. The subsequent contraction may involve both membrane potential-dependent and -independent mechanisms, utilizing both extracellular and intracellular Ca^{2+}.

We thank Professor D.H. Jenkinson for helpful comments on the manuscript, and the Sandoz Institute for Medical Research for a Research Student Scholarship (J.L.F.) and gifts of peptides. We acknowledge support from Zeneca Pharmaceuticals Group, Delaware, U.S.A., and the Wellcome Trust.

References

AARSEN, P.N. & VAN CASPEL-DE BRUYN, M. (1970). Effect of changes in ionic environment on the actions of bradykinin on the guinea-pig taenia caeci. *Eur. J. Pharmacol.*, **12**, 348–358.

BANKS, B.E.C., BROWN, C., BURGESS, G.M., BURNSTOCK, G., CLARET, M., COCKS, T.M. & JENKINSON, D.H. (1979). Apamin blocks certain neurotransmitter-induced increases in potassium permeability. *Nature*, **282**, 415–417.

BERRIDGE, M.J., DOWNES, C.P. & HANLEY, M.R. (1982). Lithium amplifies agonist-dependent phosphatidylinositol responses in brain and salivary glands. *Biochem. J.*, **206**, 587–593.

BRAMLEY, A.M., SAMHOUN, M.N. & PIPER, P.J. (1990). The role of the epithelium in modulating the responses of guinea-pig trachea induced by bradykinin *in vitro*. *Br. J. Pharmacol.*, **99**, 762–766.

BRADING, A.F., BURNETT, M. & SNEDDON, P. (1980). The effect of sodium removal on the contractile responses of the guinea-pig taenia coli to carbachol. *J. Physiol.*, **306**, 411–429.

BURCH, R.M. (1990). Kinin signal transduction: role of phosphoinositides and eicosanoids. *J. Cardiovasc. Pharmacol.*, **15**, Suppl. 6, S44–S45.

CARTER, T.D., HALL, J.M., MCCABE, D.V., MORTON, I.K.M. & SCHACHTER, M. (1986). Biphasic actions of bradykinin in the guinea-pig taenia caeci preparation. *Br. J. Pharmacol.*, **90**, 137P.

DEN HERTOG, A., NELEMANS, A. & VAN DEN AKKER, J. (1988). The multiple actions of bradykinin on smooth muscle of guinea-pig taenia caeci. *Eur. J. Pharmacol.*, **151**, 357–363.

DEN HERTOG, A., PIELKENROOD, J. & VAN DEN AKKER, J. (1985). Effector mechanisms for α,β-methylene ATP and ATP derivatives in guinea-pig taenia caeci. *Eur. J. Pharmacol.*, **110**, 95–101.

DURBIN, R.P. & JENKINSON, D.H. (1961). The effect of carbachol on the permeability of depolarized smooth muscle to inorganic ions. *J. Physiol*, **157**, 74–89.

FARMER, S.G. & BURCH, R.M. (1992). Biochemical and molecular pharmacology of kinin receptors. *Annu. Rev. Pharmacol. Toxicol.*, **32**, 511–536.

FIELD, J.L., FOX, A.J., HALL, J.M., MAGBAGBEOLA, A.O. & MORTON, I.K.M. (1988). Multiple bradykinin B_2 receptor subtypes in smooth muscle preparations? *Br. J. Pharmacol.*, **92**, 284P.

FIELD, J.L., HALL, J.M. & MORTON, I.K.M. (1992a). The nature of the bradykinin receptors involved in phosphatidylinositol hydrolysis and functional responses in the smooth muscle of the guinea-pig taenia caeci. *Br. J. Pharmacol.*, **107**, 30P.

FIELD, J.L., HALL, J.M. & MORTON, I.K.M. (1992b). Bradykinin receptors in the guinea-pig taenia caeci are similar to proposed BK_3 receptors in the guinea-pig trachea, and are blocked by Hoe 140. *Br. J. Pharmacol.*, **105**, 293–296.

FIELD, J.L., HALL, J.M. & MORTON, I.K.M. (1992c). Putative novel bradykinin B_3 receptors in the smooth muscle of the guinea-pig taenia caeci and trachea. *Agents Actions*, **38/I**, 540–545.

GARDNER, A.L., CHOO, L.K. & MITCHELSON, F. (1988). Comparison of the effects of some muscarinic agonists on smooth muscle and phosphatidylinositol turnover in the guinea-pig taenia caeci. *Br. J. Pharmacol.*, **94**, 199–211.

GATER, P.R., HAYLETT, D.G. & JENKINSON, D.H. (1985). Neuromuscular blocking agents inhibit receptor-mediated increases in the potassium permeability of intestinal smooth muscle. *Br. J. Pharmacol.*, **86**, 861–868.

HALL, J.M. (1992). Bradykinin receptors: pharmacological properties and biological roles. *Pharmacol. Ther.*, **56**, 131–190.

HALL, J.M., CAULFIELD, M.P., WATSON, S.P. & GUARD, S. (1993). Receptor subtypes or species homologues: relevance to drug discovery. *Trends Pharmacol. Sci.*, **14**, 376–383.

HALL, J.M., FIELD, J.L. & MORTON, I.K.M. (1991). Putative bradykinin BK_3 receptors in the guinea-pig taenia caeci and trachea. *Br. J. Pharmacol.*, **104**, 41P.

HALL, J.M., MCCABE, D.V. & MORTON, I.K.M. (1986). A comparison of receptor-effector coupling of histamine and analogues with that of carbachol in the guinea-pig taenia caeci. *Br. J. Pharmacol.*, **89**, 609P.

HALL, J.M. & MORTON, I.K.M. (1986). Different receptor systems in intestinal smooth muscle vary in their ability to translocate calcium. *Br. J. Pharmacol.*, **87**, 206P.

HALL, J.M. & MORTON, I.K.M. (1991a). Subtypes and excitation-contraction coupling mechanisms for neurokinin receptors in smooth muscle of the guinea-pig *Taenia caeci*. *Naunyn-Schmied. Arch. Pharmacol.*, **344**, 225–234.

HALL, J.M. & MORTON, I.K.M. (1991b). Bradykinin B_2 receptor evoked K^+ permeability increase mediates relaxation in the rat duodenum. *Eur. J. Pharmacol.*, **193**, 231–238.

HIGASHIDA, H. & BROWN, D.A. (1986). Two polyphosphatidylinositide metabolites control two K^+ currents in an neuronal cell. *Nature*, **323**, 333–335.

HOCK, F.J., WIRTH, K., ALBUS, U., LINZ, W., GERHARDS, H.J., WIEMER, G., HENKE, ST., BREIPOHL, G., KONIG, W., KNOLLE, J. & SCHOLKENS, B.A. (1991). Hoe 140 a new potent and long acting bradykinin-antagonist. *in vitro* studies. *Br. J. Pharmacol.*, **102**, 769–773.

JENKINSON, D.H. & MORTON, I.K.M. (1967a). The effect of noradrenaline on the permeability of depolarized intestinal smooth muscle to inorganic ions. *J. Physiol.*, **188**, 373–386.

JENKINSON, D.H. & MORTON, I.K.M. (1967b). The role of α- and β-adrenergic receptors in some actions of catecholamines on intestinal smooth muscle. *J. Physiol.*, **188**, 387–402.

MARSH, K.A. & HILL, S.J. (1992). Bradykinin B_2 receptor-mediated phosphoinositide hydrolysis in bovine cultured tracheal smooth muscle cells. *Br. J. Pharmacol.*, **107**, 443–447.

MARSH, K.A. & HILL, S.J. (1993). Characterisation of the bradykinin-induced changes in intracellular calcium ion concentrations of single bovine tracheal smooth muscle cells. *Br. J. Pharmacol.*, **110**, 29–35.

MORTON, I.K.M., HALL, J.M. & FOX, A.J. (1987). Mechanism of action bradykinin in the taenia caeci. *X International Congress of Pharmacology, Sydney, Australia*, p1460.

NELEMENS, A. & DEN HERTOG, A. (1987). Changes in membrane potential and phosphoinositides during α_1-adrenoceptor stimulation in smooth muscle cells of the guinea-pig taenia caeci. *Eur. J. Pharmacol.*, **133**, 215–223.

O'CONNOR, S.E., DAINTY, I.A. & LEFF, P. (1987). Further subclassification of ATP receptors based on agonist studies. *Trends Pharmacol. Sci.*, **12**, 137–141.

RANSOM, R.W., GOODMAN, C.B. & YOUNG, G.S. (1992). Bradykinin stimulation of phosphoinositide hydrolysis in guinea-pig ileum longitudinal muscle. *Br. J. Pharmacol.*, **105**, 919–924.

REGOLI, D. & BARABÉ, J. (1980). Pharmacology of bradykinin and related kinins. *Pharmacol. Rev.*, **32**, 1–46.

(Received May 12, 1994
Accepted June 2, 1994)

Br. J. Pharmacol. (1994), **113**, 614–620 © Macmillan Press Ltd, 1994

Differential effects of P_2-purinoceptor antagonists on phospholipase C- and adenylyl cyclase-coupled P_{2Y}-purinoceptors

José L. Boyer, Irene E. Zohn, *Kenneth A. Jacobson & [1]T. Kendall Harden

Department of Pharmacology, School of Medicine, University of North Carolina, Chapel Hill, NC 27599 and *Laboratory of Bioorganic Chemistry, National Institute of Diabetes and Digestive and Kidney Diseases, National Institutes of Health, Bethesda, Maryland, U.S.A.

1 Stimulation of P_{2Y}-purinoceptors on turkey erythrocytes and many other cell types results in activation of phospholipase C. In contrast, we have observed recently that P_{2Y}-purinoceptors on C6 rat glioma cells are not coupled to phospholipase C, but rather, inhibit adenylyl cyclase.

2 In this study we investigated the pharmacological selectivity of the P_2-purinoceptor antagonists, suramin, reactive blue 2, and pyridoxal phosphate 6-azophenyl 2',4'-disulphonic acid (PPADS) for phospholipase C- and adenylyl cyclase-coupled P_{2Y}-purinoceptors.

3 In C6 glioma cells, suramin and reactive blue 2 competitively antagonized the inhibitory effect of 2MeSATP on adenylyl cyclase ($pK_B = 5.4 \pm 0.2$ and 7.6 ± 0.1, respectively), whereas PPADS at concentrations up to 100 μM had no effect.

4 In contrast, in the turkey erythrocyte preparation, PPADS at concentrations up to 30 μM was a competitive antagonist of P_{2Y}-purinoceptor-stimulated phospholipase C activity ($pK_B = 5.9 \pm 0.1$). Suramin and reactive blue 2 produced both a shift to the right of the concentration-effect of 2MeSATP for the activation of phospholipase C and a significant decrease in the maximal inositol phosphate response.

5 Turkey erythrocytes also express a phospholipase C-coupled β-adrenoceptor. Concentrations of PPADS that competitively inhibited the P_{2Y}-purinoceptor-mediated response had only minimal effects on the activation of phospholipase C by β-adrenoceptors. In contrast, suramin and reactive blue 2 produced a non-competitive inhibition, characterized by decreases in the maximal response to isoprenaline with no change in the potency of this β-adrenoceptor agonist.

6 The differential effect of PPADS on P_{2Y}-purinoceptors of C6 glioma cells and turkey erythrocytes adds further support to the idea that different P_{2Y}-purinoceptor subtypes mediate coupling to adenylyl cyclic and phospholipase C.

Keywords: Reactive blue 2; suramin; PPADS; phospholipase C; inositol phosphates; P_{2Y}-purinoceptors; cyclic AMP accumulation; adenylyl cyclase inhibition; C6 rat glioma cells

Introduction

Adenosine 5'-triphosphate (ATP) is released from multiple cell types including neurones, platelets, and endothelial cells (Gordon, 1986; O'Connor *et al.*, 1991). Extracellular ATP and its derivatives interact with specific receptors on the surface of target cells and regulate a number of biological functions such as platelet aggregation, neurotransmission, cardiac performance, muscle contraction, and glucose metabolism (for review see Dubyak & El-Motassim, 1993). Purinoceptors originally were classified as P_1- and P_2-purinoceptors (Burnstock, 1978). P_1-purinoceptors, which are activated by adenosine, were further sub-classified into A_1 and A_2 subtypes (Van Calker *et al.*, 1979; Londos *et al.*, 1980), and a third adenosine receptor subtype (A_3) has been identified recently (Meyerhoff *et al.*, 1991; Zhou *et al.*, 1992). P_2-purinoceptors are activated by ATP and/or ADP. This receptor class originally was sub-divided into P_{2X}- and P_{2Y}-purinoceptors (Burnstock & Kennedy, 1985). However, additional receptor subtypes exist within this class including the P_{2U}-, P_{2Z}-, and P_{2T}-purinoceptors (Gordon, 1986; O'Connor *et al.*, 1991; Dubyak & El-Motassim, 1993).

In contrast to the P_1-purinoceptor class, classification of P_2-purinoceptors has relied exclusively on the pharmacological specificity of responses to agonist analogues of ATP and ADP. However, several compounds that are known to interact with multiple ATP binding proteins have proven useful as functional antagonists of ATP signalling responses. Reactive blue 2 has been reported to antagonise ATP actions at the P_{2Y}-purinoceptor subtype (Choo, 1981; Manzini *et al.*, 1986; Reilly *et al.*, 1987; Rice & Singleton, 1989), and the trypanocidal drug suramin is an antagonist of multiple ATP-receptor stimulated responses (Dunn & Blakely, 1988; Hoyle *et al.*, 1990; Leff *et al.*, 1990). Pyridoxal phosphate 6-azophenyl-2',4'-disulphonic acid (PPADS) recently was shown to inhibit ATP-receptor-stimulated mechanical responses of the rabbit vas deferens (Lambrecht *et al.*, 1992) and rabbit urinary bladder detrusor muscle (Ziganshin *et al.*, 1993).

The signalling mechanisms associated with P_2-purinoceptors are only partially understood. Perhaps the most widely studied P_2-purinoceptor signalling mechanism is the G-protein-regulated inositol lipid cascade and calcium mobilization that results from activation of P_{2Y}- (Charest *et al.*, 1985; Forsberg *et al.*, 1987; Pirotton *et al.*, 1987; Boyer *et al.*, 1989; Berrie *et al.*, 1989) and P_{2U}-purinoceptors (Dubyak *et al.*, 1988; Okajima *et al.*, 1989; Fine *et al.*, 1989; Stutchfield & Cockcroft, 1990; Brown *et al.*, 1991). However, activation of P_2-receptors in a number of target tissues results in a decrease in adenosine 3':5'-cyclic monophosphate (cyclic AMP) accumulation (Okajima *et al.*, 1987; Pianet *et al.*, 1989; Sato *et al.*, 1992; Valeins *et al.*, 1992; Lin & Chuang, 1993), and we recently reported that C6 rat glioma cells express a P_{2Y}-purinoceptor subtype that inhibits adenylyl cyclase (Boyer *et al.*, 1993). This observation contrasts with

[1] Author for correspondence.

the well-characterized effect of 2-methylthio-ATP (2MeSATP) on phospholipase C activity mediated by 'typical' P_{2Y}-purinoceptors. Differences in the pharmacological specificity for adenine nucleotide analogues on the two receptor responses have been observed (Boyer *et al.*, 1993; O'Tuel, Boyer & Harden, unpublished). The involvement of a different signalling pathway and the possible existence of different pharmacological specificities are consistent with the idea that a unique receptor subtype is involved in the regulation of adenylyl cyclase by P_{2Y}-purinoceptor agonists in C6 glioma cells.

In this study we compared the effect of the putative P_2-purinoceptor antagonists, reactive blue 2, suramin, and PPADS on 2MeSATP-promoted inhibition of adenylyl cyclase in C6 glioma cells and on activation of phospholipase C in turkey erythrocytes. We present evidence of differences in apparent affinity of reactive blue 2 between the two test systems and for a selective effect of PPADS for the phospholipase C-coupled P_{2Y}-purinoceptor. These results suggest that different P_{2Y}-purinoceptors regulate adenylyl cyclase and phospholipase C activities.

Methods

Cell culture

C6 rat glioma cells were grown in Dulbecco's Modified Eagle's Medium supplemented with 5% foetal calf serum in a humidified atmosphere of 95% air and 5% CO_2. Cells were passaged by trypsinization. Experiments were carried out in confluent cultures 2–4 days after plating in 12-well plates as previously described (Frederich *et al.*, 1983).

Cyclic AMP accumulation

Cells were labelled for 2 h with 1-2 μCi ml^{-1} [^{3}H]-adenine (Meeker & Harden, 1982; Frederich *et al.*, 1983). Cells were washed twice with HEPES (20 mM, pH 7.5) buffered Eagle's medium at 37°C, and then preincubated for 10 min with HEPES Eagle's medium containing 200 μM isobutyl methylxanthine (IBMX). Antagonists were added to the cells 10 min before challenge with agonist. Agonist incubations were initiated by the simultaneous addition of 10 μM isoprenaline and the indicated concentrations of the P_{2Y}-purinoceptor agonist, 2MeSATP. The reactions were stopped after 10 min by aspiration of the drug-containing medium and addition of 1 ml of ice-cold 5% trichloroacetic acid. [^{3}H]-cyclic AMP accumulation was determined by Dowex and alumina chromatography as previously described (Harden *et al.*, 1982).

Turkey erythrocyte labelling

Fresh blood was obtained from female turkeys by venous puncture and collected into a heparinized syringe. Erythrocytes were washed twice by centrifugation and resuspension with sterile DMEM, followed by a final wash in inositol-free DMEM. One ml of washed packed erythrocytes was resuspended in a final volume of 4.2 ml of inositol-free DMEM in the presence of 0.5–1 mCi [^{3}H]-inositol. Cells were incubated in a stirred glass vial for 16–20 h at 37°C in a humidified atmosphere of 95% air, 5% CO_2 as previously described in detail (Harden *et al.*, 1988; Boyer *et al.*, 1989).

Phospholipase C assay

Erythrocyte ghosts were prepared with [^{3}H]-inositol-labelled cells by hypotonic lysis in 15 volumes of a buffer containing 5 mM sodium phosphate, pH 7.4, 5 mM $MgCl_2$, and 1 mM EGTA (lysis buffer). Erythrocyte ghosts were washed three times by centrifugation and resuspension with lysis buffer. The final resuspension was in 20 mM HEPES pH 7.0 to a concentration of 6 mg protein ml^{-1}. This preparation was used immediately for the phospholipase C assay. Twenty five μl of [^{3}H]-inositol-labelled ghost preparation ($\approx$150 μg protein, 200,000 c.p.m.) were combined in a final volume of 200 μl of a medium containing 0.91 mM $MgSO_4$, 115 mM KCl, 5 mM potassium phosphate, 0.424 mM $CaCl_2$, 2 mM EGTA, 10 mM HEPES, pH 7.0 (free Ca^{2+} concentration was $\approx$1 μM). Since receptor-and G-protein activation of phospholipase C in turkey erythrocyte ghosts is strictly dependent on the presence of guanine nucleotides (Boyer *et al.*, 1989), the non-hydrolyzable analogue of GTP, GTPγS at 1 μM was included in the assay.

Ghosts were incubated for 5 min at 37°C with the indicated concentrations of 2MeSATP, in the presence or in the absence of antagonist. Incubations were terminated by the addition of 1 ml of ice cold 5% trichloroacetic acid. Samples were centrifuged, the supernatants were transferred to a fresh tube, and the trichloroacetic acid was extracted three times with 3 ml portions of ethyl ether. Neutralized samples were diluted with 8 ml of water and transferred into Dowex AG-X8 columns (formate form). Columns were washed with 8 ml of 200 mM ammonium formate, 100 mM formic acid, and the eluant was discarded. Total inositol phosphates (IP_2 through IP_4) were eluted with 5 ml of 1.2 M ammonium formate, 100 mM formic acid, and collected in scintillation vials. [^{3}H]-inositol phosphates were quantitated by scintillation spectroscopy as previously described in detail (Harden *et al.*, 1988, Boyer *et al.*, 1989).

Materials

2MeSATP was obtained from Research Biochemicals Inc. (Natick, MA, U.S.A.); reactive Blue 2 (Cibacron Blue) was from Fluka (Ronkonkowa, NY, U.S.A.); PPADS was from Cookson Chemical Ltd (Southampton, England); isoprenaline was from Sigma Chemical Co. (St. Louis, MO, U.S.A.); 2-[^{3}H]-*myo*-inositol (20 Ci mmol^{-1}) and [8-^{3}H]-adenine (27 Ci mmol^{-1}) were obtained from American Radiolabeled Chemicals, Inc. (St. Louis, MO, U.S.A.); inositol-free DMEM was from Gibco BRL, (Grand Island, NY, U.S.A.); suramin was a generous gift from the Department of Drug Services from the Center for Disease Control (Atlanta, GA, U.S.A.). The sources of other materials have been previously reported (Harden *et al.*, 1988; Boyer *et al.*, 1989; 1993).

Data analysis

Agonist potencies were calculated using a four parameter logistic equation using the GraphPad software package. In experiments where antagonists produced parallel displacements in the concentration-effect curves, dose-ratios were calculated from the $K_{0.5}$ estimates for each pair of curves and analysed according to Arunlakshana & Schild (1959).

Results

Incubation of C6 glioma cells with the P_{2Y}-purinoceptor agonist 2MeSATP resulted in a concentration-dependent inhibition of isoprenaline-stimulated cyclic AMP accumulation (Boyer *et al.*, 1993). Preincubation of cells with increasing concentrations of the putative P_2-purinoceptor antagonist, suramin, resulted in parallel shifts to the right of the concentration-effect curve of 2MeSATP (Figure 1a). Arunlakshana-Schild analysis of these data (Arunlakshana & Schild, 1959) indicated that in intact C6 cells, suramin at concentrations up to 100 μM behaves as a competitive antagonist (slope = 0.94 $\pm$ 0.04) of the P_{2Y}-purinoceptor coupled to the inhibition of adenylyl cyclase. The pK_B for

suramin derived from Arunlakshana-Schild plots (Figure 1b) was 5.4 ± 0.2 ($n = 3$ experiments).

The effect of reactive blue 2 on 2MeSATP-induced inhibition of cyclic AMP accumulation is shown in Figure 2. As was observed with suramin, reactive blue 2 at concentrations up to 10 μM produced parallel shifts to the right of the concentration-effect curve of 2MeSATP (Figure 2a). The pK_B value for reactive blue 2 obtained from four Arunlakshana-Schild plots (slope = 1.07 ± 0.08) was 7.6 ± 0.1 (Figure 2b). These results indicate that at surprisingly low concentrations, reactive blue 2 behaves as a competitive antagonist of the P_{2Y}-purinoceptor on C6 rat glioma cells. Incubation of C6 cells with concentrations of reactive blue 2 higher than 50 μM significantly decreased the maximal responses of cyclic AMP accumulation observed with isoprenaline.

Lambrecht *et al.* (1992) have reported recently that the pyridoxal phosphate derivative, PPADS is a competitive antagonist of P_2-purinoceptors in the vas deferens. In marked contrast to the effects of suramin and reactive blue 2, PPADS had no effect on the inhibition of cyclic AMP accumulation by 2MeSATP in C6 glioma cells when assayed at concentrations up to 100 μM (Figure 3).

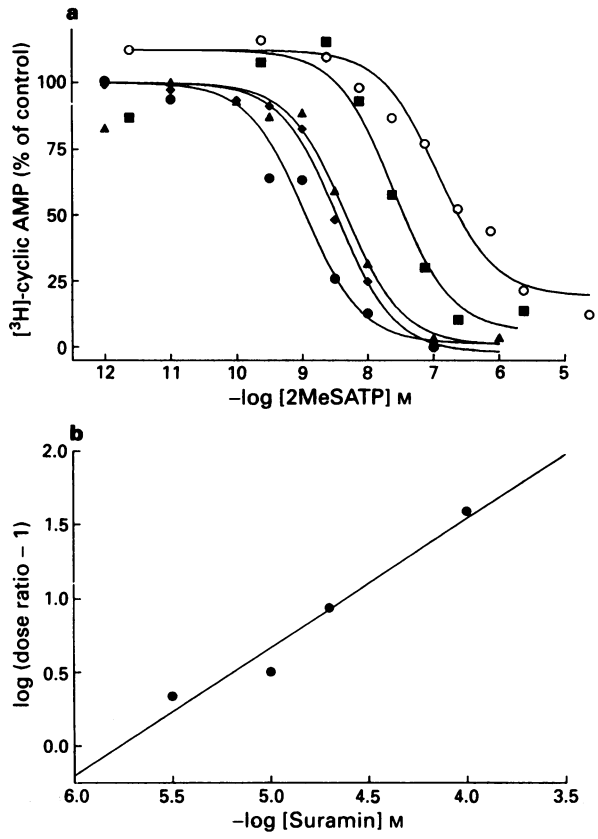


Figure 1 Effect of suramin on P_{2Y}-purinoceptor-mediated inhibition of adenylyl cyclase activity in C6 glioma cells. Cyclic AMP accumulation in [^{3}H]-adenine-labelled C6 glioma cells was quantitated as described in Methods. (a) The concentration dependence of 2MeSATP for inhibition of isoprenaline-stimulated cyclic AMP accumulation was determined in the absence (●), or in the presence of 3 (◆), 10 (▲), 20 (■), and 100 μM (○) suramin. The maximal cyclic AMP accumulation stimulated by 10 μM isoprenaline was 19000 ± 2000 c.p.m. Maximal effective concentrations of 2MeSATP resulted in 40–50% inhibition of the response to isoprenaline. Data are presented as percentage of the isoprenaline-induced cyclic AMP accumulation inhibitable by a maximally effective concentration of 2MeSATP observed in the absence of antagonist. (b) Arunlakshana-Schild plot from the data presented in (a). The slope of the plot was 0.94 and the estimated pK_B obtained from three separate experiments was 5.4 ± 0.2. Data shown are the mean of triplicate determinations and the results shown are representative of those obtained in three separate experiments.

In contrast to the P_{2Y}-purinoceptor on C6 cells, activation of P_{2Y}-purinoceptors on turkey erythrocytes results in a rapid increase in the hydrolysis of inositol lipids by phospholipase

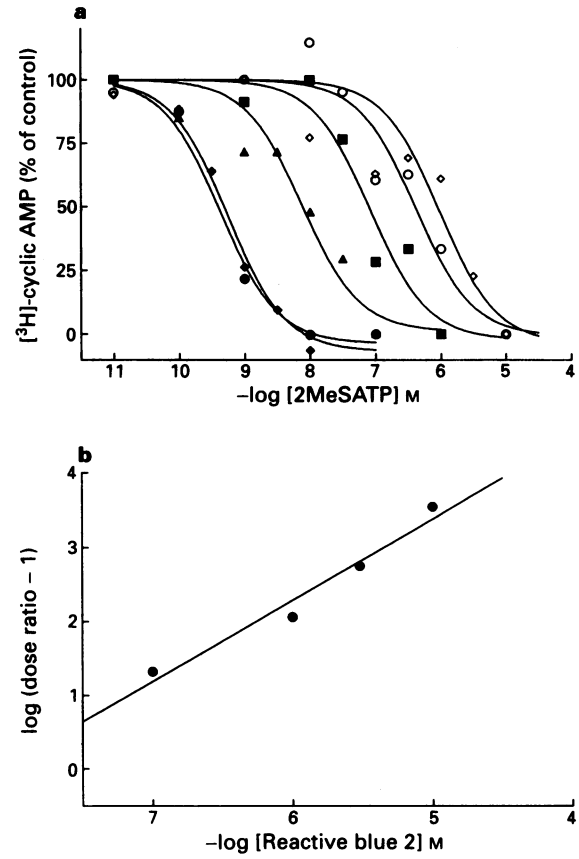


Figure 2 Effect of reactive blue 2 on P_{2Y}-purinoceptor-mediated inhibition of adenylyl cyclase activity in C6 glioma cells. Cyclic AMP accumulation in [^{3}H]-adenine-labelled C6 glioma cells was quantitated as described in Methods. (a) The concentration-dependence of 2MeSATP in inhibiting isoprenaline-stimulated cyclic AMP accumulation was determined in the absence (●), or in the presence of 0.03 (◆), 0.1 (▲), 1 (■), 3 (○) and 10 μM (◇) reactive blue 2. See legend of Figure 1 for details. (b) Arunlakshana-Schild plot from the data presented in (a). The slope of the plot was 1.07 ± 0.08. The estimated pK_B was 7.6 ± 0.1 ($n = 4$ experiments). Data shown are the mean of triplicate determinations and the results shown are representative of those obtained in four separate experiments.

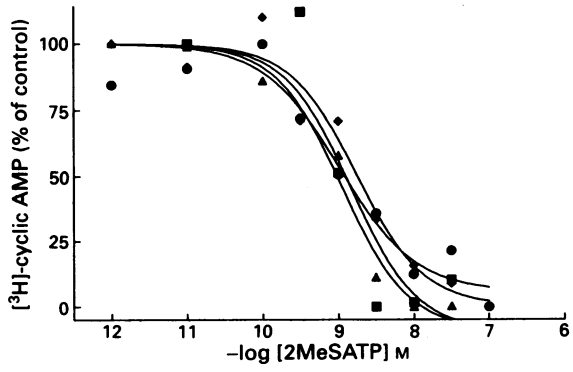


Figure 3 Lack of effect of PPADS on P_{2Y}-purinoceptor-mediated inhibtion of adenylyl cyclase activity in C6 glioma cells. Cyclic AMP accumulation in [^{3}H]-adenine-labelled C6 glioma cells was quantitated as indicated under Methods. The concentration-dependence of 2MeSATP in inhibiting isoprenaline-stimulated cyclic AMP accumulation was determined in the absence (●) or in the presence of 0.3 (◆), 30 (▲), and 100 μM (■) PPADS. See legend of Figure 1 for details. For abbreviations, see text.

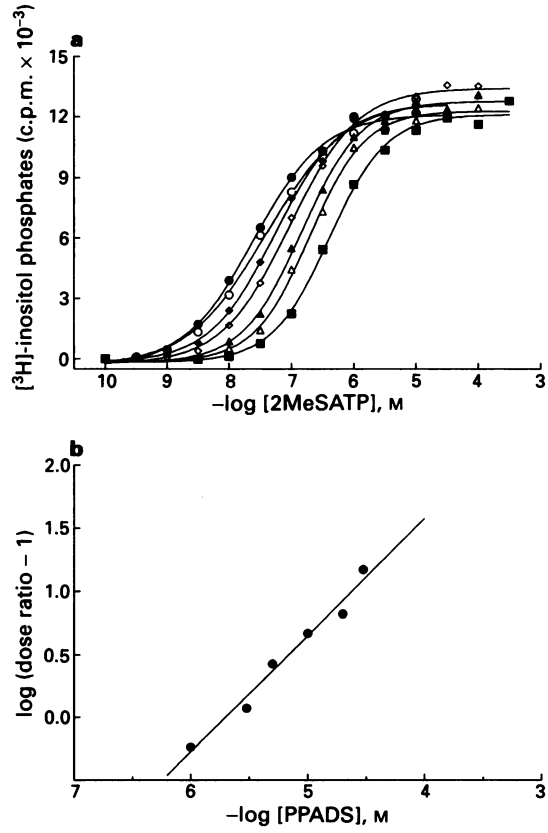


Figure 4 Effect of PPADS on P_{2Y}-purinoceptor-mediated activation of phospholipase C in turkey erythrocyte membranes. Membranes from [^{3}H]-inositol-labelled erythrocytes were prepared as described in Methods. (a) Release of [^{3}H]-inositol phosphates was measured in the presence of 1 μM GTPγS and the indicated concentrations of 2MeSATP in the absence (●), or in the presence of 1 (○), 3 (◆), 5 (◇), 10 (▲), 20 (△), or 30 μM PPADS (■). Data shown are the mean of duplicate determinations, and the results shown are representative of those obtained in three separate experiments. [^{3}H]-inositol phosphates released by 1 μM GTPγS in the absence of 2MeSATP (500 ± 200 c.p.m.) were subtracted from the data. (b) The corresponding Arunlakshana-Schild plot from the data presented in (a). The slope of the plot was 1.1 ± 0.1 and the estimated pK_B was 5.9 ± 0.1 ($n = 3$ experiments). For abbreviations, see text.

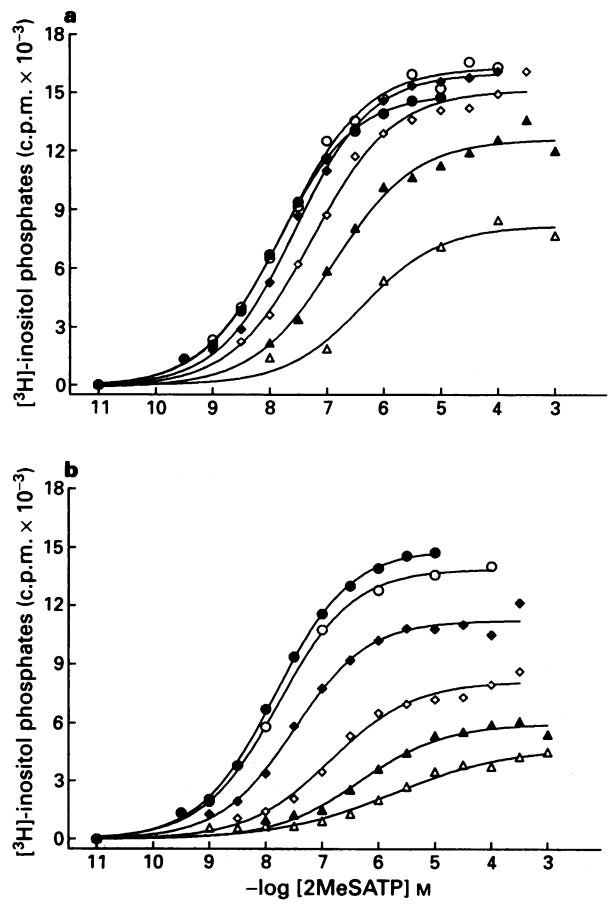


Figure 5 Effects of suramin and reactive blue 2 on P_{2Y}-purinoceptor-mediated activation of phospholipase C in turkey erythrocyte membranes. Membranes from [^{3}H]-inositol-labelled erythrocytes were prepared as described in Methods. (a) Release of [^{3}H]-inositol phosphates was measured in the presence of 1 μM GTPγS and the indicated concentrations of 2MeSATP in the absence (●), or in the presence of 1 (○), 3 (◆), 10 (◇), 30 (▲) or 100 μM suramin (△). (b) Release of [^{3}H]-inositol phosphates was measured in the presence of 1 μM GTPγS and the indicated concentrations of 2MeSATP in the absence (●) or in the presence of 1 (○), 3 (◆), 10 (◇), 30 (▲), or 100 μM reactive blue 2 (△). Data shown are the mean of duplicate determinations and the results shown are representative of those obtained in three different experiments.

C. The effects of PPADS, suramin and reactive blue 2 on the P_{2Y}-purinoceptor-stimulated inositol lipid response of turkey erythrocyte membranes were examined. In contrast to the lack of effect of PPADS on the C6 cell P_{2Y}-purinoceptor, PPADS produced a 30 to 45 fold shift to the right in the concentration-effect curve of 2MeSATP in turkey erythrocyte membranes without producing any significant effect on the maximal response (Figure 4a). Arunlakshana-Schild analysis of these data indicated that PPADS is a competitive antagonist of the phospholipase C-coupled P_{2Y}-purinoceptor. The pK_B for PPADS was 5.9 ± 0.1, and the slope of the Schild regression was 1.1 ± 0.1 (Figure 4b). Higher concentrations, i.e. greater than 50 μM PPADS, produced further shifts to the right in the concentration-effect curves for 2MeSATP but also resulted in decreases in the maximal inositol phosphate response (data not shown).

Treatment of turkey erythrocyte membranes with suramin or reactive blue 2 also produced a concentration-dependent shift to the right of the concentration-effect curve of 2MeSATP for activation of phospholipase C (Figure 5). For example, the EC_{50} for 2MeSATP increased by 10 and 50 fold in the presence of 30 μM suramin and 30 μM reactive blue 2, respectively. However, this shift in the concentration-effect curve was accompanied by a significant decrease in the maximal stimulation of inositol phosphates produced by 2MeSATP (Figure 5). These results indicate that the inhibitory effects of suramin and reactive blue 2 on the inositol phosphate response of 2MeSATP do not solely occur by competitive inhibition.

Based on the broad range of potential effects of the available P_2-antagonists, it is not unlikely that these compounds produce non-specific effects, particularly at high concentrations. This possibility is even more likely to occur in cell-free assays, as with the turkey erythrocyte membrane preparation used in this study. To determine whether the decrease in the maximal response to 2MeSATP observed in membranes treated with suramin and reactive blue 2 was related to the inactivation of the P_{2Y}-purinoceptor, the effects of the antagonists on the β-adrenoceptor promoted activation of phospholipase C (Rooney *et al.*, 1991; Vaziri & Downes, 1992) were studied. In contrast to the marked shifts to the right of the concentration-effect curves of 2MeSATP (Figure 5), no effect of suramin or reactive blue 2 on the EC_{50} for the isoprenaline response was observed (Figure 6a). However, both antagonists produced a concentration-dependent decrease in the maximal inositol phosphate response to isoprenaline (Figure 6a, and data not shown). Consistent with a specific antagonist effect, 30 μM PPADS produced a

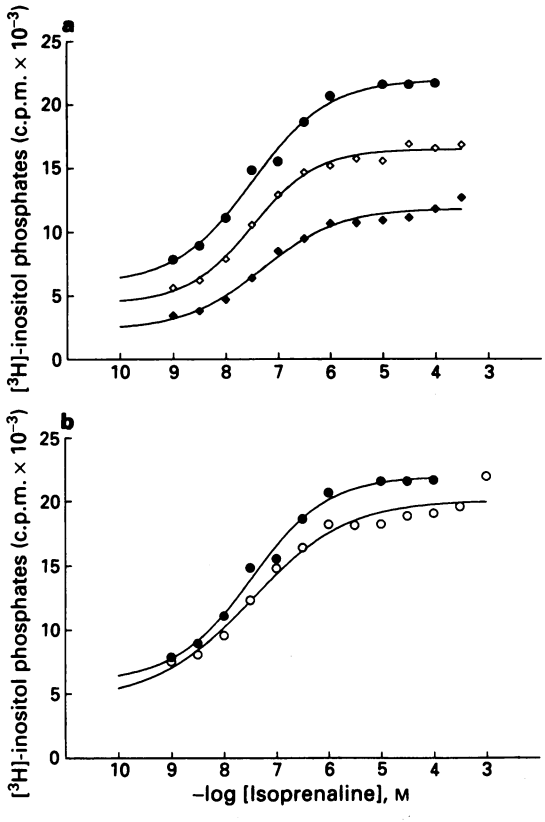


Figure 6 Effects of suramin, reactive blue 2, and PPADS on β-adrenoceptor-mediated activation of phospholipase C in turkey erythrocyte membranes. Membranes from [^{3}H]-inositol-labelled erythrocytes were prepared as described in Methods. Release of [^{3}H]-inositol phosphates was measured in the presence of 1 μM GTPγS and the indicated concentrations of isoprenaline in the absence (●), or in the presence of 30 μM suramin (◇), 30 μM reactive blue 2 (◆) (a), or 30 μM PPADS (○) (b). Data shown are the mean of duplicate determinations and the results shown are representative of those obtained in three separate experiments.

30 fold increase in the EC_{50} for 2MeSATP (Figure 4a) without modifying significatively the concentration-effect curve of isoprenaline (Figure 6b). The decrease in the maximal inositol phosphate response to isoprenaline produced by 30 μM antagonist was 6%, 23% and 46% for PPADS, suramin, and reactive blue 2, respectively. These data indicate that the inhibitory effect of suramin, reactive blue 2, and that observed with higher concentrations of PPADS on the inositol phosphate response to isoprenaline are non-competitive, and probably occur as a result of a non-specific interaction with the G-protein involved or phospholipase C. Consistent with these results, reactive blue 2 and high concentrations of suramin also inhibited the activation of phospholipase C produced by AlF_4^- whereas PPADS at concentrations up to 100 μM had no effect on the response to AlF_4^- (data not shown). Taken together, these data indicate that in the turkey erythrocyte preparation, the effects of suramin and reactive blue 2 on the response of 2MeSATP are produced by at least two independent effects: a specific effect at the P_{2Y}-purinoceptor (as evidenced by the shift to the right of the concentration-effect curve of 2MeSATP (Figure 5)) and a non-specific effect at the level of G-protein/phospholipase C (as evidenced by their effects on the response to AlF_4^- and by the decrease in the maximal phospholipase C response to isoprenaline without a change in the EC_{50} value).

Discussion

The relative simplicity of the model systems studied here, together with the exceptional sensitivity of the P_{2Y}-purinoceptor responses in turkey erythrocytes and C6 glioma cells, have allowed us to determine the pharmacological properties of putative P_2-purinoceptor antagonists at the most immediate response of the activation of the receptor, the generation of the second messenger. The pyridoxal phosphate derivative, PPADS, exhibited selectivity for the phospholipase C-coupled P_{2Y}-purinoceptor of the turkey erythrocyte, whereas no activity against the adenylyl cyclase-coupled P_{2Y}-purinoceptor in C6 glioma cells was observed (Figure 3). The effect of PPADS was competitive (Figure 4), and its selectivity was confirmed by a lack of effect on activation of phospholipase C by β-adrenoceptors (Figure 6b). These results with PPADS strongly suggest that the activation of phospholipase C and the inhibition of adenylyl cyclase are mediated by different P_{2Y}-purinoceptor subtypes. Evidence for heterogeneity within the P_{2Y}-purinoceptor subclass also has been obtained recently in studies of the effects of a large series of nucleotide analogues on the responses mediated by ATP receptors on the guinea-pig taenia coli, rabbit aorta, rabbit mesenteric artery and turkey erythrocytes (Fischer *et al.*, 1993; Burnstock *et al.*, 1994).

Lambrecht *et al.* (1992) and Ziganshin *et al.* (1993) have reported the antagonist properties of PPADS on P_{2X}-purinoceptor-mediated mechanical responses of the rabbit vas deferens and urinary bladder detrusor muscle. The effects of PPADS were found to be selective, since mechanical responses induced by α_1-adrenoceptor, M_2- and M_3-muscarinic, H_1-histamine, and A_1-adenosine receptors were not affected. The binding of [^{3}H]-α,β-methylene ATP to urinary bladder membranes was also blocked by PPADS in the same concentration-range (Ziganshin *et al.*, 1993). It is clear from our data that PPADS also interacts with P_{2Y}-purinoceptors, and therefore, a more extensive pharmacological analysis of the effects of PPADS on other P_2-purinoceptor systems is necessary to establish its overall specificity towards ATP-mediated responses.

Suramin and reactive blue 2 have been shown to produce multiple effects on a variety of biological systems (Fedan & Lamport, 1990; Voogd *et al.*, 1993). In spite of this broad range of effects, these compounds have proved useful as functional antagonists of ATP-stimulated responses in some tissues (Dunn & Blakely, 1978; Choo, 1980; Manzini *et al.*, 1986; Reilly *et al.*, 1987; Rice & Singleton, 1989; Hoyle *et al.*, 1990; Leff *et al.*, 1990). Within a defined concentration-range both suramin and reactive blue 2 behaved as competitive antagonists of the adenylyl cyclase-coupled P_{2Y}-purinoceptor of C6 cells. The apparent affinity of reactive blue 2 ($pK_B = 7.6 \pm 0.1$) is the highest that to our knowledge has been reported for this compound in any ATP response. Suramin and reactive blue 2 also shifted to the right the concentration-effect curve of 2MeSATP for the stimulation of phospholipase C in the turkey erythrocyte preparation (Figure 5). In contrast to the apparently competitive inhibition by suramin and reactive blue 2 of P_{2Y}-purinoceptors on C6 cells (Figures 1 and 2), the inhibition of the turkey erythrocyte P_{2Y}-purinoceptor was more complex; significant decreases in the maximal response of phospholipase C occurred coincidently with the rightward shifts in the concentration-effect curve for 2MeSATP (Figure 5). Suramin decreased the maximal response of phospholipase C to isoprenaline without affecting the EC_{50} for this β-adrenoceptor agonist. These data suggest that in the turkey erythrocyte preparation, suramin interacts with the P_{2Y}-purinoceptor but not with the β-adrenoceptor and that the decrease in the maximal responses to P_{2Y}-purinoceptor- and β-adrenoceptor-stimulation results from effects at sites other than the receptor, probably at the level of the G-protein or phospholipase C. Consistent with this idea, the effects of suramin on the maximal responses to P_{2Y}-purinoceptor- and β-adrenoceptor-stimulation were similar.

Reactive blue 2 also decreased the maximal response of phospholipase C to isoprenaline without affecting the EC_{50}. However, in contrast with suramin, the depression of the

response of phospholipase C to 2MeSATP produced by reactive blue 2 was larger than that of isoprenaline, consistent with a non competitive effect of reactive blue 2 on the P_{2Y}-purinoceptor.

The overall affinities of PPADS and suramin observed in these model systems were in a good agreement with the values reported in most previous studies with mammalian tissue preparations (Leff *et al.*, 1990; Lambrecht *et al.*, 1992; Wilkinson *et al.*, 1993). However, the affinity of reactive blue 2 for the adenylyl cyclase-coupled P_{2Y}-purinoceptor of C6 glioma cells ($\approx$30 nM) was at least 50 fold higher than the affinities reported for P_{2Y}-purinoceptors in other tissues (Choo, 1981; Crema *et al.*, 1983; Reilly *et al.*, 1987; Rice & Singleton, 1989; Soltoff *et al.*, 1989). As was observed here, the selectivity and specificity of the available P_2-purinoceptor antagonists is frequently limited to a set of particular experimental conditions and to a narrow range of concentrations. More selective antagonists obviously are needed. However, all three compounds studied here can be used as a starting point for the development of more potent and selective drugs.

In summary, our results show that PPADS selectively blocks the phospholipase C coupled P_{2Y}-purinoceptor of turkey erythrocytes. These results support the hypothesis that activation of phospholipase C and inhibition of adenylyl cyclase are mediated by different P_{2Y}-purinoceptors. The definitive answer to this question should come from molecular cloning of the receptors involved. The predicted amino acid sequence of a P_{2Y}-purinoceptor subtype has been reported recently (Webb *et al.*, 1993), and we have shown that this receptor couples to phospholipase C but not to adenylyl cyclase (Filtz *et al.*, 1994). Availability of the nucleotide sequence of the P_{2Y}-purinoceptor should facilitate the identification of new members of this family of receptors and the identification of their signalling mechanisms.

This work was supported by United States Public Health Service Grants GM 38213, GM 29563, and HL 32322. We gratefully acknowledge the help of Seon Kyung Judy Kim and John O'Tuel.

References

ARUNLAKSHANA, O. & SCHILD, H.O. (1959). Some quantitative uses of drug antagonists. *Br. J. Pharmacol. Chemother.*, **14**, 48–58.

BERRIE, C.P., HAWKINS, P.T., STEPHENS, L.R., HARDEN, T.K. & DOWNES, C.P. (1989). Phosphatidylinositol 4,5-bisphosphate hydrolysis in turkey erythrocytes is regulated by P_{2Y}-purinoceptors. *Mol. Pharmacol.*, **35**, 526–532.

BOYER, J.L., DOWNES, C.P. & HARDEN, T.K. (1989). Kinetics of activation of phospholipase C by P_2-purinergic receptor agonists and guanine nucleotides. *J. Biol. Chem.*, **264**, 884–890.

BOYER, J.L., LAZAROWSKI, E.R., CHEN, X.-H. & HARDEN, T.K. (1993). Identification of a P_{2Y}-purinergic receptor that inhibits adenylyl cyclase. *J. Pharmacol. Exp. Ther.*, **267**, 1140–1146.

BROWN, H.A., LAZAROWSKI, E.R., BOUCHER, R.C. & HARDEN, T.K. (1991). Evidence that UTP and ATP regulate phospholipase C through a common extracellular 5′ nucleotide receptor in airway epithelial cells. *Mol. Pharmacol.*, **40**, 648–655.

BURNSTOCK, G. (1978). A basis for distinguishing two types of purinergic receptors. In *Cell Membrane Receptors for Drugs and Hormones*, a Multidisciplinary Approach. ed. Staub R.W. & Bolis L. pp. 107–118. New York: Raven Press.

BURNSTOCK, G. & KENNEDY, C. (1985). Is there a basis for distinguishing two types of P_2-purinoceptors? *Gen. Pharmacol.*, **16**, 433–440.

BURNSTOCK, G., FISCHER, B., HOYLE, C.H.V., MAILLARD, M., ZINGASHIN, A.U., BRIZZOLARA, A.L., VON ISAKOVICS, A., BOYER, J.L., HARDEN, T.K. & JACOBSON, K.A. (1994). Structure activity relationship for derivatives of adenosine-5′-triphosphate as agonists at P_2 purinoceptors: heterogeneity within P_{2X} and P_{2Y} subtypes. *Drug Dev. Res.*, **31**, 206–219.

CHAREST, R., BLACKMORE, P.F. & EXTON, J.H. (1985). Characterization of responses of isolated hepatocytes to ATP and ADP. *J. Biol. Chem.*, **260**, 15789–15794.

CHOO, L.K. (1981). The effect of reactive blue, an antagonist of ATP, on the isolated urinary bladders of guinea-pig and rat. *J. Pharm. Pharmacol.*, **33**, 248–250.

CREMA, A., FRIGO, G.M., LECCHINI, S., MANZ, L., ONORI, L. & TONINI, M. (1983). Purine receptors in the guinea-pig internal anal sphincter. *Br. J. Pharmacol.*, **78**, 599–603.

DUBYAK, G.R., COWEN, D.S. & MUELLER, L.M. (1988). Activation of inositol phospholipid breakdown in HL60 cells by P_2-purinergic receptors for extracellular ATP. Evidence for mediation by both pertussis toxin-sensitive and pertussis toxin-insensitive mechanisms. *J. Biol. Chem.*, **263**, 18108–18117.

DUBYAK, G.R. & EL-MOTASSIM, C. (1993). Signal transduction via P_2-purinergic receptors for extracellular ATP and other nucleotides. *Am. J. Physiol.*, **34**, C577–C606.

DUNN, P. & BLAKELY, A.G.H. (1988). Suramin: a reversible P_2-purinoceptor antagonist in the mouse vas deferens. *Br. J. Pharmacol.*, **93**, 243–245.

FEDAN, J.S. & LAMPORT, S.J. (1990). P_2-purinoceptor antagonists. *Ann. N.Y. Acad. Sci.*, **603**, 182–197.

FLITZ, T.A., LI, Q., BOYER, J.L., NICHOLAS, R.A. & HRDEN, T.K. (1994). Expression of a cloned P_{2Y}-purinergic receptor that couples to phospholipase C. *Mol. Pharmacol.*, **46**, 8–14.

FINE, J., COLE, P. & DAVIDSON, J.S. (1989). Extracellular nucleotides stimulate receptor-mediated calcium mobilization and inositol phosphate production in human fibroblasts. *Biochem. J.*, **263**, 371–376.

FISCHER, B., BOYER, J.L., HOYLE, C.H.V., ZIGANSHIN, A.U., BRIZZOLARA, A.L., KNIGHT, G.E., ZIMMET, J., BURNSTOCK, G., HARDEN, T.K. & JACOBSON, K.A. (1993). Identification of potent, selective P_{2Y}-purinoceptor agonists: structure-activity relationships for 2-thioether derivatives of adenosine 5′-triphosphate. *J. Med. Chem.*, **36**, 3937–3946.

FORSBERG, E.J., FEBERSTEIN, G., SHOHAMI, E. & POLLARD, H.B. (1987). Adenosine triphosphate stimulates inositol phospholipid metabolism and prostacyclin formation in adrenal medullary endothelial cells by means of P_2-purinergic receptors. *Proc. Natl. Acad. Sci. U.S.A.*, **84**, 5630–5634.

FREDERICH, R.M., WALDO, G.L., HARDEN, T.K. & PERKINS, J.P. (1983). Characterization of agonist-induced β-adrenergic receptor-specific desensitization in C6-2B glioma cells. *J. Cyclic Nucleotide Res.*, **9**, 103–118.

GORDON, J.L. (1986). Extracellular ATP: effects, sources and fate. *Biochem. J.*, **233**, 309–319.

HARDEN, T.K., SCHEER, A.G. & SMITH, M.M. (1982). Differential modification of the interaction of cardiac muscarinic cholinergic and β-adrenergic receptors with guanine nucleotide binding site(s). *Mol. Pharmacol.*, **21**, 570–580.

HARDEN, T.K., HAWKINS, P.T., STEPHENS, L., BOYER, J.L. & DOWNES, C.P. (1988). Phosphoinositide hydrolysis of guanosine 5′-[γ-thio]triphosphate-activated phospholipase C of turkey erythrocyte membranes. *Biochem. J.*, **252**, 583–593.

HOYLE, C.H.V., KNIGHT, G.E. & BURNSTOCK, G. (1990). Suramin antagonizes responses to P_2-purinoceptor agonists and purinergic nerve stimulation in the guinea-pig urinary bladder and taenia coli. *Br. J. Pharmacol.*, **99**, 617–621.

LAMBRECHT, G., FRIEBE, T., GRIMM, U., WINDSCHEIF, U., BUNGARDT, E., HILDERBRANDT. C., BAUMERT, H., SPATZ-KUMBEL, G. & MUTSCHLER, E. (1992). PPADS, a novel functionally selective antagonist of P_2 purinoceptor-mediated responses. *Eur. J. Pharmacol.*, **271**, 217–219.

LEFF, P., WOOD, B.E. & O'CONNOR, S.E. (1990). Suramin is a slowly-equilibrating but competitive antagonist at P_{2X}-receptors in the rabbit isolated ear artery. *Br. J. Pharmacol.*, **101**, 645–649.

LIN, W.-W. & CHUANG, D.-M. (1993). Endothelin- and ATP-induced inhibition of adenylyl cyclase activity in C6 glioma cells: role of G_i and calcium. *Mol. Pharmacol.*, **44**, 158–165.

LONDOS, C., COOPER, D.M.F. & WOLFF, J. (1980). Subclasses of adenosine receptors. *Proc. Natl. Acad. Sci. U.S.A.*, **77**, 2551–2554.

MANZINI, S., HOYLE, C.H.V. & BURNSTOCK, G. (1986). An electrophysiological analysis of the effect of reactive blue 2, a putative P_2-purinergic receptor antagonist, on inhibitory junction potentials of rat cecum. *Eur. J. Pharmacol.*, **127**, 197–204.

MEEKER, R.B. & HARDEN, T.K. (1982). Muscarinic receptor-mediated activation of phosphodiesterase. *Mol. Pharmacol.*, **22**, 310–319.

MEYERHOF, W., MÜLLER-BRECHLIN, R. & RICHTER, D. (1991). Molecular cloning of a novel putative G-protein coupled receptor expressed during rat spermiogenesis. *FEBS Lett.*, **284**, 155–160.

O'CONNOR, S.E., DAINTY, I.A. & LEFF, P. (1991). Further subclassification of ATP receptors based on agonist studies. *Trends Pharmacol. Sci.*, **12**, 137–141.

OKAJIMA, F., KIOICHI, J.S., NAZAREA, M., SHO, K. & KONDO, Y. (1989). A permissive role of pertussis toxin substrate G-protein in P_2-purinergic stimulation of PI turnover and arachidonic acid release in FRTL-5 thyroid cells. *J. Biol. Chem.*, **264**, 13029–13037.

OKAJIMA, F., TOKUMITSU, Y., KONDO, Y. & UI, M. (1987). P_2-purinergic receptors are coupled to two signal transduction systems leading to inhibition of cAMP generation and to production of inositol triphosphate in rat hepatocytes. *J. Biol. Chem.*, **262**, 13483–13490.

PIANET, I., MERLE, M. & LABOUESSE, J. (1989). ADP and, indirectly, ATP are potent inhibitors of cAMP production in intact isoproterenol-stimulated C6 glioma cells. *Biochem. Biophys. Res. Commun.*, **163**, 1150–1157.

PIROTTON, S., RASPE, E., DEMOLLE, D., ERNEUX, C. & BOEYNAEMS, J.M. (1987). Involvement of inositol 1,4,5-triphosphate and calcium in the action of adenine nucleotides on aortic endothelial cells. *J. Biol. Chem.*, **262**, 17461–17466.

REILLY, W.M., SAVILLE, V.L. & BURNSTOCK, G. (1987). An assessment of the antagonistic activity of reactive blue 2 at P_1- and P_2-purinoceptors: supporting evidence for purinergic innervation of the rabbit portal vein. *Eur. J. Pharmacol.*, **140**, 47–53.

RICE, W.A. & SINGLETON, F.M. (1989). Reactive blue 2 selectively inhibits P_{2Y}-purinoceptor-stimulated surfactant phospholipid secretion from isolated alveolar type II cells. *Br. J. Pharmacol.*, **97**, 158–162.

ROONEY, T.A., HAGER, R. & THOMAS, A.P. (1991). β-Adrenergic receptor-mediated phospholipase C activation independent of cAMP formation in turkey erythrocyte membranes. *J. Biol. Chem.*, **266**, 15068–15074.

SATO, K., OKAJIMA, F. & KONDO, Y. (1992). Extracellular ATP stimulates three different receptor-signal transduction systems in FRTL-5 thyroid cells. *Biochem. J.*, **238**, 281–287.

SOLTOFF, S.P., MCMILLAN, M.K. & TALAMO, B.R. (1989). Coomassie brilliant blue G is a more potent antagonist of P_2 purinergic responses than reactive blue 2 (cibacron blue 3GA) in rat parotid acinar cells. *Biochem. Biophys. Res. Commun.*, **165**, 1279–1285.

STUTCHFIELD, J. & COCKCROFT, S. (1990). Undifferentiated HL-60 cells respond to extracellular ATP and UTP by stimulating phospholipase C activation and exocytosis. *FEBS Lett.*, **262**, 256–258.

VALEINS, H., MERLE, M. & LABOUESSE, J. (1992). Pre-steady state study of the β-adrenergic and purinergic receptor interaction in C6 cell membranes. *Mol. Pharmacol.*, **42**, 1033–1041.

VAN CALKER, D., MULLER, M. & HAMPRECHT, B. (1979). Adenosine regulates via two different types of receptors the accumulation of cyclic AMP in cultured brain cells. *J. Neurochem.*, **33**, 999–1005.

VAZIRI, C. & DOWNES, C.P. (1992). G-protein-mediated activation of turkey erythrocyte phospholipase C by β-adrenergic and P_{2Y}-purinergic receptors. *Biochem. J.*, **284**, 917–922.

VOOGD, T.E., VANSTERKENBURG, E.L.M., WILTING, J. & JANSSEN, L.H.M. (1993). Recent research on the biological activity of suramin. *Pharmacol. Rev.*, **45**, 177–203.

WEBB, T.E., SIMON, J., KRISHEK, B.J., BATESON, A.N., SMART, T.G., KING, B.F., BURNSTOCK, G. & BARNARD, E.A. (1993). Cloning and functional expression of a brain G-protein-coupled ATP receptor. *FEBS Lett.*, **324**, 219–225.

WILKINSON, G., PURKISS, J.R. & BOARDER, M.R. (1993). The regulation of aortic endothelial cells by purines and pyrimidines involves co-existing P_{2Y}-purinoceptors and nucleotide receptors linked to phospholipase C. *Br. J. Pharmacol.*, **108**, 689–693.

ZHOU, Q.-Y., LI, C., OLAH, M.E., JOHNSON, R.A., STILES, G.A. & CIVELLI, O. (1992). Molecular cloning and characterization of an adenosine receptor: the A_3 adenosine receptor. *Proc. Natl. Acad. Sci. U.S.A.*, **89**, 7432–7436.

ZIGANSHIN, A.U., HOYLE, C.H.V., BO, H., LAMBRECHT, G., MUTSCHLER, E., BÄUMERT, H.G. & BURNSTOCK, G. (1993). PPADS selectively antagonizes P_{2X}-purinoceptor-mediated responses in the rabbit urinary bladder. *Br. J. Pharmacol.*, **110**, 1491–1495.

(Received March 18, 1994
Revised May 27, 1994
Accepted June 6, 1994)

Br. J. Pharmacol. (1994), **113**, 621–627 © Macmillan Press Ltd, 1994

Muscarinic (M_1) receptor-mediated inhibition of K^+-evoked [^{3}H]-noradrenaline release from human neuroblastoma (SH-SY5Y) cells via inhibition of L- and N-type Ca^{2+} channels

R.L. McDonald, *P.F.T. Vaughan & [1]C. Peers

Departments of Pharmacology and *Cardiovascular Studies, University of Leeds, Leeds LS2 9JT

1 Human neuroblastoma (SH-SY5Y) cells were preincubated with [^{3}H]-noradrenaline ([^{3}H]-NA) in the presence of 0.2 mM pargyline to examine the modulation of K^+-evoked [^{3}H]-NA release by muscarinic agonists.

2 Release of [^{3}H]-NA evoked by 4 min exposure to 100 mM K^+ could be partially inhibited by 5 μM nifedipine and partially inhibited by 100 nM ω-conotoxin GVIA (ω-CgTx). When nifedipine and ω-CgTx were added together, evoked release was inhibited by approximately 93%.

3 K^+-evoked [^{3}H]-NA release was inhibited by >90% by pretreatment of cells for 2 min with muscarine, carbachol or oxotremorine methiodide (each at 300 μM). For muscarine, inhibition of evoked release was both time- and concentration-dependent and was reversible. Muscarine also inhibited [^{3}H]-NA release evoked by veratridine (28 μM) and replacement of extracellular Ca^{2+} with Ba^{2+}, but not that evoked by the Ca^{2+} ionophore, A23187 (19 μM).

4 Residual K^+-evoked [^{3}H]-NA release measured in the presence of either nifedipine (5 μM) or ω-CgTx (100 nM) was inhibited by muscarine with a similar potency as release evoked in the absence of either Ca^{2+} channel blocker. Pretreatment of cells for 16–24 h with pertussis toxin (200 ng ml^{-1}) did not affect K^+-evoked release *per se* or the ability of muscarine to inhibit such release.

5 Muscarinic inhibition of K^+-evoked [^{3}H]-NA release was potently antagonized by pirenzepine (pA_2 8.14) and by hexahydrosiladiphenidol (pA_2 9.03), suggesting the involvement of an M_1 receptor.

6 Our results demonstrate that 100 mM K^+-evoked release of [^{3}H]-NA from the human neuroblastoma is mediated by activation of both L- and N-type Ca^{2+} channels. Activation of muscarinic M_1 receptors can inhibit release via a pertussis toxin-insensitive mechanism which involves non-selective inhibition of L- and N-type Ca^{2+} channels.

Keywords: SH-SY5Y; calcium channels; noradrenaline release; muscarinic receptor; nifedipine; ω-conotoxin GVIA; pirenzepine; hexahydrosiladiphenidol

Introduction

Many transmitters and hormones regulate neuronal functioning by modifying the activity of voltage-gated Ca^{2+} channels (Tsien *et al.*, 1988; Anwyl, 1991; Swandulla *et al.*, 1991). These channels exert important influences on neuronal excitability and provide the pathway for Ca^{2+} influx which is required to stimulate neurotransmitter release. Numerous studies have used patch clamp techniques to demonstrate both inhibitory and stimulatory actions of neurotransmitters on neuronal Ca^{2+} channels (e.g. Anwyl, 1991; Caulfield *et al.*, 1992; Cox & Dunlap, 1992; Yang & Tsien, 1993), but for reasons of experimental ease or necessity, Ca^{2+} channels are often recorded from the cell soma rather than at neurotransmitter release sites (see for example Lipscombe *et al.*, 1989). Consequently, less direct information is available concerning the influence of Ca^{2+} channel regulation by transmitters and hormones on neurosecretion. It is apparent that in different neurones, different sub-types of Ca^{2+} channels mediate Ca^{2+} influx required to trigger neurosecretion: for example, in dorsal root ganglion cells, L-type (dihydropyridine-sensitive) Ca^{2+} channels mediate release of substance P (Perney *et al.*, 1986), and in neurohypophysial cells, both L-type and N-type Ca^{2+} channels can mediate neurosecretion (N-type being defined as ω-conotoxin GVIA (ω-CgTx)-sensitive; Nowycky, 1991). In sympathetic neurones, N-type is the dominant Ca^{2+} channel (Hirning *et al.*, 1988), but dihydropyridine agonists can enhance noradrenaline release (Perney *et al.*, 1986). In chromaffin cells, three types of Ca^{2+} channel (L-, N-, and ω-agatoxin-IVA-sensitive P-type) have been shown to influence catecholamine release to varying degrees, depending on the electrical parameters used to stimulate cells (Artalejo *et al.*, 1994).

In this study, we have used the clonal cell line SH-SY5Y to investigate the modulation of K^+-evoked [^{3}H]-noradrenaline ([^{3}H]-NA) release caused by activation of muscarinic receptors. SH-SY5Y cells are derived from human sympathetic tissue (Pahlman *et al.*, 1990) and retain the ability to release noradrenaline in response to a variety of stimuli (Murphy *et al.*, 1991a,b; Vaughan *et al.*, 1993a,b; McDonald *et al.*, 1994). Our results indicate that both L- and N-type Ca^{2+} channels mediate release of [^{3}H]-NA in response to raised $[K^+]_o$ and that activation of muscarinic M_1 receptors reduces evoked release by inhibition of both types of Ca^{2+} channel.

Methods

Culture of SH-SY5Y cells

The human neuroblastoma SH-SY5Y (kindly provided by Dr J. Beidler, Sloan-Kettering Institute for Cancer Research, Rye, New Jersey, U.S.A.) was cultured in a 1:1 mixture of Ham's F-12 and Eagle's minimal essential media containing nonessential amino acids supplemented with 10% foetal calf serum in a 98% air, 2% CO_2 humidified incubator at 37°C. When confluent, cell layers were harvested by incubation at 37°C for 10 min in Ca^{2+} and Mg^{2+}-free phosphate-buffered saline (PBS) in the absence of trypsin, to select against possible contamination of epitheloid SH-EP cells (Ciccarone *et al.*, 1989; Ogino & Costa, 1992). The cell suspension was

[1] Author for correspondence.

triturated by 3 passes through a 0.8 mm guage needle, and cell number was estimated with a Coulter Counter. Cells were then subcultured in 24-well plates at a seeding density of 10^5 cells ml^{-1}, 0.4 ml being added to each plate.

[^{3}H]-noradrenaline release assays

Release of [^{3}H]-NA was measured after 4–5 days in subculture using previously described methodology (Murphy *et al.*, 1991b; Vaughan *et al.*, 1993a). In brief, culture medium was removed from the 24-well plates and cell monolayers were washed twice with PBS. To each well was then added 0.4 ml of HEPES-buffered saline (HBS) of composition (in mM): NaCl 135, KCl 5, $MgCl_2$ 0.6, $CaCl_2$ 2.5, HEPES 10, glucose 6, pargyline 0.2, ascorbic acid 0.2 (pH 7.4) containing 40 nM [^{3}H]-NA. After incubation for 1 h at 37°C, unaccumulated [^{3}H]-NA was removed by 4 consecutive washes with 0.4 ml aliquots of HBS, each applied to cells for 10 min. Cell layers were preincubated with 0.4 ml HBS alone or containing muscarine, carbachol or other drugs for the times indicated in the relevant figures. These solutions were then replaced with 100 mM K^+-containing solutions to evoke [^{3}H]-NA release (which contained the same concentration of drugs used during the preincubation period) and incubations continued for 4 min. In solutions of high K^+ concentration (100 mM) the Na^+ concentration was reduced correspondingly to maintain isoosmolarity. Unreleased [^{3}H]-NA was extracted with 0.4 M perchloric acid and the amount of [^{3}H]-NA released during a 4 min incubation in 100 mM K^+-containing solutions in a given experiment was expressed as a percentage of the total amount of radioactivity in the cell layer at the beginning of the incubation period.

For some experiments, cells were pretreated for 16–24 h with pertussis toxin (PTX). PTX was added to culture medium from a 50% glycerol stock solution of 50 $\mu g\ ml^{-1}$ to give a final concentration of 200 $ng\ ml^{-1}$. In these studies, control cells were treated with the same volume of an identical solution, but lacking the PTX.

Drugs used were muscarine chloride, carbachol chloride, oxotremorine methiodide, atropine sulphate, pirenzepine dihydrochloride, hexahydrosiladiphenidol hydrochloride (HHSiD), nifedipine, veratridine, A23187, yohimbine hydrochloride (from Sigma Chemical Co., Poole, Dorset) and omega-conotoxin GVIA (ω-CgTx; from Calbiochem, Nottingham). To examine the effects of these drugs on [^{3}H]-NA release from SH-SY5Y cells evoked by solutions of raised $[K^+]_o$, drugs were added to the cells at varying periods (30 s to 8 min) before exposure to high $[K^+]$ solutions, and were also usually present in the solution of high $[K^+]$. Cells were always exposed to high $[K^+]$ solutions for 4 min. Since application times varied according to each experiment, further details are given in the Results section and figure legends. All results are expressed as means ± standard error of the mean (s.e.mean), taken from the number of experiments indicated. One experiment constitutes the mean of results obtained from two culture dishes i.e. experiments were always performed in duplicate. Statistical comparisons were made as indicated in the Results using the unpaired Student's *t* test.

Results

K^+-evoked [^{3}H]-NA release is coupled to L- and N-type Ca^{2+} channels

Figure 1 shows that raising extracellular $[K^+]$ from 5 mM to 100 mM evoked [^{3}H]-NA release from SH-SY5Y cells, as previously described (Murphy *et al.*, 1991a,b). In the presence of the L-type Ca^{2+} channel blocker, nifedipine (which was applied 8 min before the 100 mM K^+ solution), at a supramaximal but selective concentration (Reeve *et al.*, 1994) of 5 μM, K^+-evoked release was reduced by approximately 76%. The N-type Ca^{2+} channel blocker ω-CgTx

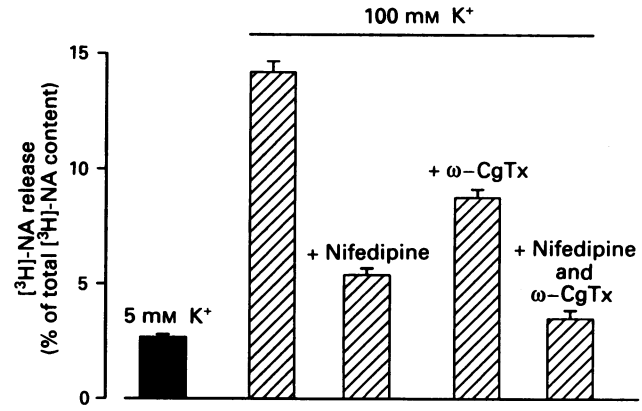


Figure 1 Release of [^{3}H]-noradrenaline ([^{3}H]-NA) from SH-SY5Y cells, expressed as mean (± s.e.mean, taken from 4 experiments in each case) percentage of total radioactivity taken up by cell monolayers (see Methods). Release determined in the presence of 5 mM K^+ represents basal release, and in all subsequent figures basal release has been subtracted. Nifedipine was added at a concentration of 5 μM, for 8 min prior to exposure to 100 mM K^+-containing solutions. ω-Conotoxin GVIA (ω-CgTx) was applied at 100 mM for 20 min prior to exposure to 100 mM K^+-containing solutions. Both blockers were also present during the 4 min exposure to 100 mM K^+-containing solutions.

(applied 20 min prior to the 100 mM K^+ solution) also inhibited evoked [^{3}H]-NA release, by approximately 47%. In the presence of both blockers, K^+-evoked [^{3}H]-NA release was reduced by over 90% (Figure 1). These data indicate that K^+-evoked release involves Ca^{2+} influx through both dihydropyridine-sensitive L-type and ω-CgTx-sensitive N-type Ca^{2+} channels in SH-SY5Y cells. It is conceivable that removal of Na^+ (which is required to maintain isoosmolarity in solutions of high K^+ concentration) might in itself evoke release, for example by reversal of Na-Ca exchange. However, such a possibility is not likely to cause a large effect on release since release was almost fully inhibited by blockers of voltage-gated Ca^{2+} channels. The inhibitory actions of the Ca^{2+} channel blockers, applied alone or together, were highly statistically significant ($P < 0.0001$).

Muscarine inhibits K^+-evoked [^{3}H]-NA release

Exposure of SH-SY5Y cells to muscarine inhibited 100 mM K^+-evoked [^{3}H]-NA release from SH-SY5Y cells in a time- and concentration-dependent manner (Figure 2). When muscarine was applied to cells simultaneously with the high $[K^+]$-containing solutions, inhibition of evoked release was only seen at concentrations > 30 μM, and appeared to saturate at approximately 25% inhibition with 300 μM muscarine (□, Figure 2a). By contrast, if cells were exposed to muscarine for 2 min prior to application of 100 mM K^+ (and muscarine was also present in the 100 mM K^+-containing solution), release could be inhibited by up to 90–95%, with an IC_{50} of 3 μM (●, Figure 2a) as determined by eye from the data shown. This inhibition-response curve was shifted further to the left (i.e. to lower muscarine concentrations) when cells were pretreated for 4 min prior to application of 100 mM K^+ (IC_{50} 0.5 μM, ○, Figure 2a). The (■) symbols of Figure 2a show that exposure of cells to 100 nM atropine 8 min prior to muscarine exposure completely abolished the inhibition of K^+-evoked release caused by 2 min pretreatment with muscarine. We also observed inhibition of K^+-evoked [^{3}H]-NA release with carbachol (300 μM causing 88.5 ± 0.8% inhibition, $n = 4$ experiments) and oxotremorine methiodide (300 μM causing 92.4 ± 0.3% inhibition, $n = 4$). Again, these agonists were present 2 min prior to, and during the 4 min exposure to 100 mM K^+. Muscarinic agonists can themselves evoke [^{3}H]-NA release from SH-SY5Y cells via

activation of M_3 receptors (Murphy *et al.*, 1991b), and so it was conceivable that the small release of [^{3}H]-NA evoked by pretreatment of cells with muscarine (0.30 ± 0.15% above basal release in the present studies, $n = 7$) could act to inhibit K^+-evoked release by stimulating α_2 receptors and hence inhibiting Ca^{2+} channels coupled to noradrenaline release. However, the ability of muscarine to inhibit K^+-evoked release was not significantly affected by the α_2 antagonist, yohimbine: in a series of 4 experiments conducted in parallel, muscarine (applied 4 min prior to, and during, 100 mM K^+ application) inhibited K^+-evoked release by 38.9 ± 0.6% and 89.3 ± 0.5% at concentrations of 0.3 μM and 30 μM respectively. In the presence of 1 μM yohimbine (added 8 min prior to, and during, 100 mM K^+ application) release was inhibited by 36.6 ± 0.2% and 90.5 ± 0.5% by these concentrations of muscarine. Yohimbine alone did not affect release during the 8 min exposure in the presence of 5 mM K^+.

The time-dependence of muscarine inhibition of K^+-evoked release was studied in greater detail using two muscarine concentrations of 0.3 and 30 μM (Figure 2b). At the higher concentration, muscarine rapidly inhibited K^+-evoked release of [^{3}H]-NA, and reached a plateau level of 90–95% within 2–4 min. At the lower concentration, muscarine inhibition developed more slowly and appeared to approach a lower plateau level of approximately 50%. To investigate the reversibility of muscarine's action, we examined the release of [^{3}H]-NA evoked by 100 mM K^+ in cells which were exposed to muscarine for 2 min and then repeatedly washed in muscarine-free solution for 4 min prior to application of 100 mM K^+ solutions. In cells treated this way, K^+ evoked release of 12.5 ± 0.3% of the total cellular ^{3}H content ($n = 3$). This value represents 87.4 ± 0.4% of release seen in cells which were never exposed to muscarine but were simply repeatedly washed before exposure to 100 mM K^+, which released 14.3 ± 0.7% of total content ($n = 3$). This contrasts with the marked suppression of release evoked in the continued presence of muscarine (Figure 2) and indicates that the actions of muscarine were largely reversible.

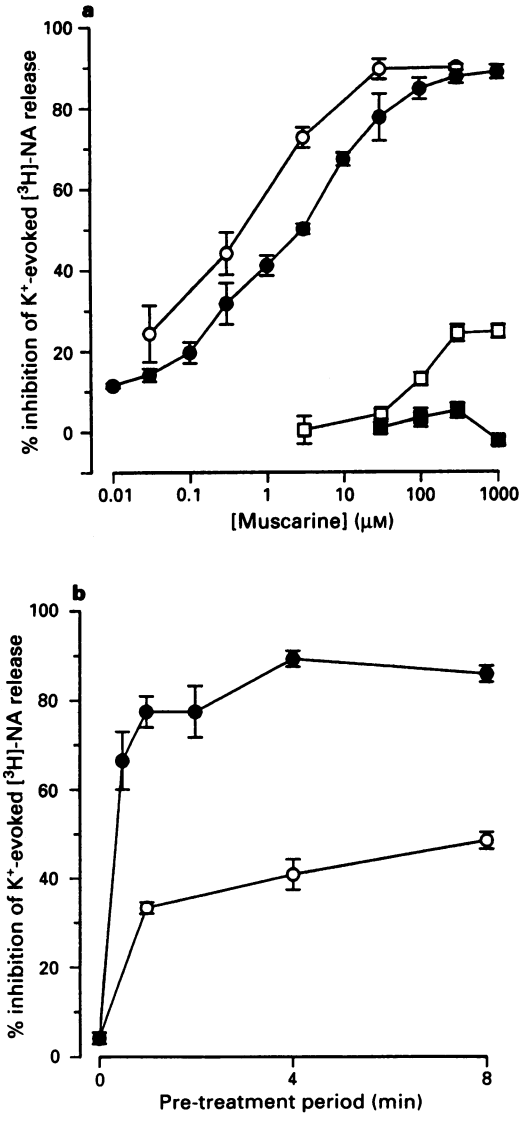


Figure 2 Inhibition of K^+-evoked [^{3}H]-noradrenaline ([^{3}H]-NA) release by muscarine: (a) percentage inhibition of 100 mM K^+-evoked release by muscarine added simultaneously with 100 mM K^+ (□) or 2 min (●) or 4 min (○) prior to application of 100 mM K^+. Muscarine was also always present during the 4 min exposure to 100 mM K^+. Atropine (100 nM), added for 8 min prior to (and during) 100 mM K^+ exposure, abolished the inhibition of evoked release caused by 2 min pretreatment with muscarine (■). (b) Time course of inhibition of K^+-evoked release by muscarine at 0.3 μM (○) and 30 μM (●), applied for varying periods before application of 100 mM K^+ as indicated (muscarine was also present during the 4 min exposure to 100 mM K^+-containing solutions). Points plotted in (a) and (b) are means with s.e.mean taken from 4 to 14 experiments in each case.

Muscarinic inhibition of [^{3}H]-NA release occurs via pertussis toxin-insensitive block of L- and N-type Ca^{2+} channels

Muscarinic agonists are known to inhibit neuronal Ca^{2+} channels (see Introduction), and given that K^+-evoked [^{3}H]-NA release in SH-SY5Y cells is mediated via L- and N-type Ca^{2+} channels (Figure 1) it seemed likely that muscarine acted to inhibit evoked release via inhibition of Ca^{2+} channels. To examine this possibility, we investigated the ability of muscarine to inhibit [^{3}H]-NA release evoked by other stimuli. We have previously shown that Ba^{2+} evokes release in these cells via depolarization and Ca^{2+} influx through voltage-gated Ca^{2+} channels (Vaughan *et al.*, 1993b). Figure 3 shows that release evoked by substitution of extracellular Ca^{2+} with Ba^{2+} (2.5 mM) for 4 min, and also by 4 min exposure to 28 μM veratridine (another commonly used depolarizing secretagogue) can be inhibited to similar degrees as K^+-evoked release with 300 μM muscarine. By contrast, release evoked by 4 min exposure to the Ca^{2+} ionophore, A23187 (19 μM), which still involves Ca^{2+} influx but not via

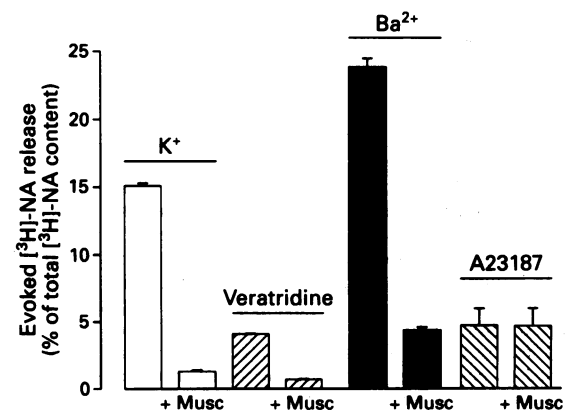


Figure 3 Release of [^{3}H]-noradrenaline ([^{3}H]-NA) (expressed as percentage of total cellular ^{3}H content; mean values ± s.e.mean, taken from 3 to 5 experiments in each case, basal release subtracted) from SH-SY5Y cells evoked by 4 min exposures to 100 mM K^+, 28 μM veratridine, replacement of extracellular Ca^{2+} with Ba^{2+} (2.5 mM) and 19 μM A23187 as indicated, in the absence or presence (+ Musc) of 300 μM muscarine (applied 2 min prior to stimulus and present during the 4 min period of exposure to the stimulus), as indicated. Note lack of effect of muscarine on A23187-evoked release.

voltage-gated Ca^{2+} channels, was unaffected by pretreatment of cells with muscarine (Figure 3). For all studies shown in Figure 3, 300 μM muscarine was added to cells 2 min prior to each stimulus, and was also present during the 2 min exposure to the stimulus. These data indicate that muscarine inhibits depolarization-mediated release via inhibition of Ca^{2+} channels.

Figure 4 indicates that muscarinic inhibition of K^+-evoked [^{3}H]-NA release involves non-selective inhibition of both L-type and N-type Ca^{2+} channels. In the presence of nifedipine (5 μM, applied for 8 min prior to and also during exposure to 100 mM K^+ solutions), residual, ω-CgTx sensitive release can be inhibited by 300 μM muscarine and, conversely, residual, nifedipine-sensitive release evoked in the presence of 100 nM ω-CgTx (applied for 8 min prior to and also during exposure to 100 mM K^+ solutions) was also inhibited (Figure 4a).

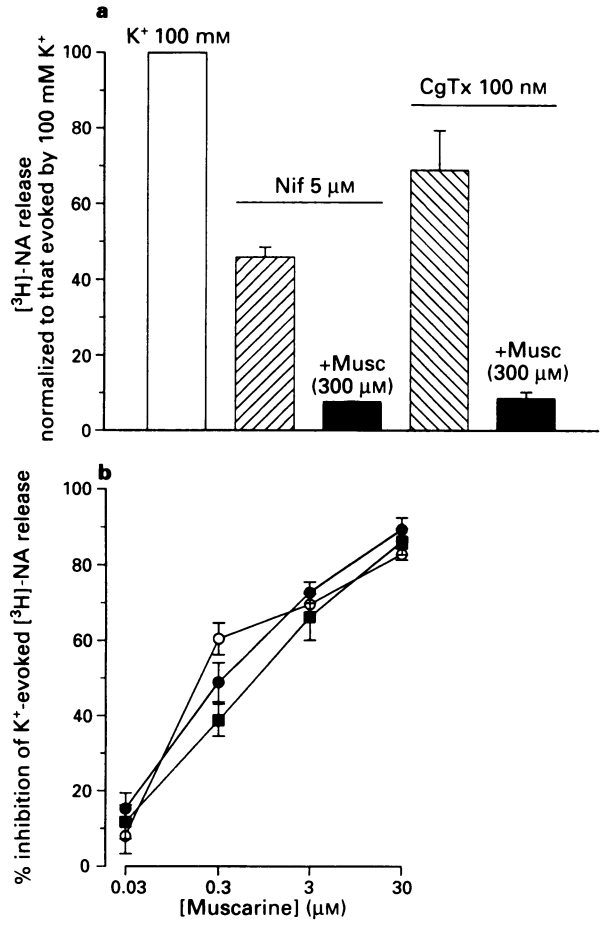


Figure 4 (a) Release of [^{3}H]-noradrenaline ([^{3}H]-NA) (means ± s.e.mean, taken from 3 experiments in each case) caused by a 4 min exposure to 100 mM K^+ in the presence of 5 μM nifedipine (Nif) or 100 nM ω-conotoxin GVIA (ω-CgTx) from untreated cells (hatched columns) or cells pretreated for 4 min with 300 μM muscarine prior to and during application of 100 mM K^+ (solid columns). Nifedipine and ω-CgTx were applied for 8 min prior to (and during) exposure to 100 mM K^+-containing solutions. Release is expressed as percentage of release measured in the absence of muscarine, nifedipine or ω-CgTx, taken as 100% (open column). Actual release was 16.6 ± 0.7% of total cellular ^{3}H content in the absence of muscarine or Ca^{2+} channel blockers. (b) Percentage inhibition of K^+-evoked [^{3}H]-NA release caused by muscarine. Release was measured in the presence of 5 μM nifedipine (○), 100 nM ω-CgTx (■) or in the absence of Ca^{2+} channel blockers (●). Nifedipine, ω-CgTx and muscarine were applied for the same time periods as in (a). In each of these 3 cases, release was normalized to 100% in the absence of muscarine, and each point plotted is a mean (with s.e.mean) taken from 3 to 5 experiments. No significant differences were found between the 3 conditions at any muscarine concentration studied.

Although ω-CgTx was applied for less time than in the experiments shown in Figure 1, the degree of inhibition of release it caused was not significantly affected. If release in the presence of either Ca^{2+} channel blocker is normalized to 100% in the absence of muscarine (Figure 4b), it can be seen that muscarine inhibits release mediated by L-type and N-type Ca^{2+} channels with similar potency, and release in the presence of either Ca^{2+} channel blocker is similarly sensitive to muscarine as in the absence of either. Thus muscarine is non-selective in its ability to inhibit 100 mM K^+-evoked release via Ca^{2+} influx through L-type or N-type Ca^{2+} channels.

To investigate whether muscarine inhibited Ca^{2+} channels via a pertussis toxin- (PTX-) sensitive G-protein, we investigated the effects of muscarine in inhibiting K^+-evoked [^{3}H]-NA release in cells pretreated for 16–24 h with 200 ng ml^{-1} PTX. Such pretreatment did not affect the inhibitory action of muscarine: for example, in 4 experiments conducted in parallel, 30 μM muscarine inhibited K^+-evoked release by 89.4 ± 2.0% in untreated cells, and in PTX-treated cells the same concentration inhibited release by 90.8 ± 2.1%. These findings suggest that the actions of muscarine are not mediated by PTX-sensitive G-proteins.

Muscarine acts at M_1 receptors to inhibit K^+-evoked [^{3}H]-NA release

SH-SY5Y cells are known to express muscarinic M_1, M_2 and M_3 receptors. To examine whether the inhibition of K^+-evoked release by muscarine is coupled to a specific muscarinic sub-type, we tested the effects of two muscarinic receptor antagonists, pirenzepine and HHSiD. Figure 5a plots the inhibitory effects of muscarine on K^+-evoked [^{3}H]-NA release in the absence and presence of three concentrations of pirenzepine. Pirenzepine was added 4 min prior to muscarine, then both drugs were incubated with the cells for 4 min prior to addition of 100 mM K^+. Both drugs were also present during the 4 min exposure to 100 mM K^+. From these data, a Schild plot was obtained (Figure 5b) which yielded a pA_2 value for pirenzepine of 8.14. Thus pirenzepine acted as a potent antagonist at the receptors mediating the effects of muscarine on K^+-evoked [^{3}H]-NA release, suggesting that the receptors involved were of the M_1 or M_4 subtype (see Discussion). Figure 5c plots the effects of three concentrations of HHSiD (applied as described above for pirenzepine) on the actions of muscarine to reduce K^+-evoked release, and from these results a Schild plot was obtained (Figure 5d) which yielded a pA_2 of 9.03 for HHSiD. Since HHSiD has been shown to be a potent antagonist at M_1 and M_3 receptors (Lambrecht *et al.*, 1988; Richards, 1991), and pirenzepine was also found to be potent in the current studies, the results presented in Figure 5 suggest that muscarinic inhibition of K^+-evoked [^{3}H]-NA release is mediated by M_1 receptors. Neither pirenzepine nor HHSiD altered basal [^{3}H]-NA release in the presence of 5 mM K^+.

Discussion

Raised extracellular K^+ concentrations can stimulate release of [^{3}H]-NA from SH-SY5Y cells via depolarization and the consequent activation of voltage-gated Ca^{2+} channels. This in agreement with previous reports (Murphy *et al.*, 1991a,b) and the present study indicates that both L-type and N-type Ca^{2+} channels are involved in this release mechanism, since 100 mM K^+-evoked release was sensitive to both nifedipine and ω-CgTx (Figure 1). These channels account for the whole-cell Ca^{2+} channel current seen in electrophysiological studies (Kennedy & Henderson, 1992; Reuveney & Narahashi, 1993; Reeve *et al.*, 1994). Muscarinic agonists inhibited 100 mM K^+-evoked release in a time- and concentration-dependent manner (Figure 2) that can be attributed to a mechanism involving inhibition of both L- and N-type Ca^{2+}

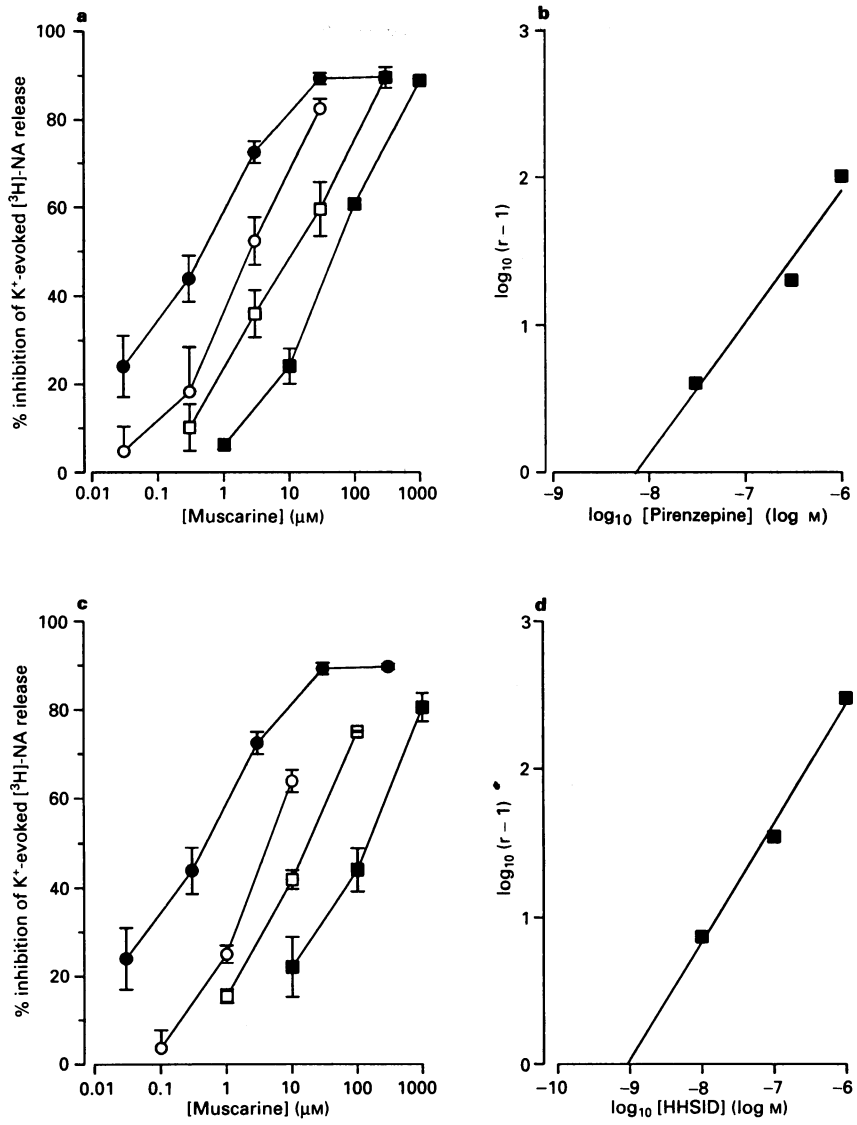


Figure 5 (a) Percentage inhibition of K^+-evoked [^{3}H]-noradrenaline ([^{3}H]-NA) release measured in cells pretreated with muscarine for 4 min in the absence of pirenzepine (●) and in the presence of 30 nM (○), 300 nM (□) and 1 μM (■) pirenzepine (pirenzepine was added for 4 min prior to application of muscarine). Cells were then incubated in the presence of muscarine and pirenzepine for 4 min prior to exposure to 100 mM K^+, and both drugs were also present during 4 min exposure to 100 mM K^+-containing solutions. (b) Schild plot obtained from data in (a), taking dose-ratios (r) at 50% inhibition. Values were determined by eye from the data shown in (a). The line was fitted by linear regression ($r^2 = 0.97$) and has a slope of 0.89. Intercept gives a pA_2 value of 8.14. (c) Percentage inhibition of K^+-evoked [^{3}H]-NA release measured in cells pretreated with muscarine for 4 min in the absence of hexahydrosiladiphenidol (HHSiD; ●) and in the presence of 10 nM (○), 100 nM (□) and 1 μM (■) HHSiD (in each case added for 4 min prior to application of muscarine; protocols were exactly as for pirenzepine, in a). (d) Schild plot obtained from data in (c), taking dose-ratios (r) at 50% inhibition. The line fitting the data by linear regression ($r^2 = 0.99$) has a slope of 0.80. Intercept gives a pA_2 value of 9.03. Each plotted point in (a) and (c) is the mean (± s.e.mean) taken from 3 to 5 experiments in each case.

channels: release evoked by Ba^{2+} which, like K^+ and veratridine, stimulates release via depolarization and consequent Ca^{2+} entry (Vaughan *et al.*, 1903b) was also strongly inhibited by muscarine, whereas release evoked by the Ca^{2+} ionophore, A23187 (which effectively bypasses Ca^{2+} channels to allow Ca^{2+} entry) was unaffected by muscarine (Figure 3).

Exposure of cells to either nifedipine or ω-CgTx caused partial inhibition of K^+-evoked [^{3}H]-NA release (Figure 1) which was always less than the maximal inhibition of release caused by muscarine. Residual release of [^{3}H]-NA measured in the presence of either nifedipine or ω-CgTx could also be inhibited by muscarine (Figure 4), indicating that the inhibition of Ca^{2+} channels by muscarine was non-selective i.e. muscarine could inhibit Ca^{2+} influx through both L- and N-type Ca^{2+} channels. Furthermore, the sensitivity to inhibition by muscarine was similar for the two channel types (Figure 4b).

The lack of effect of PTX on muscarinic inhibition of K^+-evoked release is unlikely to be due to the fact that muscarine acts via a pathway that does not involve G proteins, since all known muscarinic receptors are believed to be G protein-coupled. Instead, muscarine could be acting via a PTX-insensitive G protein, and in this respect it is noteworthy that the G protein subunit $G_z\alpha$ has recently been identified in SH-SY5Y cells (Ammer & Schulz, 1994). This subunit is classified as belonging to the G_i family of G proteins but is known to be insensitive to PTX (Hepler & Gilman, 1992). We can discount the possibility that PTX was for some reason ineffective on SH-SY5Y cells since in other parallel studies conducted in our laboratory, SH-SY5Y cells were treated with the same batch of PTX in an identical manner, and such pretreatment inhibited the suppressive actions of neuropeptide Y (NPY) on Ca^{2+} channel currents recorded with the patch-clamp technique (see Reeve *et al.*,

1994, for recording details): 100 nM NPY caused 36.5 ± 5.1% inhibition of peak inward Ca^{2+} channel currents in 8 cells which were not exposed to PTX, but this inhibitory action of 100 nM NPY was significantly reduced ($P<0.02$) to 16.8 ± 5.6% in 7 cells pretreated with 200 ng ml^{-1} PTX for 16–24 h.

SH-SY5Y cells have been shown to express M_1, M_2 and M_3 receptors (Adem *et al.*, 1987; Serra *et al.*, 1988; Lambert *et al.*, 1989; Mei *et al.*, 1989; Cioffi & Fisher, 1990; Murphy *et al.*, 1991b). Our observation that pirenzepine potently antagonized the actions of muscarine suggested that muscarine acted via a M_1 or M_4 receptor (e.g. Richards, 1991). We were able to discriminate between these two receptor types by finding that HHSiD was also a potent muscarinic antagonist in our cells: HHSiD has previously been shown to act potently at M_1 and M_3 receptors (Lambrecht *et al.*, 1988), but is a poor antagonist at M_4 receptors. Thus the muscarinic receptor mediating inhibition of K^+-evoked [^{3}H]-NA release from SH-SY5Y cells appeared to be the M_1 type.

Different presynaptic muscarinic receptor subtypes have been shown to be coupled to modulation of noradrenaline release from sympathetic nerves. For example, Costa & Majewski (1991) demonstrated inhibitory M_2 and facilitatory M_1 receptors in atrial sympathetic nerves. Facilitatory M_1 receptors have also been reported in sympathetic nerves innervating blood vessels (Casado *et al.*, 1992). By contrast, in a series of studies, Hille and colleagues described two distinct pathways by which a muscarinic agonist inhibits Ca^{2+} currents in rat sympathetic neurones (Beech *et al.*, 1991; Bernheim *et al.*, 1991; Mathie *et al.*, 1992). One pathway was rapid, mediated by M_4 receptors, blocked by PTX treatment of cells and caused selective inhibition of N-type Ca^{2+} channels. The second pathway, mediated by M_1 receptors, was slower, insensitive to PTX treatment, involved an unidentified diffusible second messenger and caused non-selective inhibition of both L- and N-type channels. Features of this second pathway (namely M_1 receptor-mediation, PTX-insensitivity, non-selective inhibition of L- and N-type Ca^{2+} channels) are remarkably similar to the data presented here, and we would suggest that the results described by those workers can account for the effects of muscarine on K^+-evoked [^{3}H]-NA release in SH-SY5Y cells. Unfortunately, it is at present impossible to compare these findings further: the second messenger involved in M_1 receptor-mediated non-selective inhibition of L- and N-type channels was not identified despite detailed investigations (Bernheim *et al.*, 1991). Ca^{2+} channel inhibition was reduced by intracellular Ca^{2+} buffers (Beech *et al.*, 1991), but we are unable to test whether Ca^{2+} buffering alters muscarinic inhibition of noradrenaline release since exposure of SH-SY5Y cells to membrane permeable Ca^{2+} buffers is likely in itself to inhibit K^+-evoked release. Nevertheless, as far as we can determine, our results are likely to occur as a consequence of Ca^{2+} channel inhibition as described earlier (Beech *et al.*, 1991; Bernheim *et al.*, 1991). Our results do not provide evidence that a fast, PTX-sensitive pathway for muscarinic receptor inhibition is involved in the suppression of K^+-evoked neurosecretion. However, we cannot at present discount such a possible mechanism in our cells. Furthermore, it must be remembered that the contribution of Ca^{2+} channel sub-types to the regulation of neurotransmitter release and therefore the importance of selective regulation of Ca^{2+} channel sub-types, depends critically on the nature and intensity of the stimulus (Artalejo *et al.*, 1994).

The support of The British Heart Foundation is gratefully acknowledged.

References

ADEM, M.A., MATTSSON, M.E., NORDBERG, A. & PAHLMAN, S. (1987). Muscarinic receptors in human SH-SY5Y neuroblastoma cell line: regulation by phorbol ester and retinoic acid. *Brain Res.*, **430**, 235–242.

AMMER, H. & SCHULZ, R. (1994). Retinoic acid-induced differentiation of human neuroblastoma SH-SY5Y cells is associated with changes in the abundance of G proteins. *J. Neurochem.*, **62**, 1310–1318.

ANWYL, R. (1991). Modulation of vertebrate calcium channels by neurotransmitters. *Brain Res. Rev.*, **16**, 265–281.

ARTALEJO, C.R., ADAMS, M.E. & FOX, A.P. (1994). Three types of Ca^{2+} channel trigger secretion with different efficacies in chromaffin cells. *Nature*, **367**, 72–76.

BEECH, D.J., BERNHEIM, L., MATHIE, A. & HILLE, B. (1991). Intracellular Ca^{2+} buffers disrupt muscarinic suppression of Ca^{2+} current and M current in rat sympathetic neurones. *Proc. Natl. Acad. Sci. U.S.A.*, **88**, 652–656.

BERNHEIM, L., BEECH, D.J. & HILLE, B. (1991). A diffusable second messenger mediates one of the pathways coupling receptors to calcium channels in rat sympathetic neurons. *Neuron*, **6**, 859–867.

CASADO, M.A., MARIN, J. & SALAICES, M. (1992). Evidence for M_1 muscarinic cholinoceptors mediating facilitation of noradrenaline release in guinea-pig carotid artery. *Naunyn-Schmied. Arch. Pharmacol.*, **346**, 391–394.

CAULFIELD, M.P., ROBBINS, J. & BROWN, D.A. (1992). Neurotransmitters inhibit the omega-conotoxin-sensitive component of Ca current in neuroblastoma x glioma hybrid (NG 108 15) cells, not the nifedipine-sensitive component. *Pflügers Arch.*, **420**, 486–492.

CICCARONE, V., SPENGLER, B.A., MEYERS, M.B., BEIDLER, J.L. & ROSS, R.A. (1989). Phenotypic diversification in human neuroblastoma cells: expression of distinct neural crest lineages. *Cancer Res.*, **49**, 219–225.

CIOFFI, C.L. & FISHER, S.K. (1990). Reduction of muscarinic receptor density and guanine nucleotide-stimulated phosphoinositide hydrolysis in human SH-SY5Y neuroblastoma cells following long term treatment with 12-O-teradecanoylphorbol 13-acetate or mezerein. *J. Neurochem.*, **54**, 1725–1734.

COSTA, M. & MAJEWSKI, H. (1991). Evidence for facilitatory and inhibitory muscarinic receptors on postganglionic sympathetic nerves in mouse isolated atria. *Br. J. Pharmacol.*, **102**, 855–860.

COX, D.H. & DUNLAP, K. (1992). Pharmacological discrimination of N-type from L-type calcium current and its selective modulation by transmitters. *J. Neurosci.*, **12**, 906–914.

HEPLER, J.R. & GILMAN, A.G. (1992). G proteins. *Trends Biochem. Sci.*, **17**, 383–387.

HIRNING, L.D., FOX, A.P., MCCLESKEY, E.W., OLIVERA, B.M., THAYER, S.A., MILLER, R.J. & TSIEN, R.W. (1988). Dominant role of N-type Ca^{2+} channels in evoked release of norepinephrine from sympathetic neurons. *Science*, **239**, 57–60.

KENNEDY, C. & HENDERSON, G. (1992). Chronic exposure to morphine does not induce dependence at the level of the calcium channel current in human SH-SY5Y cells. *Neuroscience*, **49**, 937–944.

LAMBERT, D.G., GHATAORRE, A.S. & NAHORSKI, S.R. (1989). Muscarinic receptor binding characteristics of a human neuroblastoma SK-N-SH and its clones SH-SY5Y and SH-EP1. *Eur. J. Pharmacol.*, **165**, 71–77.

LAMBRECHT, G., FEIFEL, R., FORTH, B., STROHMANN, C., TACKE, R. & MUTSCHLER, E. (1988). p-Fluoro-hexahydro-sila-difenidol: the first $M_{2\beta}$-selective muscarinic agonist. *Eur. J. Pharmacol.*, **152**, 193–194.

LIPSCOMBE, D., KONGSAMUT, S. & TSIEN, R.W. (1989). α-adrenergic inhibition of sympathetic neurotransmitter release mediated by modulation of N-type calcium channel gating. *Nature*, **340**, 639–642.

MATHIE, A., BERNHEIM, L. & HILLE, B. (1992). Inhibtion of N- and L-type calcium channels by muscarinic receptor activation in rat sympathetic neurons. *Neuron*, **8**, 907–914.

MCDONALD, R.L., KAYE, D.F., REEVE, H.L., BALL, S.G., PEERS, C. & VAUGHAN, P.F.T. (1994). Bradykinin-evoked release of [^{3}H] noradrenaline from the human neuroblastoma SH-SY5Y. *Biochem. Pharmacol.*, **48**, 23–30.

MEI, L., ROESKE, W.R. & YAMAMURA, H.I. (1989). The coupling of muscarinic receptors to hydrolysis of inositol lipids in human neuroblastoma SH-SY5Y cells. *Brain Res.*, **504**, 7–14.

MURPHY, N.P., BALL, S.G. & VAUGHAN, P.F.T. (1991a). The effect of calcium channel antagonists on the release of [^{3}H]noradrenaline in the human neuroblastoma, SH-SY5Y. *Neurosci. Lett.*, **129**, 229–232.

MURPHY, N.P., BALL, S.G. & VAUGHAN, P.F.T. (1991b). Potassium and carbachol evoked release of [^{3}H]noradrenaline release from human neuroblastoma cells, SH-SY5Y. *J. Neurochem.*, **56**, 1810–1815.

NOWYCKY, M.C. (1991). Two high-threshold Ca^{2+} channels contribute Ca^{2+} for depolarization-secretion coupling in the mammalian neurohypophysis. *Ann. N.Y. Acad. Sci.*, **635**, 45–57.

OGINO, Y. & COSTA, T. (1992). The epithelial phenotype of human neuroblastoma cells express bradykinin, endothelin and angiotensin II receptors that stimulate phosphoinositide hydrolysis. *J. Neurochem.*, **58**, 46–56.

PAHLMAN, S., MAMEVA, S., MEYERSON, G., MATTSONN, M.E.K., BJELFMAN, C., ORTOFT, E. & HAMMERLING, U. (1990). Human neuroblastoma cells in culture: a model for neuronal cell differentiation and function. *Acta Physiol. Scand.*, **592**, 25–37.

PERNEY, T.M., HIRNING, L.D., LEEMAN, S.E. & MILLER, R.J. (1986). Multiple calcium channels mediate neurotransmitter release from peripheral neurons. *Proc. Natl. Acad. Sci. U.S.A.*, **83**, 6656–6659.

REEVE, H.L., VAUGHAN, P.F.T. & PEERS, C. (1994). Calcium channel currents in undifferentiated human neuroblastoma (SH-SY5Y) cells: actions and possible interactions of dihydropyridines and ω-conotoxin. *Eur. J. Neurosci.*, **6**, 943–952.

REUVENEY, E. & NARAHASHI, T. (1993). Two types of high voltage-activated calcium channels in SH-SY5Y human neuroblastoma cells. *Brain Res.*, **603**, 64–73.

RICHARDS, M.H. (1991). Pharmacology and second messenger interactions of cloned muscarinic receptors. *Biochem. Pharmacol.*, **42**, 1645–1653.

SERRA, M., MEI, L., ROESKE, W.R., LUI, G.K., WATSON, M. & YAMAMURA, H.I. (1988). The intact human neuroblastoma cell (SH-SY5Y) exhibits high affinity [^{3}H]pirenzepine binding associated with hydrolysis of phosphoinositols. *J. Neurochem.*, **50**, 1513–1521.

SWANDULLA, D., CARBONE, E. & LUX, H.D. (1991). Do calcium channel classifications account for neuronal calcium channel diversity? *Trends Neurosci.*, **14**, 46–51.

TSIEN, R.W., LIPSCOMBE, D., MADISON, D.V., BLEY, K.R. & FOX, A.P. (1988). Multiple types of neuronal calcium channels and their selective modulation. *Trends Neurosci.*, **10**, 431–438.

VAUGHAN, P.F.T., KAYE, D., REEVE, H.L., BALL, S. & PEERS, C. (1993a). Nicotinic receptor-mediated release of noradrenaline in the human neuroblastoma SH-SY5Y. *J. Neurochem.*, **60**, 2159–2166.

VAUGHAN, P.F.T., REEVE, H.L. & PEERS, C. (1993b). The effect of barium on noradrenaline release from the human neuroblastoma SH-SY5Y. *J. Physiol.*, **467**, 359P.

YANG, J. & TSIEN, R.W. (1993). Enhancement of N- and L-type calcium channel currents by protein kinase C in frog sympathetic neurones. *Neuron*, **10**, 127–136.

(Received May 26, 1994
Revised June 7, 1994
Accepted June 9, 1994)

Br. J. Pharmacol. (1994), **113**, 628–634 © Macmillan Press Ltd, 1994

Mediation by $SRIF_1$ receptors of the contractile action of somatostatin in rat isolated distal colon; studies using some novel SRIF analogues

[1]E.S. McKeen, W. Feniuk & P.P.A. Humphrey

Glaxo Institute of Applied Pharmacology, Department of Pharmacology, University of Cambridge, Tennis Court Road, Cambridge CB2 1QJ

1 The motor effects of somatostatin-14 (SRIF), and several SRIF peptide analogues were investigated on the rat isolated distal colon. The objective of these studies was to characterize the receptor mediating the contractile action of SRIF by comparing the relative agonist potencies of a range of SRIF analogues.

2 SRIF (1 nM–1 μM) produced concentration-dependent contractions with an EC_{50} value of approximately 10 nM. Contractile responses induced by SRIF were insensitive to atropine (1 μM) or naloxone (1 μM) but abolished by tetrodotoxin (1 μM). Somatostatin-28 ($SRIF_{28}$), also induced concentration-dependent contractions and was equipotent with SRIF. Phosphoramidon (1 μM) and amastatin (10 μM) did not increase the potency of either SRIF or $SRIF_{28}$.

3 The SRIF peptide analogues, octreotide, $SRIF_{25}$, seglitide, angiopeptin and CGP23996 (1 nM–1 μM) produced contractile responses in the rat distal colon, each having similar potency and maximal activity relative to SRIF. The $SSTR_2$ receptor-selective hexapeptide, BIM23027 (0.1 nM–1 μM), and the SRIF stereoisomer, D-Trp^8-SRIF (0.1 nM–1 μM), were the most potent agonists examined being approximately 12 and 7 times more potent than SRIF, respectively. In contrast, the $SSTR_5$ receptor-selective analogue, L362,855, was approximately 120 times weaker than SRIF, whilst the $SSTR_3$ receptor-selective analogue, BIM23056, was inactive at concentrations up to 3 μM.

4 The putative SRIF receptor antagonist, (cyclo(7-aminoheptanoyl Phe-D-Trp-Lys-Thr[Bzl]))(CPP) (1 μM), had no agonist activity and had no effect on contractions induced by SRIF.

5 The contractile actions of BIM23027 and seglitide were subject to pronounced desensitization. Desensitization of preparations by BIM23027 (0.3 μM) abolished the contractile action of SRIF and $SRIF_{28}$ but had no effect on contractions produced by acetylcholine (0.1 nM–1 μM), suggesting that BIM23027, SRIF and $SRIF_{28}$ act via a common receptor mechanism.

6 In conclusion, the rat isolated distal colon contracts in response to SRIF and a number of SRIF analogues. Seglitide and octreotide exhibited similar potency and maximal activity relative to SRIF, suggesting that in the rat colon the receptor mediating contraction belongs to the $SRIF_1$-receptor group, of which the recombinant $SSTR_2$, $SSTR_3$ and $SSTR_5$ receptors appear to be subtypes. The high potency of BIM23027, the weak agonist activity of L362,855 and the lack of activity exhibited by BIM23056 suggests that the SRIF receptor mediating contraction in the rat distal colon is similar to the recombinant $SSTR_2$ receptor.

Keywords: Somatostatin receptors; SRIF; rat colon; contraction; seglitide; BIM23027; BIM23056; L362,855

Introduction

Somatostatin-14 (SRIF), a cyclic tetradecapeptide discovered originally in mammalian hypothalamus (Brazeau *et al.*, 1973), exists in high concentrations within the enteric nervous system of the human and rodent gastrointestinal tract (Costa *et al.*, 1980; Keast *et al.*, 1984; Ekbald *et al.*, 1988). Somatostatin-28 ($SRIF_{28}$), an N-terminally extended form of SRIF, is also found in the gut, but primarily in the endocrine cells of the intestinal mucosa (Pradayrol *et al.*, 1980). SRIF has been reported to be a potent inhibitor of neuroendocrine and exocrine gastrointestinal secretion, intestinal transport and splanchnic blood flow (for review see Gyr & Meier, 1993). The effects of SRIF on gastrointestinal motility are complex. For example, SRIF has been shown to inhibit migrating motor complexes originating in the stomach (Ormsbee *et al.*, 1978), whilst those originating in the intestine appear to be stimulated (Thor *et al.*, 1978; Peeters *et al.*, 1983). In the guinea-pig isolated ileum, SRIF inhibits neurogenically mediated contractions probably through a pre-junctional mechanism (Guillemin, 1976; Feniuk *et al.*, 1993). Under basal conditions in the same preparation, SRIF has been shown to evoke cholinergically mediated contractile responses (Roberts *et al.*, 1993). In conscious dogs, SRIF injected intravenously inhibits both spontaneous and cholecystokinin octapeptide (CCK8)-induced colonic motility (Atanassova *et al.*, 1993).

To date, the receptors mediating these many actions of SRIF in the gut remain poorly characterized. This is largely due to the lack of availability of specific and selective SRIF receptor blocking drugs, and the fact that most agonist potency comparisons have been based solely on differences in the relative potencies of SRIF and $SRIF_{28}$ (Meyers *et al.*, 1980; Brazeau *et al.*, 1981; Hirst *et al.*, 1982). Moreover, with few exceptions (Gu *et al.*, 1992), the potential influence of endogenous peptidases on the reactivity of these peptides appears to have been largely ignored. However, recent molecular cloning studies have revealed a large SRIF receptor family, composed at present of five distinct SRIF receptor types (for review see Bell & Reisine, 1993; Raynor *et al.*, 1993a,b). These have been termed $SSTR_1$ (Yamada *et al.*, 1992a; Li *et al.*, 1992), $SSTR_2$ (Yamada *et al.*, 1992a; Kluxen *et al.*, 1992), and $SSTR_3$ (Yasuda *et al.*, 1992; Meyerhof *et al.*, 1992; Yamada *et al.*, 1992b; Corness *et al.*, 1993) which have been structurally characterized from human, rat and mouse, together with a rat $SSTR_4$ receptor (Bruno *et al.*, 1992). A fifth receptor isolated from the rat by O'Carroll *et al.* (1992), has also been designated $SSTR_4$. It is structurally

[1] Author for correspondence.

and pharmacologically distinct from the first described rat $SSTR_4$ receptor (Bruno *et al.*, 1992) and for the purpose of the present study (and in the absence of an agreed international nomenclature) will be termed $SSTR_5$. Radioligand binding studies on several mammalian cell lines expressing the different SRIF receptors have identified several peptide analogues that appear to be highly potent, and selective for certain subtypes of SRIF receptor (Raynor *et al.*, 1993a,b). Such compounds include BIM23027 (c[N-Me-Ala-Tyr-D-Trp-Lys-Abu-Phe]), BIM23056 (D-Phe-Phe-Tyr-D-Trp-Lys-Val-Phe-D-Nal-NH_2), and L362,855 (c[Aha-Phe-Trp-D-Lys-Thr-Phe]) which selectively bind with subnanomolar affinities to $SSTR_2$, $SSTR_3$ and $SSTR_5$ receptors, respectively (Raynor *et al.*, 1993a,b). However, to date, the functional characteristics of these SRIF analogues in whole tissue preparations, naturally expressing SRIF receptors, remains unexplored.

We have recently demonstrated that SRIF causes a concentration-dependent contraction of the rat isolated colon (McKeen *et al.*, 1994). The aim of this study was to characterize the SRIF receptor mediating this effect by comparing the relative agonist potencies of a range of SRIF analogues, including the recently identified $SSTR_2$, $SSTR_3$ and $SSTR_5$ receptor-selective peptides, BIM23027, BIM23056 and L362,855, respectively. A preliminary account of some of these findings has been presented to the British Pharmacological Society (McKeen *et al.*, 1994).

Methods

Male Sprague-Dawley rats (200–300 g) were humanely killed. The distal colon was removed and placed in modified Krebs solution of the following composition (mM): NaCl 118, $NaHCO_3$ 25, KCl 4.7, $MgSO_4.7H_2O$ 0.6, KH_2PO_4 1.2, D-glucose 11.1, $CaCl_2.6H_2O$ 1.3, (pH 7.4), at room temperature and gassed with 95% O_2/5% CO_2. Preparations were gently cleared of any faecal matter and adhering connective tissue. Segments of colon (approx. 1.5 cm) were mounted in 4 ml organ baths at 37°C in gassed modified Krebs solution of the above composition. Contractile responses were measured isometrically from a resting tension of 1.5 g using a Dynamometer UF1 force transducer, and displayed on a chart recorder (Lectromed Multitrace 8). All preparations were allowed to equilibrate for 30 min during which time tension was maintained at 1.5 g and washed with fresh Krebs every 15 min.

Effect of SRIF analogues

Concentration-effect curves to SRIF were constructed non-cumulatively using increasing sequential concentrations. Each concentration of SRIF was applied for approximately 1 min during which time a peak effect was reached. A washout period of 15 min was used between each SRIF application since in preliminary experiments contractile responses to SRIF were desensitized if shorter periods were employed. The maximum concentration of agonist tested was normally 1 μM. Following a 60 min interval a second concentration-effect curve to a test agonist was established as above. Using a Latin square design, one colonic preparation always acted as a control to monitor spontaneous changes in agonist sensitivity. Thirty minute dosing intervals were used for experiments with BIM23027 and seglitide since preliminary results showed that a 30 min interval with regular washes was required between each drug concentration in order to prevent desensitization.

Effect of peptidase inhibitors and antagonists on responses to SRIF

In some experiments the influence of a combination of the peptidase inhibitors, amastatin (10 μM) and phosphoramidon (1 μM), on the contractile action of SRIF and $SRIF_{28}$ was examined. Agonist concentration-effect curves were obtained before and after a 30 min exposure to the peptidase inhibitors which were in contact with the preparation throughout the second concentration-effect curve. Unless otherwise stated, an identical protocol was used to assess any antagonistic properties of cyclo(7-aminoheptanoyl Phe-D-Trp-Lys-Thr [Bzl])(CPP) (1 μM) or BIM23056 (1 μM).

Effect of desensitization by BIM23027 on responses to SRIF, $SRIF_{28}$ and acetylcholine

Desensitization was achieved by applying BIM23027 (0.3 μM) with a contact time of 4 min, followed by a 1 min washout period before administration of various concentrations of SRIF or $SRIF_{28}$. BIM23027 was applied before each concentration of the test agonist, and a recovery period of 10 min was allowed between successive concentrations. The selectivity of BIM23027 desensitization was determined by investigating the effect of BIM23027 (0.3 μM) pretreatment on acetylcholine-induced (0.1 nM–10 μM) contractions by use of the same protocol as above.

Analysis of results

The contractile responses in the rat distal colon were expressed as a percentage of the maximum contractile response to SRIF obtained in the first (control) concentration-effect curve. When agonist potencies were determined, equi-effective molar ratios (EMRs) were measured from the concentration-effect curves at a point corresponding to 50% of the second agonist maximum (EC_{50}), and corrected for spontaneous changes in agonist sensitivity. The effect of antagonists was studied by measuring the concentration-ratio which was the ratio of the agonist EC_{50} values in the presence and absence of antagonist. All values stated are geometric means (95% confidence limits) of n observations, except for % maxima which are expressed as arithmetic mean ± s.e. mean. Tests for statistically significant differences were carried out using a Student's unpaired t test, and a probability $P<0.05$ was considered significant.

Drugs and solutions

The following drugs were obtained from Sigma Chemical Co. Ltd., SRIF, $SRIF_{28}$, $SRIF_{25}$ cyclo(7-aminoheptanoyl-Phe-D-Trp-Lys-Thr[Bzl]) (CPP), angiopeptin (β-(2-napthyl)-D-Ala-c[Cys-Tyr-D-Trp-Lys-Val-Cys]-Thr amide), phosphoramidon, amastatin, atropine methylnitrate, tetrodotoxin and acetylcholine.

CGP 23996 (cyclo [Ahep-Lys-Asn-Phe-Trp-Lys-Thr-Tyr-Thr-Ser]), BIM23027 (c[N-Me-Ala-Tyr-D-Trp-Lys-Abu-Phe]), BIM23056 (D-Phe-Phe-Tyr-D-Trp-Lys-Val-Phe-D-Nal-NH_2), and L362,855 (c[Aha-Phe-Trp-D-Lys-Thr-Phe]) and seglitide (MK 678) were synthesized by Dr J. Kitchin's team, Chemistry Division, Glaxo Group Research Ltd. Octreotide (Sandostatin) was purchased from a pharmaceutical supplier.

All peptides were initially dissolved in distilled water, divided into aliquots and stored at −20°C. Fresh aliquots were used on each experimental day and samples were kept on ice during the experiment. There was no loss of biological activity of these samples during the course of an experiment and stored samples showed similar activity to samples prepared from solid stock material and used immediately.

Results

Effect of SRIF

Preliminary studies showed that the rat distal colon was contracted by SRIF (1 μM). If a concentration of SRIF (1 μM) was repeated 5 min after a similar application, the contractile response of the peptide was greatly diminished. In

subsequent experiments pronounced desensitization was overcome by having only a 1 min agonist contact time and by leaving a period of 15 min between application. With this protocol it was possible to obtain reproducible responses over several hours.

SRIF (1 nM–1 μM) produced concentration-dependent contractions in the rat isolated distal colon (Figure 1a). The contractile response to each concentration of SRIF reached a peak within 30–50 s, and even in the continuous presence of the drug, returned rapidly towards baseline. First and second concentration-effect curves to SRIF were reproducible with mean EC_{50} values of 12.3 (8.4–15) and 9.2 (6.5–12)nM respectively, there being only a 0.53 (0.38–0.73) fold leftward shift between the first and second concentration-effect curve ($n = 20$) (Figure 2a). The maximum contractile responses (at 1 μM) for the first and second concentration-effect curve to SRIF were 1.83 ± 0.23 g and 2.28 ± 0.28 g respectively, and these were not significantly different ($P < 0.05$).

Effects of atropine and tetrodotoxin on contractile responses to SRIF

Contractile responses to SRIF (1 nM–1 μM) remained unchanged following a 30 min exposure to atropine (1 μM) (concentration ratio 1.6 (0.4–7.6), $n = 4$). Treatment of preparations with tetrodotoxin (1 μM, 20 min contact time) produced pronounced spontaneous activity (Figure 1b). In the continuous presence of tetrodotoxin (1 μM), contractile responses to a maximally effective concentration of SRIF (1 μM) were abolished. In contrast contractile responses produced by acetylcholine (30 nM) remained unchanged following tetrodotoxin (1 μM) pretreatment (Figure 1b).

Effect of analogues of SRIF

A range of SRIF analogues were tested for activity on the rat distal colon, $SRIF_{28}$, octreotide, angiopeptin, seglitide, CGP 23996, $SRIF_{25}$, BIM23027, and D-Trp^8-SRIF mimicked contractions induced by SRIF. The maximum contractile effect produced by each of these analogues was not significantly different from that produced by SRIF (Table 1). $SRIF_{28}$, octreotide, angiopeptin, CGP23996 and $SRIF_{25}$ were of similar potency to SRIF (Table 1). Seglitide was also equipotent to SRIF and produced a similar maximum contractile response (Table 1). However, at high concentrations (>0.1 μM) seglitide caused smaller contractile responses than were observed at lower concentrations, thus producing a bell shaped concentration-effect curve (Figure 2b). BIM23027 and D-Trp^8-SRIF were the most potent agonists tested being approximately 12 and 7 times more potent than SRIF, respectively (Table 1). In contrast, L362,855 was devoid of contractile activity up to concentrations of 0.3 μM (Figure 2b). Higher concentrations of L362,855 produced contractile responses, although a maximum response was not achieved at a concentration of 3 μM. Assessment of the relative agonist potency of L362,855 at the level of 50% of the SRIF maximum produced an EMR of 120(58–248), $n = 4$. BIM23056 was inactive at concentrations up to 3 μM (Figure 2b). In view of the lack of intrinsic activity of BIM23056, it was tested as a potential SRIF receptor blocking drug. However, BIM23056 (3 μM, 30 min contact time) had no significant effect on either the potency or maximum amplitude of contraction produced by SRIF (concentration ratio 1.0 (0.4–2.6), $n = 4$).

Effect of peptidase inhibitors

The influence of a combination of phosphoramidon (1 μM) and amastatin (10 μM) on the potency of SRIF and $SRIF_{28}$ was examined in the rat distal colon. Phosphoramidon and amastatin did not increase the potency or maximum amplitude of contraction produced by any of the peptides examined (concentration-ratios were 1.2(0.2–6.3) and 3.2 (1.2–8.8) respectively, $n = 4$, $P > 0.05$). BIM23056 was inac-

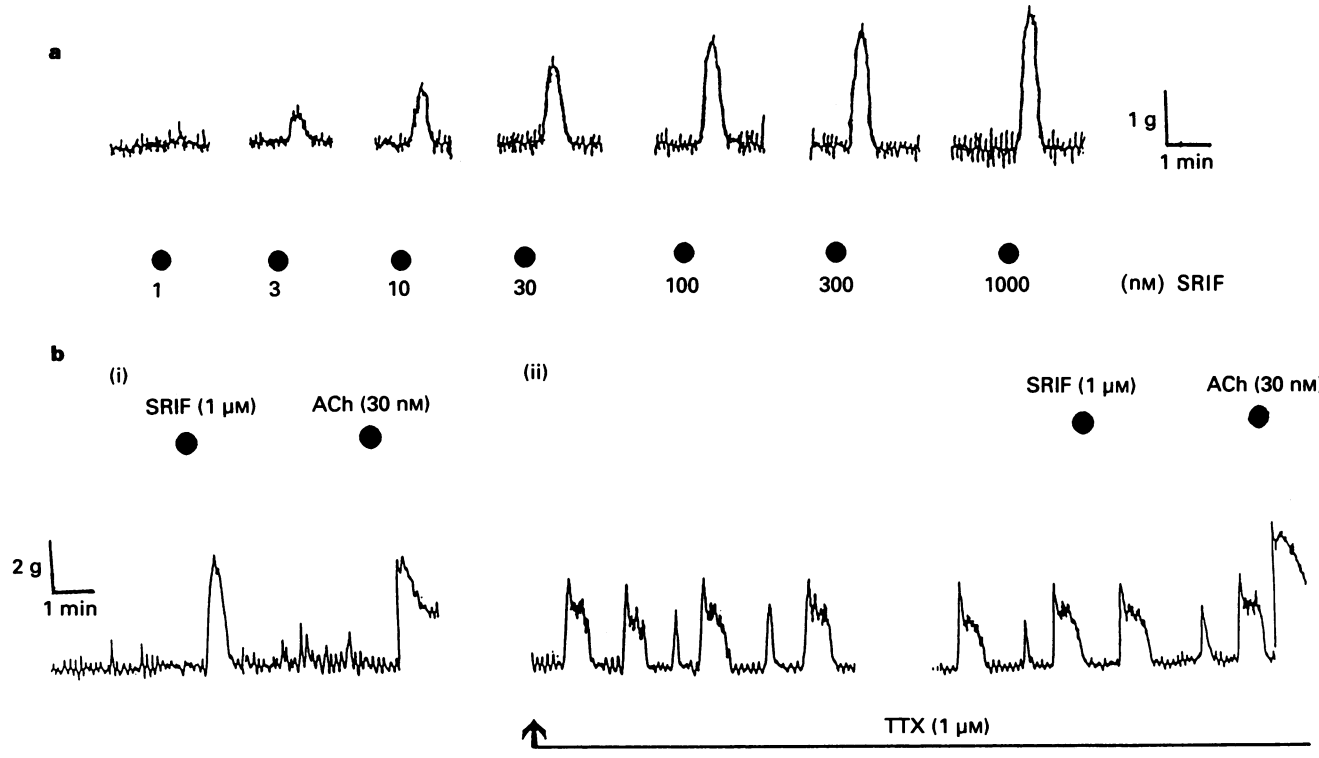


Figure 1 (a) Experimental recordings demonstrating the contractile effect of SRIF (1 nM–1 μM) in the rat isolated distal colon. Each concentration of SRIF was applied for approximately 1 min during which time the peak contractile response was reached, and returned rapidly towards baseline. A washout period of 15 min was used between each sequential dose of SRIF. (b) Contractile action of SRIF (1 μM) and acetylcholine (ACh, 30 nM), in the rat distal colon in the absence (i) and in the presence of tetrodotoxin (TTX) (1 μM) (ii). Note that TTX (1 μM) produced pronounced spontaneous activity and that the contractile responses to SRIF were abolished while the contractions to acetylcholine remained unchanged.

Table 1 A comparison of the potencies of several SRIF analogues in producing contraction in the rat isolated distal colon

Analogue	EC_{50} (nM)	*EMR*	*Maximum (% original SRIF max)*
SRIF	11.5 (8.7–15.6)	1	126 ± 4*
BIM23027	0.9 (0.1–8.3)	0.08 (0.21–0.34)	130 ± 7
[D-Trp^8]-SRIF$_{14}$	2.0 (0.2–17.2)	0.14 (0.02–0.94)	126 ± 8
MK678	2.6 (1.5–4.5)	0.45 (0.15–1.33)	106 ± 7
Octreotide	6.7 (3.0–15.0)	0.31 (0.04–2.37)	120 ± 7
CGP23996	14.9 (2.90–11.3)	0.58 (0.19–1.80)	141 ± 15
Angiopeptin	18.5 (4.9–70.1)	0.94 (0.15–5.90)	103 ± 12
SRIF$_{25}$	14.3 (11.3–17.2)	1.03 (0.53–2.00)	113 ± 7
SRIF$_{28}$	20.0 (8.0–49.2)	1.58 (0.55–4.59)	102 ± 5
L362,855	–	120 (58–248)	NA
BIM23056	>3000	>300	NA

All values are expressed as geometric mean (95% confidence limits), except values for % original SRIF max which are expressed as mean ± s.e.mean, where $n = 4–5$ observations. EMR (equieffective molar ratio) values of less than unity indicate greater potency than that of SRIF. *Values for SRIF are given for the second concentration-effect curves in the control preparations ($n = 34$). NA, maximum not achieved.

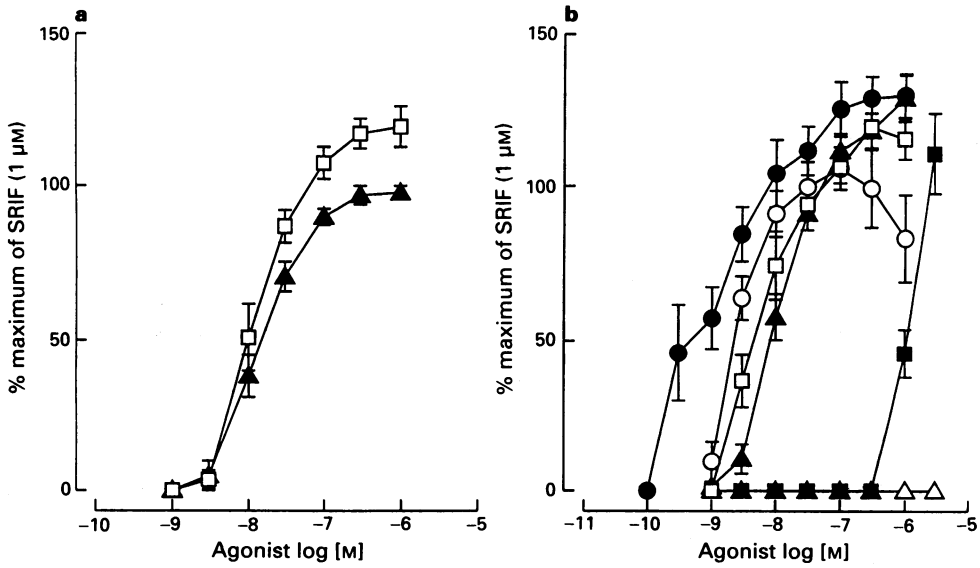


Figure 2 (a) Reproducibility of the first and second concentration-effect curves to SRIF in the rat isolated distal colon. First concentration-effect curve (▲), second concentration-effect curve (□). Each point represents the mean ± s.e.mean ($n = 20$). The abscissa scale shows the log molar concentration of drug and the ordinate scale the contractile response expressed as % of the maximum contractile response to SRIF (1 μM). (b) Comparison of the contractile responses produced by SRIF (▲), BIM23027 (●), BIM23056 (△), L362,855 (■), seglitide (○), and octreotide (□). Each point represents the mean and s.e.mean ($n = 4$, except SRIF $n = 20$). The abscissa scale shows the log molar concentration of drug and the ordinate scale the contractile response expressed as % of the maximum contractile response to SRIF (1 μM).

tive at concentrations up to 3 μM even in the presence of phosphoramidon (1 μM) and amastatin (10 μM) ($n = 4$).

Effect of BIM23027 desensitization

In view of the pronounced susceptibility of BIM23027-induced contractions to desensitization, it was used in cross-desensitization studies with SRIF and SRIF$_{28}$. Pre-exposure of preparations to BIM23027 (0.3 μM) for 4 min period followed by washout (see methods), abolished the contractile responses produced by SRIF and SRIF$_{28}$ (Figure 3a,b), whilst contractions produced by acetylcholine were unchanged (Figure 3c).

Effects of putative antagonists on contractions to SRIF

The putative SRIF receptor blocking drug, CPP (1 μM, 1 h contact time), was inactive at 1 μM, and had no significant effects on either the potency or maximum amplitude of contraction produced by SRIF (concentration ratio 0.8(0.5–1.3); $n = 4$).

Naloxone (1 μM, 30 min contact time) had no antagonistic effect on the contractile action of SRIF (concentration-ratio 0.4(0.04–3.3), $n = 4$).

Discussion

In the present study we have demonstrated that SRIF and several SRIF analogues produce concentration-dependent contractions in the rat isolated distal colon. The contractile response to SRIF appears to be neurogenic, and does not involve cholinergic stimulation since the effects of SRIF were abolished by tetrodotoxin and unaffected by atropine. In general SRIF has been reported to be a potent inhibitor of gastrointestinal motility. For example, SRIF inhibits neurogenically mediated contractile responses in the guinea-pig isolated ileum (Guillemin, 1976; Feniuk *et al.*, 1993), while in

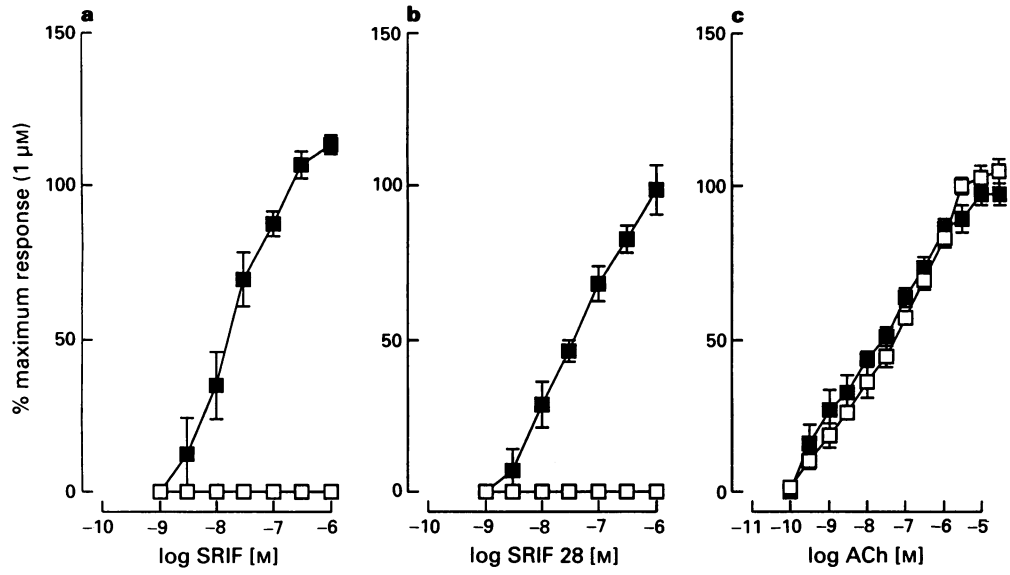


Figure 3 Effect of (a) SRIF, (b) $SRIF_{28}$ and (c) acetylcholine in the rat isolated distal colon in the absence (■) and following desensitization of preparations by BIM23027 (0.3 μM) (□). Desensitization was achieved by applying BIM23027 (0.3 μM) with a contact time of 4 min, followed by a 1 min washout period before administration of SRIF or $SRIF_{28}$. BIM23027 was applied before each concentration of the test agonist, and a recovery period of 10 min was allowed between successive concentrations. Each point represents the mean ± s.e.mean ($n = 4$). The abscissa scale shows the log molar concentration of drug and the ordinate scale the contractile response expressed as % of the maximum contractile response to SRIF (1 μM).

the conscious dogs SRIF injected intravenously inhibits both spontaneous and CCK-induced colonic motility (Atanassova *et al.*, 1993). Thus, as far as we know this is the first evidence of a stimulatory effect of SRIF on colonic motility. The main objective of this study was to study the SRIF receptor involved in this action by comparing the relative agonist potencies of some SRIF analogues that have been claimed to be selective for various SRIF receptor types.

The SRIF analogues, $SRIF_{28}$, $SRIF_{25}$, angiopeptin, and CGP23996 all induced contractile responses in the rat distal colon, each being of similar potency to SRIF. Interestingly, all of these SRIF agonists also showed similar potency to SRIF at inhibiting neurogenically mediated contractions in the guinea-pig isolated ileum (Feniuk *et al.*, 1993), suggesting that the SRIF receptor in the rat colon and the guinea-pig ileum may be similar. Endogenous SRIF and $SRIF_{28}$ are known to be substrates for the catabolic activity of endopeptidase (Marks *et al.*, 1976). Indeed, in tissues such as the guinea-pig isolated vas deferens, pretreatment with peptidase inhibitors (phosphoramidon and amastatin) has been shown to enhance the potency of SRIF by about five fold (Feniuk *et al.*, 1993). However, since the potency of SRIF or $SRIF_{28}$ was not increased by phosphoramidon and amastatin in this study, it seems unlikely that these peptides are degraded by endopeptidases in the rat distal colon.

The characteristics of the SRIF receptor mediating contraction in the rat colon obviously differs from that found in the guinea-pig vas deferens and right atrium. For example, in the guinea-pig vas deferens and right atrium, $SRIF_{28}$ has been shown to be approximately 30 times more potent than SRIF at inhibiting neurogenically mediated contractions and the negative inotropic effect of SRIF, respectively (Feniuk *et al.*, 1993). Furthermore, in the guinea-pig right atrium, the synthetic analogues octreotide and angiopeptin exhibited low intrinsic activity. Indeed, angiopeptin acted as a competitive SRIF receptor blocking drug by specifically antagonizing the negative inotropic action of both SRIF and $SRIF_{28}$ with estimated pK_B values 7.4 and 7.2, respectively. Seglitide has been shown also to act as a SRIF receptor antagonist in the guinea-pig atrium but was approximately 20 times weaker than angiopeptin in this respect (Dimech *et al.*, 1993). In the present study, both angiopeptin and seglitide were agonists with similar potency and maximal activity relative to SRIF. Interestingly, at high concentrations (>0.3 μM), seglitide produced smaller contractions, suggesting that at these concentrations, responses to seglitide may be susceptible to desensitization even with a 30 min washout period between each concentration of drug.

In the rat distal colon, the putative SRIF receptor blocking drug CPP, had no contractile action *per se* and did not antagonize the contractile action of SRIF. Interestingly, CPP has also been reported to have no effect on the inhibitory action of SRIF in the guinea-pig isolated ileum or vas deferens, nor did it antagonize the negative inotropic action of SRIF in the right atrium (Feniuk *et al.*, 1993). This is in contrast to the findings of Fries *et al.* (1982), who found that CPP antagonized SRIF-induced inhibitory effects upon GH, insulin and glucagon release in anaesthetized rats. Araujo *et al.* (1990) have also shown CPP to block the ability of SRIF to enhance acetylcholine release from hippocampal slices. These differences in the antagonistic profile of CPP may be a reflection of SRIF receptor heterogeneity. Alternatively, they may reflect a non-specific action of CPP. Further studies are needed to establish the usefulness of CPP as a tool for classifying SRIF receptors.

It has been suggested that SRIF exerts its effects by interacting with opiate μ-receptors (Terenius, 1976). However, in the rat distal colon such an interaction seems unlikely since naloxone had no effect on the contractile action of SRIF. This observation is consistent with similar findings in the guinea-pig ileum, vas deferens and atrium (Feniuk *et al.*, 1993). In the rat colon the lack of effect of naloxone would also suggest that enkephalins are unlikely to be involved in the mechanism underlying the contractile action of SRIF. Previous studies have suggested that γ-aminobutyric acid, tachykinins and vasointestinal peptide may mediate SRIF-induced contractions in the guinea-pig isolated ileum (Grider *et al.*, 1987; Roberts *et al.*, 1993). However, our unpublished studies with specific antagonists have excluded these neurotransmitters as mediators of SRIF-induced contraction in the rat colon. Further studies are needed to determine the site and mechanism of action of SRIF in the colon.

The plethora of actions exerted by SRIF in the gastrointes-

tinal tract are likely to be mediated by distinct SRIF receptor types. The earliest evidence for the existence of distinct types of SRIF receptor was based on the differential sensitivity to the native peptides SRIF and $SRIF_{28}$ (Meyers *et al.*, 1980; Brazeau *et al.*, 1981; Hirst *et al.*, 1982). The relative binding affinities of more metabolically stable analogues of SRIF such as seglitide and octreotide has been used as the basis for the subclassification of SRIF receptors into $SRIF_1$ and $SRIF_2$ in the rat brain (Tran *et al.*, 1985; Raynor & Reisine, 1992a). The $SRIF_1$ receptor has high affinity for seglitide and octreotide, whereas $SRIF_2$ receptors are insensitive to these analogues. On this basis, the SRIF receptor mediating contraction in the rat distal colon belongs to the $SRIF_1$ group, since seglitide and octreotide displayed high potency relative to SRIF. As previously mentioned (see introduction), the recent cloning of genes encoding multiple SRIF receptors has revealed a SRIF receptor family, composed of at least five distinct SRIF receptor types termed $SSTR_1$-$SSTR_5$. Pharmacological and structural comparisons suggest that there may be subgroups within the SRIF receptor family, with $SSTR_1$ and $SSTR_4$ receptors comprising one group, and $SSTR_2$, $SSTR_3$ and $SSTR_5$ receptors comprising a second group (Raynor *et al.*, 1993b). In view of the high affinity of the latter group for seglitide (Raynor *et al.*, 1993b), this group may represent members of the $SRIF_1$ receptor group, whilst, $SSTR_1$ and $SSTR_4$ represent members of the $SRIF_2$ receptor group.

Radioligand binding studies on several mammalian cell lines expressing the different recombinant SRIF receptors have identified several peptide analogues that are highly potent and selective for certain subtypes of SRIF receptors (Raynor *et al.*, 1993a,b). Such compounds include BIM 23027, BIM23056 and L362,855 which selectively bind with high affinity to $SSTR_2$, $SSTR_3$ and $SSTR_5$ receptors, respectively (Raynor *et al.*, 1993a,b). However, to date, the functional characteristics of these analogues in preparations naturally expressing SRIF receptors is unknown. In the rat distal colon, the contractile effect of SRIF would not appear to be mediated by a SRIF receptor similar to the cloned $SSTR_3$ and $SSTR_5$ receptors for several reasons. First, BIM 23056 which has high affinity and selectivity for the $SSTR_3$ receptor (Raynor *et al.*, 1993a), was inactive up to concentrations of 1 μM in the rat distal colon. Secondly, the $SSTR_5$ receptor selective analogue, L362,855, (Raynor *et al.*, 1993b) was approximately 120 times weaker than SRIF in the present study. In contrast, BIM23027, which has high affinity and selectivity for the cloned $SSTR_2$ receptor, was the most potent agonist (approximately 12 times more potent than SRIF) examined in the rat distal colon. Our contention that a SRIF-receptor similar to the cloned $SSTR_2$ receptor mediates the contractile effect of SRIF in the rat colon is clearly based on the high agonist potency of BIM23027 and its apparent selectivity for the recombinant $SSTR_2$ receptor (Raynor *et al.*, 1993a,b). Studies in our laboratories (Castro, unpublished) with BIM23027 on recombinant $SSTR_1$ and $SSTR_2$ receptors expressed in LTK^- cells, have confirmed a greater than 10,000 fold selectivity of BIM23027 for the $SSTR_2$ receptor, although the affinity estimate of BIM23027 (IC_{50} of 0.035 nM) for the $SSTR_2$ receptor was somewhat lower than that described by Raynor *et al.*, 1993a. A recent study (Bruno *et al.*, 1993) using solution hybridisation/nuclease protection analysis with sequence specific SRIF-receptor cRNA probes have identified the existence of $SSTR_2$ mRNA in several peripheral rat tissues such as the spleen, pancreas and stomach, however the colon was not examined. Further studies using either *in situ* hybridisation and/or PCR analyses should confirm the presence of $SSTR_2$ receptors in the rat colon. Recently, two splice variants of the $SSTR_2$ receptor have been cloned, the recombinant receptors being termed $SSTR_{2A}$ and $SSTR_{2B}$ (Vanetti *et al.*, 1992). These receptors exhibit similar affinities for $SSTR_2$ receptor-selective agonists such as BIM23027, both are regulated by agonist pretreatment and both mediate their effects through G proteins (Reisine *et al.*, 1993). It was not therefore possible in the present study to determine operationally which of the spliced variants might mediate the contractile effect of SRIF in the rat distal colon.

At present, the exact relationship between recombinant SRIF receptors expressed in cell lines and SRIF receptors expressed naturally in tissues is unclear. For example, there is a large discrepancy between the agonist binding affinity estimates (IC_{50} values) obtained in the radioligand binding studies on the recombinant SRIF receptors (Raynor *et al.*, 1993a,b), and their potencies (EC_{50} values) in the functional study described here and in the guinea-pig (Feniuk *et al.*, 1993). The identification of more potent and selective SRIF receptor antagonists for use in both functional and radioligand binding studies would be invaluable tools in comparing and contrasting operational characteristics of SRIF receptors, both native and recombinant.

The contractile action of all of the SRIF agonists examined in the present study were subject to desensitization, the hexapeptides BIM23027 and MK678 being most susceptible. Studies have also shown that some of the effects of SRIF are susceptible to desensitization. For example, pretreatment with SRIF in anterior pituitary tumour cells has been shown to reduce SRIF receptor coupling to adenylyl cyclase (Reisine, 1985). In contrast, SRIF receptor desensitization selectively abolishes non-adrenergic inhibitory postsynaptic potentials in sympathetically denervated guinea-pig submucosal neurones, and does not appear to involve adenylyl cyclase, protein kinase C or receptor internalization (Shen & Suprenant, 1993). Although the mechanism of desensitization to SRIF was not investigated in the present study, desensitization of preparations by BIM23027 selectively abolished contractile responses to SRIF and $SRIF_{28}$, suggesting that these agonists all act via a common receptor mechanism. Agonist-induced desensitization is a characteristic that has been used to differentiate between types of SRIF receptors. For example, chronic exposure of $SRIF_1$ receptors to SRIF or seglitide, reduces high affinity agonist binding, whilst $SRIF_2$ receptors appear unaffected (Rens-Domiano *et al.*, 1992; Raynor & Reisine, 1992b). It is also noteworthy that the cloned $SSTR_2$ receptor can be readily desensitized by prior exposure to seglitide (Rens-Domiano *et al.*, 1992). The finding that the contractile action of SRIF and $SRIF_{28}$ were readily desensitized by prior exposure to BIM23027 supports further the view that a subtype of the $SRIF_1$ receptor group mediates the contractile action of SRIF in the rat colon.

In summary, we have shown for the first time a contractile action of SRIF and several SRIF analogues in the rat distal colon. Seglitide and octreotide exhibited similar potency and efficacy to SRIF, suggesting that the SRIF receptor mediating the contractile action of SRIF belongs to the $SRIF_1$ receptor group. The high potency of recently identified SRIF receptor-selective ligands such as BIM23027, the weak agonist activity of L362,855 relative to SRIF, and the lack of activity exhibited by BIM23056 suggests that the SRIF receptor subtype mediating the contractile action of SRIF in the rat distal colon in similar to the recombinant $SSTR_2$ receptor. The contractile action of SRIF in the rat distal colon appears to involve activation of non-cholinergic nerves, however the precise site and mechanism involved remains to be elucidated.

References

ARAUJO, D.M., LAPCHAK, P.A., COLLIER, B. & QUIRION, R. (1990). Evidence that somatostatin enhances endogenous acetylcholine release in the rat hippocampus. *J. Neurochem.*, **55**, 1046–1555.

ATANASSOVA, E., BOCHEVA, A. & MILENOV, K. (1993). Effect of cholecystokinin octapeptide on the mechanical and electrical activity in the colon of conscious dogs. *J. Gastrointest. Mot.*, **5**, 57–62.

BELL, G.I. & REISINE, T. (1993). Molecular biology of somatostatin receptors. *Trends Neurol. Sci.*, **16**, 34–38.

BRAZEAU, P., LING, N., ESCH, F., BOHLER, P., BENOIT, R. & GUILLEMIN, R. (1981). High biological activity of the synthetic replicates of somatostatin-28, and somatostatin-25. *Regul. Pept.*, **1**, 255–262.

BRAZEAU, P., VALE, W., BURGUS, R., LING, N, BUTCHER, M., RIVIER, J. & GUILLEMAN, R. (1973). Hypothalamic polypeptide that inhibits the secretion of growth hormone. *Science*, **179**, 77–79.

BRUNO, J., XU, Y., SONG, J. & BERELOWITZ, M. (1992). Molecular cloning and functional expression of a brain-specific somatostatin receptor. *Proc. Natl. Acad. Sci. USA*, **89**, 10267–10271.

BRUNO, J., XU, Y., SONG, J. & BERELOWITZ, M. (1993). Tissue distribution of somatostatin receptor subtype messenger ribonucleic acid in the rat. *Endocrinology*, **133**, 2561–2567.

CORNESS, J., DEMCHYSHYN, L., SEMAN, P., VAN TOL, H.H.M., SRIKANT, C.B., KENT, G., PATEL, Y.C. & NIZNIK, H.B. (1993). The cloned human $SSTR_3$ receptor, located on chromosome 22, displays preferential affinity for somatostatin-14 like peptides. *FEBS Lett.*, **321**, 279–284.

COSTA, M.J., FURNESS, J.B., LLEWELLYN, I.J., DAVIES, B. & OLIVER, J. (1980). An immunohistochemical study of projections of somatostatin-containing neurons in guinea-pig intestine. *Neuroscience*, **5**, 841–852.

DIMECH, J., FENIUK, W. & HUMPHREY, P.P.A. (1993). Antagonist effects of seglitide (MK678) at somatostatin receptors in guinea-pig isolated right atria. *Br. J. Pharmacol.*, **109**, 898–899.

EKBALD, E., EKMAN, R., HAKANSON, J. & SUNDLER, F. (1988). Projections of peptide containing neurons in the rat colon. *Neuroscience*, **27**, 655–661.

FENIUK, W., DIMECH, J. & HUMPHREY, P.P.A. (1993). Characterization of somatostatin receptors in guinea-pig isolated ileum, vas deferens, and right atrium. *Br. J. Pharmacol.*, **110**, 1156–1164.

FRIES, J.L., MURPHY, W.A., SUEIRAS-DIAZ, D. & COY, D.H. (1982). Somatostatin analogues increase GH, insulin, and glucagon release in the rat. *Peptides*, **3**, 811–814.

GRIDER, J.R., ARIMURA, A. & MAKHLOUF, G.M. (1987). Role of somatostatin neurons in peristalsis: facilitatory interneurons in descending pathways. *Am. J. Physiol.*, **253**, G434–G438.

GU, Z.F., PRADHAN, T., COY, D.H., MANTEY, S., BUNNETT, N.W., JENSEN, R.T. & MATON, P.N. (1992). Actions of somatostatin on gastric smooth muscle cells. *Am. J. Physiol.*, **262**, G432–G438.

GUILLEMIN, R. (1976). Somatostatin inhibits the release of acetylcholine-induced electrically in the myenteric plexus. *J. Physiol.*, **303**, 315–316.

GYR, K.E. & MEIER, R. (1993). Pharmacodynamic effects of Sandostatin in the gastrointestinal tract. *Digestion*, **54**, 14–19.

HIRST, B., CONLON, J.M., COY, D.H., HOLLAND, J. & SHAW, B. (1982). Comparison of the gastric exocrine inhibition and activation and plasma kinetics of somatostatin-28 and somatostatin-14 in cat. *Regul. Pept.*, **4**, 227–237.

KEAST, J.B., FURNESS, J.B. & COSTA, M. (1984). Somatostatin in human enteric nerves. *Cell Tissue Res.*, **237**, 299–308.

KLUXEN, F.-W., BRUNS, C. & LUBBERT, H. (1992). Expression cloning of a rat brain somatostatin receptor cDNA. *Proc. Natl. Acad. U.S.A.*, **89**, 4618–4622.

LI, X.-J., FORTE, M., NORTH, R.A., ROSS, C.A. & SYNDER, S.H. (1992). Cloning and expression of a rat somatostatin receptor enriched in brain. *J. Biol. Chem.*, **267**, 21307–21312.

MARKS, N., STERNA, F. & BENUCK, M. (1976). Correlation between biological potency and biodegradation of somatostatin analogues. *Nature*, **261**, 511–512.

MCKEEN, E.S., FENIUK, W. & HUMPHREY, P.P.A. (1994). Characterization of the contractile action of somatostatin in the rat distal colon. *Br. J. Pharmacol.*, **112**, 169P.

MEYERHOF, W., WULFSEN, I., SCHONROCK, C., FEHR, S. & DICHTER, R. (1992). Molecular cloning of a somatostatin-28 receptor and comparison of its expression pattern with that of somatostatin-14 receptor in the rat brain. *Proc. Natl. Acad. Sci. U.S.A.*, **89**, 10267–10271.

MEYERS, C.A., MURPHY, W.A., REDDING, T.W., COY, D.H. & SCHALLY, A.V. (1980). Synthesis and biological actions of prosomatostatin. *Proc. Natl. Acad. Sci. U.S.A.*, **77**, 6171–6174.

O'CARROLL, A.M., LOLAIT, S.J., KONIG, M. & MAHAN, L.C. (1992). Molecular cloning and expression of a pituitary somatostatin receptor with preferential affinity for somatostatin-28. *Mol. Pharmacol.*, **42**, 939–946.

ORMSBEE, H.S., KOEHLER, S. & TELFORD, G.I. (1978). Somatostatin inhibits motilin-induced interdigestive contractile activity in the dog. *Am. J. Dig. Dis.*, **23**, 781–788.

PEETERS, T.L., JANSSENS, J. & VANTRAPPER, G.R. (1983). Somatostatin and interdigestive migrating motor complexes in man. *Regul. Pept.*, **5**, 209–217.

PRADAYROL, L., JORNALL, H. & MUTT, V. (1980). N-terminally extended somatostatin: the primary structure of somatostatin-28. *FEBS Lett.*, **109**, 55–588.

RAYNOR, K., MURPHY, W.A., COY, D.H., TAYLOR, J.E., MOREAU, J., YASUDA, K., BELL, G.I. & REISINE, T. (1993a). Cloned somatostatin receptors: identification of subtype selective peptides and demonstration of high affinity binding of linear peptides. *Mol. Pharmacol.*, **43**, 838–844.

RAYNOR, K., O'CARROLL, A.M., KONG, H., YASUDA, K., MAHAN, L.C., BELL, G.I. & REISINE, T. (1993b). Characterization of the cloned somatostatin receptor subtypes $SSTR_4$ and $SSTR_5$. *Mol. Pharmacol.*, **44**, 385–392.

RAYNOR, K. & REISINE, T. (1992a). Differential coupling of somatostatin receptors to adenylyl cyclase in rat striatum vs pituitary and other regions of the rat brain. *J. Pharmacol. Exp. Ther.*, **260**, 841–848.

RAYNOR, K. & REISINE, T. (1992b). Subtypes of somatostatin receptors are expressed in the anterior pituitary cell line GH3. *J. Pharmacol. Exp. Ther.*, **264**, 110–116.

REISINE, T. (1985). Multiple mechanisms of inhibition of adrenocorticotropin release from mouse anterior pituitary tumour cells. *Endocrinology*, **115**, 2256–2259.

REISINE, T., KONG, H., RAYNOR, K., YANO, J., YASUDA, K. & BELL, G. (1993). Splice variant of the somatostatin receptor 2 subtype, somatostatin receptor 2B, couples to adenylyl cyclase. *Mol. Pharmacol.*, **44**, 1008–1015.

RENS-DOMANIO, S., LAW, S.F., YAMADA, Y., SEINO, S., BELL, G.I. & REISINE, T. (1992). Pharmacological properties of 2 cloned somatostatin receptors. *Mol. Pharmacol.*, **42**, 28–34.

ROBERTS, D.J., HASLER, W.L. & OWYANG, C. (1993). GABA mediation of the dual effects of somatostatin on the guinea-pig ileal myenteric cholinergic transmission. *Am. J. Physiol.*, **264**, G953–G960.

SHEN, K.Z. & SUPRENANT, A. (1993). Somatostatin-mediated inhibitory postsynaptic potential in sympathetically denervated guinea-pig submucosal neurons. *J. Physiol.*, **470**, 619–635.

TERENIUS, L. (1976). Somatostatin and acetylcholine are peptides with partial antagonist-like selectivity for opiate receptors. *Eur. J. Pharmacol.*, **38**, 211–213.

THOR, P., KROL, R., KONTUREK, S.J, COY, D.H. & SCHALLY, A.V. (1978). Effect of somatostatin on myoelectric activity of the small bowel. *Am. J. Physiol.*, **235**, E249–E254.

TRAN, V.T., BEAL, M.F. & MARTIN, J.B. (1985). Two types of somatostatin receptors differentiated by cyclic somatostatin analogues. *Science*, **228**, 492–495.

VANETTI, M., KOUBA, M., WANG, G. & HOLLT, V. (1992). Cloning and expression of a novel mouse somatostatin receptor. *FEBS Lett.*, **311**, 290–294.

YAMADA, Y., POST, S.R., WANG, K., TANGER, H.S., BELL, G.I. & SEINO, S. (1992a). Cloning and functional charcterization of a family of human and mouse somatostatin receptors expressed in brain, gastrointestinal tract and kidney. *Proc. Natl. Acad. Sci. U.S.A.*, **89**, 251–255.

YAMADA, Y., REISINE, T., LAW, S., YU, I., KUBOTA, A., KAGIMOTO, S., SEINO, M., SEINO, Y., BELL, G.I. & SEINO, O. (1992b). Somatostatin receptor, an expanding gene family: cloning and functional characterization of human $SSTR_3$, a protein coupled to adenylate cyclase. *Mol. Endocrinol.*, **6**, 2136–2142.

YASUSA, K., RENS-DOMIANO, S., BREDER, S.F., LAW, S.F., CAPER, C.B., REISINE, T. & BELL, G.I. (1992). Cloning of a novel somatostatin receptor, $SSTR_3$ coupled to adenylyl cyclase. *J. Biol. Chem.*, **267**, 20422–20428.

(Received April 8, 1994
Revised June 14, 1994
Accepted June 17, 1994)

Br. J. Pharmacol. (1994), **113**, 635–641 © Macmillan Press Ltd, 1994

Effect of the tachykinin NK_1 receptor antagonists, RP 67580 and SR 140333, on electrically-evoked substance P release from rat spinal cord

Marzia Malcangio & Norman G. Bowery

Department of Pharmacology, the School of Pharmacy, 29/39 Brunswick Square, London WC1N 1AX

1 The effects of the non-peptide tachykinin NK_1 receptor antagonists, RP 67580, SR 140333, CP-96,345 and CP-99,994 have been investigated on electrically-evoked release of substance P-like immunoreactivity (SP-LI) from rat spinal cord slices.

2 RP 67580 (10 nM) and SR 140333 (1 nM), perfused 5 min prior to and during 8 min stimulation of the dorsal roots (20 V, 0.5 ms, 1 Hz), significantly enhanced SP-LI release by 213 ± 43 ($n = 8$) and 203 ± 31 ($n = 5$) % of control evoked release (187 ± 16% of basal outflow, $n = 22$) respectively. Neither compound modified basal outflow of SP-LI (15.3 ± 2.5 fmol/8 ml, $n = 10$).

3 RP 67580 (10 nM) did not modify electrically-evoked release of calcitonin gene-related peptide-LI from rat spinal cord slices.

4 CP-96,345 (10 nM) and CP-99,994 (1 and 10 nM) did not alter electrically-evoked SP-LI release; however, they both inhibited release at 1 μM. Inhibition was also induced by 1 μM RP 67580 but not 1 μM SR 140333.

5 The effect of the NK_1 receptor agonists, [$Sar^9Met(O_2)^{11}$]SP and [Sar^9]SP, could not be tested on SP-LI release due to interference with the substance P radioimmunoassay (RIA). The other NK_1 receptor agonists used, GR 73632, [Pro^9]SP and septide, which did not interfere with the RIA, increased SP-LI basal outflow by 1807 ± 713% ($n = 3$), 1259 ± 160% ($n = 3$) and 620 ± 69% ($n = 3$) at 10 nM, 1 nM and 1 μM, respectively. At the same concentrations, the three agonists also enhanced electrically-evoked SP-LI release by 204 ± 38% ($n = 6$), 753 ± 40% ($n = 3$) and 504 ± 97% ($n = 3$), respectively. The GR 73632 (10 nM)-induced increase in electrically-evoked SP-LI release, was not prevented by SR 140333 (100 nM). None of the agonists inhibited SP-LI release at lower concentrations (0.1 nM GR 73632; 0.01 and 0.1 nM [Pro^9]SP and 1–100 nM septide).

6 NKA and NKB, at concentrations up to 10 nM which did not interfere with the RIA, did not modify electrically-evoked release of SP-LI.

7 The ability of NK_1 receptor antagonists to enhance electrically-evoked SP-LI release supports the concept of an NK_1 autoreceptor control mechanism at substance P nerve terminals within the dorsal horn of the rat spinal cord.

Keywords: SR 140333; RP 67580; substance P; NK_1 receptor; autoreceptor; spinal cord

Introduction

The undecapeptide substance P (SP) is a member of the tachykinin family of peptides. It is widely distributed throughout the mammalian central nervous system (CNS), including the spinal cord where it is highly localized in the superficial layers (Hökfelt *et al.*, 1975). In particular, SP has been identified in small diameter fibres within the dorsal roots of the rat spinal cord that have been shown to terminate within laminae I and II of the dorsal horn (Tuchscherer & Seybold, 1985). Other peptides such as calcitonin gene-related peptide (CGRP) (Wiesenfeld-Hallin *et al.*, 1984), galanin (Skofitsch & Jacobowitz, 1985), somatostatin (Hökfelt *et al.*, 1976), neurokinin A (NKA) (Kanazawa *et al.*, 1984) and dicarboxylic acids like glutamate and D-aspartate (Potashner & Tran, 1984) are also present in mammalian primary afferent terminals. SP appears to coexist with CGRP, galanin (Tuchscherer & Seybold, 1989) and glutamate (Biasi & Rustioni, 1988) in varicosities within the dorsal horn. It is possible that these co-localized agents may interact in the dorsal horn, at both presynaptic and postsynaptic sites, possibly to regulate sensory information transfer at the first CNS synaptic relay (Rusin *et al.*, 1992). For example, it is known that tachykinins and CGRP can increase glutamate release from primary afferent terminals with both peptides inducing a calcium-independent increase of either basal or electrically-evoked release of glutamate *in vitro* (Kawagoe *et al.*, 1986; Kangrga *et al.*, 1990; Kangrga & Randić, 1990). SP has also been reported to increase glutamate release *in vivo* (Smullin *et al.*, 1990). A possible interaction between the peptides contained in primary afferent terminals has also been investigated and CGRP has been reported to increase SP release partly through inhibition of its degradation (Le Greves *et al.*, 1985; Oku *et al.*, 1987). However, no information is available on possible modulation by each peptide of its own release from primary afferent terminals.

We have recently reported that electrical stimulation of the dorsal roots induces a significant and consistent release of endogenous SP from lumbo-sacral horizontal slices of rat spinal cord (Malcangio & Bowery, 1993). SP release was calcium-dependent, tetrodotoxin-sensitive and inhibited by the amino acid neurotransmitter, γ-aminobutyric acid (GABA) through $GABA_B$ receptors (Malcangio & Bowery, 1993). The availability of an experimental system which readily allows the assessment of endogenous SP release, has prompted us to investigate the possible existence of a SP autoreceptor on primary afferent terminals of the rat spinal cord. Tachykinin receptors are currently classified into three types referred to as NK_1, NK_2 and NK_3 (see review by Maggi *et al.*, 1993). Recently, selective and metabolically stable antagonists with high affinity for tachykinin receptors have been developed (see Watling, 1992) and, of these, four have been examined in the present study (Figure 1). CP-96,345

was the first non-peptide NK_1 receptor antagonist to be developed (Snider *et al.*, 1991) and shows higher affinity for NK_1 receptors in guinea-pig and human tissue (pK_i 9.6 ± 0.08 in human IM9 cells, McLean *et al.*, 1993) than in rat and mouse (Watling *et al.*, 1991; Gitter *et al.*, 1991; Beresford *et al.*, 1991; Barr & Watson, 1993). However, this NK_1 receptor antagonist also possesses non-specific effects such as interference with Ca^{2+} mobilization via an interaction with the L-type calcium channel, as shown by its ability to inhibit [^{3}H]-diltiazem binding in rat cerebral cortex (IC_{50} 22.5 nM) (Schmidt *et al.*, 1992; Guard *et al.*, 1993), and depression of voltage-dependent sodium currents in neurones cultured from rat cortex (IC_{50} 18 ± 2 μM at 0.1 Hz, Caeser *et al.*, 1993). A more recent derivative, CP 99,994, has similar affinity for NK_1 receptors in human IM9 cells (pK_i 9.6 ± 0.05), but considerably lower L-type calcium channel blocking activity (IC_{50} 3 μM) (McLean *et al.*, 1993). Furthermore, this antagonist also has lower affinity for the rat caudate (pIC_{50} 6.21 ± 0.05) than for the human caudate/putamen NK_1 receptor (pIC_{50} 8.78 ± 0.07). RP 67580, is another selective non-peptide antagonist at the NK_1 receptor which has been reported to displace, competitively, [^{3}H]-SP binding from rat brain membranes (K_i 4.1 nM) and to antagonize SP-induced contractions of the guinea-pig isolated ileum (pA_2 7.16) (Garret *et al.*, 1991). However, it shows the opposite species specificity to CP-96,345 being selective for the rat NK_1 receptor. Finally, SR 140333, has been reported to be a potent non-peptide NK_1 antagonist both in *in vivo* (Jung *et al.*, 1994) and *in vitro* models and shows no species selectivity (Emonds-Alt *et al.*, 1993).

In this study, we have compared the effects of RP 67580, CP-96,345, CP-99,994 and SR 140333 on electrically-evoked SP-LI release from rat isolated spinal cord. Agonists for tachykinin receptors were also employed (Figure 1) to investigate whether SP can regulate its own release from primary afferent fibres through an autoreceptor control mechanism. One such selective NK_1 receptor agonist used in this study was septide ([pGlu^6,L-Pro^9]SP(6-11); Figure 1), a hexapeptide derivative of the SP C-terminal sequence (Laufer *et al.*, 1986), which shows higher affinity for the NK_1 binding sites in the guinea-pig ileum than for those in the rat brain (Lee *et al.*, 1986).

Methods

Rat spinal cord slice preparation and superfusion

Horizontal spinal cord slices were obtained from adult male Wistar rats (~250 g) as previously described (Malcangio & Bowery, 1993). Briefly, hemisected dorsal lumbosacral slices with attached dorsal roots were cut using a Vibratome (Campden Instruments, London) and mounted in a three-compartment chamber. The tissue was positioned in the central compartment where it was continuously perfused with Krebs solution at 1 ml min^{-1} and the dorsal roots were placed across two pairs of bipolar electrodes and immersed in mineral oil in the lateral compartments. Leak-proof partition barriers of perspex and paraffin grease ensured electrical isolation. After 1 h wash, normal Krebs solution (in mM: NaCl 118, KCl 4, $MgSO_4$ 1.2, KH_2PO_4 1.2, $NaHCO_3$ 25, $CaCl_2$ 2.5 and glucose, 11) was substituted with Krebs solution containing 0.1% bovine serum albumin, 100 μM captopril, 1 μM phosphoramidon, 20 μg ml^{-1} bacitracin and dithiothreitol (6 μM) to prevent metabolic breakdown of SP. Eight-minute fractions were collected in the following order: 3 fractions to measure basal outflow, one fraction to evaluate release following electrical stimulation of 20 V, 0.5 ms, 1 Hz (SP) or 10 Hz (CGRP) either in the absence or presence of drugs and 3 fractions to evaluate recovery to basal levels. It is worth noting that a higher stimulation frequency was necessary to release consistent and significant amounts of

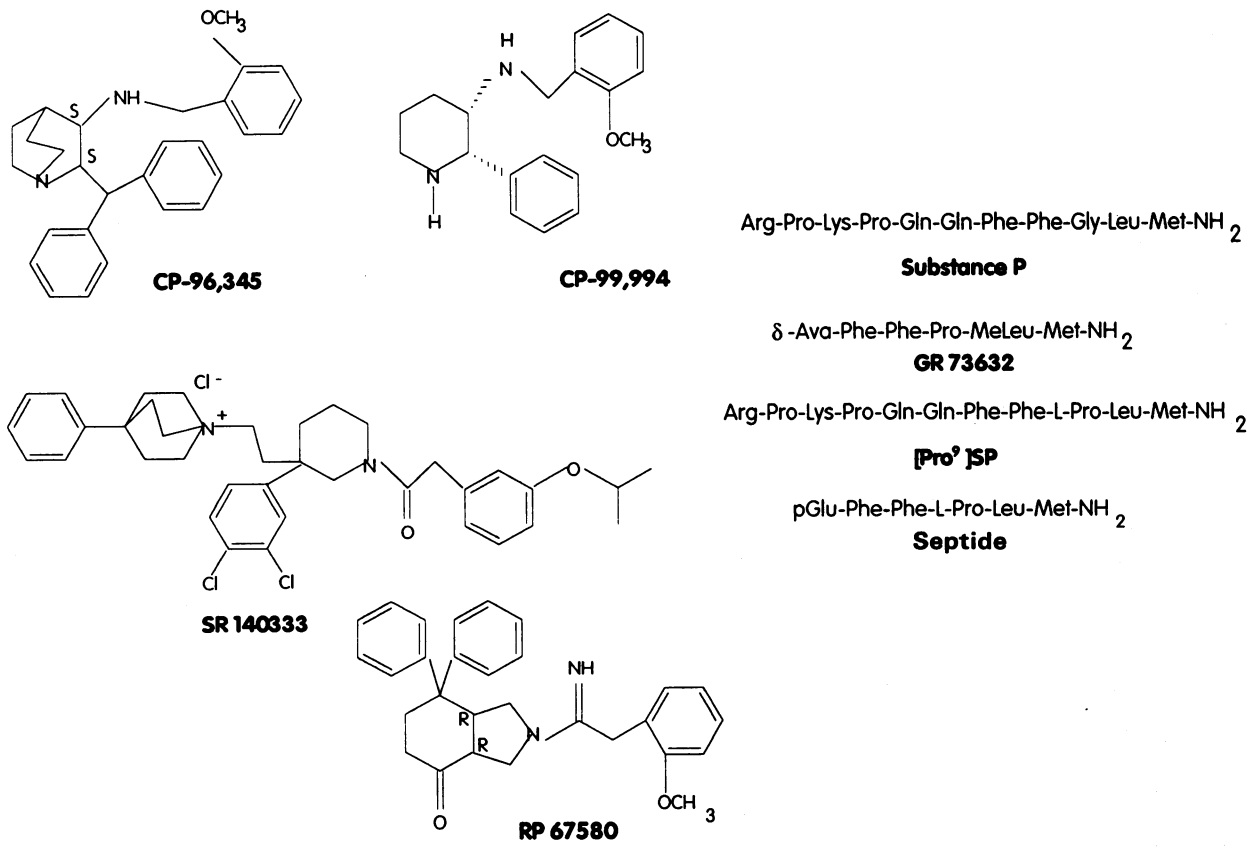


Figure 1 Structure of NK_1 receptor agonists and antagonists used in this study.

CGRP-LI. At the completion of each experiment, the slice was blotted, weighed and extracted. Samples (8 ml volume) were desalted by using 100 mg SEP-PAK C_{18} reverse phase silica gel cartridges (Millipore) as already described for SP (Malcangio & Bowery, 1993). In the case of CGRP, cartridges were treated with 3 ml methanol followed by 6 ml trifluoroacetic acid 0.1% (TFA) and NaCl (3.5 g l^{-1}). Samples were then loaded into the catridge followed by 6 ml TFA:NaCl and 4 ml TFA:methanol (6:4). CGRP was then eluted by using 2 ml methanol. The eluates were dried by evaporation at 55°C under nitrogen and stored at − 80°C until they could be assayed for SP-LI or CGRP-LI content by RIA using the scintillation proximity assay bead technique (Amersham International, UK) (see Malcangio & Bowery, 1993).

SP and CGRP radioimmunoassays (RIA)

In each experiment, RIA standard curves were constructed for SP or CGRP by using known amounts of synthetic peptides ranging between 1 and 100 fmol per tube. The dried samples were resuspended in 300 µl of 50 mM phosphate buffer (pH 7.4) containing bovine serum albumin and 10 mM ethylenediaminetetracetic acid (EDTA) and assayed in amounts of SP immunoreactivity sufficient to place them within the range of the standard curve. SP or CGRP content were measured by using a polyclonal rabbit antiserum specific for the whole SP undecapeptide (Amersham International, UK) or for human CGRP (Peninsula Laboratories, U.S.A.). The incubation mixtures of each assay contained sample or standard (100 µl), tracer containing ~6000 c.p.m. of the isotope (100 µl), diluted antiserum (100 µl) and 50 µl of scintillation proximity assay protein A reagent. All samples were assayed in duplicate. The reaction mixture was vortexed and incubated at room temperature on a shaker for 48 h before being placed in the scintillation-counter.

Most of the compounds used in this study were checked for possible interference with the specific RIA for SP and only concentrations below the assay sensitivity (1 fmol per tube) were employed (Table 1).

Drugs

GR 73632 (δ-Ava-Phe-Phe-Pro-MeLeu-Met-NH_2) was a kind gift of Dr C.C. Jordan, Glaxo Group Research, Hertfordshire, U.K. Peptides were purchased from the following sources: NKA, NKB, [Sar^9]SP,[Sar^{9}Met$(O_2)^{11}$]SP, [Pro^9]SP and septide (Neosystem, Strasbourg, France/SNPE Croydon, U.K.); SP and CGRP (Sigma), CP-96,345 ([2(S,3S)-*cis*-2(diphenylmethyl)-N-[(2-methoxyphenyl)-methyl-1-azabicyclo) 2.2.2)] octan-3-amine and CP 99,994 (+)-(2S,3S)-3-methoxybenzylamino)-2-phenylpiperidine were a gift of Dr Kadin, Pfizer Inc, Groton, U.S.A.; RP 67580 ([3a**R**,7a**R**]-7,7-diphenyl-2-[1-imino-2-(2-methoxyphenyl)-ethyl] perhydroisoindol-4-one) and RP 68651 ([3a**S**,7a**S**] -7,7-diphenyl-2-[1-imino-2-(2-methoxyphenyl)-ethyl]perhydroisoindol-4-one) were kindly provided by Dr C. Garret, Rhône-Poulenc Rorer, Vitry, France; SR 140333 ((S)-1-[2-[3-(3,4-dichlorophenyl)-1-(3-isopropoxyphenylacetyl)-piperidin-3-yl]ethyl]-4-phenyl-1-azoniabicyclo [2.2.2] octane chloride) was kindly supplied by Dr X. Emonds-Alt, Sanofi Recherche, Montpellier, France. [^{125}I]-Bolton Hunter SP, [^{125}I]-CGRP and rabbit antiserum raised against SP (Amersham Internation, UK), rabbit antiserum against CGRP (Peninsula Laboratories, U.S.A.)

[Sar^9]SP, [Sar^{9}Met$(O_2)^{11}$]SP, NKA and NKB were dissolved in dimethylsulphoxide in stock solutions (1 mM) and stored at − 20°C. SP was dissolved in 0.1% acetic acid and stored at − 80°C; [Pro^9]SP, GR 73632 and CGRP were dissolved in water and stored at − 80°C; septide was dissolved in acetic acid 11% and stored at − 80°C. NK_1 receptor antagonists were dissolved in distilled water just before use except for RP 67580 which was previously dissolved in 0.1 M HCl.

Statistical analysis and calculation

Values were calculated as fmol SP-LI released by electrical stimulation after subtraction of basal outflow. Statistical analysis of the data was performed using a non-parametric test (Mann-Whitney U test). Values for Figure 3 and Tables 2 and 4 were calculated according to the formula:

$$100 \times \frac{\text{fmol evoked } (NK_1 \text{ receptor agonist or antagonist}) - \text{fmol (basal)}}{\text{fmol evoked (control)} - \text{fmol (basal)}}$$

Results

Electrical stimulation (20 V, 0.5 ms, 1 Hz) of the dorsal roots for 8 min induced a significant release (210 ± 0.1 fmol μg^{-1} tissue, $n = 10$ $P < 0.01$) of substance P-like immunoreactivity (SP-LI) from rat spinal cord slices, which was approximately twice the basal level (90 ± 0.01 fmol μg^{-1} tissue). This evoked release was Ca^{2+}-dependent and inhibited by tetrodotoxin (1 µM) (Malcangio & Bowery, 1993) (data not shown).

In an attempt to determine whether the amount released

Table 1 Cross-reactivity between substance P (SP), neurokinin A (NKA), NKB and NK_1 receptor agonists and antagonists in the specific radioimmunossay (RIA) for SP

Drug	*Amount added*	*Apparent amount detected as SP*
[Sar^9]SP	1–100 fmol	1–100 fmol
[Sar^{9}Met$(O_2)^{11}$]SP	1–100 fmol	1–100 fmol
[Pro^9]SP	1–100 pmol	0–75 pmol
Septide	1–100 pmol	0–3 pmol
GR 73632	1–100 pmol	0–3.9 pmol
NKA	1–100 pmol	0 pmol
NKB	1–100 pmol	0 pmol
RP 67580	1–100 pmol	0 pmol

SP was used as standard (1–100 fmol per tube) for the RIA.

Table 2 Comparison between the effects of RP 67580, SR 140333, CP-96,345 and CP-99,994 on electrically-evoked substance P-like immunoreactivity (SP-LI) release from rat spinal cord slices

Drug	[nM]	n	*SP-LI release* (% of control evoked release)
RP 67580	1	3	94 ± 13
	3	3	170 ± 59
	10	8	213 ± 43*
	100	4	81 ± 8.5
	1000	6	57 ± 9.8*
SR 140333	0.1	4	154 ± 37
	1	5	203 ± 31*
	10	3	72 ± 25
	100	3	107 ± 36.3
CP-96,345	10	3	92.6 ± 22.4
	1000	3	26.4 ± 7.0*
CP-99,994	1	3	106.8 ± 30.8
	10	3	124 ± 41.7
	100	3	61.6 ± 3.17
	1000	5	50 ± 10.4*

Drugs were perfused 5 min prior to and during 8 min stimulation (20 V, 0.5 ms, 1 Hz). In control slices, electrically-evoked release − basal outflow was 16.8 ± 2.7 fmol per fraction ($n = 22$).
*$P < 0.05$, Mann-Whitney U test.

by stimulation was limited by possible feedback inhibition, the tissue was superfused with the NK_1 receptor antagonist, RP 67580, at concentrations between 1–1000 nM. RP 67580 (10 nM) significantly increased the amount of SP-LI released (Figure 2). This effect was concentration-dependent and also stereospecific since the inactive isomer, RP 68651, was without effect at 10 nM and 100 nM (Figure 3). The concentration-response curve to RP 67580 appeared to be 'bell-shaped' in that concentrations above 10 nM failed to enhance the evoked release of SP-LI. In fact, at 1 μM, a significant inhibition of the evoked release was observed (Figure 3).

The NK_1 receptor antagonist, SR 140333, also induced a significant increase in the electrically-evoked release of SP-LI at concentrations even lower (1 nM) than for RP 67580 (Table 2). However, at no concentration was any inhibition of release detected. The NK_1 receptor antagonist, CP-96,345, at a concentration of 10 nM, failed to modify the evoked release of SP-LI but, like RP 67580, it significantly inhibited release at 1 μM (Table 2). At this concentration and at 100 nM, CP-99,994 also inhibited SP-LI release, whereas it did not modify the release at 1 and 10 nM (Table 2). None of the NK_1 receptor antagonists altered basal outflow of SP-LI at any concentration tested (Table 3).

The enhancement of SP-LI release produced by RP 67580 appeared to be selective in that the evoked release of CGRP-LI was unaltered by the same concentration (10 nM) of the NK_1 receptor antagonist (Figure 4).

To characterize further the modulation of SP release in spinal cord, an attempt was made to investigate the effects of the selective NK_1 receptor agonists, [Sar^9]SP, [Pro^9]SP, [Sar^{9}Met(O$_2$)^{11}]SP, septide and GR 73632. Unfortunately, [Sar^{9}Met(O$_2$)^{11}]SP and [Sar^9]SP interfered with the RIA even at low concentrations (1–100 fmol per tube, Table 1) and could not therefore be used. However, GR 73632, [Pro^9]SP and septide did not appear to interfere with the RIA even at 50–100 pmol/tube and were therefore tested. GR 73632

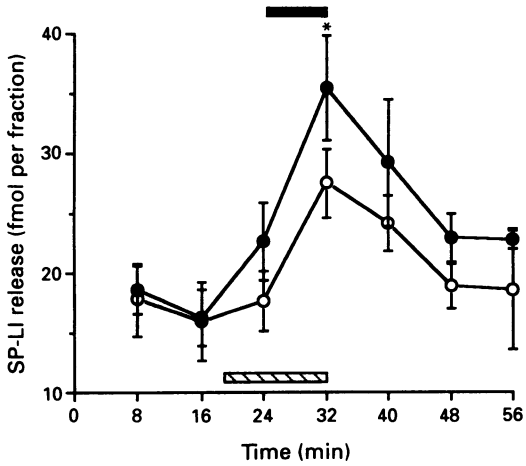


Figure 2 Effect of RP 67580 10 nM (● $n = 3$) on substance P-like immunoreactivity (SP-LI) release from rat spinal cord slices induced by electrical stimulation of the dorsal roots for 8 min (solid horizontal bar) as compared to control slices (○, $n = 3$). Drug was perfused 5 min prior to and during stimulation (hatched horizontal bar). Stimulation parameters were as follows: 20 V, 0.5 ms, 1 Hz. *$P < 0.05$ Mann-Whitney U test.

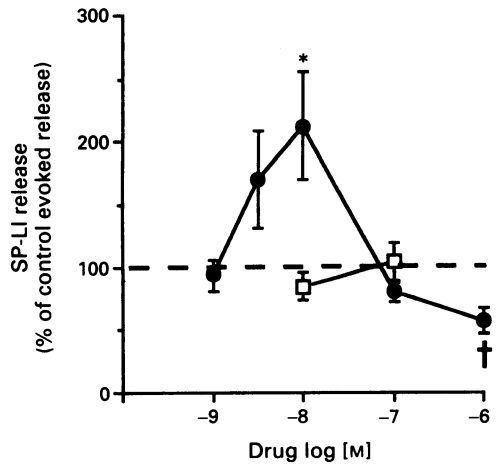


Figure 3 Concentration-dependent increase of electrically-evoked release of substance P-like immunoreactivity (SP-LI) from rat spinal cord slices induced by RP 67580 (●), and lack of effect of RP 68651 (□). Values are mean ± s.e.mean of 4–8 experiments and are calculated according to the formula in the Methods section. Stimulation parameters and drug perfusion were as described in Figure 2. In the absence of drug, stimulated control SP-LI release was 27.5 ± 2.9 fmol per fraction including 15.0 ± 1.2 fmol per fraction of basal outflow, $n = 9$. *$P < 0.05$ RP 67580 versus control, †$P = 0.05$ RP 67580 versus control, Mann-Whitney U test.

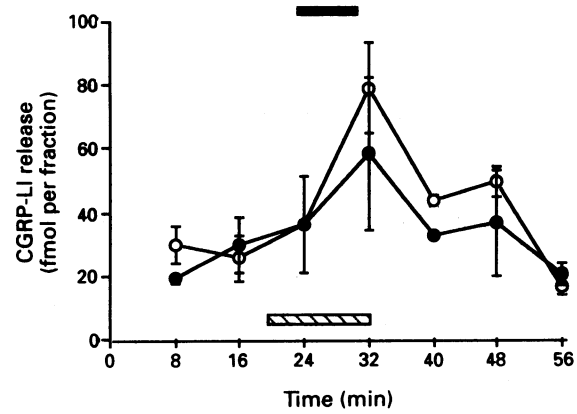


Figure 4 Effect of RP 67580 10 nM (●) on calcitonin gene-related peptide-like immunoreactivity (CGRP-LI) release from rat spinal cord induced by electrical stimulation of the dorsal roots for 8 min (solid horizontal bar) compared to control slices (○). Drug was present 5 min prior to and during stimulation (hatched horizontal bar). Stimulation parameters were as follows: 20 V, 0.5 ms, 10 Hz. Values are means ± s.e.mean of 3 experiments.

Table 3 Comparison of the effects of RP 67580, SR 140333, CP-96,345 and CP-99,994 on substance P-like immunoreactivity (SP-LI) basal outflow from rat spinal cord slices

Drug	[nM]	n	*SP-LI release* (% of control evoked release)
RP 67580	1	3	89.4 ± 12.8
	3	3	102 ± 12.3
	10	8	133.0 ± 18.1
	100	4	135.0 ± 23.5
	1000	6	111.0 ± 14.5
SR 140333	0.1	4	96.6 ± 10.2
	1	5	111.0 ± 6.9
	10	3	100.0 ± 1.0
	100	3	110.0 ± 4.5
CP-96,345	10	3	100.6 ± 6.3
	1000	3	114.3 ± 15.5
CP-99,994	1	3	115.0 ± 4.0
	10	3	112.3 ± 4.3
	100	3	153.0 ± 48.4
	1000	5	126.0 ± 11.5

Drugs were present for 5 min out of 8 min collection period. Basal outflow of SP-LI was 15.3 ± 2.5 fmol per fraction ($n = 10$) in the presence of peptidase inhibitors.

(10 nM), [Pro^9]SP (1 nM) and septide (1 μM) significantly increased the basal outflow of SP-LI in the absence of peptidase inhibitors (Figure 5) and electrically-evoked SP-LI release (Table 4). GR 73632 (10 nM) also induced a significant increase in basal outflow in the presence of peptidase inhibitors (22 ± 5.6 fmol per fraction over basal, $n = 3$, $P < 0.05$) and enhanced electrically-evoked release of SP-LI (Figure 6a and b). However, neither the effects on basal nor electrically-evoked release could be antagonized by SR 140333 (100 nM) (Figure 6b). [Pro^9]SP, perfused at a concentration of 0.01 nM which did not interfere with the RIA or increase SP-LI basal outflow, inhibited ($P = 0.05$) electrically-evoked SP-LI release (Table 4). Higher concentrations of [Pro^9]SP (0.1 and 1 nM) appeared to enhance the release of SP-LI (Table 4) which could be attributed to the apparent increase in basal outflow (Figure 5). Septide, did not modify electrically-evoked SP-LI release in the concentration range 1–100 nM (Table 4). The tachykinins NKA and NKB could be examined at concentrations up to 10 nM without interfering with the RIA. At this concentration, neither modified the electrically-evoked SP-LI release (104 ± 0.5 and 114.5 ± 2.5% of control evoked release, respectively, $n = 3$) or basal outflow (data not shown).

Table 4 Comparison between the effects of GR 73632, [Pro^9]SP and septide on electrically-evoked substance P-like immunoreactivity (SP-LI) release from rat spinal cord slices

Drug	[nM]	n	*SP-LI release* (% of control evoked release)
GR 73632	0.1	4	192 ± 67
	10	6	204 ± 38*
[Pro^9]SP	0.01	4	38 ± 12†
	0.1	2	180
	1	3	753 ± 40
Septide	1	3	121 ± 56
	10	3	97 ± 32
	100	4	219 ± 78
	1000	3	504 ± 97

Drugs were perfused 1 min prior to and during 8 min stimulation (20 V, 0.5 ms, 1 Hz). In control slices, electrically-evoked release – basal outflow was 19.5 ± 2.9 fmol per fraction ($n = 12$).
*$P < 0.05$, †$P = 0.05$, Mann-Whitney U test.

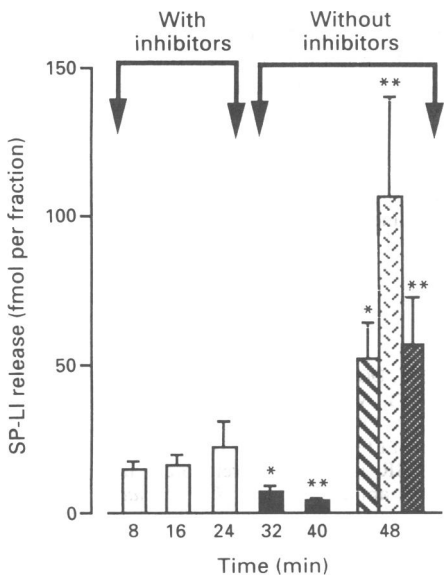


Figure 5 Effect of [Pro^9]SP (1 nM), ( ) GR 73632 (10 nM), ( ) and septide (1 μM) ( ) on basal outflow of substance P-like immunoreactivity (SP-LI) detected in the absence of peptidase inhibitors. Abscissae indicate time at which 8 ml fractions were collected. Open columns represent SP-LI content in presence of peptidase inhibitors which was reduced significantly in the absence of peptidase inhibitors (solid columns). See methods for details of peptidase inhibitors used. $n = 9$ experiments for initial 5 columns and 3 experiments for final 3 columns. *$P < 0.05$, **$P < 0.01$.

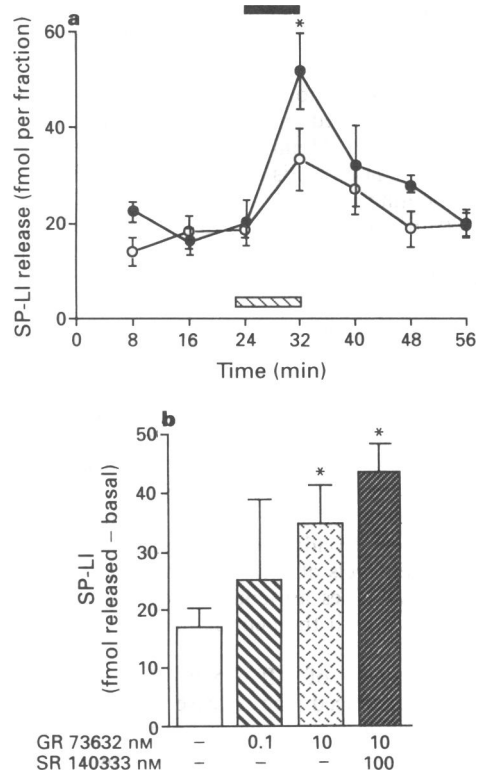


Figure 6 Effect of GR 73632 (10 nM, $n = 6$) (●) on substance P-like immunoreactivity (SP-LI) release from rat spinal cord slices induced by electrical stimulation of the dorsal roots for 8 min (solid horizontal bar). Control slices, $n = 4$ (○). Drug was present 1 min prior to and during stimulation (hatched horizontal bar) (a). Lack of antagonism of GR 73632 (10 mM)-induced increase in SP-LI release by SR 140333 (100 nM) (b). Stimulation parameters were as follows: 20 V, 0.5 ms, 1 Hz. Values are means ± s.e. mean of 3–5 experiments. *$P < 0.05$ Mann-Whitney U test.

Discussion

In the present study, the specific antagonist for the rodent tachykinin NK_1 receptor, RP 67580, but not its inactive isomer RP 68651, dose-dependently increased the electrically-evoked release of SP-LI from rat spinal cord whilst producing no effect on basal SP-LI release. This effect was mimicked by the NK_1 receptor antagonist, SR 140333, which has similar or greater affinity for rat and human NK_1 receptors, but not by CP-99,994 and CP-96,345 which have low affinity for the rodent NK_1 receptor.

RP 67580- and SR 140333-induced increases in electrically-evoked SP-LI release support the concept of an autoreceptor control mechanism through which SP could modulate its own release from primary afferent terminals in the dorsal horn. It has already been suggested that SP, together with CGRP, may regulate glutamate and aspartate release from the same terminals (Kawagoe *et al.*, 1986; Kangrga *et al.*, 1990; Kangrga & Randić, 1990). On this basis, SP and CGRP autoreceptors have been proposed to exist on neuropeptide-containing primary afferent terminals (Levine *et al.*, 1993). Our data now provide evidence for this existence, thus providing a mechanism through which SP could exert a negative feed-back on its own release from primary afferent terminals since the NK_1 receptor antagonists, RP 67580 and

SR 140333, enhanced the release of SP-LI. Unfortunately, we could not demonstrate any inhibition of SP-LI release under our conditions since the available agonists all increased the apparent SP concentration in the perfusates, when used at concentrations reported to be effective in other studies (Petitet *et al.*, 1992; Meini *et al.*, 1994, Lee *et al.*, 1986; Hagan *et al.*, 1991) and this increase was not blocked by the NK_1 receptor antagonists.

RP 67580 did not modify CGRP-LI evoked release suggesting that, if there was any control exerted by endogenous SP on its release from primary afferent fibres, it could not be detected in our system.

The existence of an autoreceptor for SP on primary afferent terminals has previously been excluded on the basis of autoradiographic studies in which binding sites for SP increased in the dorsal horn of neonatally capsaicin-treated rats (Helke *et al.*, 1986). However, any loss of presynaptic sites could be missed by an up regulation of postsynaptic SP binding sites due to the removal of SP innervation and the number of presynaptic sites may be much lower than the postsynaptic levels. In addition, mismatch occurs for SP and its receptor at all levels of the brain and spinal cord and only when receptor subtypes are considered does there appear to be a better match with the peptide distribution (Herkenham, 1987).

The concentrations of RP 67580 (10 nM) and SR 14033 (1 nM) which enhanced the release of SP-LI through a putative presynaptic NK_1 receptor are in the range reported to be effective in *in vitro* models for postsynaptic NK_1 receptor activation (Garret *et al.*, 1991; Oury-Donat *et al.*, 1994). The present results provide no evidence to suggest that the putative autoreceptor and the postsynaptic receptor have different characteristics, but this is an important consideration requiring further study.

The lack of effect of RP 67580 and SR 140333 on basal SP-LI release suggests that there is no SP 'tone' at autoreceptors in the spinal cord, at least under our experimental conditions. The low basal level of SP-LI detected in our system is presumably too low to affect the autoreceptor and just reflects the small amount which is spontaneously released from stores within the tissue. The highest concentrations of RP 67580 and CP-96,345 used in this study inhibited the release of SP and this might be due to an interference with calcium entry into the primary afferent fibre terminals. In fact, it has recently been reported that racemic RP 67580 can inhibit [^{3}H]-diltiazem binding to rabbit skeletal membranes (IC_{50} 290 nM) and depresses high threshold calcium current in neurones cultured from rat cortex (10% inhibition at 10 μM) (Rupniak *et al.*, 1993). Since we know that the electrically-evoked release of SP in our preparation is Ca^{2+}-dependent and can be blocked by tetrodotoxin (Malcangio & Bowery, 1993), it seems reasonable to assume that the inhibitory effect of higher concentrations of RP 67580 (1 μM) is unrelated to SP receptor antagonism, but more to non-specific effects on neurotransmission (Wang *et al.*, 1994). The Ca^{2+}-blocking effect of RP 67580 is shared by the former non-peptide NK_1 receptor antagonist CP-96,345 (Schmidt *et al.*, 1992; Guard *et al.*, 1993). This compound has been shown to interact with L-type calcium channels in rat cerebral cortex membranes and furthermore to block voltage-dependent sodium currents in neurones cultured from rat cortex (Caeser *et al.*, 1993). This latter property might be more of a determinant for the block of SP release since the same effect was also induced by the same concentration of CP-99,994 which possesses less calcium channel-blocking activity than CP-96,345 (McLean *et al.*, 1993).

Experiments with the NK_1 receptor agonists, [Pro^9]SP, GR 73632 and septide, revealed they could greatly increase the basal SP-LI content in the spinal cord perfusion, even at concentrations that did not cross-react with SP antiserum. The fact that they exerted this effect in the absence of peptidase inhibitors to a much greater extent than in their presence, may suggest a possible inhibition of the peptide breakdown. GR 73632 has been suggested to be a metabolically stable NK_1 receptor agonist (Hagan *et al.*, 1991), although this does not exclude the possibility that it itself might inhibit peptidase activity, thus reducing SP degradation.

Modulation of SP-LI release by activation of either NK_2 or NK_3 receptors is unlikely to be responsible since NKA and NKB did not modify SP-LI release. NKB is not contained in the primary afferent terminals (Ogawa *et al.*, 1985) whereas NKA is co-localized with SP-LI and has also been shown to increase glutamate release, from primary afferent terminals (Kangrga *et al.*, 1990). Its lack of effect on SP-LI release could be either attributed to the limited concentration we could use without interfering with the RIA or to an absence of NK_2-mediated modulation of SP-LI release from primary afferent terminals. This last possibility appears most likely in view of the fact that once released, NKA diffuses through the dorsal horn towards the deeper layers of the spinal cord (Duggan *et al.*, 1990), whereas SP remains localized in the substantia gelatinosa (Morton *et al.*, 1990).

In conclusion, we suggest the existence of an NK_1 autoreceptor for SP on primary afferent fibre terminals in the rat spinal cord. Whether this receptor is the same as that which is believed to regulate the release of coexisting transmitters (Levine *et al.*, 1993) remains to be determined.

This study was supported by grant B0196 from the Arthritis and Rheumatism Council.

References

BARR, A.J. & WATSON, S.P. (1993). Non-peptide antagonists, CP-96,345 and RP 67580, distinguish species variants in tachykinin NK_1 receptors. *Br. J. Pharmacol.*, **108**, 223–227.

BERESFORD, I.J.M., BIRCH, P.J., HAGAN, R.M. & IRELAND, S.J. (1991). Investigation into species variants in tachykinin NK_1 receptors by use of the non-peptide antagonist, CP-96,345. *Br. J. Pharmacol.*, **104**, 292–293.

CAESER, M., SEABROOK, G.R. & KEMP, J.A. (1993). Block of voltage dependent sodium currents by the substance P receptor antagonist (±)-CP-96,345 in neurones cultured from rat cortex. *Br. J. Pharmacol.*, **109**, 918–924.

DE BIASI, S. & RUSTIONI, A. (1988). Glutamate and substance P coexist in primary afferent terminals in the superficial laminae of spinal cord. *Proc. Natl. Acad. Soc. U.S.A.*, **85**, 7820–7824.

DUGGAN, A.W., HOPE, P.J., JARROTT, B., SCHAIBLE, H.G. & FLEETWOOD-WALKER, S.M. (1990). Release, spread and persistence of immunoreactive neurokinin A in the dorsal horn of the cat following noxious cutaneous stimulation. Studies with antibody microprobes. *Neuroscience*, **35**, 195–202.

EMONDS-ALT, X., DOUTREMEPUICH, J.-D., HEAULME, M., NELIAT, G., SANTUCCI, V., STEINBERG, R., VILAIN, P., BICHON, D., DUCOUX, J.-P., PROIETTO, V., VAN BROECK, D., SOUBRIÉ, P., LE FUR, G. & BRELIÈRE, J.-C. (1993). In vitro and in vivo biological activities of SR 140333, a novel potent non-peptide tachykinin NK_1 receptor antagonist. *Eur. J. Pharmacol.*, **250**, 403–413.

GARRET, C., CARRUETTE, A., FARDIN, V., MOUSSAOUI, S., PEYRONEL, J.-F., BLANCHARD, J.-C. & LADURON, P.M. (1991). Pharmacological properties of a potent and selective nonpeptide substance P antagonist. *Proc. Natl. Acad. Soc. U.S.A.*, **88**, 10208–10212.

GITTER, B.D., WATERS, D.C., BRUNS, E.F., MASON, N.R., NIXON, J.A. & HOWBERT, J.J. (1991). Species differences in affinities of non-peptide antagonists for substance P receptors. *Eur. J. Pharmacol.*, **197**, 237–238.

GUARD, S., BOYLE, S.J., TANG, K.-W., WATLING, K.J., MCKNIGHT, A.T. & WOODRUFF, G.N. (1993). The interaction of the NK_1 receptor antagonist CP-96,345 with L-type calcium channels and its functional consequences. *Br. J. Pharmacol.*, **110**, 385–391.

HAGAN, R.M., IRELAND, S.J., JORDAN, C.C., BERESFORD, I.J.M., DEAL M.J. & WARD, P. (1991). Receptor-selective, peptidase-resistant agonists at neurokinin NK_1 and NK_2 receptors: new tools for investigating neurokinin function. *Neuropeptides*, **19**, 127–135.

HELKE, C.J., CHARLTON, C.G. & WILEY, R.G. (1986). Studies on the cellular localization of the spinal cord substance P receptors. *Neuroscience*, **19**, 523–533.

HERKENHAM, M. (1987). Mismatches between neurotransmitter and receptor localization in brain: observations and implications. *Neuroscience*, **23**, 1–38.

HÖKFELT, T., ELDE, R., JOHANSSON, O., LUFT, R., NILSSON, G. & ARIMURA, A. (1976). Immunohistochemical evidence for separate populations of somatostatin-containing and substance P-containing primary afferent neurons in the rat. *Neuroscience*, **1**, 131–136.

HÖKFELT, T., KELLERTH, J.-O., NILSSON, G. & PERNOW, B. (1975). Substance P: localization in the central nervous system and some primary sensory neurons. *Science*, **190**, 889–890.

JUNG, M., CALASSI, R., MARUANI, J., BARNOUIN, M.C., SOUILHAC, J., PONCELET, M., GUEDET, C., EMONDS-ALT, X., SOUBRIÉ, J.C., BRELIÈRE, J.C. & LE FUR, G. (1994). Neuropharmacological characterization of SR 140333, a non peptide antagonist of NK_1 receptors. *Neuropharmacol.*, **33**, 167–179.

KANAZAWA, I., TOGAWA, T., SKIMURA, S. & MUNEKATA, E. (1984). Regional distribution of substance P, neurokinin α and neurokinin β in rat central nervous system. *Neurosci. Res.*, **2**, 111–120.

KANGRGA, I. & RANDIĆ, M. (1990). Tachykinin and calcitonin gene-related peptide enhance release of endogenous glutamate and aspartate from the rat spinal dorsal horn slice. *J. Neurosci.*, **10**, 2026–2038.

KANGRGA, I., LAREAU, J.S.A. & RANDIĆ, M. (1990). The effect of substance P and calcitonin-gene-related peptide on the efflux of endogenous glutamate and aspartate from the rat spinal dorsal horn in vitro. *Neurosci. Lett.*, **108**, 155–160.

KAWAGOE, R., ONODERA, K. & TAKEUCHI, A. (1986). The release of endogenous glutamate from the newborn rat spinal cord induced by dorsal root stimulation and substance P. *Biomed. Res.*, **7**, 253–259.

LAUFER, R., GILON, C., CHOREV, M. & SELINGER, Z. (1986). $[pGlu^6, Pro^9]SP_{6-11}$, a selective agonist for the substance P P-receptor subtype. *J. Med. Chem.*, **29**, 1284–1288.

LEE, C.-M., CAMPBELL, N.J., WILLIAMS, B.J. & IVERSEN, L.L. (1986). Multiple tachykinin binding sites in peripheral tissues and in brain. *Eur. J. Pharmacol.*, **130**, 209–217.

LE GREVES, P., NYBERG, F., TERENIUS, L. & HÖKFELT, T. (1985). Calcitonin-gene-related peptide is a potent inhibitor of substance P degradation. *Eur. J. Pharmacol.*, **115**, 309–311.

LEVINE, J.D., FIELDS, H.L. & BASBAUM, A.I. (1993). Peptides and the primary afferent nociceptor. *J. Neurosci.*, **13**, 2273–2286.

MAGGI, C.A., PATACCHINI, R., ROVERO, P. & GIACHETTI, A. (1993). Tachykinin receptors and tachykinin receptor antagonists. *J. Autonom. Pharmacol.*, **13**, 23–93.

MALCANGIO, M. & BOWERY, N.G. (1993). γ-Aminobutyric $Acid_B$, but not γ-Aminobutyric $Acid_A$ activation, inhibits electrically evoked substance P-like immunoreactivity release from the rat spinal cord in vitro. *J. Pharmacol. Exp. Ther.*, **266**, 1490–1496.

MCLEAN, S.R., GANOG, A., SEYMOUR, P.A., SNIDER, R.M., DESAI, M.C., ROSEN, T., BRYCE, D.K., LONGO, K.P., REYNOLDS, L.S., ROBINSON, A.W., SCHMIDT, A.W., SIOK, C. & HEYM, J. (1993). Pharmacology of CP 99,994: a non peptide antagonist of the tachykinin NK_1 receptor. *J. Pharmacol. Exp. Ther.*, **267**, 472–479.

MEINI, S., PATACCHINI, R. & MAGGI, C.A. (1994). Tachykinin NK_1 receptor subtypes in the rat urinary bladder. *Br. J. Pharmacol.*, **111**, 739–746.

MORTON, C.R., HUTCHINSON, W.D., DUGGAN, A.W. & HENDRY, I.A. (1990). Morphine and substance P release in the spinal cord. *Exp. Brain Res.*, **80**, 89–96.

OGAWA, T., KANAZAWA, I. & KIMURA, S. (1985). Regional distribution of substance P, neurokinin A and neurokinin B in rat spinal cord, nerve roots and dorsal root ganglia, and the effects of dorsal root section on spinal transection. *Brain Res.*, **359**, 152–157.

OKU, R., SATOH, M., FUJU, N., OTAKA, A., YAJIMA, H. & TAKAGI, H. (1987). Calcitonin-gene-related peptide promotes mechanical nociception by potentiating release of substance P from the spinal dorsal horn in rat. *Brain Res.*, **403**, 350–354.

OURY-DONAT, F., LEFEVRE, I.A., THURNEYSSEN, O., GAUTHIER, T., BORDEY, A., FELTZ, P., EMONDS-ALT, X., LE FUR, G. & SOUBRIÉ, P. (1994). SR 140333, a novel, selective and potent non peptide antagonist of the NK_1 tachykinin receptor: characterization on the U373MG cell line. *J. Neurochem.*, (in press).

PETITET, F., SAFFROY, M., TORRENS, Y., LAVIELLE, S., CHASSAING, G., LOEUILLET, D., GLOWINSKI, J. & BEAUHOUAN, J.C. (1992). Possible existence of a new tachykinin receptor subtype in the guinea-pig ileum. *Peptides*, **13**, 383–388.

POTASHNER, S.J. & TRAN, P.L. (1984). Decreased uptake and release of D-aspartate in the guinea-pig spinal cord after dorsal root section. *J. Neurochem.*, **42**, 1135–1144.

RUPNIAK, N.M.J., BOYCE, S., WILLIAMS, A.R., COOK, G., LONGMORE, J., SEABROOK, G.R., CAESAR, M., IVERSEN, S.D. & HILL, R.G. (1993). Antinociceptive activity of NK_1 receptor antagonists: non-specific effects of racemic RP 67580. *Br. J. Pharmacol.*, **110**, 1607–1613.

RUSIN, K.I., RYU, P.D. & RANDIĆ, M. (1992). Modulation of excitatory amino acid responses in rat dorsal horn neurons by tachykinins. *J. Neurophysiol.*, **68**, 265–286.

SCHMIDT, A.W., MCLEAN, S.R. & HEYM, J. (1992). The substance P receptor antagonist CP-96,345 interacts with Ca^{2+} channels. *Eur. J. Pharmacol.*, **219**, 491–492.

SKOFITSCH, G. & JACOBOWITZ, D.M. (1985). Galanin-like immunoreactivity in capsaicin sensitive sensory neurons and sensory ganglia of the rat. *Peptides*, **6**, 747–754.

SMULLIN, D.H., SKILLING, S.R. & LARSON, A.A. (1990). Interaction between substance P, calcitonin gene-related peptide, taurine and excitatory amino acids in the spinal cord. *Pain*, **42**, 93–101.

SNIDER, R.M., CONSTANTINE, J.W., LOWE III, J.A., LONGO, K.P., LEBEL, W.S., WOODY, H.A., DROUZDA, S.E., DESAI, M.C., VINICK, F.J., SPENCER, R.W. & HESS, H.-J. (1991). A potent nonpeptide antagonist of the substance P (NK_1) receptor. *Science*, **251**, 435–437.

TUCHSCHERER, M.M. & SEYBOLD, V.S. (1985). Immunohistochemical studies of substance P, cholecystokinin-octapeptide and somatostatin in dorsal root ganglia of the rat. *J. Neurosci.*, **14**, 593–605.

TUCHSCHERER, M.M. & SEYBOLD, V.S. (1989). A quantitative study of the coexistence of peptides in varicosities within the superficial laminae of the dorsal horn of the rat spinal cord. *J. Neurosci.*, **9**, 195–205.

WANG, Z.-Y., TUNG, S.R., STRICHARTZ, G.R. & HÅKANSON, R. (1994). Non-specific actions of the non-peptide tachykinin receptor antagonists, CP-96,345, RP 67580 and SR 48968, on neurotransmission. *Br. J. Pharmacol.*, **111**, 179–184.

WATLING, K.J. (1992). Nonpeptide antagonists herald new era in tachykinin research. *Trends Pharmacol. Sci.*, **13**, 266–269.

WATLING, K.J., GUARD, S., HOWSON, W. & WALTON, L. (1991). Inhibition of binding to tachykinin NK_1 receptor sites in rat, guinea-pig and human brain by the non-peptide antagonist (±)-CP 96,345. *Br. J. Pharmacol.*, **104**, 28P.

WIESENFELD-HALLIN, Z., HÖKFELT, T., LUNDBERG, J.M., FORSSMANN, W.G., REINECKE, M., TSCHOPP, F.A. & FISCHER, J.A. (1984). Immunoreactive calcitonin gene-related peptide and substance P coexist in sensory neurons to the spinal cord and interact in spinal behavioural responses of the rat. *Neurosci. Lett.*, **52**, 199–204.

(Received January 28, 1994
Revised May 25, 1994
Accepted June 16, 1994)

Br. J. Pharmacol. (1994), **113**, 642–648

© Macmillan Press Ltd, 1994

In vitro potency and mode of action of ANQ9040: a novel fast acting muscle relaxant

[1]G. Lees, I.T. Munday, M.D. Edwards & R.M. Jones

Department of Anaesthetics, Imperial College of Medicine, (St Mary's Hospital Medical School), London W2 1NY

1 The *in vitro* potency and mode of action of the novel, rapid-onset steroidal relaxant ANQ9040 were characterized in the rat isolated phrenic nerve hemidiaphragm.

2 At 32°C, ANQ9040 antagonized neurally evoked contractures with EC_{50}s of 21.5 μM for unitary twitches; 14.4 μM for 2 Hz 'trains of four'; and 7.5 μM for 50 Hz (2 s) tetanic stimulus trains.

3 (+)-Tubocurarine was 22–24 times more potent than ANQ9040 in comparative organ bath experiments.

4 Intracellular recording from endplates revealed that ANQ9040 (0.53–10.0 μM) dose-dependently and reversibly decreased the amplitude of miniature-endplate potentials (IC_{50} of *circa* 0.95 μM) without changing transmembrane potential.

5 Surmountable antagonism of subthreshold responses to exogenous (ionophoretic) acetylcholine provided evidence for a non-depolarizing and competitive blockade of post-junctional nicotinic receptors.

6 Sucrose gap recordings of phrenic nerve action potentials revealed that, at concentrations up to 32 μM, ANQ9040 produced no tonic or frequency-dependent antagonism of axonic Na^+ channels.

7 We conclude that ANQ9040 is a relatively low-affinity, non-depolarizing, nicotinic antagonist. The *in vitro* results are discussed in relation to factors impinging on relaxant kinetics and current models for frequency-dependent fade.

Keywords: ANQ9040; (+)-tubocurarine; acetylcholine; nicotinic; electrophysiology; mode-of-action; rat hemidiaphragm; phrenic-nerve; endplate; muscle-relaxant

Introduction

ANQ9040, or 3-β-(1′-hexamethyleneiminomethyl)-3-α-acetoxy-17a-methyl-17a-aza-D-homo-5-α-androstane 17a-*N*-methyl besylate, is a novel steroidal muscle relaxant with a rate of onset in humans comparable to the depolarizing blocker, suxamethonium (Munday *et al.*, 1992). However, at twice the ED_{95} in a volunteer study it resulted in tachycardia and hypotension as a result of consistent and significant histamine release (Munday *et al.*, 1994). Such a steep dose-dependent toxicological response to steroidal relaxants is unusual but led to the withdrawal of the drug from further clinical assessment. Because of its promising kinetic profile we have examined both its potency and mode-of-action *in vitro*. The rat hemidiaphragm-phrenic nerve preparation was selected for these studies because it has been used extensively for both pharmacodynamic characterization and bioassay of a broad range of relaxant molecules. Data from such experiments can be obtained at steady-state for known drug concentrations in the absence of complicating pharmokinetic factors.

The rate of onset of non-depolarizing relaxants is inversely related to their potency at equilibrium (Bowman *et al.*, 1988b; Kopman, 1989). In contrast depolarizing relaxants (which do not need to deplete endplate receptor reserve) block rapidly as a consequence of agonist actions at the nicotinic receptor: the fulminant increase in cation conductance results in transient fasciculations and ultimately the blocking action may be secondary to localized inactivation of voltage-gated sodium channels (Delisle Burns & Paton, 1951; Zaimis & Head, 1976). Most nicotinic antagonists induce frequency-dependent fade in twitch tension. The extent of this tetanic fade is clearly structure-dependent and is virtually absent for toxiferine VI and bungarotoxin (Gibb & Marshall, 1986; 1987). Postsynaptic responses to ionophoretic acetylcholine do not exhibit fading in the presence of relevant concentrations of tubocurarine. This has led to the suggestion that the phenomenon reflects blockade of prejunctional nicotinic autoreceptors which promote transmitter release under physiological conditions (Bowman *et al.*, 1990) rather than postsynaptic channel block reported for tubocurarine at higher concentrations (Lambert *et al.*, 1983; Gibb & Marshall, 1987). Frequency- or use-dependence is an acknowledged property of certain drugs or toxins (Usherwood *et al.*, 1984) which are classified as 'open channel blockers' (reviewed by Hille, 1984). Experiments with CNS neurones and cell lines have demonstrated that selective depression of burst firing by anticonvulsants (Lees & Leach, 1993) reflects frequency-dependent antagonism of voltage-gated sodium currents (Lang *et al.*, 1993). As well as clinically useful anticonvulsants, class I anti-arrhythmics and local anaesthetics also perturb the sodium channel in a similar frequency-, voltage- and state-dependent manner (Catterall, 1987). For the first time we have characterized the *in vitro* potency of ANQ9040 and compared it with (+)-tubocurarine in organ bath experiments. We have used electrophysiology to determine the mode of action of the compound and seek pharmacodynamic factors which may underpin its promising kinetic profile. In addition experiments on phrenic nerve have been conducted to assess the speculative possibility that tetanic fade produced by this drug may reflect a frequency-dependent inhibition of axonal Na^+ channels.

Methods

Tension recording

Left hemidiaphragms were isolated from male Sprague-Dawley rats (250–300 g) and mounted, together with the phrenic nerve, in an organ bath. Preparations were bathed in

[1] Author for correspondence.

Krebs-Henseleit solution of the following composition (mM): NaCl 118, KCl 5, $CaCl_2$ 2.5, $NaHCO_3$ 25, KH_2PO_4 1, $MgCl_2$ 1 and (+)-glucose 11, maintained at 32.1°C (s.e. 0.02°) and pH 7.4 when equilibrated with 95% O_2 and 5% CO_2. The phrenic nerve was stimulated with bipolar silver electrodes using 0.2 ms pulses of 10–12 V (greater than 2 × intensity for maximal response) delivered from a Grass stimulator and isolation unit. Tension was recorded under semi-isometric conditions with a Grass (FT03) transducer connected to a Gould chart recorder. Throughout the experiments, trains of four (2 Hz) were delivered every 12 s but tetanic stimulation (50 Hz train for 2 s) was used only after 60 min exposure to drugs or treatment blanks (to avoid prolonged periods of post-tetanic changes in contractility encountered in the absence of relaxants).

Twitch tension (T_1 in the train of four) was measured as a percentage of control. Train of four fade (at steady state) and tetanic-fade (in response to the first 50 Hz train after treatment) were calculated by standard methods (Gibb & Marshall, 1986). Each preparation was exposed to a single drug at one concentration and each concentration was tested in 3–4 preparations. Sigmoid log dose-response curves were produced by fitting raw data by non-linear regression to a three term logistic function using a maximum-likelihood method ('Inplot' and 'MLP' software) to calculate EC_{50}s (and confidence limits) for each of the parameters measured.

Electrophysiology

Intracellular recordings 1 cm strips of diaphragm were mounted in rapidly flowing (circa 5 ml min^{-1}) oxygenated Krebs-Henseleit solution at room temperature, 22–24°C. Endplates were visible under dissecting optics using transmitted light following gentle lateral and longitudinal stretching of the fibres; 15–30 MΩ electrodes (Mecanex BBCH puller) backfilled with 3 M KCl were placed over the endplates (Narishige M0203 manipulators) and following impalement, resting membrane potentials and miniature endplate potentials (m.e.p.ps) were monitored (via WPI 767 pre-amp). Cells with resting membrane potentials which were unstable or less negative than − 65 mV were not used for pharmacological studies. Pulses of ionophoretic acetylcholine (0.2–1 s, 1 M) resulting in subthreshold depolarizations were delivered from a second microelectrode adjacent to the impaled fibre within 10 μm of the endplate. Data were recorded real-time on a Gould brush recorder and on a tape recorder (Racal Store Four) for analysis off-line using a CED (1401) A/D converter, a PC, and 'Scan' software (kindly provided by John Dempster, University of Strathclyde).

Mannitol gap recordings 1–2 cm of phrenic nerve was isolated and draped through a series of perspex chambers and sealed in with vaseline. The cut-end and the reference electrode were immersed in isotonic KCl, which was separated from the test chamber and recording electrode by a non-conducting gap filled with rapidly flowing isotonic mannitol. Oxygenated Krebs-Henseleit saline (above) was again used in the test chamber. Rectangular pulses (0.2 ms) were applied with bipolar silver electrodes to evoke compound action potentials at 0.1–50 Hz. Evoked signals were monitored with a WPI electrometer and digitized real time (CED 1401: 25–30 kHz) for display and analysis with SCAN software. All reported pharmacological responses were observed in a minimum of four preparations unless otherwise stated.

Drugs

Solutions of ANQ9040 (Anaquest) were freshly prepared each day in 0.3% acetic acid and diluted 1:500 to achieve the stated concentrations in buffered saline. (+)-Tubocurarine chloride (Sigma) was dissolved in purified water and formulated using the 1:500 dilution factor. A total of nine control experiments were conducted using these vehicles as blanks but produced no significant effects on the parameters reported here. All other drugs and reagents were from Sigma or BDH.

Results

Twitch tension: potency and frequency-dependence

In a total of 58 preparations, pretreatment twitch tension ranged from 7.8–32.3 g: mean, 15.3 g and s.e. 0.55 g. In all treatment blanks ($n = 9$) twitch tension (and the TOF response) was stable for 60 min: at this time application of a tetanic stimulus did not result in fade in any of these drug-free preparations. Sixty minutes exposure was sufficient to achieve equilibrium with both (+)-tubocurarine and ANQ 9040 (assessed by continuous monitoring of TOF responses). Steady-state concentration-effect relationships are shown in Figure 1 for the three stimulus parameters. EC_{50} values determined from these curves, relative potencies and twitch: fade ratios were given in Table 1. ANQ9040 was consistently less potent (22–24 fold) than (+)-tubocurarine. Both drugs were more potent at higher stimulus frequencies but ANQ9040 and (+)-tubocurarine produced similar degrees of tetanic fade. Neither drug produced fasciculations, spontaneous contractures or consistent/dose-dependent change in muscle tone.

Intracellular recording

Resting membrane potentials typically ranged from − 65 to − 75 mV and were stable for up to 45 min. Proximity to endplates was assessed from the 5–95% rise times (< 1.2 ms) of m.e.p.ps which typically ranged in amplitude between 0.25–2.0 mV. By averaging 100–150 of these (at steady-state) before, during and after drug application we were able to monitor and quantify the effects of ANQ9040. The drug reversibly and dose-dependently depressed the amplitude of m.e.p.ps with an IC_{50} of circa 0.95 μM (Figure 2) without changing the transmembrane potential in the endplate region. M.e.p.p. frequency and kinetics were not overtly altered by the compound although this was not analysed in detail. Subthreshold depolarizations (1–15 mV) in response to exogenous acetylcholine were reversibly depressed but could be restored by raising the ionophoretic ejection current or its duration. This apparently-competitive antagonism (Figure 3) was effected with almost identical onset and recovery kinetics to the depression of tonic synaptic events described above.

Phrenic nerve sodium spikes

Compound phrenic-nerve action potentials (CAP) of 25–35 mV in amplitude and 0.3–0.75 ms duration (at half-height) could be monitored in the mannitol gap for periods in excess of 90 min. In control oxygenated saline the CAP was stable throughout 2 s stimulus trains at 0.5–50 Hz. Pilot experiments using 1 μM tetrodotoxin (Figure 4a, $n = 2$) and 500 μM lignocaine (not shown, $n = 2$) resulted in a significant tonic block (0.1 Hz) of these axonic spikes. In contrast, 45 min exposure to concentrations of 18 μM ($n = 2$) to 32 μM ANQ 9040 produced no demonstrable tonic (Figure 4b) or frequency-dependent block (Figure 4c) of the CAP in ensheathed nerve trunks.

Discussion

In vivo studies with ANQ9040 in animals (Anaquest unpublished data) and man (Munday *et al.*, 1994) describe a blocking action without transient contractures/fasciculations which could be reversed with anticholinesterases, featuring train-of-four fade: all characteristic features of non-depolarizing nicotinic antagonists. Our *in vitro* results are consistent with

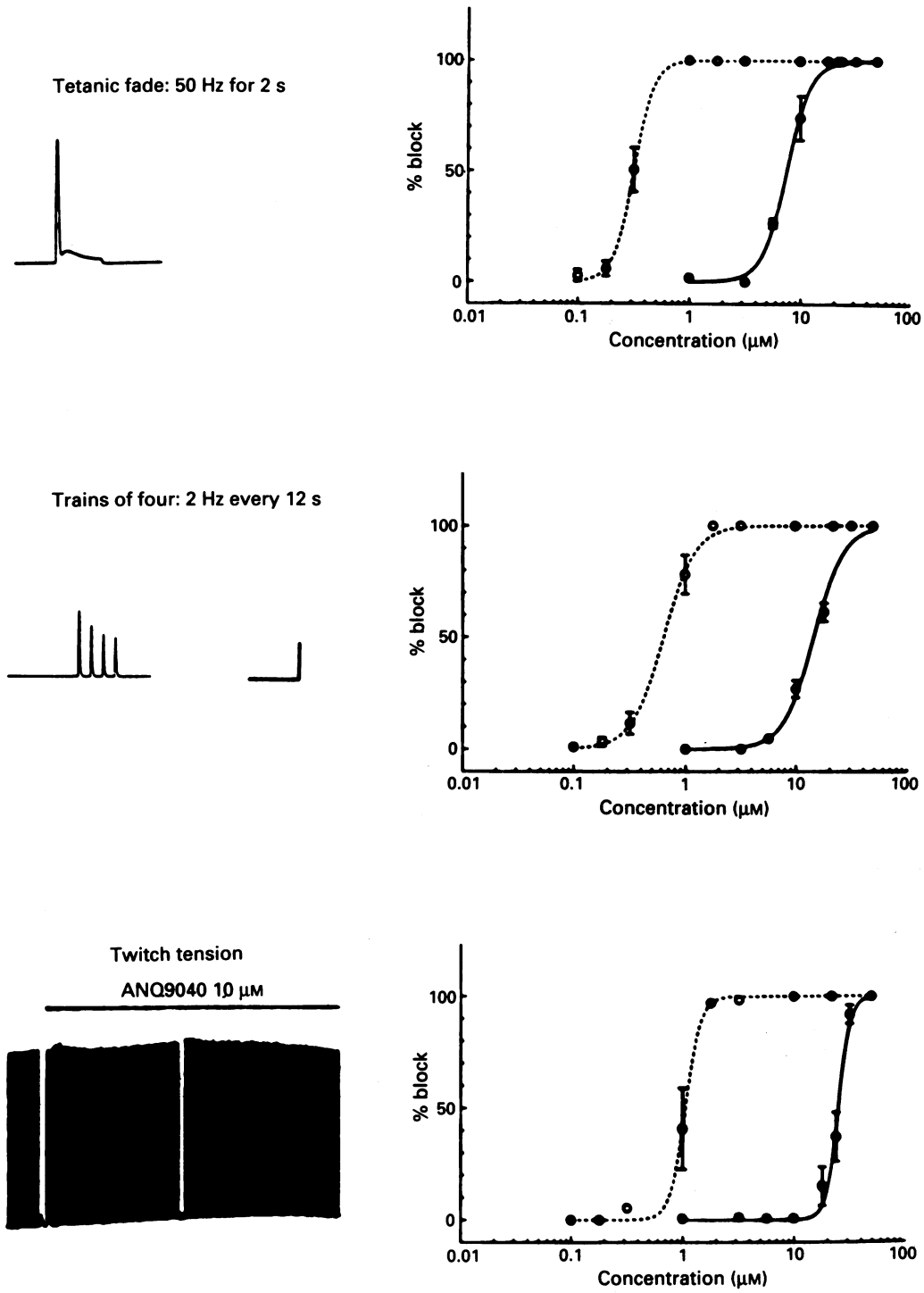


Figure 1 Frequency-dependent fade and comparative potency of ANQ9040 and (+)-tubocurarine. Left column: illustration of frequency-dependent fade after equilibration with ANQ9040 at 10 μM. The compound did not notably change the amplitude of T_1, the first twitch in a train of four, (depicted in the compressed lower trace: scale bars; 3 g, 10 min). After 60 min exposure, in the same hemidiaphragm, the compound induced marked train of four fade and almost complete tetanic fade (scale bars; 7.5 g, 2 s) in this representative illustration. Right column: dose-effect plots for the three parameters: mean ± s.e. (+)-Tubocurarine (○); ANQ9040 (●). Note the relatively low potency of ANQ9040 and the marked left-shift in curves for both compounds as stimulus frequency is increased.

Table 1 EC_{50} values (μM) for neuromuscular blockade in rat diaphragm

	Tetanic fade	*TOF fade*	*Twitch block*	*Twitch: Fade ratio*
(+)-Tubocurarine	0.32 (0.297–0.342)	0.64 (0.553–0.744)	1.06 (0.940–1.196)	3.3
ANQ9040	7.55 (6.879–8.292)	14.35 (13.43–15.34)	25.06 (23.88–26.30)	3.3
Relative potency	× 24 (21.21–26.45)	× 22 (19.22–26.10)	× 24 (20.93–26.71)	

Figures in parentheses denote 95% confidence intervals.

these observations and confirm that the steroid depresses excitation-contraction coupling by an apparently competitive action at endplate receptors. It is notable that effective concentrations (as well as onset and recovery kinetics) for suppression of m.e.p.ps or subthreshold depolarizations produced by ionophoretic acetylcholine were comparable which suggests a predominantly postsynaptic locus for these tonic effects. The apparent EC_{50} for m.e.p.p. suppression (0.95 μM) was considerably lower than concentrations required to effect depression of twitch tension regardless of stimulus frequency.

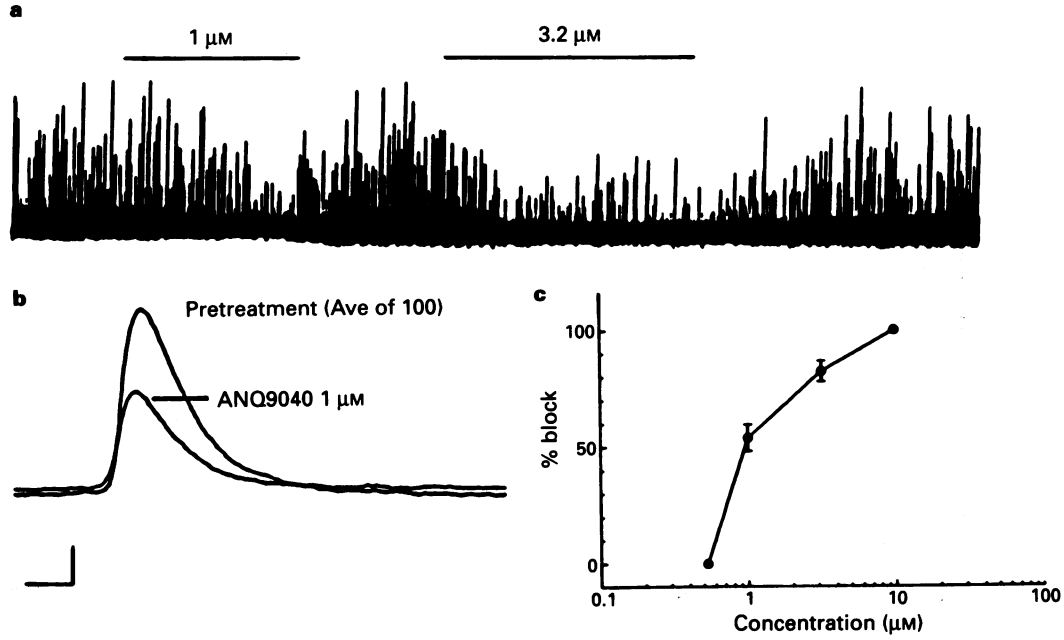


Figure 2 ANQ9040 and miniature endplate potentials (m.e.p.ps). (a) a.c.-coupled high gain recording of m.e.p.ps before, during and after ANQ9040 at the indicated concentrations. The consistent dose-dependent reduction of m.e.p.p. amplitude was not associated with notable changes in postsynaptic membrane potential or m.e.p.p. frequency. Calibration: 0.5 mV, 2 min. (b) Averaged data (100 m.e.p.ps aligned by their maximum rate of rise) from the cell depicted in (a) before and after equilibration with ANQ9040 at 1 μM. Calibration: 0.15 mV, 1.7 ms. (c) Compounded data from a total of 17 similar experiments (mean ± s.e.) suggests that ANQ9040 depressed m.e.p.p. amplitude with an IC_{50} of 0.95 μM.

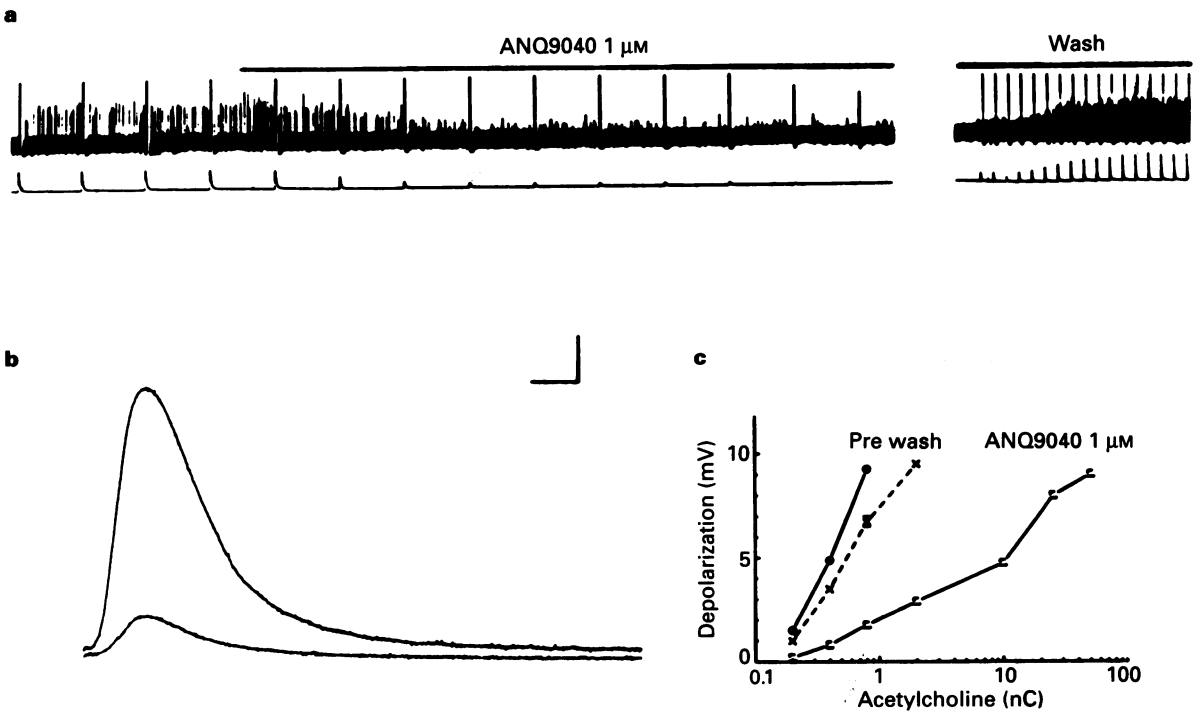


Figure 3 ANQ9040 and ionophoretic acetylcholine. (a) Superimposed high gain, a.c.-coupled m.e.p.ps (upper traces: calibration; 0.25 mV, 24 ms) and d.c. recording of depolarizations (cal.: 5 mV) evoked by 100 ms pulses of acetylcholine from the same cell. Both were markedly depressed by ANQ9040 with similar kinetics of onset and recovery (compressed inset: cal 2 min). (b) Higher gain recordings showing steady-state depression of responses to exogenous acetylcholine in a different preparation (2 mV, 150 ms). (c) Ionophoretic dose-response plot from the cell in (a) showing that the reversible antagonistic action could be overcome by increasing agonist ejection current or duration.

This reflects, in part, the significant nicotinic 'receptor reserve' at the endplate although this is insufficient to account for the drastic shift observed in the dose-effect plots. This rightward shift is further evidence for competition with acetylcholine in the synaptic cleft: evoked-release synchronously liberates >200 quanta from neurotransmitter pools whereas m.e.p.ps are associated with the release of single quanta (Del Castillo & Katz, 1954).

ANQ9040, like (+)-tubocurarine, produced significant degrees of TOF and tetanic fade and was more potent at higher

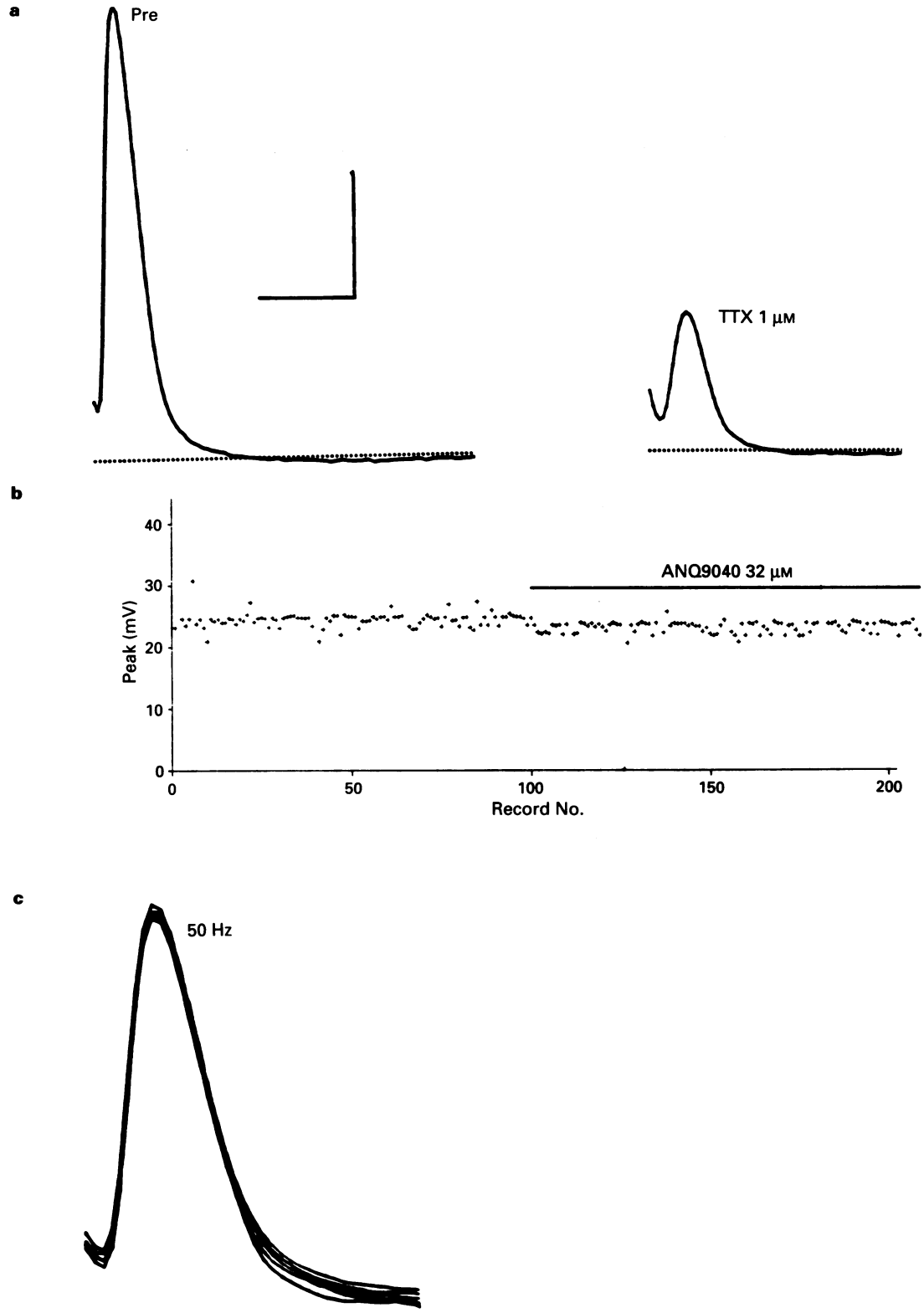


Figure 4 Phrenic nerve action potentials. (a) Typical recording of the compound action potential, inverted for clarity, illustrating the depressant effect of 1 μM tetrodotoxin (right) in this partially desheathed preparation. Dotted line indicates pre-stimulus resting potential. Calibration: 10 mV, 2 ms. (b) Amplitude of evoked spikes plotted in control saline and after equilibration (20 min) with 32 μM ANQ9040 in a typical cell. Even at this high concentration, no tonic block of the compound action potential was produced. (c) Six superimposed sweeps sampled throughout a 2 s/50 Hz stimulus train, after 45 min exposure to 32 μM ANQ9040. No significant fading was observed which might account for frequency-dependent fade in twitch tension. Calibration: 10 mV, 0.75 ms.

stimulus frequencies. Our experiments suggest that this does not reflect frequency-dependent depression of sodium spikes in the phrenic nerve. These observations were made in sheathed nerve trunks, to reflect the organ bath experiments, so the concentrations of the polar molecule cited are not indicative of those at the axon plane. No elegant vertebrate preparations are yet available to examine potential for use-dependent antagonism of either voltage-gated Na^+ or Ca^{2+} channels in more-exposed terminal membranes closely apposed to presumptive sites for transmitter release. Voltage/use-dependent channel block of nicotinic receptors has been documented for a variety of structurally diverse relaxants (Gibb & Marshall, 1987) including (+)-tubocurarine (Lambert *et al.*, 1983). The relatively high doses required to effect postsynaptic channel block cannot account for the 'generic' phenomenon of frequency-dependent fade in response to potent curareform relaxants (Gibb & Marshall, 1987) but may contribute to the effects of certain drugs like hexamethonium (Gibb & Marshall, 1986) or trimethaphan (Gibb & Marshall, 1982). The potential contribution of frequency-dependent nicotinic channel block to the fade produced by ANQ9040 has not yet been examined under voltage-clamp conditions. Fade on recovery in clinical studies was cited as 'unremarkable' (Munday *et al.*, 1994) but effects of cholinesterase inhibition (which one would expect to enhance use-dependent fade/open-channel block) were not noted. Presynaptic nicotinic receptors may facilitate mobilisation of transmitter under high-frequency discharge and their antagonism, concurrently with erosion of postsynaptic receptor reserve, has been proposed as a mechanism for tetanic fade (Bowman *et al.*, 1988a). This hypothesis encompasses the distinct pharmacology of nicotinic drugs and toxins which elicit differing degrees of fade (or none at all). Twitch to fade ratios were identical for ANQ9040 and (+)-tubocurarine. In the absence of evidence on potential for channel block, this could be interpreted as evidence that the two relaxants have similar selectivities for such presumptive presynaptic autoreceptors. However, as previously discussed (Gibb & Marshall, 1986), a more rigorous way to quantify propensity to produce fade is to compare tetanic fade with suppression of peak tetanic tension (not determined in this study).

In human volunteers at a dose of 2.6 mg kg^{-1} ($2 \times ED_{95}$), ANQ9040 (Munday *et al.*, 1994) had an onset of action at least as fast as succinylcholine 1 mg kg^{-1} (see Ferguson & Bevan, 1981). These clinically promising kinetic features appear to reflect the relatively low potency of this molecule rather than any unique pharmacodynamic actions. No consistent or dose-dependent changes in basal tension or resting membrane potential were seen to suggest depolarizing or desensitizing block (secondary to agonist or partial agonist activity for the steroid). Our organ bath experiments confirm in the absence of potential contributory pharmacokinetic factors that ANQ9040 is a low-potency antagonist of twitch tension in comparison with (+)-tubocurarine. EC_{50}s determined for (+)-tubocurarine are very similar to those previously published using the same preparation under identical assay conditions (Gibb & Marshall, 1986). Related bioassay data (Gibb & Marshall, 1987) permits the ranking of *in vitro* EC_{50}s for twitch depression (μM), at steady state, in order of decreasing potency: (+)-tubocurarine, 1.1 (1.4, Gibb & Marshall, 1986); pancuronium, 4.2; vecuronium, 7.5; ANQ9040, 25.1. Different methods are used to compare relaxant potency in patients but an appropriate ranking of ED_{50} can be produced and compared with mean onset times: vecuronium, 0.021 mg kg^{-1}, 5.1 min (O'Hara *et al.*, 1985); mivacurium, 0.05 mg kg^{-1}, 5.3 min (Savarese *et al.*, 1988); atracurium, 0.10 mg kg^{-1} (Basta *et al.*, 1982) and ANQ9040, 0.60 mg kg^{-1}, 1.4 min (Munday *et al.*, 1994). Variation in protocols, pharmacokinetics and excipient drugs makes detailed comparison difficult but ANQ9040 appears to have a lower potency than other commonly used neuromuscular blocking agents (with the exception of gallamine). This is broadly consistent with theories derived from *in vivo* experiments in laboratory animals which show an inverse correlation between receptor potency at equilibrium and rate of onset (Bowman *et al.*, 1988b; Kopman, 1989). We have not attempted a comparison of onset kinetics at equi-efficacious concentrations as drug access in the organ bath appears to be limited by bulk diffusion into the diaphragm. Equilibration times in electrophysiological experiments were drastically shorter because we were working with peripheral fibres and can be reduced even further (to more closely approximate true kinetics of receptor interaction) by release of relaxant from ionophoretic pipettes into the microenvironment of the endplate (Law Min *et al.*, 1992). These observations reinforce the proposal that the process of diffusion into endplates, presumed to be first order, is the primary determinant of rates of onset and recovery. Administration of a larger bolus of drug molecules (as required for clinical utility of drugs with low intrinsic potency) will more rapidly erode receptor reserve to produce functional block as a consequence. ORG9426 (rocuronium) may represent a notable exception to this trend as its onset time is faster than predicted from its molar potency (Witkowski *et al.*, 1992). A similarly fast acting but safe (not exhibiting dose-dependent histamine release) non-depolarizing relaxant would represent a significant clinical advance.

We thank ANAQUEST, U.S.A. for the sample of ANQ9040 (besylate salt) used in this study.

References

BASTA, S.J., ALI, H.H., SAVARESE, J.J., SUNDER, N., GIONFRIDDO, M., CLOUTIER, G., LINEBERRY, C. & CATO, A.E. (1982). Clinical pharmacology of atracurium besylate (BW33A): a new non-depolarising muscle relaxant. *Anesth. Analg.*, **61**, 723–729.

BOWMAN, W.C., MARSHALL, I.G., GIBB, I.J. & HARBORNE, A.J. (1988a). Feedback control of transmitter release at the neuromuscular junction. *Trends Pharmacol. Sci.*, **9**, 16–20.

BOWMAN, W.C., PRIOR, C. & MARSHALL, I.G. (1990). Presynaptic receptors in the neuromuscular junction. *Ann. N.Y. Acad. Sci.*, **604**, 69–81.

BOWMAN, W.C., RODGER, I.W., HOUSTON, J., MARSHALL, R.J. & MCINDEWAR, I. (1988b). Structure: action relationships among some desacetoxy analogues of pancuronium and vecuronium in the anesthetized cat. *Anesthesiology*, **69**, 57–62.

CATTERALL, W.A. (1987). Common modes of drug action on Na^+ channels: local anaesthetics, antiarrhythmics and anticonvulsants. *Trends Pharmacol. Sci.*, **8**, 57–65.

DEL CASTILLO, J. & KATZ, B. (1954). The effect of magnesium on the activity of motor nerve endings. *J. Physiol.*, **124**, 553–559.

DELISLE BURNS, B. & PATON, W.D.M. (1951). Depolarization of the motor end-plate by decamethonium and acetylcholine. *J. Physiol.*, **115**, 41–73.

FERGUSON, A. & BEVAN, D.R. (1981). Mixed neuromuscular block: the effects of precurarization. *Anaesthesia*, **36**, 661–666.

GIBB, A.J. & MARSHALL, I.G. (1982). The effects of trimetaphan on tetanic fade and on endplate ion channels at the rat neuromuscular junction. *Br. J. Pharmacol.*, **187**, 187P.

GIBB, A.J. & MARSHALL, I.G. (1986). Nicotinic antagonists produce differing amounts of tetanic fade in the isolated diaphragm of the rat. *Br. J. Pharmacol.*, **89**, 619–624.

GIBB, A.J. & MARSHALL, I.G. (1987). Examination of the mechanisms involved in tetanic fade produced by vecuronium and related analogues in the rat diaphragm. *Br. J. Pharmacol.*, **90**, 511–521.

HILLE, B. (1984). Mechanisms of block. In *Ionic Channels of Excitable Membranes*. pp. 272–302. Sunderland, Massachusetts, U.S.A.: Sinauer Associates Inc.

KOPMAN, A.F. (1989). Pancuronium, gallamine, and d-tubocurarine compared: is speed of onset inversely related to drug potency. *Anesthesiology*, **70**, 915–920.

LAMBERT, J.J., DURANT, N.N. & HENDERSON, E.G. (1983). Drug induced modification of ionic conductances at the neuromuscular junction. *Annu. Rev. Pharmacol. Toxicol.*, **23**, 505–539.

LANG, D.G., WANG, C.M. & COOPER, B.R. (1993). Lamotrigine, phenytoin and carbamezepine interactions on the sodium current present in N4TG1 mouse neuroblastoma cells. *J. Pharmacol. Exp. Ther.*, **266**, 829–835.

LAW MIN, J.C., BEKAVAC, I., GLAVINOVIC, M.I., DONATI, F. & BEVAN, D.R. (1992). Iontophoretic study of speed of action of various muscle relaxants. *Anesthesiology*, **77**, 351–356.

LEES, G. & LEACH, M.J. (1993). Studies on the mechanism of action of the novel anticonvulsant lamotrigine (Lamictal) using primary neuroglial cultures from rat cortex. *Brain Res.*, **612**, 190–199.

MUNDAY, I.T., JONES, R.M., DONATI, F., MANT, T.G.K. & DAMASK, M.C. (1992). ANQ9040: dose-response, safety, and cardiovascular effects. *Anesthesiology*, **77**, A969.

MUNDAY, I.T., JONES, R.M., DONATI, F., MANT, T.G.K. & DAMASK, M.C. (1994). Safety and potency of ANQ9040 in male volunteers. *Anesthesiology*, **80**, 97–103.

O'HARA, D.A., FRAGEN, R.J. & SHANKS, C.A. (1985). The effects of age on the dose-response curves for vecuronium in adults. *Anesthesiology*, **63**, 542–544.

SAVARESE, J.J., ALI, H.H., BASTA, S.J., EMBREE, P.B., SCOTT, R.P.H., SUNDER, N., WEAKLY, J.N., WASTILA, W.B. & EL-SAYAD, H.A. (1988). The clinical neuromuscular pharmacology of mivacurium chloride (BW B1090U). *Anesthesiology*, **68**, 723–732.

USHERWOOD, P.N.R., DUCE, I.R. & BOWDEN, P. (1984). Slowly-reversible block of glutamate receptor-channels by venoms of the spiders, *Argiope trifasciata and Araneus gemma*. *J. Physiol. Paris*, **79**, 241–245.

WITKOWSKI, T.A., BARTKOWSKI, R.R., AZAD, S.S., MARR, A., LESSIN, J. & EPSTEIN, R.H. (1992). ORG9426 onset of action: a comparison with atracurium and vecuronium. *Anesthesiology*, **77**, A964.

ZAIMIS, E. & HEAD, S. (1976). Depolarizing neuromuscular blocking drugs. In *Neuromuscular Junction*. ed. Zaimis, E. pp. 365–420. Springer-Verlag.

(Received April 14, 1994
Revised June 16, 1994
Accepted June 20, 1994)

Br. J. Pharmacol. (1994), **113**, 649–655 © Macmillan Press Ltd, 1994

Inhibition of substance P-induced microvascular leakage by inhaled methoxamine in rat airways

*Fabrice Larrazet, *Michel Chauveau, **Simon Weber, *Alain Lockhart & [1]*†Nelly Frossard

*Laboratoire de physiologie respiratoire, **Service de cardiologie, UFR Cochin Port-Royal, Paris and †Neuroimmunopharmacologie Pulmonaire, INSERM CJF 91-05, BP 24, 67401 Illkirch Cedex, France

1 The effect of the inhaled α-adrenoceptor agonist, methoxamine (MTX), was studied on experimental airway oedema induced by injection of substance P (SP) in the rat. Sprague-Dawley rats (300–350 g) were anaesthetized with sodium thiopentone, tracheotomized and artificially ventilated.

2 MTX or its vehicle was administered by inhalation. Airway resistance and blood pressure were monitored continuously. Evans Blue dye (EB, 20 mg kg^{-1}) was injected through a jugular catheter 1 min before SP (14.8 nmol kg^{-1}). Airways were dissected out, weighed and placed in formamide for EB extraction and determination by spectrophotometry.

3 EB extravasation induced by SP was significantly reduced in distal intraparenchymal bronchi by inhaled MTX at doses of 50 μg kg^{-1} (58 ± 9 vs 96 ± 9 ng EB mg^{-1} tissue after vehicle, $P<0.001$) and 100 μg kg^{-1} (69 ± 11 vs 137 ± 26 ng EB mg^{-1} tissue after vehicle, $P<0.01$). Inhaled MTX by itself (100 μg kg^{-1}) increased blood pressure: 172 ± 6 vs 132 ± 10 mmHg baseline ($P<0.02$), but neither induced extravasation nor increased airway resistance.

4 In another set of experiments without SP, MTX was administered intravenously 1 min after EB. At 100 μg kg^{-1}, i.v. MTX increased blood pressure to a similar extent as inhaled MTX (180 vs 147 mmHg baseline, $P<0.01$), increased airway resistance and caused leakage of plasma proteins in distal intraparenchymal bronchi (79 ± 7 vs 47 ± 1 ng EB mg^{-1} tissue, $P<0.02$).

5 Similarly, after sequential i.v. injections of doubling doses of MTX (50–800 μg kg^{-1}), a marked EB extravasation was found in the airways. This was abrogated by pretreatment with prazosin (100 μg kg^{-1}) but not with propranolol (2 mg kg^{-1}).

6 These results suggest that microvascular leakage and airway oedema induced by i.v. MTX may be linked to an increase in pressure in the pulmonary circulation, resulting from vasoconstriction of the pulmonary vasculature and acute cardiac dysfunction due to systemic hypertension.

7 Our results with inhaled MTX show that direct deposition of MTX at the bronchial vasculature induces a reduction in SP-induced microvascular leakage in rat airways and that inhaled MTX does not share the untoward effect of i.v. MTX inducing airway oedema.

Keywords: α-Adrenoceptor agonist; bronchial circulation; airways; substance P; microvascular leakage; oedema; cardiac asthma

Introduction

The α-adrenoceptor agonist, methoxamine (MTX), is a potent vasoconstrictor of the tracheobronchial circulation (Armendia *et al.*, 1962; Lung *et al.*, 1976; Salonen *et al.*, 1990). Inhaled MTX reduces bronchial hyperresponsiveness to methacholine and exercise-induced dyspnoea in patients with severely impaired left ventricular function (Cabanes *et al.*, 1989; 1992) as well as exercise-induced asthma in some patients suffering from mild asthma (Dinh Xuan *et al.*, 1989). Both methacholine and exercise cause vasodilatation of the tracheobronchial circulation (Regnard & Lockhart, 1992). Our group suggested, therefore, that the preventive effect of MTX could be explained by vasoconstriction of these vessels and by reduction of congestion and microvascular leakage which are facilitated in the airway wall by an increased outflow pressure of the bronchial circulation in left ventricular failure or by inflammation in asthma (Regnard & Lockhart, 1992). However, direct evidence that inhaled MTX causes local vasoconstriction and inhibition of microvascular leakage in the airways was lacking.

There is evidence in animals that intravenously administered vasoconstrictor agents, e.g. adrenaline, inhibit i.v. histamine- and PAF-induced increase in microvascular permeability in the tracheobronchial tree (Boschetto *et al.*, 1989; Persson & Erjefält, 1979). In addition, both i.v. phenylephrine and MTX inhibit the acute bronchial obstruction caused by i.v. acetylcholine, histamine and 5-hydroxytryptamine in the guinea-pig (Advenier & Floch-Saint-Aubin, 1984).

In the present study, we have investigated the ability of inhaled MTX to inhibit microvascular leakage in the airways of rats. Microvascular leakage was induced by intravenous administration of exogenous substance P (SP) (Saria *et al.*, 1983; Rogers *et al.*, 1988). We have used the Evans blue dye (EB) technique to quantitate plasma protein extravasation. As high doses of inhaled MTX elicited a rise in arterial blood pressure, indicating systemic diffusion of the drug, we have also investigated the effect of i.v. MTX on blood pressure, heart rate, respiratory resistance, and airway microvascular leakage.

Methods

The study followed a blind, randomized, placebo-controlled and parallel design. EB which binds to serum albumin (Rawson, 1943; Steinwall & Klatzo, 1966) was used to quantitate microvascular leakage of plasma proteins from the tracheobronchial microvasculature (Persson & Erjefält, 1979; Lundberg & Saria, 1982; Boschetto *et al.*, 1989).

Sprague Dawley rats (300–350 g, Iffa Credo, L'Arbresle, France) were anaesthetized with thiopentone sodium (60 mg

[1] Author for correspondence at: Neuroimmunopharmacologie, BP 24, 67401 Illkirch Cedex, France.

kg^{-1}) intubated and mechanically ventilated (pump Harvard model 683) with warm humidified air to prevent dry air-induced damage of airway epithelium (Barbet *et al.*, 1988). The animals were placed in a thermostated plethysmographic box that allowed measurements of ventilation (Fleisch pneumotachograph, No. 000 and pressure transducer: ± 1 mbar, Schlumberger 5105/0, France) and tracheal pressure (± 50 mbar, Schlumberger 5020/5, France).

Drugs were administered by inhalation or via the jugular veins. EB (20 mg kg^{-1}) was injected and allowed to circulate for 1 min before injection of drugs inducing plasma extravasation or control vehicles. Five minutes later, the animals were perfused to remove intravascular dye. The thorax was opened and the ascending aorta was perfused with 50 ml of a buffered (pH 3.5) paraformaldehyde solution which was allowed to drain freely through a large opening in the right atrium. Trachea, main bronchi, lungs, oesophagus and urinary bladder were quickly removed. Lung parenchyma was carefully stripped out with a razor blade, avoiding damage of the intraparenchymal bronchi. These were then divided into proximal bronchi (first 3 mm) and distal bronchi. All organs were wiped with absorbent paper and their wet weight measured. EB was extracted by incubating all tissues in 2 ml of formamide at 50°C for 24 h. Light absorbance of the extracts was measured at a wavelength of 620 nm (UV 160A, Shimadzu, Japan). The actual concentration of EB was determined by interpolation from a standard curve constructed with EB concentrations ranging from 0.625 to 10 μg ml^{-1}.

Tracheal pressure, flow and tidal volume were recorded on a strip chart recorder (Gould model 2600) connected to an Apple 2e microcomputer, programmed for off-line calculation of respiratory resistance according to the isovolume method. The calculated value is the total resistance of the respiratory system, including resistance of the tracheal canula (0.11 cmH_2O s ml^{-1}) as previously described (Chauveau *et al.*, 1992). Mean arterial pressure (MAP) was measured from the right carotid artery via a polyethylene catheter filled with heparinized saline connected to a pressure transducer and amplifier (Gould models P10 EZ and 13-4615-50). Heart rate was derived from the MAP signal (Biotach Amplifier, Gould model 13-4615-66) and recorded continuously throughout the experiment.

Inhalation of MTX

We used either a De Vilbiss nebulizer (No. 646) driven by compressed air (1.5 atm) (Cabanes *et al.*, 1989) or an ultrasonic nebulizer (Portasonic, De Vilbiss, France) to deliver the desired amount of inhaled MTX into the airways. The aerosol was delivered directly into the tracheal canula by a fully automated, home-made electrovalve system allowing control of insufflation pressure and duration leading to the delivery of a precise dose of drug (Chauveau *et al.*, 1992). Quantification of the delivered aerosol has been made *in vitro* by measuring the liquid expelled at the tip of the tracheal canula while the system was run in the same mechanical conditions as in the *in vivo* experiments (outflow pressure, timing and insufflated volume). The amount of liquid expelled into the airways was 4.1 ± 0.5 nl ml^{-1} gas (mean ± s.d.) with the compressed air nebulizer and 35.7 ± 7.7 nl ml^{-1} gas (mean ± s.d.) with the ultrasonic nebulizer (Chauveau *et al.*, 1992).

The 20 μg kg^{-1} dose of inhaled MTX was obtained with the compressed air nebulizer from a 4% MTX solution (300 mosmol l^{-1}) by ten successive lung inflations of 4 ml. The 50 μg kg^{-1} dose was obtained from a 10% MTX solution (950 mosmol l^{-1}) with a similar nebulization sequence (10 × 4 ml). To increase the dose of MTX further to that active in man (Cabanes *et al.*, 1989), the nebulizer was changed since a change in other parameters could have led to artefactual results: (1) the volume of insufflation (4 ml) could not be increased due to risks of pulmonary barotrauma and (2) a higher number of insufflations would have led to an incorrect decreased amount of liquid expelled at the tip of the tracheal canula (data not shown). We have used an ultrasonic nebulizer yielding a 9 times greater concentration of droplets in the aerosol for the two higher doses (100 and 150 μg kg^{-1}), thus allowing a small number of insufflations (6 and 9, respectively) from an isoosmolar 4% MTX solution (300 mosmol l^{-1}).

Corresponding placebos were saline or a 15% glucose solution (G15, 950 mosmol l^{-1}). All solutions were buffered at pH 7.0.

Protocol

The effect of inhaled MTX (20, 50 and 100 μg kg^{-1}) on SP-induced microvascular leakage was studied in two groups of 24 rats (20 and 50 μg kg^{-1}) and in one group of 20 rats (100 μg kg^{-1}). Each group was subdivided in 4 sets of 5–6 rats: inhaled placebo and i.v. saline (double placebo), inhaled MTX and i.v. saline, inhaled placebo and i.v. SP and inhaled MTX and i.v. SP. Pretreatment with inhaled MTX or placebo took place 9 min before i.v. injection of EB. SP (14.8 nmol kg^{-1}) was injected 1 min after EB. We also studied the effect of a higher dose (150 μg kg^{-1}) of inhaled MTX on extravasation of EB.

In additional experiments without SP, MTX was administered i.v. and EB extravasation was measured. Two sets of experiments were performed. In 12 rats, single doses of MTX (50, 100, 200 μg kg^{-1}; $n = 3$ for each dose) or placebo (saline, $n = 3$) were administered i.v. 1 min after EB.

Table 1 Effect of inhaled methoxamine (MTX, 20, 50, 100 μg kg^{-1}) compared with placebo (saline or 15% glucose [G15] as appropriate) on Evans blue (EB) dye extravasation induced by substance P (SP, 14.8 nmol kg^{-1}) in trachea, main bronchi, oesophagus and urinary bladder

	EB extravasation (ng mg^{-1} tissue)			
Inhaled/i.v.	*Trachea*	*Main bronchi*	*Oesophagus*	*Urinary bladder*
MTX 20 μg kg^{-1}				
Saline/saline	38	52	11	9
$n = 6$	(2)	(3)	(2)	(3)
MTX/saline	37	56	20	28
$n = 6$	(6)	(9)	(7)	(13)
Saline/SP	96*†	156*†	86*†	123*†
$n = 6$	(12)	(14)	(17)	(*27)
MTX/SP	109*†	151*†	54	96*
$n = 6$	(13)	(16)	(11)	(21)
MTX 50 μg kg^{-1}				
G15/saline	34	50	9	11
$n = 6$	(8)	(7)	(1)	(2)
MTX/saline	26	42	11	8
$n = 6$	(4)	(3)	(2)	(2)
G15/SP	68*†	138*†	65*†	91*†
$n = 6$	(12)	(18)	(15)	(17)
MTX/SP	97	98	44*†	79*†
$n = 6$	(13)	(14)	(4)	(10)
MTX 100 μg kg^{-1}				
Saline/Saline	37	52	9	7
$n = 5$	(7)	(5)	(1)	(2)
MTX/saline	31	42	11	9
$n = 5$	(5)	(4)	(2)	(2)
Saline/SP	114*†	164*†	66*†	82*†
$n = 5$	(12)	(14)	(5)	(4)
MTX/SP	113*†	134*†	53*†	78*†
$n = 5$	(22)	(24)	(12)	(24)

Values are means and s.e.mean (parentheses) of n experiments in 3 groups of rats.
*$P < 0.001$ between placebo/SP or MTX/SP and placebo/saline.
†$P < 0.001$ between placebo/SP or MTX/SP and MTX/saline.

EB extravasation in airways was studied as a function of the dose of MTX used. In 9 other rats, we studied effects on EB extravasation, on systemic haemodynamics and respiratory resistance of increasing doubling doses of i.v. MTX (25, 50, 100, 200, 400, 800 $\mu g\,kg^{-1}$) administered every 7 min after intravenous administration either of solvent ($n = 3$), of the α_1-adrenoceptor antagonist, prazosin (100 $\mu g\,kg^{-1}$, $n = 3$) or of the β-adrenoceptor antagonist, propranolol (2 $mg\,kg^{-1}$, $n = 3$). After completion of the dose-response curves, the animals were killed and extravasation of EB in airways was measured. Injection of similar volumes of saline according to the same schedule was performed in 3 other rats and had no effect.

Drugs and chemicals

Drugs and chemicals were obtained from the following sources: methoxamine hydrochloride (MTX, Synthélabo, Paris, France), Evans Blue dye, formamide, prazosin HCl, (±)-propranolol HCl (Sigma, St-Louis, U.S.A.); substance P (SP, Neosystem, Strasbourg, France), sodium thiopentone (Abbott, St Rémy sur Avre, France). Intravenous drugs were diluted in order to obtain injection volumes of 1 $ml\,kg^{-1}$ except for the study involving doubling doses of i.v. MTX that were diluted to inject 0.3 $ml\,kg^{-1}$. Intravenous drugs were prepared in saline, except prazosin which was diluted in 50% ethanol in saline.

Expression of the results and statistical analysis

Extravasation of EB was expressed as mean ± s.e.mean in ng of EB mg^{-1} wet weight tissue. Respiratory resistance was expressed as $cmH_2O\,s\,ml^{-1}$. Since baseline values were not statistically different between groups, results are presented as percentages of baseline in Figure 4. Statistical differences between groups and between subgroups in a given group were analysed by a two-way analysis of variance (Statview II, Abacus Concepts, U.S.A.) followed by a Scheffe's F-test.

Results

Effect of inhaled MTX

Extravasation of EB With the double placebo, there was no difference between groups in control EB extravasation in any of the tissues studied (Table 1, Figure 1). Following pretreatment with placebo, injection of SP (14.8 $nmol\,kg^{-1}$) induced a similar increase in extravasation in the three groups of rats for each tissue studied (Table 1). Although the increase was lower in the presence of G15 than saline (Table 1), this was not significant. Compared with the appropriate placebo, pretreatment with 20 $\mu g\,kg^{-1}$ inhaled MTX had no significant effect on SP-induced extravasation in any of the tissues studied (Table 1, Figure 1). MTX, 50 $\mu g\,kg^{-1}$, significantly

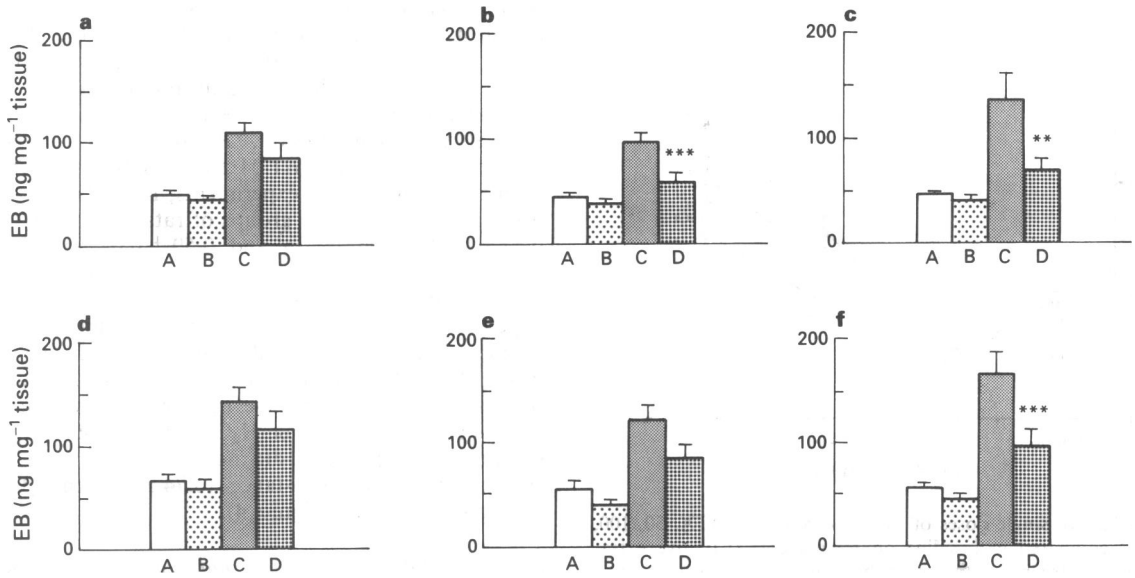


Figure 1 Effect of inhaled-methoxamine (MTX) on Evan's blue (EB) dye extravasation induced by substance P (SP, 14.8 $nmol\,kg^{-1}$, i.v.) in distal (a,b,c) and proximal (d,e,f) intraparenchymal bronchi. MTX: 20 $\mu g\,kg^{-1}$ (a,d), 50 $\mu g\,kg^{-1}$ (b,e) and 100 $\mu g\,kg^{-1}$ (c,f). (A) saline-inhaled saline-injected, (B) MTX-inhaled, saline-injected, (C) saline-inhaled, SP-injected and (D) MTX-inhaled SP-injected. Values are means ± s.e.mean of 6 (25 and 50 $\mu g\,kg^{-1}$) or 5 experiments (100 $\mu g\,kg^{-1}$). $^{**}P < 0.01$; $^{***}P < 0.001$.

Table 2 Effect of inhaled methoxamine (MTX) (150 $\mu g\,kg^{-1}$) compared with placebo (saline) on Evan's blue (EB) dye extravasation (ng mg^{-1} tissue)

	EB dye extravasation (ng mg^{-1} tissue)					
			Bronchi			
	Trachea	*Main*	*Parenchymal proximal*	*Parenchymal distal*	*Oesophagus*	*Urinary bladder*
Saline	46	64	54	50	9	5
	(14)	(16)	(6)	(6)	(1)	(1)
MTX	24	51	52	52	14	8
	(4)	(5)	(6)	(3)	(2)	(2)

Values are means and s.e.mean (parentheses) of 3 experiments. Comparisons with controls receiving only saline were non significant.

inhibited SP-induced extravasation in the distal bronchi (Figure 1, $P<0.001$) (58 ± 9 ng EB mg^{-1} tissue vs 96 ± 9 after vehicle) whereas leakage in the urinary bladder and oesophagus was unchanged (Table 1).

MTX, 100 $\mu g\ kg^{-1}$, induced a significant inhibition of SP-induced EB extravasation in both proximal and distal intraparenchymal bronchi (Figure 1, $P<0.001$ and $P<0.01$, respectively) (69 ± 11 ng EB mg^{-1} tissue vs 137 ± 26 after vehicle in distal bronchi). There was a trend towards inhibition in the main bronchi (NS). MTX had almost no effect in the other tissues studied (Table 1).

Inhaled MTX by itself, even at the highest dose used (150 $\mu g\ kg^{-1}$), did not affect baseline EB extravasation in the airways as compared with saline (Table 2).

Respiratory resistance Inhaled MTX had no effect on baseline respiratory resistance even at 100 $\mu g\ kg^{-1}$. Similarly, i.v. SP caused no change in airway resistance compared with baseline after pretreatment with inhaled placebo (0.66 ± 0.02 vs 0.62 ± 0.02 $cmH_2O\ s\ l^{-1}$) or MTX (100 $\mu g\ kg^{-1}$) (0.69 ± 0.02 vs 0.65 ± 0.02 $cmH_2O\ s\ l^{-1}$).

Mean arterial pressure and heart rate Baseline MAP was unchanged after placebo (139 ± 4 before and 141 ± 5 mmHg after, respectively, $n = 13$) as well as after inhalation of 20 or 50 $\mu g\ kg^{-1}$ of MTX (Table 3). Conversely, 100 $\mu g\ kg^{-1}$ of inhaled MTX caused a marked and transitory rise in MAP over baseline that peaked 1 min after nebulization of MTX (Table 3). MAP had returned to baseline in approximately 10 min, i.e. just before the injection of SP took place (146 ± 3 compared with 132 ± 10 mmHg). Five minutes after SP, MAP had fallen to about 50% of baseline in both placebo and MTX-inhaled animals (20, 50 and 100 $\mu g\ kg^{-1}$) with no significant difference between groups.

Heart rate was not significantly modified by inhaled MTX (100 $\mu g\ kg^{-1}$) (393 ± 21 before and 378 ± 21 beats min^{-1} after, respectively, $n = 5$) compared with saline (390 ± 21 before and 380 ± 22 beats min^{-1} after, respectively, $n = 5$).

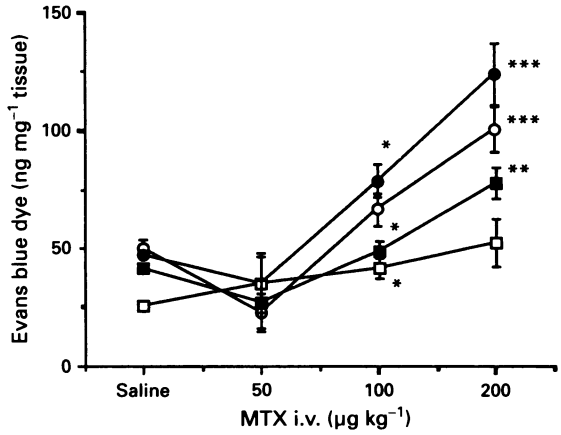


Figure 2 Effect of single doses of i.v. methoxamine (MTX, 50, 100, 200 $\mu g\ kg^{-1}$) compared with saline on Evan's blue (EB) dye extravasation in (□) trachea, (■) main bronchi, (○) proximal intraparenchymal bronchi, (●) distal intraparenchymal bronchi. Values are means ± s.e.mean of 3 experiments. $*P<0.02$; $**P<0.01$; and $***P<0.001$.

Intravenous MTX

Extravasation of EB When single i.v. doses of MTX were administered, there was no effect of the lowest dose (50 $\mu g\ kg^{-1}$) (Figure 2). With higher doses, significant extravasation was observed in the trachea, in main and distal intraparenchymal bronchi (100 $\mu g\ kg^{-1}$: 79 ± 7 vs saline: 47 ± 1 ng EB mg^{-1} tissue in distal bronchi, $P<0.02$) and also in main and intrapulmonary bronchi (200 $\mu g\ kg^{-1}$) (Figure 2). Conversely, there was no increase over control value of extravasation in urinary bladder and oesophagus even at 200 $\mu g\ kg^{-1}$ (not shown).

Marked EB extravasation was found in the airways after sequential i.v. injections of doubling doses of MTX (25–800 $\mu g\ kg^{-1}$) (Figure 3). This was abrogated by pretreatment with prazosin (100 $\mu g\ kg^{-1}$) whereas solvent (50% ethanol in saline) (not shown) or propranolol (2 mg kg^{-1}) (Figure 3) did not modify i.v. MTX-induced extravasation of EB.

Respiratory resistance When single i.v. doses of MTX were administered, there was no effect of the lowest dose (50 $\mu g\ kg^{-1}$, from 0.58 ± 0.01 baseline to 0.59 ± 0.02 $cmH_2O\ s\ l^{-1}$). With higher doses, significant increase in respiratory resistance was observed at 100 $\mu g\ kg^{-1}$ (0.58 ± 0.02 baseline to 0.80 ± 0.07 $cmH_2O\ s\ l^{-1}$, $P<0.02$) and at 200 $\mu g\ ml^{-1}$ (0.59 ± 0.03 baseline to 1.04 ± 0.1 $cmH_2O\ s\ l^{-1}$, $P< 0.05$).

In the second set of experiments, mean baseline resistance was similar in the three groups of rats (0.58 ± 0.02 for saline, 0.57 ± 0.03 for prazosin and 0.59 ± 0.02 $cmH_2O\ ml^{-1}\ s$ for propranolol). After sequential i.v. injections of increasing doubling doses of MTX (25–800 $\mu g\ kg^{-1}$), a marked dose-dependent increase in respiratory resistance was observed (Figure 4) which was already significant with the 100 $\mu g\ kg^{-1}$ dose (0.82 ± 0.06 $cmH_2O\ s\ l^{-1}$, $P<0.05$). Pretreatment by prazosin suppressed the rise in airway resistance caused by i.v. MTX (0.59 ± 0.02 $cmH_2O\ s\ l^{-1}$ at 100 $\mu g\ kg^{-1}$ MTX) (Figure 4). Propranolol did not abrogate i.v. MTX-induced rise in respiratory resistance (0.74 ± 0.09 $cmH_2O\ ml^{-1}\ s$ at 100 $\mu g\ kg^{-1}$ MTX) (Figure 4).

Mean arterial blood pressure and heart rate Single doses of i.v. MTX (50, 100 and 200 $\mu g\ kg^{-1}$) increased MAP above baseline (Table 3). Intravenous MTX induced a marked transient bradycardia at doses of 100 $\mu g\ kg^{-1}$ and higher

Table 3 Changes in mean arterial pressure (MAP) on administration of methoxamine (MTX) by inhalation (20, 50 and 100 $\mu g\ kg^{-1}$) or by single i.v. injection (50, 100 and 200 $\mu g\ kg^{-1}$)

		MAP (mmHg) *MTX* ($\mu g\ kg^{-1}$)	
Inhaled	20	50	100
Baseline	143 ± 4	137 ± 6	132 ± 10
Drug	144 ± 6	139 ± 7	172 ± 6**
		MTX ($\mu g\ kg^{-1}$)	
Intravenous	50	100	200
Baseline	142 (134–155)	147 (137–158)	153 (135–165)
Drug	179 (173–184)***	180 (175–185)***	183 (179–188)*

Values are means ± s.e.mean of 4–5 experiments for inhaled MTX and are medians (range) of 3 experiments for i.v. MTX. $*P<0.05$; $**P<0.02$ and $***P<0.01$.

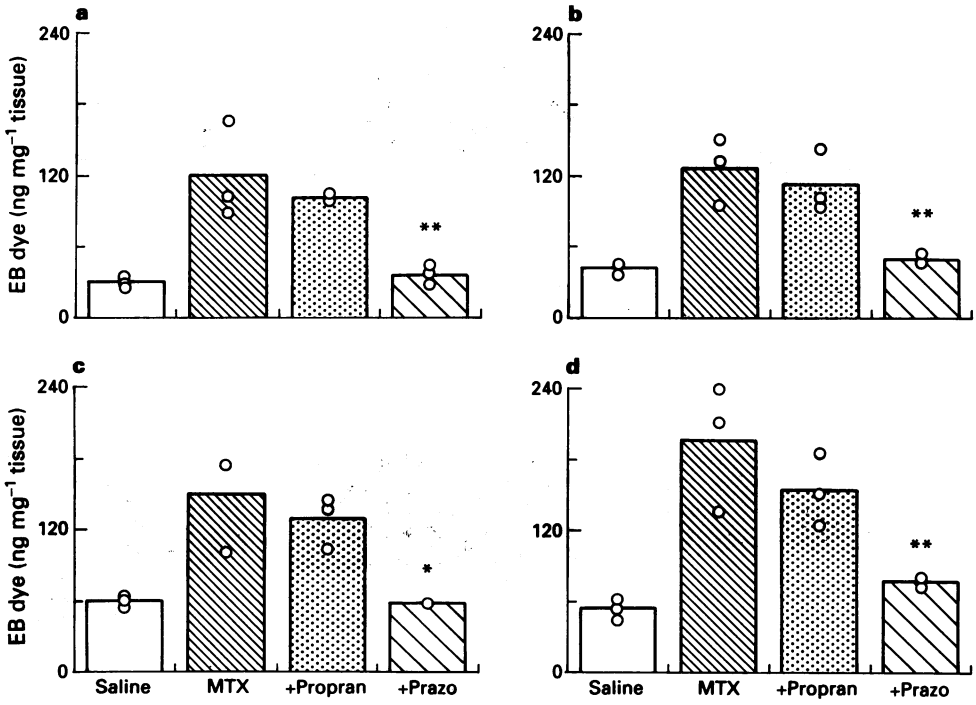


Figure 3 Evan's blue (EB) dye extravasation after sequential i.v. injections of methoxamine (MTX, 25–800 μg kg^{-1}) after pretreatment with propranolol (Propran, 2 mg kg^{-1}) or prazosin (Prazo, 100 μg kg^{-1}). Open columns (saline) represent control extravasation. (a) Trachea, (b) main bronchi, (c) proximal intraparenchymal bronchi and (d) distal intraparenchymal bronchi. Values are means (columns) and individual values (dots). $*P<0.02$; $**P<0.01$.

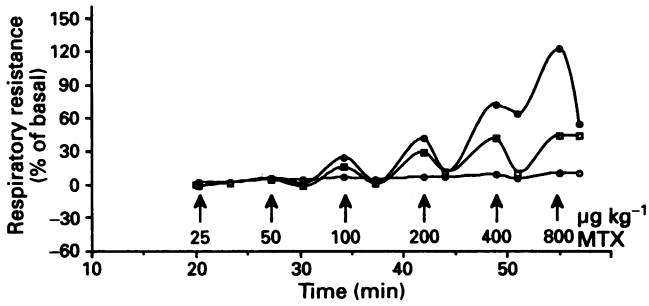


Figure 4 Representative traces of the effect of prazosin (100 μg kg^{-1}; ○), propranolol (2 mg kg^{-1}; □) and solvent (●) on the increase in respiratory resistance induced by increasing doses of i.v. methoxamine (MTX, 25–800 μg kg^{-1}) injected every 7 min (arrows). Respiratory resistance is expressed as % of basal resistance.

(413 ± 30 before and 317 ± 58 beats min^{-1} after, $n=3$, $P<0.01$). An illustrative example of the dose-effect of i.v. MTX is shown in Figure 5.

Intravenous MTX (25–800 μg kg^{-1}) induced a dose-dependent increase in MAP that was already significant at a dose of 25 μg kg^{-1}. The changes in MAP were also reduced by prior administration of prazosin (data not shown).

Discussion

Our study shows that administration of methoxamine by inhalation protects against exogenous SP induced-microvascular leakage in rat airways. Whereas inhaled MTX by itself did not cause plasma protein extravasation, intravenous MTX induced marked microvascular leakage in the airways together with systemic hypertension and increase in respiratory resistance at doses ⩾ 100 μg kg^{-1}.

The preventive effect of inhaled MTX on SP-induced plasma extravasation in the airways is best explained by a topical effect of MTX inducing reduction in bronchial blood flow probably by acting through activation of the α-adrenoceptors of the bronchial vessels (Lung *et al.*, 1976). This preventive effect occurred in the intraparenchymal bronchi but not in the trachea and main bronchi. Since the trachea was cannulated, the site of deposition of inhaled MTX was distal in the airways. This probably explains why inhaled MTX had no preventive effect on SP-induced microvascular leakage in the trachea and a borderline effect in the main bronchi ($P=0.06$, NS), in contrast to previous studies in the guinea-pig where vasoconstrictor agents were administered intravenously (Persson & Erjefält, 1979; Advenier & Floch-Saint-Aubin, 1984; Boschetto *et al.*, 1989).

Inhaled MTX (50 μg kg^{-1}) caused no modification of MAP and heart rate and prevented SP-induced plasma protein extravasation in distal airways. This suggests that the systemic diffusion of inhaled MTX was unimportant and that the action of the drug administered by inhalation was essentially local. In accordance with this, no reduction of SP-induced EB extravasation in the oesophagus and urinary bladder was observed. At 100 μg kg^{-1} of inhaled MTX, a transitory rise in arterial pressure took place and had subsided at the time of injection of SP. This pressor effect did not suppress the preventive effect of MTX on airway microvascular leakage.

Since inhaled MTX caused a rise in systemic blood pressure, we wondered whether systemic passage of the drug might act as a confounding factor. To study the role of MTX on systemic and local vasculature, we compared effects of inhaled and intravenous MTX. At a dose of 100 μg kg^{-1}, inhaled and i.v. MTX caused a similar increase in MAP. However, i.v. but not inhaled MTX caused a marked plasma protein extravasation in the airways. In contrast, no leak was observed in organs supplied by the systemic circulation, e.g. oesophagus and urinary bladder. When the rise in systemic blood pressure was abrogated by pretreatment with the α-adrenoceptor antagonist, prazosin, i.v. MTX-induced airway wall oedema was also prevented. Pulmonary oedema is a well

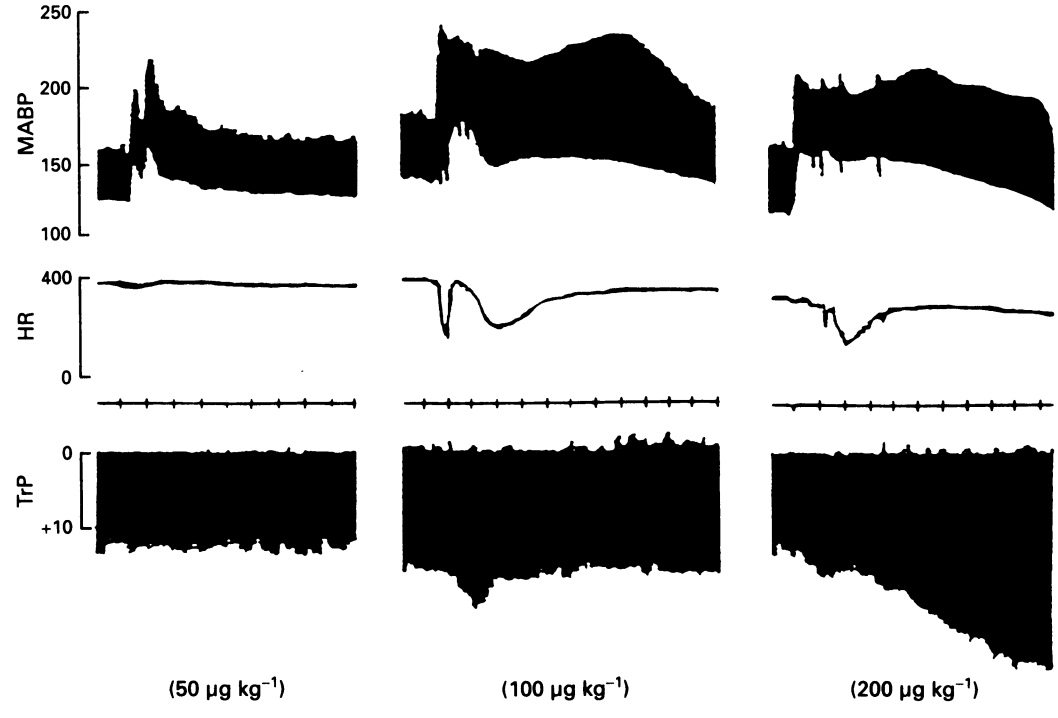


Figure 5 Representative records of the effect of methoxamine (MTX, i.v. 50 μg kg^{-1}; 100 μg kg^{-1}; 200 μg kg^{-1}) on mean arterial pressure (MAP, mmHg; top panels), heart rate (HR, beats min^{-1}; middle panels) and tracheal pressure (TrP, cmH_2O; lower panels).

known sequela of high doses of i.v. adrenaline (Hoffman & Lefkowitz, 1990). It is attributed to the combined effects of the sudden increase in left ventricular afterload and of the shift of blood from the venous compartment into the pulmonary circuit mediated by the powerful venoconstrictor effect of adrenaline. Hence, pulmonary oedema might also have occurred following i.v. MTX. Since the bronchial microvasculature drains into pulmonary veins and anastomoses exist between the pulmonary and bronchial vessels (Deffebach *et al.*, 1987), it is not surprising that airway wall oedema occurred in rats receiving high doses of i.v. MTX.

Together with the extravasation of plasma proteins in the bronchial tree, i.v. MTX caused a dose-dependent increase in airway resistance. This increase in airway resistance was unlikely to be due to a direct effect of MTX on the bronchial smooth muscle since inhaled MTX did not induce bronchoconstriction. Airway oedema and the concomitant increase in airway wall thickness can reduce airway lumen diameter and cause an increase in airway resistance (Freedman, 1972; Hogg *et al.*, 1987), particularly in small airways (Hogg *et al.*, 1972). In our experiments in Sprague-Dawley rats, both plasma protein extravasation and rise in respiratory resistance occurred at 100 μg kg^{-1} i.v. MTX. Both effects were attributable to the α-adrenoceptor effect of MTX since they were blocked by the selective α-adrenoceptor antagonist, prazosin and were unchanged by the β-adrenoceptor antagonist, propranolol. In contrast to the effects of i.v. MTX, inhaled MTX did not cause either plasma protein extravasation in airways or increase in airway resistance up to a dose of 150 μg kg^{-1} in spite of the transitory rise in systemic arterial pressure that occurred with the highest doses of inhaled MTX used. Therefore, it is tempting to attribute the rise in respiratory resistance to airway wall oedema. However, it should be emphasized that SP-induced plasma extravasation in the airways was not accompanied by an increase in respiratory resistance, even though the amount of extravasated plasma was about the same with i.v. SP and i.v. MTX. Respiratory resistance, as measured in our study, is the sum of airway, lung and chest wall resistances. Whereas there is no reason to believe chest wall resistance was different in our different subgroups of rats, it is likely that pulmonary oedema was present in rats receiving i.v. MTX but not in rats receiving i.v. SP and was responsible for the increase in respiratory resistance in the former group of rats.

In conclusion, administration of MTX by inhalation in the rat inhibits microvascular leakage induced by SP in the intraparenchymal bronchi. These findings support our contention that the beneficial antidyspnoeic effect of inhaled MTX might be linked to concomitant reduction of airway oedema and reduced thickness of the airway wall in patients with impaired left ventricular function. Whether the inhibitory effect of inhaled MTX is linked to activation of α-adrenoceptors on the bronchial vessel or to a direct effect on epithelial cells remains to be determined.

The authors express their thanks to J. Maccario for statistical analyses, to B. Scatton (LERS, France) and to L. Cabanes and J. Regnard for helpful suggestions. This work was supported by grants from INSERM (CRE No. 88-5012), by Direction de la Recherche et des Etudes Doctorales and by laboratoire Synthélabo, Paris, France.

References

ADVENIER, C. & FLOCH-SAINT-AUBIN, A. (1984). Bronchopulmonary effects of phenylephrine and methoxamine in the guinea-pig, interaction with bronchoconstrictor drugs. *Eur. J. Pharmacol.*, **100**, 59–69.

ARMENDIA, P., DE LETONA, J.M.L. & AVIADO, D.M. (1962). Responses of the bronchial veins in heart-lung bronchial preparation. *Circ. Res.*, **10**, 3–10.

BARBET, J.P., CHAUVEAU, M., LABBE, S. & LOCKHART, A. (1988). Breathing dry air causes acute epithelial damage and inflammation in the guinea pig trachea. *J. Appl. Physiol.*, **64**, 1851–1857.

BOSCHETTO, P., ROBERTS, N.M., ROGERS, D.F. & BARNES, P.J. (1989). Effect of anti-asthma drugs on microvascular leakage in guinea pig airways. *Am. Rev. Respir. Dis.*, **139**, 416–421.

CABANES, L., COSTES, F., WEBER, S., REGNARD, J., BENVENUTI, C., CASTAIGNE, A., GUERIN, F. & LOCKHART, A. (1992). Improvement of exercise capacity by inhalation of an alpha-adrenergic agonist in congestive heart failure. *N. Engl. J. Med.*, **326**, 1661–1665.

CABANES, L., WEBER, S., MATRAN, R., REGNARD, J., RICHARD, M., DEGEORGES, M. & LOCKHART, A. (1989). Bronchial hyperresponsiveness to methacholine in patients with impaired left ventricular function. *N. Engl. J. Med.*, **320**, 1317–1322.

CHAUVEAU, M., LEROY, M., LE GALL, G. & LOCKHART, A. (1992). Bronchial provocation tests in small animals: a quantified and automated procedure. *J. Appl. Physiol.*, **73**, 410–419.

DEFFEBACH, M.E., CHARAN, N.B., LAKSHMINARAYAN, S. & BUTLER, J. (1987). The bronchial circulation: small, but a vital attribute of the lung. *Am. Rev. Respir. Dis.*, **135**, 463–481.

DINH XUAN, A.T., CHAUSSAIN, M., REGNARD, J. & LOCKHART, A. (1989). Pretreatment with an inhaled alpha 1-adrenergic agonist, methoxamine, reduces exercise-induced asthma. *Eur. Respir. J.*, **2**, 409–414.

FREEDMAN, R.J. (1972). The functional geometry of the bronchi: the relationship between changes in external diameter and calibre, and a consideration of the passive role played by the mucosa in bronchoconstriction. *Bull. Physiopathol. Respir.*, **8**, 545–552.

HOFFMAN, B.B. & LEFKOWITZ, R.J. (1990). Catecholamines and sympathomimetic drugs. In *Goodman and Gilman's The Pharmacological Basis of Therapeutics*. ed. Goodman Gilman, A., Rall, T.W., Nies, A.S. & Taylor, P. p. 194. New York: Pergamon Press.

HOGG, J.C., AGRAWAL, J.B., GARDINER, A.J.S., PALMER, W.H. & MACKLEM, P.T. (1972). Distribution of airway resistance with developing pulmonary edema in dogs. *J. Appl. Physiol.*, **32**, 80–84.

HOGG, J.C., PARÉ, P.D. & MORENO, R. (1987). The effect of submucosal edema on airway resistance. *Am. Rev. Respir. Dis.*, **135**, S54–S56.

LUNDBERG, J.M. & SARIA, A. (1982). Capsaicin-sensitive vagal neurons involved in control of vascular permeability in rat trachea. *Acta Physiol. Scand.*, **115**, 521–523.

LUNG, M.A., WANG, J.C. & CHENG, K.K. (1976). Bronchial circulation: an auto-perfusion method for assessing its vasomotor activity and the study of alpha- and beta-adrenoceptors in the bronchial artery. *Life Sci.*, **19**, 577–580.

PERSSON, C.G.A. & ERJEFÄLT, I. (1979). Terbutaline and adrenaline inhibit leakage of fluid and protein in guinea-pig lung. *Eur. J. Pharmacol.*, **55**, 199–201.

RAWSON, R.A. (1943). The binding of T-1824 and structurally related diazo dyes by plasma proteins. *Am. J. Physiol.*, **138**, 708–717.

REGNARD, J. & LOCKHART, A. (1992). Vascular factors in bronchial hyperresponsiveness and asthma. *Respir. Med.*, **86**, 179–181.

ROGERS, D.F., BELVISI, M.G., AURSUDKIJ, B., EVANS, T.W. & BARNES, P.J. (1988). Effects and interactions of sensory neuropeptides on airway microvascular leakage in guinea-pigs. *Br. J. Pharmacol.*, **95**, 1109–1116.

SALONEN, R.O., WEBBER, S.E. & WIDDICOMBE, J.G. (1990). Effects of neurotransmitters on tracheobronchial blood flow. *Eur. Respir. J.*, **3**, Suppl 12), 630S–637S.

SARIA, A., LUNDBERG, J.M., SKOFITSCH, G. & LEMBECK, F. (1983). Vascular protein leakage in various tissues induced by substance P, capsaicin, bradykinin, serotonin, histamine and by antigen challenge. *Naunyn-Schmied. Arch. Pharmacol.*, **324**, 212–218.

STEINWALL, O. & KLATZO, I. (1966). Selective vulnerability of the blood brain barrier in chemically induced lesions. *J. Neuropath. Exp. Neurol.*, **25**, 542–559.

(Received February 25, 1993
Revised June 13, 1994
Accepted June 23, 1994)

 © Macmillan Press Ltd, 1994

Erratum

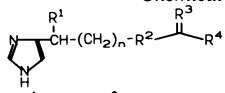
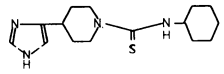
Br. J. Pharmacol. (1994), **112**, 1043–1048

E. Schlicker, M. Kathmann, S. Reidemeister, H. Stark & W. Schunack. Novel histamine H_3 receptor antagonists: affinities in an H_3 receptor binding assay and potencies in two functional H_3 receptor models.

In the above article, Table 1 was published incorrectly owing to a typesetting error. The publishers would like to apologise for any inconvenience this may have caused.

The correct version of Table 1 is reproduced below.

Table 1 Chemical structures, affinities for H_3 binding sites and antagonistic potencies in two functional H_3 receptor models of ten newly synthesized compounds and of thioperamide

Compound	*Chemical structure*					*Binding experiments*	*Functional experiments*	
						pK_i	Apparent pA_2	
	n	R^1	R^2	R^3	R^4	Rat brain cortex membranes[a]	Mouse brain cortex slices[b]	Guinea-pig ileum strips[c]
1	2	H	NH	NH	NH-CH_2-⬡	8.68	9.20	8.81
2	2	H	0	0	$(CH_2)_2$-⬠	8.52	8.28	7.23
3	2	H	NH	N-C(=O)-$OC(CH_3)_3$	NH-CH_2-⬡	7.98	8.67	7.38
4	3	H	NH	N-C(=O)-$OC(CH_3)_3$	NH-⬡	7.86	7.28	6.93
5	2	CH_3	NH	0	$(CH_2)_2$-⬡	7.76	7.98	7.27
6	2	H	NH	0	$(CH_2)_2$-⬡	7.66	7.47	6.81
7	2	H	NH	0	$(CH_2)_2$-⬠	7.63	7.18	7.21
8	2	H	NH	0	NH-⬡	7.58	7.07	7.26
9	2	H	NH	S	$(CH_2)_2$-⬠	7.57	7.40	7.51
10	2	H	NH	0	$(CH_2)_2$-⬡	7.56	7.27	6.64
Thioperamide						8.31, 7.19[d]	8.67[e]	8.79

[a]pK_i values were determined from the concentration-response curves (shown in Figure 1) of the novel H_3 receptor antagonists for their inhibitory effect on [^{3}H]-N$^\alpha$-methylhistamine binding to rat brain cortex membranes. Means of 4–8 experiments; the s.e.mean values (not shown) ranged from 0.02 to 0.10.

[b]The apparent pA_2 value of **1** was obtained from the concentration-response curves (shown in Figure 2) of histamine for its inhibitory effect on the electrically-evoked tritium overflow from superfused mouse brain cortex slices (preincubated with [^{3}H]-noradrenaline). The apparent pA_2 values of the other newly synthesized compounds were obtained from corresponding concentration-response curves (not shown). Means of 4–11 experiments; the s.e.mean values (not shown) ranged from 0.06 to 0.26.

[c]The apparent pA_2 value of **1** was obtained from the concentration-response curves (shown in Figure 3) of **R**-(−)-α-methylhistamine for its inhibitory effect on the electrically induced contraction in guinea-pig ileum strips. The apparent pA_2 values of the other newly synthesized compounds and of thioperamide were obtained from corresponding concentration-response curves (not shown). Means of 8–20 experiments; the s.e.mean values (not shown) ranged from 0.04 to 0.16.

[d]The values, which represent the pK_i for H_{3A} and H_{3B} binding sites, respectively, are taken from West *et al.* (1990; almost identical binding assay as in the present study).

[e]From Schlicker *et al.* (1992).

Also in the above article, point **1** of the summary was reproduced incorrectly. This point should read as follows:

> **1** We determined the affinities of ten novel H_3 receptor antagonists in an H_3 receptor binding assay and their potencies in two functional H_3 receptor models. The novel compounds differ from histamine in that the aminoethyl side chain is replaced by a propyl or butyl chain linked to a polar group (amide, thioamide, ester, guanidine, guanidine ester or urea) which, in turn, is connected to a hexocyclic ring or to an alicyclic ring-containing alkyl residue.

British Journal of Pharmacology

VOLUME 113 (2) OCTOBER 1994

SPECIAL REPORTS

H.T. Schambye, B. v. Wijk, S.A. Hjorth, W. Wienen, M. Entzeroth, D.J. Bergsma & T.W. Schwartz. Mutations in transmembrane segment VII of the AT_1 receptor differentiate between closely related insurmountable and competitive angiotensin antagonists 331

C.P. Baines, R.S. Szwarc & H.A. Ball. Parallel tolerance between platelet cyclic GMP and preload effects of nitroglycerin in anaesthetized mini-pigs 334

T. Fukuroda, S. Ozaki, M. Ihara, K. Ishikawa, M. Yano & M. Nishikibe. Synergistic inhibition by BQ-123 and BQ-788 of endothelin-1-induced contractions of the rabbit pulmonary artery 336

J.M. Barnes, K.K. Dev & J.M. Henley. Cyclothiazide unmasks AMPA-evoked stimulation of [^{3}H]-L-glutamate release from rat hippocampal synaptosomes 339

PAPERS

R.P. Coppes, F. Brouwer, I. Freie, J. Smit & J. Zaagsma. Sustained prejunctional facilitation of noradrenergic neurotransmission by adrenaline as a co-transmitter in the portal vein of freely moving rats 342

T. Jun & Å. Wennmalm. NO-dependent and -independent elevation of plasma levels of insulin and glucose in rats by L-arginine 345

R. Bültmann, M. Trendelenburg & K. Starke. Blockage of P_{2x}-purinoceptors by trypan blue in rat vas deferens 349

F.P. Jansen, T.S. Wu, H.-P. Voss, H.W.M. Steinbusch, R.C. Vollinga, B. Rademaker, A. Bast & H. Timmerman. Characterization of the binding of the first selective radiolabelled histamine H_3-receptor antagonist, [^{125}I]-iodophenpropit, to rat brain 355

E. Thorin, C. Capdeville-Atkinson, B. Corman & J. Atkinson. Sympathetic neurotransmission in the tail artery of aging rats 363

Y.-M. Qian, R.L. Jones, K.-M. Chan, A.I. Stock & J.K.S. Ho. Potent contractile actions of prostanoid EP_3-receptor agonists on human isolated pulmonary artery 369

R.S. Redman & E.M. Silinsky. Decrease in calcium currents induced by aminoglycoside antibiotics in frog motor nerve endings 375

R.A. Keith, T.J. Mangano, P.A. DeFeo, G.E. Ernst & E.J. Warawa. Differential inhibition of neuronal calcium entry and [^{3}H]-D-aspartate release by the quaternary derivatives of verapamil and emopamil 379

Y. Kita, Y. Hirasawa, K. Yoshida & K. Maeda. Antiplatelet activities of FK409, a new spontaneous NO releaser 385

J.P. Galizzi, M.C. Bodinier, B. Chapelain, S.M. Ly, L. Coussy, S. Giraud, G. Neliat & T. Jean. Up-regulation of [^{3}H]-des-Arg^{10}-kallidin binding to the bradykinin B_1 receptor by interleukin-1β in isolated smooth muscle cells: correlation with B_1 agonist-induced PGI_2 production 389

J. Su, N. Renaud, A. Carayon, B. Crozatier & L. Hittinger, with the technical assistance of Monique Laplace. Effects of the calcium channel blockers, diltiazem and Ro 40-5967, on systemic haemodynamics and plasma noradrenaline levels in conscious dogs with pacing-induced heart failure 395

A. Laniyonu, M. Saifeddine, S. Ahmad & M.D. Hollenberg. Regulation of vascular and gastric smooth muscle contractility by pervanadate 403

G. Erdemli & K. Krnjević. Actions of cromakalim on outward currents of CA1 neurones in hippocampal slices 411

M.C. Martínez, J.M. Vila, M. Aldasoro, P. Medina, B. Flor & S. Lluch. Relaxation of human isolated mesenteric arteries by vasopressin and desmopressin 419

M. Ballarin, A. Carceller & X. Guitart. Effect of acute administration of the 5-HT_{1A} receptor ligand, lesopitron, on rat cortical 5-HT and dopamine turnover 425

Y. Zhang & R.J. Lang. Effects of intrinsic prostaglandins on the spontaneous contractile and electrical activity of the proximal renal pelvis of the guinea-pig 431

R. Gniadecki, M. Gniadecka & J. Serup. Inhibition of glucocorticoid-induced epidermal and dermal atrophy with KH 1060 – a potent 20-epi analogue of 1,25-dihydroxyvitamin D_3 439

A.E. Eckly & C. Lugnier. Role of phosphodiesterases III and IV in the modulation of vascular cyclic AMP content by the NO/cyclic GMP pathway 445

R. Okuyama, S. Adachi-Akahane & T. Nagao. Differential potential by depolarization of the effects of calcium antagonists on contraction and Ca^{2+} current in guinea-pig heart 451

P. Pacaud, G. Grégoire & G. Loirand. Release of Ca^{2+} from intracellular store in smooth muscle cells of rat portal vein by ATP-induced Ca^{2+} entry 457

D.J. Trezise, N.J. Bell, I. Kennedy & P.P.A. Humphrey. Effects of divalent cations on the potency of ATP and related agonists in the rat isolated vagus nerve: implications for P_2 purinoceptor classification 463

G.A.J. Kuijpers, L.A. Vergara, S. Calvo & G. Yadid. Inhibitory effect of strychnine on acetylcholine receptor activation in bovine adrenal medullary chromaffin cells 471

J..S. Lacroix, L.G. Ulman & E.K. Potter. Modulation by neuropeptide Y of parasympathetic nerve-evoked nasal vasodilatation via Y_2 prejunctional receptor 479

P. Blier & C. Bouchard. Modulation of 5-HT release in the guinea-pig brain following long-term administration of antidepressant drugs 485

R.J. Kiff, D.W. Moss & S. Moncada. Effect of nitric oxide gas on the generation of nitric oxide by isolated blood vessels: implications for inhalation therapy 496

J. Church, E.J. Fletcher, K. Baxter & J.F. MacDonald. Blockade by ifenprodil of high voltage-activated Ca^{2+} channels in rat and mouse cultured hippocampal pyramidal neurones: comparison with N-methyl-D-aspartate receptor antagonist actions **499**

F.L.M. Ricciardolo, J.A. Nadel, P.D. Graf, C. Bertrand, S. Yoshihara & P. Geppetti. Role of kinins in anaphylactic-induced bronchoconstriction mediated by tachykinins in guinea-pigs **508**

M.J. Sanz, V.B. Weg, D.T. Walsh, T.J. Williams & S. Nourshargh. Differential effects of the PAF receptor antagonist UK-74,505 on neutrophil and eosinophil accumulation in guinea-pig skin **513**

J.M. Hall & S.D. Brain. Inhibition by SR140333 of NK_1 tacykinin receptor-evoked, nitric oxide-dependent vasodilatation in the hamster cheek pouch microvasculature *in vivo* **522**

F.G. de Lorenzi, T.R. Bridal & W. Spinelli. Block of the delayed rectifier current (I_K) by the $5\text{-}HT_3$ antagonists ondansetron and granisetron in feline ventricular myocytes **527**

G.J. McBean. Inhibition of the glutamate transporter and glial enzymes in rat striatum by the gliotoxin, αaminoadipate **536**

D. Currò, P. Preziosi, E. Ragazzoni & G. Ciabattoni. Peptide histidine isoleucine-like immunoreactivity release from the rat gastric fundus **541**

N. Fernández, L. Monge, A.L. García-Villalón, J.L. García, B. Gómez & G. Diéguez. Cooling effects on nitric oxide production by rabbit ear and femoral arteries during cholinergic stimulation **550**

R.W. Peoples & F.F. Weight. Trichloroethanol potentiation of γ-aminobutyric acid-activated chloride current in mouse hippocampal neurones **555**

S.-I. Shimizu, M. Nomoto, T. Yamamoto & K. Momose. Reduction by N^G-nitro-L-arginine of H_2O_2-induced endothelial cell injury **564**

P. Charoonroje, Y. Tokumitsu & Y. Numura. Developmental changes in ANP-stimulated guanylyl cyclase activity enhanced by ATP in rat lung membrane fractions **569**

D.J. Otter & R. Chess-Williams. The effects of aldose reductase inhibition with ponalrestat on changes in vascular function in streptozotocin diabetic rats **576**

H. Wise & R.L. Jones. Characterization of prostanoid receptors on rat neutrophils **581**

P. Santicioli & C.A. Maggi. Inhibitory transmitter action of calcitonin gene-related peptide in guinea-pig ureter via activation of glibenclamide-sensitive K channels **588**

D.J. Brayden & A.W. Baird. A distinctive electrophysiological signature from the Peyer's patches of rabbit intestine **593**

N.A. Brown, J.A. Kemp & G.R. Seabrook. Block of human voltage-sensitive Na^+ currents in differentiated SH-SY5Y cells by lifarizine **600**

J.L. Field, S.K. Butt, I.K.M. Morton & J.M. Hall. Bradykinin B_2 receptors and coupling mechanisms in the smooth muscle of the guinea-pig taenia caeci **607**

J.L. Boyer, I.E. Zohn, K.A. Jacobson & T.K. Harden. Differential effects of P_2-purinoceptor antagonists on phospholipase C- and adenylyl cyclase-coupled P_{2Y}-purinoceptors **614**

R.L. McDonald, P.F.T. Vaughan & C. Peers. Muscarinic (M_1) receptor-mediated inhibition of K^+-evoked [^{3}H]-noradrenaline release from human neuroblastoma (SH-SY5Y) cells via inhibition of L- and N-type Ca^{2+} channels **621**

E.S. McKeen, W. Feniuk & P.P.A. Humphrey. Mediation by $SRIF_1$ receptors of the contractile action of somatostatin in rat isolated distal colon; studies using some novel SRIF analogues **628**

M. Malcangio & N.G. Bowery. Effect of the tachykinin NK_1 receptor antagonists, RP 67580 and SR 140333, on electrically-evoked substance P release from rat spinal cord **635**

G. Lees, I.T. Munday, M.D. Edwards & R.M. Jones. *In vitro* potency and mode of action of ANQ9040: a novel fast acting muscle relaxant **642**

F. Larrazet, M. Chauveau, S. Weber, A. Lockhart & N. Frossard. Inhibition of substance P-induced microvascular leakage by inhaled methoxamine in rat airways **649**

Erratum **657**

BRITISH JOURNAL OF PHARMACOLOGY

The *British Journal of Pharmacology* welcomes contributions in all fields of experimental pharmacology including neuroscience, biochemical, cellular and molecular pharmacology. The Board of Editors represents a wide range of expertise and ensures that well-presented work is published as promptly as possible, consistent with maintaining the overall quality of the journal.

Edited for the British Pharmacological Society by

A.T. Birmingham
(Chairman)

R.W. Horton **W.A. Large**
(Secretaries)

Editorial Board

J.A. Angus *Melbourne, Australia*
M.L.J. Ashford *Cambridge*
G.W. Bennett *Nottingham*
W.C. Bowman *Glasgow*
N.G. Bowery *London*
Alison F. Brading *Oxford*
S.D. Brain *London*
K.D. Butler *Horsham*
M. Caulfield *London*
R. Chess-Williams *Sheffield*
M.K. Church *Southampton*
T. Cocks *Melbourne, Australia*
S.J. Coker *Liverpool*
R.A. Coleman *Ware*
Helen M. Cox *London*
A.J. Cross *London*
V. Crunelli *Cardiff*
T.C. Cunnane *Oxford*
F. Cunningham *London*
A. Dray *London*
J.R. Docherty *Dublin*
J.M. Edwardson *Cambridge*
P.C. Emson *Cambridge*
W. Feniuk *Cambridge*
J.R. Fozard *Basle, Switzerland*
Allison D. Fryer *Baltimore, USA*
Sheila M. Gardiner *Nottingham*
C.J. Garland *Bristol*
L.G. Garland *Beckenham*
A. Gibson *London*
R. W. Gristwood *Cambridge*
D.W.P. Hay *Philadelphia, USA*
P.G. Hellewell *London*
P.E. Hicks *Edinburgh*
S.J. Hill *Nottingham*
S.M.O. Hourani *Guildford*
J.C. Hunter *Cambridge*
C.C. Jordan *Ware*
D.A. Kendall *Nottingham*
P. Leff *Loughborough*
H.D. Lux *Planegg, Germany*
R. McMillan *Macclesfield*
J. Maclagan *London*
C.A. Maggi *Florence, Italy*
Janice M. Marshall *Birmingham*
G. Martin *Beckenham*
W. Martin *Glasgow*
A. Mathie *London*
D.N. Middlemiss *Harlow*
P.K. Moore *London*
R.J. Naylor *Bradford*
C.D. Nicholson *Oss, The Netherlands*
C.P. Page *London*
A.N. Payne *Beckenham*
F.L. Pearce *London*
J.D. Pearson *London*
A.G. Renwick *Southampton*
M.H.T. Roberts *Cardiff*
C. Robinson *London*
G.J. Sanger *Harlow*
M.A. Simmonds *London*
J.M. Sneddon *Sunderland*
P. Sneddon *Glasgow*
K. Starke *Freiburg, Germany*
R.J. Summers *Melbourne, Australia*
P.V. Taberner *Bristol*
J. Tamargo *Madrid, Spain*
C. Thiemermann *London*
M.D. Tricklebank *Harlow*
M.B. Tyers *Ware*
S.P. Watson *Oxford*
K.J. Watling *Boston, USA*
A.H. Weston *Manchester*
B.J.R. Whittle *Beckenham*
Eileen Winslow *Riom, France*
B. Woodward *Bath*
E.H.F. Wong *California, USA*

Corresponding Editors

P.R. Adams *Stony Brook, U.S.A.*
C. Bell *Melbourne, Australia*
F.E. Bloom *La Jolla, U.S.A.*
A.L.A. Boura *Newcastle, Australia*
N.J. Dun *Toledo, U.S.A.*
R.F. Furchgott *New York, U.S.A.*
T. Godfraind *Brussels, Belgium*
S.Z. Langer *Paris, France*
R.J. Miller *Chicago, U.S.A.*
R.C. Murphy *Denver, U.S.A.*
E. Muscholl *Mainz, Germany*
R.A. North *Portland, U.S.A.*
M. Otsuka *Tokyo, Japan*
M.J. Rand *Melbourne, Australia*
S. Rosell *Södertalje, Sweden*
P. Seeman *Toronto, Canada*
L. Szekeres *Szeged, Hungary*
B. Uvnas *Stockholm, Sweden*
P.A. Van Zwieten *Amsterdam, Netherlands*
V.M. Varagič *Belgrade, Yugoslavia*
G. Velo *Verona, Italy*
Wang Zhen Gang *Beijing, China*
M.B.H. Youdim *Haifa, Israel*

Submission of manuscripts: Manuscripts (two copies) should be sent to The Editorial Office, British Journal of Pharmacology, St. George's Hospital Medical School, Cranmer Terrace, London SW17 0RE.

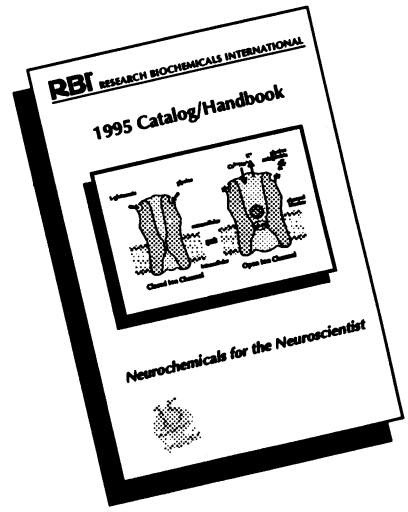
Authors should consult the Instructions to Authors and the Nomenclature Guidelines for Authors in Vol. **111**, 378–387. These Instructions and Guidelines also appear with the journal Index for Volumes **108–110**, 1993. A checklist of the essential requirements is summarised in each issue of the journal, or as the last page of the issue.

Whilst every effort is made by the publishers and editorial committee to see that no inaccurate or misleading data, opinion or statement appears in this Journal, they and the *British Pharmacological Society* wish to make it clear that the data and opinions appearing in the articles and advertisements herein are the responsibility of the contributor or advertiser concerned. Accordingly, the *British Pharmacological Society*, the publishers and the editorial committee and their respective employees, officers and agents accept no liability whatsoever for the consequences of any such inaccurate or misleading data, opinion or statement.

RBI THE RESEARCHER'S GOLD STANDARD

Look here first for new...

- Adenosines/Purinergics
- Adrenergics
- β-Amyloid Proteins
- Benzodiazepines
- Cholecystokinins
- Cholinergics
- Cocaine Receptor Ligands
- Controlled Substances
- Dopaminergics
- Drug Metabolites
- Enzyme Inhibitors
- Excitatory Amino Acids
- GABA-ergics
- Gangliosides
- Histaminergics
- Ion Channel Modulators
- Neuropeptides
- Neurotoxins
- Neurosteroids
- Opioids
- PCP/Sigma Receptor Ligands
- PET/SPECT Agents
- Reference Standards
- Serotonergics
- Signal Transduction Agents
- Tachykinins



Fax or write for our latest Catalog/Handbook, *Neurochemicals for the Neuroscientist*, listing over 1,100 pharmacologically active compounds.

RBI RESEARCH BIOCHEMICALS INTERNATIONAL

One Strathmore Road, Natick, MA 01760-2447 USA
508-651-8151 • 800-736-3690 • Fax 508-655-1359 • 800-736-2480

The *British Journal of Pharmacology* is published by Macmillan Press Ltd.

Scope The *British Journal of Pharmacology* is published monthly. It welcomes contribution in all field of experimental pharmacology including neuroscience, biochemical, cellular and molecular pharmacology. The Board of Editors represents a wide range of expertise and ensures that well-presented work is published as promptly as possible, consistent with maintaining the overall qulaity of the journal

This journal is covered by Current Contents, Excerpta Medica, BIOSIS and Index Medicus.

Editorial Manuscripts (plus two copies) and all editorial correspondence should be sent to: The Editorial Office, British Journal of Pharmacology, St George's Hospital Medical School, Cranmere Terrace, London SW17 0RE, UK. Tel: +44 81 767 6765; Fax: +44 81 767 5645.

Advertisements Enquires concerning advertisements should be addressed to: Michael Rowley, Hasler House, High Street, Great Dunmow, Essex CM6 1AP. Tel: +44 371 874613; Fax: +44 371 872273.

Publisher All business correspondence, supplement enquiries and reprint requests should be addressed to British Journal of Pharmacology, Scientific and Medical Division, Macmillan Press Ltd, Houndmills, Basingstoke, Hampshire RG21 2XS, UK. Tel: +44 256 29242; Fax: +44 256 810526. Publisher: Marija Vukovojac. Editorial Assistant: Alice Ellingham. Production Controller: Kath Parr.

Subscription Subscription price per annum (one volume, twelve issues) £540, rest of world £714 (Airmail), £595 (Surface mail) or equivalent in any other currency. Orders must be accompanied by remittance. Cheques should be made payable to Macmillan Magazines and sent to: The Subscription Department, Macmillan Press Ltd, Houndmills, Basingstoke, Hampshire RG21 2XS, UK. Where appropriate, subscribers may make payments into UK Post Office Giro Account No. 519 2455. Full details must accompany the payment. Subscribers from EC territories should add sales tax at the local rate.

British Journal of Pharmacology (ISSN 0007–1188) is published monthly by Macmillan Press Ltd, c/o Mercury Airfreight International Ltd, 2323 Randolph Avenue, Avenel, NJ 07001, USA. Subscription price for institutions is $950 per annum. 2nd class postage is paid at Rahway NJ. Postmaster: send address corrections to Macmillan Press Ltd, c/o Mercury Airfreight International Ltd, 2323 Randolph Avenue, Avenel NJ 07001.

Reprints of any article in this journal are available from Scientific and Medical Division, Macmillan Press Ltd, Houndmills, Basingstoke, Hampshire RG21 2XS, UK. Tel: +44 256 29242; Fax: +44 256 810526.

Copyright © 1994 The Macmillan Press Ltd

ISSN 0007–1188

All rights of reproduction are reserved in respect of all papers, articles, illustrations, etc., published in this journal in all countries of the world.

All material published in this journal is protected by copyright, which covers exclusive rights to reproduce and distribute the material. No material published in this journal may be reproduced or stored on microfilm or in electronic, optical or magnetic form without the written authorisation of the Publisher.

Authorisation to photocopy items for internal or personal use of specific clients, is granted by Macmillan Press Ltd, for libraries and other users registered with the Copyright Clearance Center (CCC) Transaction Reporting Service, provided that the base fee of $9.00 per copy is paid directly to CCC, 21 Congress St., Salem, MA 01970, USA. 0007-1188/94 $9.00 + $0.00.

Apart from any fair dealing for the purposes of research or private study, or criticism or review, as permitted under the Copyright, Designs and Patent Act 1988, this publication may be reproduced, stored or transmitted, in any form or by any means, only with the prior permission in writing of the publishers, or in the case of reprographic reproduction, in accordance with the terms of licences issued by the Copyright Licensing Agency.

Official publication of the British Pharmacological Society.

PREPARATION OF MANUSCRIPTS

Authors are strongly recommended to read the full *Instructions to Authors* and *Nomenclature Guidelines for Authors* (*Br. J. Pharmacol.* 1994, **111**, 378–387) before submitting a manuscript for publication in the *British Journal of Pharmacology*. The manuscript and cover letter should be checked against the following list before mailing.

The original and one copy of the manuscript must be supplied. Manuscripts must be typed in double-line spacing on one side of A4 paper, in type not smaller than 12 characters per inch or 10 point. Both copies to include Tables and a set of labelled Figures. One set of Figures without numbers or letters is also to be included. The text to be arranged in the following subsections:

1. **Title**—To have no more than 150 characters on a separate page, which should also include a Short Title (50 characters maximum) and the name and address of the author for correspondence.
2. **Summary**—To be arranged in numbered paragraphs (Full Papers) or a single paragraph (Special Reports).
   —to include aims, principal results and conclusions.
   —to include Key words (10 maximum) at end of summary.
3. **Introduction**—To contain concise statements of the problem and the aims of the investigation.
4. **Methods**—To have brief but adequate account of the procedures; *full names of drugs* (*including those referred to by manufacturer's code*), sources of drugs and statistical tests to be stated.
5. **Results**—To have no repetition of data in Figures, Tables and text.
6. **Discussion**—Findings and conclusions to be placed in context of other relevant work.
   NB Simple repetition of results and unwarranted speculation are not acceptable.
7. **Acknowledgements**—Sources of support. Sources of drugs not widely available commercially.
8. **References**—All references in the text to be included in the Reference List and *vice versa*. References in alphabetical order with complete citations; Journals publishing 'in press' papers identified.
   References to manuscripts submitted to other journals but not yet accepted are not allowed.
9. **Tables**—Each on a separate page and prepared in accordance with current requirements of the Journal.
10. **Figures**—Both labelled and non-labelled Figures to be prepared in accordance with current requirements of the Journal (see *Instructions to Authors*, 1993, **108**, 275–281) and provided with Figure Number and Authors' names on back (*in pencil*).
    —each legend to be typed on a separate page and carrying keys to symbols.
    —keys to symbols and histograms must not appear on the figures themselves, but in the respective legends.
    —'box style' figures are not in keeping with the Journal style; line drawings etc must have only left-hand and bottom axes.
11. **Manuscripts**—To be accompanied by a declaration signed by each author that
    (a) results are original
    (b) approval of all persons concerned has been given to submit manuscripts for consideration (see also 12b)
    (c) the same material is neither 'in press' (i.e. is in proof or has definitely been accepted for publication) nor under consideration elsewhere. Furthermore it will not be submitted or published elsewhere before a decision has been reached by the Editorial Board of the *British Journal of Pharmacology* and will not be submitted elsewhere if accepted by the *British Journal of Pharmacology*.
    (d) Copyright assignment is included.
12. **Cover letter**—To state clearly
    (a) Corresponding author's full postal address, telephone, telex or Fax number
    (b) where appropriate, that *either* ethical approval has been given for investigation *or* Company or Institutional permission to publish work has been received.
13. **Reminder**—Packaging to be sufficiently robust to protect Figures and to withstand mailing.

Failure to comply with *Instructions to Authors* may lead to substantial delays in processing, review and publication and may even jeopardize acceptance of the manuscript.

NOMENCLATURE

Authors are reminded that accepted receptor and associated terminology is laid out in *Nomenclature Guidelines for Authors*, as published in the *British Journal of Pharmacology*, *Br. J. Pharmacol.*, 1994, **111**, 385–387.

SPECIAL REPORTS

The purpose of *Special Reports* is to provide rapid publication for **new** and **important** results which the Editorial Board considers are likely to be of special pharmacological significance. *Special Reports* will have publication priority over all other material and so authors are asked to consider carefully the status of their work before submission.

In order to speed publication there is normally no revision allowed beyond very minor typographical or grammatical corrections. If significant revision is required, the Board may either invite rapid re-submission or, more probably, propose that it be re-written as a Full Paper and be re-submitted for consideration. In order to reduce delays, proofs of *Special Reports* will be sent to authors but **essential corrections must reach the Production Office within 48 hours of receipt.** Authors should ensure that their submitted material conforms exactly to the following requirements.

Special Reports should normally occupy no more than two printed pages of the Journal; two illustrations (Figures or Tables, with legends) are permitted. As a guideline, with type face of 12 pitch and double-line spacing, a page of A4 paper could contain about 400 words. The absolute maximum length of the *Special Report* is 1700 words. For each Figure or Table, please deduct 200 words. The manuscript should comprise a Title page with key words (maximum of 10), a Summary consisting of a single short paragraph, followed by Introduction, Methods, Results, Discussion and References (maximum of 10). In all other respects, the requirements are the same as for Full Papers (see current 'Instructions to Authors').

BRITISH JOURNAL OF PHARMACOLOGY VOLUME 113 (2) 1994

SPECIAL REPORTS

H.T. Schambye, B. v. Wijk, S.A. Hjorth, W. Wienen, M. Entzeroth, D.J. Bergsma & T.W. Schwartz. Mutations in transmembrane segment VII of the AT_1 receptor differentiate between closely related insurmountable and competitive angiotensin antagonists 331

C.P. Baines, R.S. Szwarc & H.A. Ball. Parallel tolerance between platelet cyclic GMP and preload effects of nitroglycerin in anaesthetized mini-pigs 334

T. Fukuroda, S. Ozaki, M. Ihara, K. Ishikawa, M. Yano & M. Nishikibe. Synergistic inhibition by BQ-123 and BQ-788 of endothelin-1-induced contractions of the rabbit pulmonary artery 336

J.M. Barnes, K.K. Dev & J.M. Henley. Cyclothiazide unmasks AMPA-evoked stimulation of [^{3}H]-L-glutamate release from rat hippocampal synaptosomes 339

PAPERS

R.P. Coppes, F. Brouwer, I. Freie, J. Smit & J. Zaagsma. Sustained prejunctional facilitation of noradrenergic neurotransmission by adrenaline as a co-transmitter in the portal vein of freely moving rats 342

T. Jun & Å. Wennmalm. NO-dependent and -independent elevation of plasma levels of insulin and glucose in rats by L-arginine 345

R. Bültmann, M. Trendelenburg & K. Starke. Blockage of P_{2x}-purinoceptors by trypan blue in rat vas deferens 349

F.P. Jansen, T.S. Wu, H.-P. Voss, H.W.M. Steinbusch, R.C. Vollinga, B. Rademaker, A. Bast & H. Timmerman. Characterization of the binding of the first selective radiolabelled histamine H_3-receptor antagonist, [^{125}I]-iodophenpropit, to rat brain 355

E. Thorin, C. Capdeville-Atkinson, B. Corman & J. Atkinson. Sympathetic neurotransmission in the tail artery of aging rats 363

Y.-M. Qian, R.L. Jones, K.-M. Chan, A.I. Stock & J.K.S. Ho. Potent contractile actions of prostanoid EP_3-receptor agonists on human isolated pulmonary artery 369

R.S. Redman & E.M. Silinsky. Decrease in calcium currents induced by aminoglycoside antibiotics in frog motor nerve endings 375

R.A. Keith, T.J. Mangano, P.A. DeFeo, G.E. Ernst & E.J. Warawa. Differential inhibition of neuronal calcium entry and [^{3}H]-D-aspartate release by the quaternary derivatives of verapamil and emopamil 379

Y. Kita, Y. Hirasawa, K. Yoshida & K. Maeda. Antiplatelet activities of FK409, a new spontaneous NO releaser 385

J.P. Galizzi, M.C. Bodinier, B. Chapelain, S.M. Ly, L. Coussy, S. Giraud, G. Neliat & T. Jean. Up-regulation of [^{3}H]-des-Arg^{10}-kallidin binding to the bradykinin B_1 receptor by interleukin-1β in isolated smooth muscle cells: correlation with B_1 agonist-induced PGI_2 production 389

J. Su, N. Renaud, A. Carayon, B. Crozatier & L. Hittinger, with the technical assistance of Monique Laplace. Effects of the calcium channel blockers, diltiazem and Ro 40-5967, on systemic haemodynamics and plasma noradrenaline levels in conscious dogs with pacing-induced heart failure 395

A. Laniyonu, M. Saifeddine, S. Ahmad & M.D. Hollenberg. Regulation of vascular and gastric smooth muscle contractility by pervanadate 403

G. Erdemli & K. Krnjević. Actions of cromakalim on outward currents of CA1 neurones in hippocampal slices 411

M.C. Martínez, J.M. Vila, M. Aldasoro, P. Medina, B. Flor & S. Lluch. Relaxation of human isolated mesenteric arteries by vasopressin and desmopressin 419

M. Ballarin, A. Carceller & X. Guitart. Effect of acute administration of the 5-HT_{1A} receptor ligand, lesopitron, on rat cortical 5-HT and dopamine turnover 425

Y. Zhang & R.J. Lang. Effects of intrinsic prostaglandins on the spontaneous contractile and electrical activity of the proximal renal pelvis of the guinea-pig 431

R. Gniadecki, M. Gniadecka & J. Serup. Inhibition of glucocorticoid-induced epidermal and dermal atrophy with KH 1060 – a potent 20-epi analogue of 1,25-dihydroxyvitamin D_3 439

A.E. Eckly & C. Lugnier. Role of phosphodiesterases III and IV in the modulation of vascular cyclic AMP content by the NO/cyclic GMP pathway 445

R. Okuyama, S. Adachi-Akahane & T. Nagao. Differential potential by depolarization of the effects of calcium antagonists on contraction and Ca^{2+} current in guinea-pig heart 451

P. Pacaud, G. Grégoire & G. Loirand. Release of Ca^{2+} from intracellular store in smooth muscle cells of rat portal vein by ATP-induced Ca^{2+} entry 457

D.J. Trezise, N.J. Bell, I. Kennedy & P.P.A. Humphrey. Effects of divalent cations on the potency of ATP and related agonists in the rat isolated vagus nerve: implications for P_2 purinoceptor classification 463

G.A.J. Kuijpers, L.A. Vergara, S. Calvo & G. Yadid. Inhibitory effect of strychnine on acetylcholine receptor activation in bovine adrenal medullary chromaffin cells 471

J.S. Lacroix, L.G. Ulman & E.K. Potter. Modulation by neuropeptide Y of parasympathetic nerve-evoked nasal vasodilatation via Y_2 prejunctional receptor 479

P. Blier & C. Bouchard. Modulation of 5-HT release in the guinea-pig brain following long-term administration of antidepressant drugs 485

R.J. Kiff, D.W. Moss & S. Moncada. Effect of nitric oxide gas on the generation of nitric oxide by isolated blood vessels: implications for inhalation therapy 496

J. Church, E.J. Fletcher, K. Baxter & J.F. MacDonald. Blockade by ifenprodil of high voltage-activated Ca^{2+} channels in rat and mouse cultured hippocampal pyramidal neurones: comparison with N-methyl-D-aspartate receptor antagonist actions 499

F.L.M. Ricciardolo, J.A. Nadel, P.D. Graf, C. Bertrand, S. Yoshihara & P. Geppetti. Role of kinins in anaphylactic-induced bronchoconstriction mediated by tachykinins in guinea-pigs 508

M.J. Sanz, V.B. Weg, D.T. Walsh, T.J. Williams & S. Nourshargh. Differential effects of the PAF receptor antagonist UK-74,505 on neutrophil and eosinophil accumulation in guinea-pig skin 513

J.M. Hall & S.D. Brain. Inhibition by SR140333 of NK_1 tacykinin receptor-evoked, nitric oxide-dependent vasodilatation in the hamster cheek pouch microvasculature *in vivo* 522

F.G. de Lorenzi, T.R. Bridal & W. Spinelli. Block of the delayed rectifier current (I_K) by the 5-HT_3 antagonists ondansetron and granisetron in feline ventricular myocytes 527

G.J. McBean. Inhibition of the glutamate transporter and glial enzymes in rat striatum by the gliotoxin, αaminoadipate 536

D. Currò, P. Preziosi, E. Ragazzoni & G. Ciabattoni. Peptide histidine isoleucine-like immunoreactivity release from the rat gastric fundus 541

N. Fernández, L. Monge, A.L. García-Villalón, J.L. García, B. Gómez & G. Diéguez. Cooling effects on nitric oxide production by rabbit ear and femoral arteries during cholinergic stimulation 550

R.W. Peoples & F.F. Weight. Trichloroethanol potentiation of γ-aminobutyric acid-activated chloride current in mouse hippocampal neurones 555

S.-I. Shimizu, M. Nomoto, T. Yamamoto & K. Momose. Reduction by N^G-nitro-L-arginine of H_2O_2-induced endothelial cell injury 564

P. Charoonroje, Y. Tokumitsu & Y. Numura. Developmental changes in ANP-stimulated guanylyl cyclase activity enhanced by ATP in rat lung membrane fractions 569

Contents continue inside back cover

Typeset by Elite Typesetting Techniques, Southampton, Hampshire
and printed in Great Britain by Unwin Brothers Ltd., The Gresham Press, Old Woking, Surrey

D.J. Otter & R. Chess-Williams. The effects of aldose reductase inhibition with ponalrestat on changes in vascular function in streptozotocin diabetic rats **576**

H. Wise & R.L. Jones. Characterization of prostanoid receptors on rat neutrophils **581**

P. Santicioli & C.A. Maggi. Inhibitory transmitter action of calcitonin gene-related peptide in guinea-pig ureter via activation of glibenclamide-sensitive K channels **588**

D.J. Brayden & A.W. Baird. A distinctive electrophysiological signature from the Peyer's patches of rabbit intestine **593**

N.A. Brown, J.A. Kemp & G.R. Seabrook. Block of human voltage-sensitive Na^+ currents in differentiated SH-SY5Y cells by lifarizine **600**

J.L. Field, S.K. Butt, I.K.M. Morton & J.M. Hall. Bradykinin B_2 receptors and coupling mechanisms in the smooth muscle of the guinea-pig taenia caeci **607**

J.L. Boyer, I.E. Zohn, K.A. Jacobson & T.K. Harden. Differential effects of P_2-purinoceptor antagonists on phospholipase C- and adenylyl cyclase-coupled P_{2Y}-purinoceptor **614**

R.L. McDonald, P.F.T. Vaughan & C. Peers. Muscarinic (M_1) receptor-mediated inhibition of K^+-evoked [^{3}H]-noradrenaline release from human neuroblastoma (SH-SY5Y) cells via inhibition of L- and N-type Ca^{2+} channels **621**

E.S. McKeen, W. Feniuk & P.P. A. Humphrey. Mediation by $SRIF_1$ receptors of the contractile action of somatostatin in rat isolated distal colon; studies using some novel SRIF analogues **628**

M. Malcangio & N.G. Bowery. Effect of the tachykinin NK_1 receptor antagonists, RP 67580 and SR 140333, on electrically-evoked substance P release from rat spinal cord **635**

G. Lees, I.T. Munday, M.D. Edwards & R.M. Jones. *In vitro* potency and mode of action of ANQ9040: a novel fast acting muscle relaxant **642**

F. Larrazet, M. Chauveau, S. Weber, A. Lockhart & N. Frossard. Inhibition of substance P-induced microvascular leakage by inhaled methoxamine in rat airways **649**

Erratum **657**